APPENDIX B.1.1

# Downhole Data

# Appendix B.1.1
# Downhole Data

The following data reports were prepared for the SR 710 Tunnel Technical Study Final Geotechnical Summary Report (CH2M HILL, 2010). However, only data relevant to the SR 710 North Study are provided herein. To view the reports in their entirety, refer to the Technical Study (CH2M HILL, 2010).

GEOVision
geophysical services

# SR-710 TUNNEL TECHNICAL STUDY
# BORING GEOPHYSICS

## BORINGS Z1-B3, Z1-B5, Z1-B6, Z1-B7, Z2-B1, Z2-B4, Z3-B1, Z3-B3, Z3-B4, Z3-B6, Z3-B8, Z3-B12 AND Z4-B4

**Report 9014-01 rev 0**

**October 5, 2009**

# SR-710 TUNNEL TECHNICAL STUDY
# BORING GEOPHYSICS

# BORINGS Z1-B3, Z1-B5, Z1-B6, Z1-B7, Z2-B1, Z2-B4, Z3-B1, Z3-B3, Z3-B4, Z3-B6, Z3-B8, Z3-B12 AND Z4-B4

**Report 9014-01 rev 0**

**October 5, 2009**

**Prepared for:**

**Cascade Drilling, Inc.**
**555 South Harbor Boulevard**
**La Habra, California 90631**
**562-929-8176**

**Prepared by**

**GEOVision Geophysical Services**
**1124 Olympic Drive**
**Corona, California 92881**
**(951) 549-1234**

# TABLE OF CONTENTS

# Table of Figures

# Table of Tables

## APPENDICES

## INTRODUCTION

Boring geophysical measurements were collected in thirteen uncased borings located within four zones of the SR-710 tunnel technical study. Geophysical data acquisition was performed between January 14 and March 31, 2009 by Robert Steller, Charles Carter and Lauren Annis of **GEO***Vision*. Data analysis was performed by Robert Steller and reviewed by John Diehl of **GEO***Vision*. Report preparation was performed by Robert Steller and reviewed by John Diehl of **GEO***Vision*. The work was performed under subcontract with Cascade Drilling for CH2M Hill, Inc. (CH2M) with Ravee Raveendra serving as the point of contact for CH2M.

This report describes the field measurements, data analysis, and results of this work.

## SCOPE OF WORK

This report presents the results of boring geophysical measurements collected between January 14 and March 31, 2009, in thirteen borings, as detailed in Table 1. The purpose of these studies was to supplement stratigraphic information obtained during CH2M's soil and rock sampling program and to acquire shear wave velocities and compressional wave velocities as a function of depth, as a component of the SR-710 tunnel study.

The OYO/Robertson Suspension PS Logging System (Suspension System) was used to obtain in-situ horizontal shear ($S_H$) and compressional (P) wave velocity measurements in all borings, except Z3-B8, at 1.6-foot intervals. Measurements followed **GEO***Vision* Procedure for P-S Suspension Seismic Velocity Logging, revision 1.3. The acquired data was analyzed and a profile of velocity versus depth was produced for both compressional and horizontally polarized shear waves.

A detailed reference for the suspension PS velocity measurement techniques used in this study is:

> Guidelines for Determining Design Basis Ground Motions, Report TR-102293, Electric Power Research Institute, Palo Alto, California, November 1993, Sections 7 and 8.

The Robertson 3ACS probe was used to collect 3-arm mechanical caliper and natural gamma data at 0.05-foot intervals in all borings to aid in identification of stratagraphic transitions. Measurement procedures followed these ASTM standards:

- ASTM D5753, "Planning and Conducting Borehole Geophysical Surveys
- ASTM D6274, "Conducting Borehole Geophysical Logging – Gamma ASTM D6274-98 (Re-approved 2004), Conducting Borehole Geophysical Logging - Gamma"
- ASTM D6167-97 (Re-approved 2004) "Conducting Borehole Geophysical Logging – Mechanical Caliper"

The acquired data was combined and a profile of these parameters versus depth was produced.

The Robertson High Resolution Acoustic Televiewer (HiRAT) was used to collect deviation data and acoustic televiewer images of the rock at 0.008-foot intervals in all borings except Z3-B8. Measurements followed the **GEO***Vision* HiRAT Field Procedure, revision 1.0. In addition, the boring images were analyzed and planar features such as bedding planes and fractures were identified for dip, azimuth and stereonet processing to identify dominant fracture and bedding planes.

# INSTRUMENTATION

## Suspension Velocity Instrumentation

Suspension velocity measurements were performed using the suspension PS logging system, manufactured by OYO Corporation, and their subsidiary, Robertson Geologging. This system directly determines the average velocity of a 3.28-foot high segment of the soil column surrounding the boring of interest by measuring the elapsed time between arrivals of a wave propagating upward through the soil column. The receivers that detect the wave, and the source that generates the wave, are moved as a unit in the boring producing relatively constant amplitude signals at all depths.

The suspension system probe consists of a combined reversible polarity solenoid horizontal shear-wave source ($S_H$) and compressional-wave source (P), joined to two biaxial receivers by a flexible isolation cylinder, as shown in Figure 1. The separation of the two receivers is 3.28 feet, allowing average wave velocity in the region between the receivers to be determined by inversion of the wave travel time between the two receivers. The total length of the probe as used in these surveys is 19 feet, with the center point of the receiver pair 12.1 feet above the bottom end of the probe.

The probe receives control signals from, and sends the digitized receiver signals to, instrumentation on the surface via an armored 4 conductor cable. The cable is wound onto the drum of a winch and is used to support the probe. Cable travel is measured to provide probe depth data, using a 3.28-foot circumference sheave fitted with a digital rotary encoder.

The entire probe is suspended in the boring by the cable, therefore, source motion is not coupled directly to the boring walls; rather, the source motion creates a horizontally propagating impulsive pressure wave in the fluid filling the boring and surrounding the source. This pressure wave is converted to P and $S_H$-waves in the surrounding soil and rock as it passes through the casing and grout annulus and impinges upon the wall of the boring. These waves propagate

through the soil and rock surrounding the boring, in turn causing a pressure wave to be generated in the fluid surrounding the receivers as the soil waves pass their location. Separation of the P and $S_H$-waves at the receivers is performed using the following steps:

1. Orientation of the horizontal receivers is maintained parallel to the axis of the source, maximizing the amplitude of the recorded $S_H$ -wave signals.
2. At each depth, $S_H$-wave signals are recorded with the source actuated in opposite directions, producing $S_H$-wave signals of opposite polarity, providing a characteristic $S_H$-wave signature distinct from the P-wave signal.
3. The 7.0-foot separation of source and receiver 1 permits the P-wave signal to pass and damp significantly before the slower $S_H$-wave signal arrives at the receiver. In faster soils or rock, the isolation cylinder is extended to allow greater separation of the P- and $S_H$-wave signals.
4. In saturated soils, the received P-wave signal is typically of much higher frequency than the received $S_H$-wave signal, permitting additional separation of the two signals by low pass filtering.
5. Direct arrival of the original pressure pulse in the fluid is not detected at the receivers because the wavelength of the pressure pulse in fluid is significantly greater than the dimension of the fluid annulus surrounding the probe (foot versus inch scale), preventing significant energy transmission through the fluid medium.

In operation, a distinct, repeatable pattern of impulses is generated at each depth as follows:

1. The source is fired in one direction producing dominantly horizontal shear with some vertical compression, and the signals from the horizontal receivers situated parallel to the axis of motion of the source are recorded.
2. The source is fired again in the opposite direction and the horizontal receiver signals are recorded.
3. The source is fired again and the vertical receiver signals are recorded. The repeated source pattern facilitates the picking of the P and $S_H$-wave arrivals; reversal of the source changes the polarity of the $S_H$-wave pattern but not the P-wave pattern.

The data from each receiver during each source activation is recorded as a different channel on the recording system. The Suspension PS system has six channels (two simultaneous recording channels), each with a 1024 sample record. The recorded data are displayed as six channels with a common time scale. Data are stored on disk for further processing. Up to 8 sampling sequences can be summed to improve the signal to noise ratio of the signals.

Review of the displayed data on the recorder or computer screen allows the operator to set the gains, filters, delay time, pulse length (energy), sample rate, and summing number to optimize the quality of the data before recording. Verification of the calibration of the Suspension PS digital recorder is performed every twelve months using a NIST traceable frequency source and counter, as outlined in Appendix D.

## Caliper / Natural Gamma Instrumentation

Caliper and natural gamma data were collected using a Model 3ACS 3-arm caliper probe, serial number 5368, manufactured by Robertson Geologging, Ltd. With the short arm configuration used in these surveys, the probe permitted measurement of boring diameters between 1.6 and 16 inches. With this tool, caliper measurements were collected concurrent with measurement of natural gamma emission from the boring walls. The probe is 6.82 feet long, and 1.5 inches in diameter.

This probe is useful in the following studies:

- Measurement of boring diameter and volume
- Location of hard and soft formations
- Location of fissures, caving, pinching and casing damage
- Bed boundary identification
- Strata correlation between borings

The probe receives control signals from, and sends the digitized measurement values to, a Robertson Micrologger II on the surface via an armored 4 conductor cable. The cable is wound onto the drum of a winch and is used to support the probe. Cable travel is measured to provide probe depth data, using a 3.28-foot circumference sheave fitted with a digital rotary encoder. The probe and depth data are transmitted by USB link from the Micrologger unit to a laptop computer where it is displayed and stored on hard disk.

The caliper consists of three arms, each with a toothed quadrant at their base, pivoted in the lower probe body. A toothed rack engages with each quadrant, thus constraining the arms to move together. Linear movement of the rack is converted to opening and closing of the arms. Springs hold the arms open in the operating position. A motor drive is provided to retract the arms, allowing the probe to be lowered into the boring. The rack is coupled to a potentiometer which converts movement into a voltage sensed by the probe's microprocessor.

Natural gamma measurements rely upon small quantities of radioactive material contained in all soil and rocks to emit gamma radiation as they decay. Trace amounts of Uranium and Thorium are present in a few minerals, where potassium-bearing minerals such as feldspar, mica and clays will include traces of a radioactive isotope of Potassium. These emit gamma radiation as they decay with an extremely long half-life. This radiation is detected by scintillation - the production of a tiny flash of light when gamma rays strike a crystal of sodium iodide. The light is converted into an electrical pulse by a photomultiplier tube. Pulses above a threshold value of 60 thousand electron Volts (KeV) are counted by the probe's microprocessor. The measurement is useful because the radioactive elements are concentrated in certain soil and rock types e.g. clay or shale, and depleted in others e.g. sandstone or coal.

## Acoustic Televiewer / Boring Deviation Instrumentation

An acoustic image and boring deviation data were collected using a High Resolution Acoustic Televiewer probe (HiRAT), serial number 5174, manufactured by Robertson Geologging, Ltd. The probe is 5.2 feet long, 1.6 inches in diameter, and may be fitted with upper and lower four-band centralizers.

In this application, this probe is useful in the following studies:

- Measurement of boring inclination and deviation from vertical
- Determination of need to correct soil and geophysical log depths to true vertical depths
- Acoustic imaging of the boring wall to identify fractures, dikes, and weathered zones, and determine dip and azimuth of these features

The probe receives control signals from, and sends the digitized measurement values to, a Robertson Micrologger II on the surface via an armored 4 conductor cable. The cable is wound onto the drum of a winch and is used to support the probe. Cable travel is measured to provide probe depth data, using a 3.28-foot circumference sheave fitted with a digital rotary encoder. The probe and depth data are transmitted by USB link from the Micrologger unit to a laptop computer where it is displayed and stored on hard disk.

This system produces images of the boring wall based upon the amplitude and travel time of an ultrasonic beam reflected from the formation wall. The ultrasonic energy is generated by a piezoelectric transducer at a frequency of 1.4 MHz. A periodic acoustic energy wave is emitted by the transducer and travels through the acoustic head and boring fluid until it reaches the interface between the boring fluid and the boring wall. Here a portion of the energy is reflected back to the transducer, the remainder continuing on into the formation. By careful time sequencing, the piezoelectric transducer acts as both the transmitter of the ultrasonic pulse and receiver of the reflected wave. The travel time of the energy wave is the period between transmission of the source energy pulse and the return of the reflected wave measured at the point of maximum wave amplitude. The magnitude of the wave energy is measured in dB, a

unit-less ratio of the detected echo wave amplitude divided by the amplitude of the transmitted wave. The strength of the reflected signal depends primarily upon the impedance contrast of the boring fluid and the boring wall formation. In a number of these borings, there was significant clay "wall cake" which attenuated the acoustic signal, and created a low impedance contrast at the boring wall.

The acoustic wave propagates along the axis of the probe and then is reflected perpendicular to this axis by a reflector that focuses the beam to a 0.1-inch diameter spot about 2 inches from the central axis of the probe. This reflector is mounted on the shaft of a stepper motor enabling the position of the measurement to be rotated through 360°. Sampling rates of 90, 180 and 360 measured points per revolution are available. During these surveys, data were collected at 360 samples per revolution, providing an equivalent horizontal pixel size of approximately 0.05 inches on the boring wall. It should be noted that during logging the probe is moving in the boring, so that the measured points describe a very fine pitch spiral.

The probe contains a fluxgate magnetometer to monitor magnetic north, and all raw televiewer data are referenced to magnetic north. The processed data is referenced to true north, using a declination of 12.9 degrees east for these sites and dates, obtained from the NOAA declination web site (http://www.ngdc.noaa.gov/geomagmodels/Declination.jsp). Also, a three-axis accelerometer is enclosed in the probe, and boring deviation data are recorded during the logging runs, to permit correction of structure dip angle from apparent dip, (referenced to boring axis), to true dip (referenced to a vertical axis) in non-vertical borings.

The data are presented on a computer screen for operator review during the logging run, and stored on hard disk for later processing.

# MEASUREMENT PROCEDURES

## Suspension Velocity Measurement Procedures

Twelve borings (excluding Z3-B8) were logged while filled with bentonite or polymer based drilling mud. Measurements followed the **GEO***Vision* Procedure for P-S Suspension Seismic Velocity Logging, revision 1.31, as presented in Appendix E. These procedures were supplied and approved in advance of the work. Prior to each logging run, the probe was positioned with the top of the probe at the top of the surface casing, and the electronic depth counter was set to 8.2 feet, the distance between the mid-point of the receiver and the top of the probe, minus the height of the casing stick-up, as verified with a tape measure, and recorded on the field logs. The probe was lowered to the bottom of the boring, stopping at 1.6-foot intervals to collect data, as summarized in Table 2.

At each measurement depth the measurement sequence of two opposite horizontal records and one vertical record was performed, and the gains were adjusted as required. The data from each depth were viewed on the computer display, checked, and recorded on disk before moving to the next depth.

Upon completion of the measurements, the probe zero depth indication at the depth reference point was verified prior to removal from the boring, and after survey depth error (ASDE) was calculated, as listed in Table 3.

## Caliper / Natural Gamma Procedures

The borings were filled with bentonite or polymer based drilling mud and logged from the bottom of the boring up until the caliper entered the bottom of the surface casing or reached the surface, as listed in Table 2. Measurements followed ASTM D6167-97 (Re-approved 2004) Conducting Borehole Geophysical Logging – Mechanical Caliper.

Prior to and following each logging run, the caliper tool was verified, using the manufacturer's supplied three point calibration jig. The three point jig is a circular plate with a series of holes in the top surface into which the tips of the caliper arms fit. This has circles of diameters from 2 to 12 inches. The calibration jig is placed over a bucket with the probe standing upright with its nose section passing through the jig's central hole. The caliper probe arms are opened under program control, and a log is recorded as the tips of the arms are placed in the holes on the calibration jig. The measured dimensions, as displayed on the recording computer screen was recorded on the field log sheet, as well as in the digital files, and compared with the calibration jig dimensions. These files are presented in LAS 2.0 format in the boring specific sub-directories of the data directory on the data disk (CD-R) labeled Report 9014-02 that accompanies this report. If the verification records did not fall within +/- 0.05 inches of the calibration jig values, the caliper tool was re-calibrated, using the three point calibration jig, and the log repeated. As with the verification, the tips of the caliper arms are placed in the holes marked with the required diameter. During calibration, the value of the current calibration point, as stamped on the jig, is entered via the control computer. The system counts for 15 seconds to make an average of the response. The procedure is repeated for the second and third required openings. The computation and generation of the calibration coefficient file is entirely automatic. The calibration file is simply the set of coefficients of a quadratic curve which fits the three data points.

Natural gamma was not calibrated in the field, as it is a qualitative measurement, not a quantitative value, and is used only to assist in picking transitions between stratigraphic units, as described in ASTM D6274-98 (Re-approved 2004), Conducting Borehole Geophysical Logging - Gamma.

In each boring, the probe was positioned with the top of the probe at the top of the casing, and the electronic depth counter was set to the specified length of the probe, minus the height of the casing stick-up, as verified with a tape measure, and recorded on the field logs. The probe was lowered to the bottom of the boring, where the caliper legs were opened, and data collection begun. The probe was then returned to the surface at 10 feet/minute, collecting data continuously at 0.05-foot spacing, as summarized in Table 2.

Upon completion of the measurements, the probe zero depth indication at the depth reference point was verified prior to removal from the boring, and after survey depth error (ASDE) was calculated, as listed in Table 3.

## Acoustic Televiewer / Boring Deviation Measurement Procedures

Twelve borings (excluding Z3-B8) were logged while filled with bentonite or polymer based drilling mud. Measurements followed the **GEO***Vision* standard field procedures, as presented in Appendix E.

Prior to use, the HiRAT probe tiltmeter and compass functions were checked by comparison with a Brunton surveyors' compass, and the results recorded on the field logs.

In each boring, the HiRAT probe was positioned with the top of the probe at the top of the casing, and the electronic depth counter was set to the specified length of the probe, minus the height of the casing stick-up, as verified with a tape measure, and recorded on the field logs. The probe was lowered to the bottom of the boring, and data collection begun. The rotational scan resolution was set to 360 samples per revolution, giving a horizontal pixel size of approximately 0.05 inches. The probe was returned to the surface at a nominal rate of 3 feet/minute, with an acquisition rate of 125 samples/foot, giving an equivalent vertical pixel size of 0.008 feet (approximately 0.1 inches).

Upon completion of the measurements, the probe zero depth indication at grade was verified prior to removal from the boring, and after survey depth error (ASDE) was calculated, as listed in Table 3.

# DATA ANALYSIS

## Suspension Velocity Analysis

Using the proprietary OYO program PSLOG.EXE version 1.0, the recorded digital waveforms were analyzed to locate the most prominent first minima, first maxima, or first break on the vertical axis records, indicating the arrival of P-wave energy.

The difference in travel time between receiver 1 and receiver 2 (R1-R2) arrivals was used to calculate the P-wave velocity for that 3.28-foot segment of the soil column. When observable, P-wave arrivals on the horizontal axis records were used to verify the velocities determined from the vertical axis data. The time picks were then transferred into an EXCEL template (EXCEL version 2003 SP2) to complete the velocity calculations based upon the arrival time picks made in PSLOG. The EXCEL analysis files are included in the boring specific directories on the data disk (CD-R) labeled Report 9014-02 that accompanies this report.

The P-wave velocity over the 7.0-foot interval from source to receiver 1 (S-R1) was also picked using PSLOG, and calculated and plotted in EXCEL, for quality assurance of the velocity derived from the travel time between receivers. In this analysis, the depth values as recorded were increased by 5.2 feet to correspond to the mid-point of the7.0-foot S-R1 interval. Travel times were obtained by picking the first break of the P-wave signal at receiver 1 and subtracting 0.3 milliseconds, the calculated and experimentally verified delay from source trigger pulse (beginning of record) to source impact. This delay corresponds to the duration of acceleration of the solenoid before impact.

As with the P-wave records, the recorded digital waveforms were analyzed to locate clear $S_H$-wave pulses, as indicated by the presence of opposite polarity pulses on each pair of horizontal records. Ideally, the $S_H$-wave signals from the 'normal' and 'reverse' source pulses are very nearly inverted images of each other. Digital Fast Fourier Transform – Inverse Fast Fourier Transform (FFT – IFFT) lowpass filtering was used to remove the higher frequency P-wave

signal from the $S_H$-wave signal. Different filter cutoffs were used to separate P- and $S_H$-waves at different depths, ranging from 600 Hz in the slowest zones to 3000 Hz in the regions of highest velocity. At each depth, the filter frequency was selected to be at least twice the fundamental frequency of the $S_H$-wave signal being filtered.

Generally, the first maxima were picked for the 'normal' signals and the first minima for the 'reverse' signals, although other points on the waveform were used if the first pulse was distorted. The absolute arrival time of the 'normal' and 'reverse' signals may vary by +/- 0.2 milliseconds, due to differences in the actuation time of the solenoid source caused by constant mechanical bias in the source or by boring inclination. This variation does not affect the R1-R2 velocity determinations, as the differential time is measured between arrivals of waves created by the same source actuation. The final velocity value is the average of the values obtained from the 'normal' and 'reverse' source actuations.

As with the P-wave data, $S_H$-wave velocity calculated from the travel time over the 7.0-foot interval from source to receiver 1 was calculated and plotted for verification of the velocity derived from the travel time between receivers. In this analysis, the depth values were increased by 5.2 feet to correspond to the mid-point of the 7.0-foot S-R1 interval. Travel times were obtained by picking the first break of the $S_H$-wave signal at the near receiver and subtracting 0.3 milliseconds, the calculated and experimentally verified delay from the beginning of the record at the source trigger pulse to source impact.

These data and analysis were reviewed by John Diehl as a component of **GEO***Vision*'s in-house Quality assurance program.

Figure 2 shows an example of R1 - R2 measurements on a sample filtered suspension record. In Figure 2, the time difference over the 3.28-foot interval of 1.88 milliseconds for the horizontal signals is equivalent to an $S_H$-wave velocity of 1745 feet/second. Whenever possible, time differences were determined from several phase points on the $S_H$-waveform records to verify the data obtained from the first arrival of the $S_H$-wave pulse. Figure 3 displays the same record before filtering of the $S_H$-waveform record with a 1400 Hz FFT - IFFT digital lowpass filter,

illustrating the presence of higher frequency P-wave energy at the beginning of the record, and distortion of the lower frequency $S_H$-wave by residual P-wave signal.

## Caliper / Natural Gamma Analysis

No analysis is required with the caliper or natural gamma data; however depths to identifiable boring features on the acoustic televiewer and suspension logs were compared to verify compatible depth readings on all logs. Using Robertson Geologging Winlogger software version 1.5, build 401J, these data were converted to LAS 2.0 and PDF formats for transmittal to the client.

## Acoustic Televiewer / Boring Deviation Analysis

The acoustic televiewer data were processed using Robertson's RGLDIP software, version 6.2. Sinusoidal projections of fractures observed in the boring walls were interactively picked on the un-wrapped televiewer image, and are presented on the logs as red sinusoids superimposed over the televiewer image. Bedding features, where identifiable, were picked on the same images, and are presented on the logs as green sinusoids. The sinusoidal projections were processed using the mechanical caliper diameter data to calculate apparent dip angle. True dip was calculated, correcting for the plunge of the borings using the recorded data from the accelerometer located in the probes, and presented in arrow format, with true dip indicated by the arrow position across the plot. Azimuth of dip (not strike), is indicated by the direction of the arrow tail, with true north being "up". These values are presented with the comments to the right of the arrow plots, as dip azimuth followed by dip angle.

The televiewer images were also processed to create a simulated core image of the borings. It must be noted that the simulated core image represents a core that would have the full diameter of the boring, not the diameter of the cores removed during drilling, so that direct comparison between the two is not possible. Also, the unwrapped image is viewed from the perspective of an observer in the center of the boring looking outward. The simulated core image is viewed form the "outside" of the boring looking inward, so there is a reversal of the position of east and west relative to north between the two images.

The televiewer data were also processed to extract the deviation data and produce an ASCII file and plots of boring deviation. Stereonet analysis of the identified features was performed with Robertson's RGLDIP software, version 6.2, to assist in identifying dominant fracture and bedding planes in the borings. Concentrations of similarly oriented features were enclosed in three to five small circles on the stereonet image, and the vector mean dip and azimuth for each small circle was calculated.

# RESULTS

## Suspension Velocity Results

Suspension R1-R2 P- and $S_H$-wave velocities are plotted in Figures 4, 8, 12, 16, 20, 24, 28, 32, 36, 40, 45, and 49. The suspension velocity data presented in these figures are presented in Tables 5, 7, 9, 11, 13, 15, 17, 19, 21, 23, 25, and 27. The EXCEL analysis file for each boring are included in the boring specific directories on the data disk (CD-R) labeled Report 9014-02 that accompanies this report.

P- and $S_H$-wave velocity data from R1-R2 analysis and quality assurance analysis of S-R1 data are plotted together in Figures A-1 through A-12 to aid in visual comparison. It should be noted that R1-R2 data are an average velocity over a 3.28-foot segment of the soil column; S-R1 data are an average over 7.0 feet, creating a significant smoothing relative to the R1-R2 plots. S-R1 data are presented in Tables A-1 through A-12, and included in the EXCEL analysis files for each boring on the data disk (CD-R) labeled Report 9014-02 that accompanies this report. The EXCEL analysis files include Poisson's Ratio calculations, tabulated data and plots.

Calibration procedures and records for the suspension PS measurement system are presented in Appendix D.

The **GEO***Vision* standard field procedures, as provided to CH2M for approval prior to field work, are reproduced in Appendix E.

## Caliper / Natural Gamma Results

Caliper and natural gamma data are presented as single page logs in Figures 5, 9, 13, 17, 21, 25, 29, 33, 37, 41, 44, 46 and 50, as well as multi-page logs in Appendix B. LAS 2.0 data and Acrobat files for each boring are included in the boring specific sub-directories in the data directory on the data disk (CD-R) labeled Report 9014-02 that accompanies this report.

## Acoustic Televiewer / Boring Deviation Results

Acoustic televiewer amplitude images and picked sinusoids are presented in Appendix C. The same logs are presented in .pdf format in the boring specific sub-directories of the data disk (CD-R) labeled Report 9014-02 that accompanies this report. Fracture and bedding depth, dip and azimuth of dip data are provided on the multi-page log sheets in Appendix C, and in Tables 6, 8, 10, 12, 14, 16, 18, 20, 22, 24, 26 and 28 as well as in .txt and EXCEL format.

Upper hemisphere stereonet plots are presented in Figures 6, 10, 14, 18, 22, 26, 30, 34, 38, 42, 47, and 51, as well as in PDF format. These borings did not exhibit different zones of feature orientation; the feature orientations appeared to be fairly evenly distributed over the boring depths, so they were processed as single zone models.

The mean dips for each of the stereonet small circles are presented in Figures 6, 10, 14, 18, 22, 26, 30, 34, 38, 42, 47, and 51, and in ASCII format. Feature distribution histograms and Rose diagrams are presented in the boring specific sub-directories of the data disk (CD-R).

Boring deviation data is presented graphically in Figures 7, 11, 15, 19, 23, 27, 31, 35, 39, 43, 48 and 52, and summarized in Table 4. Deviation data plots in Acrobat format and deviation data at 1.0-foot stations are presented in text format in the boring specific sub-directories of the data disk (CD-R).

# SUMMARY

## Discussion of Suspension Velocity Results

Suspension PS velocity data are ideally collected in an uncased fluid filled boring, drilled with rotary mud (rotary wash) methods. The borings at these sites were well suited for collection of suspension PS velocity data, though in some cases the shallow portions of the borings were eroded out to large diameters, which degraded the quality of the velocity data.

Suspension PS velocity data quality is judged based upon 5 criteria:

1. Consistent data between receiver to receiver (R1 – R2) and source to receiver (S – R1) data.
2. Consistent relationship between P-wave and $S_H$ -wave (excluding transition to saturated soils)
3. Consistency between data from adjacent depth intervals.
4. Clarity of P-wave and $S_H$-wave onset, as well as damping of later oscillations.
5. Consistency of profile between adjacent borings, if available.

Generally, these data show excellent correlation between R1 – R2 and S – R1 data, as well as excellent correlation between P-wave and $S_H$-wave velocities. P-wave and $S_H$-wave onsets are very clear, and later oscillations are well damped, with the exception of the borings that showed larger diameters due to erosion, Z1-B6, Z1-B7, Z2-B1 and Z3-B12, some which had diameters approaching 12 inches.

## Discussion of Caliper / Natural Gamma Results

Caliper and natural gamma data were collected in each boring. The caliper logs for these borings generally show nominal bit diameters of below about 100 feet, with the softer material above 100 feet eroded out to almost 12 inches in some locations. Natural gamma data were collected with this tool in all the borings, and shows a number of thin layers that correspond to

features on the acoustic televiewer logs. One such example is at 361 – 362 feet in Z1-B6, where there is a significant drop in natural gamma, and an apparent hard sandstone layer on the acoustic televiewer image. A significant velocity increase can be seen at the same depth.

## Discussion of Acoustic Televiewer / Boring Deviation Results

Despite the large nominal diameter (5.5 inches) of the Cascade Drilling borings, the acoustic televiewer data quality in borings with good diameter control and clean walls, like Z1-B3, Z1-B5 are quite clear, showing contacts between soft and harder rock units, fractures in the rock, and even spiral marks form the coring bit.

Boring Z1-B6 has good diameter control below 100 feet, but the images are not as clear due to a thick wall cake. This is illustrated by the presence of interference patterns caused by standing acoustic waves in the wall cake, similar to optical moiré patterns. These can be seen clearly in Z1-B6 at 333 – 334 feet. Heavy wall cake was a regular problem, with the probe completely covered in clay at the end of logging runs.

Boring Z2-B1 is eroded out to 8 inches or more for the entire depth, and yields almost no acoustic image. Z3-B1 does not show many planar features, but the image quality is good. This boring shows a number of hard inclusions in a softer matrix, but few planar features.

The twelve borings in which deviation data were collected were inclined at 2.0 degrees, or less, from vertical, and the maximum error in depth value was 0.3 feet in 319 feet, or less than 0.1 percent, as presented in Table 4. This error is less than depth errors from other causes, and no adjustment of log depths is indicated.

## Quality Assurance

These boring geophysical measurements were performed using industry-standard or better methods for measurements and analyses. All work was performed under **GEO***Vision* quality assurance procedures, which include:

- Use of NIST-traceable calibrations, where applicable, for field and laboratory instrumentation
- Use of standard field data logs
- Use of independent verification of velocity data by comparison of receiver-to-receiver and source-to-receiver velocities
- Independent review of calculations and results by a registered professional engineer, geologist, or geophysicist.

## Suspension Velocity Data Reliability

P- and $S_H$-wave velocity measurement using the Suspension Method gives average velocities over a 3.28-foot interval of depth. This high resolution results in the scatter of values shown in the graphs. Individual measurements are very reliable with estimated precision of +/- 5%. Standardized field procedures and quality assurance checks contribute to the reliability of these data.

## CERTIFICATION

All geophysical data, analysis, interpretations, conclusions, and recommendations in this document have been prepared under the supervision of and reviewed by a **GEO***Vision* California Professional Geophysicist.

7/31/09

Antony J. Martin — Date
California Professional Geophysicist GP989
**GEO***Vision* Geophysical Services

* This geophysical investigation was conducted under the supervision of a California Professional Geophysicist using industry standard methods and equipment. A high degree of professionalism was maintained during all aspects of the project from the field investigation and data acquisition, through data processing interpretation and reporting. All original field data files, field notes and observations, and other pertinent information are maintained in the project files and are available for the client to review for a period of at least one year.

  A professional geophysicist's certification of interpreted geophysical conditions comprises a declaration of his/her professional judgment. It does not constitute a warranty or guarantee, expressed or implied, nor does it relieve any other party of its responsibility to abide by contract documents, applicable codes, standards, regulations or ordinances.

| BORING DESIGNATION | DATES LOGGED | COORDINATES (FEET, ZONE 5, NAD83) [1] | | ELEVATION [1] (FEET NAVD88) |
|---|---|---|---|---|
| | | NORTH | EAST | |
| Z1-B3 | 1/30/2009 | 1855594.07 | 6492810.43 | 343.23 |
| Z1-B5 | 2/25/2009 | 1850576.02 | 6499981.20 | 442.15 |
| Z1-B6 | 2/10/2009 | 1852836.59 | 6503970.85 | 447.22 |
| Z1-B7 | 1/26/2009 | 1849941.30 | 6506175.09 | 480.52 |
| Z2-B1 | 1/21/2009 | 1866308.10 | 6492663.29 | 451.02 |
| Z2-B4 | 3/31/2009 | 1858027.66 | 6507350.57 | 558.11 |
| Z3-B1 | 3/19/2009 | 1873601.92 | 6507232.68 | 885.14 |
| Z3-B3 | 2/11/2009 | 1870194.48 | 6514774.44 | 801.99 |
| Z3-B4 | 3/6/2009 | 1870813.73 | 6516733.49 | 768.04 |
| Z3-B6 | 3/5/2009 | 1868062.70 | 6516722.28 | 750.00 |
| Z3-B8 | 3/23/2009 | 1860993.95 | 6514198.81 | 594.27 |
| Z3-B12 | 1/14/2009 | 1856063.15 | 6513380.17 | 501.00 |
| Z4-B4 | 3/17/2009 | 1851895.71 | 6514496.46 | 454.42 |

[1] Coordinates and elevation provided by CH2M dated 6/17/09

Table 1. Boring locations and logging dates

| BORING NUMBER | TOOL AND RUN NUMBER | DEPTH RANGE (FEET) | BOTTOM OF BOREHOLE CASING | SAMPLE OR MEASUREMENT INTERVAL (FEET) | DATE LOGGED |
|---|---|---|---|---|---|
| Z1-B3 | CALIPER/GAMMA 1 | 300.7 – 71.0 | 86 | 0.05 | 1/30/2009 |
| Z1-B3 | ACOUSTIC TELEVIEWER 1 | 300.9 – 82.3 | 86 | 0.008 | 1/30/2009 |
| Z1-B3 | SUSPENSION PS 1 | 88.6 – 288.7 | 86 | 1.6 | 1/30/2009 |
| Z1-B5 | CALIPER/GAMMA 1 | 500.1 – 4.1 | 8 | 0.05 | 2/25/2009 |
| Z1-B5 | ACOUSTIC TELEVIEWER 1 | 499.4 – 35.0 | 8 | 0.008 | 2/25/2009 |
| Z1-B5 | SUSPENSION PS 1 | 11.8 – 487.2 | 8 | 1.6 | 2/25/2009 |
| Z1-B6 | CALIPER/GAMMA 1 | 400.1 – 1.0 | 4 | 0.05 | 2/10/2009 |
| Z1-B6 | ACOUSTIC TELEVIEWER 1 | 400.0 – 65.0 | 4 | 0.008 | 2/10/2009 |
| Z1-B6 | SUSPENSION PS 1 | 6.6 – 390.4 | 4 | 1.6 | 2/10/2009 |
| Z1-B7 | CALIPER/GAMMA 1 | 299.0 - 0 | 11 | 0.05 | 1/26/2009 |
| Z1-B7 | ACOUSTIC TELEVIEWER 1 | 299.0 – 145.0 | 11 | 0.008 | 1/26/2009 |
| Z1-B7 | SUSPENSION PS 1 | 13.1 – 290.4 | 11 | 1.6 | 1/26/2009 |
| Z2-B1 | CALIPER/GAMMA 1 | 149.0 – 1.0 | 19 | 0.05 | 1/21/2009 |
| Z2-B1 | ACOUSTIC TELEVIEWER 1 | 149.0 – 18.5 | 19 | 0.008 | 1/21/2009 |
| Z2-B1 | SUSPENSION PS 1 | 21.3 – 137.8 | 19 | 1.6 | 1/21/2009 |
| Z2-B4 | CALIPER/GAMMA 1 | 358.3 – 6.0 | 6 | 0.05 | 3/31/2009 |
| Z2-B4 | CALIPER/GAMMA 2 | 374.5 – 325.0 | 6 | 0.05 | 3/31/2009 |
| Z2-B4 | ACOUSTIC TELEVIEWER 1 | 358.7 – 1.8 | 6 | 0.008 | 3/31/2009 |
| Z2-B4 | ACOUSTIC TELEVIEWER 2 | 374.2 – 347.0 | 6 | 0.008 | 3/31/2009 |
| Z2-B4 | SUSPENSION PS 1 | 3.3 – 305.1 | 6 | 1.6 | 3/31/2009 |
| Z2-B4 | SUSPENSION PS 2 | 306.8 – 360.9 | 6 | 1.6 | 3/31/2009 |
| Z3-B1 | CALIPER/GAMMA 1 | 300.2 – 14.8 | 26 | 0.05 | 3/19/2009 |
| Z3-B1 | ACOUSTIC TELEVIEWER 1 | 300.2 – 22.2 | 26 | 0.008 | 3/19/2009 |
| Z3-B1 | SUSPENSION PS 1 | 4.0 – 287.1 | 26 | 1.6 | 3/19/2009 |

- PROBE DID NOT TOUCH BOTTOM OF BORING

Table 2. Logging dates and depth ranges

| BORING NUMBER | TOOL AND RUN NUMBER | DEPTH RANGE (FEET) | BOTTOM OF BOREHOLE CASING | SAMPLE OR MEASUREMENT INTERVAL (FEET) | DATE LOGGED |
|---|---|---|---|---|---|
| Z3-B3 | CALIPER/GAMMA 1 | 273.0 – 165.1 | 174.5 | 0.05 | 2/11/2009 |
| Z3-B3 | CALIPER/GAMMA 2 | 273.0 – 50.0 | 55 | 0.05 | 2/11/2009 |
| Z3-B3 | ACOUSTIC TELEVIEWER 1 | 274.0 – 173.0 | 174.5 | 0.008 | 2/11/2009 |
| Z3-B3 | SUSPENSION PS 1 | 177.2 – 262.5 | 174.5 | 1.6 | 2/11/2009 |
| Z3-B3 | SUSPENSION PS 2 | 57.4 – 183.7 | 55 | 1.6 | 2/11/2009 |
| Z3-B4 | CALIPER/GAMMA 1 | 274.9 – 2.1 | 3.5 | 0.05 | 3/6/2009 |
| Z3-B4 | ACOUSTIC TELEVIEWER 1 | 275.3 – 2.5 | 3.5 | 0.008 | 3/6/2009 |
| Z3-B4 | SUSPENSION PS 1 | 2.8 – 262.5 | 3.5 | 1.6 | 3/6/2009 |
| Z3-B6 | CALIPER/GAMMA 1 | 325.0 - 5.3 | 10.5 | 0.05 | 3/5/2009 |
| Z3-B6 | ACOUSTIC TELEVIEWER 1 | 320.4 – 308.9 | 10.5 | 0.008 | 3/5/2009 |
| Z3-B6 | ACOUSTIC TELEVIEWER 2 | 318.7 – 28.3 | 10.5 | 0.008 | 3/5/2009 |
| Z3-B6 | SUSPENSION PS 1 | 43.0 – 311.7 | 10.5 | 1.6 | 3/5/2009 |
| Z3-B8 | CALIPER/GAMMA 1 | 275.7 – 4.2 | 4 | 0.05 | 3/23/2009 |
| Z3-B12 | CALIPER/GAMMA 1 | 273.0 – 50.0 | 57.5 | 0.05 | 1/14/2009 |
| Z3-B12 | CALIPER/GAMMA 2 | 273.0 – 245.5 | 57.5 | 0.05 | 1/14/2009 |
| Z3-B12 | CALIPER/GAMMA 3 | 258.0 – 54.0 | 57.5 | 0.05 | 1/14/2009 |
| Z3-B12 | ACOUSTIC TELEVIEWER 1 | 67.5 – 186.8 | 57.5 | 0.008 | 1/14/2009 |
| Z3-B12 | ACOUSTIC TELEVIEWER 2 | 182.6 – 57.0 | 57.5 | 0.008 | 1/14/2009 |
| Z3-B12 | SUSPENSION PS 1 | 59.0 – 185.4 | 57.5 | 1.6 | 1/14/2009 |
| Z3-B12 | SUSPENSION PS 2 | 173.9 – 251.0<br>8.2 – 62.3 | 5 | 1.6 | 1/14/2009 |
| Z4-B4 | CALIPER/GAMMA 1 | 275.0 – 2.0 | 7 | 0.05 | 3/17/2009 |
| Z4-B4 | ACOUSTIC TELEVIEWER 1 | 275.1 – 270.3 | 7 | 0.008 | 3/17/2009 |
| Z4-B4 | ACOUSTIC TELEVIEWER 2 | 275.1 – 4.7 | 7 | 0.008 | 3/17/2009 |
| Z4-B4 | SUSPENSION PS 1 | 4.7 – 262.5 | 7 | 1.6 | 3/17/2009 |

- PROBE DID NOT TOUCH BOTTOM OF BORING

Table 2, continued. Logging dates and depth ranges

| BORING NUMBER | MEAN DEVIATION AND AZIMUTH (DEGREES TN) | SURVEY DEPTH (FEET) | VERTICAL DEPTH (FEET) | DEPTH ERROR (FEET) | HORIZONTAL OFFSET (FEET) |
|---|---|---|---|---|---|
| Z1-B3 | 0.7 – N213 | 300.8 | 300.7 | 0.1 | 3.8 |
| Z1-B5 | 0.5 – N292 | 499.3 | 499.3 | 0 | 4.7 |
| Z1-B6 | 1.3 – N031 | 400.0 | 399.8 | 0.2 | 9.0 |
| Z1-B7 | 1.5 – N226 | 299.0 | 298.9 | 0.1 | 7.6 |
| Z2-B1 | 1.2 – N178 | 148.9 | 148.0 | 0 | 3.0 |
| Z2-B4 | 0.9 – N000 | 374.6 | 374.5 | 0.1 | 6.0 |
| Z3-B1 | 1.8 – N307 | 300.2 | 300.0 | 0.2 | 9.3 |
| Z3-B3 | 0.5 – N265 | 273.9 | 273.9 | 0 | 2.2 |
| Z3-B4 | 0.2 – N033 | 275.2 | 275.2 | 0 | 1.1 |
| Z3-B6 | 2.0 – N081 | 318.7 | 318.4 | 0.3 | 11.3 |
| Z3-B12 | 0.3 – N264 | 182.5 | 182.5 | 0 | 0.9 |
| Z4-B4 | 0.6 – N000 | 275.1 | 275.0 | 0.1 | 2.6 |

Table 3. Boring Deviation Data Summary

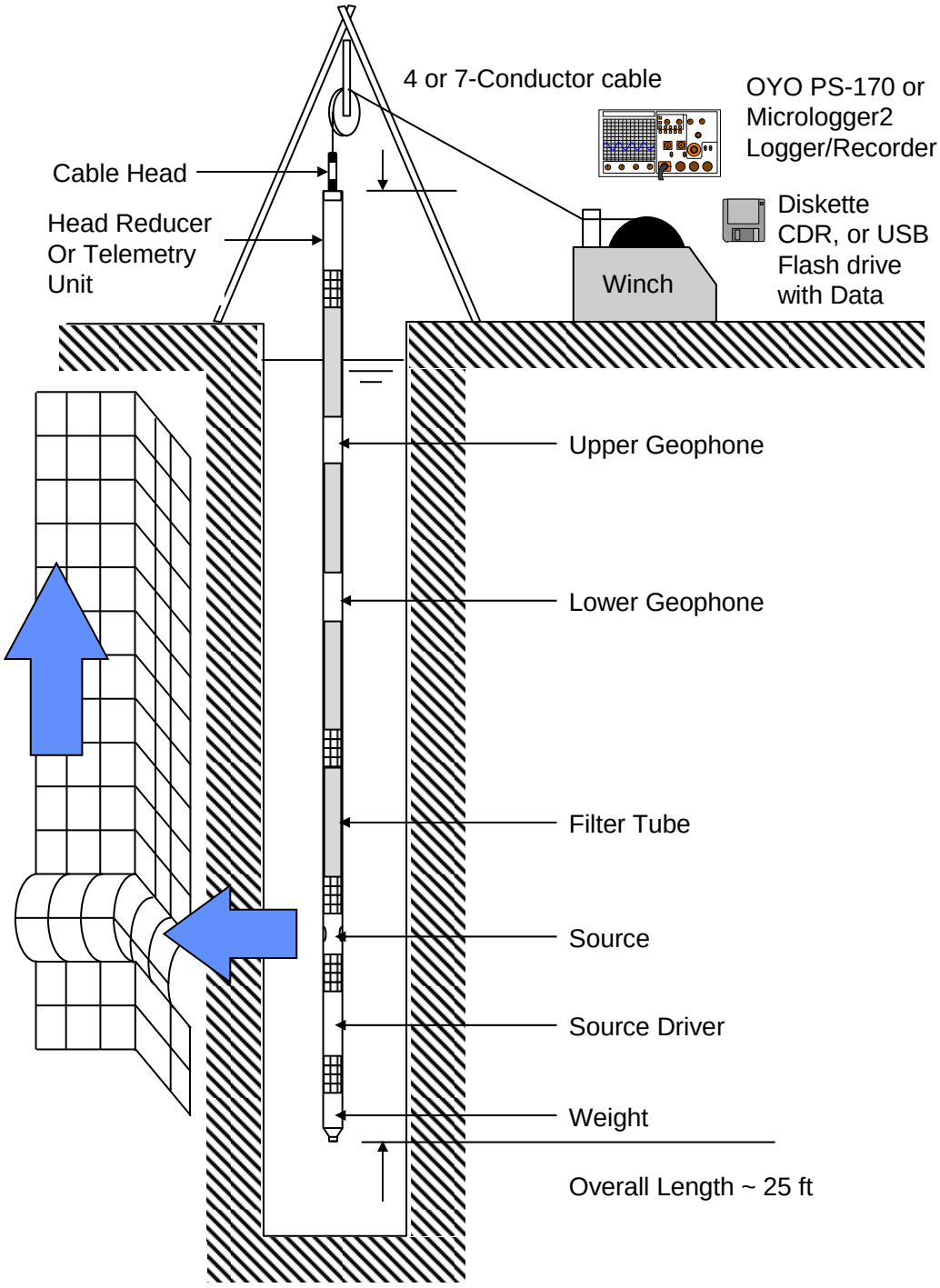


Figure 1: Concept illustration of Suspension P S logging system

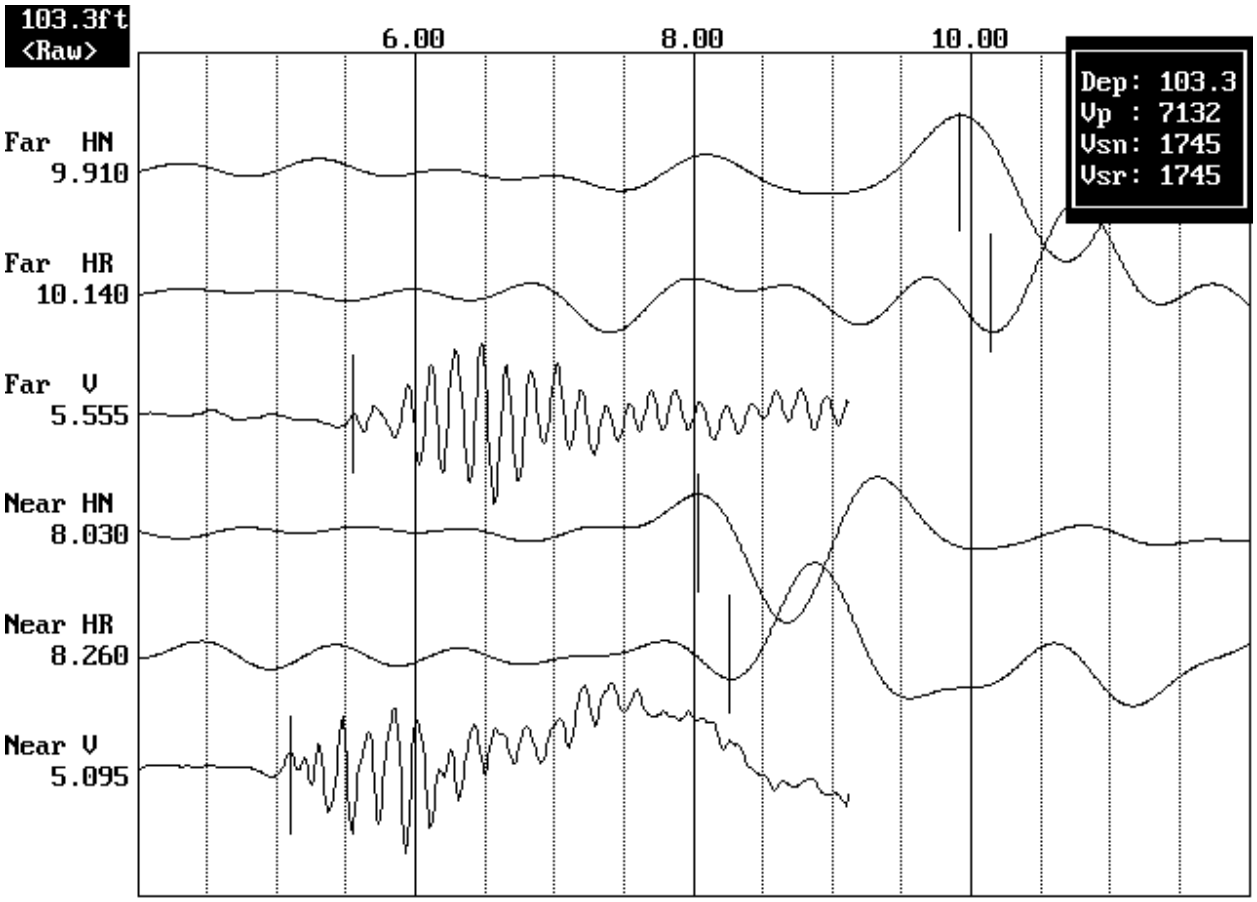


Figure 2: Example of filtered (1400 Hz lowpass) suspension record

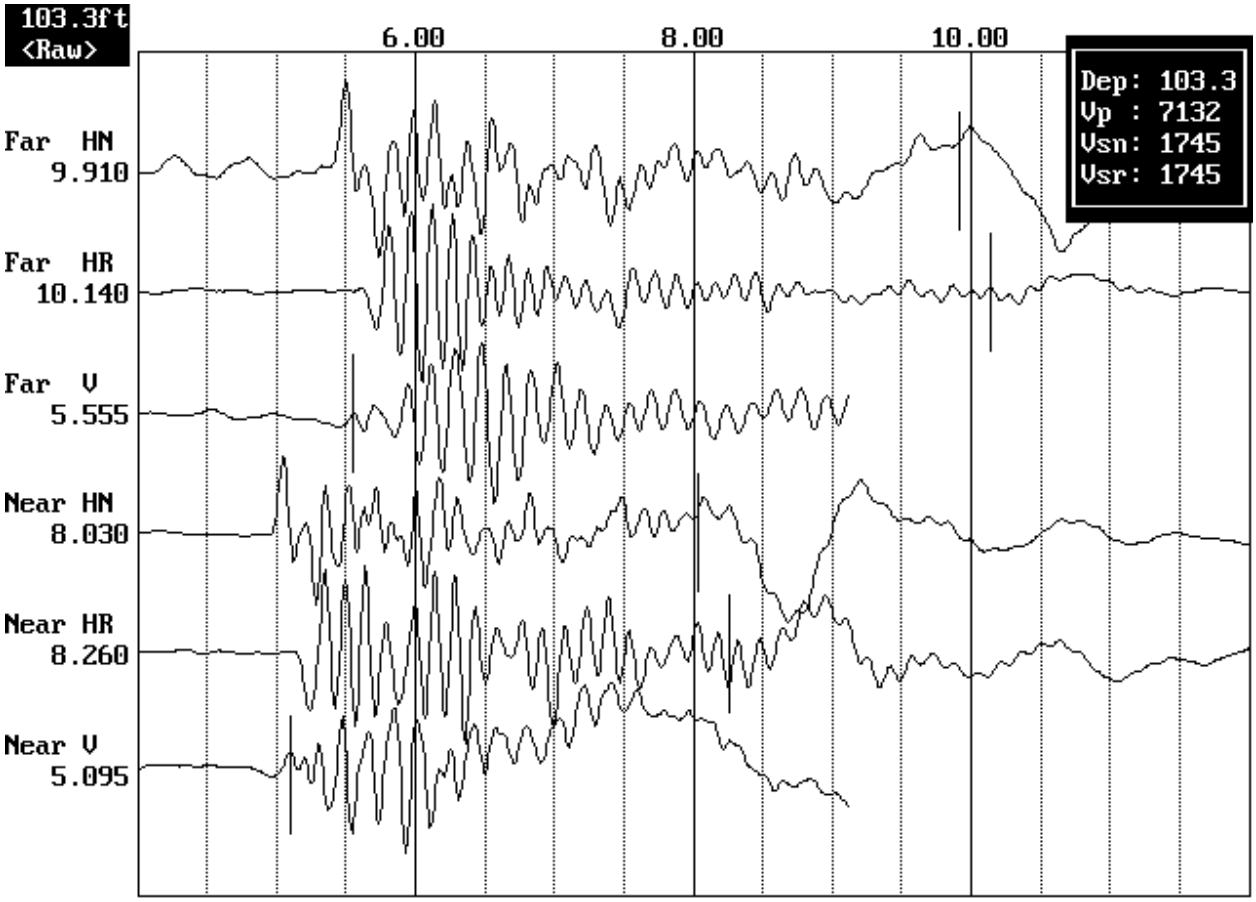


Figure 3. Example of unfiltered suspension record

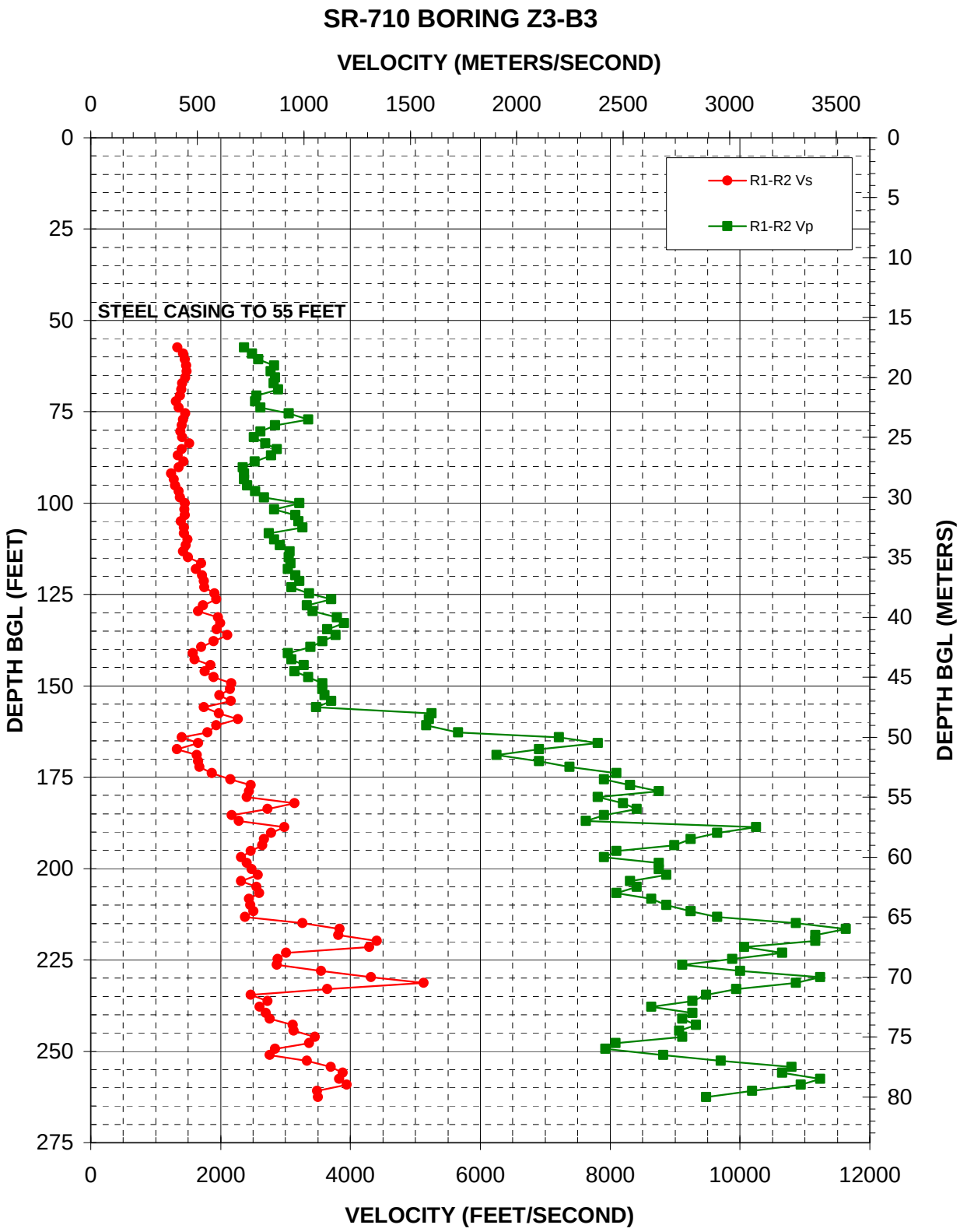


Figure 32: Boring Z3-B3, Suspension R1-R2 P- and $S_H$-wave velocities

| Depth (feet) | $V_s$ (feet/sec) | $V_p$ (feet/sec) |
|---|---|---|
| 57.41 | 1334 | 2360 |
| 59.06 | 1426 | 2485 |
| 60.70 | 1448 | 2583 |
| 62.34 | 1468 | 2828 |
| 63.98 | 1481 | 2769 |
| 65.62 | 1458 | 2841 |
| 67.26 | 1408 | 2816 |
| 68.90 | 1393 | 2891 |
| 70.54 | 1379 | 2553 |
| 72.18 | 1312 | 2533 |
| 73.82 | 1353 | 2614 |
| 75.46 | 1455 | 3052 |
| 77.10 | 1423 | 3348 |
| 78.74 | 1402 | 2841 |
| 80.38 | 1384 | 2614 |
| 82.02 | 1411 | 2514 |
| 83.66 | 1515 | 2689 |
| 85.30 | 1405 | 2865 |
| 86.94 | 1345 | 2780 |
| 88.58 | 1433 | 2524 |
| 90.22 | 1353 | 2343 |
| 91.86 | 1240 | 2360 |
| 93.50 | 1282 | 2360 |
| 95.14 | 1299 | 2412 |
| 96.78 | 1356 | 2533 |
| 98.43 | 1379 | 2667 |
| 100.07 | 1452 | 3217 |
| 101.71 | 1445 | 2828 |
| 103.35 | 1448 | 3155 |
| 104.99 | 1387 | 3201 |
| 106.63 | 1439 | 3265 |
| 108.27 | 1439 | 2745 |
| 109.91 | 1491 | 2828 |
| 111.55 | 1465 | 2916 |
| 113.19 | 1426 | 3066 |
| 114.83 | 1498 | 3052 |
| 116.47 | 1704 | 3081 |
| 118.11 | 1624 | 3038 |
| 119.75 | 1713 | 3155 |
| 121.39 | 1740 | 3217 |
| 123.03 | 1750 | 3095 |
| 124.67 | 1907 | 3365 |
| 126.31 | 1936 | 3707 |
| 127.95 | 1731 | 3331 |
| 129.59 | 1657 | 3418 |
| 131.23 | 1959 | 3793 |
| 132.87 | 1994 | 3906 |
| 134.51 | 1941 | 3645 |
| 136.15 | 2103 | 3771 |
| 137.80 | 1896 | 3566 |
| 139.44 | 1700 | 3382 |
| 141.08 | 1574 | 3038 |
| 142.72 | 1600 | 3095 |
| 144.36 | 1848 | 3281 |
| 146.00 | 1759 | 3140 |
| 147.64 | 1896 | 3348 |
| 149.28 | 2166 | 3566 |
| 150.92 | 2144 | 3566 |
| 152.56 | 1982 | 3605 |
| 154.20 | 2158 | 3707 |
| 155.84 | 1745 | 3472 |
| 157.48 | 1976 | 5249 |
| 159.12 | 2270 | 5208 |
| 160.76 | 1936 | 5167 |
| 162.73 | 1798 | 5657 |
| 164.04 | 1402 | 7211 |
| 165.68 | 1657 | 7812 |
| 167.32 | 1331 | 6907 |
| 168.96 | 1632 | 6249 |
| 170.60 | 1657 | 6907 |
| 172.24 | 1674 | 7373 |
| 173.88 | 1864 | 8101 |
| 175.52 | 2151 | 7906 |
| 177.17 | 2467 | 8306 |
| 178.81 | 2439 | 8749 |
| 180.45 | 2404 | 7812 |
| 182.09 | 3140 | 8202 |
| 183.73 | 2723 | 8412 |
| 185.37 | 2173 | 7906 |
| 187.01 | 2278 | 7630 |
| 188.65 | 2983 | 10253 |
| 190.29 | 2780 | 9650 |
| 191.93 | 2667 | 9242 |
| 193.57 | 2646 | 8989 |
| 195.21 | 2467 | 8101 |
| 196.85 | 2319 | 7906 |
| 198.49 | 2404 | 8749 |
| 200.13 | 2476 | 8749 |
| 201.77 | 2573 | 8867 |
| 203.41 | 2319 | 8306 |
| 205.05 | 2553 | 8412 |
| 206.69 | 2594 | 8101 |
| 208.33 | 2439 | 8634 |
| 209.97 | 2458 | 8867 |
| 211.61 | 2504 | 9242 |
| 213.25 | 2377 | 9650 |
| 214.90 | 3265 | 10864 |
| 216.54 | 3837 | 11634 |
| 218.18 | 3815 | 11159 |
| 219.82 | 4404 | 11159 |
| 221.46 | 4289 | 10064 |
| 223.10 | 3010 | 10652 |
| 224.74 | 2878 | 9882 |
| 226.38 | 2865 | 9113 |
| 228.02 | 3547 | 10003 |
| 229.66 | 4317 | 11236 |
| 231.30 | 5126 | 10864 |
| 232.94 | 3645 | 9942 |
| 234.58 | 2467 | 9482 |
| 236.22 | 2723 | 9268 |
| 237.86 | 2604 | 8634 |
| 239.50 | 2700 | 9268 |
| 241.14 | 2757 | 9113 |
| 242.78 | 3110 | 9321 |
| 244.42 | 3125 | 9063 |
| 246.06 | 3454 | 9113 |
| 247.70 | 3365 | 8081 |
| 249.34 | 2841 | 7925 |
| 250.98 | 2757 | 8819 |
| 252.62 | 3331 | 9707 |
| 254.27 | 3697 | 10792 |
| 255.91 | 3883 | 10652 |
| 257.55 | 3826 | 11236 |
| 259.19 | 3941 | 10936 |
| 260.83 | 3490 | 10189 |
| 262.47 | 3500 | 9482 |
| | | |

Table 18. Boring Z3-B3, Suspension R1-R2 depths and P- and $S_H$-wave velocities

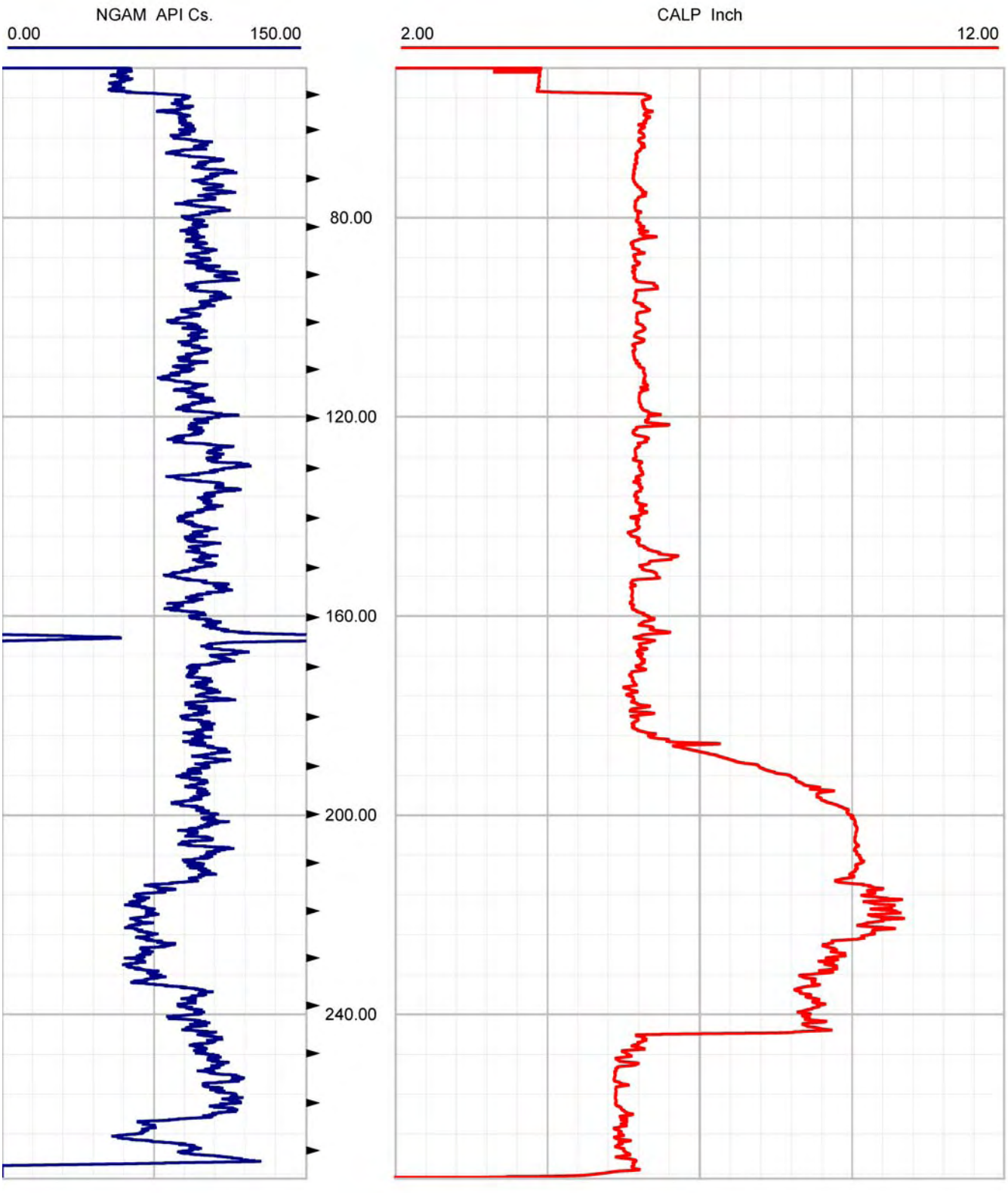


Figure 33. Boring Z3-B3, Caliper and Natural Gamma logs

DIP DATA INTERPRETATION
RGLDIP vsn 6.2
FRACTURE ANALYSIS STEREOGRAMS

CASCADE DRILLING

Borehole: Z3-B3

SR-710 TUNNEL INVESTIGATION

top of borehole.....
East:_
North:_
Elev:_

North ref: true
Depth units are feet

Zone from 273.652 to 271.984ft
Mean dip format: dip-azimuth and dip

Interpretation 1

Dip data sets .....
BHTV dips

Z3-B3
Zone 0. 271.984 - 273.642ft
Deviation 1.60 N308.50

dipdata sets.....
BHTV dips
• Highlighted dips: Fracture Planar Hairline-fracture

| | mean dip | n | f |
|---|---|---|---|
| N348 52 | N348 52 | 2 | 2.04 |
| N123 29 | N123 29 | 1 | ( 0.00) |

intersections

| | N348 52 | N123 29 |
|---|---|---|
| N348 52 | | 16 N065 |
| N123 29 | 16 N065 | |

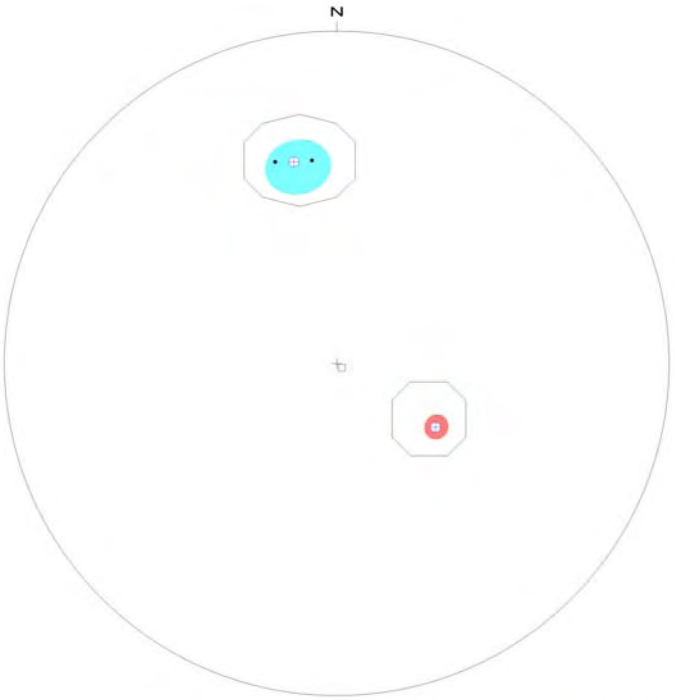


equal-area upper-hemisphere 0-90
contour-levels 1,

Z3-B3, Interpretation 1 273.642 to 271.984ft 1

Figure 34. Boring Z3-B3, Stereonet Plot

| Depth (feet) | Dip azimuth | Dip | Structure description |
|---|---|---|---|
| 273.15 | N343 | 53 | Primary-structure Planar Bedding |
| 272.68 | N353 | 52 | Primary-structure Planar Bedding |
| 272.48 | N123 | 29 | Fracture Planar Hairline-fracture |
| | | | |

Table 19. Boring Z3-B3, Structure depth, dip azimuth, dip and description

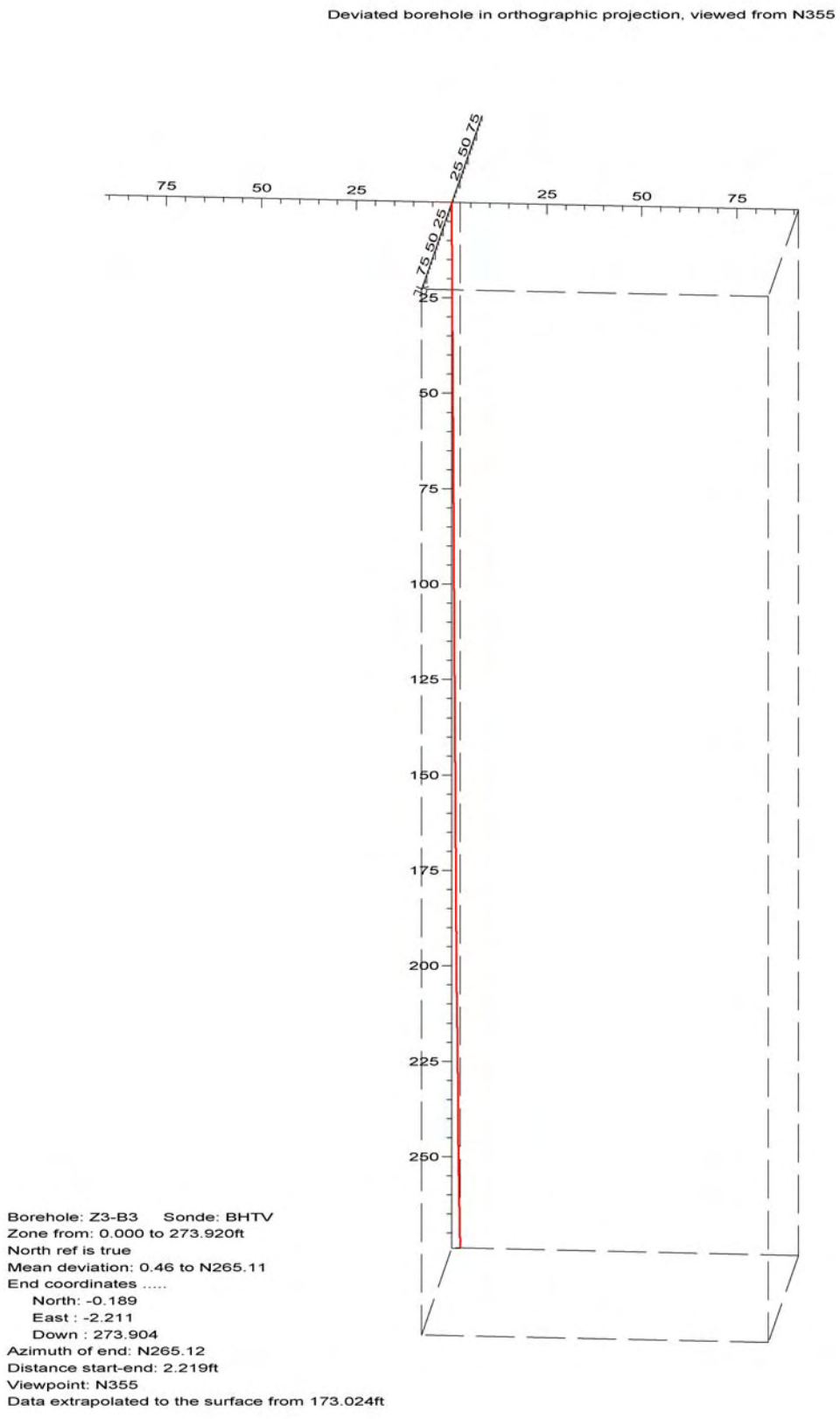


Figure 35. Boring Z3-B3, Deviation Projection

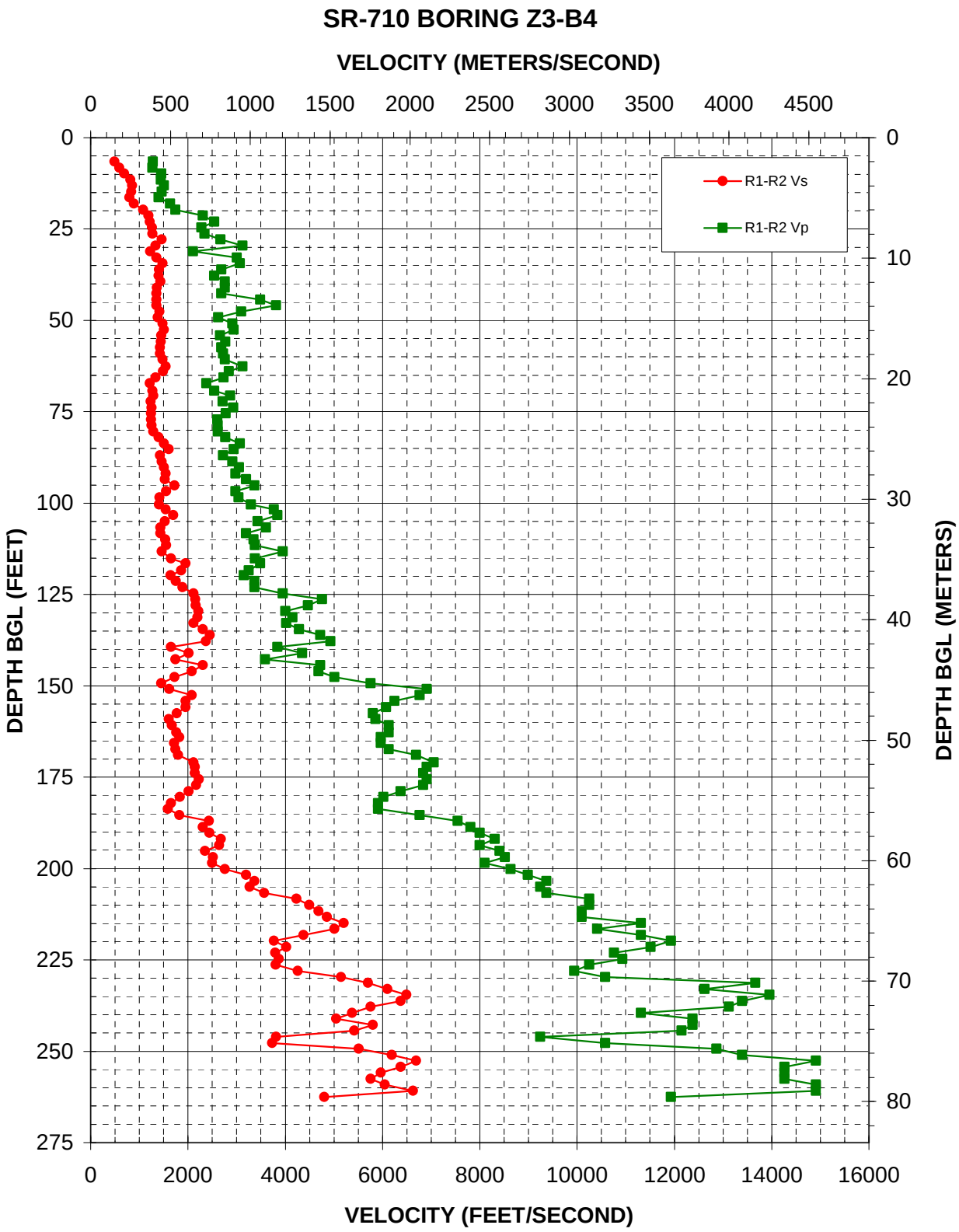


Figure 36: Boring Z3-B4, Suspension R1-R2 P- and $S_H$-wave velocities

| Depth (feet) | $V_s$ (feet/sec) | $V_p$ (feet/sec) |
|---|---|---|
| 6.56 | 489 | 1277 |
| 8.20 | 594 | 1272 |
| 9.84 | 689 | 1452 |
| 11.48 | 814 | 1445 |
| 13.12 | 857 | 1505 |
| 14.76 | 833 | 1458 |
| 16.40 | 800 | 1402 |
| 18.04 | 894 | 1632 |
| 19.69 | 1079 | 1745 |
| 21.33 | 1189 | 2310 |
| 22.97 | 1215 | 2543 |
| 24.61 | 1267 | 2278 |
| 26.25 | 1272 | 2343 |
| 27.89 | 1458 | 2667 |
| 29.53 | 1334 | 3125 |
| 31.17 | 1224 | 2103 |
| 32.81 | 1356 | 3010 |
| 34.45 | 1485 | 3066 |
| 36.09 | 1408 | 2689 |
| 37.73 | 1396 | 2543 |
| 39.37 | 1433 | 2757 |
| 41.01 | 1361 | 2757 |
| 42.65 | 1356 | 2689 |
| 44.29 | 1350 | 3490 |
| 45.93 | 1356 | 3815 |
| 47.57 | 1420 | 3095 |
| 49.21 | 1384 | 2625 |
| 50.85 | 1478 | 2916 |
| 52.49 | 1505 | 2942 |
| 54.13 | 1452 | 2657 |
| 55.77 | 1445 | 2769 |
| 57.41 | 1426 | 2689 |
| 59.06 | 1426 | 2723 |
| 60.70 | 1478 | 2757 |
| 62.66 | 1540 | 3125 |
| 63.98 | 1491 | 2841 |
| 65.62 | 1334 | 2734 |
| 67.26 | 1215 | 2377 |
| 69.23 | 1272 | 2543 |
| 70.54 | 1287 | 2865 |
| 72.18 | 1233 | 2711 |
| 73.82 | 1252 | 2929 |
| 75.46 | 1247 | 2780 |
| 77.10 | 1247 | 2604 |
| 78.74 | 1252 | 2614 |
| 80.38 | 1292 | 2614 |
| 82.02 | 1402 | 2769 |
| 83.66 | 1512 | 3066 |
| 85.30 | 1608 | 2942 |
| 86.94 | 1426 | 2723 |
| 88.58 | 1465 | 2916 |
| 90.22 | 1512 | 3052 |
| 91.86 | 1548 | 2983 |
| 93.50 | 1526 | 3201 |
| 95.14 | 1727 | 3365 |
| 96.78 | 1555 | 2983 |
| 98.43 | 1414 | 3038 |
| 100.39 | 1408 | 3297 |
| 101.71 | 1540 | 3771 |
| 103.35 | 1700 | 3837 |
| 104.99 | 1526 | 3435 |
| 106.63 | 1433 | 3605 |
| 108.27 | 1433 | 3201 |
| 109.91 | 1533 | 3348 |
| 111.55 | 1555 | 3382 |
| 113.19 | 1458 | 3953 |
| 115.16 | 1649 | 3382 |
| 116.47 | 1953 | 3490 |
| 118.44 | 1864 | 3248 |
| 119.75 | 1640 | 3155 |
| 121.39 | 1754 | 3365 |
| 123.03 | 1886 | 3365 |
| 124.67 | 2117 | 3953 |
| 126.31 | 2151 | 4755 |
| 127.95 | 2158 | 4464 |
| 129.59 | 2217 | 4001 |
| 131.23 | 2202 | 4153 |
| 132.87 | 2117 | 4026 |
| 134.51 | 2310 | 4289 |
| 136.15 | 2448 | 4721 |
| 137.80 | 2369 | 4934 |
| 139.44 | 1649 | 3837 |
| 141.08 | 2013 | 4345 |
| 142.72 | 1745 | 3586 |
| 144.36 | 2310 | 4721 |
| 146.00 | 2076 | 4687 |
| 147.64 | 1727 | 5009 |
| 149.28 | 1452 | 5756 |
| 150.92 | 1620 | 6907 |
| 152.56 | 2083 | 6765 |
| 154.20 | 1953 | 6249 |
| 155.84 | 1953 | 6076 |
| 157.48 | 1773 | 5807 |
| 159.12 | 1608 | 5859 |
| 160.76 | 1674 | 6132 |
| 162.73 | 1759 | 6132 |
| 164.04 | 1828 | 5965 |
| 165.68 | 1713 | 5965 |
| 167.32 | 1745 | 6132 |
| 168.96 | 1798 | 6696 |
| 170.93 | 2117 | 7056 |
| 172.24 | 2144 | 6907 |
| 173.88 | 2144 | 6835 |
| 175.52 | 2224 | 6907 |
| 177.17 | 2173 | 6835 |
| 178.81 | 2019 | 6371 |
| 180.45 | 1838 | 6020 |
| 182.09 | 1657 | 5911 |
| 183.73 | 1589 | 5911 |
| 185.37 | 1823 | 6765 |
| 187.01 | 2430 | 7542 |
| 188.65 | 2310 | 7812 |
| 190.29 | 2439 | 8002 |
| 191.93 | 2678 | 8306 |
| 193.57 | 2646 | 8002 |
| 195.21 | 2352 | 8412 |
| 196.85 | 2514 | 8522 |
| 198.49 | 2495 | 8101 |
| 200.13 | 2757 | 8634 |
| 201.77 | 3201 | 8989 |
| 203.41 | 3365 | 9374 |
| 205.05 | 3265 | 9242 |
| 206.69 | 3566 | 9374 |
| 208.33 | 4233 | 10253 |
| 209.97 | 4494 | 10253 |
| 211.61 | 4687 | 10095 |
| 213.25 | 4861 | 10095 |
| 214.90 | 5208 | 11313 |
| 216.54 | 5009 | 10415 |
| 218.18 | 4374 | 11313 |
| 219.82 | 3771 | 11930 |
| 221.46 | 4026 | 11512 |
| 223.10 | 3793 | 10757 |
| 224.74 | 3871 | 10936 |
| 226.38 | 3804 | 10253 |
| 228.02 | 4261 | 9942 |
| 229.66 | 5146 | 10583 |
| 231.30 | 5706 | 13670 |
| 232.94 | 6104 | 12619 |
| 234.58 | 6497 | 13961 |
| 236.22 | 6371 | 13391 |
| 237.86 | 5756 | 13123 |
| 239.50 | 5378 | 11313 |
| 241.14 | 5047 | 12381 |
| 242.78 | 5807 | 12381 |
| 244.42 | 5423 | 12151 |
| 246.06 | 3815 | 9242 |
| 247.70 | 3728 | 10583 |
| 249.34 | 5514 | 12866 |
| 250.98 | 6190 | 13391 |

Table 20. Boring Z3-B4, Suspension R1-R2 depths and P- and $S_H$-wave velocities

| Depth (feet) | $V_s$ (feet/sec) | $V_p$ (feet/sec) |
|---|---|---|
| 252.62 | 6696 | 14913 |
| 254.27 | 6371 | 14265 |
| 255.91 | 5965 | 14265 |
| 257.55 | 5756 | 14265 |
| 259.19 | 6048 | 14913 |
| 260.83 | 6628 | 14913 |
| 262.47 | 4807 | 11930 |
| | | |

Table 20, continued. Boring Z3-B4, Suspension R1-R2 depths and P- and $S_H$-wave velocities

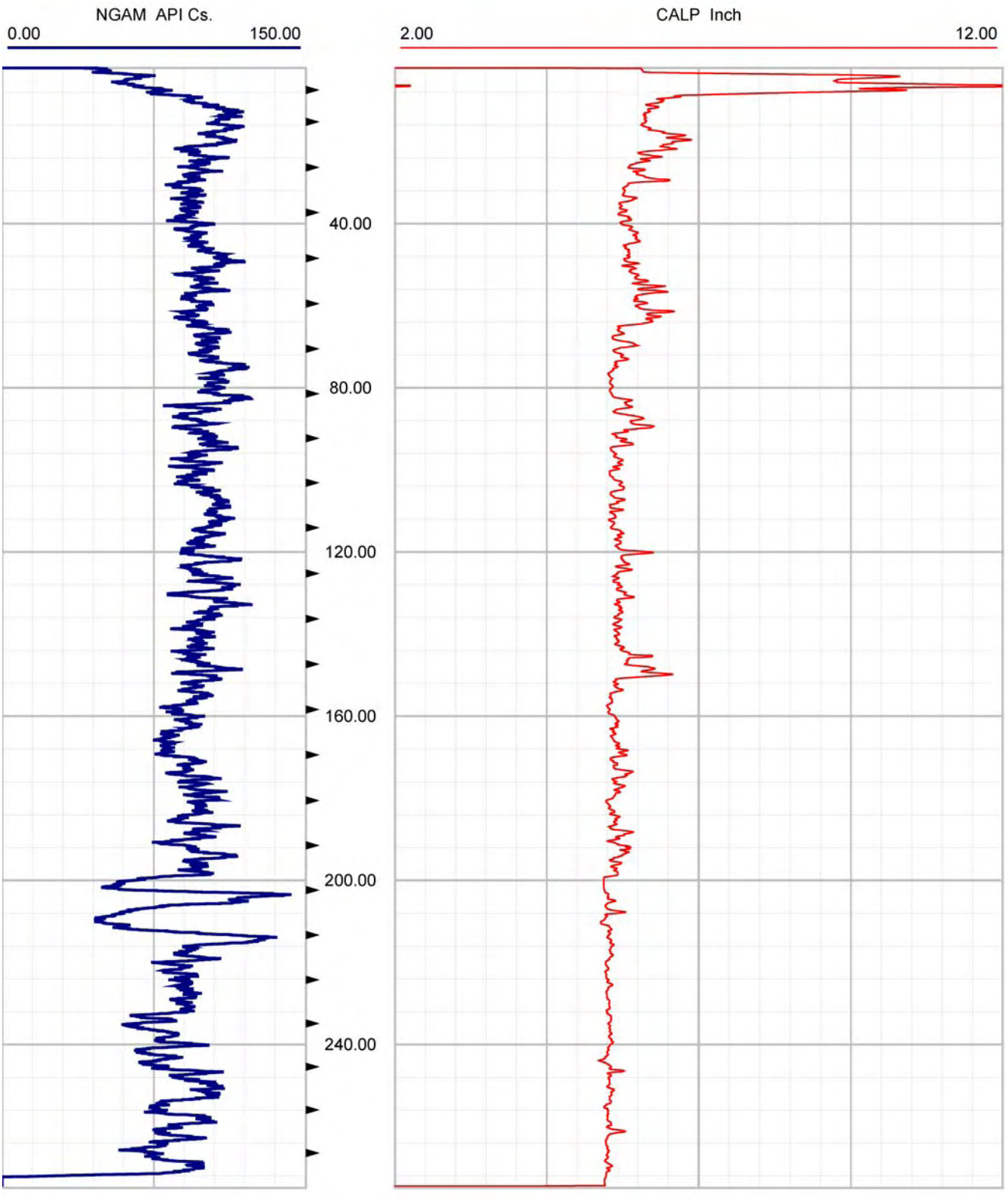


Figure 37. Boring Z3-B4, Caliper and Natural Gamma logs

DIP DATA INTERPRETATION
RGLDIP vsn 6.2
FRACTURE ANALYSIS STEREOGRAMS

CASCADE DRILLING

Borehole: Z3-B4

SR-710 TUNNEL INVESTIGATION

top of borehole.....
East:_
North:_
Elev:_

North ref: true
Depth units are feet

Zone from 275.196 to 64.540ft
Mean dip format: dip-azimuth and dip

Interpretation 1

Dip data sets .....
BHTV dips

Z3-B4
Zone 0. 64.540 - 275.196ft
Deviation 0.30 N 25.80

dipdata sets.....
BHTV dips
• Highlighted dips: Fracture Planar Hairline-fracture

| | mean dip | n | f |
|---|---|---|---|
| N334 53 | N334 53 | 7 | ( 0.06) |
| N072 58 | N072 58 | 3 | ( 0.03) |
| N157 59 | N157 59 | 7 | ( 0.06) |
| N181 11 | N181 11 | 10 | ( 0.05) |

intersections

| | N334 53 | N072 58 | N157 59 | N181 11 |
|---|---|---|---|---|
| N334 53 | | 43 N018 | 02 N246 | 04 N247 |
| N072 58 | 43 N018 | | 50 N113 | 10 N156 |
| N157 59 | 02 N246 | 50 N113 | | 05 N244 |
| N181 11 | 04 N247 | 10 N156 | 05 N244 | |

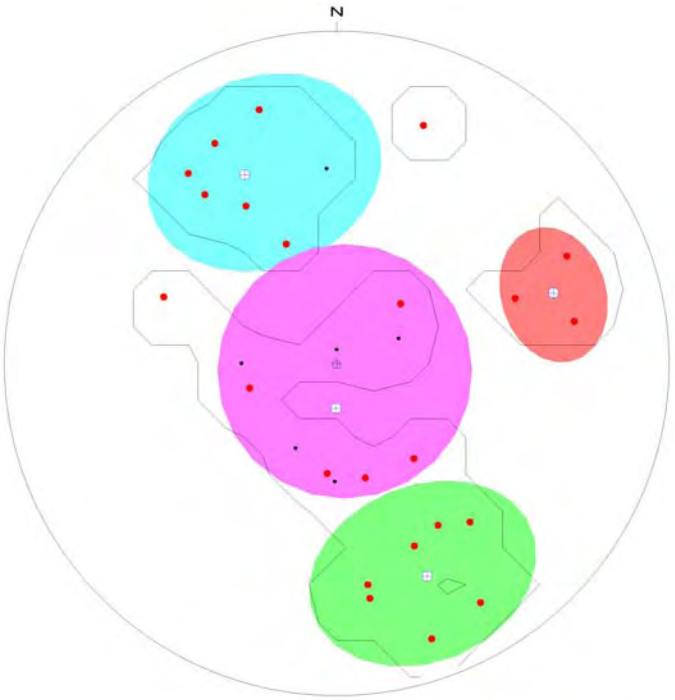


equal-area upper-hemisphere 0-90
contour-levels 1,

Z3-B4, Interpretation 1 275.196 to 64.540ft 1

Figure 38. Boring Z3-B4, Stereonet Plot

| Depth (feet) | Dip azimuth | Dip | Structure description |
|---|---|---|---|
| 274.74 | N141 | 30 | Fracture Planar Hairline-fracture |
| 274.42 | N065 | 65 | Fracture Planar Hairline-fracture |
| 274.33 | N020 | 65 | Fracture Planar Hairline-fracture |
| 273.39 | N331 | 65 | Fracture Planar Hairline-fracture |
| 273.13 | N080 | 62 | Fracture Planar Hairline-fracture |
| 271.88 | N185 | 27 | Fracture Planar Hairline-fracture |
| 271.42 | N157 | 50 | Fracture Planar Hairline-fracture |
| 271.18 | N148 | 48 | Fracture Planar Hairline-fracture |
| 270.43 | N161 | 77 | Fracture Planar Hairline-fracture |
| 270.26 | N181 | 29 | Primary-structure Planar Bedding |
| 267.93 | N149 | 73 | Fracture Planar Hairline-fracture |
| 265.43 | N166 | 29 | Fracture Planar Hairline-fracture |
| 265.05 | N343 | 69 | Fracture Planar Hairline-fracture |
| 259.99 | N330 | 45 | Fracture Planar Hairline-fracture |
| 258.86 | N322 | 54 | Fracture Planar Hairline-fracture |
| 258.15 | N291 | 47 | Fracture Planar Hairline-fracture |
| 257.82 | N047 | 21 | Fracture Planar Hairline-fracture |
| 252.67 | N070 | 48 | Fracture Planar Hairline-fracture |
| 250.25 | N254 | 22 | Fracture Planar Hairline-fracture |
| 248.28 | N172 | 61 | Fracture Planar Hairline-fracture |
| 247.64 | N359 | 3 | Primary-structure Planar Bedding |
| 245.30 | N322 | 62 | Fracture Planar Hairline-fracture |
| 236.66 | N172 | 57 | Fracture Planar Hairline-fracture |
| 215.95 | N140 | 52 | Fracture Planar Hairline-fracture |
| 199.28 | N337 | 32 | Fracture Planar Hairline-fracture |
| 191.94 | N357 | 49 | Primary-structure Planar Bedding |
| 190.56 | N206 | 23 | Primary-structure Planar Bedding |
| 133.02 | N270 | 23 | Primary-structure Planar Bedding |
| 65.04 | N068 | 16 | Primary-structure Planar Bedding |
| | | | |

Table 21. Boring Z3-B4, Structure depth, dip azimuth, dip and description

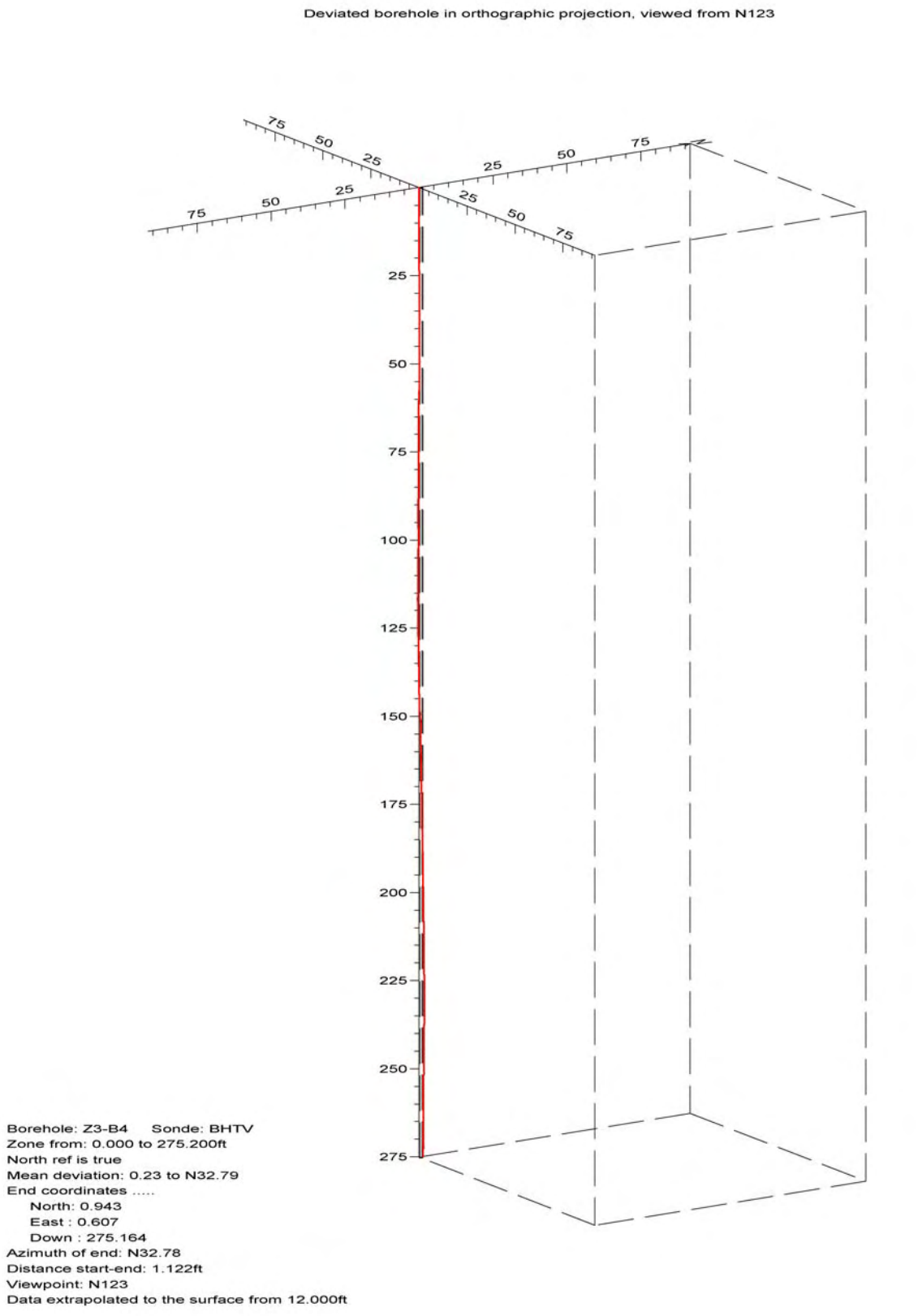


Figure 39. Boring Z3-B4, Deviation Projection

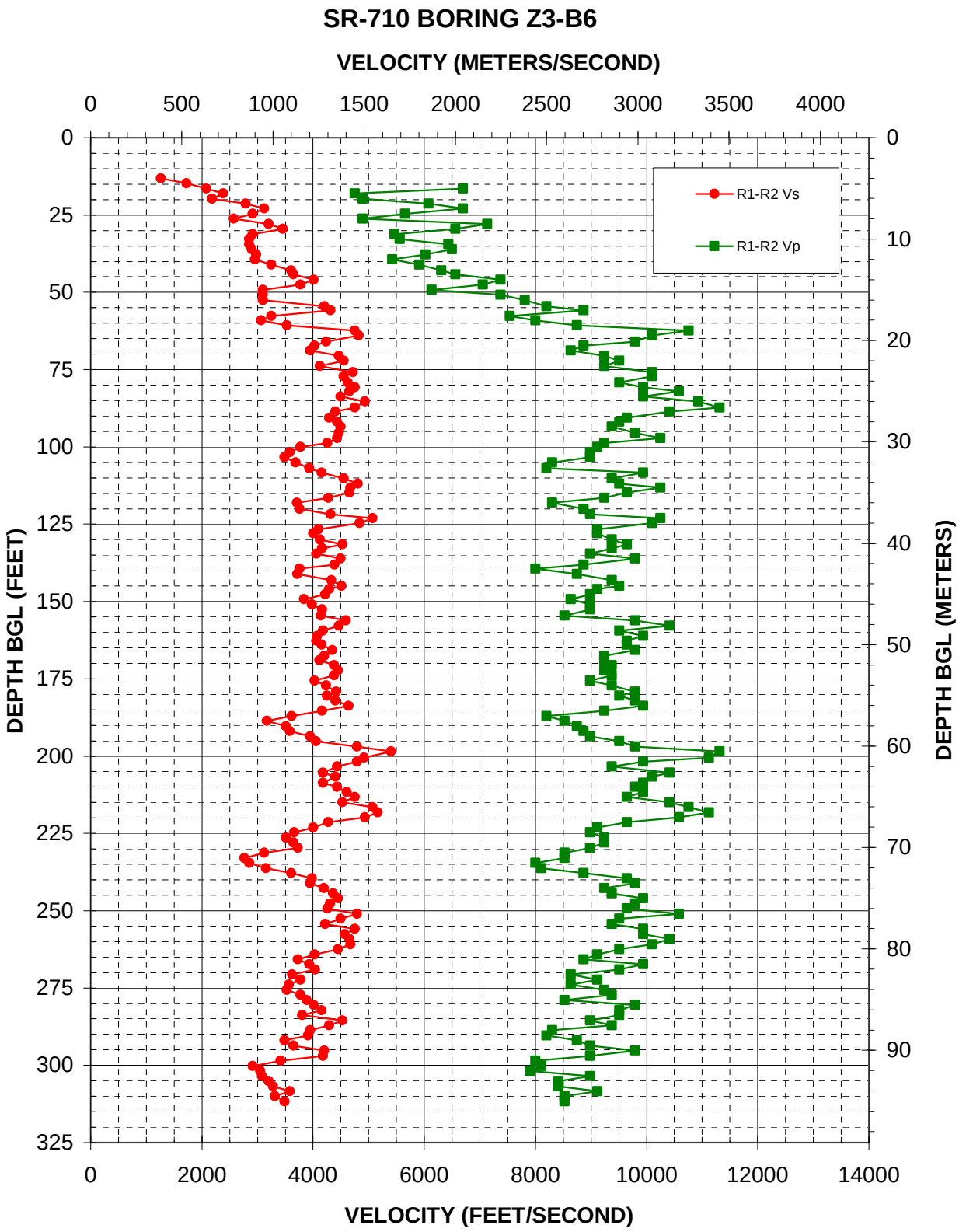


Figure 40: Boring Z3-B6, Suspension R1-R2 P- and $S_H$-wave velocities

| Depth (feet) | $V_s$ (feet/sec) | $V_p$ (feet/sec) |
|---|---|---|
| 13.12 | 1262 | |
| 14.76 | 1727 | |
| 16.40 | 2083 | 6696 |
| 18.04 | 2386 | 4755 |
| 19.69 | 2187 | 4897 |
| 21.33 | 2792 | 6076 |
| 22.97 | 3125 | 6696 |
| 24.61 | 2916 | 5657 |
| 26.25 | 2573 | 4897 |
| 27.89 | 3201 | 7132 |
| 29.53 | 3454 | 6562 |
| 31.17 | 2916 | 5468 |
| 32.81 | 2853 | 5561 |
| 34.45 | 2853 | 6433 |
| 36.09 | 2903 | 6497 |
| 37.73 | 2983 | 6020 |
| 39.37 | 2956 | 5423 |
| 41.01 | 3248 | 5911 |
| 42.98 | 3605 | 6309 |
| 44.29 | 3645 | 6562 |
| 45.93 | 4013 | 7373 |
| 47.57 | 3771 | 7056 |
| 49.21 | 3095 | 6132 |
| 50.85 | 3095 | 7373 |
| 52.49 | 3095 | 7812 |
| 54.46 | 4206 | 8202 |
| 55.77 | 4317 | 8867 |
| 57.74 | 3248 | 7542 |
| 59.06 | 3066 | 8002 |
| 60.70 | 3528 | 8749 |
| 62.34 | 4755 | 10757 |
| 63.98 | 4825 | 10095 |
| 65.94 | 4233 | 9794 |
| 67.26 | 4026 | 8867 |
| 68.90 | 3953 | 8634 |
| 70.54 | 4464 | 9242 |
| 72.18 | 4557 | 9510 |
| 73.82 | 4127 | 9242 |
| 75.79 | 4721 | 10095 |
| 77.10 | 4557 | 10095 |
| 79.07 | 4621 | 9510 |
| 80.71 | 4755 | 9942 |
| 82.02 | 4654 | 10583 |
| 83.66 | 4494 | 9942 |
| 85.30 | 4934 | 10936 |
| 87.27 | 4755 | 11313 |
| 88.58 | 4404 | 10415 |
| 90.55 | 4289 | 9650 |
| 91.86 | 4434 | 9510 |
| 93.50 | 4494 | 9374 |
| 95.47 | 4464 | 9794 |
| 97.11 | 4434 | 10253 |
| 98.75 | 4261 | 9242 |
| 100.07 | 3771 | 9113 |
| 101.71 | 3586 | 8989 |
| 103.35 | 3490 | 8989 |
| 104.99 | 3686 | 8306 |
| 106.96 | 3929 | 8202 |
| 108.27 | 4153 | 9942 |
| 110.24 | 4557 | 9374 |
| 111.88 | 4807 | 9510 |
| 113.19 | 4670 | 10253 |
| 114.83 | 4654 | 9650 |
| 116.47 | 4275 | 9242 |
| 118.11 | 3707 | 8306 |
| 120.08 | 3760 | 8867 |
| 121.72 | 4317 | 8989 |
| 123.03 | 5067 | 10253 |
| 124.67 | 4843 | 10095 |
| 126.64 | 4101 | 9113 |
| 127.95 | 4001 | 9113 |
| 129.92 | 4127 | 9374 |
| 131.56 | 4525 | 9650 |
| 132.87 | 4166 | 9374 |
| 134.51 | 4063 | 8989 |
| 136.15 | 4494 | 9794 |
| 138.12 | 4389 | 8867 |
| 139.44 | 3760 | 8002 |
| 141.08 | 3718 | 8749 |
| 143.04 | 4331 | 9374 |
| 145.01 | 4510 | 9510 |
| 146.00 | 4289 | 9113 |
| 147.64 | 4220 | 8989 |
| 149.28 | 3837 | 8634 |
| 150.92 | 3977 | 8989 |
| 152.56 | 4166 | 8989 |
| 154.53 | 4140 | 8522 |
| 156.17 | 4589 | 9794 |
| 157.81 | 4464 | 10415 |
| 159.45 | 4179 | 9510 |
| 161.09 | 4076 | 9942 |
| 162.73 | 4063 | 9650 |
| 164.04 | 4153 | 9650 |
| 165.68 | 4345 | 9794 |
| 167.65 | 4206 | 9242 |
| 168.96 | 4114 | 9242 |
| 170.60 | 4374 | 9374 |
| 172.24 | 4449 | 9242 |
| 173.88 | 4374 | 9374 |
| 175.52 | 4026 | 8989 |
| 177.17 | 4233 | 9374 |
| 179.13 | 4419 | 9794 |
| 180.45 | 4247 | 9510 |
| 182.09 | 4404 | 9794 |
| 183.73 | 4637 | 9942 |
| 185.37 | 4166 | 9242 |
| 187.01 | 3615 | 8202 |
| 188.65 | 3170 | 8522 |
| 190.29 | 3509 | 8749 |
| 191.93 | 3586 | 8867 |
| 193.57 | 3953 | 8989 |
| 195.21 | 4050 | 9510 |
| 196.85 | 4790 | 9794 |
| 198.49 | 5401 | 11313 |
| 200.46 | 4915 | 11121 |
| 201.77 | 4790 | 9942 |
| 203.41 | 4434 | 9374 |
| 205.38 | 4179 | 10415 |
| 206.69 | 4404 | 10095 |
| 208.66 | 4179 | 9942 |
| 209.97 | 4434 | 9794 |
| 211.61 | 4605 | 9942 |
| 213.25 | 4755 | 9650 |
| 214.90 | 4525 | 10415 |
| 216.54 | 5067 | 10757 |
| 218.18 | 5167 | 11121 |
| 219.82 | 4934 | 10583 |
| 221.46 | 4275 | 9650 |
| 223.10 | 4001 | 9113 |
| 224.74 | 3666 | 8989 |
| 226.38 | 3509 | 9242 |
| 228.02 | 3645 | 9242 |
| 229.66 | 3728 | 8989 |
| 231.30 | 3125 | 8522 |
| 232.94 | 2769 | 8522 |
| 234.58 | 2853 | 8002 |
| 236.22 | 3155 | 8101 |
| 237.86 | 3605 | 8867 |
| 239.50 | 3977 | 9650 |
| 241.14 | 3953 | 9794 |
| 242.78 | 4193 | 9242 |
| 244.42 | 4360 | 9374 |
| 246.06 | 4449 | 9942 |
| 247.70 | 4303 | 9794 |
| 249.34 | 4261 | 9650 |
| 250.98 | 4790 | 10583 |
| 252.62 | 4494 | 9510 |
| 254.27 | 4220 | 9374 |
| 255.91 | 4755 | 9942 |
| 257.55 | 4573 | 9942 |

Table 22. Boring Z3-B6, Suspension R1-R2 depths and P- and $S_H$-wave velocities

| Depth (feet) | $V_s$ (feet/sec) | $V_p$ (feet/sec) |
|---|---|---|
| 259.19 | 4654 | 10415 |
| 260.83 | 4670 | 10095 |
| 262.47 | 4449 | 9510 |
| 264.11 | 4026 | 9113 |
| 265.75 | 3728 | 8867 |
| 267.39 | 3929 | 9942 |
| 269.03 | 4038 | 9510 |
| 270.67 | 3625 | 8634 |
| 272.31 | 3771 | 9113 |
| 273.95 | 3566 | 8634 |
| 275.59 | 3528 | 9242 |
| 277.23 | 3771 | 9374 |
| 278.87 | 3883 | 8522 |
| 280.51 | 4013 | 9794 |
| 282.15 | 4153 | 9510 |
| 283.79 | 3804 | 9510 |
| 285.43 | 4525 | 8989 |
| 287.07 | 4289 | 9374 |
| 288.71 | 3953 | 8306 |
| 290.35 | 3906 | 8202 |
| 291.99 | 3490 | 8749 |
| 293.64 | 3645 | 8989 |
| 295.28 | 4206 | 9794 |
| 296.92 | 4179 | 8989 |
| 298.56 | 3418 | 8002 |
| 300.20 | 2916 | 8101 |
| 301.84 | 3052 | 7906 |
| 303.48 | 3081 | 8989 |
| 305.12 | 3201 | 8412 |
| 306.76 | 3281 | 8412 |
| 308.40 | 3586 | 9113 |
| 310.04 | 3314 | 8522 |
| 311.68 | 3490 | 8522 |
| | | |

Table 22, continued. Boring Z3-B6, Suspension R1-R2 depths and P- and $S_H$-wave velocities

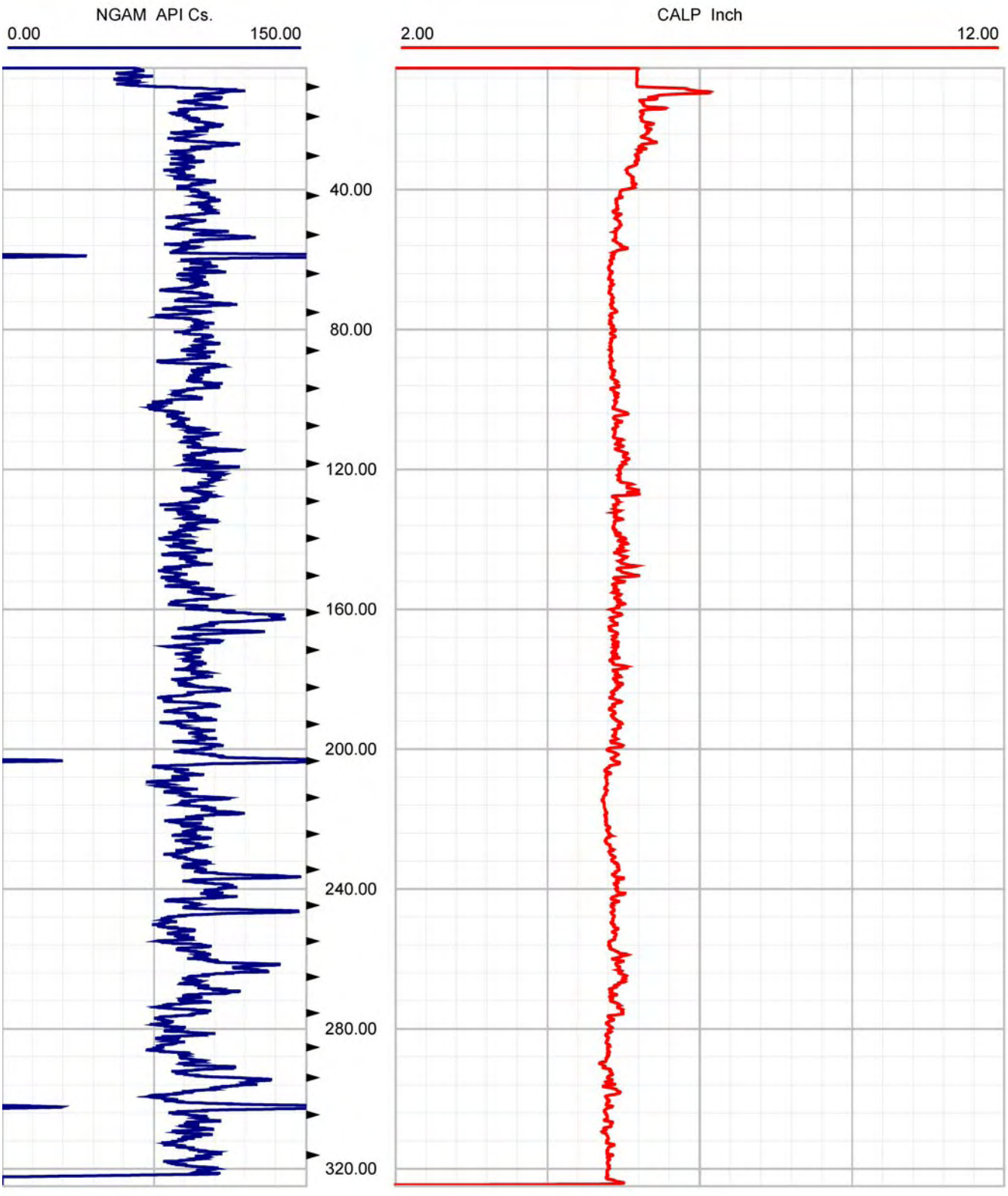


Figure 41. Boring Z3-B6, Caliper and Natural Gamma logs

DIP DATA INTERPRETATION
RGLDIP vsn 6.2
FRACTURE ANALYSIS STEREOGRAMS

CASCADE DRILLING

Borehole: Z3-B6

SR-710 TUNNEL INVESTIGATION

top of borehole.....
East:_
North:_
Elev:_

North ref: true
Depth units are feet

Zone from 285.973 to 45.665ft
Mean dip format: dip-azimuth and dip

Interpretation 1

Dip data sets .....
BHTV dips

Z3-B6
Zone 0. 45.665 - 285.973ft
Deviation 2.10 N 78.30

dipdata sets.....
BHTV dips
• Highlighted dips: Fracture Planar Hairline-fracture

| | mean dip | n | f |
|---|---|---|---|
| N293 51 | N293 51 | 7 | ( 0.04) |
| N347 35 | N347 35 | 4 | ( 0.02) |

intersections

| | N293 51 | N347 35 |
|---|---|---|
| N293 51 | | 35 N348 |
| N347 35 | 35 N348 | |

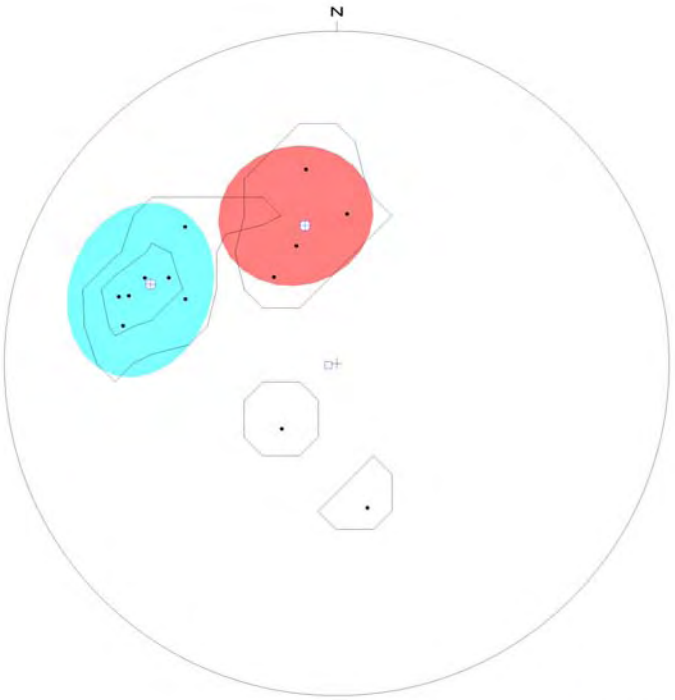


mean dip
well axis

equal-area upper-hemisphere 0-90
contour-levels 1,3,

Z3-B6, Interpretation 1 285.973 to 45.665ft 1

Figure 42. Boring Z3-B6, Stereonet Plot

| Depth (feet) | Dip azimuth | Dip | Structure description |
|---|---|---|---|
| 285.47 | N351 | 49 | Primary-structure Planar Bedding |
| 267.80 | N324 | 26 | Primary-structure Planar Bedding |
| 256.46 | N004 | 37 | Primary-structure Planar Bedding |
| 255.27 | N341 | 31 | Primary-structure Planar Bedding |
| 219.30 | N312 | 52 | Primary-structure Planar Bedding |
| 108.50 | N280 | 55 | Primary-structure Planar Bedding |
| 108.43 | N288 | 56 | Primary-structure Planar Bedding |
| 97.24 | N294 | 53 | Primary-structure Planar Bedding |
| 97.13 | N287 | 58 | Primary-structure Planar Bedding |
| 63.31 | N168 | 37 | Primary-structure Planar Bedding |
| 61.26 | N220 | 21 | Primary-structure Planar Bedding |
| 46.68 | N293 | 41 | Primary-structure Planar Bedding |
| 46.17 | N297 | 47 | Primary-structure Planar Bedding |
| | | | |

Table 23. Boring Z3-B6, Structure depth, dip azimuth, dip and description

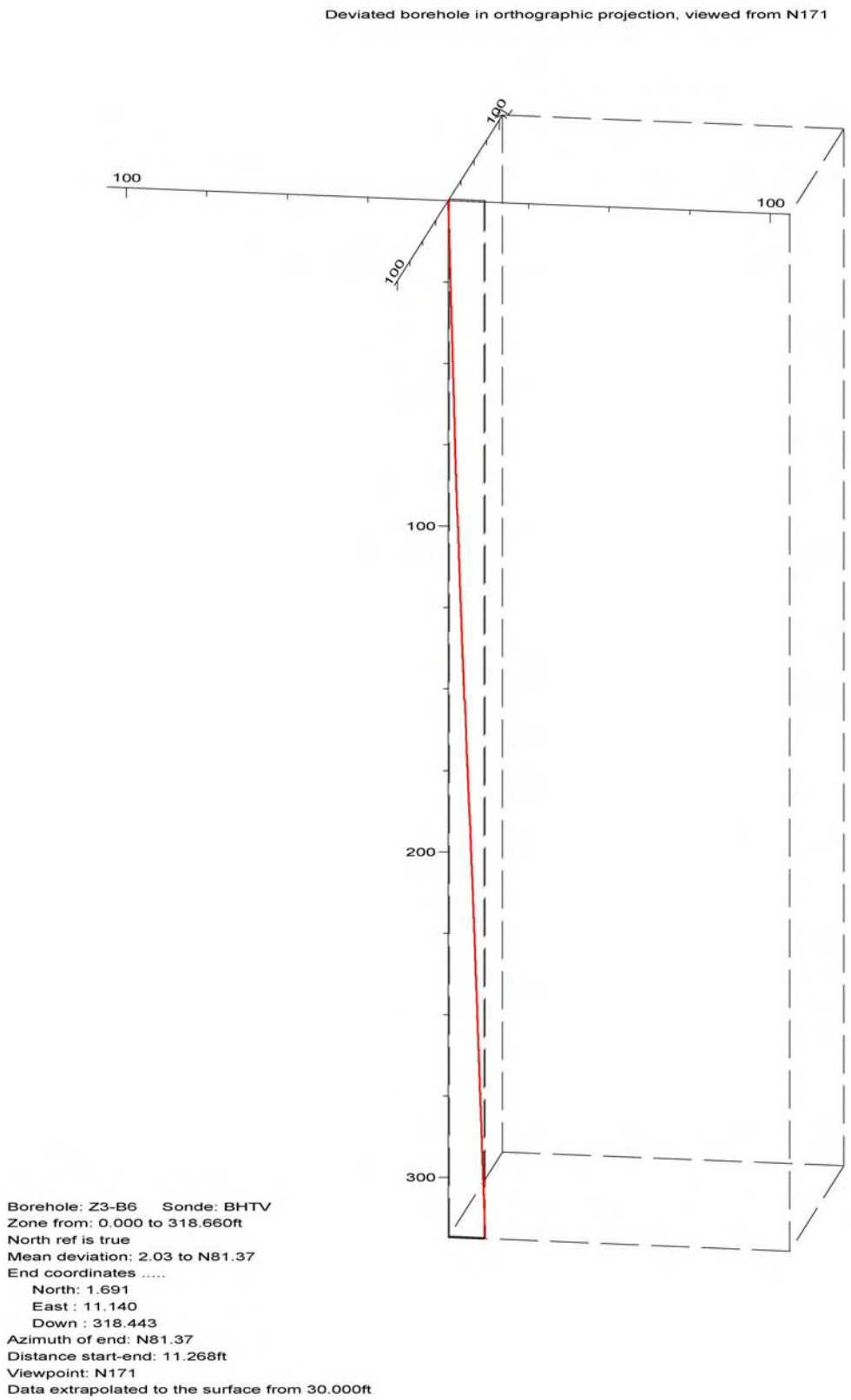


Figure 43. Boring Z3-B6, Deviation Projection

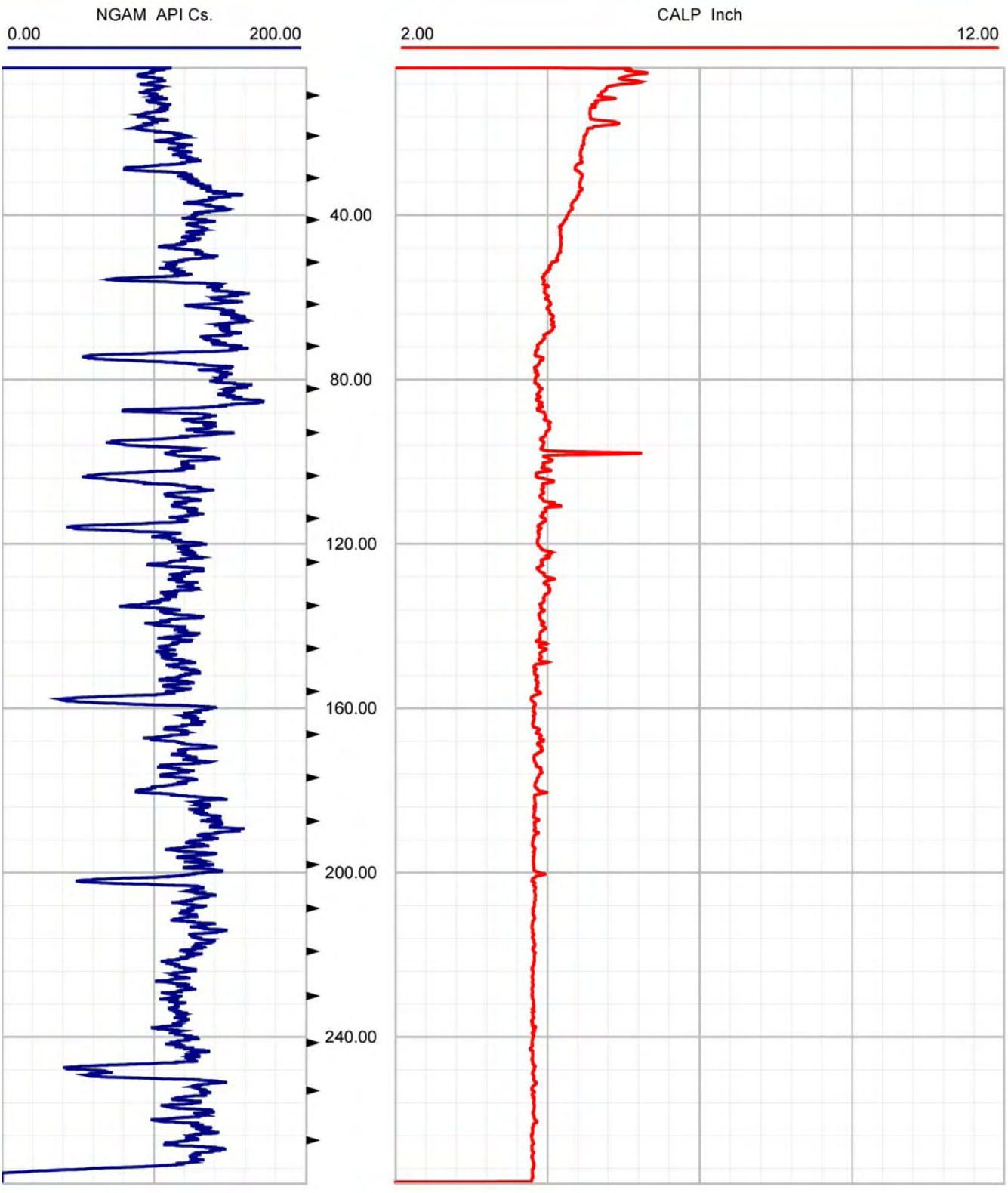


Figure 44. Boring Z3-B8, Caliper and Natural Gamma logs

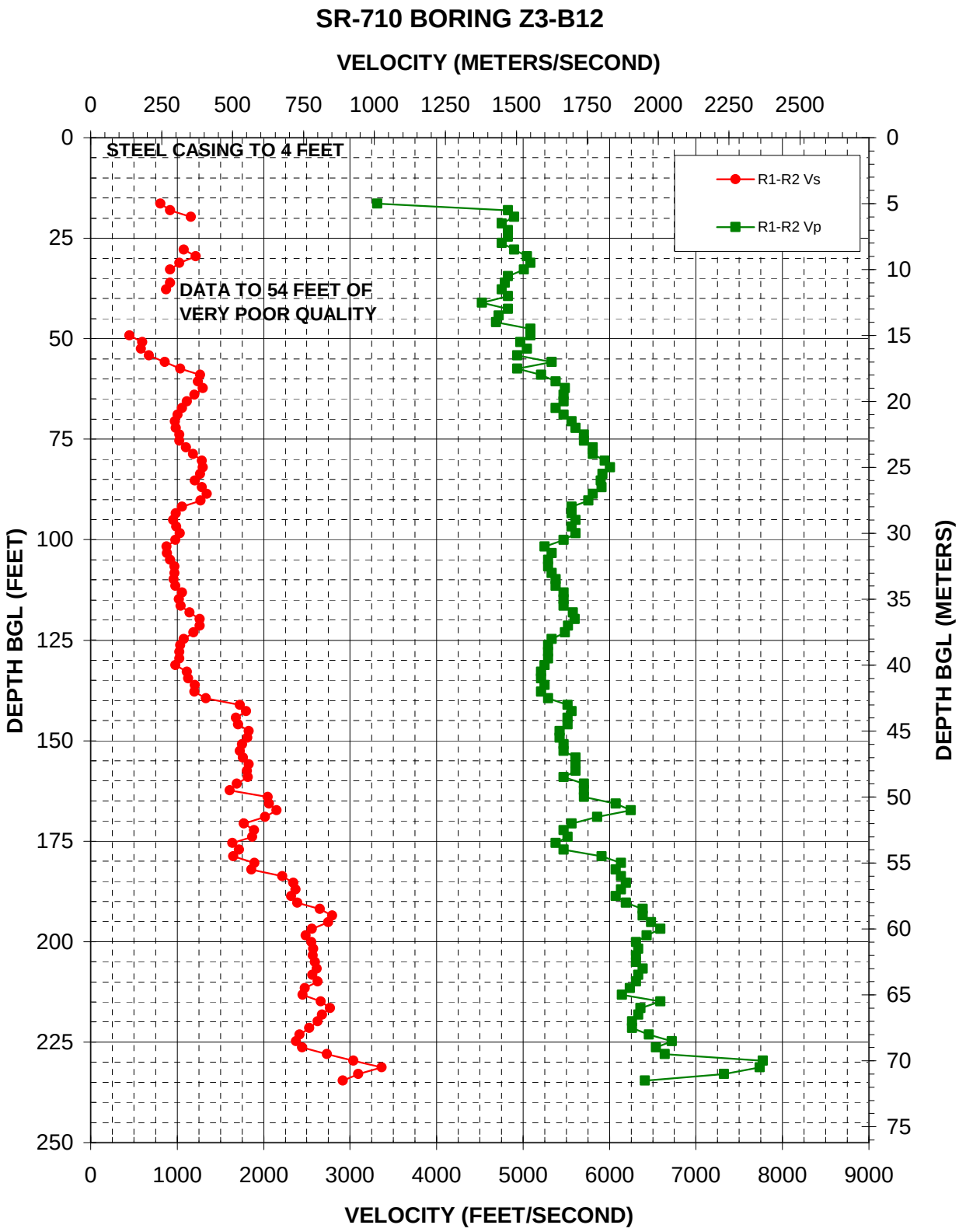


Figure 45: Boring Z3-B12, Suspension R1-R2 P- and $S_H$-wave velocities

| Depth (feet) | $V_s$ (feet/sec) | $V_p$ (feet/sec) |
|---|---|---|
| 8.20 | | |
| 16.40 | 805 | 3314 |
| 18.04 | 918 | 4825 |
| 19.69 | 1161 | 4897 |
| 21.33 | | 4755 |
| 22.97 | | 4825 |
| 24.61 | | 4825 |
| 26.25 | | 4755 |
| 27.89 | 1076 | 4897 |
| 29.53 | 1215 | 5047 |
| 31.17 | 1025 | 5087 |
| 32.81 | 918 | 5009 |
| 34.45 | | 4825 |
| 36.09 | 918 | 4790 |
| 37.73 | 875 | 4755 |
| 39.37 | | 4825 |
| 41.01 | | 4525 |
| 42.65 | | 4825 |
| 44.29 | | 4721 |
| 45.93 | | 4687 |
| 47.57 | | 5087 |
| 49.21 | 449 | 5087 |
| 50.85 | 599 | 4971 |
| 52.49 | 583 | 5047 |
| 54.13 | 676 | 4934 |
| 55.77 | 859 | 5335 |
| 57.41 | 1038 | 4934 |
| 59.06 | 1267 | 5208 |
| 60.70 | 1243 | 5378 |
| 62.34 | 1297 | 5486 |
| 63.98 | 1202 | 5468 |
| 65.62 | 1116 | 5468 |
| 67.26 | 1055 | 5378 |
| 68.90 | 1006 | 5468 |
| 70.54 | 976 | 5561 |
| 72.18 | 988 | 5608 |
| 73.82 | 1028 | 5706 |
| 75.46 | 1025 | 5706 |
| 77.10 | 1105 | 5807 |
| 78.74 | 1184 | 5807 |
| 80.38 | 1289 | 5944 |
| 82.02 | 1299 | 6009 |
| 83.66 | 1267 | 5922 |
| 85.30 | 1206 | 5901 |
| 86.94 | 1287 | 5911 |
| 88.58 | 1345 | 5807 |
| 90.22 | 1272 | 5756 |
| 91.86 | 1058 | 5561 |
| 93.50 | 988 | 5561 |
| 95.14 | 954 | 5608 |
| 96.78 | 991 | 5561 |
| 98.43 | 1032 | 5608 |
| 100.07 | 982 | 5468 |
| 101.71 | 877 | 5249 |
| 103.35 | 882 | 5335 |
| 104.99 | 922 | 5292 |
| 106.63 | 971 | 5292 |
| 108.27 | 971 | 5335 |
| 109.91 | 959 | 5378 |
| 111.55 | 979 | 5378 |
| 113.19 | 1058 | 5468 |
| 114.83 | 1020 | 5468 |
| 116.47 | 1043 | 5468 |
| 118.11 | 1143 | 5580 |
| 119.75 | 1262 | 5599 |
| 121.39 | 1259 | 5523 |
| 123.03 | 1191 | 5486 |
| 124.67 | 1079 | 5335 |
| 126.31 | 1035 | 5292 |
| 127.95 | 1025 | 5292 |
| 129.59 | 1028 | 5292 |
| 131.23 | 982 | 5249 |
| 132.87 | 1112 | 5208 |
| 134.51 | 1131 | 5208 |
| 136.15 | 1206 | 5249 |
| 137.80 | 1202 | 5208 |
| 139.44 | 1334 | 5292 |
| 141.08 | 1727 | 5514 |
| 142.72 | 1798 | 5561 |
| 144.36 | 1682 | 5514 |
| 146.00 | 1704 | 5514 |
| 147.64 | 1828 | 5423 |
| 149.28 | 1813 | 5423 |
| 150.92 | 1750 | 5468 |
| 152.56 | 1727 | 5468 |
| 154.20 | 1764 | 5608 |
| 155.84 | 1828 | 5608 |
| 157.48 | 1808 | 5608 |
| 159.12 | 1818 | 5468 |
| 160.76 | 1691 | 5706 |
| 162.40 | 1608 | 5706 |
| 164.04 | 2051 | 5706 |
| 165.68 | 2063 | 6076 |
| 167.32 | 2151 | 6249 |
| 168.96 | 2019 | 5859 |
| 170.60 | 1773 | 5561 |
| 172.24 | 1891 | 5468 |
| 173.88 | 1869 | 5514 |
| 175.52 | 1640 | 5378 |
| 177.17 | 1718 | 5468 |
| 178.81 | 1649 | 5911 |
| 180.45 | 1896 | 6132 |
| 182.09 | 1859 | 6076 |
| 183.73 | 2217 | 6132 |
| 185.37 | 2343 | 6190 |
| 187.01 | 2369 | 6132 |
| 188.65 | 2319 | 6076 |
| 190.29 | 2390 | 6190 |
| 191.93 | 2651 | 6383 |
| 193.57 | 2792 | 6383 |
| 195.21 | 2745 | 6484 |
| 196.85 | 2558 | 6588 |
| 198.49 | 2485 | 6433 |
| 200.13 | 2553 | 6309 |
| 201.77 | 2573 | 6334 |
| 203.41 | 2568 | 6309 |
| 205.05 | 2594 | 6309 |
| 206.69 | 2614 | 6383 |
| 208.33 | 2563 | 6334 |
| 209.97 | 2625 | 6309 |
| 211.61 | 2476 | 6237 |
| 213.25 | 2453 | 6144 |
| 214.90 | 2662 | 6588 |
| 216.54 | 2769 | 6358 |
| 218.18 | 2678 | 6334 |
| 219.82 | 2625 | 6261 |
| 221.46 | 2529 | 6261 |
| 223.10 | 2417 | 6458 |
| 224.74 | 2377 | 6723 |
| 226.38 | 2448 | 6536 |
| 228.02 | 2734 | 6641 |
| 229.66 | 3038 | 7774 |
| 231.30 | 3365 | 7738 |
| 232.94 | 3095 | 7323 |
| 234.58 | 2916 | 6408 |
| | | |

NOTE: “blank” space indicates data of insufficient quality for good pick. See Appendix A for Source-to-Receiver measurement.

Table 24. Boring Z3-B12, Suspension R1-R2 depths and P- and $S_H$-wave velocities

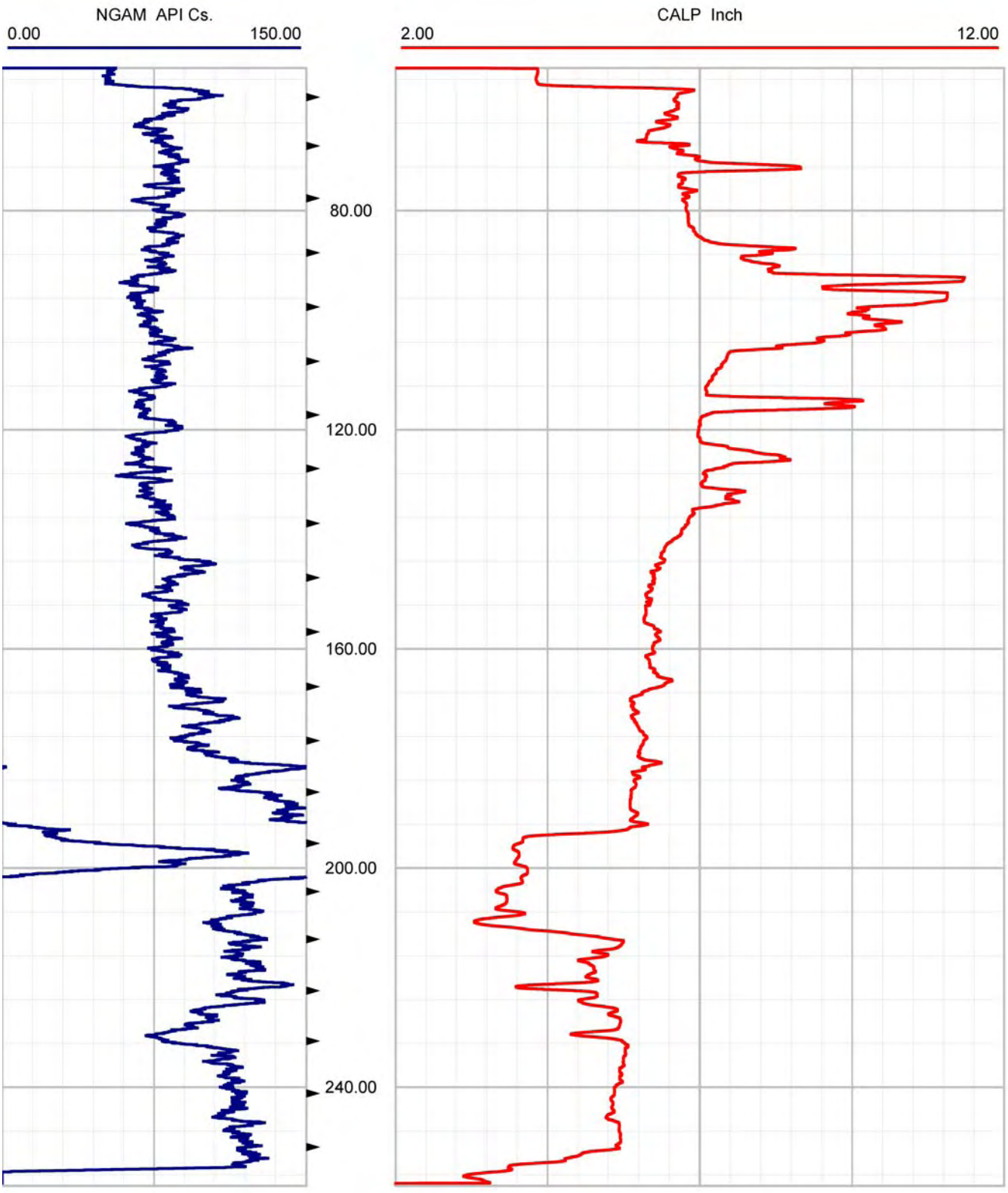


Figure 46. Boring Z3-B12, Caliper and Natural Gamma logs

DIP DATA INTERPRETATION
RGLDIP vsn 6.2
FRACTURE ANALYSIS STEREOGRAMS

CASCADE DRILLING

Borehole: Z3-B12

SR-710 TUNNEL INVESTIGATION

top of borehole.....
East:_
North:_
Elev:_

North ref: true
Depth units are feet

Zone from 179.361 to 113.631ft
Mean dip format: dip-azimuth and dip

Interpretation 1

Dip data sets .....
BHTV dips

Z3-B12
Zone 0. 113.631 - 179.351ft
Deviation 0.20 N234.00

dipdata sets.....
BHTV dips
• Highlighted dips: Fracture Planar Open-fracture

| | mean dip | n | f |
|---|---|---|---|
| N175 56 | N175 56 | 17 | 0.47 |
| N351 26 | N351 26 | 1 | ( 0.00) |

intersections

| | N175 56 | N351 26 |
|---|---|---|
| N175 56 | | 01 N264 |
| N351 26 | 01 N264 | |

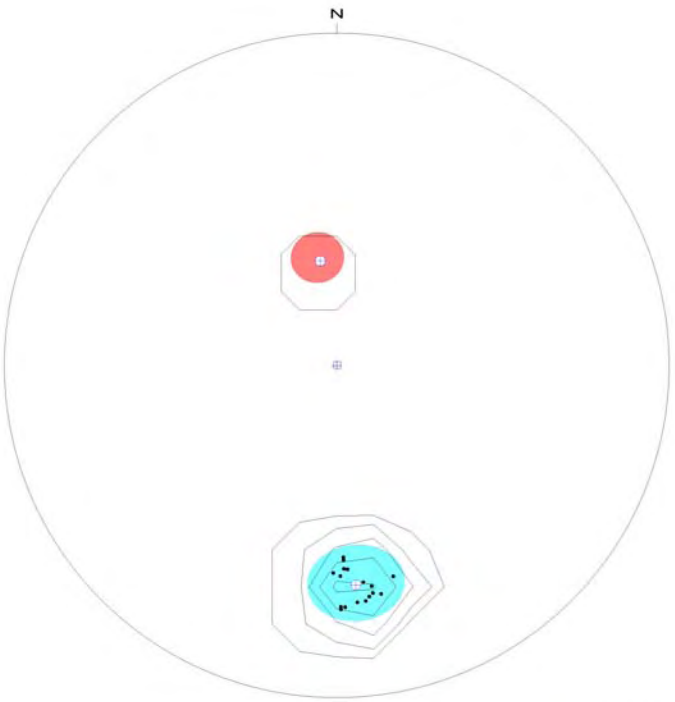


equal-area upper-hemisphere 0-90
contour-levels 1,3,6,10,15,

Z3-B12, Interpretation 1 179.351 to 113.631ft 1

Figure 47. Boring Z3-B12, Stereonet Plot

| Depth (feet) | Dip azimuth | Dip | Structure description |
|---|---|---|---|
| 178.86 | N179 | 62 | Primary-structure Planar Bedding |
| 178.55 | N179 | 63 | Primary-structure Planar Bedding |
| 177.99 | N178 | 62 | Primary-structure Planar Bedding |
| 176.93 | N175 | 61 | Primary-structure Planar Bedding |
| 176.29 | N173 | 61 | Primary-structure Planar Bedding |
| 174.71 | N172 | 60 | Primary-structure Planar Bedding |
| 162.82 | N171 | 57 | Primary-structure Planar Bedding |
| 162.36 | N169 | 59 | Primary-structure Planar Bedding |
| 161.74 | N165 | 55 | Primary-structure Planar Bedding |
| 159.94 | N171 | 59 | Primary-structure Planar Bedding |
| 157.05 | N179 | 53 | Primary-structure Planar Bedding |
| 156.16 | N173 | 55 | Primary-structure Planar Bedding |
| 152.02 | N178 | 49 | Primary-structure Planar Bedding |
| 150.86 | N178 | 48 | Primary-structure Planar Bedding |
| 148.50 | N178 | 51 | Primary-structure Planar Bedding |
| 146.45 | N181 | 53 | Primary-structure Planar Bedding |
| 131.08 | N177 | 52 | Primary-structure Planar Bedding |
| 114.13 | N351 | 26 | Primary-structure Planar Bedding |
| | | | |

Table 25. Boring Z3-B12, Structure depth, dip azimuth, dip and description

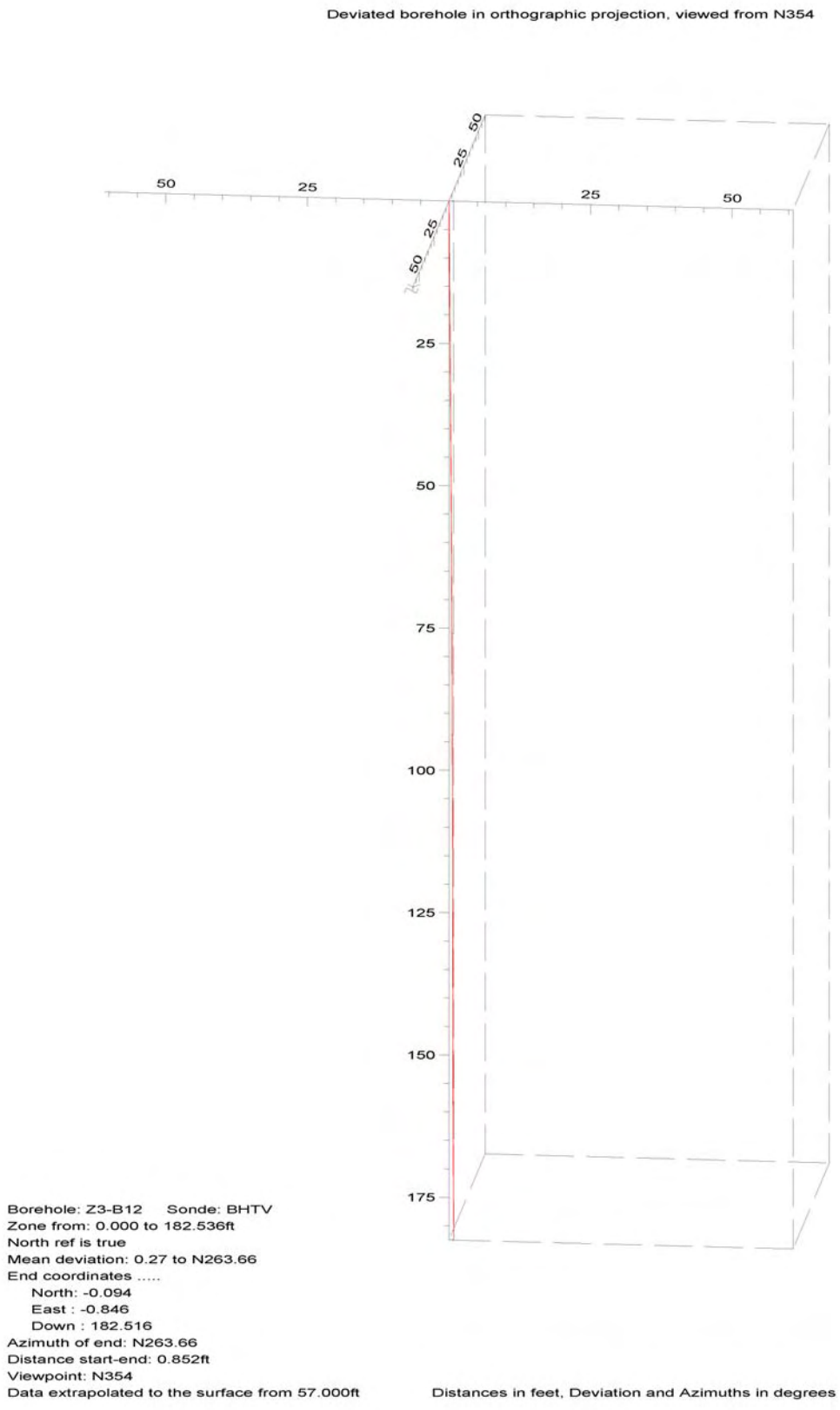


Figure 48. Boring Z3-B12, Deviation Projection

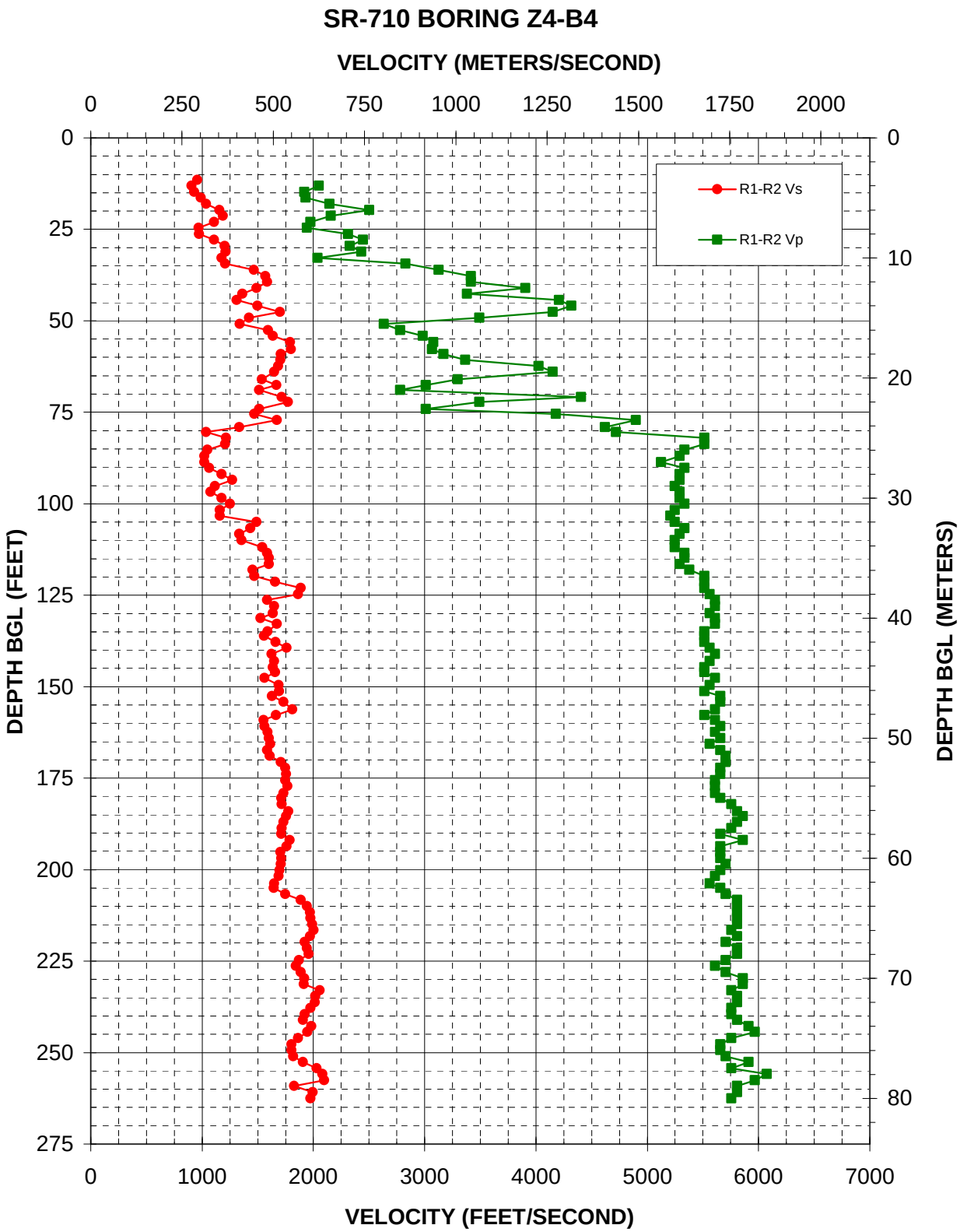


Figure 49: Boring Z4-B4, Suspension R1-R2 P- and $S_H$-wave velocities

| Depth (feet) | $V_s$ (feet/sec) | $V_p$ (feet/sec) |
|---|---|---|
| 11.48 | 958 | |
| 13.12 | 904 | 2051 |
| 14.76 | 929 | 1919 |
| 16.40 | 991 | 1930 |
| 18.04 | 1035 | 2144 |
| 19.69 | 1155 | 2504 |
| 21.33 | 1189 | 2158 |
| 22.97 | 1108 | 1976 |
| 24.61 | 968 | 1941 |
| 26.25 | 974 | 2310 |
| 27.89 | 1108 | 2448 |
| 29.53 | 1202 | 2327 |
| 31.17 | 1211 | 2430 |
| 32.81 | 1176 | 2038 |
| 34.45 | 1206 | 2828 |
| 36.09 | 1465 | 3125 |
| 37.73 | 1570 | 3418 |
| 39.37 | 1585 | 3418 |
| 41.01 | 1491 | 3906 |
| 42.65 | 1361 | 3382 |
| 44.29 | 1312 | 4206 |
| 45.93 | 1498 | 4317 |
| 47.57 | 1700 | 4153 |
| 49.21 | 1420 | 3490 |
| 50.85 | 1339 | 2635 |
| 52.49 | 1593 | 2780 |
| 54.13 | 1636 | 2983 |
| 55.77 | 1793 | 3081 |
| 57.74 | 1798 | 3066 |
| 59.06 | 1709 | 3170 |
| 60.70 | 1704 | 3365 |
| 62.34 | 1682 | 4026 |
| 63.98 | 1649 | 4153 |
| 65.94 | 1537 | 3297 |
| 67.59 | 1670 | 3010 |
| 68.90 | 1512 | 2780 |
| 70.87 | 1718 | 4404 |
| 72.18 | 1773 | 3490 |
| 74.15 | 1512 | 3010 |
| 75.46 | 1471 | 4179 |
| 77.10 | 1674 | 4897 |
| 79.07 | 1334 | 4621 |
| 80.38 | 1038 | 4721 |
| 82.02 | 1215 | 5514 |
| 83.66 | 1206 | 5514 |
| 85.30 | 1048 | 5335 |
| 86.94 | 1022 | 5292 |
| 88.58 | 1022 | 5126 |
| 90.22 | 1065 | 5335 |
| 91.86 | 1176 | 5292 |
| 93.50 | 1272 | 5292 |
| 95.14 | 1116 | 5249 |
| 96.78 | 1076 | 5292 |
| 98.43 | 1176 | 5292 |
| 100.07 | 1252 | 5335 |
| 101.71 | 1159 | 5249 |
| 103.35 | 1159 | 5208 |
| 104.99 | 1491 | 5249 |
| 106.63 | 1433 | 5335 |
| 108.27 | 1334 | 5292 |
| 109.91 | 1356 | 5249 |
| 111.88 | 1540 | 5249 |
| 113.52 | 1585 | 5335 |
| 114.83 | 1600 | 5335 |
| 116.47 | 1600 | 5292 |
| 118.11 | 1455 | 5378 |
| 119.75 | 1468 | 5514 |
| 121.39 | 1657 | 5514 |
| 123.03 | 1886 | 5514 |
| 124.67 | 1864 | 5561 |
| 126.31 | 1585 | 5608 |
| 127.95 | 1649 | 5608 |
| 129.92 | 1636 | 5561 |
| 131.23 | 1526 | 5608 |
| 132.87 | 1674 | 5608 |
| 134.84 | 1589 | 5514 |
| 136.15 | 1559 | 5514 |
| 137.80 | 1661 | 5514 |
| 139.44 | 1759 | 5561 |
| 141.08 | 1624 | 5608 |
| 143.04 | 1649 | 5561 |
| 144.69 | 1636 | 5514 |
| 146.00 | 1657 | 5514 |
| 147.64 | 1562 | 5608 |
| 149.61 | 1687 | 5561 |
| 151.25 | 1691 | 5514 |
| 152.56 | 1628 | 5657 |
| 154.20 | 1731 | 5657 |
| 156.17 | 1813 | 5608 |
| 157.81 | 1665 | 5514 |
| 159.12 | 1555 | 5608 |
| 160.76 | 1562 | 5657 |
| 162.40 | 1589 | 5608 |
| 164.04 | 1600 | 5657 |
| 165.68 | 1612 | 5561 |
| 167.32 | 1585 | 5657 |
| 168.96 | 1608 | 5706 |
| 170.60 | 1709 | 5706 |
| 172.24 | 1750 | 5657 |
| 173.88 | 1754 | 5657 |
| 175.52 | 1750 | 5608 |
| 177.17 | 1769 | 5608 |
| 179.13 | 1731 | 5608 |
| 180.45 | 1713 | 5657 |
| 182.09 | 1718 | 5756 |
| 184.06 | 1776 | 5807 |
| 185.37 | 1754 | 5859 |
| 187.01 | 1731 | 5807 |
| 188.65 | 1718 | 5756 |
| 190.29 | 1713 | 5657 |
| 191.93 | 1788 | 5859 |
| 193.57 | 1759 | 5657 |
| 195.21 | 1704 | 5657 |
| 196.85 | 1713 | 5657 |
| 198.49 | 1709 | 5706 |
| 200.13 | 1696 | 5657 |
| 201.77 | 1687 | 5608 |
| 203.74 | 1649 | 5561 |
| 205.05 | 1645 | 5657 |
| 206.69 | 1750 | 5706 |
| 208.33 | 1886 | 5807 |
| 209.97 | 1941 | 5807 |
| 211.61 | 1970 | 5807 |
| 213.25 | 1976 | 5807 |
| 214.90 | 1988 | 5807 |
| 216.54 | 2001 | 5756 |
| 218.18 | 1970 | 5807 |
| 219.82 | 1924 | 5706 |
| 221.46 | 1941 | 5807 |
| 223.10 | 1959 | 5807 |
| 224.74 | 1869 | 5706 |
| 226.38 | 1843 | 5608 |
| 228.02 | 1886 | 5706 |
| 229.66 | 1919 | 5859 |
| 231.30 | 1913 | 5859 |
| 232.94 | 2057 | 5756 |
| 234.58 | 2019 | 5807 |
| 236.22 | 2013 | 5807 |
| 237.86 | 1976 | 5756 |
| 239.50 | 1924 | 5756 |
| 241.14 | 1907 | 5807 |
| 242.78 | 1982 | 5911 |
| 244.42 | 1947 | 5965 |
| 246.06 | 1864 | 5756 |
| 247.70 | 1803 | 5657 |
| 249.34 | 1803 | 5657 |
| 250.98 | 1818 | 5706 |
| 252.62 | 1907 | 5911 |
| 254.27 | 2031 | 5756 |
| 255.91 | 2083 | 6076 |

Table 26. Boring Z4-B4, Suspension R1-R2 depths and P- and $S_H$-wave velocities

| Depth (feet) | $V_s$ (feet/sec) | $V_p$ (feet/sec) |
|---|---|---|
| 257.55 | 2096 | 5965 |
| 259.19 | 1828 | 5807 |
| 260.83 | 1994 | 5807 |
| 262.47 | 1976 | 5756 |
| | | |

Table 26, continued. Boring Z4-B4, Suspension R1-R2 depths and P- and $S_H$-wave velocities

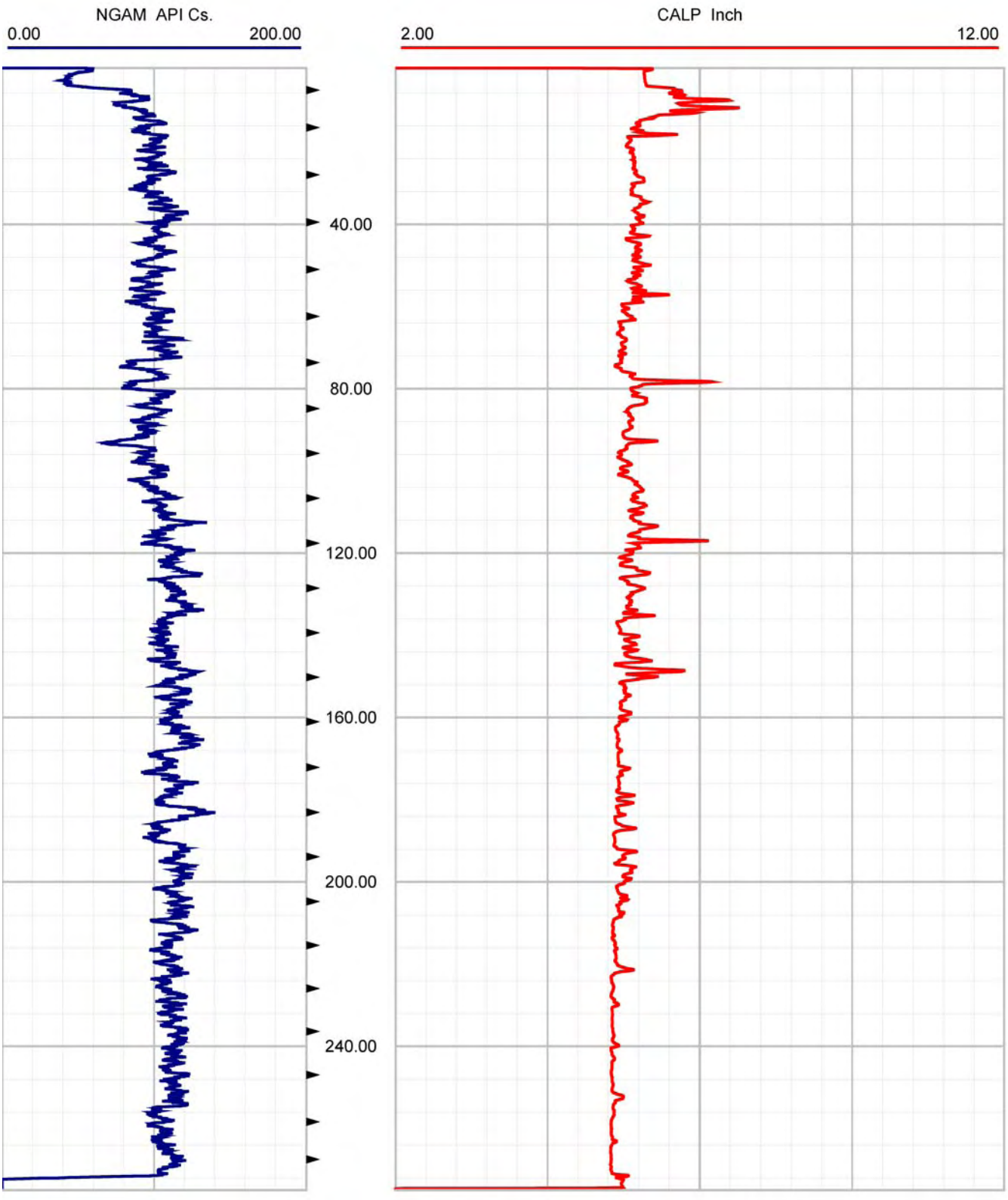


Figure 50. Boring Z4-B4, Caliper and Natural Gamma logs

DIP DATA INTERPRETATION
RGLDIP vsn 6.2
FRACTURE ANALYSIS STEREOGRAMS

CASCADE DRILLING

Borehole: Z4-B4

SR-710 TUNNEL INVESTIGATION

top of borehole.....
East:_
North:_
Elev:_

North ref: true
Depth units are feet

Zone from 274.222 to 17.723ft
Mean dip format: dip-azimuth and dip

Interpretation 1

Dip data sets .....
BHTV dips

Z4-B4
Zone 0. 17.723 - 274.222ft
Deviation 0.60 N356.10

dipdata sets.....
BHTV dips
• Highlighted dips: Fracture Planar Hairline-fracture

| | mean dip | n | f |
|---|---|---|---|
| N088 72 | N088 72 | 10 | ( 0.13) |
| N238 37 | N238 37 | 5 | ( 0.02) |
| N156 6 | N156 6 | 7 | ( 0.03) |
| N314 68 | N314 68 | 3 | ( 0.03) |

intersections

| | N088 72 | N238 37 | N156 6 | N314 68 |
|---|---|---|---|---|
| N088 72 | | 17 N172 | 06 N176 | 47 N018 |
| N238 37 | 17 N172 | | 06 N156 | 37 N242 |
| N156 6 | 06 N176 | 06 N156 | | 02 N225 |
| N314 68 | 47 N018 | 37 N242 | 02 N225 | |

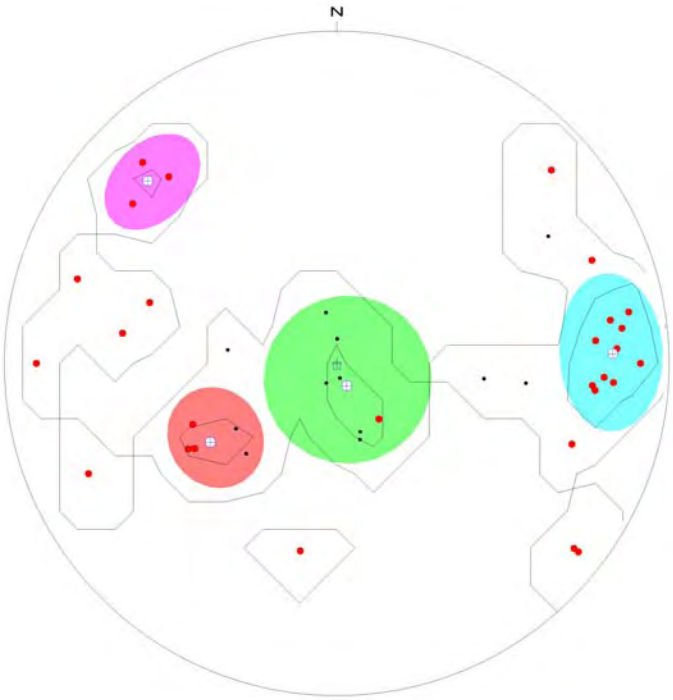


equal-area upper-hemisphere 0-90
contour-levels 1,3,

Z4-B4, Interpretation 1 274.222 to 17.723ft 1

Figure 51. Boring Z4-B4, Stereonet Plot

| Depth (feet) | Dip azimuth | Dip | Structure description |
|---|---|---|---|
| 273.72 | N318 | 65 | Fracture Planar Hairline-fracture |
| 273.28 | N316 | 73 | Fracture Planar Hairline-fracture |
| 269.47 | N308 | 67 | Fracture Planar Hairline-fracture |
| 257.47 | N239 | 41 | Fracture Planar Hairline-fracture |
| 245.93 | N109 | 64 | Fracture Planar Hairline-fracture |
| 208.70 | N143 | 17 | Fracture Planar Hairline-fracture |
| 187.06 | N001 | 6 | Primary-structure Planar Bedding |
| 182.56 | N128 | 81 | Fracture Planar Hairline-fracture |
| 173.49 | N128 | 80 | Fracture Planar Hairline-fracture |
| 172.05 | N068 | 72 | Fracture Planar Hairline-fracture |
| 168.70 | N208 | 6 | Primary-structure Planar Bedding |
| 168.04 | N168 | 4 | Primary-structure Planar Bedding |
| 159.96 | N083 | 75 | Fracture Planar Hairline-fracture |
| 159.55 | N240 | 43 | Fracture Planar Hairline-fracture |
| 155.97 | N247 | 39 | Fracture Planar Hairline-fracture |
| 152.85 | N288 | 50 | Fracture Planar Hairline-fracture |
| 152.03 | N191 | 48 | Fracture Planar Hairline-fracture |
| 150.23 | N094 | 72 | Fracture Planar Hairline-fracture |
| 146.46 | N085 | 67 | Fracture Planar Hairline-fracture |
| 145.99 | N081 | 72 | Fracture Planar Hairline-fracture |
| 144.45 | N246 | 71 | Fracture Planar Hairline-fracture |
| 142.84 | N087 | 73 | Fracture Planar Hairline-fracture |
| 140.85 | N288 | 71 | Fracture Planar Hairline-fracture |
| 121.97 | N080 | 78 | Fracture Planar Hairline-fracture |
| 121.13 | N095 | 66 | Fracture Planar Hairline-fracture |
| 120.84 | N096 | 67 | Fracture Planar Hairline-fracture |
| 120.50 | N093 | 69 | Fracture Planar Hairline-fracture |
| 118.41 | N090 | 81 | Fracture Planar Hairline-fracture |
| 118.05 | N278 | 55 | Fracture Planar Hairline-fracture |
| 117.53 | N225 | 32 | Primary-structure Planar Bedding |
| 117.11 | N096 | 37 | Primary-structure Planar Bedding |
| 114.88 | N277 | 27 | Primary-structure Planar Bedding |
| 113.08 | N270 | 80 | Fracture Planar Hairline-fracture |
| 112.28 | N048 | 76 | Fracture Planar Hairline-fracture |
| 98.48 | N059 | 63 | Primary-structure Planar Bedding |
| 78.32 | N096 | 48 | Primary-structure Planar Bedding |
| 43.39 | N237 | 30 | Primary-structure Planar Bedding |
| 35.14 | N348 | 13 | Primary-structure Planar Bedding |
| 18.61 | N161 | 18 | Primary-structure Planar Bedding |
| 18.22 | N163 | 20 | Primary-structure Planar Bedding |
| | | | |

Table 27. Boring Z4-B4, Structure depth, dip azimuth, dip and description

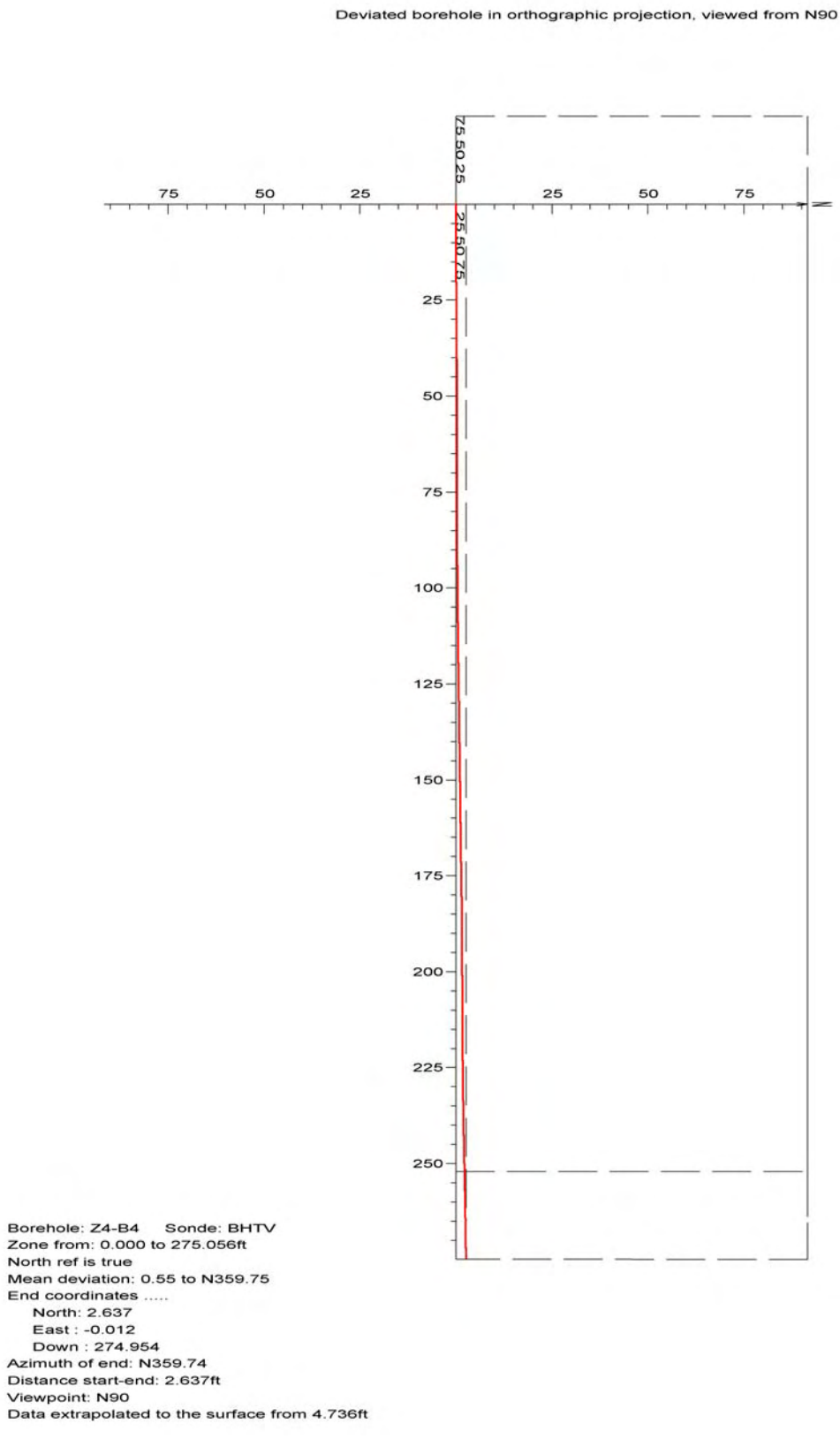


Figure 52. Boring Z4-B4, Deviation Projection

This page left intentionally blank

# APPENDIX A

# SUSPENSION VELOCITY MEASUREMENT QUALITY ASSURANCE SUSPENSION SOURCE TO RECEIVER ANALYSIS RESULTS

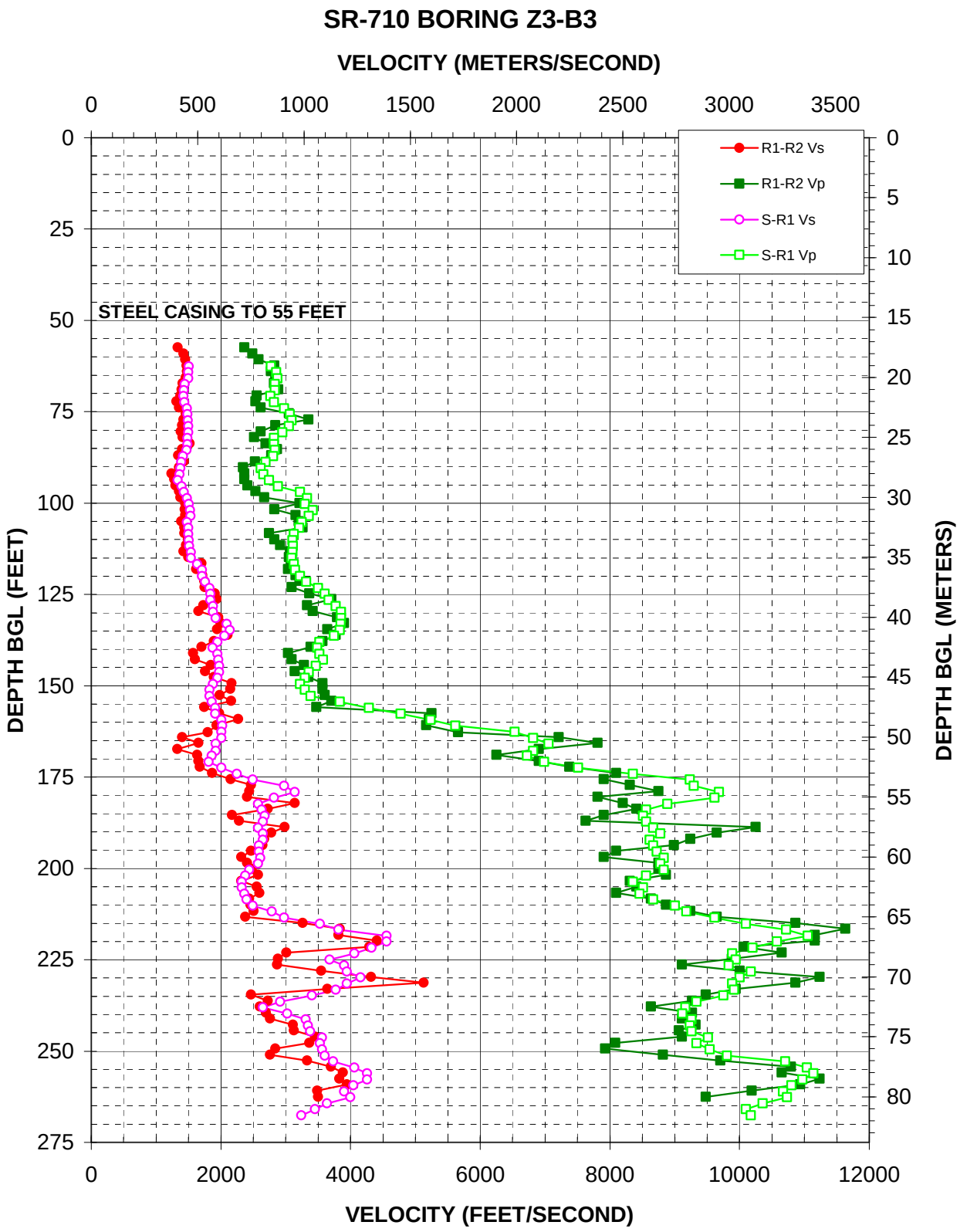


Figure A-8. Boring Z3-B3, R1 - R2 high resolution analysis and S - R1 quality assurance analysis P- and $S_H$-wave data

| Depth (feet) | $V_s$ (feet/sec) | $V_p$ (feet/sec) |
|---|---|---|
| 62.57 | 1503 | 2775 |
| 64.21 | 1497 | 2854 |
| 65.85 | 1497 | 2872 |
| 67.49 | 1445 | 2831 |
| 69.13 | 1430 | 2831 |
| 70.77 | 1424 | 2764 |
| 72.41 | 1437 | 2820 |
| 74.05 | 1478 | 2975 |
| 75.69 | 1484 | 3066 |
| 77.33 | 1491 | 3093 |
| 78.97 | 1497 | 3053 |
| 80.61 | 1497 | 2950 |
| 82.25 | 1484 | 2820 |
| 83.89 | 1484 | 2820 |
| 85.53 | 1469 | 2831 |
| 87.17 | 1418 | 2803 |
| 88.81 | 1388 | 2690 |
| 90.45 | 1377 | 2615 |
| 92.09 | 1363 | 2654 |
| 93.73 | 1337 | 2743 |
| 95.37 | 1399 | 2877 |
| 97.01 | 1430 | 3221 |
| 98.65 | 1478 | 3327 |
| 100.30 | 1503 | 3296 |
| 101.94 | 1526 | 3417 |
| 103.58 | 1533 | 3359 |
| 105.22 | 1478 | 3250 |
| 106.86 | 1497 | 3206 |
| 108.50 | 1497 | 3127 |
| 110.14 | 1505 | 3107 |
| 111.78 | 1510 | 3114 |
| 113.42 | 1540 | 3107 |
| 115.06 | 1540 | 3093 |
| 116.70 | 1633 | 3127 |
| 118.34 | 1712 | 3148 |
| 119.98 | 1712 | 3221 |
| 121.62 | 1760 | 3320 |
| 123.26 | 1828 | 3502 |
| 124.90 | 1838 | 3601 |
| 126.54 | 1838 | 3666 |
| 128.18 | 1882 | 3775 |
| 129.82 | 1882 | 3858 |
| 131.46 | 1924 | 3858 |
| 133.10 | 2090 | 3847 |
| 134.74 | 2141 | 3837 |
| 136.38 | 2059 | 3745 |
| 138.02 | 1950 | 3519 |
| 139.67 | 1872 | 3484 |
| 141.31 | 1950 | 3519 |
| 142.95 | 1961 | 3573 |
| 144.59 | 1972 | 3467 |
| 146.23 | 1972 | 3359 |
| 147.87 | 1950 | 3296 |
| 149.51 | 1882 | 3221 |
| 151.15 | 1828 | 3296 |
| 152.79 | 1828 | 3384 |
| 154.43 | 1857 | 3837 |
| 156.07 | 1913 | 4281 |
| 157.71 | 1913 | 4776 |
| 159.35 | 2012 | 5240 |
| 160.99 | 2023 | 5617 |
| 162.63 | 2012 | 6531 |
| 164.27 | 2012 | 6817 |
| 165.91 | 1924 | 7056 |
| 167.88 | 1924 | 6817 |
| 169.19 | 1857 | 6719 |
| 170.83 | 1810 | 6986 |
| 172.47 | 2012 | 7509 |
| 174.11 | 2250 | 8358 |
| 175.75 | 2490 | 9238 |
| 177.40 | 2975 | 9299 |
| 179.04 | 3141 | 9684 |
| 180.68 | 2820 | 9618 |
| 182.32 | 2572 | 8887 |
| 183.96 | 2630 | 8562 |
| 185.60 | 2675 | 8510 |
| 187.24 | 2649 | 8562 |
| 188.88 | 2572 | 8668 |
| 190.52 | 2649 | 8776 |
| 192.16 | 2649 | 8615 |
| 193.80 | 2591 | 8668 |
| 195.44 | 2591 | 8722 |
| 197.08 | 2610 | 8831 |
| 198.72 | 2572 | 8776 |
| 200.36 | 2438 | 8831 |
| 202.00 | 2380 | 8562 |
| 203.64 | 2325 | 8358 |
| 205.28 | 2325 | 8510 |
| 206.92 | 2364 | 8459 |
| 208.56 | 2396 | 8668 |
| 210.20 | 2490 | 9001 |
| 211.84 | 2786 | 9178 |
| 213.48 | 2975 | 9618 |
| 215.12 | 3528 | 10102 |
| 216.77 | 3816 | 10719 |
| 218.41 | 4559 | 11057 |
| 220.05 | 4559 | 10574 |
| 221.69 | 4323 | 10205 |
| 223.33 | 4058 | 9889 |
| 224.97 | 3676 | 9945 |
| 226.61 | 3901 | 9833 |
| 228.25 | 3944 | 10175 |
| 229.89 | 4154 | 10001 |
| 231.53 | 3944 | 9889 |
| 233.17 | 3775 | 9917 |
| 234.81 | 3408 | 9751 |
| 236.45 | 2913 | 9336 |
| 238.09 | 2649 | 9166 |
| 239.73 | 3026 | 9118 |
| 241.37 | 3312 | 9263 |
| 243.01 | 3343 | 9238 |
| 244.65 | 3375 | 9263 |
| 246.29 | 3564 | 9514 |
| 247.93 | 3528 | 9336 |
| 249.57 | 3564 | 9539 |
| 251.21 | 3601 | 9806 |
| 252.85 | 3735 | 10703 |
| 254.49 | 4058 | 11039 |
| 256.14 | 4255 | 11144 |
| 257.78 | 4255 | 10970 |
| 259.42 | 4047 | 10802 |
| 261.06 | 3901 | 10670 |
| 262.70 | 4001 | 10735 |
| 264.34 | 3638 | 10355 |
| 265.98 | 3450 | 10102 |
| 267.62 | 3243 | 10175 |
| | | |

Table A-8. Boring Z3-B3, S - R1 quality assurance analysis P- and $S_H$-wave data

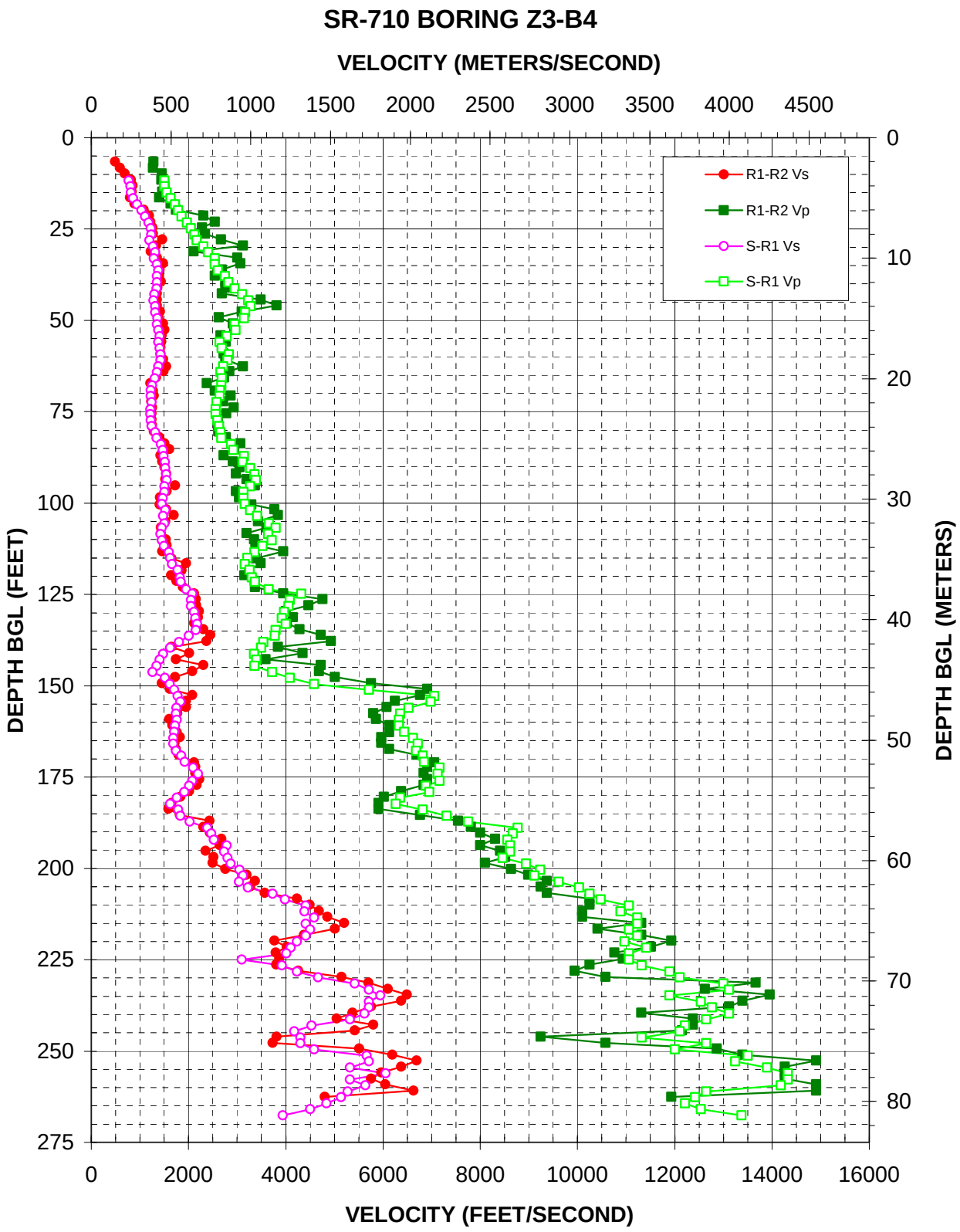


Figure A-9. Boring Z3-B4, R1 - R2 high resolution analysis and S - R1 quality assurance analysis P- and $S_H$-wave data

| Depth (feet) | $V_s$ (feet/sec) | $V_p$ (feet/sec) |
|---|---|---|
| 11.71 | 767 | 1510 |
| 13.35 | 807 | 1510 |
| 14.99 | 815 | 1550 |
| 16.63 | 858 | 1633 |
| 18.27 | 941 | 1721 |
| 19.91 | 1034 | 1791 |
| 21.56 | 1111 | 1862 |
| 23.20 | 1182 | 1972 |
| 24.84 | 1227 | 2053 |
| 26.48 | 1236 | 2128 |
| 28.12 | 1198 | 2174 |
| 29.76 | 1272 | 2302 |
| 31.40 | 1315 | 2404 |
| 33.04 | 1286 | 2544 |
| 34.68 | 1350 | 2544 |
| 36.32 | 1382 | 2610 |
| 37.96 | 1355 | 2753 |
| 39.60 | 1355 | 2820 |
| 41.24 | 1340 | 2950 |
| 42.88 | 1295 | 3107 |
| 44.52 | 1281 | 3235 |
| 46.16 | 1315 | 3281 |
| 47.80 | 1315 | 3170 |
| 49.44 | 1361 | 3141 |
| 51.08 | 1355 | 2950 |
| 52.72 | 1377 | 2969 |
| 54.36 | 1410 | 2786 |
| 56.00 | 1377 | 2644 |
| 57.64 | 1410 | 2690 |
| 59.28 | 1427 | 2837 |
| 60.93 | 1427 | 2803 |
| 62.57 | 1377 | 2711 |
| 64.21 | 1350 | 2659 |
| 65.85 | 1305 | 2690 |
| 67.81 | 1254 | 2680 |
| 69.13 | 1227 | 2654 |
| 70.77 | 1227 | 2639 |
| 72.41 | 1240 | 2581 |
| 74.38 | 1219 | 2562 |
| 75.69 | 1219 | 2562 |
| 77.33 | 1227 | 2600 |
| 78.97 | 1245 | 2630 |
| 80.61 | 1315 | 2659 |
| 82.25 | 1345 | 2675 |
| 83.89 | 1433 | 2877 |
| 85.53 | 1469 | 2925 |
| 87.17 | 1487 | 3141 |
| 88.81 | 1513 | 3114 |
| 90.45 | 1526 | 3273 |
| 92.09 | 1540 | 3359 |
| 93.73 | 1553 | 3384 |
| 95.37 | 1507 | 3273 |
| 97.01 | 1507 | 3134 |
| 98.65 | 1469 | 3134 |
| 100.30 | 1451 | 3163 |
| 101.94 | 1526 | 3273 |
| 103.58 | 1481 | 3417 |
| 105.54 | 1507 | 3657 |
| 106.86 | 1457 | 3795 |
| 108.50 | 1427 | 3638 |
| 110.14 | 1451 | 3715 |
| 111.78 | 1500 | 3519 |
| 113.42 | 1596 | 3359 |
| 115.06 | 1625 | 3213 |
| 116.70 | 1664 | 3163 |
| 118.34 | 1782 | 3258 |
| 120.31 | 1828 | 3304 |
| 121.62 | 1848 | 3367 |
| 123.59 | 1950 | 3647 |
| 124.90 | 2077 | 4321 |
| 126.54 | 2053 | 4082 |
| 128.18 | 2053 | 4058 |
| 129.82 | 2115 | 3967 |
| 131.46 | 2141 | 3922 |
| 133.10 | 2180 | 4001 |
| 134.74 | 2154 | 3795 |
| 136.38 | 2006 | 3775 |
| 138.02 | 1810 | 3546 |
| 139.67 | 1625 | 3493 |
| 141.31 | 1478 | 3351 |
| 142.95 | 1404 | 3400 |
| 144.59 | 1348 | 3359 |
| 146.23 | 1258 | 3725 |
| 147.87 | 1513 | 4082 |
| 149.51 | 1618 | 4589 |
| 151.15 | 1704 | 5708 |
| 152.79 | 1782 | 7056 |
| 154.43 | 1838 | 6986 |
| 156.07 | 1755 | 6531 |
| 157.71 | 1747 | 6354 |
| 159.35 | 1760 | 6325 |
| 160.99 | 1721 | 6325 |
| 162.63 | 1708 | 6441 |
| 164.27 | 1688 | 6624 |
| 165.91 | 1692 | 6719 |
| 167.88 | 1747 | 6687 |
| 169.19 | 1853 | 6817 |
| 170.83 | 1924 | 6850 |
| 172.47 | 2102 | 7164 |
| 174.11 | 2194 | 7128 |
| 176.08 | 2077 | 7164 |
| 177.40 | 2012 | 6883 |
| 179.04 | 1918 | 6951 |
| 180.68 | 1764 | 6354 |
| 182.32 | 1621 | 6269 |
| 183.96 | 1791 | 6817 |
| 185.60 | 1833 | 7314 |
| 187.24 | 2023 | 7758 |
| 188.88 | 2388 | 8776 |
| 190.52 | 2472 | 8668 |
| 192.16 | 2526 | 8562 |
| 193.80 | 2786 | 8615 |
| 195.44 | 2732 | 8615 |
| 197.08 | 2808 | 8459 |
| 198.72 | 2866 | 8944 |
| 200.36 | 3053 | 9238 |
| 202.00 | 3120 | 9118 |
| 203.64 | 3039 | 9618 |
| 205.28 | 3221 | 10030 |
| 206.92 | 3735 | 10250 |
| 208.56 | 3989 | 10479 |
| 210.20 | 4416 | 11057 |
| 211.84 | 4388 | 10885 |
| 213.48 | 4589 | 11234 |
| 215.12 | 4416 | 11234 |
| 216.77 | 4501 | 11057 |
| 218.41 | 4416 | 11234 |
| 220.05 | 4230 | 10970 |
| 221.69 | 4106 | 11416 |
| 223.33 | 4012 | 11057 |
| 224.97 | 3093 | 11057 |
| 226.61 | 3922 | 11324 |
| 228.25 | 4230 | 11900 |
| 229.89 | 4665 | 12105 |
| 231.53 | 5422 | 13002 |
| 233.17 | 5708 | 13123 |
| 234.81 | 5950 | 11900 |
| 236.45 | 5708 | 12537 |
| 238.09 | 5708 | 12765 |
| 239.73 | 5617 | 13123 |
| 241.37 | 5319 | 12650 |
| 243.01 | 4530 | 12210 |
| 244.65 | 4179 | 12105 |
| 246.29 | 4307 | 11324 |
| 247.93 | 4307 | 12650 |
| 249.57 | 4589 | 12002 |
| 251.21 | 5662 | 13502 |
| 252.85 | 5708 | 13247 |
| 254.49 | 5319 | 13903 |
| 256.14 | 6053 | 14329 |

Table A-9. Boring Z3-B4, S - R1 quality assurance analysis P- and $S_H$-wave data

| Depth (feet) | $V_s$ (feet/sec) | $V_p$ (feet/sec) |
|---|---|---|
| 257.78 | 5319 | 14329 |
| 259.42 | 5639 | 14184 |
| 261.06 | 5279 | 12650 |
| 262.70 | 5144 | 12427 |
| 264.34 | 4842 | 12210 |
| 265.98 | 4501 | 12537 |
| 267.62 | 3944 | 13373 |
| | | |

Table A-9, continued. Boring Z3-B4, S - R1 quality assurance analysis P- and $S_H$-wave data

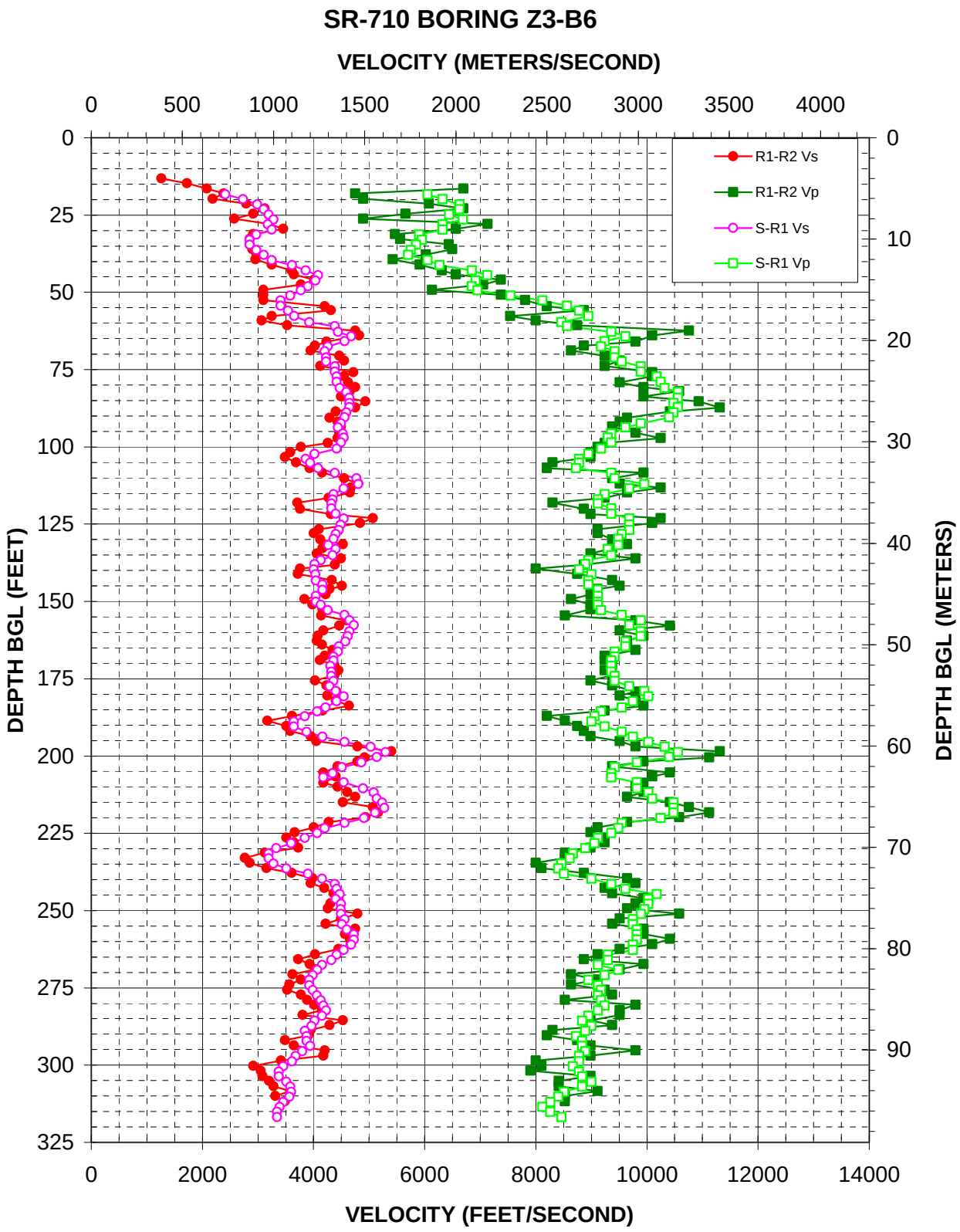


Figure A-10. Boring Z3-B6, R1 - R2 high resolution analysis and S - R1 quality assurance analysis P- and $S_H$-wave data

| Depth (feet) | $V_s$ (feet/sec) | $V_p$ (feet/sec) |
|---|---|---|
| 18.27 | 2413 | 6053 |
| 19.91 | 2732 | 6325 |
| 21.56 | 2988 | 6624 |
| 23.20 | 3107 | 6624 |
| 24.84 | 3191 | 6441 |
| 26.48 | 3281 | 6687 |
| 28.12 | 3177 | 6325 |
| 29.76 | 3250 | 6325 |
| 31.40 | 2975 | 5900 |
| 33.04 | 2854 | 5950 |
| 34.68 | 2854 | 5851 |
| 36.32 | 2975 | 5755 |
| 37.96 | 3107 | 5708 |
| 39.60 | 3250 | 6053 |
| 41.24 | 3619 | 6269 |
| 42.88 | 3858 | 6850 |
| 44.52 | 4082 | 7128 |
| 46.16 | 4035 | 6917 |
| 48.13 | 3901 | 6850 |
| 49.44 | 3775 | 6951 |
| 51.08 | 3582 | 7549 |
| 52.72 | 3408 | 8117 |
| 54.36 | 3408 | 8562 |
| 56.00 | 3546 | 8776 |
| 57.64 | 3657 | 8944 |
| 59.61 | 3922 | 8459 |
| 60.93 | 4388 | 8562 |
| 62.89 | 4444 | 9361 |
| 64.21 | 4681 | 9618 |
| 65.85 | 4559 | 9238 |
| 67.49 | 4255 | 9178 |
| 69.13 | 4204 | 9424 |
| 71.10 | 4230 | 9424 |
| 72.41 | 4230 | 9552 |
| 74.05 | 4388 | 9889 |
| 75.69 | 4388 | 9889 |
| 77.33 | 4416 | 10175 |
| 78.97 | 4416 | 10250 |
| 80.94 | 4472 | 10325 |
| 82.25 | 4589 | 10558 |
| 84.22 | 4650 | 10558 |
| 85.86 | 4650 | 10479 |
| 87.17 | 4650 | 10558 |
| 88.81 | 4589 | 10479 |
| 90.45 | 4559 | 10401 |
| 92.42 | 4501 | 9889 |
| 93.73 | 4444 | 9618 |
| 95.70 | 4530 | 9361 |
| 97.01 | 4544 | 9299 |
| 98.65 | 4501 | 9361 |
| 100.62 | 4416 | 9178 |
| 102.26 | 4023 | 8944 |
| 103.90 | 3858 | 8776 |
| 105.22 | 3944 | 8776 |
| 106.86 | 4082 | 8722 |
| 108.50 | 4388 | 9361 |
| 110.14 | 4776 | 9424 |
| 112.11 | 4809 | 9959 |
| 113.42 | 4544 | 9684 |
| 115.39 | 4361 | 9238 |
| 117.03 | 4347 | 9118 |
| 118.34 | 4321 | 9118 |
| 119.98 | 4321 | 9361 |
| 121.62 | 4402 | 9361 |
| 123.26 | 4544 | 9684 |
| 125.23 | 4486 | 9684 |
| 126.87 | 4458 | 9684 |
| 128.18 | 4402 | 9552 |
| 129.82 | 4361 | 9488 |
| 131.79 | 4268 | 9488 |
| 133.10 | 4402 | 9299 |
| 135.07 | 4347 | 9361 |
| 136.71 | 4130 | 8944 |
| 138.02 | 4023 | 8887 |
| 139.67 | 4001 | 8776 |
| 141.31 | 4035 | 9001 |
| 143.27 | 4047 | 8944 |
| 144.59 | 4167 | 8944 |
| 146.23 | 4167 | 9118 |
| 148.20 | 4047 | 9118 |
| 150.16 | 4047 | 9118 |
| 151.15 | 4130 | 9118 |
| 152.79 | 4255 | 9178 |
| 154.43 | 4559 | 9552 |
| 156.07 | 4650 | 9889 |
| 157.71 | 4728 | 9684 |
| 159.68 | 4650 | 9889 |
| 161.32 | 4619 | 9889 |
| 162.96 | 4574 | 9618 |
| 164.60 | 4458 | 9618 |
| 166.24 | 4444 | 9424 |
| 167.88 | 4361 | 9424 |
| 169.19 | 4361 | 9361 |
| 170.83 | 4307 | 9361 |
| 172.80 | 4321 | 9361 |
| 174.11 | 4321 | 9424 |
| 175.75 | 4361 | 9424 |
| 177.40 | 4294 | 9684 |
| 179.04 | 4402 | 9959 |
| 180.68 | 4544 | 10030 |
| 182.32 | 4416 | 9751 |
| 184.28 | 4217 | 9552 |
| 185.60 | 4070 | 9178 |
| 187.24 | 3847 | 9059 |
| 188.88 | 3647 | 9001 |
| 190.52 | 3647 | 9238 |
| 192.16 | 3879 | 9552 |
| 193.80 | 4167 | 9751 |
| 195.44 | 4559 | 10030 |
| 197.08 | 5033 | 10325 |
| 198.72 | 5299 | 10558 |
| 200.36 | 5144 | 10401 |
| 202.00 | 4859 | 9820 |
| 203.64 | 4515 | 9424 |
| 205.61 | 4347 | 9361 |
| 206.92 | 4179 | 9361 |
| 208.56 | 4544 | 9820 |
| 210.53 | 4893 | 9820 |
| 211.84 | 5088 | 10030 |
| 213.81 | 5144 | 10102 |
| 215.12 | 5240 | 10479 |
| 216.77 | 5279 | 10479 |
| 218.41 | 5106 | 10479 |
| 220.05 | 4910 | 10250 |
| 221.69 | 4559 | 9552 |
| 223.33 | 4204 | 9488 |
| 224.97 | 4070 | 9361 |
| 226.61 | 3847 | 9118 |
| 228.25 | 3601 | 9059 |
| 229.89 | 3327 | 8887 |
| 231.53 | 3191 | 8668 |
| 233.17 | 3191 | 8615 |
| 234.81 | 3281 | 8459 |
| 236.45 | 3510 | 8408 |
| 238.09 | 3901 | 8510 |
| 239.73 | 4154 | 9001 |
| 241.37 | 4388 | 9361 |
| 243.01 | 4416 | 9618 |
| 244.65 | 4472 | 10175 |
| 246.29 | 4402 | 10030 |
| 247.93 | 4501 | 10030 |
| 249.57 | 4486 | 9959 |
| 251.21 | 4501 | 9889 |
| 252.85 | 4559 | 9751 |
| 254.49 | 4515 | 9751 |
| 256.14 | 4604 | 9820 |
| 257.78 | 4728 | 9820 |
| 259.42 | 4728 | 9820 |
| 261.06 | 4681 | 9751 |
| 262.70 | 4544 | 9751 |

Table A-10. Boring Z3-B6, S - R1 quality assurance analysis P- and $S_H$-wave data

| Depth (feet) | $V_s$ (feet/sec) | $V_p$ (feet/sec) |
|---|---|---|
| 264.34 | 4416 | 9299 |
| 265.98 | 4321 | 9299 |
| 267.62 | 4154 | 9118 |
| 269.26 | 4070 | 9488 |
| 270.90 | 3989 | 9238 |
| 272.54 | 3922 | 8944 |
| 274.18 | 3922 | 9118 |
| 275.82 | 3989 | 9178 |
| 277.46 | 4058 | 9118 |
| 279.10 | 4130 | 9178 |
| 280.74 | 4179 | 9238 |
| 282.38 | 4230 | 9118 |
| 284.02 | 4154 | 8944 |
| 285.66 | 4023 | 8831 |
| 287.30 | 3967 | 9001 |
| 288.94 | 3847 | 8887 |
| 290.58 | 3879 | 8722 |
| 292.22 | 3879 | 8831 |
| 293.86 | 3944 | 8831 |
| 295.51 | 3795 | 8887 |
| 297.15 | 3676 | 8776 |
| 298.79 | 3619 | 8776 |
| 300.43 | 3459 | 8668 |
| 302.07 | 3375 | 8776 |
| 303.71 | 3375 | 8831 |
| 305.35 | 3510 | 9001 |
| 306.99 | 3582 | 8831 |
| 308.63 | 3601 | 8510 |
| 310.27 | 3564 | 8408 |
| 311.91 | 3459 | 8260 |
| 313.55 | 3392 | 8117 |
| 315.19 | 3343 | 8260 |
| 316.83 | 3343 | 8459 |
| | | |

Table A-10, continued. Boring Z3-B6, S - R1 quality assurance analysis
P- and $S_H$-wave data

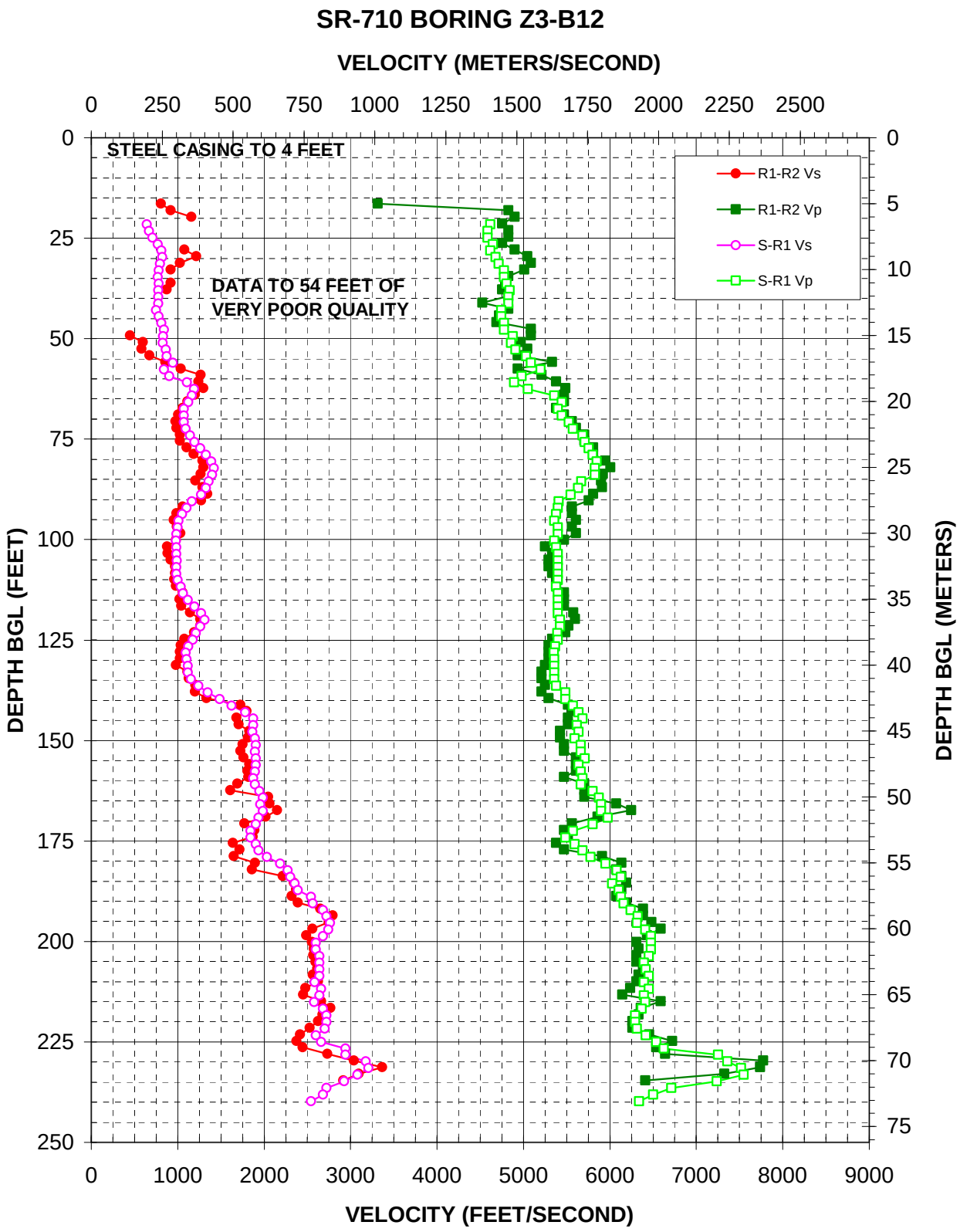


Figure A-11. Boring Z3-B12, R1 - R2 high resolution analysis and S - R1 quality assurance analysis P- and $S_H$-wave data

| Depth (feet) | $V_s$ (feet/sec) | $V_p$ (feet/sec) |
|---|---|---|
| 13.35 | | |
| 21.56 | 645 | 4619 |
| 23.20 | 669 | 4589 |
| 24.84 | 711 | 4589 |
| 26.48 | 769 | 4650 |
| 28.12 | 814 | 4619 |
| 29.76 | 823 | 4681 |
| 31.40 | 795 | 4712 |
| 33.04 | 782 | 4776 |
| 34.68 | 773 | 4776 |
| 36.32 | 782 | 4809 |
| 37.96 | 778 | 4842 |
| 39.60 | 778 | 4825 |
| 41.24 | 778 | 4825 |
| 42.88 | 749 | 4744 |
| 44.52 | 782 | 4744 |
| 46.16 | 814 | 4776 |
| 47.80 | 843 | 4776 |
| 49.44 | 833 | 4876 |
| 51.08 | 828 | 4859 |
| 52.72 | 864 | 4910 |
| 54.36 | 874 | 5033 |
| 56.00 | 945 | 5088 |
| 57.64 | 843 | 5201 |
| 59.28 | 906 | 4979 |
| 60.93 | 1111 | 4893 |
| 62.57 | 1188 | 5051 |
| 64.21 | 1164 | 5360 |
| 65.85 | 1122 | 5443 |
| 67.49 | 1072 | 5401 |
| 69.13 | 1072 | 5443 |
| 70.77 | 1072 | 5528 |
| 72.41 | 1092 | 5572 |
| 74.05 | 1142 | 5685 |
| 75.69 | 1196 | 5708 |
| 77.33 | 1261 | 5755 |
| 78.97 | 1327 | 5802 |
| 80.61 | 1390 | 5851 |
| 82.25 | 1418 | 5827 |
| 83.89 | 1401 | 5827 |
| 85.53 | 1358 | 5671 |
| 87.17 | 1327 | 5635 |
| 88.81 | 1272 | 5546 |
| 90.45 | 1164 | 5409 |
| 92.09 | 1102 | 5401 |
| 93.73 | 1053 | 5380 |
| 95.37 | 1010 | 5360 |
| 97.01 | 1002 | 5401 |
| 98.65 | 985 | 5401 |
| 100.30 | 979 | 5360 |
| 101.94 | 985 | 5380 |
| 103.58 | 985 | 5401 |
| 105.22 | 993 | 5401 |
| 106.86 | 985 | 5401 |
| 108.50 | 985 | 5401 |
| 110.14 | 1002 | 5401 |
| 111.78 | 1037 | 5380 |
| 113.42 | 1062 | 5401 |
| 115.06 | 1120 | 5401 |
| 116.70 | 1196 | 5401 |
| 118.34 | 1274 | 5401 |
| 119.98 | 1312 | 5426 |
| 121.62 | 1261 | 5426 |
| 123.26 | 1211 | 5392 |
| 124.90 | 1174 | 5401 |
| 126.54 | 1122 | 5368 |
| 128.18 | 1092 | 5351 |
| 129.82 | 1102 | 5360 |
| 131.46 | 1120 | 5360 |
| 133.10 | 1120 | 5360 |
| 134.74 | 1153 | 5360 |
| 136.38 | 1244 | 5380 |
| 138.02 | 1348 | 5485 |
| 139.67 | 1484 | 5485 |
| 141.31 | 1625 | 5572 |
| 142.95 | 1782 | 5639 |
| 144.59 | 1872 | 5685 |
| 146.23 | 1872 | 5617 |
| 147.87 | 1862 | 5639 |
| 149.51 | 1892 | 5594 |
| 151.15 | 1903 | 5662 |
| 152.79 | 1892 | 5662 |
| 154.43 | 1903 | 5708 |
| 156.07 | 1903 | 5639 |
| 157.71 | 1892 | 5662 |
| 159.35 | 1872 | 5685 |
| 160.99 | 1892 | 5662 |
| 162.63 | 1945 | 5802 |
| 164.27 | 1989 | 5875 |
| 165.91 | 1956 | 5900 |
| 167.55 | 1989 | 5900 |
| 169.19 | 1934 | 5975 |
| 170.83 | 1903 | 5802 |
| 172.47 | 1843 | 5572 |
| 174.11 | 1845 | 5485 |
| 175.75 | 1903 | 5594 |
| 177.40 | 1934 | 5685 |
| 179.04 | 2035 | 5779 |
| 180.68 | 2187 | 5950 |
| 182.32 | 2272 | 6079 |
| 183.96 | 2302 | 6132 |
| 185.60 | 2356 | 6027 |
| 187.24 | 2388 | 6105 |
| 188.88 | 2544 | 6132 |
| 190.52 | 2562 | 6159 |
| 192.16 | 2680 | 6241 |
| 193.80 | 2721 | 6325 |
| 195.44 | 2764 | 6314 |
| 197.08 | 2743 | 6412 |
| 198.72 | 2680 | 6477 |
| 200.36 | 2600 | 6477 |
| 202.00 | 2600 | 6477 |
| 203.64 | 2639 | 6453 |
| 205.28 | 2639 | 6394 |
| 206.92 | 2639 | 6418 |
| 208.56 | 2639 | 6453 |
| 210.20 | 2583 | 6394 |
| 211.84 | 2659 | 6453 |
| 213.48 | 2639 | 6394 |
| 215.12 | 2581 | 6412 |
| 216.77 | 2680 | 6371 |
| 218.41 | 2721 | 6291 |
| 220.05 | 2721 | 6291 |
| 221.69 | 2700 | 6314 |
| 223.33 | 2600 | 6418 |
| 224.97 | 2659 | 6537 |
| 226.61 | 2944 | 6624 |
| 228.25 | 2944 | 7253 |
| 229.89 | 3177 | 7360 |
| 231.53 | 3206 | 7517 |
| 233.17 | 3079 | 7549 |
| 234.81 | 2925 | 7238 |
| 236.45 | 2721 | 6712 |
| 238.09 | 2680 | 6501 |
| 239.73 | 2544 | 6337 |
| | | |

Table A-11. Boring Z3-B12, S - R1 quality assurance analysis P- and $S_H$-wave data

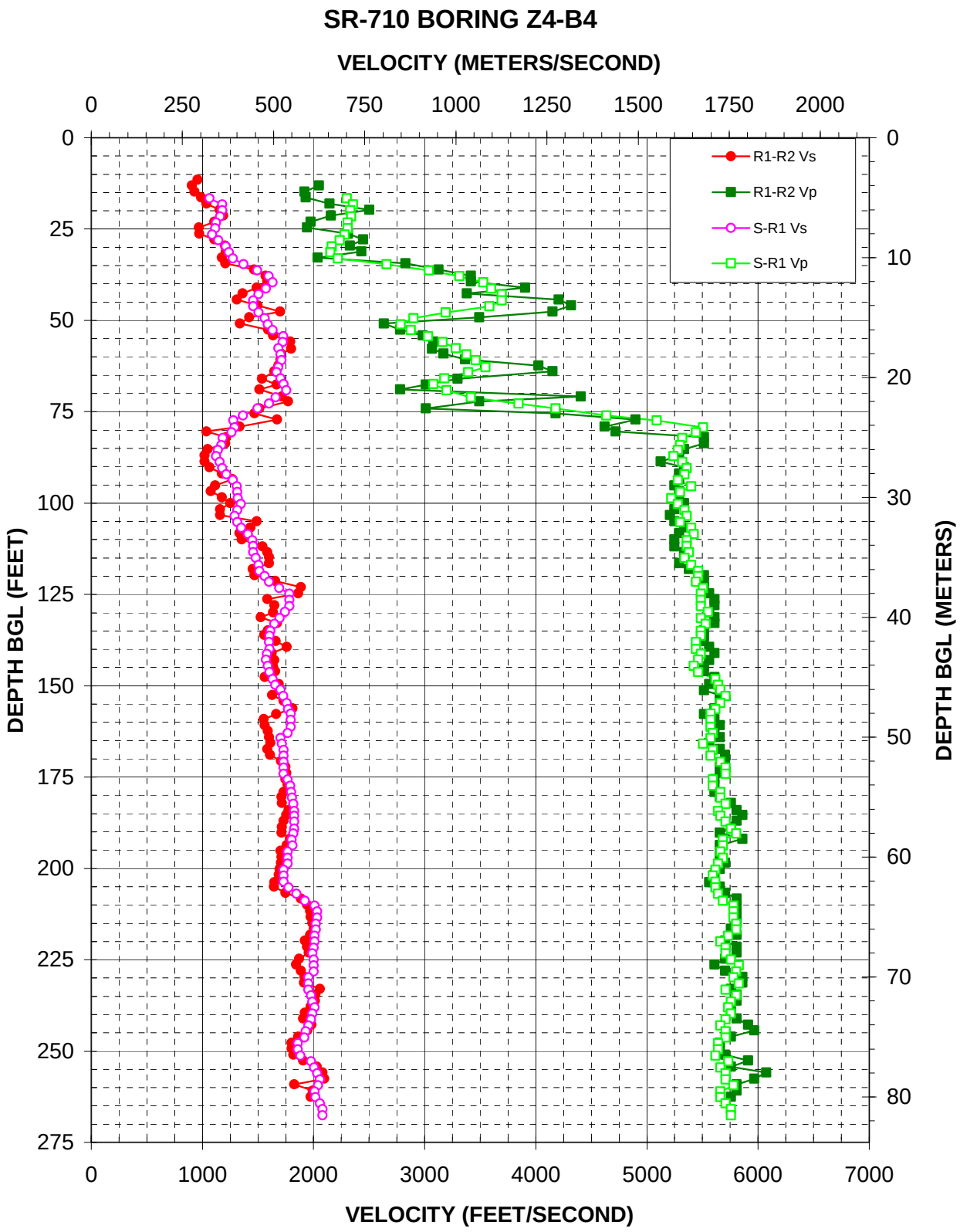


Figure A-12. Boring Z4-B4, R1 - R2 high resolution analysis and S - R1 quality assurance analysis P- and $S_H$-wave data

| Depth (feet) | $V_s$ (feet/sec) | $V_p$ (feet/sec) |
|---|---|---|
| 16.63 | 1064 | 2302 |
| 18.27 | 1178 | 2356 |
| 19.91 | 1178 | 2333 |
| 21.56 | 1159 | 2340 |
| 23.20 | 1125 | 2310 |
| 24.84 | 1114 | 2310 |
| 26.48 | 1087 | 2280 |
| 28.12 | 1143 | 2236 |
| 29.76 | 1211 | 2167 |
| 31.40 | 1240 | 2154 |
| 33.04 | 1277 | 2222 |
| 34.68 | 1371 | 2659 |
| 36.32 | 1494 | 3039 |
| 37.96 | 1596 | 3312 |
| 39.60 | 1633 | 3528 |
| 41.24 | 1574 | 3601 |
| 42.88 | 1507 | 3695 |
| 44.52 | 1457 | 3695 |
| 46.16 | 1457 | 3582 |
| 47.80 | 1507 | 3191 |
| 49.44 | 1560 | 2901 |
| 51.08 | 1588 | 2786 |
| 52.72 | 1633 | 2877 |
| 54.36 | 1729 | 3033 |
| 56.00 | 1723 | 3163 |
| 57.64 | 1686 | 3281 |
| 59.28 | 1704 | 3375 |
| 60.93 | 1712 | 3459 |
| 62.89 | 1686 | 3546 |
| 64.21 | 1668 | 3392 |
| 65.85 | 1704 | 3177 |
| 67.49 | 1734 | 3079 |
| 69.13 | 1755 | 3199 |
| 71.10 | 1660 | 3417 |
| 72.74 | 1599 | 3847 |
| 74.05 | 1497 | 4179 |
| 76.02 | 1366 | 4634 |
| 77.33 | 1281 | 5088 |
| 79.30 | 1291 | 5507 |
| 80.61 | 1263 | 5443 |
| 82.25 | 1182 | 5319 |
| 84.22 | 1170 | 5299 |
| 85.53 | 1140 | 5279 |
| 87.17 | 1125 | 5240 |
| 88.81 | 1155 | 5319 |
| 90.45 | 1178 | 5360 |
| 92.09 | 1215 | 5339 |
| 93.73 | 1277 | 5279 |
| 95.37 | 1310 | 5401 |
| 97.01 | 1314 | 5299 |
| 98.65 | 1320 | 5220 |
| 100.30 | 1348 | 5279 |
| 101.94 | 1315 | 5339 |
| 103.58 | 1291 | 5360 |
| 105.22 | 1315 | 5299 |
| 106.86 | 1350 | 5401 |
| 108.50 | 1410 | 5422 |
| 110.14 | 1451 | 5360 |
| 111.78 | 1457 | 5360 |
| 113.42 | 1457 | 5380 |
| 115.06 | 1481 | 5339 |
| 117.03 | 1507 | 5401 |
| 118.67 | 1513 | 5464 |
| 119.98 | 1560 | 5464 |
| 121.62 | 1599 | 5443 |
| 123.26 | 1692 | 5507 |
| 124.90 | 1782 | 5485 |
| 126.54 | 1782 | 5485 |
| 128.18 | 1782 | 5485 |
| 129.82 | 1742 | 5550 |
| 131.46 | 1696 | 5485 |
| 133.10 | 1650 | 5528 |
| 135.07 | 1614 | 5485 |
| 136.38 | 1607 | 5485 |
| 138.02 | 1599 | 5443 |
| 139.99 | 1607 | 5443 |
| 141.31 | 1583 | 5485 |
| 142.95 | 1574 | 5464 |
| 144.59 | 1588 | 5422 |
| 146.23 | 1607 | 5464 |
| 148.20 | 1633 | 5617 |
| 149.84 | 1656 | 5639 |
| 151.15 | 1704 | 5662 |
| 152.79 | 1729 | 5708 |
| 154.76 | 1760 | 5662 |
| 156.40 | 1773 | 5617 |
| 157.71 | 1796 | 5572 |
| 159.35 | 1796 | 5572 |
| 161.32 | 1796 | 5572 |
| 162.96 | 1769 | 5594 |
| 164.27 | 1704 | 5572 |
| 165.91 | 1717 | 5507 |
| 167.55 | 1734 | 5594 |
| 169.19 | 1734 | 5572 |
| 170.83 | 1734 | 5662 |
| 172.47 | 1734 | 5708 |
| 174.11 | 1734 | 5708 |
| 175.75 | 1769 | 5594 |
| 177.40 | 1791 | 5594 |
| 179.04 | 1800 | 5662 |
| 180.68 | 1810 | 5662 |
| 182.32 | 1819 | 5708 |
| 184.28 | 1828 | 5639 |
| 185.60 | 1828 | 5662 |
| 187.24 | 1828 | 5708 |
| 189.21 | 1828 | 5755 |
| 190.52 | 1819 | 5802 |
| 192.16 | 1803 | 5685 |
| 193.80 | 1812 | 5685 |
| 195.44 | 1769 | 5662 |
| 197.08 | 1766 | 5685 |
| 198.72 | 1766 | 5639 |
| 200.36 | 1734 | 5617 |
| 202.00 | 1734 | 5594 |
| 203.64 | 1734 | 5617 |
| 205.28 | 1777 | 5617 |
| 206.92 | 1848 | 5639 |
| 208.89 | 1924 | 5685 |
| 210.20 | 2012 | 5779 |
| 211.84 | 2035 | 5779 |
| 213.48 | 2035 | 5779 |
| 215.12 | 2023 | 5802 |
| 216.77 | 2023 | 5802 |
| 218.41 | 2012 | 5731 |
| 220.05 | 2012 | 5662 |
| 221.69 | 2000 | 5708 |
| 223.33 | 1989 | 5708 |
| 224.97 | 2000 | 5755 |
| 226.61 | 2000 | 5827 |
| 228.25 | 2000 | 5802 |
| 229.89 | 1956 | 5779 |
| 231.53 | 1956 | 5827 |
| 233.17 | 1956 | 5708 |
| 234.81 | 1978 | 5802 |
| 236.45 | 1989 | 5755 |
| 238.09 | 2012 | 5731 |
| 239.73 | 1989 | 5755 |
| 241.37 | 1978 | 5708 |
| 243.01 | 1956 | 5662 |
| 244.65 | 1929 | 5708 |
| 246.29 | 1918 | 5708 |
| 247.93 | 1857 | 5639 |
| 249.57 | 1857 | 5639 |
| 251.21 | 1882 | 5617 |
| 252.85 | 1978 | 5731 |
| 254.49 | 2006 | 5662 |
| 256.14 | 2035 | 5708 |
| 257.78 | 2059 | 5708 |
| 259.42 | 2041 | 5779 |
| 261.06 | 2012 | 5662 |

Table A-12. Boring Z4-B4, S - R1 quality assurance analysis P- and $S_H$-wave data

| Depth (feet) | $V_s$ (feet/sec) | $V_p$ (feet/sec) |
|---|---|---|
| 262.70 | 2018 | 5662 |
| 264.34 | 2059 | 5708 |
| 265.98 | 2083 | 5755 |
| 267.62 | 2083 | 5755 |
| | | |

Table A-12, continued. Boring Z4-B4, S - R1 quality assurance analysis P- and $S_H$-wave data

# APPENDIX B

# CALIPER AND
# NATURAL GAMMA LOGS

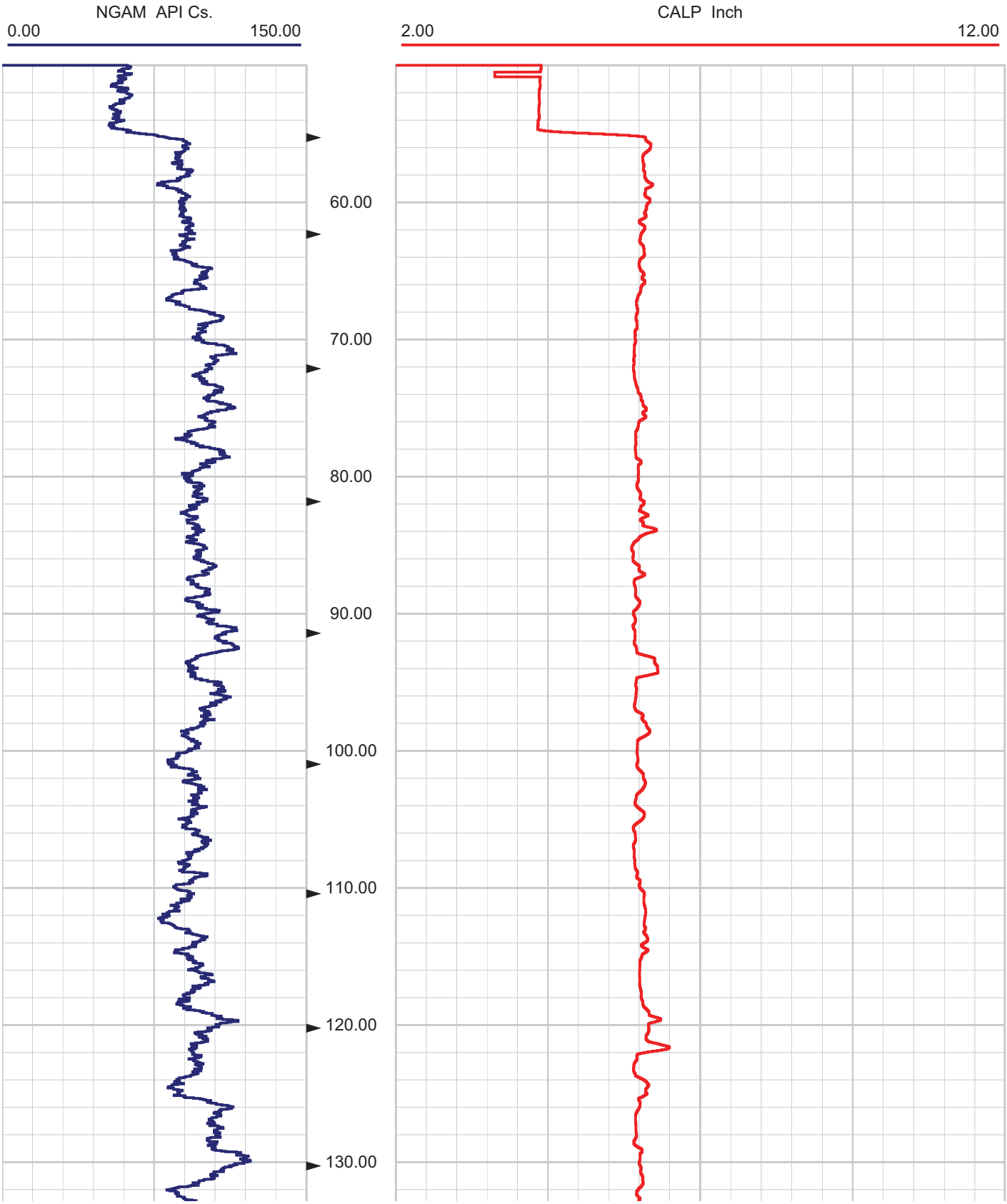


SR-710 Boring Z3-B3 Caliper and Natural Gamma rev 1.1 Sheet 1 of 3

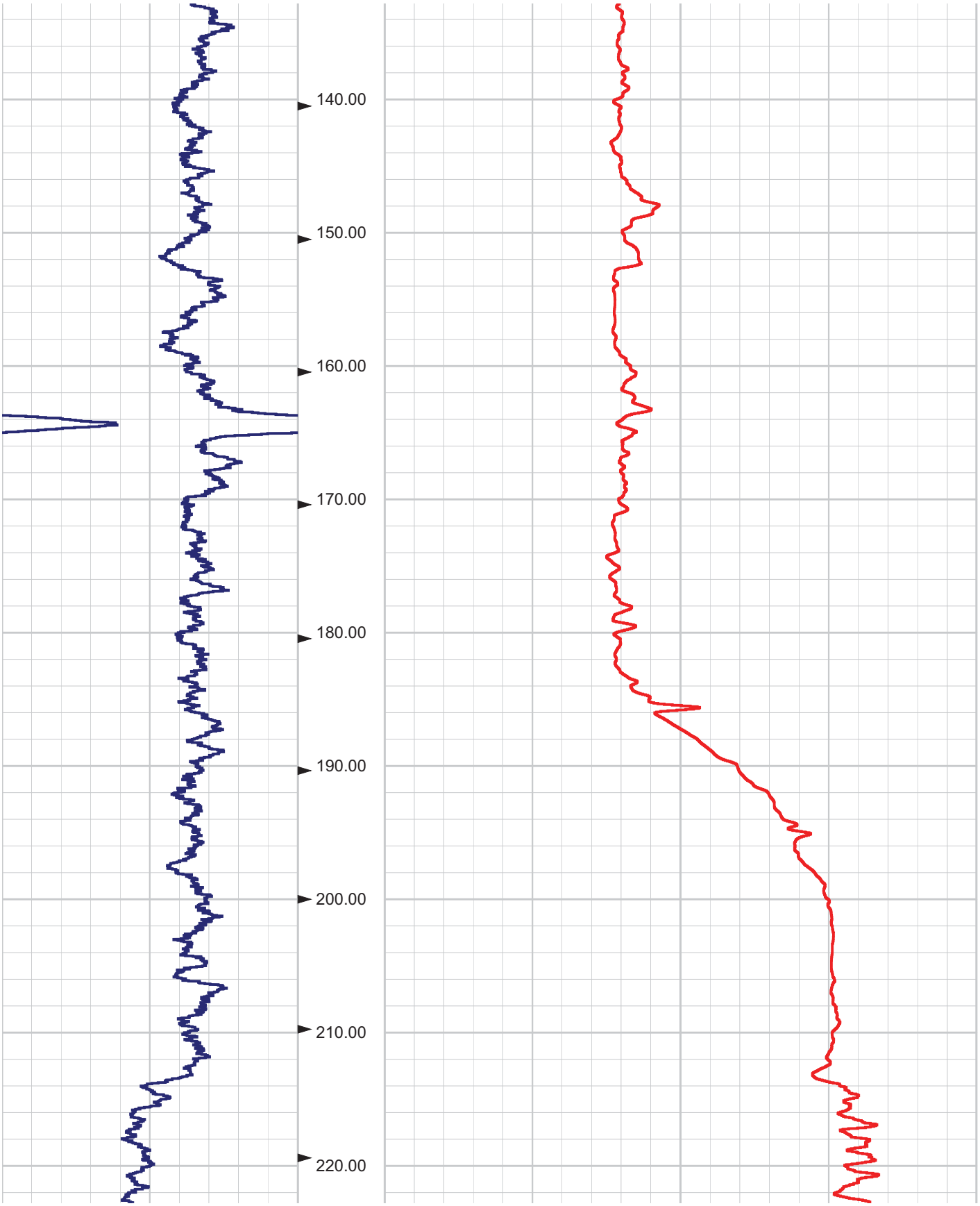


SR-710 Boring Z3-B3 Caliper and Natural Gamma rev 1.1 Sheet 2 of 3

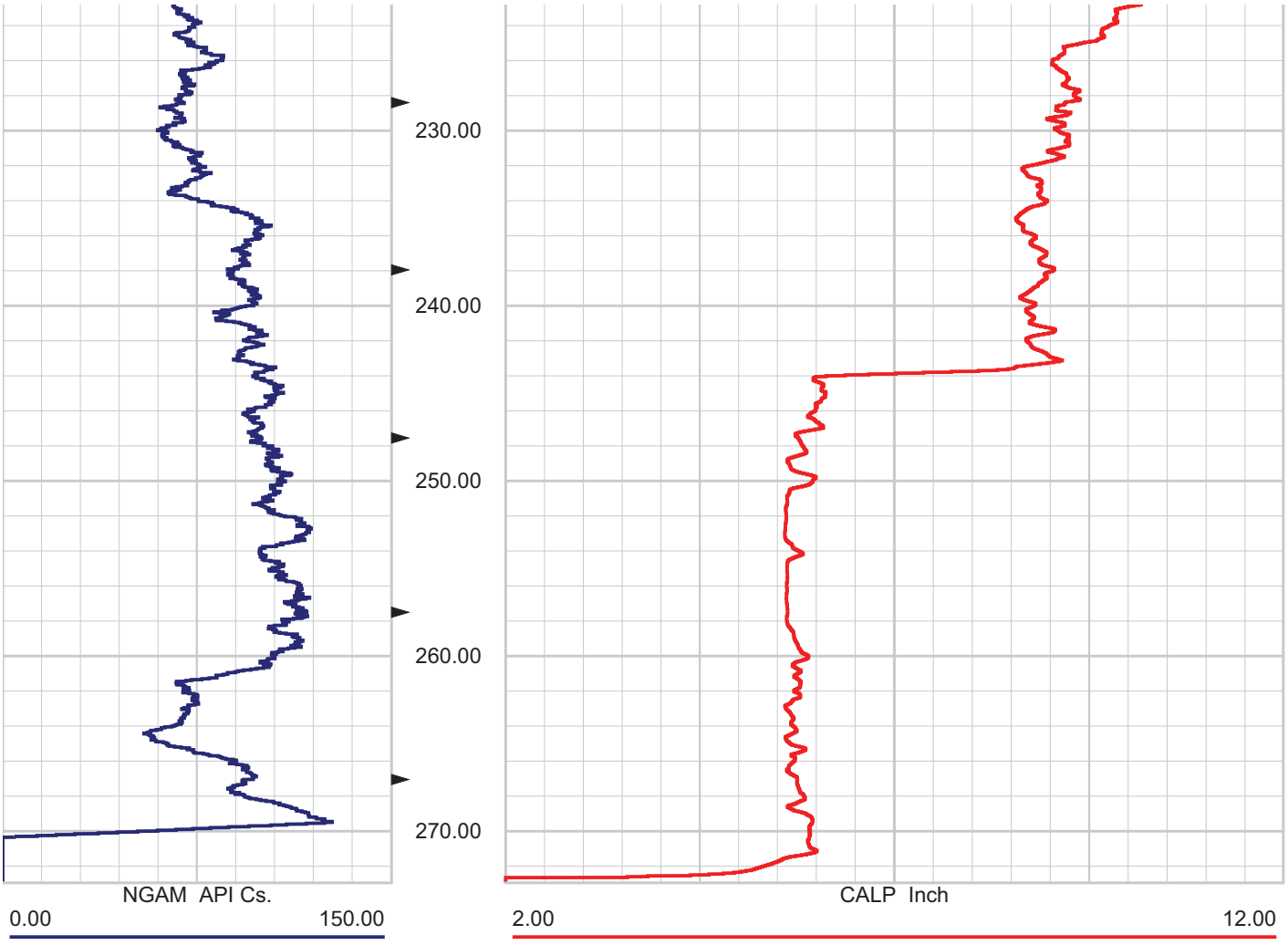
230.00
240.00
250.00
260.00
270.00
NGAM API Cs.
0.00
150.00
CALP Inch
2.00
12.00

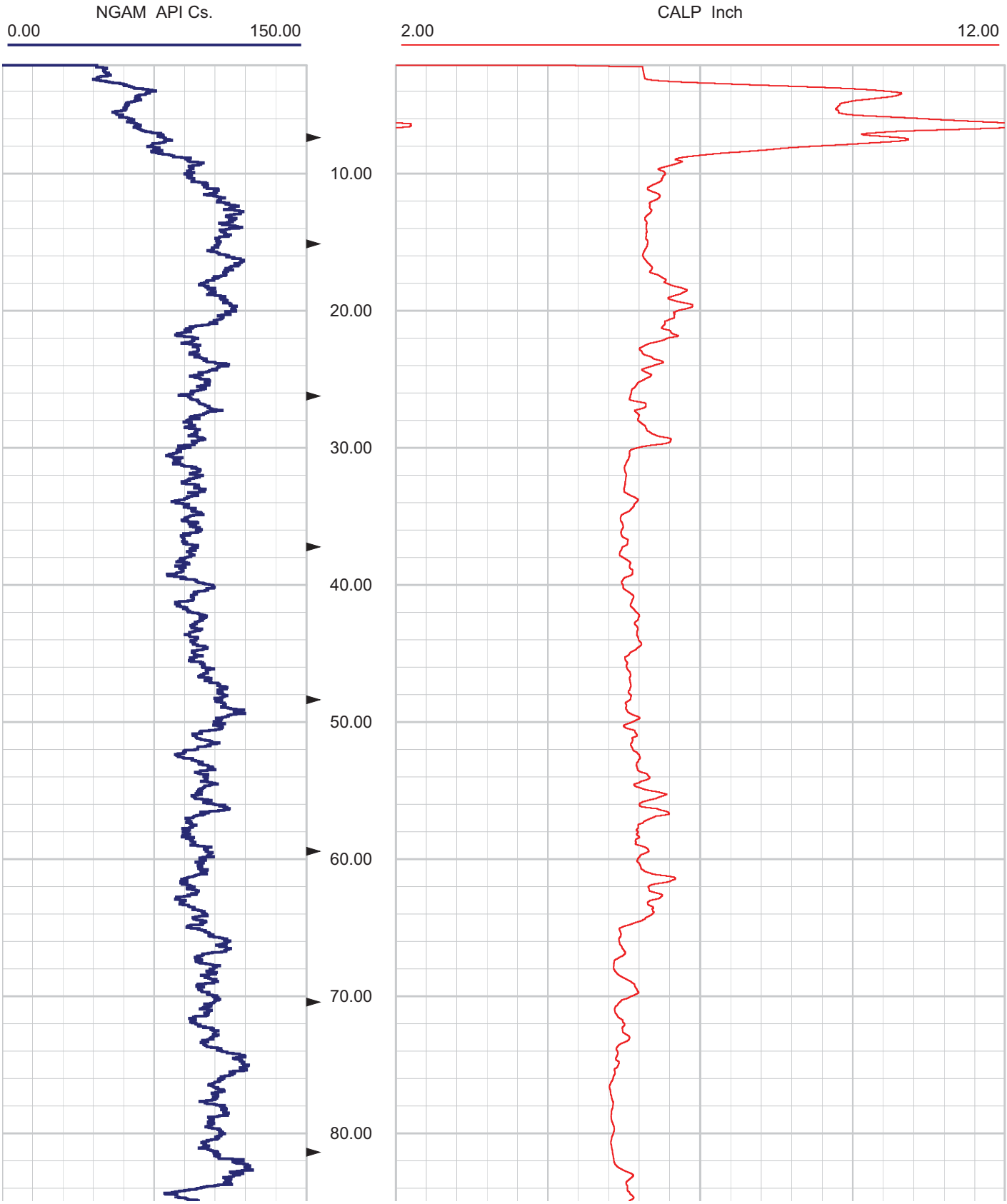


SR-710 Boring Z3-B4 Caliper and Natural Gamma rev 1.1 Sheet 1 of 4

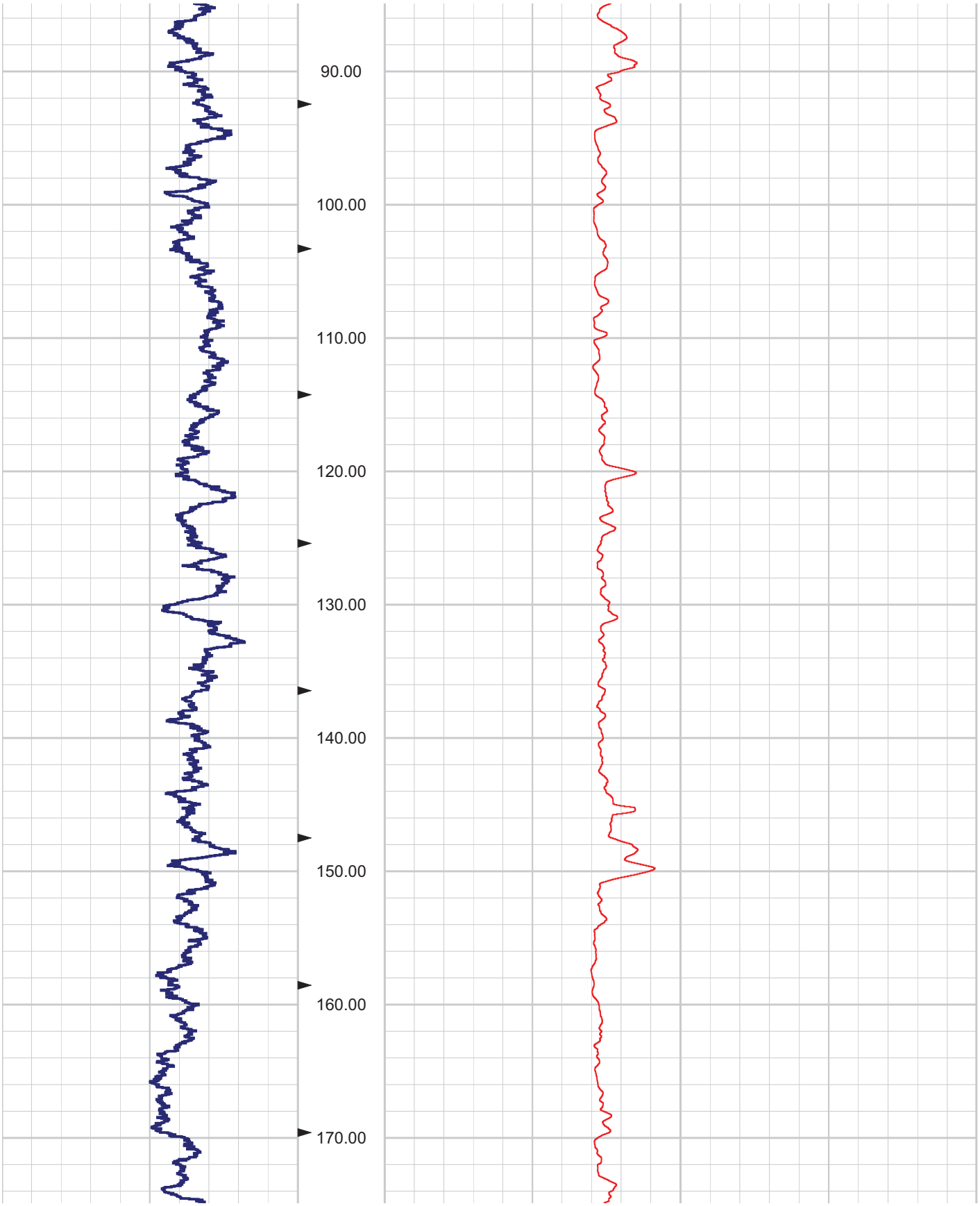


SR-710 Boring Z3-B4 Caliper and Natural Gamma rev 1.1 Sheet 2 of 4

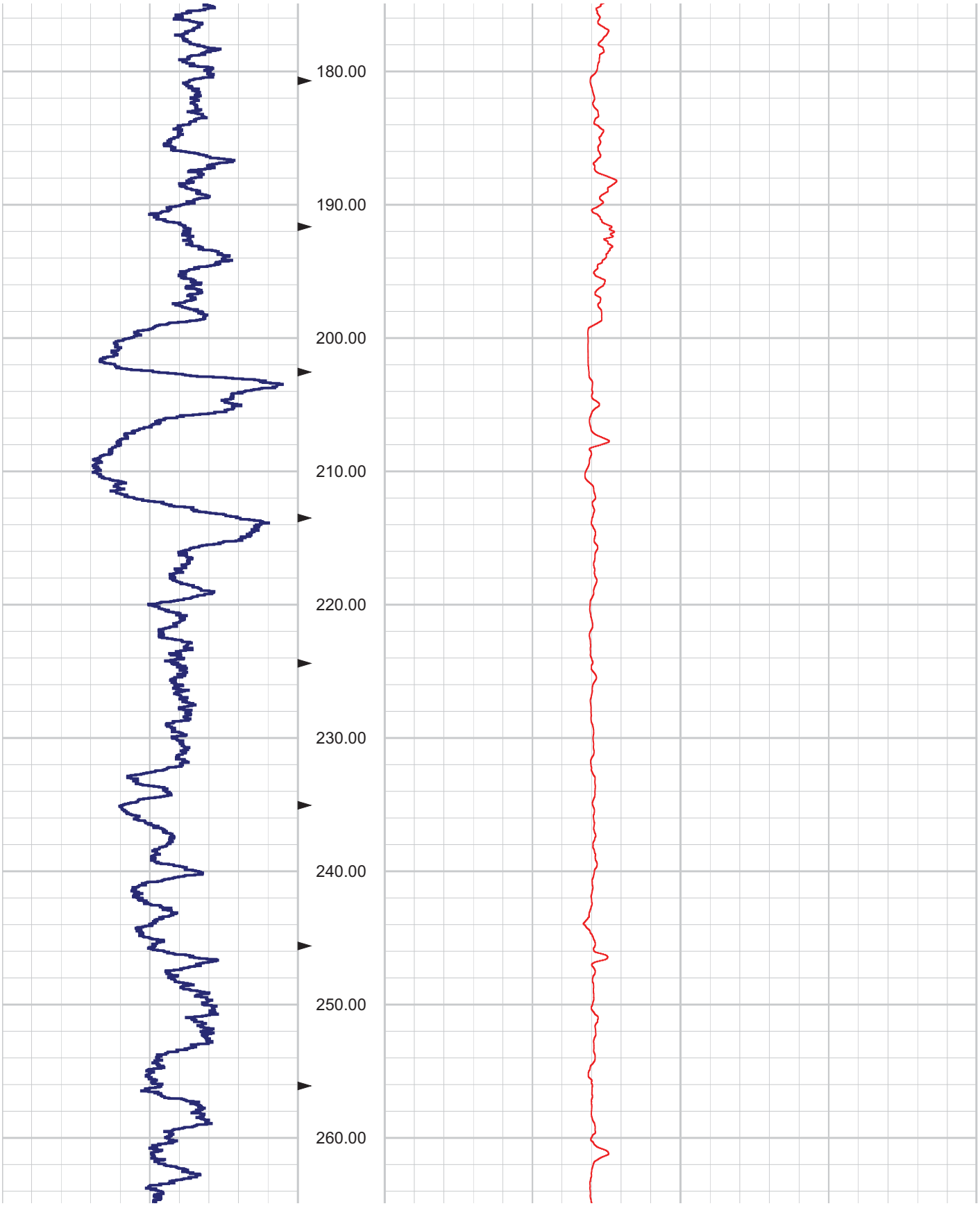


SR-710 Boring Z3-B4 Caliper and Natural Gamma rev 1.1 Sheet 3 of 4

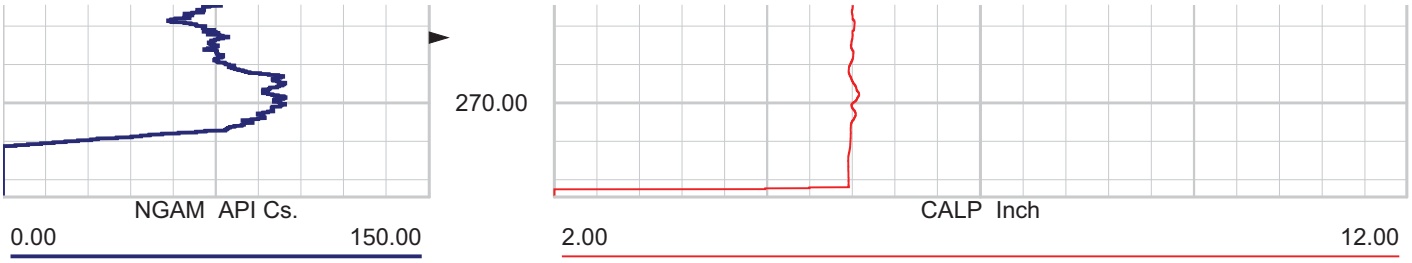
270.00
NGAM API Cs.
0.00
150.00
CALP Inch
2.00
12.00

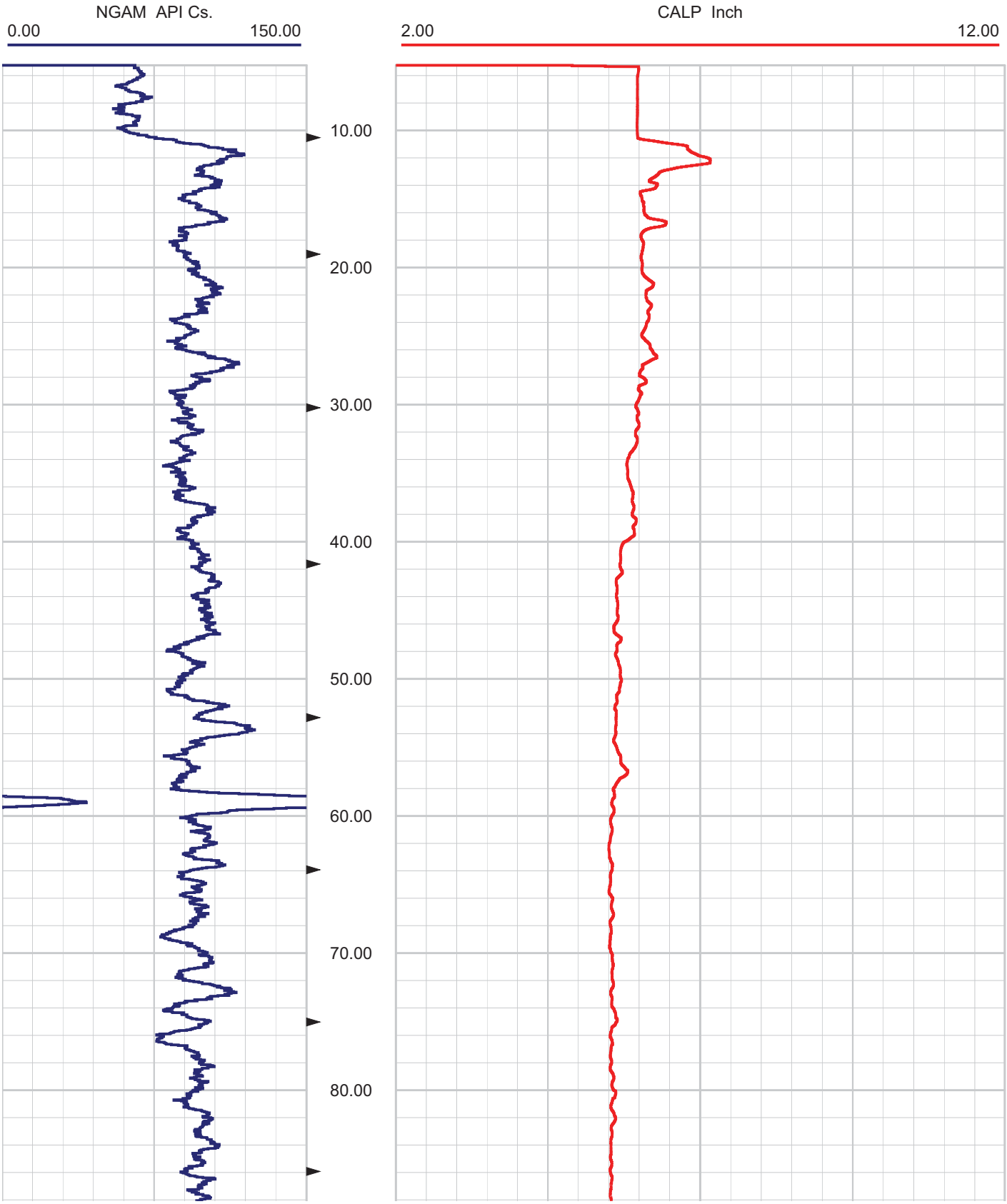


SR-710 Boring Z3-B6 Caliper and Natural Gamma rev 1.1 Sheet 1 of 4

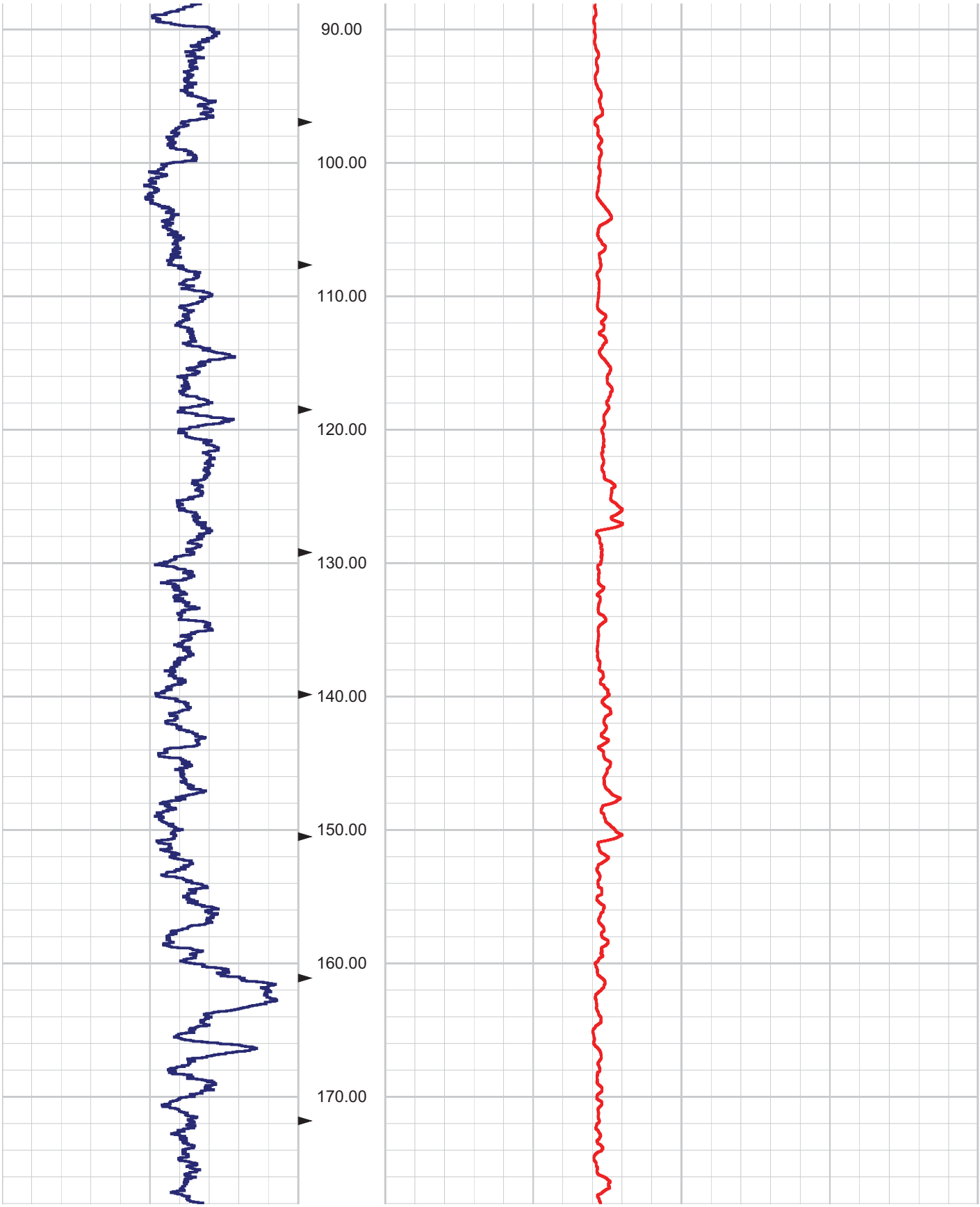


SR-710 Boring Z3-B6 Caliper and Natural Gamma rev 1.1 Sheet 2 of 4

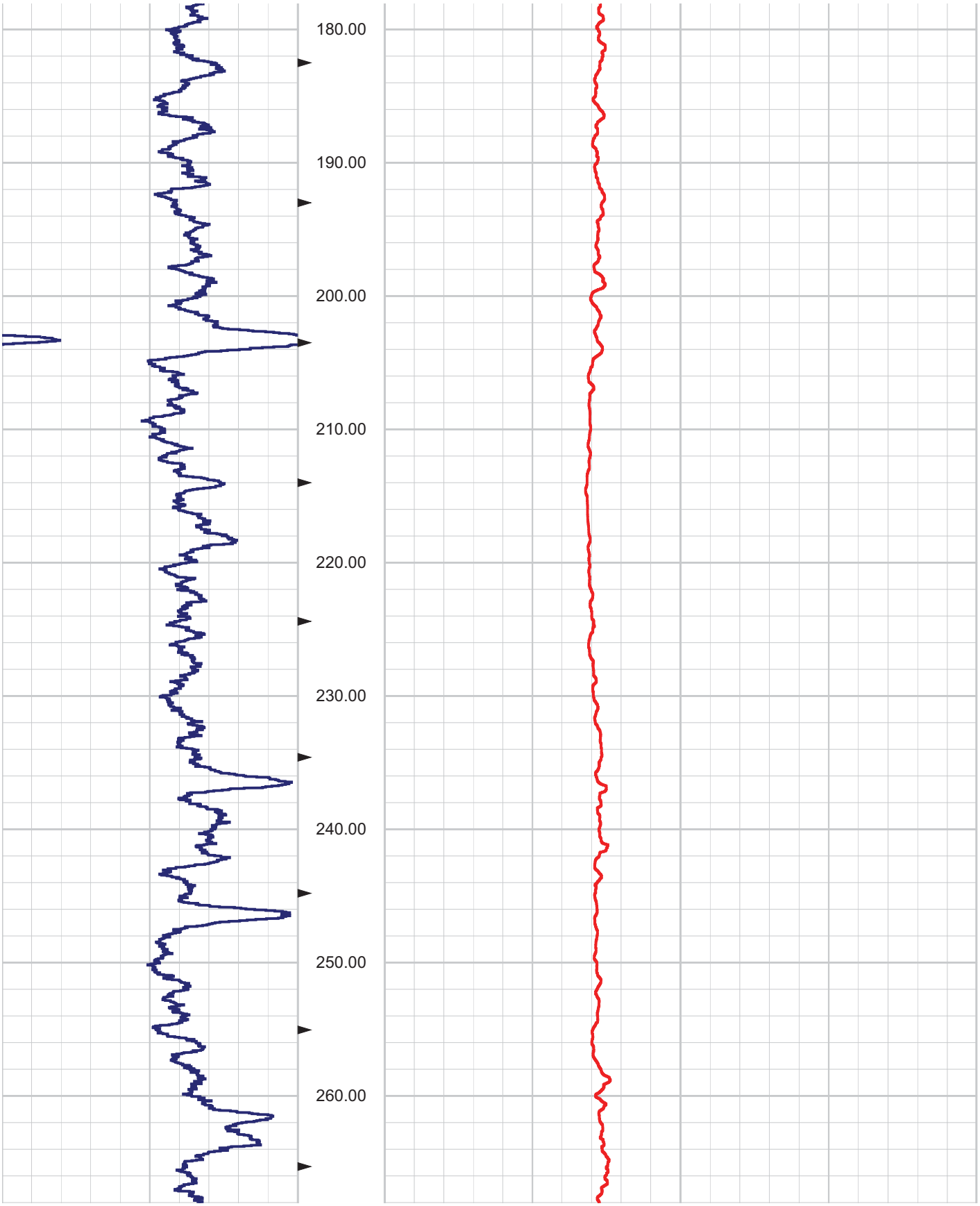


SR-710 Boring Z3-B6 Caliper and Natural Gamma rev 1.1 Sheet 3 of 4

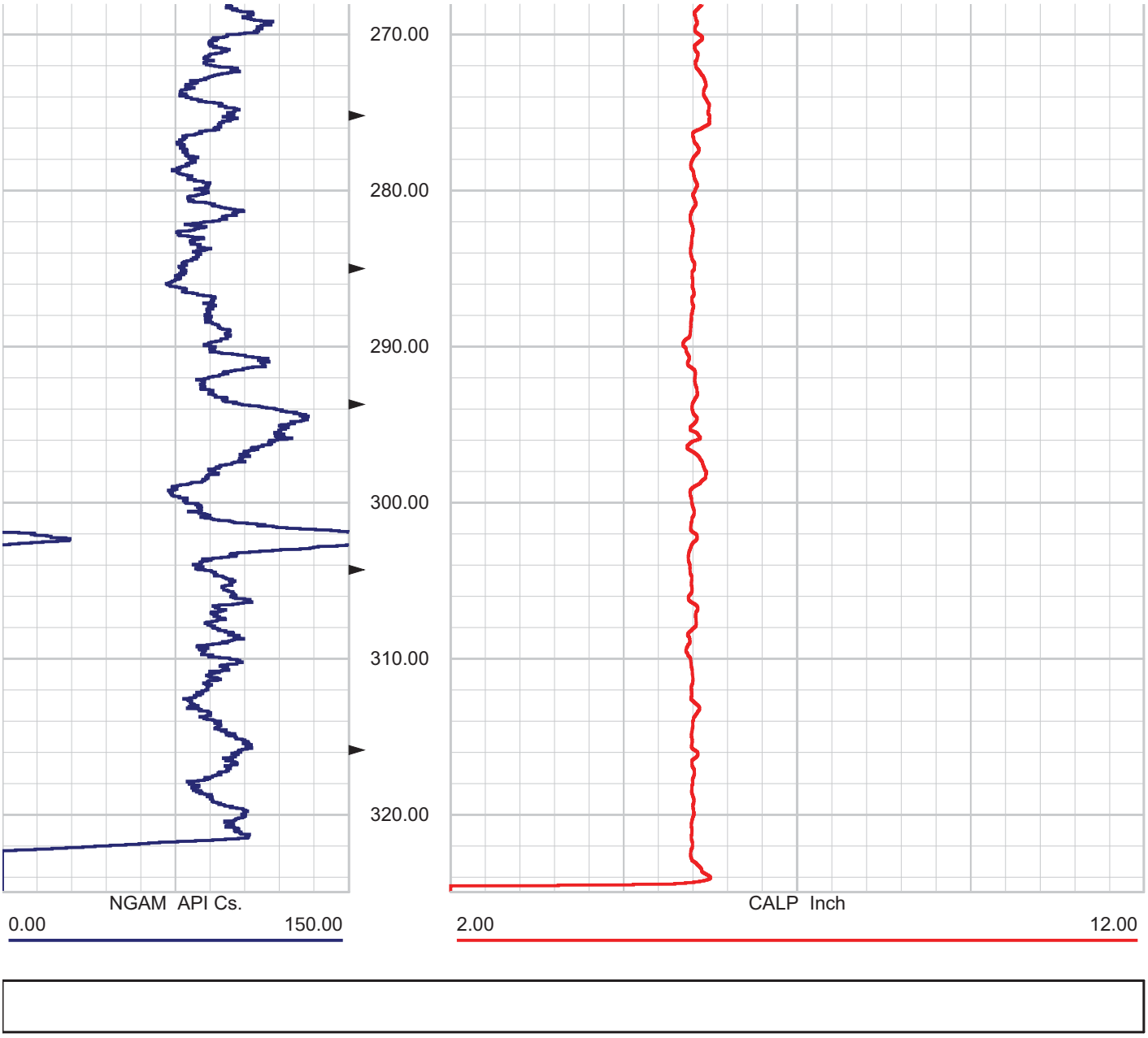
270.00
280.00
290.00
300.00
310.00
320.00
NGAM API Cs.
0.00
150.00
CALP Inch
2.00
12.00

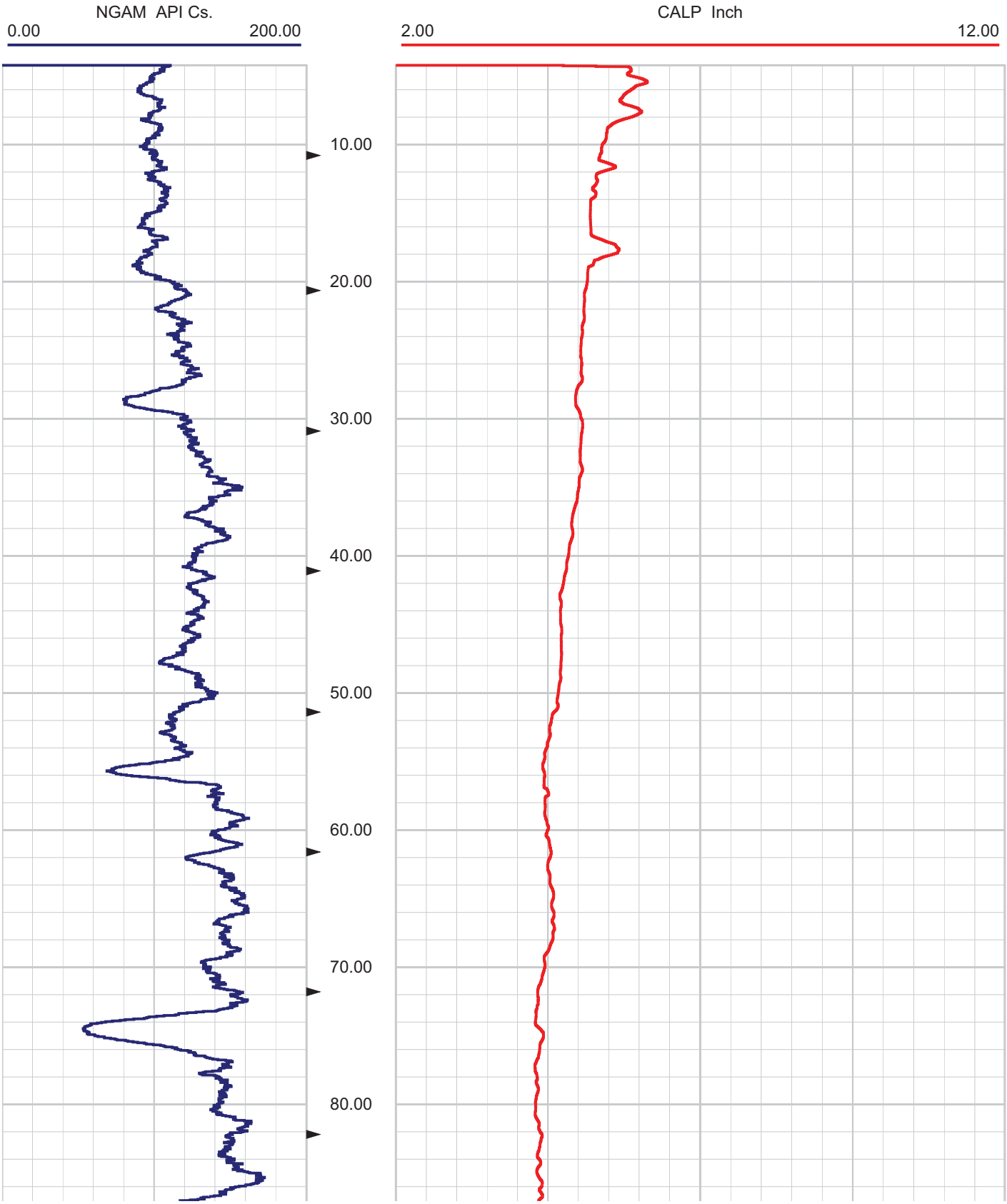


SR-710 Boring Z3-B8 Caliper and Natural Gamma rev 1.1 Sheet 1 of 4

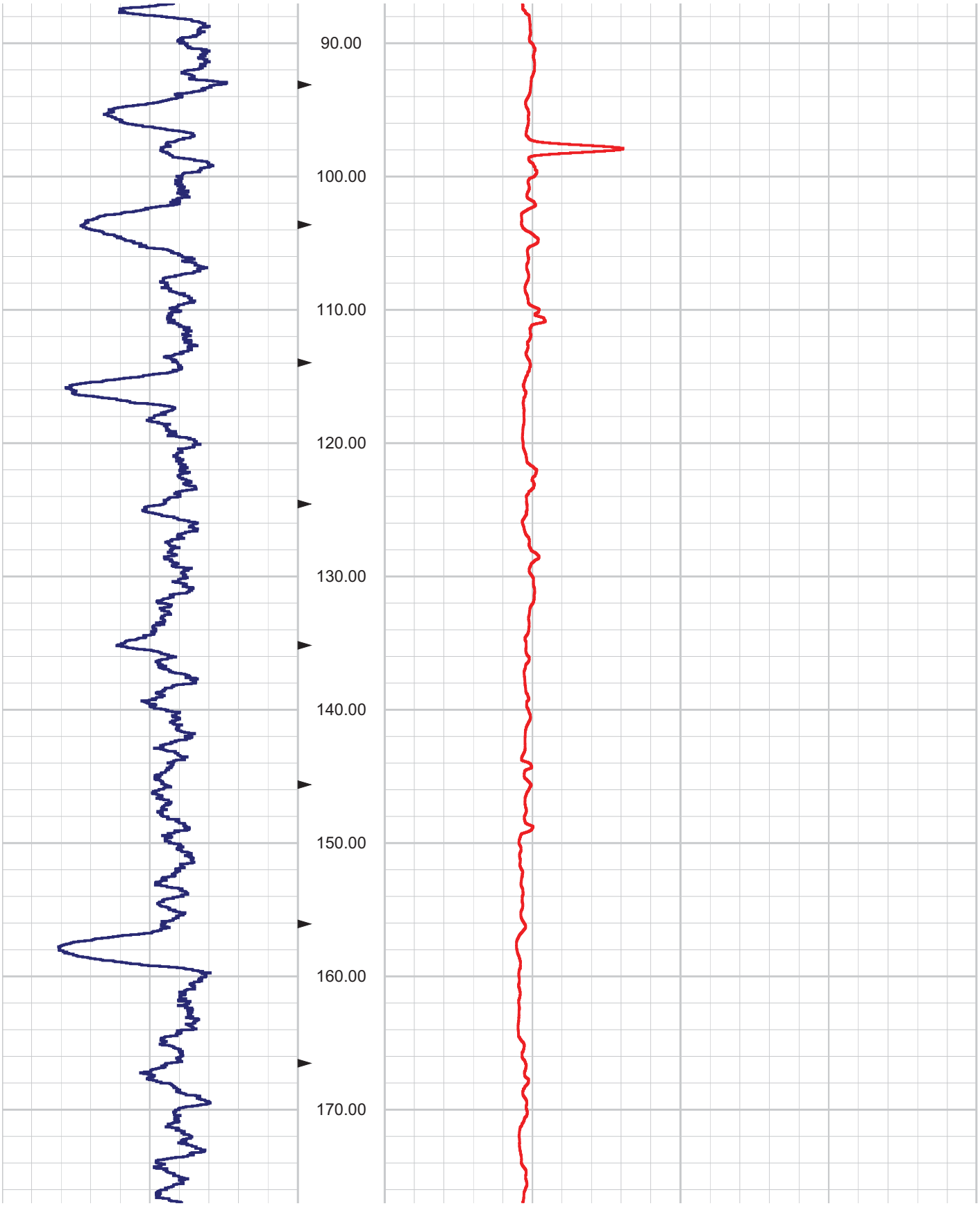


SR-710 Boring Z3-B8 Caliper and Natural Gamma rev 1.1 Sheet 2 of 4

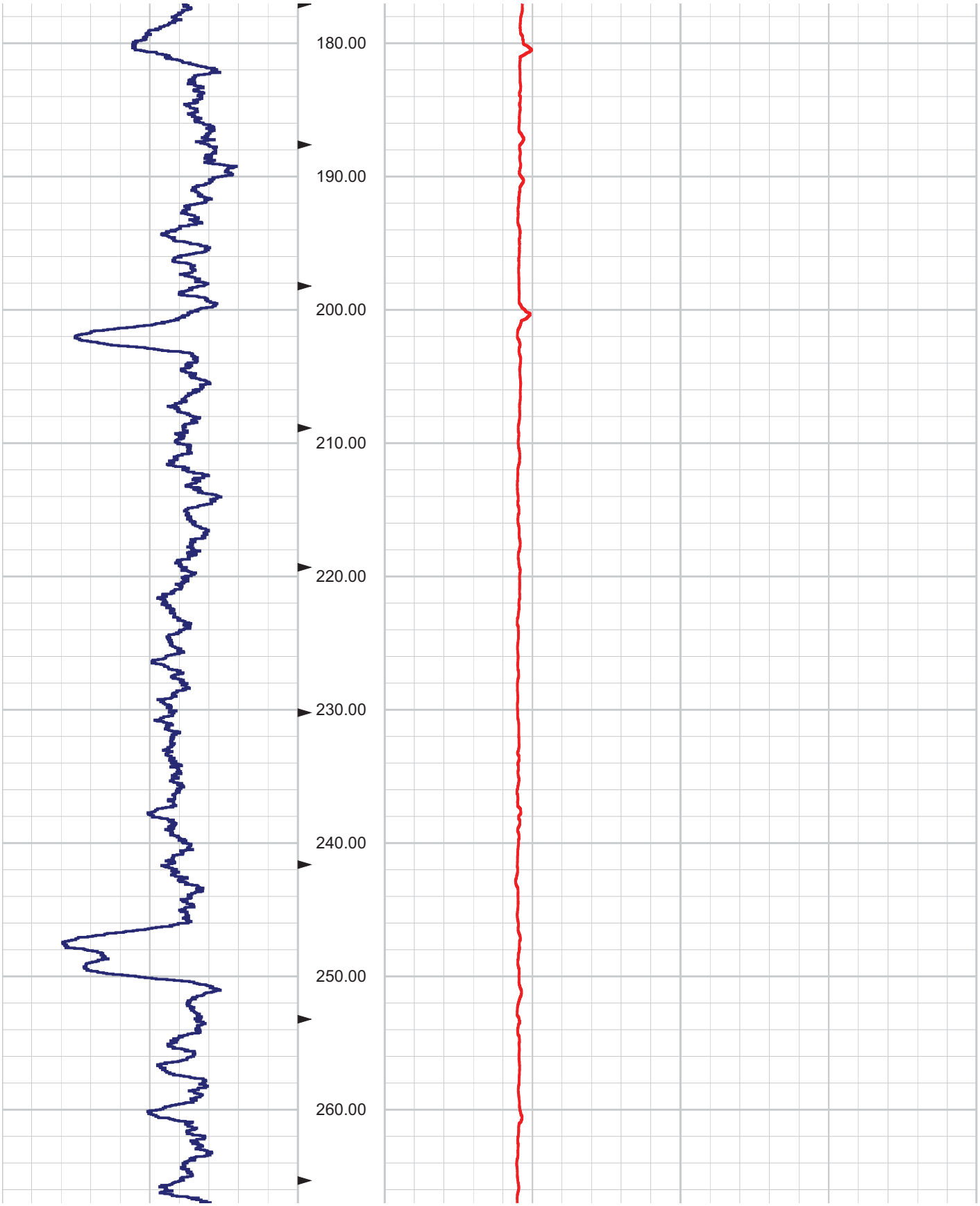


SR-710 Boring Z3-B8 Caliper and Natural Gamma rev 1.1 Sheet 3 of 4

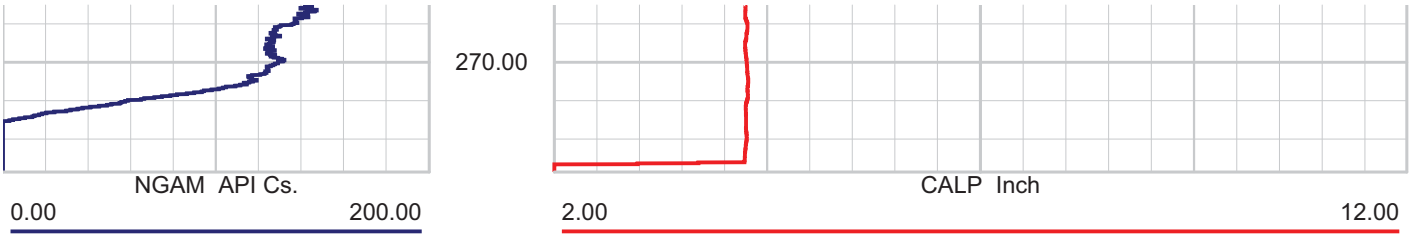


Depth: 3.00 ft Date: 23 Mar 2009 Time: 14:16:54 File: "C:\Winlogger401\Data\SR710\Z3-B8\Z3B8CALUP01.LOG"

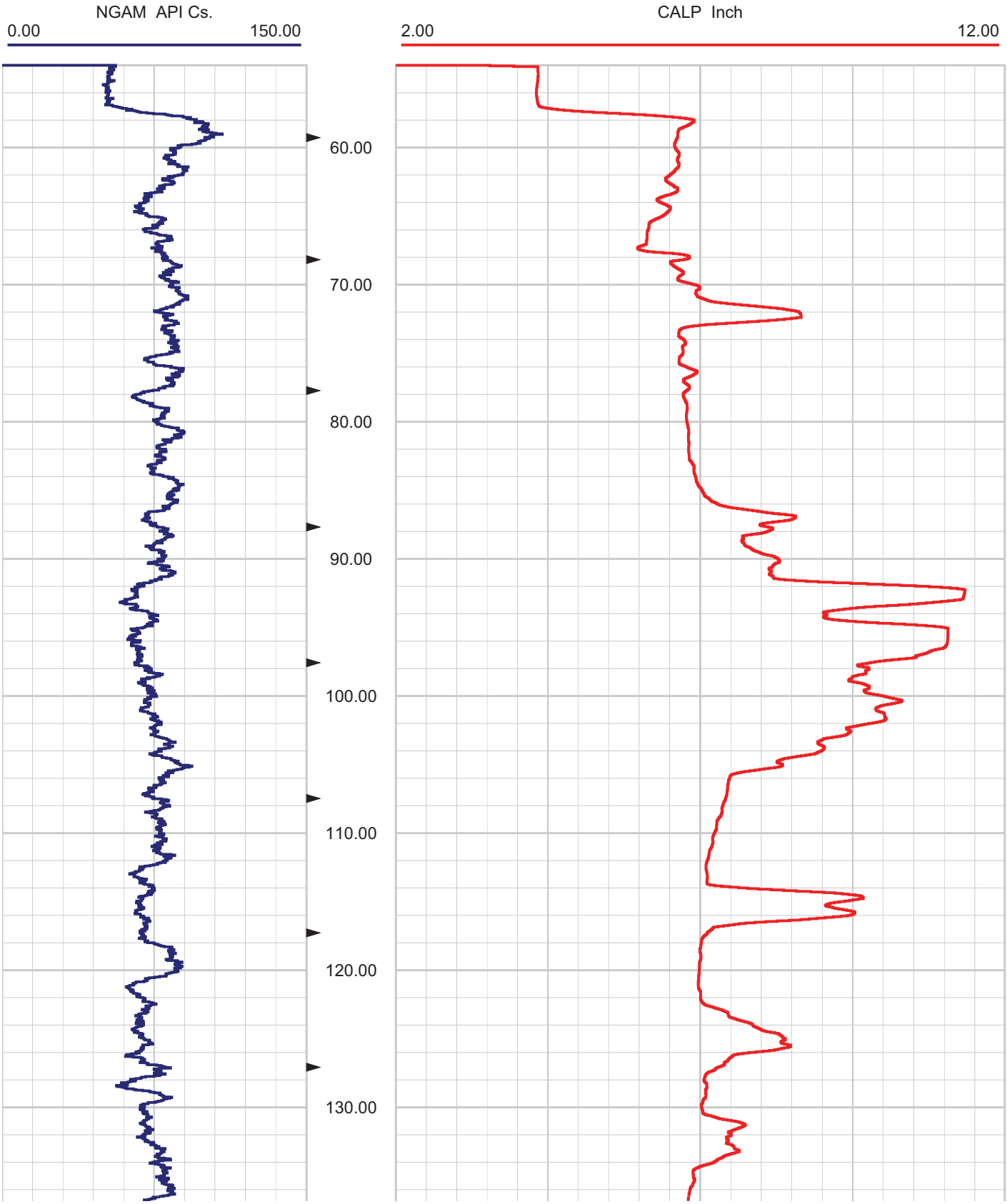


SR-710 Boring Z3-B12 Caliper and Natural Gamma rev 1.1 Sheet 1 of 3

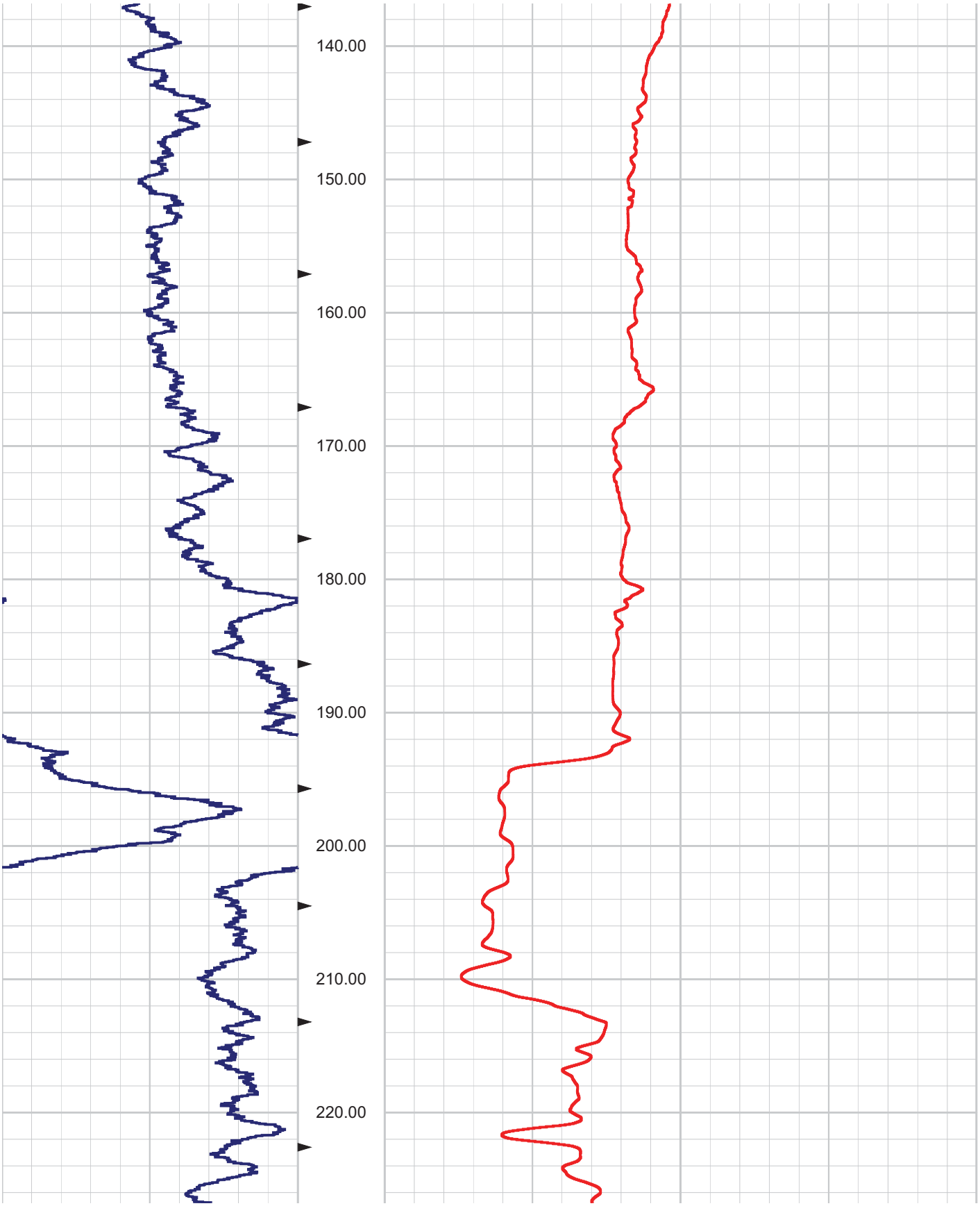


SR-710 Boring Z3-B12 Caliper and Natural Gamma rev 1.1 Sheet 2 of 3

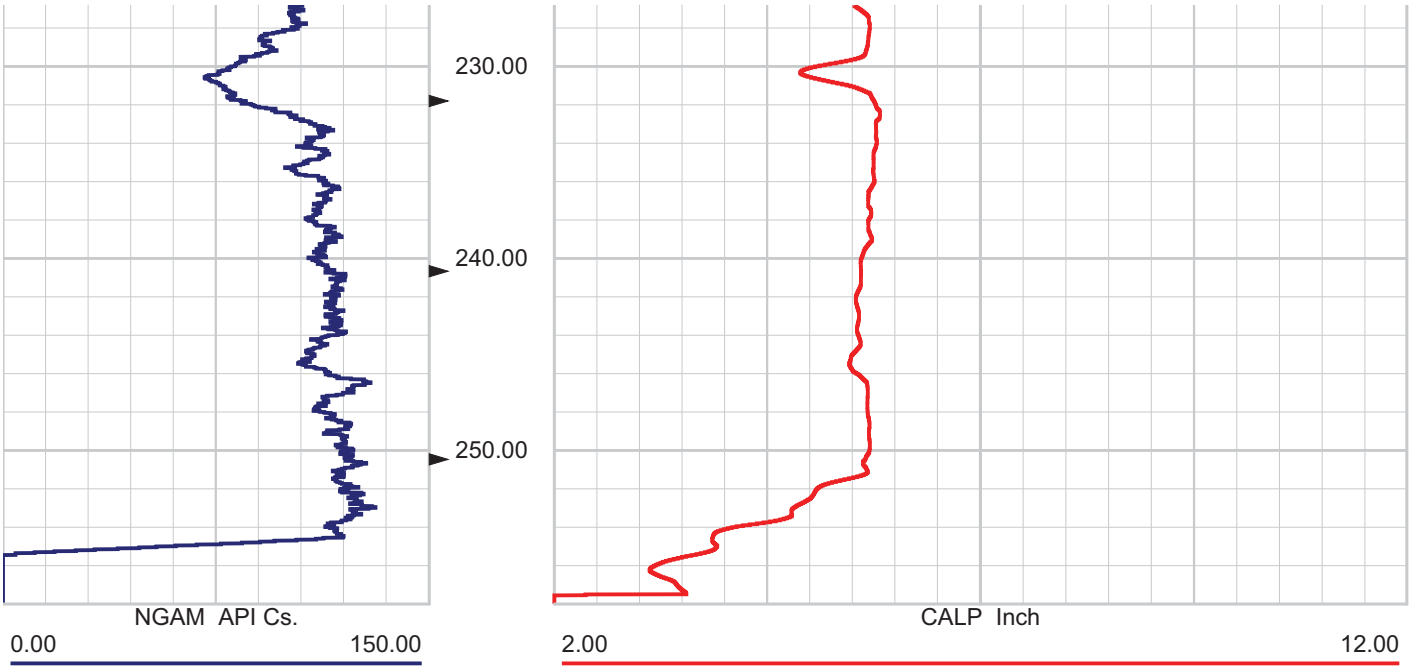
230.00
240.00
250.00
NGAM API Cs.
0.00
150.00
CALP Inch
2.00
12.00

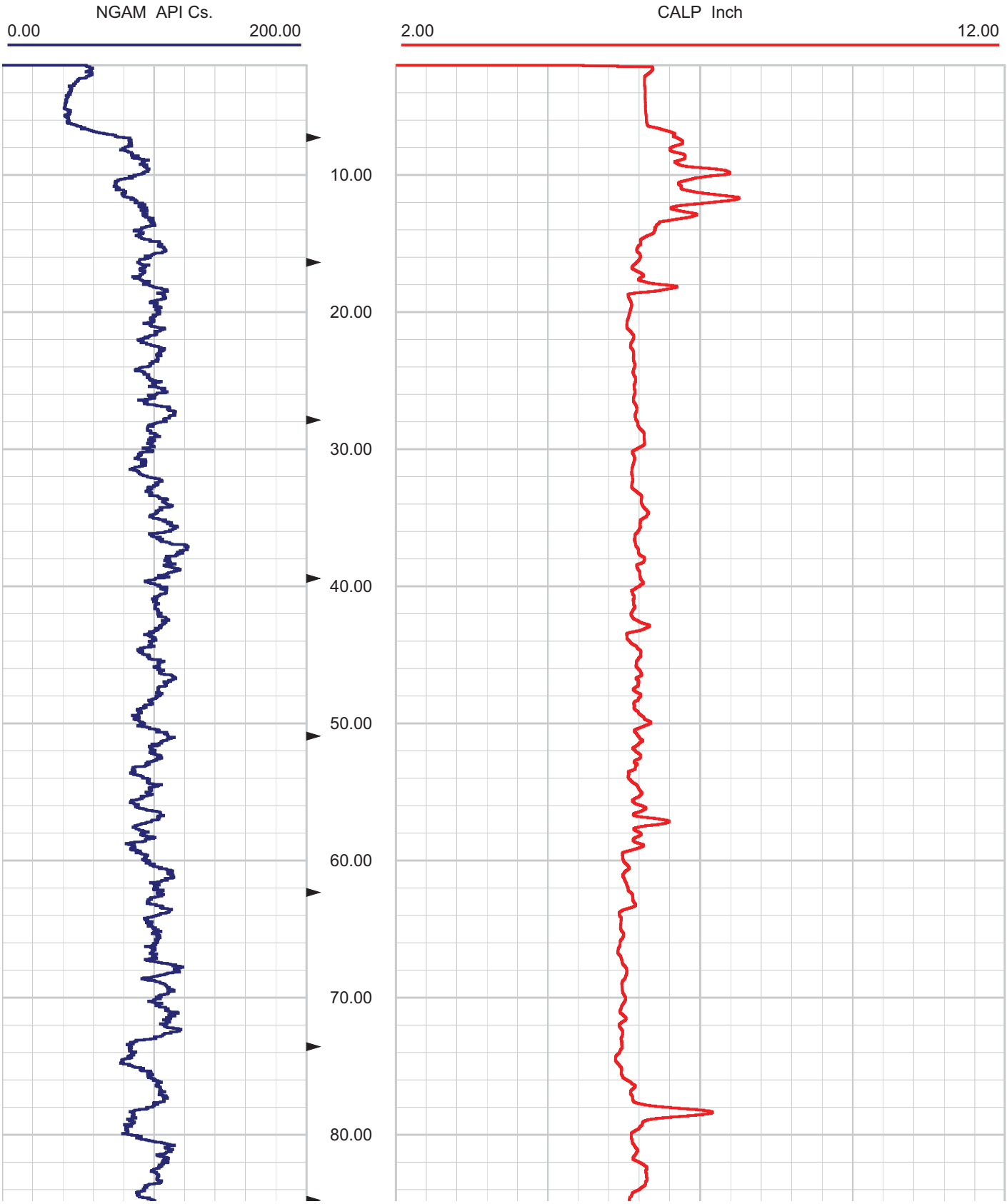


SR-710 Boring Z4-B4 Caliper and Natural Gamma rev 1.1 Sheet 1 of 4

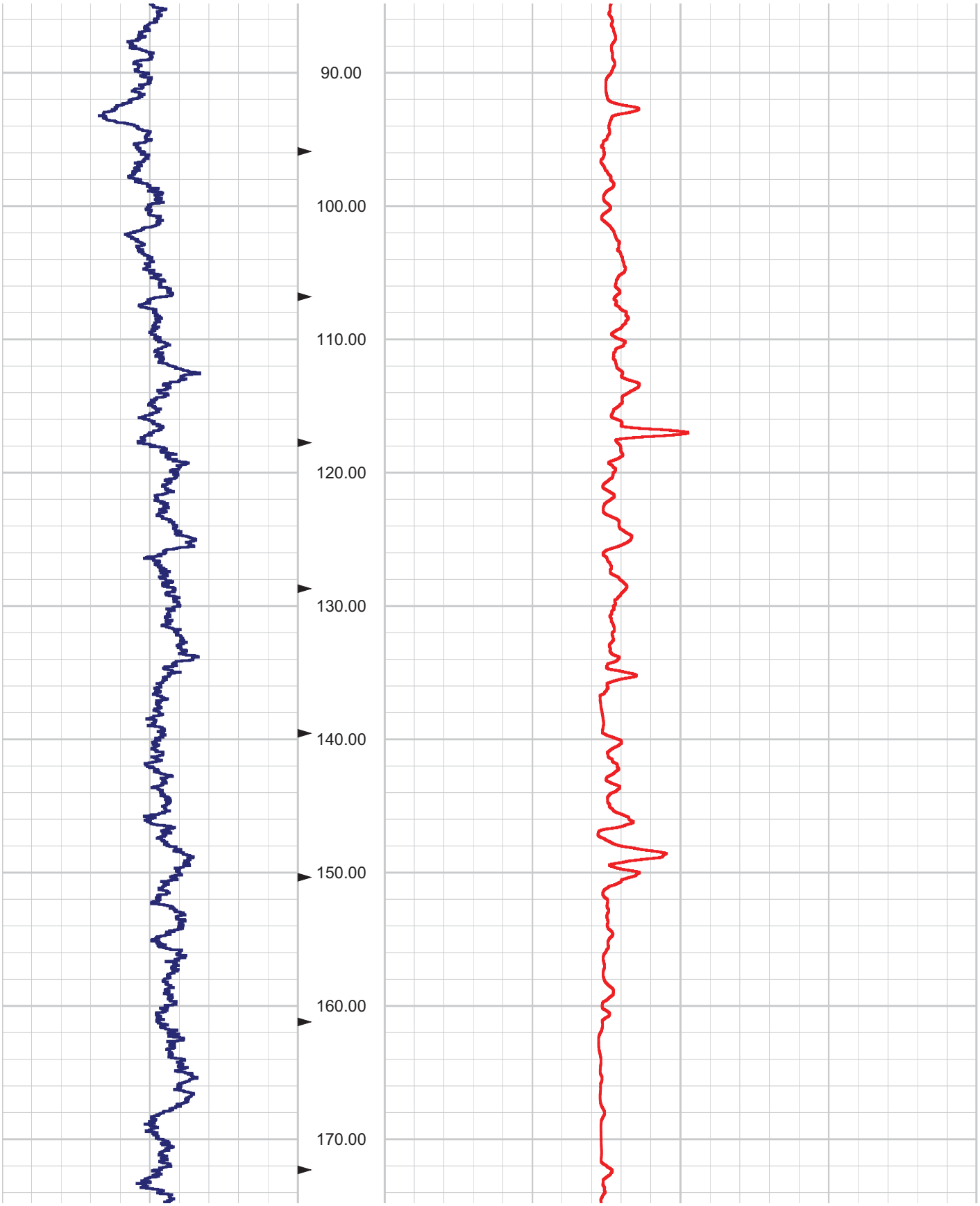


SR-710 Boring Z4-B4 Caliper and Natural Gamma rev 1.1 Sheet 2 of 4

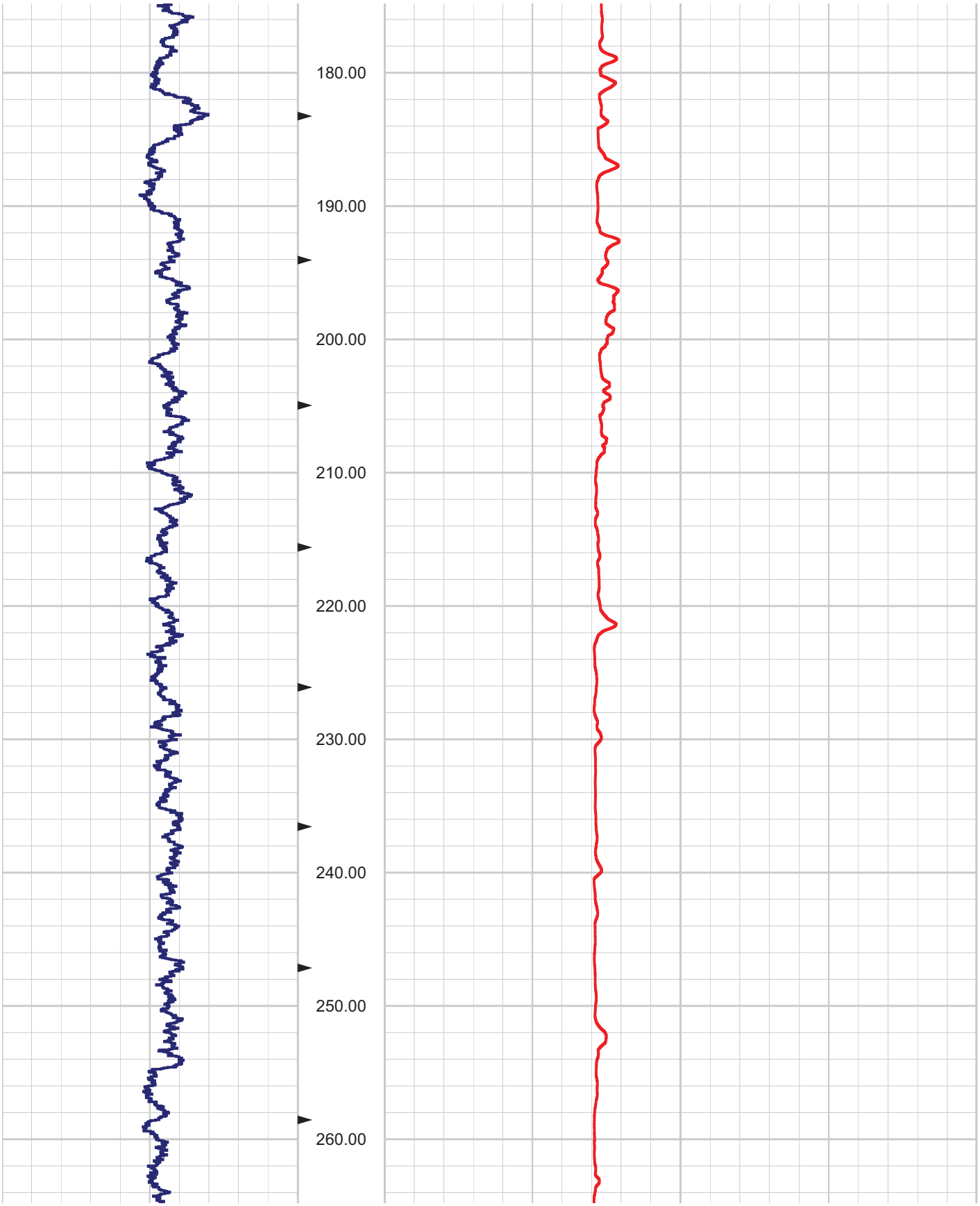


SR-710 Boring Z4-B4 Caliper and Natural Gamma rev 1.1 Sheet 3 of 4

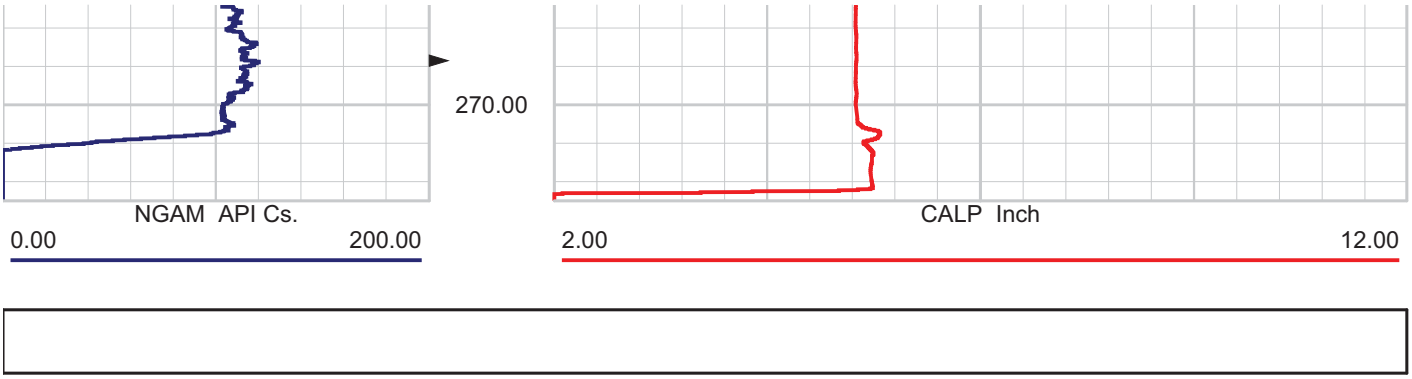
270.00
NGAM API Cs.
0.00
200.00
CALP Inch
2.00
12.00

# APPENDIX C

# ACOUSTIC TELEVIEWER DIPS LOGS

BHTV DATA PROCESSING
RGLDIP vsn 6.2
INTERPRETED BHTV DIPS LOG

CASCADE DRILLING

Borehole: Z3-B3

SR-710 TUNNEL INVESTIGATION

top of borehole.....
East: _
North: _
Elev: _

North ref. is true
Depth units are feet
Vertical scale: 1/10
Horiz scale = 1.00x Vert scale

Zone from 273.984 to 173.200ft
Format: BHTV-NESWN

Borehole diam: 5.600inch
Vertical = borehole-axis
Image: Amplitude

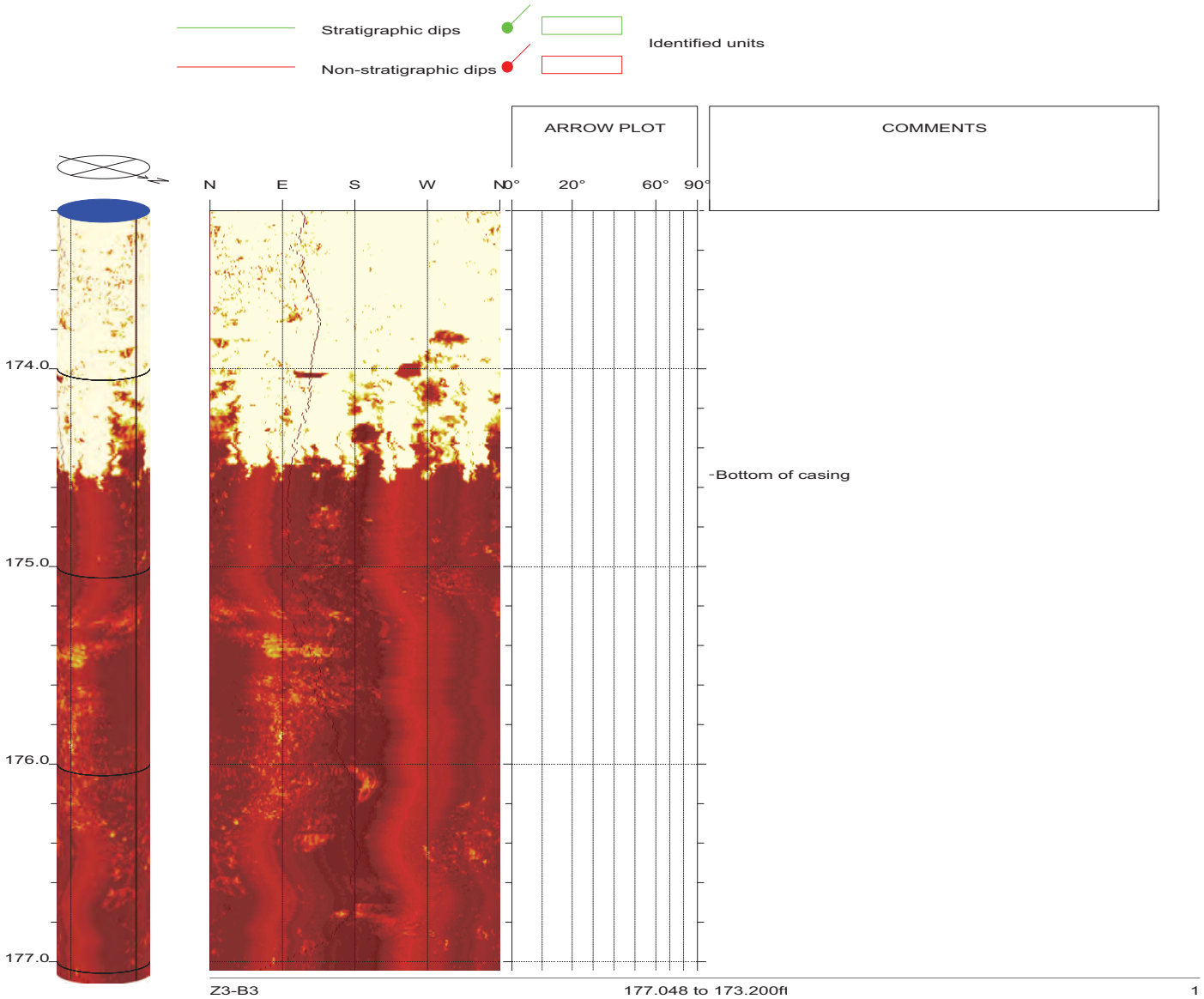


SR-710 Boring Z3-B3 Acoustic Televiewer Dips rev 1 Sheet 1 of 15

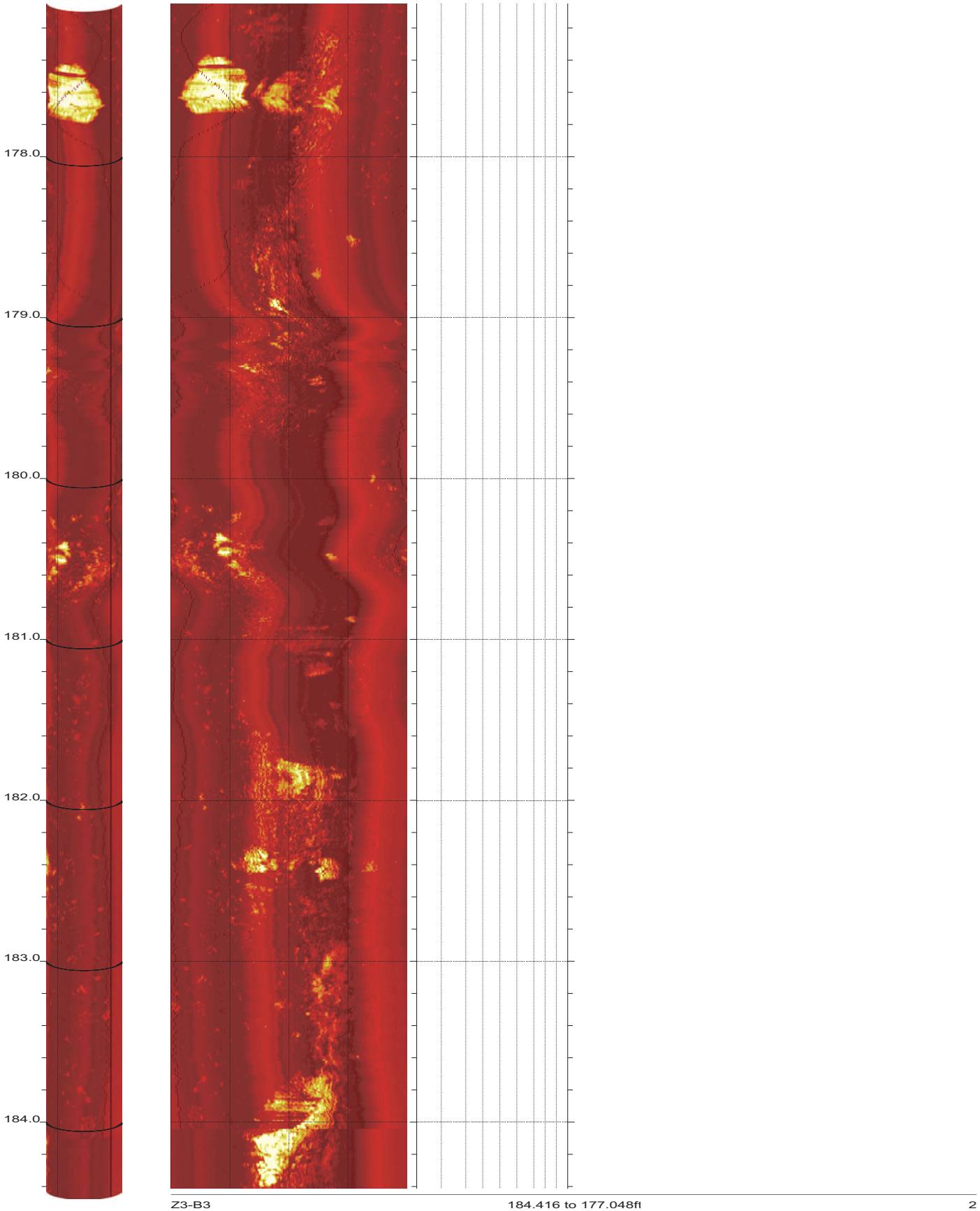


SR-710 Boring Z3-B3 Acoustic Televiewer Dips rev 1 Sheet 2 of 15

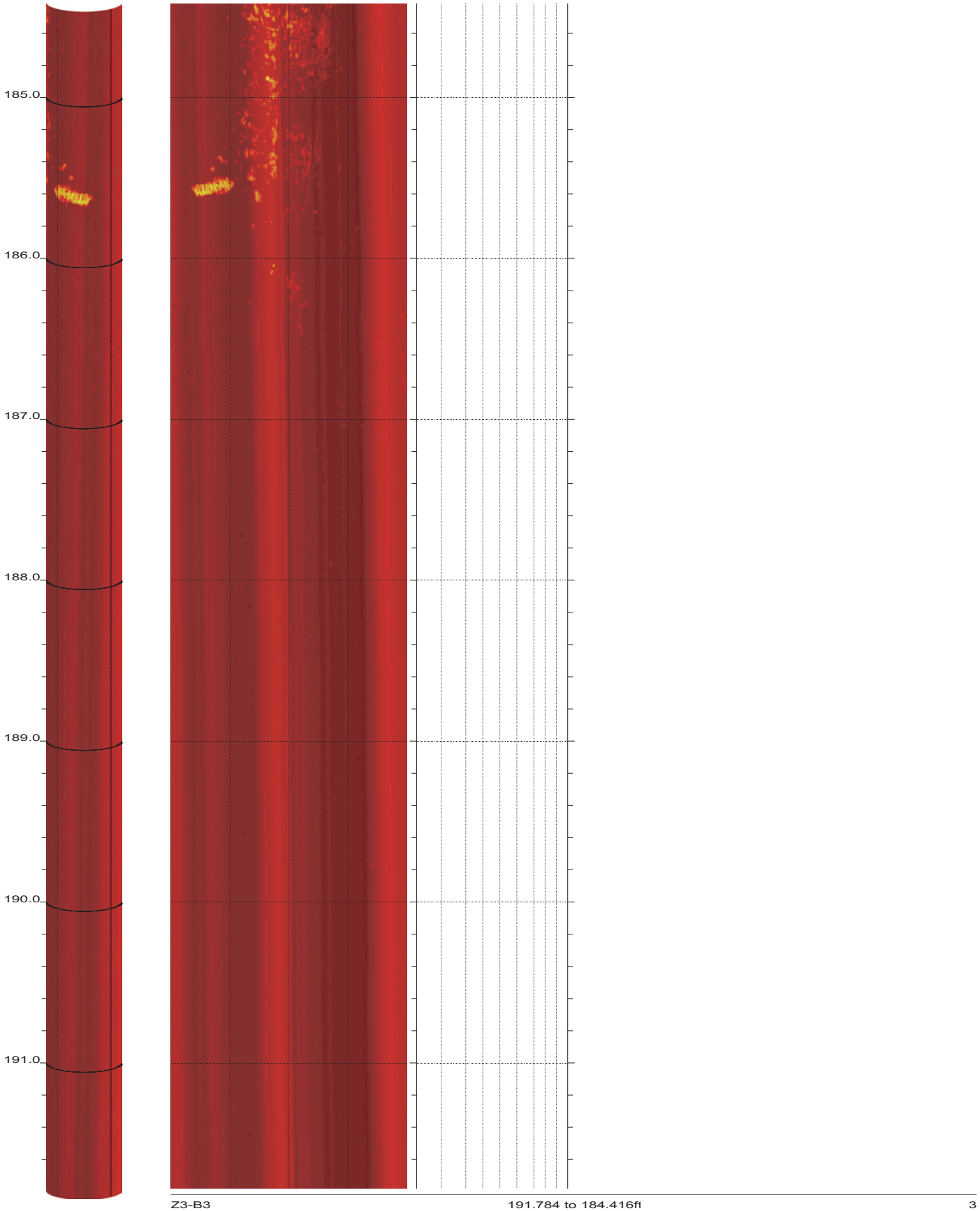


SR-710 Boring Z3-B3 Acoustic Televiewer Dips rev 1 Sheet 3 of 15

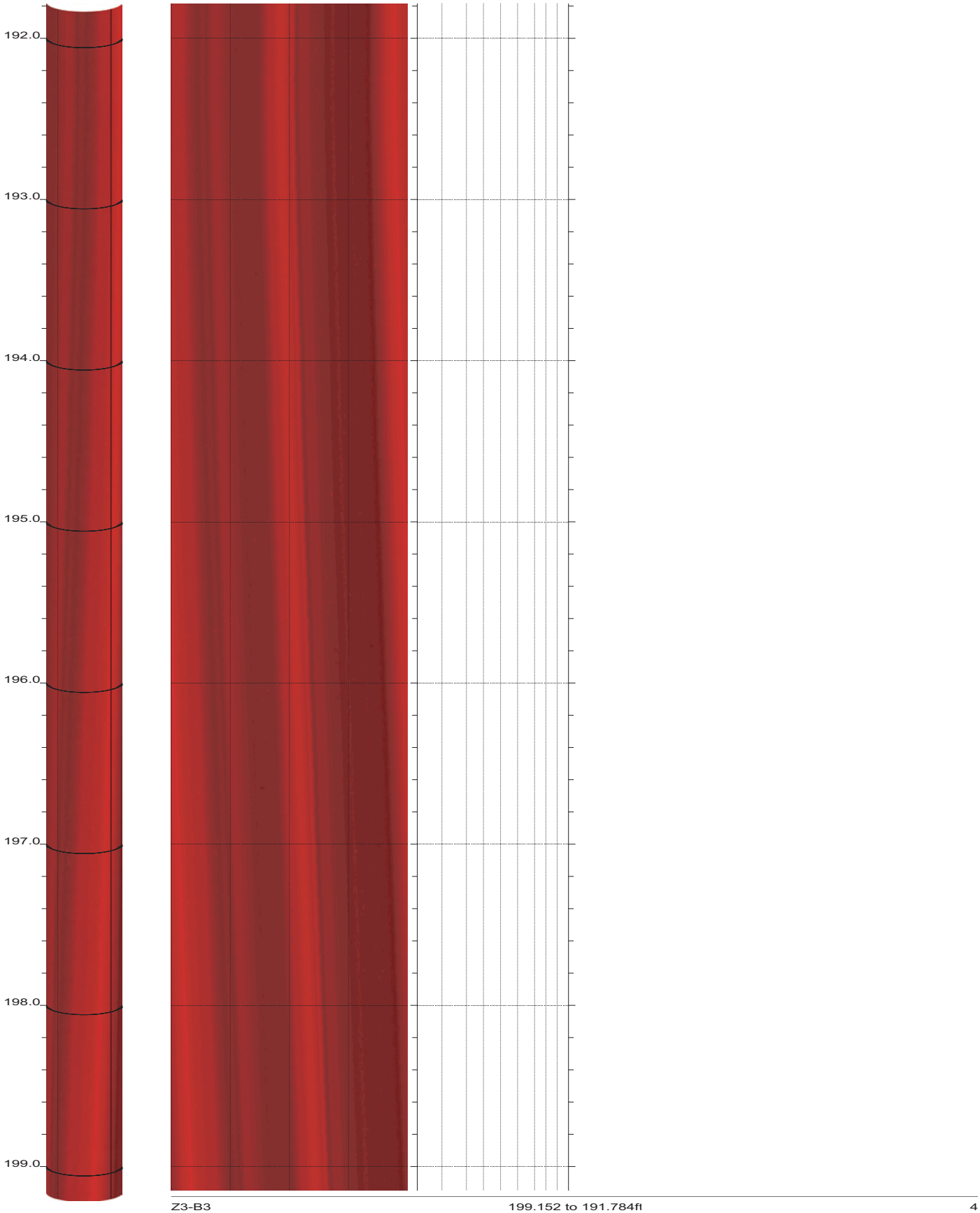


SR-710 Boring Z3-B3 Acoustic Televiewer Dips rev 1 Sheet 4 of 15

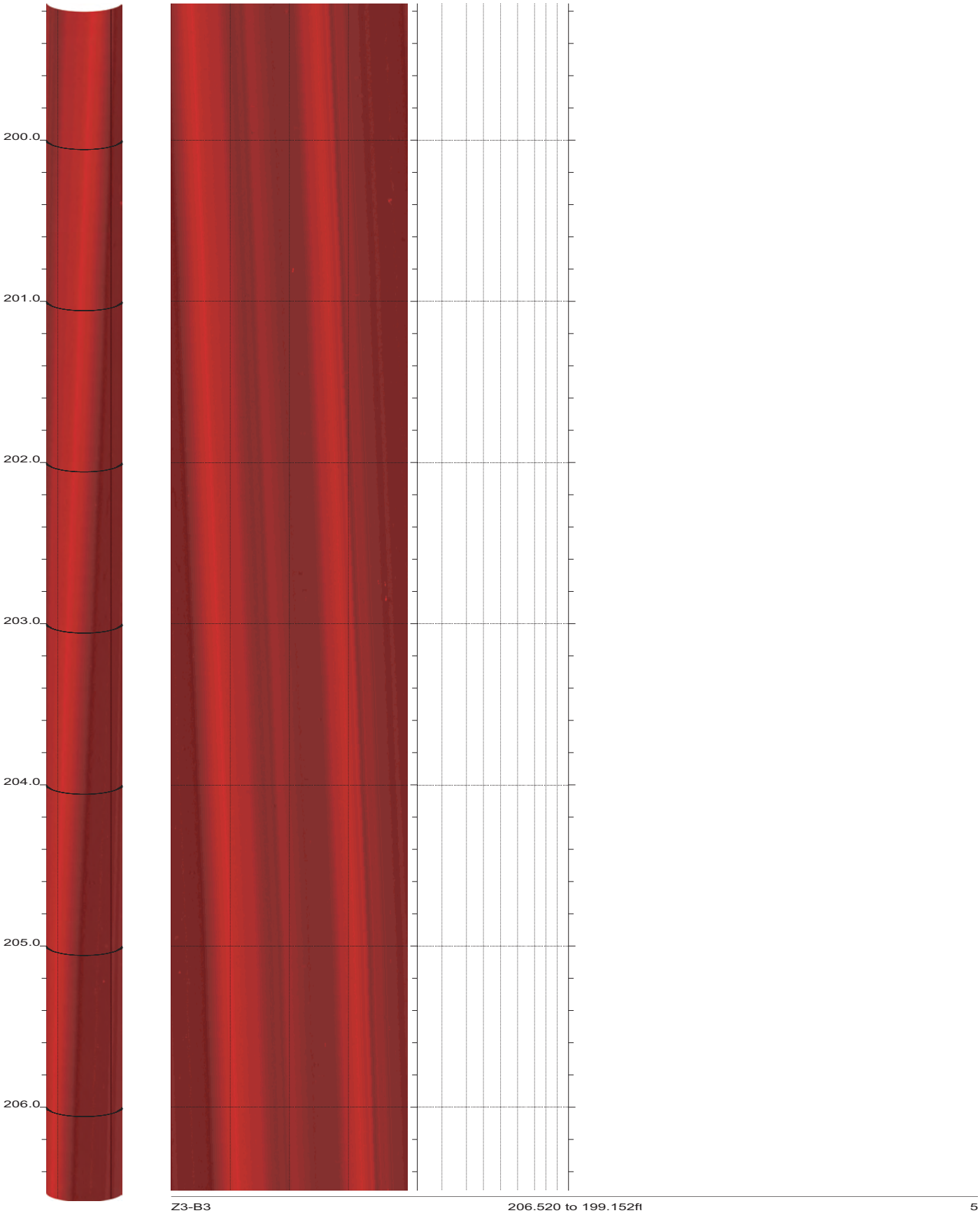


SR-710 Boring Z3-B3 Acoustic Televiewer Dips rev 1 Sheet 5 of 15

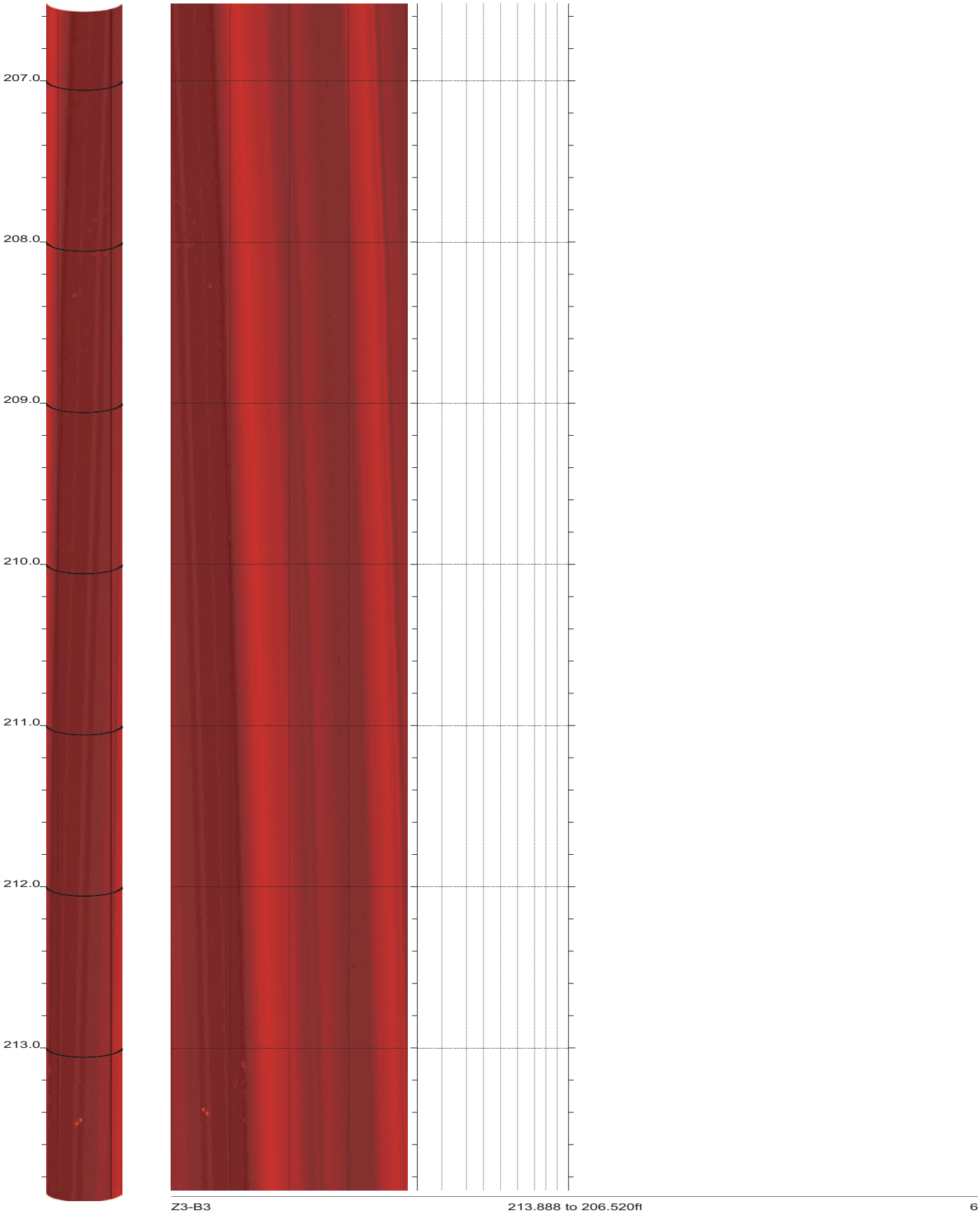


SR-710 Boring Z3-B3 Acoustic Televiewer Dips rev 1 Sheet 6 of 15

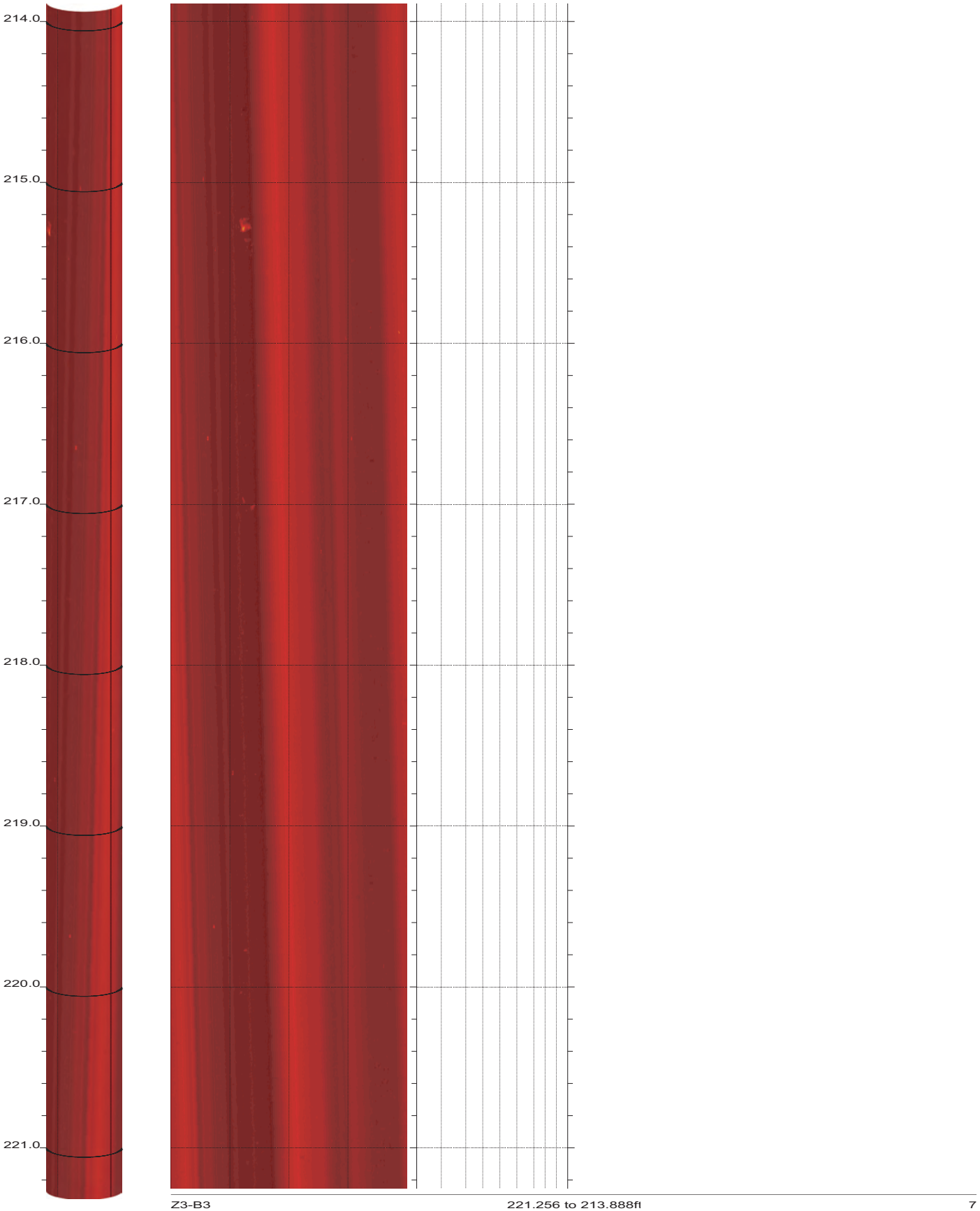


SR-710 Boring Z3-B3 Acoustic Televiewer Dips rev 1 Sheet 7 of 15

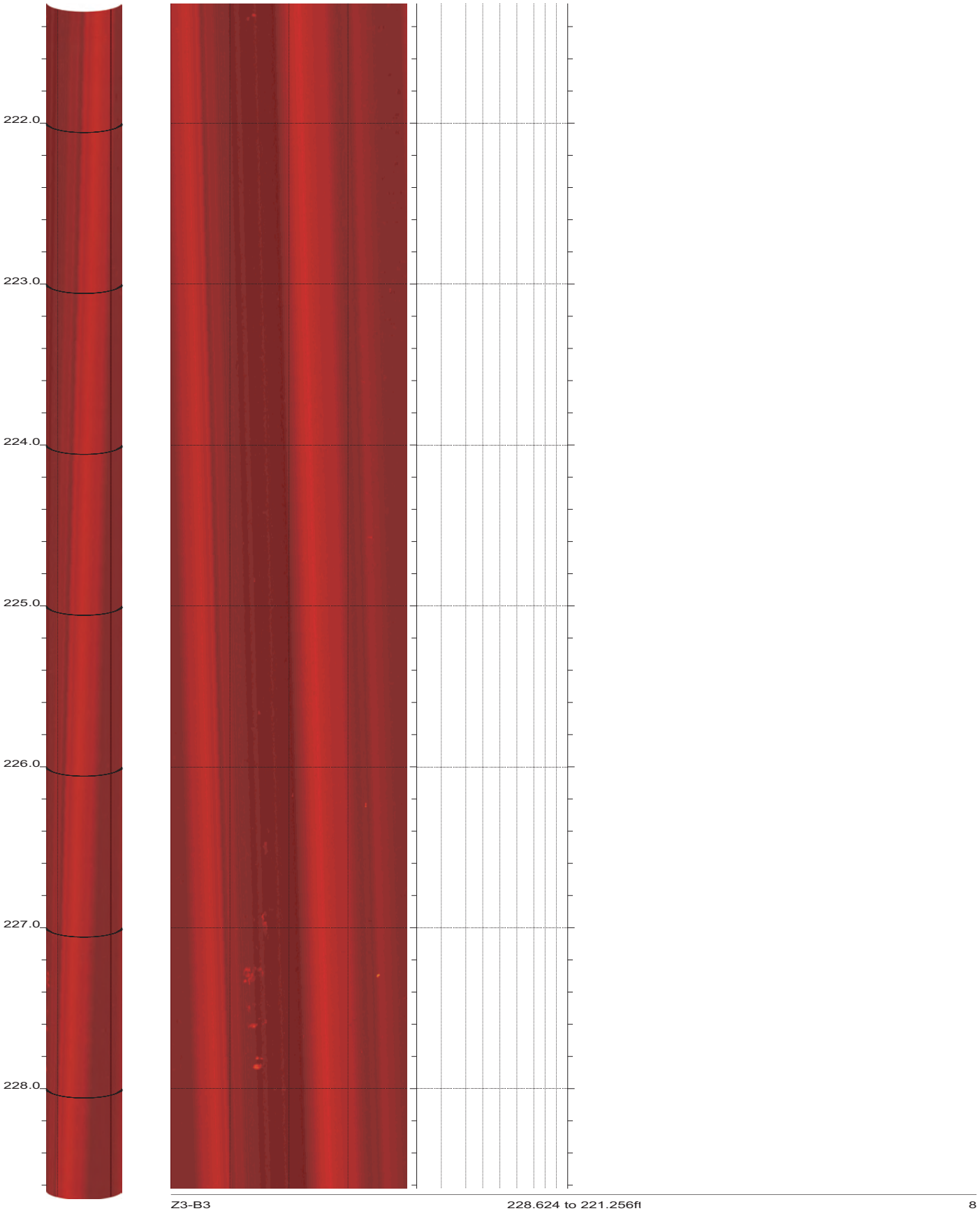


SR-710 Boring Z3-B3 Acoustic Televiewer Dips rev 1 Sheet 8 of 15

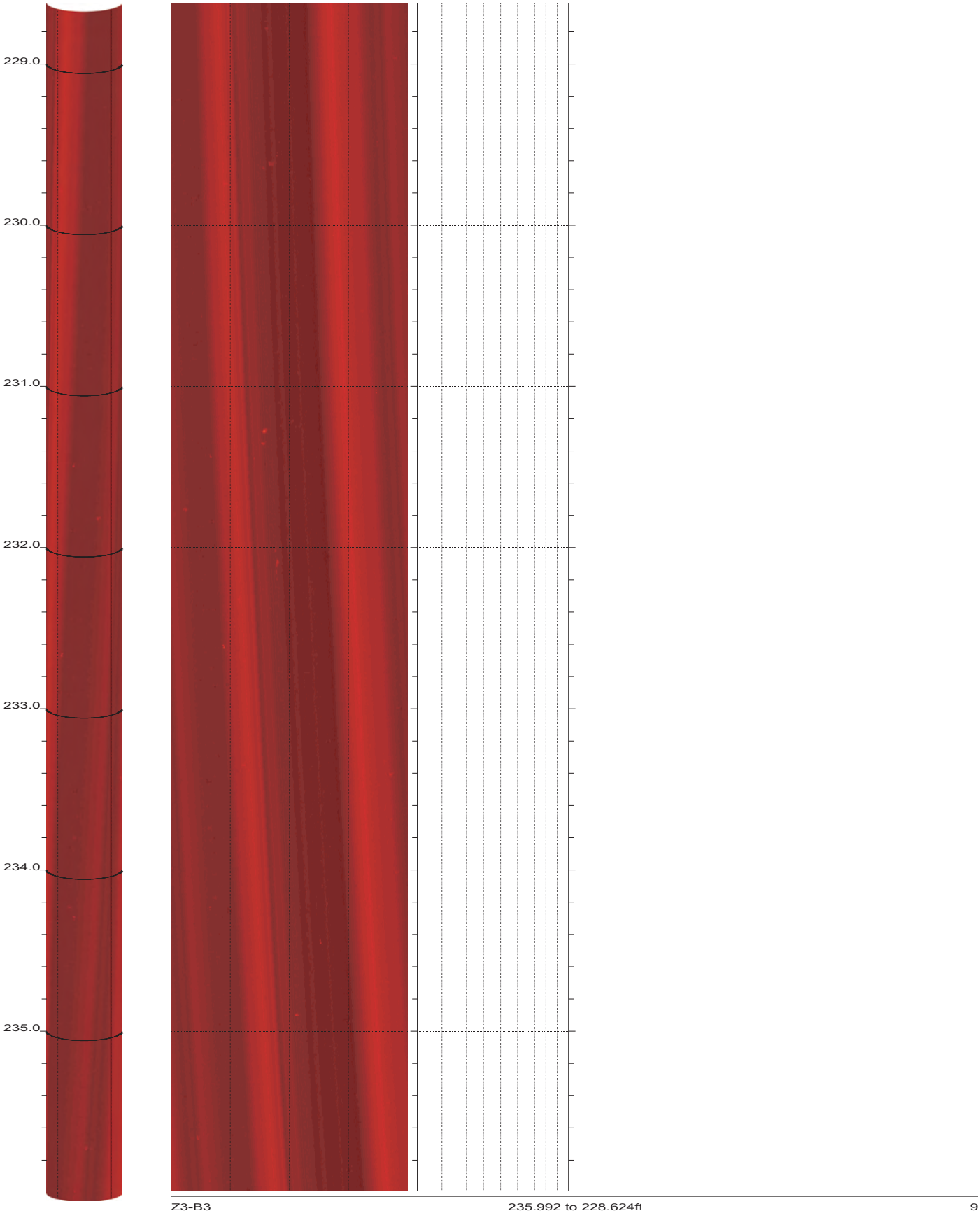


SR-710 Boring Z3-B3 Acoustic Televiewer Dips rev 1 Sheet 9 of 15

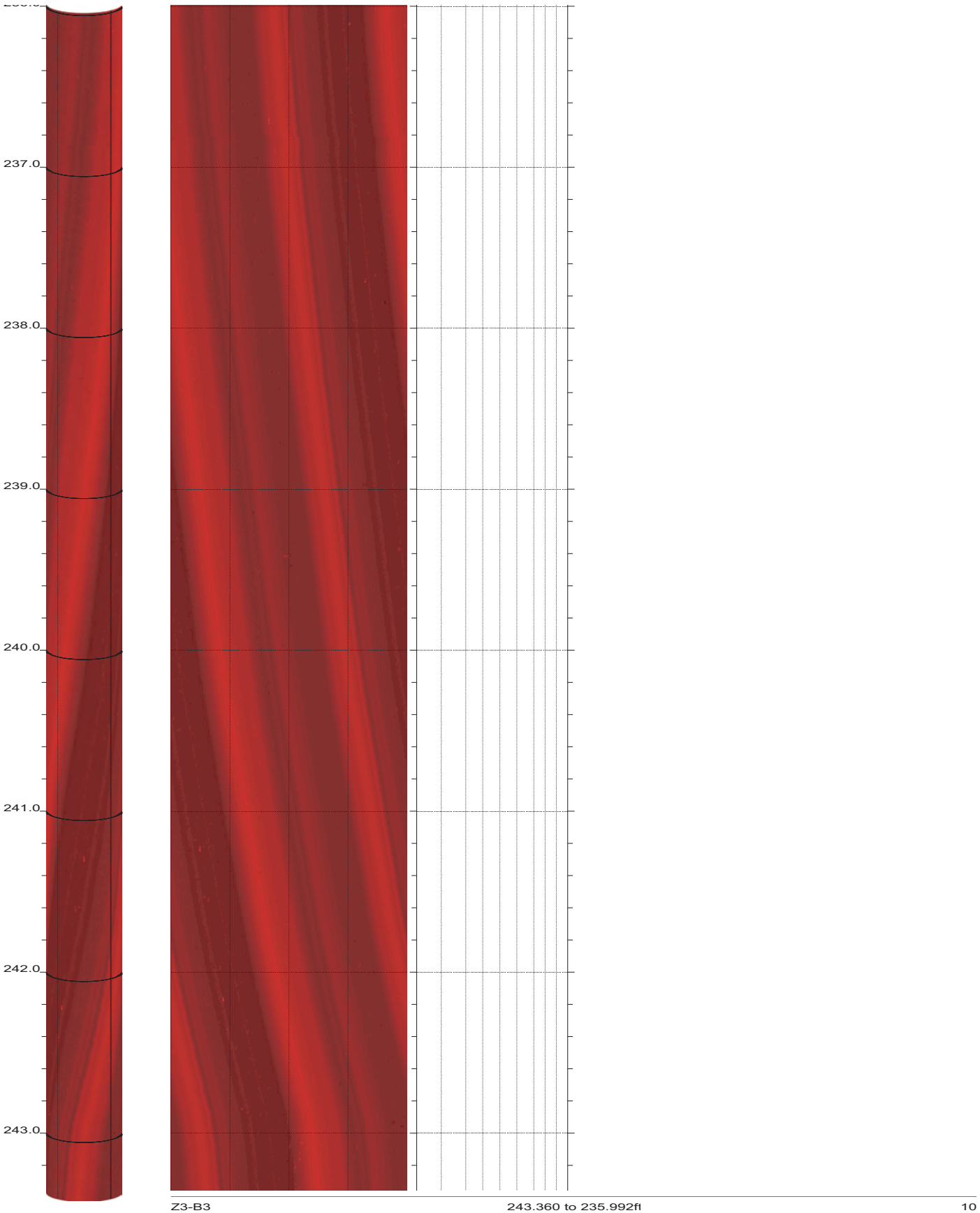


SR-710 Boring Z3-B3 Acoustic Televiewer Dips rev 1 Sheet 10 of 15

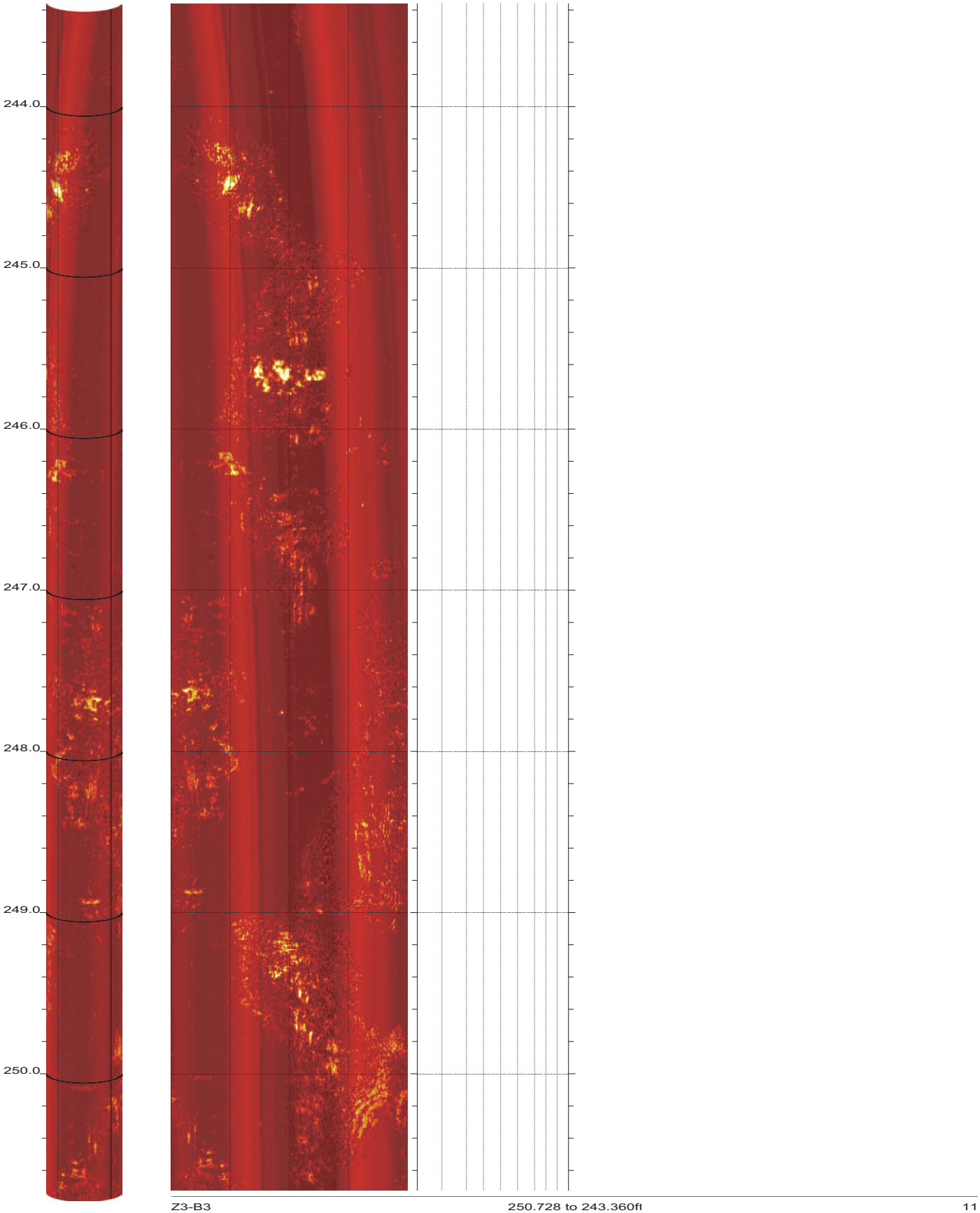


SR-710 Boring Z3-B3 Acoustic Televiewer Dips rev 1 Sheet 11 of 15

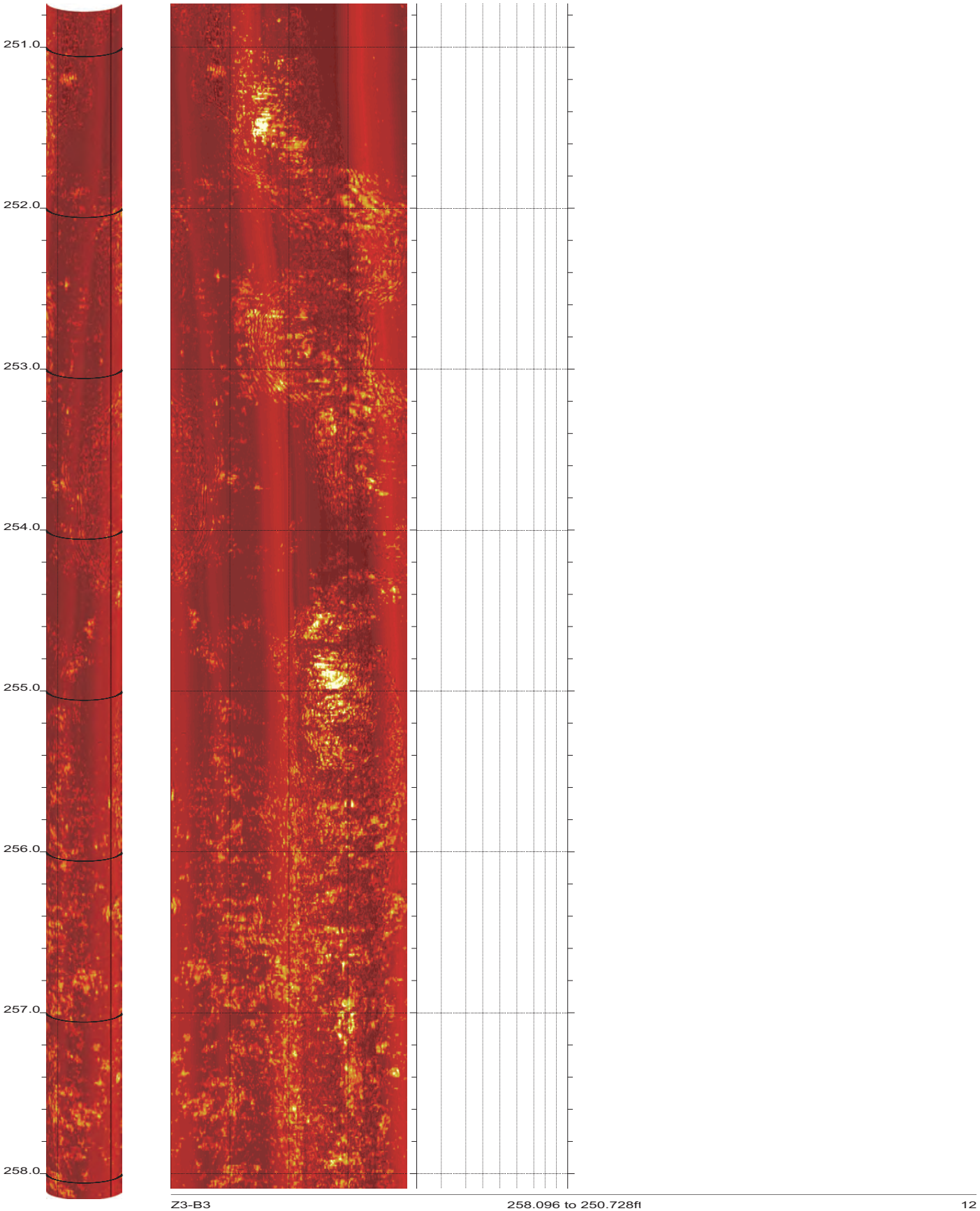
251.0
252.0
253.0
254.0
255.0
256.0
257.0
258.0
Z3-B3
258.096 to 250.728fl
12

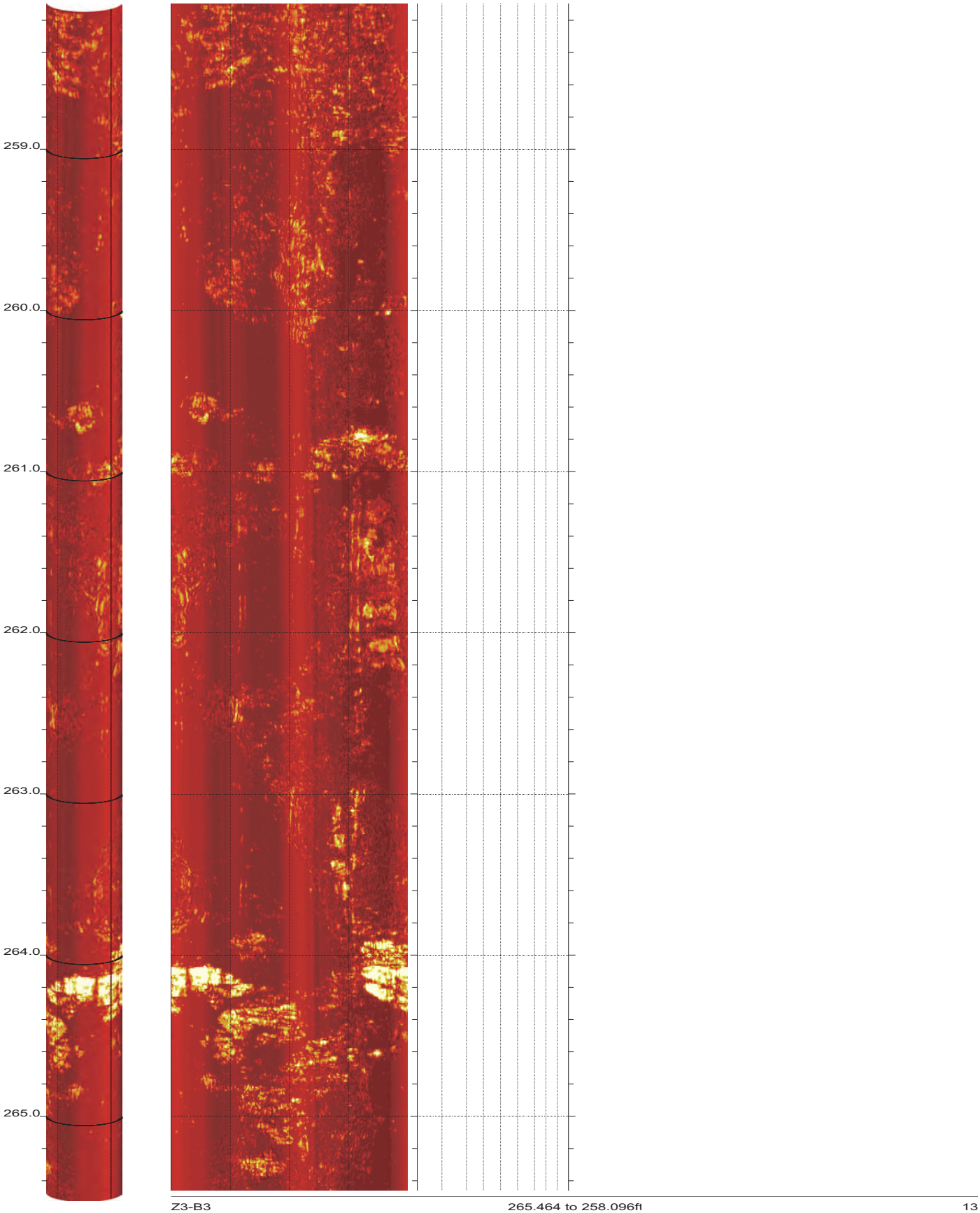


SR-710 Boring Z3-B3 Acoustic Televiewer Dips rev 1 Sheet 13 of 15

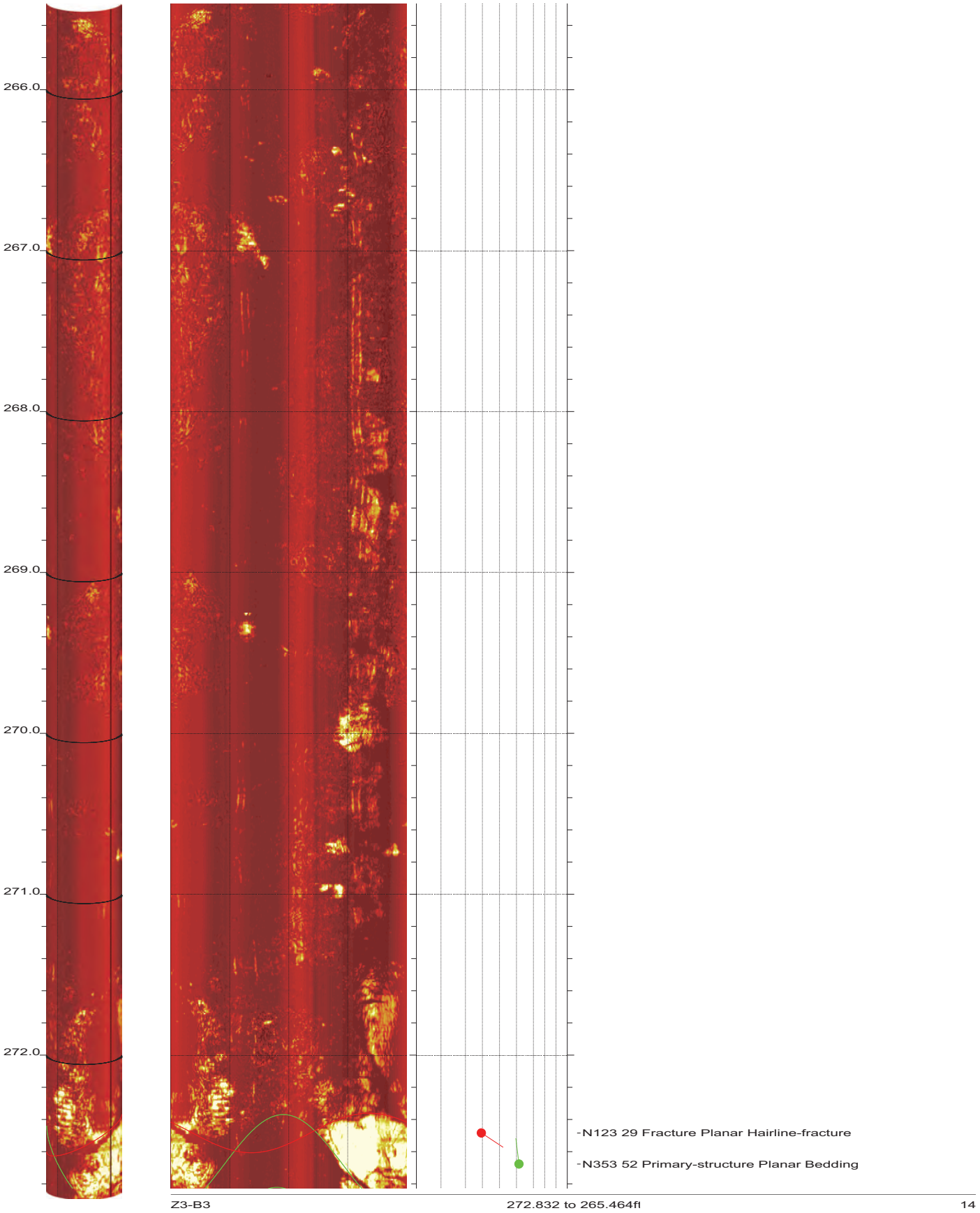


SR-710 Boring Z3-B3 Acoustic Televiewer Dips rev 1 Sheet 14 of 15

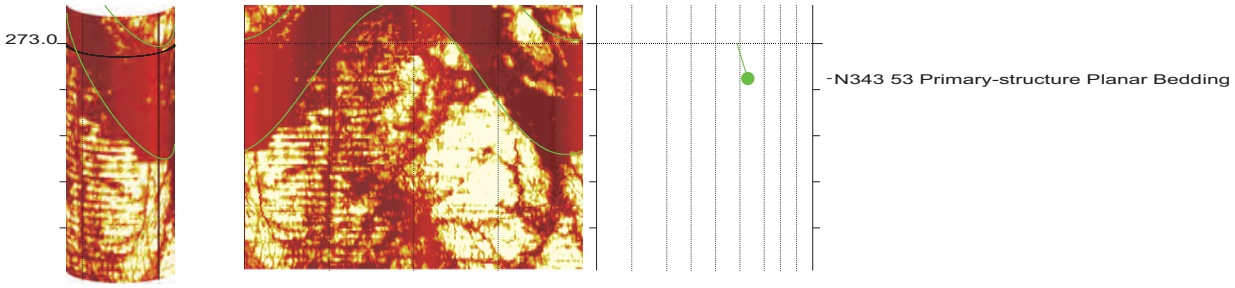
273.0
-N343 53 Primary-structure Planar Bedding

BHTV DATA PROCESSING
RGLDIP vsn 6.2
INTERPRETED BHTV DIPS LOG

CASCADE DRILLING

Borehole: Z3-B4

SR-710 TUNNEL INVESTIGATION

top of borehole.....
East: _
North: _
Elev: _

North ref. is true
Depth units are feet
Vertical scale: 1/10
Horiz scale = 1.00x Vert scale

Zone from 275.000 to 2.600ft
Format: BHTV-NESWN

Borehole diam: 5.600inch
Vertical = borehole-axis
Image: Amplitude

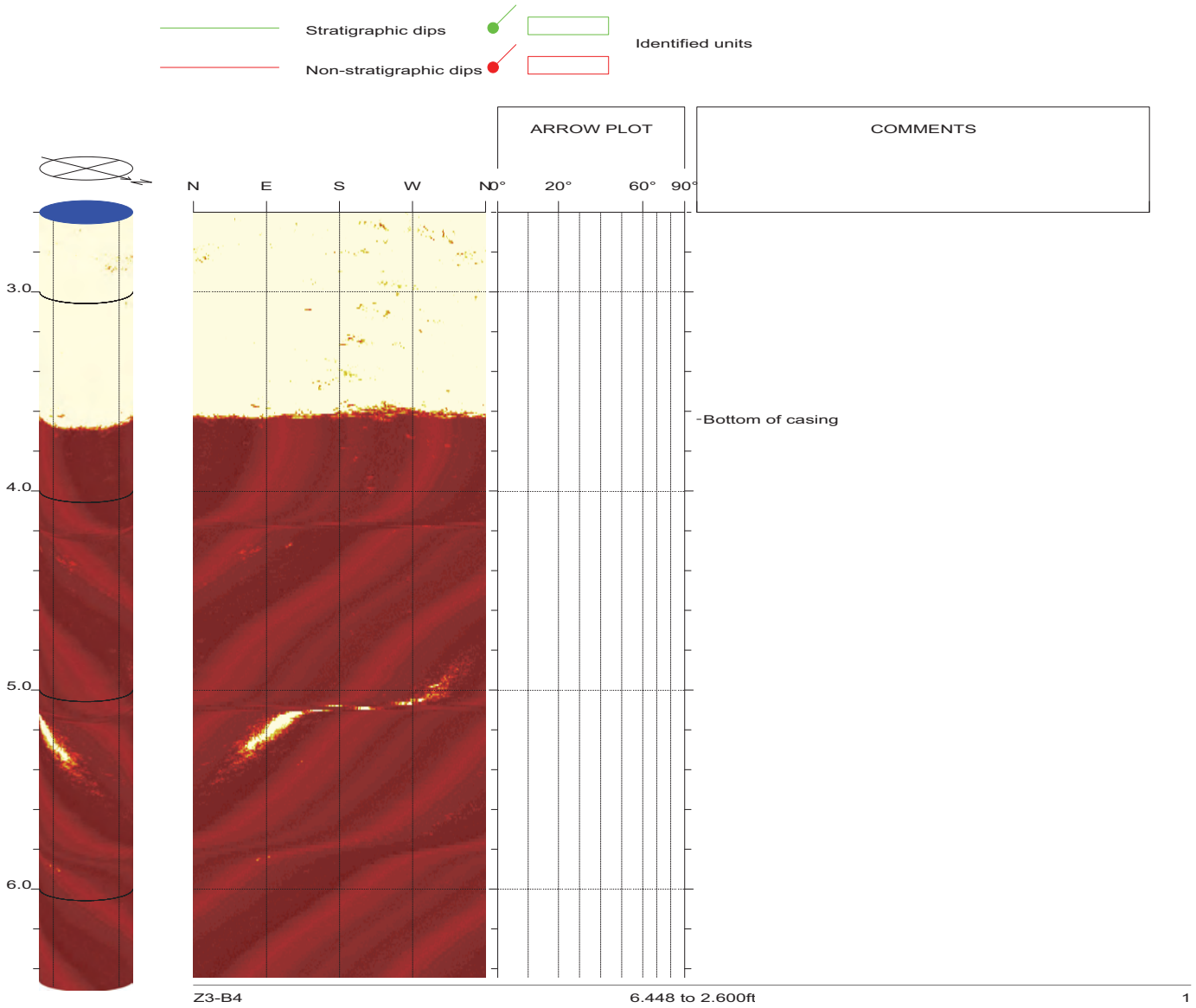

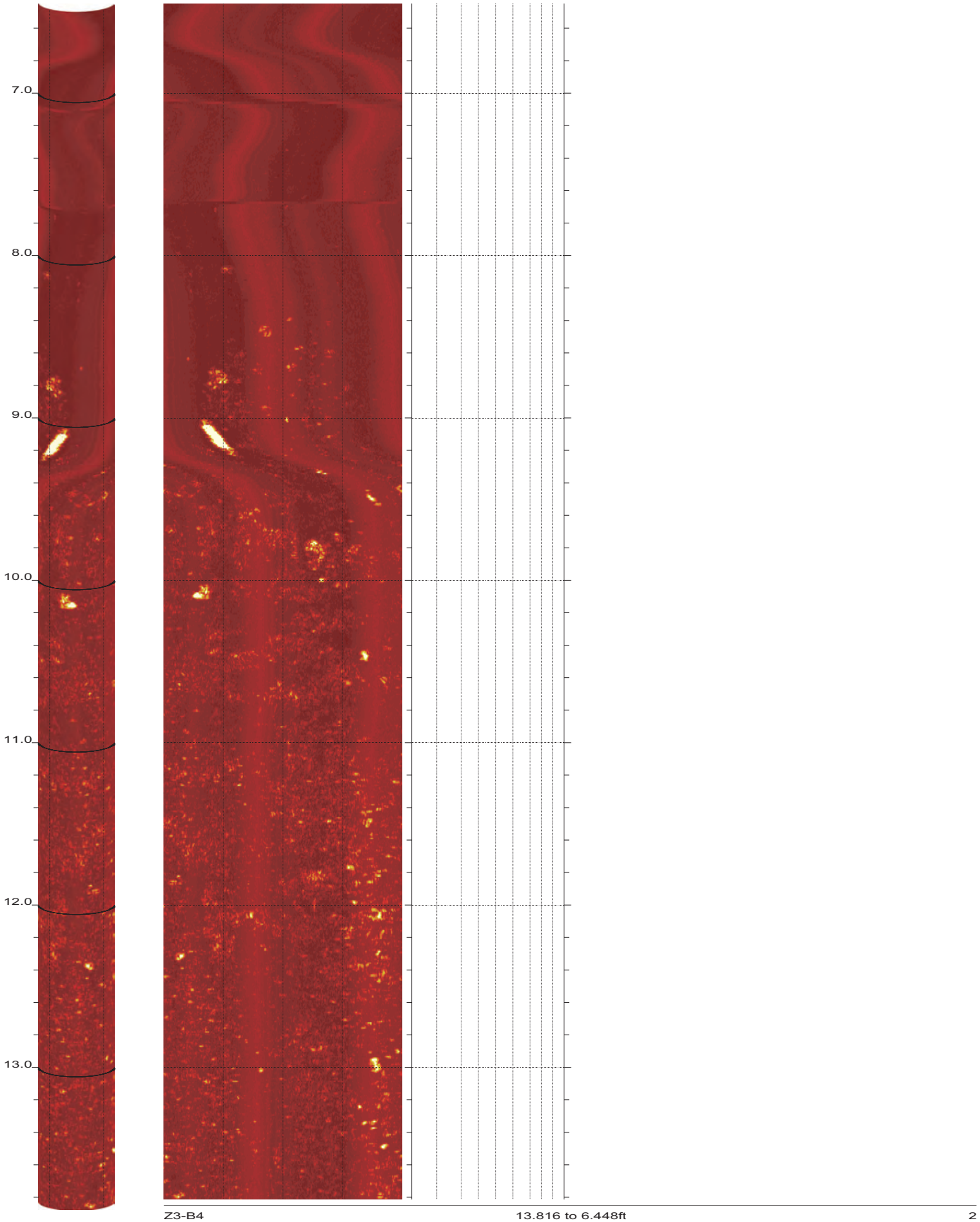
7.0
8.0
9.0
10.0
11.0
12.0
13.0
Z3-B4
13.816 to 6.448ft
2

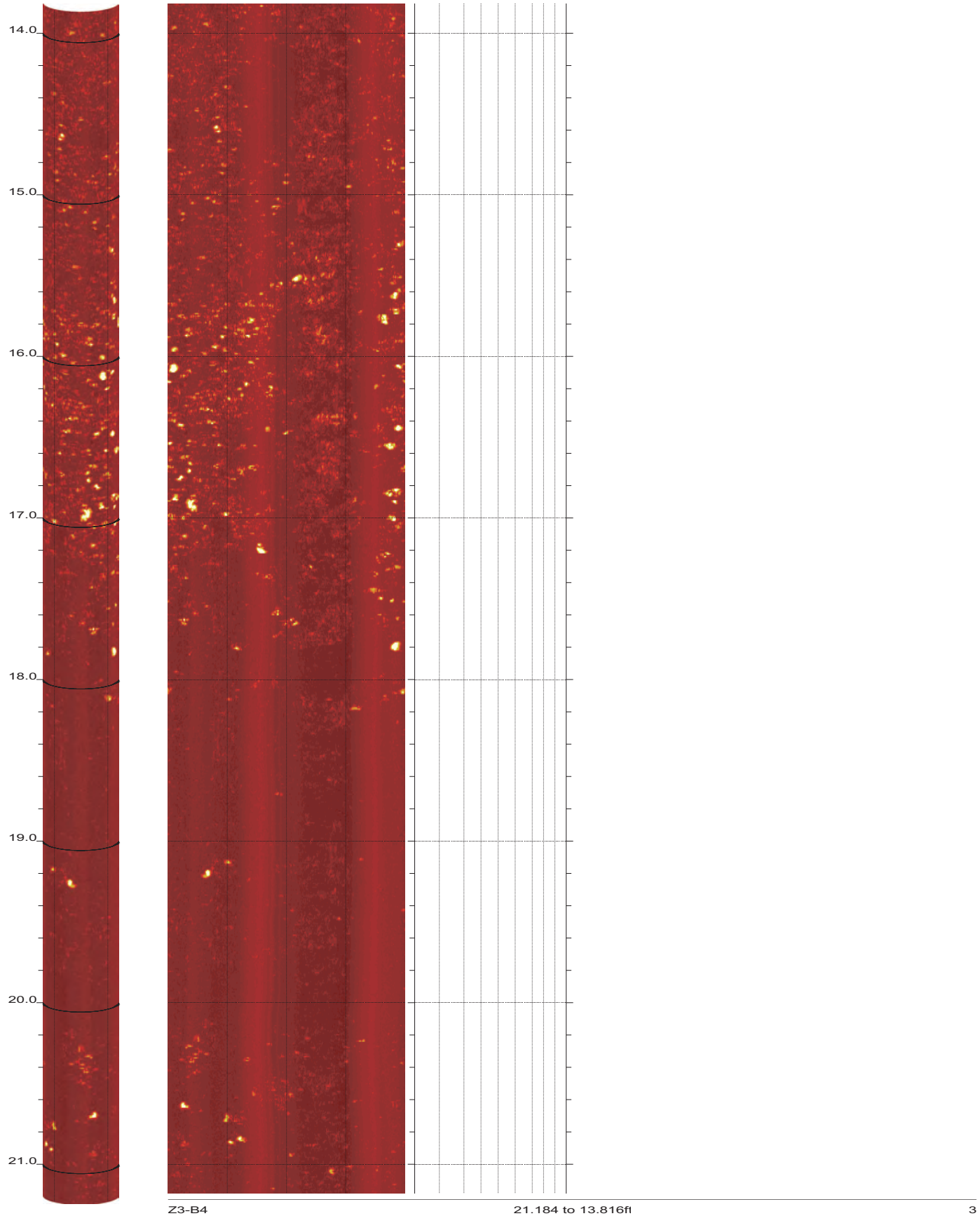


SR-710 Boring Z3-B4 Acoustic Televiewer Dips rev 1 Sheet 3 of 38

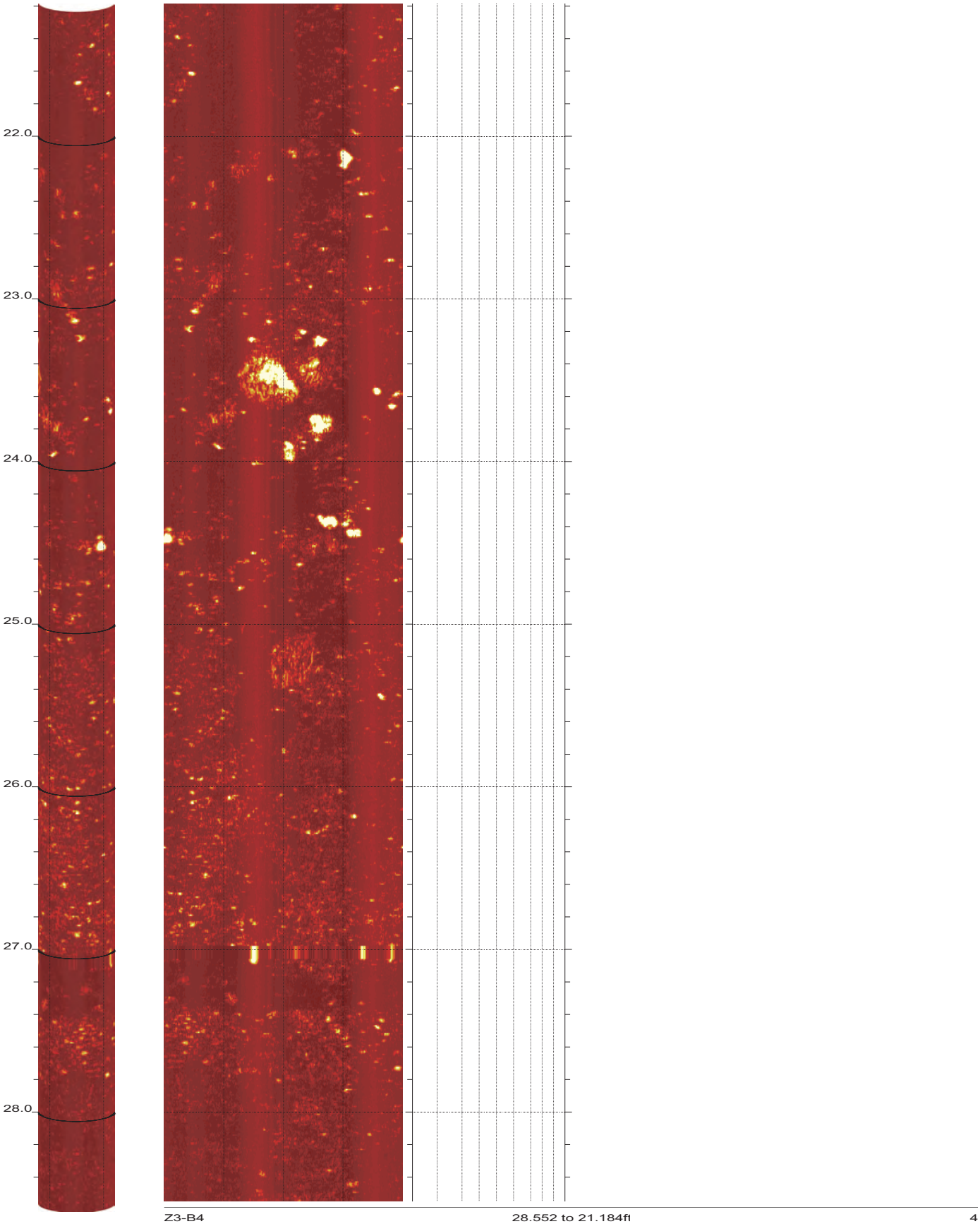


SR-710 Boring Z3-B4 Acoustic Televiewer Dips rev 1 Sheet 4 of 38

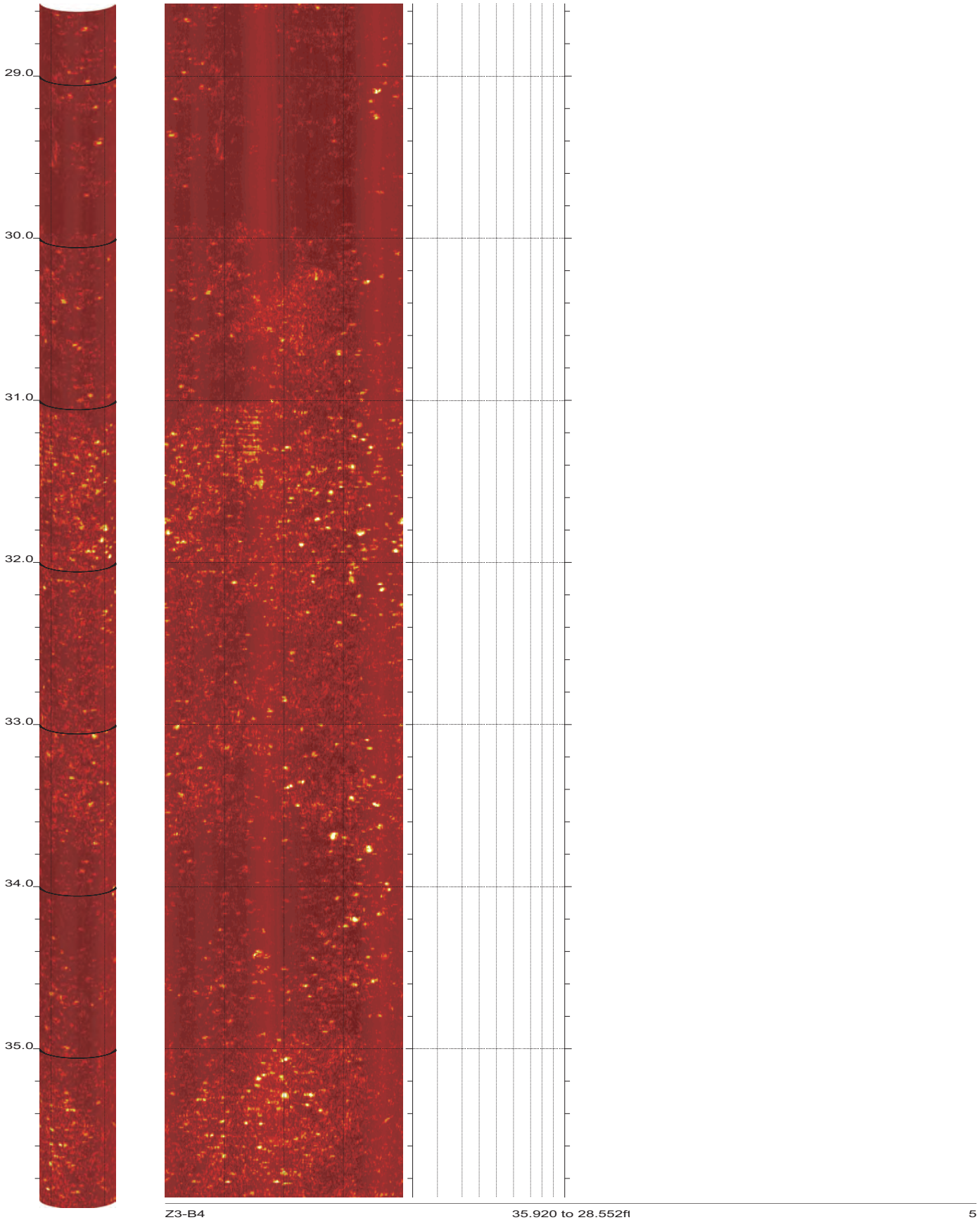


SR-710 Boring Z3-B4 Acoustic Televiewer Dips rev 1 Sheet 5 of 38

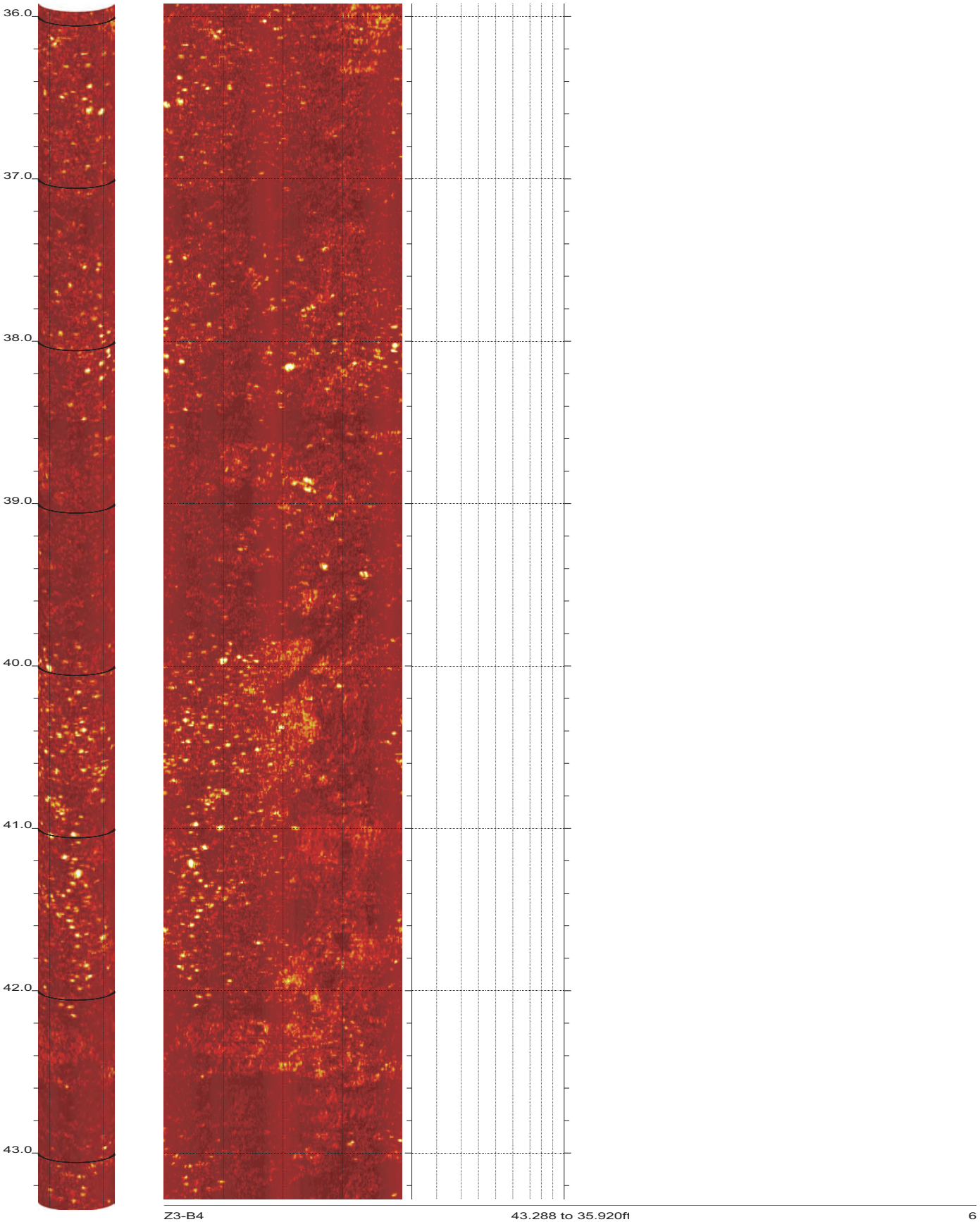


SR-710 Boring Z3-B4 Acoustic Televiewer Dips rev 1 Sheet 6 of 38

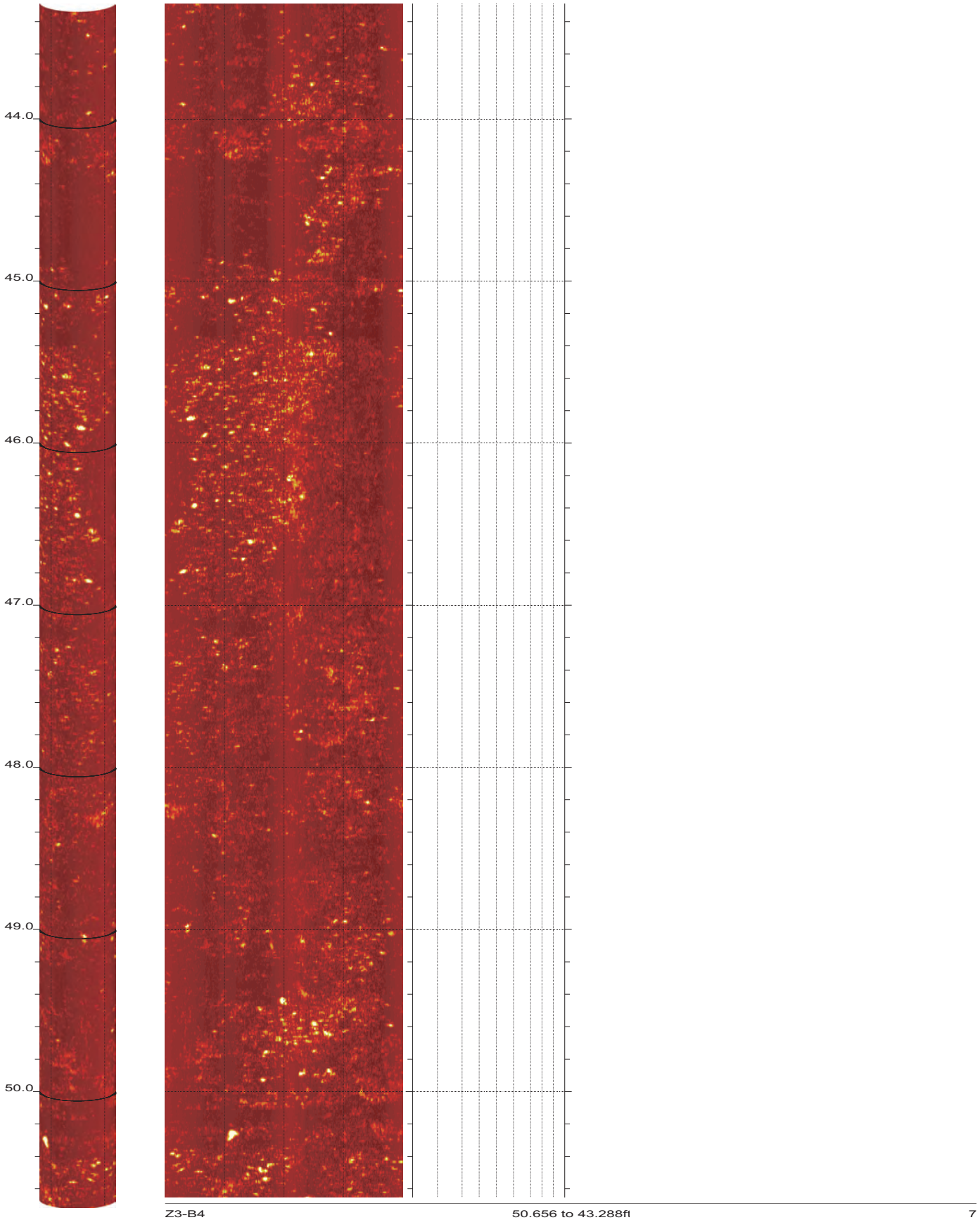
44.0
45.0
46.0
47.0
48.0
49.0
50.0
Z3-B4
50.656 to 43.288ft
7

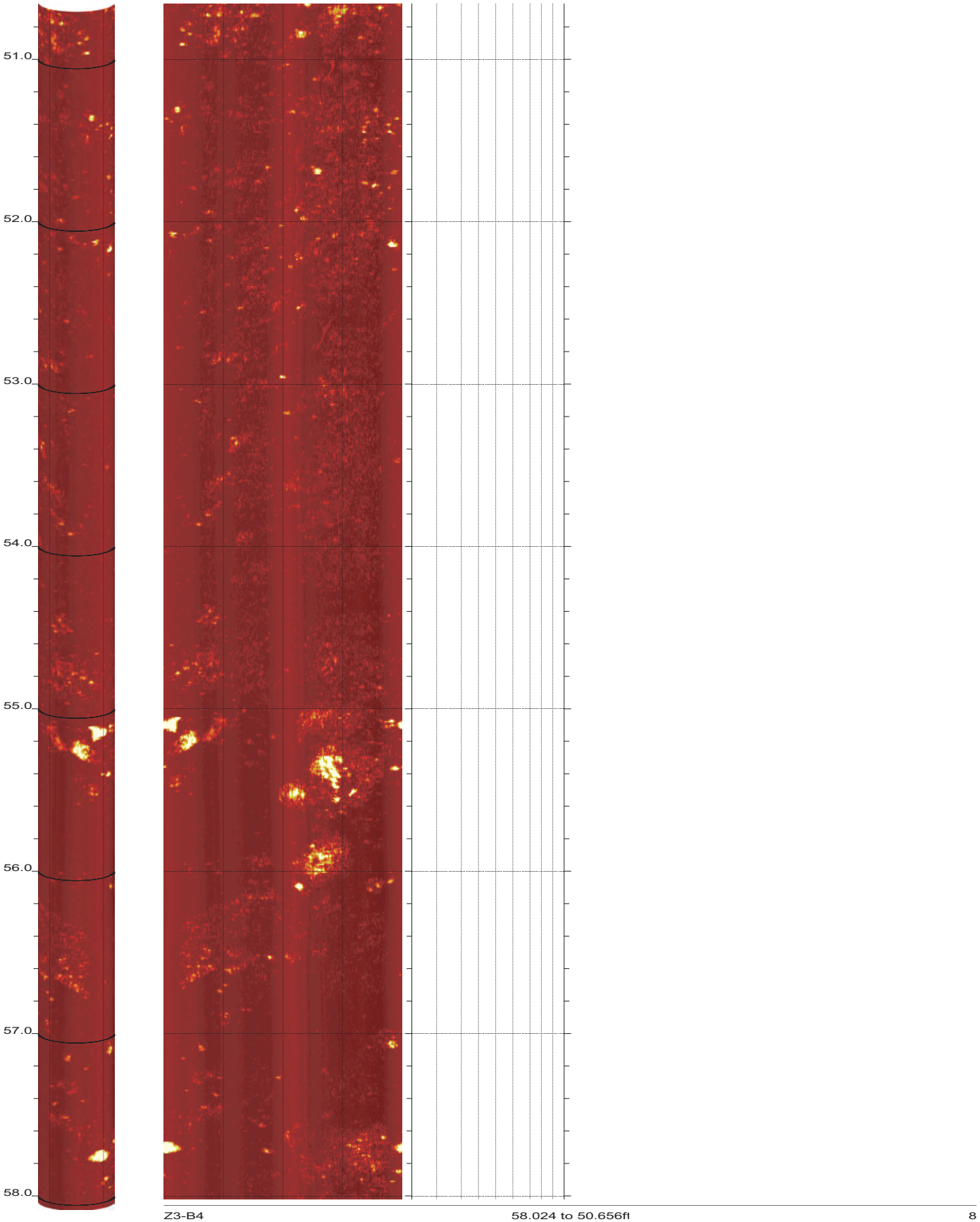


SR-710 Boring Z3-B4 Acoustic Televiewer Dips rev 1 Sheet 8 of 38

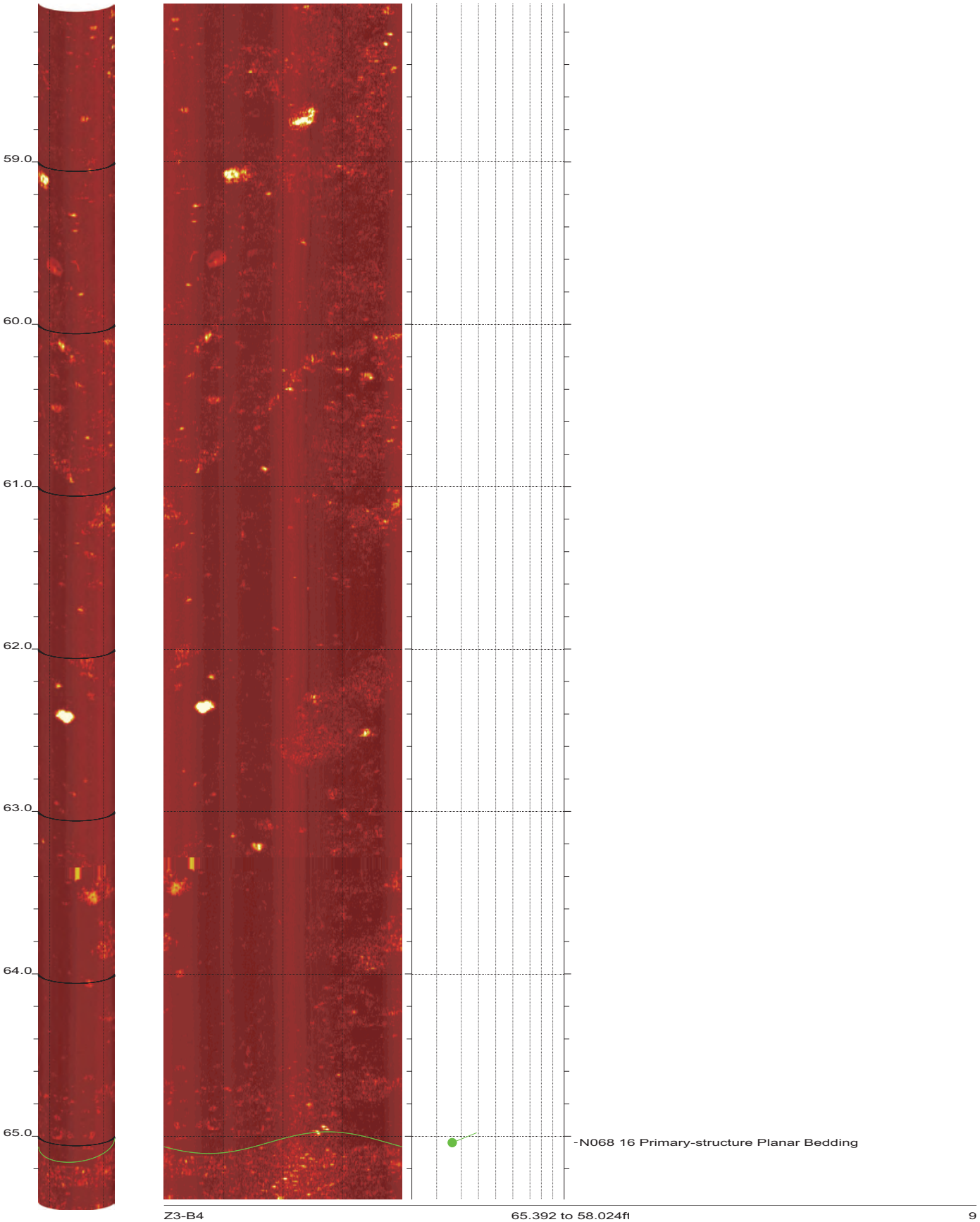


SR-710 Boring Z3-B4 Acoustic Televiewer Dips rev 1 Sheet 9 of 38

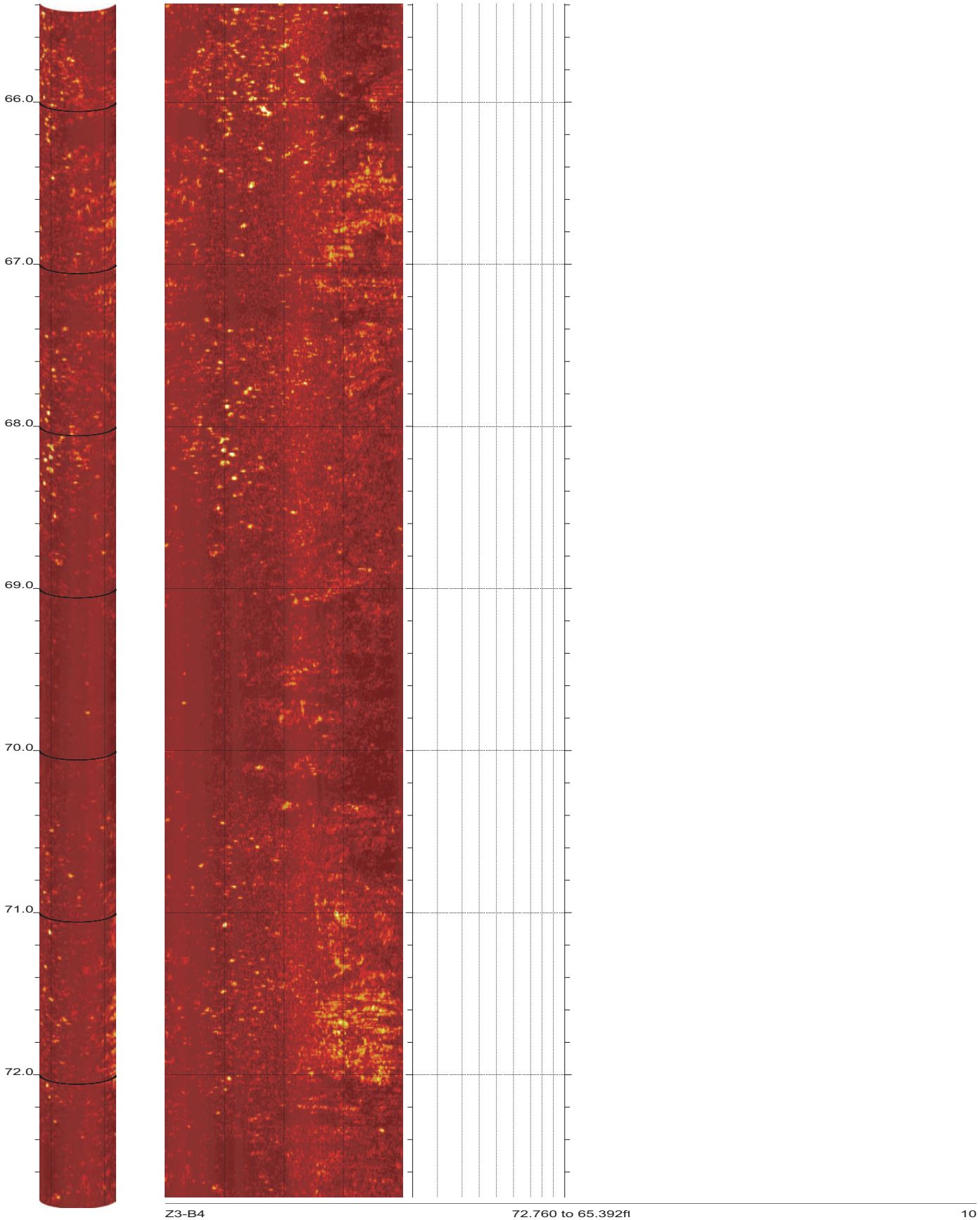


SR-710 Boring Z3-B4 Acoustic Televiewer Dips rev 1 Sheet 10 of 38

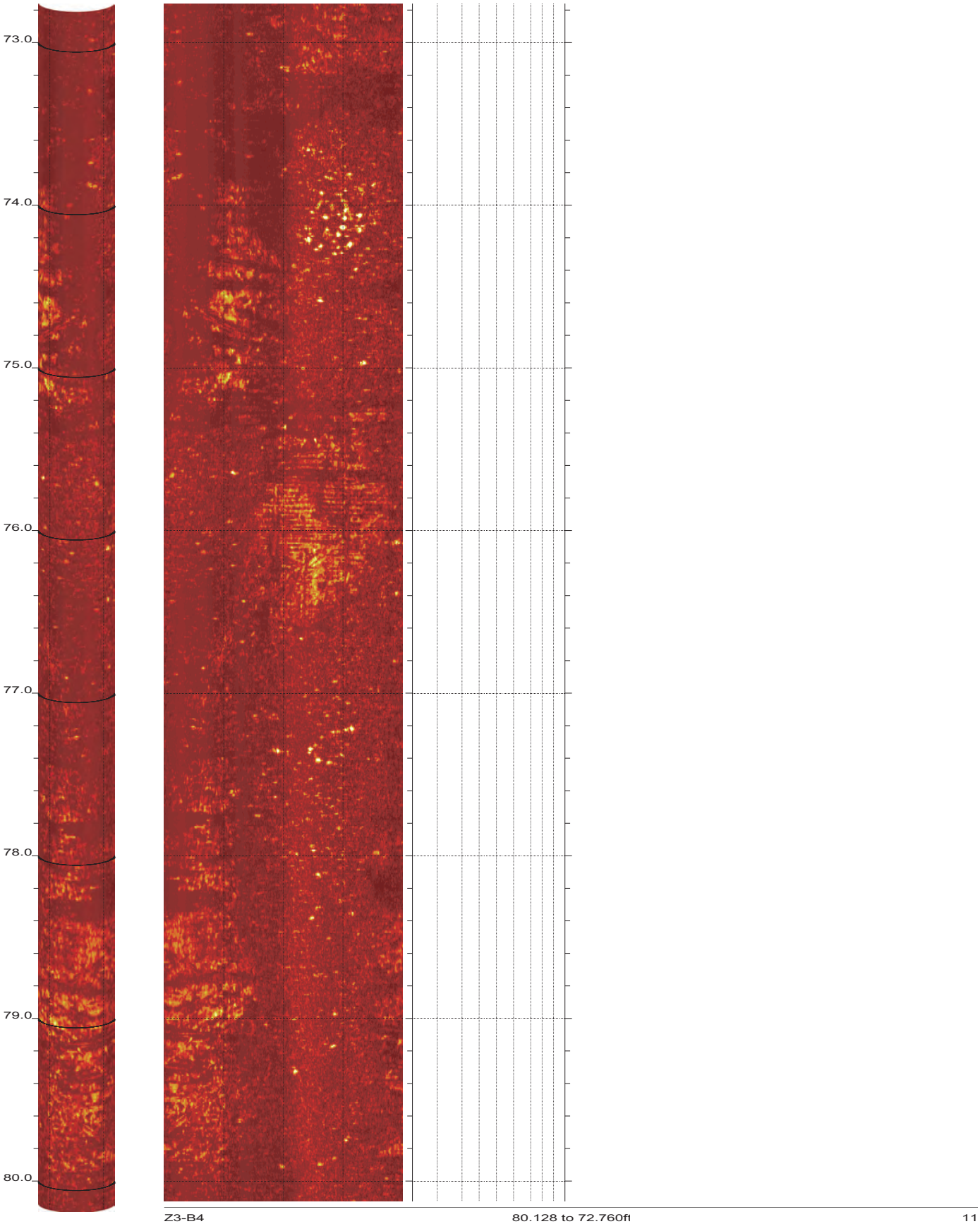
73.0
74.0
75.0
76.0
77.0
78.0
79.0
80.0
Z3-B4
80.128 to 72.760ft
11

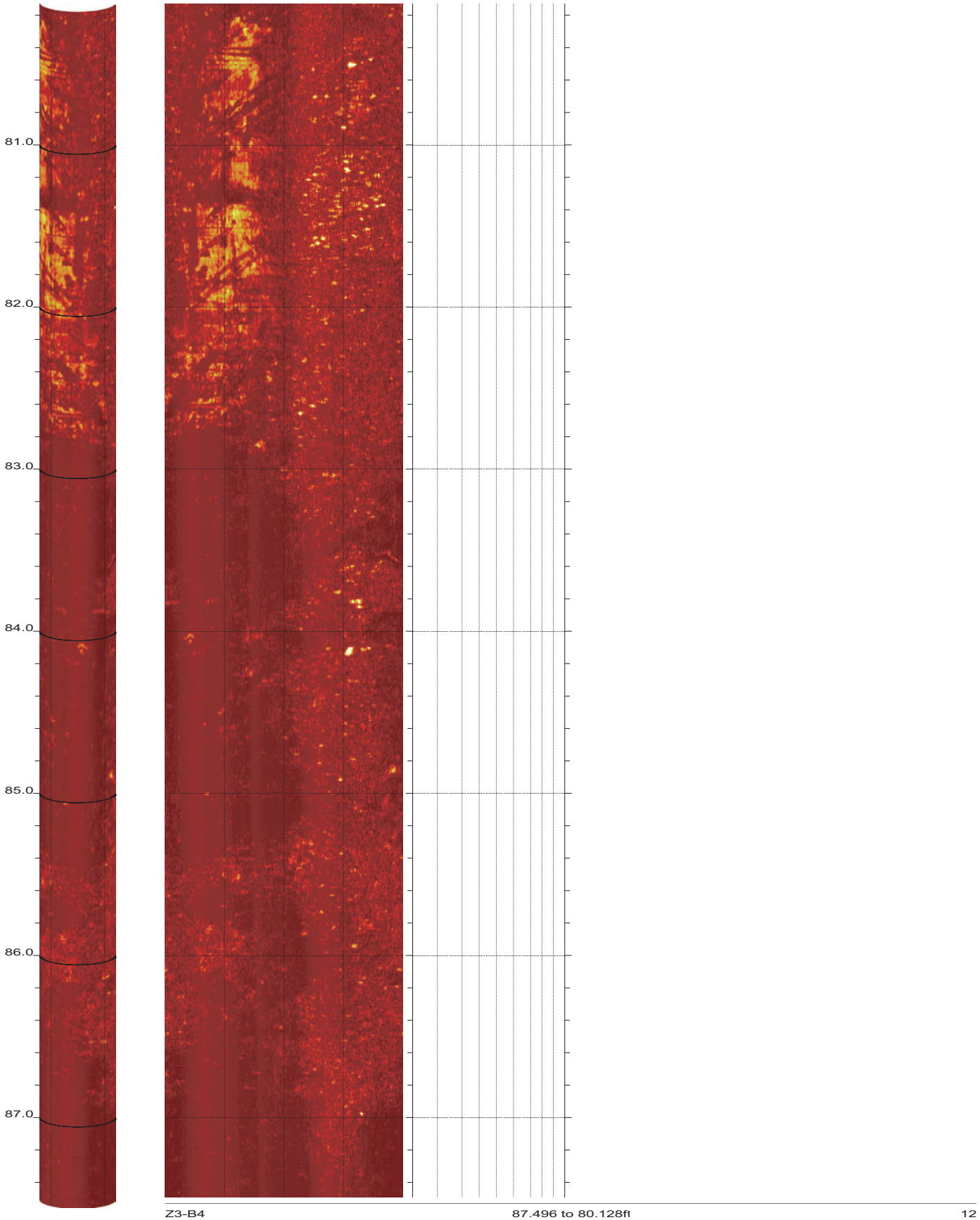
81.0
82.0
83.0
84.0
85.0
86.0
87.0
Z3-B4
87.496 to 80.128ft
12

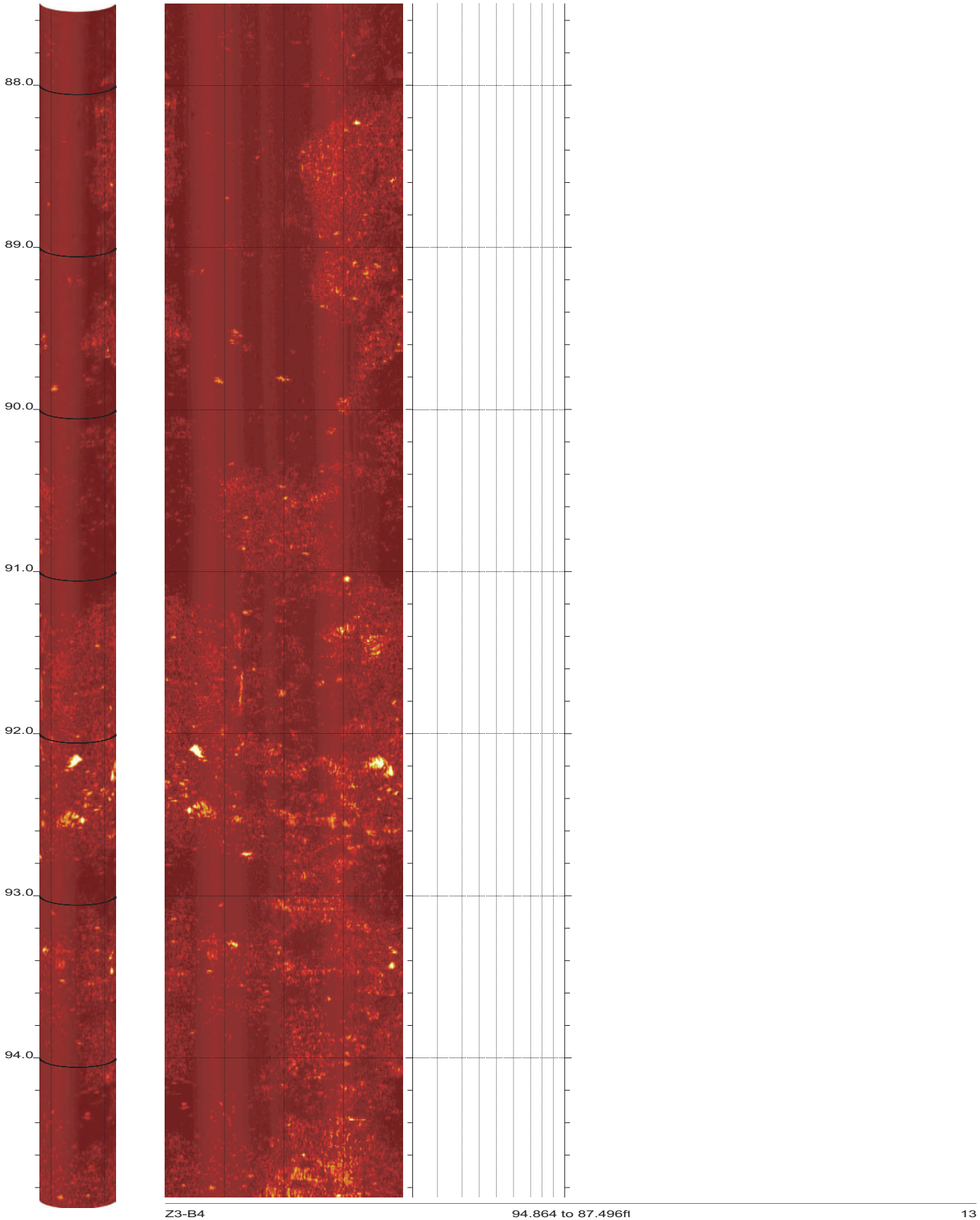
88.0
89.0
90.0
91.0
92.0
93.0
94.0
Z3-B4
94.864 to 87.496fl
13

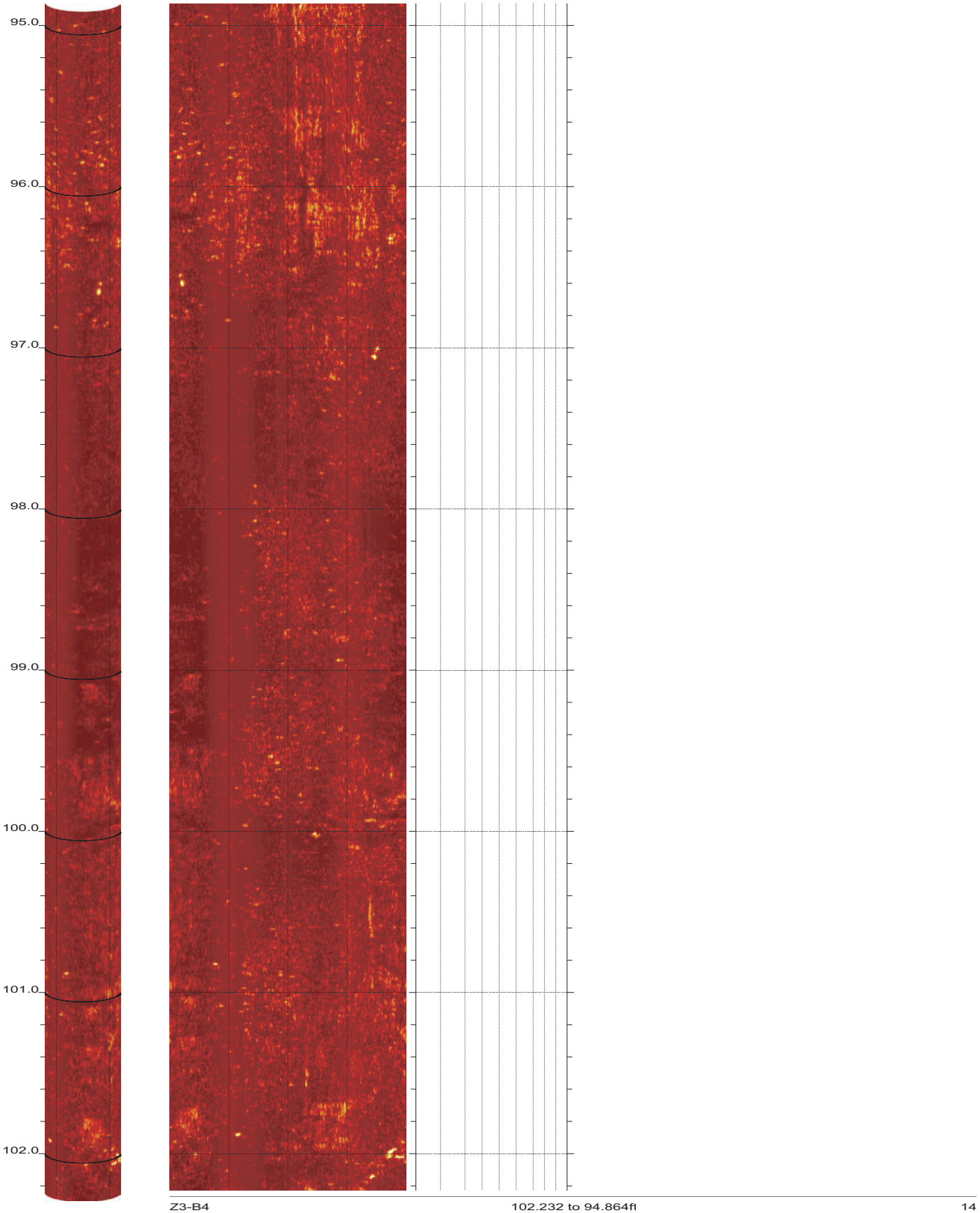
95.0
96.0
97.0
98.0
99.0
100.0
101.0
102.0
Z3-B4
102.232 to 94.864ft
14

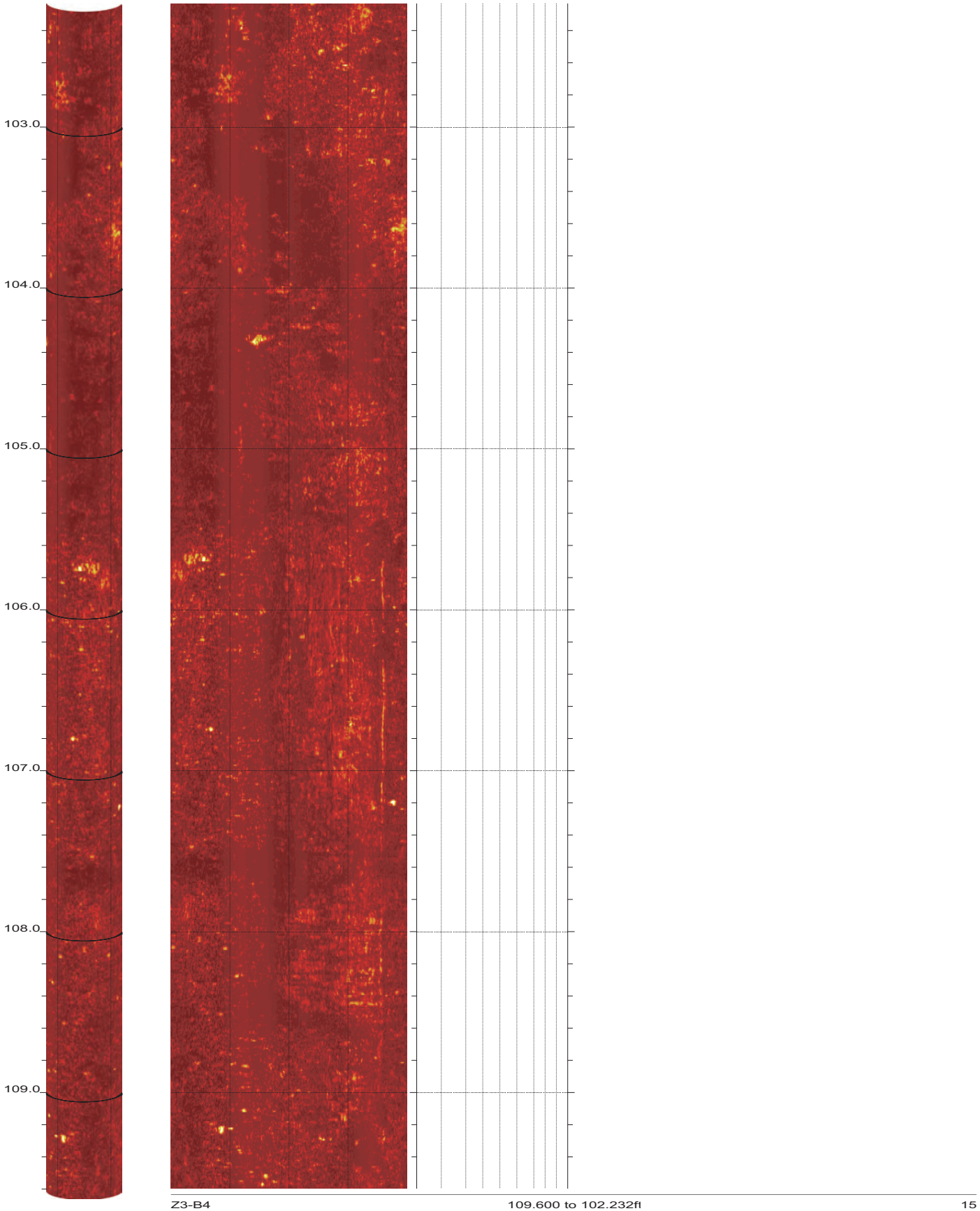


SR-710 Boring Z3-B4 Acoustic Televiewer Dips rev 1 Sheet 15 of 38

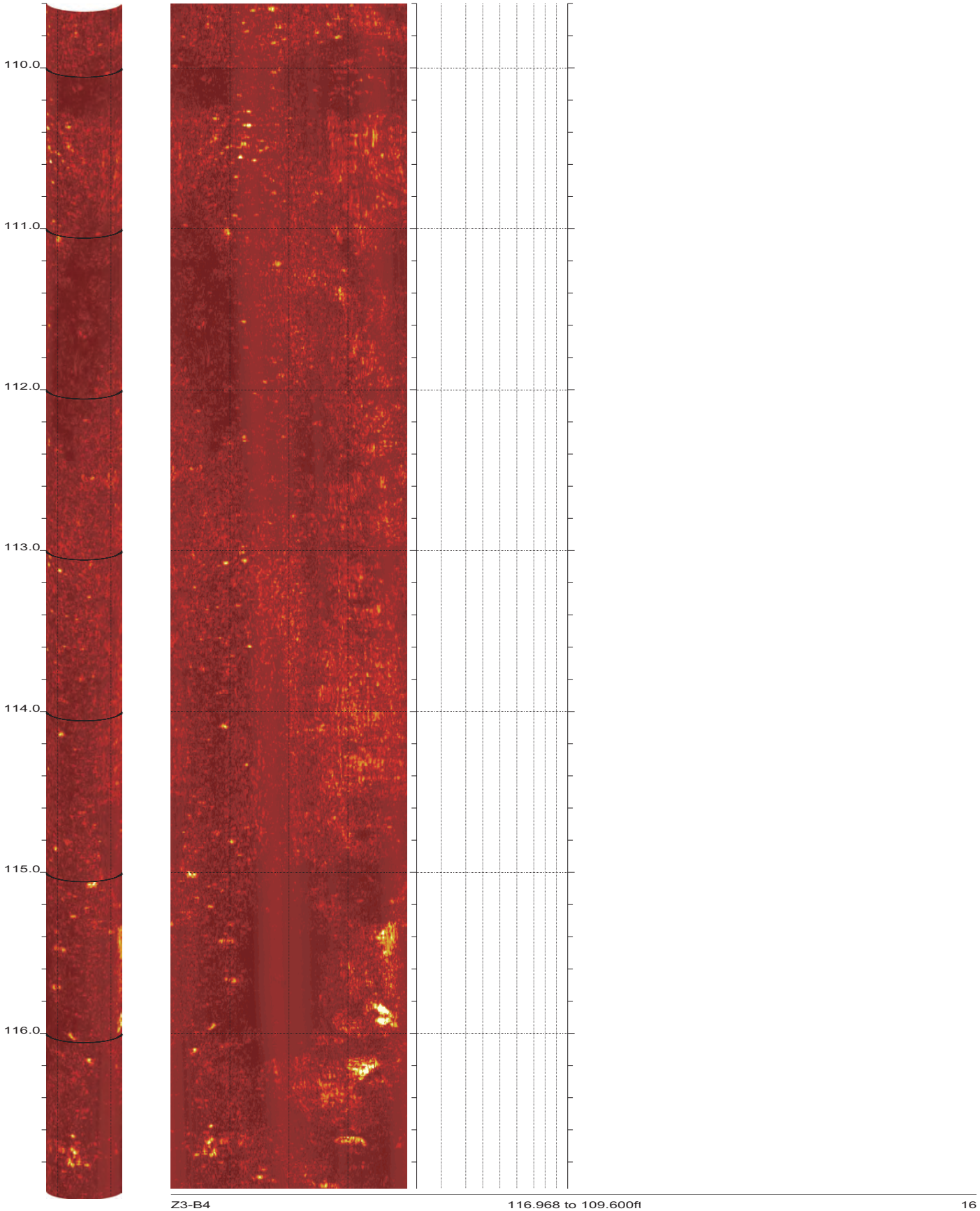
110.0
111.0
112.0
113.0
114.0
115.0
116.0
Z3-B4
116.968 to 109.600ft
16

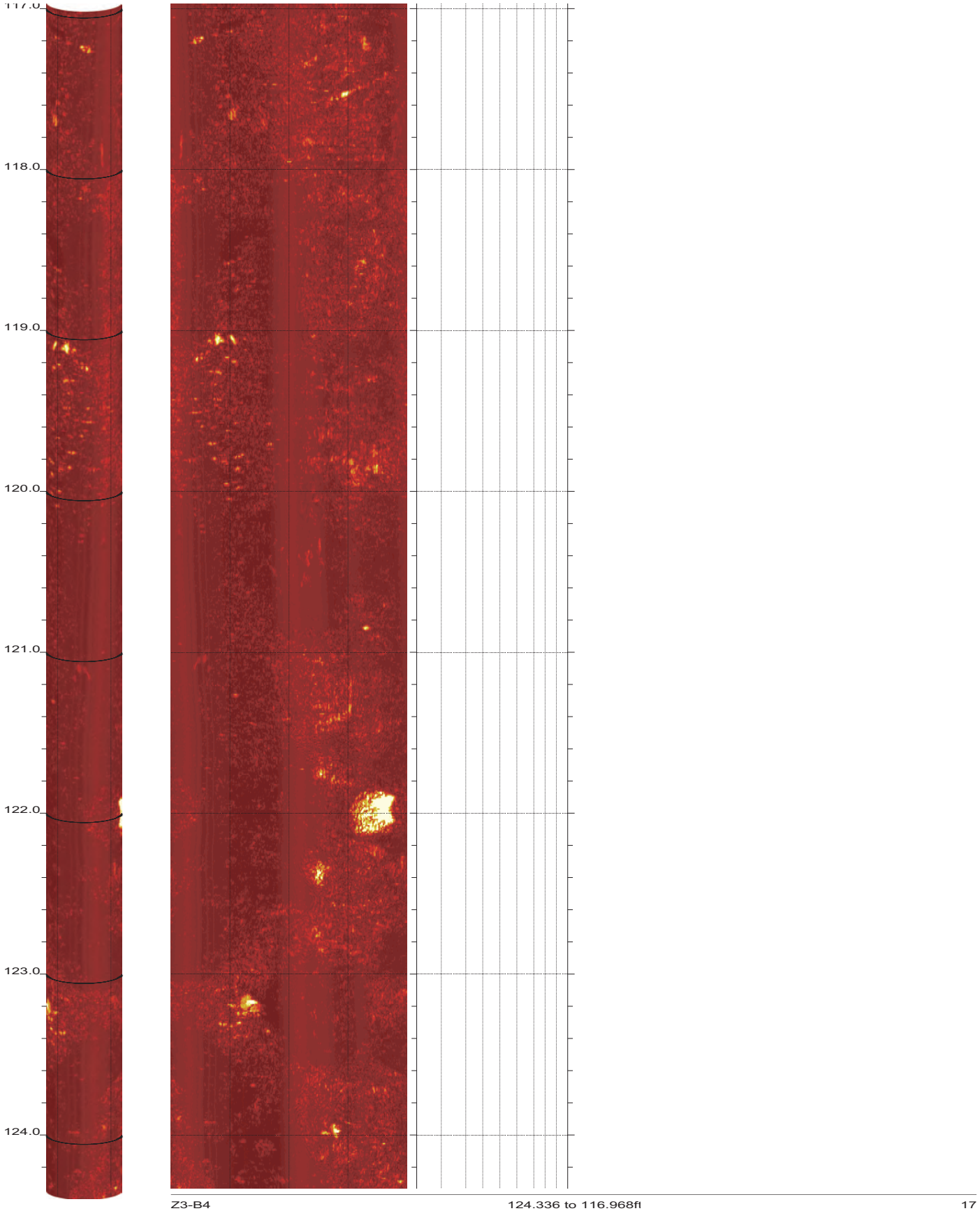
117.0
118.0
119.0
120.0
121.0
122.0
123.0
124.0
Z3-B4
124.336 to 116.968ft
17

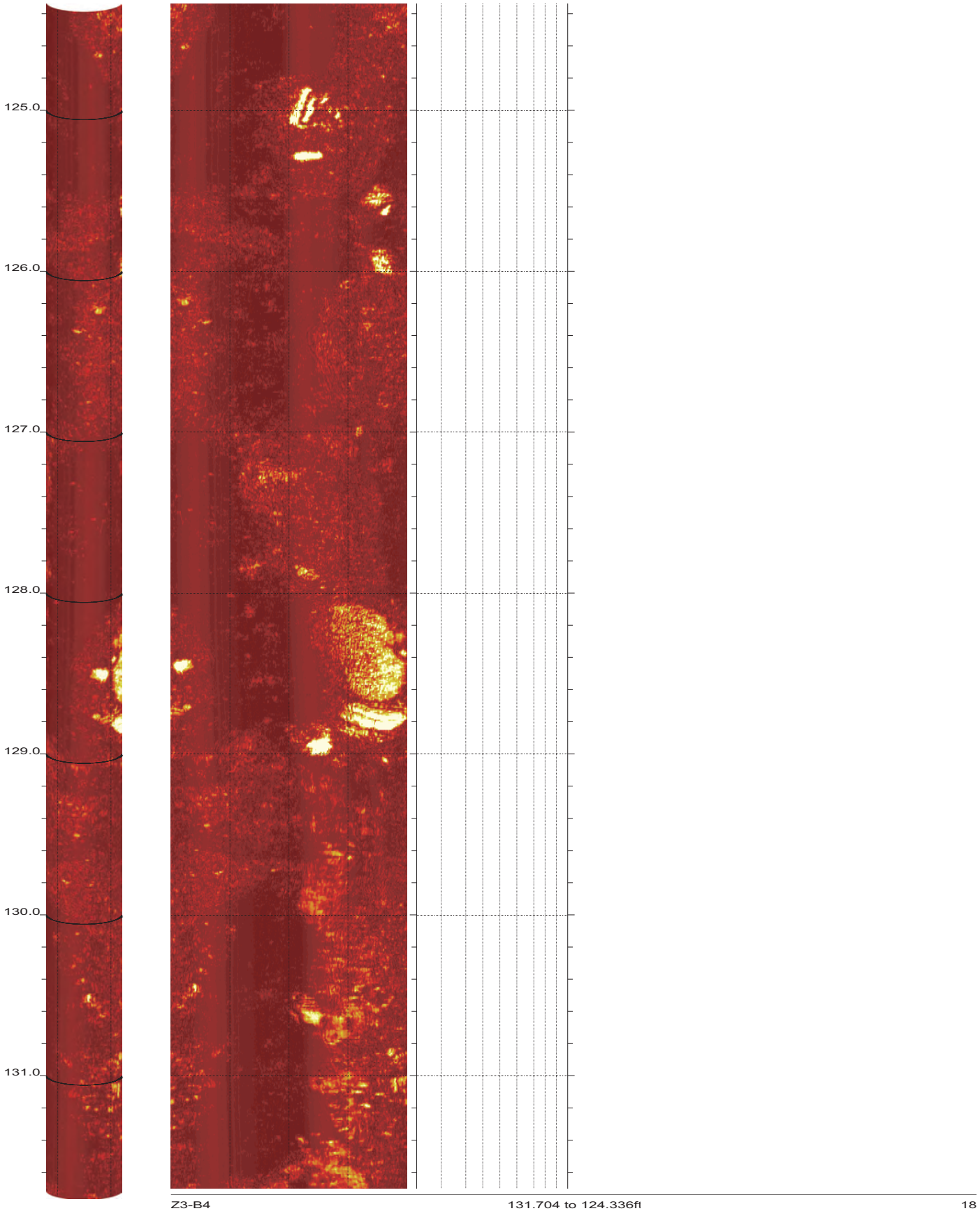


SR-710 Boring Z3-B4 Acoustic Televiewer Dips rev 1 Sheet 18 of 38

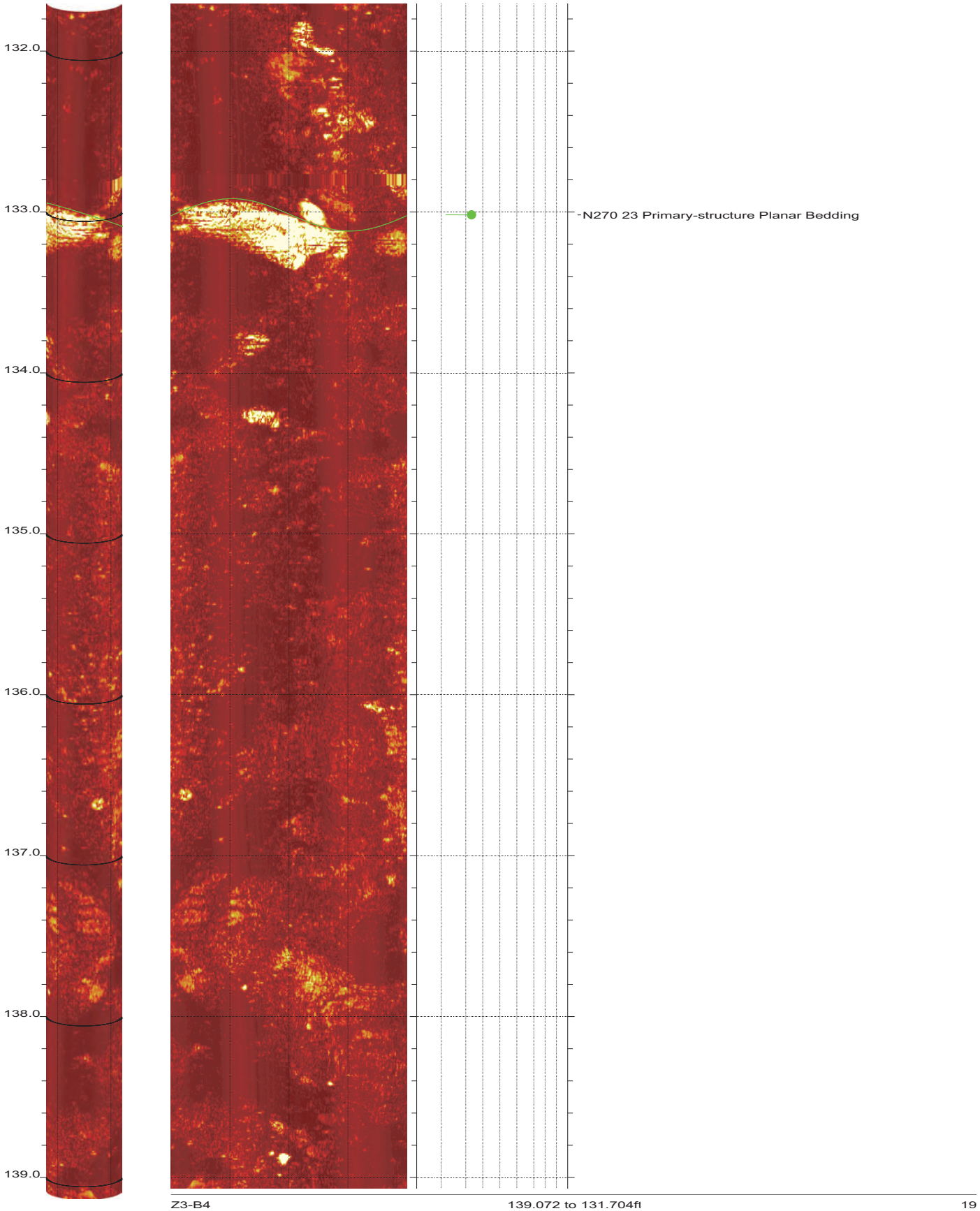


SR-710 Boring Z3-B4 Acoustic Televiewer Dips rev 1 Sheet 19 of 38

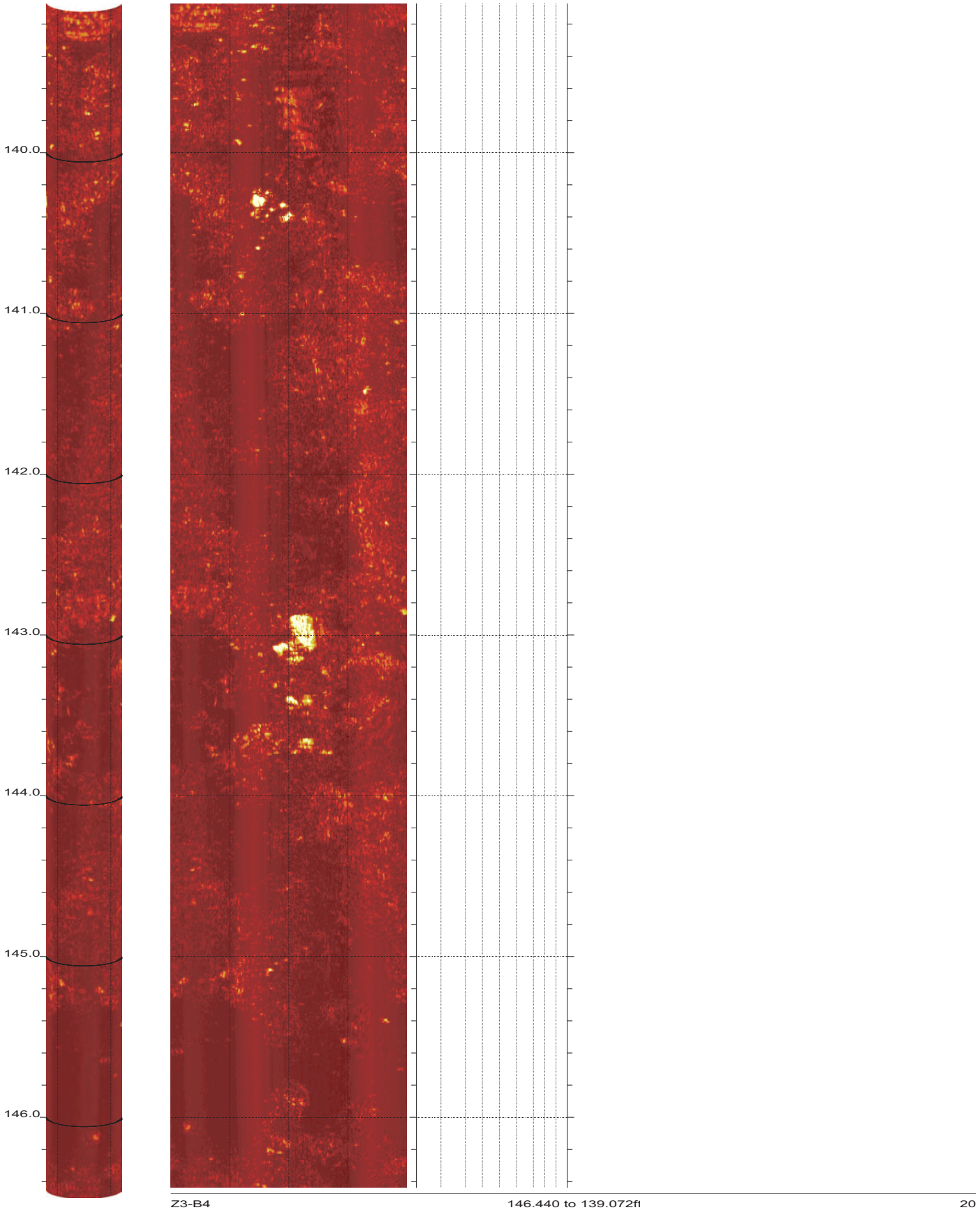


SR-710 Boring Z3-B4 Acoustic Televiewer Dips rev 1 Sheet 20 of 38

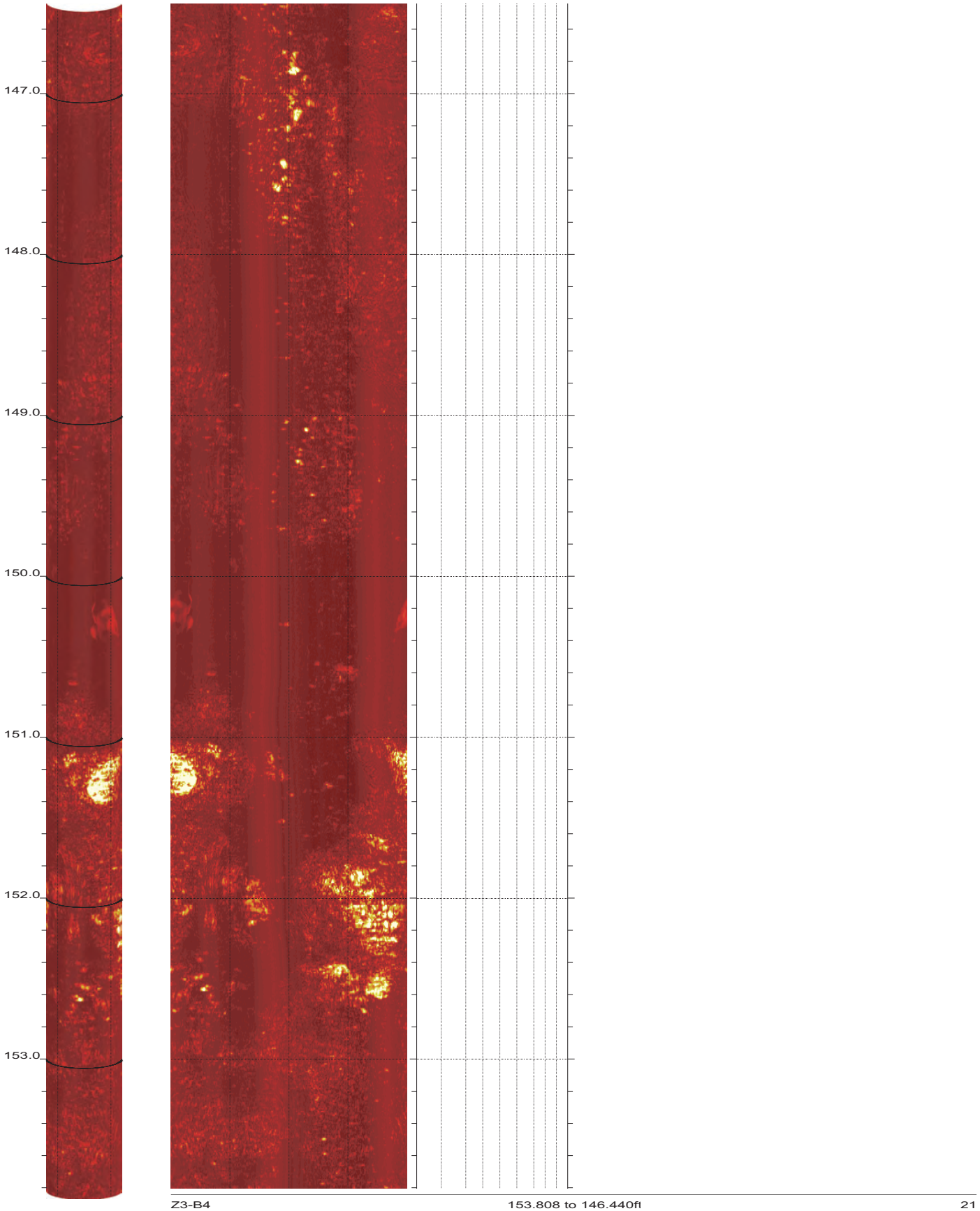


SR-710 Boring Z3-B4 Acoustic Televiewer Dips rev 1 Sheet 21 of 38

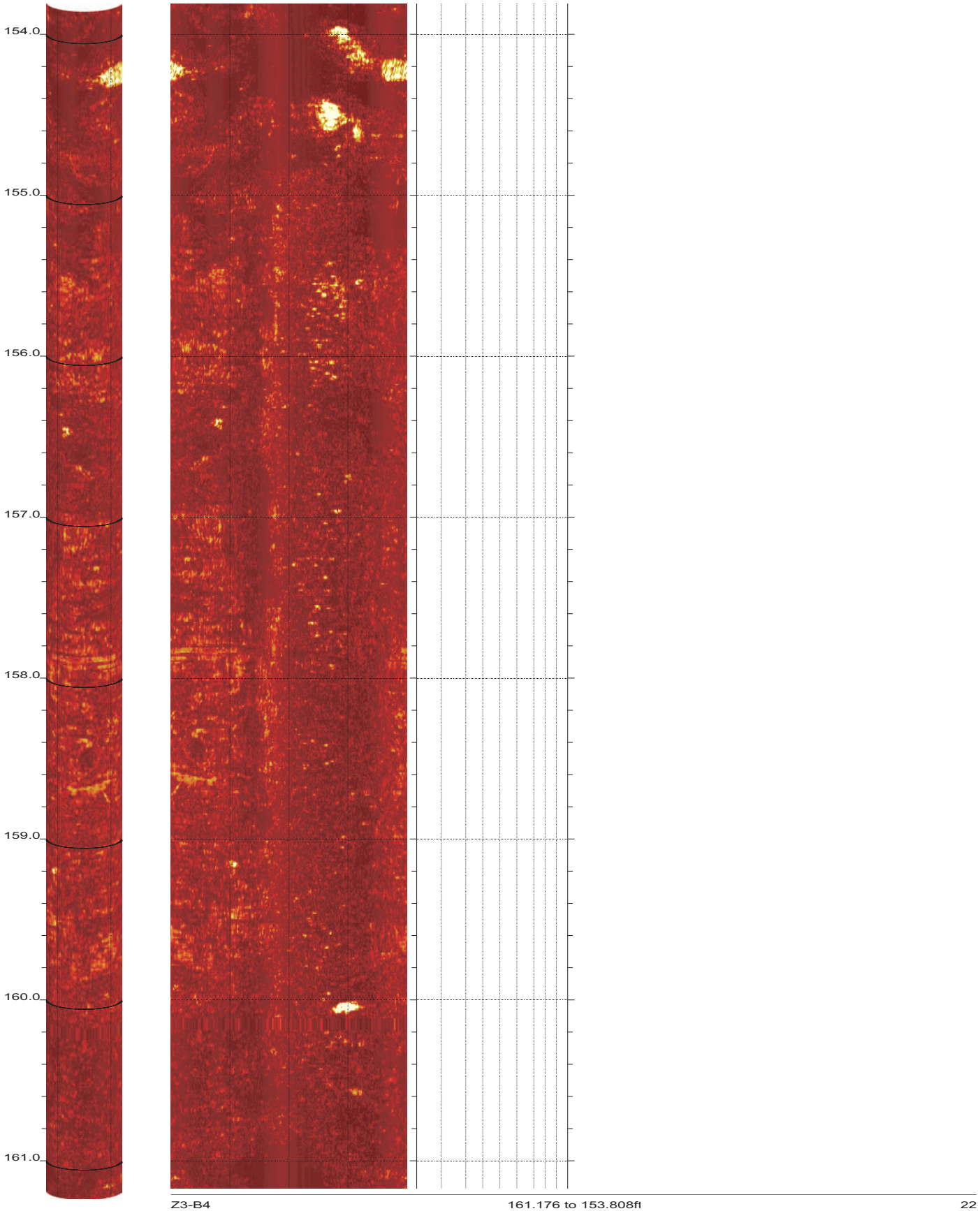
154.0
155.0
156.0
157.0
158.0
159.0
160.0
161.0
Z3-B4
161.176 to 153.808ft
22

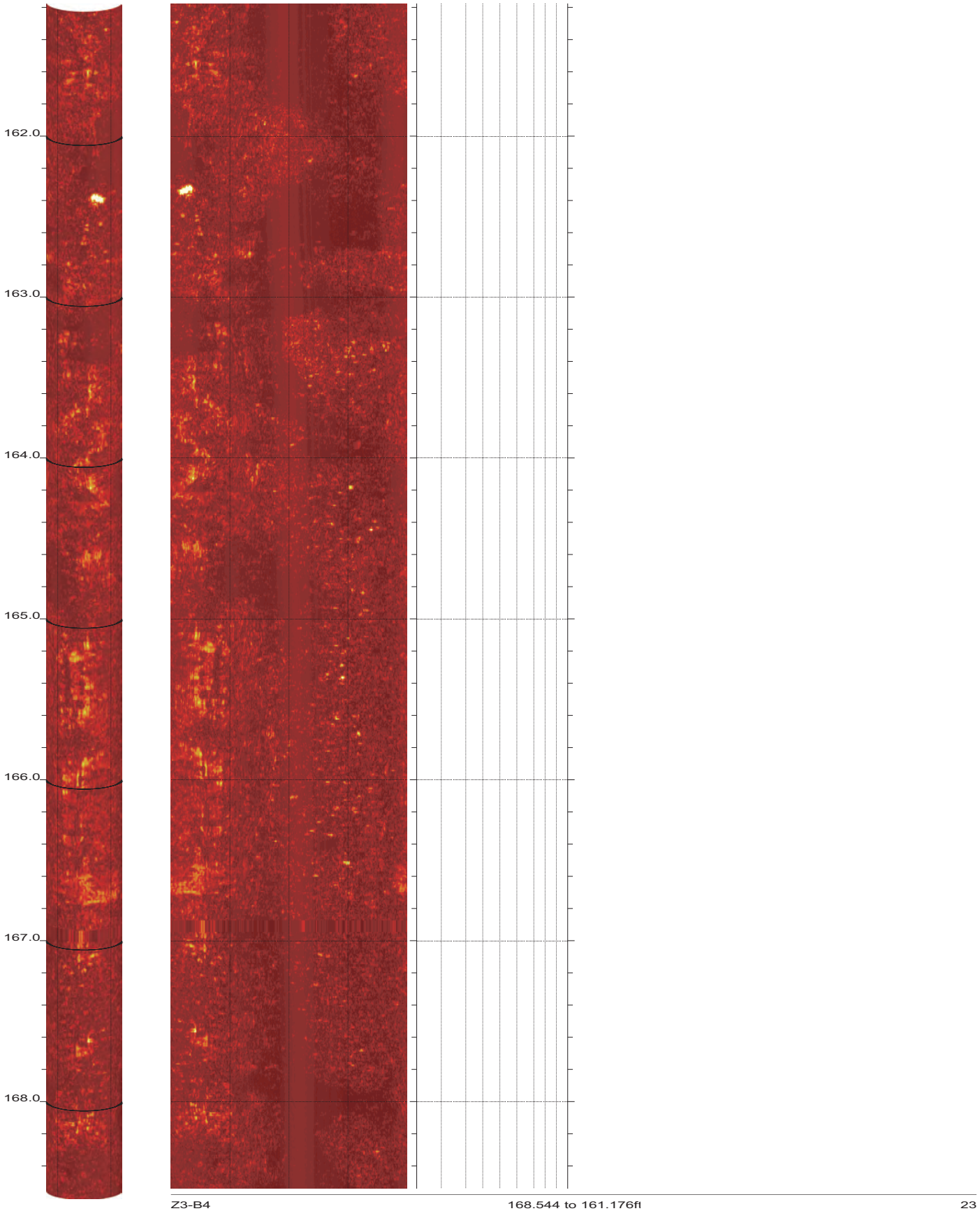
162.0
163.0
164.0
165.0
166.0
167.0
168.0
Z3-B4
168.544 to 161.176fl
23

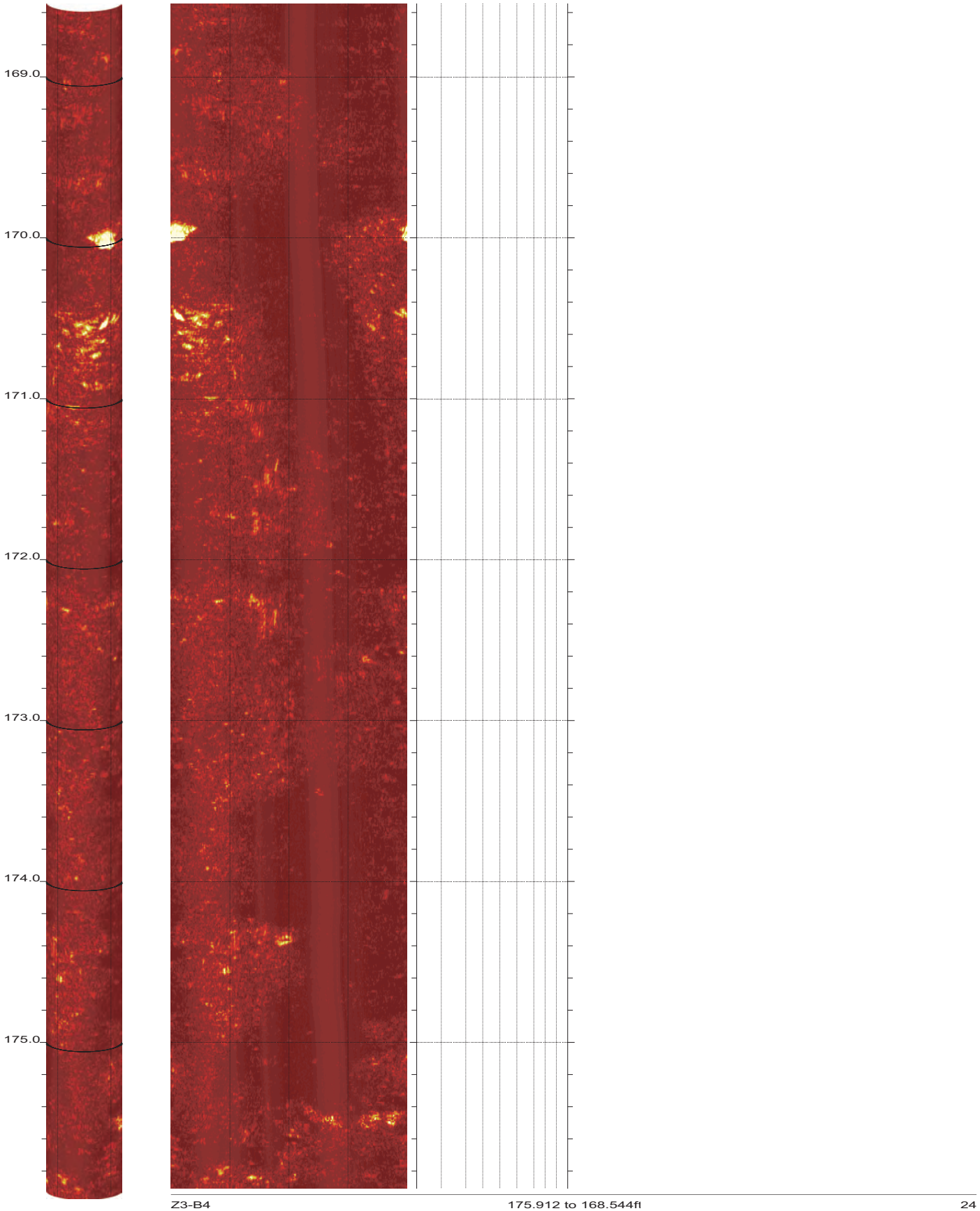
169.0
170.0
171.0
172.0
173.0
174.0
175.0
Z3-B4
175.912 to 168.544fl
24

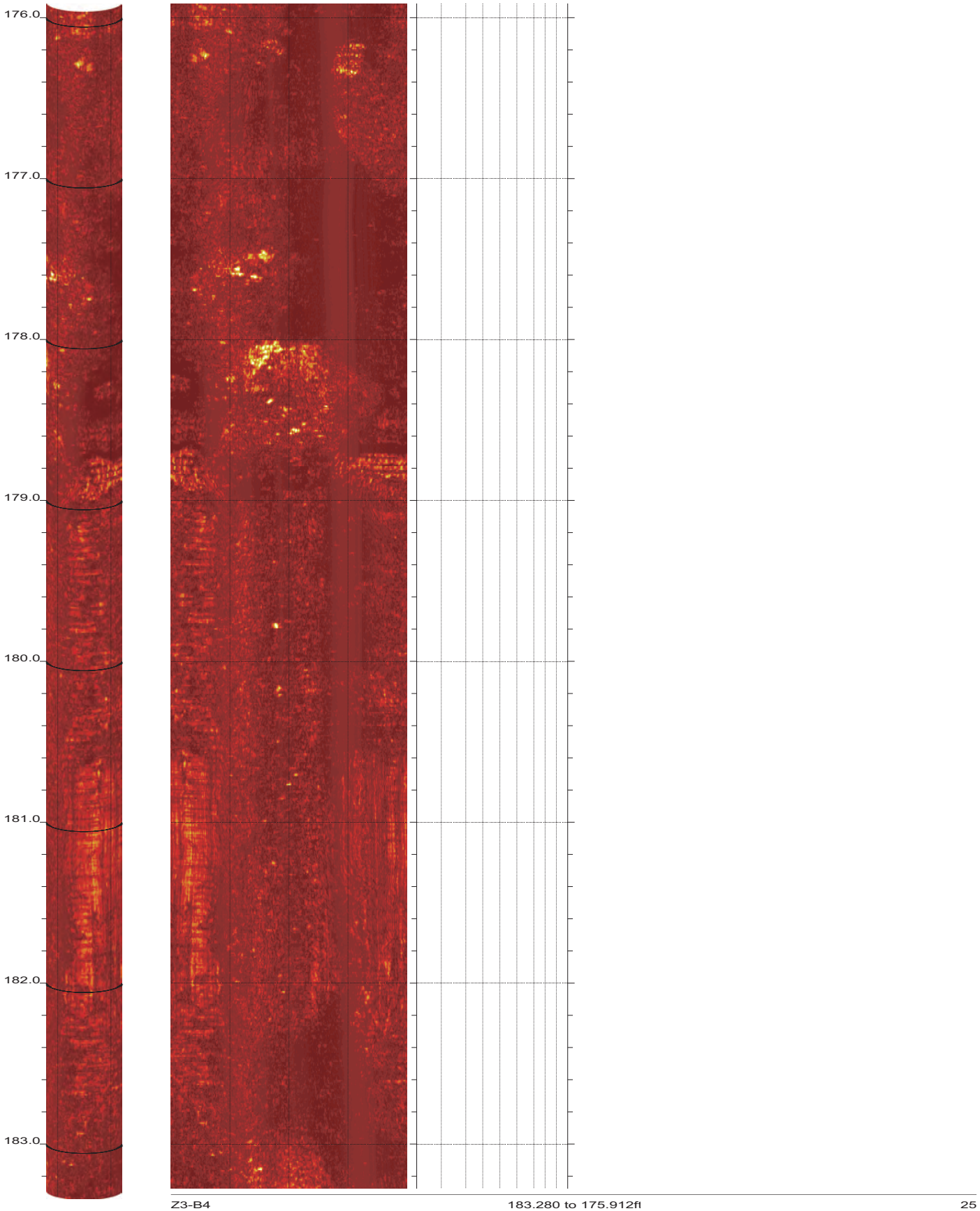
176.0
177.0
178.0
179.0
180.0
181.0
182.0
183.0
Z3-B4
183.280 to 175.912fl
25

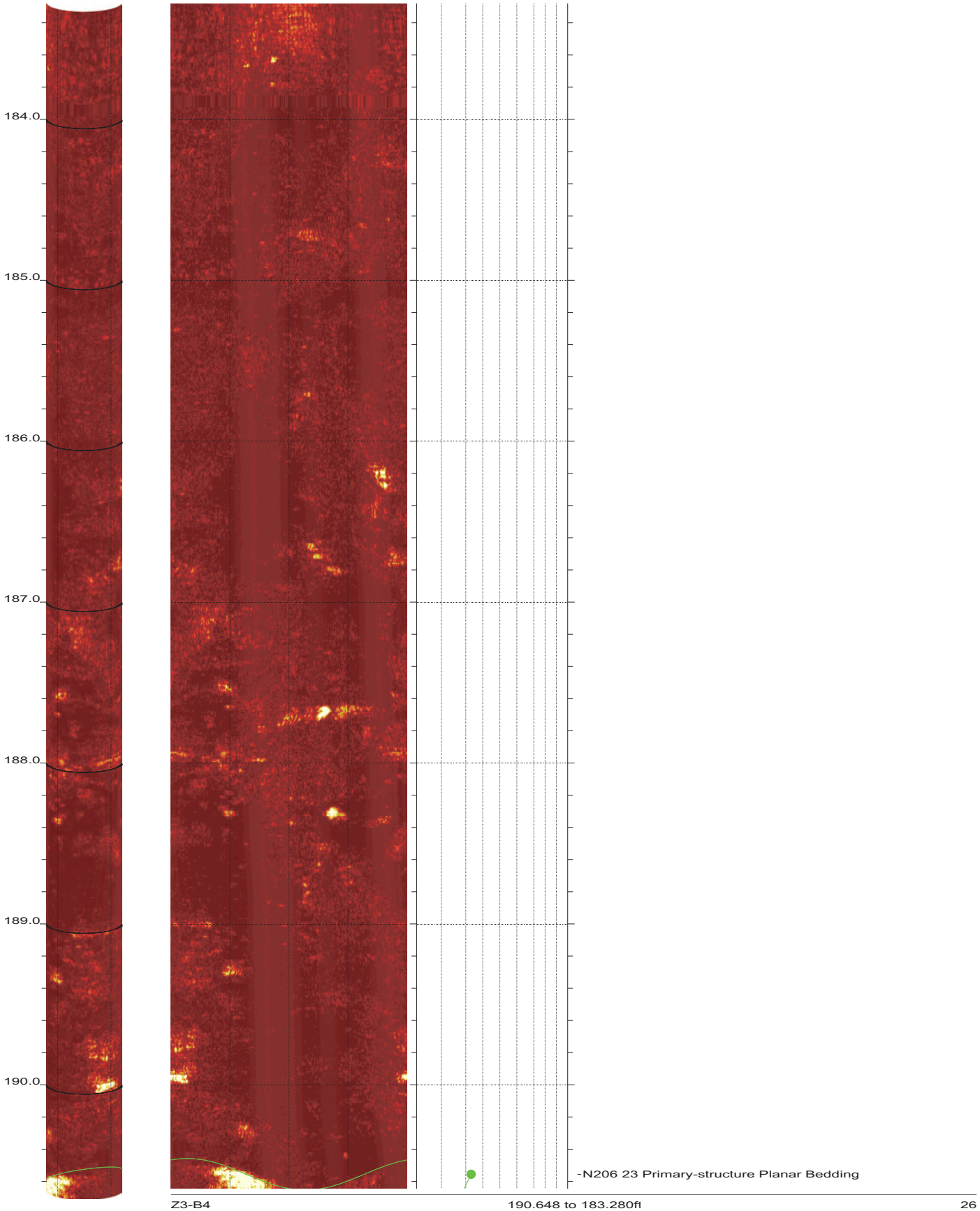


SR-710 Boring Z3-B4 Acoustic Televiewer Dips rev 1 Sheet 26 of 38

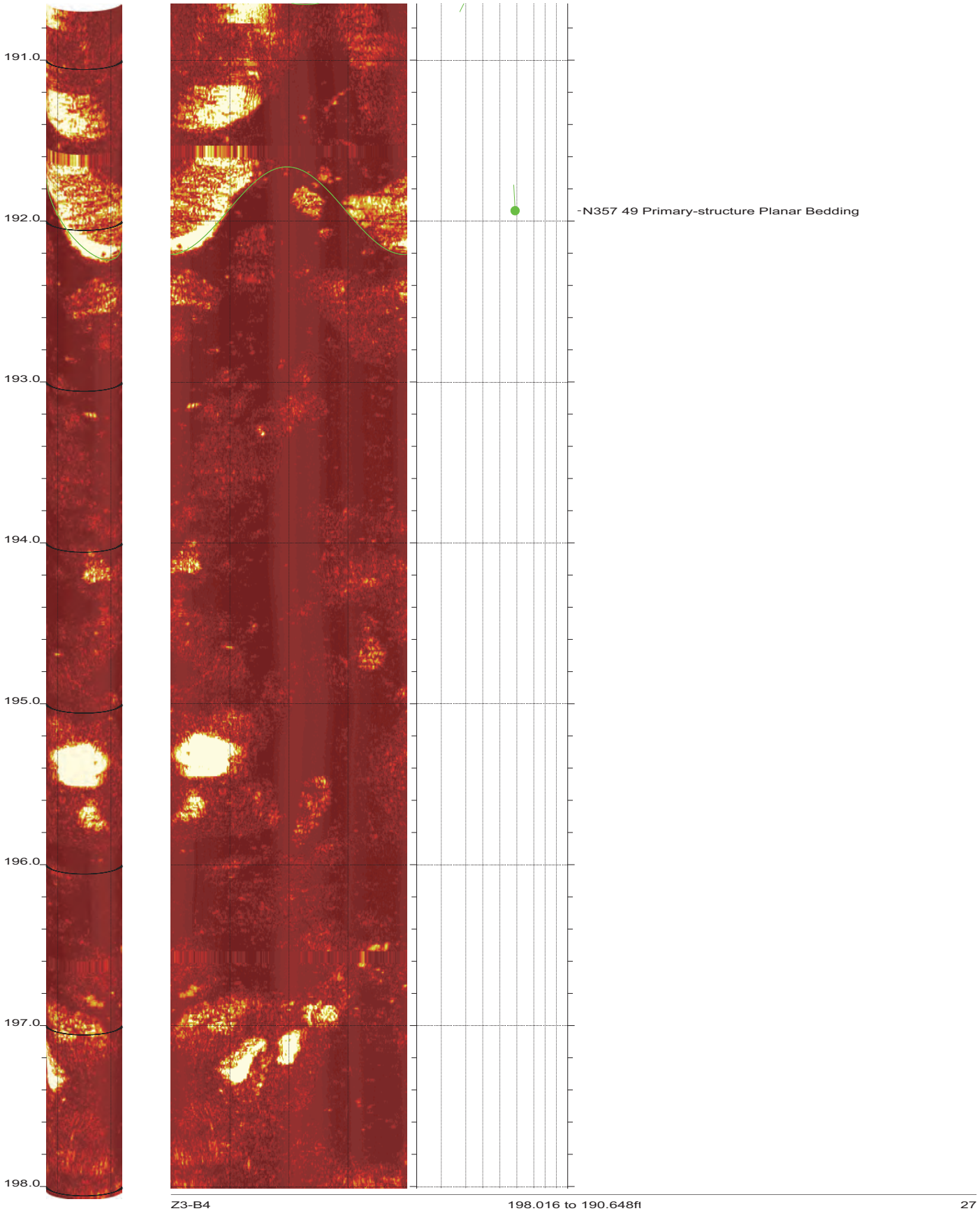


SR-710 Boring Z3-B4 Acoustic Televiewer Dips rev 1 Sheet 27 of 38

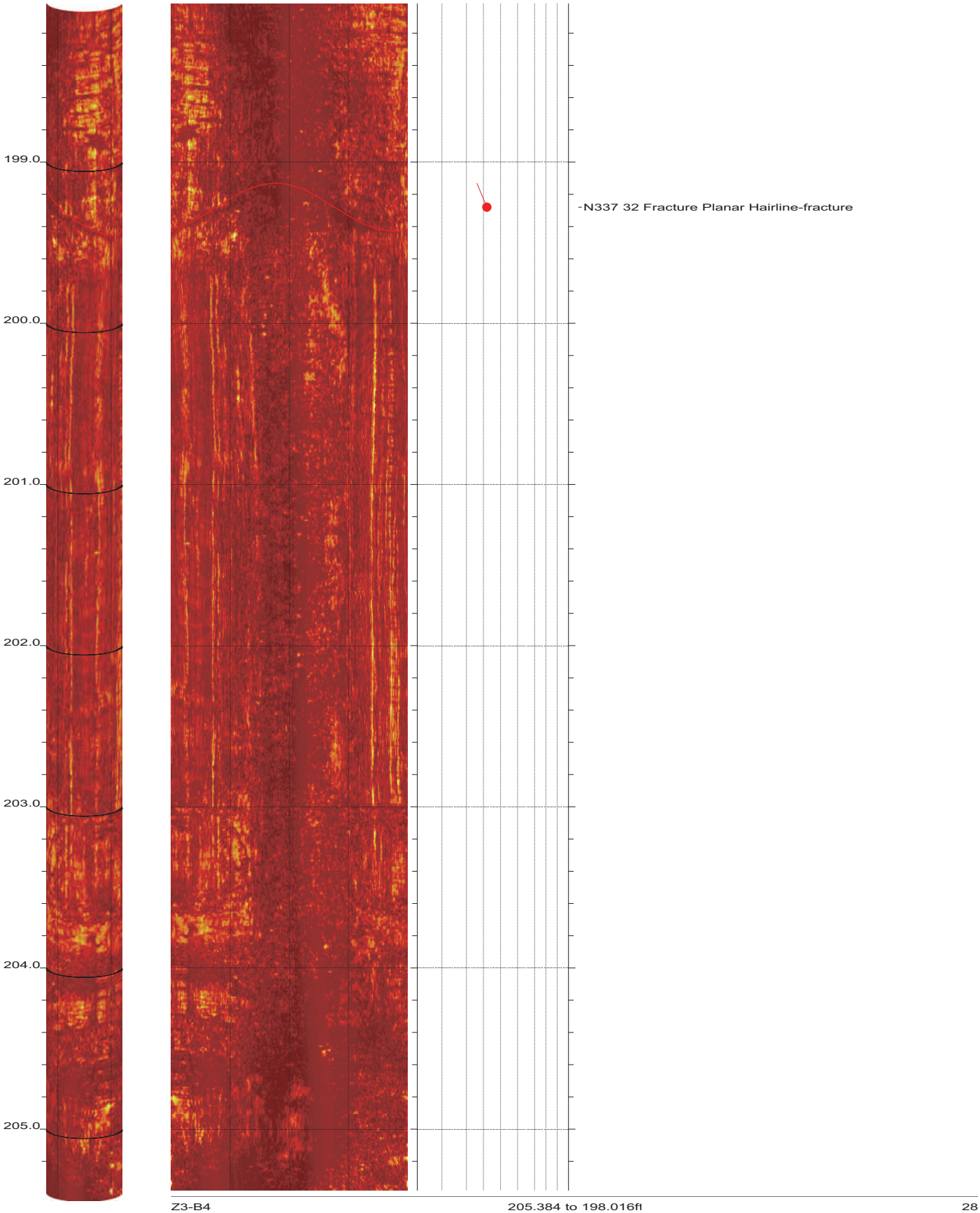


SR-710 Boring Z3-B4 Acoustic Televiewer Dips rev 1 Sheet 28 of 38

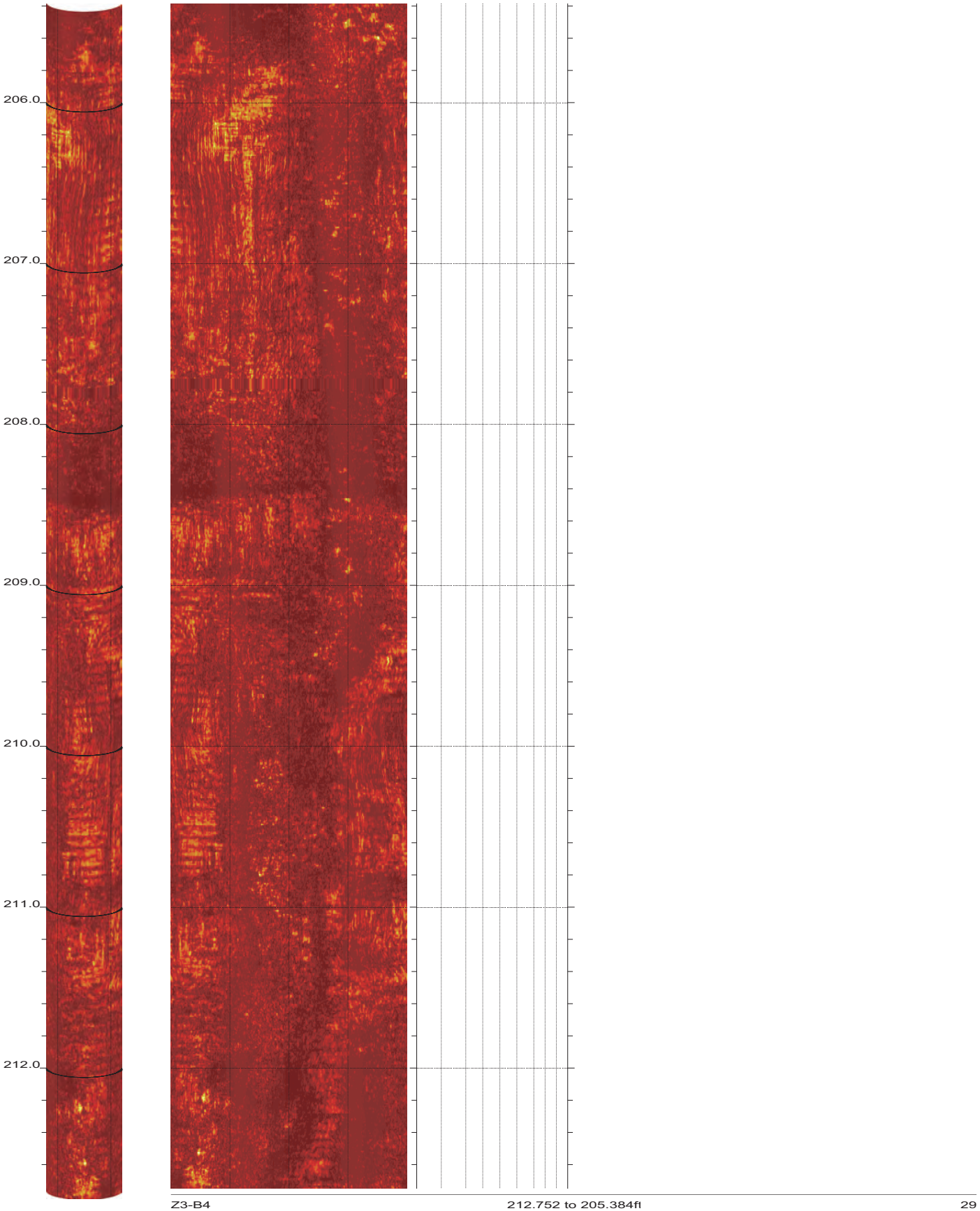


SR-710 Boring Z3-B4 Acoustic Televiewer Dips rev 1 Sheet 29 of 38

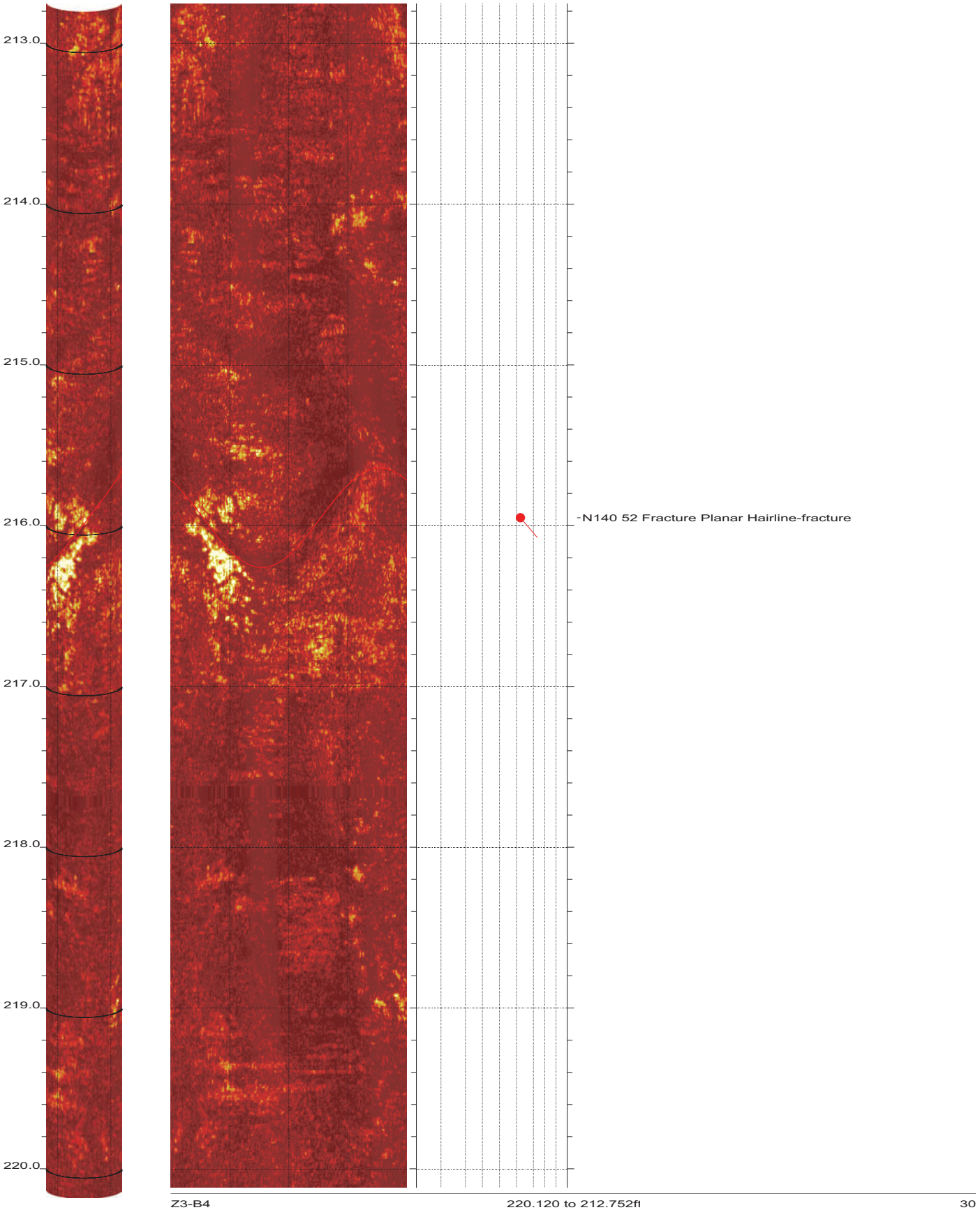


SR-710 Boring Z3-B4 Acoustic Televiewer Dips rev 1 Sheet 30 of 38

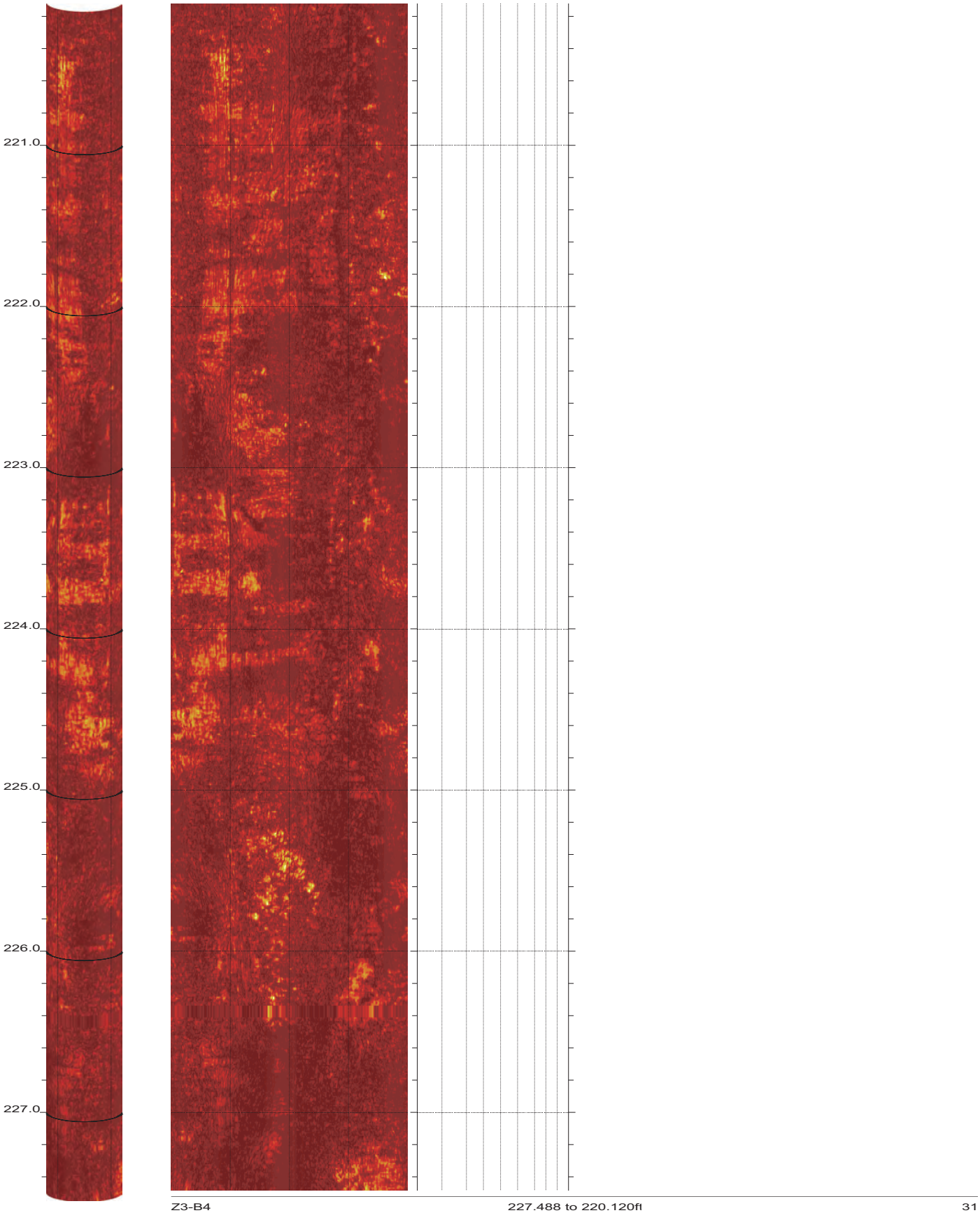


SR-710 Boring Z3-B4 Acoustic Televiewer Dips rev 1 Sheet 31 of 38

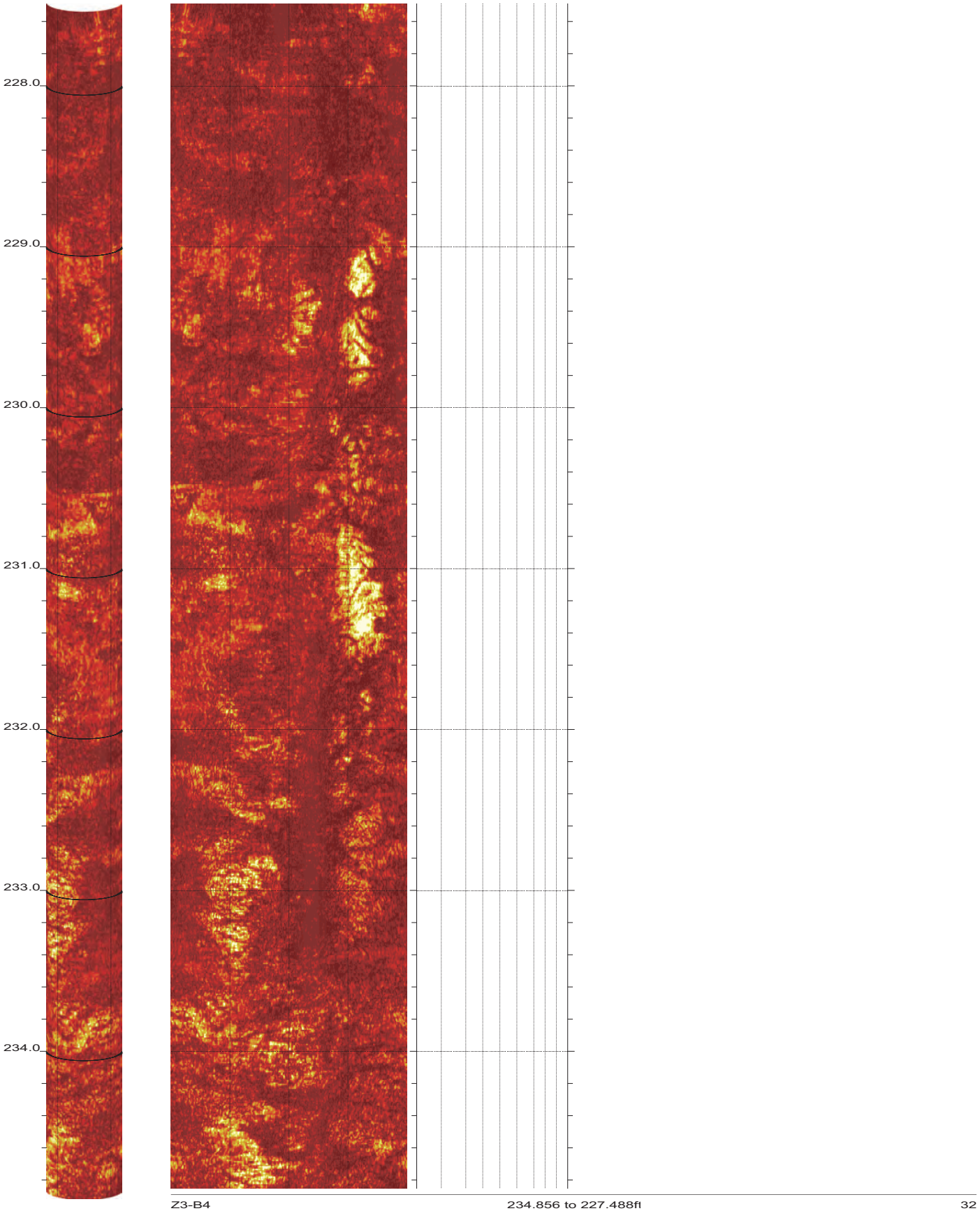


SR-710 Boring Z3-B4 Acoustic Televiewer Dips rev 1 Sheet 32 of 38

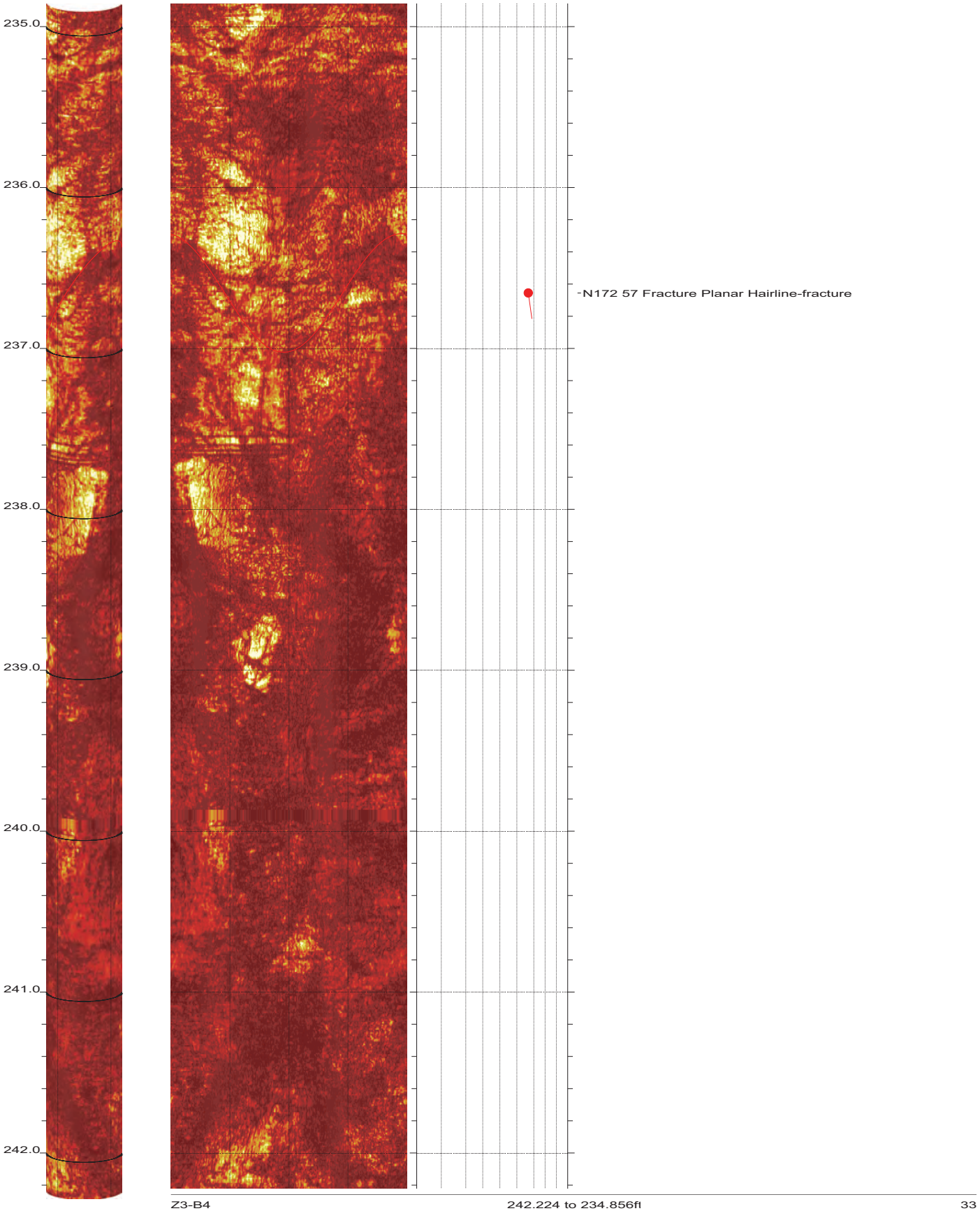


SR-710 Boring Z3-B4 Acoustic Televiewer Dips rev 1 Sheet 33 of 38

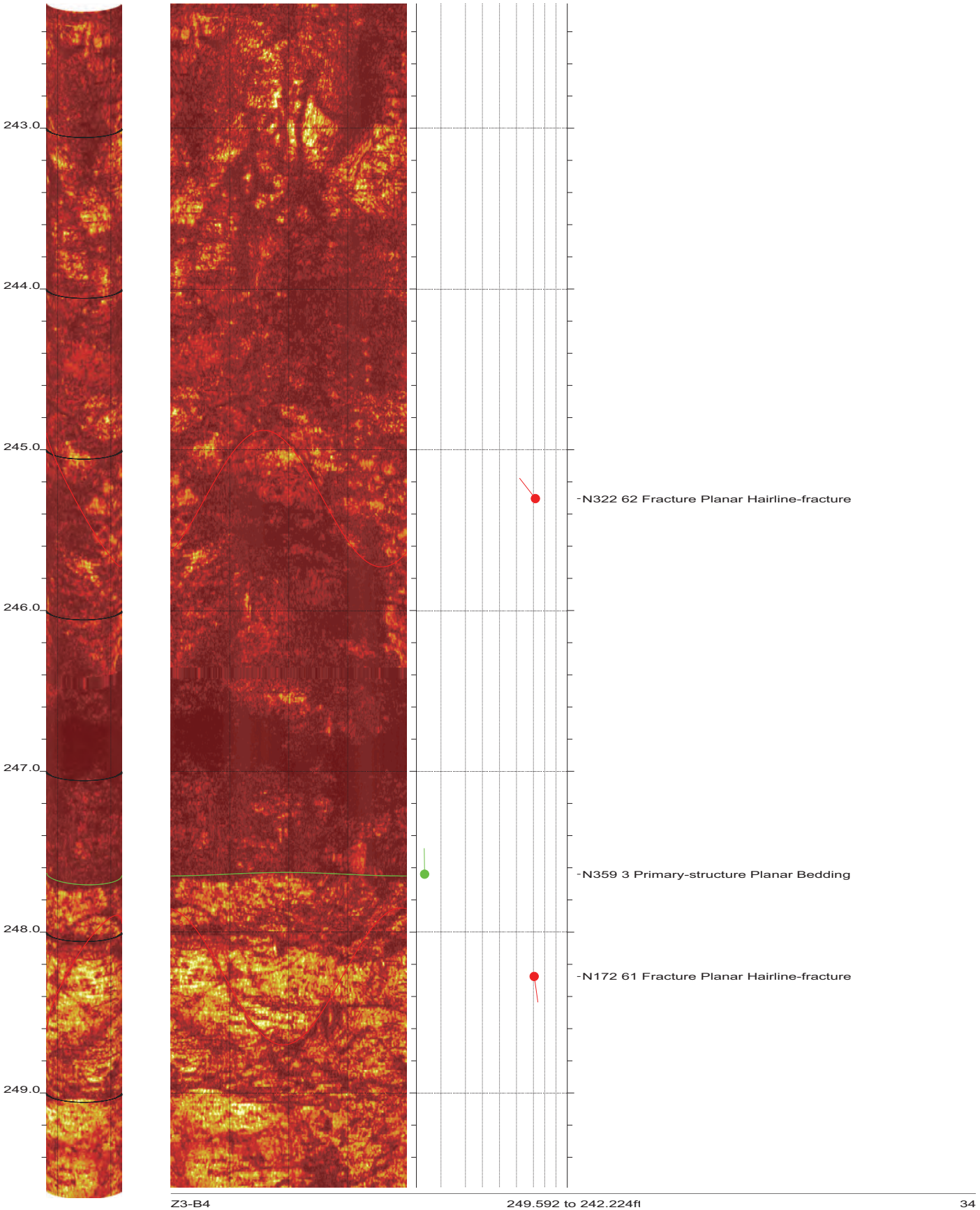


SR-710 Boring Z3-B4 Acoustic Televiewer Dips rev 1 Sheet 34 of 38

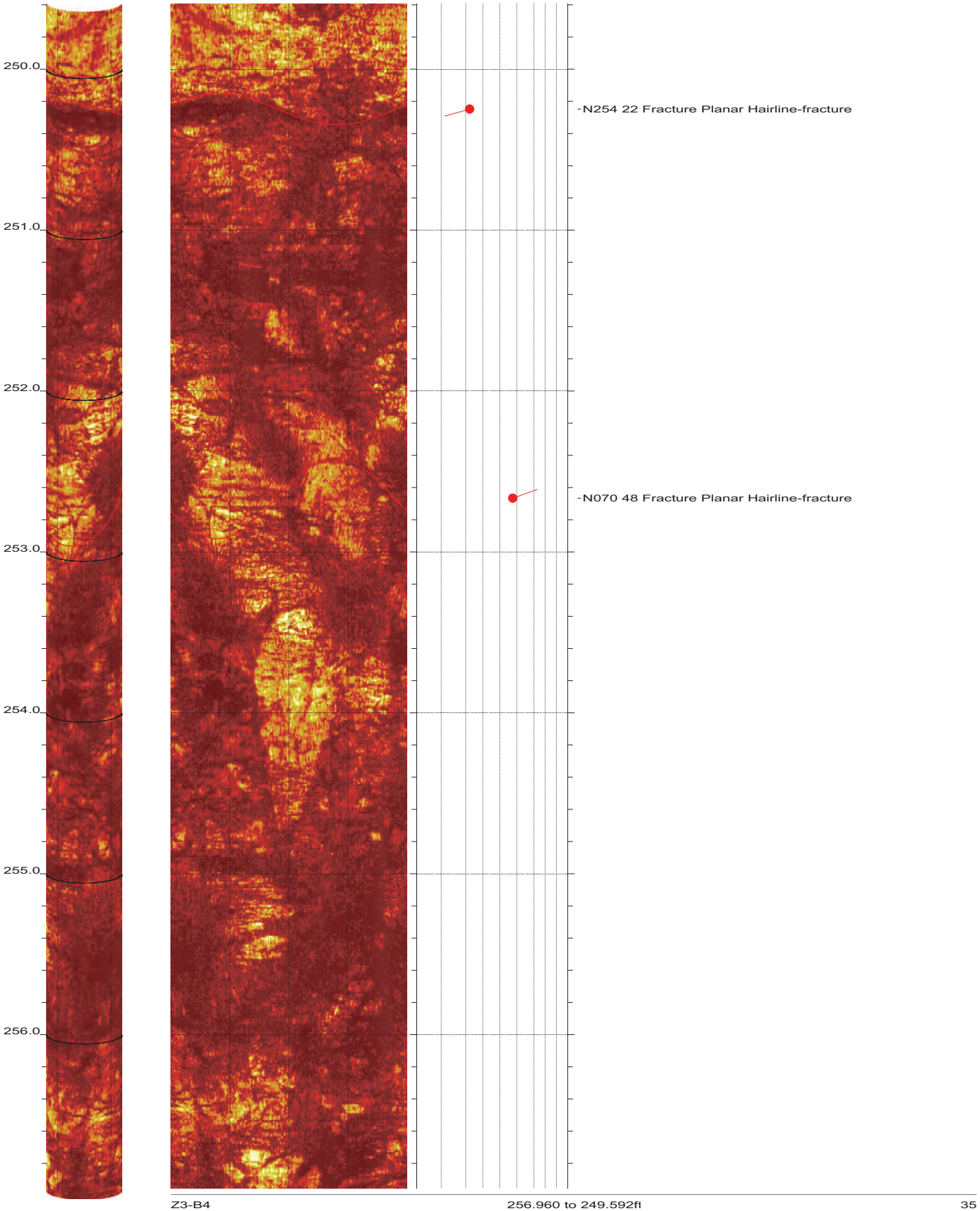


SR-710 Boring Z3-B4 Acoustic Televiewer Dips rev 1 Sheet 35 of 38

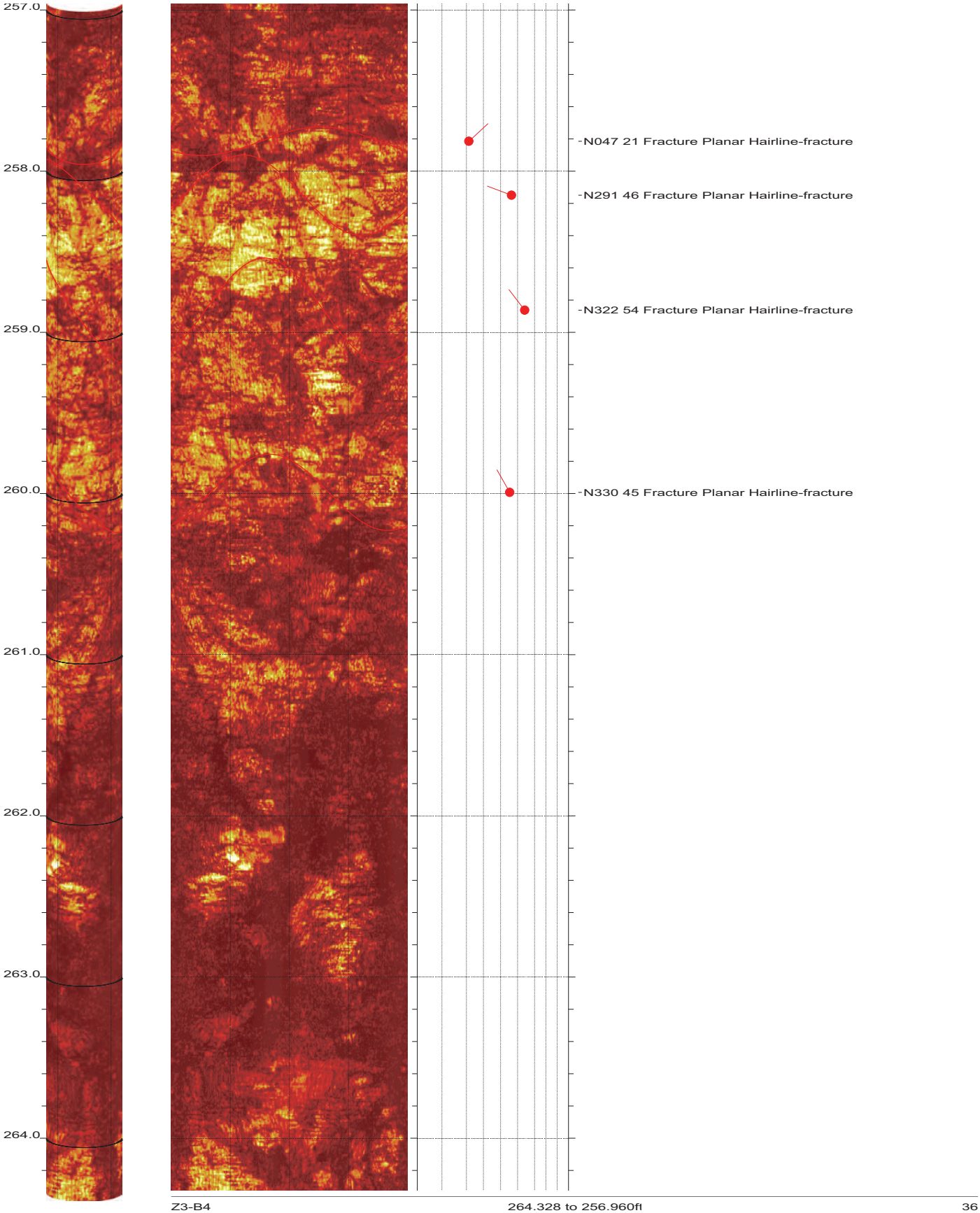


SR-710 Boring Z3-B4 Acoustic Televiewer Dips rev 1 Sheet 36 of 38

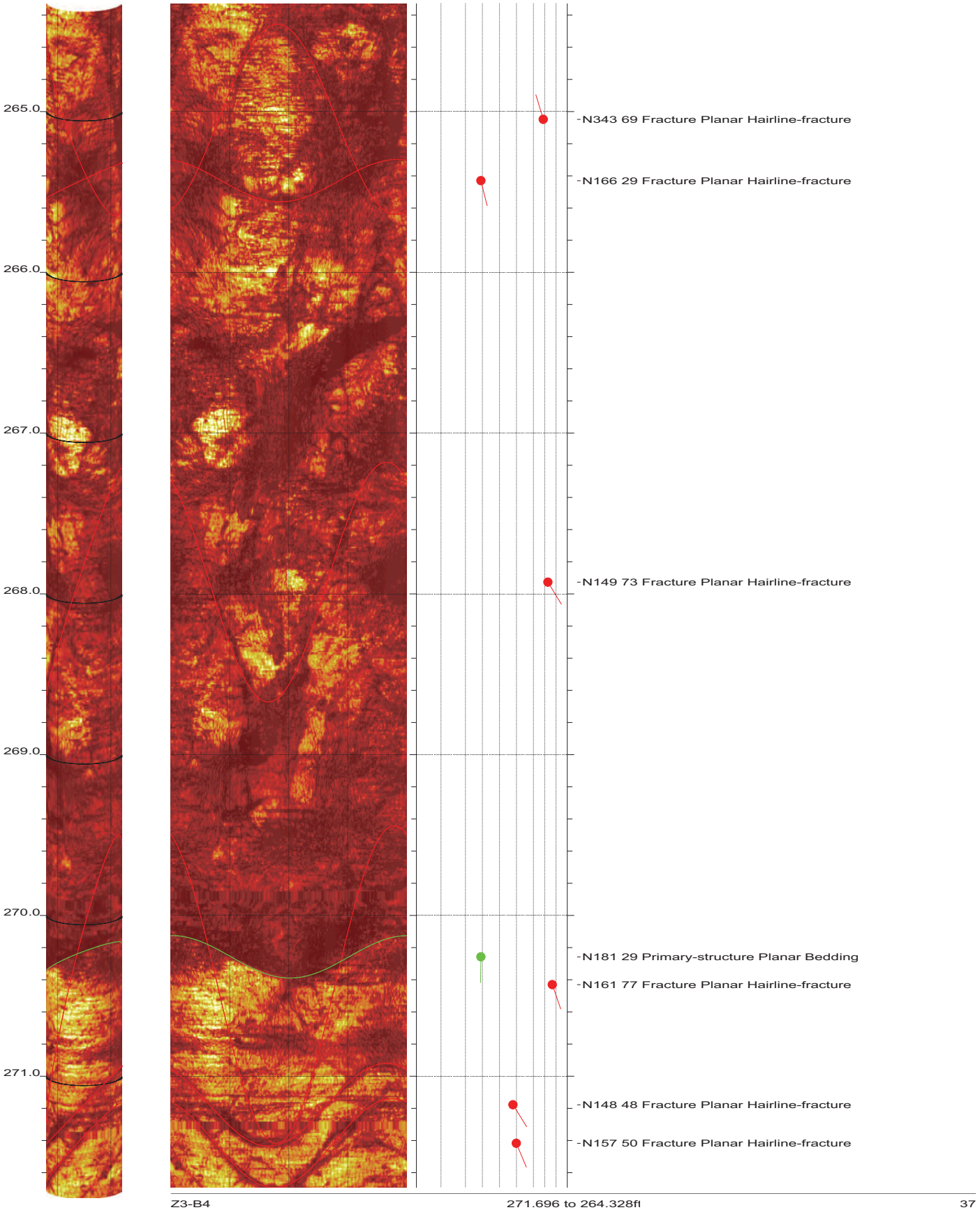


SR-710 Boring Z3-B4 Acoustic Televiewer Dips rev 1 Sheet 37 of 38

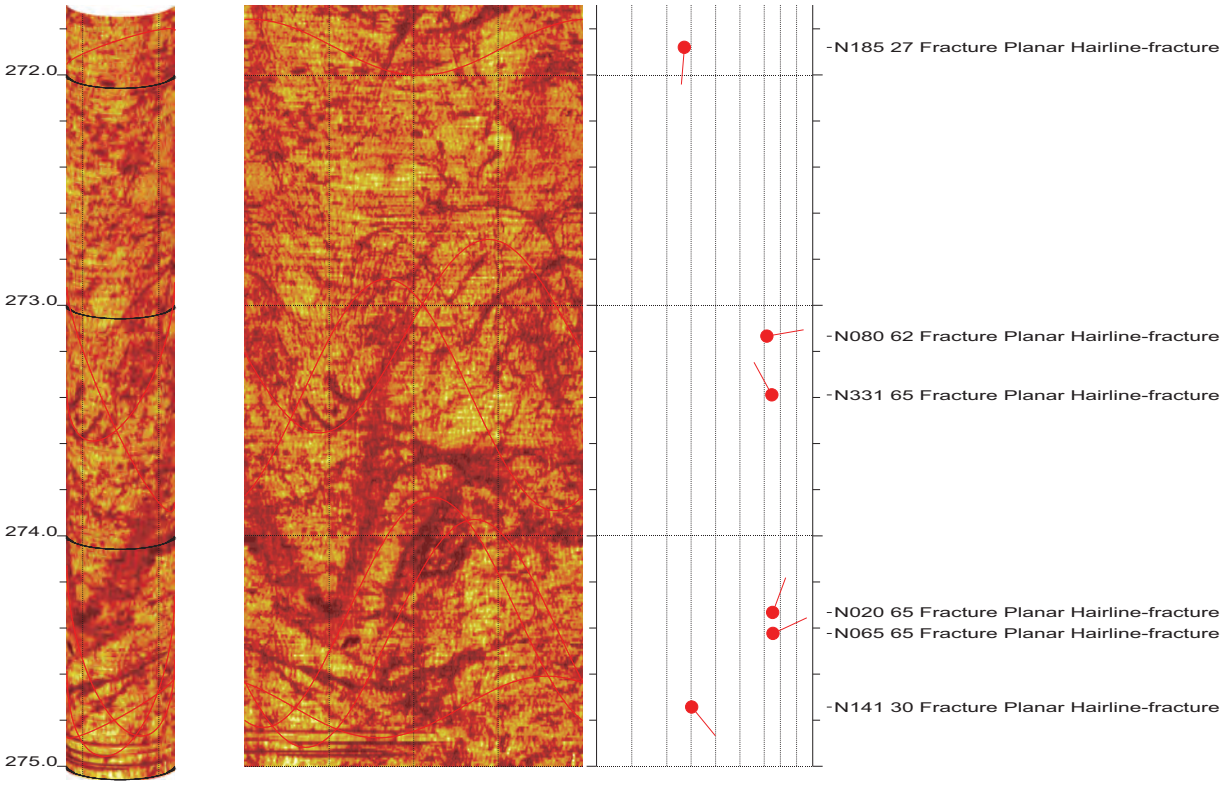
272.0
273.0
274.0
275.0
-N185 27 Fracture Planar Hairline-fracture
-N080 62 Fracture Planar Hairline-fracture
-N331 65 Fracture Planar Hairline-fracture
-N020 65 Fracture Planar Hairline-fracture
-N065 65 Fracture Planar Hairline-fracture
-N141 30 Fracture Planar Hairline-fracture

BHTV DATA PROCESSING
RGLDIP vsn 6.2
INTERPRETED BHTV DIPS LOG

CASCADE DRILLING

Borehole: Z3-B6

SR-710 TUNNEL INVESTIGATION

top of borehole.....
East: _
North: _
Elev: _

North ref. is true
Depth units are feet
Vertical scale: 1/10
Horiz scale = 1.00x Vert scale

Zone from 318.600 to 28.400ft
Format: BHTV-NESWN

Borehole diam: 5.600inch
Vertical = borehole-axis
Image: Amplitude

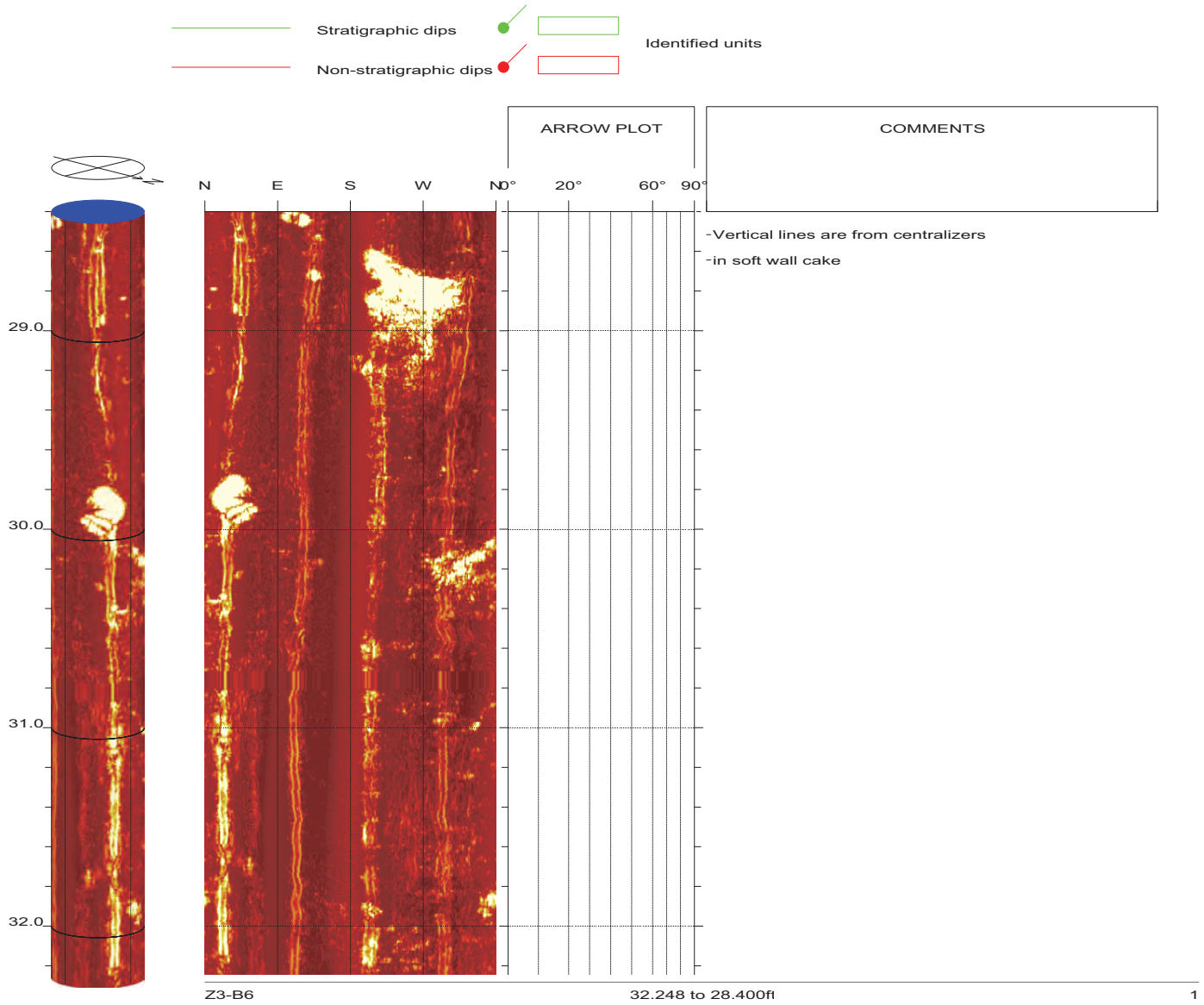

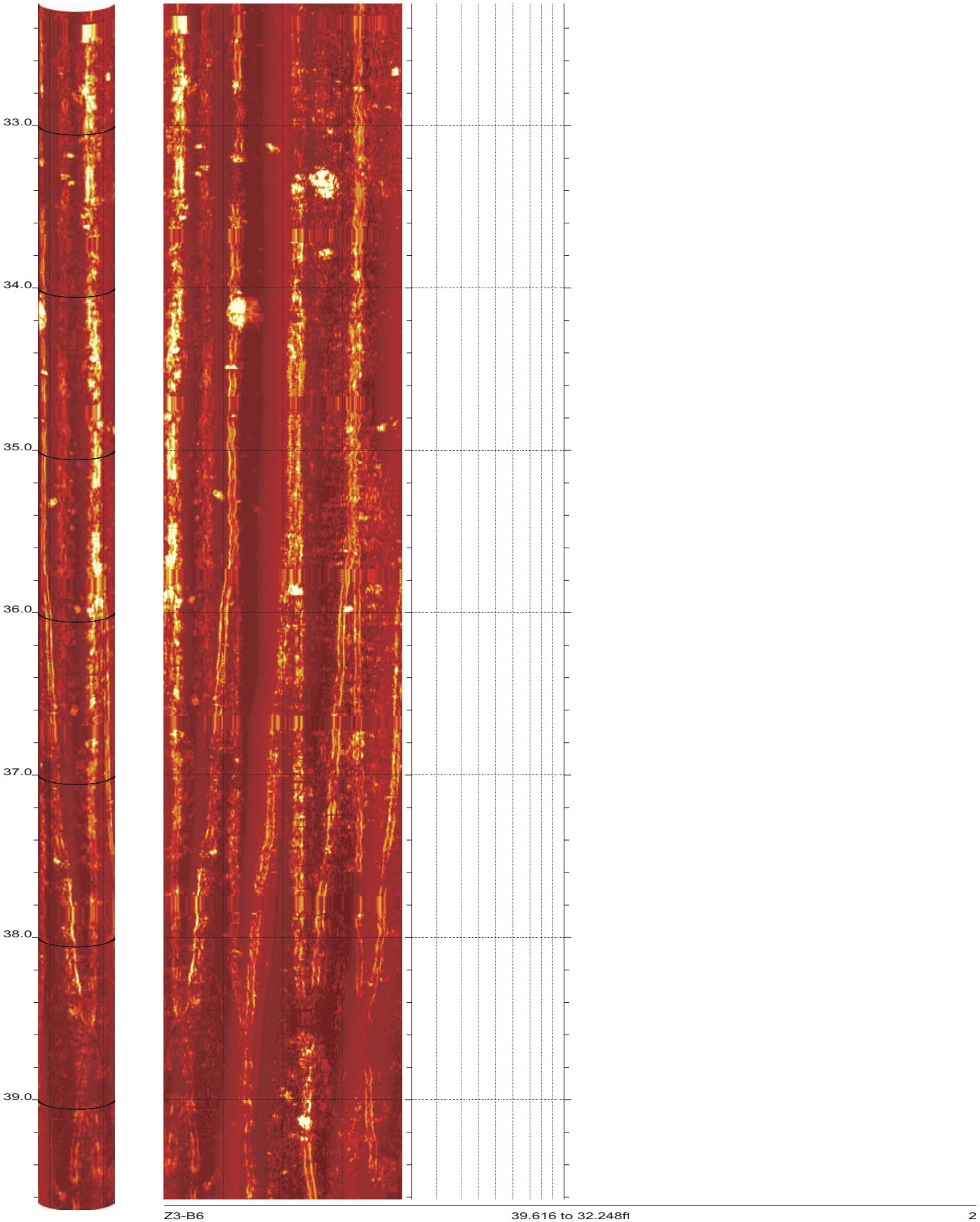
33.0
34.0
35.0
36.0
37.0
38.0
39.0
Z3-B6
39.616 to 32.248fl
2

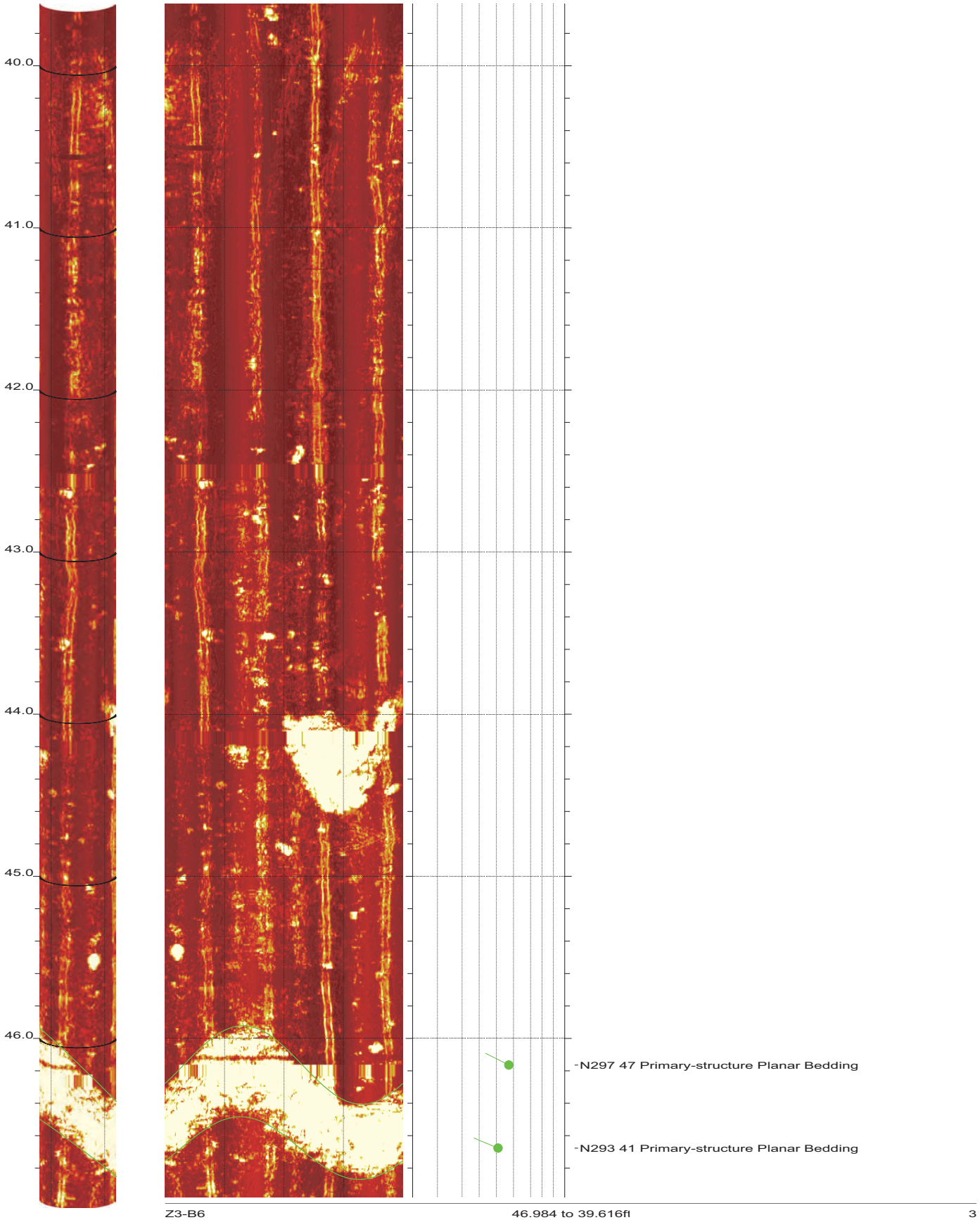


SR-710 Boring Z3-B6 Acoustic Televiewer Dips rev 1 Sheet 3 of 40

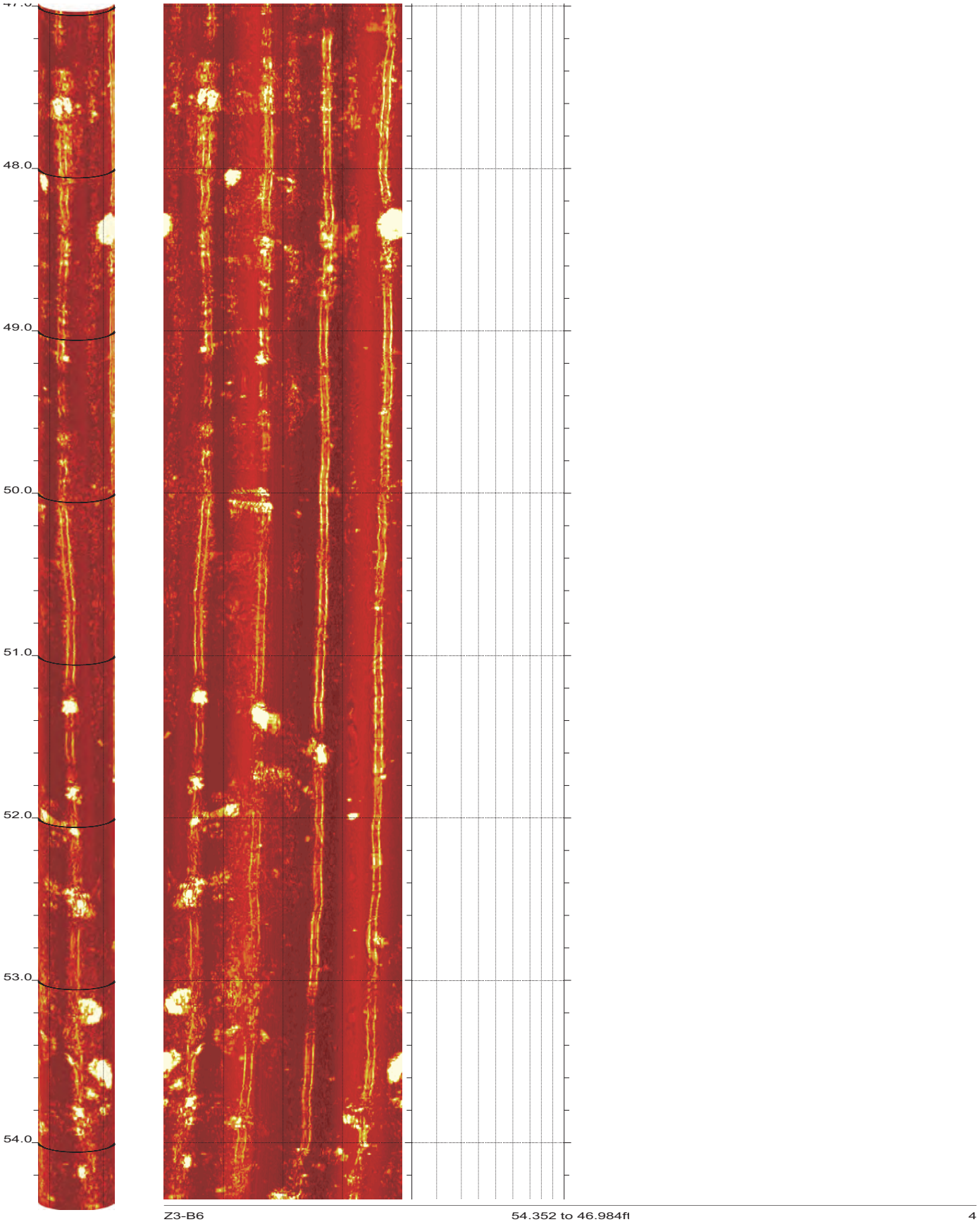


SR-710 Boring Z3-B6 Acoustic Televiewer Dips rev 1 Sheet 4 of 40

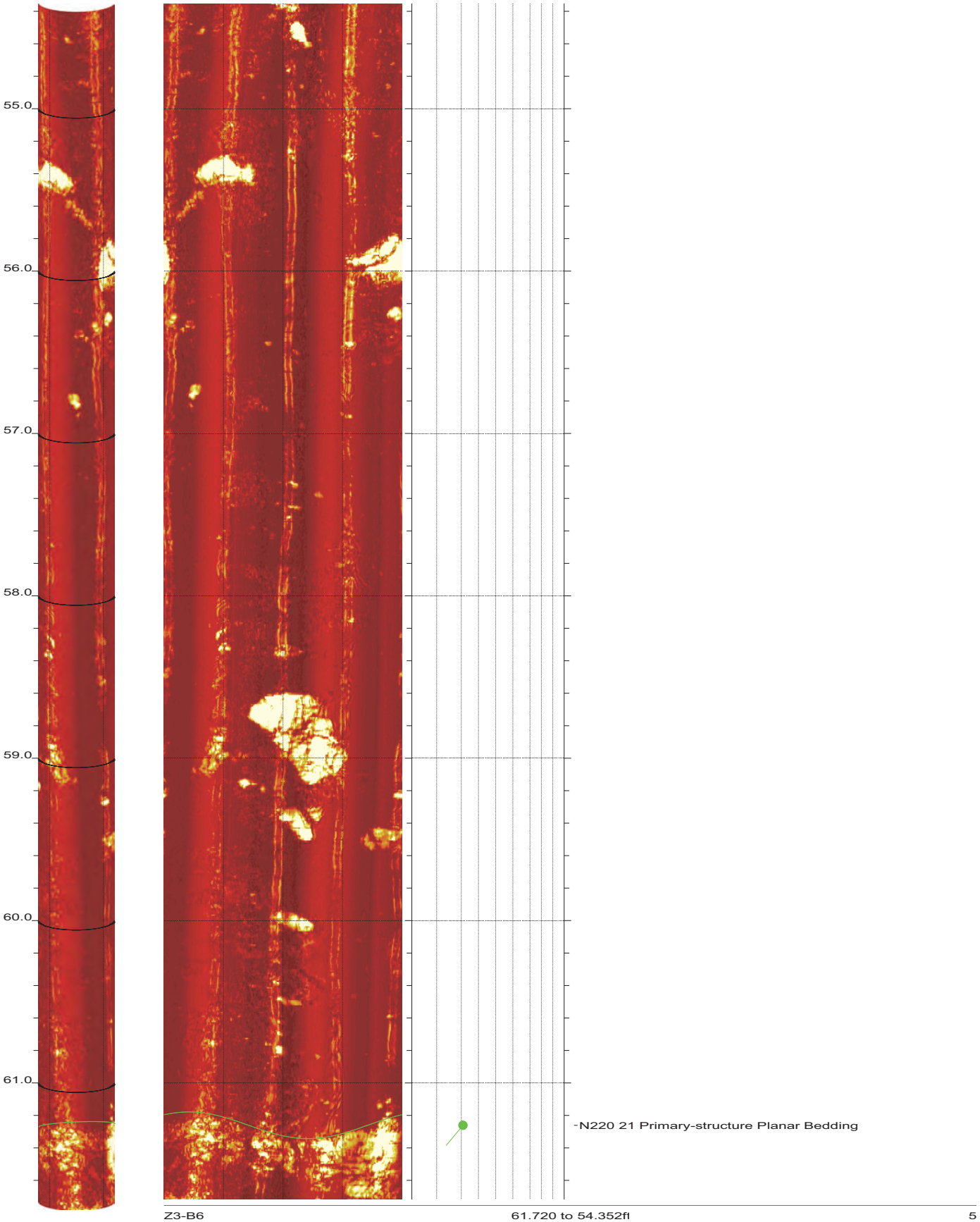


SR-710 Boring Z3-B6 Acoustic Televiewer Dips rev 1 Sheet 5 of 40

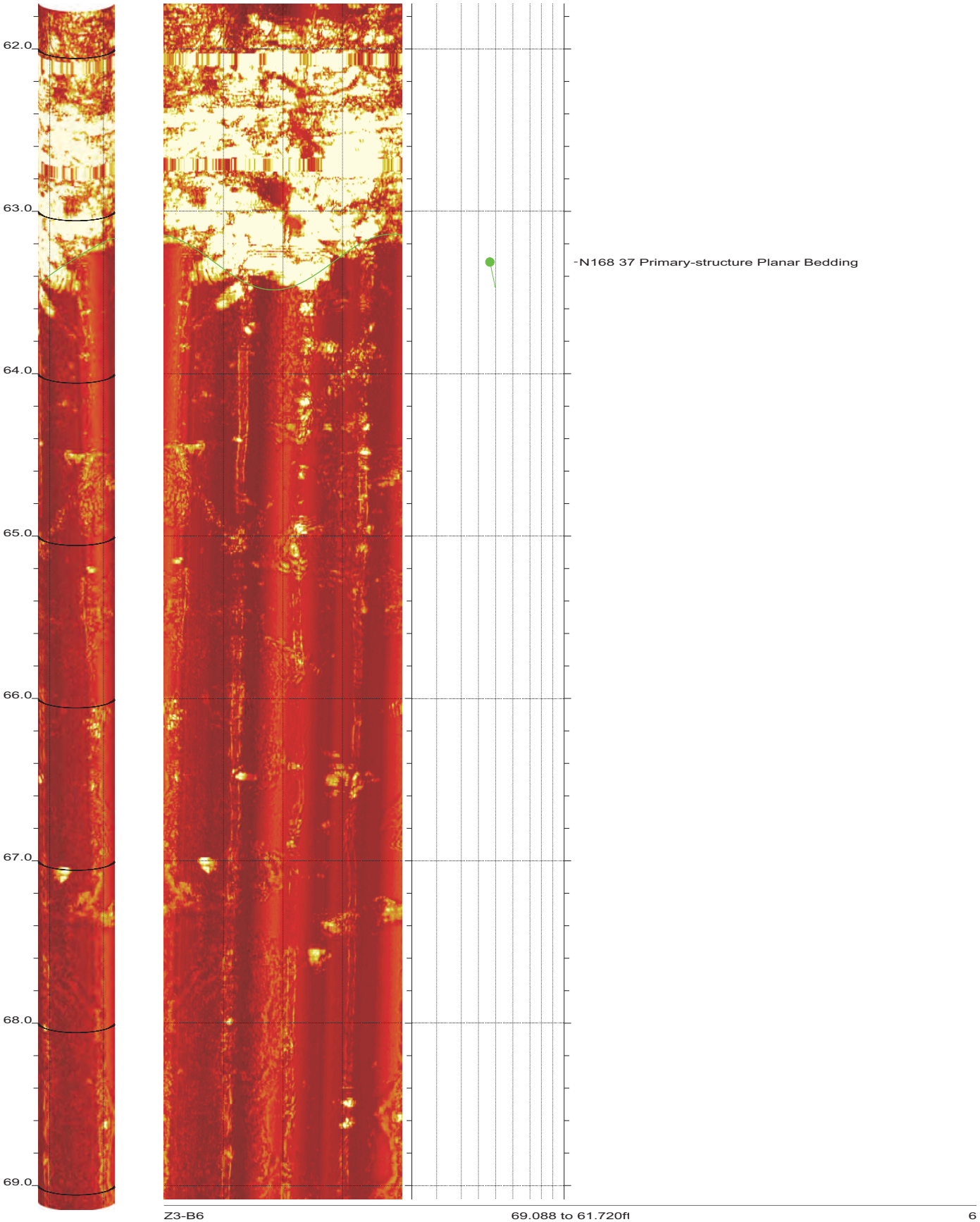


SR-710 Boring Z3-B6 Acoustic Televiewer Dips rev 1 Sheet 6 of 40

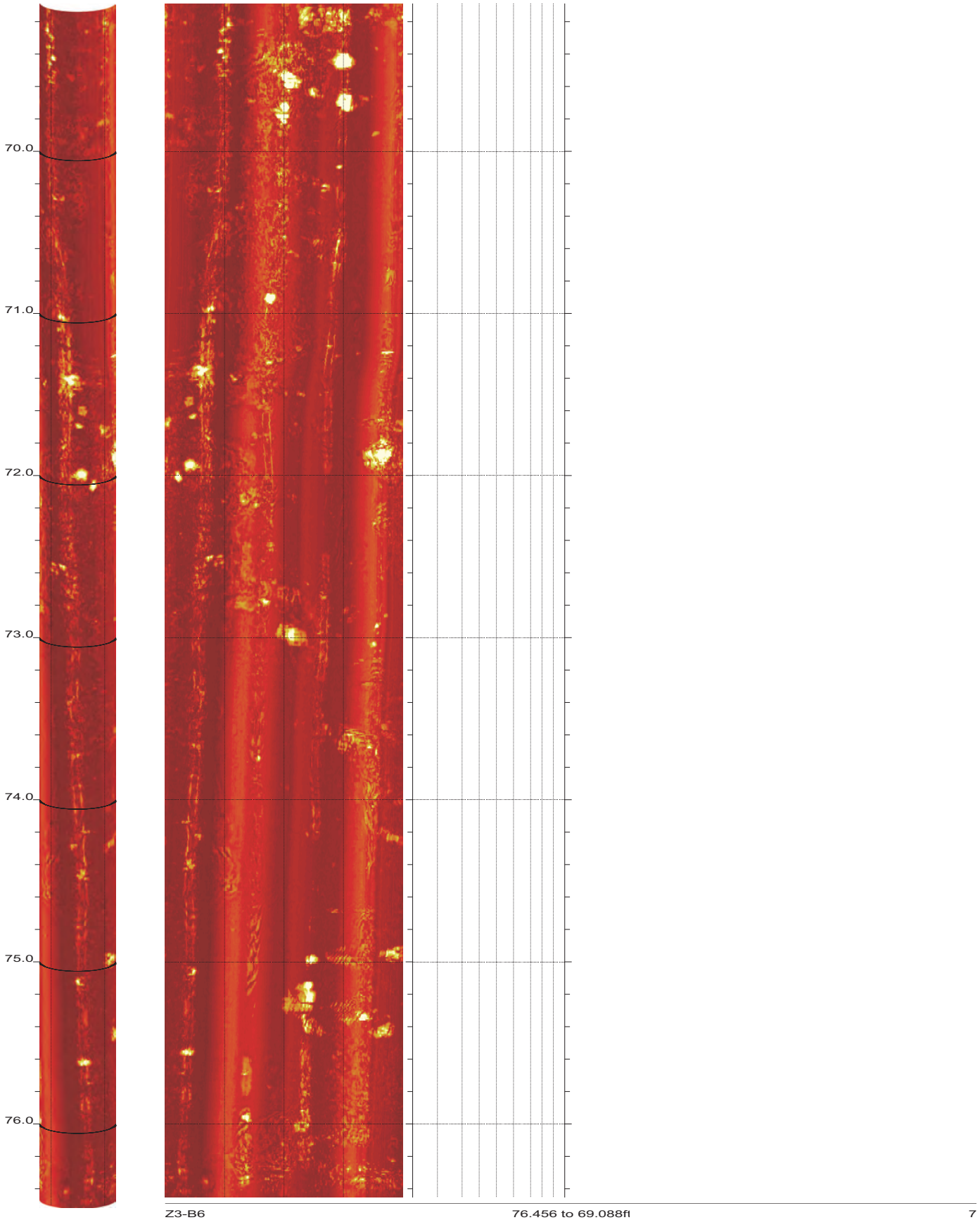


SR-710 Boring Z3-B6 Acoustic Televiewer Dips rev 1 Sheet 7 of 40

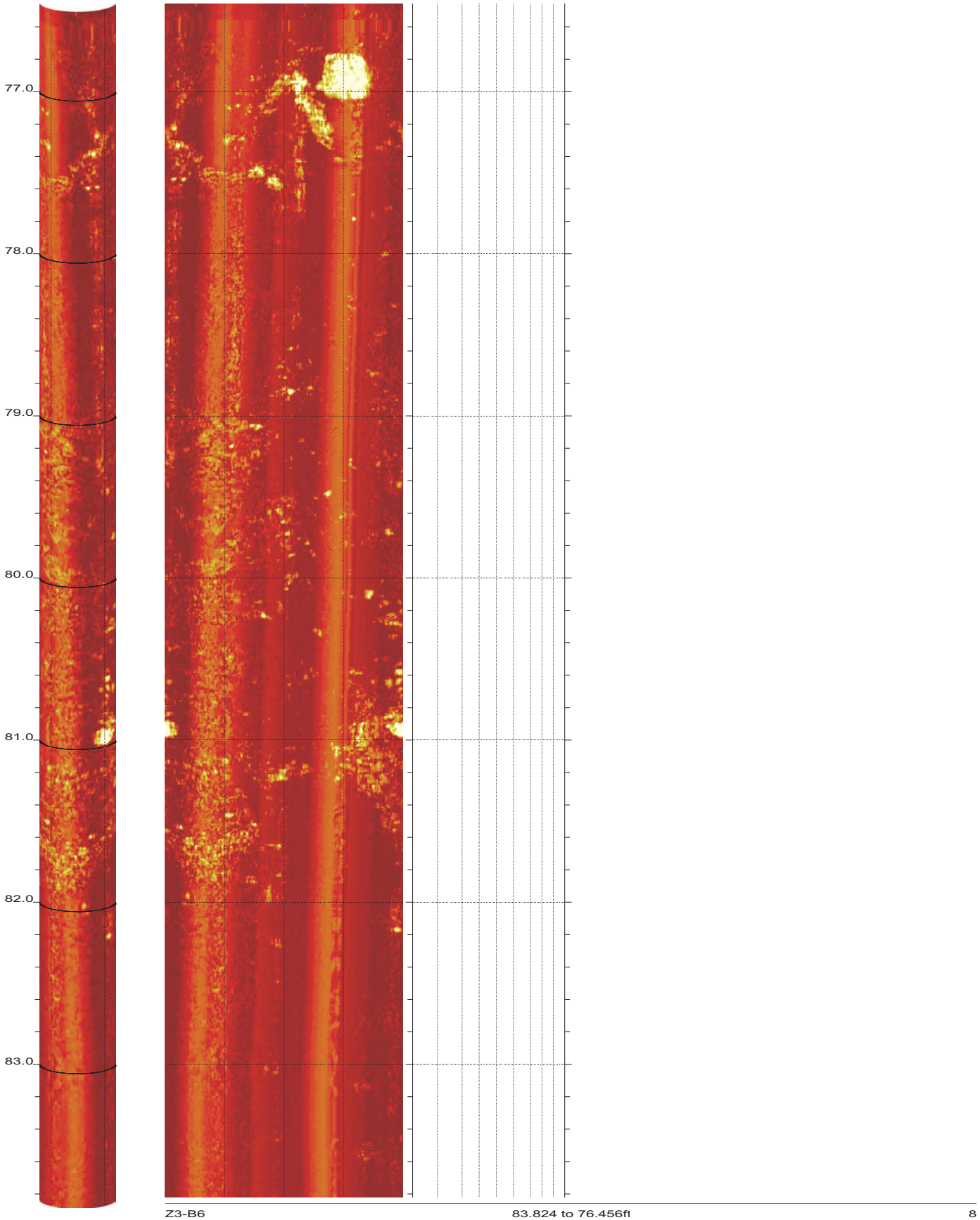


SR-710 Boring Z3-B6 Acoustic Televiewer Dips rev 1 Sheet 8 of 40

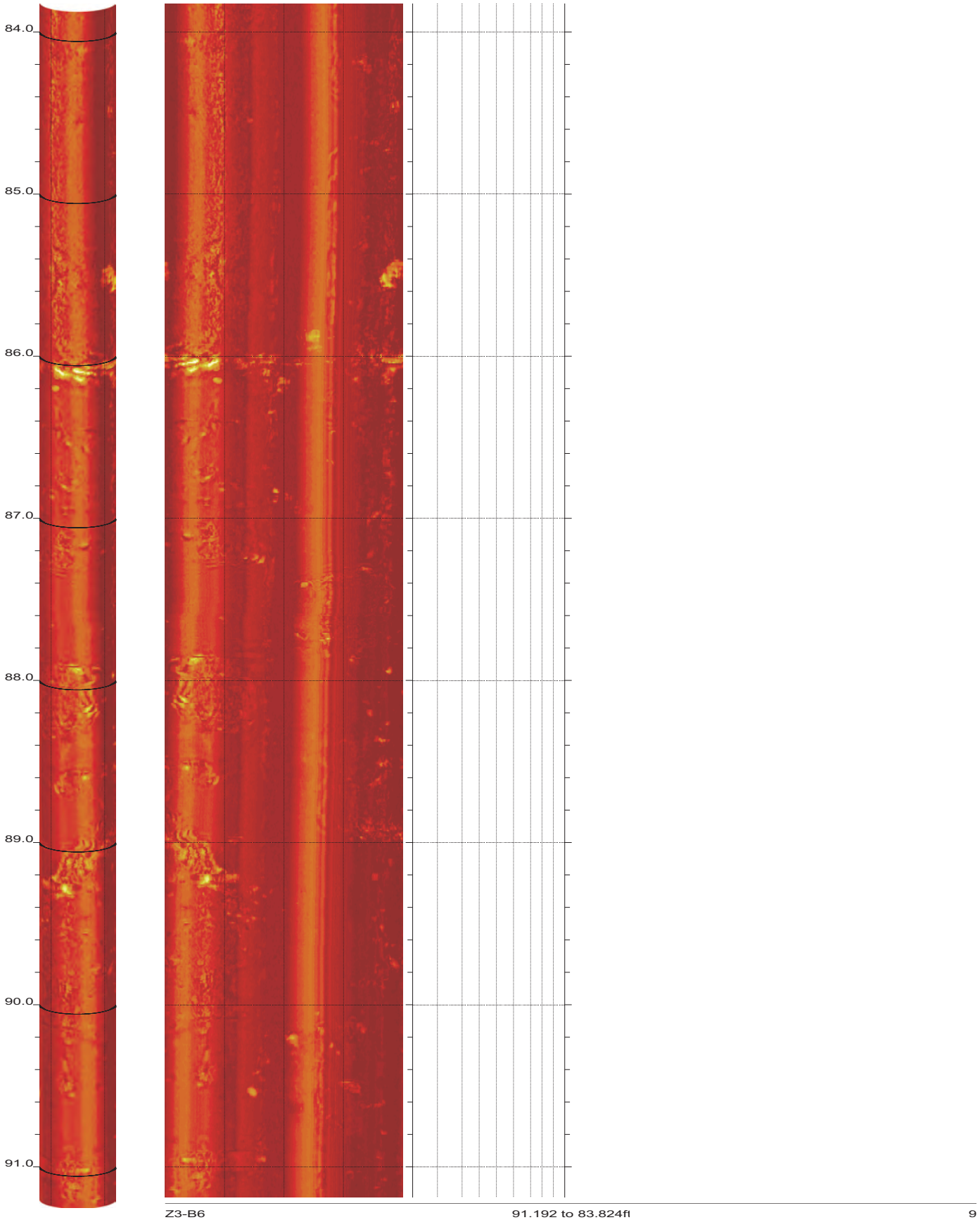


SR-710 Boring Z3-B6 Acoustic Televiewer Dips rev 1 Sheet 9 of 40

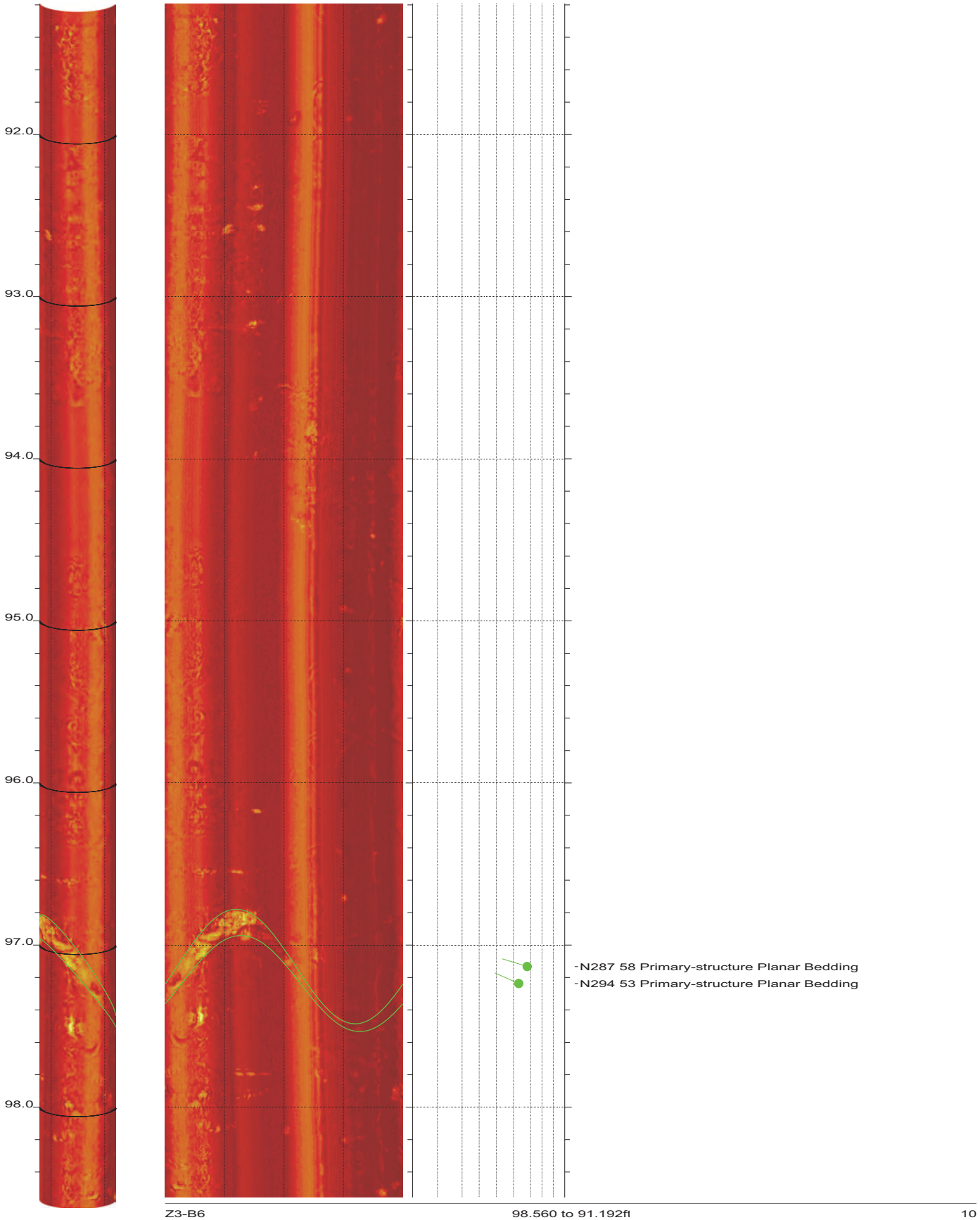


SR-710 Boring Z3-B6 Acoustic Televiewer Dips rev 1 Sheet 10 of 40

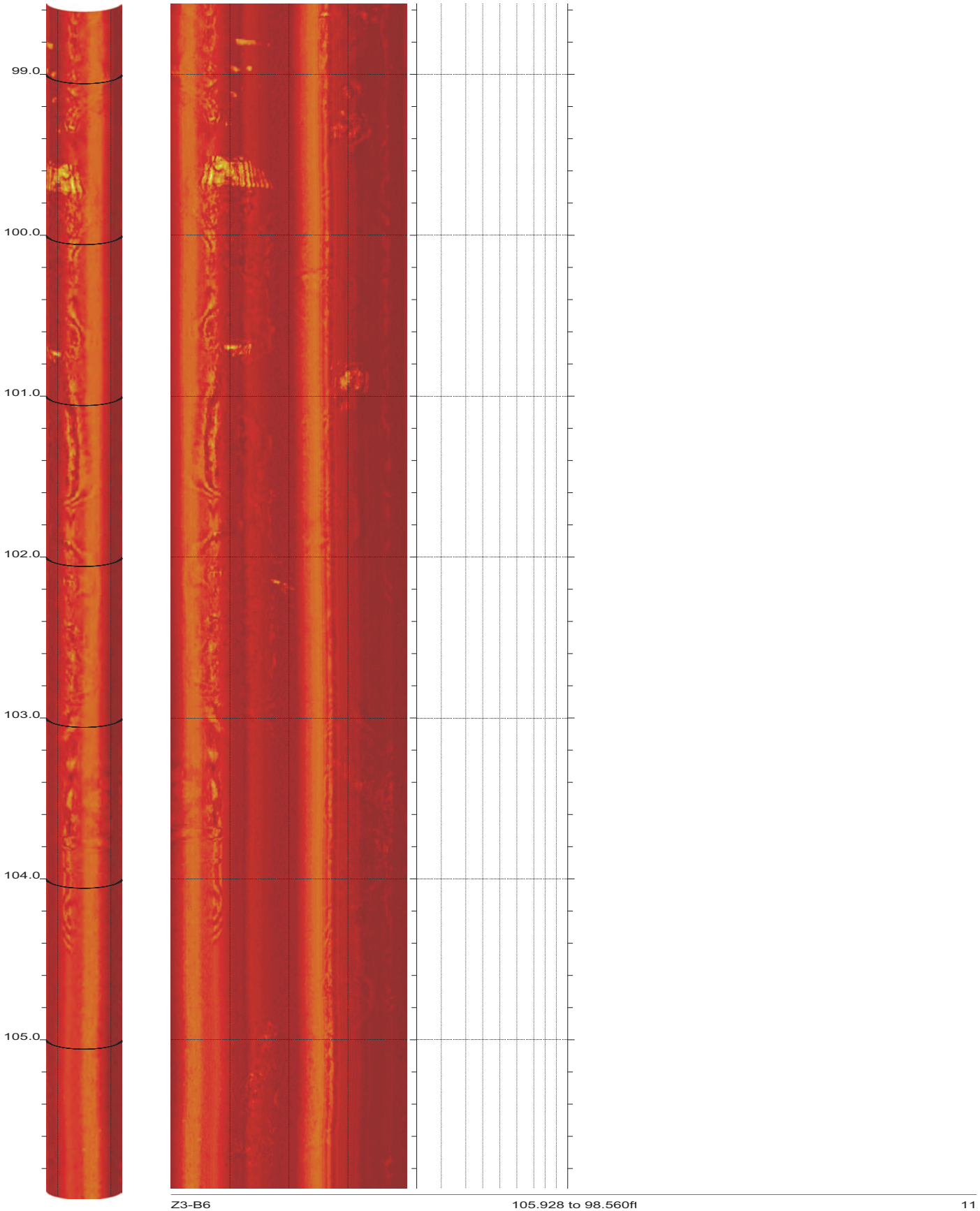
99.0
100.0
101.0
102.0
103.0
104.0
105.0
Z3-B6
105.928 to 98.560ft
11


106.0
107.0
108.0
109.0
110.0
111.0
112.0
113.0
N288 55 Primary-structure Planar Bedding
N280 55 Primary-structure Planar Bedding
Z3-B6
113.296 to 105.928ft
12

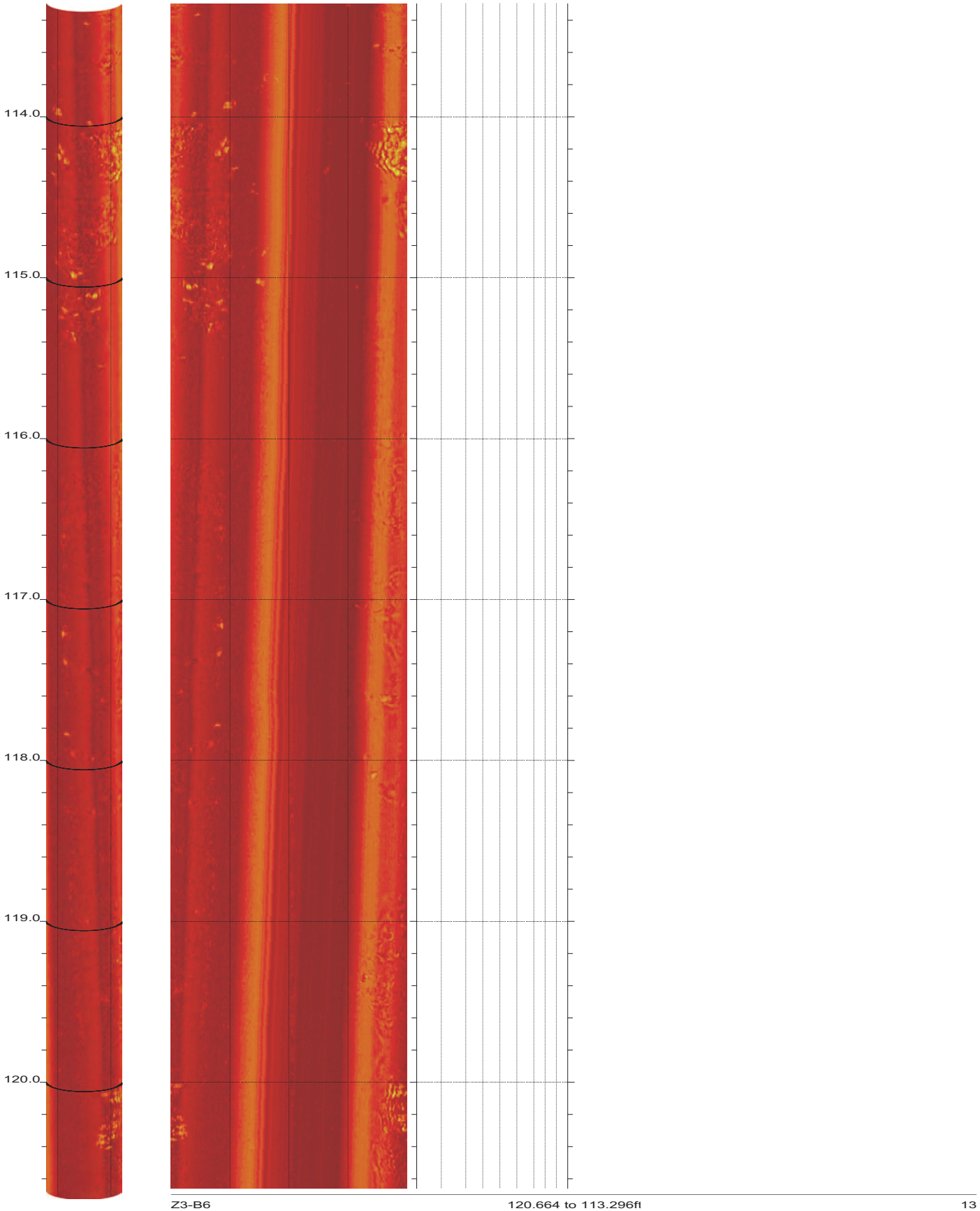
114.0
115.0
116.0
117.0
118.0
119.0
120.0
Z3-B6
120.664 to 113.296fl
13

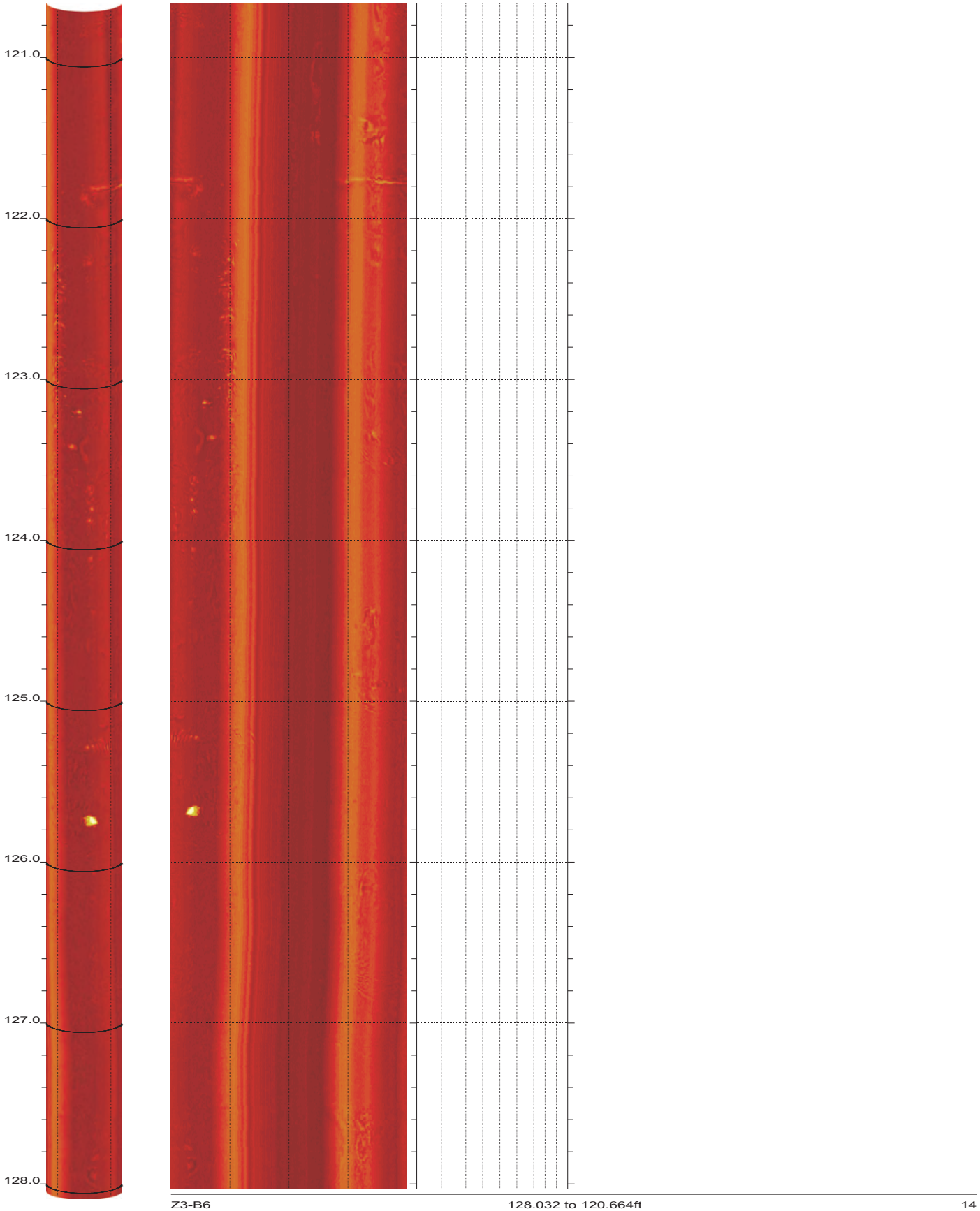
121.0
122.0
123.0
124.0
125.0
126.0
127.0
128.0
Z3-B6
128.032 to 120.664ft
14

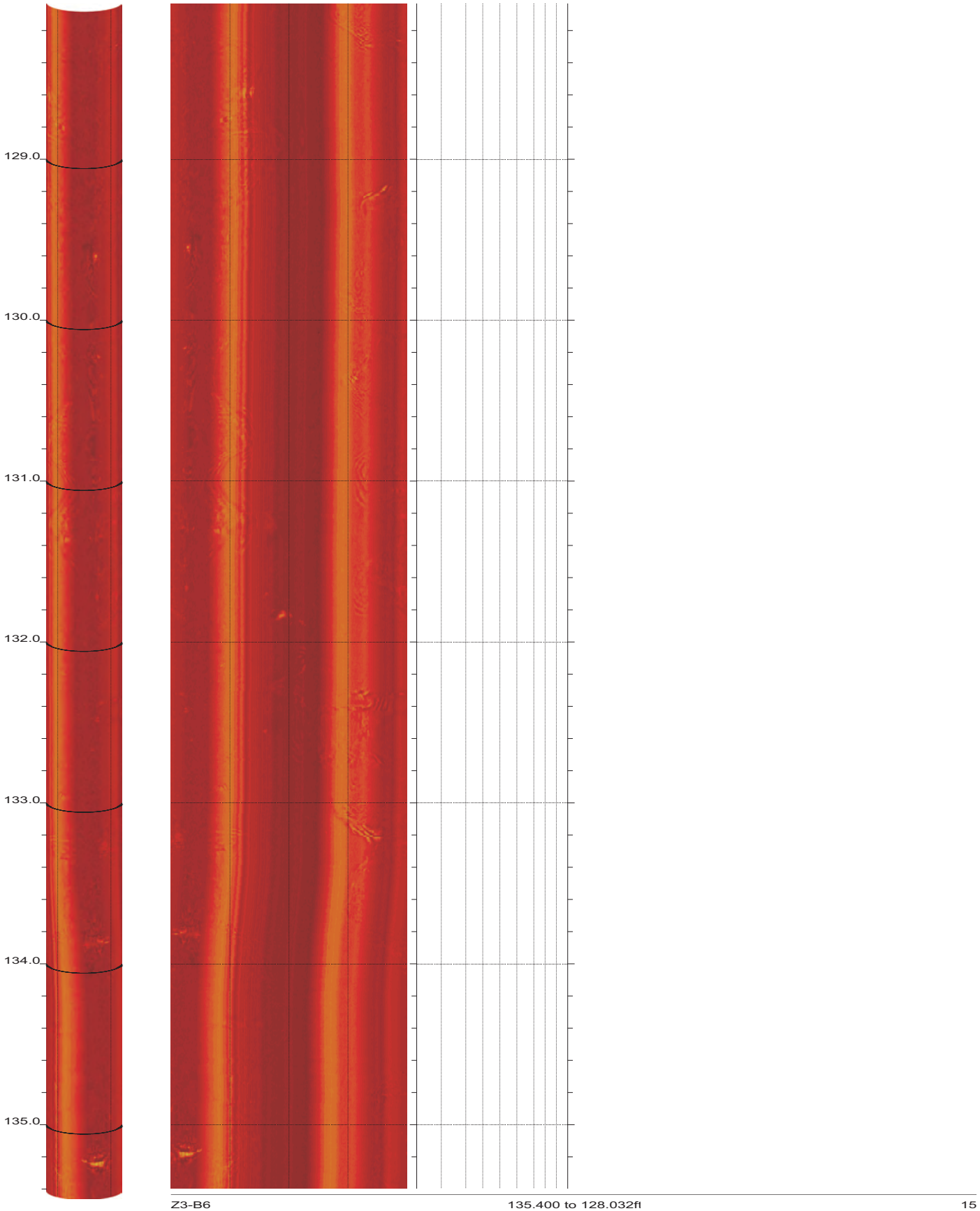
129.0
130.0
131.0
132.0
133.0
134.0
135.0
Z3-B6
135.400 to 128.032fl
15

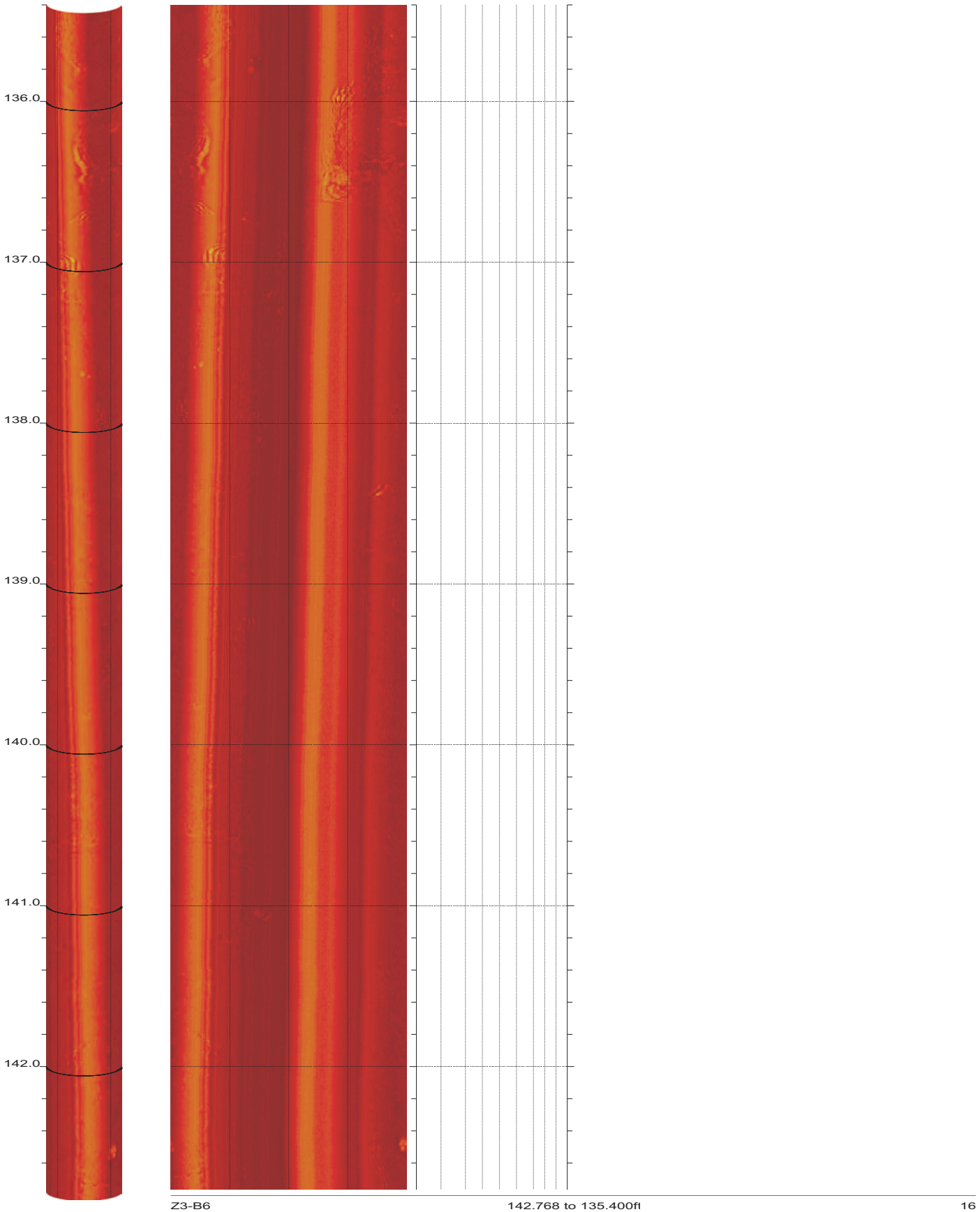
136.0
137.0
138.0
139.0
140.0
141.0
142.0
Z3-B6
142.768 to 135.400ft
16

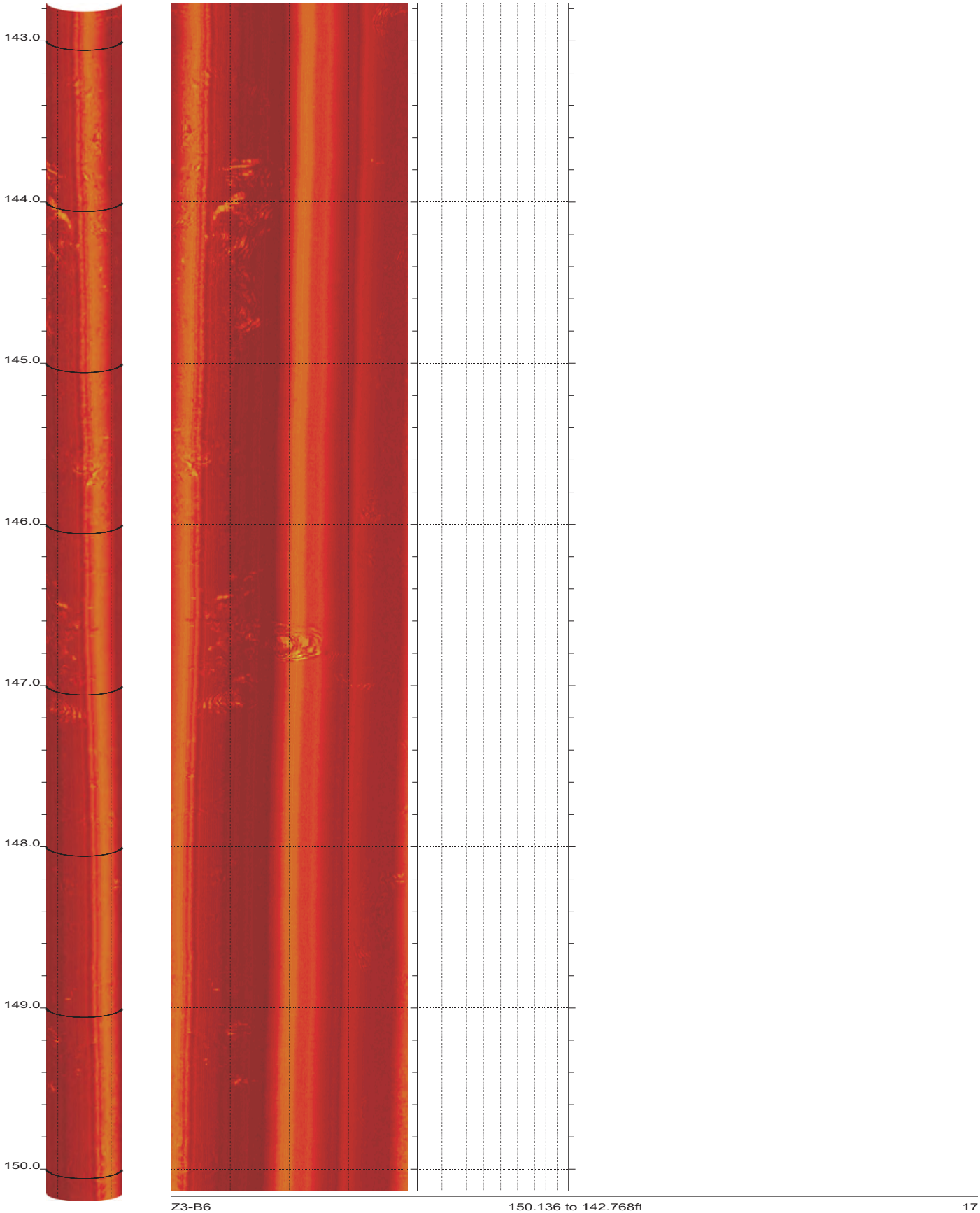
143.0
144.0
145.0
146.0
147.0
148.0
149.0
150.0
Z3-B6
150.136 to 142.768ft
17

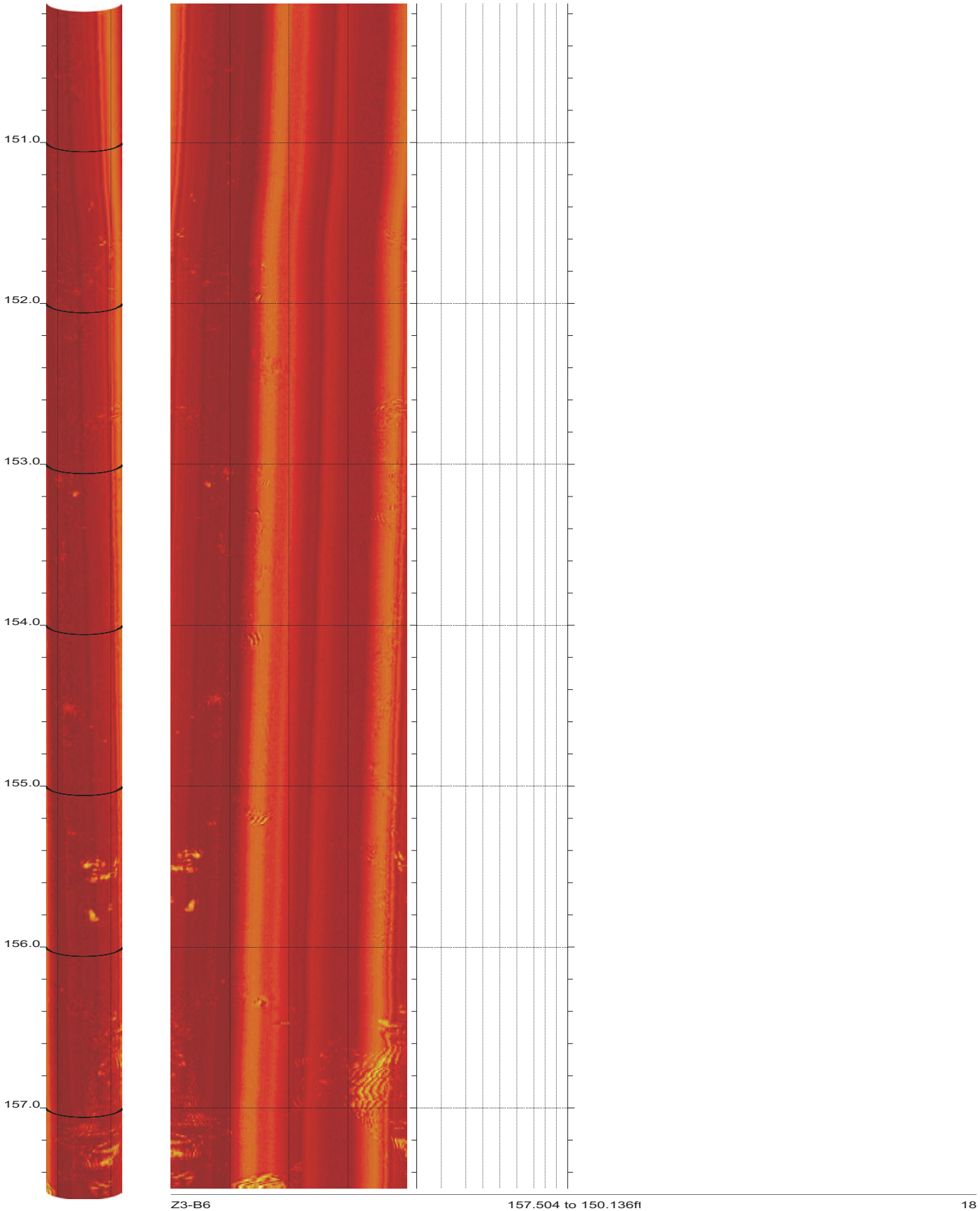
151.0
152.0
153.0
154.0
155.0
156.0
157.0
Z3-B6
157.504 to 150.136ft
18

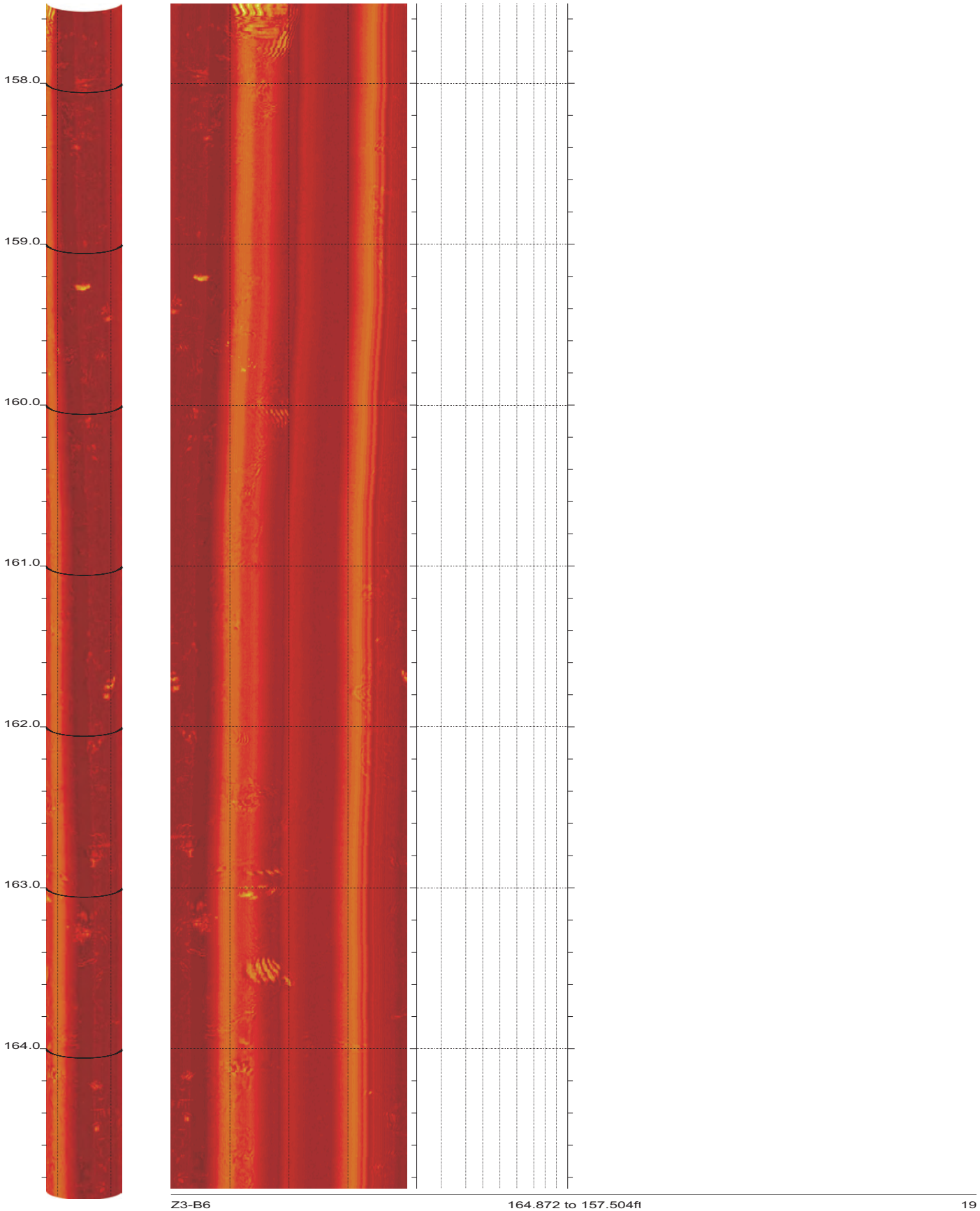
158.0
159.0
160.0
161.0
162.0
163.0
164.0
Z3-B6
164.872 to 157.504ft
19

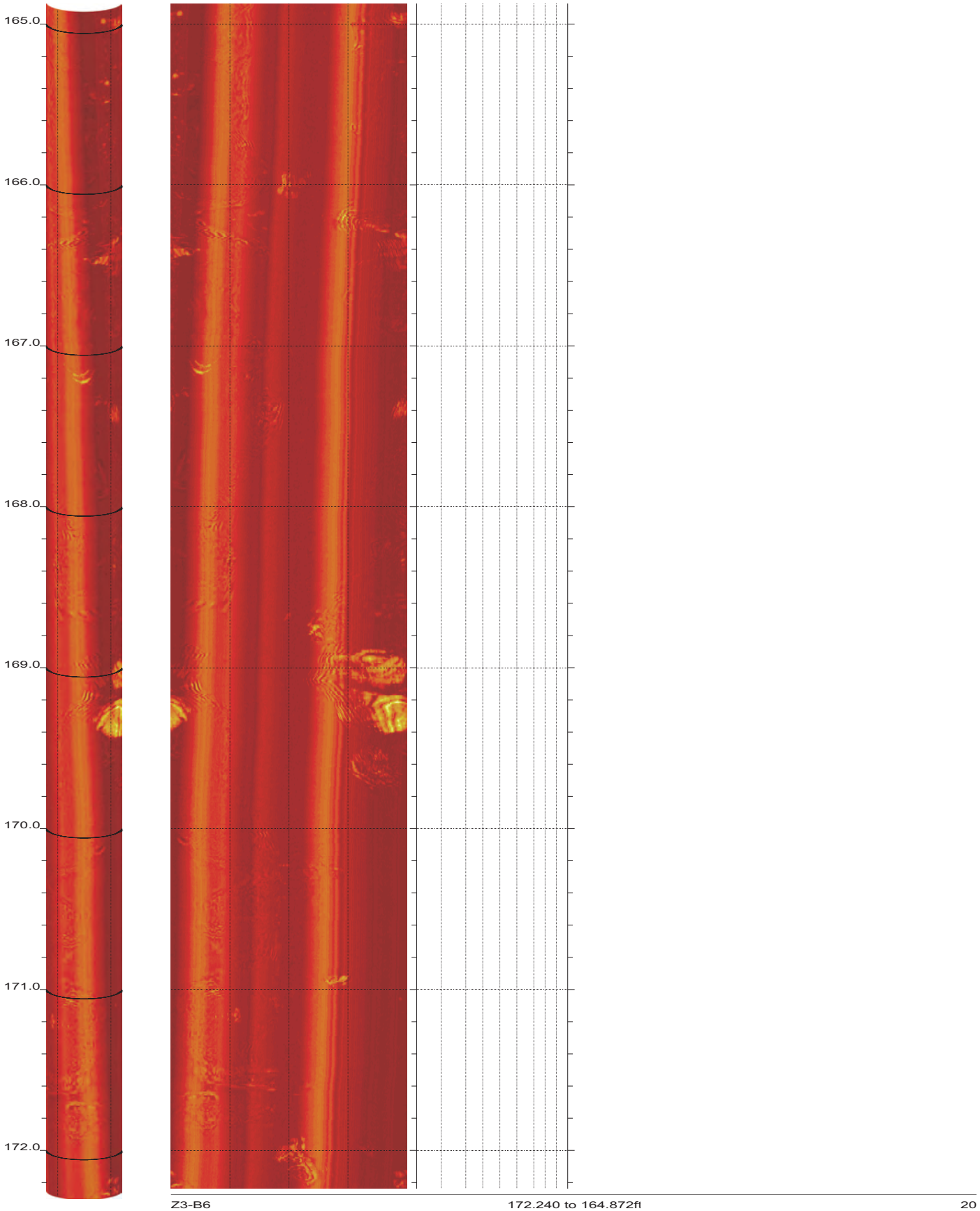


SR-710 Boring Z3-B6 Acoustic Televiewer Dips rev 1 Sheet 20 of 40

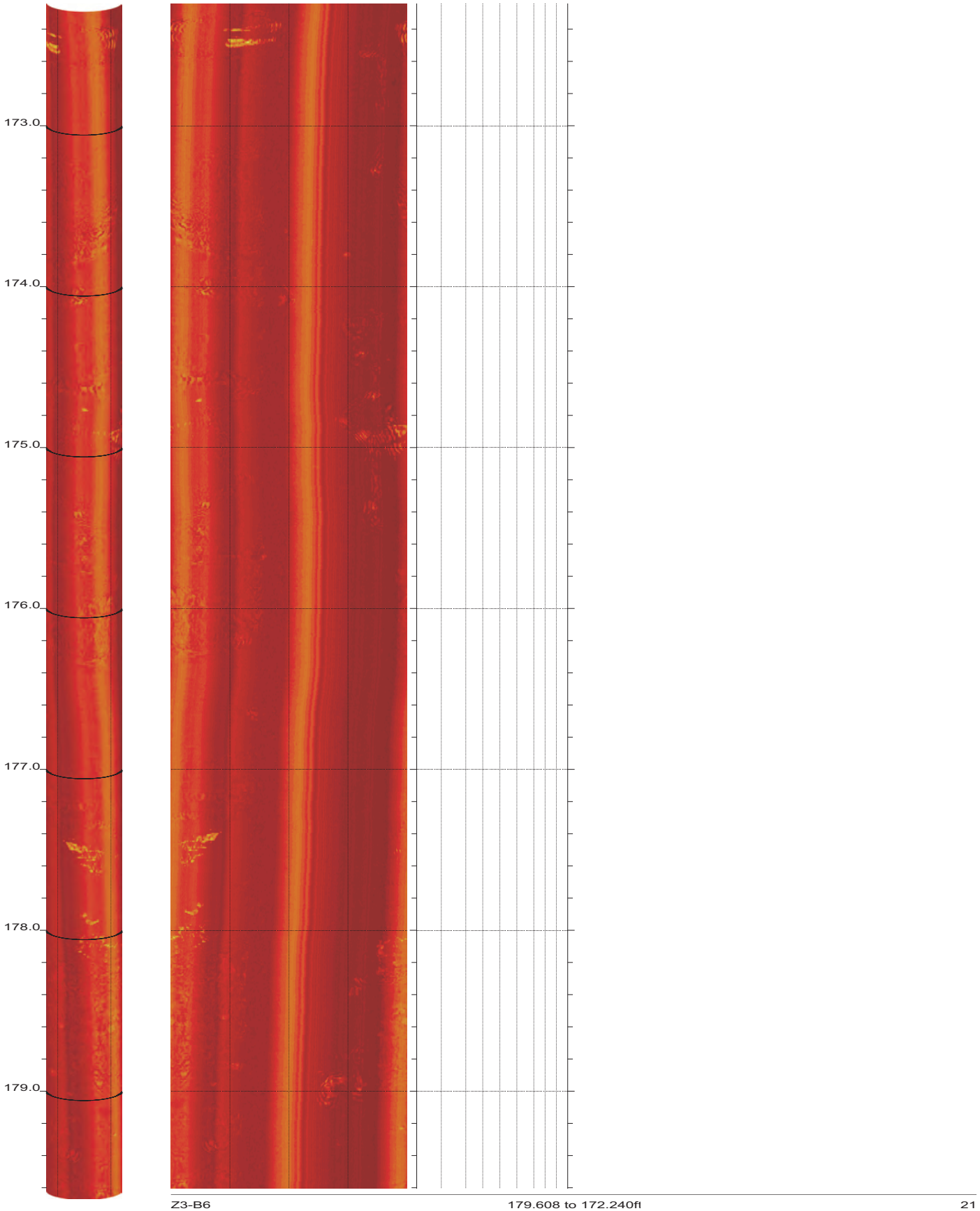


SR-710 Boring Z3-B6 Acoustic Televiewer Dips rev 1 Sheet 21 of 40

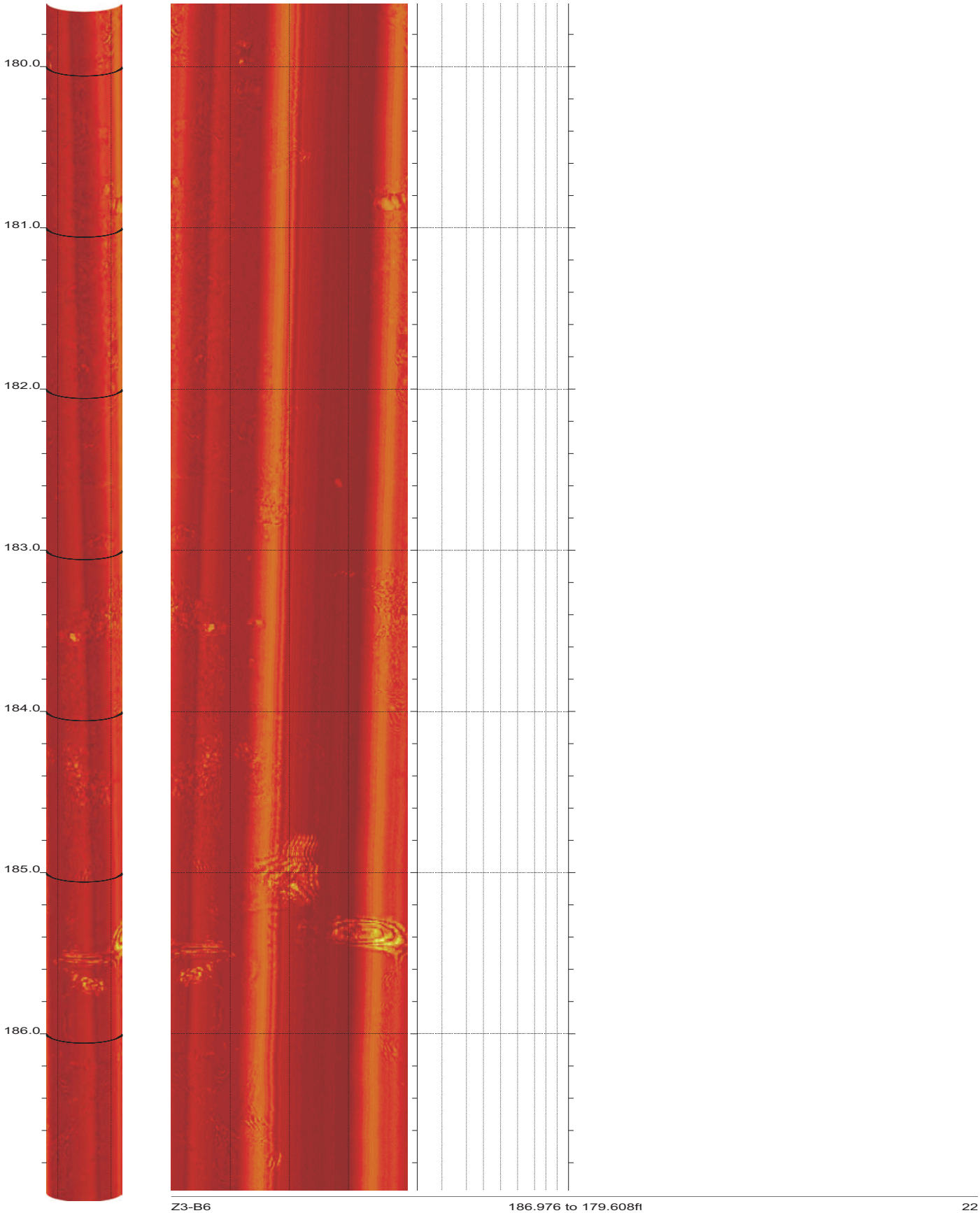
180.0
181.0
182.0
183.0
184.0
185.0
186.0
Z3-B6
186.976 to 179.608ft
22

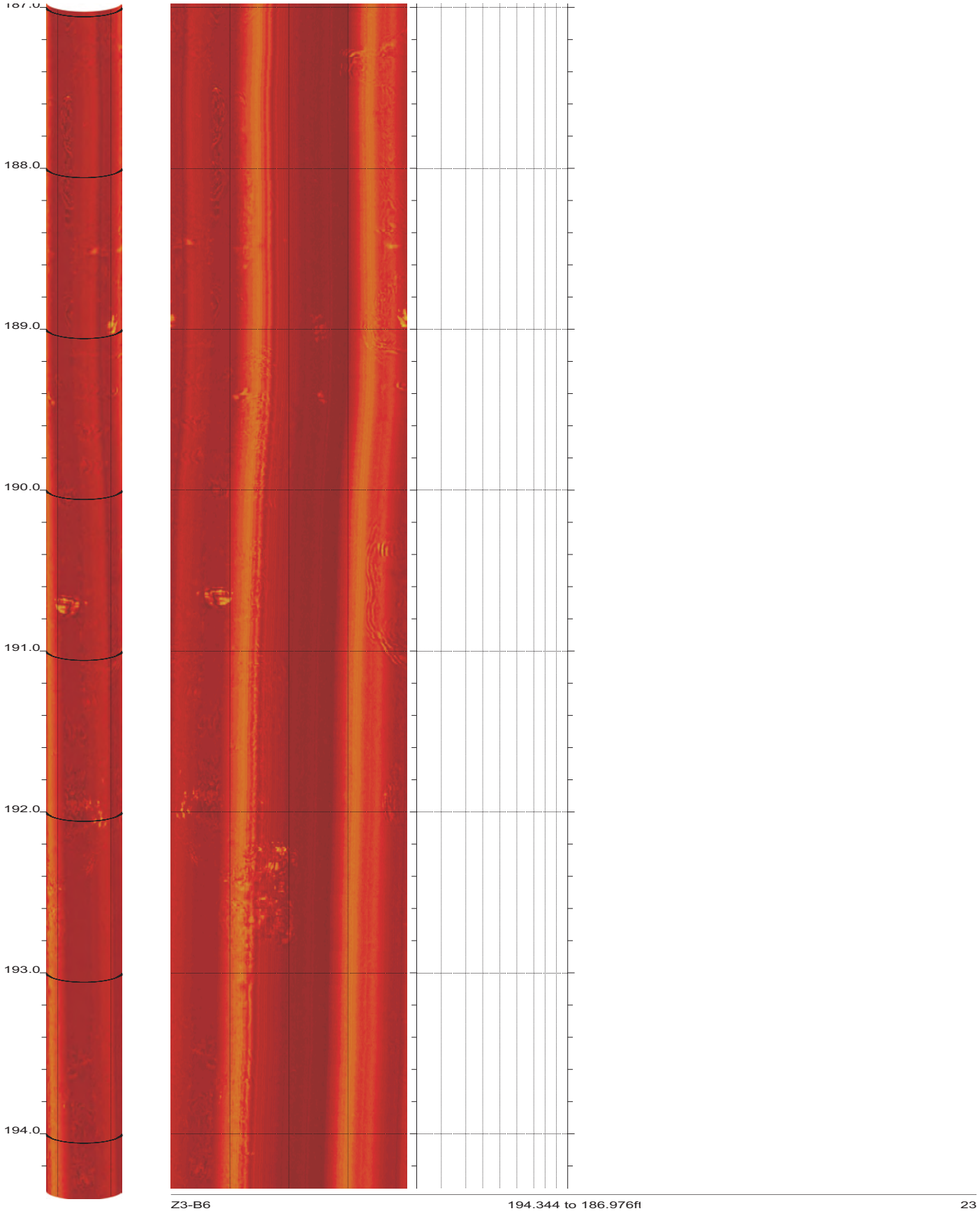
188.0
189.0
190.0
191.0
192.0
193.0
194.0
Z3-B6
194.344 to 186.976fl
23

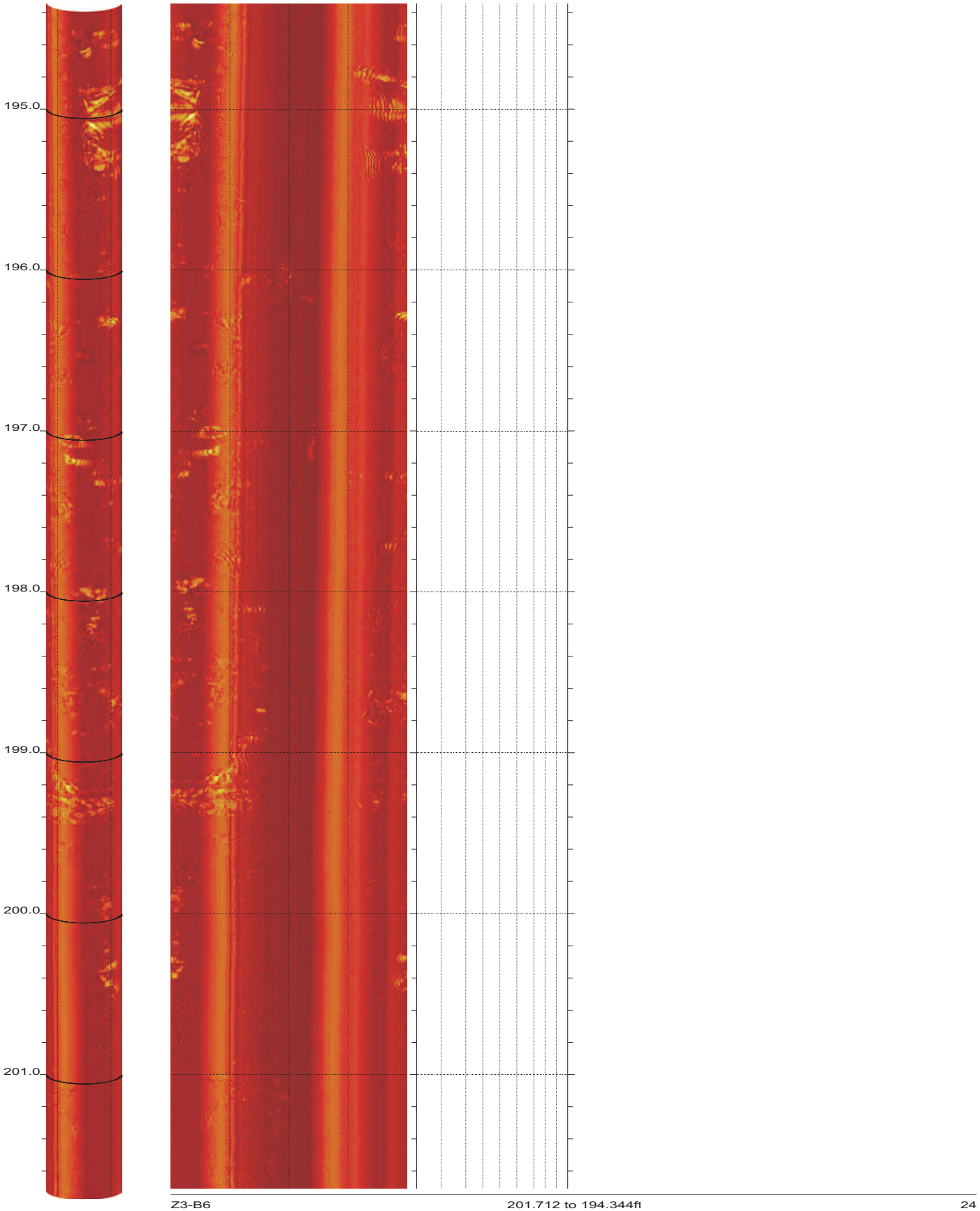


SR-710 Boring Z3-B6 Acoustic Televiewer Dips rev 1 Sheet 24 of 40

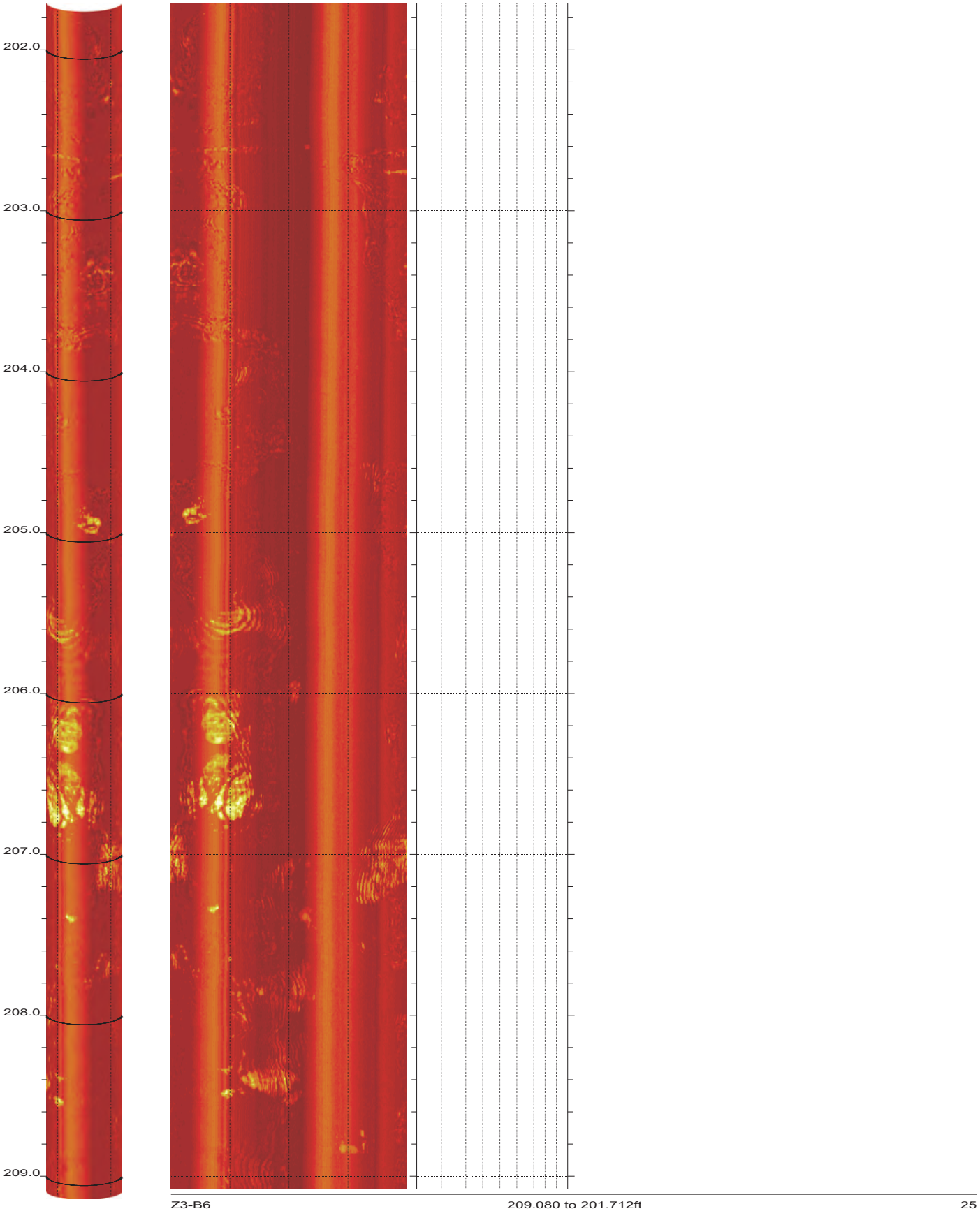


SR-710 Boring Z3-B6 Acoustic Televiewer Dips rev 1 Sheet 25 of 40

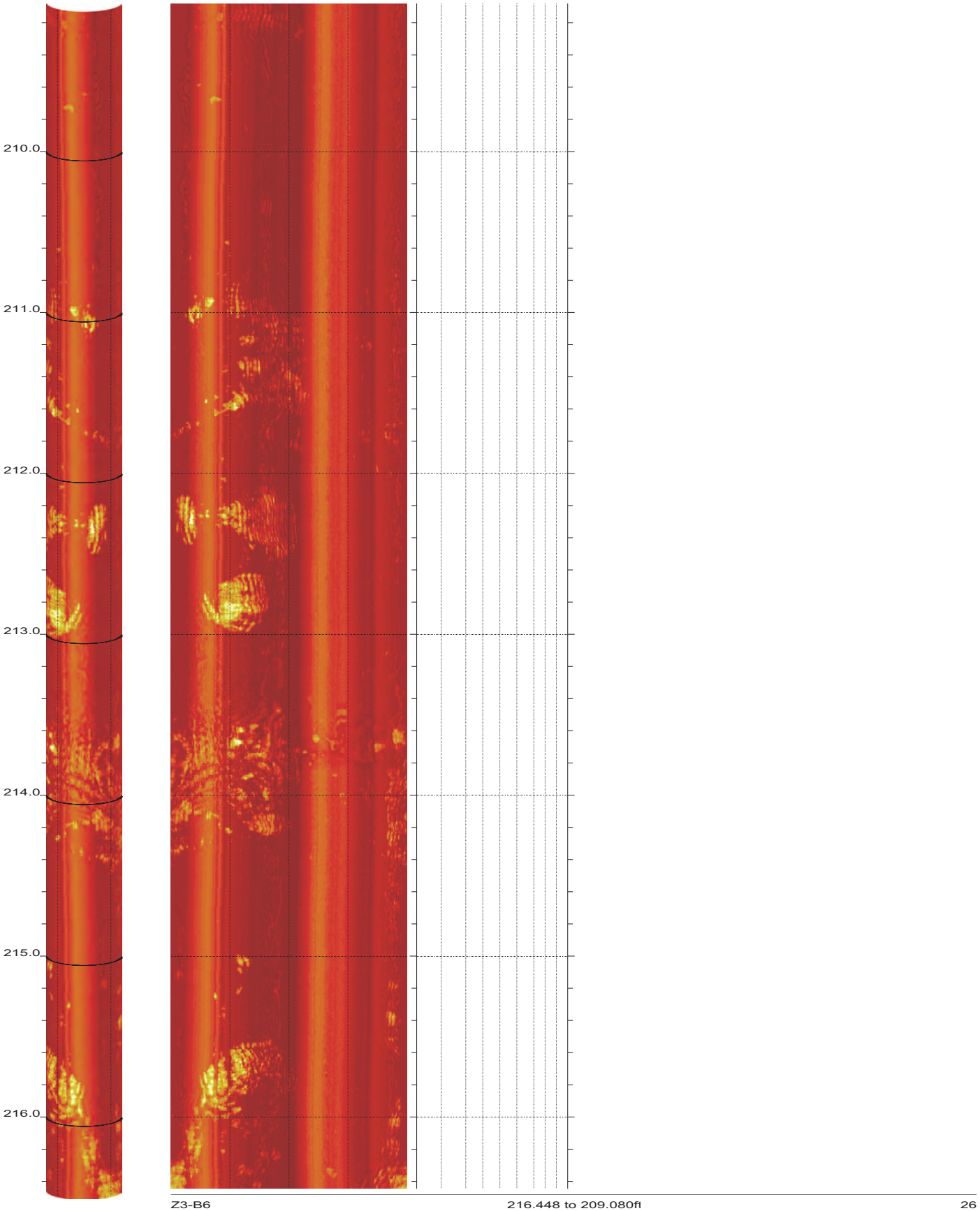


SR-710 Boring Z3-B6 Acoustic Televiewer Dips rev 1 Sheet 26 of 40

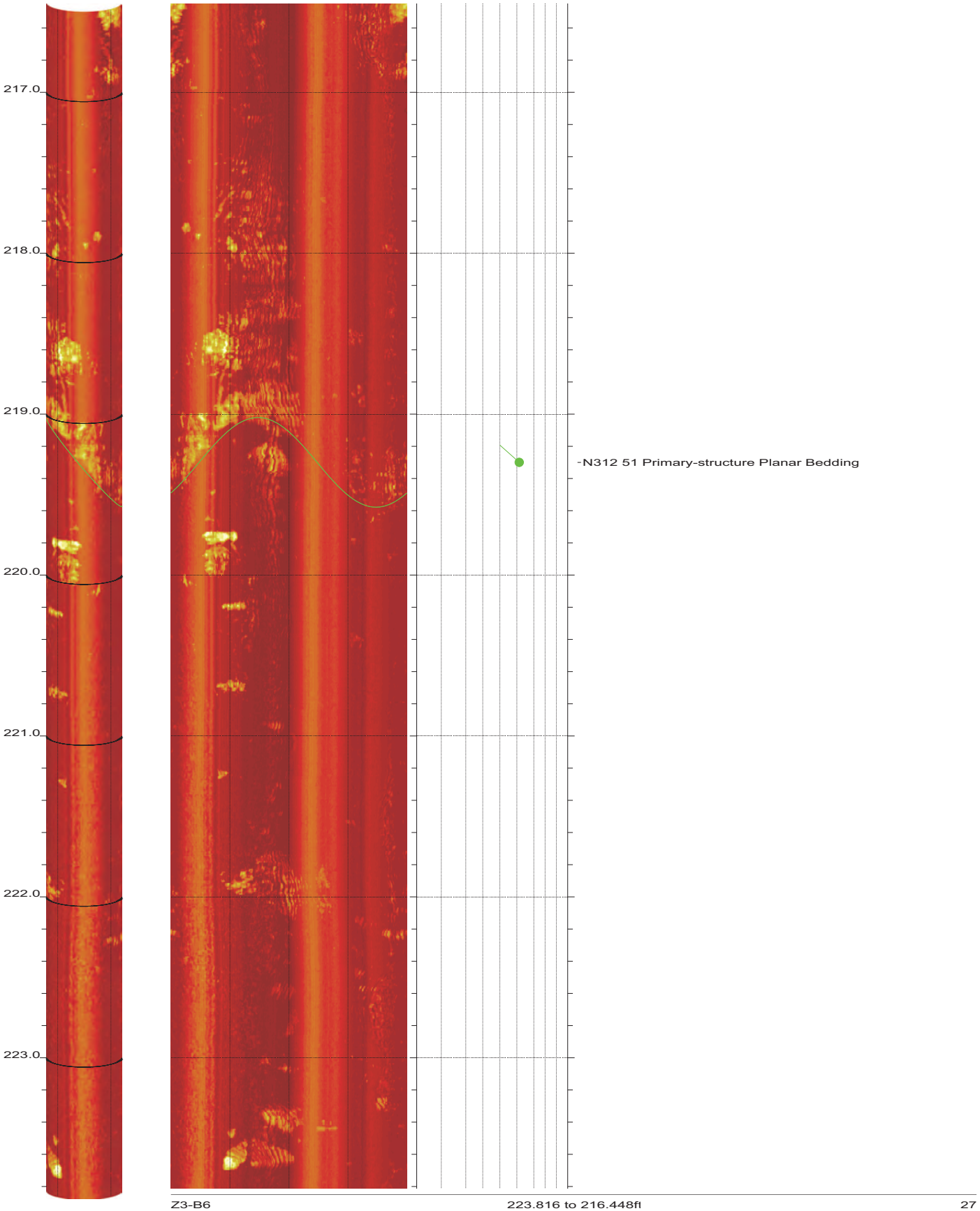


SR-710 Boring Z3-B6 Acoustic Televiewer Dips rev 1 Sheet 27 of 40

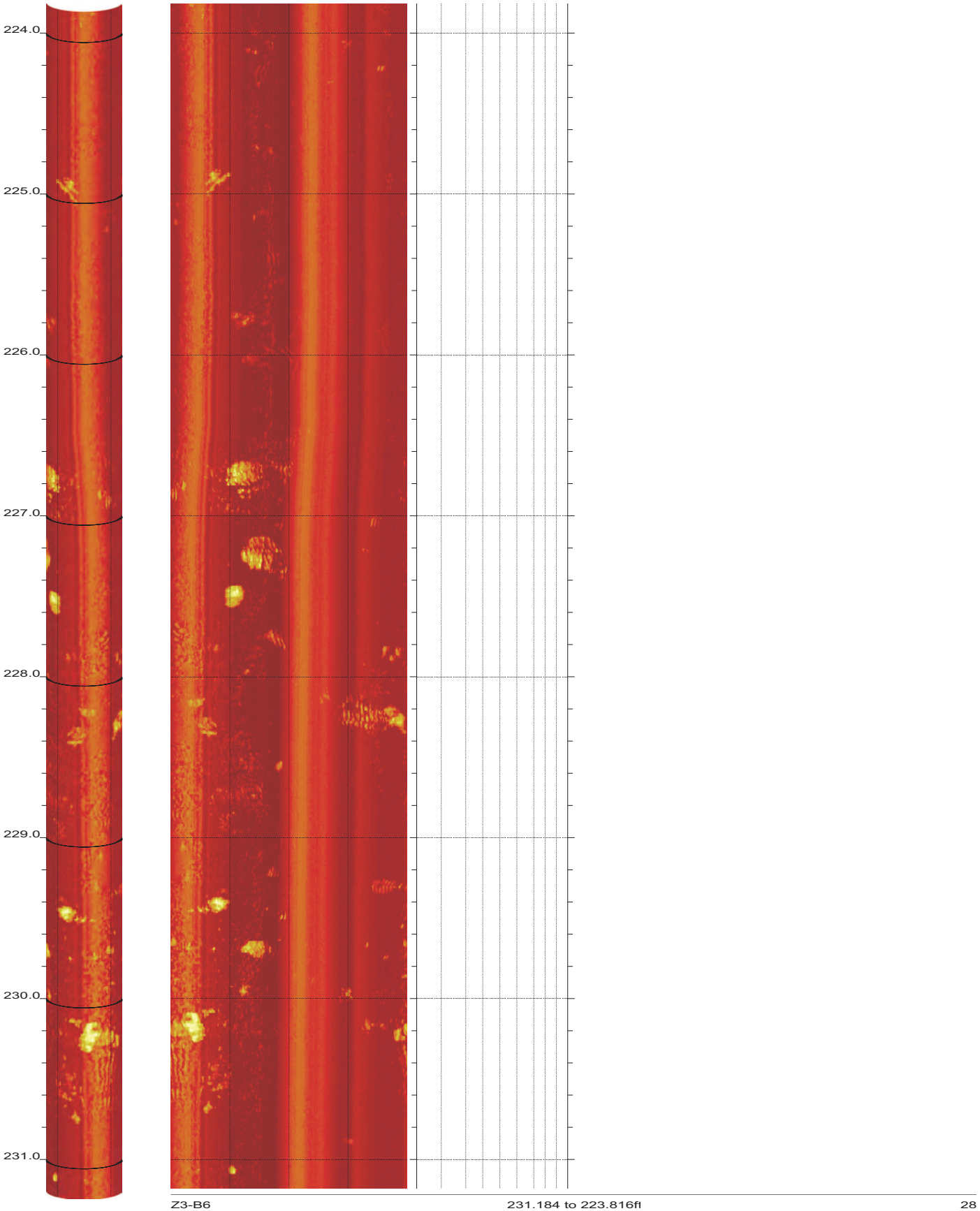


SR-710 Boring Z3-B6 Acoustic Televiewer Dips rev 1 Sheet 28 of 40

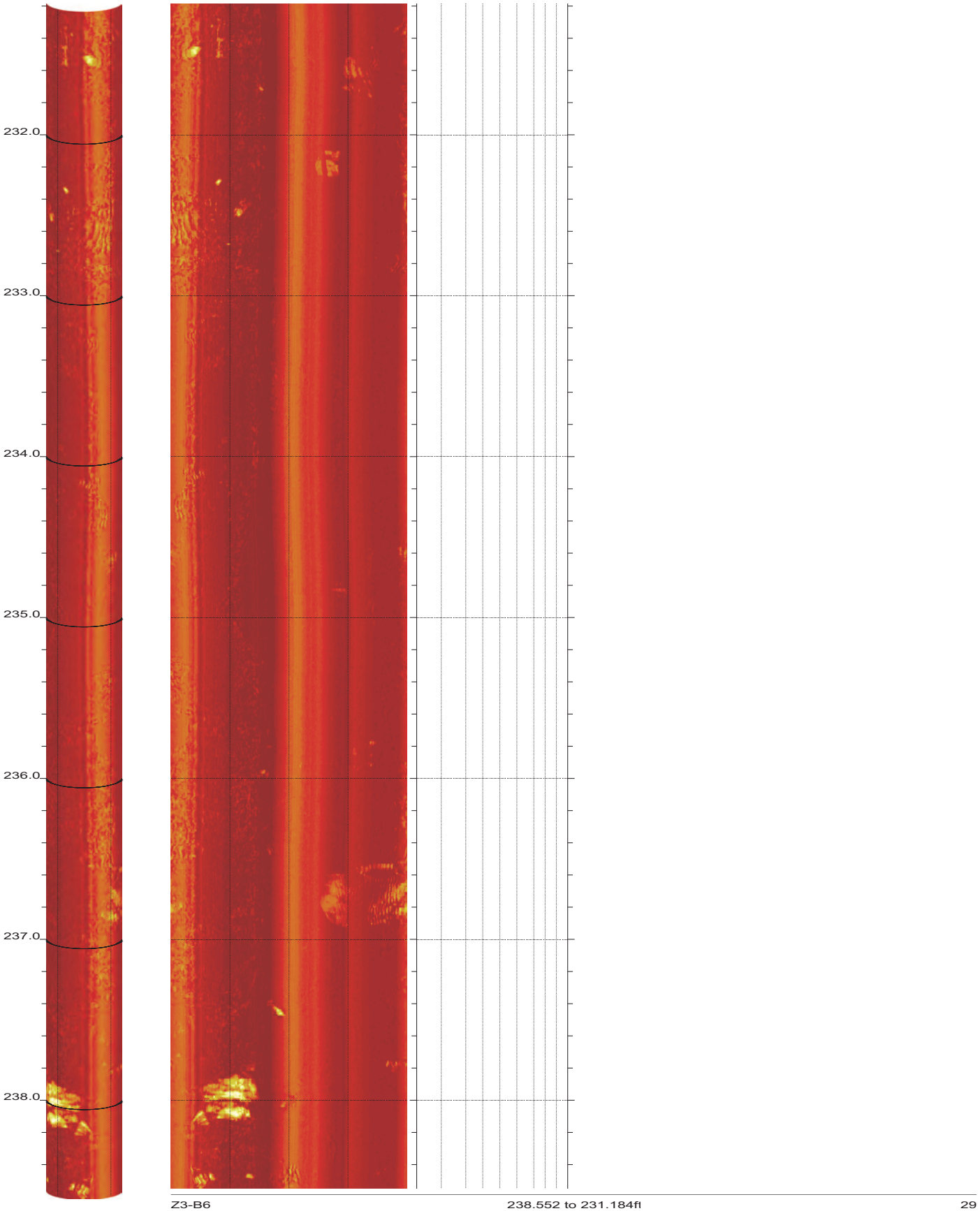
232.0
233.0
234.0
235.0
236.0
237.0
238.0
Z3-B6
238.552 to 231.184fl
29

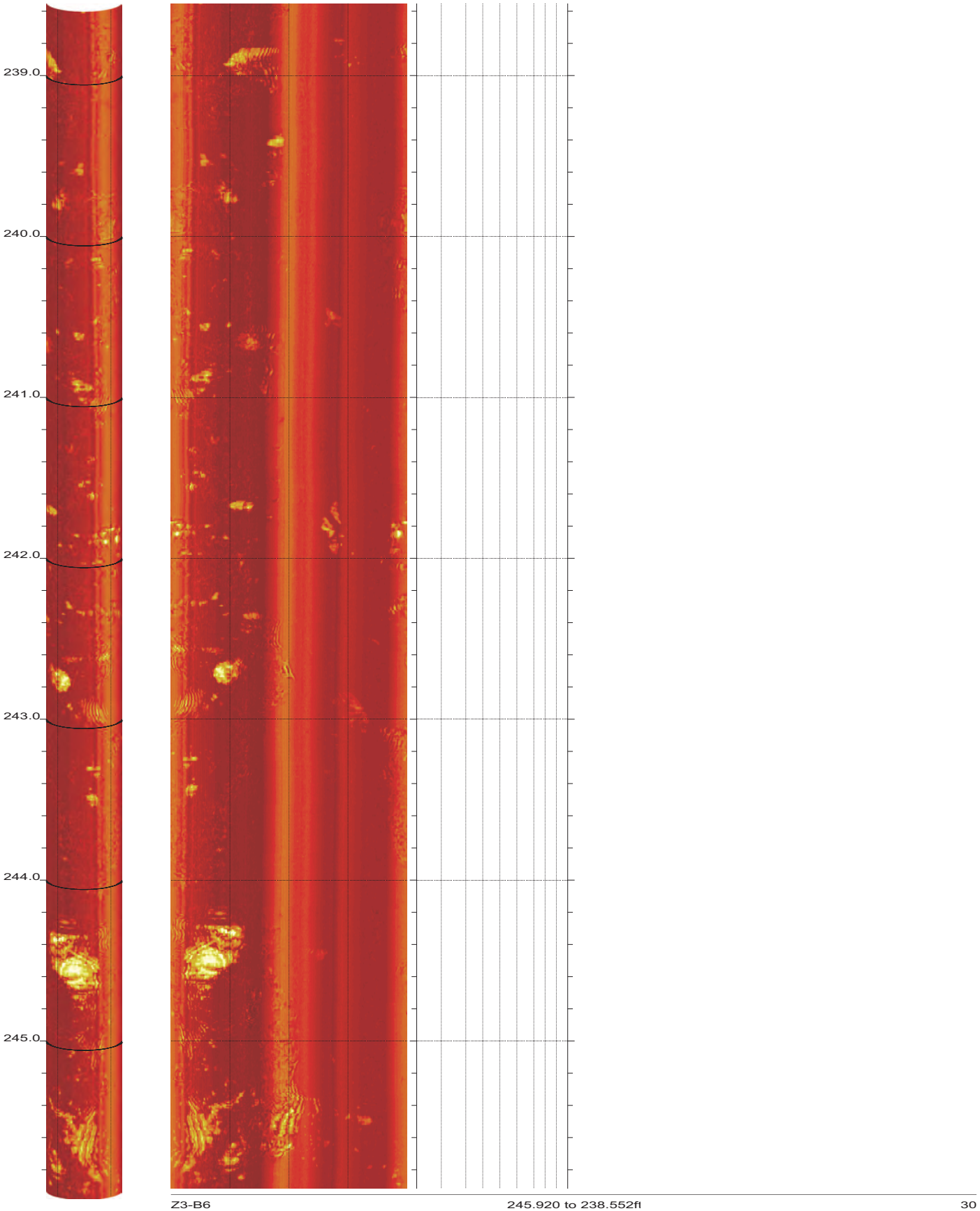


SR-710 Boring Z3-B6 Acoustic Televiewer Dips rev 1 Sheet 30 of 40

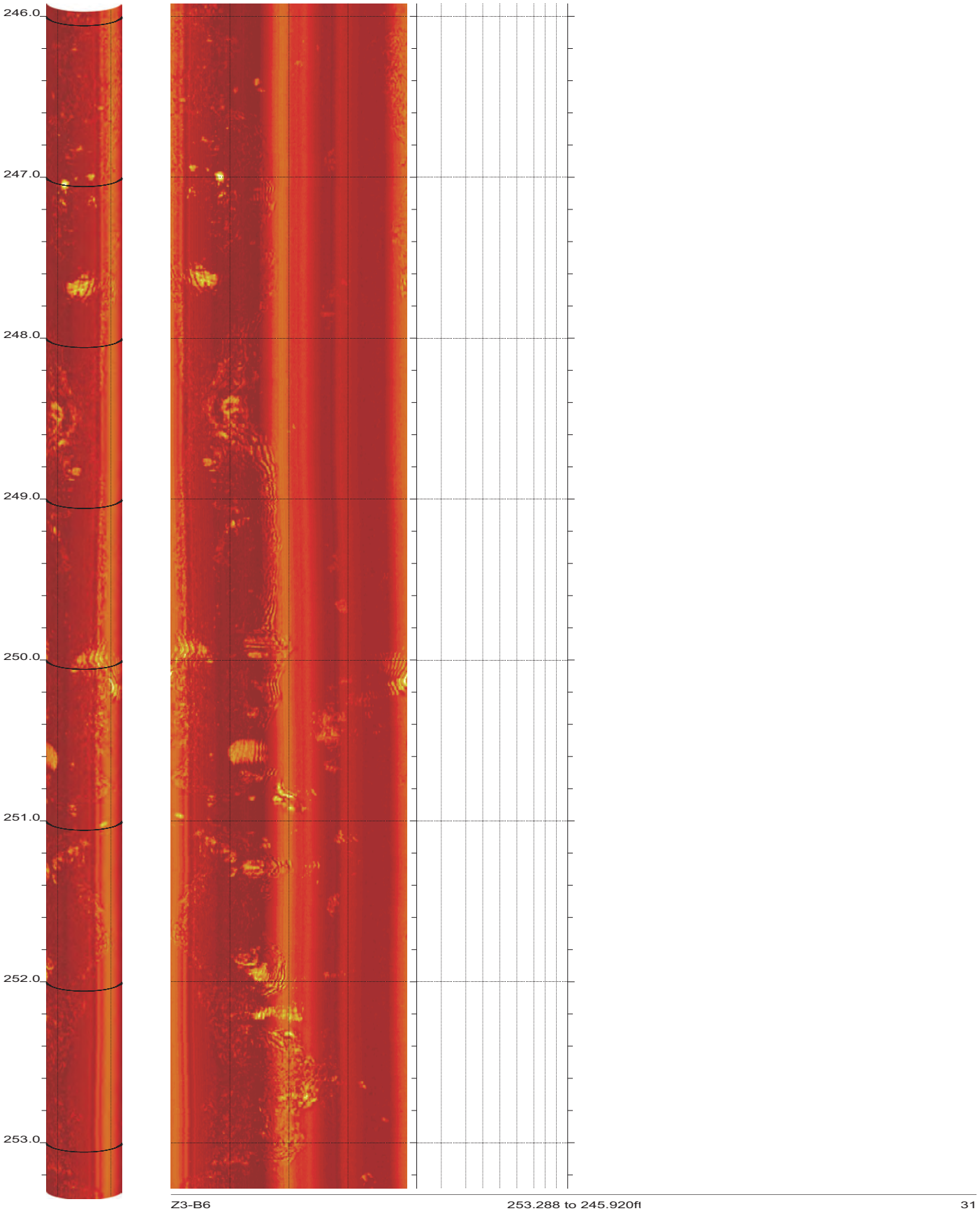


SR-710 Boring Z3-B6 Acoustic Televiewer Dips rev 1 Sheet 31 of 40

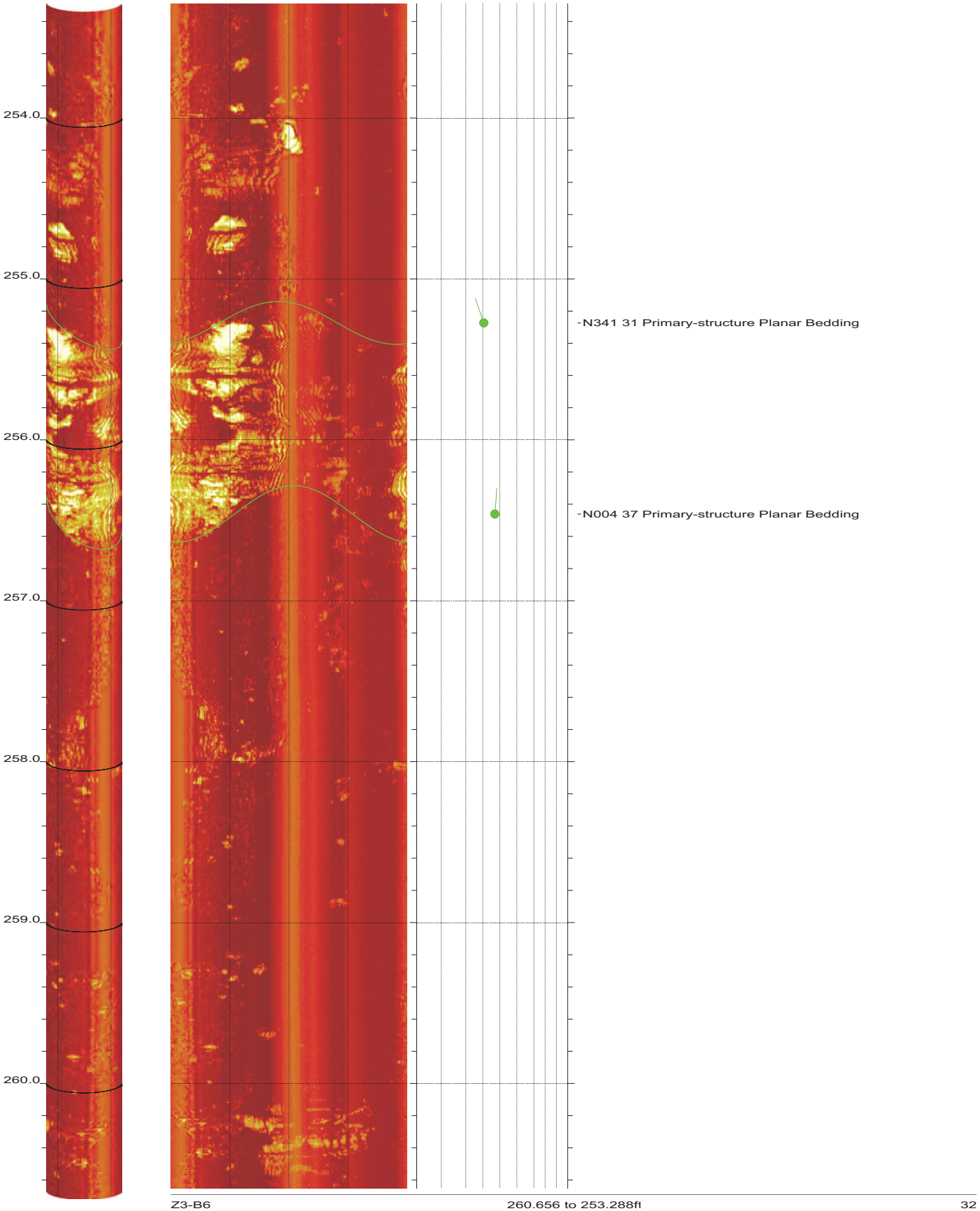


SR-710 Boring Z3-B6 Acoustic Televiewer Dips rev 1 Sheet 32 of 40

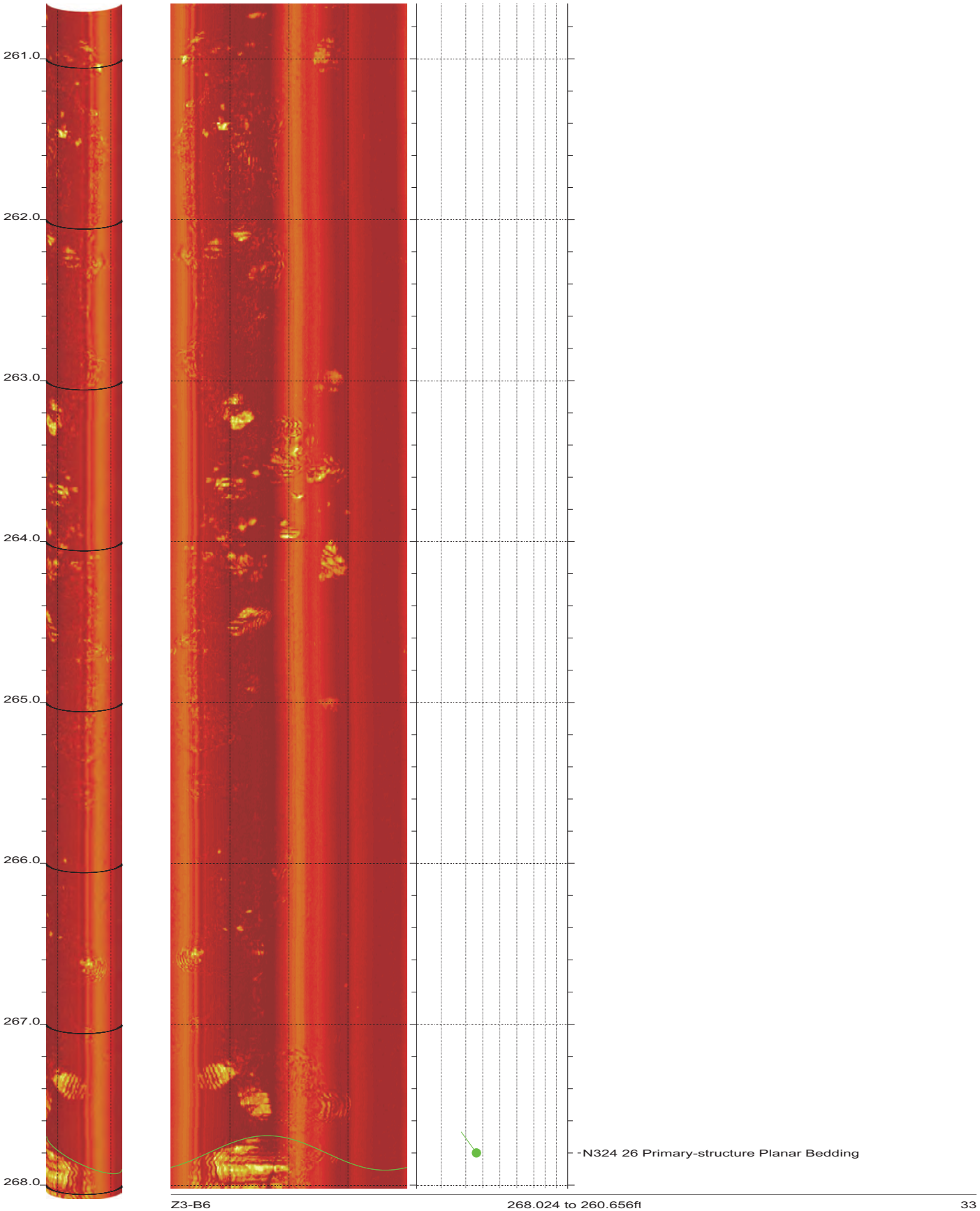


SR-710 Boring Z3-B6 Acoustic Televiewer Dips rev 1 Sheet 33 of 40

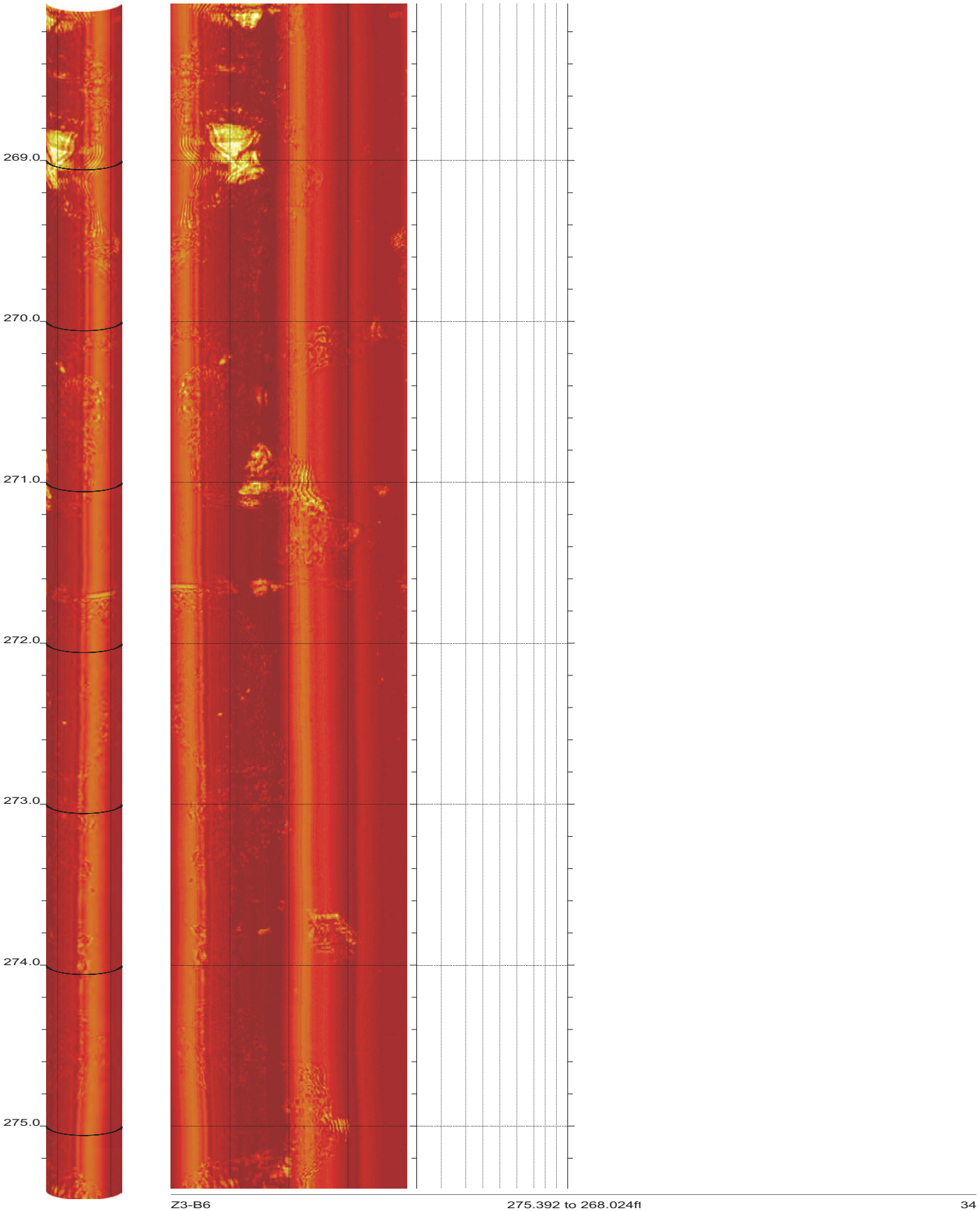


SR-710 Boring Z3-B6 Acoustic Televiewer Dips rev 1 Sheet 34 of 40

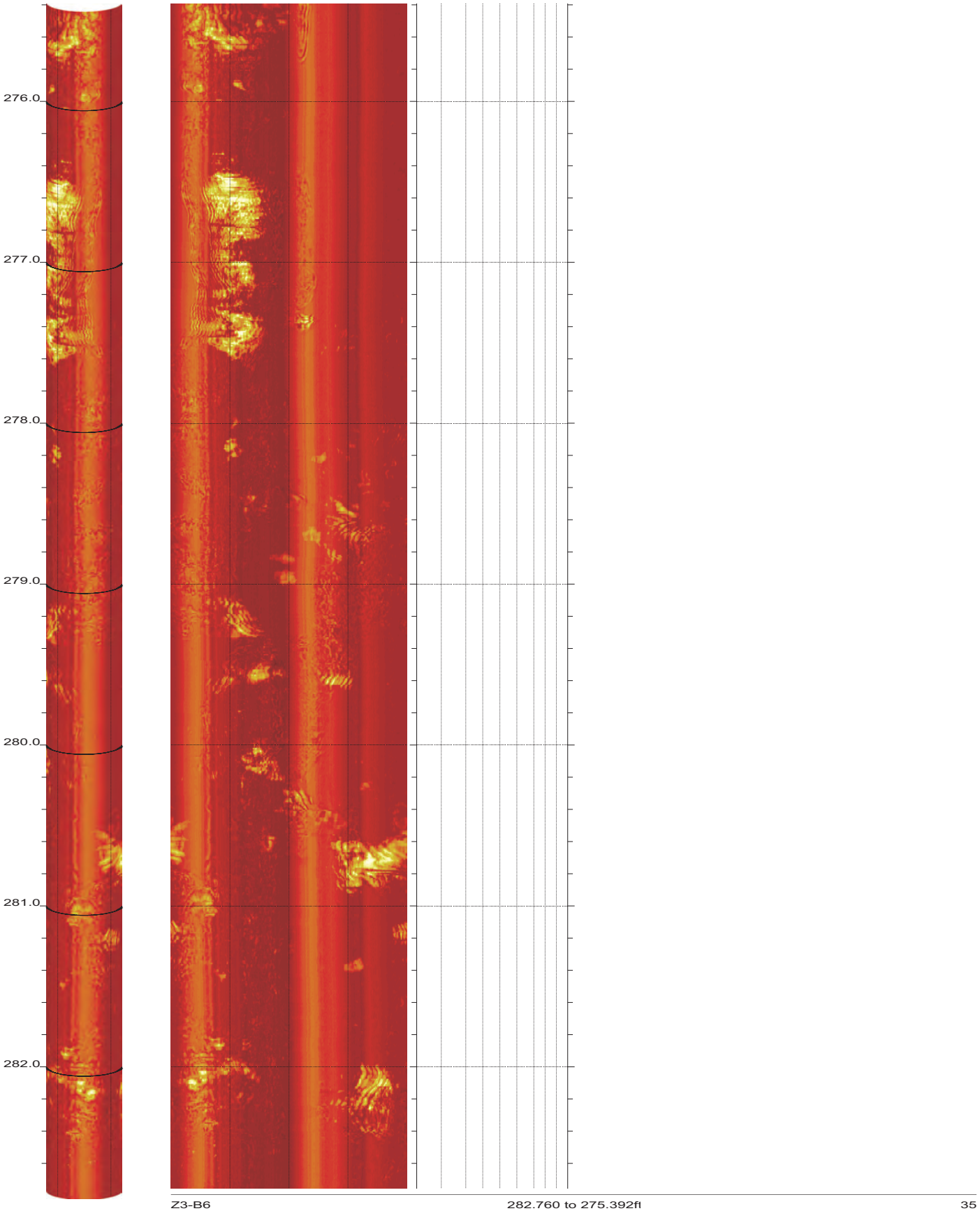


SR-710 Boring Z3-B6 Acoustic Televiewer Dips rev 1 Sheet 35 of 40

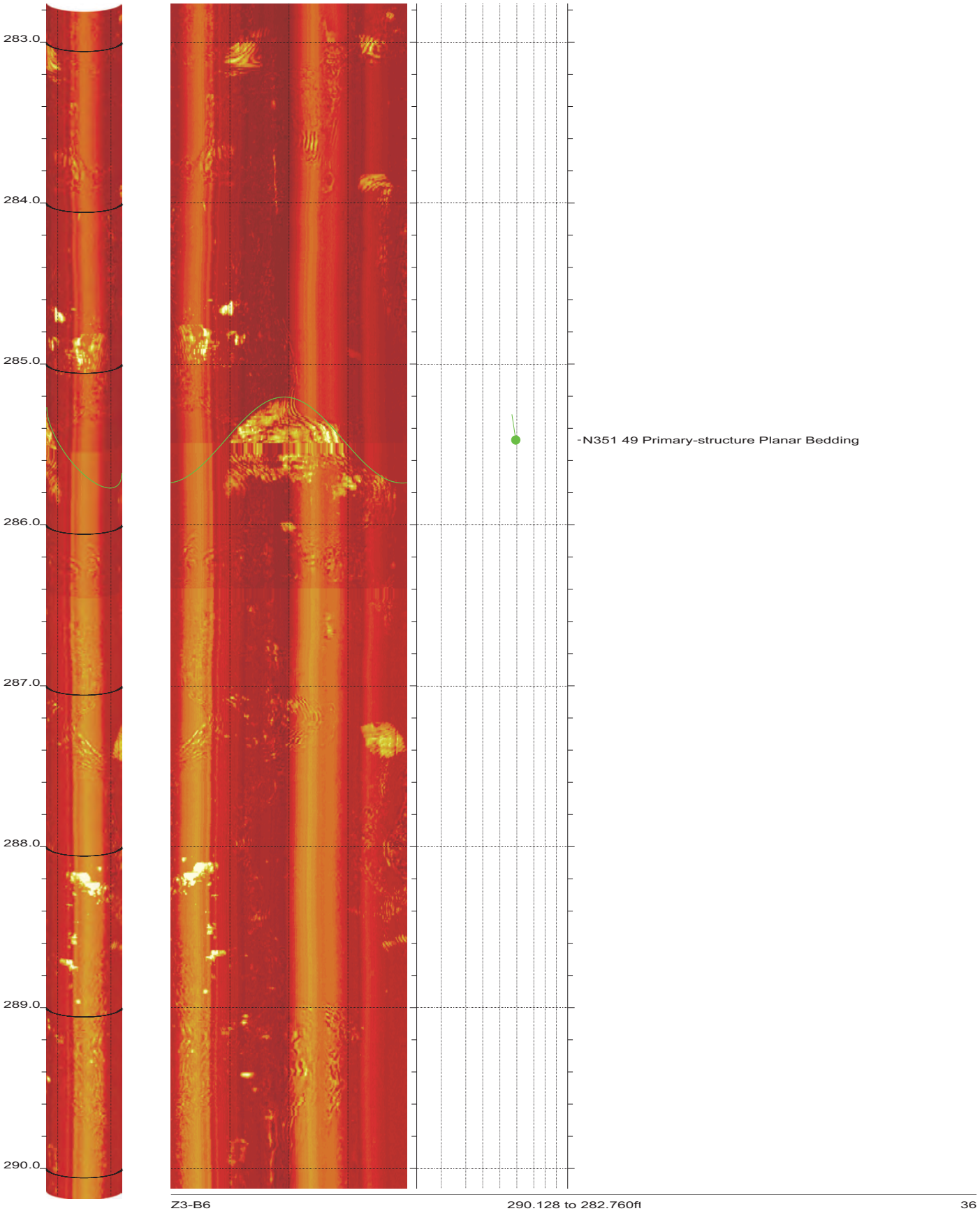


SR-710 Boring Z3-B6 Acoustic Televiewer Dips rev 1 Sheet 36 of 40

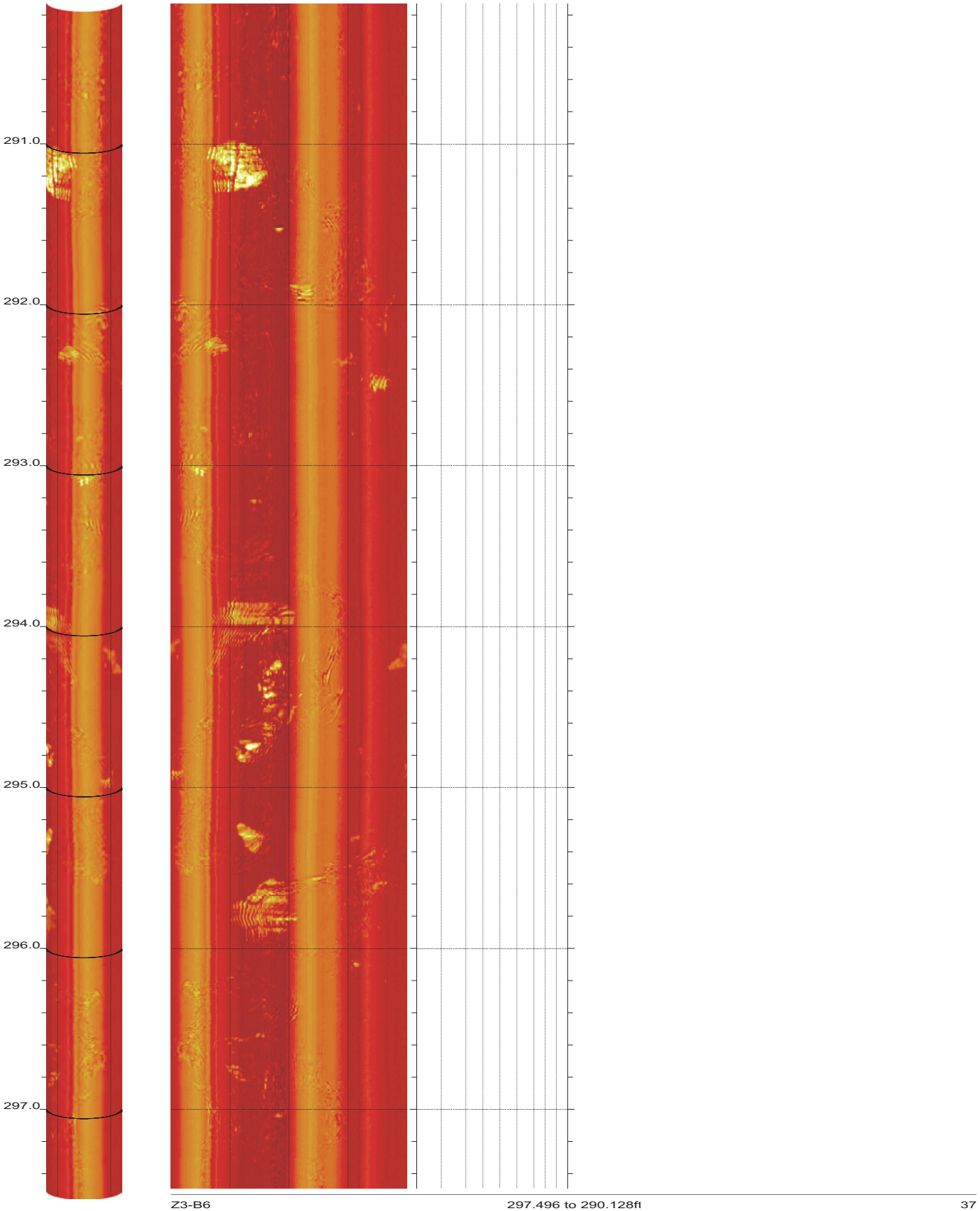


SR-710 Boring Z3-B6 Acoustic Televiewer Dips rev 1 Sheet 37 of 40

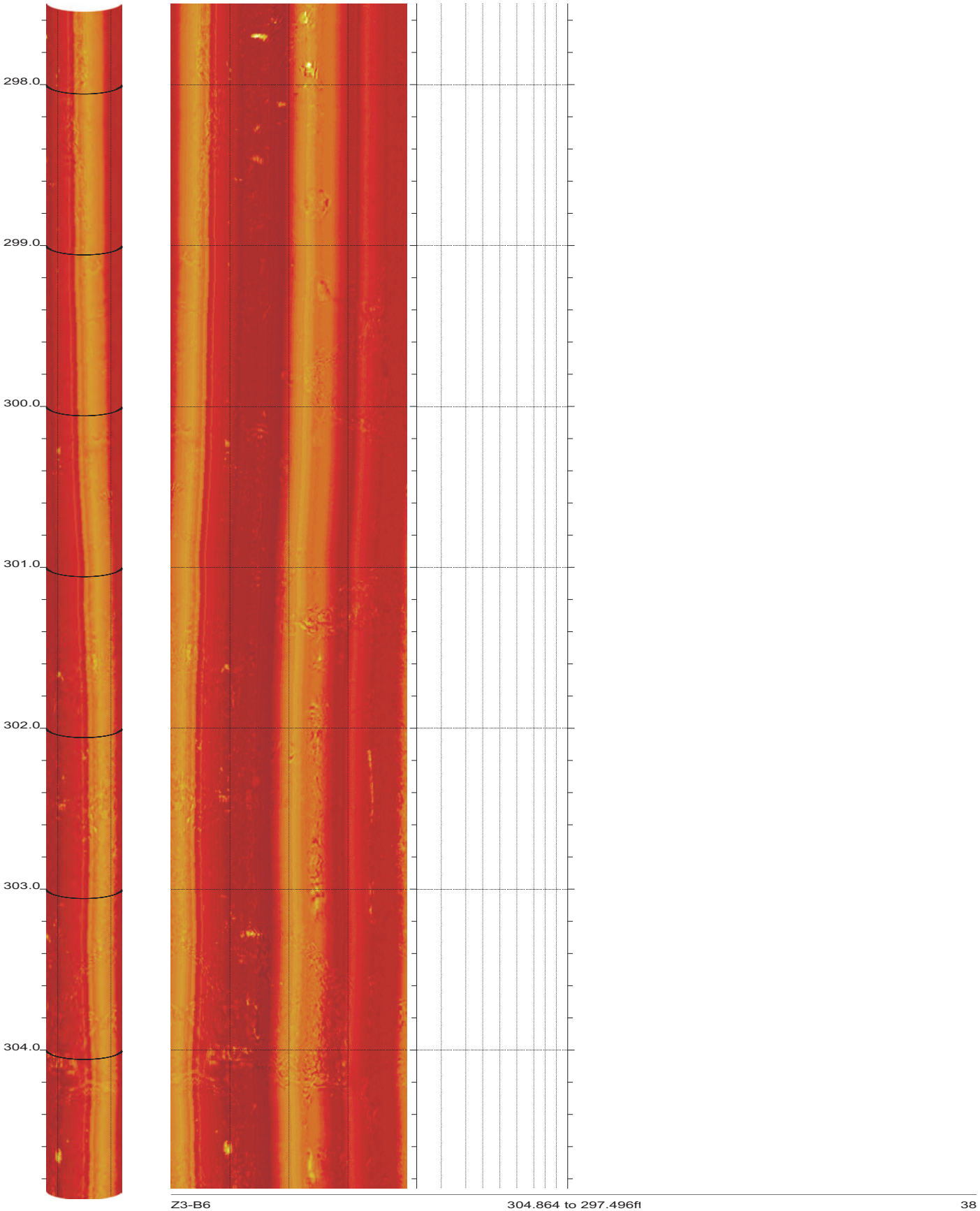


SR-710 Boring Z3-B6 Acoustic Televiewer Dips rev 1 Sheet 38 of 40

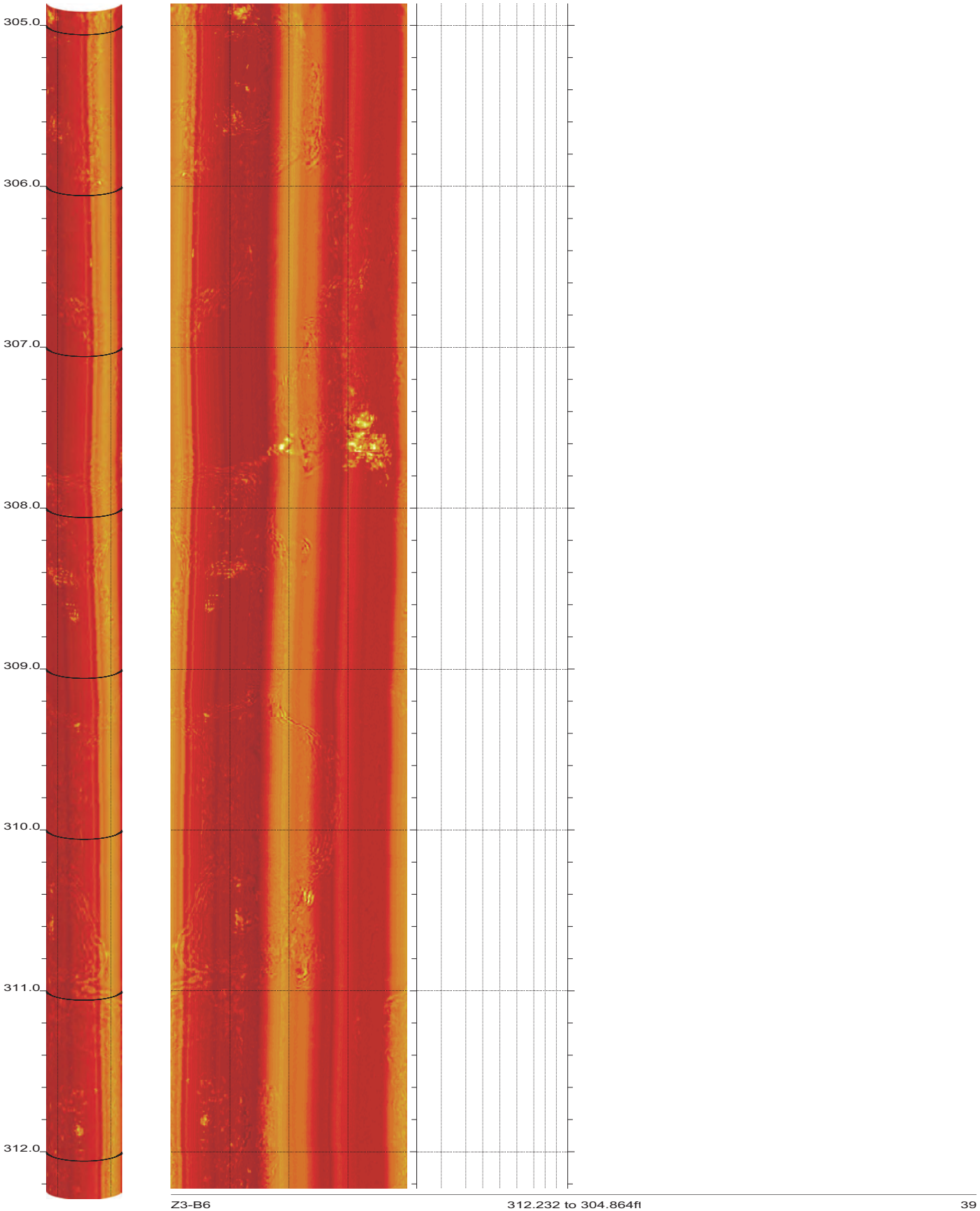


SR-710 Boring Z3-B6 Acoustic Televiewer Dips rev 1 Sheet 39 of 40

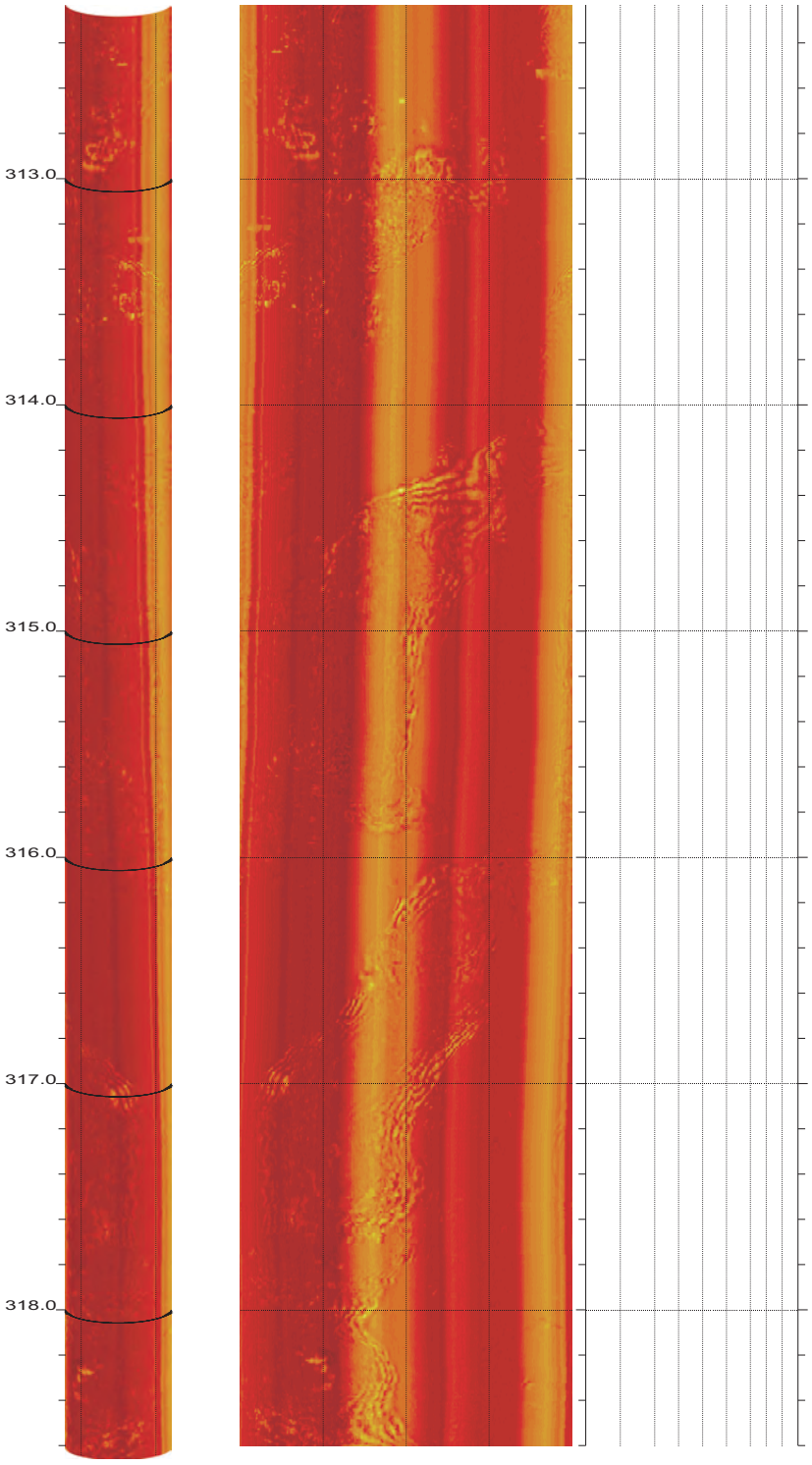
313.0
314.0
315.0
316.0
317.0
318.0

BHTV DATA PROCESSING
RGLDIP vsn 6.2
INTERPRETED BHTV DIPS LOG

CASCADE DRILLING

Borehole: Z3-B12

SR-710 TUNNEL INVESTIGATION

top of borehole.....
East: _
North: _
Elev: _

North ref. is true
Depth units are feet
Vertical scale: 1/10
Horiz scale = 1.00x Vert scale

Zone from 182.400 to 57.000ft
Format: BHTV-NESWN

Borehole diam: 7.000inch
Vertical = borehole-axis
Image: Amplitude

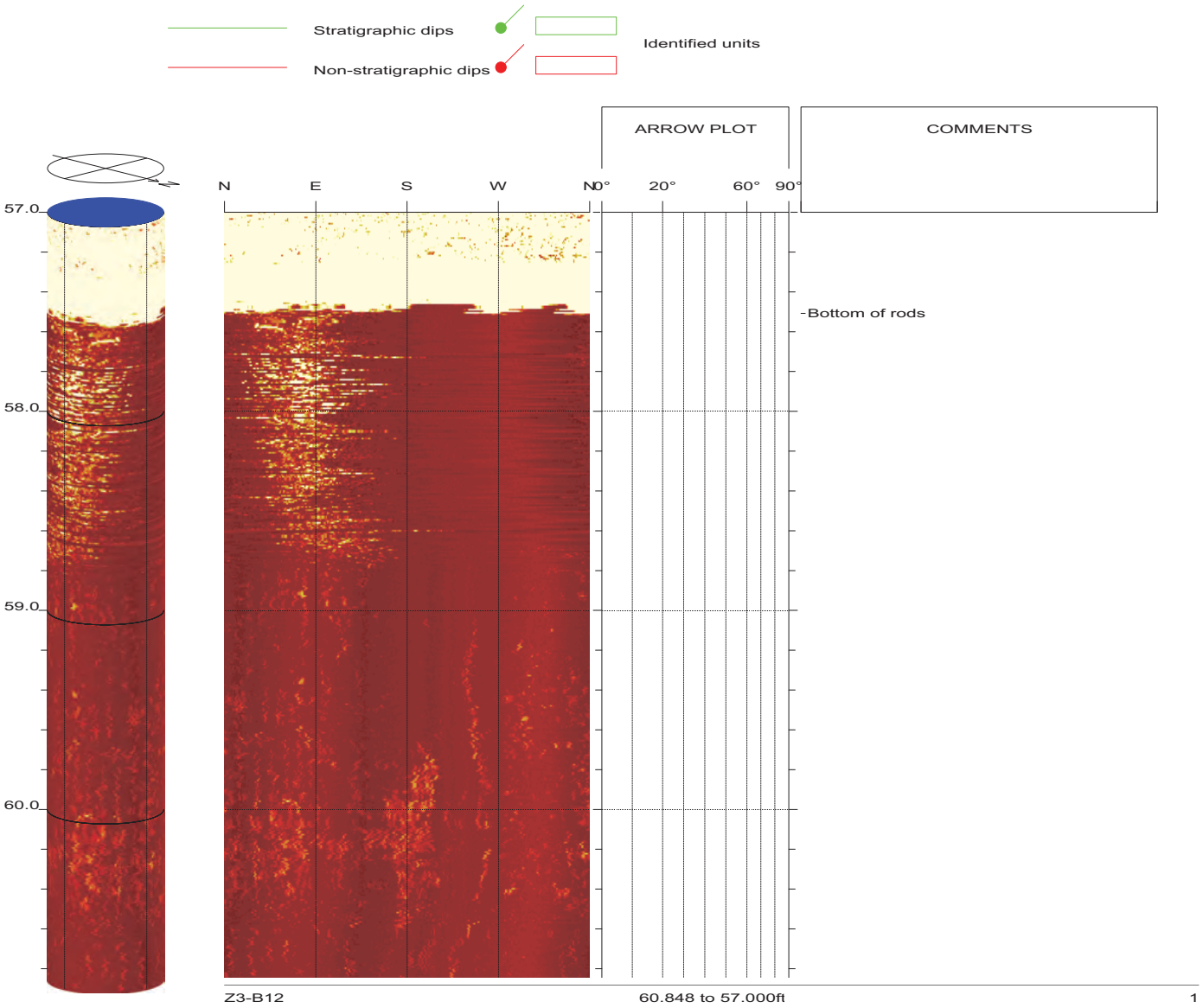

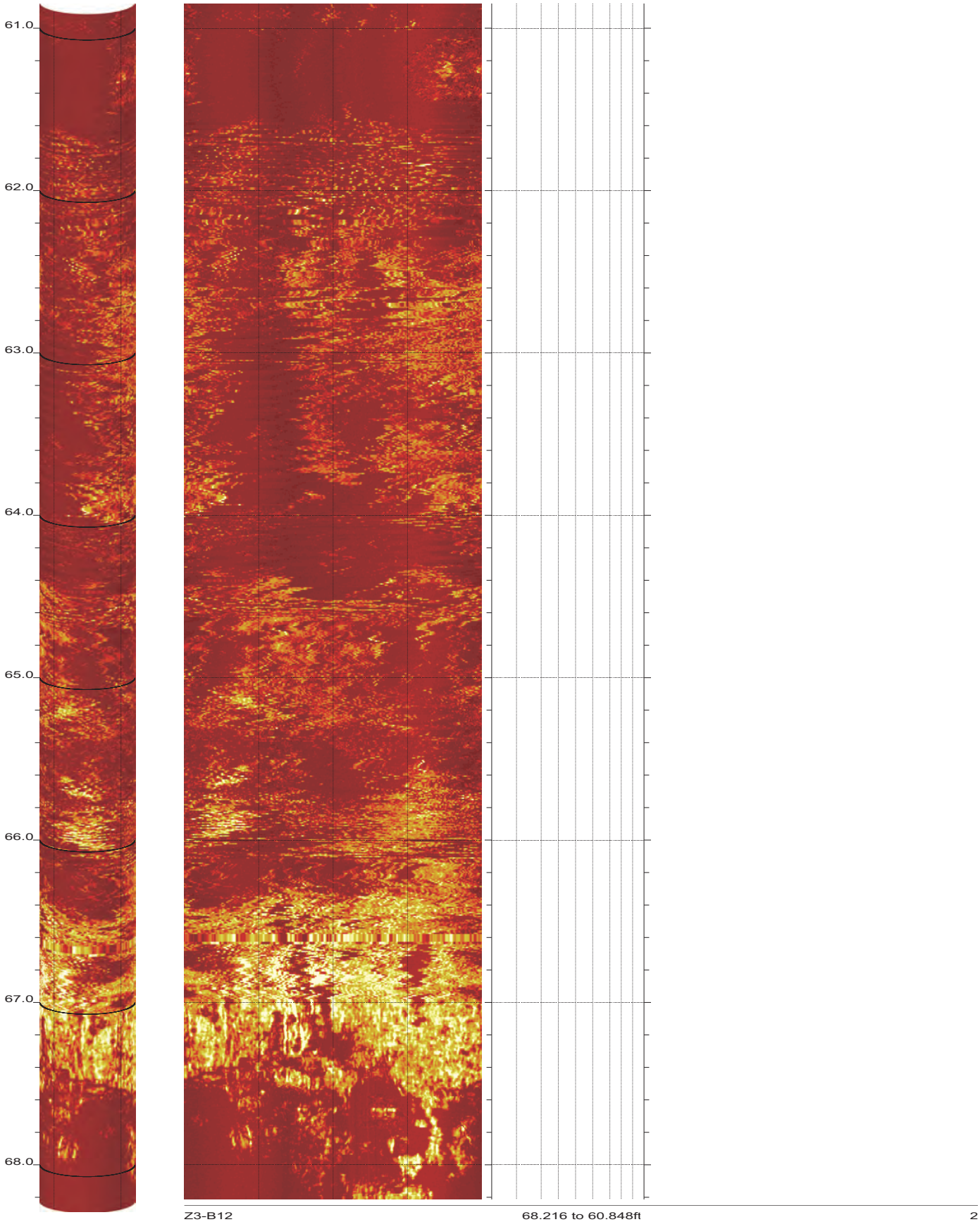
61.0
62.0
63.0
64.0
65.0
66.0
67.0
68.0
Z3-B12
68.216 to 60.848ft
2

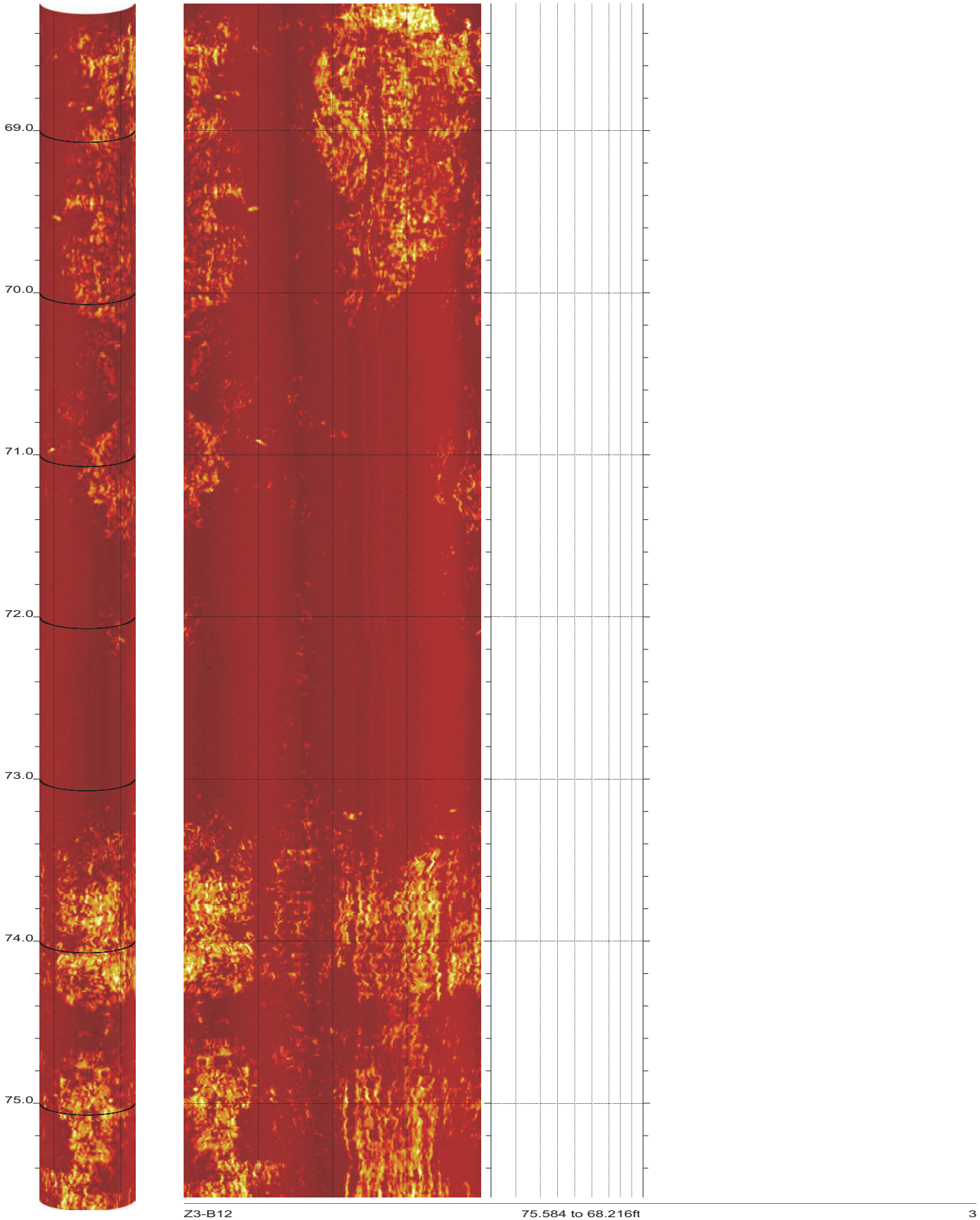


SR-710 Boring Z3-B12 Acoustic Televiewer Dips rev 1 Sheet 3 of 18

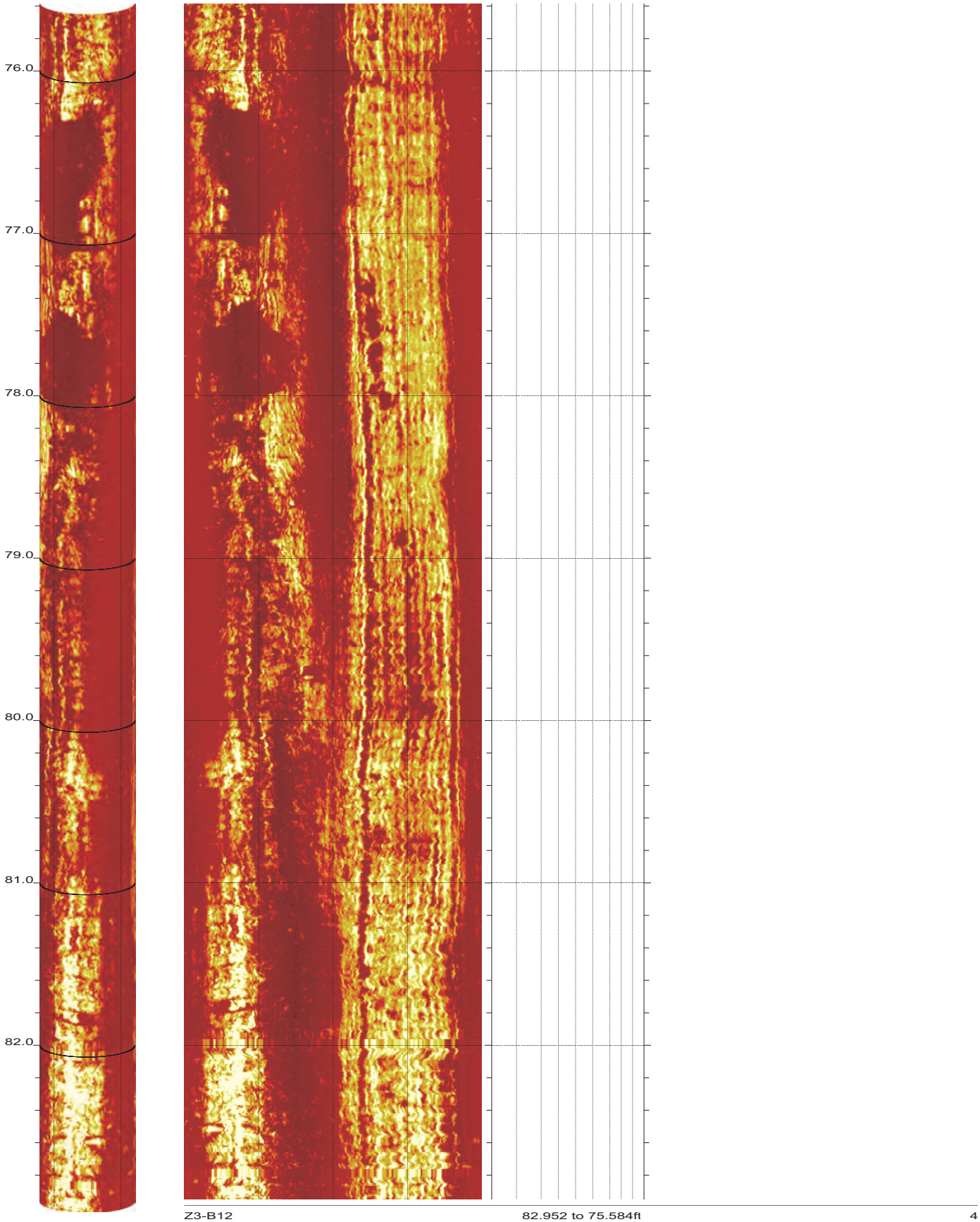


SR-710 Boring Z3-B12 Acoustic Televiewer Dips rev 1 Sheet 4 of 18

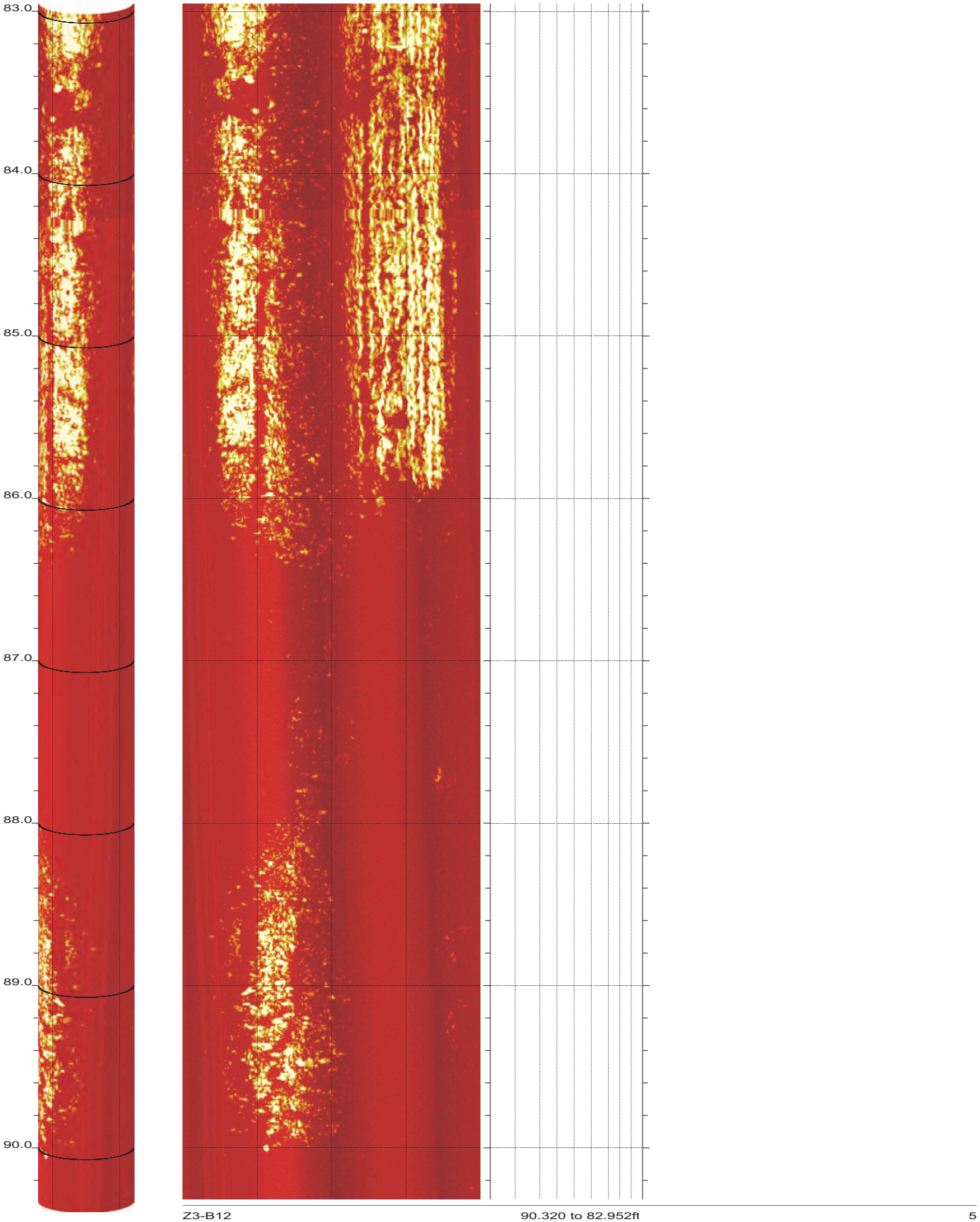


SR-710 Boring Z3-B12 Acoustic Televiewer Dips rev 1 Sheet 5 of 18

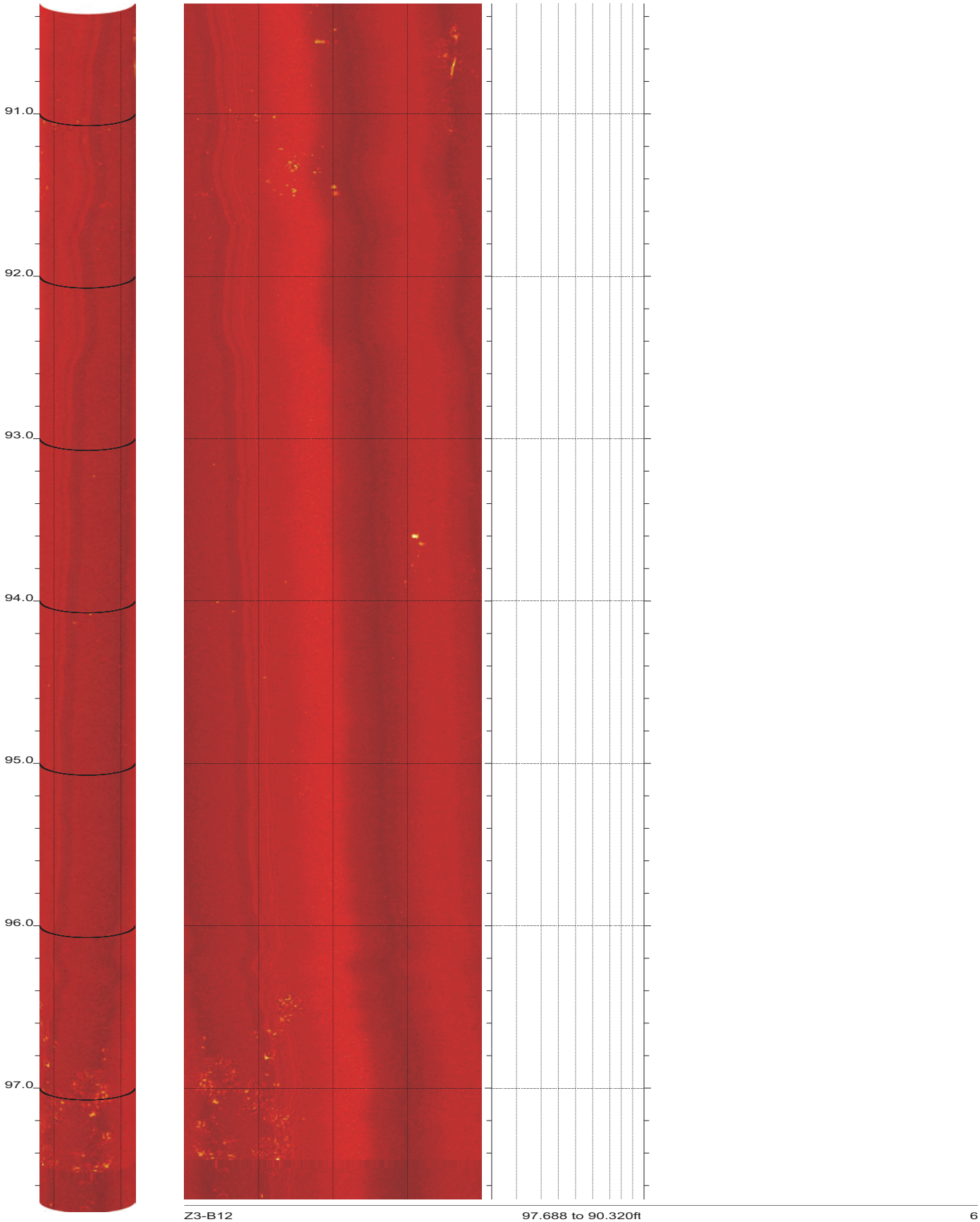


SR-710 Boring Z3-B12 Acoustic Televiewer Dips rev 1 Sheet 6 of 18

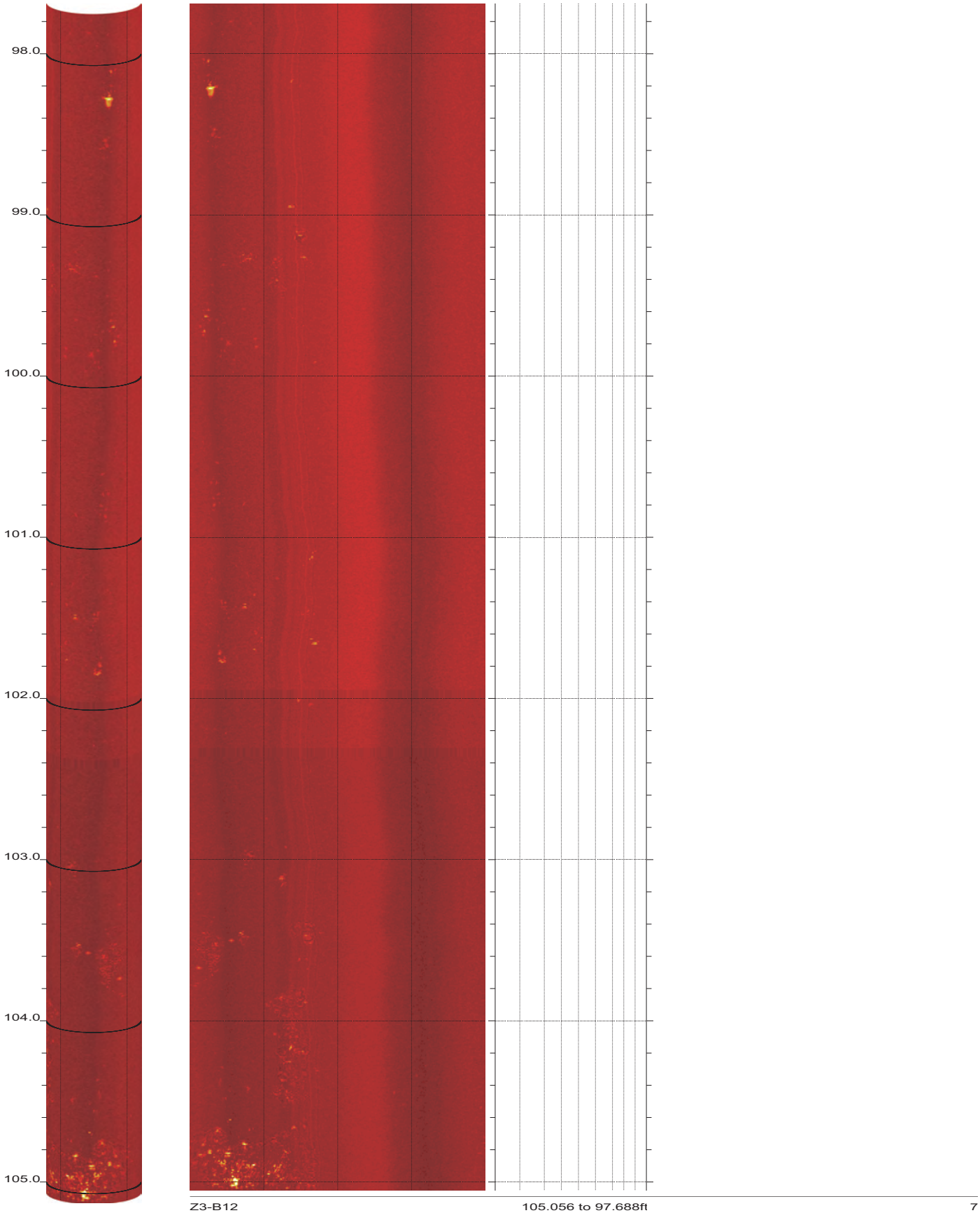


SR-710 Boring Z3-B12 Acoustic Televiewer Dips rev 1 Sheet 7 of 18

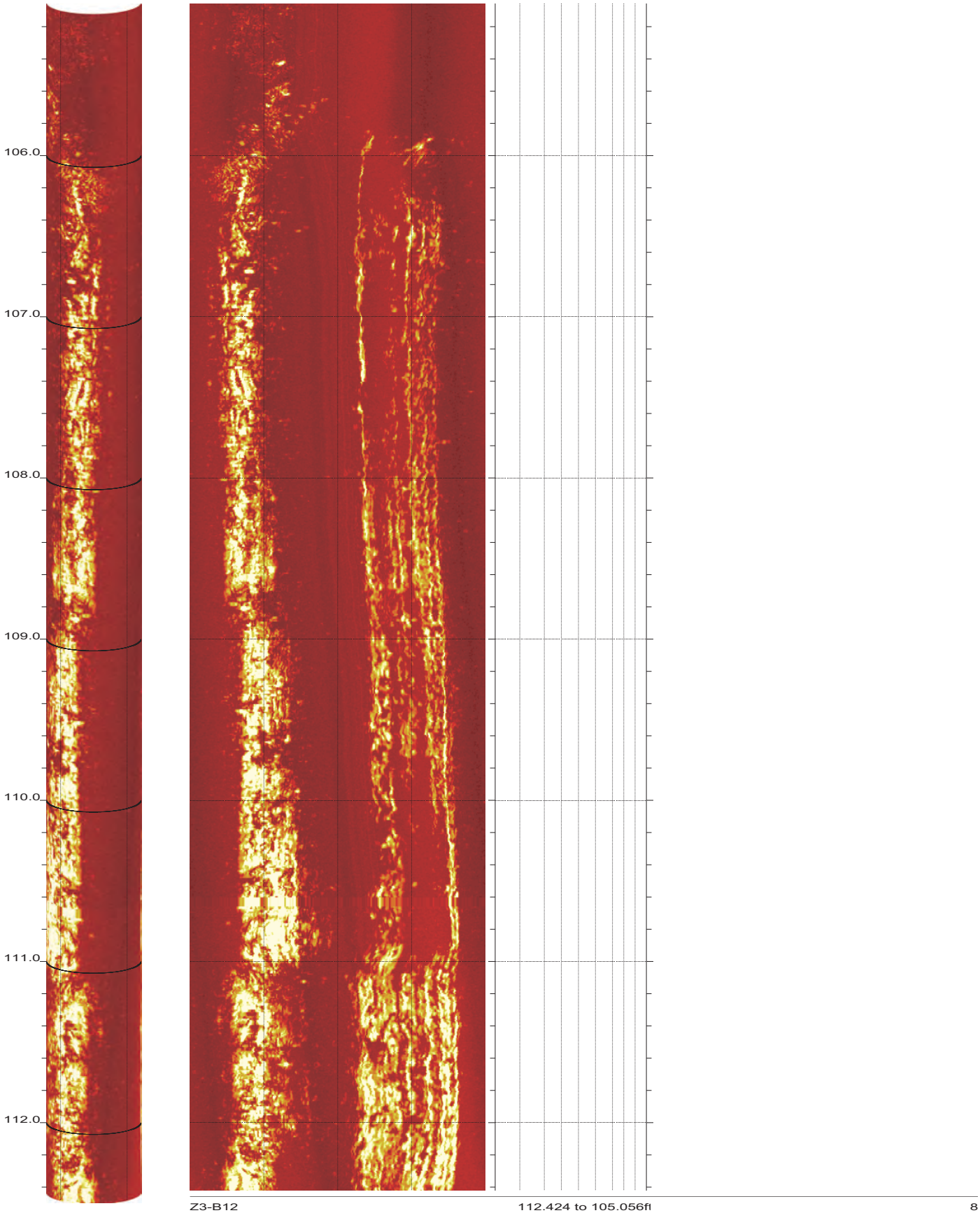


SR-710 Boring Z3-B12 Acoustic Televiewer Dips rev 1 Sheet 8 of 18

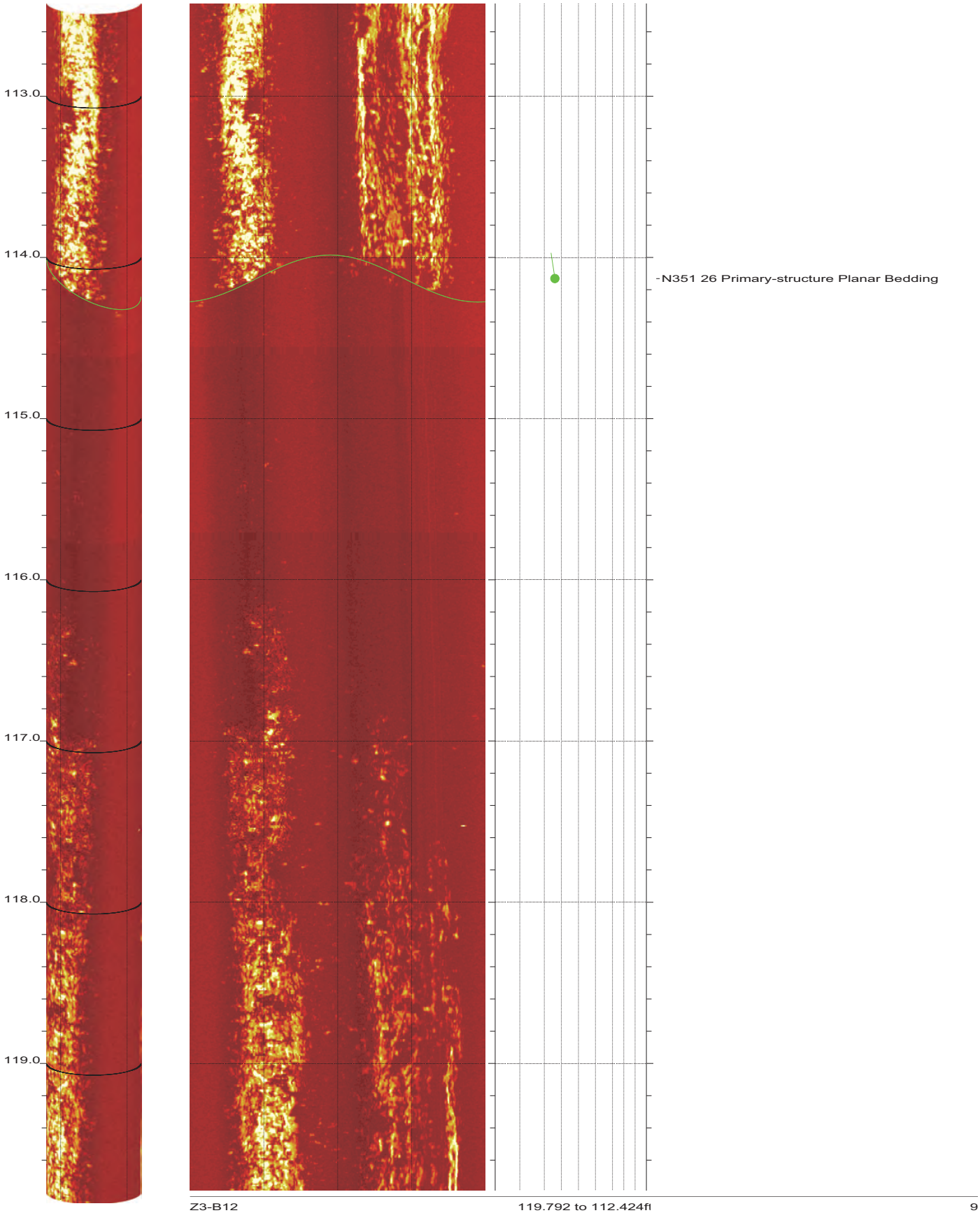
113.0
114.0
115.0
116.0
117.0
118.0
119.0
N351 26 Primary-structure Planar Bedding
Z3-B12
119.792 to 112.424ft
9

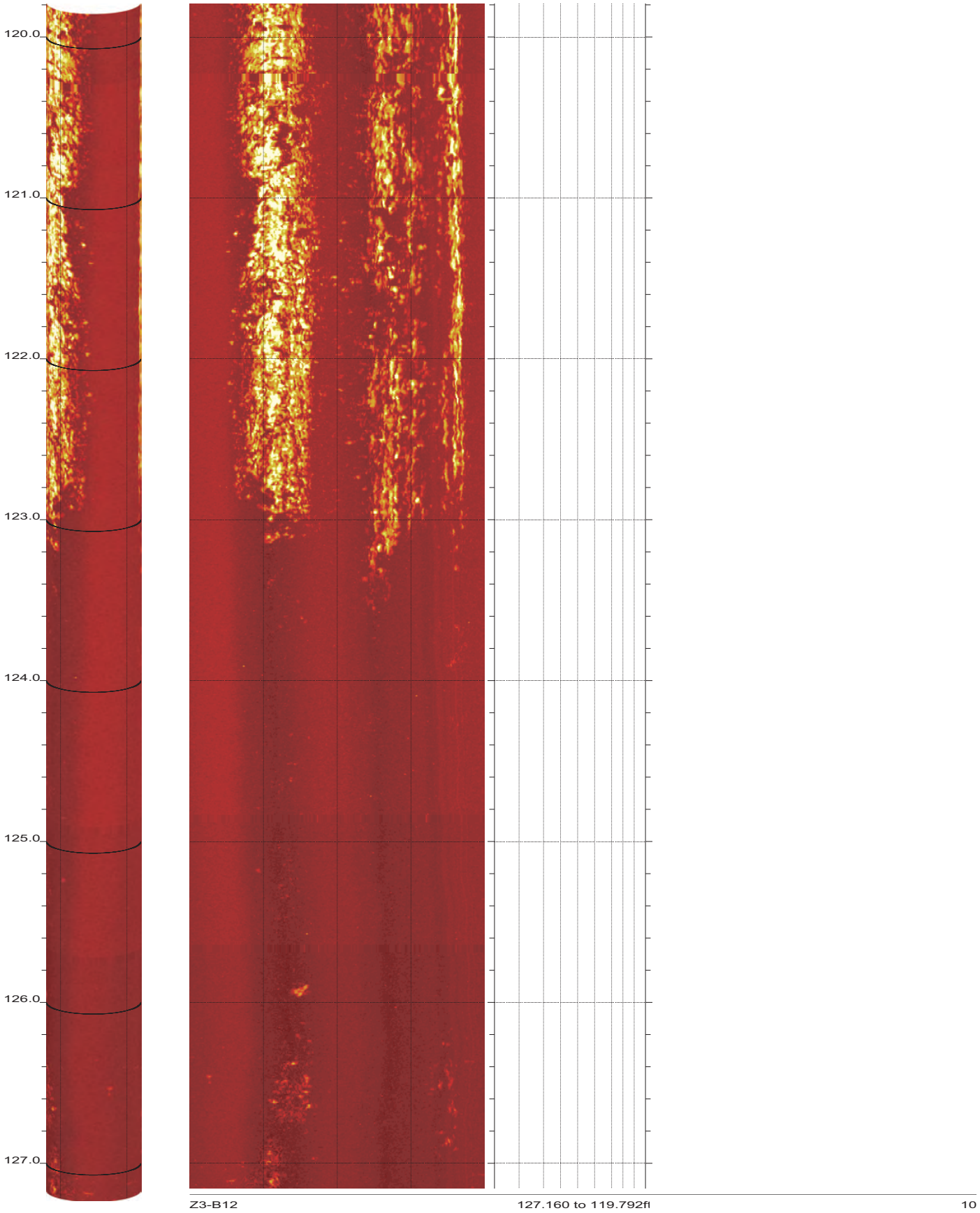
120.0
121.0
122.0
123.0
124.0
125.0
126.0
127.0
Z3-B12
127.160 to 119.792fl
10

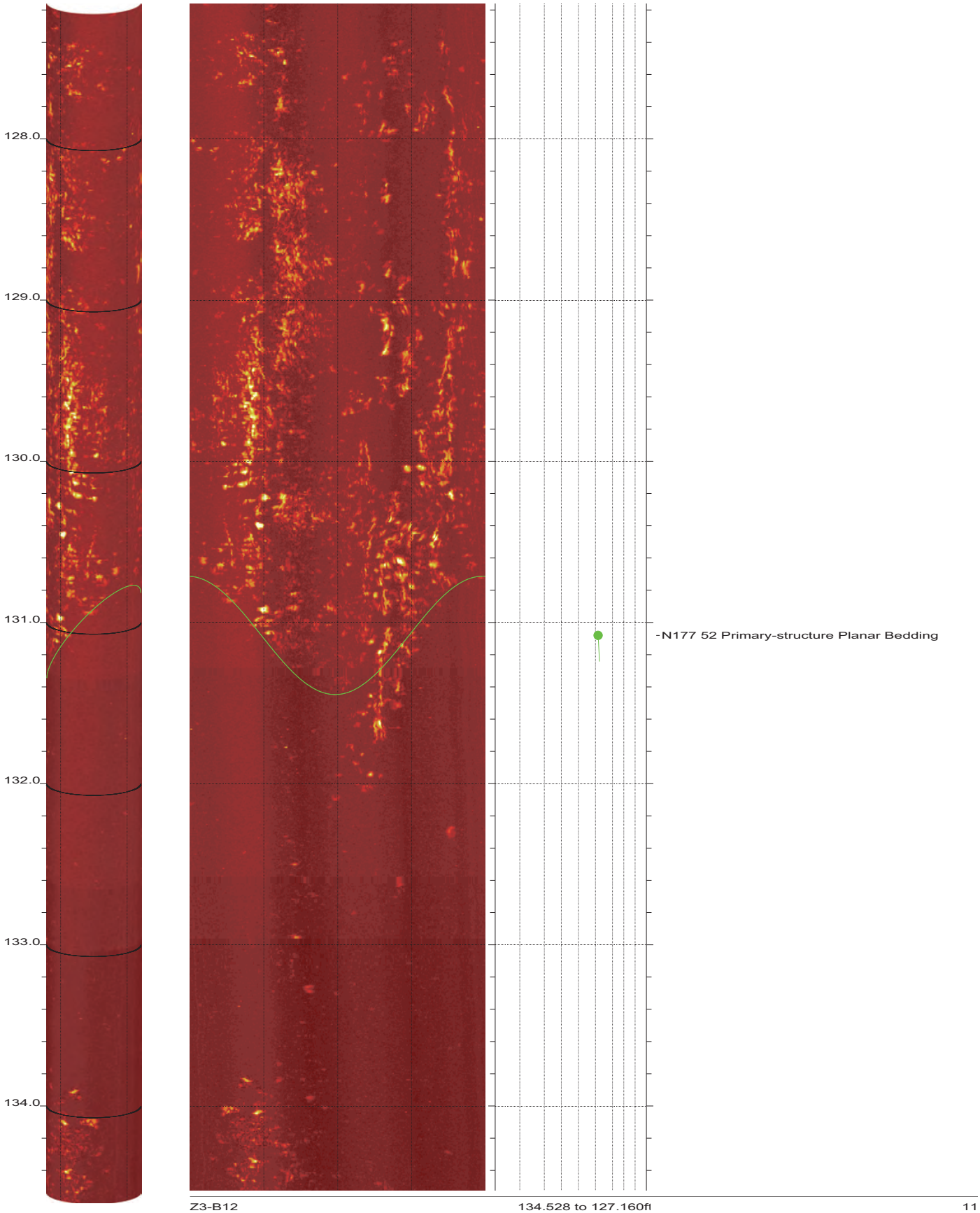
128.0
129.0
130.0
131.0
132.0
133.0
134.0
-N177 52 Primary-structure Planar Bedding
Z3-B12
134.528 to 127.160ft
11

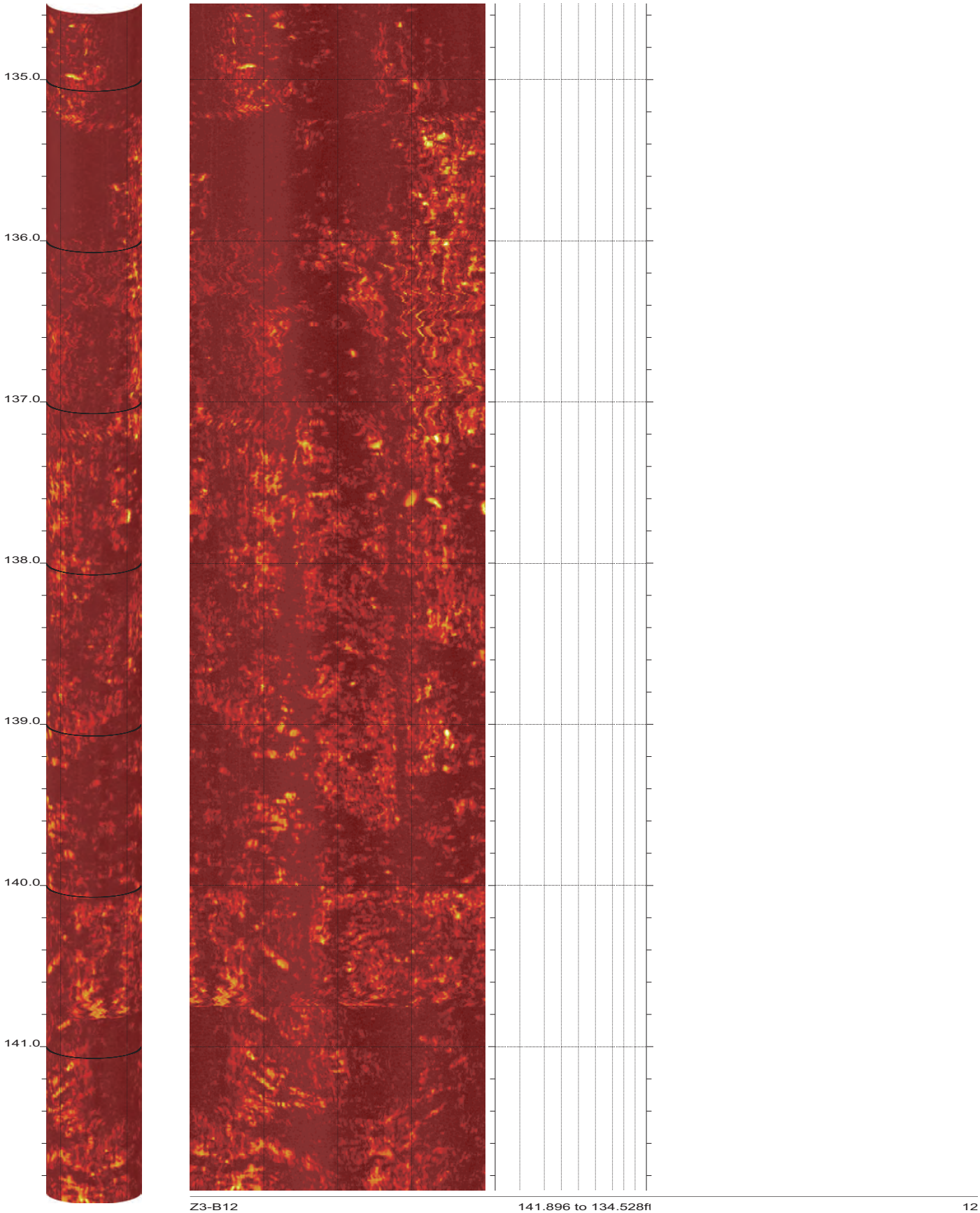
135.0
136.0
137.0
138.0
139.0
140.0
141.0
Z3-B12
141.896 to 134.528fl
12

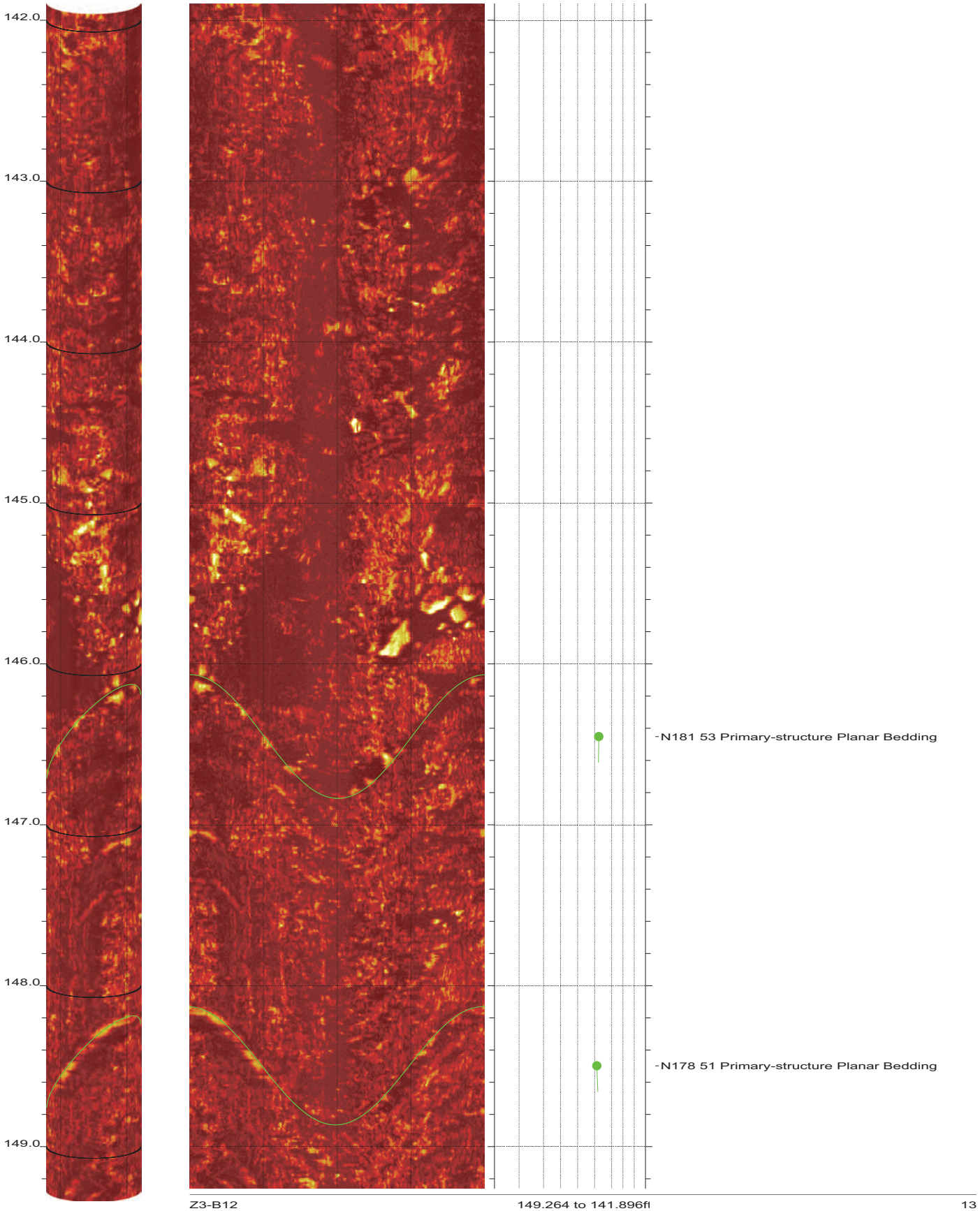
142.0
143.0
144.0
145.0
146.0
147.0
148.0
149.0
N181 53 Primary-structure Planar Bedding
N178 51 Primary-structure Planar Bedding
Z3-B12
149.264 to 141.896fl
13

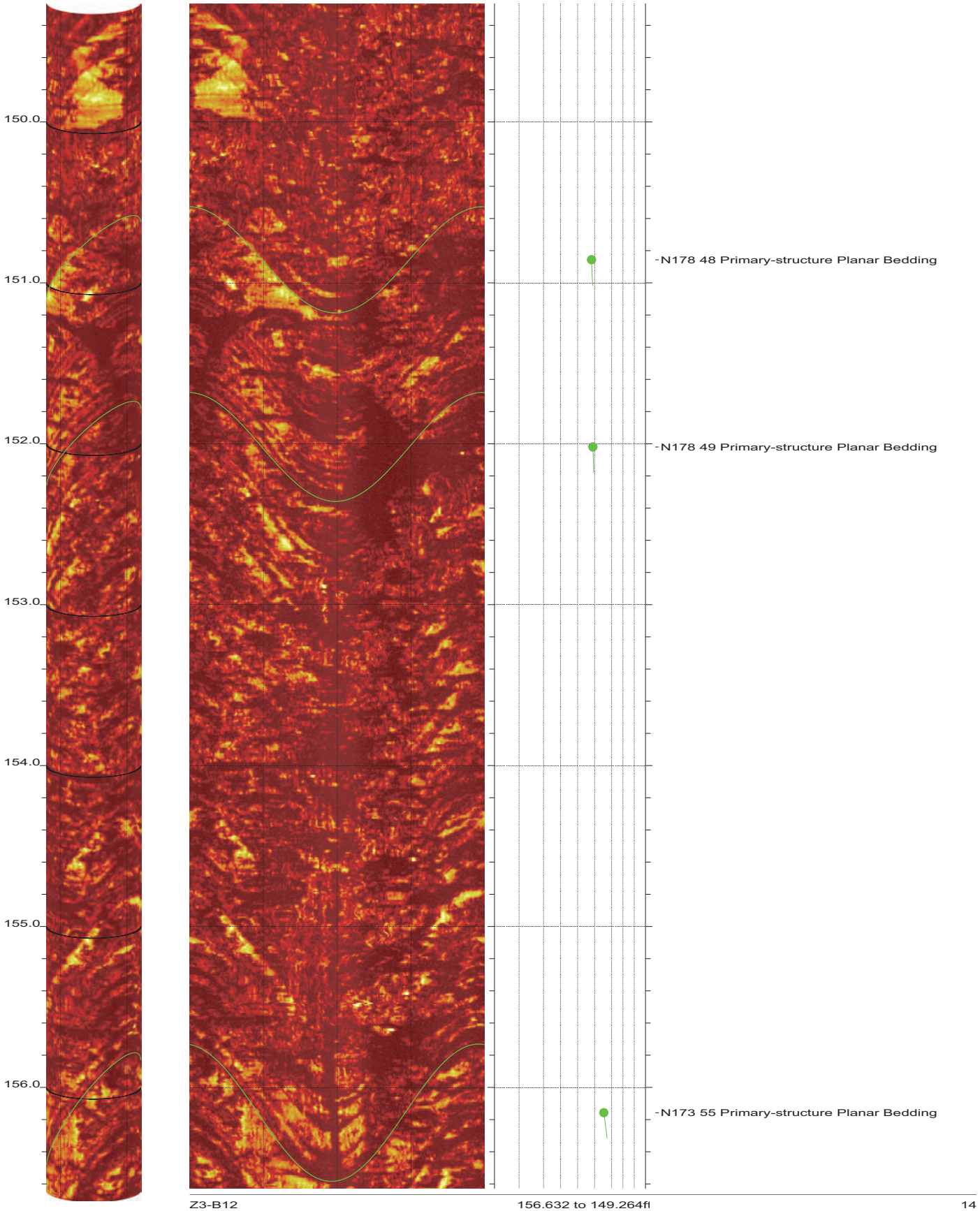
150.0
151.0
152.0
153.0
154.0
155.0
156.0
N178 48 Primary-structure Planar Bedding
N178 49 Primary-structure Planar Bedding
N173 55 Primary-structure Planar Bedding
Z3-B12
156.632 to 149.264ft
14

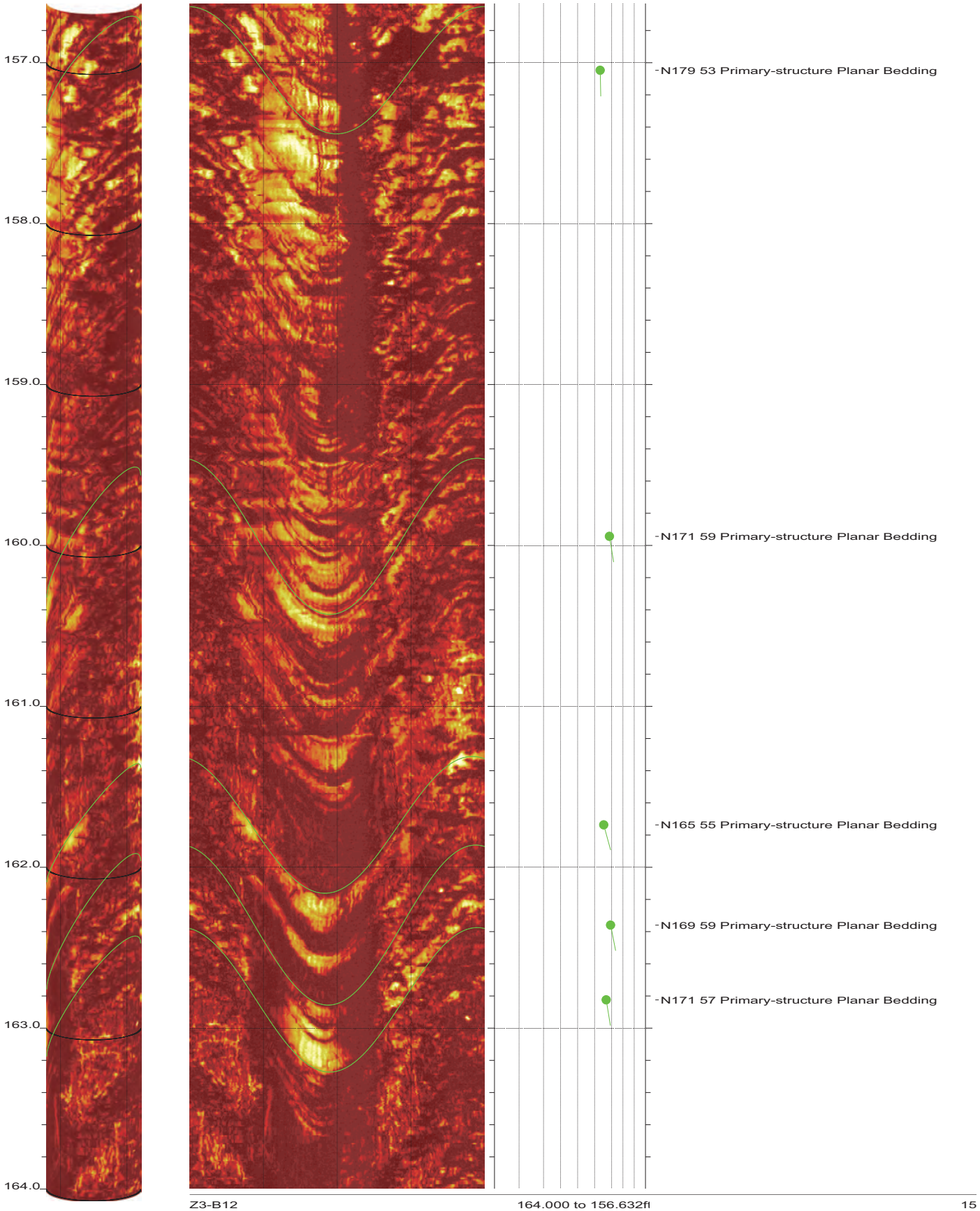
157.0
158.0
159.0
160.0
161.0
162.0
163.0
164.0
N179 53 Primary-structure Planar Bedding
N171 59 Primary-structure Planar Bedding
N165 55 Primary-structure Planar Bedding
N169 59 Primary-structure Planar Bedding
N171 57 Primary-structure Planar Bedding
Z3-B12
164.000 to 156.632fl
15

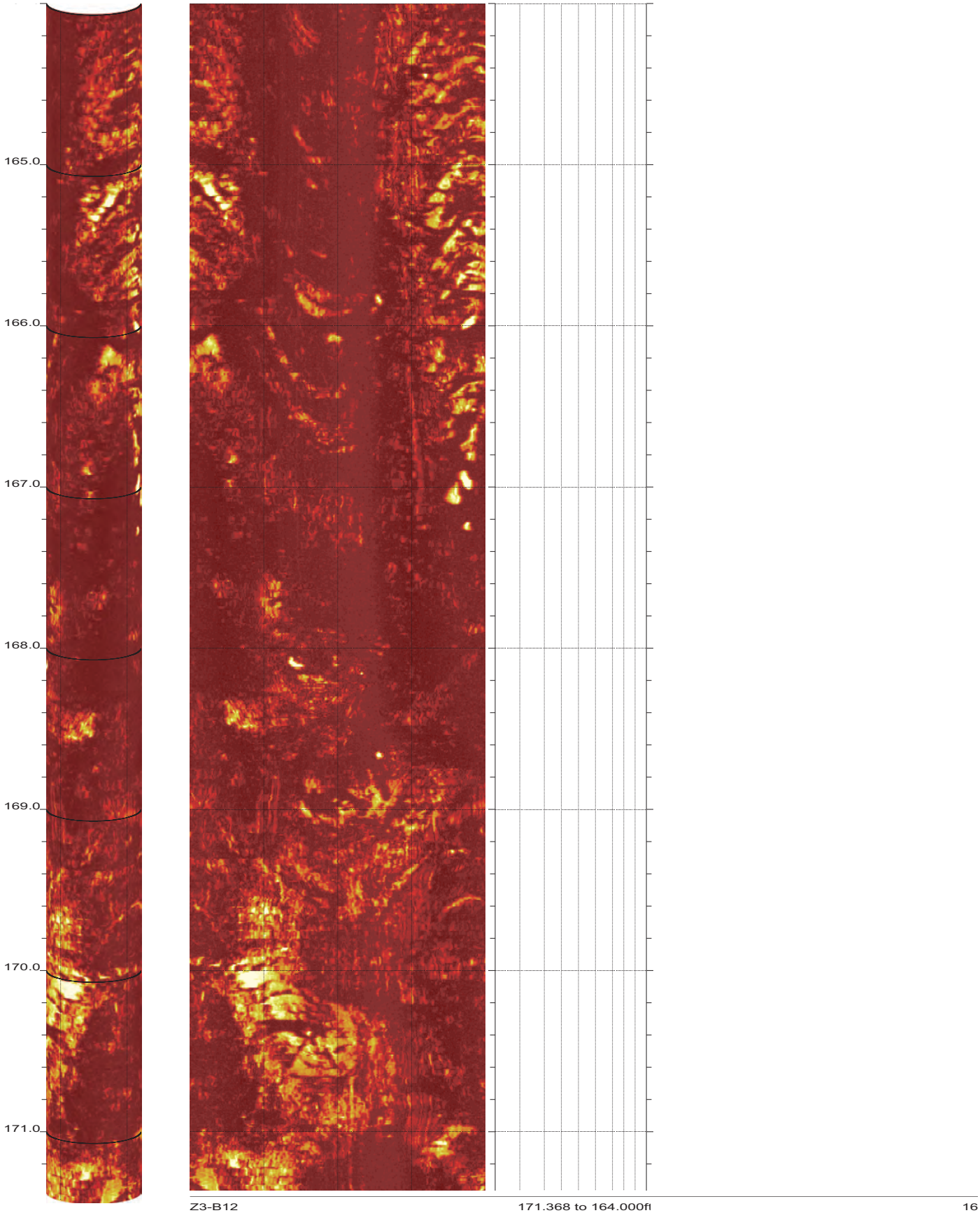


SR-710 Boring Z3-B12 Acoustic Televiewer Dips rev 1 Sheet 16 of 18

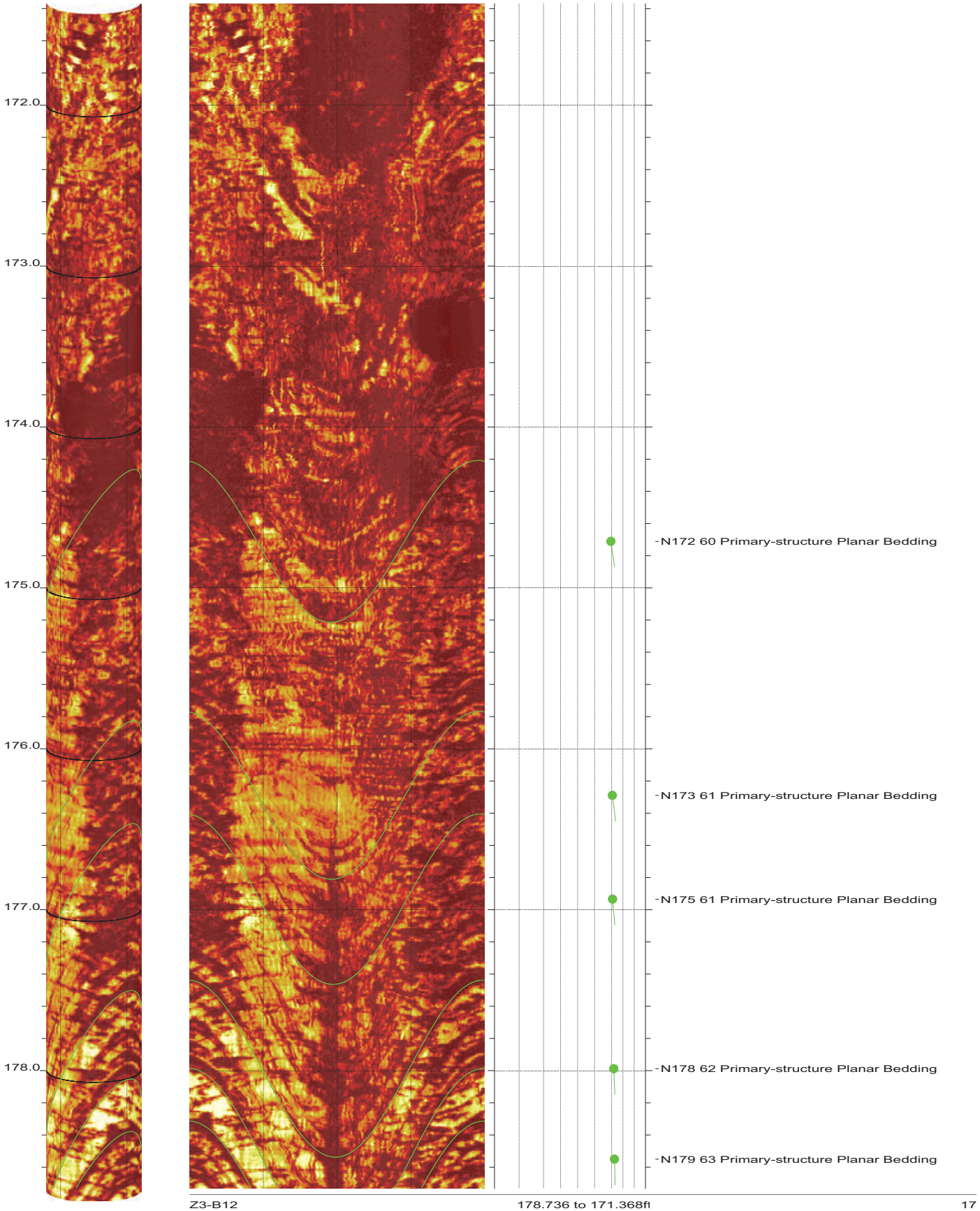
172.0
173.0
174.0
175.0
176.0
177.0
178.0
N172 60 Primary-structure Planar Bedding
N173 61 Primary-structure Planar Bedding
N175 61 Primary-structure Planar Bedding
N178 62 Primary-structure Planar Bedding
N179 63 Primary-structure Planar Bedding
Z3-B12
178.736 to 171.368fl
17

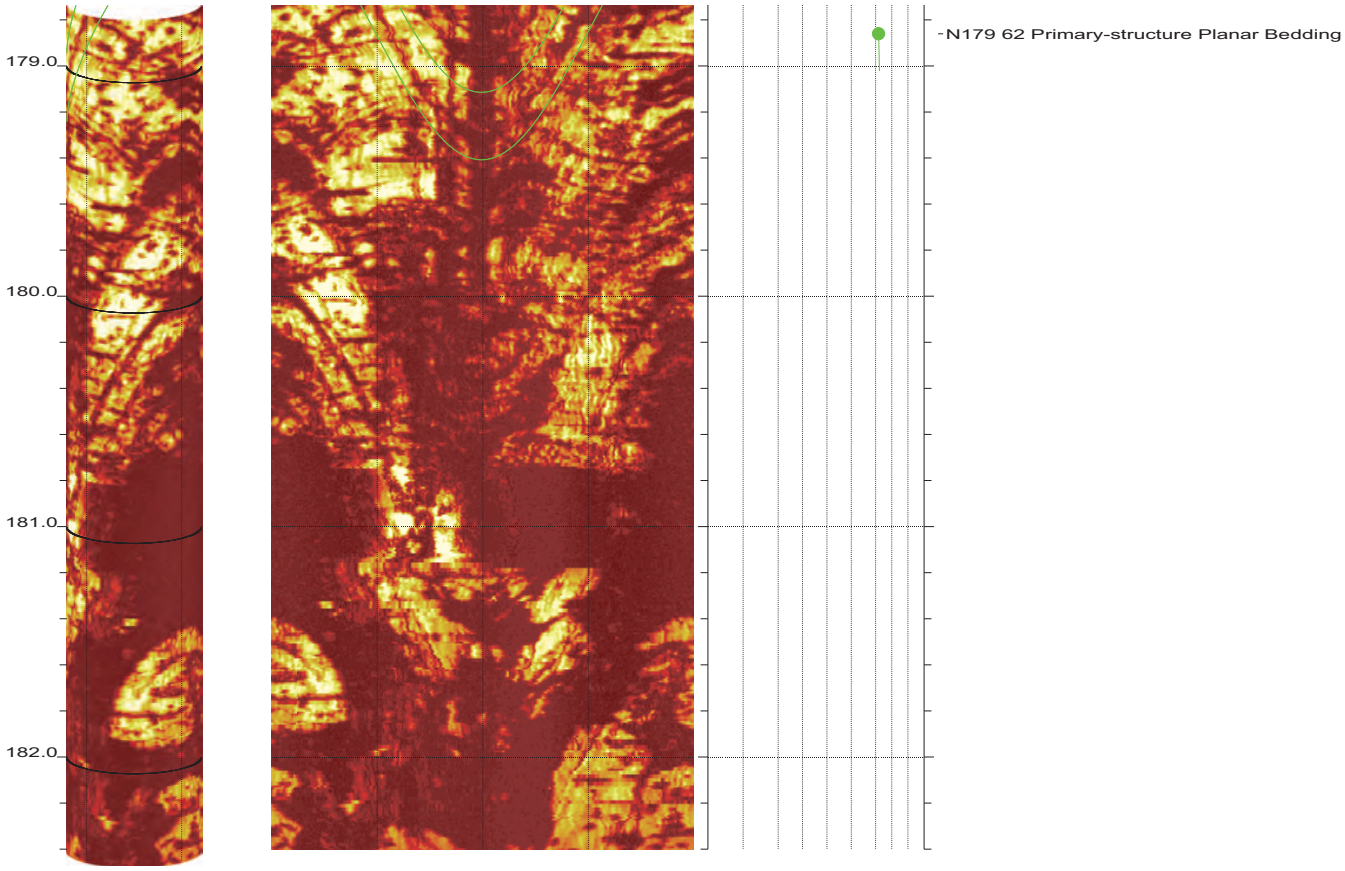
179.0
180.0
181.0
182.0
N179 62 Primary-structure Planar Bedding

BHTV DATA PROCESSING
RGLDIP vsn 6.2
INTERPRETED BHTV DIPS LOG

CASCADE DRILLING

Borehole: Z4-B4

SR-710 TUNNEL INVESTIGATION

top of borehole.....
East: _
North: _
Elev: _

North ref. is true
Depth units are feet
Vertical scale: 1/10
Horiz scale = 1.00x Vert scale

Zone from 275.000 to 6.800ft
Format: BHTV-NESWN

Borehole diam: 5.700inch
Vertical = borehole-axis
Image: Amplitude

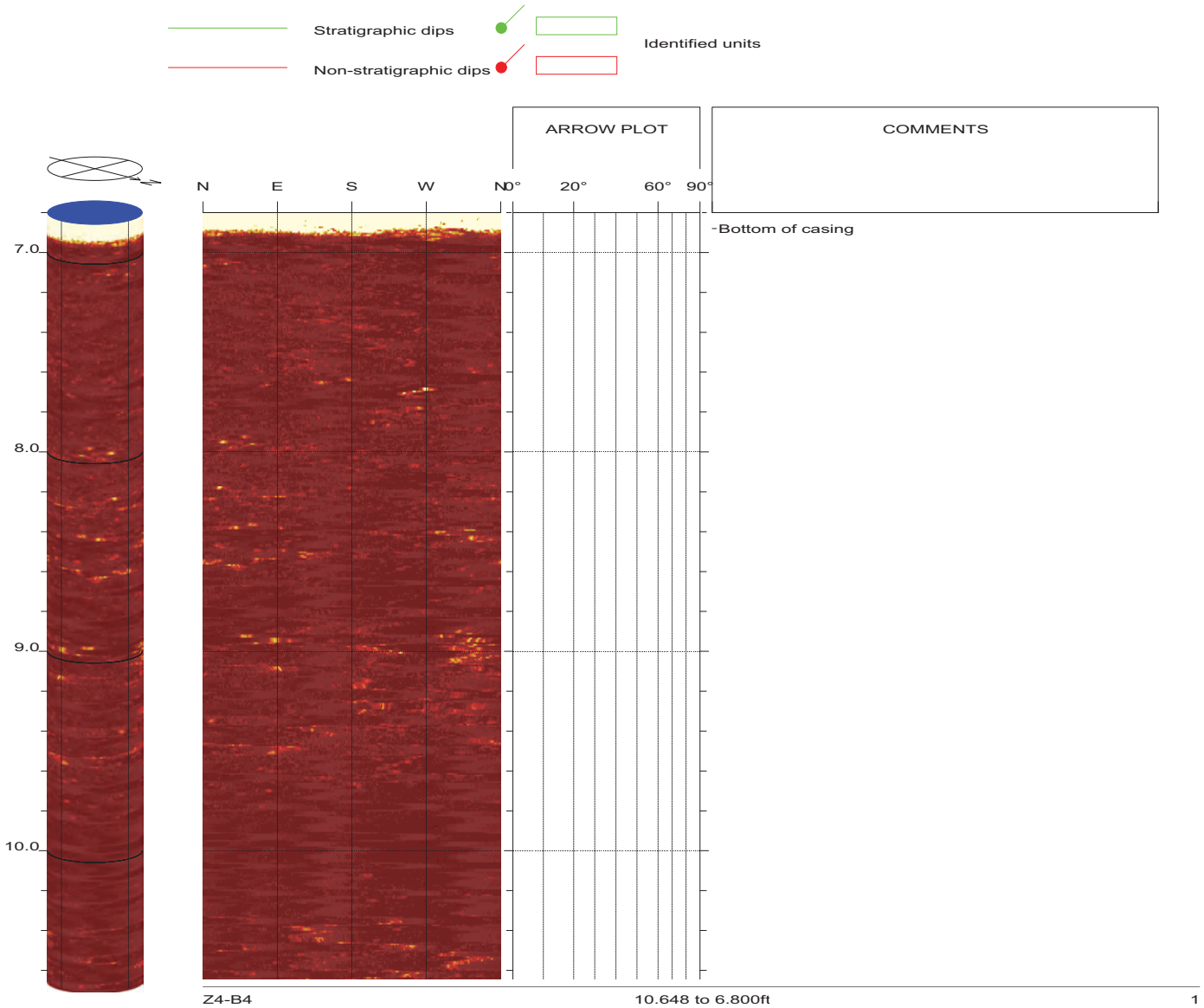

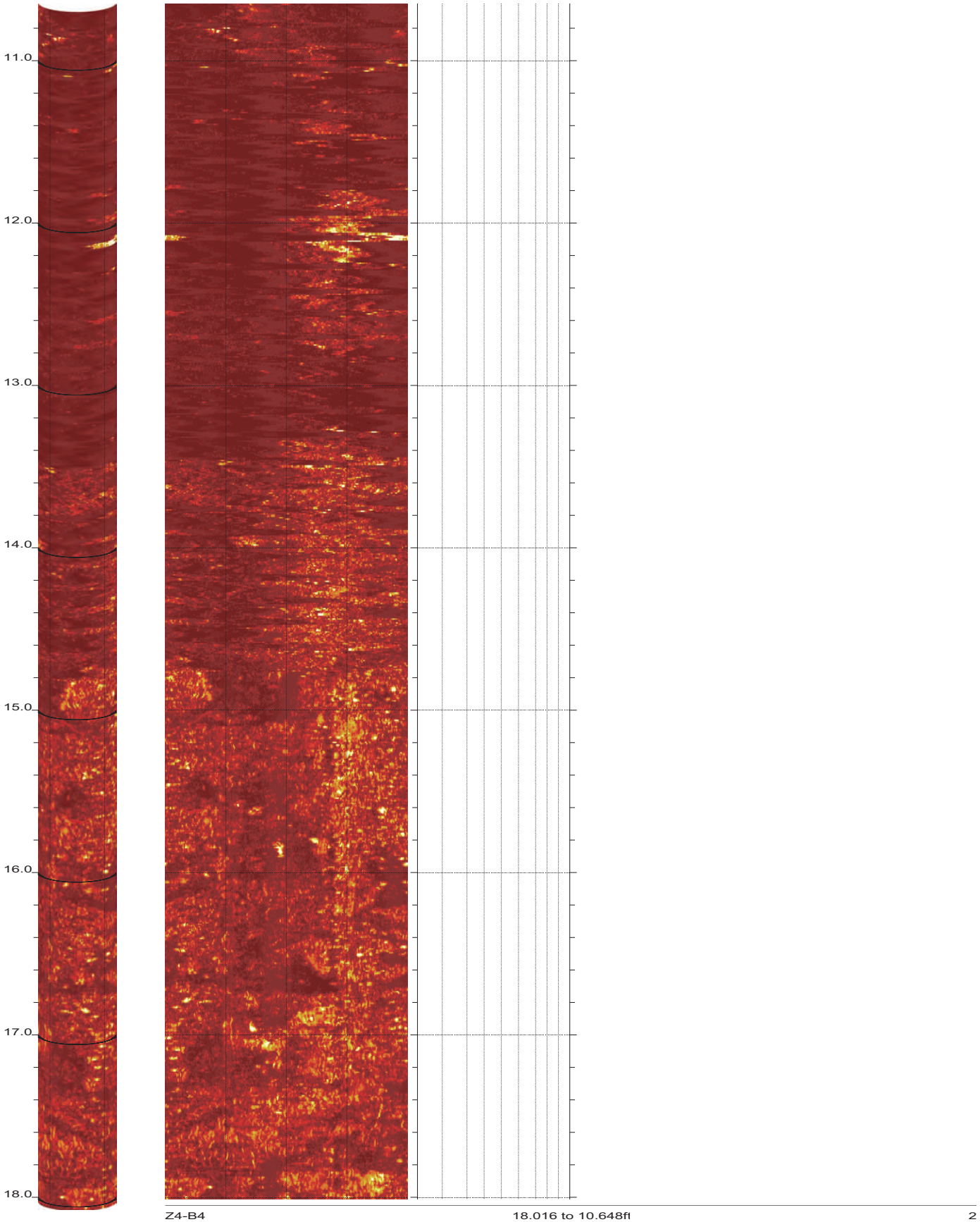


SR-710 Boring Z4-B4 Acoustic Televiewer Dips rev 1 Sheet 2 of 37

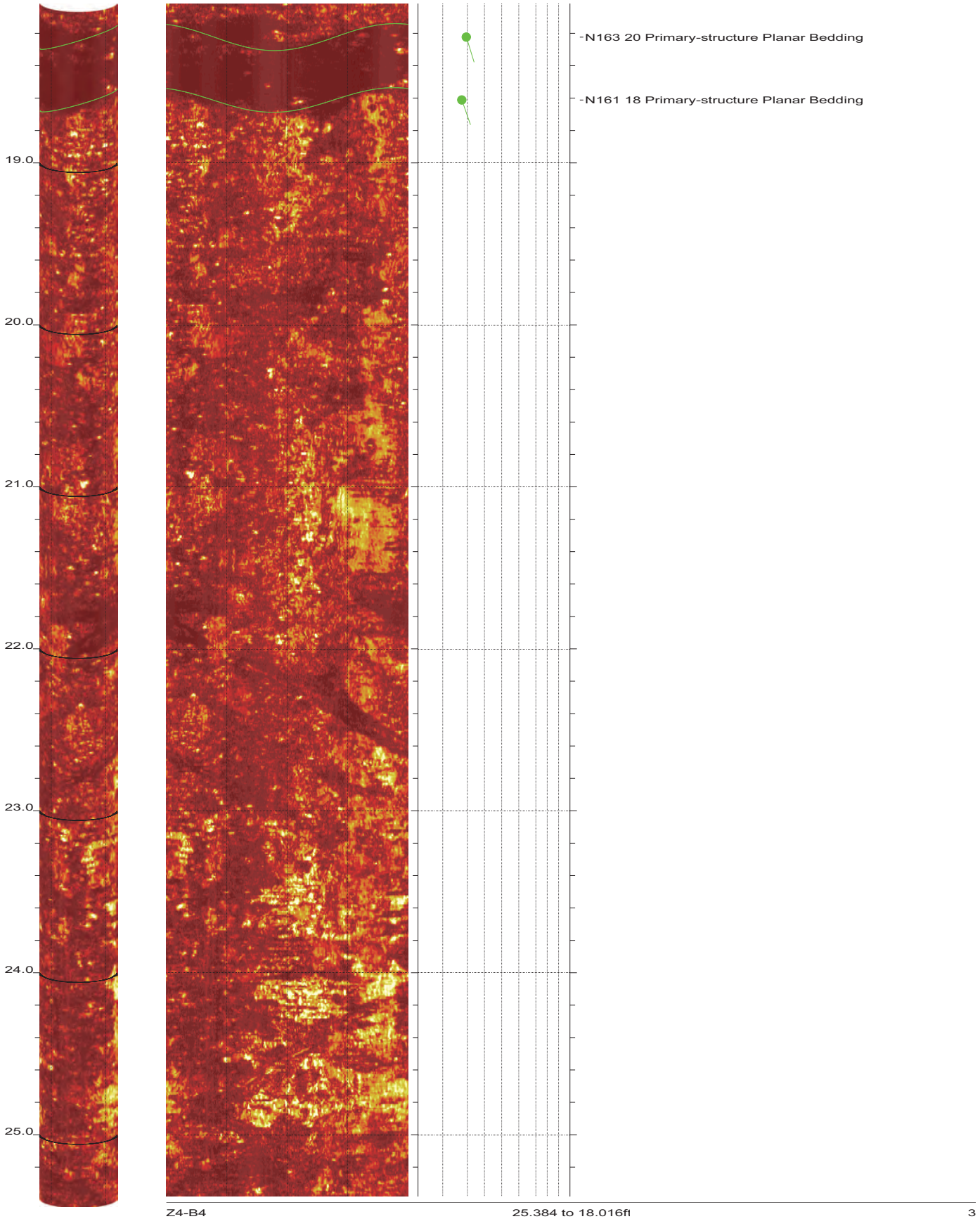


SR-710 Boring Z4-B4 Acoustic Televiewer Dips rev 1 Sheet 3 of 37

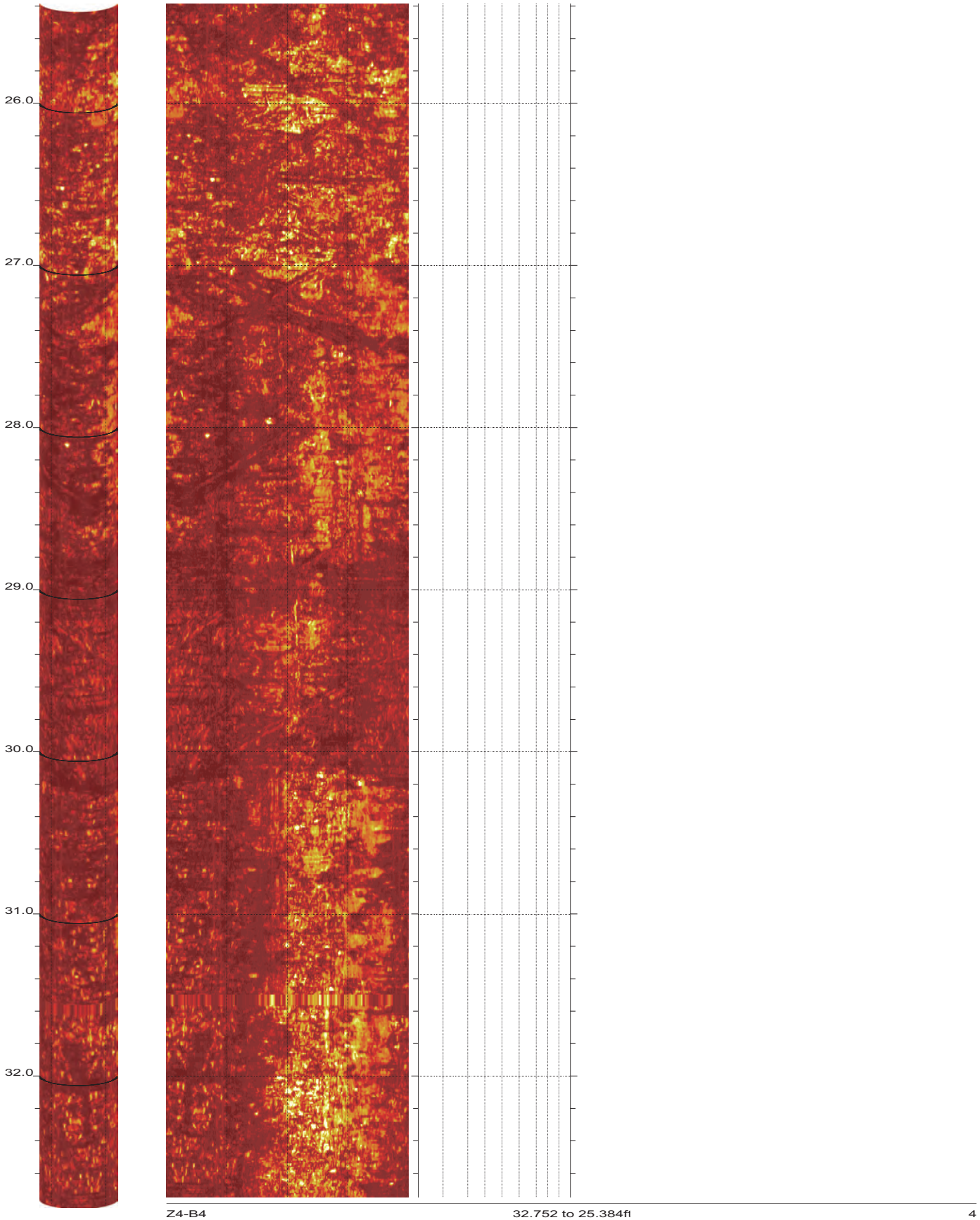
26.0
27.0
28.0
29.0
30.0
31.0
32.0
Z4-B4
32.752 to 25.384fl
4

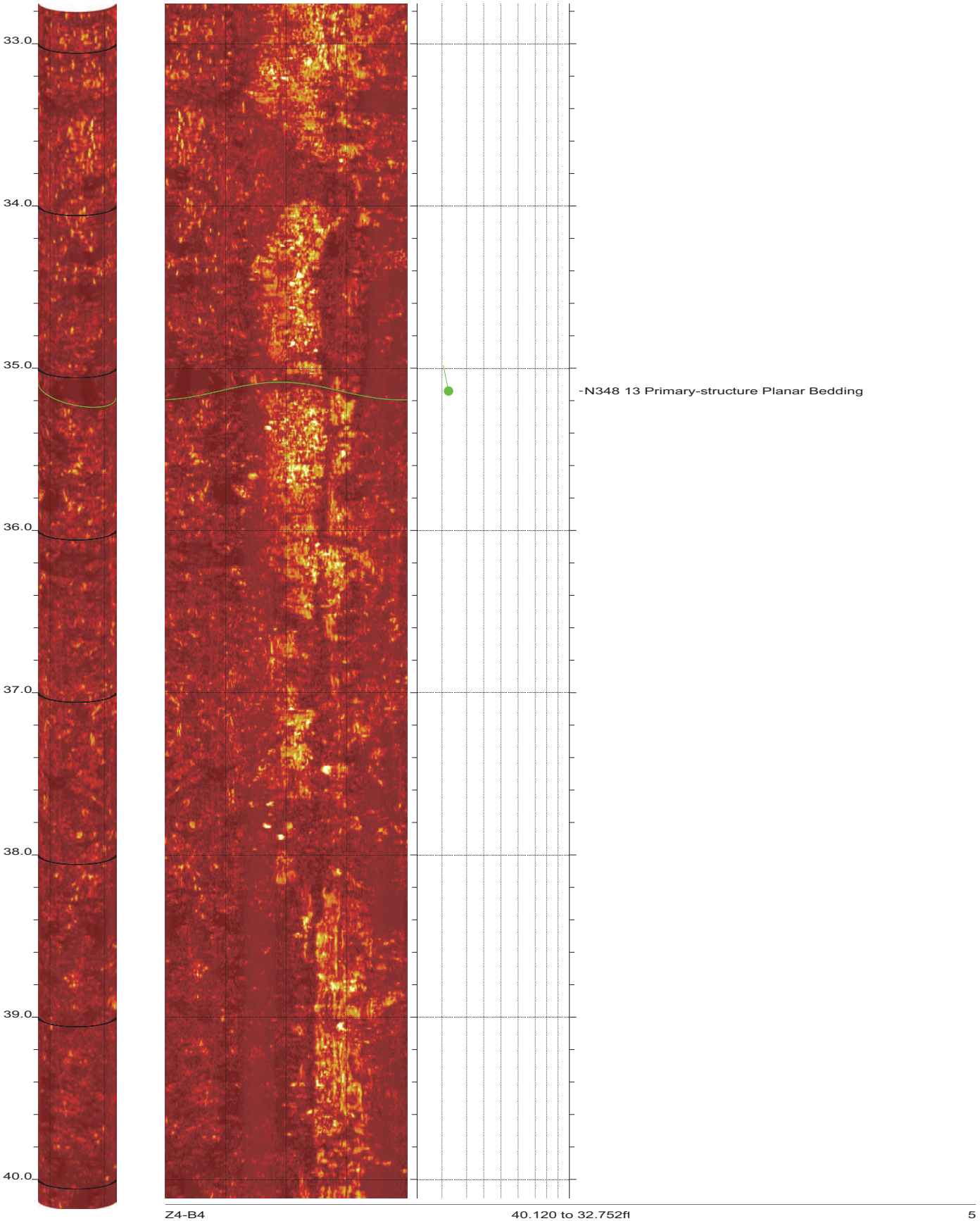


SR-710 Boring Z4-B4 Acoustic Televiewer Dips rev 1 Sheet 5 of 37

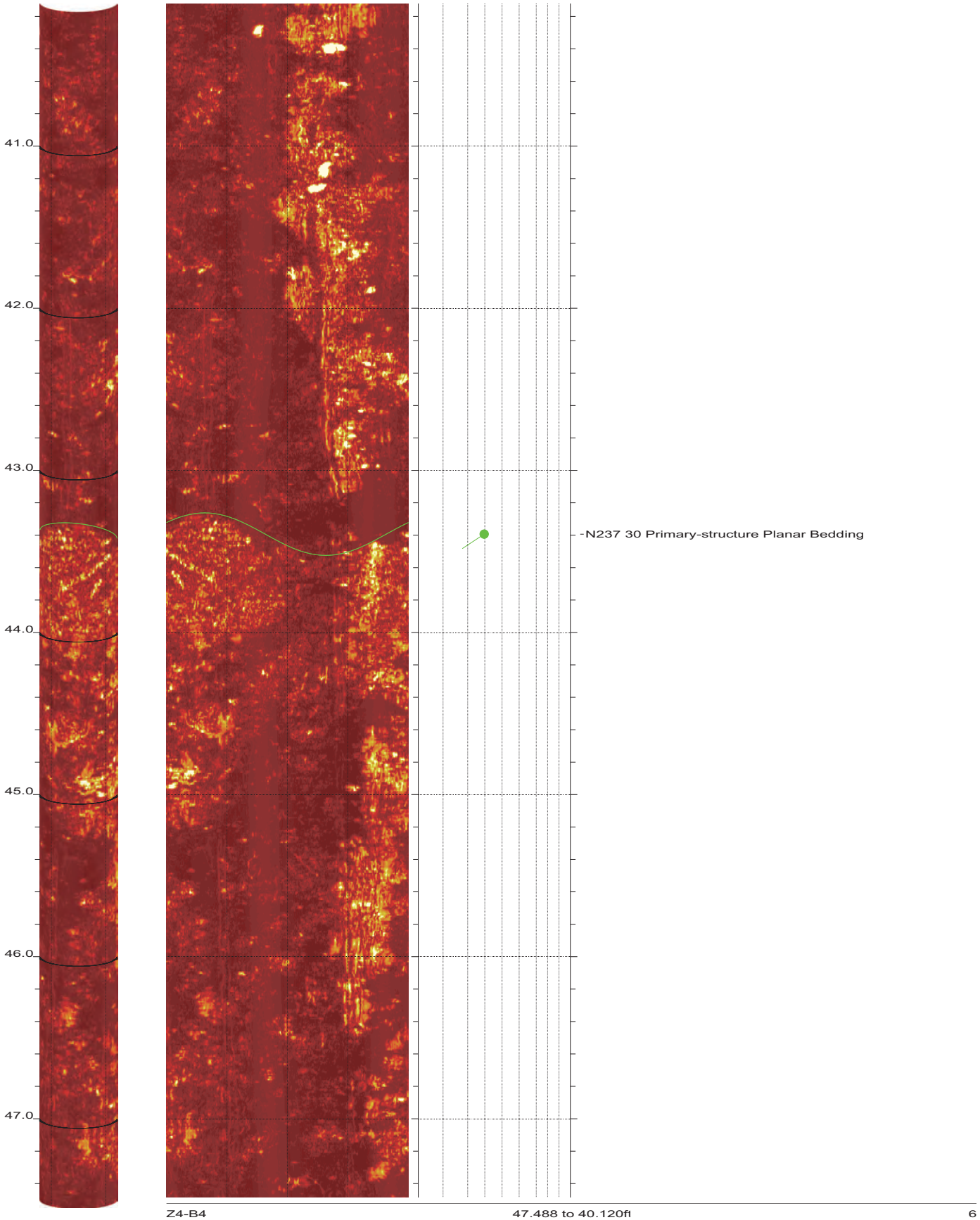


SR-710 Boring Z4-B4 Acoustic Televiewer Dips rev 1 Sheet 6 of 37

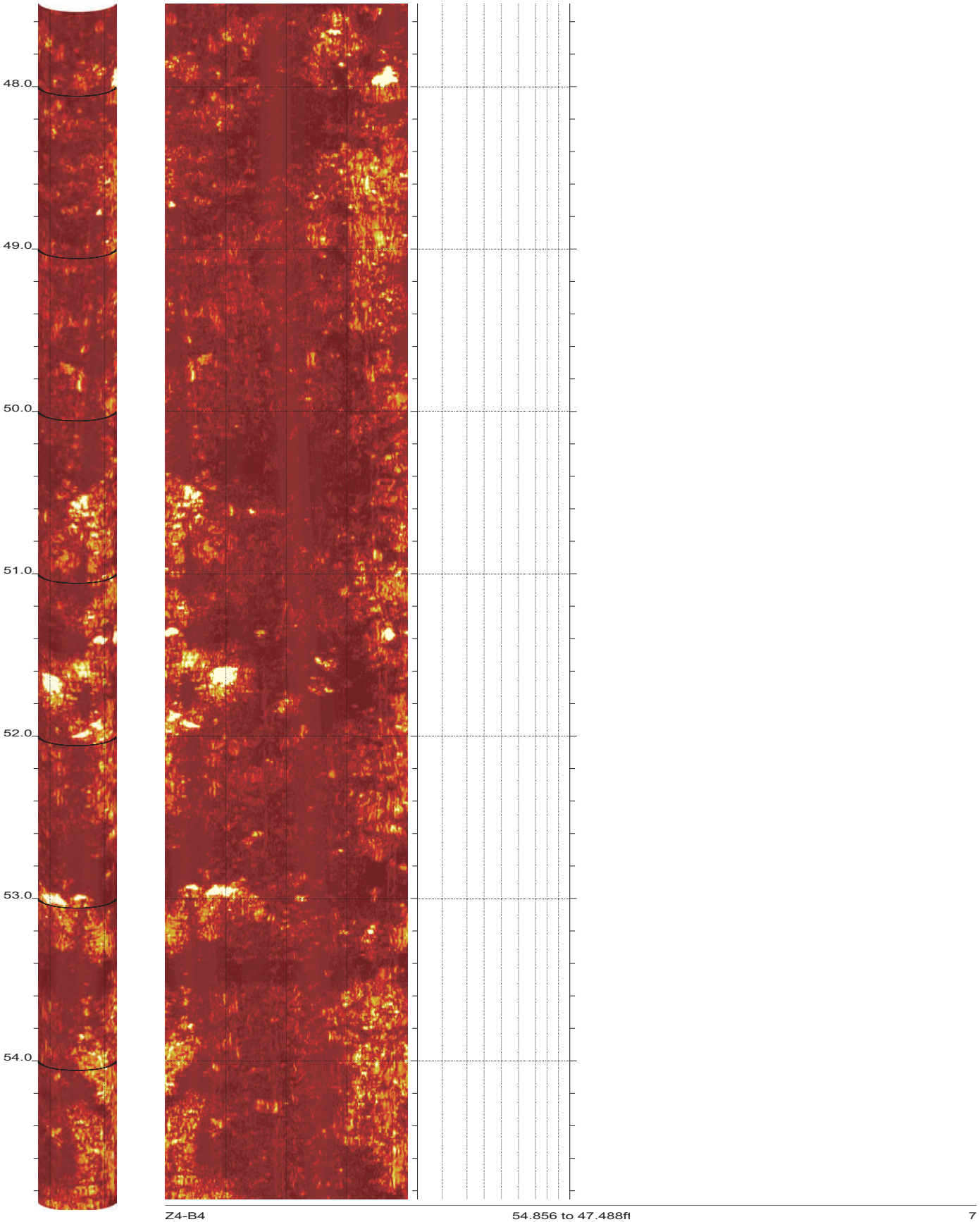


SR-710 Boring Z4-B4 Acoustic Televiewer Dips rev 1 Sheet 7 of 37

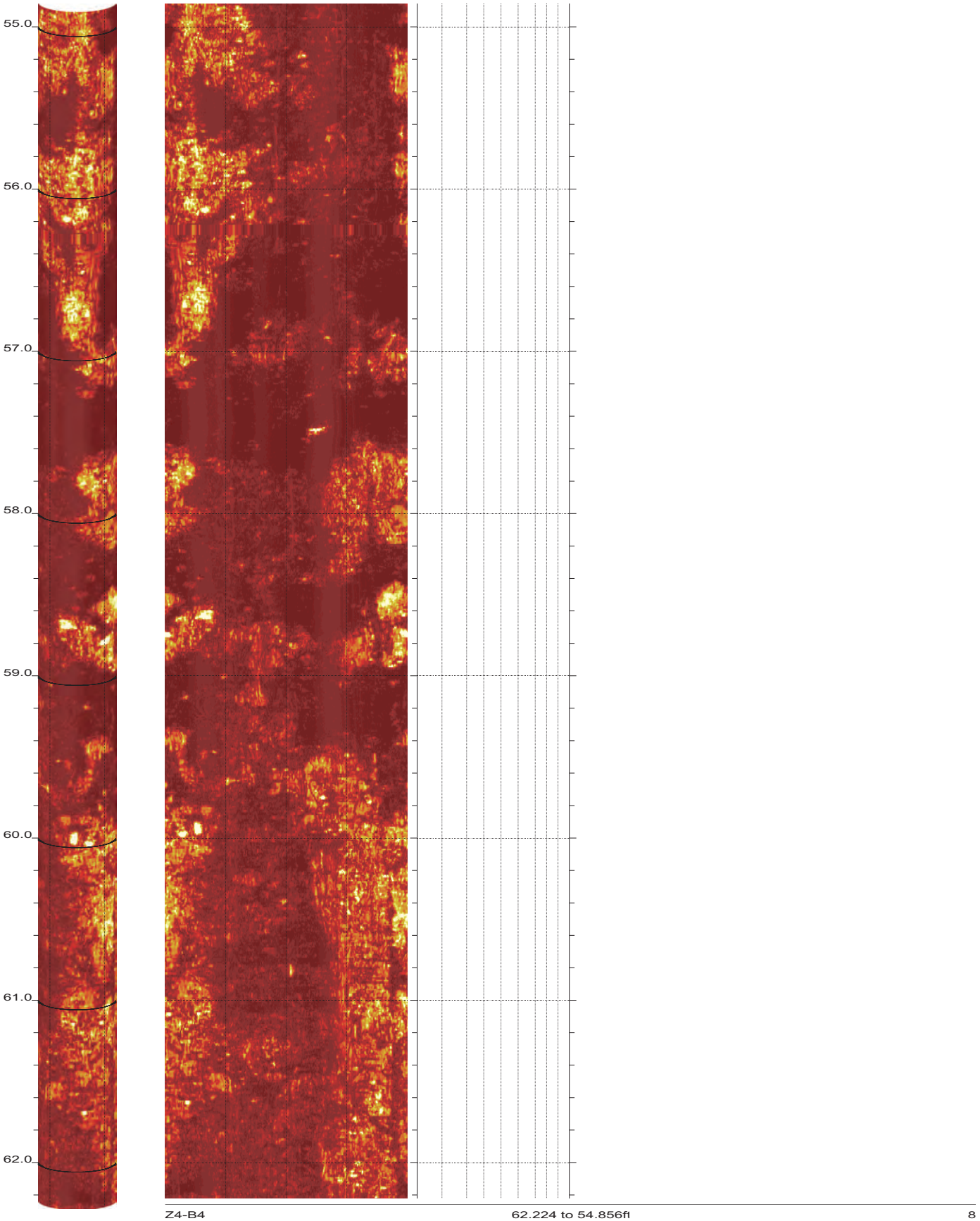


SR-710 Boring Z4-B4 Acoustic Televiewer Dips rev 1 Sheet 8 of 37

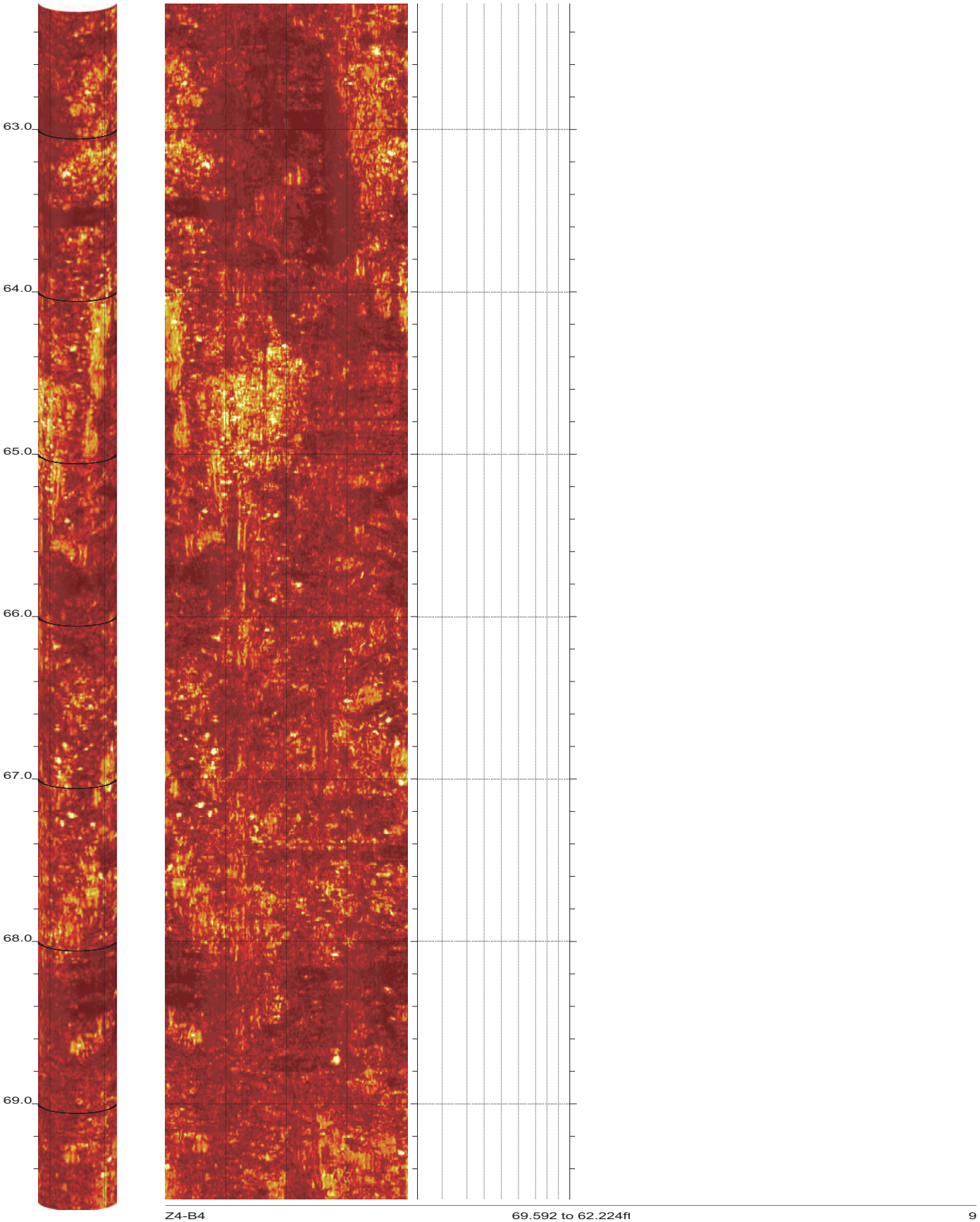
63.0
64.0
65.0
66.0
67.0
68.0
69.0
Z4-B4
69.592 to 62.224ft
9

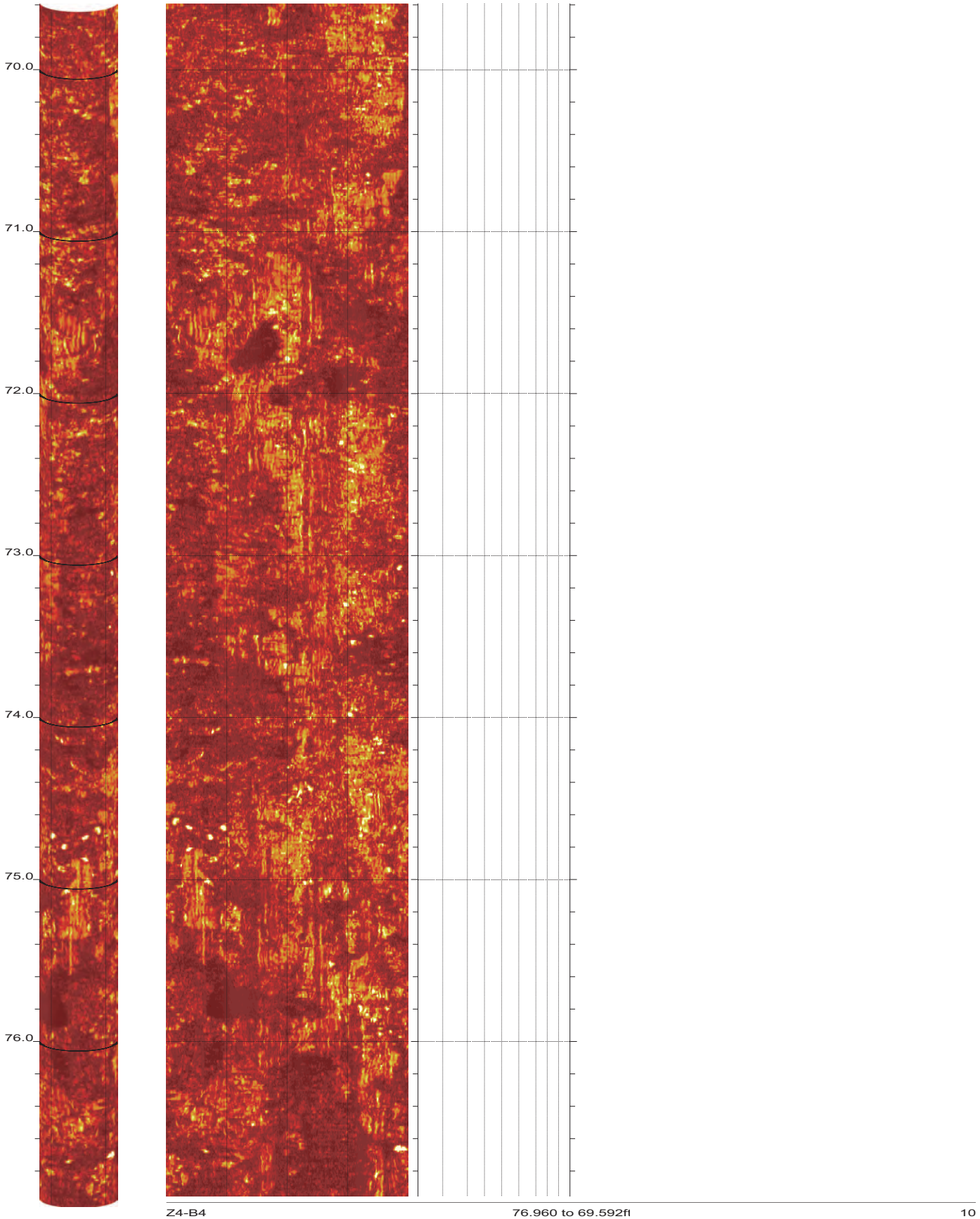


SR-710 Boring Z4-B4 Acoustic Televiewer Dips rev 1 Sheet 10 of 37

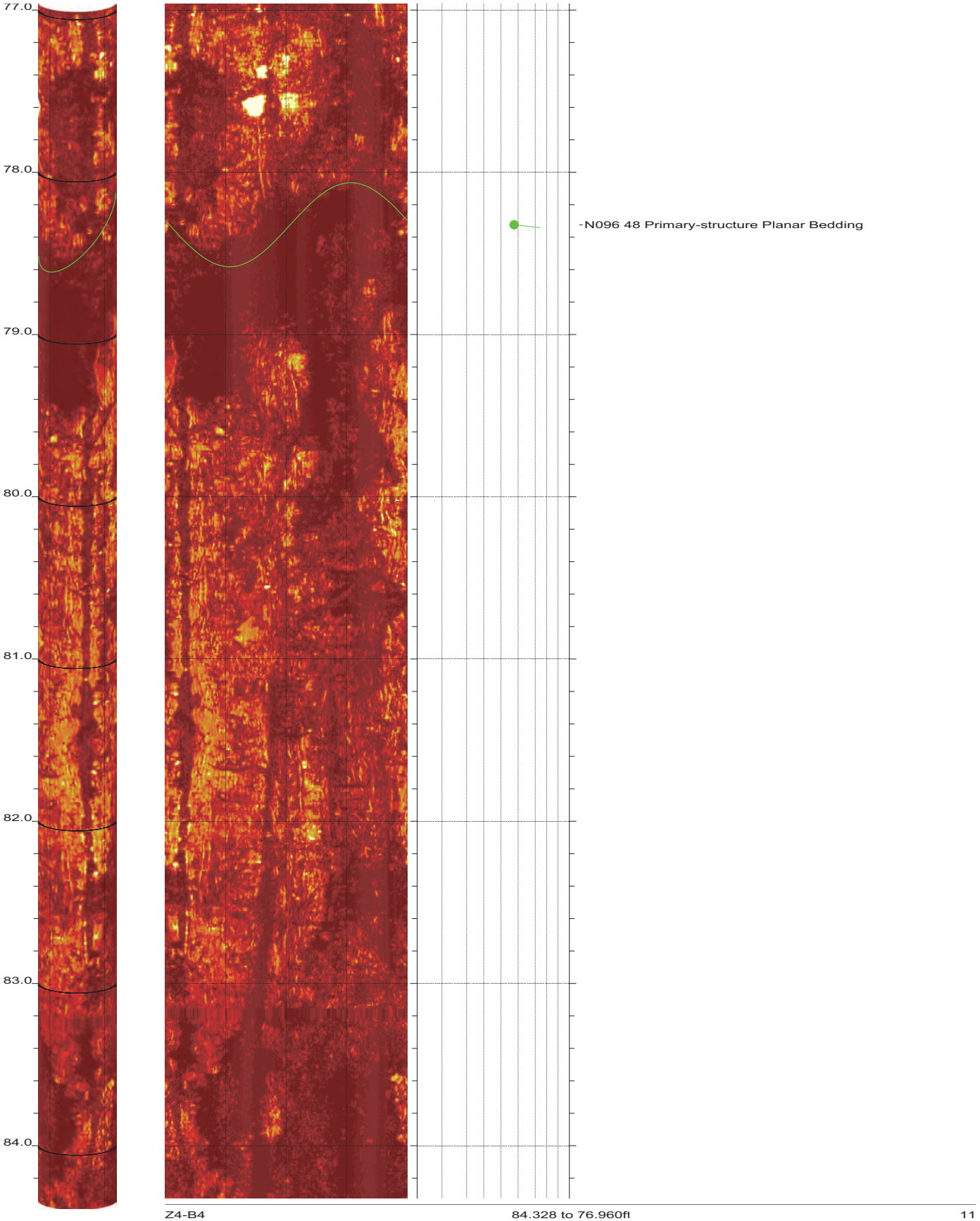
77.0
78.0
79.0
80.0
81.0
82.0
83.0
84.0
N096 48 Primary-structure Planar Bedding
Z4-B4
84.328 to 76.960fl
11

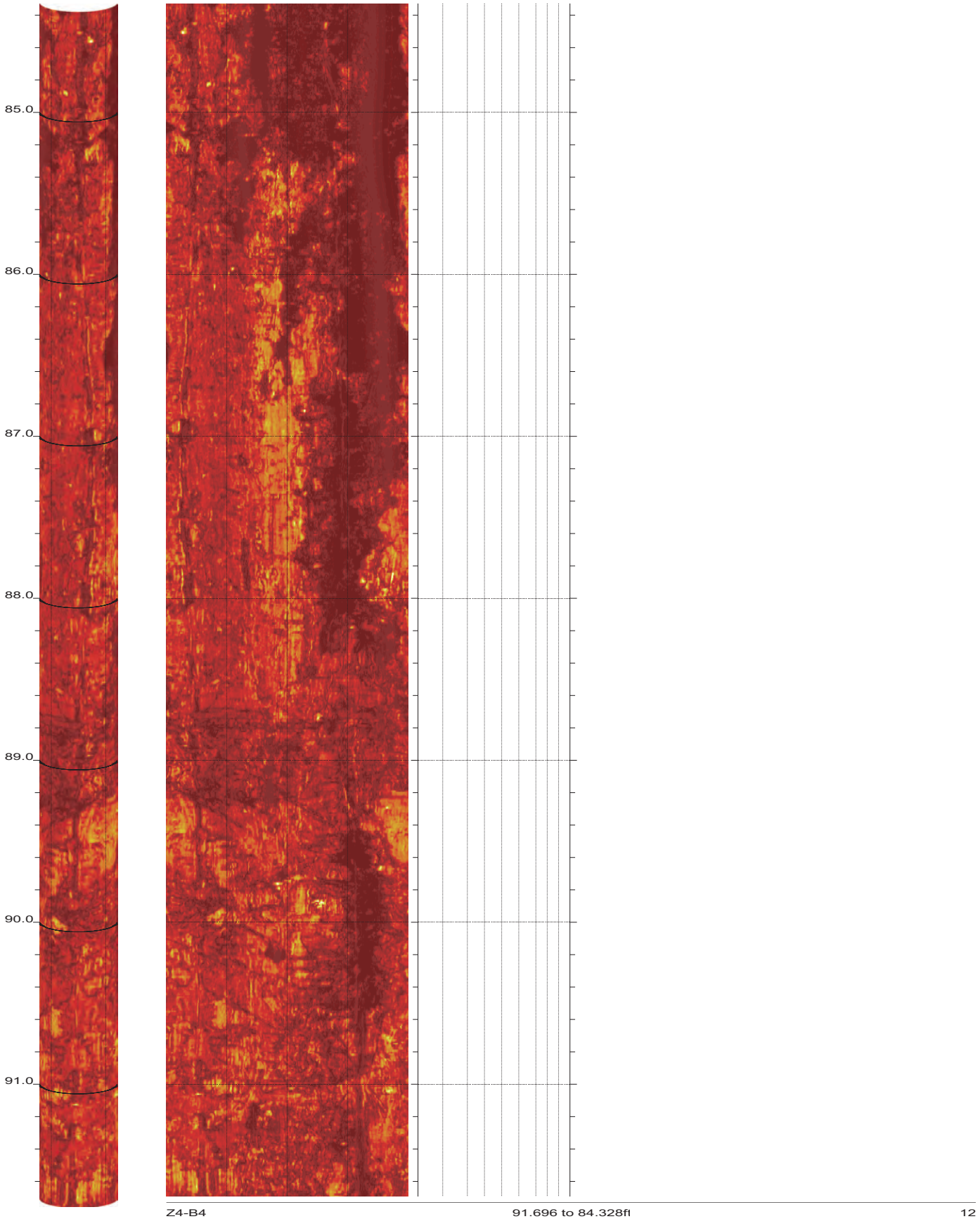
85.0
86.0
87.0
88.0
89.0
90.0
91.0
Z4-B4
91.696 to 84.328fl
12

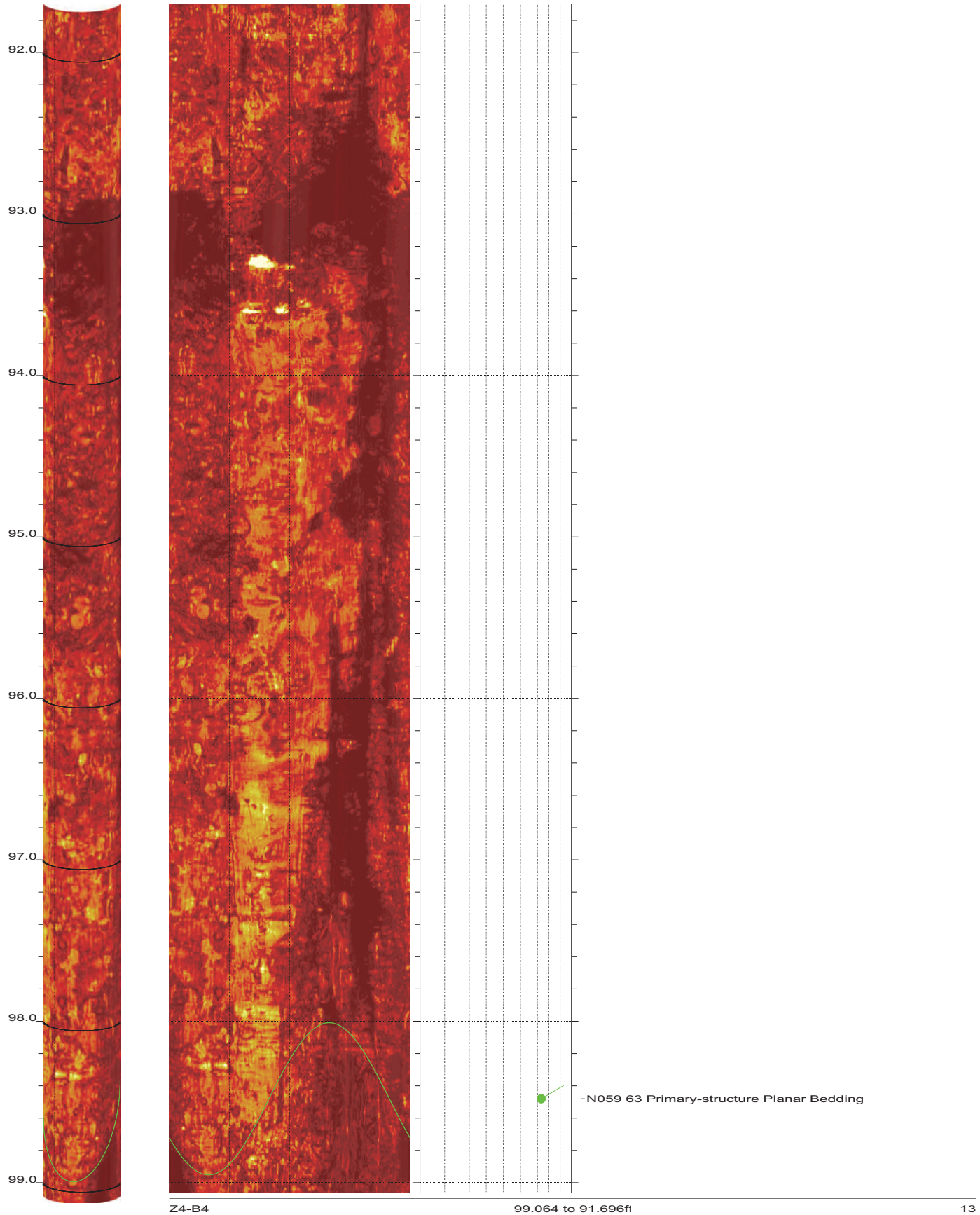


SR-710 Boring Z4-B4 Acoustic Televiewer Dips rev 1 Sheet 13 of 37

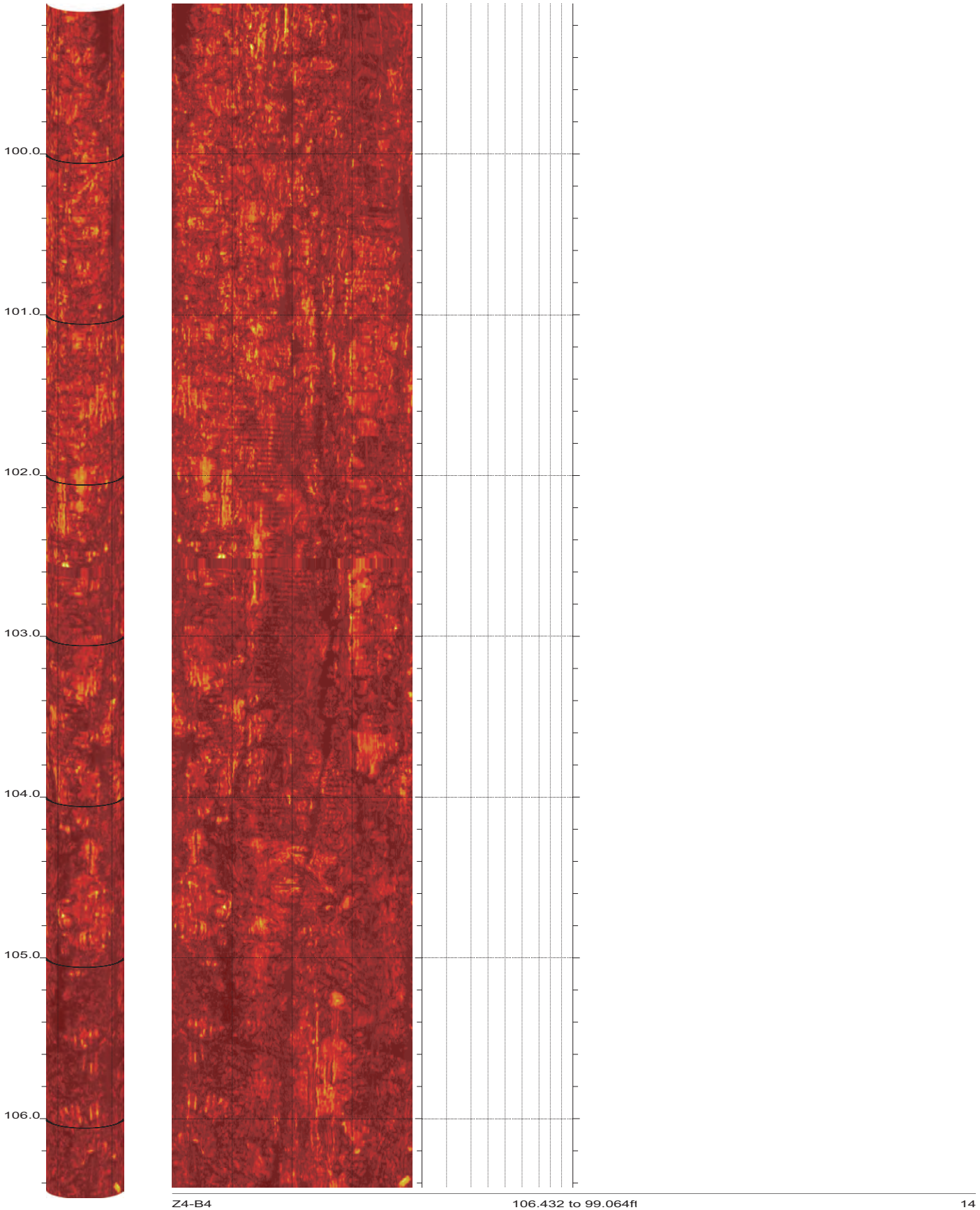
100.0
101.0
102.0
103.0
104.0
105.0
106.0
Z4-B4
106.432 to 99.064ft
14

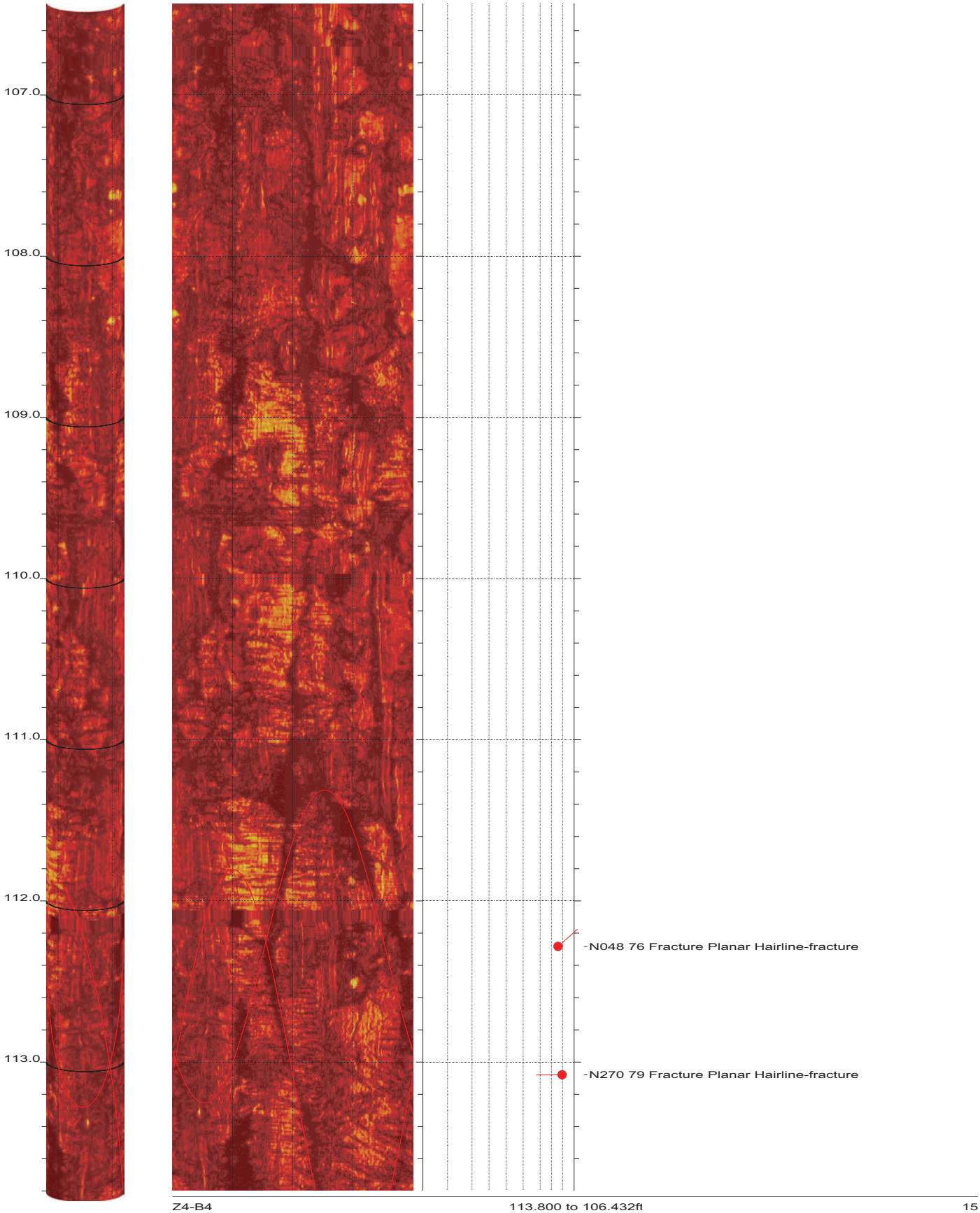


SR-710 Boring Z4-B4 Acoustic Televiewer Dips rev 1 Sheet 15 of 37

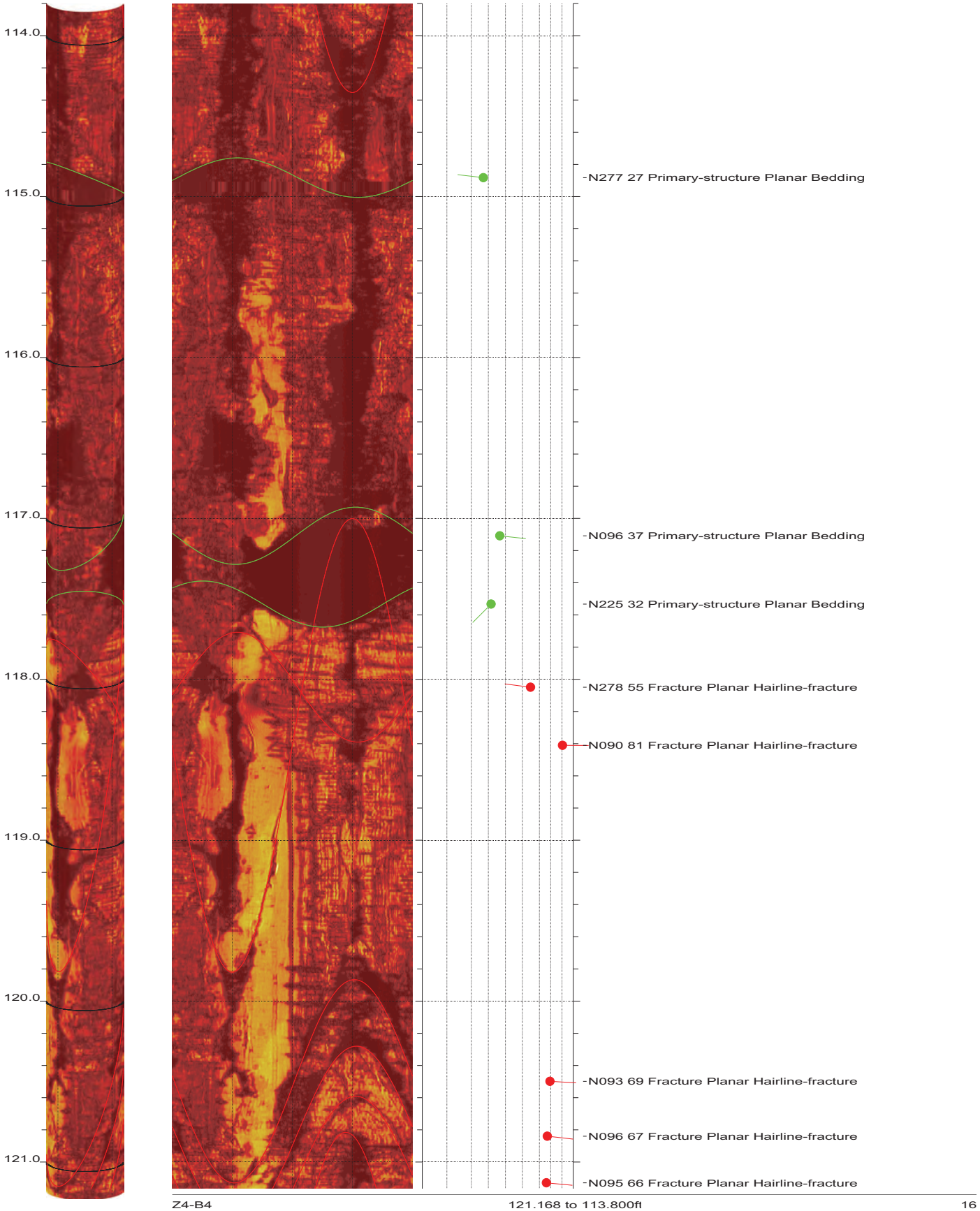


SR-710 Boring Z4-B4 Acoustic Televiewer Dips rev 1 Sheet 16 of 37

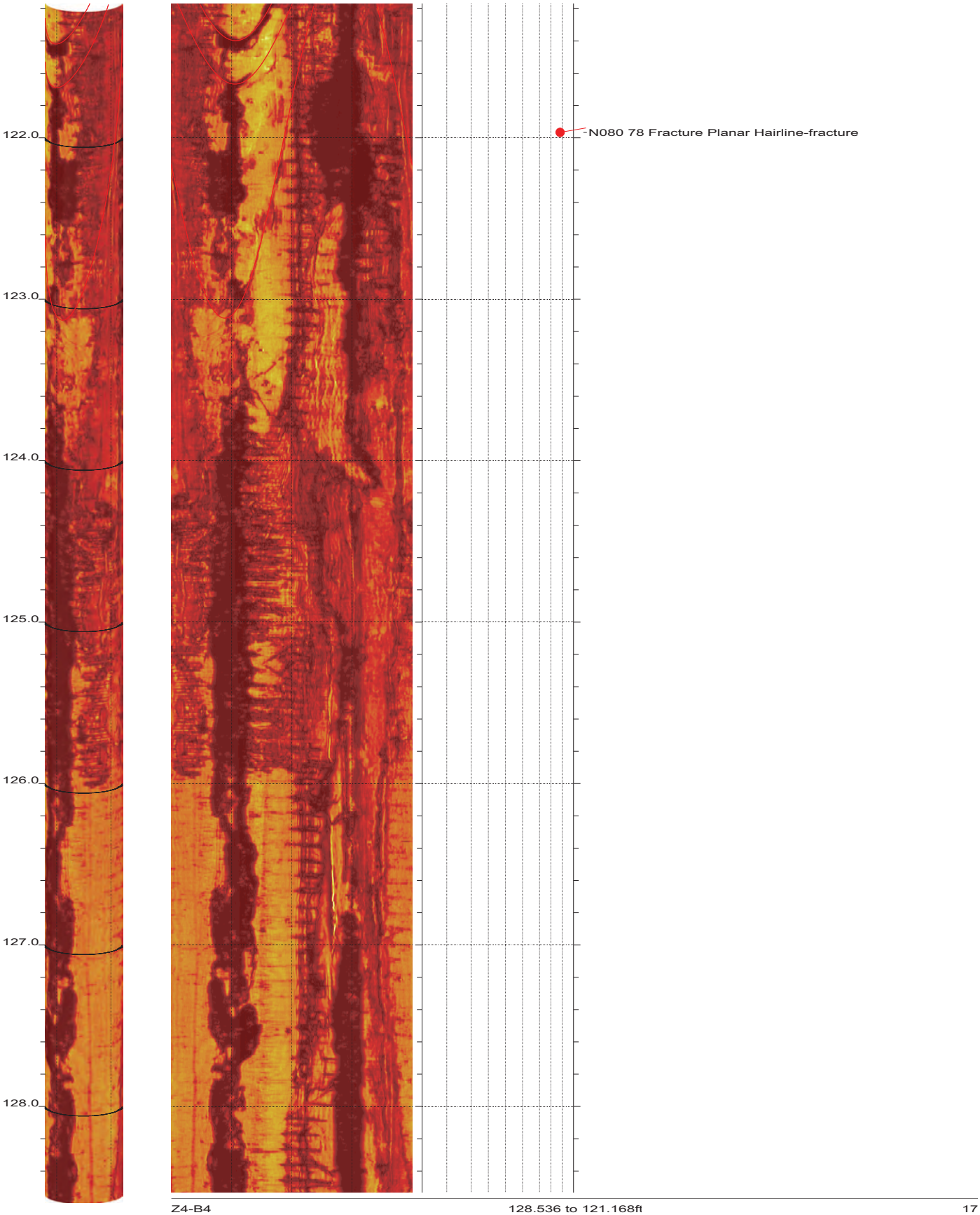
122.0
123.0
124.0
125.0
126.0
127.0
128.0
N080 78 Fracture Planar Hairline-fracture
Z4-B4
128.536 to 121.168ft
17

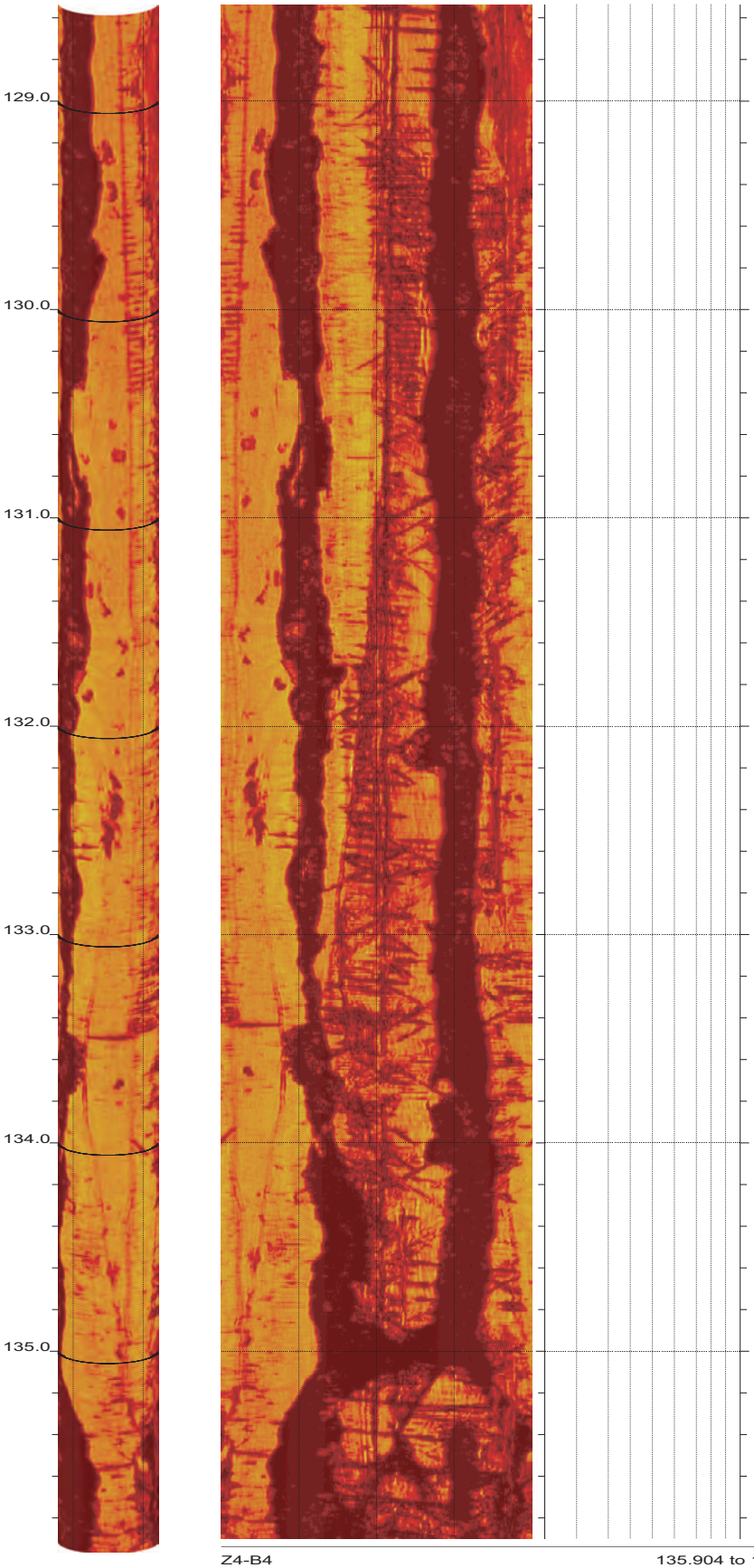


Z4-B4 135.904 to 128.536ft 18

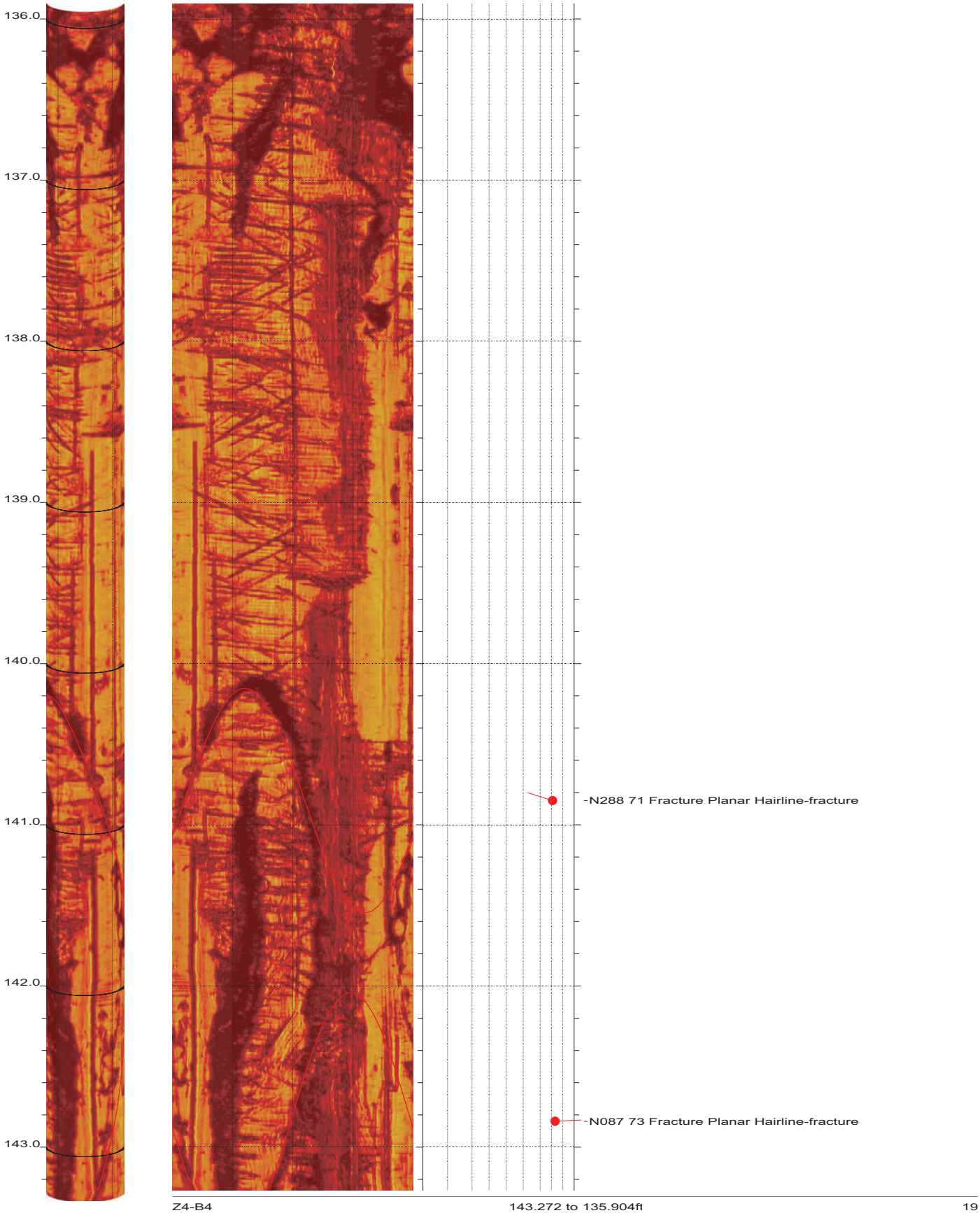
136.0
137.0
138.0
139.0
140.0
141.0
142.0
143.0
N288 71 Fracture Planar Hairline-fracture
N087 73 Fracture Planar Hairline-fracture
Z4-B4
143.272 to 135.904ft
19

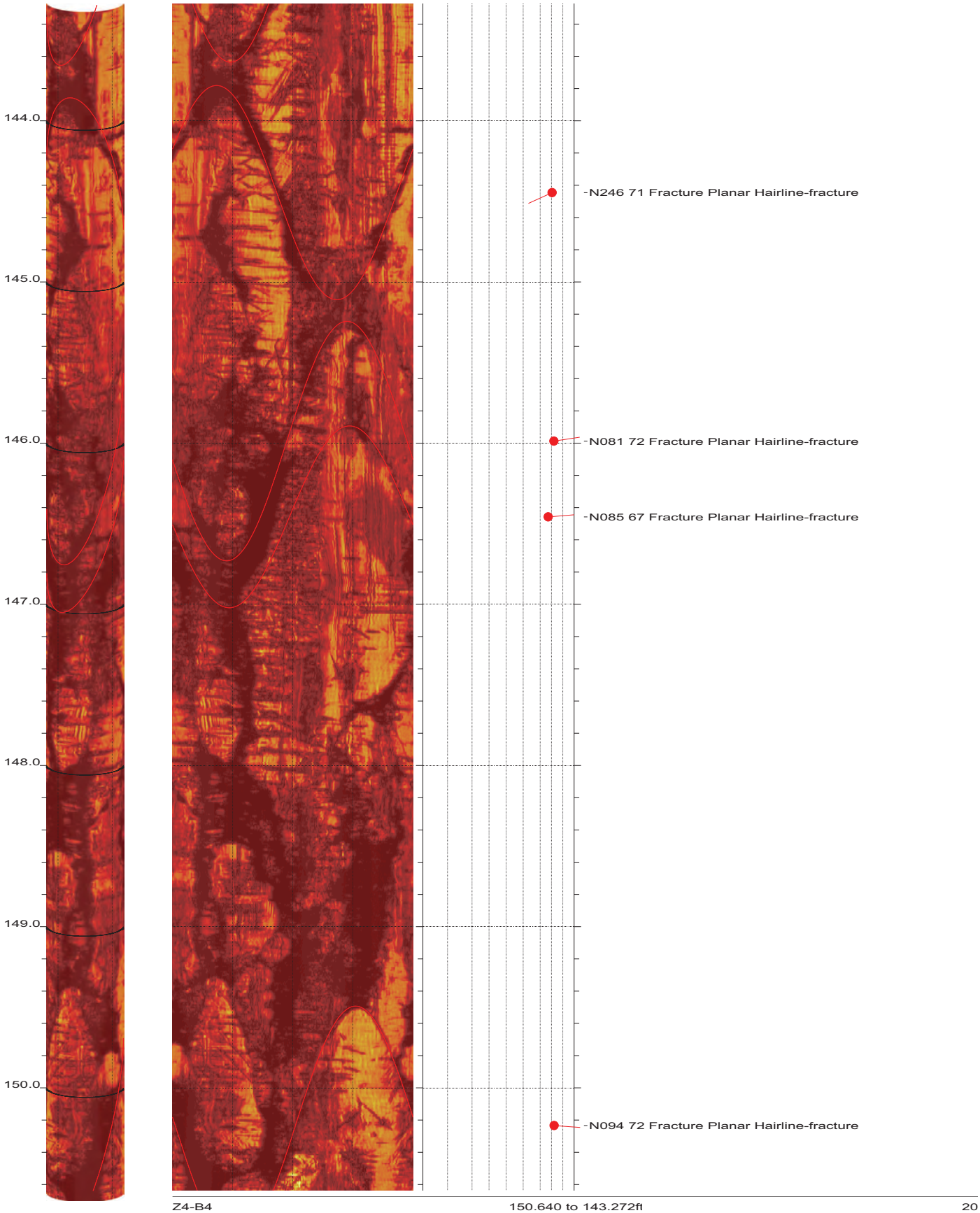


SR-710 Boring Z4-B4 Acoustic Televiewer Dips rev 1 Sheet 20 of 37

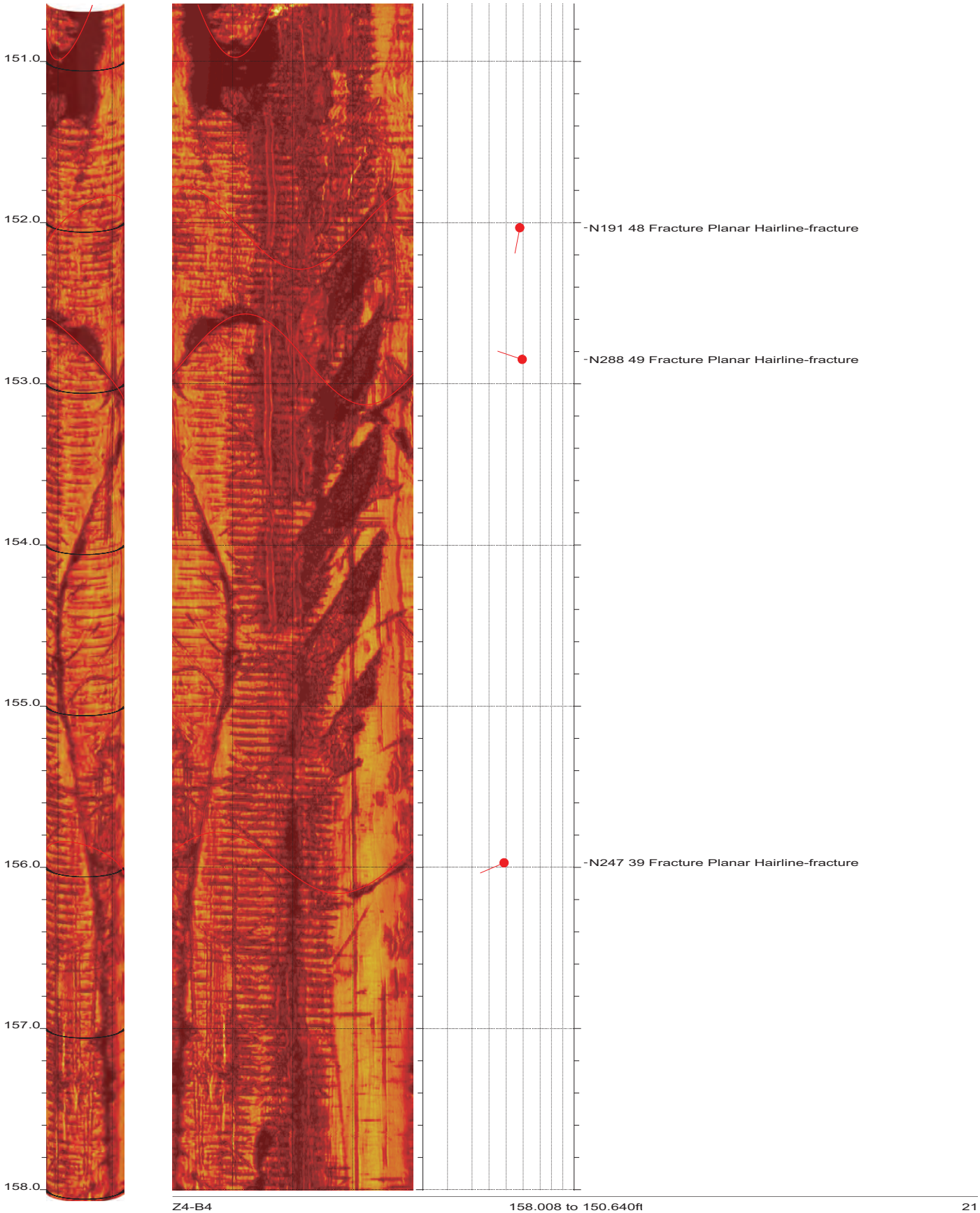


SR-710 Boring Z4-B4 Acoustic Televiewer Dips rev 1 Sheet 21 of 37

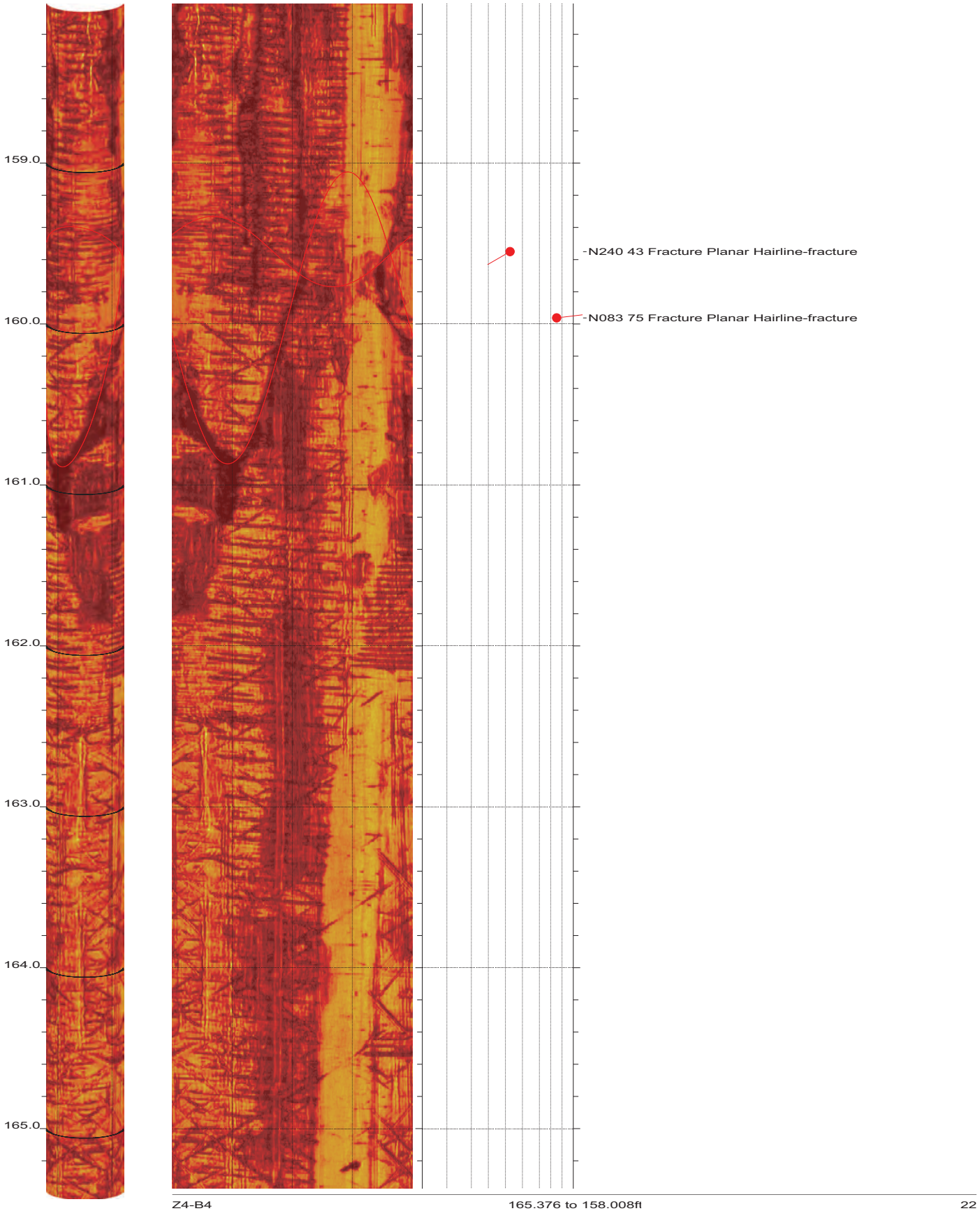


SR-710 Boring Z4-B4 Acoustic Televiewer Dips rev 1 Sheet 22 of 37

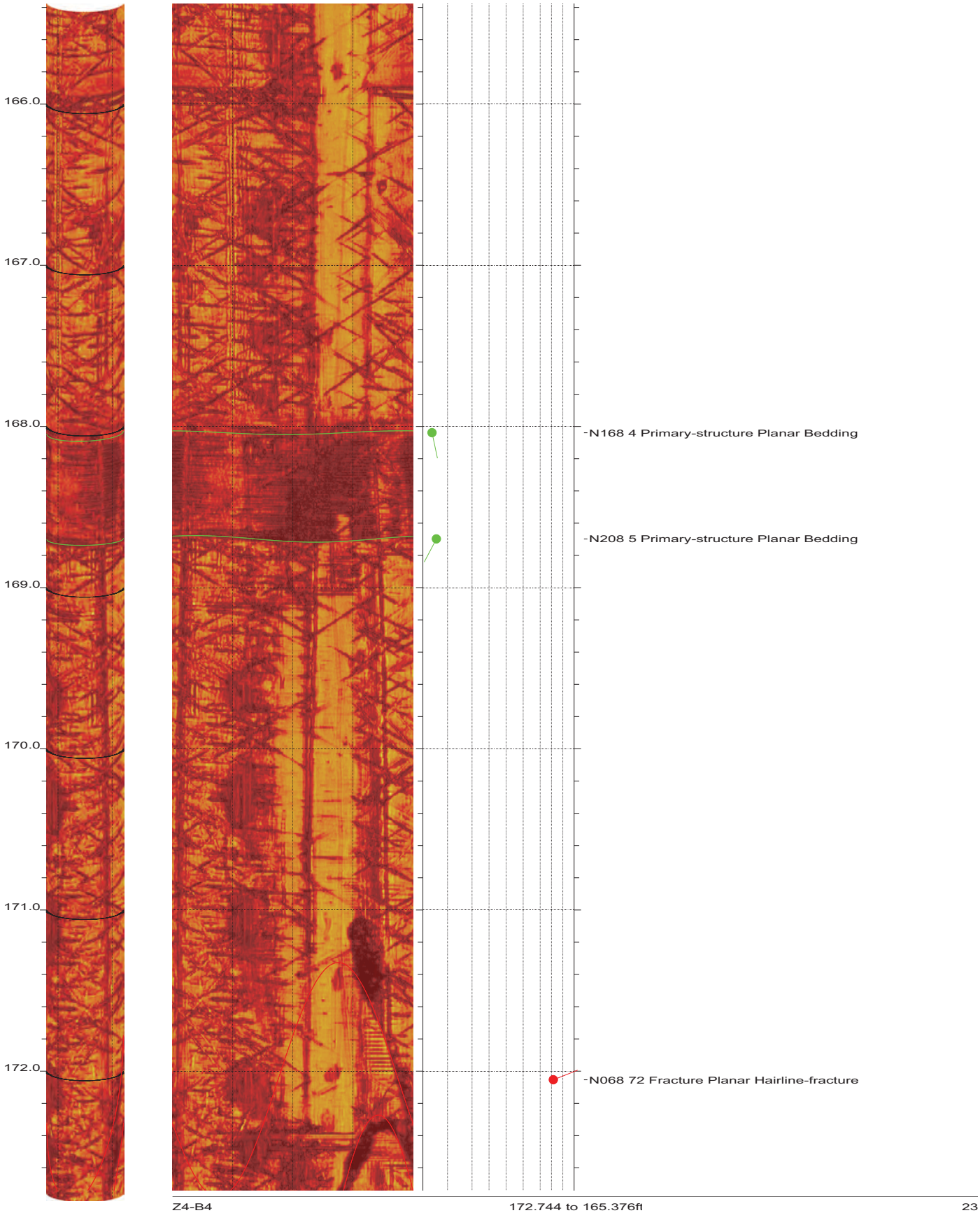


SR-710 Boring Z4-B4 Acoustic Televiewer Dips rev 1 Sheet 23 of 37

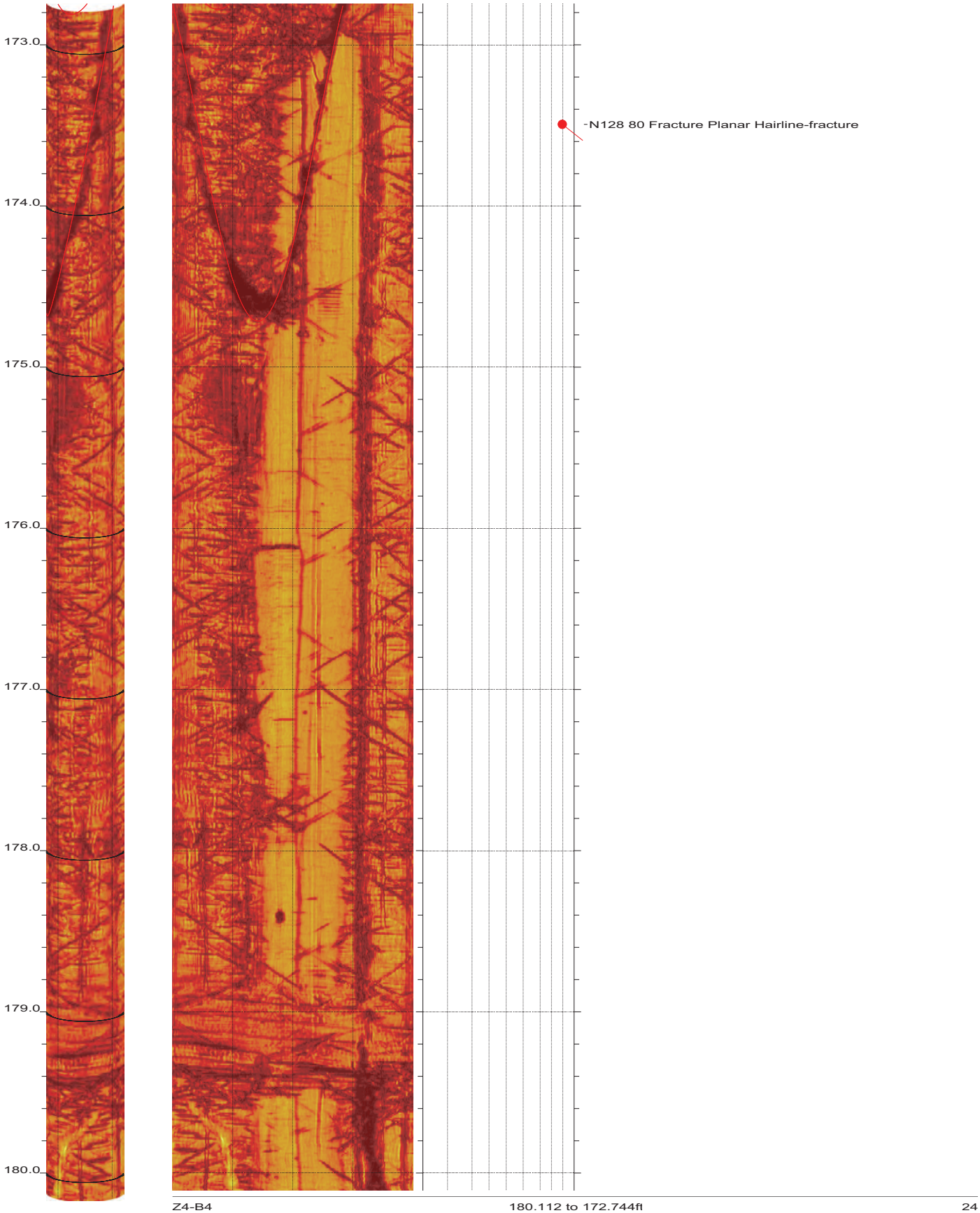
173.0
174.0
175.0
176.0
177.0
178.0
179.0
180.0
N128 80 Fracture Planar Hairline-fracture
Z4-B4
180.112 to 172.744ft
24

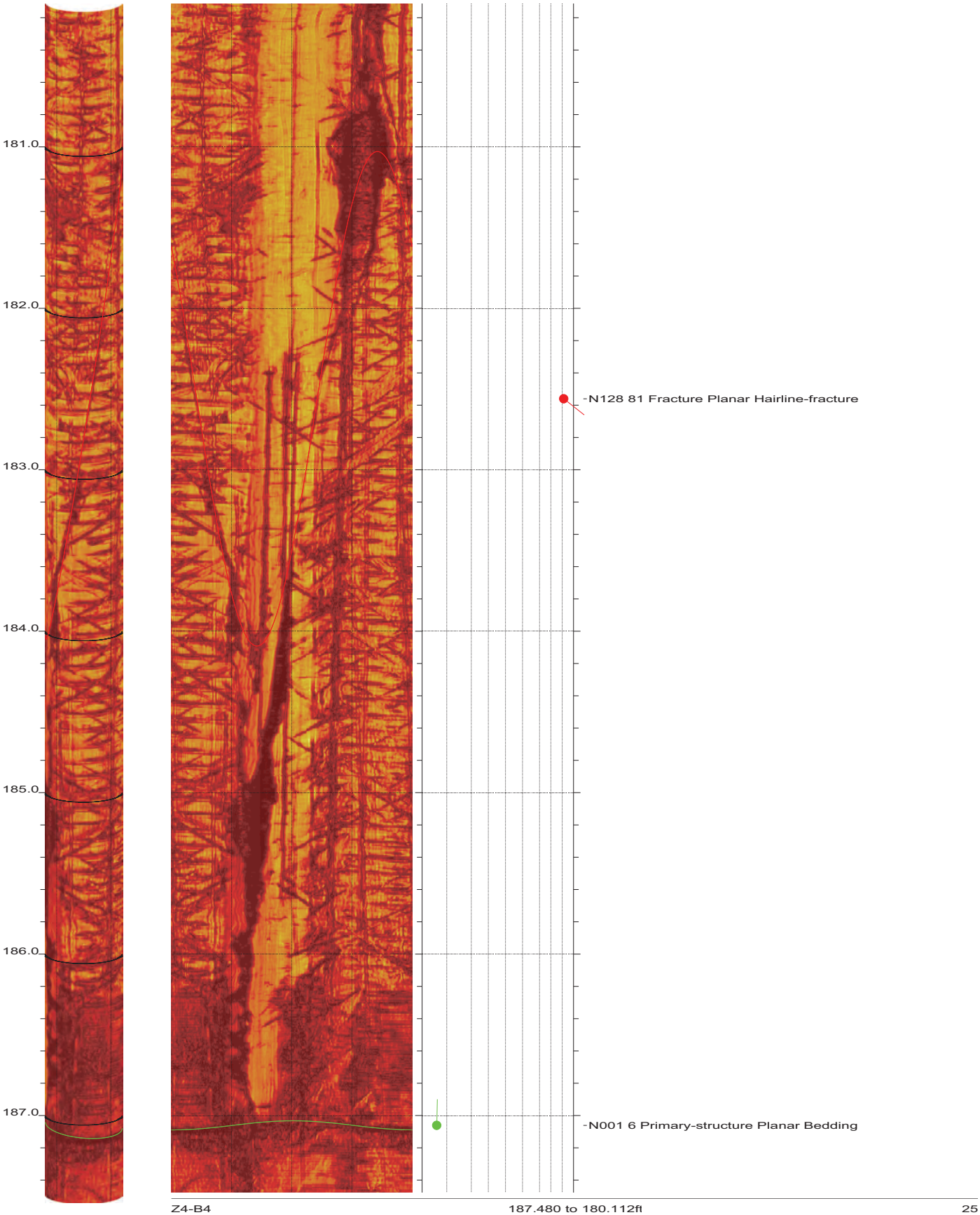


SR-710 Boring Z4-B4 Acoustic Televiewer Dips rev 1 Sheet 25 of 37

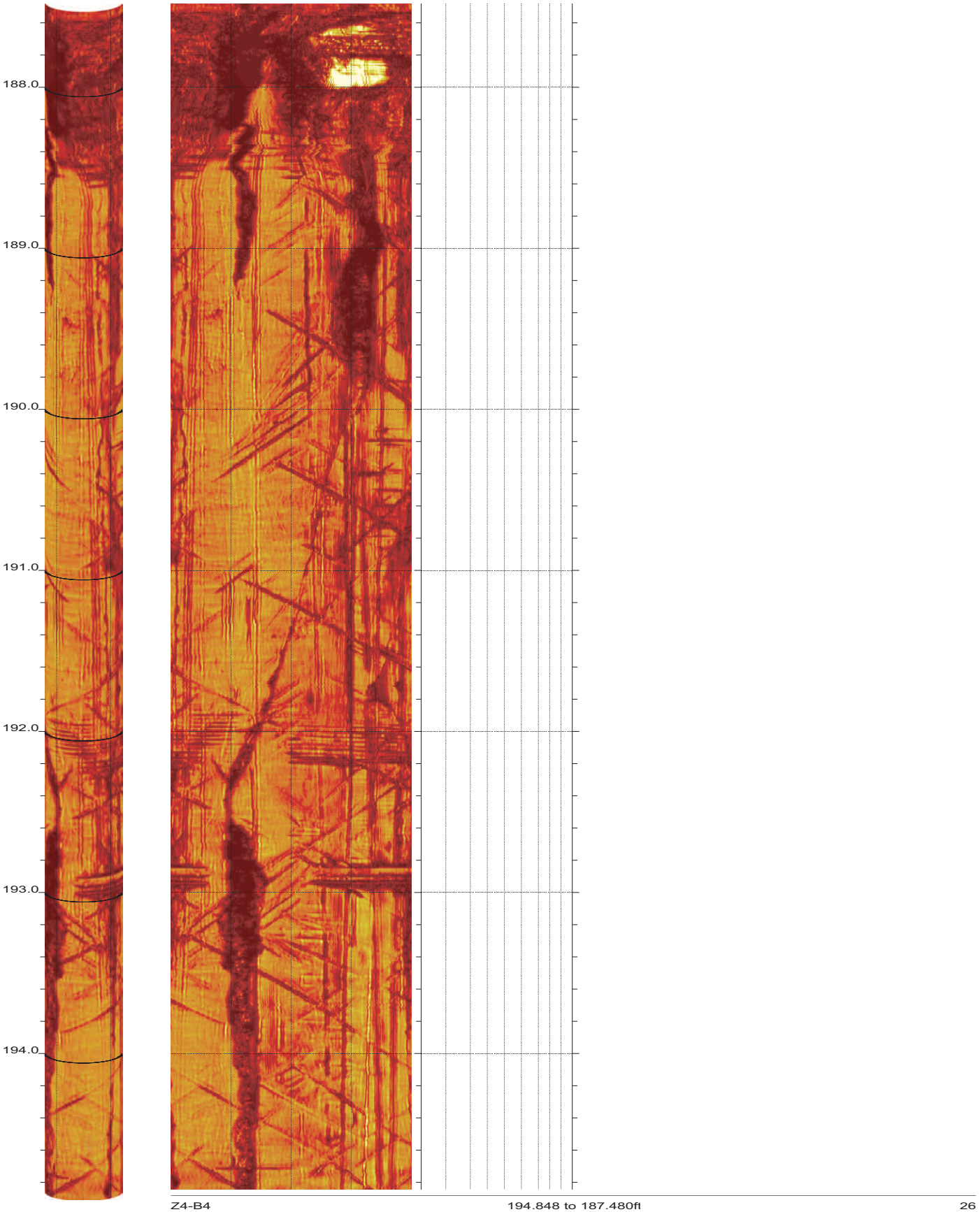
188.0
189.0
190.0
191.0
192.0
193.0
194.0
Z4-B4
194.848 to 187.480ft
26

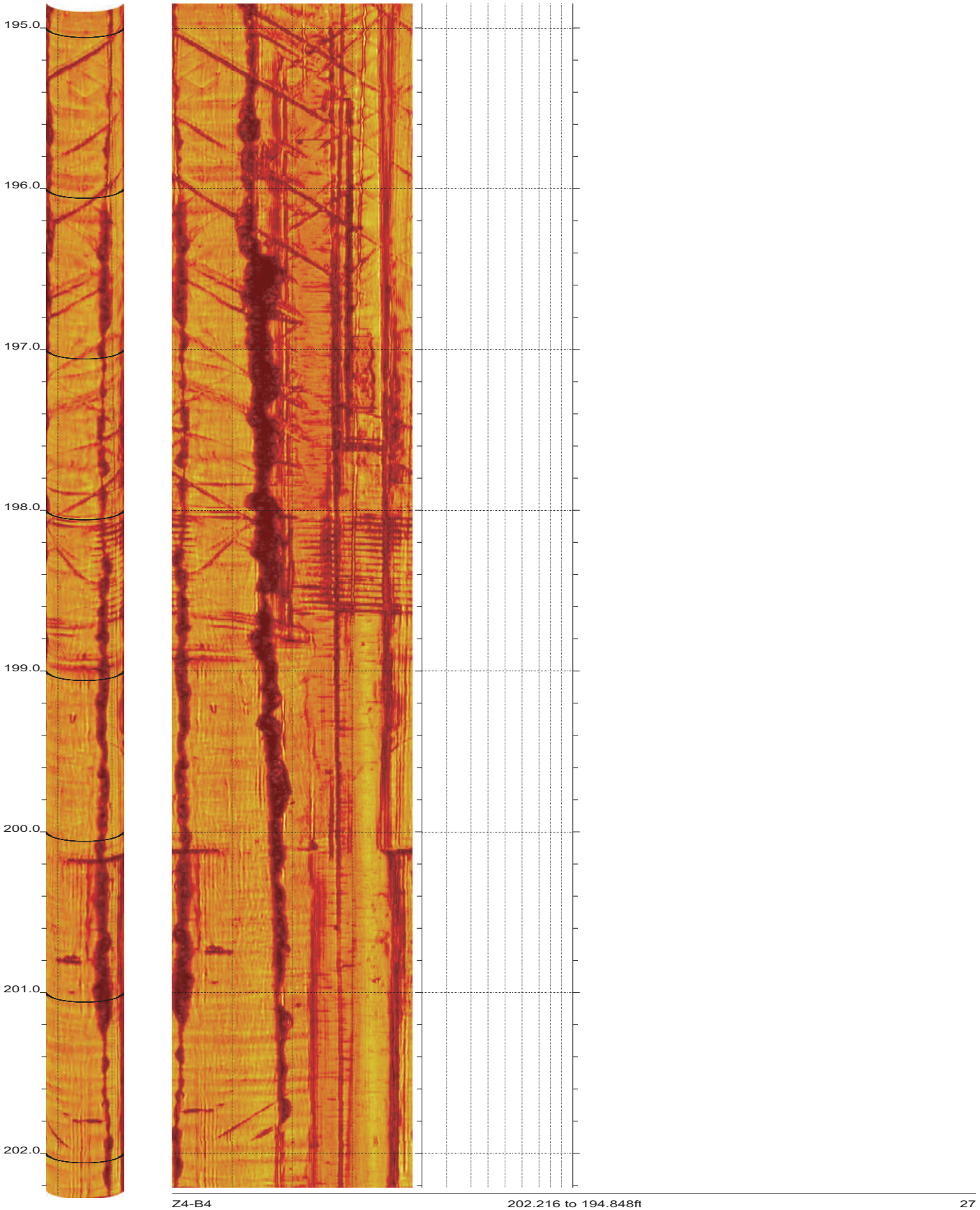


SR-710 Boring Z4-B4 Acoustic Televiewer Dips rev 1 Sheet 27 of 37

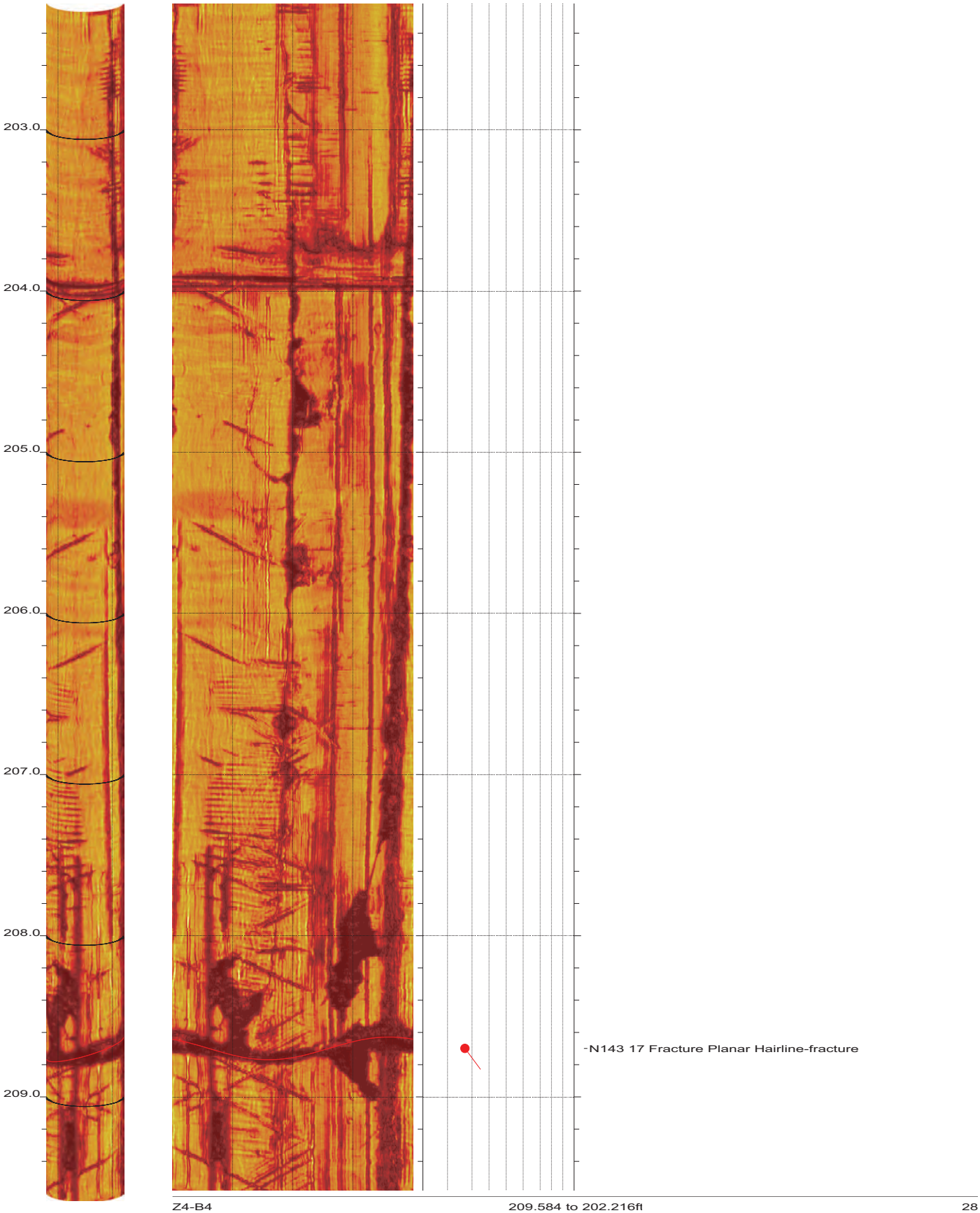


SR-710 Boring Z4-B4 Acoustic Televiewer Dips rev 1 Sheet 28 of 37

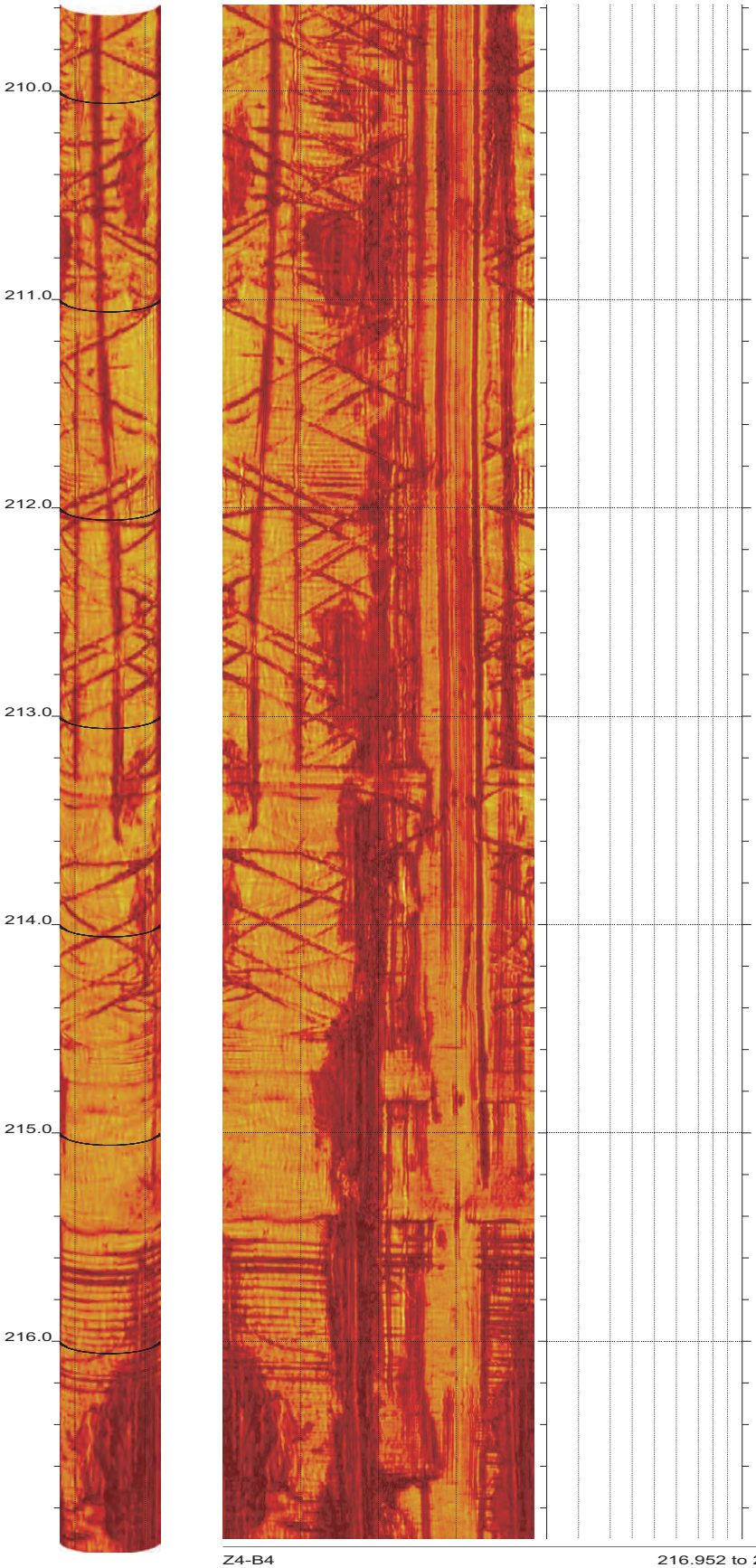


Z4-B4 216.952 to 209.584ft 29

SR-710 Boring Z4-B4 Acoustic Televiewer Dips rev 1 Sheet 29 of 37

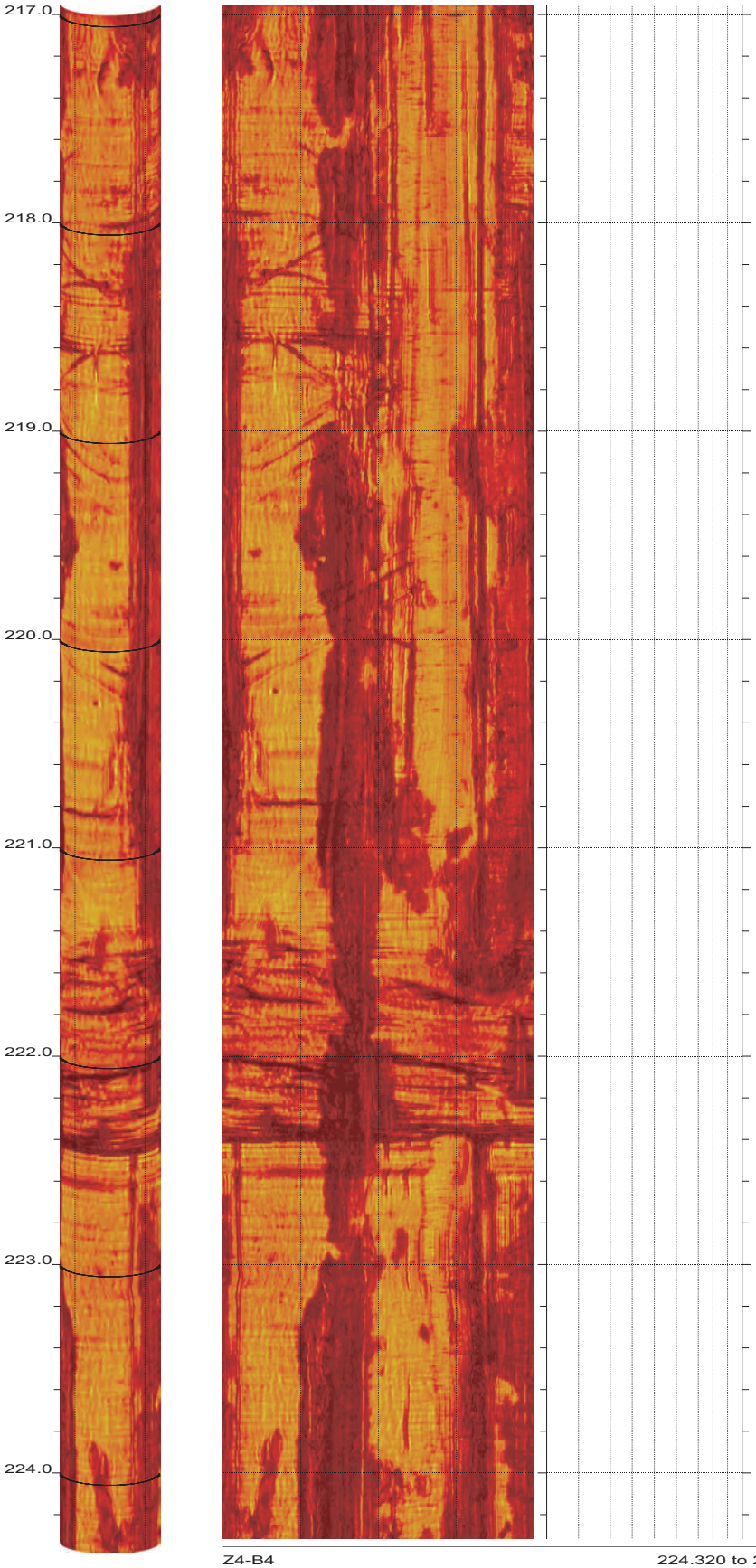


Z4-B4 224.320 to 216.952ft 30

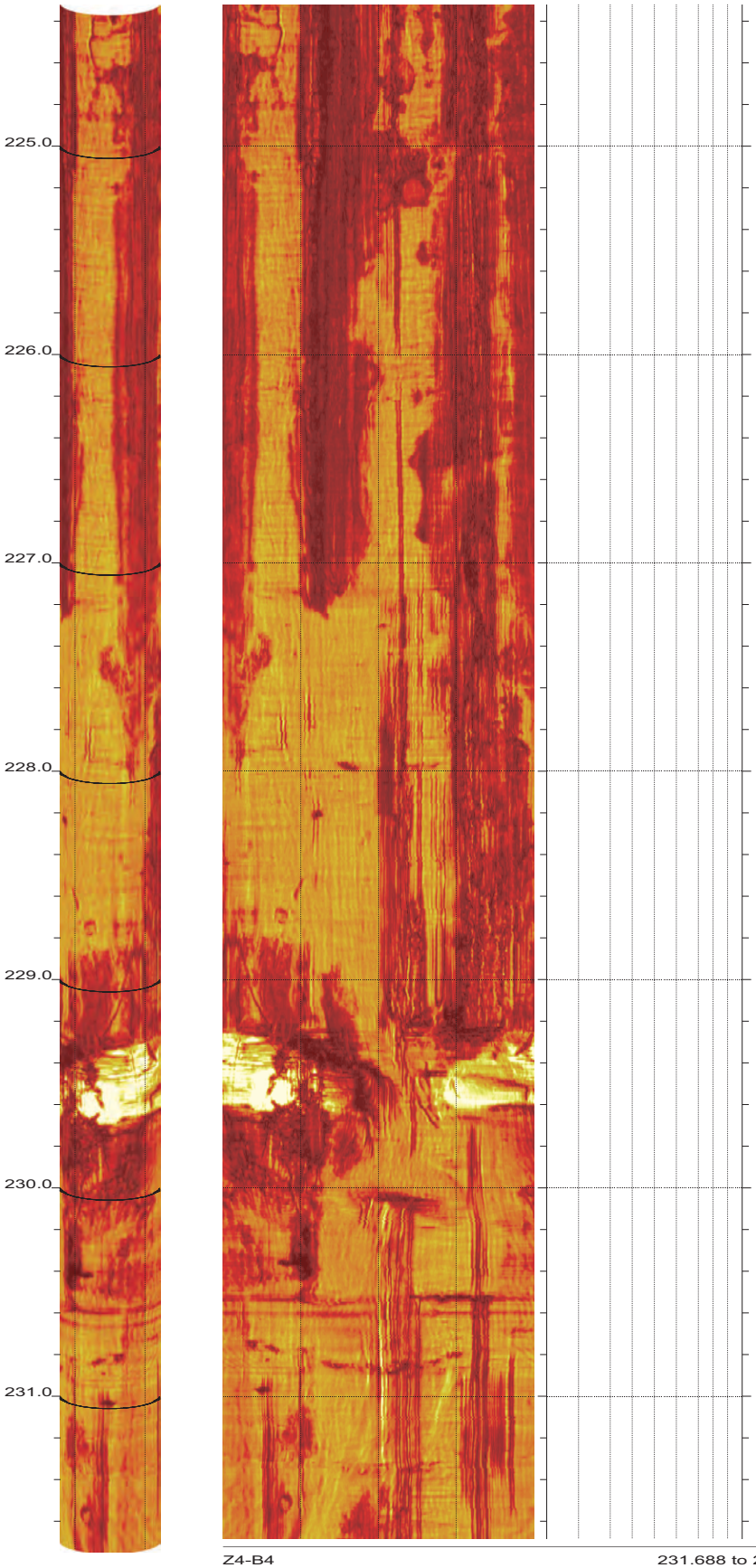


Z4-B4 231.688 to 224.320ft 31

SR-710 Boring Z4-B4 Acoustic Televiewer Dips rev 1 Sheet 31 of 37

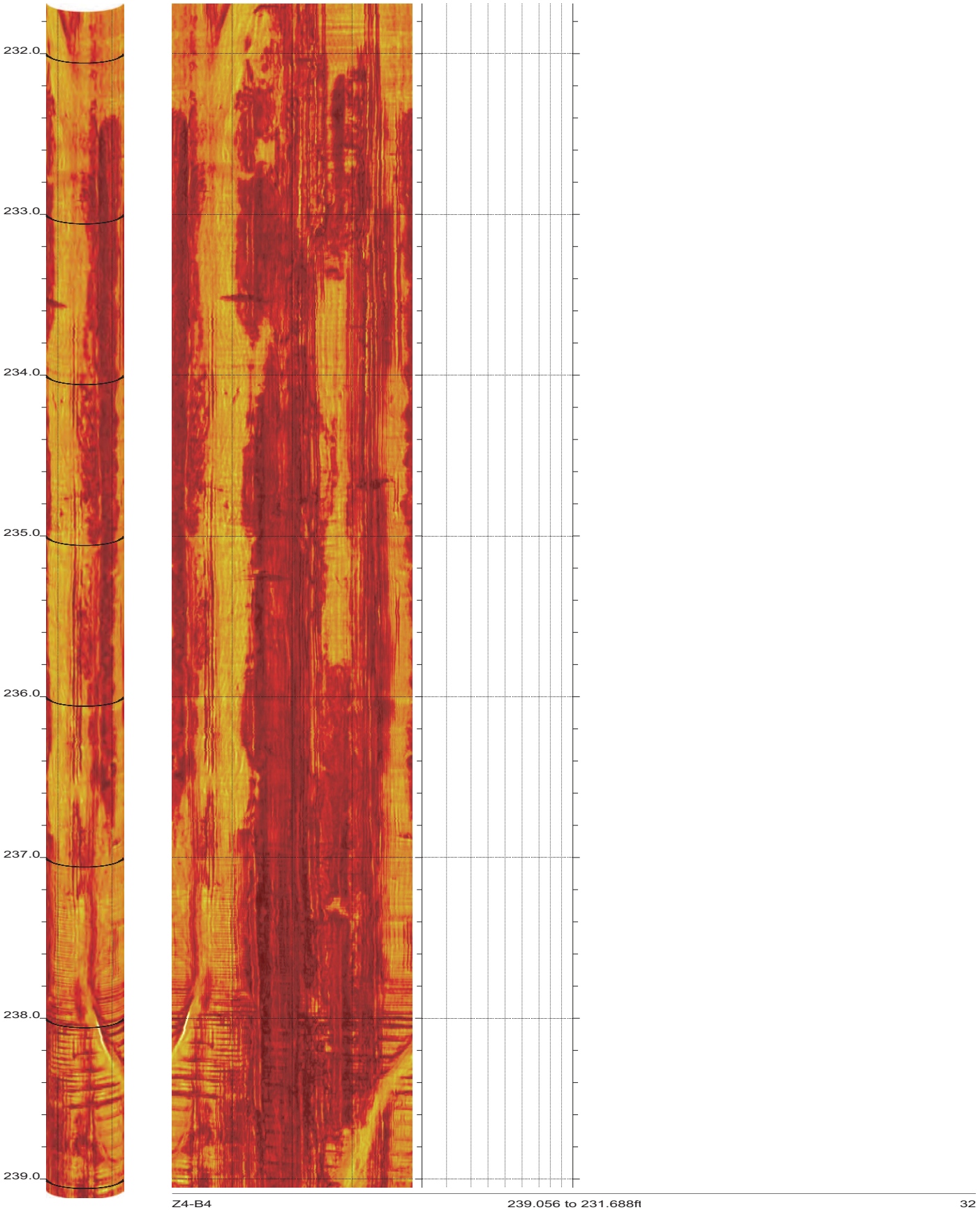
232.0
233.0
234.0
235.0
236.0
237.0
238.0
239.0
Z4-B4
239.056 to 231.688ft
32

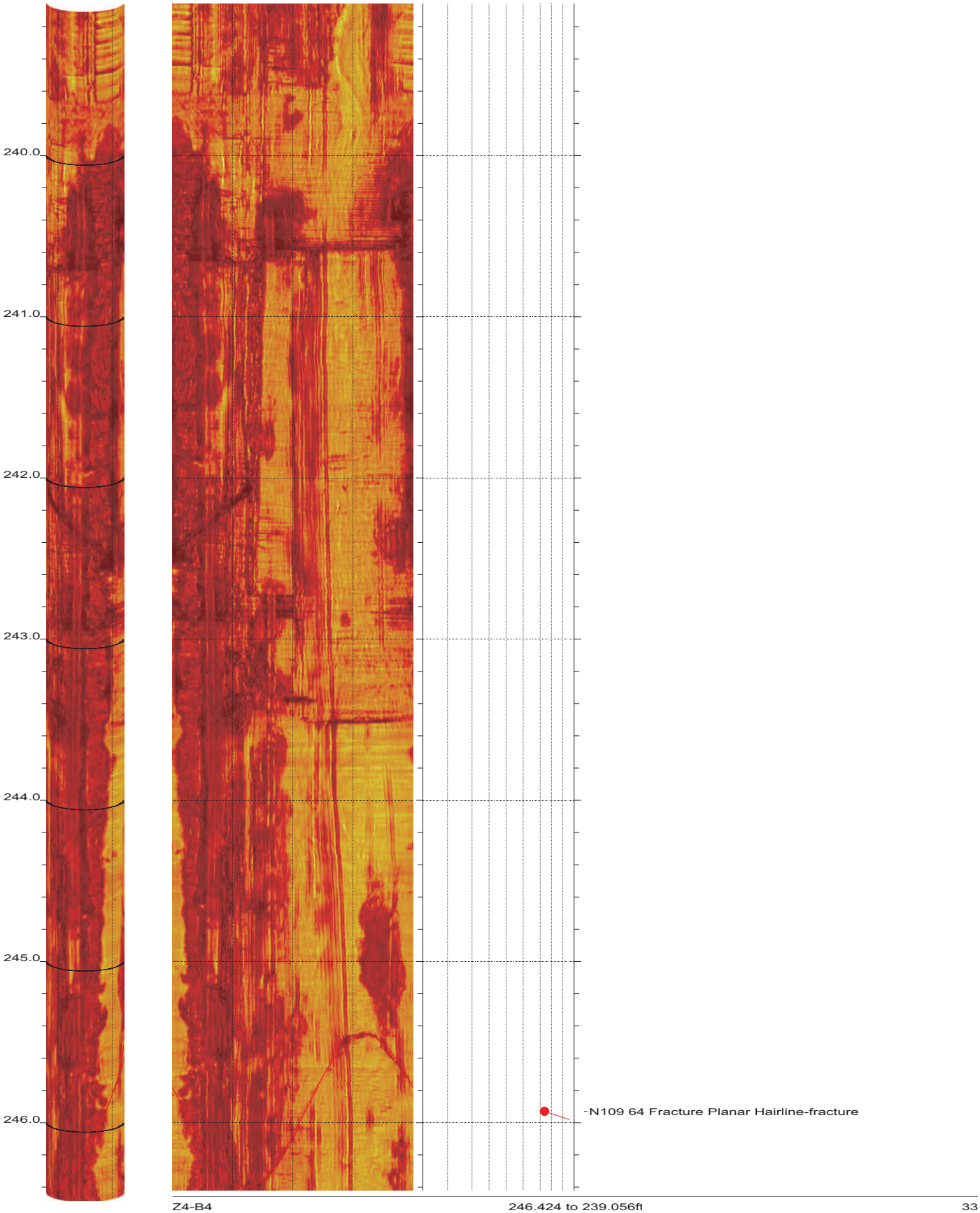


SR-710 Boring Z4-B4 Acoustic Televiewer Dips rev 1 Sheet 33 of 37

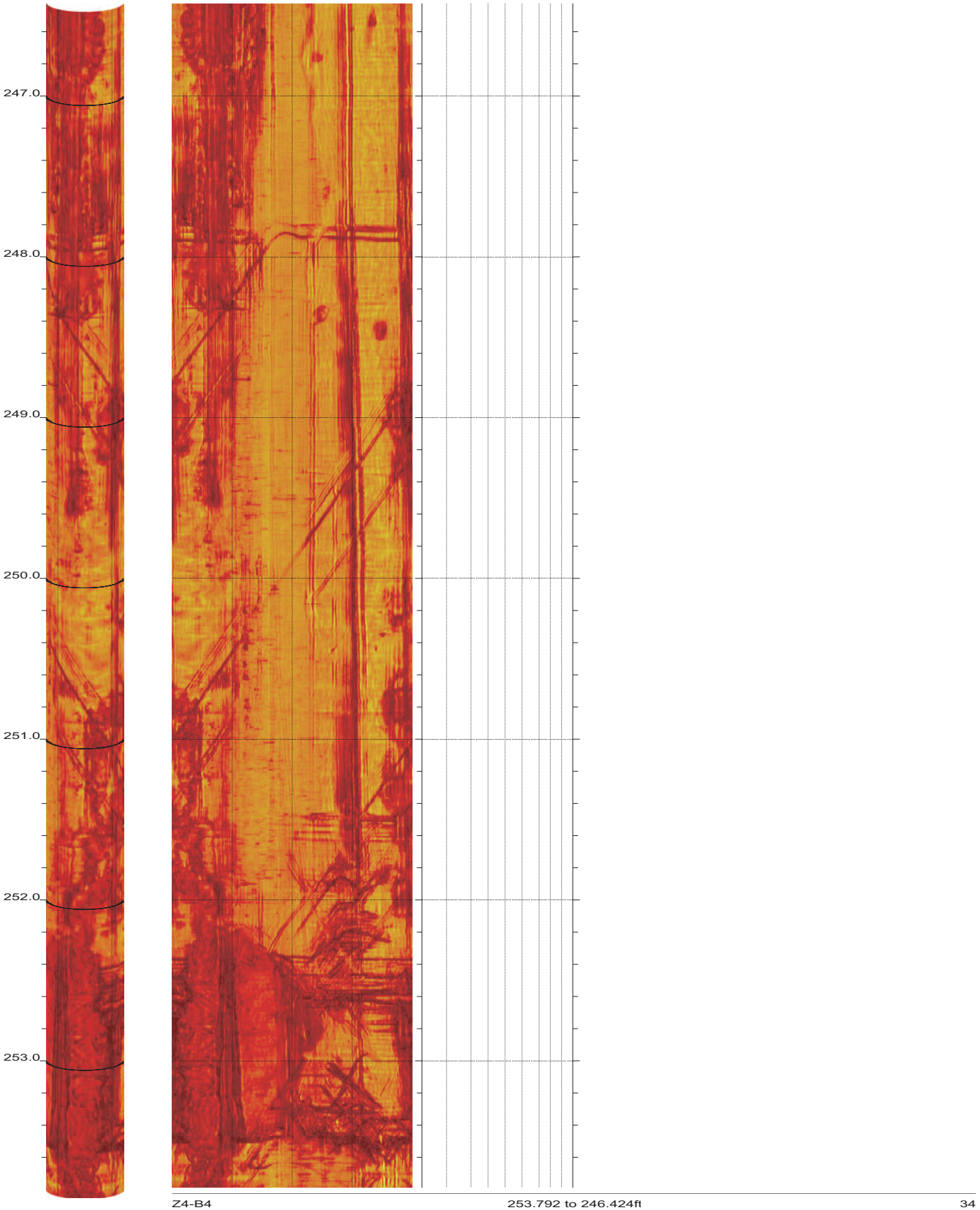


SR-710 Boring Z4-B4 Acoustic Televiewer Dips rev 1 Sheet 34 of 37

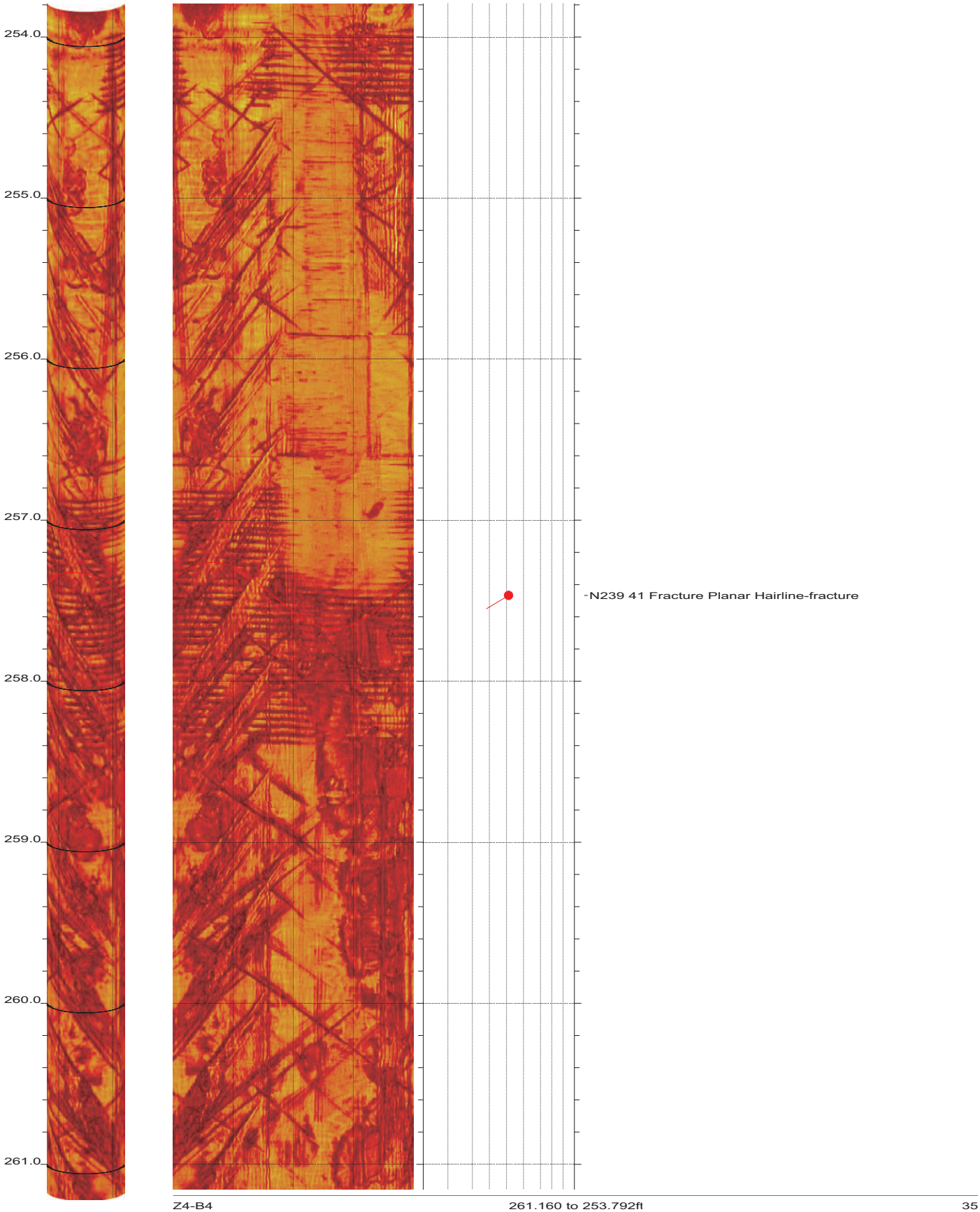


SR-710 Boring Z4-B4 Acoustic Televiewer Dips rev 1 Sheet 35 of 37

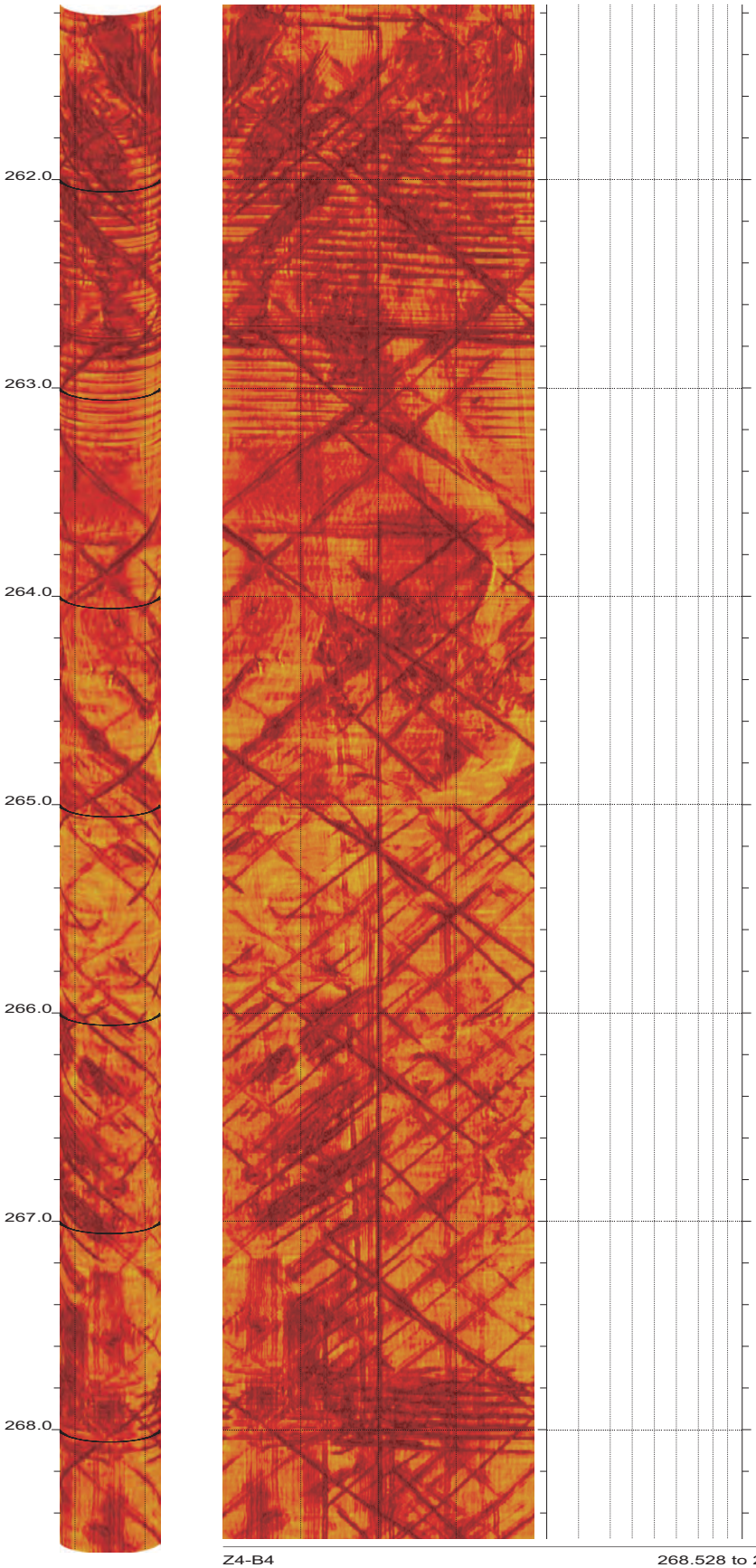


Z4-B4 268.528 to 261.160ft 36

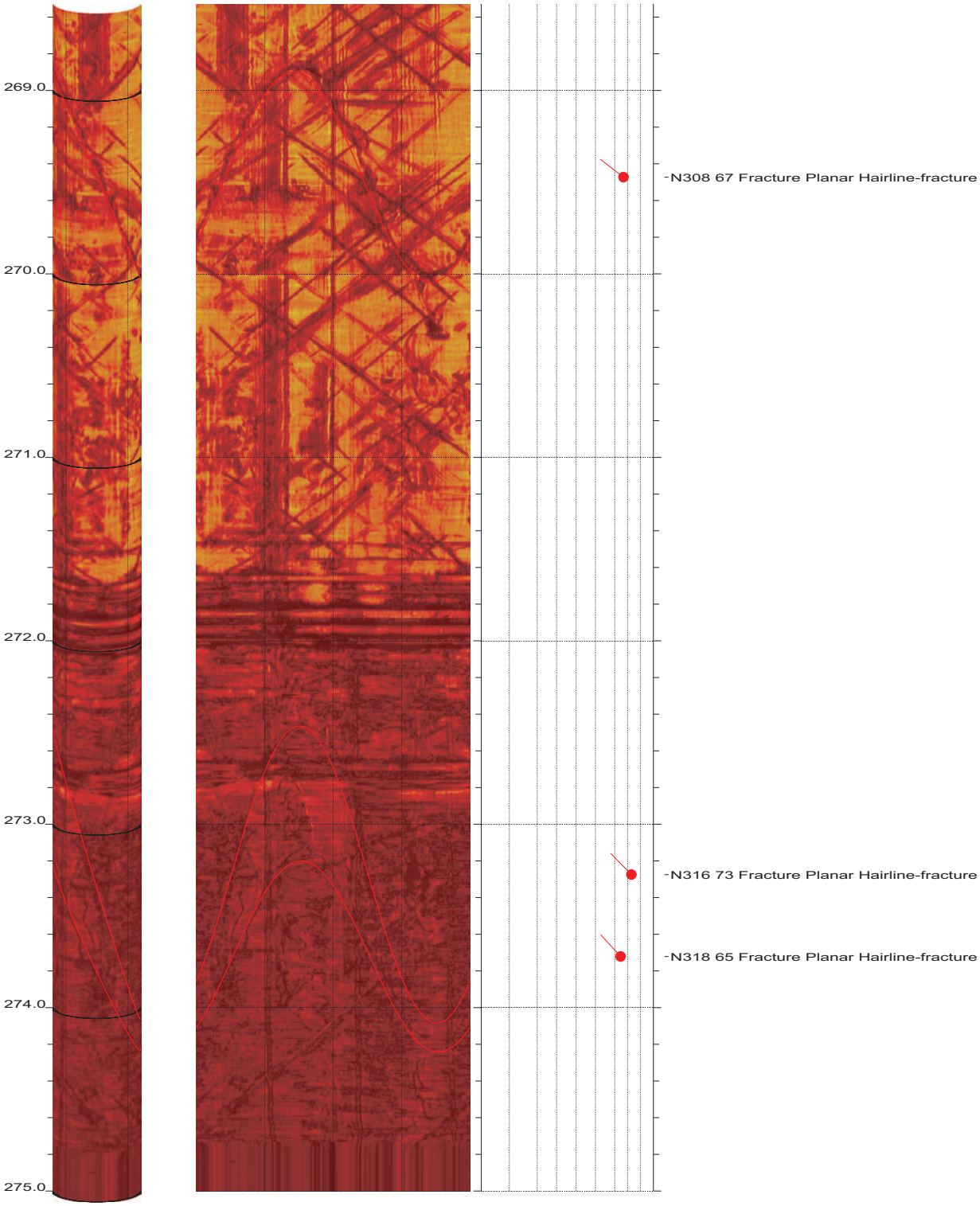
269.0
270.0
271.0
272.0
273.0
274.0
275.0
N308 67 Fracture Planar Hairline-fracture
N316 73 Fracture Planar Hairline-fracture
N318 65 Fracture Planar Hairline-fracture

# APPENDIX D

# GEOPHYSICAL LOGGING SYSTEMS – NIST TRACEABLE CALIBRATION PROCEDURES AND CALIBRATION RECORDS

# CALIBRATION PROCEDURE FOR

# GEOVision SEISMIC RECORDER/LOGGER

Reviewed 4/6/06

## Objective

The timing/sampling accuracy of seismic recorders or data loggers is required for several GEOVision field procedures including Seismic Refraction, Downhole Seismic Velocity Logging, and P-S Suspension Logging. This procedure describes the method for measuring the timing accuracy of a seismic data logger, such as the OYO Model 170, OYO/Robertson Model 3403, Geometrics Strataview or Geometrics Geode. The objective of this procedure is to verify that the timing accuracy of the recorder is accurate to within 1%.

## Frequency of Calibration

The calibration of each GEOVision seismic data logger is twelve (12) months. In the case of rented seismic data loggers, calibration must be performed prior to use.

## Test Equipment Required

The following equipment is required. Item #2 must have current NIST traceable calibration.

1. Function generator, Krohn Hite 5400B or equivalent
2. Frequency counter, HP 5315A or equivalent
3. Test cables, from item 1 to item 2, and from item 1 to subject data logger.

## Procedure

This procedure is designed to be performed using the accompanying Seismograph Calibration Data Sheet with the same revision number. All data must be entered and the procedure signed by the technician performing the test.

1. Record all identification data on the form provided.
2. Connect function generator to data logger (such as OYO Model 170) using test cable
3. Connect the function generator to the frequency counter using test cable.

4. Set up generator to produce a 100.0 Hz, 0.25 volt (amplitude is approximate, modify as necessary to yield less than full scale waveforms on logger display) peak square wave or sine wave. Verify frequency using the counter and initial space on the data sheet.

5. Initialize data logger and record a data record of at least 0.1 second using a 100 microsecond or less sample period.

6. Measure the recorded square wave frequency by measuring the duration of 9 cycles of data. This measurement can be made using the data logger display device, or by printing out a paper tape. If a paper tape can be printed, the resulting printout must be attached to this procedure. Record the data in the space provided.

7. Repeat steps 5 and 6 three more times using separate files.

**Criteria**

The duration for 9 cycles in any file must be 90.0 milliseconds plus or minus 0.9 milliseconds, corresponding to an average frequency for the nine cycles of 100.0 Hz plus or minus 1 Hz (obtained by dividing 9 cycles by the duration in milliseconds).

If the results are outside this range, the data logger must be marked with a GEOVision REJECT tag until it can be repaired and retested.

If results are acceptable affix label indicating the initials of the person performing the calibration, the date of calibration, and the due date for the next calibration (12 months).

**Procedure Approval**

Approved by:

| | |
|---|---|
| John G. Diehl | President |
| Name | Title |
| Signature | April 6, 2006 |
| | Date |

Client Approval (if required):

| | |
|---|---|
| | |
| Name | Title |
| | |
| Signature | Date |

# GEOVision SUSPENSION PS SEISMIC LOGGER/RECORDER

# CALIBRATION PROCEDURE

Reviewed 7/21/08

## Objective

The timing/sampling accuracy of seismic recorders or data loggers is required for several GEOVision field procedures including Seismic Refraction, Downhole P-S Seismic Velocity Logging, and Suspension P-S Seismic Velocity Logging. This procedure describes the method for measuring the timing accuracy of a seismic data logger, such as the OYO Model 170 or OYO/Robertson Model 3403. The objective of this procedure is to verify that the timing accuracy of the recorder is accurate to within 1%.

## Frequency of Calibration

The calibration of each GEOVision seismic data logger is twelve (12) months. In the case of rented seismic logger/recorders, calibration must be performed prior to use.

## Test Equipment Required

The following equipment is required. Item #2 must have current NIST traceable calibration.

1. Function generator, Krohn Hite 5400B or equivalent
2. Frequency counter, HP 5315A or equivalent
3. Test cables, from item 1 to item 2, and from item 1 to subject data logger.

## Procedure

This procedure is designed to be performed using the accompanying Suspension P-S Seismic Logger/Recorder Calibration Data Form with the same revision number. All data must be entered and the procedure signed by the technician performing the test.

1. Record all identification data on the form provided.
2. Connect function generator to data logger (such as OYO Model 170) using test cable
3. Connect the function generator to the frequency counter using test cable.
4. Set signal generator to target frequency specified on data form, 0.25 volt (amplitude is approximate, modify as necessary to yield less than full scale waveforms on

logger display) peak sine wave. Verify frequency using the counter and note actual frequency on the data form.

5. Set data logger to file length specified on data form and record a data file to disk. Note file name on data form.

6. Measure the duration of 9 complete sine wave cycles on the data file. This measurement must be made using the analysis program PSLOG.EXE version 1.00, and saved as a .sps pick file. Note the duration in milliseconds in the spaces provided on the data form. Calculate average recorded sine wave frequency for each channel pair (Hn, Hr, V) by dividing the duration by 9. Note the average frequency of each channel pair on the data form.

7. Repeat steps 4 through 6 until all target frequencies have been recorded, producing 6 separate data and pick files.

**Criteria**

The average frequency for the nine cycles (obtained by dividing 9 cycles by the duration in seconds) must be within plus or minus 1% of the actual frequency for each of the 6 records.

If the results are outside this range, the data logger must be marked with a GEOVision REJECT tag until it can be repaired and retested.

If results are acceptable affix label indicating the initials of the person performing the calibration, the date of calibration, and the due date for the next calibration (12 months).

**Procedure Approval**

Approved by:

| | |
|---|---|
| John G. Diehl | President |
| Name | Title |
| Signature | July 21, 2008 |
| | Date |

Calibration Laboratory Approval (if required):

| | |
|---|---|
| _____ | _____ |
| Name | Title |
| _____ | _____ |
| Signature | Date |

EDISON ESI℠

A SOUTHERN CALIFORNIA EDISON® Company

**Metrology**
7300 Fenwick Lane
Westminster, CA 92683
Phone: 866-723-2257

# Calibration Report

*NVLAP Accredited*
*Calibration*

**GEOVision Geophysical Services**
1124 Olympic Drive
Corona, CA 92881-3390

TEST NUMBER
558549

NVLAP®
**Lab Code:105014-0**

| | |
|---|---|
| **Manufacturer:** | Oyo |
| **Model Number:** | 3403 |
| **Description:** | Unit, Suspension Telemetry, |
| **Asset Number:** | 160024 |
| **Serial Number:** | 160024 |
| **PO Number:** | 8200-080122-01 |

| | |
|---|---|
| **Condition As Found:** | In Tolerance |
| **Condition As Left:** | In Tolerance |
| **Calibration Date:** | 08/01/2008 |
| **Calibration Due Date:** | 08/01/2009 |
| **Calibration Interval:** | 12 Months |

**Remarks:**

This unit was calibrated with the customer's old procedure and specifications which have been reviewed by Metrology Engineering and documented in SCE Document M013684. The data can be found on page 2 of this report with the original observation data on page 3. The unit was then calibrated with the customer's new procedure and specification's which have been reviewed by Metrology Engineering and documented in SCE Document M013987. The data can be found on pages 4 and 5 of this report with the original observation data on page 6 of this report. Corrected Copy: This record created to add missing maximum error calculations on page 6 of 6. CAB 8-5-08

**Standards Utilized**

| I.D. No. | Mfg. | Model No. | Description | Cal. Date | Due Date |
|---|---|---|---|---|---|
| S1-01252 | Hewlett Packard | 5335A OPT 010,203040 | Counter, Universal, | 07/17/2008 | 01/17/2009 |
| S1-01347 | Hewlett Packard | 3325A | Generator, Function, Synthesizer | 04/24/2008 | 10/24/2008 |
| S1-03686 | Fluke | 910 | Standard, Frequency, Controlled, Gps | 01/22/2008 | 01/22/2009 |

**Procedure:** Customer
**Temperature:** 23° C
**Humidity:** 52% RH
**Test No.:** 558549

| Calibration Performed By: | | | Quality Reviewer: | |
|---|---|---|---|---|
| Branson, Craig A CAB | Metrologist | 714-895-0714 | | 8-5-08 |
| Name | Title | Phone | Name | Date |

Test No. 558549
Asset No. 160024

# Custom Specification Report

**Oyo 3403 Unit, Suspension Telemetry,**



| STEP NUM | FUNCTION TESTED | NOMINAL VALUE | AS FOUND | AS LEFT | Out of Tol | CALIBRATION TOLERANCE |
|---|---|---|---|---|---|---|
| | CH HN Frequency Square Wave | 100.0 Hz | 100.0 | Same | | 99.0 to 101.0 Hz [EMU 0.000500 Hz] |
| | " | 100.0 Hz | 100.0 | Same | | 99.0 to 101.0 Hz [EMU 0.000500 Hz] |
| | Sine Wave | 100.0 Hz | 100.0 | Same | | 99.0 to 101.0 Hz [EMU 0.000500 Hz] |
| | " | 100.0 Hz | 100.0 | Same | | 99.0 to 101.0 Hz [EMU 0.000500 Hz] |
| | CH HR Frequency Square Wave | 100.0 Hz | 100.0 | Same | | 99.0 to 101.0 Hz [EMU 0.000500 Hz] |
| | " | 100.0 Hz | 100.0 | Same | | 99.0 to 101.0 Hz [EMU 0.000500 Hz] |
| | Sine Wave | 100.0 Hz | 100.0 | Same | | 99.0 to 101.0 Hz [EMU 0.000500 Hz] |
| | " | 100.0 Hz | 100.0 | Same | | 99.0 to 101.0 Hz [EMU 0.000500 Hz] |
| | CH V Frequency Square Wave | 100.0 Hz | 100.0 | Same | | 99.0 to 101.0 Hz [EMU 0.000500 Hz] |
| | " | 100.0 Hz | 100.0 | Same | | 99.0 to 101.0 Hz [EMU 0.000500 Hz] |
| | Sine Wave | 100.0 Hz | 100.0 | Same | | 99.0 to 101.0 Hz [EMU 0.000500 Hz] |
| | " | 100.0 Hz | 100.0 | Same | | 99.0 to 101.0 Hz [EMU 0.000500 Hz] |
| | | | | | | |
| | | | | | | |
| | | | | | | |
| | | | | | | |

**Remarks:**

*MudCats CPM: Version 2.2.2 (Professional)*
*Src DUI: {4A70366A-164D-4E33-8F79-34E3FDFFA198} (c)*
*Doc DUI: {293A3A00-D536-43A0-A1E5-945133CD4CF7} (o)*

**ATTACHMENT 1**
**Page 1 of 1**

**Customer**

## SEISMOGRAPH CALIBRATION DATA SHEET REV 4/6/06

**INSTRUMENT DATA**

| | | | |
|---|---|---|---|
| SYSTEM MFR: | OYO | MODEL NO.: | 3403 |
| SERIAL NO.: | 160024 | CALIBRATION DATE: | 8/1/2008 |
| BY: | CRAIG BRANSON | DUE DATE: | 8/1/2009 |
| COUNTER MFR: | HEWLETT PACKARD | MODEL NO.: | 5335A |
| SERIAL NO.: | 2626A09881 | CALIBRATION DATE: | 7/17/2008 |
| BY: | SCE #S1-01252 | DUE DATE: | 1/17/2009 |
| FCTN GEN MFR: | HEWLETT PACKARD | MODEL NO.: | 3325A |
| SERIAL NO.: | 2652A25647 | CALIBRATION DATE: | 4/24/2008 |
| BY: | SCE #S1-01347 | DUE DATE: | 10/24/2008 |

**SYSTEM SETTINGS:**

| | |
|---|---|
| GAIN: | 2 |
| FILTER: | 10 KHZ |
| RANGE: | 100 MILLISEC |
| DELAY: | 0 |
| STACK: 1 (STD) | 1 |
| PULSE: | 1.6 |
| DISPLAY: | NA |
| SYSTEM: DATE = CORRECT DATE & TIME | 8/1/2008 715 |

**PROCEDURE:**

SET FREQUENCY TO 100.0HZ SQUAREWAVE WITH AMPLITUDE APPROXIMATELY 0.25 VOLT PEAK. RECORD BOTH ON DISK AND PAPER TAPE, IF AVAILABLE. ANALYZE AND PRINT WAVEFORMS FROM ANALYSIS UTILITY. ATTACH PAPER COPIES OF PRINTOUT AND PAPER TAPES, IF AVAILABLE, TO THIS FORM. AVERAGE FREQUENCY MUST BE BETWEEN 99.0 AND 101.0 HZ.

AS FOUND 100.0 HZ AS LEFT 100.0 HZ

| WAVEFORM | FILE NO | FREQUENCY | TIME FOR 9 CYCLES Hn | TIME FOR 9 CYCLES Hr | TIME FOR 9 CYCLES V | AVERAGE FREQ. |
|---|---|---|---|---|---|---|
| SQUARE | 501 | 100.0 | 90.00 MS | 90.00 MS | 90.00 MS | 100.0 HZ |
| SQUARE | 502 | 100.0 | 90.00 MS | 90.00 MS | 90.00 MS | 100.0 HZ |
| SINE | 503 | 100.0 | 90.00 MS | 90.00 MS | 90.00 MS | 100.0 HZ |
| SINE | 504 | 100.0 | 90.00 MS | 90.00 MS | 90.00 MS | 100.0 HZ |

CALIBRATED BY: CRAIG BRANSON (NAME) 8/1/2008 (DATE) Craig Branson (SIGNATURE)

Seismic recorder/Logger Calibration Data Sheet Rev 1.30 4-6-06

Test No. 558549
Asset No. 160024

# Custom Specification Report

## Oyo 3403 Logger/Recorder, Seismic, PS Suspension



| STEP NUM | FUNCTION TESTED | NOMINAL VALUE | AS FOUND | AS LEFT | Out of Tol | CALIBRATION TOLERANCE |
|---|---|---|---|---|---|---|
| | CH HN Frequency Sine Wave | 50.00 Hz | 50.00 | Same | | 49.50 to 50.50 Hz [EMU 0.000250] |
| | " | 100.0 Hz | 100.0 | Same | | 99.0 to 101.0 Hz [EMU 0.000500] |
| | " | 200.0 Hz | 200.0 | Same | | 198.0 to 202.0 Hz [EMU 0.001000] |
| | " | 500.0 Hz | 500.0 | Same | | 495.0 to 505.0 Hz [EMU 0.002500] |
| | " | 1000 Hz | 1000 | Same | | 990 to 1010 Hz [EMU 0.005000] |
| | " | 2000 Hz | 2000 | Same | | 1980 to 2020 Hz [EMU 0.010000] |
| | CH HR Frequency Sine Wave | 50.00 Hz | 49.95 | Same | | 49.50 to 50.50 Hz [EMU 0.000250] |
| | " | 100.0 Hz | 100.0 | Same | | 99.0 to 101.0 Hz [EMU 0.000500] |
| | " | 200.0 Hz | 200.2 | Same | | 198.0 to 202.0 Hz [EMU 0.001000] |
| | " | 500.0 Hz | 500.0 | Same | | 495.0 to 505.0 Hz [EMU 0.002500] |
| | " | 1000 Hz | 1001 | Same | | 990 to 1010 Hz [EMU 0.005000] |
| | " | 2000 Hz | 2000 | Same | | 1980 to 2020 Hz [EMU 0.010000] |
| | CH V Frequency Sine Wave | 50.00 Hz | 50.00 | Same | | 49.50 to 50.50 Hz [EMU 0.000250] |
| | " | 100.0 Hz | 100.0 | Same | | 99.0 to 101.0 Hz [EMU 0.000500] |
| | " | 200.0 Hz | 199.8 | Same | | 198.0 to 202.0 Hz [EMU 0.001000] |
| | " | 500.0 Hz | 500.0 | Same | | 495.0 to 505.0 Hz [EMU 0.002500] |

**Remarks:**

Test No. 558549
Asset No. 160024

# Custom Specification Report

## Oyo 3403 Logger/Recorder, Seismic, PS Suspension



| STEP NUM | FUNCTION TESTED | NOMINAL VALUE | AS FOUND | AS LEFT | Out of Tol | CALIBRATION TOLERANCE |
|---|---|---|---|---|---|---|
| | CH V Frequency Sine Wave | 1000 Hz | 1000 | Same | | 990 to 1010 Hz [EMU 0.005000] |
| | \| | 2000 Hz | 1998 | Same | | 1980 to 2020 Hz [EMU 0.010000] |
| | | | | | | |
| | | | | | | |
| | | | | | | |
| | | | | | | |
| | | | | | | |
| | | | | | | |
| | | | | | | |
| | | | | | | |
| | | | | | | |
| | | | | | | |
| | | | | | | |
| | | | | | | |
| | | | | | | |
| | | | | | | |

**Remarks:**

GEOVision geophysical services PAGE 6 OF 6

## SUSPENSION PS SEISMIC LOGGER/RECORDER CALIBRATION DATA FORM

**INSTRUMENT DATA**

| | | | |
|---|---|---|---|
| System mfg.: | Oyo | Model no.: | 3403 |
| Serial no.: | 160024 | Calibration date: | 8/1/2008 |
| By: | Craig Branson | Due date: | 8/1/2009 |
| Counter mfg.: | Hewlett-Packard | Model no.: | 5335A |
| Serial no.: | 2626A09881 | Calibration date: | 7/17/2008 |
| By: | SCE #S1-01252 | Due date: | 1/17/2009 |
| Signal generator mfg.: | Hewlett-Packard | Model no.: | 3325A |
| Serial no.: | 2652A25647 | Calibration date: | 4/24/2008 |
| By: | SCE #S1-01347 | Due date: | 10/24/2008 |

**SYSTEM SETTINGS:**

| | |
|---|---|
| Gain: | 2 |
| Filter | 10KHz |
| Range: | See sample period in table below |
| Delay: | 0 |
| Stack (1 std) | 1 |
| System date = correct date and time | 8/1/2008 728 |

**PROCEDURE:**

Set sine wave frequency to target frequency with amplitude of approximately 0.25 volt peak
Note actual frequency on data form.
Set sample period and record data file to disk. Note file name on data form.
Pick duration of 9 cycles using PSLOG.EXE program, note duration on data form, and save as .sps file. Calculate average frequency for each channel pair and note on data form.

Average frequency must be within +/- 1% of actual frequency at all data points.

Maximum error ((AVG-ACT)/ACT*100)% As found 0.10% As left 0.10%

| Target Frequency (Hz) | Actual Frequency (Hz) | Sample Period (microS) | File Name | Time for 9 cycles Hn (msec) | Average Frequency Hn (Hz) | Time for 9 cycles Hr (msec) | Average Frequency Hr (Hz) | Time for 9 cycles V (msec) | Average Frequency V (Hz) |
|---|---|---|---|---|---|---|---|---|---|
| 50.00 | 50.00 | 200 | 505 | 180.0 | 50.00 | 180.2 | 49.95 | 180.0 | 50.00 |
| 100.0 | 100.0 | 100 | 506 | 90.00 | 100.0 | 90.00 | 100.0 | 90.00 | 100.0 |
| 200.0 | 200.0 | 50 | 507 | 45.00 | 200.0 | 44.95 | 200.2 | 45.05 | 199.8 |
| 500.0 | 500.0 | 20 | 508 | 18.00 | 500.0 | 18.00 | 500.0 | 18.00 | 500.0 |
| 1000 | 1000 | 10 | 509 | 9.000 | 1000 | 8.990 | 1001 | 9.000 | 1000 |
| 2000 | 2000 | 5 | 510 | 4.500 | 2000 | 4.500 | 2000 | 4.505 | 1998 |

Calibrated by: Craig Branson (Name) 8/1/2008 (Date) Craig Branson (Signature)

Witnessed by: Robert Steller (Name) 8/1/2008 (Date) (Signature)

Suspension PS Seismic Recorder/Logger Calibration Data Form Rev 2.0 July 21, 2008

## GEOVision Borehole Geophysics depth wheel verification

Performed by Robert Steller

| | Depth reading in #1 | Depth reading out | Depth reading in #2 |
|---|---|---|---|
| Depth wheel<br>S/N 101<br>500 pulse/revolution<br>(gear 1:5, encoder 100 ppr)<br>Circumference = 983mm<br>(3225.07 millifeet) | 100.1 feet<br>(30.51 m)<br>September 23, 2006 | 99.95 feet<br>(30.46 m)<br>September 23, 2006 | 100.05 feet<br>(30.50 m)<br>September 23, 2006 |
| Depth wheel<br>S/N 103<br>500 pulse/revolution<br>(gear 1:5, encoder 100 ppr)<br>Circumference = 994mm<br>(3261.15 millifeet) | 100.00 feet<br>(30.48) m<br>September 23, 2006 | 100.00 feet<br>(30.48 m)<br>September 23, 2006 | 100.00 feet<br>(30.48) m<br>September 23, 2006 |
| Aries winch<br>200 pulse/revolution<br>(gear 1:1, encoder 200 ppr)<br>Circumference = 305.9mm<br>(1003.51 millifeet) | 100.05 feet<br>(30.50 m)<br>September 23, 2006 | 100.05 feet<br>(30.50 m)<br>September 23, 2006 | 100.00 feet<br>(30.48 m)<br>September 23, 2006 |
| Robertson Depth wheel<br>For MiniWinch<br>1000 pulse/revolution<br>(gear 1:1, encoder 1000 ppr)<br>Circumference = 400mm<br>(1312 millifeet) | 99.92 feet<br>(30.46 m)<br>Re-verified<br>June 7, 2007 | 100.10 feet<br>(30.51 m)<br>Re-verified<br>June 7, 2007 | 99.90 feet<br>(30.45 m)<br>Re-verified<br>June 7, 2007 |
| Robertson Smartwinch 200<br>S/N 5802<br>5000 pulse/revolution<br>(gear 1:4, encoder 1250 ppr)<br>Circumference = 404mm<br>(1326 millifeet) | 99.99 feet<br>(30.48 m)<br>June 6, 2007 | 99.97 feet<br>(30.47 m)<br>June 6, 2007 | 100.00 feet<br>(30.48 m)<br>June 6, 2007 |
| Comprobe winch<br>500 pulse/revolution<br>(gear 1:1, encoder 500 ppr)<br>Circumference = 1000mm<br>(3.281 feet) | 100.1 feet<br>(30.5 m)<br>Re-verified<br>June 7, 2007 | 100.1 feet<br>(30.5 m)<br>Re-verified<br>June 7, 2007 | 100.1 feet<br>(30.5 m)<br>Re-verified<br>June 7, 2007 |

All measurements taken with a Stanley 100-foot flexible stainless steel tape model number 34-130, and a Keeson 300-foot fiberglass tape, both marked in feet, inches and 1/8ths of inches. Enough cable was spooled off of the winch to allow the cable and tape measures to be laid flat on the parking lot surface side-by-side. A permanent marker was used to mark a 100.0-foot interval on the cable, and the marks were also tagged with electrical tape for visibility. The cable was then spooled back onto the winch. When the first mark was at the top of the measuring wheel, a matching permanent mark was placed, and the recording system (Robertson Micrologger) was set to 0.0 feet depth. The cable was spooled in to the second mark, and the distance was recorded. The recording system was set to 0.0 feet again, and the cable spooled out to the first mark again, and the distance was recorded. The process was repeated one more time to spool the cable back onto the winch, and the distance was recorded.

Estimated accuracy is of these measurements is +/- 0.1 foot or +/- 0.03m.

## GEOVision Suspension PS probe Receiver 1–Receiver 2 (R1-R2) spacing verification

Performed by Robert Steller on September 23, 2006

| | R2 center to R1 center hanging dry | R2 center to R1 center hanging submerged | R1 bottom to source center hanging submerged with 1m isolation tube S/N 280068 | R1 center to source center hanging submerged with 1m isolation tube S/N 280068 |
|---|---|---|---|---|
| Receiver S/N 30086 | 40.2in<br>1.02m | 40.0in<br>1.02m | 76.0in<br>1.93m | 83.5in<br>2.12m |
| | | | | |
| Receiver S/N 20042 | 39.8in<br>1.01m | 39.6in<br>1.01m | 75.7in<br>1.92m | 83.2in<br>2.11m |
| | | | | |
| Receiver S/N 12008 | 40.2in<br>1.02m | 40.0in<br>1.02m | 76.0in<br>1.93m | 83.5in<br>2.12m |
| | | | | |

All measurements taken with a Lufkin 3.7m flexible steel tape model number HV1034DM, marked in mm and 100$^{th}$ of feet. Probe suspended in 3-inch diameter clear PVC pipe, using chain clamp placed between bottom and center of Receiver 2 hard section (See Figure). Probe "bounced" to establish unrestricted hanging length before measurement. Probe allowed to relax for 5 minutes prior to each measurement. Water level set to submerge bottom of Receiver 2 hard section.. Estimated accuracy due to hysterisis in rubber section approximately +/- 0.01' or +/- 0.003m.

# APPENDIX E

# BORING GEOPHYSICAL LOGGING FIELD MEASUREMENT PROCEDURES

# PROCEDURE FOR

# OYO P-S SUSPENSION SEISMIC VELOCITY LOGGING

## Background

This procedure describes a method for measuring shear and compressional wave velocities in soil and rock. The OYO P-S Suspension Method is applied by generating shear and compressional waves in a borehole using the OYO P-S Suspension Logger borehole tool and measuring the travel time between two receiver geophones or hydrophones located in the same tool.

## Objective

The outcome of this procedure is a plot and table of P and $S_H$ wave velocity versus depth for each borehole. Standard analysis is performed on receiver to receiver data. Data is presented in report format, with digital data files transmitted in Excel, Word or ASCII format.

## Instrumentation

1. OYO Model 170 Digital Logging Recorder or equivalent
2. OYO P-S Suspension Logger probe or equivalent, including two sets horizontal and vertical geophones, seismic source, and power supply for the source and receivers
3. Winch and winch controller, with logging cable
4. Batteries to operate P-S Logger and winch

The Suspension P-S Logger system, manufactured by OYO Corporation, or the Robertson Digital P-S Suspension Probe with the Robertson Micrologger2 are currently the only commercially available suspension logging systems. As shown in Figure 1, these systems consists of a borehole probe suspended by a cable and a recording/control electronics package on the surface.

The suspension system probe consists of a combined reversible polarity solenoid horizontal shear-wave generator ($S_H$) and compressional-wave generator (P), joined to

two biaxial geophones by a flexible isolation cylinder. The separation of the two geophones is one meter, allowing average wave velocity in the region between the geophones to be determined by inversion of the wave travel time between the two geophones. The total length of the probe is approximately 7 meters; the center point of the geophones is approximately 4 meters above the bottom end of the probe.

The probe receives control signals from, and sends the amplified geophone signals to, the instrumentation package on the surface via an armored 4 or 7 conductor cable. The cable is wound onto the drum of a winch and is used to support the probe. Cable travel is measured by a rotary encoder to provide probe depth data.

The entire probe is suspended by the cable and may be centered in the borehole by nylon "whiskers." Therefore, source motion is not coupled directly to the borehole walls; rather, the source motion creates a horizontally propagating pressure wave in the fluid filling the borehole and surrounding the source. This pressure wave produces a horizontal displacement of the soil forming the wall of the borehole. This displacement propagates up and down the borehole wall, in turn causing a pressure wave to be generated in the fluid surrounding the geophones as the soil displacement wave passes their location.

**Environmental Conditions**

The OYO P-S Suspension Logging Method can be used in either cased or uncased boreholes. For best results, the uncased borehole must be between 10 and 20 cm in diameter, or 4 to 8 inches. A cased borehole may be as small as 3 inches, if properly grouted (see below) and the grout annulus does not exceed 1 inch.

Uncased boreholes are preferred because the effects of the casing and grouting are removed. It is recommended that the borehole be drilled using the rotary mud method. This method does little damage to the borehole wall, and the drilling fluid coats and seals the borehole wall reducing fluid loss and wall collapse. The borehole fluid is required for the logging, and must be well circulated prior to logging.

If the borehole must be cased, the casing must be PVC and properly installed and grouted. Any voids in the grout will cause problems with the data. Likewise, large grout bulbs used to fill cavities will also cause problems. The grout must be set before testing. This means the grouting must take place at least 48 hours before testing.

For borehole casing, applicable preparation procedures are presented in ASTM Standard D4428/D4428M-91 Section 4.1 (see ASTM website for copy).

**Calibration**

Calibration of the digital recorder is required. Calibration is limited to the timing accuracy of the recorder. GEOVision's Seismograph Calibration Procedure or equivalent should be used. Calibration must be performed on an annual basis.

**Measurement Procedure**

The entire probe is lowered into the borehole to a specific measurement depth by the winch. A measurement sequence is then initiated by the operator from the instrumentation package control panel. No further operator intervention is then needed to complete the measurement sequence described below.

The system electronics activates the SH-wave source in one direction and records the output of the two horizontally oriented geophone axes which are situated parallel to the axis of motion of the source. The source is then activated in the opposite direction, and the horizontal output signals are again recorded, producing a SH-wave record of polarity opposite to the previous record. The source is finally actuated in the first direction again, and the responses of the vertical geophone axes to the resultant P-wave are recorded during this sampling.

The data from each geophone during each source activation is recorded as a different channel on the recording system. The seismograph has at least six channels (two simultaneous recording channels), each with at least a 12 bit 1024 sample record. Newer seismographs may have longer record lengths. The recorded data is displayed on a CRT or LCD display and possibly on paper tape output as six channels with a common time scale. Data is stored on digital media for further processing. Up to 8 sampling sequences can be stacked (averaged) to improve the signal to noise ratio of the signals.

Review of the data on the display or paper tape allows the operator to set the gains, filters, delay time, pulse length (energy), sample rate, and stacking number in order to optimize the quality of the data before recording. In the case of the Model 170, printed data is verified by the operator prior to moving the probe. In the case of the Robertson Micrologger2, storage on the hard disk should be verified from time-to-time, certainly before exiting the borehole.

Typical depth spacing for measurements is 1.0 meters, or 3.3 feet. Alternative spacing is 0.5 meter, or 1.6 feet.

**Required Field Records**

1) Field log for each borehole showing

   a) Borehole identification

   b) Date of test

   c) Tester or data recorder

d) Description of measurement

e) Any deviations from test plan and action taken as a result

f) QA Review

2) Paper output records are no longer required, since the Micrologger2 cannot generate them. However, data must be stored in at least 2 places prior to leaving the site

3) List of record ID numbers (for data on digital media) and corresponding depth

4) Diskettes, CDRom, or USB flash drives with backup copies of data on hard disk, labeled with borehole designation, record ID numbers, date, and tester name.

An example Field Log is attached to this procedure.

**Analysis**

Following completion of field work, the recorded digital records are processed by computer using the OYO Corporation software program PSLOG and interactively analyzed by an experienced geophysicist to produce plots and tables of P and $S_H$ wave velocity versus depth.

The digital time series records from each depth are transferred to a personal computer for analysis. Figure 2 shows a sample of the data from a single depth. These digital records are analyzed to locate the first minima on the vertical axis records, indicating the arrival of P-wave energy. The difference in travel time between these arrivals is used to calculate the P-wave velocity for that 1-meter interval. When observable, P-wave arrivals on the horizontal axis records are used to verify the velocities determined from the vertical axis data. In addition, the soil velocity calculated from the travel time from source to first receiver is compared to the velocity derived from the travel time between receivers.

The digital records are studied to establish the presence of clear SH-wave pulses, as indicated by the presence of opposite polarity pulses on each pair of horizontal records. Ideally, the SH-wave signals from the ‘normal’ and ‘reverse’ source pulses are very nearly inverted images of each other. Digital FFT – IFFT lowpass filtering are used to remove the higher frequency P-wave signal from the SH-wave signal.

The first maxima are picked for the ‘normal’ signals and the first minima are picked for the 'reverse' signals. The absolute arrival time of the ‘normal’ and ‘reverse’ signals may vary by +/- 0.2 milliseconds, due to differences in actuation time of the solenoid source caused by constant mechanical bias in the source or by borehole inclination. This variation does not affect the velocity determinations, as the differential time is measured between arrivals of waves created by the same source actuation. The final velocity

value is the average of the values obtained from the 'normal' and 'reverse' source actuations.

In Figure 2, the time difference over the 1-meter interval of 1.70 millisecond is equivalent to a SH-wave velocity of 588 m/sec. Whenever possible, time differences are determined from several phase points on the $S_H$ -wave pulse trains to verify the data obtained from the first arrival of the $S_H$ -wave pulse. In addition, the soil velocity calculated from the travel time from source to first receiver is compared to the velocity derived from the travel time between receivers.

Figure 3 is a sample composite plot of the far normal horizontal geophone records for a range of depths. This plot shows the waveforms at each depth, clearly showing the S-wave arrivals. This display format is used during analysis to observe trends in velocity with changing depth.

Once the proper picks are entered in PSLOG, the picks are transferred to an Excel spreadsheet where Vs and Vp are calculated. The spreadsheet allows output for presentation in charts and tables.

Standard analysis is performed on receiver 1 to receiver 2 data, with separate analysis performed on source to receiver data as a quality assurance procedure.

Registered Geophysicist Antony Martin Date 9/11/06

QA Review 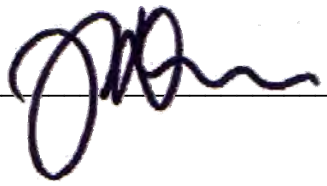 Date 9/11/06

References:


1. "In Situ P and S Wave Velocity Measurement", Ohya, S. 1986. Proceedings of In-Situ '86, *Use of In-Situ Tests In Geotechnical Engineering*, an ASCE Specialty Conference sponsored by the Geotechnical Engineering Division of ASCE and co-sponsored by the Civil Engineering Dept of Virginia Tech.

2. Guidelines for Determining Design Basis Ground Motions, Report TR-102293, Electric Power Research Institute, Palo Alto, California, November 1993, Sections 7 and 8.

3. "Standard test Methods for Crosshole Seismic Testing", ASTM Standard D4428/D4428M-91, July 1991, Philadelphia, PA

# OYO SUSPENSION P-S VELOCITY LOGGING SETUP

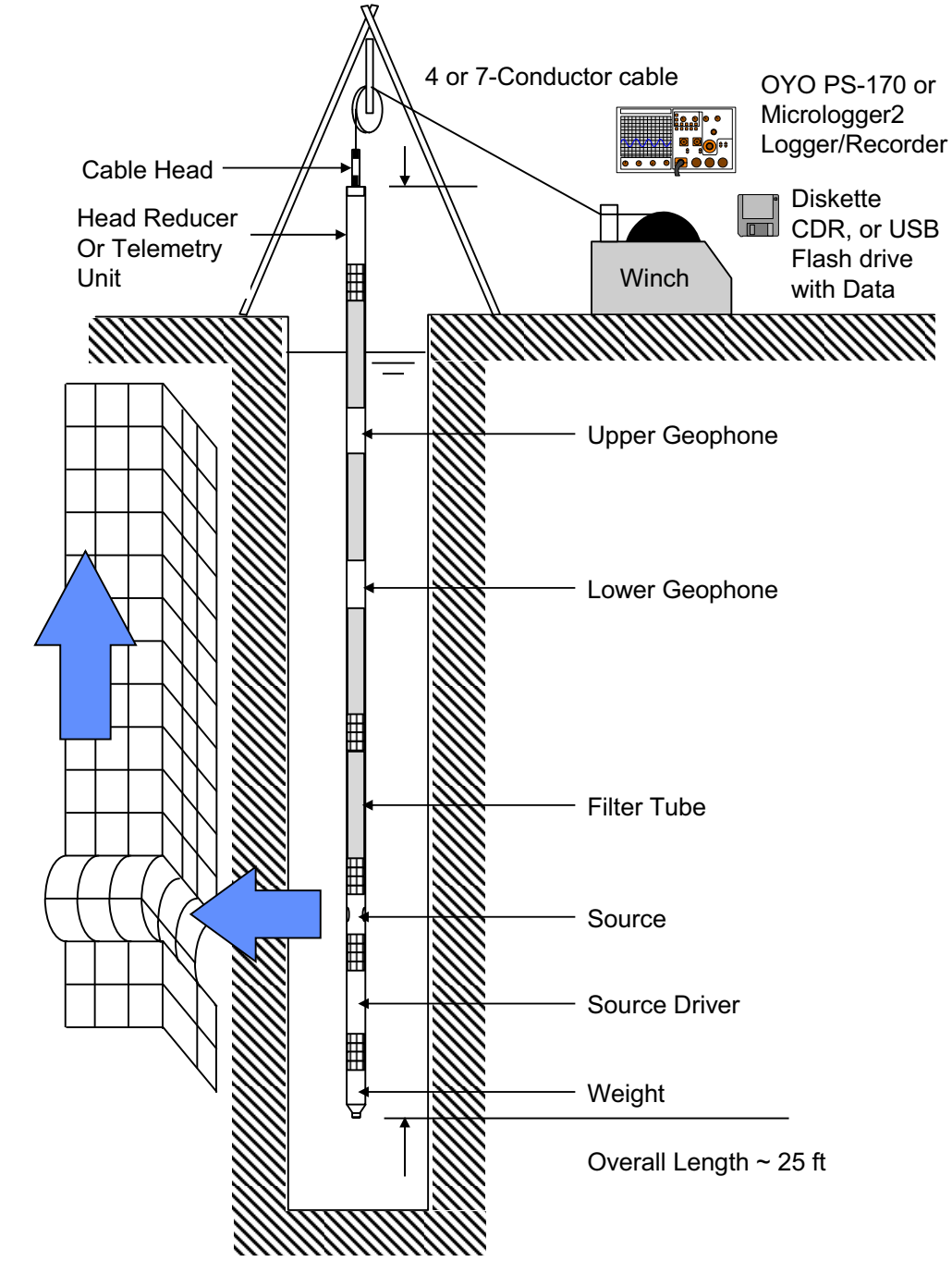


Figure 1. Suspension PS logging method setup

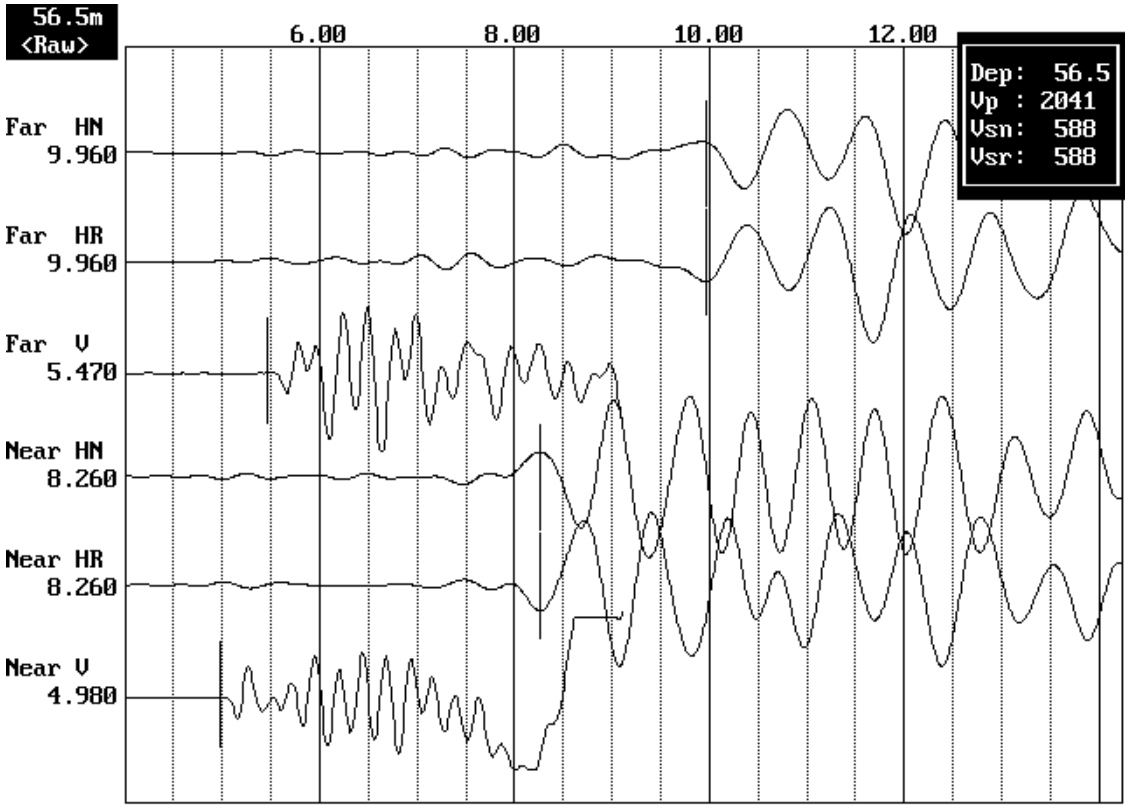


Figure 2. Sample suspension method waveform data showing horizontal normal and reversed (HR and HN), and vertical (V) waveforms received at the near (bottom 3 channels) and far (top 3 channels) geophones. The arrivals in milliseconds for each pick are shown on the left. The box in the upper right corner shows the depth in the borehole and the velocities calculated based on the picks.

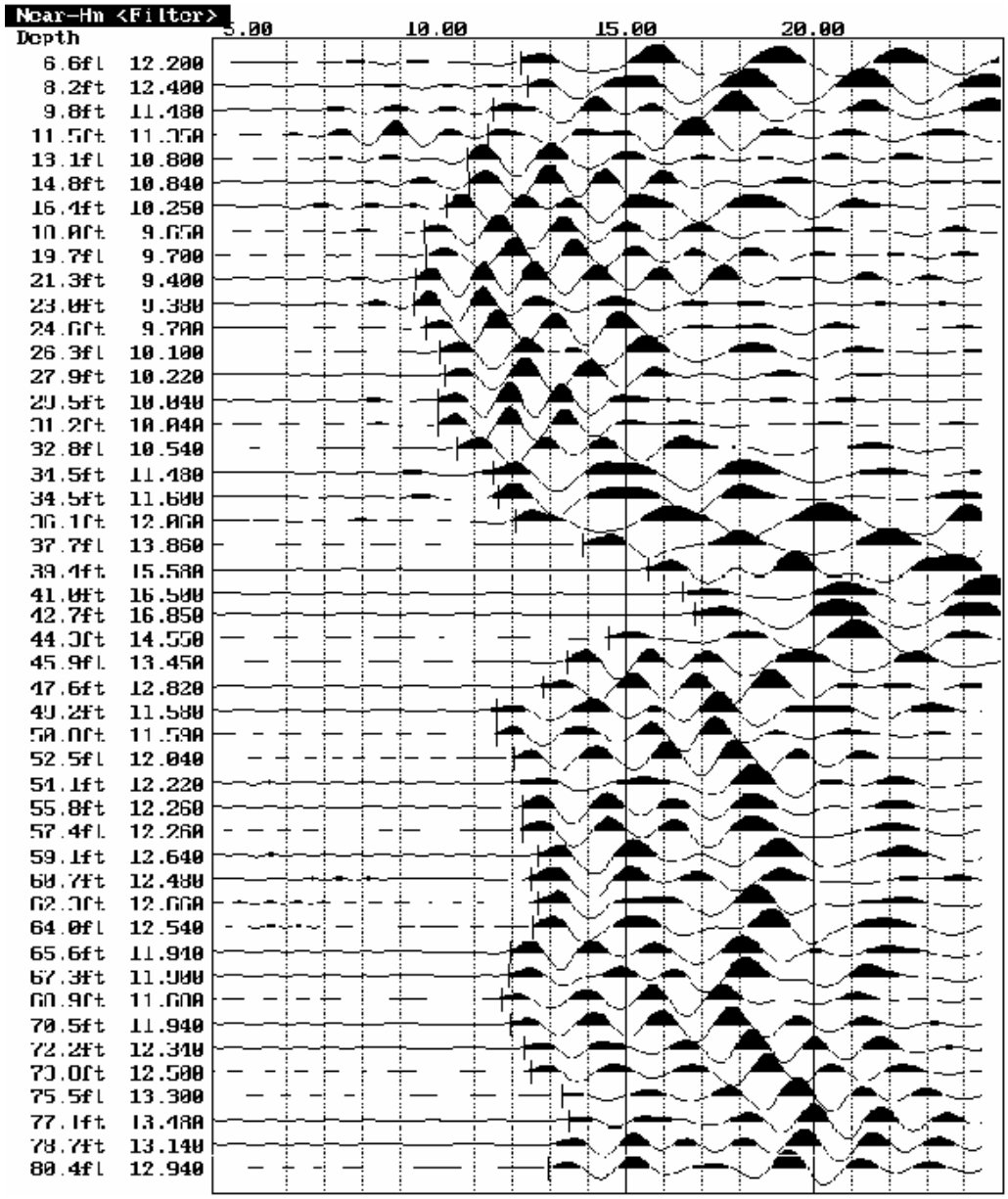


Figure 3. Sample composite waveform plot for normal shear waves received at the near geophone in a single borehole

GEOVision
geophysical services

# P-S SUSPENSION VELOCITY FIELD LOG

SITE:_____ DATE:_____
CLIENT:_____ JOB:_____
AUTHOR:_____ PAGE 1 OF _____

CONTACT:_____ _OFFICE__ PHONE:_____
_____ PHONE:_____
CONTACT:_____ _OFFICE__ PHONE:_____
_____ PHONE:_____
CONTACT:_____ _____ PHONE:_____
_____ PHONE:_____
CONTACT:_____ _____ PHONE:_____
_____ PHONE:_____
DRILLER:_____ _____ PHONE:_____
COMPANY:_____ _____ PHONE:_____

DIRECTIONS TO SITE:_____
_____
_____
_____
_____

GENERAL SITE CONDITIONS/LOCATION:_____
_____

EA#:_____
BOREHOLE DESIGNATION:_____LOCATION:_____
_____
COUNTY:_____RANGE:_____TOWNSHIP:_____SECTION:_____
BOREHOLE CONSTRUCTION: CASED_____ UNCASED_____
DIAMETERS AND DEPTH RANGES: _____ 0 TO _____ ; _____, _____ TO _____
BOREHOLE TOTAL DEPTH AS DRILLED:_____
CONDUCTOR CASING?: YES____ DEPTH TO BOTTOM OF CASING_____; NO____
DEPTH TO BEDROCK:_____ DEPTH TO WATER TABLE:_____
BOREHOLE FLUID: WATER_____; FRESH WATER MUD_____; SALT WATER MUD _____;
OTHER:_____
DEPTH TO BOREHOLE FLUID:_____ TIME SINCE LAST CIRCULATION:_____

GEOVision
geophysical services

SITE:_____ DATE:_____
CLIENT:_____ JOB:_____
AUTHOR:_____ PAGE 2 OF _____

LOGGING CREW:_____
VEHICLE(S) USED AND MILEAGE: _____
MOBILIZED FROM:_____ DEPARTURE TIME:_____
ARRIVED ON SITE:_____
STANDBY TIME:_____ CAUSE:_____
LOGGING STARTED:_____ LOGGING COMPLETED:_____
STANDBY TIME:_____ CAUSE:_____
LOGGING STARTED:_____ LOGGING COMPLETED:_____
DEMOBILIZED TO:_____ ARRIVAL TIME:_____
ADDITIONAL DEMOB TIME:_____ REASON:_____

BATTERIES CHANGED BEFORE LOGGING: YES_____; NO_____; STORED WITH NEW_____

| | | | | | | | | | |
|---|---|---|---|---|---|---|---|---|---|
| WINCH | COMPROBE ☐ | | GREY ☐ | OYO ☐ | RG ☐ | OTH ☐ | | | |
| INSTRUMENT | OYO | 12004 ☐ | 15014 ☐ | 19029 ☐ | | RG | 160023 ☐ | 160024 ☐ | |
| RECEIVER S/N | | 12008 ☐ | 20042 ☐ | 26066 ☐ | 11001 ☐ | | 23053 ☐ | | |

MAINTENANCE PERFORMED ON SITE:_____
_____
_____
_____
EQUIPMENT PROBLEMS OR FAILURES:_____
_____
_____

SUGGESTIONS, ADDITIONS, CHANGES:_____
_____
_____

COMMENTS:_____
_____
_____
_____
_____
_____

GEOVision Geophysical Services 1151 Pomona Road, Suite P, Corona, CA 92882 Ph (951) 549-1234 Fx (951) 549-1236

# GEOVISION SUSPENSION LOGGING FIELD NOTES

SITE: _____ DATE: _____

CLIENT: _____ JOB: _____

AUTHOR: _____ PAGE _____ OF _____

| DEPTH METERS | DEPTH FEET | UNFILTERED FILE NO. | FILTERED FILE NO. | COMMENTS CASING, WATER, ROCK, ETC |
|---|---|---|---|---|
| 0.5 | 1.64 | | | |
| 1.0 | 3.28 | | | |
| 1.5 | 4.92 | | | |
| 2.0 | 6.56 | | | |
| 2.5 | 8.20 | | | |
| 3.0 | 9.84 | | | |
| 3.5 | 11.48 | | | |
| 4.0 | 13.12 | | | |
| 4.5 | 14.76 | | | |
| 5.0 | 16.40 | | | |
| 5.5 | 18.04 | | | |
| 6.0 | 19.69 | | | |
| 6.5 | 21.33 | | | |
| 7.0 | 22.97 | | | |
| 7.5 | 24.61 | | | |
| 8.0 | 26.25 | | | |
| 8.5 | 27.89 | | | |
| 9.0 | 29.53 | | | |
| 9.5 | 31.17 | | | |
| 10.0 | 32.81 | | | |
| 10.5 | 34.45 | | | |
| 11.0 | 36.09 | | | |
| 11.5 | 37.73 | | | |
| 12.0 | 39.37 | | | |
| 12.5 | 41.01 | | | |
| 13.0 | 42.65 | | | |
| 13.5 | 44.29 | | | |
| 14.0 | 45.93 | | | |
| 14.5 | 47.57 | | | |
| 15.0 | 49.21 | | | |
| 15.5 | 50.85 | | | |
| 16.0 | 52.49 | | | |
| 16.5 | 54.13 | | | |
| 17.0 | 55.77 | | | |
| 17.5 | 57.41 | | | |
| 18.0 | 59.06 | | | |

# GEOVISION SUSPENSION LOGGING FIELD NOTES

SITE: _____ DATE: _____

CLIENT: _____ JOB: _____

AUTHOR: _____ PAGE _____ OF

| DEPTH METERS | DEPTH FEET | UNFILTERED FILE NO. | FILTERED FILE NO. | COMMENTS CASING, WATER, ROCK, ETC |
|---|---|---|---|---|
| 18.5 | 60.70 | | | |
| 19.0 | 62.34 | | | |
| 19.5 | 63.98 | | | |
| 20.0 | 65.62 | | | |
| 20.5 | 67.26 | | | |
| 21.0 | 68.90 | | | |
| 21.5 | 70.54 | | | |
| 22.0 | 72.18 | | | |
| 22.5 | 73.82 | | | |
| 23.0 | 75.46 | | | |
| 23.5 | 77.10 | | | |
| 24.0 | 78.74 | | | |
| 24.5 | 80.38 | | | |
| 25.0 | 82.02 | | | |
| 25.5 | 83.66 | | | |
| 26.0 | 85.30 | | | |
| 26.5 | 86.94 | | | |
| 27.0 | 88.58 | | | |
| 27.5 | 90.22 | | | |
| 28.0 | 91.86 | | | |
| 28.5 | 93.50 | | | |
| 29.0 | 95.14 | | | |
| 29.5 | 96.78 | | | |
| 30.0 | 98.43 | | | |
| 30.5 | 100.07 | | | |
| 31.0 | 101.71 | | | |
| 31.5 | 103.35 | | | |
| 32.0 | 104.99 | | | |
| 32.5 | 106.63 | | | |
| 33.0 | 108.27 | | | |
| 33.5 | 109.91 | | | |
| 34.0 | 111.55 | | | |
| 34.5 | 113.19 | | | |
| 35.0 | 114.83 | | | |
| 35.5 | 116.47 | | | |
| 36.0 | 118.11 | | | |

## PROCEDURE FOR USING THE ROBERTSON GEOLOGGING HI-RESOLUTION ACOUSTIC TELEVIEWER (HiRAT)

### Reviewed 2/13/06

### Background

The acoustic televiewer is a device for producing a qualitative image of the wall of a borehole. Because it uses ultrasound rather than visible light it is able to work in dirty or opaque borehole fluids, although heavy drilling mud will cause excessive dispersion of the acoustic beam. The picture below shows the sonde's lower nylon section, and one of the bowspring attachments which are used to centralize the sonde in the borehole.

Pulses of ultrasound (0.5 - 1.5MHz) are generated by a piezo-electric resonator. The pulses are transmitted through the oil in which the resonator is immersed, through the wall of the acoustic housing, then propagate through the borehole fluid and are reflected from the wall of the borehole. The reflected energy is picked up by the same transducer, from which is recorded both the ***amplitude*** of the returned pulse and the ***travel-time*** which have elapsed. Blanking must be applied to prevent the transducer from registering reflections from the inside surface of the acoustic housing. The material of the housing is chosen so that its acoustic properties are similar to the oil which fills it. The housing is not designed to withstand borehole fluid pressures, but has a piston device to allow equalization between inside and outside pressure.

The ***amplitude*** of the returned pulse is a function of the acoustic reflectivity of the borehole wall. If the beam strikes a hard borehole wall normally to the surface the energy will be returned to the transducer and a strong return will be recorded. If the formation is softer, then less energy will be reflected. Also, if the surface of the borehole is rough, or effectively missing because of the presence of a fracture or other structure, then energy will be dispersed and a poor return will be recorded.

The ***travel-time*** is a simple function of the diameter of the borehole and the velocity of sound in the borehole fluid (typically 1.5Km/sec). An A/D converter monitors the output from the transducer once the blanking period has expired and a comparator is used to detect the peak amplitude during the sampling window.

The coaxially-mounted transducer has a planar radiating surface, but the vibration characteristics are such that the acoustic pulse is emitted as a 'pencil' beam. The emitted beam is deflected by a planar mirror so that it leaves the acoustic housing at right angles to the sonde axis. The mirror is rotated to scan the borehole wall. The ultrasound pulses are synchronized with rotation of the mirror so that up to 360 pulses are emitted in every revolution. Because of the time which must elapse for the two-way transit of the borehole fluid, there is an upper limit upon the number of radial samples that may be acquired from a borehole of a particular radius. In larger boreholes, therefore, it may be necessary to reduce the number of radial samples. The sonde is able to operate at 90, 180 or 360 samples per revolution.

An image of the borehole wall is produced by moving the sonde along the borehole axis while it is scanning radially. By the same logic as shown above, it can be seen that any horizontal point will be imaged by more than one sweep of the acoustic beam so long as the axial movement of the sonde during one complete sweep is no greater than the beam diameter. An upper limit is therefore imposed upon the logging speed which will be a function of the rotational speed of the transducer, the radial sampling interval and borehole diameter.

## Objective

The objective of this procedure is to provide a pseudo “core” of the borehole, and map the orientation and angles of cracks and voids in rock boreholes.

## Instrumentation

This procedure is written specifically for the Robertson Geologging High-Resolution Acoustic Televiewer (HiRAT). The required equipment includes:

1. The Robertson High-Resolution Acoustic Televiewer (HiRAT) sonde with centralizers
2. A 4-conductor wire-line winch with cable at least 30m (100ft) longer than the depth of the borehole (RG Smart Winch or equivalent. GEOVision has adapted all our 4-conductor winches)
3. A sheave with depth encoder with minimum 500 pulse/revolution
4. A Robertson Geologging Micrologger II
5. A laptop with Winlogger installed and the following minimum system requirements:
    - Windows 98SE or above
    - 64M System memory
    - 800x600x24 SVGA Display with DirectX 8.0
    - 500Mhz CPU
    - USB 2.0 connection
6. Battery power supply with cables

## Environmental Conditions

This tool is designed for fluid-filled boreholes between 67 and 150mm (3-6in) in rock. Since fine cracks are usually not visible in the walls of soil borings, the televiewers add very little information from a soil boring than a simple video. Now if the boring has soil AND rock, televiewer visuals in the soil may still be useful.

## Calibration

The acoustic televiewer uses the variability in reflectance and the travel time to make an image of the borehole wall, mostly resulting from relative differences of materials and the physical characteristics of the wall. Since these are relative measurements, no field calibration of the sonde is required. However, it is important that the same location in the borehole be checked at the start and finish of the logging to make sure that the response or functionality haven't changed during the measurement.

A test fixture may be used to check function of the acoustic televiewer prior to use. This test fixture should comprise a plastic pipe, with a known internal diameter between 3 and 6 inches. This should be filled with water and the sonde stood upright in the fixture. A target made of metal or metal foil is glued on the inside of the container, or optionally on a seal and shaft so that it can be moved in and out on a line radial to the center-line of the pipe. A representation of this is shown in the figure below.

The purpose of this test fixture is to check the ability of the sonde to differentiate between materials of different acoustic reflectances, and different travel times, and to check the calibration of the caliper function of the sensor using the measured diameter of the pipe. However, if calibrated caliper measurements are required, it is recommended that a mechanical 3-arm caliper tool be used for this purpose because it can be calibrated in the field prior to use. The HiRAT will give very accurate results but this procedure does not cover calibration.

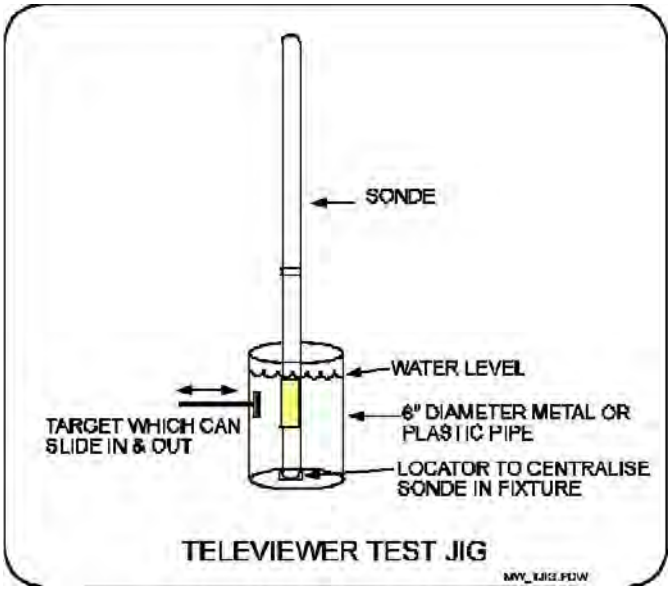

## Hi-RAT Field Procedure

Because the logging software is a standalone module, there are a number of settings which must be initialized independently of the WinLogger software. These include the depth measurement subsystem and sonde operating modes. Click on 'System' on the menu bar to show the following dialog boxes:

### 1.0 Log Mode

The sonde can operate in three distinct modes:

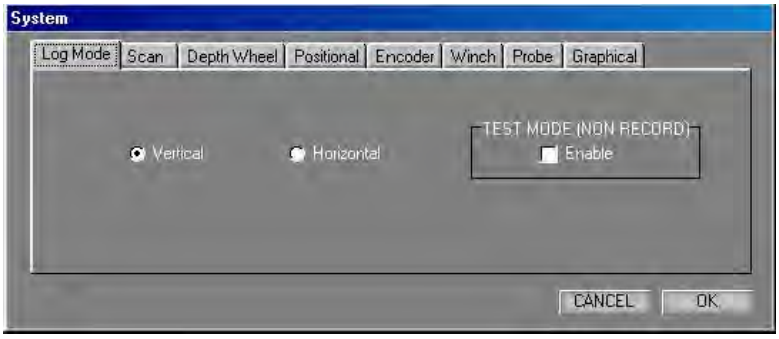


- Vertical mode is used for boreholes which are drilled from the surface and are deviated at less than 70 degrees from the vertical. Most exploration boreholes will fall into this class. In this mode the image is orientated according to compass directions (magnetic co-ordinates).

- Horizontal mode is used for boreholes which are sub-horizontal so their inclination will probably exceed 70 degrees from the vertical. Boreholes in this class would normally be drilled as part of ground investigations for tunneling and mining, drilling ahead of a drive to determine the nature and extent of fracturing. In this mode the image is orientated according to gravitational coordinates (up/down) since there is no unique point of the image circle which can be orientated to North with any precision.

- Test mode is used to exercise all sonde functions without creating a log. The image will scroll on the screen in the normal fashion, and orientation readouts will be refreshed continuously.

### 2.0 Scan Parameters

The scan parameters control the radial sampling of the borehole. The values will be retained between logging sessions, so the sonde will be initialized correctly at power-on. There are three parameters in the dialog:

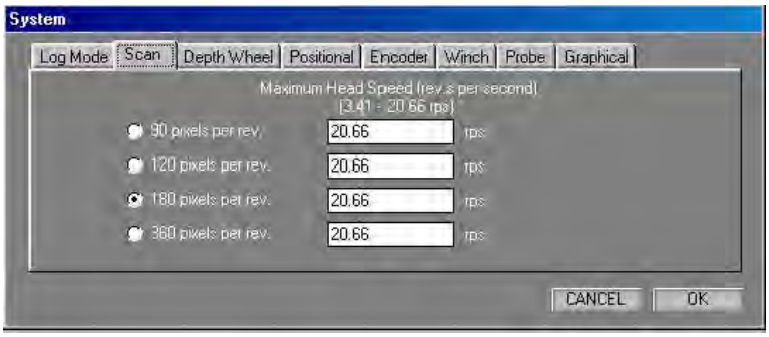


- The radial sampling rate can be set to one of 90, 120, 180, 360 samples per revolution. There is a relationship between the logging speed and the radial sampling rate, since the time taken to send the dataset to the surface depends upon its length. The size of the log file is also determined by the radial sampling rate. The probe will always try to use the maximum head speed entered. If limited by a low Baud rate or a large 'window' setting then the probe will reduce its head speed automatically to compensate - see sonde operation section.

### 3.0 Depth Wheel Configuration

The depth measurement system is dependent upon the combination of depth measurement wheel with its calibrated groove, and the shaft encoder which translates rotation into pulses which are counted by the logging system controller. Two parameters are therefore required: depth wheel circumference and encoder pulse rate. The encoder parameters are covered in a subsequent topic.

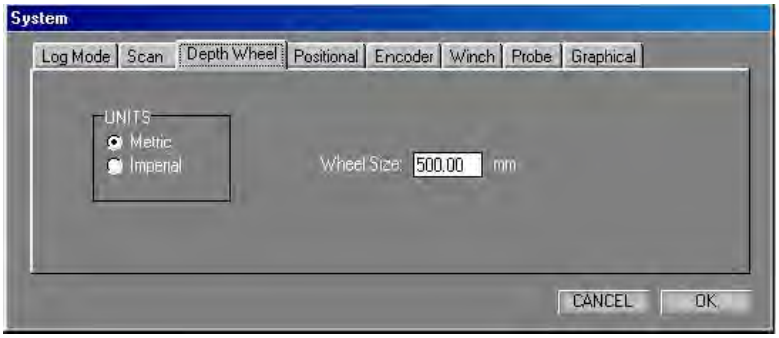


- Select Metric or Imperial depth measurement units from the left-hand pane.

- Type the circumference of the depth measurement wheel into the 'wheel size' box. The standard sizes of GEOVision wheels are 1000mm. If you are measuring in Imperial units (or changing back to metric units), the standard wheel size can be converted automatically by clicking the left mouse button and choosing the appropriate conversion. The size is always specified in units of 1/1000 of the depth unit i.e. millimetres (mm) or millifeet (mft).

## 4.0 Encoder Configuration

The depth measurement system is dependent upon the combination of depth measurement wheel with its calibrated groove, and the shaft encoder which translates rotation into pulses which are counted by the logging system controller. The depth wheel circumference is covered in a previous topic. In order to accommodate a variety of encoders, their operational characteristics can be configured in the software.


- Select supply voltage from the radio buttons in the left-hand pane. The options are 5 Volt and 12 Volt. GEOVision encoders are always specified for 5 Volt operation.

- Type the number of pulses emitted per revolution into the central box. The standard values for all GEOVision winches are 500 pulses/rev.

- The logical direction of movement can be reversed if required to accommodate the directional characteristics (phase lead or lag) of the different encoder types.

## 5.0 Winch and Cable Configuration

Support for remote control of the RG Smart Winch is provided, and can be enabled by checking the ***Enable*** control in the left-hand Smart Winch pane. If the Smart Winch control is enabled, it is also necessary to select the measure units in force - select ***Metric*** or ***Imperial*** from the radio buttons on offer.

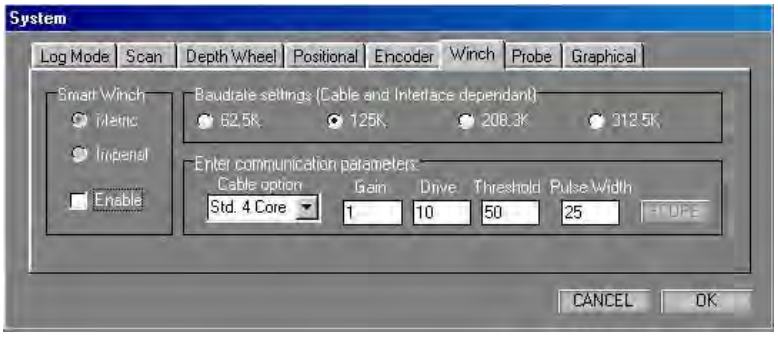

The Baud settings can be chosen to match the *quality* of the communication channel. The channel will be effected by cable type and length. Typically a Baudrate of 312.5K is used. The remaining controls in the dialog relate to the communications parameters. The operation is entirely compatible with the WinLogger software operation and the values would be expected to be the same as those in force for logging six-channel type sondes with that software. (Certain probe types may be fitted with a digital interface that does not require set-up and in this case the parameter edit boxes will not appear.)

- ***Cable Option*** is used to select the logging cable type which is available on the winch. The options are *Not Connected*, *Std. 4 Core*, *Differential* and *Monocable*. The only cable types used in GEOVision systems is Std. 4 Core. Select the appropriate type from the drop-down menu box. Note this value can only be changed when the probe power is turned off.

- ***Gain*** is related to cable length and uphole signal attenuation. Gain values range from 0-3 and control the amplification applied to the incoming signal. Use the *Scope* dialog to visualize the incoming signals. Gain should be set so that the signal reaches between 70% and 100% of the height of the display, generally obtained with a setting of 0 for GEOVision winches. If the peak height exceeds this level, clipping will result in artifacts which will be detected erroneously. Click *Apply* to set the parameters before proceeding to the *Scope* dialog.

- ***Threshold*** is the level at which the incoming signals are detected. Gain and Threshold are related, and can be visualized using the *Scope* dialog. Set the gain so that the signal reaches between 70% and 100% of the height of the display. Then adjust the threshold so that it is between 50% and 70% of the height of the pulses displayed and clear of any region of 'overshoot' of the positive and negative pulses. This will ensure that peaks are detected and noise is ignored. Generally a setting of 25 is used for GEOVision winches. When the scope dialog is displayed, the position of the mouse is reported as a threshold value to make it simpler to infer the correct setting. The scope option is greyed out when the probe power is turned off.

- ***Drive*** sets the strength of the downhole signal. It is not possible to visualize the downhole signal, but the effect of insufficient drive is to disable downhole communication, which will result in the commands being ignored by the sonde. Values range from 0 -127, and for GEOVision winches will be around 10. Increase the drive for longer cables.

- ***Pulse Width*** This is the width of the transmitted communication pulses in 100nS steps. The default is 25 equivalent to 2.5uS. The range is from 8 to 64. The pulse width can be reduced to prevent signal overshoot on short cables. The default value is used in most cases. Note any changes only come into effect during a log. (Note setting too large a pulse width when using the highest Baud rates will automatically be prevented within the probe and the pulse width reduced.)

**IMPORTANT** Please note the effects of changing 'Baud' will not appear until the first new log is made. The setting for 'threshold' may be effected by an increase in the 'Baud' rate please recheck 'threshold' if 'Baud' is altered using the 'Scope' function after making a short test log.

The parameters which are entered will be applied automatically if you close the dialog with ***OK***. The above parameters once set correctly will be remembered by the system and should never need to be altered.

### 6.0 Probe Configuration

The probe is normally energized at 90 Volts from the surface. However, it may be necessary to compensate for voltage drop on longer cables due to the higher power draw of this sonde. The voltage at

the surface may be increased in order to deliver 90 Volts at the sonde. Simply type the value into the text box provided. The voltage should be set at 90V for all GEOVision winches. Values outside the indicated range will be rejected.

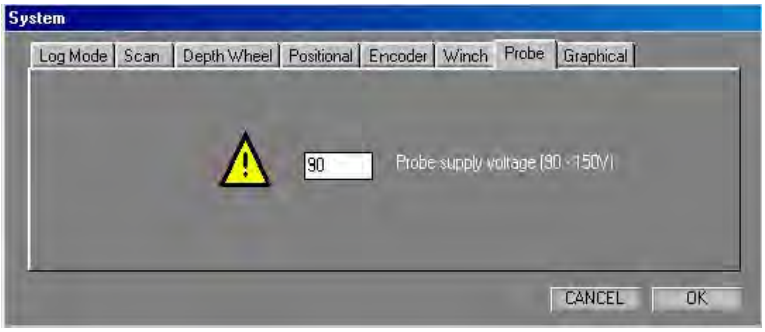


## 7.0 Positional Configuration

The probe includes a 3-axis orientation package, and is capable of producing a borehole image aligned to geographic North. This is achieved by determining and applying two image rotation parameters:

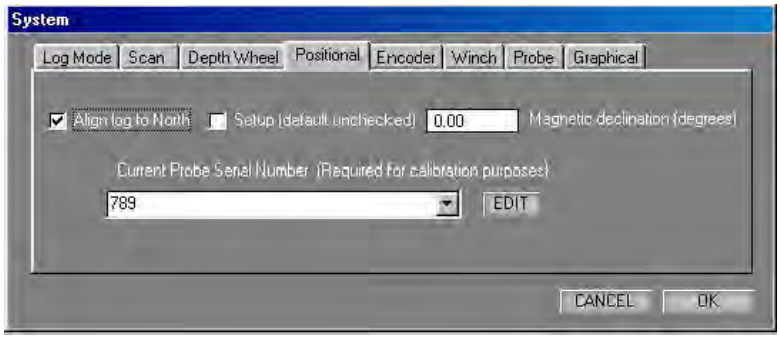


- ***Magnetic Declination*** is used to correct for the difference between Magnetic North and True North. The value varies from place to place, so the local value must be inserted here if you wish to perform this correction during data collection. This correction may also be made during processing. If the value is zero, the log will be referred to Magnetic North.
- ***Align to North*** is a check-box used to select image rotation to start at Magnetic North. If in addition a value is set for Magnetic Declination (see above) the image will be rotated to start at True North. If the box is not checked, the image will not be oriented to geographic co-ordinates, but will use the local co-ordinate frame of the sonde (X, Y, Z axis of the orientation module). This mode may be used to inspect the inside of magnetic casing, where an orientated image would be subjected to random effects caused by the metalwork.
- Set-up mode is selected by checking the ***Setup*** box, and is used to determine the required image rotation offset to correct for the angle between the axis of the orientation package and the index mark of the rotating transducer section. In set-up mode the normal sonde azimuth display is modified, and will instead show the 'relative bearing' which is measured between the high side of the borehole and the orientation sensor index. Check ***Setup***, then OK to close the dialog. The icon adjacent to the sonde azimuth readout at the top of the screen is modified with the legend CAL when the system is in set-up mode. The sonde must now be placed in a stand or jig so that it

is inclined at about 20 degrees to the vertical, and adjacent to a target fixed to the jig so that it is directly above the transducer in the vertical plane. Lower the sonde with its attachment into a large bucket of water so that the transducer and target are fully immersed. Start the radial amplitude display, when it will be possible to see the strong signal returning from the target. Rotate the sonde so that the image of the target moves to the top of the display. When the two are coincident, the 'relative bearing' reads out the image rotation offset. This value is fixed for the sonde unless it is disassembled and rebuilt, at which point the procedure MUST be repeated. Please see the additional topic on the Radial Amplitude Display for further details.

- The ***Serial Number*** list box is used to select the sonde which is in use. When the appropriate sonde is selected, the image rotation offset determined by the above procedure is selected. To edit the image offset click the '***Edit***' and enter the new offset. Several serial numbers and associated offsets can be stored and selected as required.

## 8.0 Graphical

The palette can be changed between a colored and grey scale setting. The changes affect the log screen palette display and are also applied when replaying a log. Selecting Full range in the 'AGC Palette' will cause the software to spread the palette over the full 16bit signal. 'Mid range' will spread the palette over the first quarter of the 16bit range and 'Low range' will spread the palette over the first eighth of the 16 bit range. In most cases the 'Low range' selection is used. Note these settings do not affect the stored log data in any way. The 'Filter Width' is applied to the Natural Gamma trace data and is a simply running average filter. The range of the filter width is from 1 to 50 ( x 10 millidepth units ie. mm or mft).

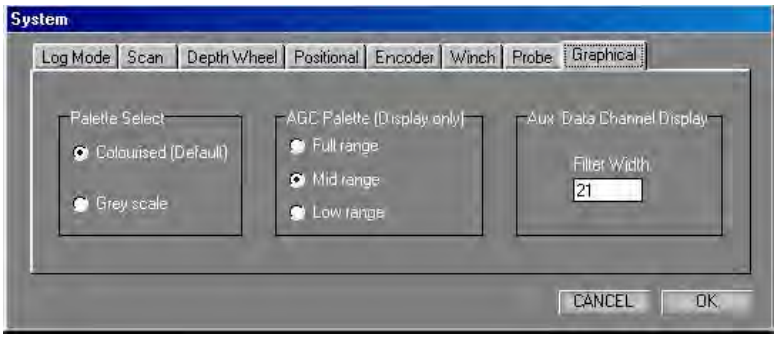


## 9.0 Sonde Operation

When the operations specified above have been reviewed and the correct settings have been selected, the system is ready for use. The main screen area is divided into 3 horizontal elements. At the top is the depth and orientation readout, together with the scale headings for the scrolling display of unwrapped borehole image.

On the left side of the depth track is the travel time display, with text boxes for sonde inclination, azimuth and head temperature.

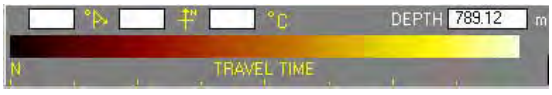

On the right side is the display of amplitude and indication of current operating mode. Located in the center above the depth track are the text boxes for depth and cable speed (computed at the surface). The ranges for the 'Natural Gamma' channel overlay (optional) are shown above the Amplitude.


The central area is utilized for the scrolling display of unwrapped borehole data. The display is orientated with the left edge corresponding to North point of the aligned image data (if orientation is selected) according to the outputs of the sonde's orientation package.

The lower area has controls for the winch (applicable to RG Smart Winch only), depth initialization and sonde control.


The winch control area is only displayed when RG SmartWinch operation is enabled - see section 5 - and has four controls. Set Target Speed by typing the required speed into the window and pressing Enter.

Cable movement is initiated by clicking on either the UP or DOWN arrow control.

Cable movement is halted by clicking on the square STOP control.


Depth is initialized by typing the required value into the entry box and pressing Enter. The entry box is not available at times when the system is in logging mode and the depth should not be changed by user entry.

Sonde power is applied by clicking on the green-colored 1 button. Power is turned off by clicking on the red-colored 0 button. There is no indicator for the state of the power supply on the desktop, so the external indicators should be observed for this purpose.

To make a log ensure that the Test Mode is disabled - see section 1, Log Mode setting. Click File|New Log and select a filename. Old logs may be overwritten if necessary -TAKE CARE. The header editor will be started automatically. A previous set of header data may be loaded by clicking LOAD and choosing a template.

To start logging, click on the red Record (circle) control. The log data will start to scroll down the screen after a brief pause for synchronization. The messages "DSP2: Detecting data stream" and "Updating probe settings" will be observed at the bottom of the screen during this process. Note that the screen scrolling direction is not affected by the actual direction of movement of the sonde. To cease logging, click on the black STOP control (square). The data should be immediately backed up to a USB drive, CD, or other data storage prior to beginning another log.

If the data display from a probe which is properly connected appears to occupy only half of the track area,

with the remainder filled with random colors such as green which are not part of the regular palette, then it is most likely that the downhole data communication is not functioning properly. This symptom is due to the fact that the probe settings cannot be communicated properly, and it is operating in its default power-up mode. If this is the case, the Drive setting of the System|Winch dialog should be increased or decreased accordingly. See section 5 for full details.

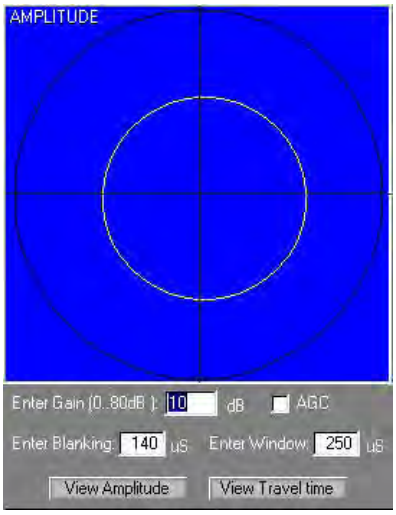



To adjust the sonde gain it is necessary to use the Radial Amplitude plot, which is enabled by clicking on the circle with cross-hairs symbol. When the dialog is active a new window will open on top of the unwrapped data display. In this display, the data is presented as a 'polar' plot. Press the 'View Amplitude' button to display the amplitude plot. This plot shows amplitude increasing towards the outside of the circle and the compass direction following the sweep of the transducer. The line indicating the data is drawn in the regular palette, so that high amplitudes are drawn in white and low amplitudes in black/brown. The picture here shows the image of the inside of a cylinder.

If the data is concentrated in a small circle at the center, the gain is too low and should be increased. If the data is obviously clipped at the outside of the circle, then the gain should be reduced. Type the new gain value into the entry box and press Enter. The ideal would be to set a gain value which allows the peak values to be displayed without clipping, with the majority of the data around the half-way level. It may also be necessary to adjust the blanking to ensure that internal reflections from the acoustic housing are not detected at the new gain value. This will be apparent in the unwrapped data display as pronounced patterning unrelated to the true target. The AGC option causes the probe to set gain automatically thus preventing signal saturation in most cases. (The gain is varied in 6dB steps

Blanking Period and window length can be set independently. Blanking is set to avoid reflections from the housing of the acoustic transducer or random reflections from a rugose borehole, and window length is set to accommodate the range of borehole radius that might be expected. An error will be indicated if the sum of the blanking period and window length would be greater than 409 microseconds, which is the maximum range of the timer. The default value for the blanking period is 145 microseconds, which is the minimum required for the two-way transit from the transceiver to the outer surface of the acoustic housing. It is not advisable to reduce this value beyond the default setting, although it may be increased for larger boreholes at the rate of 1.5mm of one-way travel per microsecond.

Window Length (sample time) defines the period during which the arrival gate remains open to detect the returned acoustic pulse. The acoustic pulse will travel in water at a speed of approximately 1.5mm per microsecond. The default window length is 150 microseconds, which is equivalent to 225 mm of (two-way) travel in the borehole fluid, or approximately 110mm of borehole diameter. If this is added to the default blanking period, which is equivalent to the outside diameter of the acoustic housing, it can be seen that the default set-up will be correct for boreholes up to 150mm. An error will be indicated if the sum of the blanking period and window length would be greater than 409 microseconds, which is the maximum range of the timer. Choose your window setting to best match the borehole diameter.

Pressing the ‘View Travel time’ button changes the display to that shown below:

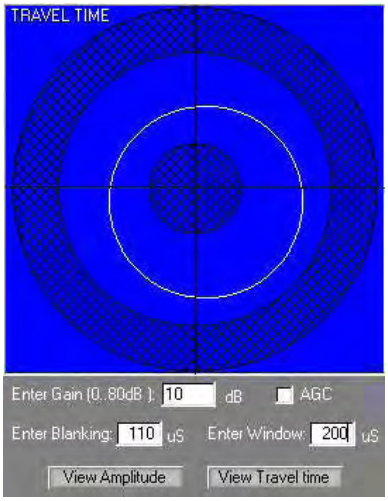


The unhatched ring between the two cross hatched zones represents the sample window. The width of this ring will vary with window length value. The profile of a cylinder is represented here appearing as a circle in the sample window.

Pressing this button displays the following dialog box:


This box allows you to enable the Natural Gamma option by checking the ‘Enable Overlay’ check box. The Overlay appears as a trace upon the Amplitude plot. The trace range and color can also be set by this dialog. The level of filtering can also be altered (see section 8) (note that any displayed trace data is automatically aligned with the acoustic scan data but only when logging up. The Natural Gamma sensor occupies a higher position in the probe so sufficient data has to be prebuffered so that the acoustic data can depth aligned with gamma. The prebuffering results in a delay at the start of a log before correct gamma data appears this is normal.)

## Data Analysis and Interpretation

RG-DIP, the manufacturer’s image interpretation package, offers manual and automatic feature recognition options. Feature orientations (dip/strike and azimuth) are automatically calculated. Display options include stereographic projections of zone axes, orientation frequency plots and 'synthetic cores' for comparison with real core data. The last option is invaluable for orientating core samples, particularly in the case of incomplete recovery.

## Reporting

The final report will include the objective and scope of the survey, location of the boreholes, discussion of instrumentation and procedures in the field and lab. For each borehole there will be a plot showing the dip/strike and azimuth of features. The next page shows an example.

Assumptions and limitations of the results will be discussed. Supporting references will be listed as necessary

## Required Field Records

Field log for each borehole showing

a) Location and description of the borehole

b) Date of test

c) Field personnel

d) Instrumentation

e) Any deviations from test plan and action taken as a result

This procedure has been reviewed and approved by the undersigned:

Professional Geophysicist Antony Marks Date Feb 13. 2006

QA Review 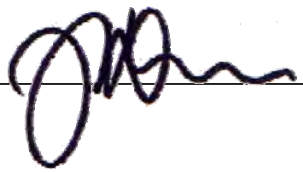 Date Feb 13. 2006

| B-XXX | Company | Geovision Geophysical Services |
|---|---|---|
| | Location | Somewhere Dam |

| | | | |
|---|---|---|---|
| BH | B-XXX Acoustic Televiewer | | |
| Date | 7/8/05 | BH Fluid | Air/Water |
| Casing | 4" Steel to 15 ft | | |
| File Name | BXXXdown1 | | |
| Depth Drilled | 300 feet | | |
| Depth Logged | 299.3 feet | | |
| Logged by | Rob Steller | | |
| Client | Best Customer Inc. | | |

Notes:

1) All orientations referenced to True North

2) Tadpole tails indicate dip direction with True North as up.

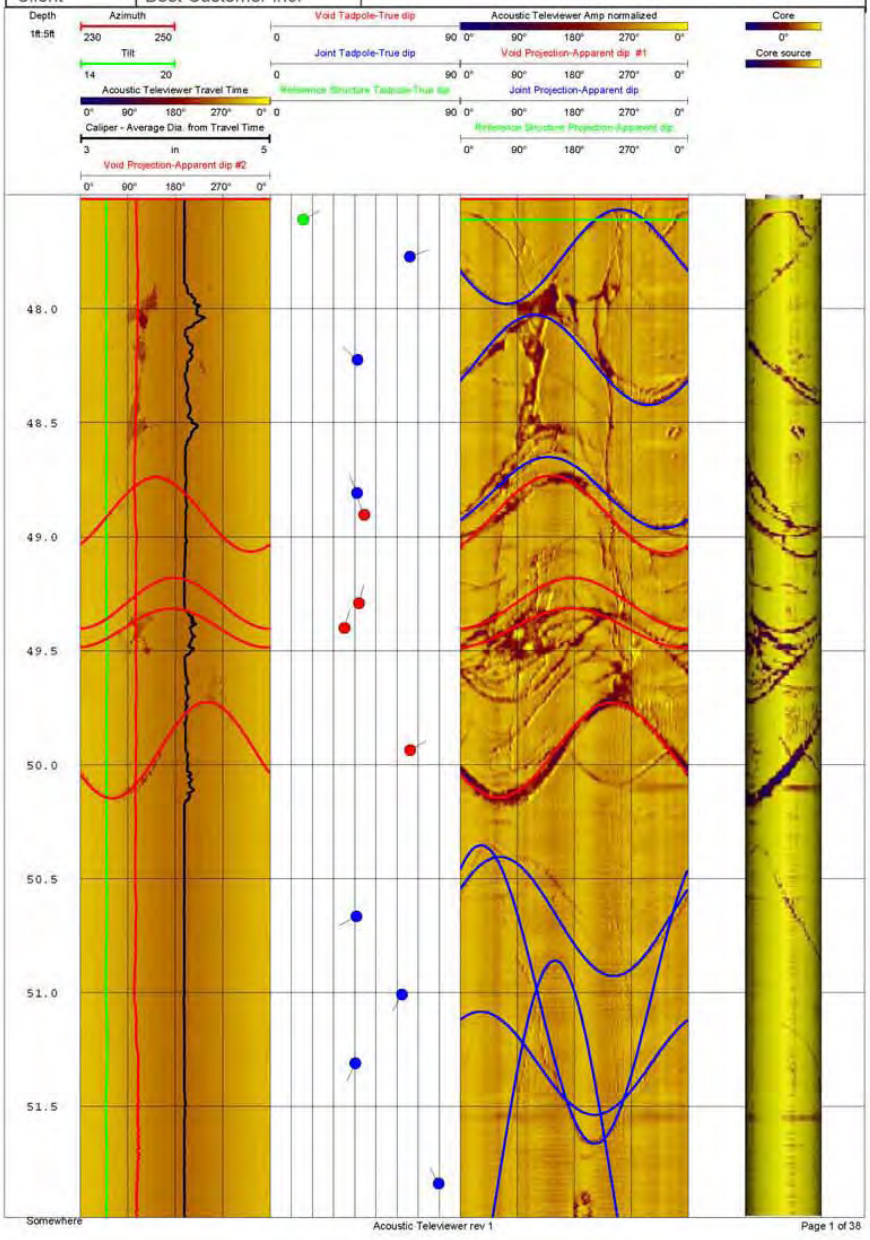

The following downhole data was prepared by Caltrans Drilling Services (See CH2M HILL, 2010)


LA 710 Tunnel boring Z1 B8

| | | | | | |
|---|---|---|---|---|---|
| COMPANY | : CALTRANS | | | | |
| WELL | : Z1 B8 | | | | |
| LOCATION/FIELD | : LA 710 TUNNEL | | | | |
| COUNTY | : LA | | | | |
| LOCATION | : CA | | | | |
| SECTION | : None | TOWNSHIP | : None | RANGE | : None |
| DATE | : 1/08/09 | PERMANENT DATUM | : None | | |
| DEPTH DRILLER | : 200 FT | | | KB | : NA |
| LOG BOTTOM | : 201.5 | LOG MEASURED FROM: | GL | DF | : NA |
| LOG TOP | : -0.2 | DRL MEASURED FROM: | GL | GL | : NA |
| CASING DIAMETER | : 3.9 | LOGGING UNIT | : 7311 | | |
| CASING TYPE | : none | FIELD OFFICE | : 7311 | | |
| CASING THICKNESS: | 0 | RECORDED BY | : DH/DL | | |
| BIT SIZE | : 3.95 IN | BOREHOLE FLUID | : 0 | FILE | : PROCESSE |
| MAGNETIC DECL. | : 12.85 | RM | : 0 | TYPE | : 9065A |
| MATRIX DENSITY | : 2.71 | RM TEMPERATURE | : 0 | LGDATE | : 1/08/09. |
| NEUTRON MATRIX | : DOLOMITE | MATRIX DELTA T | : 140 | | |
| | | | | THRESH: | 2500 |

OTHER SERVICES:
IND-CAL
AC TEL
PSLOG

THIS LOG MEASURED IN FEET, CALIPER MEASURED IN INCHES
EA: 07-187900. GL ELEVATION ESTIMATED FROM HANDHELD GPS 377 FT

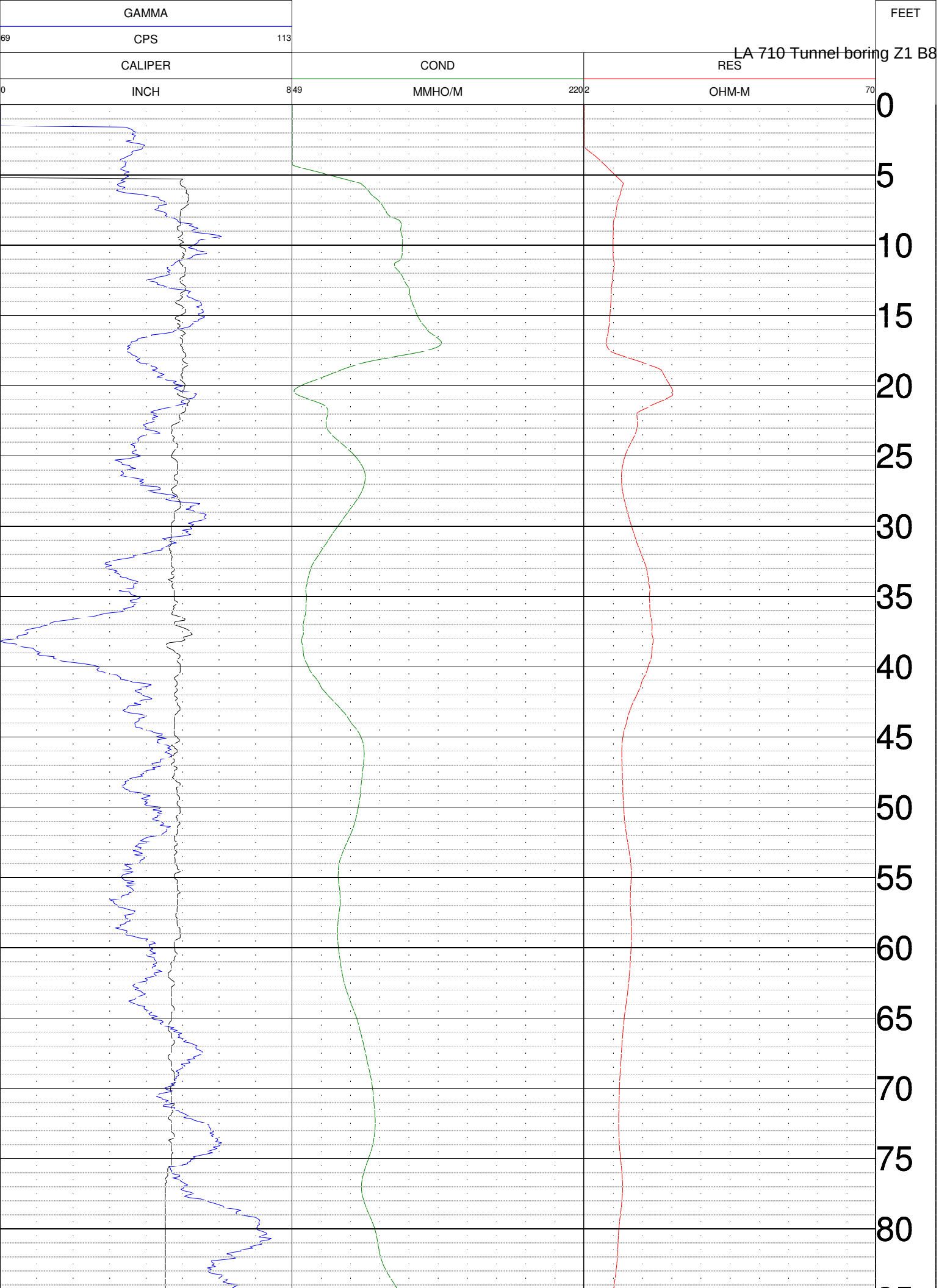
GAMMA
69
CPS
113
CALIPER
0
INCH
8
COND
49
MMHO/M
220
RES
2
OHM-M
70
FEET
LA 710 Tunnel boring Z1 B8
0
5
10
15
20
25
30
35
40
45
50
55
60
65
70
75
80

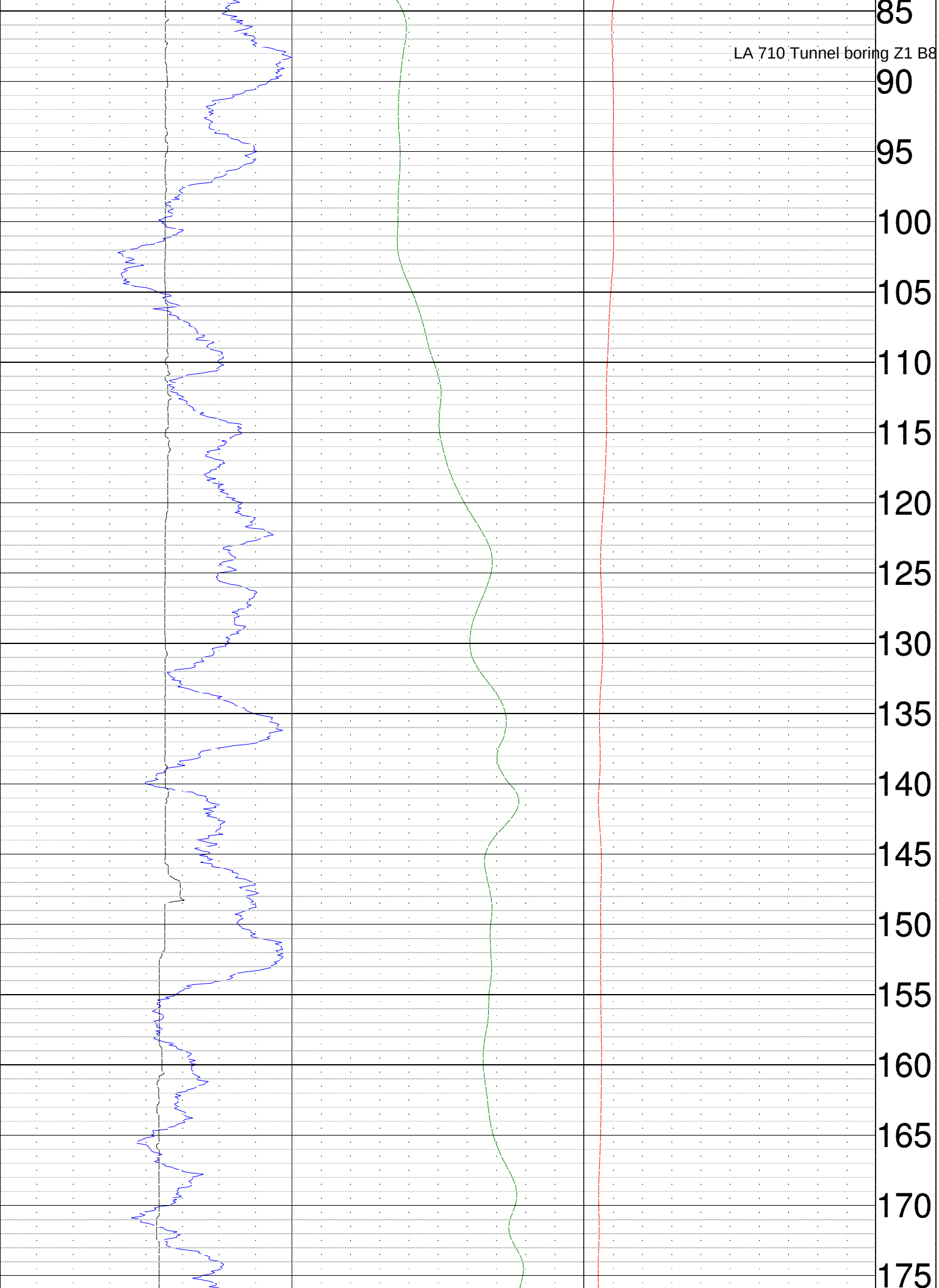
LA 710 Tunnel boring Z1 B8
85
90
95
100
105
110
115
120
125
130
135
140
145
150
155
160
165
170
175

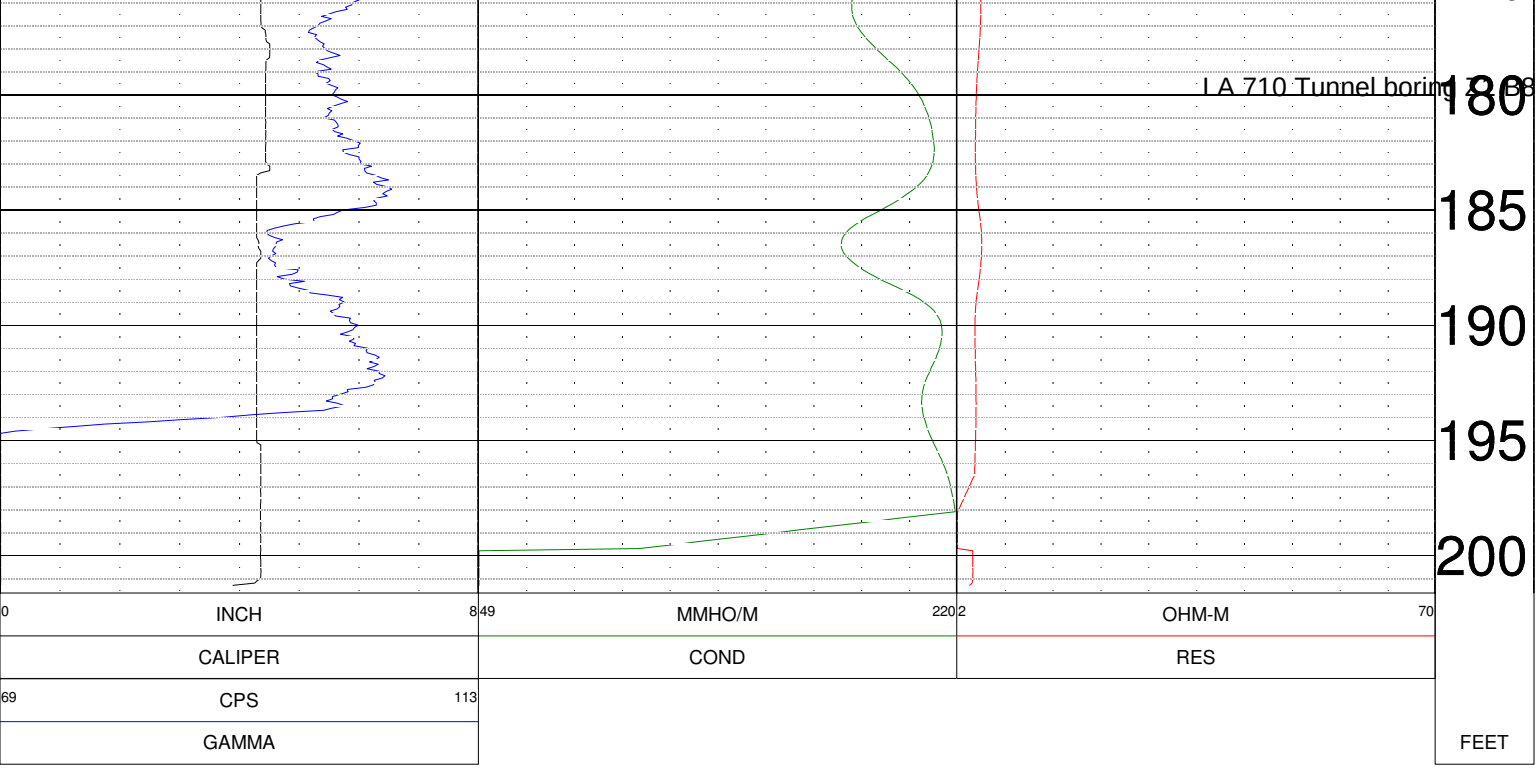
I A 710 Tunnel boring 2 of 8
180
185
190
195
200
0
INCH
8
49
MMHO/M
220
2
OHM-M
70
CALIPER
COND
RES
69
CPS
113
GAMMA
FEET

**Table 2.** LA 710 Tunnel
Boring Z1 B8
PS Suspension Log Data Summary



| Top of Hole Elevation (m) | Depth (m) | Depth (ft) | Vs (m/s) | Vs (ft/s) | Vp (m/s) | Vp (ft/s) | $\gamma$ | $\rho$(Vp) (g/cc) | $\rho$(Vp) ($lb/ft^3$) | G (GPa) | E (GPa) | K (GPa) | G ($10^3 lb/ft^2$) | E ($10^3 lb/ft^2$) | K ($10^3 lb/ft^2$) |
|---|---|---|---|---|---|---|---|---|---|---|---|---|---|---|---|
| Not Provided | 1 | 3.3 | 214 | 702 | | NA | NA | NA | NA | NA | NA | NA | NA | NA | NA |
| | 1.5 | 4.9 | 203 | 666 | | NA | NA | NA | NA | NA | NA | NA | NA | NA | NA |
| | 2 | 6.6 | 215 | 706 | | NA | NA | NA | NA | NA | NA | NA | NA | NA | NA |
| | 2.5 | 8.2 | 242 | 795 | | NA | NA | NA | NA | NA | NA | NA | NA | NA | NA |
| | 3 | 9.8 | 255 | 836 | | NA | NA | NA | NA | NA | NA | NA | NA | NA | NA |
| | 3.5 | 11.5 | 258 | 847 | | NA | NA | NA | NA | NA | NA | NA | NA | NA | NA |
| | 4 | 13.1 | 233 | 763 | | NA | NA | NA | NA | NA | NA | NA | NA | NA | NA |
| | 4.5 | 14.8 | 198 | 650 | | NA | NA | NA | NA | NA | NA | NA | NA | NA | NA |
| | 5 | 16.4 | 196 | 643 | | NA | NA | NA | NA | NA | NA | NA | NA | NA | NA |
| | 5.5 | 18.0 | 242 | 795 | | NA | NA | NA | NA | NA | NA | NA | NA | NA | NA |
| | 6 | 19.7 | 299 | 979 | | NA | NA | NA | NA | NA | NA | NA | NA | NA | NA |
| | 6.5 | 21.3 | 241 | 791 | 515 | 1691 | NA | NA | NA | NA | NA | NA | NA | NA | NA |
| | 7 | 23.0 | 194 | 637 | 382 | 1252 | NA | NA | NA | NA | NA | NA | NA | NA | NA |
| | 7.5 | 24.6 | 187 | 613 | 495 | 1624 | NA | NA | NA | NA | NA | NA | NA | NA | NA |
| | 8 | 26.2 | 198 | 650 | 833 | 2734 | NA | NA | NA | NA | NA | NA | NA | NA | NA |
| | 8.5 | 27.9 | 219 | 717 | 1163 | 3815 | NA | NA | NA | NA | NA | NA | NA | NA | NA |
| | 9 | 29.5 | 237 | 777 | 1613 | 5292 | 0.49 | 1.94 | 121.09 | 0.109 | 0.324 | 4.901 | 2269 | 6758 | 102358 |
| | 9.5 | 31.2 | 242 | 795 | 1786 | 5859 | 0.49 | 2.06 | 128.62 | 0.121 | 0.361 | 6.408 | 2529 | 7539 | 133836 |
| | 10 | 32.8 | 261 | 858 | 2000 | 6562 | 0.49 | 2.18 | 136.25 | 0.149 | 0.445 | 8.531 | 3116 | 9292 | 178175 |
| | 10.5 | 34.4 | 253 | 831 | 1613 | 5292 | 0.49 | 1.94 | 121.09 | 0.124 | 0.370 | 4.880 | 2596 | 7723 | 101922 |
| | 11 | 36.1 | 267 | 875 | 1471 | 4825 | NA | NA | NA | NA | NA | NA | NA | NA | NA |
| | 11.5 | 37.7 | 290 | 951 | 1563 | 5126 | NA | NA | NA | NA | NA | NA | NA | NA | NA |
| | 12 | 39.4 | 328 | 1076 | 1667 | 5468 | 0.48 | 1.98 | 123.58 | 0.213 | 0.630 | 5.215 | 4445 | 13155 | 108922 |
| | 12.5 | 41.0 | 286 | 937 | 1613 | 5292 | 0.48 | 1.94 | 121.09 | 0.158 | 0.470 | 4.835 | 3307 | 9814 | 100975 |
| | 13 | 42.7 | 274 | 899 | 1613 | 5292 | 0.49 | 1.94 | 121.09 | 0.146 | 0.432 | 4.852 | 3041 | 9032 | 101330 |
| | 13.5 | 44.3 | 317 | 1042 | 1613 | 5292 | 0.48 | 1.94 | 121.09 | 0.195 | 0.579 | 4.785 | 4083 | 12083 | 99940 |
| | 14 | 45.9 | 339 | 1112 | 1667 | 5468 | 0.48 | 1.98 | 123.58 | 0.227 | 0.673 | 5.196 | 4751 | 14048 | 108513 |
| | 14.5 | 47.6 | 333 | 1094 | 1667 | 5468 | 0.48 | 1.98 | 123.58 | 0.220 | 0.651 | 5.206 | 4594 | 13590 | 108723 |
| | 14.9 | 48.9 | 342 | 1122 | 1667 | 5468 | 0.48 | 1.98 | 123.58 | 0.231 | 0.684 | 5.190 | 4833 | 14285 | 108405 |
| | 14.9 | 48.9 | 308 | 1009 | 1724 | 5657 | 0.48 | 2.02 | 126.09 | 0.191 | 0.567 | 5.749 | 3994 | 11850 | 120076 |
| | 15.4 | 50.5 | 348 | 1141 | 1667 | 5468 | 0.48 | 1.98 | 123.58 | 0.240 | 0.708 | 5.180 | 5002 | 14778 | 108179 |
| | 15.5 | 50.9 | 360 | 1182 | 1724 | 5657 | 0.48 | 2.02 | 126.09 | 0.262 | 0.775 | 5.655 | 5478 | 16184 | 118097 |
| | 15.9 | 52.2 | 354 | 1161 | 1667 | 5468 | 0.48 | 1.98 | 123.58 | 0.248 | 0.732 | 5.168 | 5181 | 15297 | 107940 |
| | 16 | 52.5 | 370 | 1215 | 1724 | 5657 | 0.48 | 2.02 | 126.09 | 0.277 | 0.818 | 5.635 | 5787 | 17080 | 117685 |
| | 16.4 | 53.8 | 345 | 1131 | 1613 | 5292 | 0.48 | 1.94 | 121.09 | 0.231 | 0.681 | 4.738 | 4817 | 14220 | 98961 |
| | 16.5 | 54.1 | 400 | 1312 | 1667 | 5468 | 0.47 | 1.98 | 123.58 | 0.317 | 0.931 | 5.077 | 6615 | 19441 | 106028 |
| | 16.9 | 55.4 | 412 | 1353 | 1667 | 5468 | 0.47 | 1.98 | 123.58 | 0.337 | 0.988 | 5.050 | 7031 | 20634 | 105474 |

$\gamma$ = Poisson's Ratio  $\rho$(Vp) = Vp-derived density  G = Shear Modulus  E = Young's Modulus  K = Bulk Modulus
Shaded cells denote questionable data.

**Table 2.** LA 710 Tunnel
Boring Z1 B8
PS Suspension Log Data Summary



| Top of Hole Elevation (m) | Depth (m) | Depth (ft) | Vs (m/s) | Vs (ft/s) | Vp (m/s) | Vp (ft/s) | γ | ρ(Vp) (g/cc) | ρ(Vp) ($lb/ft^3$) | G (GPa) | E (GPa) | K (GPa) | G ($10^3 lb/ft^2$) | E ($10^3 lb/ft^2$) | K ($10^3 lb/ft^2$) |
|---|---|---|---|---|---|---|---|---|---|---|---|---|---|---|---|
| | 17 | 55.8 | 354 | 1161 | 1563 | 5126 | NA | NA | NA | NA | NA | NA | NA | NA | NA |
| | 17.4 | 57.1 | 333 | 1094 | 1613 | 5292 | 0.48 | 1.94 | 121.09 | 0.216 | 0.637 | 4.758 | 4501 | 13302 | 99383 |
| | 17.5 | 57.4 | 348 | 1141 | 1667 | 5468 | 0.48 | 1.98 | 123.58 | 0.240 | 0.708 | 5.180 | 5002 | 14778 | 108179 |
| | 17.9 | 58.7 | 348 | 1141 | 1724 | 5657 | 0.48 | 2.02 | 126.09 | 0.244 | 0.723 | 5.678 | 5104 | 15094 | 118596 |
| | 18 | 59.1 | 377 | 1238 | 1724 | 5657 | 0.47 | 2.02 | 126.09 | 0.288 | 0.848 | 5.621 | 6007 | 17719 | 117392 |
| | 18.5 | 60.7 | 357 | 1172 | 1724 | 5657 | 0.48 | 2.02 | 126.09 | 0.258 | 0.761 | 5.661 | 5381 | 15901 | 118227 |
| | 18.5 | 60.7 | 374 | 1226 | 1724 | 5657 | 0.48 | 2.02 | 126.09 | 0.282 | 0.833 | 5.628 | 5895 | 17395 | 117540 |
| | 19 | 62.3 | 400 | 1312 | 1786 | 5859 | 0.47 | 2.06 | 128.62 | 0.330 | 0.971 | 6.130 | 6885 | 20290 | 128029 |
| | 19 | 62.3 | 364 | 1193 | 1786 | 5859 | 0.48 | 2.06 | 128.62 | 0.272 | 0.805 | 6.206 | 5690 | 16823 | 129621 |
| | 19.5 | 64.0 | 364 | 1193 | 1667 | 5468 | 0.48 | 1.98 | 123.58 | 0.262 | 0.772 | 5.150 | 5467 | 16128 | 107558 |
| | 19.5 | 64.0 | 348 | 1141 | 1724 | 5657 | 0.48 | 2.02 | 126.09 | 0.244 | 0.723 | 5.678 | 5104 | 15094 | 118596 |
| | 20 | 65.6 | 354 | 1161 | 1667 | 5468 | 0.48 | 1.98 | 123.58 | 0.248 | 0.732 | 5.168 | 5181 | 15297 | 107940 |
| | 20 | 65.6 | 364 | 1193 | 1724 | 5657 | 0.48 | 2.02 | 126.09 | 0.267 | 0.789 | 5.648 | 5578 | 16475 | 117964 |
| | 20.5 | 67.3 | 339 | 1112 | 1667 | 5468 | 0.48 | 1.98 | 123.58 | 0.227 | 0.673 | 5.196 | 4751 | 14048 | 108513 |
| | 21 | 68.9 | 315 | 1033 | 1667 | 5468 | 0.48 | 1.98 | 123.58 | 0.196 | 0.582 | 5.237 | 4101 | 12153 | 109379 |
| | 21.5 | 70.5 | 331 | 1085 | 1667 | 5468 | 0.48 | 1.98 | 123.58 | 0.216 | 0.640 | 5.211 | 4518 | 13370 | 108824 |
| | 22 | 72.2 | 357 | 1172 | 1667 | 5468 | 0.48 | 1.98 | 123.58 | 0.253 | 0.745 | 5.162 | 5274 | 15567 | 107816 |
| | 22.5 | 73.8 | 345 | 1131 | 1667 | 5468 | 0.48 | 1.98 | 123.58 | 0.235 | 0.696 | 5.185 | 4916 | 14529 | 108293 |
| | 23 | 75.5 | 364 | 1193 | 1667 | 5468 | 0.48 | 1.98 | 123.58 | 0.262 | 0.772 | 5.150 | 5467 | 16128 | 107558 |
| | 23.5 | 77.1 | 385 | 1262 | 1724 | 5657 | 0.47 | 2.02 | 126.09 | 0.299 | 0.881 | 5.606 | 6240 | 18394 | 117081 |
| | 24 | 78.7 | 385 | 1262 | 1563 | 5126 | NA | NA | NA | NA | NA | NA | NA | NA | NA |
| | 24 | 78.7 | 377 | 1238 | 1667 | 5468 | 0.47 | 1.98 | 123.58 | 0.282 | 0.830 | 5.123 | 5888 | 17344 | 106998 |
| | 24.5 | 80.4 | 388 | 1274 | 1724 | 5657 | 0.47 | 2.02 | 126.09 | 0.305 | 0.898 | 5.598 | 6362 | 18746 | 116918 |
| | 25 | 82.0 | 400 | 1312 | 1724 | 5657 | 0.47 | 2.02 | 126.09 | 0.323 | 0.951 | 5.573 | 6750 | 19865 | 116402 |
| | 25.5 | 83.7 | 392 | 1287 | 1724 | 5657 | 0.47 | 2.02 | 126.09 | 0.311 | 0.915 | 5.590 | 6487 | 19109 | 116751 |
| | 26 | 85.3 | 370 | 1215 | 1667 | 5468 | 0.47 | 1.98 | 123.58 | 0.272 | 0.801 | 5.137 | 5671 | 16720 | 107286 |
| | 26.5 | 86.9 | 392 | 1287 | 1667 | 5468 | 0.47 | 1.98 | 123.58 | 0.304 | 0.895 | 5.093 | 6358 | 18702 | 106370 |
| | 27 | 88.6 | 440 | 1442 | 1724 | 5657 | 0.47 | 2.02 | 126.09 | 0.390 | 1.144 | 5.484 | 8151 | 23885 | 114534 |
| | 27.5 | 90.2 | 455 | 1491 | 1724 | 5657 | 0.46 | 2.02 | 126.09 | 0.417 | 1.221 | 5.448 | 8716 | 25497 | 113780 |
| | 28 | 91.9 | 460 | 1508 | 1724 | 5657 | 0.46 | 2.02 | 126.09 | 0.427 | 1.248 | 5.435 | 8917 | 26070 | 113511 |
| | 28.5 | 93.5 | 440 | 1442 | 1724 | 5657 | 0.47 | 2.02 | 126.09 | 0.390 | 1.144 | 5.484 | 8151 | 23885 | 114534 |
| | 29 | 95.1 | 455 | 1491 | 1724 | 5657 | 0.46 | 2.02 | 126.09 | 0.417 | 1.221 | 5.448 | 8716 | 25497 | 113780 |
| | 29.5 | 96.8 | 471 | 1544 | 1724 | 5657 | 0.46 | 2.02 | 126.09 | 0.447 | 1.306 | 5.408 | 9342 | 27274 | 112945 |
| | 30 | 98.4 | 488 | 1600 | 1786 | 5859 | 0.46 | 2.06 | 128.62 | 0.490 | 1.431 | 5.916 | 10239 | 29891 | 123556 |
| | 30.5 | 100.1 | 506 | 1661 | 1786 | 5859 | 0.46 | 2.06 | 128.62 | 0.528 | 1.538 | 5.865 | 11031 | 32129 | 122500 |
| | 31 | 101.7 | 513 | 1682 | 1852 | 6076 | 0.46 | 2.10 | 131.15 | 0.552 | 1.612 | 6.468 | 11539 | 33658 | 135081 |
| | 31.5 | 103.3 | 533 | 1750 | 1786 | 5859 | 0.45 | 2.06 | 128.62 | 0.586 | 1.701 | 5.788 | 12239 | 35519 | 120889 |

γ = Poisson's Ratio  ρ(Vp) = Vp-derived density  G = Shear Modulus  E = Young's Modulus  K = Bulk Modulus
Shaded cells denote questionable data.

**Table 2.** LA 710 Tunnel
Boring Z1 B8
PS Suspension Log Data Summary



| Top of Hole Elevation (m) | Depth (m) | Depth (ft) | Vs (m/s) | Vs (ft/s) | Vp (m/s) | Vp (ft/s) | $\gamma$ | $\rho$(Vp) (g/cc) | $\rho$(Vp) ($lb/ft^3$) | G (GPa) | E (GPa) | K (GPa) | G ($10^3 lb/ft^2$) | E ($10^3 lb/ft^2$) | K ($10^3 lb/ft^2$) |
|---|---|---|---|---|---|---|---|---|---|---|---|---|---|---|---|
| | 32 | 105.0 | 526 | 1727 | 1786 | 5859 | 0.45 | 2.06 | 128.62 | 0.571 | 1.658 | 5.809 | 11919 | 34624 | 121316 |
| | 32.5 | 106.6 | 656 | 2151 | 1786 | 5859 | 0.42 | 2.06 | 128.62 | 0.886 | 2.520 | 5.388 | 18502 | 52622 | 112539 |
| | 33 | 108.3 | 588 | 1930 | 1667 | 5468 | 0.43 | 1.98 | 123.58 | 0.685 | 1.958 | 4.586 | 14306 | 40883 | 95773 |
| | 33.5 | 109.9 | 465 | 1526 | 1667 | 5468 | 0.46 | 1.98 | 123.58 | 0.428 | 1.249 | 4.928 | 8944 | 26078 | 102922 |
| | 34 | 111.5 | 367 | 1204 | 1613 | 5292 | 0.47 | 1.94 | 121.09 | 0.261 | 0.769 | 4.698 | 5455 | 16068 | 98110 |
| | 34.5 | 113.2 | 317 | 1042 | 1667 | 5468 | 0.48 | 1.98 | 123.58 | 0.200 | 0.591 | 5.233 | 4167 | 12344 | 109292 |
| | 35 | 114.8 | 276 | 905 | 1724 | 5657 | 0.49 | 2.02 | 126.09 | 0.154 | 0.457 | 5.799 | 3210 | 9546 | 121121 |
| | 35.5 | 116.5 | 345 | 1131 | 1786 | 5859 | 0.48 | 2.06 | 128.62 | 0.245 | 0.725 | 6.243 | 5116 | 15151 | 130386 |
| | 36 | 118.1 | 460 | 1508 | 1852 | 6076 | 0.47 | 2.10 | 131.15 | 0.444 | 1.303 | 6.612 | 9275 | 27215 | 138099 |
| | 36.5 | 119.8 | 449 | 1475 | 1852 | 6076 | 0.47 | 2.10 | 131.15 | 0.424 | 1.246 | 6.639 | 8863 | 26033 | 138649 |
| | 37 | 121.4 | 430 | 1411 | 1724 | 5657 | 0.47 | 2.02 | 126.09 | 0.374 | 1.096 | 5.506 | 7804 | 22894 | 114996 |
| | 37.5 | 123.0 | 417 | 1367 | 1667 | 5468 | 0.47 | 1.98 | 123.58 | 0.344 | 1.008 | 5.041 | 7178 | 21056 | 105277 |
| | 38.5 | 126.3 | 465 | 1526 | 1724 | 5657 | 0.46 | 2.02 | 126.09 | 0.437 | 1.277 | 5.422 | 9126 | 26662 | 113233 |
| | 39 | 128.0 | 460 | 1508 | 1667 | 5468 | 0.46 | 1.98 | 123.58 | 0.418 | 1.221 | 4.941 | 8740 | 25500 | 103195 |
| | 39.5 | 129.6 | 455 | 1491 | 1724 | 5657 | 0.46 | 2.02 | 126.09 | 0.417 | 1.221 | 5.448 | 8716 | 25497 | 113780 |
| | 40 | 131.2 | 460 | 1508 | 1724 | 5657 | 0.46 | 2.02 | 126.09 | 0.427 | 1.248 | 5.435 | 8917 | 26070 | 113511 |
| | 40.5 | 132.9 | 426 | 1396 | 1667 | 5468 | 0.47 | 1.98 | 123.58 | 0.358 | 1.050 | 5.021 | 7487 | 21938 | 104866 |
| | 41 | 134.5 | 421 | 1381 | 1613 | 5292 | 0.46 | 1.94 | 121.09 | 0.344 | 1.006 | 4.587 | 7182 | 21020 | 95808 |
| | 41.5 | 136.2 | 488 | 1600 | 1724 | 5657 | 0.46 | 2.02 | 126.09 | 0.481 | 1.400 | 5.363 | 10038 | 29241 | 112017 |
| | 42 | 137.8 | 635 | 2083 | 1786 | 5859 | 0.43 | 2.06 | 128.62 | 0.831 | 2.371 | 5.462 | 17346 | 49527 | 114080 |
| | 42.5 | 139.4 | 667 | 2187 | 1667 | 5468 | 0.40 | 1.98 | 123.58 | 0.880 | 2.472 | 4.326 | 18376 | 51627 | 90347 |
| | 43 | 141.1 | 513 | 1682 | 1724 | 5657 | 0.45 | 2.02 | 126.09 | 0.531 | 1.542 | 5.296 | 11094 | 32205 | 110609 |
| | 43.5 | 142.7 | 494 | 1620 | 1724 | 5657 | 0.46 | 2.02 | 126.09 | 0.493 | 1.434 | 5.348 | 10287 | 29943 | 111685 |
| | 44 | 144.4 | 513 | 1682 | 1724 | 5657 | 0.45 | 2.02 | 126.09 | 0.531 | 1.542 | 5.296 | 11094 | 32205 | 110609 |
| | 44.5 | 146.0 | 526 | 1727 | 1786 | 5859 | 0.45 | 2.06 | 128.62 | 0.571 | 1.658 | 5.809 | 11919 | 34624 | 121316 |
| | 45 | 147.6 | 541 | 1773 | 1786 | 5859 | 0.45 | 2.06 | 128.62 | 0.602 | 1.745 | 5.767 | 12572 | 36449 | 120445 |
| | 45.5 | 149.3 | 541 | 1773 | 1786 | 5859 | 0.45 | 2.06 | 128.62 | 0.602 | 1.745 | 5.767 | 12572 | 36449 | 120445 |
| | 46 | 150.9 | 533 | 1750 | 1786 | 5859 | 0.45 | 2.06 | 128.62 | 0.586 | 1.701 | 5.788 | 12239 | 35519 | 120889 |
| | 46.5 | 152.6 | 541 | 1773 | 1786 | 5859 | 0.45 | 2.06 | 128.62 | 0.602 | 1.745 | 5.767 | 12572 | 36449 | 120445 |
| | 47 | 154.2 | 548 | 1798 | 1786 | 5859 | 0.45 | 2.06 | 128.62 | 0.619 | 1.791 | 5.745 | 12919 | 37414 | 119983 |
| | 47 | 154.2 | 541 | 1773 | 1786 | 5859 | 0.45 | 2.06 | 128.62 | 0.602 | 1.745 | 5.767 | 12572 | 36449 | 120445 |
| | 47.5 | 155.8 | 556 | 1823 | 1786 | 5859 | 0.45 | 2.06 | 128.62 | 0.636 | 1.839 | 5.722 | 13280 | 38418 | 119501 |
| | 48 | 157.5 | 506 | 1661 | 1786 | 5859 | 0.46 | 2.06 | 128.62 | 0.528 | 1.538 | 5.865 | 11031 | 32129 | 122500 |
| | 48.5 | 159.1 | 513 | 1682 | 1786 | 5859 | 0.46 | 2.06 | 128.62 | 0.542 | 1.577 | 5.847 | 11316 | 32930 | 122120 |
| | 49 | 160.8 | 548 | 1798 | 1786 | 5859 | 0.45 | 2.06 | 128.62 | 0.619 | 1.791 | 5.745 | 12919 | 37414 | 119982 |
| | 49.5 | 162.4 | 635 | 2083 | 1786 | 5859 | 0.43 | 2.06 | 128.62 | 0.831 | 2.371 | 5.462 | 17346 | 49527 | 114080 |
| | 50 | 164.0 | 851 | 2792 | 1786 | 5859 | 0.35 | 2.06 | 128.62 | 1.492 | 4.038 | 4.580 | 31166 | 84338 | 95653 |

$\gamma$ = Poisson's Ratio  $\rho$(Vp) = Vp-derived density  G = Shear Modulus  E = Young's Modulus  K = Bulk Modulus
Shaded cells denote questionable data.

**Table 2.** LA 710 Tunnel
Boring Z1 B8
PS Suspension Log Data Summary



| Top of Hole Elevation (m) | Depth (m) | Depth (ft) | Vs (m/s) | Vs (ft/s) | Vp (m/s) | Vp (ft/s) | $\gamma$ | $\rho$(Vp) (g/cc) | $\rho$(Vp) ($lb/ft^3$) | G (GPa) | E (GPa) | K (GPa) | G ($10^3 lb/ft^2$) | E ($10^3 lb/ft^2$) | K ($10^3 lb/ft^2$) |
|---|---|---|---|---|---|---|---|---|---|---|---|---|---|---|---|
| | 50.5 | 165.7 | 513 | 1682 | 1724 | 5657 | 0.45 | 2.02 | 126.09 | 0.531 | 1.542 | 5.296 | 11094 | 32205 | 110609 |
| | 51 | 167.3 | 348 | 1141 | 1724 | 5657 | 0.48 | 2.02 | 126.09 | 0.244 | 0.723 | 5.678 | 5104 | 15094 | 118596 |
| | 51.5 | 169.0 | 404 | 1326 | 1724 | 5657 | 0.47 | 2.02 | 126.09 | 0.330 | 0.970 | 5.565 | 6887 | 20260 | 116219 |
| | 52 | 170.6 | 460 | 1508 | 1724 | 5657 | 0.46 | 2.02 | 126.09 | 0.427 | 1.248 | 5.435 | 8917 | 26070 | 113511 |
| | 52.5 | 172.2 | 488 | 1600 | 1786 | 5859 | 0.46 | 2.06 | 128.62 | 0.490 | 1.431 | 5.916 | 10239 | 29891 | 123556 |
| | 53 | 173.9 | 494 | 1620 | 1786 | 5859 | 0.46 | 2.06 | 128.62 | 0.502 | 1.466 | 5.900 | 10493 | 30610 | 123217 |
| | 53.5 | 175.5 | 526 | 1727 | 1786 | 5859 | 0.45 | 2.06 | 128.62 | 0.571 | 1.658 | 5.809 | 11919 | 34624 | 121315 |
| | 54 | 177.2 | 556 | 1823 | 1852 | 6076 | 0.45 | 2.10 | 131.15 | 0.648 | 1.881 | 6.340 | 13542 | 39286 | 132410 |
| | 54.5 | 178.8 | 548 | 1798 | 1639 | 5378 | 0.44 | 1.96 | 122.33 | 0.588 | 1.691 | 4.482 | 12288 | 35319 | 93605 |
| | 55 | 180.4 | 506 | 1661 | 1724 | 5657 | 0.45 | 2.02 | 126.09 | 0.518 | 1.505 | 5.314 | 10815 | 31424 | 110981 |
| | 55.5 | 182.1 | 513 | 1682 | 1724 | 5657 | 0.45 | 2.02 | 126.09 | 0.531 | 1.542 | 5.296 | 11094 | 32205 | 110609 |
| | 56 | 183.7 | 417 | 1367 | 1724 | 5657 | 0.47 | 2.02 | 126.09 | 0.351 | 1.030 | 5.537 | 7324 | 21517 | 115636 |
| | 56.5 | 185.4 | 500 | 1640 | 1923 | 6309 | 0.46 | 2.14 | 133.69 | 0.535 | 1.567 | 7.206 | 11182 | 32735 | 150502 |
| | 56.5 | 185.4 | 513 | 1682 | 1923 | 6309 | 0.46 | 2.14 | 133.69 | 0.563 | 1.646 | 7.169 | 11763 | 34387 | 149728 |
| | 57 | 187.0 | 526 | 1727 | 2000 | 6562 | 0.46 | 2.18 | 136.25 | 0.605 | 1.769 | 7.924 | 12627 | 36941 | 165494 |
| | 57 | 187.0 | 513 | 1682 | 1923 | 6309 | 0.46 | 2.14 | 133.69 | 0.563 | 1.646 | 7.169 | 11763 | 34387 | 149728 |
| | 57.5 | 188.6 | 552 | 1813 | 1786 | 5859 | 0.45 | 2.06 | 128.62 | 0.629 | 1.820 | 5.731 | 13134 | 38012 | 119696 |

$\gamma$ = Poisson's Ratio  $\rho$(Vp) = Vp-derived density  G = Shear Modulus  E = Young's Modulus  K = Bulk Modulus
Shaded cells denote questionable data.

# Figure 1. LA 710 Tunnel
# Boring Z1 B8
# Downhole Interval Velocities

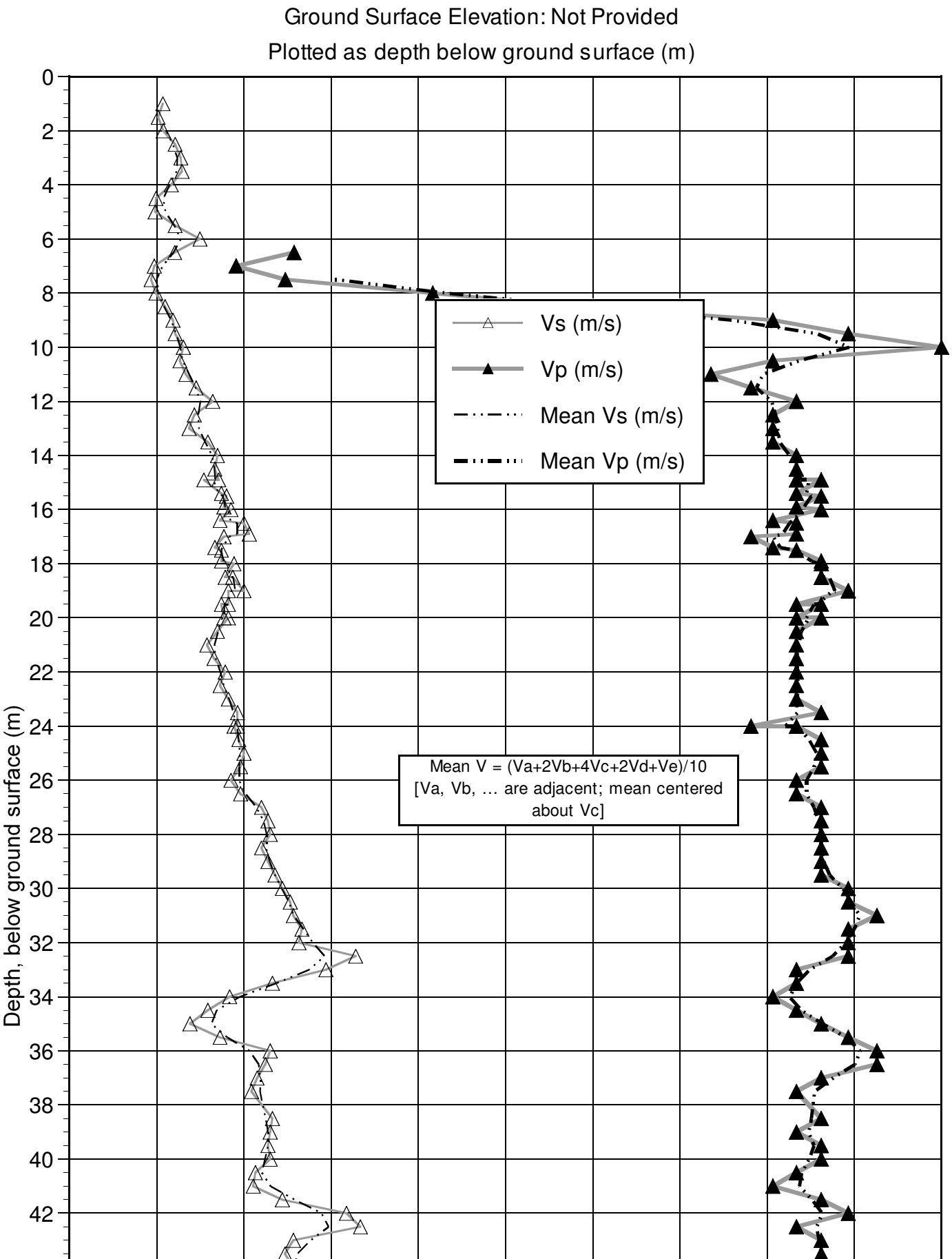

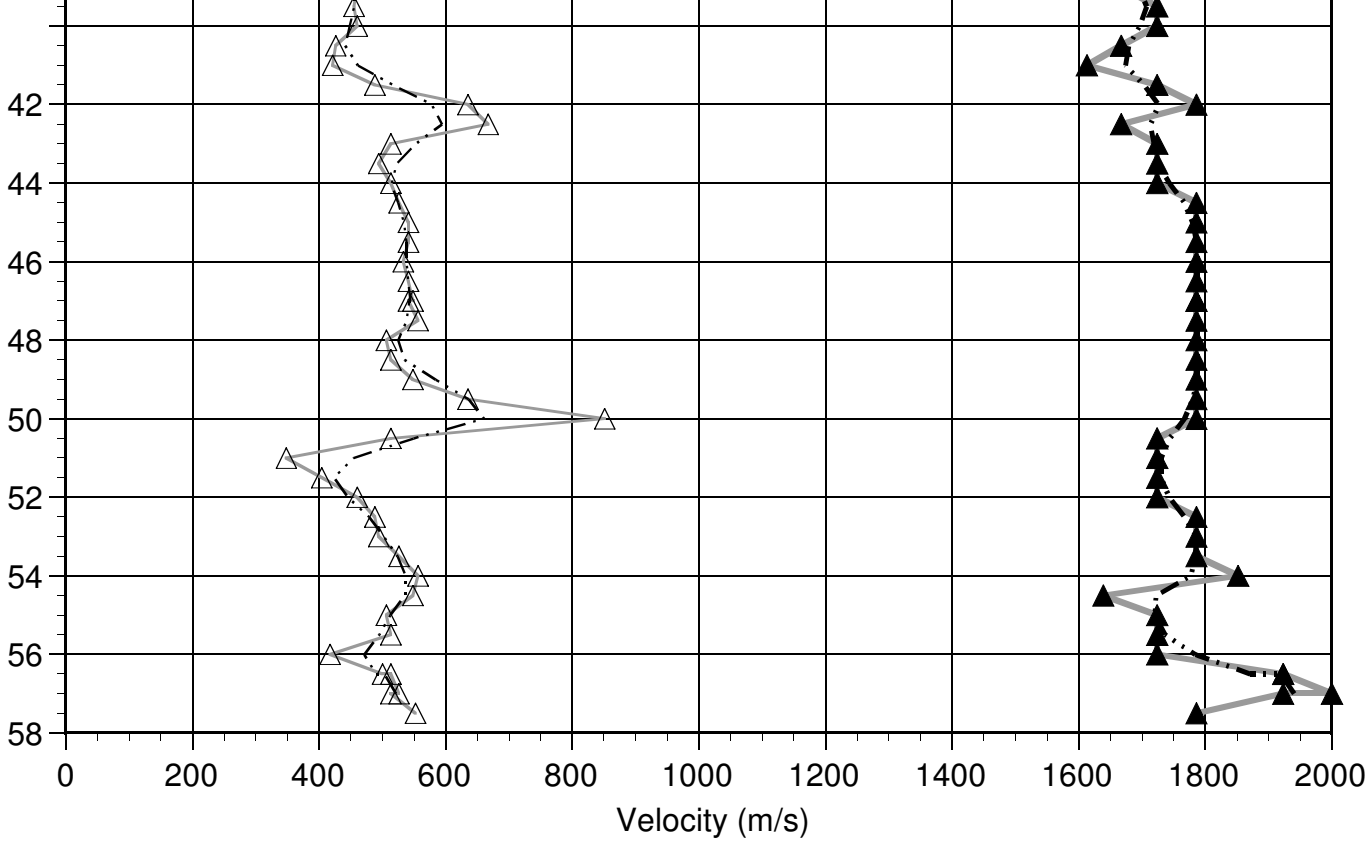
42
44
46
48
50
52
54
56
58
0
200
400
600
800
1000
1200
1400
1600
1800
2000
Velocity (m/s)


LA 710 Tunnel boring Z2 B5

| | | | | | |
|---|---|---|---|---|---|
| COMPANY | : CALTRANS | | | | |
| WELL | : Z2 B5 | | | | |
| LOCATION/FIELD | : LA 710 TUNNEL | | | | |
| COUNTY | : LA | | | | |
| LOCATION | : CA | | | | |
| SECTION | : None | TOWNSHIP | : NONE | RANGE | : None |
| DATE | : 4/14/09 | PERMANENT DATUM | : None | | |
| DEPTH DRILLER | : 91.44 | | | KB | : NA |
| LOG BOTTOM | : 90.6 | LOG MEASURED FROM: | GL | DF | : NA |
| LOG TOP | : 1.2 | DRL MEASURED FROM: | GL | GL | : NA |
| CASING DIAMETER | : n/a | LOGGING UNIT | : 7311 | | |
| CASING TYPE | : N/A | FIELD OFFICE | : 7311 | | |
| CASING THICKNESS: | N/A | RECORDED BY | : DH/DL | | |
| BIT SIZE | : 10.8CM | BOREHOLE FLUID | : 0 | FILE | : PROCESSE |
| MAGNETIC DECL. | : 12.85 | RM | : 0 | TYPE | : 9065A |
| MATRIX DENSITY | : 2.71 | RM TEMPERATURE | : 0 | LGDATE | : 4/14/09. |
| NEUTRON MATRIX | : DOLOMITE | MATRIX DELTA T | : 140 | | |
| | | | | THRESH: | 2500 |

OTHER SERVICES:
IND-CAL
AC TEL
PS LOG

CALIPER LOG IS APPROXIMATE, AND STARTS AT ~82M DEPTH
EA: 07-187900. GL ELEVATION ESTIMATED FROM HANDHELD GPS 143.9M

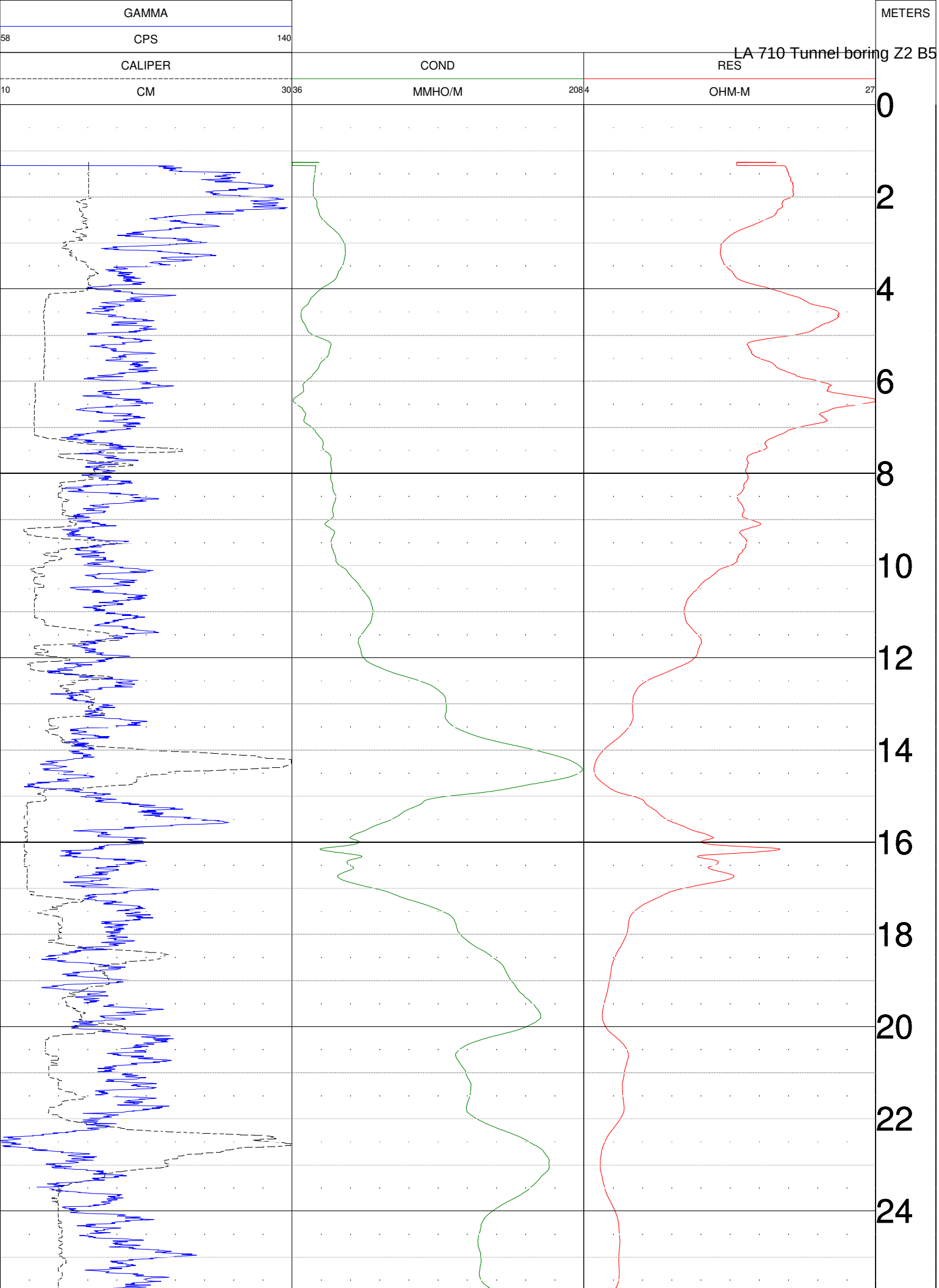
GAMMA
58
CPS
140
CALIPER
10
CM
30
COND
36
MMHO/M
208
RES
4
OHM-M
27
METERS
LA 710 Tunnel boring Z2 B5
0
2
4
6
8
10
12
14
16
18
20
22
24

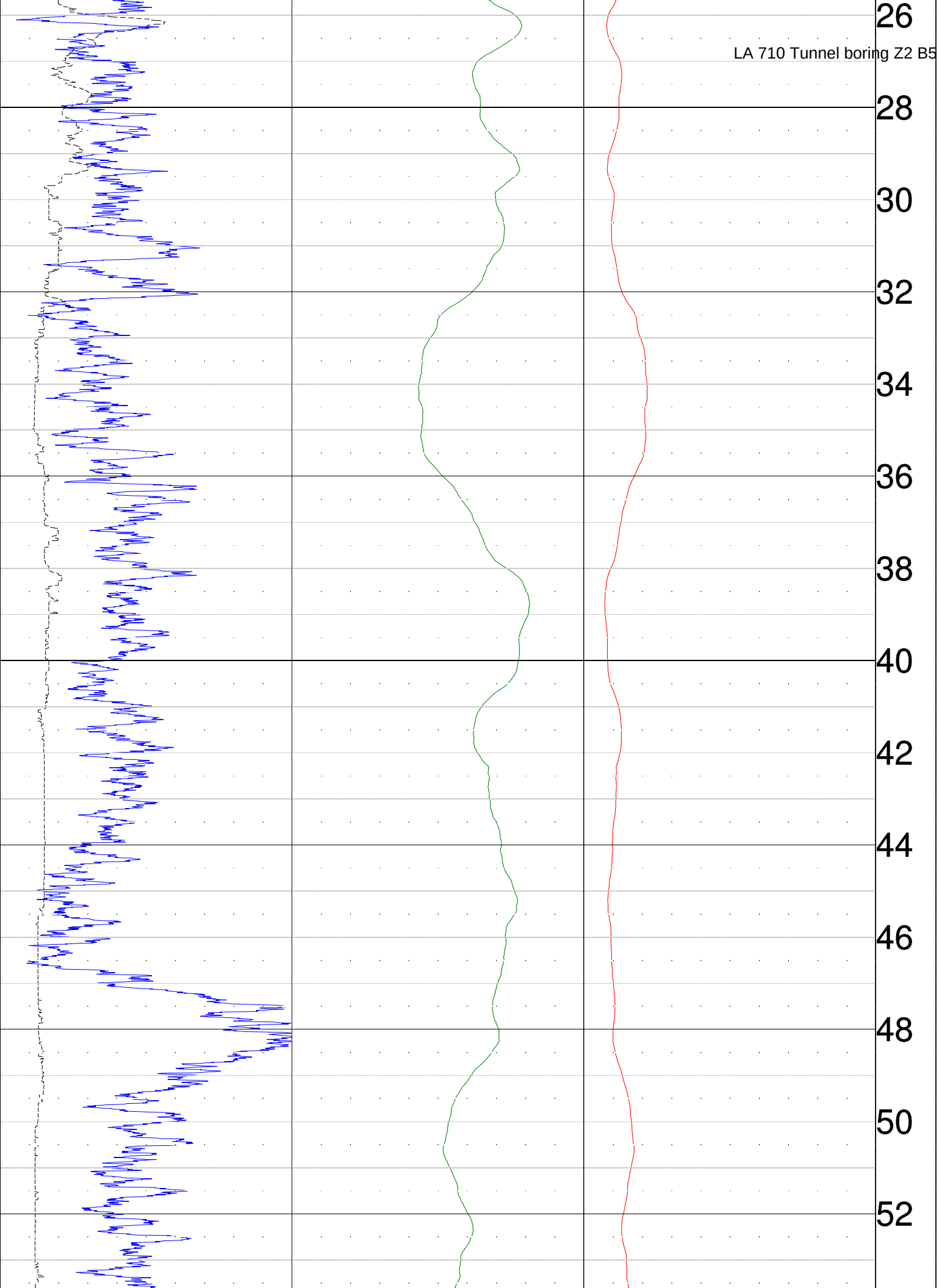
LA 710 Tunnel boring Z2 B5
26
28
30
32
34
36
38
40
42
44
46
48
50
52

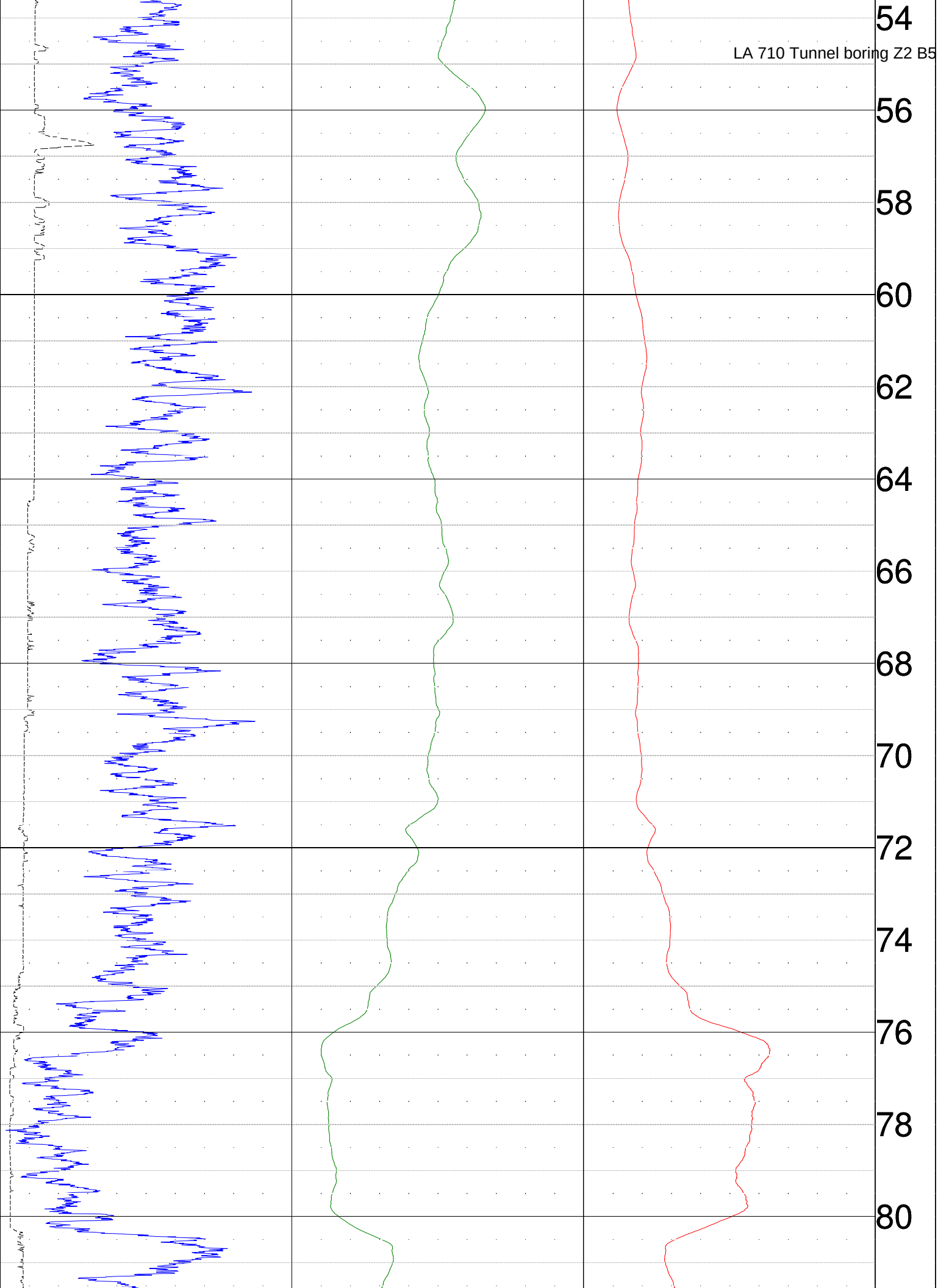
LA 710 Tunnel boring Z2 B5
54
56
58
60
62
64
66
68
70
72
74
76
78
80

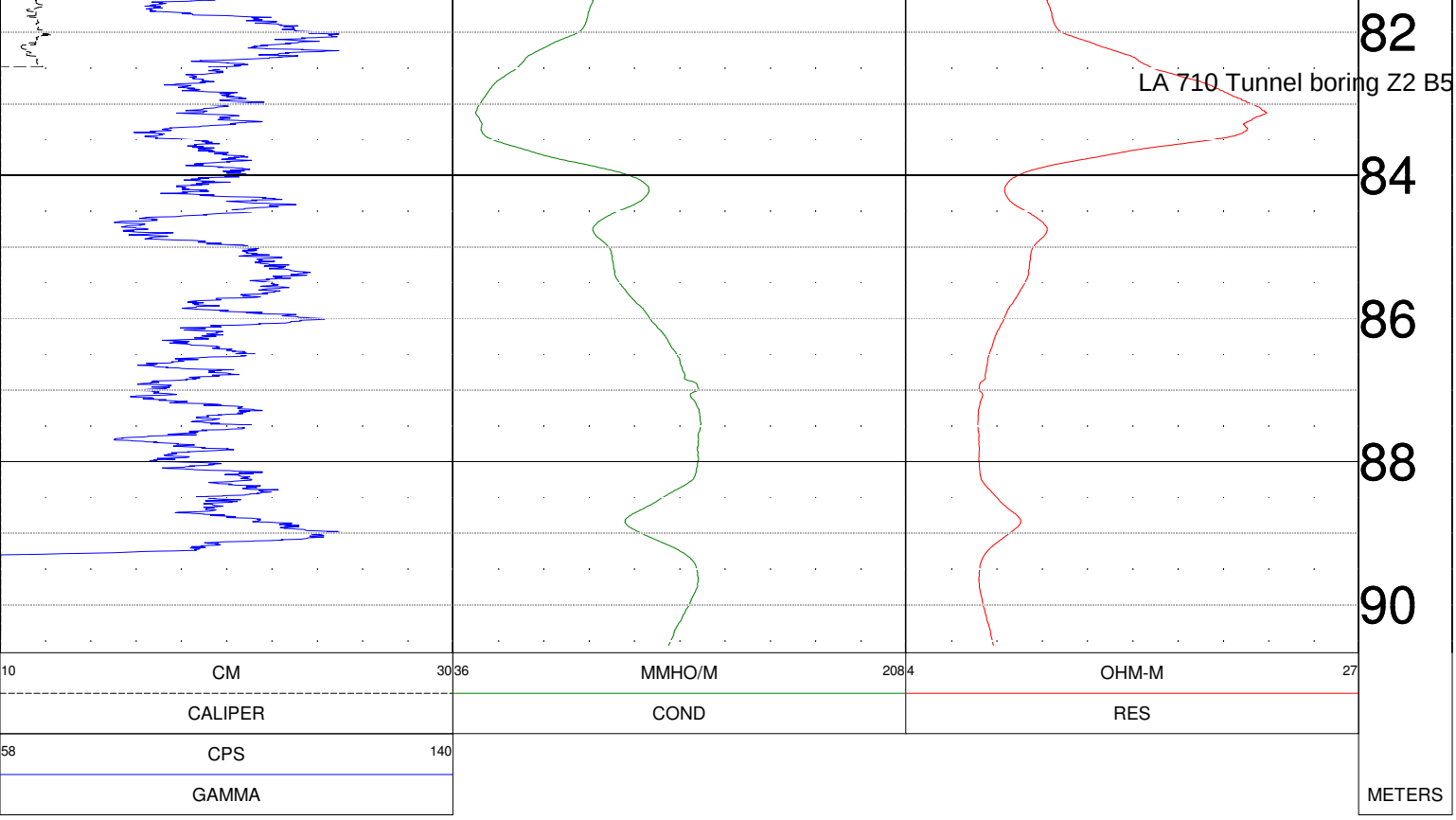
LA 710 Tunnel boring Z2 B5
82
84
86
88
90
10
CM
30
CALIPER
36
MMHO/M
208
COND
4
OHM-M
27
RES
58
CPS
140
GAMMA
METERS

**Table 2.** LA 710 tunnel
Boring Z2 B5
PS Suspension Log Data Summary



| Top of Hole Elevation (m) | Depth (m) | Depth (ft) | Vs (m/s) | Vs (ft/s) | Vp (m/s) | Vp (ft/s) | $\gamma$ | $\rho$(Vp) (g/cc) | $\rho$(Vp) ($lb/ft^3$) | G (GPa) | E (GPa) | K (GPa) | G ($10^3 lb/ft^2$) | E ($10^3 lb/ft^2$) | K ($10^3 lb/ft^2$) |
|---|---|---|---|---|---|---|---|---|---|---|---|---|---|---|---|
| Not Provided | 2 | 6.6 | 323 | 1058 | | NA | NA | NA | NA | NA | NA | NA | NA | NA | NA |
| | 2.5 | 8.2 | 336 | 1101 | | NA | NA | NA | NA | NA | NA | NA | NA | NA | NA |
| | 3 | 9.8 | 279 | 916 | | NA | NA | NA | NA | NA | NA | NA | NA | NA | NA |
| | 3.5 | 11.5 | 239 | 785 | | NA | NA | NA | NA | NA | NA | NA | NA | NA | NA |
| | 4 | 13.1 | 336 | 1101 | | NA | NA | NA | NA | NA | NA | NA | NA | NA | NA |
| | 4.5 | 14.8 | 357 | 1172 | 625 | 2051 | NA | NA | NA | NA | NA | NA | NA | NA | NA |
| | 5 | 16.4 | 321 | 1052 | 641 | 2103 | NA | NA | NA | NA | NA | NA | NA | NA | NA |
| | 5.5 | 18.0 | 314 | 1032 | 806 | 2646 | NA | NA | NA | NA | NA | NA | NA | NA | NA |
| | 6 | 19.7 | 365 | 1197 | 735 | 2412 | NA | NA | NA | NA | NA | NA | NA | NA | NA |
| | 6.5 | 21.3 | 357 | 1172 | 714 | 2343 | NA | NA | NA | NA | NA | NA | NA | NA | NA |
| | 7 | 23.0 | 342 | 1124 | 685 | 2247 | NA | NA | NA | NA | NA | NA | NA | NA | NA |
| | 7.5 | 24.6 | 279 | 916 | 943 | 3095 | NA | NA | NA | NA | NA | NA | NA | NA | NA |
| | 8 | 26.2 | 282 | 927 | 1515 | 4971 | NA | NA | NA | NA | NA | NA | NA | NA | NA |
| | 8.5 | 27.9 | 282 | 924 | 1724 | 5657 | 0.49 | 2.02 | 126.09 | 0.160 | 0.476 | 5.791 | 3347 | 9950 | 120938 |
| | 9 | 29.5 | 313 | 1025 | 1613 | 5292 | 0.48 | 1.94 | 121.09 | 0.189 | 0.561 | 4.793 | 3956 | 11714 | 100109 |
| | 9.5 | 31.2 | 281 | 922 | 1613 | 5292 | 0.48 | 1.94 | 121.09 | 0.153 | 0.454 | 4.842 | 3196 | 9489 | 101122 |
| | 10 | 32.8 | 248 | 812 | 1493 | 4897 | NA | NA | NA | NA | NA | NA | NA | NA | NA |
| | 10.5 | 34.4 | 331 | 1086 | 1449 | 4755 | NA | NA | NA | NA | NA | NA | NA | NA | NA |
| | 11 | 36.1 | 379 | 1243 | 1563 | 5126 | NA | NA | NA | NA | NA | NA | NA | NA | NA |
| | 11.5 | 37.7 | 360 | 1180 | 1563 | 5126 | NA | NA | NA | NA | NA | NA | NA | NA | NA |
| | 12 | 39.4 | 347 | 1139 | 1613 | 5292 | 0.48 | 1.94 | 121.09 | 0.234 | 0.690 | 4.734 | 4884 | 14415 | 98872 |
| | 12.5 | 41.0 | 287 | 943 | 1613 | 5292 | 0.48 | 1.94 | 121.09 | 0.160 | 0.475 | 4.832 | 3345 | 9925 | 100924 |
| | 13 | 42.7 | 230 | 756 | 1695 | 5561 | 0.49 | 2.00 | 124.84 | 0.106 | 0.317 | 5.603 | 2217 | 6610 | 117023 |
| | 13.5 | 44.3 | 286 | 937 | 1818 | 5965 | 0.49 | 2.08 | 129.88 | 0.170 | 0.505 | 6.651 | 3547 | 10551 | 138913 |
| | 14 | 45.9 | 301 | 988 | 1724 | 5657 | 0.48 | 2.02 | 126.09 | 0.183 | 0.544 | 5.760 | 3827 | 11361 | 120298 |
| | 14.5 | 47.6 | 227 | 746 | 1613 | 5292 | 0.49 | 1.94 | 121.09 | 0.100 | 0.299 | 4.912 | 2092 | 6235 | 102594 |
| | 15 | 49.2 | 244 | 800 | 1695 | 5561 | 0.49 | 2.00 | 124.84 | 0.119 | 0.354 | 5.586 | 2485 | 7401 | 116666 |
| | 15.5 | 50.9 | 394 | 1292 | 1818 | 5965 | 0.48 | 2.08 | 129.88 | 0.322 | 0.952 | 6.448 | 6735 | 19874 | 134662 |
| | 16 | 52.5 | 424 | 1390 | 1818 | 5965 | 0.47 | 2.08 | 129.88 | 0.374 | 1.099 | 6.380 | 7802 | 22957 | 133240 |
| | 16.5 | 54.1 | 417 | 1367 | 1786 | 5859 | 0.47 | 2.06 | 128.62 | 0.358 | 1.052 | 6.093 | 7470 | 21981 | 127248 |
| | 17 | 55.8 | 345 | 1131 | 1667 | 5468 | 0.48 | 1.98 | 123.58 | 0.235 | 0.696 | 5.185 | 4916 | 14529 | 108293 |
| | 17.5 | 57.4 | 266 | 873 | 1613 | 5292 | 0.49 | 1.94 | 121.09 | 0.137 | 0.408 | 4.863 | 2865 | 8516 | 101563 |
| | 18 | 59.1 | 262 | 859 | 1724 | 5657 | 0.49 | 2.02 | 126.09 | 0.138 | 0.412 | 5.820 | 2891 | 8604 | 121547 |
| | 18.5 | 60.7 | 292 | 959 | 1818 | 5965 | 0.49 | 2.08 | 129.88 | 0.178 | 0.529 | 6.640 | 3715 | 11046 | 138688 |
| | 19 | 62.3 | 314 | 1032 | 1754 | 5756 | 0.48 | 2.04 | 127.35 | 0.202 | 0.599 | 6.010 | 4213 | 12500 | 125518 |
| | 19 | 62.3 | 292 | 959 | 1754 | 5756 | 0.49 | 2.04 | 127.35 | 0.174 | 0.518 | 6.046 | 3643 | 10824 | 126279 |
| | 19.5 | 64.0 | 294 | 965 | 1754 | 5756 | 0.49 | 2.04 | 127.35 | 0.176 | 0.524 | 6.044 | 3686 | 10950 | 126222 |

$\gamma$ = Poisson's Ratio  $\rho$(Vp) = Vp-derived density  G = Shear Modulus  E = Young's Modulus  K = Bulk Modulus
Shaded cells denote questionable data.

**Table 2.** LA 710 tunnel
Boring Z2 B5
PS Suspension Log Data Summary



| Top of Hole Elevation (m) | Depth (m) | Depth (ft) | Vs (m/s) | Vs (ft/s) | Vp (m/s) | Vp (ft/s) | γ | ρ(Vp) (g/cc) | ρ(Vp) ($lb/ft^3$) | G (GPa) | E (GPa) | K (GPa) | G ($10^3 lb/ft^2$) | E ($10^3 lb/ft^2$) | K ($10^3 lb/ft^2$) |
|---|---|---|---|---|---|---|---|---|---|---|---|---|---|---|---|
| | 19.5 | 64.0 | 291 | 954 | 1724 | 5657 | 0.49 | 2.02 | 126.09 | 0.171 | 0.507 | 5.777 | 3565 | 10590 | 120648 |
| | 19.5 | 64.0 | 289 | 948 | 1754 | 5756 | 0.49 | 2.04 | 127.35 | 0.170 | 0.506 | 6.052 | 3559 | 10578 | 126391 |
| | 20 | 65.6 | 287 | 943 | 1724 | 5657 | 0.49 | 2.02 | 126.09 | 0.167 | 0.496 | 5.782 | 3483 | 10351 | 120757 |
| | 20 | 65.6 | 289 | 948 | 1695 | 5561 | 0.49 | 2.00 | 124.84 | 0.167 | 0.496 | 5.522 | 3489 | 10361 | 115327 |
| | 20 | 65.6 | 282 | 924 | 1695 | 5561 | 0.49 | 2.00 | 124.84 | 0.159 | 0.472 | 5.533 | 3314 | 9848 | 115560 |
| | 20.5 | 67.3 | 313 | 1025 | 1754 | 5756 | 0.48 | 2.04 | 127.35 | 0.199 | 0.591 | 6.013 | 4161 | 12346 | 125588 |
| | 21 | 68.9 | 340 | 1116 | 1818 | 5965 | 0.48 | 2.08 | 129.88 | 0.241 | 0.713 | 6.557 | 5027 | 14899 | 136939 |
| | 21.5 | 70.5 | 345 | 1131 | 1818 | 5965 | 0.48 | 2.08 | 129.88 | 0.247 | 0.733 | 6.548 | 5167 | 15307 | 136753 |
| | 22 | 72.2 | 355 | 1163 | 1852 | 6076 | 0.48 | 2.10 | 131.15 | 0.264 | 0.782 | 6.852 | 5517 | 16342 | 143109 |
| | 22.5 | 73.8 | 336 | 1101 | 1754 | 5756 | 0.48 | 2.04 | 127.35 | 0.230 | 0.680 | 5.973 | 4798 | 14211 | 124739 |
| | 23 | 75.5 | 282 | 927 | 1695 | 5561 | 0.49 | 2.00 | 124.84 | 0.160 | 0.474 | 5.532 | 3333 | 9903 | 115535 |
| | 23.5 | 77.1 | 254 | 833 | 1724 | 5657 | 0.49 | 2.02 | 126.09 | 0.130 | 0.387 | 5.831 | 2717 | 8092 | 121778 |
| | 24 | 78.7 | 265 | 868 | 1695 | 5561 | 0.49 | 2.00 | 124.84 | 0.140 | 0.416 | 5.558 | 2923 | 8696 | 116082 |
| | 24.5 | 80.4 | 262 | 859 | 1724 | 5657 | 0.49 | 2.02 | 126.09 | 0.138 | 0.412 | 5.820 | 2891 | 8604 | 121546 |
| | 25 | 82.0 | 278 | 911 | 1724 | 5657 | 0.49 | 2.02 | 126.09 | 0.156 | 0.463 | 5.796 | 3255 | 9678 | 121061 |
| | 25.5 | 83.7 | 317 | 1042 | 1818 | 5965 | 0.48 | 2.08 | 129.88 | 0.210 | 0.622 | 6.598 | 4379 | 13000 | 137803 |
| | 26 | 85.3 | 316 | 1038 | 1786 | 5859 | 0.48 | 2.06 | 128.62 | 0.206 | 0.612 | 6.294 | 4309 | 12787 | 131463 |
| | 26.5 | 86.9 | 292 | 959 | 1724 | 5657 | 0.49 | 2.02 | 126.09 | 0.173 | 0.513 | 5.774 | 3607 | 10713 | 120592 |
| | 27 | 88.6 | 294 | 965 | 1724 | 5657 | 0.49 | 2.02 | 126.09 | 0.175 | 0.519 | 5.771 | 3649 | 10838 | 120535 |
| | 27.6 | 90.6 | 292 | 959 | 1695 | 5561 | 0.48 | 2.00 | 124.84 | 0.171 | 0.508 | 5.517 | 3571 | 10603 | 115218 |
| | 28 | 91.9 | 286 | 937 | 1695 | 5561 | 0.49 | 2.00 | 124.84 | 0.163 | 0.485 | 5.527 | 3409 | 10128 | 115433 |
| | 28.6 | 93.8 | 289 | 948 | 1695 | 5561 | 0.49 | 2.00 | 124.84 | 0.167 | 0.496 | 5.522 | 3489 | 10361 | 115327 |
| | 29.1 | 95.5 | 275 | 901 | 1724 | 5657 | 0.49 | 2.02 | 126.09 | 0.152 | 0.453 | 5.801 | 3184 | 9469 | 121156 |
| | 29.6 | 97.1 | 267 | 877 | 1667 | 5468 | 0.49 | 1.98 | 123.58 | 0.142 | 0.421 | 5.310 | 2956 | 8789 | 110907 |
| | 30.1 | 98.8 | 279 | 916 | 1724 | 5657 | 0.49 | 2.02 | 126.09 | 0.158 | 0.469 | 5.794 | 3291 | 9786 | 121012 |
| | 30.6 | 100.4 | 296 | 971 | 1724 | 5657 | 0.48 | 2.02 | 126.09 | 0.177 | 0.525 | 5.769 | 3693 | 10966 | 120478 |
| | 31.1 | 102.0 | 321 | 1052 | 1724 | 5657 | 0.48 | 2.02 | 126.09 | 0.207 | 0.615 | 5.728 | 4334 | 12846 | 119623 |
| | 31.6 | 103.7 | 345 | 1131 | 1754 | 5756 | 0.48 | 2.04 | 127.35 | 0.243 | 0.718 | 5.955 | 5066 | 14995 | 124381 |
| | 32.1 | 105.3 | 342 | 1124 | 1754 | 5756 | 0.48 | 2.04 | 127.35 | 0.239 | 0.708 | 5.960 | 4997 | 14793 | 124474 |
| | 33.1 | 108.6 | 331 | 1086 | 1724 | 5657 | 0.48 | 2.02 | 126.09 | 0.221 | 0.656 | 5.709 | 4625 | 13699 | 119234 |
| | 33.1 | 108.6 | 338 | 1108 | 1724 | 5657 | 0.48 | 2.02 | 126.09 | 0.231 | 0.682 | 5.697 | 4815 | 14252 | 118981 |
| | 33.6 | 110.2 | 331 | 1086 | 1724 | 5657 | 0.48 | 2.02 | 126.09 | 0.221 | 0.656 | 5.709 | 4625 | 13699 | 119234 |
| | 34.1 | 111.9 | 325 | 1065 | 1695 | 5561 | 0.48 | 2.00 | 124.84 | 0.211 | 0.624 | 5.464 | 4403 | 13040 | 114109 |
| | 34.6 | 113.5 | 321 | 1052 | 1724 | 5657 | 0.48 | 2.02 | 126.09 | 0.207 | 0.615 | 5.728 | 4334 | 12846 | 119623 |
| | 35 | 114.8 | 311 | 1019 | 1724 | 5657 | 0.48 | 2.02 | 126.09 | 0.195 | 0.578 | 5.745 | 4069 | 12069 | 119976 |
| | 35.6 | 116.8 | 316 | 1038 | 1754 | 5756 | 0.48 | 2.04 | 127.35 | 0.204 | 0.606 | 6.006 | 4267 | 12657 | 125447 |
| | 36.1 | 118.4 | 311 | 1019 | 1754 | 5756 | 0.48 | 2.04 | 127.35 | 0.197 | 0.584 | 6.017 | 4109 | 12195 | 125658 |

γ = Poisson's Ratio  ρ(Vp) = Vp-derived density  G = Shear Modulus  E = Young's Modulus  K = Bulk Modulus
Shaded cells denote questionable data.

**Table 2.** LA 710 tunnel
Boring Z2 B5
PS Suspension Log Data Summary



| Top of Hole Elevation (m) | Depth (m) | Depth (ft) | Vs (m/s) | Vs (ft/s) | Vp (m/s) | Vp (ft/s) | γ | ρ(Vp) (g/cc) | ρ(Vp) ($lb/ft^3$) | G (GPa) | E (GPa) | K (GPa) | G ($10^3 lb/ft^2$) | E ($10^3 lb/ft^2$) | K ($10^3 lb/ft^2$) |
|---|---|---|---|---|---|---|---|---|---|---|---|---|---|---|---|
| | 36.6 | 120.1 | 303 | 994 | 1754 | 5756 | 0.48 | 2.04 | 127.35 | 0.187 | 0.556 | 6.029 | 3912 | 11617 | 125920 |
| | 37.1 | 121.7 | 299 | 982 | 1754 | 5756 | 0.49 | 2.04 | 127.35 | 0.183 | 0.543 | 6.035 | 3819 | 11343 | 126044 |
| | 37.6 | 123.4 | 294 | 965 | 1724 | 5657 | 0.49 | 2.02 | 126.09 | 0.175 | 0.519 | 5.771 | 3649 | 10838 | 120535 |
| | 38.1 | 125.0 | 291 | 954 | 1724 | 5657 | 0.49 | 2.02 | 126.09 | 0.171 | 0.507 | 5.777 | 3565 | 10590 | 120648 |
| | 38.6 | 126.6 | 299 | 982 | 1667 | 5468 | 0.48 | 1.98 | 123.58 | 0.177 | 0.526 | 5.262 | 3706 | 10995 | 109906 |
| | 39.6 | 129.9 | 379 | 1243 | 1667 | 5468 | 0.47 | 1.98 | 123.58 | 0.284 | 0.837 | 5.120 | 5932 | 17474 | 106938 |
| | 40.1 | 131.6 | 373 | 1224 | 1639 | 5378 | 0.47 | 1.96 | 122.33 | 0.273 | 0.804 | 4.903 | 5698 | 16783 | 102391 |
| | 40.6 | 133.2 | 397 | 1302 | 1667 | 5468 | 0.47 | 1.98 | 123.58 | 0.312 | 0.916 | 5.083 | 6511 | 19141 | 106167 |
| | 41.1 | 134.8 | 424 | 1390 | 1695 | 5561 | 0.47 | 2.00 | 124.84 | 0.359 | 1.053 | 5.266 | 7499 | 21996 | 109981 |
| | 41.6 | 136.5 | 424 | 1390 | 1695 | 5561 | 0.47 | 2.00 | 124.84 | 0.359 | 1.053 | 5.266 | 7499 | 21996 | 109981 |
| | 42.1 | 138.1 | 424 | 1390 | 1695 | 5561 | 0.47 | 2.00 | 124.84 | 0.359 | 1.053 | 5.266 | 7499 | 21996 | 109981 |
| | 43.1 | 141.4 | 417 | 1367 | 1695 | 5561 | 0.47 | 2.00 | 124.84 | 0.347 | 1.019 | 5.282 | 7251 | 21286 | 110311 |
| | 43.1 | 141.4 | 424 | 1390 | 1667 | 5468 | 0.47 | 1.98 | 123.58 | 0.355 | 1.042 | 5.025 | 7423 | 21757 | 104950 |
| | 43.6 | 143.0 | 410 | 1345 | 1639 | 5378 | 0.47 | 1.96 | 122.33 | 0.329 | 0.965 | 4.827 | 6874 | 20165 | 100823 |
| | 44.1 | 144.7 | 385 | 1262 | 1613 | 5292 | 0.47 | 1.94 | 121.09 | 0.287 | 0.843 | 4.663 | 5993 | 17616 | 97394 |
| | 44.6 | 146.3 | 376 | 1233 | 1587 | 5208 | 0.47 | 1.92 | 119.84 | 0.271 | 0.798 | 4.475 | 5666 | 16662 | 93460 |
| | 45 | 147.6 | 382 | 1252 | 1613 | 5292 | 0.47 | 1.94 | 121.09 | 0.283 | 0.831 | 4.669 | 5901 | 17354 | 97515 |
| | 45.1 | 148.0 | 391 | 1282 | 1587 | 5208 | 0.47 | 1.92 | 119.84 | 0.293 | 0.860 | 4.446 | 6118 | 17959 | 92859 |
| | 45.5 | 149.3 | 395 | 1297 | 1639 | 5378 | 0.47 | 1.96 | 122.33 | 0.306 | 0.900 | 4.858 | 6394 | 18787 | 101464 |
| | 45.6 | 149.6 | 413 | 1356 | 1613 | 5292 | 0.46 | 1.94 | 121.09 | 0.331 | 0.970 | 4.604 | 6917 | 20265 | 96161 |
| | 46 | 150.9 | 400 | 1312 | 1639 | 5378 | 0.47 | 1.96 | 122.33 | 0.314 | 0.921 | 4.848 | 6548 | 19230 | 101258 |
| | 46.1 | 151.2 | 435 | 1426 | 1639 | 5378 | 0.46 | 1.96 | 122.33 | 0.370 | 1.083 | 4.772 | 7737 | 22625 | 99673 |
| | 46.5 | 152.6 | 424 | 1390 | 1639 | 5378 | 0.46 | 1.96 | 122.33 | 0.352 | 1.030 | 4.797 | 7348 | 21519 | 100191 |
| | 47 | 154.2 | 495 | 1624 | 1695 | 5561 | 0.45 | 2.00 | 124.84 | 0.490 | 1.425 | 5.091 | 10235 | 29752 | 106332 |
| | 47.1 | 154.5 | 467 | 1533 | 1667 | 5468 | 0.46 | 1.98 | 123.58 | 0.432 | 1.260 | 4.923 | 9028 | 26314 | 102811 |
| | 47.1 | 154.5 | 526 | 1727 | 1695 | 5561 | 0.45 | 2.00 | 124.84 | 0.554 | 1.603 | 5.006 | 11569 | 33473 | 104553 |
| | 47.5 | 155.8 | 500 | 1640 | 1695 | 5561 | 0.45 | 2.00 | 124.84 | 0.500 | 1.452 | 5.078 | 10441 | 30328 | 106057 |
| | 47.6 | 156.2 | 575 | 1886 | 1695 | 5561 | 0.44 | 2.00 | 124.84 | 0.660 | 1.896 | 4.864 | 13795 | 39592 | 101586 |
| | 48 | 157.5 | 490 | 1608 | 1639 | 5378 | 0.45 | 1.96 | 122.33 | 0.471 | 1.366 | 4.638 | 9834 | 28538 | 96876 |
| | 48 | 157.5 | 521 | 1709 | 1695 | 5561 | 0.45 | 2.00 | 124.84 | 0.542 | 1.571 | 5.021 | 11329 | 32807 | 104873 |
| | 48.5 | 159.1 | 633 | 2076 | 1667 | 5468 | 0.42 | 1.98 | 123.58 | 0.793 | 2.245 | 4.442 | 16562 | 46895 | 92766 |
| | 48.5 | 159.1 | 459 | 1505 | 1667 | 5468 | 0.46 | 1.98 | 123.58 | 0.417 | 1.216 | 4.944 | 8700 | 25387 | 103248 |
| | 49 | 160.8 | 510 | 1674 | 1695 | 5561 | 0.45 | 2.00 | 124.84 | 0.521 | 1.510 | 5.051 | 10872 | 31532 | 105483 |
| | 49 | 160.8 | 433 | 1420 | 1613 | 5292 | 0.46 | 1.94 | 121.09 | 0.363 | 1.062 | 4.561 | 7592 | 22185 | 95261 |
| | 49.5 | 162.4 | 402 | 1318 | 1754 | 5756 | 0.47 | 2.04 | 127.35 | 0.329 | 0.969 | 5.840 | 6872 | 20236 | 121974 |
| | 49.5 | 162.4 | 435 | 1426 | 1667 | 5468 | 0.46 | 1.98 | 123.58 | 0.374 | 1.095 | 5.000 | 7816 | 22877 | 104427 |
| | 50 | 164.0 | 481 | 1577 | 1695 | 5561 | 0.46 | 2.00 | 124.84 | 0.462 | 1.346 | 5.128 | 9653 | 28116 | 107108 |

γ = Poisson's Ratio  ρ(Vp) = Vp-derived density  G = Shear Modulus  E = Young's Modulus  K = Bulk Modulus
Shaded cells denote questionable data.

**Table 2.** LA 710 tunnel
Boring Z2 B5
PS Suspension Log Data Summary



| Top of Hole Elevation (m) | Depth (m) | Depth (ft) | Vs (m/s) | Vs (ft/s) | Vp (m/s) | Vp (ft/s) | γ | ρ(Vp) (g/cc) | ρ(Vp) ($lb/ft^3$) | G (GPa) | E (GPa) | K (GPa) | G ($10^3 lb/ft^2$) | E ($10^3 lb/ft^2$) | K ($10^3 lb/ft^2$) |
|---|---|---|---|---|---|---|---|---|---|---|---|---|---|---|---|
| | 50.5 | 165.7 | 472 | 1548 | 1961 | 6433 | 0.47 | 2.16 | 134.97 | 0.481 | 1.414 | 7.671 | 10047 | 29523 | 160208 |
| | 50.5 | 165.7 | 398 | 1307 | 1786 | 5859 | 0.47 | 2.06 | 128.62 | 0.327 | 0.964 | 6.134 | 6830 | 20132 | 128102 |
| | 50.5 | 165.7 | 543 | 1783 | 1754 | 5756 | 0.45 | 2.04 | 127.35 | 0.603 | 1.744 | 5.475 | 12585 | 36418 | 114357 |
| | 51 | 167.3 | 521 | 1709 | 1786 | 5859 | 0.45 | 2.06 | 128.62 | 0.559 | 1.625 | 5.824 | 11672 | 33931 | 121645 |
| | 51 | 167.3 | 476 | 1562 | 1786 | 5859 | 0.46 | 2.06 | 128.62 | 0.467 | 1.366 | 5.947 | 9757 | 28524 | 124199 |
| | 51.5 | 169.0 | 521 | 1709 | 1754 | 5756 | 0.45 | 2.04 | 127.35 | 0.553 | 1.607 | 5.541 | 11558 | 33556 | 115726 |
| | 51.5 | 169.0 | 476 | 1562 | 1613 | 5292 | 0.45 | 1.94 | 121.09 | 0.440 | 1.277 | 4.459 | 9186 | 26680 | 93136 |
| | 52 | 170.6 | 476 | 1562 | 1724 | 5657 | 0.46 | 2.02 | 126.09 | 0.458 | 1.336 | 5.394 | 9566 | 27907 | 112647 |
| | 52 | 170.6 | 481 | 1577 | 1754 | 5756 | 0.46 | 2.04 | 127.35 | 0.472 | 1.376 | 5.650 | 9848 | 28744 | 118006 |
| | 52.5 | 172.2 | 472 | 1548 | 1754 | 5756 | 0.46 | 2.04 | 127.35 | 0.454 | 1.326 | 5.674 | 9480 | 27701 | 118497 |
| | 53 | 173.9 | 467 | 1533 | 1786 | 5859 | 0.46 | 2.06 | 128.62 | 0.450 | 1.317 | 5.970 | 9396 | 27496 | 124680 |
| | 53 | 173.9 | 467 | 1533 | 1754 | 5756 | 0.46 | 2.04 | 127.35 | 0.445 | 1.302 | 5.685 | 9303 | 27200 | 118732 |
| | 53 | 173.9 | 472 | 1548 | 1754 | 5756 | 0.46 | 2.04 | 127.35 | 0.454 | 1.326 | 5.674 | 9480 | 27701 | 118496 |
| | 53.5 | 175.5 | 476 | 1562 | 1563 | 5126 | NA | NA | NA | NA | NA | NA | NA | NA | NA |
| | 53.5 | 175.5 | 505 | 1657 | 1786 | 5859 | 0.46 | 2.06 | 128.62 | 0.526 | 1.531 | 5.869 | 10976 | 31972 | 122574 |
| | 54 | 177.2 | 455 | 1491 | 1724 | 5657 | 0.46 | 2.02 | 126.09 | 0.417 | 1.221 | 5.448 | 8716 | 25497 | 113780 |
| | 54 | 177.2 | 510 | 1674 | 1786 | 5859 | 0.46 | 2.06 | 128.62 | 0.536 | 1.561 | 5.855 | 11201 | 32606 | 122274 |
| | 54.5 | 178.8 | 532 | 1745 | 1754 | 5756 | 0.45 | 2.04 | 127.35 | 0.577 | 1.673 | 5.509 | 12055 | 34944 | 115064 |
| | 54.5 | 178.8 | 500 | 1640 | 1818 | 5965 | 0.46 | 2.08 | 129.88 | 0.520 | 1.518 | 6.184 | 10863 | 31700 | 129158 |
| | 55 | 180.4 | 541 | 1773 | 1786 | 5859 | 0.45 | 2.06 | 128.62 | 0.602 | 1.745 | 5.767 | 12572 | 36449 | 120445 |
| | 55 | 180.4 | 532 | 1745 | 1887 | 6190 | 0.46 | 2.12 | 132.42 | 0.600 | 1.749 | 6.751 | 12534 | 36521 | 140998 |
| | 55.5 | 182.1 | 575 | 1886 | 1786 | 5859 | 0.44 | 2.06 | 128.62 | 0.680 | 1.963 | 5.662 | 14212 | 40994 | 118258 |
| | 55.5 | 182.1 | 556 | 1823 | 1818 | 5965 | 0.45 | 2.08 | 129.88 | 0.642 | 1.860 | 6.021 | 13411 | 38852 | 125761 |
| | 56 | 183.7 | 515 | 1691 | 1852 | 6076 | 0.46 | 2.10 | 131.15 | 0.558 | 1.628 | 6.460 | 11658 | 33995 | 134922 |
| | 56 | 183.7 | 556 | 1823 | 1818 | 5965 | 0.45 | 2.08 | 129.88 | 0.642 | 1.860 | 6.021 | 13411 | 38852 | 125760 |
| | 56.5 | 185.4 | 510 | 1674 | 1852 | 6076 | 0.46 | 2.10 | 131.15 | 0.547 | 1.596 | 6.475 | 11421 | 33326 | 135237 |
| | 56.5 | 185.4 | 495 | 1624 | 1887 | 6190 | 0.46 | 2.12 | 132.42 | 0.520 | 1.521 | 6.858 | 10857 | 31768 | 143235 |
| | 57 | 187.0 | 474 | 1555 | 1887 | 6190 | 0.47 | 2.12 | 132.42 | 0.476 | 1.397 | 6.916 | 9951 | 29182 | 144444 |
| | 57 | 187.0 | 526 | 1727 | 2174 | 7132 | 0.47 | 2.26 | 141.40 | 0.627 | 1.843 | 9.867 | 13104 | 38496 | 206085 |
| | 57.5 | 188.6 | 556 | 1823 | 1786 | 5859 | 0.45 | 2.06 | 128.62 | 0.636 | 1.839 | 5.722 | 13280 | 38418 | 119501 |
| | 57.5 | 188.6 | 578 | 1896 | 1923 | 6309 | 0.45 | 2.14 | 133.69 | 0.716 | 2.076 | 6.966 | 14944 | 43349 | 145485 |
| | 58 | 190.3 | 562 | 1843 | 1852 | 6076 | 0.45 | 2.10 | 131.15 | 0.663 | 1.922 | 6.320 | 13848 | 40140 | 132002 |
| | 58 | 190.3 | 532 | 1745 | 1724 | 5657 | 0.45 | 2.02 | 126.09 | 0.571 | 1.654 | 5.242 | 11936 | 34551 | 109487 |
| | 58.5 | 191.9 | 524 | 1718 | 1818 | 5965 | 0.45 | 2.08 | 129.88 | 0.570 | 1.659 | 6.117 | 11911 | 34655 | 127761 |
| | 58.5 | 191.9 | 503 | 1649 | 1786 | 5859 | 0.46 | 2.06 | 128.62 | 0.520 | 1.516 | 5.876 | 10866 | 31662 | 122721 |
| | 59 | 193.6 | 500 | 1640 | 1852 | 6076 | 0.46 | 2.10 | 131.15 | 0.525 | 1.534 | 6.504 | 10969 | 32044 | 135841 |
| | 59 | 193.6 | 508 | 1665 | 1818 | 5965 | 0.46 | 2.08 | 129.88 | 0.536 | 1.563 | 6.163 | 11196 | 32642 | 128713 |

γ = Poisson's Ratio  ρ(Vp) = Vp-derived density  G = Shear Modulus  E = Young's Modulus  K = Bulk Modulus
Shaded cells denote questionable data.

**Table 2.** LA 710 tunnel
Boring Z2 B5
PS Suspension Log Data Summary



| Top of Hole Elevation (m) | Depth (m) | Depth (ft) | Vs (m/s) | Vs (ft/s) | Vp (m/s) | Vp (ft/s) | γ | ρ(Vp) (g/cc) | ρ(Vp) ($lb/ft^3$) | G (GPa) | E (GPa) | K (GPa) | G ($10^3 lb/ft^2$) | E ($10^3 lb/ft^2$) | K ($10^3 lb/ft^2$) |
|---|---|---|---|---|---|---|---|---|---|---|---|---|---|---|---|
| | 59.5 | 195.2 | 602 | 1976 | 1852 | 6076 | 0.44 | 2.10 | 131.15 | 0.762 | 2.197 | 6.188 | 15922 | 45883 | 129236 |
| | 59.5 | 195.2 | 571 | 1875 | 1852 | 6076 | 0.45 | 2.10 | 131.15 | 0.686 | 1.986 | 6.290 | 14327 | 41473 | 131363 |
| | 60 | 196.9 | 532 | 1745 | 1852 | 6076 | 0.46 | 2.10 | 131.15 | 0.594 | 1.730 | 6.412 | 12414 | 36126 | 133914 |
| | 60 | 196.9 | 521 | 1709 | 1786 | 5859 | 0.45 | 2.06 | 128.62 | 0.559 | 1.625 | 5.824 | 11672 | 33931 | 121645 |
| | 60 | 196.9 | 500 | 1640 | 1818 | 5965 | 0.46 | 2.08 | 129.88 | 0.520 | 1.518 | 6.184 | 10863 | 31700 | 129158 |
| | 60.5 | 198.5 | 549 | 1803 | 1818 | 5965 | 0.45 | 2.08 | 129.88 | 0.628 | 1.821 | 6.040 | 13118 | 38035 | 126151 |
| | 60.5 | 198.5 | 538 | 1764 | 1786 | 5859 | 0.45 | 2.06 | 128.62 | 0.596 | 1.727 | 5.776 | 12437 | 36072 | 120625 |
| | 61 | 200.1 | 521 | 1709 | 1852 | 6076 | 0.46 | 2.10 | 131.15 | 0.570 | 1.661 | 6.445 | 11902 | 34684 | 134596 |
| | 61 | 200.1 | 515 | 1691 | 1852 | 6076 | 0.46 | 2.10 | 131.15 | 0.558 | 1.628 | 6.460 | 11658 | 33995 | 134922 |
| | 61 | 200.1 | 521 | 1709 | 1852 | 6076 | 0.46 | 2.10 | 131.15 | 0.570 | 1.661 | 6.445 | 11902 | 34684 | 134596 |
| | 61.5 | 201.8 | 495 | 1624 | 1818 | 5965 | 0.46 | 2.08 | 129.88 | 0.510 | 1.489 | 6.198 | 10649 | 31094 | 129443 |
| | 61.5 | 201.8 | 549 | 1803 | 1852 | 6076 | 0.45 | 2.10 | 131.15 | 0.634 | 1.841 | 6.359 | 13246 | 38459 | 132805 |
| | 62 | 203.4 | 667 | 2187 | 1786 | 5859 | 0.42 | 2.06 | 128.62 | 0.916 | 2.599 | 5.349 | 19124 | 54274 | 111710 |
| | 62 | 203.4 | 532 | 1745 | 1818 | 5965 | 0.45 | 2.08 | 129.88 | 0.589 | 1.711 | 6.093 | 12294 | 35731 | 127250 |
| | 62.5 | 205.1 | 556 | 1823 | 1852 | 6076 | 0.45 | 2.10 | 131.15 | 0.648 | 1.881 | 6.340 | 13542 | 39286 | 132410 |
| | 62.5 | 205.1 | 588 | 1930 | 1786 | 5859 | 0.44 | 2.06 | 128.62 | 0.713 | 2.052 | 5.619 | 14889 | 42854 | 117356 |
| | 63 | 206.7 | 602 | 1976 | 1852 | 6076 | 0.44 | 2.10 | 131.15 | 0.762 | 2.197 | 6.188 | 15922 | 45883 | 129236 |
| | 63 | 206.7 | 641 | 2103 | 1818 | 5965 | 0.43 | 2.08 | 129.88 | 0.855 | 2.443 | 5.738 | 17855 | 51030 | 119835 |
| | 63.5 | 208.3 | 610 | 2001 | 1786 | 5859 | 0.43 | 2.06 | 128.62 | 0.766 | 2.197 | 5.548 | 15998 | 45883 | 115877 |
| | 63.5 | 208.3 | 587 | 1924 | 1818 | 5965 | 0.44 | 2.08 | 129.88 | 0.716 | 2.064 | 5.923 | 14947 | 43105 | 123712 |
| | 64 | 210.0 | 602 | 1976 | 1667 | 5468 | 0.42 | 1.98 | 123.58 | 0.718 | 2.047 | 4.541 | 15004 | 42758 | 94843 |
| | 64.5 | 211.6 | 585 | 1919 | 1818 | 5965 | 0.44 | 2.08 | 129.88 | 0.711 | 2.052 | 5.929 | 14860 | 42865 | 123829 |
| | 64.5 | 211.6 | 602 | 1976 | 1786 | 5859 | 0.44 | 2.06 | 128.62 | 0.748 | 2.147 | 5.573 | 15615 | 44840 | 116388 |
| | 65 | 213.3 | 543 | 1783 | 1667 | 5468 | 0.44 | 1.98 | 123.58 | 0.585 | 1.685 | 4.719 | 12212 | 35183 | 98565 |
| | 65 | 213.3 | 541 | 1773 | 1667 | 5468 | 0.44 | 1.98 | 123.58 | 0.578 | 1.667 | 4.728 | 12080 | 34821 | 98741 |
| | 65 | 213.3 | 575 | 1886 | 1818 | 5965 | 0.44 | 2.08 | 129.88 | 0.687 | 1.985 | 5.961 | 14352 | 41462 | 124506 |
| | 65.5 | 214.9 | 543 | 1783 | 1818 | 5965 | 0.45 | 2.08 | 129.88 | 0.615 | 1.783 | 6.058 | 12834 | 37244 | 126529 |
| | 66 | 216.5 | 513 | 1682 | 1754 | 5756 | 0.45 | 2.04 | 127.35 | 0.536 | 1.559 | 5.564 | 11205 | 32568 | 116196 |
| | 66.5 | 218.2 | 493 | 1616 | 1818 | 5965 | 0.46 | 2.08 | 129.88 | 0.505 | 1.475 | 6.204 | 10544 | 30797 | 129583 |
| | 67 | 219.8 | 518 | 1700 | 1786 | 5859 | 0.45 | 2.06 | 128.62 | 0.553 | 1.608 | 5.832 | 11552 | 33593 | 121806 |
| | 67.5 | 221.5 | 571 | 1875 | 1754 | 5756 | 0.44 | 2.04 | 127.35 | 0.666 | 1.919 | 5.391 | 13912 | 40086 | 112586 |
| | 68 | 223.1 | 625 | 2051 | 1786 | 5859 | 0.43 | 2.06 | 128.62 | 0.805 | 2.302 | 5.497 | 16808 | 48078 | 114797 |
| | 68.5 | 224.7 | 625 | 2051 | 1818 | 5965 | 0.43 | 2.08 | 129.88 | 0.813 | 2.329 | 5.794 | 16973 | 48645 | 121011 |
| | 68.5 | 224.7 | 641 | 2103 | 1852 | 6076 | 0.43 | 2.10 | 131.15 | 0.863 | 2.472 | 6.053 | 18029 | 51633 | 126427 |
| | 69.5 | 228.0 | 617 | 2025 | 1818 | 5965 | 0.43 | 2.08 | 129.88 | 0.793 | 2.275 | 5.821 | 16557 | 47513 | 121566 |
| | 70 | 229.7 | 637 | 2090 | 1887 | 6190 | 0.44 | 2.12 | 132.42 | 0.861 | 2.471 | 6.404 | 17973 | 51607 | 133747 |
| | 70.5 | 231.3 | 667 | 2187 | 1852 | 6076 | 0.43 | 2.10 | 131.15 | 0.934 | 2.662 | 5.959 | 19500 | 55598 | 124465 |

γ = Poisson's Ratio  ρ(Vp) = Vp-derived density  G = Shear Modulus  E = Young's Modulus  K = Bulk Modulus
Shaded cells denote questionable data.

**Table 2.** LA 710 tunnel
Boring Z2 B5
PS Suspension Log Data Summary



| Top of Hole Elevation (m) | Depth (m) | Depth (ft) | Vs (m/s) | Vs (ft/s) | Vp (m/s) | Vp (ft/s) | γ | ρ(Vp) (g/cc) | ρ(Vp) ($lb/ft^3$) | G (GPa) | E (GPa) | K (GPa) | G ($10^3 lb/ft^2$) | E ($10^3 lb/ft^2$) | K ($10^3 lb/ft^2$) |
|---|---|---|---|---|---|---|---|---|---|---|---|---|---|---|---|
| | 71 | 232.9 | 610 | 2001 | 1786 | 5859 | 0.43 | 2.06 | 128.62 | 0.766 | 2.197 | 5.548 | 15998 | 45883 | 115877 |
| | 71.5 | 234.6 | 535 | 1754 | 1754 | 5756 | 0.45 | 2.04 | 127.35 | 0.583 | 1.690 | 5.501 | 12184 | 35304 | 114891 |
| | 71.5 | 234.6 | 565 | 1854 | 1852 | 6076 | 0.45 | 2.10 | 131.15 | 0.671 | 1.943 | 6.310 | 14005 | 40577 | 131793 |
| | 72.5 | 237.9 | 538 | 1764 | 1818 | 5965 | 0.45 | 2.08 | 129.88 | 0.601 | 1.746 | 6.076 | 12560 | 36476 | 126895 |
| | 72.5 | 237.9 | 621 | 2038 | 1852 | 6076 | 0.44 | 2.10 | 131.15 | 0.810 | 2.329 | 6.124 | 16927 | 48635 | 127896 |
| | 73 | 239.5 | 588 | 1930 | 1852 | 6076 | 0.44 | 2.10 | 131.15 | 0.727 | 2.099 | 6.235 | 15182 | 43842 | 130223 |
| | 74 | 242.8 | 617 | 2025 | 1852 | 6076 | 0.44 | 2.10 | 131.15 | 0.800 | 2.301 | 6.137 | 16718 | 48065 | 128175 |
| | 74 | 242.8 | 592 | 1941 | 1852 | 6076 | 0.44 | 2.10 | 131.15 | 0.736 | 2.123 | 6.224 | 15362 | 44340 | 129983 |
| | 74.5 | 244.4 | 671 | 2202 | 1887 | 6190 | 0.43 | 2.12 | 132.42 | 0.955 | 2.728 | 6.277 | 19955 | 56973 | 131105 |
| | 75.5 | 247.7 | 714 | 2343 | 1852 | 6076 | 0.41 | 2.10 | 131.15 | 1.072 | 3.028 | 5.775 | 22386 | 63244 | 120618 |
| | 75.5 | 247.7 | 690 | 2263 | 1887 | 6190 | 0.42 | 2.12 | 132.42 | 1.009 | 2.871 | 6.206 | 21071 | 59963 | 129617 |
| | 76 | 249.3 | 671 | 2202 | 1961 | 6433 | 0.43 | 2.16 | 134.97 | 0.974 | 2.792 | 7.014 | 20339 | 58317 | 146485 |
| | 77 | 252.6 | 578 | 1896 | 1923 | 6309 | 0.45 | 2.14 | 133.69 | 0.716 | 2.076 | 6.966 | 14944 | 43349 | 145485 |
| | 77.5 | 254.3 | 658 | 2158 | 1786 | 5859 | 0.42 | 2.06 | 128.62 | 0.892 | 2.535 | 5.381 | 18624 | 52947 | 112376 |
| | 77.5 | 254.3 | 613 | 2013 | 1786 | 5859 | 0.43 | 2.06 | 128.62 | 0.775 | 2.222 | 5.536 | 16195 | 46418 | 115615 |
| | 77.5 | 254.3 | 658 | 2158 | 1786 | 5859 | 0.42 | 2.06 | 128.62 | 0.892 | 2.535 | 5.381 | 18624 | 52947 | 112376 |
| | 78 | 255.9 | 627 | 2057 | 1754 | 5756 | 0.43 | 2.04 | 127.35 | 0.802 | 2.288 | 5.210 | 16748 | 47791 | 108806 |
| | 78.5 | 257.5 | 485 | 1593 | 1724 | 5657 | 0.46 | 2.02 | 126.09 | 0.476 | 1.387 | 5.370 | 9941 | 28967 | 112147 |
| | 79 | 259.2 | 538 | 1764 | 1786 | 5859 | 0.45 | 2.06 | 128.62 | 0.596 | 1.727 | 5.776 | 12437 | 36072 | 120625 |
| | 79.5 | 260.8 | 575 | 1886 | 1786 | 5859 | 0.44 | 2.06 | 128.62 | 0.680 | 1.963 | 5.662 | 14212 | 40994 | 118259 |
| | 80 | 262.5 | 457 | 1498 | 1818 | 5965 | 0.47 | 2.08 | 129.88 | 0.434 | 1.272 | 6.299 | 9060 | 26569 | 131562 |
| | 80.5 | 264.1 | 490 | 1608 | 1887 | 6190 | 0.46 | 2.12 | 132.42 | 0.510 | 1.492 | 6.872 | 10645 | 31165 | 143517 |
| | 81 | 265.7 | 662 | 2173 | 1923 | 6309 | 0.43 | 2.14 | 133.69 | 0.939 | 2.691 | 6.668 | 19616 | 56210 | 139256 |
| | 81.5 | 267.4 | 505 | 1657 | 1887 | 6190 | 0.46 | 2.12 | 132.42 | 0.541 | 1.581 | 6.830 | 11300 | 33028 | 142644 |
| | 82 | 269.0 | 654 | 2144 | 2083 | 6835 | 0.45 | 2.22 | 138.82 | 0.950 | 2.746 | 8.385 | 19839 | 57352 | 175117 |
| | 82.5 | 270.7 | 658 | 2158 | 2500 | 8202 | 0.46 | 2.39 | 149.21 | 1.035 | 3.027 | 13.559 | 21606 | 63210 | 283181 |
| | 83 | 272.3 | 873 | 2865 | 2778 | 9113 | 0.45 | 2.47 | 154.48 | 1.887 | 5.455 | 16.577 | 39420 | 113936 | 346210 |
| | 83.5 | 274.0 | 885 | 2903 | 2632 | 8634 | 0.44 | 2.43 | 151.84 | 1.905 | 5.471 | 14.304 | 39782 | 114273 | 298739 |
| | 84 | 275.6 | 595 | 1953 | 1961 | 6433 | 0.45 | 2.16 | 134.97 | 0.766 | 2.220 | 7.291 | 15999 | 46372 | 152272 |
| | 84.5 | 277.2 | 658 | 2158 | 2000 | 6562 | 0.44 | 2.18 | 136.25 | 0.945 | 2.719 | 7.471 | 19729 | 56794 | 156024 |
| | 85 | 278.9 | 826 | 2711 | 2000 | 6562 | 0.40 | 2.18 | 136.25 | 1.491 | 4.165 | 6.742 | 31133 | 86989 | 140818 |
| | 85.5 | 280.5 | 741 | 2430 | 1923 | 6309 | 0.41 | 2.14 | 133.69 | 1.175 | 3.320 | 6.353 | 24542 | 69349 | 132689 |
| | 86 | 282.2 | 709 | 2327 | 1852 | 6076 | 0.41 | 2.10 | 131.15 | 1.057 | 2.988 | 5.795 | 22069 | 62414 | 121040 |
| | 86.5 | 283.8 | 597 | 1959 | 1818 | 5965 | 0.44 | 2.08 | 129.88 | 0.742 | 2.135 | 5.889 | 15487 | 44590 | 122992 |
| | 87 | 285.4 | 629 | 2063 | 1786 | 5859 | 0.43 | 2.06 | 128.62 | 0.815 | 2.329 | 5.483 | 17020 | 48650 | 114515 |
| | 87 | 285.4 | 623 | 2044 | 1818 | 5965 | 0.43 | 2.08 | 129.88 | 0.808 | 2.315 | 5.801 | 16868 | 48359 | 121152 |
| | 87.4 | 286.7 | 592 | 1941 | 1786 | 5859 | 0.44 | 2.06 | 128.62 | 0.721 | 2.075 | 5.608 | 15065 | 43338 | 117121 |

γ = Poisson's Ratio  ρ(Vp) = Vp-derived density  G = Shear Modulus  E = Young's Modulus  K = Bulk Modulus
Shaded cells denote questionable data.

# Figure 1. LA 710 Tunnel
# Boring Z2 B5
# Downhole Interval Velocities

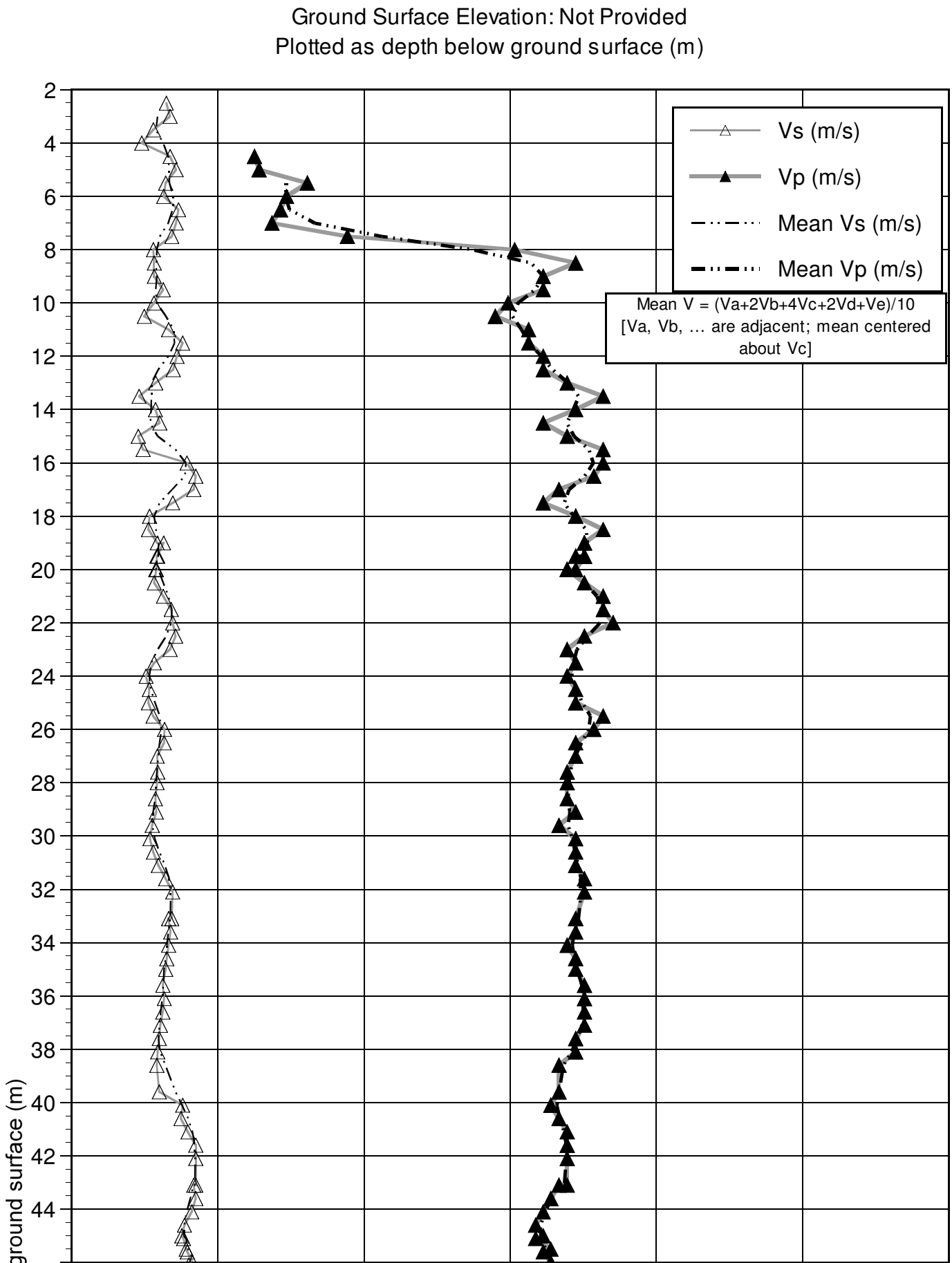

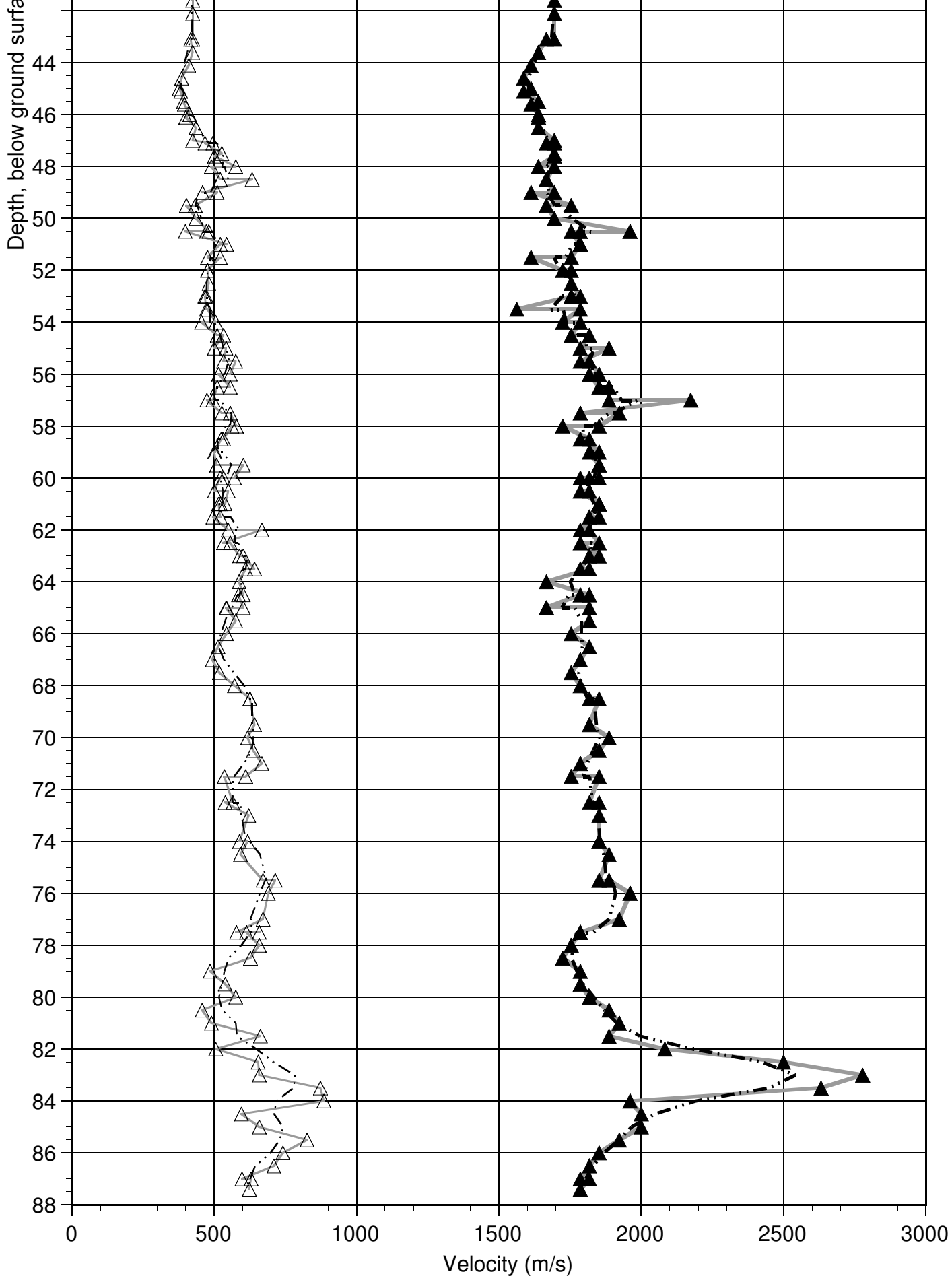
Depth, below ground surfa
44
46
48
50
52
54
56
58
60
62
64
66
68
70
72
74
76
78
80
82
84
86
88
0
500
1000
1500
2000
2500
3000
Velocity (m/s)

California Department of Transportation
Geophysical Services

# Z2 B5

| | | | |
|---|---|---|---|
| COMPANY | : CALTRANS | OTHER SERVICES: | |
| WELL | : Z2 B5 | | IND-CAL. |
| FIELD | : LA-710 Tunnel. | | AC TEL. |
| COUNTY | : LA | | PSLOG. |
| STATE | : CA | | |
| LOCATION | : | | |
| SECTION | : None | | |
| TOWNSHIP | : NONE | | |
| RANGE | : None | | |
| API NO. | : | | |
| UNIQUE WELL ID. | : | | |
| PERMANENT DATUM | : None | ELEVATION KB | : NA |
| LOG MEASURED FROM | : GL | ELEVATION DF | : NA |
| DRL MEASURED FROM | : GL | ELEVATION GL | : 143.86 |
| DATE | : 04/14/09 | RIG NUMBER | : |
| DEPTH DRILLER | : 91.44m | LOGGER TD | : |
| BIT SIZE | : 10.8cm. | ARRIVAL TIME | : |
| LOG TOP | : 5.00 | DEPARTURE TIME | : |
| LOG BOTTOM | : 90.00 | CIRC STOPPED | : 4/14 AM |
| CASING OD | : | | |
| CASING BOTTOM | : n/a | | |
| CASING TYPE | : n/a | | |
| BOREHOLE FLUID | : 0 | | |
| RM TEMPERATURE | : 0 | | |
| MUD RES | : 0 | | |
| MUD WEIGHT | : | | |
| WITNESSED BY | : | | |
| RECORDED BY | : DH/DL | | |
| REMARKS 1 | : POORLY INDUR., SOIL-LIKE MATERIAL, POOR QUAL. ATV LOG. | | |
| REMARKS 2 | : BH COLLAPSE NEAR BOTTOM, NO MECH. CAL. AVAIL BELOW -82.6 M | | |

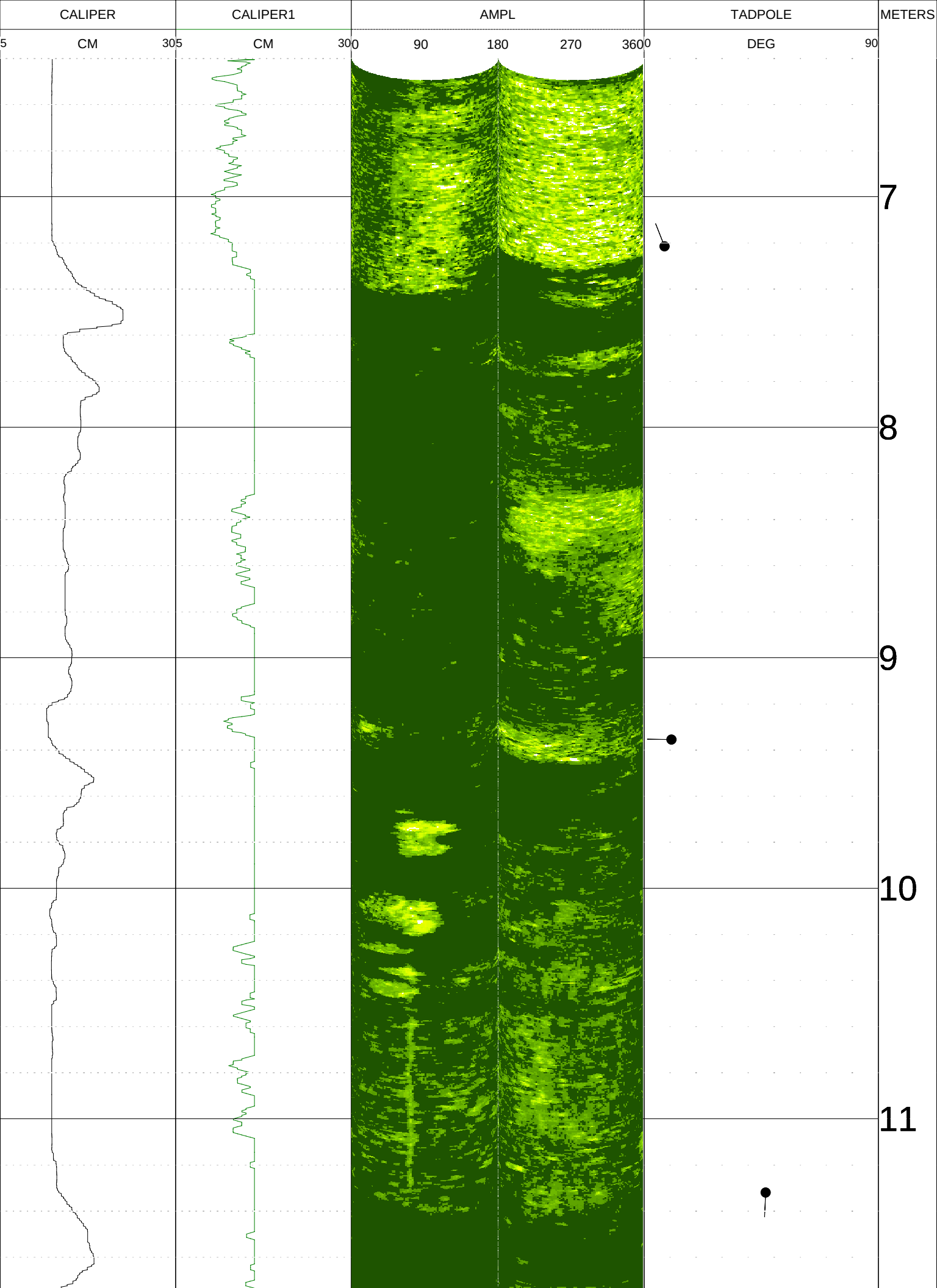
CALIPER
5
CM
30
CALIPER1
5
CM
30
AMPL
0
90
180
270
360
TADPOLE
0
DEG
90
METERS
7
8
9
10
11

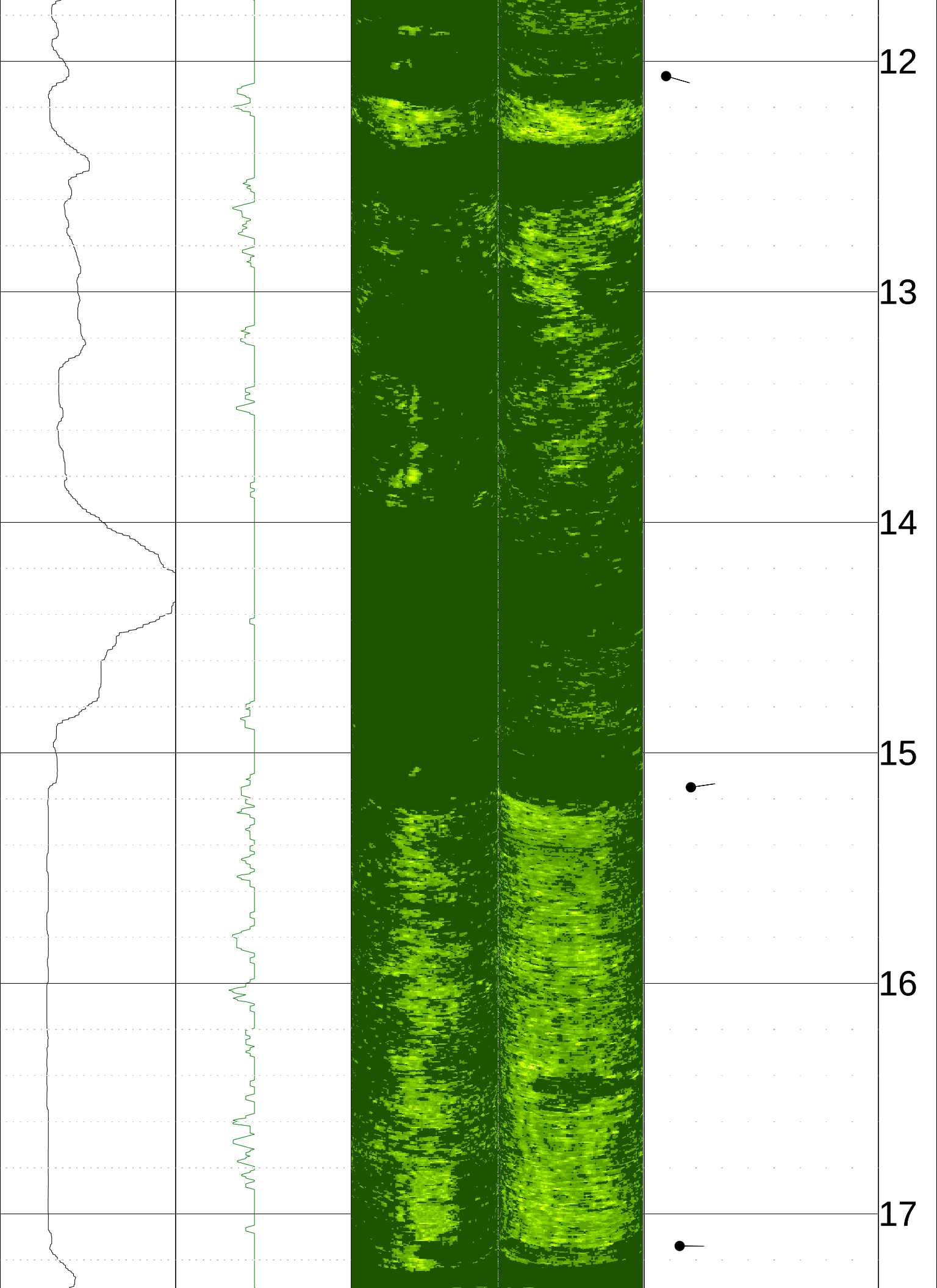
12
13
14
15
16
17

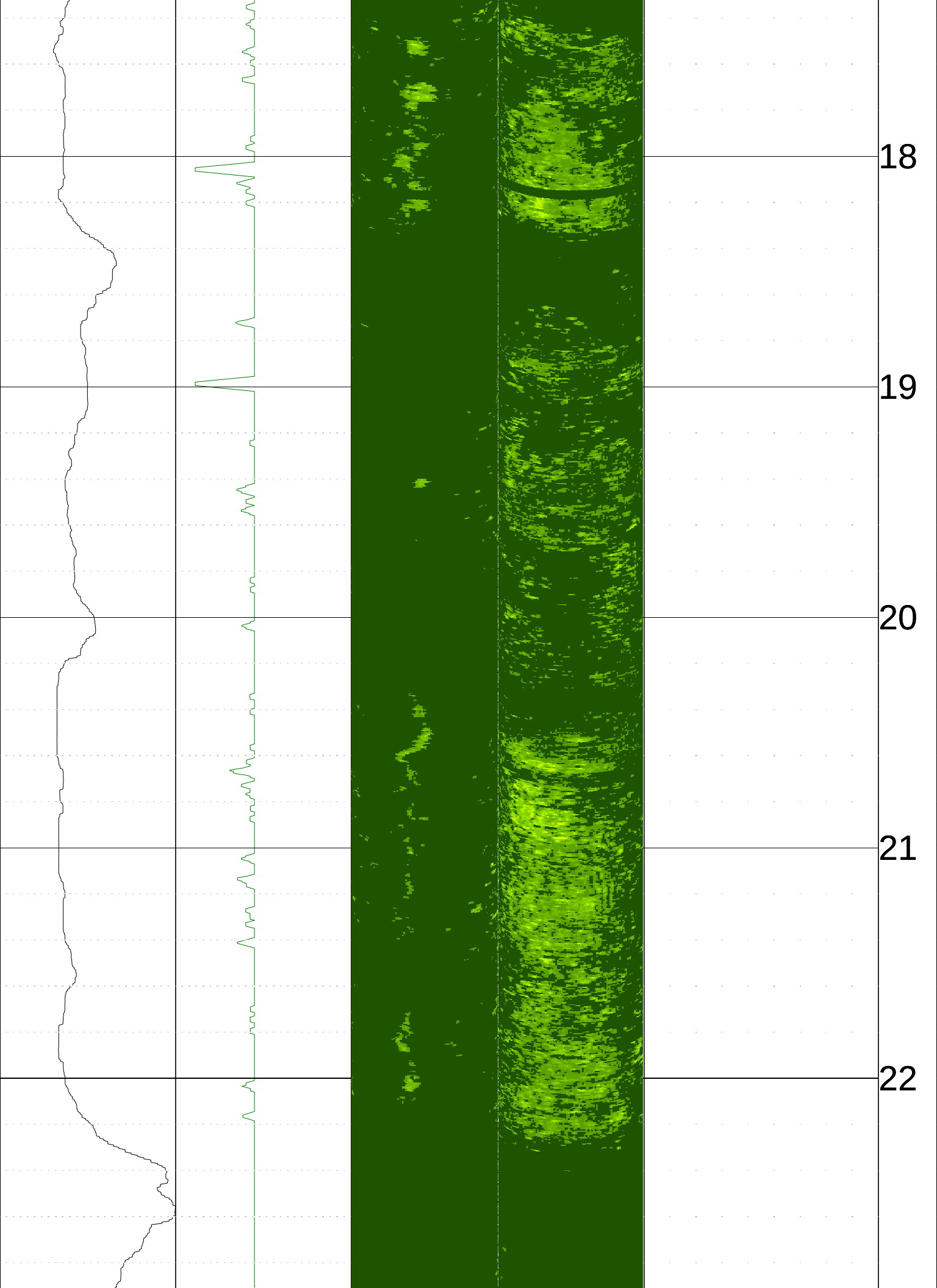
18
19
20
21
22

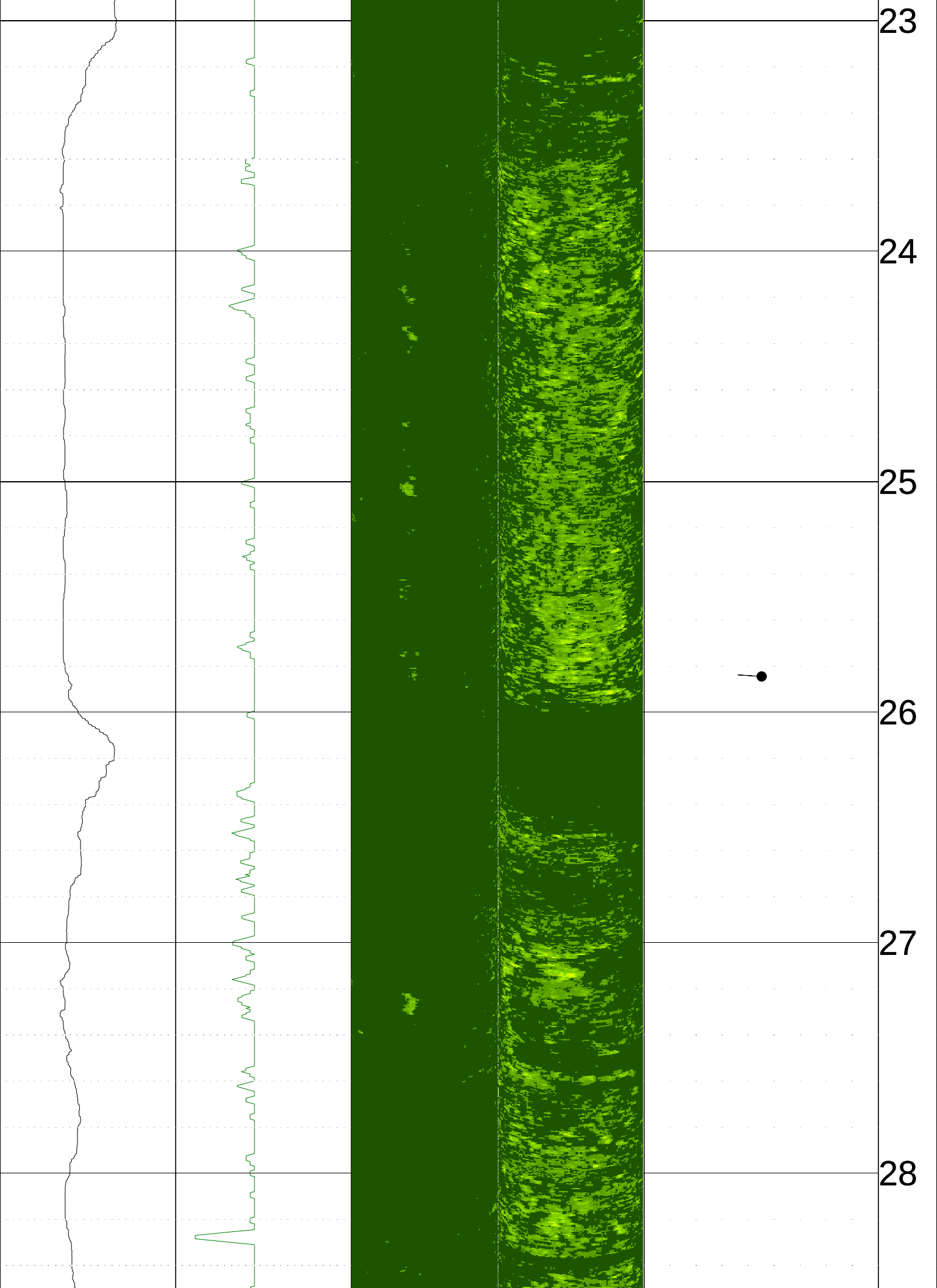
23
24
25
26
27
28

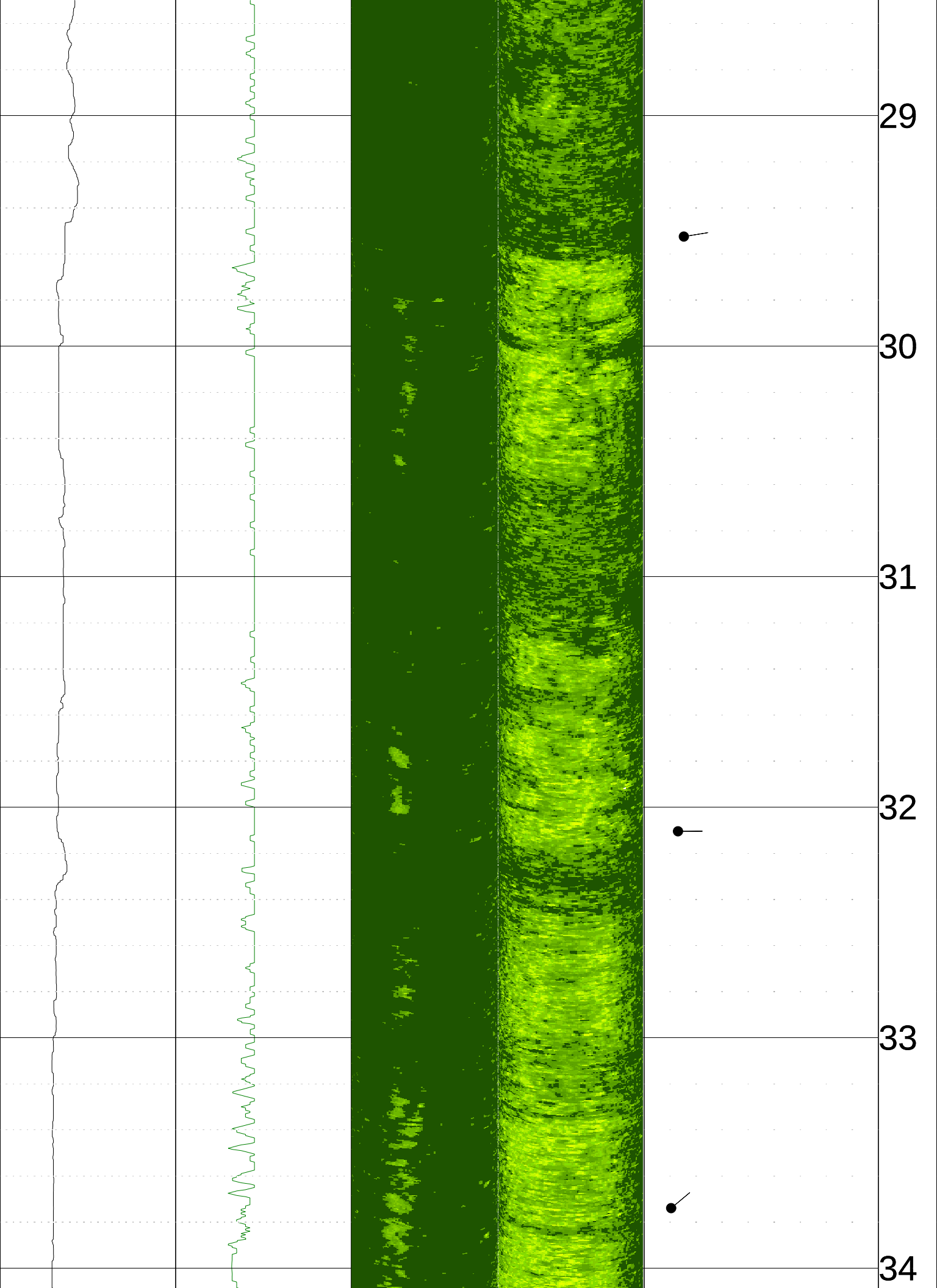
29
30
31
32
33
34

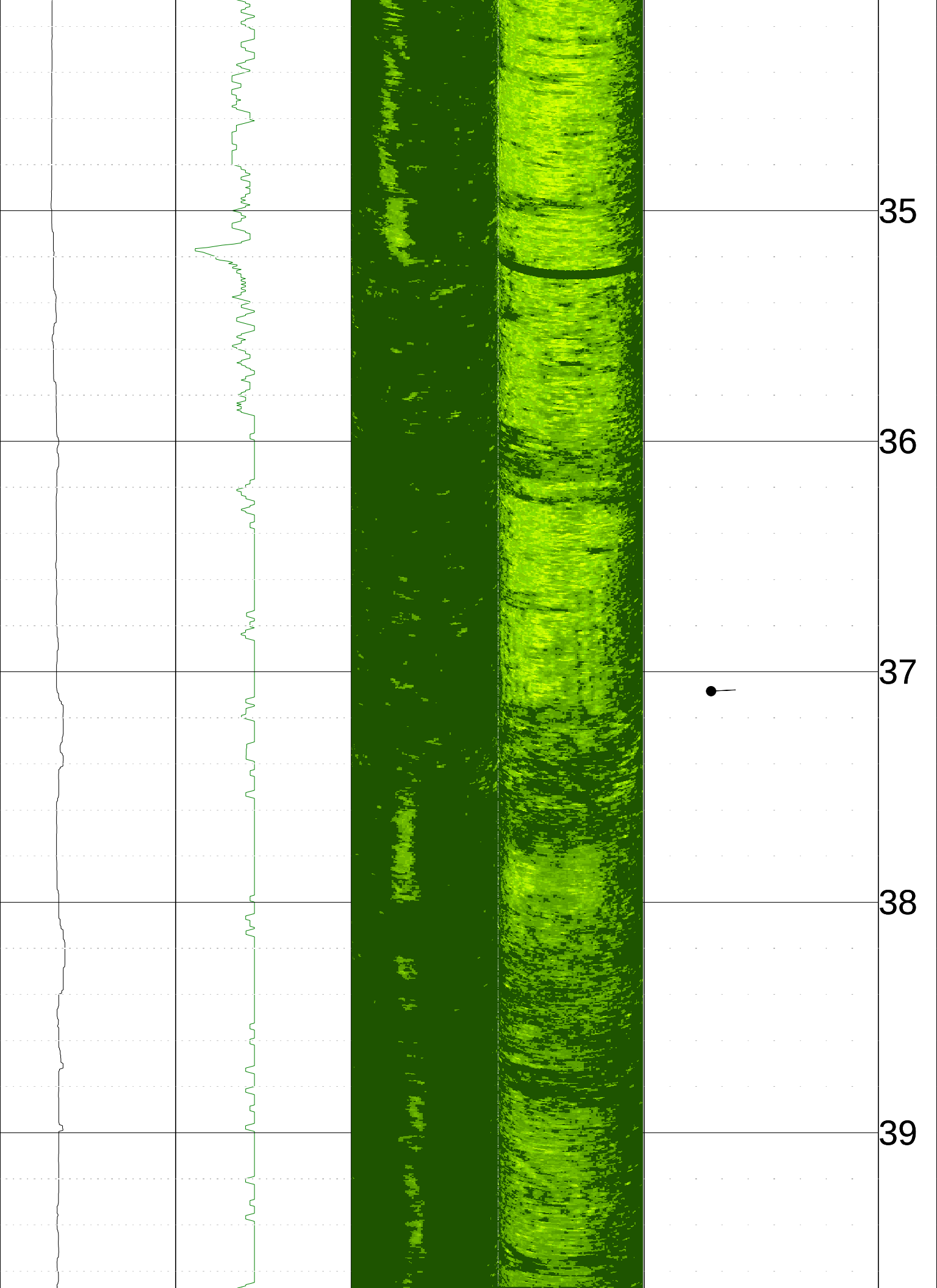
35
36
37
38
39

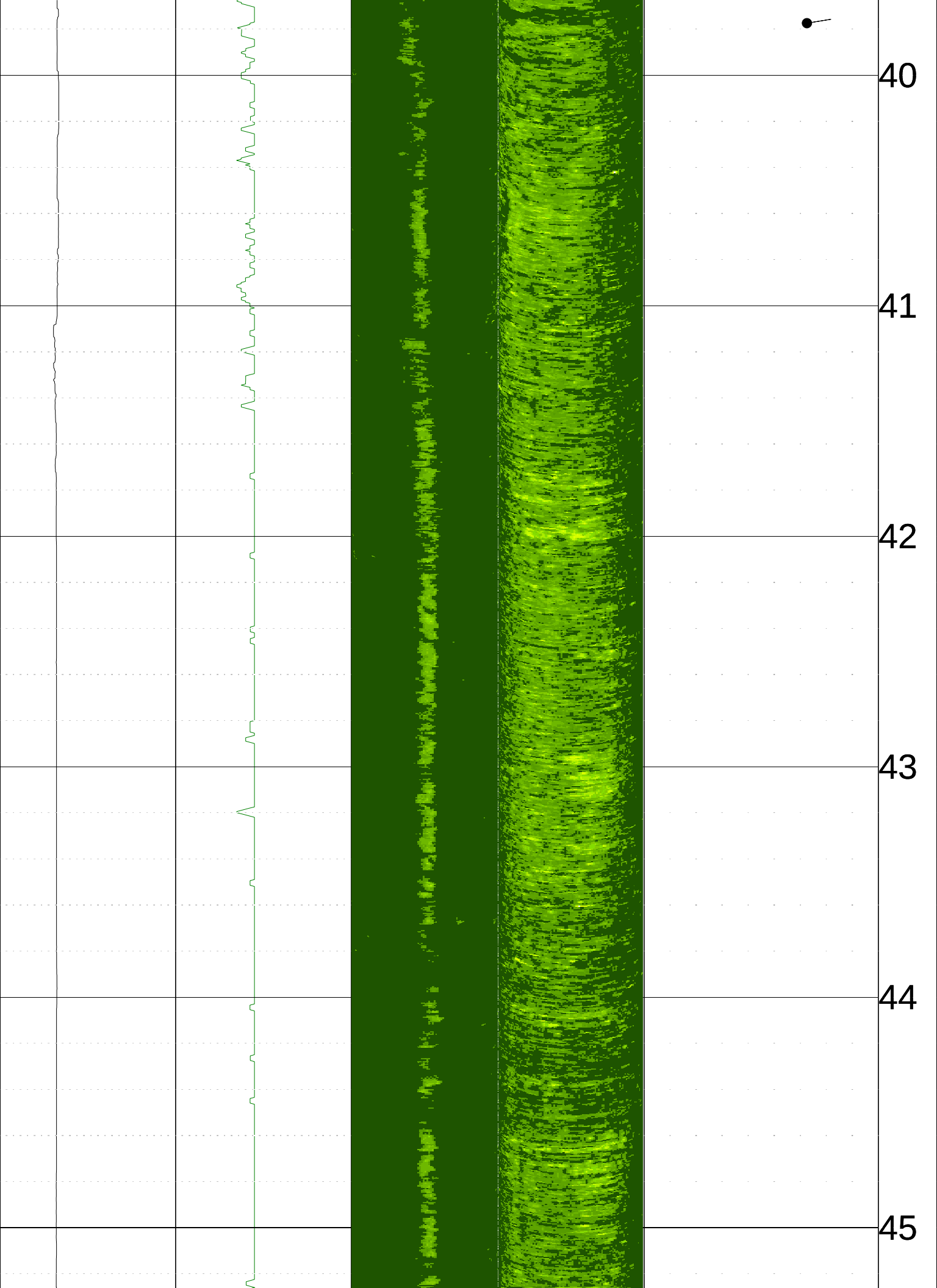
40
41
42
43
44
45

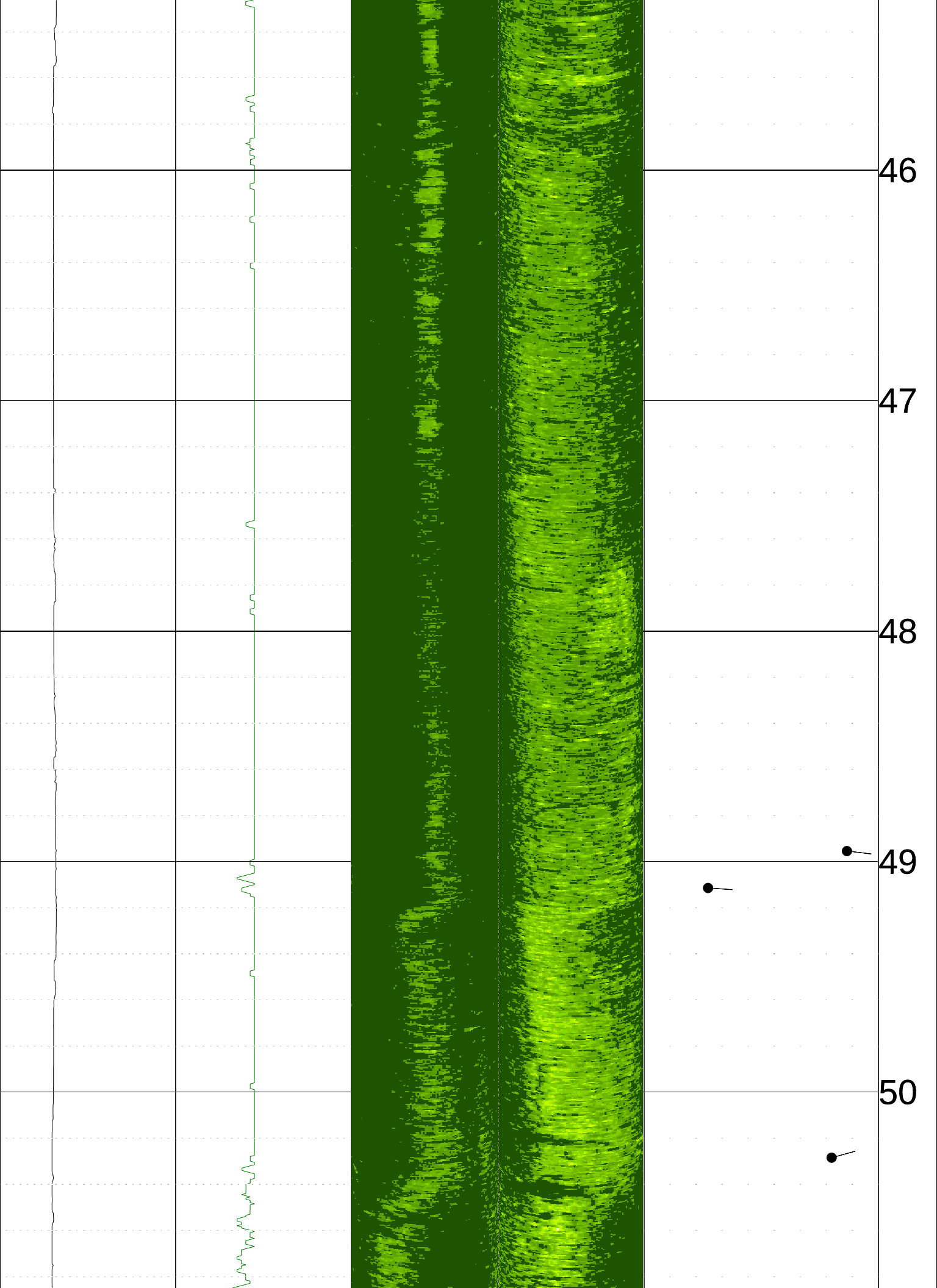
46
47
48
49
50

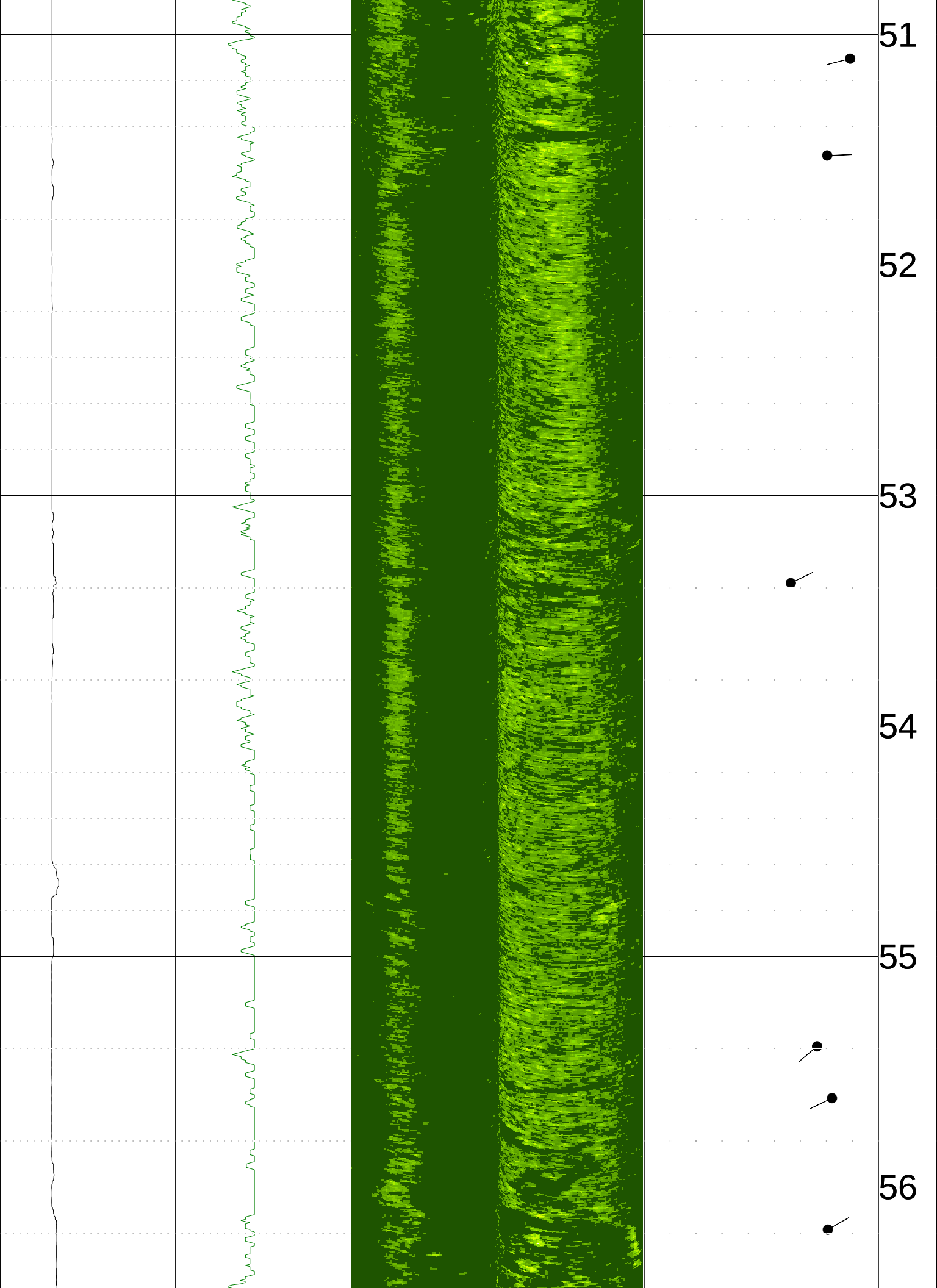
51
52
53
54
55
56

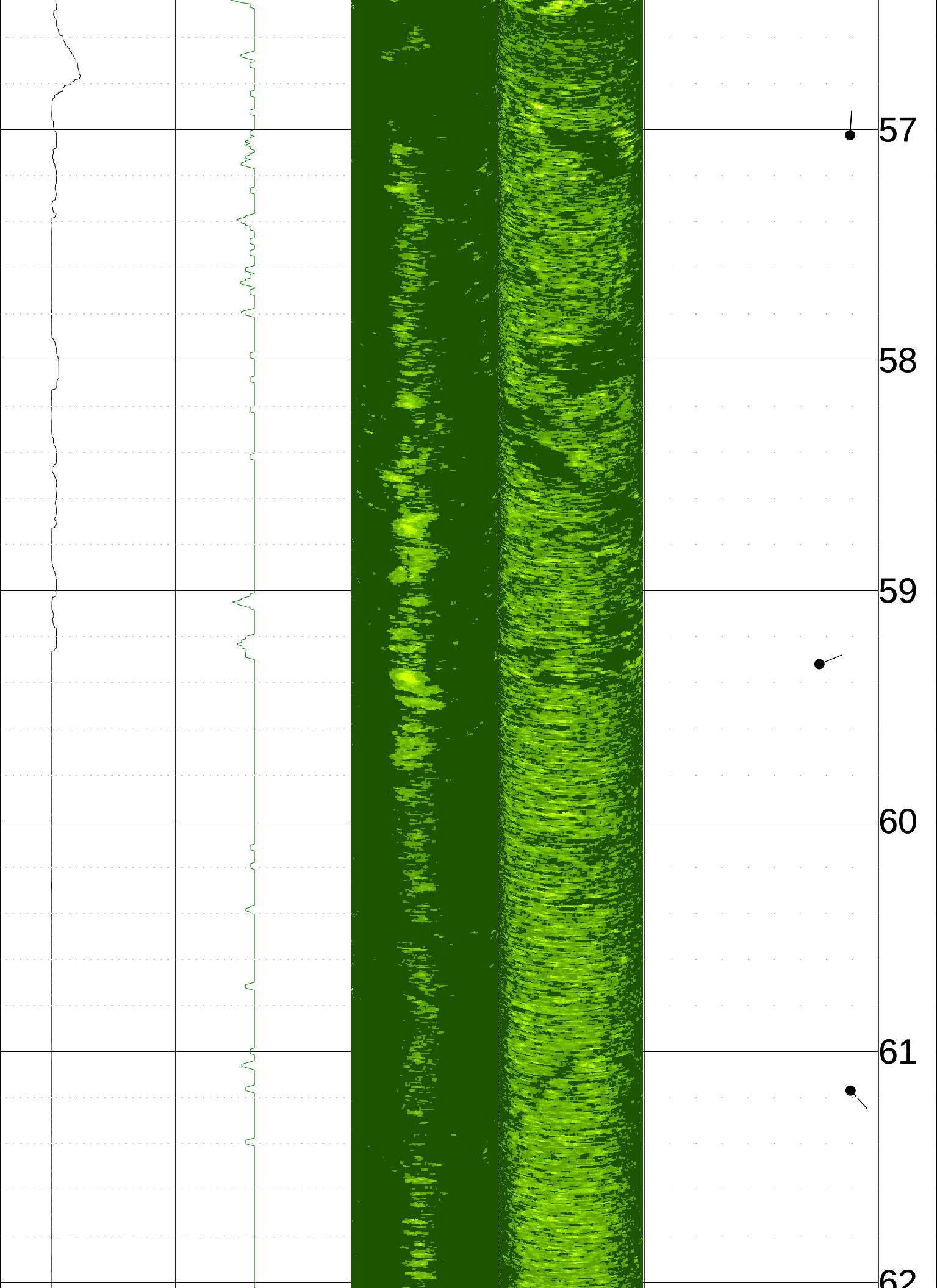
57
58
59
60
61
62

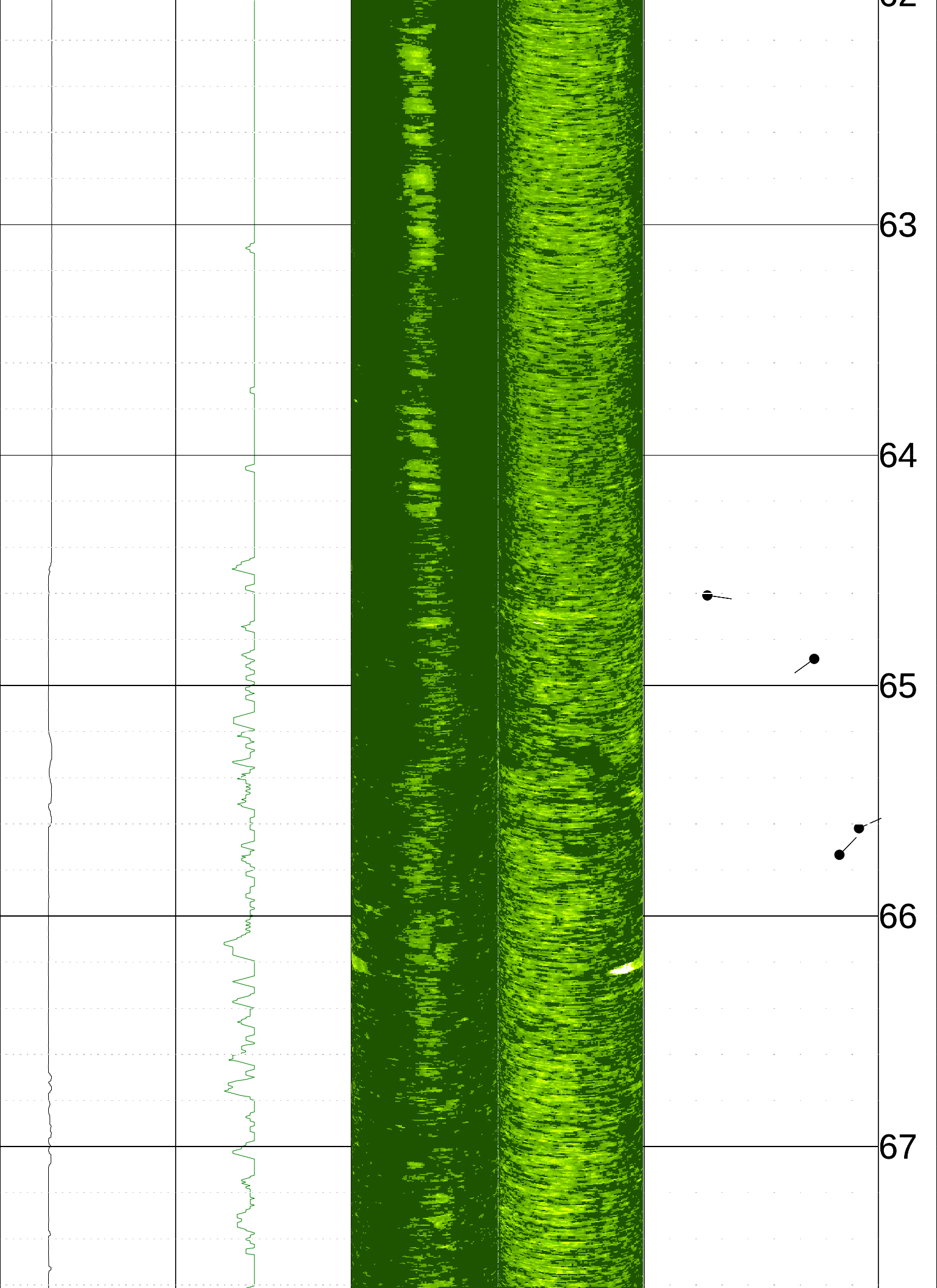
63
64
65
66
67

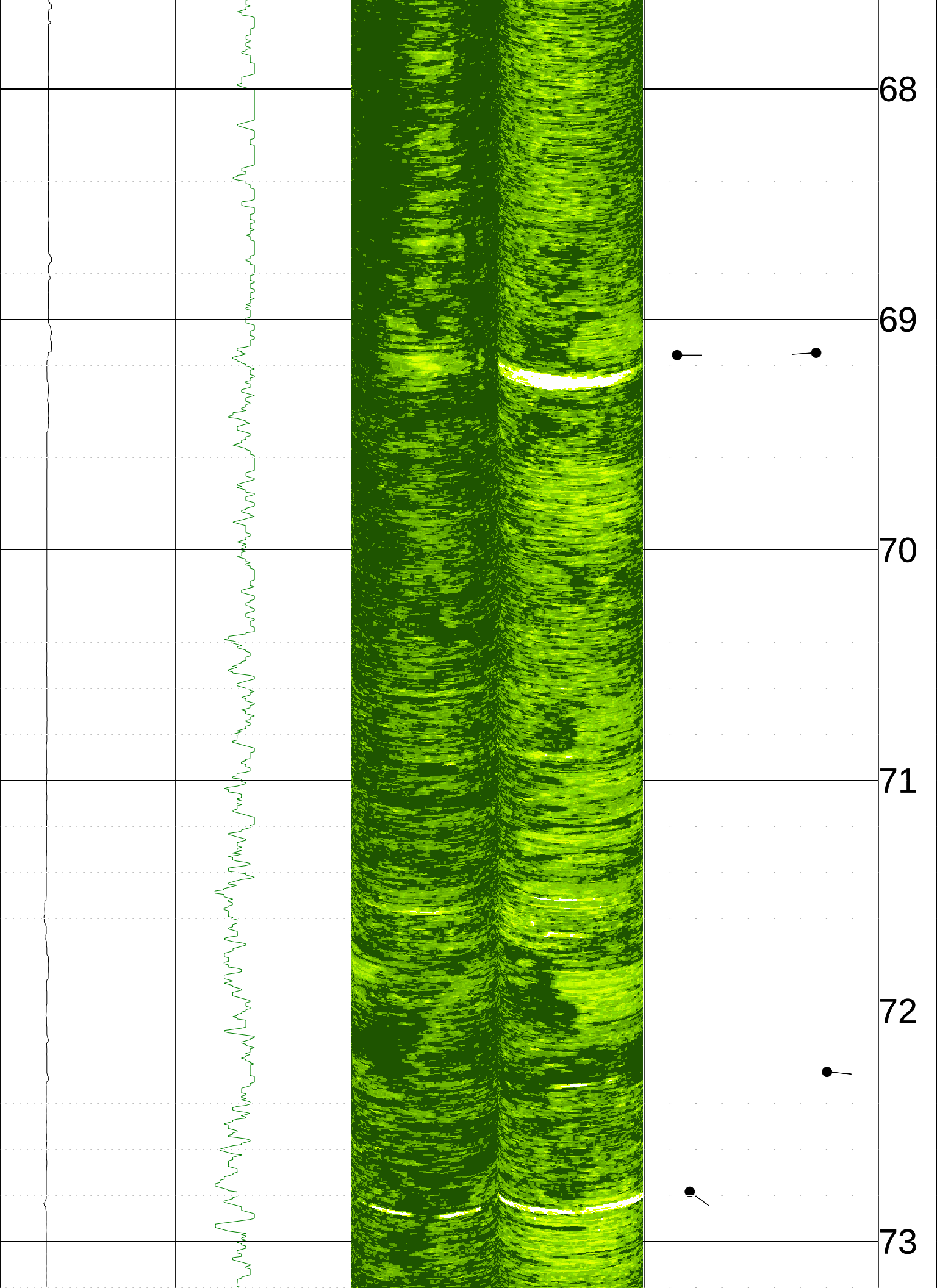
68
69
70
71
72
73

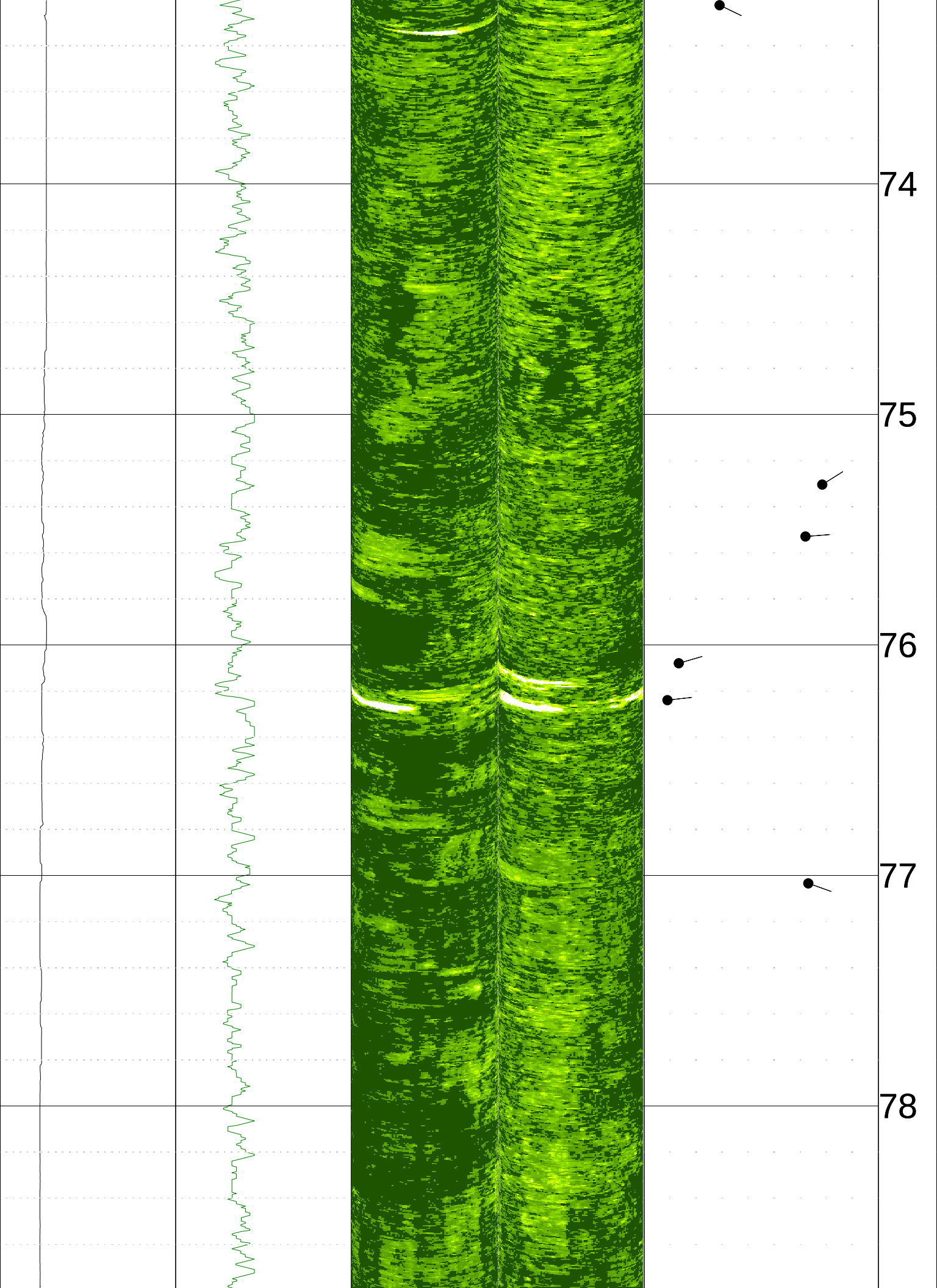
74
75
76
77
78

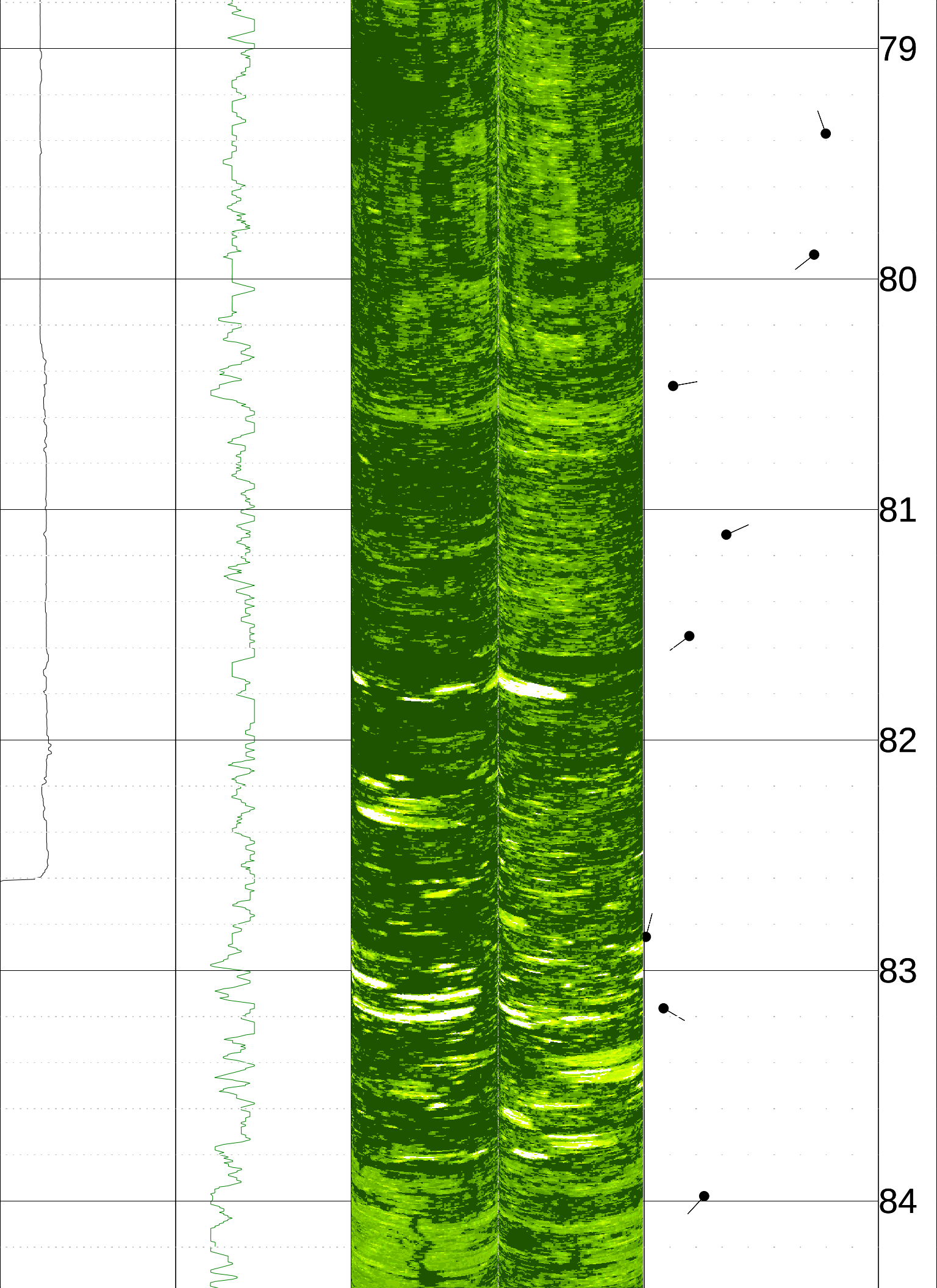
79
80
81
82
83
84

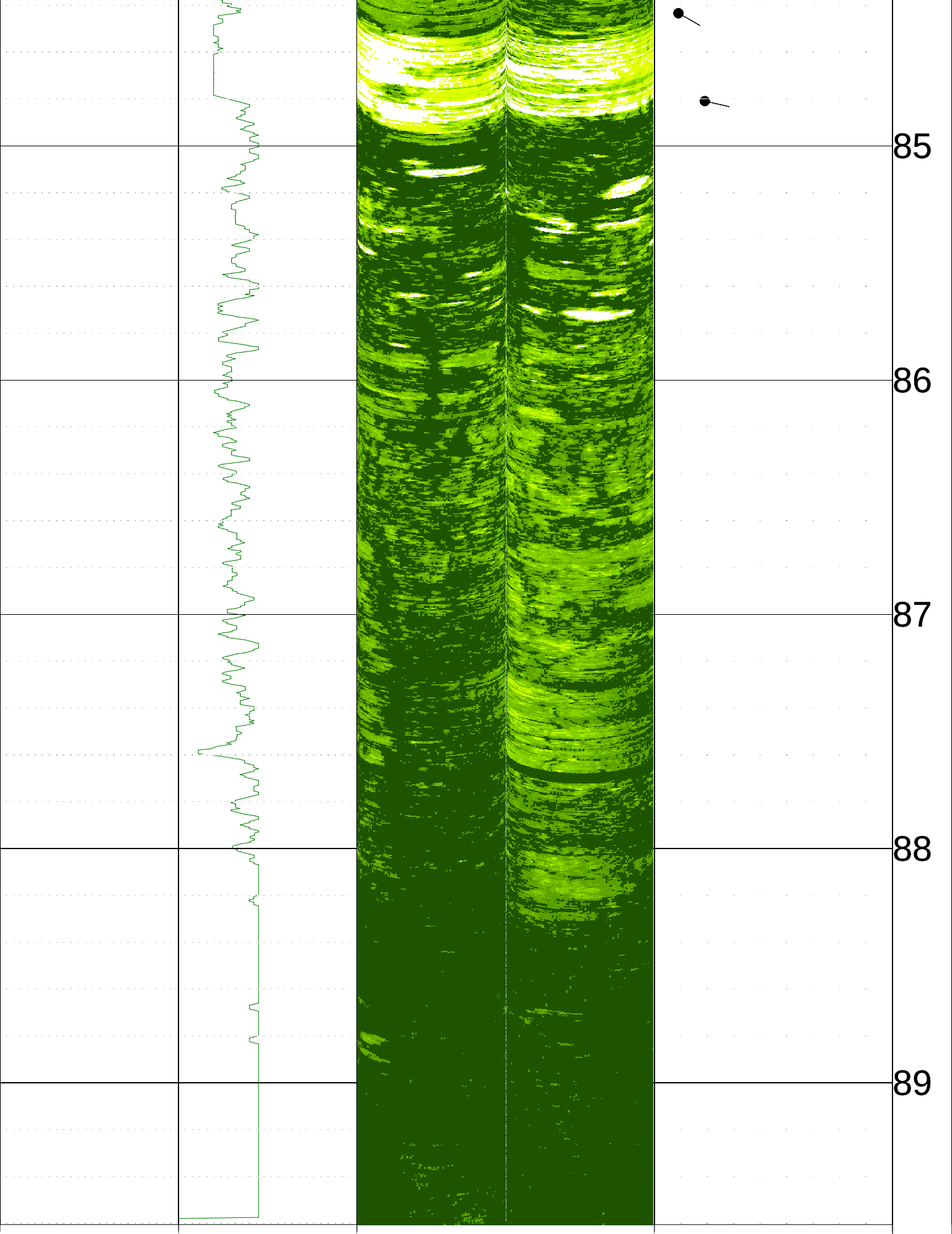
85
86
87
88
89
5
CM
30
5
CM
30
0
90
180
270
360
0
DEG
90
CALIPER
CALIPER1
AMPL
TADPOLE
METERS

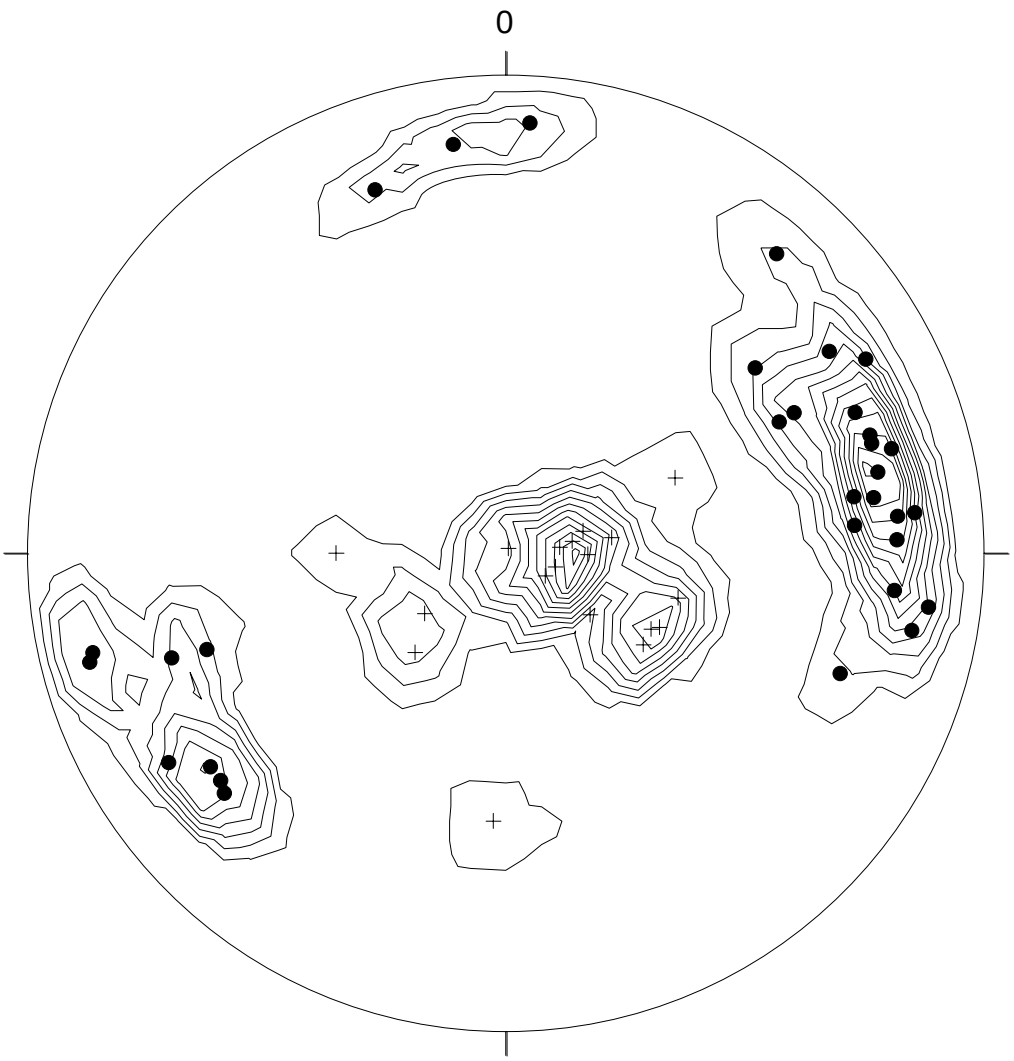


LA 710 Tunnel, boring Z2 B5

+ n=18 (P)
• n=32 (P)

Stereonet contour plot of poles to planes,
Both bedding and fractures

n=50
max. dens.=13.26 (at 76/ 24)
min. dens.=0.00
Contours at every integer between
1 and 13, inclusive:
(Multiples of random distribution)

Apparent bedding denoted as cross
Apparent fractures denoted as solid circle
Plotted on upper hemisphere


LA 710 Tunnel boring Z3 B2

| | | | | | |
|---|---|---|---|---|---|
| COMPANY | : CALTRANS | | | | |
| WELL | : Z3 B2 | | | | |
| LOCATION/FIELD | : LA 710 TUNNEL | | | | |
| COUNTY | : LA | | | | |
| LOCATION | : CA | | | | |
| SECTION | : None | TOWNSHIP | : None | RANGE | : None |
| DATE | : 1/20/09 | PERMANENT DATUM | : None | | |
| DEPTH DRILLER | : 83.8M | | | KB | : NA |
| LOG BOTTOM | : 83.8 | LOG MEASURED FROM: | GL | DF | : NA |
| LOG TOP | : 1.8 | DRL MEASURED FROM: | GL | GL | : NA |
| CASING DIAMETER | : N/A | LOGGING UNIT | : 7311 | | |
| CASING TYPE | : none | FIELD OFFICE | : 7311 | | |
| CASING THICKNESS: | 0 | RECORDED BY | : DH/DL | | |
| BIT SIZE | : 9.4CM | BOREHOLE FLUID | : 0 | FILE | : PROCESSE |
| MAGNETIC DECL. | : 12.85 | RM | : 0 | TYPE | : 9065A |
| MATRIX DENSITY | : 2.71 | RM TEMPERATURE | : 0 | LGDATE | : 1/20/09. |
| NEUTRON MATRIX | : DOLOMITE | MATRIX DELTA T | : 140 | | |
| | | | | THRESH: | 2500 |

OTHER SERVICES:
CAL-IND
AC TEL
PSLOG

CALIPER MEASUREMENT UNITS ARE CM DIAMETER
CALIPER MEASUREMENTS REPORTED AS "UNKNOWN", "UNDER" UNITS ARE CM DIA
GL ELEVATION NOT REPORTED, MEASURED AS 24.2M BY HANDHELD GPS

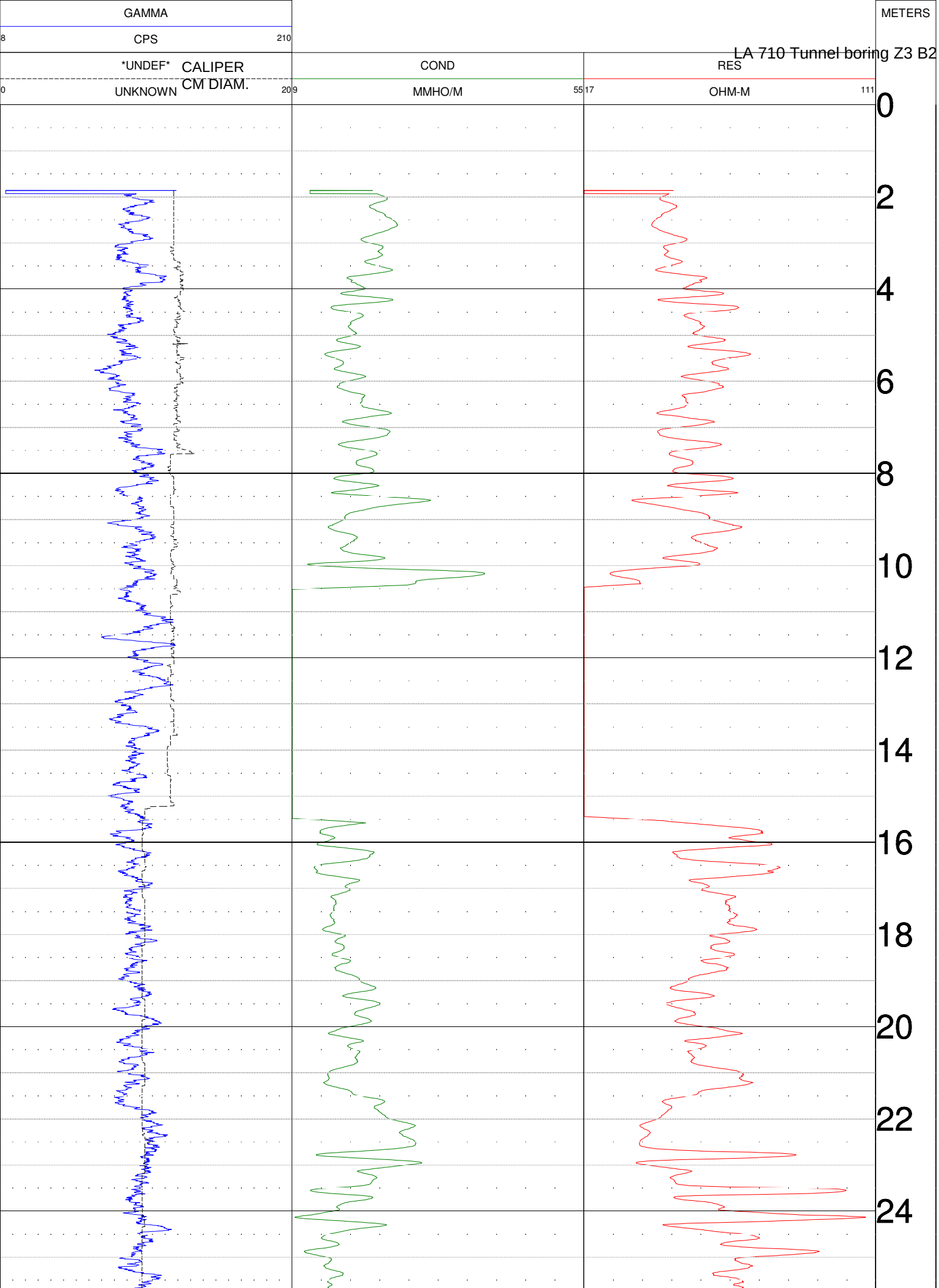
GAMMA
8
CPS
210
*UNDEF*
CALIPER
CM DIAM.
0
UNKNOWN
20
9
COND
MMHO/M
55
17
RES
OHM-M
111
METERS
LA 710 Tunnel boring Z3 B2
0
2
4
6
8
10
12
14
16
18
20
22
24

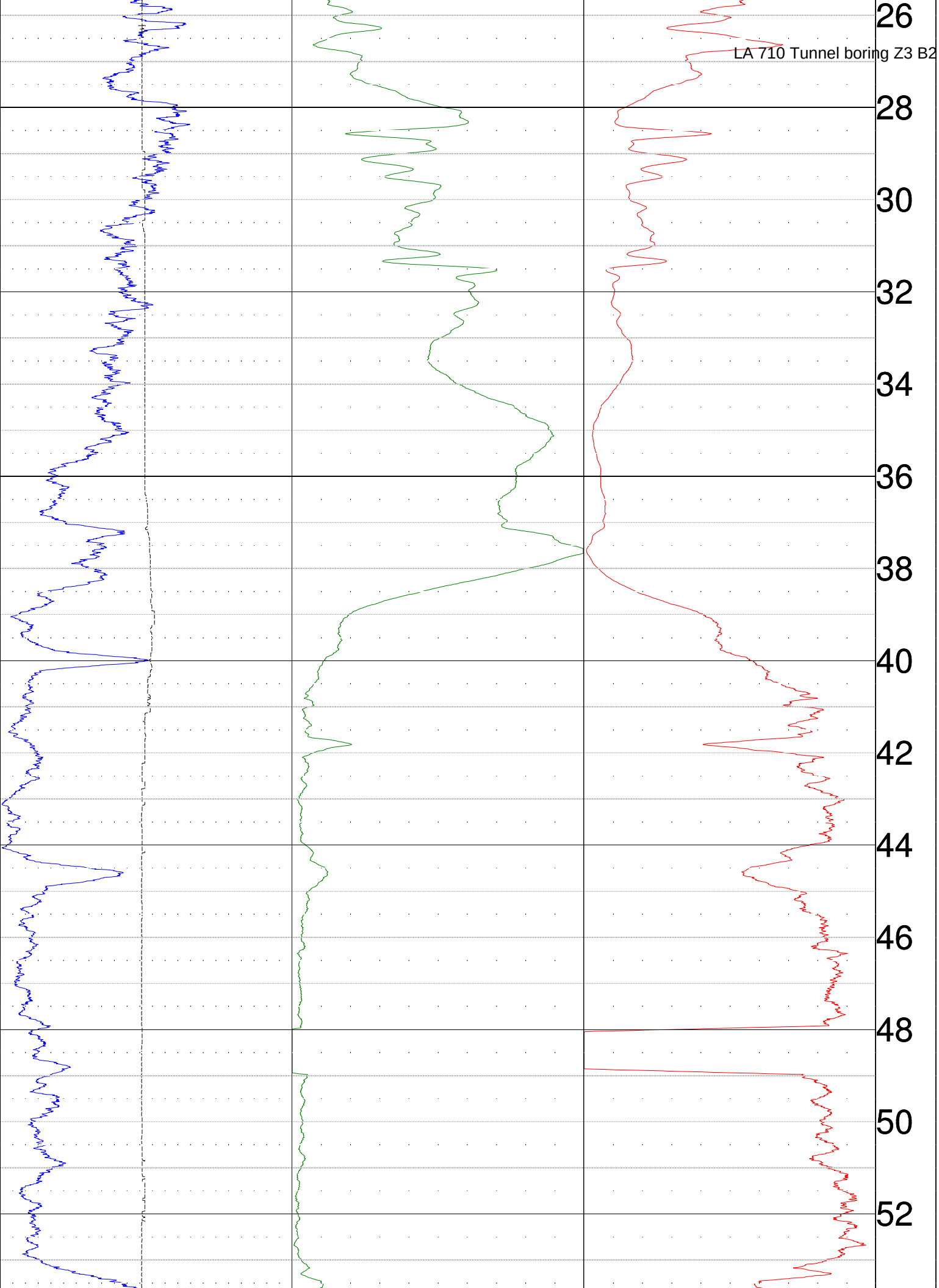
LA 710 Tunnel boring Z3 B2
26
28
30
32
34
36
38
40
42
44
46
48
50
52

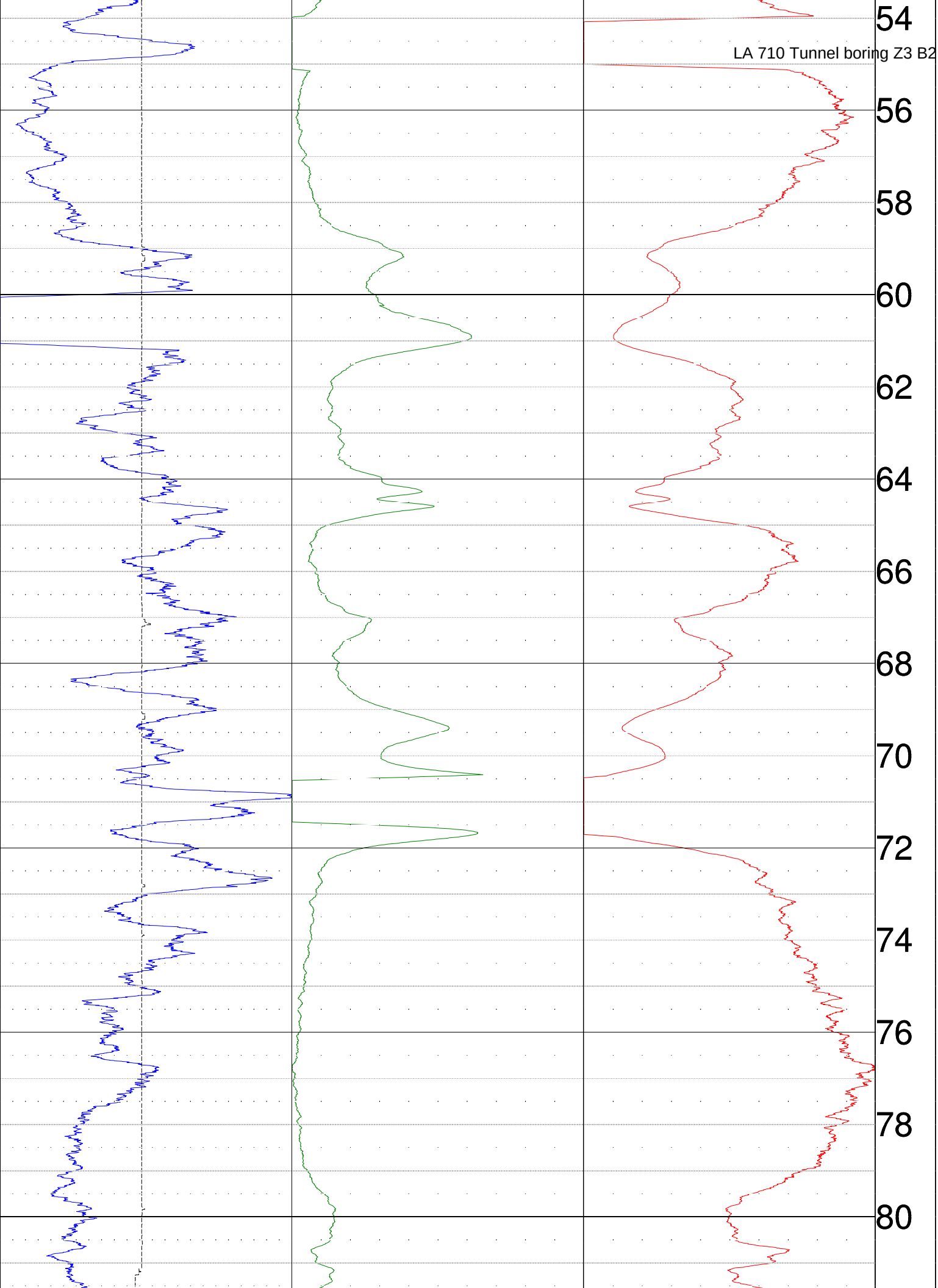
LA 710 Tunnel boring Z3 B2
54
56
58
60
62
64
66
68
70
72
74
76
78
80

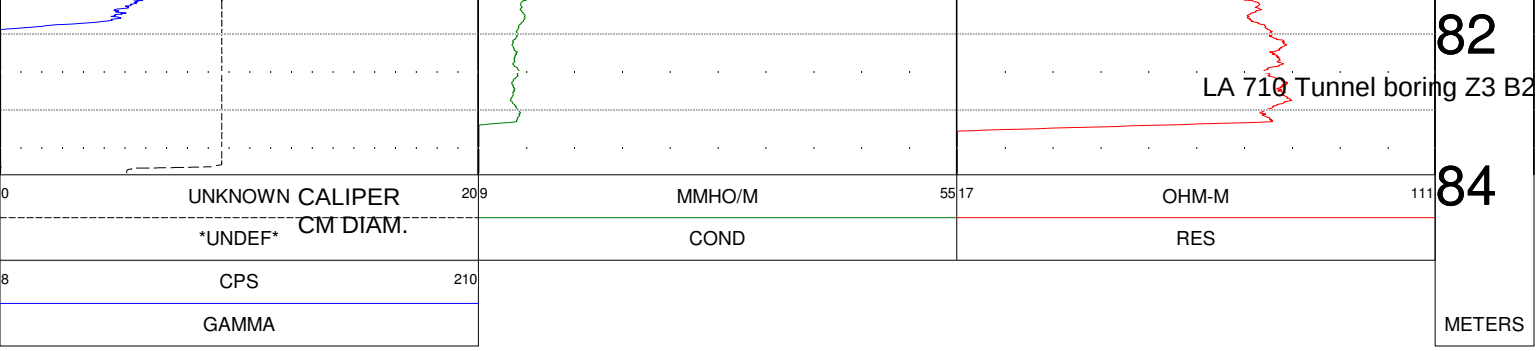
82
LA 710 Tunnel boring Z3 B2
84
0
UNKNOWN
CALIPER
CM DIAM.
20
9
MMHO/M
55
17
OHM-M
111
*UNDEF*
COND
RES
8
CPS
210
GAMMA
METERS

**Table 2.** LA 710 Tunnel
Boring Z3 B2
PS Suspension Log Data Summary



| Top of Hole Elevation (m) | Depth (m) | Depth (ft) | Vs (m/s) | Vs (ft/s) | Vp (m/s) | Vp (ft/s) | $\gamma$ | $\rho$(Vp) (g/cc) | $\rho$(Vp) ($lb/ft^3$) | G (GPa) | E (GPa) | K (GPa) | G ($10^3 lb/ft^2$) | E ($10^3 lb/ft^2$) | K ($10^3 lb/ft^2$) |
|---|---|---|---|---|---|---|---|---|---|---|---|---|---|---|---|
| Not Provided | 1.5 | 4.9 | 353 | 1159 | | NA | NA | NA | NA | NA | NA | NA | NA | NA | NA |
| | 2 | 6.6 | 402 | 1318 | | NA | NA | NA | NA | NA | NA | NA | NA | NA | NA |
| | 2.5 | 8.2 | 350 | 1147 | | NA | NA | NA | NA | NA | NA | NA | NA | NA | NA |
| | 3 | 9.8 | 372 | 1220 | | NA | NA | NA | NA | NA | NA | NA | NA | NA | NA |
| | 3.5 | 11.5 | 369 | 1211 | | NA | NA | NA | NA | NA | NA | NA | NA | NA | NA |
| | 4 | 13.1 | 356 | 1168 | | NA | NA | NA | NA | NA | NA | NA | NA | NA | NA |
| | 4.5 | 14.8 | 385 | 1262 | | NA | NA | NA | NA | NA | NA | NA | NA | NA | NA |
| | 5 | 16.4 | 433 | 1420 | | NA | NA | NA | NA | NA | NA | NA | NA | NA | NA |
| | 5.5 | 18.0 | 426 | 1396 | | NA | NA | NA | NA | NA | NA | NA | NA | NA | NA |
| | 6 | 19.7 | 556 | 1823 | | NA | NA | NA | NA | NA | NA | NA | NA | NA | NA |
| | 6.5 | 21.3 | 375 | 1229 | 699 | 2294 | NA | NA | NA | NA | NA | NA | NA | NA | NA |
| | 7 | 23.0 | 350 | 1147 | 610 | 2001 | NA | NA | NA | NA | NA | NA | NA | NA | NA |
| | 7.5 | 24.6 | 353 | 1159 | 769 | 2524 | NA | NA | NA | NA | NA | NA | NA | NA | NA |
| | 8 | 26.2 | 379 | 1243 | | NA | NA | NA | NA | NA | NA | NA | NA | NA | NA |
| | 8.5 | 27.9 | 412 | 1350 | 709 | 2327 | NA | NA | NA | NA | NA | NA | NA | NA | NA |
| | 9 | 29.5 | 433 | 1420 | 758 | 2485 | NA | NA | NA | NA | NA | NA | NA | NA | NA |
| | 9.5 | 31.2 | 439 | 1439 | | NA | NA | NA | NA | NA | NA | NA | NA | NA | NA |
| | 10 | 32.8 | 418 | 1373 | 699 | 2294 | NA | NA | NA | NA | NA | NA | NA | NA | NA |
| | 10.5 | 34.4 | 397 | 1302 | 775 | 2543 | NA | NA | NA | NA | NA | NA | NA | NA | NA |
| | 11 | 36.1 | 429 | 1408 | | NA | NA | NA | NA | NA | NA | NA | NA | NA | NA |
| | 11.5 | 37.7 | 418 | 1373 | 877 | 2878 | NA | NA | NA | NA | NA | NA | NA | NA | NA |
| | 12 | 39.4 | 386 | 1267 | 699 | 2294 | NA | NA | NA | NA | NA | NA | NA | NA | NA |
| | 12.5 | 41.0 | 495 | 1624 | 775 | 2543 | NA | NA | NA | NA | NA | NA | NA | NA | NA |
| | 13 | 42.7 | 513 | 1682 | 775 | 2543 | NA | NA | NA | NA | NA | NA | NA | NA | NA |
| | 13.5 | 44.3 | 505 | 1657 | 746 | 2448 | NA | NA | NA | NA | NA | NA | NA | NA | NA |
| | 14 | 45.9 | 495 | 1624 | 746 | 2448 | NA | NA | NA | NA | NA | NA | NA | NA | NA |
| | 14.5 | 47.6 | 532 | 1745 | 781 | 2563 | NA | NA | NA | NA | NA | NA | NA | NA | NA |
| | 15 | 49.2 | 541 | 1773 | 787 | 2583 | NA | NA | NA | NA | NA | NA | NA | NA | NA |
| | 15.5 | 50.9 | 518 | 1700 | 746 | 2448 | NA | NA | NA | NA | NA | NA | NA | NA | NA |
| | 16.5 | 54.1 | 521 | 1709 | 752 | 2467 | NA | NA | NA | NA | NA | NA | NA | NA | NA |
| | 17 | 55.8 | 532 | 1745 | 820 | 2689 | NA | NA | NA | NA | NA | NA | NA | NA | NA |
| | 17.5 | 57.4 | 552 | 1813 | 806 | 2646 | NA | NA | NA | NA | NA | NA | NA | NA | NA |
| | 18 | 59.1 | 562 | 1843 | 813 | 2667 | NA | NA | NA | NA | NA | NA | NA | NA | NA |
| | 18.5 | 60.7 | 599 | 1965 | 971 | 3185 | NA | NA | NA | NA | NA | NA | NA | NA | NA |
| | 19 | 62.3 | 595 | 1953 | 1000 | 3281 | NA | NA | NA | NA | NA | NA | NA | NA | NA |
| | 19.5 | 64.0 | 538 | 1764 | 952 | 3125 | NA | NA | NA | NA | NA | NA | NA | NA | NA |
| | 20 | 65.6 | 552 | 1813 | 952 | 3125 | NA | NA | NA | NA | NA | NA | NA | NA | NA |

$\gamma$ = Poisson's Ratio  $\rho$(Vp) = Vp-derived density  G = Shear Modulus  E = Young's Modulus  K = Bulk Modulus
Shaded cells denote questionable data.

**Table 2.** LA 710 Tunnel
Boring Z3 B2
PS Suspension Log Data Summary



| Top of Hole Elevation (m) | Depth (m) | Depth (ft) | Vs (m/s) | Vs (ft/s) | Vp (m/s) | Vp (ft/s) | $\gamma$ | $\rho$(Vp) (g/cc) | $\rho$(Vp) ($lb/ft^3$) | G (GPa) | E (GPa) | K (GPa) | G ($10^3 lb/ft^2$) | E ($10^3 lb/ft^2$) | K ($10^3 lb/ft^2$) |
|---|---|---|---|---|---|---|---|---|---|---|---|---|---|---|---|
| | 20.5 | 67.3 | 538 | 1764 | 971 | 3185 | NA | NA | NA | NA | NA | NA | NA | NA | NA |
| | 21 | 68.9 | 483 | 1585 | 926 | 3038 | NA | NA | NA | NA | NA | NA | NA | NA | NA |
| | 21.5 | 70.5 | 513 | 1682 | 1235 | 4050 | NA | NA | NA | NA | NA | NA | NA | NA | NA |
| | 22 | 72.2 | 610 | 2001 | 2083 | 6835 | 0.45 | 2.22 | 138.82 | 0.827 | 2.403 | 8.549 | 17267 | 50184 | 178546 |
| | 22.5 | 73.8 | 559 | 1833 | 1020 | 3348 | NA | NA | NA | NA | NA | NA | NA | NA | NA |
| | 23 | 75.5 | 488 | 1600 | 909 | 2983 | NA | NA | NA | NA | NA | NA | NA | NA | NA |
| | 23.5 | 77.1 | 505 | 1657 | 926 | 3038 | NA | NA | NA | NA | NA | NA | NA | NA | NA |
| | 24 | 78.7 | 495 | 1624 | 893 | 2929 | NA | NA | NA | NA | NA | NA | NA | NA | NA |
| | 24.5 | 80.4 | 476 | 1562 | 806 | 2646 | NA | NA | NA | NA | NA | NA | NA | NA | NA |
| | 25 | 82.0 | 490 | 1608 | 909 | 2983 | NA | NA | NA | NA | NA | NA | NA | NA | NA |
| | 25.5 | 83.7 | 500 | 1640 | 909 | 2983 | NA | NA | NA | NA | NA | NA | NA | NA | NA |
| | 26 | 85.3 | 488 | 1600 | 855 | 2804 | NA | NA | NA | NA | NA | NA | NA | NA | NA |
| | 26.4 | 86.6 | 457 | 1498 | 840 | 2757 | NA | NA | NA | NA | NA | NA | NA | NA | NA |
| | 26.8 | 87.9 | 513 | 1682 | 885 | 2903 | NA | NA | NA | NA | NA | NA | NA | NA | NA |
| | 27.5 | 90.2 | 515 | 1691 | 926 | 3038 | NA | NA | NA | NA | NA | NA | NA | NA | NA |
| | 28 | 91.9 | 498 | 1632 | 885 | 2903 | NA | NA | NA | NA | NA | NA | NA | NA | NA |
| | 28.5 | 93.5 | 510 | 1674 | 901 | 2956 | NA | NA | NA | NA | NA | NA | NA | NA | NA |
| | 29 | 95.1 | 578 | 1896 | 1053 | 3454 | NA | NA | NA | NA | NA | NA | NA | NA | NA |
| | 29.5 | 96.8 | 606 | 1988 | 1449 | 4755 | NA | NA | NA | NA | NA | NA | NA | NA | NA |
| | 30 | 98.4 | 568 | 1864 | 1010 | 3314 | NA | NA | NA | NA | NA | NA | NA | NA | NA |
| | 30 | 98.4 | 562 | 1843 | 1053 | 3454 | NA | NA | NA | NA | NA | NA | NA | NA | NA |
| | 30.5 | 100.1 | 541 | 1773 | 917 | 3010 | NA | NA | NA | NA | NA | NA | NA | NA | NA |
| | 31 | 101.7 | 588 | 1930 | 719 | 2360 | NA | NA | NA | NA | NA | NA | NA | NA | NA |
| | 31.5 | 103.3 | 595 | 1953 | 769 | 2524 | NA | NA | NA | NA | NA | NA | NA | NA | NA |
| | 32 | 105.0 | 513 | 1682 | 1124 | 3686 | NA | NA | NA | NA | NA | NA | NA | NA | NA |
| | 32.4 | 106.3 | 500 | 1640 | 1031 | 3382 | NA | NA | NA | NA | NA | NA | NA | NA | NA |
| | 32.9 | 107.9 | 546 | 1793 | 1449 | 4755 | NA | NA | NA | NA | NA | NA | NA | NA | NA |
| | 33.4 | 109.6 | 613 | 2013 | 1852 | 6076 | 0.44 | 2.10 | 131.15 | 0.791 | 2.275 | 6.150 | 16514 | 47506 | 128447 |
| | 33.9 | 111.2 | 602 | 1976 | 1961 | 6433 | 0.45 | 2.16 | 134.97 | 0.785 | 2.272 | 7.266 | 16386 | 47451 | 151755 |
| | 34.4 | 112.9 | 562 | 1843 | 2041 | 6696 | 0.46 | 2.20 | 137.53 | 0.695 | 2.029 | 8.248 | 14522 | 42375 | 172272 |
| | 34.9 | 114.5 | 508 | 1665 | 2083 | 6835 | 0.47 | 2.22 | 138.82 | 0.573 | 1.683 | 8.887 | 11967 | 35145 | 185614 |
| | 35.5 | 116.5 | 461 | 1512 | 2041 | 6696 | 0.47 | 2.20 | 137.53 | 0.468 | 1.378 | 8.552 | 9771 | 28788 | 178607 |
| | 36 | 118.1 | 481 | 1577 | 1852 | 6076 | 0.46 | 2.10 | 131.15 | 0.486 | 1.422 | 6.557 | 10141 | 29691 | 136944 |
| | 36.5 | 119.8 | 510 | 1674 | 1818 | 5965 | 0.46 | 2.08 | 129.88 | 0.542 | 1.578 | 6.156 | 11311 | 32966 | 128561 |
| | 36.9 | 121.1 | 599 | 1965 | 1724 | 5657 | 0.43 | 2.02 | 126.09 | 0.724 | 2.073 | 5.039 | 15126 | 43303 | 105233 |
| | 37.5 | 123.0 | 592 | 1941 | 2041 | 6696 | 0.45 | 2.20 | 137.53 | 0.771 | 2.243 | 8.147 | 16110 | 46851 | 170154 |
| | 38 | 124.7 | 662 | 2173 | 2222 | 7291 | 0.45 | 2.29 | 142.69 | 1.002 | 2.910 | 9.951 | 20937 | 60770 | 207827 |

$\gamma$ = Poisson's Ratio  $\rho$(Vp) = Vp-derived density  G = Shear Modulus  E = Young's Modulus  K = Bulk Modulus
Shaded cells denote questionable data.

**Table 2.** LA 710 Tunnel
Boring Z3 B2
PS Suspension Log Data Summary



| Top of Hole Elevation (m) | Depth (m) | Depth (ft) | Vs (m/s) | Vs (ft/s) | Vp (m/s) | Vp (ft/s) | γ | ρ(Vp) (g/cc) | ρ(Vp) ($lb/ft^3$) | G (GPa) | E (GPa) | K (GPa) | G ($10^3 lb/ft^2$) | E ($10^3 lb/ft^2$) | K ($10^3 lb/ft^2$) |
|---|---|---|---|---|---|---|---|---|---|---|---|---|---|---|---|
| | 38.5 | 126.3 | 641 | 2103 | 1923 | 6309 | 0.44 | 2.14 | 133.69 | 0.880 | 2.530 | 6.747 | 18379 | 52840 | 140906 |
| | 39 | 128.0 | 595 | 1953 | 1563 | 5126 | NA | NA | NA | NA | NA | NA | NA | NA | NA |
| | 39.5 | 129.6 | 629 | 2063 | 1408 | 4621 | NA | NA | NA | NA | NA | NA | NA | NA | NA |
| | 39.9 | 130.9 | 658 | 2158 | 1429 | 4687 | NA | NA | NA | NA | NA | NA | NA | NA | NA |
| | 40.4 | 132.5 | 662 | 2173 | 1111 | 3645 | NA | NA | NA | NA | NA | NA | NA | NA | NA |
| | 40.9 | 134.2 | 671 | 2202 | 1163 | 3815 | NA | NA | NA | NA | NA | NA | NA | NA | NA |
| | 41.5 | 136.2 | 746 | 2448 | 1429 | 4687 | NA | NA | NA | NA | NA | NA | NA | NA | NA |
| | 42 | 137.8 | 862 | 2828 | 1695 | 5561 | 0.33 | 2.00 | 124.84 | 1.486 | 3.940 | 3.763 | 31038 | 82282 | 78595 |
| | 42.5 | 139.4 | 893 | 2929 | 1471 | 4825 | NA | NA | NA | NA | NA | NA | NA | NA | NA |
| | 43 | 141.1 | 952 | 3125 | 1389 | 4557 | NA | NA | NA | NA | NA | NA | NA | NA | NA |
| | 43.5 | 142.7 | 962 | 3155 | 1429 | 4687 | NA | NA | NA | NA | NA | NA | NA | NA | NA |
| | 44 | 144.4 | 935 | 3066 | 1818 | 5965 | 0.32 | 2.08 | 129.88 | 1.817 | 4.799 | 4.455 | 37952 | 100228 | 93039 |
| | 44.6 | 146.3 | 1000 | 3281 | 2000 | 6562 | 0.33 | 2.18 | 136.25 | 2.183 | 5.820 | 5.820 | 45582 | 121553 | 121553 |
| | 45 | 147.6 | 847 | 2780 | 2381 | 7812 | 0.43 | 2.35 | 146.59 | 1.686 | 4.815 | 11.063 | 35222 | 100556 | 231059 |
| | 45.6 | 149.6 | 1010 | 3314 | 2703 | 8867 | 0.42 | 2.45 | 153.16 | 2.503 | 7.103 | 14.583 | 52279 | 148349 | 304572 |
| | 46.1 | 151.2 | 1087 | 3566 | 2857 | 9374 | 0.42 | 2.50 | 155.80 | 2.949 | 8.347 | 16.442 | 61583 | 174327 | 343390 |
| | 46.6 | 152.9 | 885 | 2903 | 2778 | 9113 | 0.44 | 2.47 | 154.48 | 1.938 | 5.595 | 16.509 | 40474 | 116849 | 344805 |
| | 46.6 | 152.9 | 893 | 2929 | 2857 | 9374 | 0.45 | 2.50 | 155.80 | 1.990 | 5.753 | 17.720 | 41553 | 120161 | 370097 |
| | 46.6 | 152.9 | 943 | 3095 | 2778 | 9113 | 0.43 | 2.47 | 154.48 | 2.202 | 6.320 | 16.157 | 45996 | 131990 | 337444 |
| | 47.1 | 154.5 | 980 | 3217 | 3030 | 9942 | 0.44 | 2.54 | 158.46 | 2.440 | 7.034 | 20.056 | 50955 | 146907 | 418867 |
| | 47.6 | 156.2 | 1010 | 3314 | 2941 | 9650 | 0.43 | 2.52 | 157.13 | 2.568 | 7.361 | 18.349 | 53635 | 153734 | 383227 |
| | 48.1 | 157.8 | 917 | 3010 | 2778 | 9113 | 0.44 | 2.47 | 154.48 | 2.083 | 5.993 | 16.316 | 43499 | 125170 | 340773 |
| | 48.1 | 157.8 | 930 | 3052 | 2778 | 9113 | 0.44 | 2.47 | 154.48 | 2.141 | 6.153 | 16.238 | 44721 | 128514 | 339142 |
| | 48.1 | 157.8 | 909 | 2983 | 2778 | 9113 | 0.44 | 2.47 | 154.48 | 2.045 | 5.890 | 16.367 | 42711 | 123010 | 341821 |
| | 48.6 | 159.4 | 833 | 2734 | 2941 | 9650 | 0.46 | 2.52 | 157.13 | 1.748 | 5.091 | 19.443 | 36505 | 106330 | 406065 |
| | 49.1 | 161.1 | 714 | 2343 | 2778 | 9113 | 0.46 | 2.47 | 154.48 | 1.262 | 3.698 | 17.410 | 26368 | 77236 | 363613 |
| | 50.1 | 164.4 | 488 | 1600 | 2632 | 8634 | 0.48 | 2.43 | 151.84 | 0.579 | 1.716 | 16.072 | 12087 | 35832 | 335665 |
| | 50.6 | 166.0 | 571 | 1875 | 2778 | 9113 | 0.48 | 2.47 | 154.48 | 0.808 | 2.388 | 18.016 | 16875 | 49880 | 376269 |
| | 51.1 | 167.7 | 645 | 2117 | 2778 | 9113 | 0.47 | 2.47 | 154.48 | 1.030 | 3.031 | 17.720 | 21511 | 63307 | 370088 |
| | 51.6 | 169.3 | 870 | 2853 | 2778 | 9113 | 0.45 | 2.47 | 154.48 | 1.871 | 5.410 | 16.599 | 39078 | 112988 | 346666 |
| | 52.1 | 170.9 | 909 | 2983 | 2778 | 9113 | 0.44 | 2.47 | 154.48 | 2.045 | 5.890 | 16.367 | 42711 | 123010 | 341821 |
| | 52.5 | 172.2 | 870 | 2853 | 2778 | 9113 | 0.45 | 2.47 | 154.48 | 1.871 | 5.410 | 16.599 | 39078 | 112988 | 346666 |
| | 53.1 | 174.2 | 1250 | 4101 | 3125 | 10253 | 0.40 | 2.56 | 159.79 | 3.999 | 11.237 | 19.664 | 83530 | 234680 | 410690 |
| | 53.6 | 175.9 | 1333 | 4374 | 3571 | 11717 | 0.42 | 2.65 | 165.16 | 4.703 | 13.348 | 27.474 | 98230 | 278782 | 573803 |
| | 54.1 | 177.5 | 1600 | 5249 | 3333 | 10936 | 0.35 | 2.60 | 162.47 | 6.663 | 17.993 | 20.034 | 139149 | 375788 | 418411 |
| | 54.6 | 179.1 | 1290 | 4233 | 2941 | 9650 | 0.38 | 2.52 | 157.13 | 4.191 | 11.573 | 16.186 | 87522 | 241706 | 338043 |
| | 55.1 | 180.8 | 1176 | 3860 | 2381 | 7812 | 0.34 | 2.35 | 146.59 | 3.250 | 8.700 | 8.978 | 67880 | 181712 | 187515 |

γ = Poisson's Ratio  ρ(Vp) = Vp-derived density  G = Shear Modulus  E = Young's Modulus  K = Bulk Modulus
Shaded cells denote questionable data.

**Table 2.** LA 710 Tunnel
Boring Z3 B2
PS Suspension Log Data Summary



| Top of Hole Elevation (m) | Depth (m) | Depth (ft) | Vs (m/s) | Vs (ft/s) | Vp (m/s) | Vp (ft/s) | γ | ρ(Vp) (g/cc) | ρ(Vp) ($lb/ft^3$) | G (GPa) | E (GPa) | K (GPa) | G ($10^3 lb/ft^2$) | E ($10^3 lb/ft^2$) | K ($10^3 lb/ft^2$) |
|---|---|---|---|---|---|---|---|---|---|---|---|---|---|---|---|
| | 55.6 | 182.4 | 870 | 2853 | 2941 | 9650 | 0.45 | 2.52 | 157.13 | 1.903 | 5.527 | 19.236 | 39749 | 115439 | 401741 |
| | 56.1 | 184.1 | 952 | 3125 | 2941 | 9650 | 0.44 | 2.52 | 157.13 | 2.283 | 6.582 | 18.729 | 47681 | 137457 | 391165 |
| | 56.6 | 185.7 | 1176 | 3860 | 3333 | 10936 | 0.43 | 2.60 | 162.47 | 3.602 | 10.294 | 24.114 | 75232 | 214990 | 503634 |
| | 57.1 | 187.3 | 1333 | 4374 | 3125 | 10253 | 0.39 | 2.56 | 159.79 | 4.551 | 12.639 | 18.929 | 95039 | 263965 | 395345 |
| | 57.6 | 189.0 | 1333 | 4374 | 3333 | 10936 | 0.40 | 2.60 | 162.47 | 4.627 | 12.999 | 22.748 | 96631 | 271487 | 475101 |
| | 58.1 | 190.6 | 1333 | 4374 | 3333 | 10936 | 0.40 | 2.60 | 162.47 | 4.627 | 12.999 | 22.748 | 96631 | 271487 | 475103 |
| | 58.6 | 192.3 | 1333 | 4374 | 3333 | 10936 | 0.40 | 2.60 | 162.47 | 4.627 | 12.999 | 22.748 | 96631 | 271487 | 475101 |
| | 59.1 | 193.9 | 1111 | 3645 | 2941 | 9650 | 0.42 | 2.52 | 157.13 | 3.107 | 8.805 | 17.630 | 64899 | 183892 | 368208 |
| | 59.6 | 195.5 | 667 | 2187 | 2632 | 8634 | 0.47 | 2.43 | 151.84 | 1.081 | 3.169 | 15.402 | 22577 | 66182 | 321680 |
| | 60 | 196.9 | 769 | 2524 | 2564 | 8412 | 0.45 | 2.41 | 150.52 | 1.427 | 4.139 | 13.950 | 29797 | 86445 | 291351 |
| | 60.5 | 198.5 | 893 | 2929 | 2778 | 9113 | 0.44 | 2.47 | 154.48 | 1.973 | 5.691 | 16.463 | 41199 | 118851 | 343838 |
| | 60.6 | 198.8 | 769 | 2524 | 2500 | 8202 | 0.45 | 2.39 | 149.21 | 1.414 | 4.095 | 13.052 | 29537 | 85523 | 272605 |
| | 60.6 | 198.8 | 606 | 1988 | 2500 | 8202 | 0.47 | 2.39 | 149.21 | 0.878 | 2.579 | 13.768 | 18335 | 53861 | 287541 |
| | 61 | 200.1 | 1163 | 3815 | 3030 | 9942 | 0.41 | 2.54 | 158.46 | 3.432 | 9.703 | 18.733 | 71678 | 202658 | 391235 |
| | 61.1 | 200.5 | 588 | 1930 | 2632 | 8634 | 0.47 | 2.43 | 151.84 | 0.842 | 2.481 | 15.721 | 17577 | 51806 | 328346 |
| | 61.5 | 201.8 | 1250 | 4101 | 2941 | 9650 | 0.39 | 2.52 | 157.13 | 3.933 | 10.931 | 16.529 | 82137 | 228306 | 345223 |
| | 61.6 | 202.1 | 1176 | 3860 | 2778 | 9113 | 0.39 | 2.47 | 154.48 | 3.425 | 9.526 | 14.527 | 71530 | 198955 | 303396 |
| | 62 | 203.4 | 1250 | 4101 | 3125 | 10253 | 0.40 | 2.56 | 159.79 | 3.999 | 11.237 | 19.664 | 83530 | 234680 | 410690 |
| | 62 | 203.4 | 1282 | 4206 | 3125 | 10253 | 0.40 | 2.56 | 159.79 | 4.207 | 11.770 | 19.387 | 87869 | 245825 | 404907 |
| | 62.5 | 205.1 | 1282 | 4206 | 3226 | 10583 | 0.41 | 2.58 | 161.13 | 4.242 | 11.931 | 21.202 | 88604 | 249191 | 442805 |
| | 62.5 | 205.1 | 1299 | 4261 | 3030 | 9942 | 0.39 | 2.54 | 158.46 | 4.281 | 11.880 | 17.600 | 89413 | 248122 | 367588 |
| | 62.5 | 205.1 | 1250 | 4101 | 3333 | 10936 | 0.42 | 2.60 | 162.47 | 4.066 | 11.534 | 23.495 | 84930 | 240891 | 490703 |
| | 63 | 206.7 | 1250 | 4101 | 3030 | 9942 | 0.40 | 2.54 | 158.46 | 3.966 | 11.085 | 18.020 | 82833 | 231515 | 376362 |
| | 63 | 206.7 | 1250 | 4101 | 3125 | 10253 | 0.40 | 2.56 | 159.79 | 3.999 | 11.237 | 19.664 | 83530 | 234680 | 410692 |
| | 63.5 | 208.3 | 1190 | 3906 | 2941 | 9650 | 0.40 | 2.52 | 157.13 | 3.567 | 10.003 | 17.017 | 74501 | 208906 | 355405 |
| | 63.5 | 208.3 | 833 | 2734 | 2857 | 9374 | 0.45 | 2.50 | 155.80 | 1.733 | 5.038 | 18.062 | 36197 | 105226 | 377238 |
| | 64 | 210.0 | 1075 | 3528 | 2857 | 9374 | 0.42 | 2.50 | 155.80 | 2.886 | 8.181 | 16.526 | 60266 | 170853 | 345146 |
| | 64 | 210.0 | 1087 | 3566 | 3030 | 9942 | 0.43 | 2.54 | 158.46 | 2.999 | 8.554 | 19.310 | 62634 | 178652 | 403295 |
| | 64.5 | 211.6 | 926 | 3038 | 2857 | 9374 | 0.44 | 2.50 | 155.80 | 2.140 | 6.168 | 17.520 | 44688 | 128819 | 365915 |
| | 64.5 | 211.6 | 1351 | 4434 | 3333 | 10936 | 0.40 | 2.60 | 162.47 | 4.753 | 13.323 | 22.580 | 99260 | 278259 | 471595 |
| | 65 | 213.3 | 1471 | 4825 | 3704 | 12151 | 0.41 | 2.67 | 166.51 | 5.768 | 16.225 | 28.897 | 120471 | 338866 | 603514 |
| | 65.1 | 213.6 | 1613 | 5292 | 2941 | 9650 | 0.28 | 2.52 | 157.13 | 6.548 | 16.827 | 13.043 | 136753 | 351447 | 272402 |
| | 65.5 | 214.9 | 1282 | 4206 | 3571 | 11717 | 0.43 | 2.65 | 165.16 | 4.348 | 12.402 | 27.947 | 90820 | 259024 | 583684 |
| | 65.6 | 215.2 | 1389 | 4557 | 3333 | 10936 | 0.39 | 2.60 | 162.47 | 5.020 | 14.006 | 22.223 | 104851 | 292526 | 464143 |
| | 66 | 216.5 | 1389 | 4557 | 3704 | 12151 | 0.42 | 2.67 | 166.51 | 5.145 | 14.593 | 29.727 | 107457 | 304788 | 620866 |
| | 66 | 216.5 | 1190 | 3906 | 3226 | 10583 | 0.42 | 2.58 | 161.13 | 3.658 | 10.397 | 21.981 | 76398 | 217149 | 459077 |
| | 66.5 | 218.2 | 1389 | 4557 | 4000 | 13123 | 0.43 | 2.71 | 169.22 | 5.229 | 14.970 | 36.398 | 109205 | 312644 | 760184 |

γ = Poisson's Ratio  ρ(Vp) = Vp-derived density  G = Shear Modulus  E = Young's Modulus  K = Bulk Modulus
Shaded cells denote questionable data.

**Table 2.** LA 710 Tunnel
Boring Z3 B2
PS Suspension Log Data Summary



| Top of Hole Elevation (m) | Depth (m) | Depth (ft) | Vs (m/s) | Vs (ft/s) | Vp (m/s) | Vp (ft/s) | $\gamma$ | $\rho$(Vp) (g/cc) | $\rho$(Vp) ($lb/ft^3$) | G (GPa) | E (GPa) | K (GPa) | G ($10^3 lb/ft^2$) | E ($10^3 lb/ft^2$) | K ($10^3 lb/ft^2$) |
|---|---|---|---|---|---|---|---|---|---|---|---|---|---|---|---|
| | 66.5 | 218.2 | 980 | 3217 | 2941 | 9650 | 0.44 | 2.52 | 157.13 | 2.419 | 6.955 | 18.548 | 50527 | 145264 | 387372 |
| | 67 | 219.8 | 794 | 2604 | 3571 | 11717 | 0.47 | 2.65 | 165.16 | 1.666 | 4.913 | 31.523 | 34804 | 102604 | 658372 |
| | 67 | 219.8 | 1064 | 3490 | 3333 | 10936 | 0.44 | 2.60 | 162.47 | 2.945 | 8.502 | 24.990 | 61515 | 177570 | 521922 |
| | 67.5 | 221.5 | 962 | 3155 | 3030 | 9942 | 0.44 | 2.54 | 158.46 | 2.347 | 6.778 | 20.179 | 49014 | 141554 | 421453 |
| | 67.5 | 221.5 | 962 | 3155 | 3448 | 11313 | 0.46 | 2.62 | 163.81 | 2.426 | 7.074 | 27.967 | 50670 | 147737 | 584096 |
| | 68 | 223.1 | 893 | 2929 | 2778 | 9113 | 0.44 | 2.47 | 154.48 | 1.973 | 5.691 | 16.463 | 41199 | 118851 | 343837 |
| | 68 | 223.1 | 847 | 2780 | 3226 | 10583 | 0.46 | 2.58 | 161.13 | 1.854 | 5.424 | 24.387 | 38715 | 113275 | 509323 |
| | 68.5 | 224.7 | 1190 | 3906 | 2941 | 9650 | 0.40 | 2.52 | 157.13 | 3.567 | 10.003 | 17.017 | 74501 | 208906 | 355406 |
| | 68.5 | 224.7 | 893 | 2929 | 2941 | 9650 | 0.45 | 2.52 | 157.13 | 2.007 | 5.816 | 19.098 | 41907 | 121466 | 398864 |
| | 69 | 226.4 | 943 | 3095 | 2703 | 8867 | 0.43 | 2.45 | 153.16 | 2.183 | 6.247 | 15.009 | 45602 | 130479 | 313474 |
| | 69.5 | 228.0 | 943 | 3095 | 2941 | 9650 | 0.44 | 2.52 | 157.13 | 2.240 | 6.463 | 18.786 | 46785 | 134990 | 392360 |
| | 70 | 229.7 | 1220 | 4001 | 3226 | 10583 | 0.42 | 2.58 | 161.13 | 3.839 | 10.876 | 21.740 | 80170 | 227143 | 454049 |
| | 70.1 | 230.0 | 1087 | 3566 | 3448 | 11313 | 0.44 | 2.62 | 163.81 | 3.100 | 8.959 | 27.068 | 64750 | 187106 | 565323 |
| | 70.5 | 231.3 | 1282 | 4206 | 3333 | 10936 | 0.41 | 2.60 | 162.47 | 4.278 | 12.090 | 23.214 | 89341 | 252512 | 484824 |
| | 71 | 232.9 | 1190 | 3906 | 3448 | 11313 | 0.43 | 2.62 | 163.81 | 3.719 | 10.653 | 26.243 | 77670 | 222501 | 548095 |
| | 71.5 | 234.6 | 1429 | 4687 | 4000 | 13123 | 0.43 | 2.71 | 169.22 | 5.532 | 15.787 | 35.994 | 115534 | 329712 | 751744 |
| | 72.1 | 236.5 | 1250 | 4101 | 3448 | 11313 | 0.42 | 2.62 | 163.81 | 4.100 | 11.680 | 25.735 | 85632 | 243940 | 537480 |
| | 72.6 | 238.2 | 1667 | 5468 | 3571 | 11717 | 0.36 | 2.65 | 165.16 | 7.349 | 20.001 | 23.947 | 153485 | 417723 | 500130 |
| | 73.1 | 239.8 | 1471 | 4825 | 3448 | 11313 | 0.39 | 2.62 | 163.81 | 5.675 | 15.763 | 23.635 | 118521 | 329215 | 493627 |
| | 73.5 | 241.1 | 1429 | 4687 | 3704 | 12151 | 0.41 | 2.67 | 166.51 | 5.443 | 15.379 | 29.330 | 113686 | 321187 | 612562 |
| | 74 | 242.8 | 1429 | 4687 | 4167 | 13670 | 0.43 | 2.73 | 170.58 | 5.576 | 15.986 | 40.002 | 116462 | 333873 | 835455 |
| | 74.5 | 244.4 | 1471 | 4825 | 3704 | 12151 | 0.41 | 2.67 | 166.51 | 5.768 | 16.225 | 28.897 | 120471 | 338866 | 603514 |
| | 75 | 246.1 | 1429 | 4687 | 3571 | 11717 | 0.40 | 2.65 | 165.16 | 5.399 | 15.169 | 26.546 | 112765 | 316815 | 554427 |
| | 75.4 | 247.4 | 1316 | 4317 | 3571 | 11717 | 0.42 | 2.65 | 165.16 | 4.580 | 13.022 | 27.638 | 95662 | 271963 | 577229 |
| | 75.9 | 249.0 | 1370 | 4494 | 3571 | 11717 | 0.41 | 2.65 | 165.16 | 4.965 | 14.037 | 27.126 | 103687 | 293174 | 566531 |
| | 76.4 | 250.7 | 1471 | 4825 | 3704 | 12151 | 0.41 | 2.67 | 166.51 | 5.768 | 16.225 | 28.897 | 120472 | 338867 | 603514 |
| | 77 | 252.6 | 1538 | 5047 | 4348 | 14265 | 0.43 | 2.75 | 171.94 | 6.519 | 18.623 | 43.372 | 136147 | 388954 | 905843 |
| | 77.5 | 254.3 | 1563 | 5126 | 3704 | 12151 | 0.39 | 2.67 | 166.51 | 6.512 | 18.126 | 27.905 | 136001 | 378557 | 582808 |
| | 78 | 255.9 | 1190 | 3906 | 3333 | 10936 | 0.43 | 2.60 | 162.47 | 3.688 | 10.526 | 23.999 | 77034 | 219838 | 501231 |
| | 78.5 | 257.5 | 1429 | 4687 | 3333 | 10936 | 0.39 | 2.60 | 162.47 | 5.311 | 14.739 | 21.835 | 110928 | 307826 | 456038 |
| | 79 | 259.2 | 1429 | 4687 | 4167 | 13670 | 0.43 | 2.73 | 170.58 | 5.576 | 15.986 | 40.002 | 116462 | 333872 | 835452 |
| | 79.5 | 260.8 | 1163 | 3815 | 3846 | 12619 | 0.45 | 2.69 | 167.86 | 3.636 | 10.541 | 34.929 | 75931 | 220154 | 729503 |
| | 80 | 262.5 | 1429 | 4687 | 3125 | 10253 | 0.37 | 2.56 | 159.79 | 5.224 | 14.291 | 18.032 | 109101 | 298479 | 376596 |
| | 80 | 262.5 | 1333 | 4374 | 3333 | 10936 | 0.40 | 2.60 | 162.47 | 4.627 | 12.999 | 22.748 | 96631 | 271487 | 475101 |

$\gamma$ = Poisson's Ratio  $\rho$(Vp) = Vp-derived density  G = Shear Modulus  E = Young's Modulus  K = Bulk Modulus
Shaded cells denote questionable data.

# Figure 1. LA 710 Tunnel
# Boring Z3 B2
# Downhole Interval Velocities

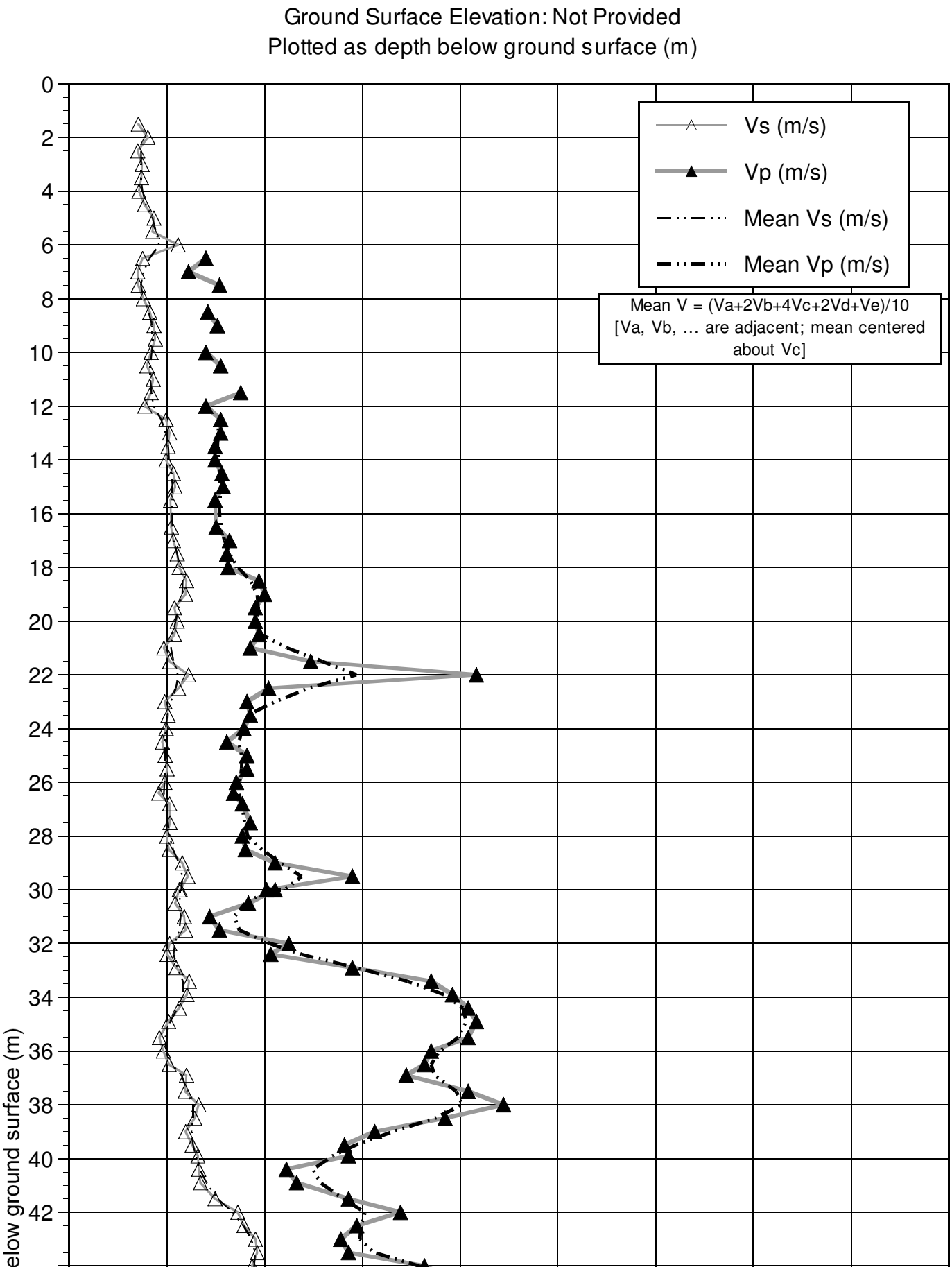

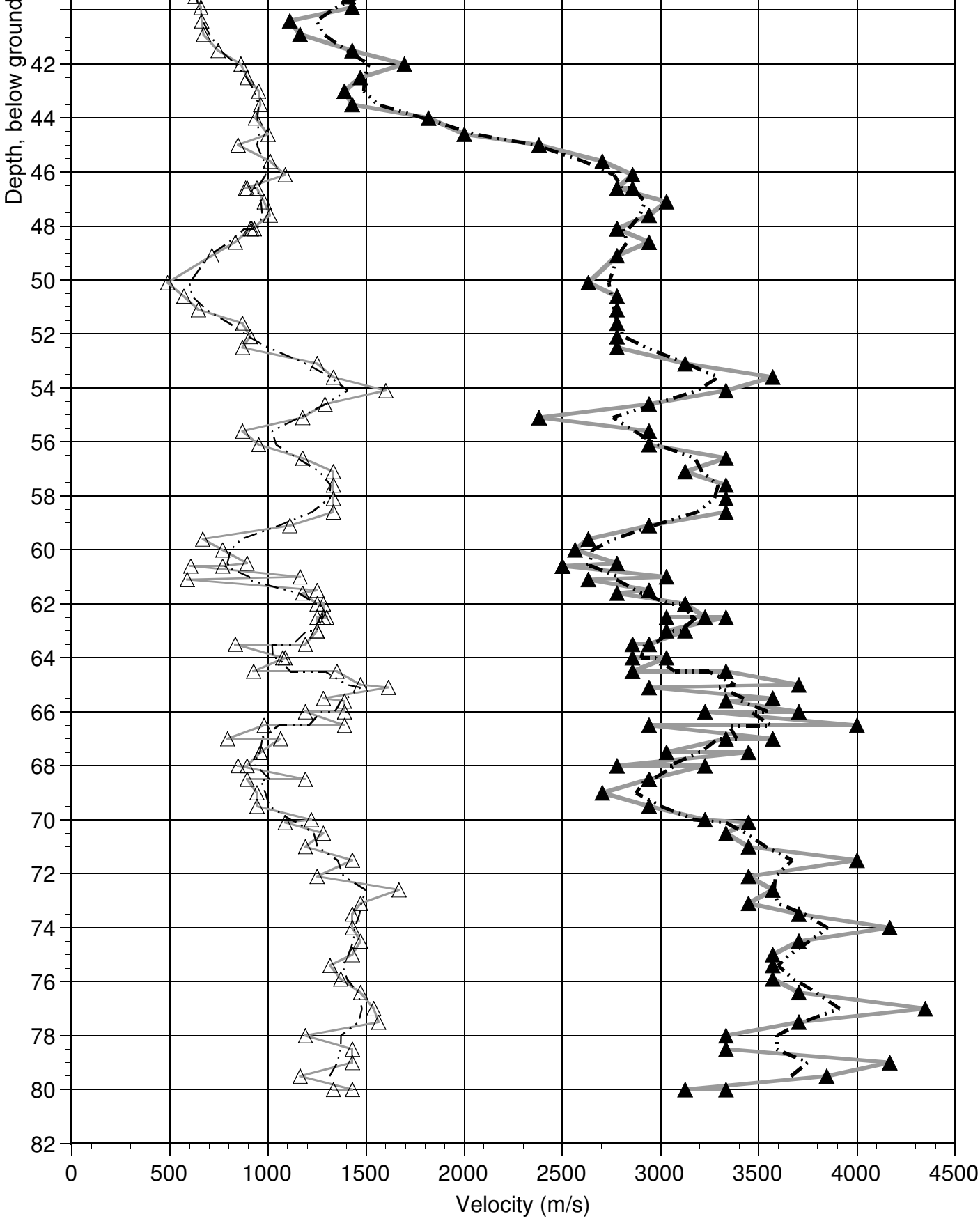
Depth, below ground
42
44
46
48
50
52
54
56
58
60
62
64
66
68
70
72
74
76
78
80
82
0
500
1000
1500
2000
2500
3000
3500
4000
4500
Velocity (m/s)


# Z3 B2.

| | | | |
|---|---|---|---|
| COMPANY | : CALTRANS. | OTHER SERVICES: | |
| WELL | : Z3 B2. | | |
| FIELD | : LA 710 TUNNEL. | | |
| COUNTY | : LA | | |
| STATE | : CA | | |
| LOCATION | : | | |
| SECTION | : None | | |
| TOWNSHIP | : None | | |
| RANGE | : None | | |
| API NO. | : | | |
| UNIQUE WELL ID. | : | | |
| PERMANENT DATUM | : None | ELEVATION KB | : NA |
| LOG MEASURED FROM | : GL | ELEVATION DF | : NA |
| DRL MEASURED FROM | : GL | ELEVATION GL | : 795ft. |
| DATE | : 1/20/09. | RIG NUMBER | : |
| DEPTH DRILLER | : 275 | LOGGER TD | : |
| BIT SIZE | : 9.4 | ARRIVAL TIME | : |
| LOG TOP | : 3.05 | DEPARTURE TIME | : |
| LOG BOTTOM | : 83.85 | CIRC STOPPED | : 0930 |
| CASING OD | : | | |
| CASING BOTTOM | : NA | | |
| CASING TYPE | : none | | |
| BOREHOLE FLUID | : 0 | | |
| RM TEMPERATURE | : 0 | | |
| MUD RES | : 0 | | |
| MUD WEIGHT | : | | |
| WITNESSED BY | : | | |
| RECORDED BY | : DH/DL | | |
| REMARKS 1 | : IND, Acoustic Tel, PSLog, CAL | | |
| REMARKS 2 | : EA: 07-187900 | | |

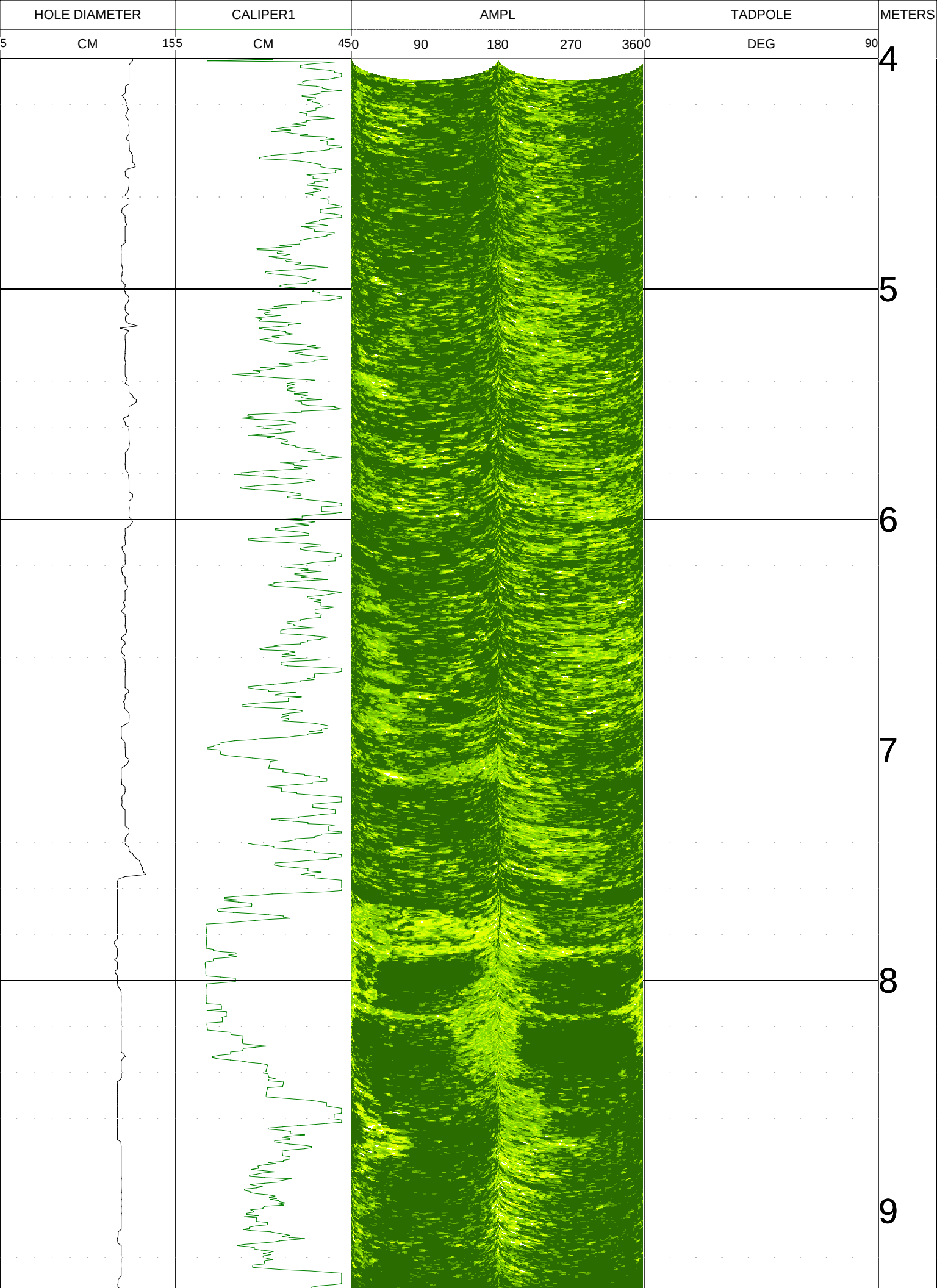
HOLE DIAMETER
5
CM
15
CALIPER1
5
CM
45
AMPL
0
90
180
270
360
TADPOLE
0
DEG
90
METERS
4
5
6
7
8
9

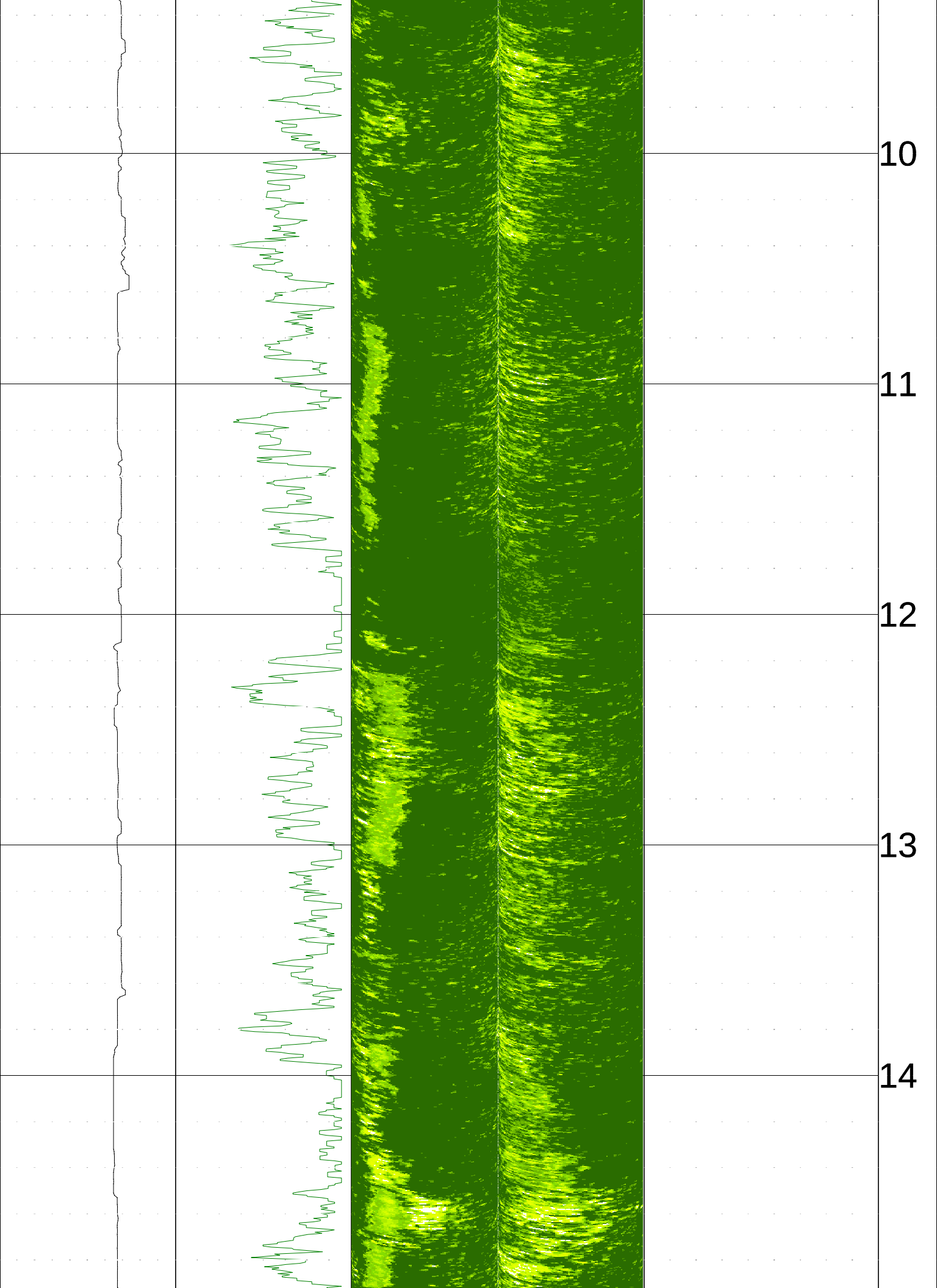
10
11
12
13
14

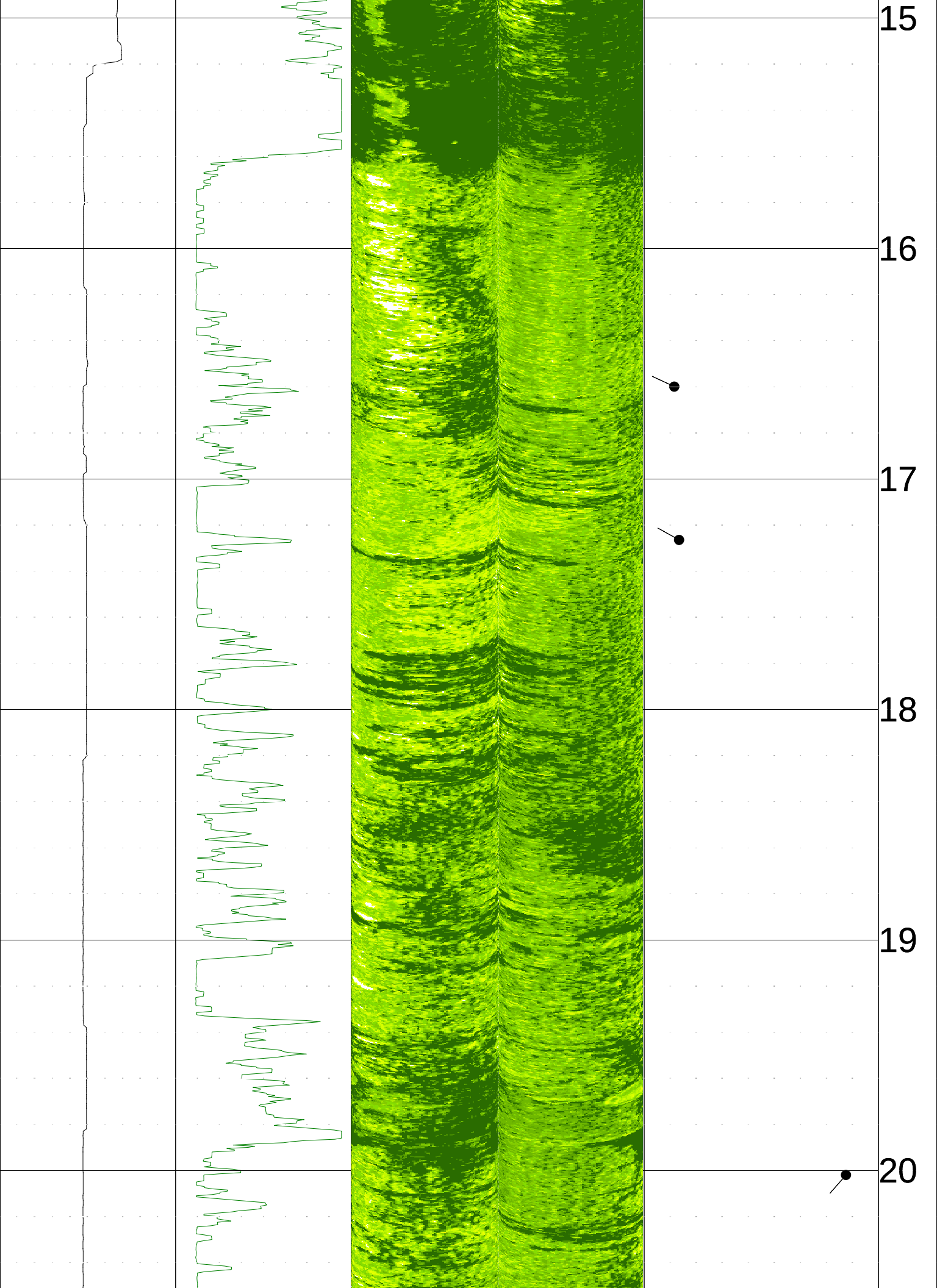
15
16
17
18
19
20

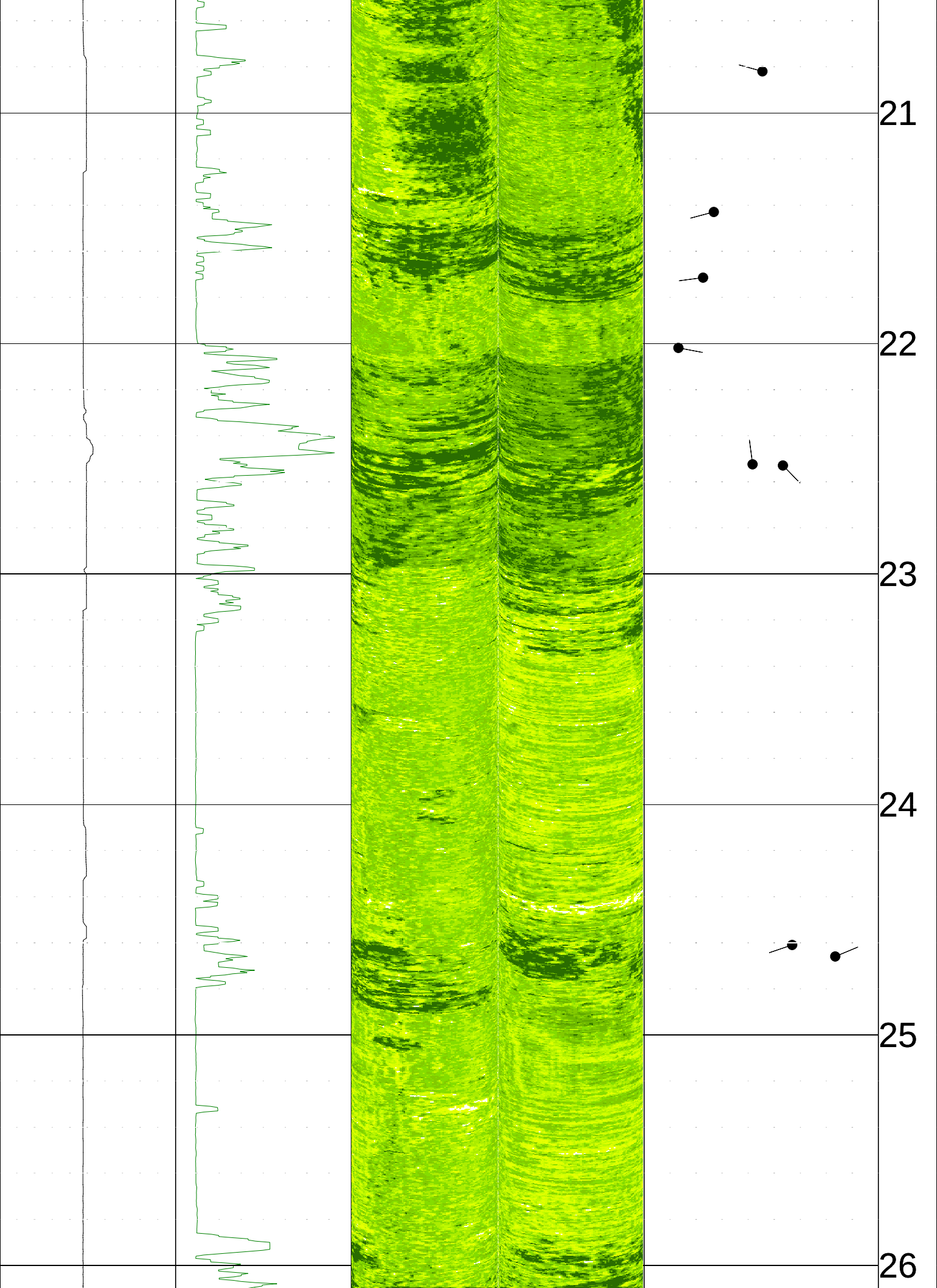
21
22
23
24
25
26

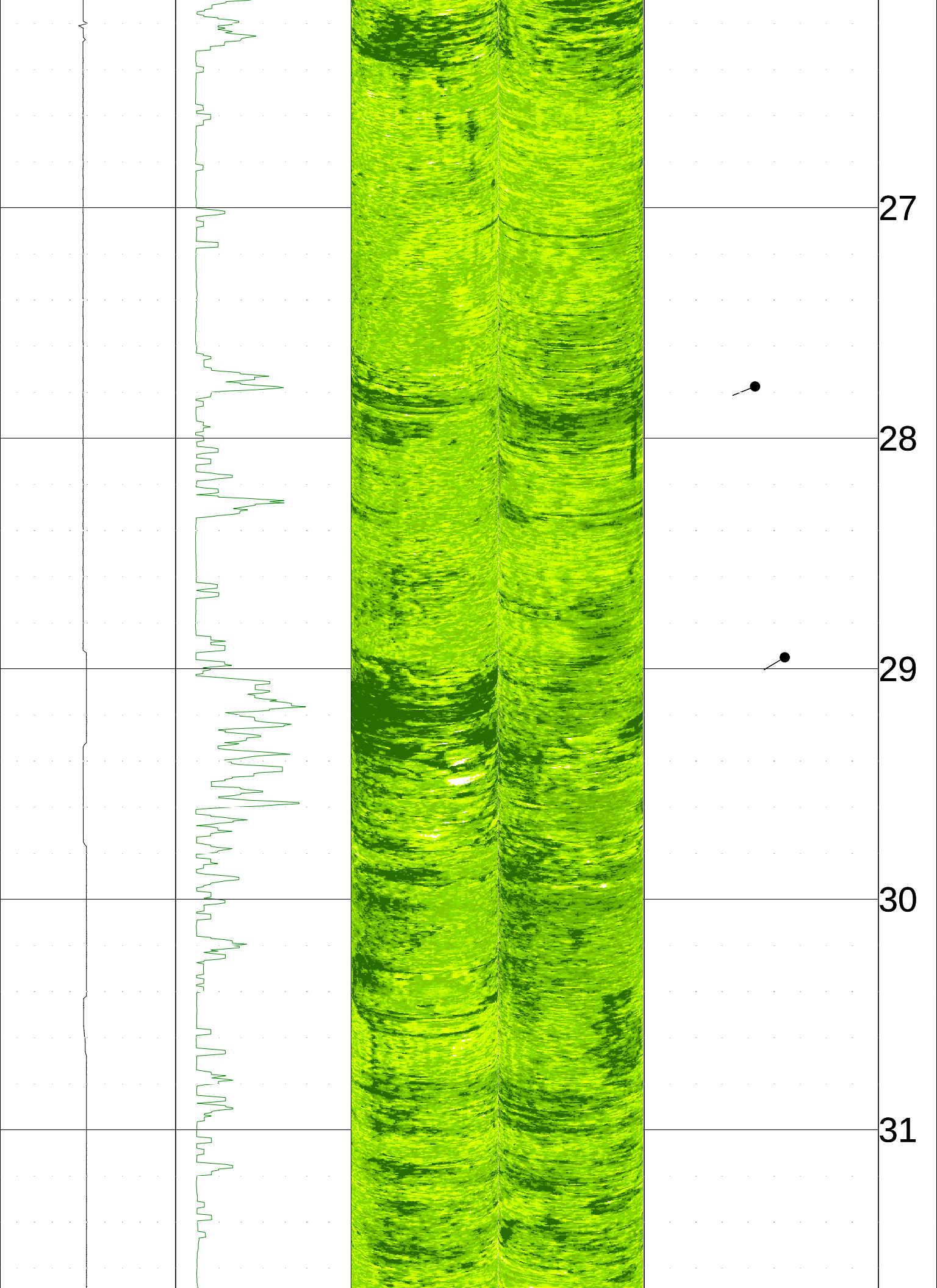
27
28
29
30
31

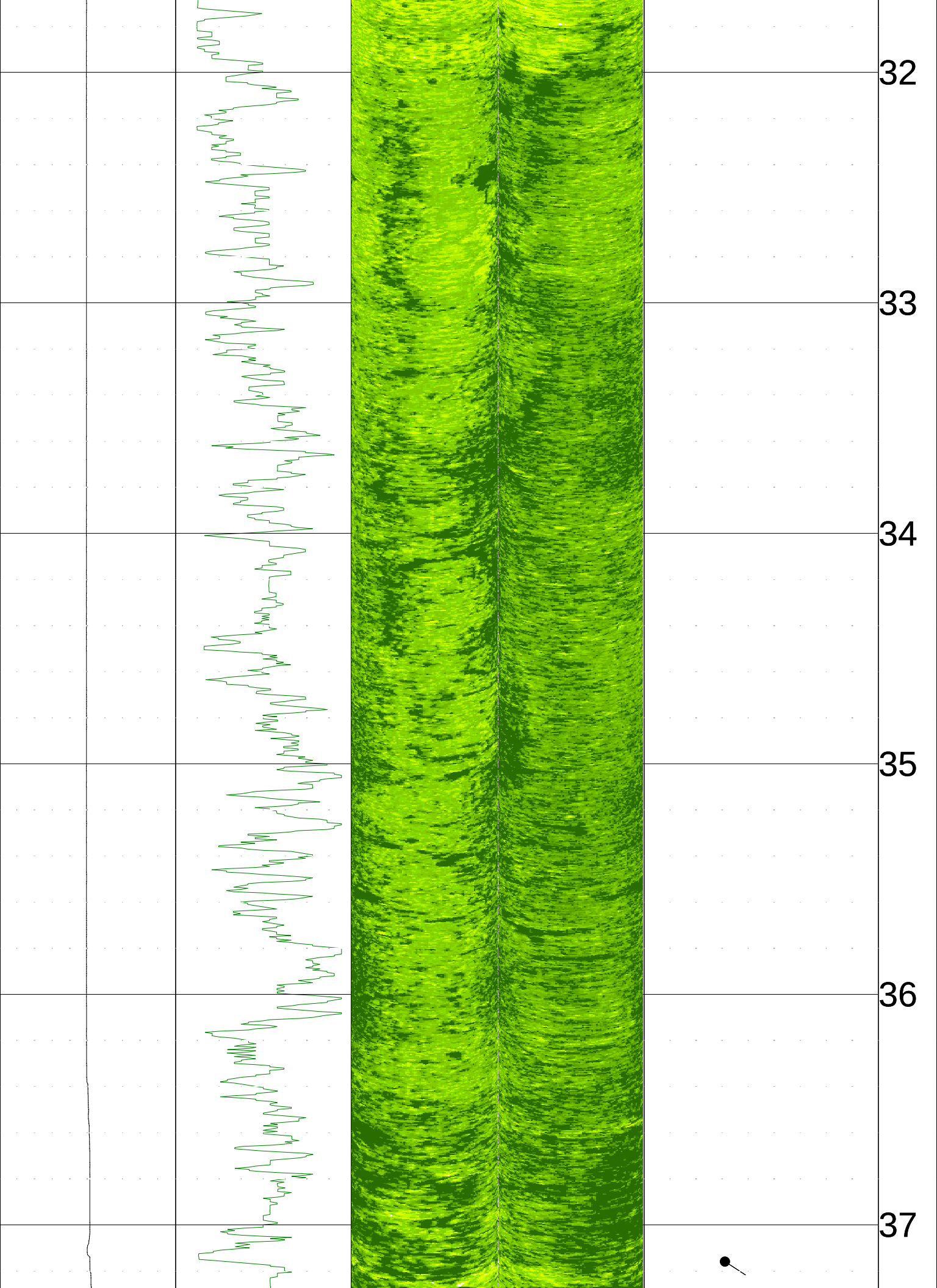
32
33
34
35
36
37

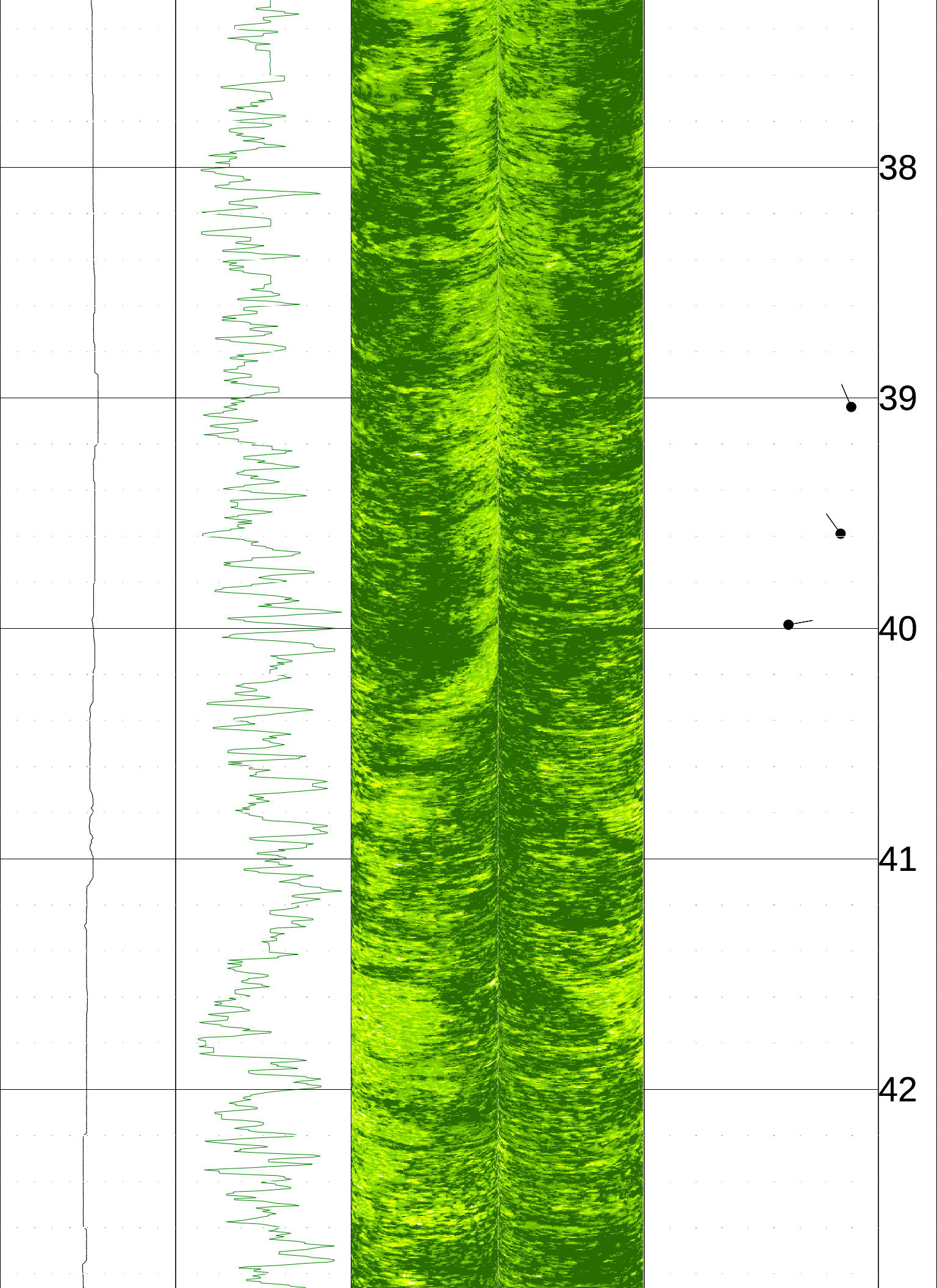
38
39
40
41
42

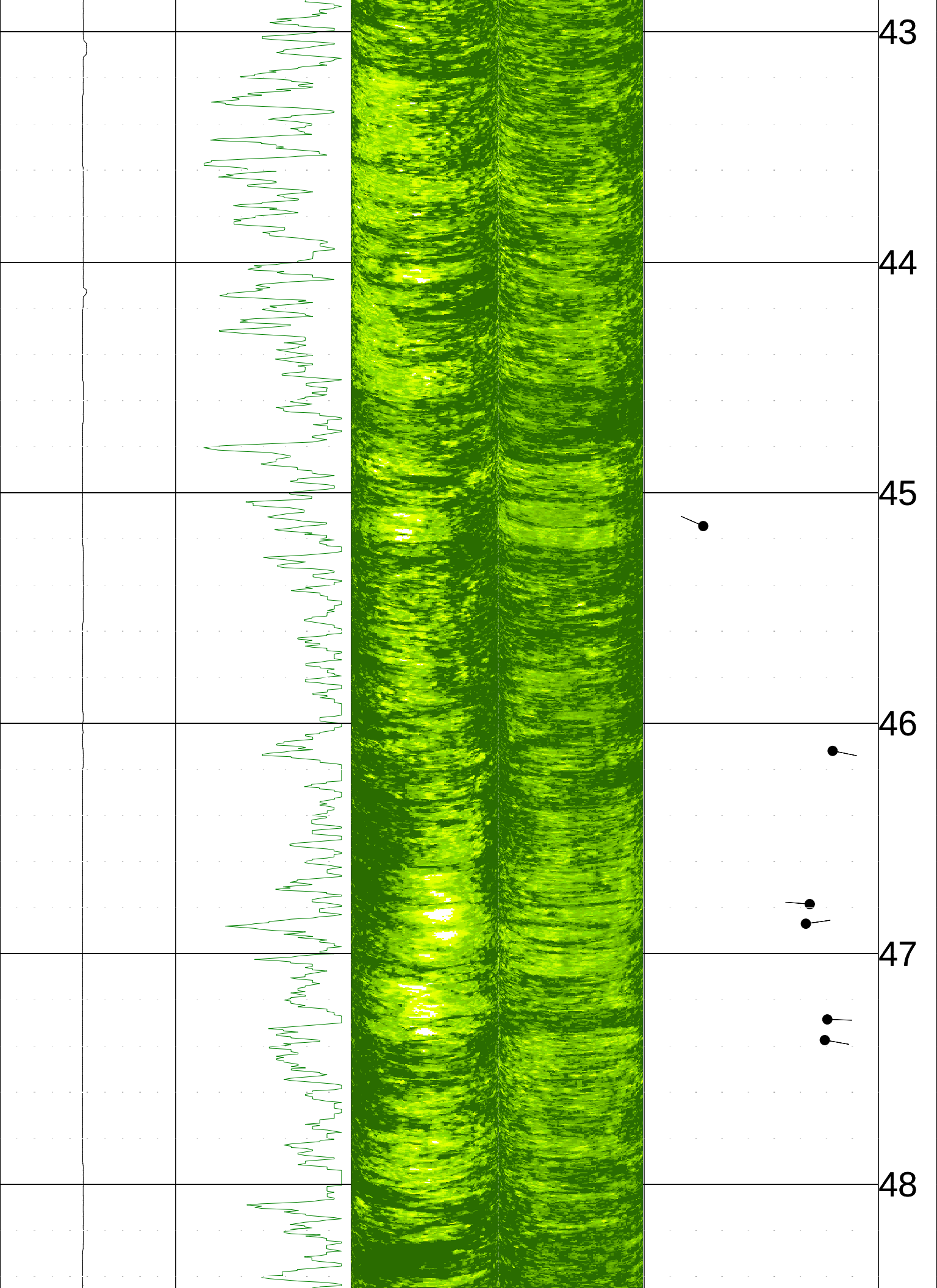
43
44
45
46
47
48

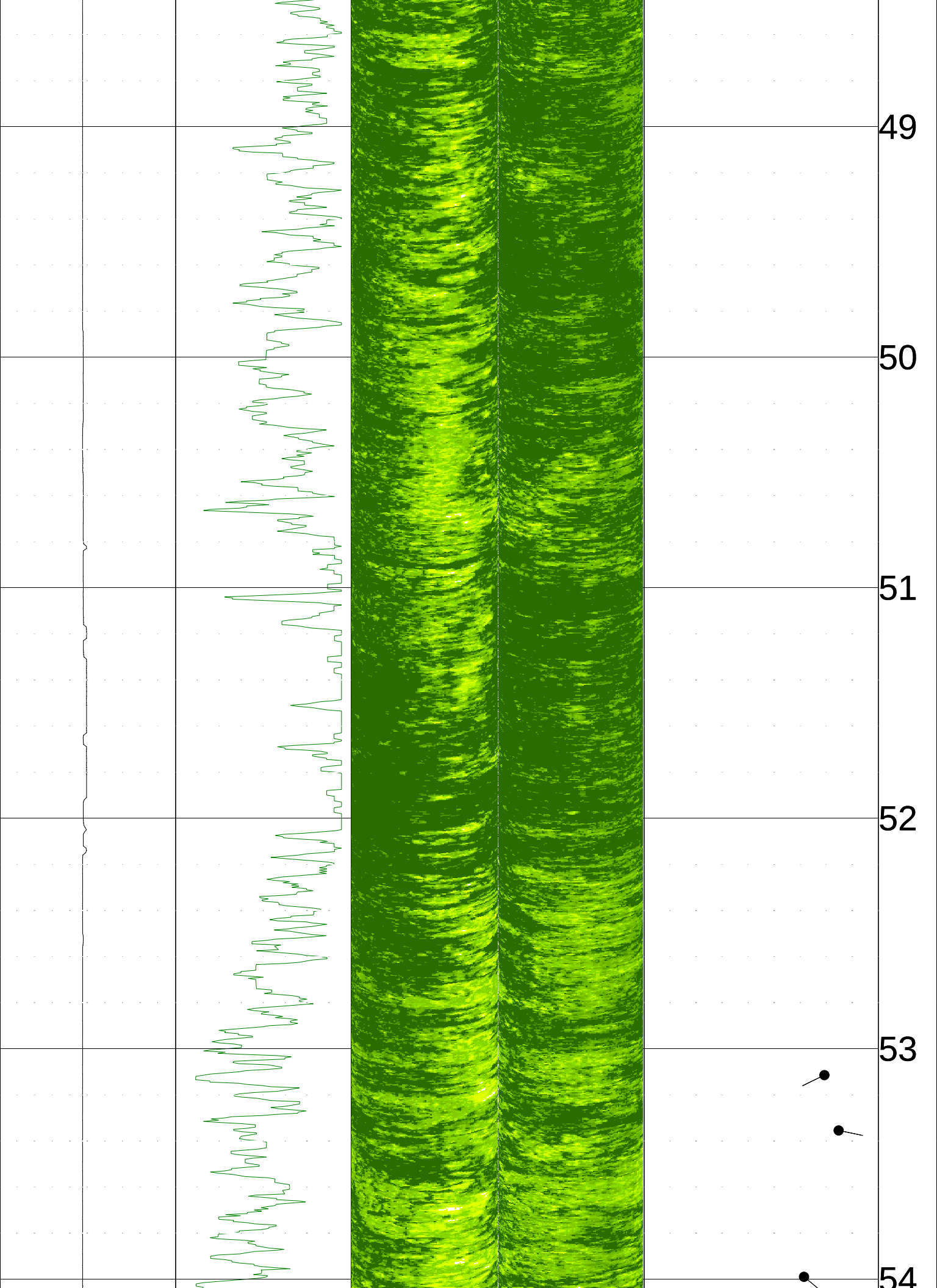
49
50
51
52
53
54

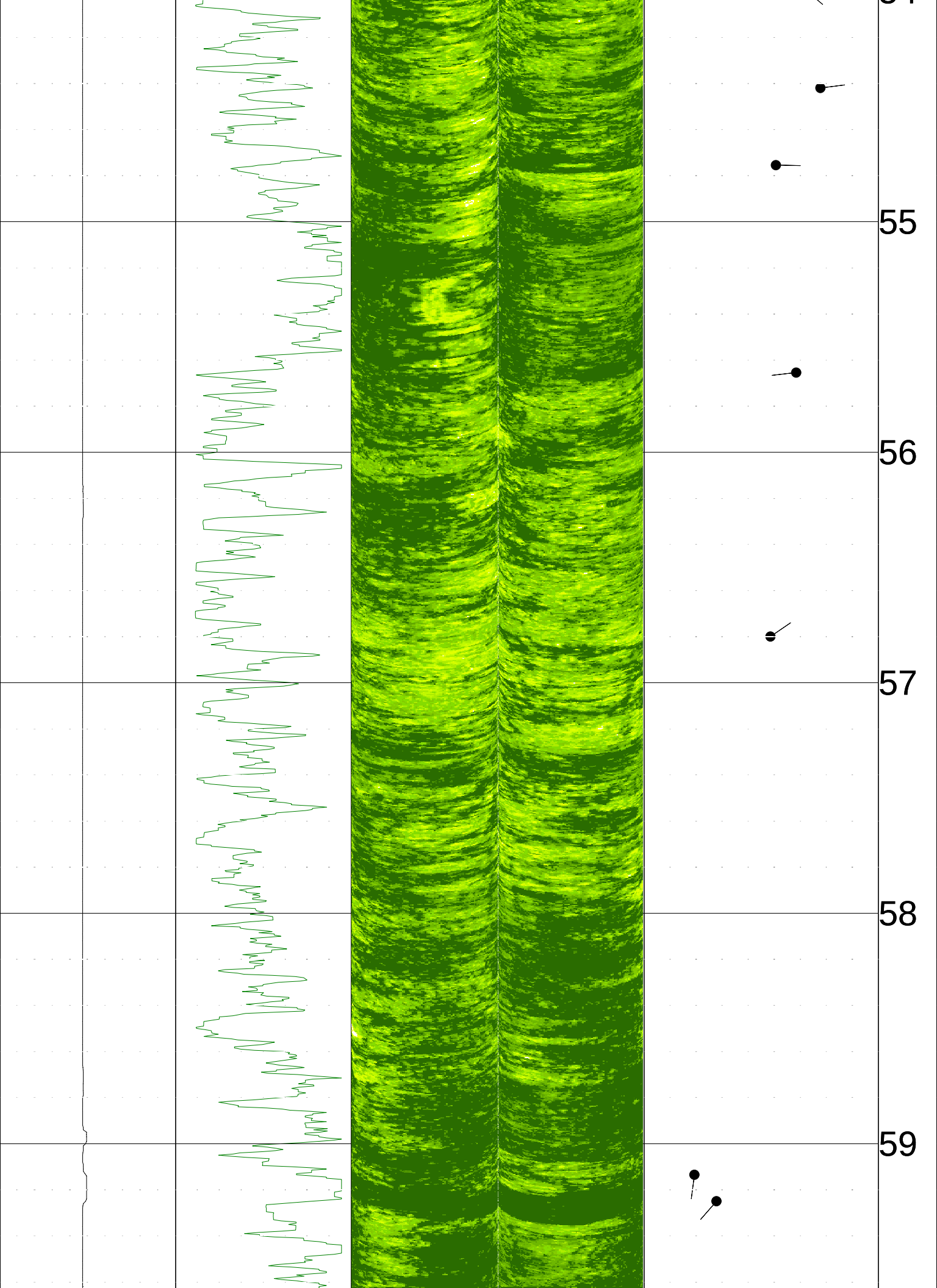
55
56
57
58
59

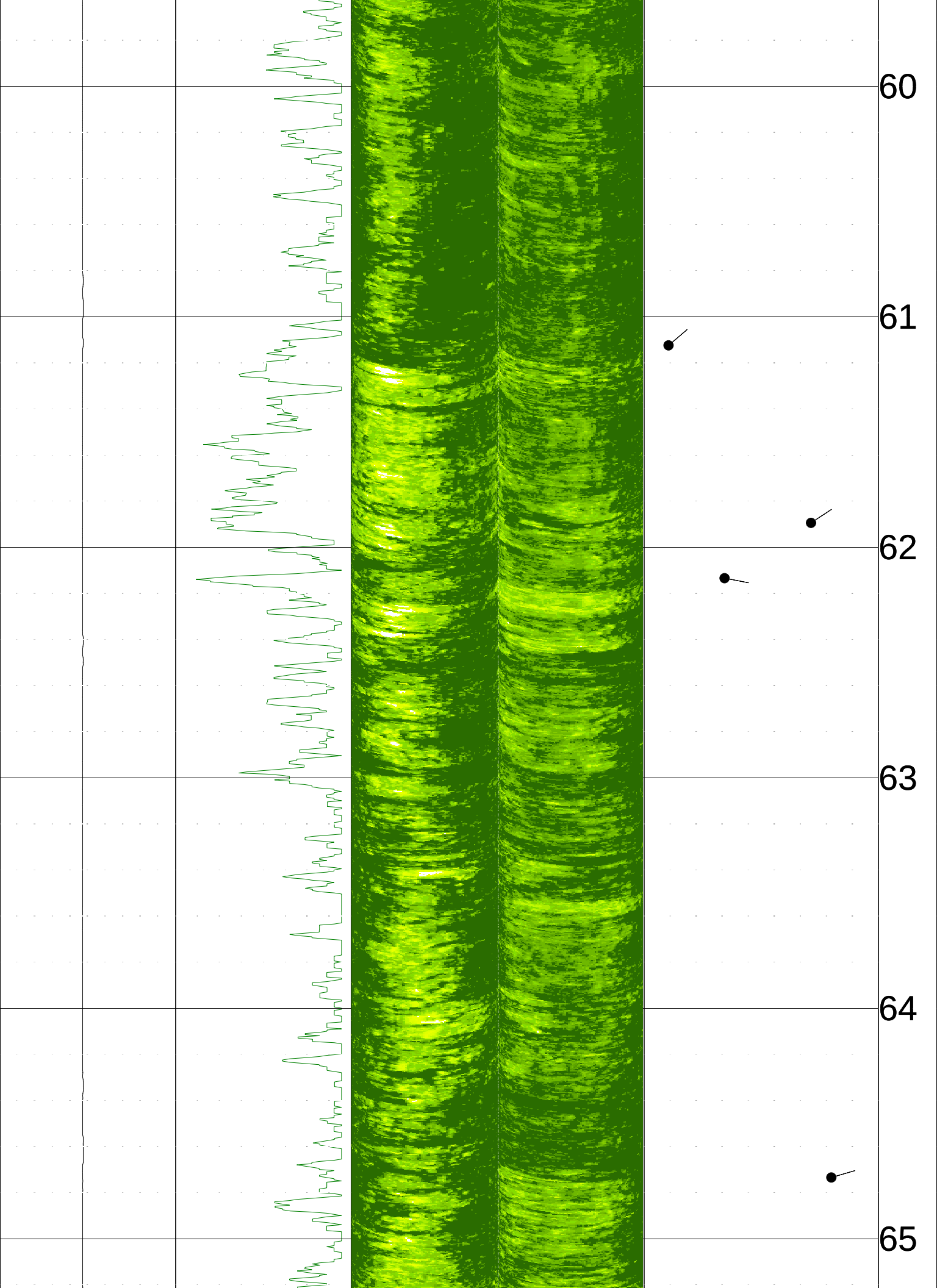
60
61
62
63
64
65

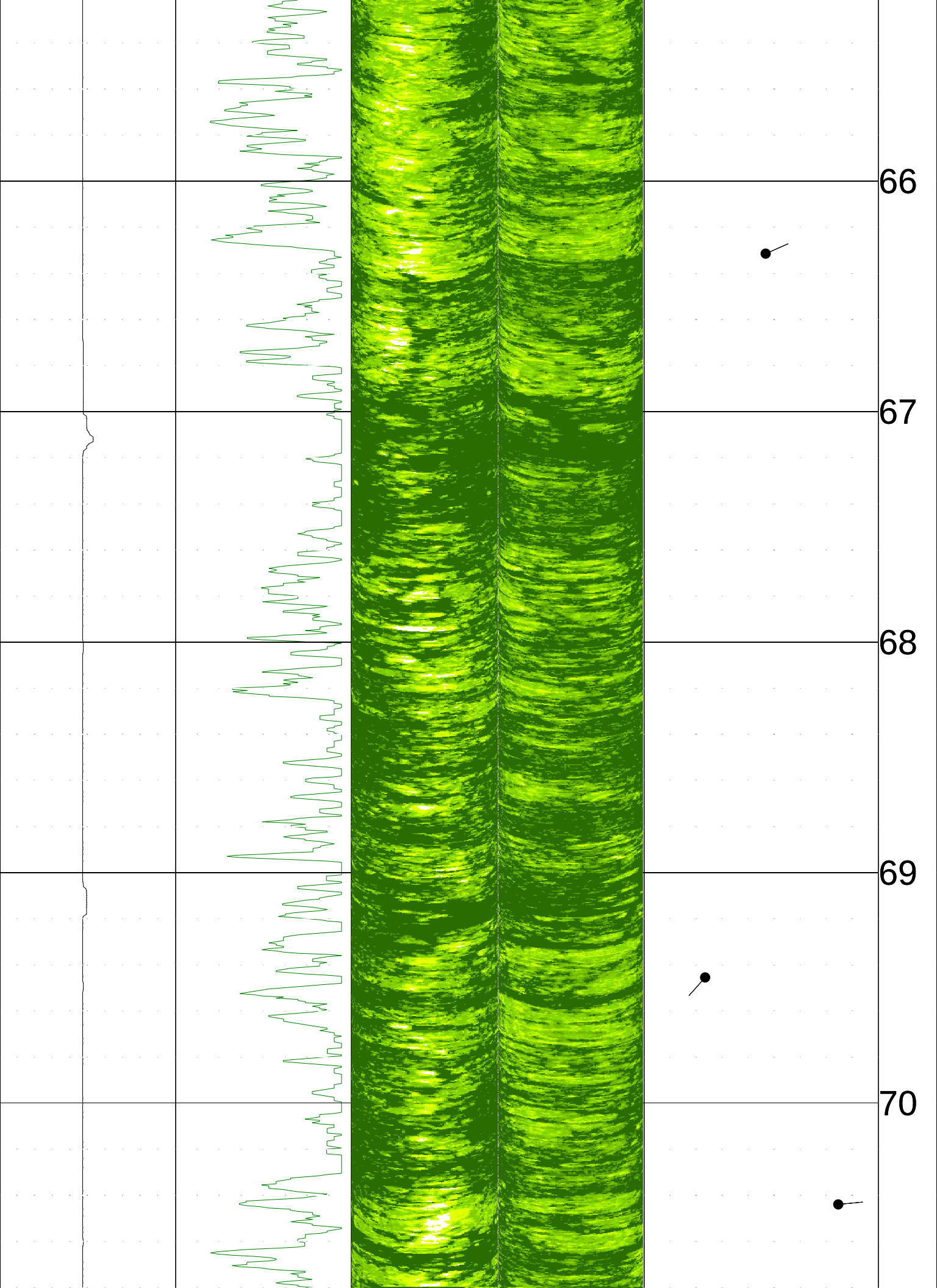
66
67
68
69
70

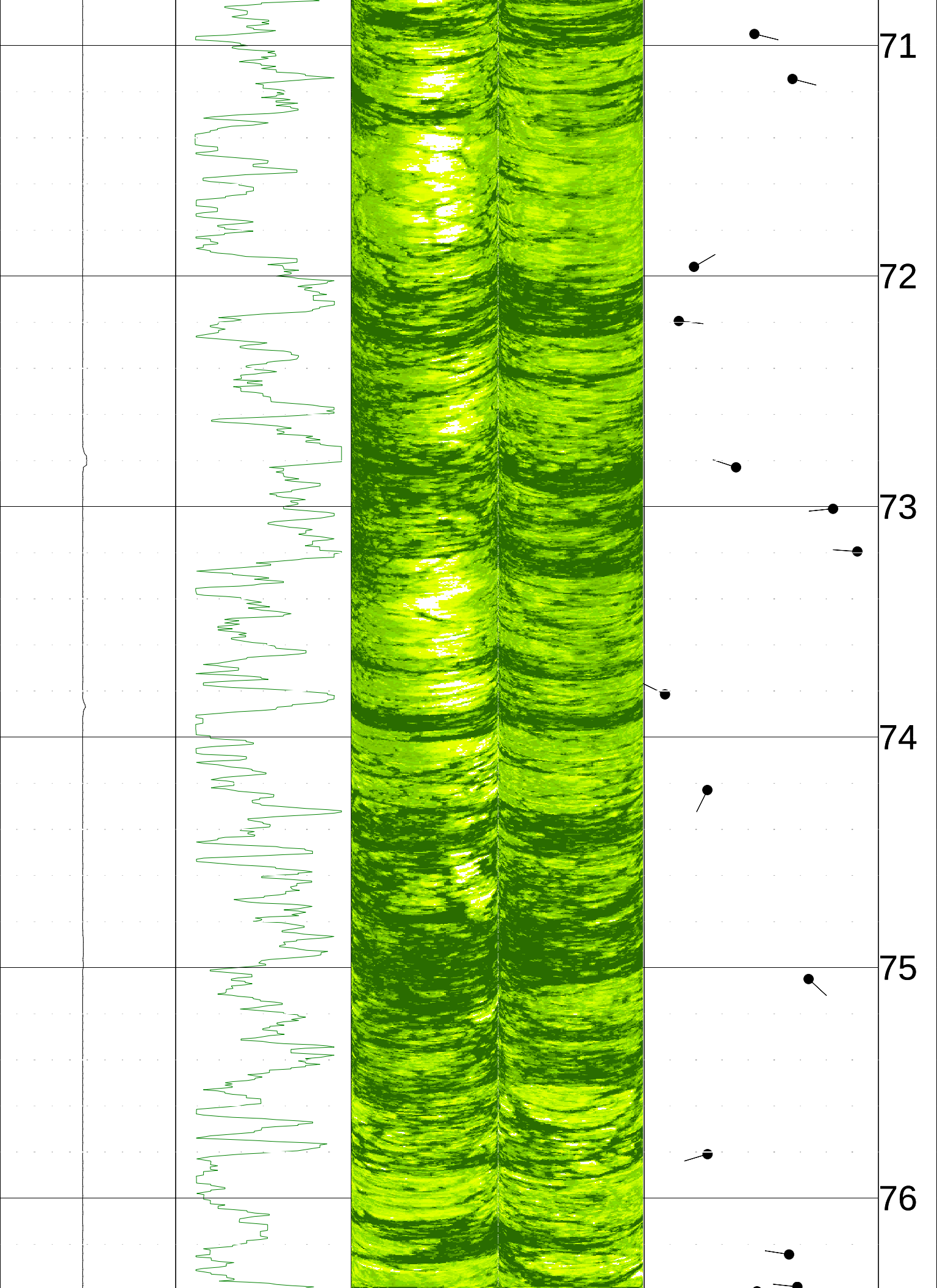
71
72
73
74
75
76

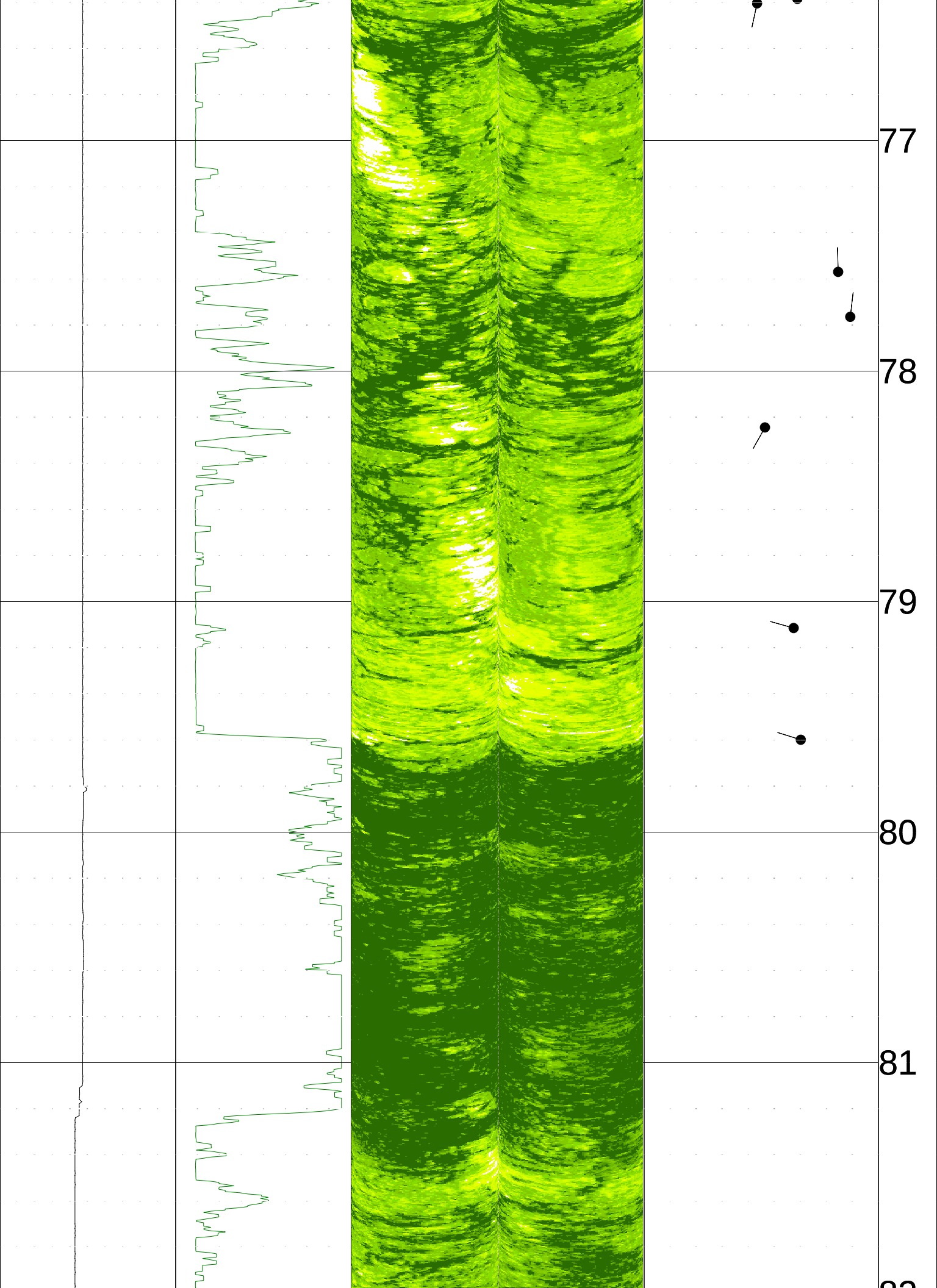
77
78
79
80
81

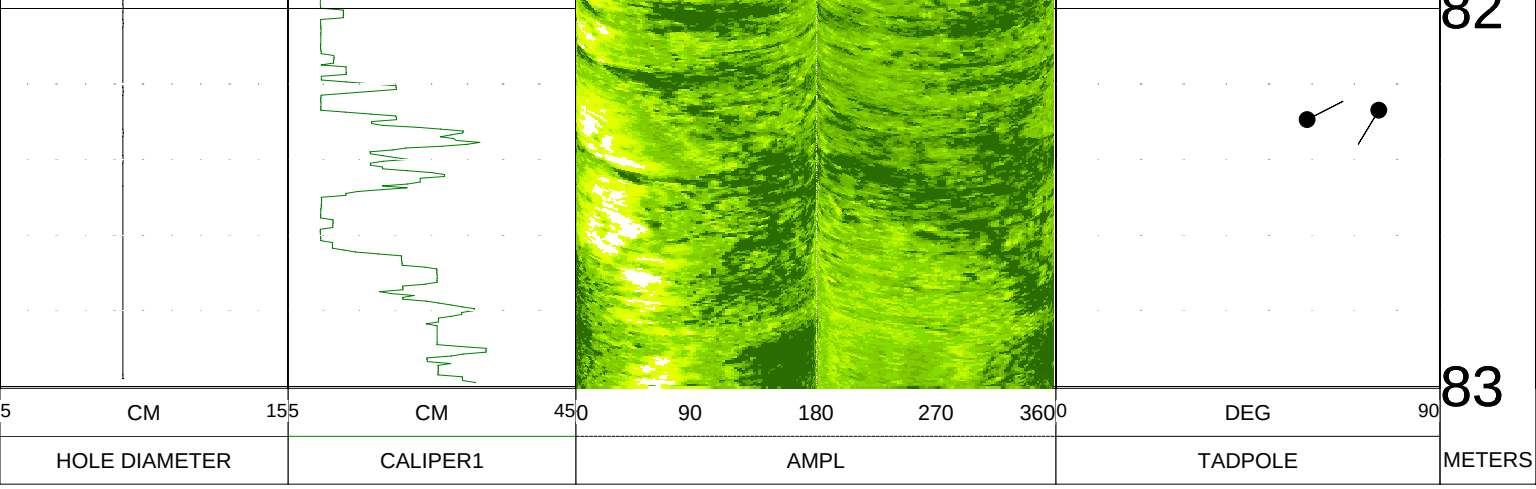
82
83
5
CM
155
CM
450
90
180
270
360
0
DEG
90
HOLE DIAMETER
CALIPER1
AMPL
TADPOLE
METERS

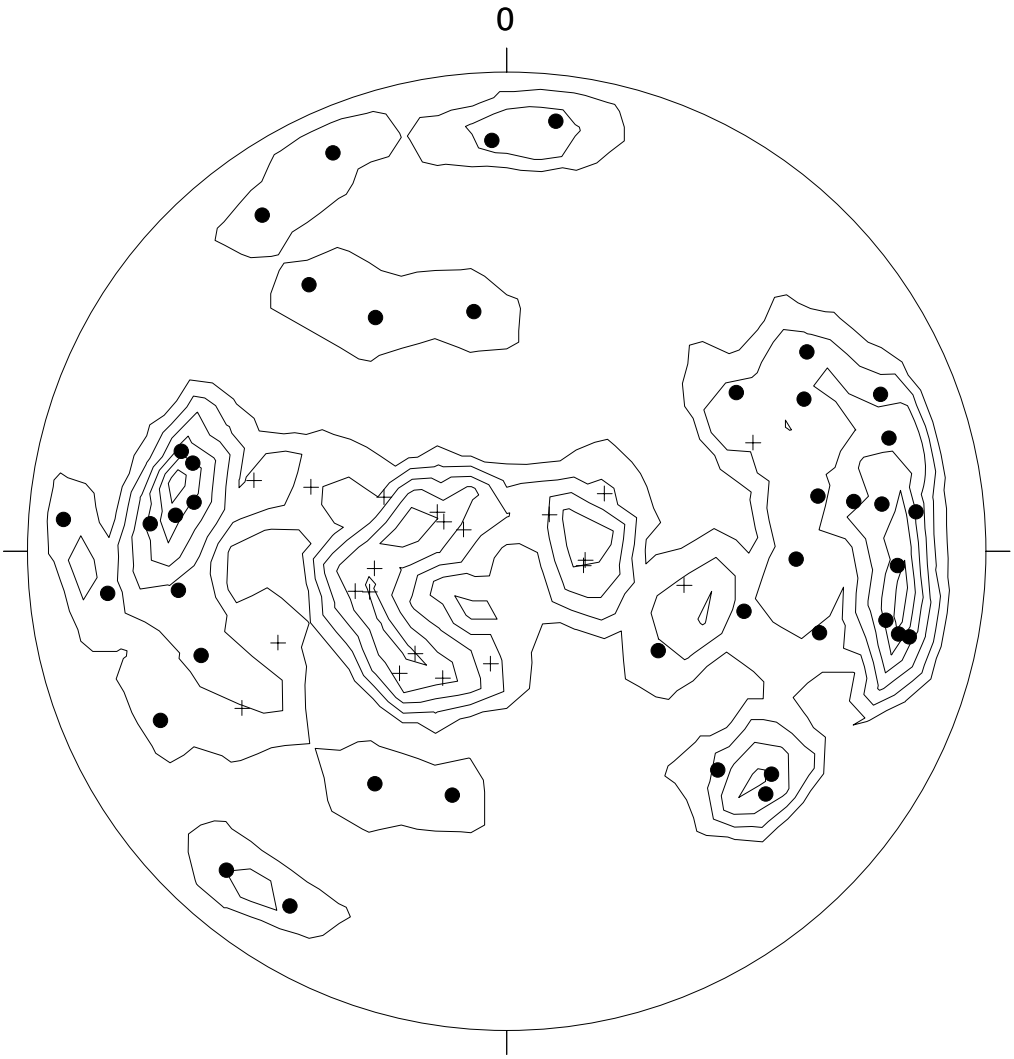


LA 710 Tunnel, boring Z3 B2

+ n=21 (P)
• n=41 (P)

Stereonet contour plot of poles to planes,
Both bedding and fractures

n=62
max. dens.= 6.72 (at 282/ 30)
min. dens.=0.00
Contours at every integer between
1 and 6, inclusive:
(Multiples of random distribution)

Apparent bedding denoted as cross
Apparent fractures denoted as solid circle
Plotted on upper hemisphere


LA 710 Tunnel boring Z3 B8

| | | | | | |
|---|---|---|---|---|---|
| COMPANY | : CALTRANS | | | | |
| WELL | : Z3 B8 | | | | |
| LOCATION/FIELD | : LA 710 TUNNEL | | | | |
| COUNTY | : LA | | | | |
| LOCATION | : CA | | | | |
| SECTION | : None | TOWNSHIP | : None | RANGE | : None |
| DATE | : 3/18/09 | PERMANENT DATUM | : None | | |
| DEPTH DRILLER | : 83.82M | | | KB | : NA |
| LOG BOTTOM | : 83.4 | LOG MEASURED FROM: | GL | DF | : NA |
| LOG TOP | : 1.3 | DRL MEASURED FROM: | GL | GL | : NA |
| CASING DIAMETER | : N/A | LOGGING UNIT | : 7311 | | |
| CASING TYPE | : N/A | FIELD OFFICE | : 7311 | | |
| CASING THICKNESS: | N/A | RECORDED BY | : DH/DG | | |
| BIT SIZE | : 10.5CM | BOREHOLE FLUID | : 0 | FILE | : ORIGINA |
| MAGNETIC DECL. | : 12.85 | RM | : 0 | TYPE | : 9511C |
| MATRIX DENSITY | : 2.71 | RM TEMPERATURE | : 0 | LGDATE | : 3/18/09. |
| NEUTRON MATRIX | : DOLOMITE | MATRIX DELTA T | : 140 | | |
| | | | | THRESH: | 2500 |

OTHER SERVICES:
INDUCT
AC TEL
PS LOG

CALIPER TOOL FAILED AT SITE, NO CALTRANS CALIPER LOG
EA: 07-187900. GL ELEVATION ESTIMATED FROM HANDHELD GPS 172.8M

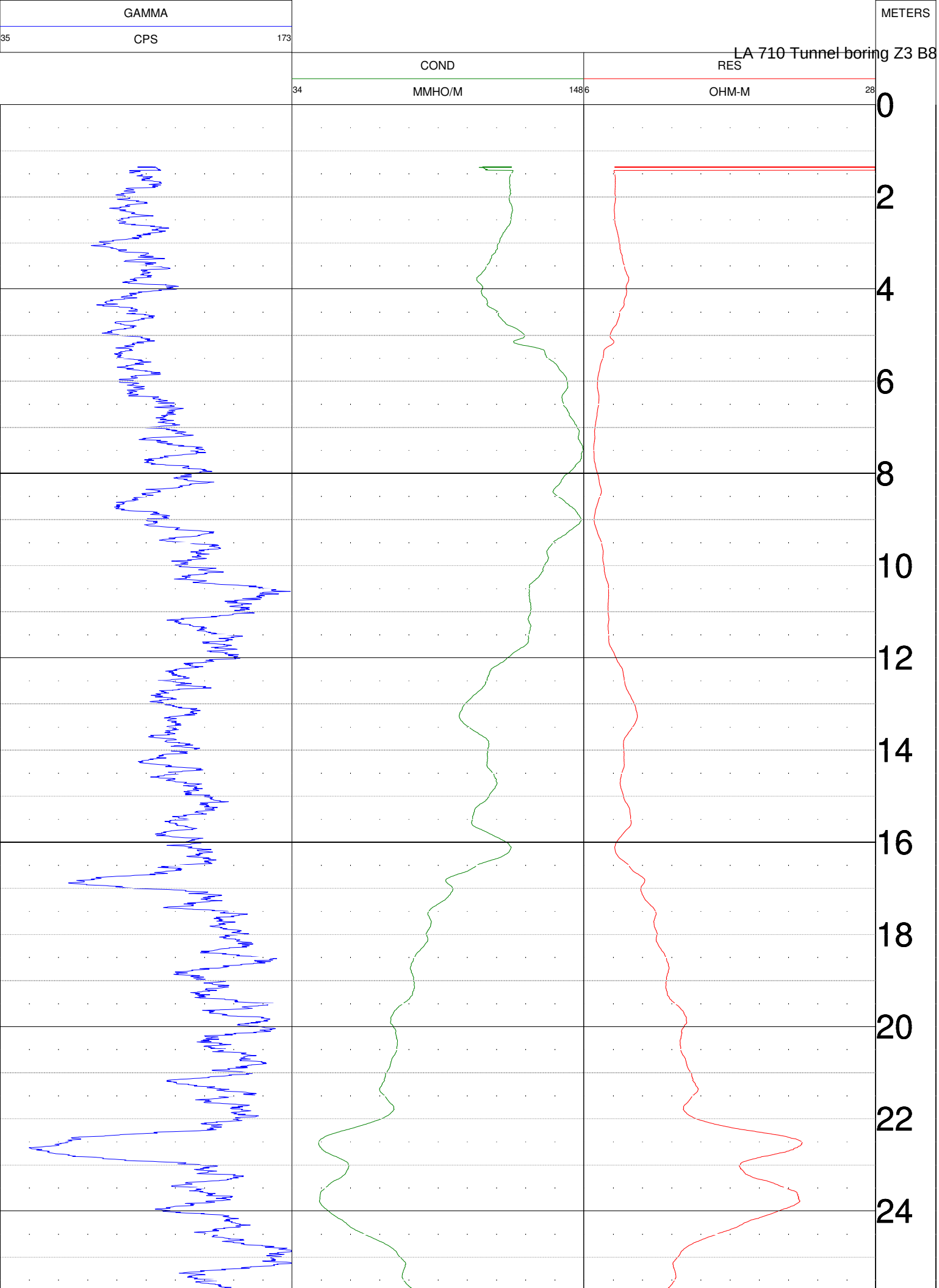
GAMMA
35
CPS
173
LA 710 Tunnel boring Z3 B8
COND
34
MMHO/M
148
RES
6
OHM-M
28
METERS
0
2
4
6
8
10
12
14
16
18
20
22
24

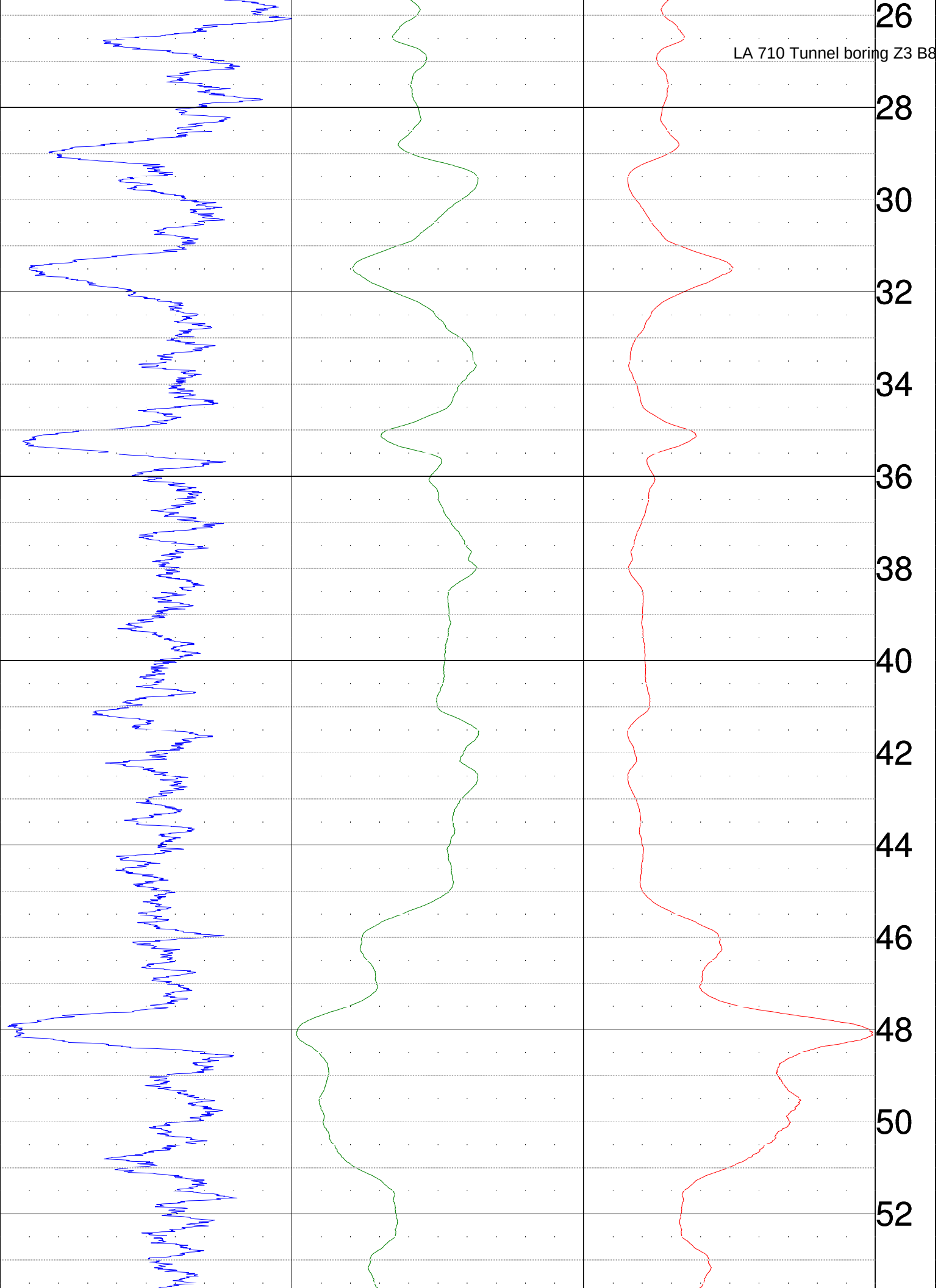
LA 710 Tunnel boring Z3 B8
26
28
30
32
34
36
38
40
42
44
46
48
50
52

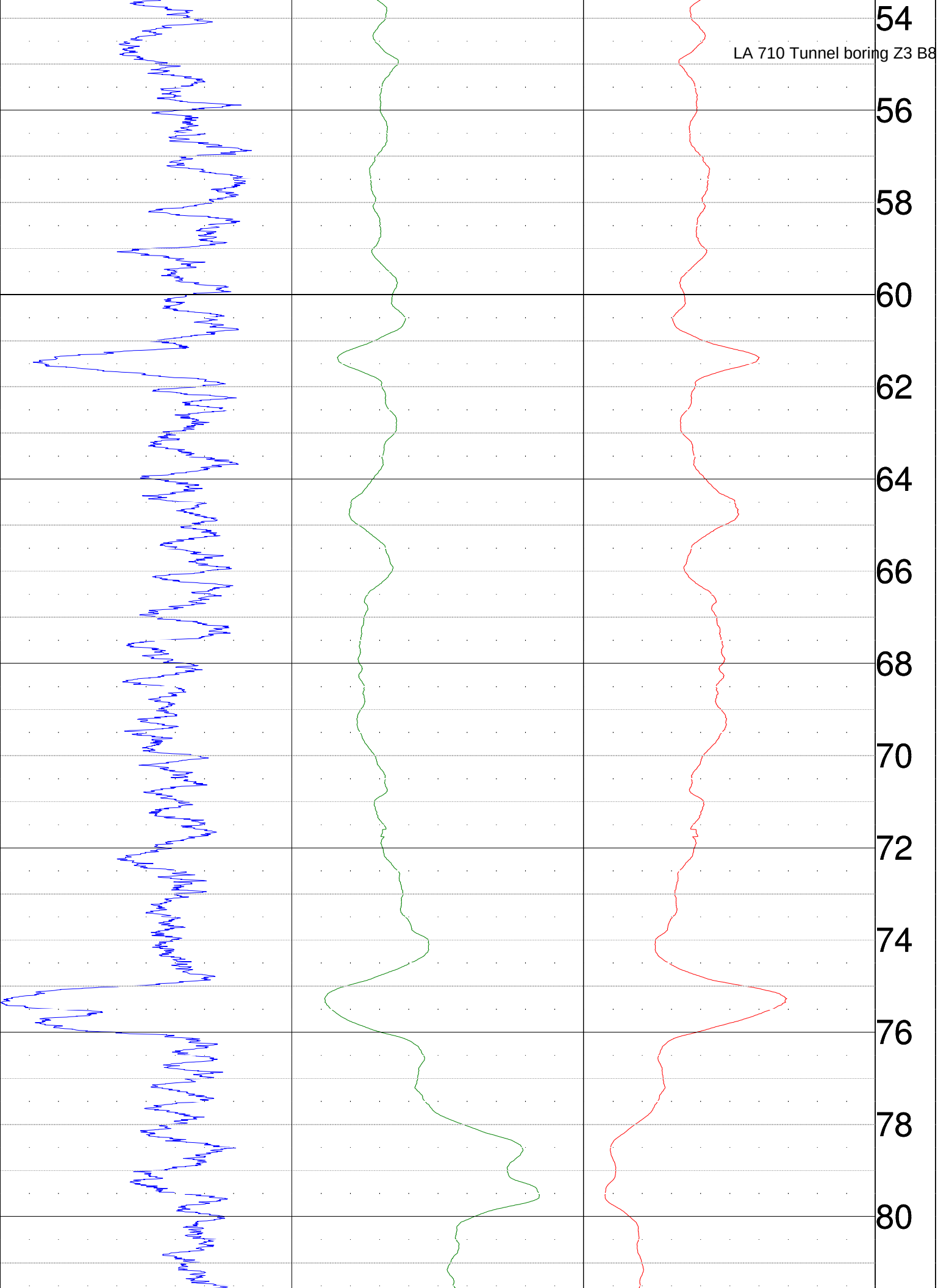
LA 710 Tunnel boring Z3 B8
54
56
58
60
62
64
66
68
70
72
74
76
78
80

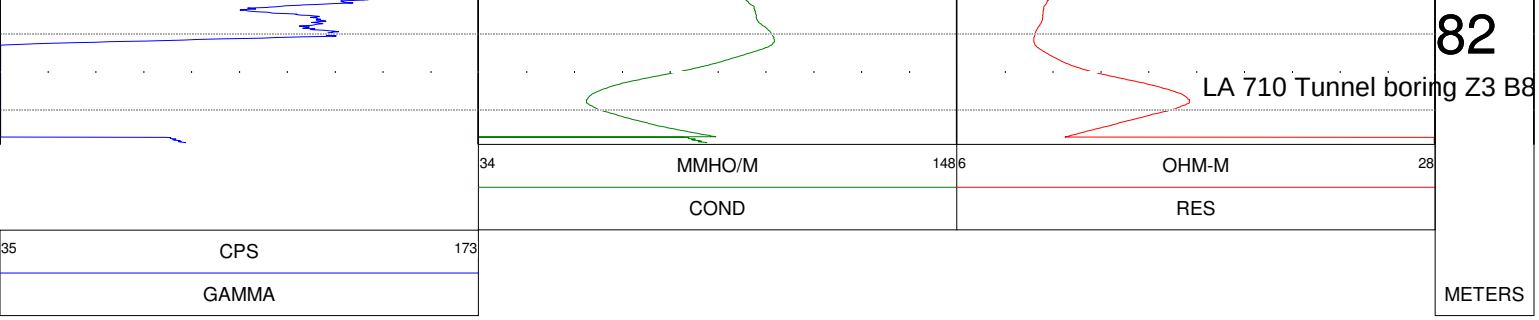
82
LA 710 Tunnel boring Z3 B8
34
MMHO/M
148
6
OHM-M
28
COND
RES
35
CPS
173
GAMMA
METERS

**Table 2.** LA 710 Tunnel
Boring Z3 B8
PS Suspension Log Data Summary



| Top of Hole Elevation (m) | Depth (m) | Depth (ft) | Vs (m/s) | Vs (ft/s) | Vp (m/s) | Vp (ft/s) | γ | ρ(Vp) (g/cc) | ρ(Vp) ($lb/ft^3$) | G (GPa) | E (GPa) | K (GPa) | G ($10^3 lb/ft^2$) | E ($10^3 lb/ft^2$) | K ($10^3 lb/ft^2$) |
|---|---|---|---|---|---|---|---|---|---|---|---|---|---|---|---|
| Not Provided | 1.5 | 4.9 | 189 | 619 | | NA | NA | NA | NA | NA | NA | NA | NA | NA | NA |
| | 2 | 6.6 | 168 | 551 | | NA | NA | NA | NA | NA | NA | NA | NA | NA | NA |
| | 2.4 | 7.9 | 165 | 542 | | NA | NA | NA | NA | NA | NA | NA | NA | NA | NA |
| | 2.4 | 7.9 | 164 | 538 | | NA | NA | NA | NA | NA | NA | NA | NA | NA | NA |
| | 2.4 | 7.9 | 167 | 549 | | NA | NA | NA | NA | NA | NA | NA | NA | NA | NA |
| | 3 | 9.8 | 166 | 543 | | NA | NA | NA | NA | NA | NA | NA | NA | NA | NA |
| | 3.5 | 11.5 | 195 | 641 | | NA | NA | NA | NA | NA | NA | NA | NA | NA | NA |
| | 4.1 | 13.5 | 235 | 770 | | NA | NA | NA | NA | NA | NA | NA | NA | NA | NA |
| | 4.6 | 15.1 | 244 | 800 | | NA | NA | NA | NA | NA | NA | NA | NA | NA | NA |
| | 5.1 | 16.7 | 255 | 837 | | NA | NA | NA | NA | NA | NA | NA | NA | NA | NA |
| | 5.1 | 16.7 | 251 | 824 | | NA | NA | NA | NA | NA | NA | NA | NA | NA | NA |
| | 5.6 | 18.4 | 250 | 820 | 515 | 1691 | NA | NA | NA | NA | NA | NA | NA | NA | NA |
| | 6.1 | 20.0 | 282 | 927 | 649 | 2130 | NA | NA | NA | NA | NA | NA | NA | NA | NA |
| | 6.6 | 21.7 | 331 | 1086 | 1136 | 3728 | NA | NA | NA | NA | NA | NA | NA | NA | NA |
| | 7.1 | 23.3 | 355 | 1163 | 1316 | 4317 | NA | NA | NA | NA | NA | NA | NA | NA | NA |
| | 7.6 | 24.9 | 417 | 1367 | 1316 | 4317 | NA | NA | NA | NA | NA | NA | NA | NA | NA |
| | 8.1 | 26.6 | 476 | 1562 | 1515 | 4971 | NA | NA | NA | NA | NA | NA | NA | NA | NA |
| | 8.5 | 27.9 | 296 | 971 | 1250 | 4101 | NA | NA | NA | NA | NA | NA | NA | NA | NA |
| | 9 | 29.5 | 239 | 785 | 1220 | 4001 | NA | NA | NA | NA | NA | NA | NA | NA | NA |
| | 9.6 | 31.5 | 352 | 1155 | 1515 | 4971 | NA | NA | NA | NA | NA | NA | NA | NA | NA |
| | 10.1 | 33.1 | 385 | 1262 | 1786 | 5859 | 0.48 | 2.06 | 128.62 | 0.305 | 0.899 | 6.163 | 6365 | 18786 | 128721 |
| | 11 | 36.1 | 373 | 1224 | 1667 | 5468 | 0.47 | 1.98 | 123.58 | 0.276 | 0.812 | 5.131 | 5756 | 16966 | 107173 |
| | 11.5 | 37.7 | 357 | 1172 | 1667 | 5468 | 0.48 | 1.98 | 123.58 | 0.253 | 0.745 | 5.162 | 5274 | 15567 | 107817 |
| | 12.5 | 41.0 | 431 | 1414 | 1786 | 5859 | 0.47 | 2.06 | 128.62 | 0.383 | 1.125 | 6.059 | 7994 | 23488 | 126549 |
| | 13 | 42.7 | 455 | 1491 | 1786 | 5859 | 0.47 | 2.06 | 128.62 | 0.426 | 1.248 | 6.002 | 8890 | 26055 | 125354 |
| | 13.5 | 44.3 | 455 | 1491 | 1786 | 5859 | 0.47 | 2.06 | 128.62 | 0.426 | 1.248 | 6.002 | 8890 | 26055 | 125354 |
| | 14 | 45.9 | 455 | 1491 | 1786 | 5859 | 0.47 | 2.06 | 128.62 | 0.426 | 1.248 | 6.002 | 8890 | 26055 | 125354 |
| | 14.5 | 47.6 | 450 | 1478 | 1786 | 5859 | 0.47 | 2.06 | 128.62 | 0.418 | 1.226 | 6.012 | 8731 | 25599 | 125567 |
| | 15 | 49.2 | 450 | 1478 | 1852 | 6076 | 0.47 | 2.10 | 131.15 | 0.426 | 1.252 | 6.636 | 8903 | 26148 | 138596 |
| | 15.5 | 50.9 | 450 | 1478 | 1786 | 5859 | 0.47 | 2.06 | 128.62 | 0.418 | 1.226 | 6.012 | 8731 | 25599 | 125567 |
| | 16 | 52.5 | 439 | 1439 | 1786 | 5859 | 0.47 | 2.06 | 128.62 | 0.396 | 1.164 | 6.041 | 8277 | 24300 | 126172 |
| | 16.5 | 54.1 | 521 | 1709 | 2083 | 6835 | 0.47 | 2.22 | 138.82 | 0.603 | 1.769 | 8.847 | 12598 | 36954 | 184772 |
| | 17 | 55.8 | 641 | 2103 | 2174 | 7132 | 0.45 | 2.26 | 141.40 | 0.931 | 2.703 | 9.463 | 19438 | 56463 | 197640 |
| | 17.5 | 57.4 | 658 | 2158 | 2083 | 6835 | 0.44 | 2.22 | 138.82 | 0.962 | 2.781 | 8.368 | 20101 | 58077 | 174768 |
| | 17.5 | 57.4 | 658 | 2158 | 2083 | 6835 | 0.44 | 2.22 | 138.82 | 0.962 | 2.781 | 8.368 | 20101 | 58077 | 174768 |
| | 18 | 59.1 | 685 | 2247 | 2083 | 6835 | 0.44 | 2.22 | 138.82 | 1.043 | 3.003 | 8.260 | 21787 | 62721 | 172520 |
| | 18.5 | 60.7 | 714 | 2343 | 2174 | 7132 | 0.44 | 2.26 | 141.40 | 1.156 | 3.327 | 9.163 | 24135 | 69484 | 191377 |

γ = Poisson's Ratio  ρ(Vp) = Vp-derived density  G = Shear Modulus  E = Young's Modulus  K = Bulk Modulus
Shaded cells denote questionable data.

**Table 2.** LA 710 Tunnel
Boring Z3 B8
PS Suspension Log Data Summary



| Top of Hole Elevation (m) | Depth (m) | Depth (ft) | Vs (m/s) | Vs (ft/s) | Vp (m/s) | Vp (ft/s) | γ | ρ(Vp) (g/cc) | ρ(Vp) ($lb/ft^3$) | G (GPa) | E (GPa) | K (GPa) | G ($10^3 lb/ft^2$) | E ($10^3 lb/ft^2$) | K ($10^3 lb/ft^2$) |
|---|---|---|---|---|---|---|---|---|---|---|---|---|---|---|---|
| | 19 | 62.3 | 735 | 2412 | 2083 | 6835 | 0.43 | 2.22 | 138.82 | 1.202 | 3.436 | 8.048 | 25109 | 71754 | 168091 |
| | 19.5 | 64.0 | 735 | 2412 | 2174 | 7132 | 0.44 | 2.26 | 141.40 | 1.225 | 3.516 | 9.071 | 25576 | 73423 | 189456 |
| | 20 | 65.6 | 781 | 2563 | 2273 | 7456 | 0.43 | 2.31 | 143.99 | 1.408 | 4.035 | 10.037 | 29402 | 84266 | 209620 |
| | 20 | 65.6 | 676 | 2217 | 2174 | 7132 | 0.45 | 2.26 | 141.40 | 1.034 | 2.992 | 9.325 | 21596 | 62480 | 194763 |
| | 20 | 65.6 | 735 | 2412 | 2174 | 7132 | 0.44 | 2.26 | 141.40 | 1.225 | 3.516 | 9.071 | 25576 | 73423 | 189457 |
| | 20 | 65.6 | 746 | 2448 | 2174 | 7132 | 0.43 | 2.26 | 141.40 | 1.261 | 3.616 | 9.022 | 26345 | 75515 | 188431 |
| | 20 | 65.6 | 746 | 2448 | 2174 | 7132 | 0.43 | 2.26 | 141.40 | 1.261 | 3.616 | 9.022 | 26345 | 75515 | 188431 |
| | 20.5 | 67.3 | 746 | 2448 | 2174 | 7132 | 0.43 | 2.26 | 141.40 | 1.261 | 3.616 | 9.022 | 26345 | 75515 | 188431 |
| | 21 | 68.9 | 704 | 2310 | 2174 | 7132 | 0.44 | 2.26 | 141.40 | 1.123 | 3.238 | 9.206 | 23460 | 67629 | 192277 |
| | 21.5 | 70.5 | 735 | 2412 | 2273 | 7456 | 0.44 | 2.31 | 143.99 | 1.247 | 3.595 | 10.251 | 26044 | 75089 | 214096 |
| | 22 | 72.2 | 806 | 2646 | 2632 | 8634 | 0.45 | 2.43 | 151.84 | 1.582 | 4.582 | 14.734 | 33037 | 95686 | 307733 |
| | 22.4 | 73.5 | 746 | 2448 | 2941 | 9650 | 0.47 | 2.52 | 157.13 | 1.402 | 4.109 | 19.904 | 29276 | 85814 | 415705 |
| | 23 | 75.5 | 704 | 2310 | 2273 | 7456 | 0.45 | 2.31 | 143.99 | 1.143 | 3.308 | 10.390 | 23875 | 69090 | 216988 |
| | 23.5 | 77.1 | 685 | 2247 | 2273 | 7456 | 0.45 | 2.31 | 143.99 | 1.082 | 3.139 | 10.471 | 22603 | 65552 | 218684 |
| | 24 | 78.7 | 676 | 2217 | 2500 | 8202 | 0.46 | 2.39 | 149.21 | 1.091 | 3.188 | 13.483 | 22790 | 66573 | 281602 |
| | 24.5 | 80.4 | 893 | 2929 | 2381 | 7812 | 0.42 | 2.35 | 146.59 | 1.872 | 5.310 | 10.816 | 39097 | 110893 | 225892 |
| | 25 | 82.0 | 769 | 2524 | 2273 | 7456 | 0.44 | 2.31 | 143.99 | 1.365 | 3.918 | 10.094 | 28504 | 81824 | 210816 |
| | 25.5 | 83.7 | 806 | 2646 | 2273 | 7456 | 0.43 | 2.31 | 143.99 | 1.500 | 4.284 | 9.914 | 31329 | 89475 | 207050 |
| | 25.9 | 85.0 | 725 | 2377 | 2381 | 7812 | 0.45 | 2.35 | 146.59 | 1.233 | 3.573 | 11.668 | 25752 | 74629 | 243685 |
| | 26.4 | 86.6 | 704 | 2310 | 2273 | 7456 | 0.45 | 2.31 | 143.99 | 1.144 | 3.310 | 10.389 | 23890 | 69133 | 216968 |
| | 26.9 | 88.3 | 641 | 2103 | 2174 | 7132 | 0.45 | 2.26 | 141.40 | 0.931 | 2.704 | 9.463 | 19438 | 56463 | 197640 |
| | 27.4 | 89.9 | 667 | 2187 | 2174 | 7132 | 0.45 | 2.26 | 141.40 | 1.007 | 2.915 | 9.362 | 21024 | 60890 | 195525 |
| | 28 | 91.9 | 685 | 2247 | 2083 | 6835 | 0.44 | 2.22 | 138.82 | 1.043 | 3.003 | 8.260 | 21787 | 62721 | 172520 |
| | 28.5 | 93.5 | 735 | 2412 | 2083 | 6835 | 0.43 | 2.22 | 138.82 | 1.202 | 3.436 | 8.048 | 25109 | 71754 | 168091 |
| | 29 | 95.1 | 735 | 2412 | 2273 | 7456 | 0.44 | 2.31 | 143.99 | 1.247 | 3.595 | 10.251 | 26044 | 75089 | 214096 |
| | 29.5 | 96.8 | 541 | 1773 | 2000 | 6562 | 0.46 | 2.18 | 136.25 | 0.638 | 1.863 | 7.880 | 13318 | 38906 | 164572 |
| | 30 | 98.4 | 513 | 1682 | 2000 | 6562 | 0.46 | 2.18 | 136.25 | 0.574 | 1.682 | 7.965 | 11987 | 35119 | 166346 |
| | 30 | 98.4 | 532 | 1745 | 2083 | 6835 | 0.47 | 2.22 | 138.82 | 0.629 | 1.844 | 8.812 | 13140 | 38503 | 184049 |
| | 30 | 98.4 | 549 | 1803 | 2000 | 6562 | 0.46 | 2.18 | 136.25 | 0.659 | 1.923 | 7.852 | 13761 | 40160 | 163981 |
| | 30.5 | 100.1 | 549 | 1803 | 2083 | 6835 | 0.46 | 2.22 | 138.82 | 0.671 | 1.964 | 8.756 | 14021 | 41013 | 182875 |
| | 31 | 101.7 | 833 | 2734 | 2381 | 7812 | 0.43 | 2.35 | 146.59 | 1.631 | 4.664 | 11.138 | 34058 | 97418 | 232611 |
| | 31.5 | 103.3 | 893 | 2929 | 2941 | 9650 | 0.45 | 2.52 | 157.13 | 2.007 | 5.816 | 19.098 | 41907 | 121467 | 398865 |
| | 32 | 105.0 | 833 | 2734 | 2381 | 7812 | 0.43 | 2.35 | 146.59 | 1.631 | 4.664 | 11.138 | 34058 | 97418 | 232611 |
| | 32.5 | 106.6 | 826 | 2711 | 2222 | 7291 | 0.42 | 2.29 | 142.69 | 1.561 | 4.433 | 9.206 | 32606 | 92583 | 192268 |
| | 32.5 | 106.6 | 893 | 2929 | 2273 | 7456 | 0.41 | 2.31 | 143.99 | 1.839 | 5.181 | 9.462 | 38402 | 108198 | 197619 |
| | 32.9 | 107.9 | 752 | 2467 | 2222 | 7291 | 0.44 | 2.29 | 142.69 | 1.292 | 3.709 | 9.565 | 26987 | 77473 | 199759 |
| | 33.5 | 109.9 | 633 | 2076 | 2128 | 6981 | 0.45 | 2.24 | 140.11 | 0.899 | 2.610 | 8.961 | 18776 | 54505 | 187155 |

γ = Poisson's Ratio  ρ(Vp) = Vp-derived density  G = Shear Modulus  E = Young's Modulus  K = Bulk Modulus
Shaded cells denote questionable data.

**Table 2.** LA 710 Tunnel
Boring Z3 B8
PS Suspension Log Data Summary



| Top of Hole Elevation (m) | Depth (m) | Depth (ft) | Vs (m/s) | Vs (ft/s) | Vp (m/s) | Vp (ft/s) | γ | ρ(Vp) (g/cc) | ρ(Vp) ($lb/ft^3$) | G (GPa) | E (GPa) | K (GPa) | G ($10^3 lb/ft^2$) | E ($10^3 lb/ft^2$) | K ($10^3 lb/ft^2$) |
|---|---|---|---|---|---|---|---|---|---|---|---|---|---|---|---|
| | 34 | 111.5 | 676 | 2217 | 2174 | 7132 | 0.45 | 2.26 | 141.40 | 1.034 | 2.992 | 9.325 | 21596 | 62480 | 194762 |
| | 34.5 | 113.2 | 813 | 2667 | 2439 | 8002 | 0.44 | 2.37 | 147.90 | 1.566 | 4.502 | 12.006 | 32705 | 94028 | 250742 |
| | 35 | 114.8 | 885 | 2903 | 2857 | 9374 | 0.45 | 2.50 | 155.80 | 1.955 | 5.656 | 17.767 | 40821 | 118130 | 371073 |
| | 35.5 | 116.5 | 840 | 2757 | 2632 | 8634 | 0.44 | 2.43 | 151.84 | 1.718 | 4.958 | 14.554 | 35871 | 103541 | 303955 |
| | 36 | 118.1 | 769 | 2524 | 2326 | 7630 | 0.44 | 2.33 | 145.29 | 1.377 | 3.962 | 10.751 | 28762 | 82751 | 224534 |
| | 36.5 | 119.8 | 813 | 2667 | 2222 | 7291 | 0.42 | 2.29 | 142.69 | 1.511 | 4.299 | 9.273 | 31554 | 89785 | 193671 |
| | 37 | 121.4 | 741 | 2430 | 2000 | 6562 | 0.42 | 2.18 | 136.25 | 1.198 | 3.402 | 7.133 | 25011 | 71056 | 148981 |
| | 37.5 | 123.0 | 680 | 2232 | 2128 | 6981 | 0.44 | 2.24 | 140.11 | 1.039 | 2.998 | 8.775 | 21691 | 62604 | 183268 |
| | 38 | 124.7 | 662 | 2173 | 2128 | 6981 | 0.45 | 2.24 | 140.11 | 0.984 | 2.847 | 8.847 | 20557 | 59467 | 184780 |
| | 38.5 | 126.3 | 730 | 2395 | 2222 | 7291 | 0.44 | 2.29 | 142.69 | 1.218 | 3.506 | 9.664 | 25434 | 73227 | 201830 |
| | 39 | 128.0 | 781 | 2563 | 2174 | 7132 | 0.43 | 2.26 | 141.40 | 1.382 | 3.942 | 8.861 | 28873 | 82336 | 185061 |
| | 39.5 | 129.6 | 775 | 2543 | 2174 | 7132 | 0.43 | 2.26 | 141.40 | 1.361 | 3.885 | 8.889 | 28427 | 81139 | 185656 |
| | 39.9 | 130.9 | 763 | 2504 | 2222 | 7291 | 0.43 | 2.29 | 142.69 | 1.332 | 3.818 | 9.512 | 27818 | 79731 | 198652 |
| | 40.4 | 132.5 | 800 | 2625 | 2273 | 7456 | 0.43 | 2.31 | 143.99 | 1.476 | 4.220 | 9.946 | 30830 | 88130 | 207715 |
| | 40.9 | 134.2 | 826 | 2711 | 2326 | 7630 | 0.43 | 2.33 | 145.29 | 1.590 | 4.539 | 10.467 | 33199 | 94799 | 218616 |
| | 41.4 | 135.8 | 781 | 2563 | 2222 | 7291 | 0.43 | 2.29 | 142.69 | 1.395 | 3.989 | 9.427 | 29137 | 83301 | 196893 |
| | 42 | 137.8 | 763 | 2504 | 2273 | 7456 | 0.44 | 2.31 | 143.99 | 1.344 | 3.861 | 10.122 | 28071 | 80642 | 211394 |
| | 42.5 | 139.4 | 794 | 2604 | 2273 | 7456 | 0.43 | 2.31 | 143.99 | 1.453 | 4.157 | 9.977 | 30343 | 86814 | 208365 |
| | 43 | 141.1 | 826 | 2711 | 2273 | 7456 | 0.42 | 2.31 | 143.99 | 1.575 | 4.486 | 9.813 | 32902 | 93692 | 204952 |
| | 43.5 | 142.7 | 877 | 2878 | 2381 | 7812 | 0.42 | 2.35 | 146.59 | 1.807 | 5.137 | 10.903 | 37737 | 107284 | 227705 |
| | 44 | 144.4 | 813 | 2667 | 2273 | 7456 | 0.43 | 2.31 | 143.99 | 1.525 | 4.350 | 9.881 | 31841 | 90850 | 206367 |
| | 44.5 | 146.0 | 820 | 2689 | 2222 | 7291 | 0.42 | 2.29 | 142.69 | 1.536 | 4.365 | 9.240 | 32073 | 91169 | 192978 |
| | 45 | 147.6 | 813 | 2667 | 2273 | 7456 | 0.43 | 2.31 | 143.99 | 1.525 | 4.350 | 9.881 | 31841 | 90850 | 206367 |
| | 45.5 | 149.3 | 962 | 3155 | 2439 | 8002 | 0.41 | 2.37 | 147.90 | 2.190 | 6.168 | 11.173 | 45747 | 128823 | 233353 |
| | 46 | 150.9 | 1099 | 3605 | 2500 | 8202 | 0.38 | 2.39 | 149.21 | 2.886 | 7.968 | 11.090 | 60280 | 166405 | 231615 |
| | 46.5 | 152.6 | 1220 | 4001 | 2500 | 8202 | 0.34 | 2.39 | 149.21 | 3.555 | 9.554 | 10.199 | 74239 | 199535 | 213003 |
| | 47 | 154.2 | 935 | 3066 | 2778 | 9113 | 0.44 | 2.47 | 154.48 | 2.161 | 6.208 | 16.212 | 45140 | 129658 | 338583 |
| | 47.4 | 155.5 | 1053 | 3454 | 3030 | 9942 | 0.43 | 2.54 | 158.46 | 2.813 | 8.052 | 19.559 | 58740 | 168160 | 408486 |
| | 48.1 | 157.8 | 1053 | 3454 | 2857 | 9374 | 0.42 | 2.50 | 155.80 | 2.765 | 7.862 | 16.686 | 57755 | 164194 | 348494 |
| | 48.5 | 159.1 | 962 | 3155 | 2439 | 8002 | 0.41 | 2.37 | 147.90 | 2.190 | 6.168 | 11.173 | 45747 | 128823 | 233352 |
| | 49 | 160.8 | 962 | 3155 | 2500 | 8202 | 0.41 | 2.39 | 149.21 | 2.210 | 6.246 | 11.992 | 46152 | 130444 | 250453 |
| | 49.4 | 162.1 | 926 | 3038 | 2564 | 8412 | 0.43 | 2.41 | 150.52 | 2.067 | 5.891 | 13.096 | 43173 | 123046 | 273516 |
| | 50 | 164.0 | 952 | 3125 | 2564 | 8412 | 0.42 | 2.41 | 150.52 | 2.187 | 6.211 | 12.936 | 45676 | 129717 | 270180 |
| | 50 | 164.0 | 926 | 3038 | 2564 | 8412 | 0.43 | 2.41 | 150.52 | 2.067 | 5.891 | 13.096 | 43173 | 123046 | 273515 |
| | 50 | 164.0 | 917 | 3010 | 2564 | 8412 | 0.43 | 2.41 | 150.52 | 2.029 | 5.790 | 13.146 | 42385 | 120931 | 274567 |
| | 50.5 | 165.7 | 1042 | 3418 | 2703 | 8867 | 0.41 | 2.45 | 153.16 | 2.662 | 7.522 | 14.371 | 55597 | 157092 | 300146 |
| | 50.6 | 166.0 | 1020 | 3348 | 2703 | 8867 | 0.42 | 2.45 | 153.16 | 2.554 | 7.239 | 14.515 | 53351 | 151184 | 303142 |

γ = Poisson's Ratio  ρ(Vp) = Vp-derived density  G = Shear Modulus  E = Young's Modulus  K = Bulk Modulus
Shaded cells denote questionable data.

**Table 2.** LA 710 Tunnel
Boring Z3 B8
PS Suspension Log Data Summary



| Top of Hole Elevation (m) | Depth (m) | Depth (ft) | Vs (m/s) | Vs (ft/s) | Vp (m/s) | Vp (ft/s) | $\gamma$ | $\rho$(Vp) (g/cc) | $\rho$(Vp) ($lb/ft^3$) | G (GPa) | E (GPa) | K (GPa) | G ($10^3 lb/ft^2$) | E ($10^3 lb/ft^2$) | K ($10^3 lb/ft^2$) |
|---|---|---|---|---|---|---|---|---|---|---|---|---|---|---|---|
| | 51 | 167.3 | 980 | 3217 | 2326 | 7630 | 0.39 | 2.33 | 145.29 | 2.237 | 6.227 | 9.604 | 46719 | 130061 | 200590 |
| | 51.1 | 167.7 | 1042 | 3418 | 2703 | 8867 | 0.41 | 2.45 | 153.16 | 2.662 | 7.522 | 14.371 | 55597 | 157092 | 300147 |
| | 51.5 | 169.0 | 917 | 3010 | 2381 | 7812 | 0.41 | 2.35 | 146.59 | 1.976 | 5.585 | 10.677 | 41278 | 116638 | 222983 |
| | 51.6 | 169.3 | 943 | 3095 | 2326 | 7630 | 0.40 | 2.33 | 145.29 | 2.071 | 5.806 | 9.825 | 43260 | 121259 | 205202 |
| | 52 | 170.6 | 901 | 2956 | 2439 | 8002 | 0.42 | 2.37 | 147.90 | 1.923 | 5.465 | 11.530 | 40159 | 114133 | 240804 |
| | 52.1 | 170.9 | 893 | 2929 | 2326 | 7630 | 0.41 | 2.33 | 145.29 | 1.855 | 5.245 | 10.113 | 38749 | 109548 | 211217 |
| | 52.5 | 172.2 | 862 | 2828 | 2273 | 7456 | 0.42 | 2.31 | 143.99 | 1.714 | 4.854 | 9.628 | 35800 | 101382 | 201089 |
| | 52.5 | 172.2 | 990 | 3248 | 2500 | 8202 | 0.41 | 2.39 | 149.21 | 2.343 | 6.593 | 11.814 | 48935 | 137701 | 246742 |
| | 53 | 173.9 | 1010 | 3314 | 2500 | 8202 | 0.40 | 2.39 | 149.21 | 2.439 | 6.840 | 11.687 | 50932 | 142858 | 244080 |
| | 53.1 | 174.2 | 1000 | 3281 | 2439 | 8002 | 0.40 | 2.37 | 147.90 | 2.369 | 6.629 | 10.935 | 49480 | 138442 | 228375 |
| | 53.5 | 175.5 | 943 | 3095 | 2439 | 8002 | 0.41 | 2.37 | 147.90 | 2.109 | 5.955 | 11.282 | 44037 | 124364 | 235633 |
| | 53.6 | 175.9 | 980 | 3217 | 2381 | 7812 | 0.40 | 2.35 | 146.59 | 2.257 | 6.310 | 10.302 | 47139 | 131792 | 215170 |
| | 54 | 177.2 | 893 | 2929 | 2381 | 7812 | 0.42 | 2.35 | 146.59 | 1.872 | 5.310 | 10.816 | 39097 | 110893 | 225893 |
| | 54.1 | 177.5 | 893 | 2929 | 2439 | 8002 | 0.42 | 2.37 | 147.90 | 1.889 | 5.374 | 11.575 | 39445 | 112232 | 241755 |
| | 54.3 | 178.1 | 855 | 2804 | 2381 | 7812 | 0.43 | 2.35 | 146.59 | 1.715 | 4.892 | 11.025 | 35827 | 102180 | 230253 |
| | 54.6 | 179.1 | 862 | 2828 | 2326 | 7630 | 0.42 | 2.33 | 145.29 | 1.730 | 4.913 | 10.281 | 36123 | 102614 | 214719 |
| | 55 | 180.4 | 893 | 2929 | 2326 | 7630 | 0.41 | 2.33 | 145.29 | 1.855 | 5.245 | 10.113 | 38749 | 109548 | 211217 |
| | 55.1 | 180.8 | 847 | 2780 | 2174 | 7132 | 0.41 | 2.26 | 141.40 | 1.627 | 4.589 | 8.535 | 33974 | 95833 | 178259 |
| | 55.4 | 181.8 | 917 | 3010 | 2381 | 7812 | 0.41 | 2.35 | 146.59 | 1.976 | 5.585 | 10.677 | 41278 | 116638 | 222983 |
| | 55.6 | 182.4 | 893 | 2929 | 2326 | 7630 | 0.41 | 2.33 | 145.29 | 1.855 | 5.245 | 10.113 | 38749 | 109548 | 211216 |
| | 55.9 | 183.4 | 909 | 2983 | 2273 | 7456 | 0.40 | 2.31 | 143.99 | 1.906 | 5.355 | 9.372 | 39811 | 111851 | 195740 |
| | 56 | 183.7 | 980 | 3217 | 2326 | 7630 | 0.39 | 2.33 | 145.29 | 2.237 | 6.227 | 9.604 | 46719 | 130061 | 200590 |
| | 56.4 | 185.0 | 885 | 2903 | 2222 | 7291 | 0.41 | 2.29 | 142.69 | 1.790 | 5.033 | 8.901 | 37386 | 105111 | 185894 |
| | 56.6 | 185.7 | 833 | 2734 | 2222 | 7291 | 0.42 | 2.29 | 142.69 | 1.587 | 4.502 | 9.171 | 33151 | 94029 | 191541 |
| | 56.9 | 186.7 | 794 | 2604 | 2273 | 7456 | 0.43 | 2.31 | 143.99 | 1.453 | 4.157 | 9.977 | 30343 | 86814 | 208365 |
| | 57.1 | 187.3 | 735 | 2412 | 2273 | 7456 | 0.44 | 2.31 | 143.99 | 1.247 | 3.595 | 10.251 | 26044 | 75089 | 214096 |
| | 57.4 | 188.3 | 855 | 2804 | 2326 | 7630 | 0.42 | 2.33 | 145.29 | 1.700 | 4.835 | 10.320 | 35508 | 100979 | 215538 |
| | 57.6 | 189.0 | 820 | 2689 | 2326 | 7630 | 0.43 | 2.33 | 145.29 | 1.564 | 4.469 | 10.502 | 32657 | 93339 | 219339 |
| | 58 | 190.3 | 962 | 3155 | 2381 | 7812 | 0.40 | 2.35 | 146.59 | 2.171 | 6.090 | 10.417 | 45343 | 127193 | 217564 |
| | 58 | 190.3 | 909 | 2983 | 2500 | 8202 | 0.42 | 2.39 | 149.21 | 1.975 | 5.625 | 12.304 | 41255 | 117478 | 256983 |
| | 58.5 | 191.9 | 980 | 3217 | 2439 | 8002 | 0.40 | 2.37 | 147.90 | 2.277 | 6.393 | 11.057 | 47559 | 133511 | 230937 |
| | 58.5 | 191.9 | 1010 | 3314 | 2381 | 7812 | 0.39 | 2.35 | 146.59 | 2.396 | 6.662 | 10.117 | 50039 | 139133 | 211303 |
| | 59 | 193.6 | 1020 | 3348 | 2500 | 8202 | 0.40 | 2.39 | 149.21 | 2.489 | 6.968 | 11.620 | 51976 | 145539 | 242687 |
| | 59 | 193.6 | 1031 | 3382 | 2500 | 8202 | 0.40 | 2.39 | 149.21 | 2.540 | 7.100 | 11.551 | 53054 | 148291 | 241250 |
| | 59.4 | 194.9 | 1042 | 3418 | 2439 | 8002 | 0.39 | 2.37 | 147.90 | 2.571 | 7.139 | 10.666 | 53689 | 149090 | 222763 |
| | 59.4 | 194.9 | 1053 | 3454 | 2439 | 8002 | 0.39 | 2.37 | 147.90 | 2.625 | 7.274 | 10.593 | 54825 | 151927 | 221248 |
| | 59.9 | 196.5 | 1031 | 3382 | 2381 | 7812 | 0.38 | 2.35 | 146.59 | 2.496 | 6.911 | 9.984 | 52123 | 144343 | 208524 |

$\gamma$ = Poisson's Ratio  $\rho$(Vp) = Vp-derived density  G = Shear Modulus  E = Young's Modulus  K = Bulk Modulus
Shaded cells denote questionable data.

**Table 2.** LA 710 Tunnel
Boring Z3 B8
PS Suspension Log Data Summary



| Top of Hole Elevation (m) | Depth (m) | Depth (ft) | Vs (m/s) | Vs (ft/s) | Vp (m/s) | Vp (ft/s) | γ | ρ(Vp) (g/cc) | ρ(Vp) ($lb/ft^3$) | G (GPa) | E (GPa) | K (GPa) | G ($10^3 lb/ft^2$) | E ($10^3 lb/ft^2$) | K ($10^3 lb/ft^2$) |
|---|---|---|---|---|---|---|---|---|---|---|---|---|---|---|---|
| | 59.9 | 196.5 | 1020 | 3348 | 2381 | 7812 | 0.39 | 2.35 | 146.59 | 2.445 | 6.785 | 10.052 | 51065 | 141706 | 209935 |
| | 60.1 | 197.2 | 1031 | 3382 | 2439 | 8002 | 0.39 | 2.37 | 147.90 | 2.518 | 7.006 | 10.736 | 52588 | 146325 | 224231 |
| | 60.4 | 198.2 | 990 | 3248 | 2381 | 7812 | 0.40 | 2.35 | 146.59 | 2.302 | 6.425 | 10.243 | 48077 | 134178 | 213919 |
| | 60.6 | 198.8 | 980 | 3217 | 2381 | 7812 | 0.40 | 2.35 | 146.59 | 2.257 | 6.310 | 10.302 | 47139 | 131792 | 215170 |
| | 61 | 200.1 | 862 | 2828 | 2632 | 8634 | 0.44 | 2.43 | 151.84 | 1.808 | 5.205 | 14.433 | 37751 | 108714 | 301448 |
| | 61 | 200.1 | 952 | 3125 | 2703 | 8867 | 0.43 | 2.45 | 153.16 | 2.225 | 6.360 | 14.954 | 46475 | 132835 | 312311 |
| | 61.5 | 201.8 | 1010 | 3314 | 2778 | 9113 | 0.42 | 2.47 | 154.48 | 2.525 | 7.189 | 15.727 | 52730 | 150155 | 328463 |
| | 61.5 | 201.8 | 909 | 2983 | 2857 | 9374 | 0.44 | 2.50 | 155.80 | 2.063 | 5.955 | 17.623 | 43077 | 124380 | 368062 |
| | 62 | 203.4 | 1087 | 3566 | 2564 | 8412 | 0.39 | 2.41 | 150.52 | 2.849 | 7.922 | 12.054 | 59496 | 165454 | 251752 |
| | 62.1 | 203.7 | 1064 | 3490 | 2632 | 8634 | 0.40 | 2.43 | 151.84 | 2.753 | 7.720 | 13.173 | 57489 | 161237 | 275130 |
| | 62.5 | 205.1 | 1000 | 3281 | 2381 | 7812 | 0.39 | 2.35 | 146.59 | 2.348 | 6.542 | 10.181 | 49043 | 136625 | 212631 |
| | 62.6 | 205.4 | 1000 | 3281 | 2439 | 8002 | 0.40 | 2.37 | 147.90 | 2.369 | 6.629 | 10.935 | 49480 | 138442 | 228375 |
| | 63 | 206.7 | 935 | 3066 | 2326 | 7630 | 0.40 | 2.33 | 145.29 | 2.033 | 5.707 | 9.877 | 42455 | 119188 | 206275 |
| | 63.1 | 207.0 | 926 | 3038 | 2381 | 7812 | 0.41 | 2.35 | 146.59 | 2.013 | 5.681 | 10.628 | 42046 | 118647 | 221959 |
| | 63.5 | 208.3 | 917 | 3010 | 2326 | 7630 | 0.41 | 2.33 | 145.29 | 1.959 | 5.516 | 9.975 | 40911 | 115194 | 208334 |
| | 63.6 | 208.7 | 909 | 2983 | 2381 | 7812 | 0.41 | 2.35 | 146.59 | 1.941 | 5.491 | 10.724 | 40531 | 114677 | 223979 |
| | 64 | 210.0 | 820 | 2689 | 2326 | 7630 | 0.43 | 2.33 | 145.29 | 1.564 | 4.469 | 10.502 | 32657 | 93339 | 219339 |
| | 64.1 | 210.3 | 833 | 2734 | 2222 | 7291 | 0.42 | 2.29 | 142.69 | 1.587 | 4.502 | 9.171 | 33151 | 94029 | 191541 |
| | 64.5 | 211.6 | 885 | 2903 | 2439 | 8002 | 0.42 | 2.37 | 147.90 | 1.855 | 5.285 | 11.620 | 38750 | 110376 | 242682 |
| | 64.6 | 211.9 | 926 | 3038 | 2381 | 7812 | 0.41 | 2.35 | 146.59 | 2.013 | 5.681 | 10.628 | 42046 | 118647 | 221959 |
| | 65 | 213.3 | 1075 | 3528 | 2564 | 8412 | 0.39 | 2.41 | 150.52 | 2.788 | 7.768 | 12.135 | 58223 | 162246 | 253448 |
| | 65.1 | 213.6 | 1111 | 3645 | 2632 | 8634 | 0.39 | 2.43 | 151.84 | 3.003 | 8.357 | 12.840 | 62713 | 174533 | 268166 |
| | 65.1 | 213.6 | 1087 | 3566 | 2632 | 8634 | 0.40 | 2.43 | 151.84 | 2.874 | 8.030 | 13.012 | 60016 | 167702 | 271761 |
| | 65.1 | 213.6 | 1087 | 3566 | 2632 | 8634 | 0.40 | 2.43 | 151.84 | 2.874 | 8.030 | 13.012 | 60016 | 167702 | 271762 |
| | 65.1 | 213.6 | 1087 | 3566 | 2632 | 8634 | 0.40 | 2.43 | 151.84 | 2.874 | 8.030 | 13.012 | 60016 | 167702 | 271761 |
| | 65.5 | 214.9 | 1111 | 3645 | 2632 | 8634 | 0.39 | 2.43 | 151.84 | 3.003 | 8.357 | 12.840 | 62713 | 174533 | 268165 |
| | 66.1 | 216.9 | 1020 | 3348 | 2632 | 8634 | 0.41 | 2.43 | 151.84 | 2.532 | 7.149 | 13.467 | 52892 | 149316 | 281259 |
| | 66.5 | 218.2 | 1000 | 3281 | 2564 | 8412 | 0.41 | 2.41 | 150.52 | 2.411 | 6.801 | 12.637 | 50357 | 142038 | 263937 |
| | 67 | 219.8 | 1020 | 3348 | 2941 | 9650 | 0.43 | 2.52 | 157.13 | 2.621 | 7.504 | 18.279 | 54735 | 156716 | 381759 |
| | 67.5 | 221.5 | 1111 | 3645 | 2439 | 8002 | 0.37 | 2.37 | 147.90 | 2.925 | 8.009 | 10.194 | 61087 | 167262 | 212900 |
| | 68 | 223.1 | 1205 | 3953 | 2564 | 8412 | 0.36 | 2.41 | 150.52 | 3.500 | 9.508 | 11.186 | 73098 | 198582 | 233616 |
| | 68.5 | 224.7 | 1235 | 4050 | 2703 | 8867 | 0.37 | 2.45 | 153.16 | 3.739 | 10.232 | 12.935 | 78096 | 213695 | 270150 |
| | 69 | 226.4 | 1299 | 4261 | 2326 | 7630 | 0.27 | 2.33 | 145.29 | 3.925 | 9.997 | 7.353 | 81982 | 208792 | 153574 |
| | 69.5 | 228.0 | 1351 | 4434 | 2703 | 8867 | 0.33 | 2.45 | 153.16 | 4.480 | 11.947 | 11.947 | 93569 | 249518 | 249518 |
| | 70 | 229.7 | 1282 | 4206 | 2703 | 8867 | 0.35 | 2.45 | 153.16 | 4.032 | 10.926 | 12.544 | 84218 | 228203 | 261986 |
| | 70.5 | 231.3 | 1220 | 4001 | 2703 | 8867 | 0.37 | 2.45 | 153.16 | 3.649 | 10.013 | 13.056 | 76202 | 209126 | 272674 |
| | 71 | 232.9 | 1250 | 4101 | 2632 | 8634 | 0.35 | 2.43 | 151.84 | 3.800 | 10.294 | 11.776 | 79371 | 214987 | 245954 |

γ = Poisson's Ratio  ρ(Vp) = Vp-derived density  G = Shear Modulus  E = Young's Modulus  K = Bulk Modulus
Shaded cells denote questionable data.

**Table 2.** LA 710 Tunnel
Boring Z3 B8
PS Suspension Log Data Summary



| Top of Hole Elevation (m) | Depth (m) | Depth (ft) | Vs (m/s) | Vs (ft/s) | Vp (m/s) | Vp (ft/s) | $\gamma$ | $\rho$(Vp) (g/cc) | $\rho$(Vp) ($lb/ft^3$) | G (GPa) | E (GPa) | K (GPa) | G ($10^3 lb/ft^2$) | E ($10^3 lb/ft^2$) | K ($10^3 lb/ft^2$) |
|---|---|---|---|---|---|---|---|---|---|---|---|---|---|---|---|
| | 71.5 | 234.6 | 1282 | 4206 | 2703 | 8867 | 0.35 | 2.45 | 153.16 | 4.032 | 10.926 | 12.544 | 84218 | 228202 | 261986 |
| | 72 | 236.2 | 1266 | 4153 | 2703 | 8867 | 0.36 | 2.45 | 153.16 | 3.931 | 10.688 | 12.679 | 82100 | 223230 | 264811 |
| | 72.5 | 237.9 | 1190 | 3906 | 2778 | 9113 | 0.39 | 2.47 | 154.48 | 3.507 | 9.732 | 14.417 | 73244 | 203251 | 301112 |
| | 73 | 239.5 | 1205 | 3953 | 2703 | 8867 | 0.38 | 2.45 | 153.16 | 3.561 | 9.800 | 13.172 | 74377 | 204686 | 275107 |
| | 73.4 | 240.8 | 1220 | 4001 | 2778 | 9113 | 0.38 | 2.47 | 154.48 | 3.680 | 10.162 | 14.187 | 76860 | 212229 | 296291 |
| | 74 | 242.8 | 1136 | 3728 | 2703 | 8867 | 0.39 | 2.45 | 153.16 | 3.168 | 8.824 | 13.697 | 66165 | 184288 | 286056 |
| | 74.5 | 244.4 | 1250 | 4101 | 2778 | 9113 | 0.37 | 2.47 | 154.48 | 3.866 | 10.617 | 13.938 | 80751 | 221749 | 291103 |
| | 75 | 246.1 | 1449 | 4755 | 3704 | 12151 | 0.41 | 2.67 | 166.51 | 5.602 | 15.794 | 29.118 | 117005 | 329859 | 608136 |
| | 75.5 | 247.7 | 1639 | 5378 | 5000 | 16404 | 0.44 | 2.82 | 176.04 | 7.578 | 21.822 | 60.394 | 158277 | 455768 | 1261342 |
| | 76 | 249.3 | 1389 | 4557 | 3125 | 10253 | 0.38 | 2.56 | 159.79 | 4.938 | 13.597 | 18.413 | 103124 | 283987 | 384565 |
| | 76.5 | 251.0 | 1190 | 3906 | 2703 | 8867 | 0.38 | 2.45 | 153.16 | 3.477 | 9.594 | 13.285 | 72617 | 200370 | 277454 |
| | 76.5 | 251.0 | 1205 | 3953 | 2703 | 8867 | 0.38 | 2.45 | 153.16 | 3.561 | 9.800 | 13.172 | 74377 | 204686 | 275107 |
| | 77 | 252.6 | 1190 | 3906 | 2857 | 9374 | 0.39 | 2.50 | 155.80 | 3.537 | 9.868 | 15.657 | 73872 | 206095 | 327005 |
| | 77.5 | 254.3 | 1282 | 4206 | 2632 | 8634 | 0.34 | 2.43 | 151.84 | 3.998 | 10.749 | 11.513 | 83493 | 224496 | 240459 |
| | 78 | 255.9 | 1087 | 3566 | 2500 | 8202 | 0.38 | 2.39 | 149.21 | 2.824 | 7.813 | 11.173 | 58977 | 163183 | 233353 |
| | 78 | 255.9 | 1235 | 4050 | 2778 | 9113 | 0.38 | 2.47 | 154.48 | 3.772 | 10.386 | 14.065 | 78769 | 216919 | 293745 |
| | 78.5 | 257.5 | 1190 | 3906 | 2632 | 8634 | 0.37 | 2.43 | 151.84 | 3.447 | 9.454 | 12.248 | 71992 | 197451 | 255793 |
| | 79 | 259.2 | 1020 | 3348 | 2381 | 7812 | 0.39 | 2.35 | 146.59 | 2.445 | 6.785 | 10.052 | 51065 | 141706 | 209934 |
| | 79.5 | 260.8 | | NA | 2273 | 7456 | NA | NA | NA | NA | NA | NA | NA | NA | NA |

$\gamma$ = Poisson's Ratio  $\rho$(Vp) = Vp-derived density  G = Shear Modulus  E = Young's Modulus  K = Bulk Modulus
Shaded cells denote questionable data.

# Figure 1. LA 710 Tunnel
# Boring Z3 B8
# Downhole Interval Velocities

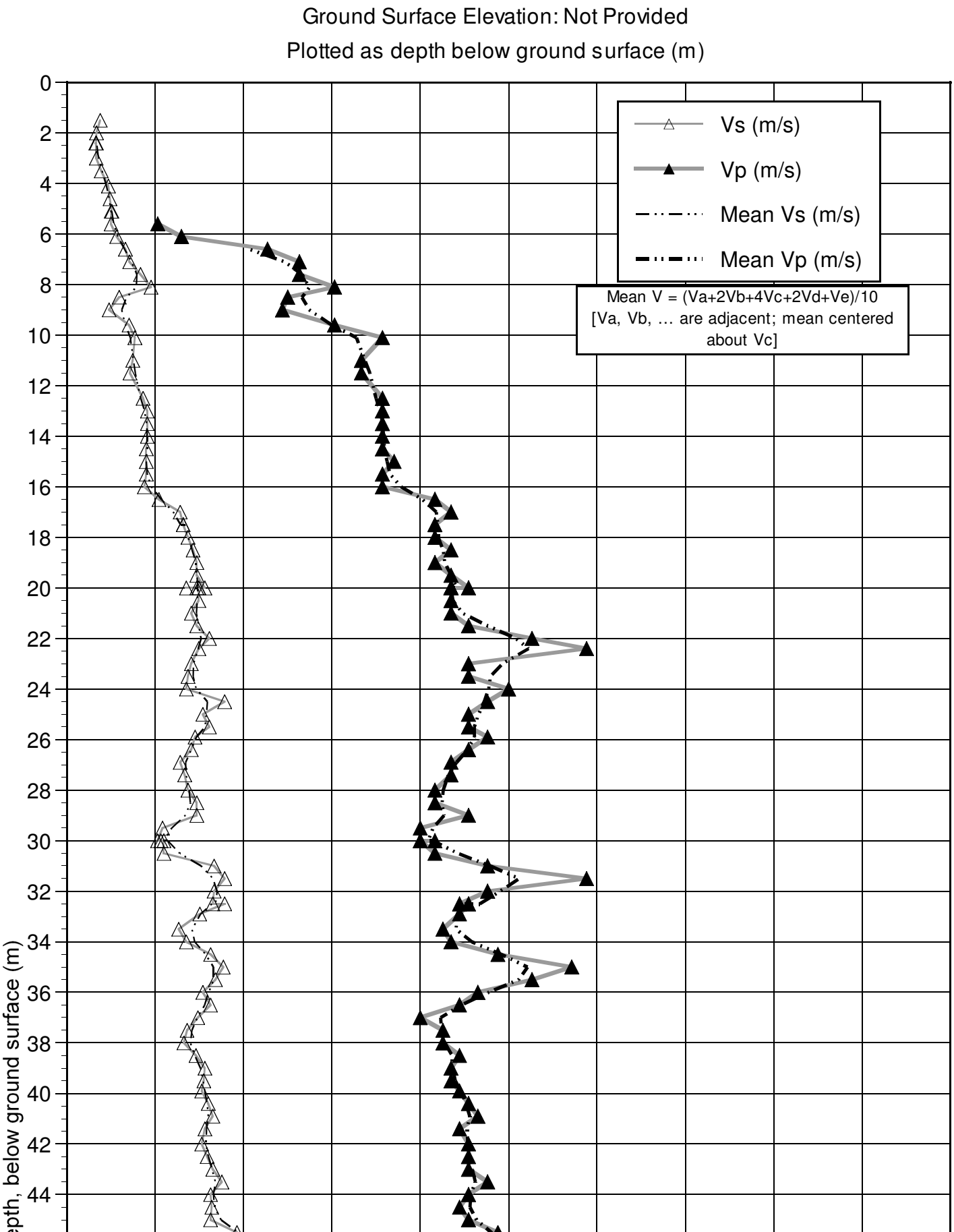

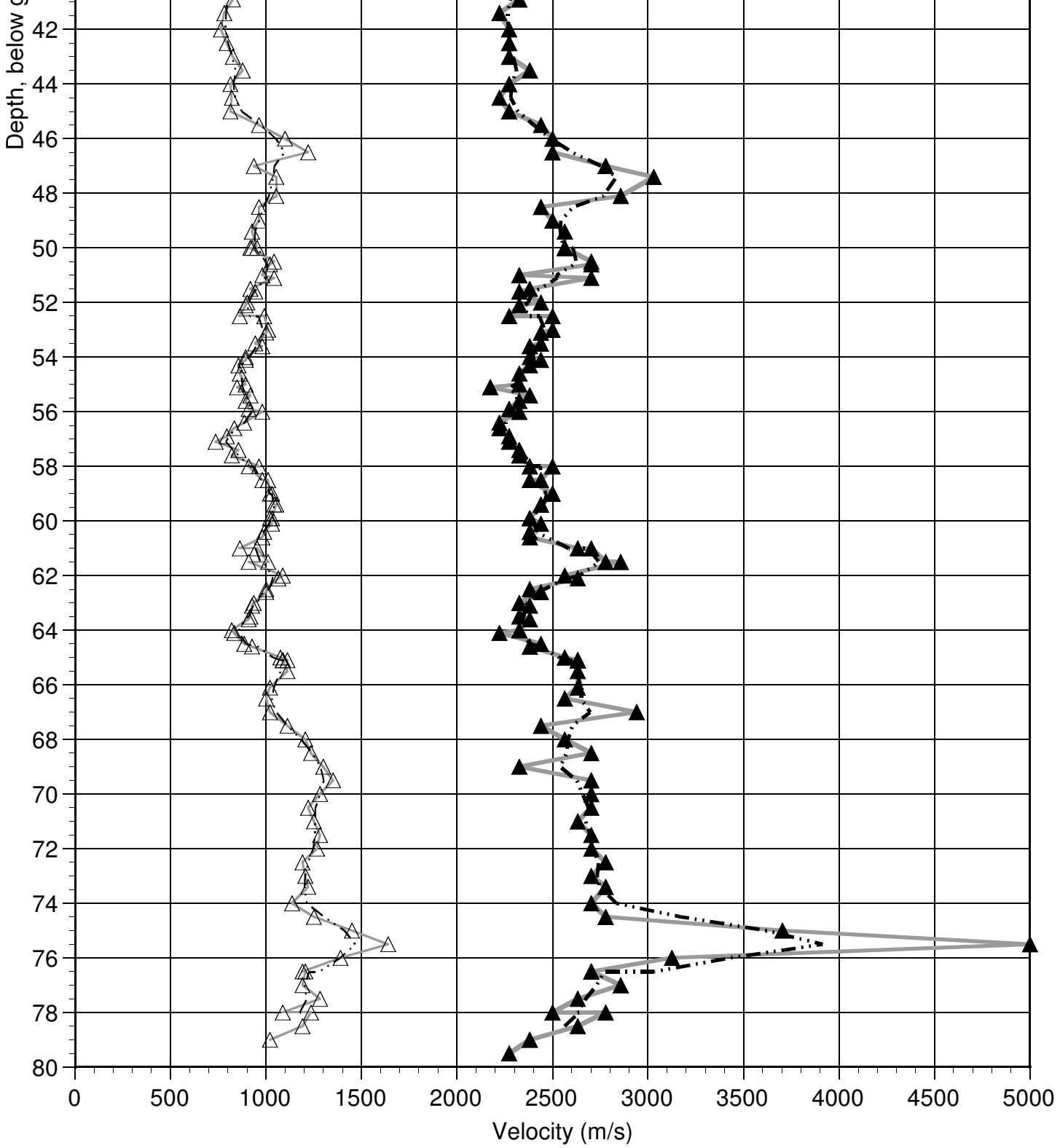
Depth, below g
42
44
46
48
50
52
54
56
58
60
62
64
66
68
70
72
74
76
78
80
0
500
1000
1500
2000
2500
3000
3500
4000
4500
5000
Velocity (m/s)


# 07-187900 Z3 B8..

| | | | |
|---|---|---|---|
| COMPANY | : Caltrans | | OTHER SERVICES: |
| WELL | : 07-187900 Z3 B8.. | | |
| FIELD | : LA Co. | | |
| COUNTY | : LA | | |
| STATE | : CA | | |
| LOCATION | : | | |
| SECTION | : None | | |
| TOWNSHIP | : None | | |
| RANGE | : None | | |
| API NO. | : | | |
| UNIQUE WELL ID. | : | | |
| PERMANENT DATUM | : None | ELEVATION KB | : NA |
| LOG MEASURED FROM | : GL | ELEVATION DF | : NA |
| DRL MEASURED FROM | : GL | ELEVATION GL | : 172.8m. |
| DATE | : 03/19/09 | RIG NUMBER | : |
| DEPTH DRILLER | : 83.82m. | LOGGER TD | : |
| BIT SIZE | : 10.5cm. | ARRIVAL TIME | : |
| LOG TOP | : 3.11 | DEPARTURE TIME | : |
| LOG BOTTOM | : 83.80 | CIRC STOPPED | : 3/18 PM |
| CASING OD | : | | |
| CASING BOTTOM | : N/A | | |
| CASING TYPE | : N/A | | |
| BOREHOLE FLUID | : 0 | | |
| RM TEMPERATURE | : 0 | | |
| MUD RES | : 0 | | |
| MUD WEIGHT | : | | |
| WITNESSED BY | : | | |
| RECORDED BY | : DH/DG | | |
| REMARKS 1 | : IND, Acoustic Tel, PSLog, CAL | | |
| REMARKS 2 | : EA: 07-187900 | | |

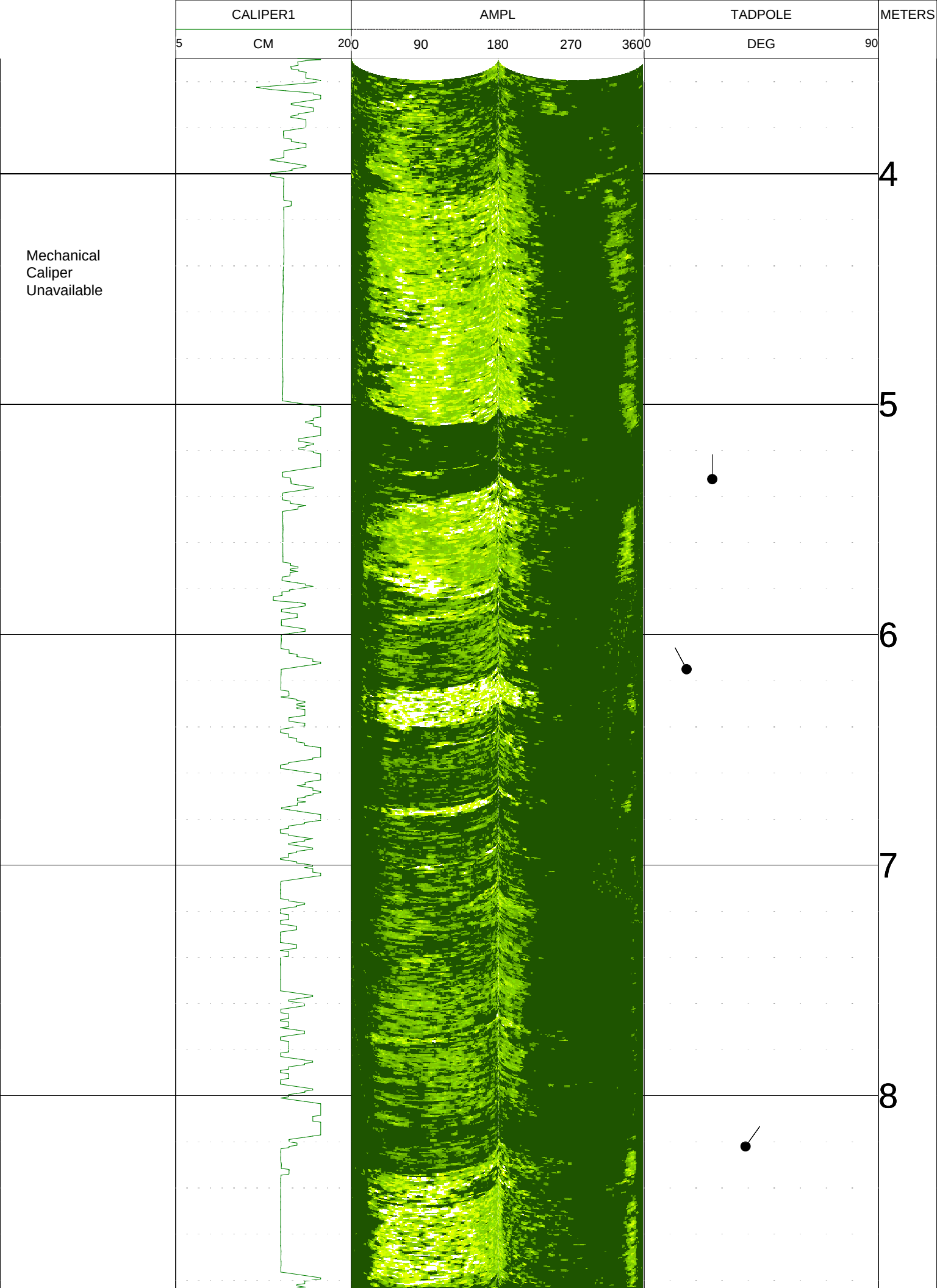
CALIPER1
AMPL
TADPOLE
METERS
5
CM
20
0
90
180
270
360
0
DEG
90
Mechanical
Caliper
Unavailable
4
5
6
7
8

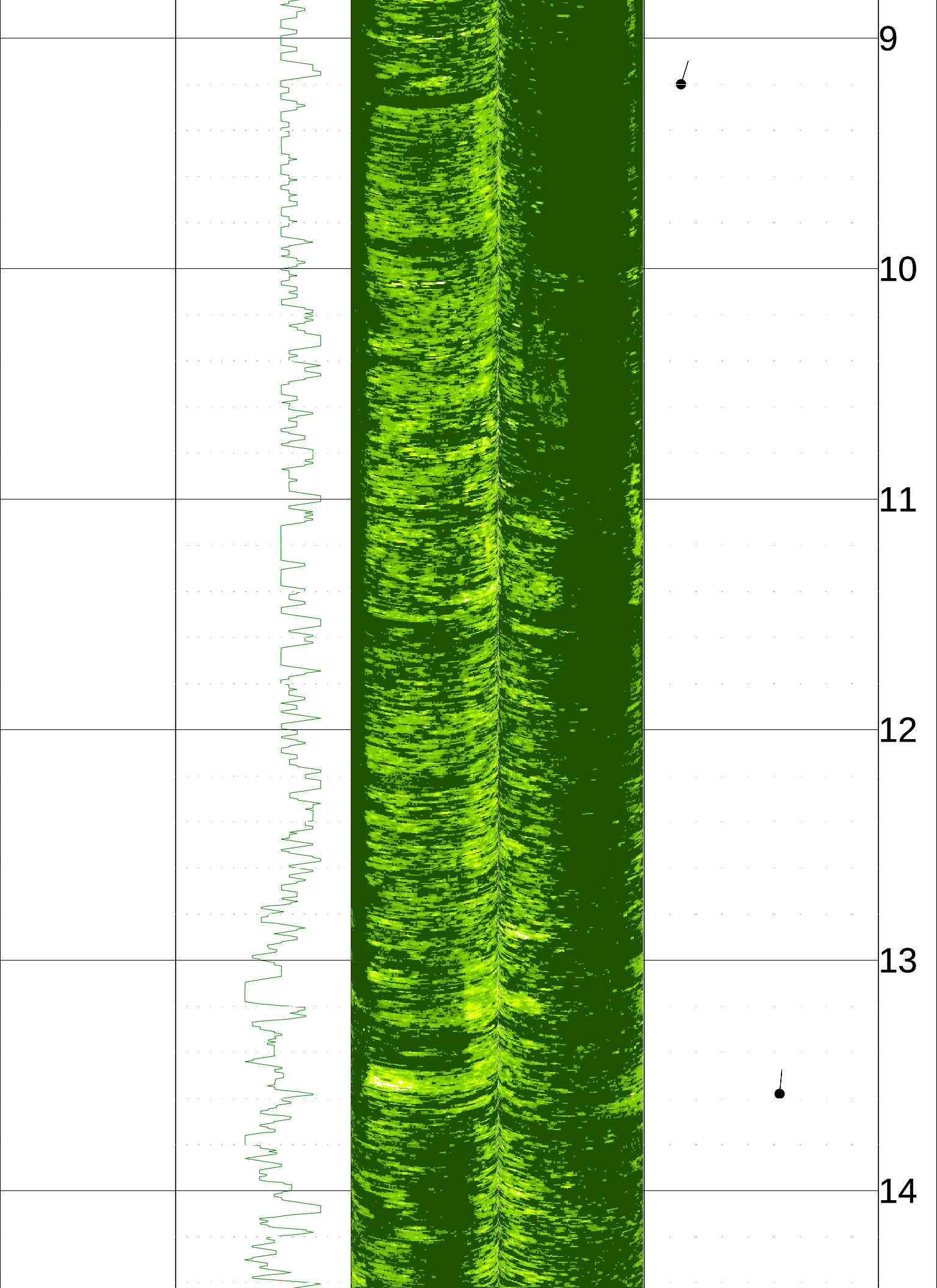
9
10
11
12
13
14

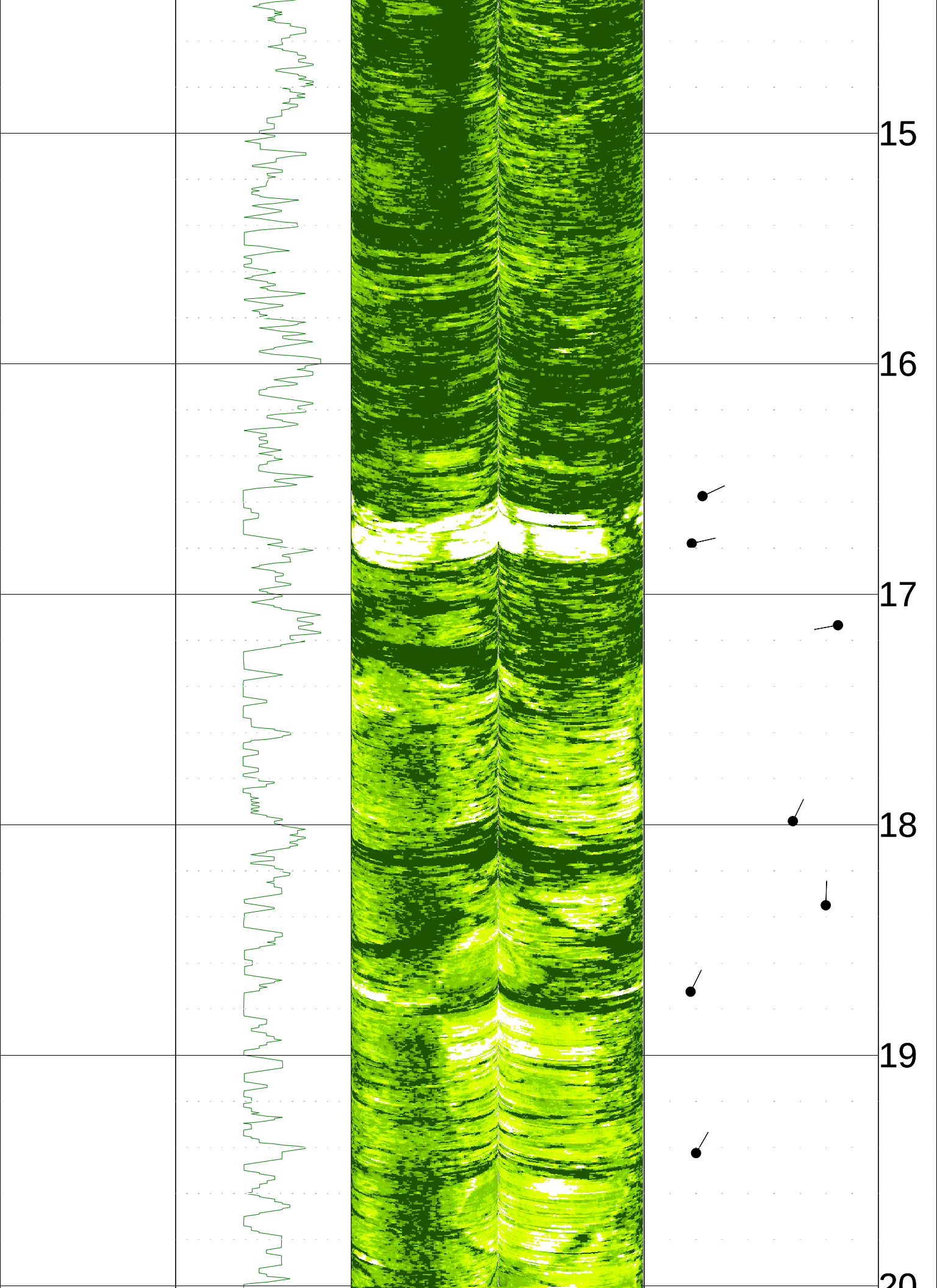
15
16
17
18
19
20

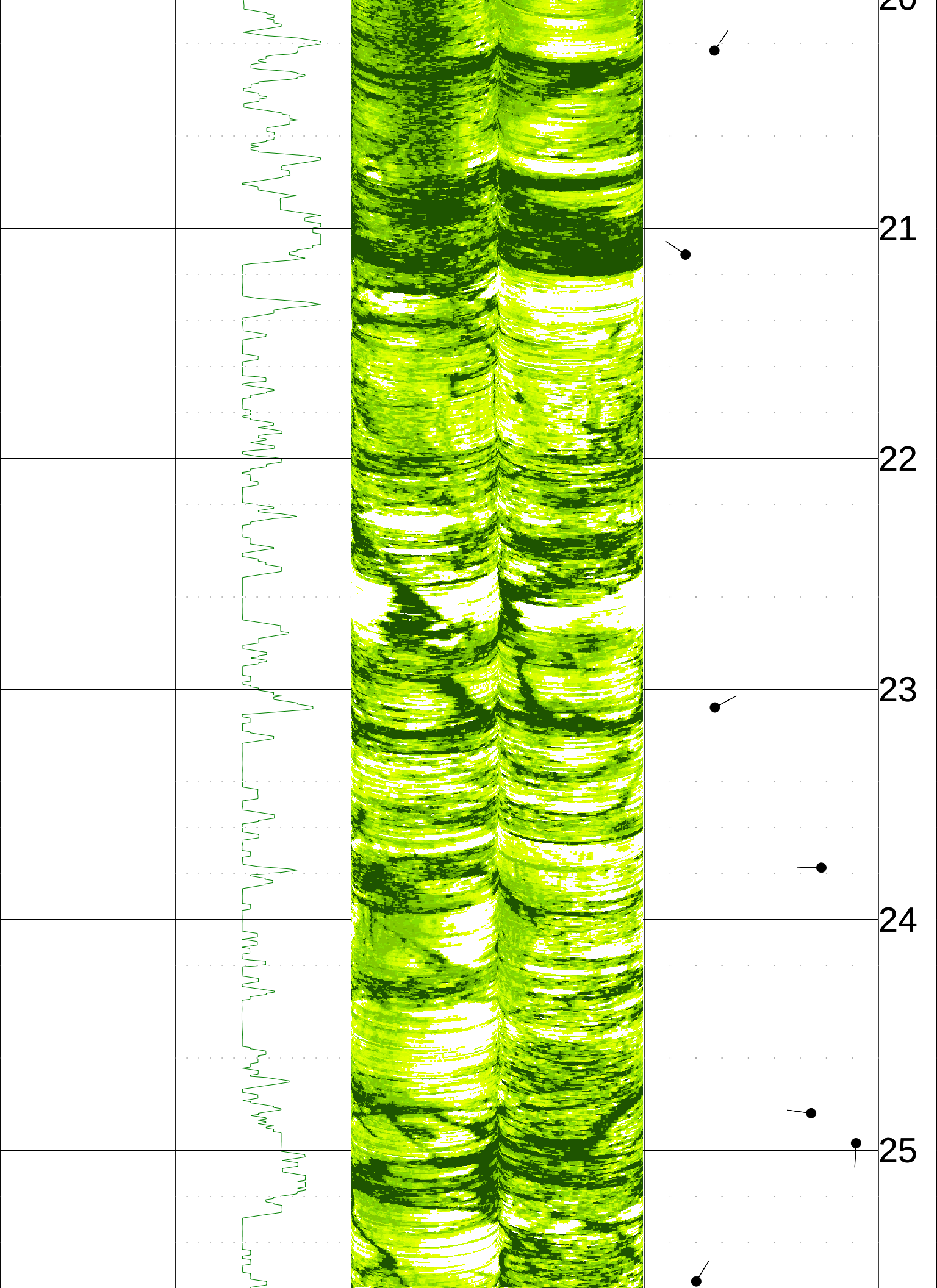
20
21
22
23
24
25

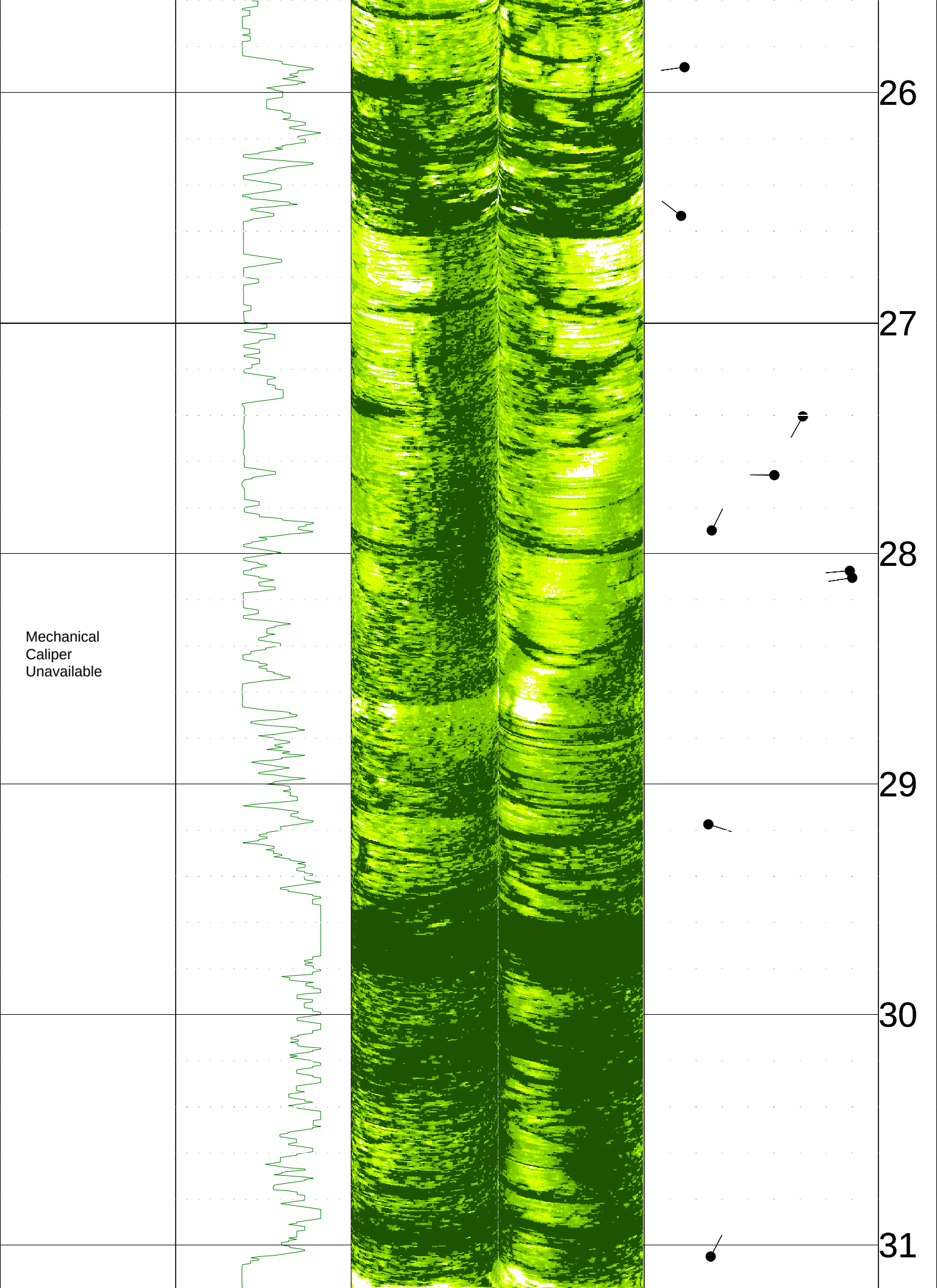
Mechanical
Caliper
Unavailable
26
27
28
29
30
31

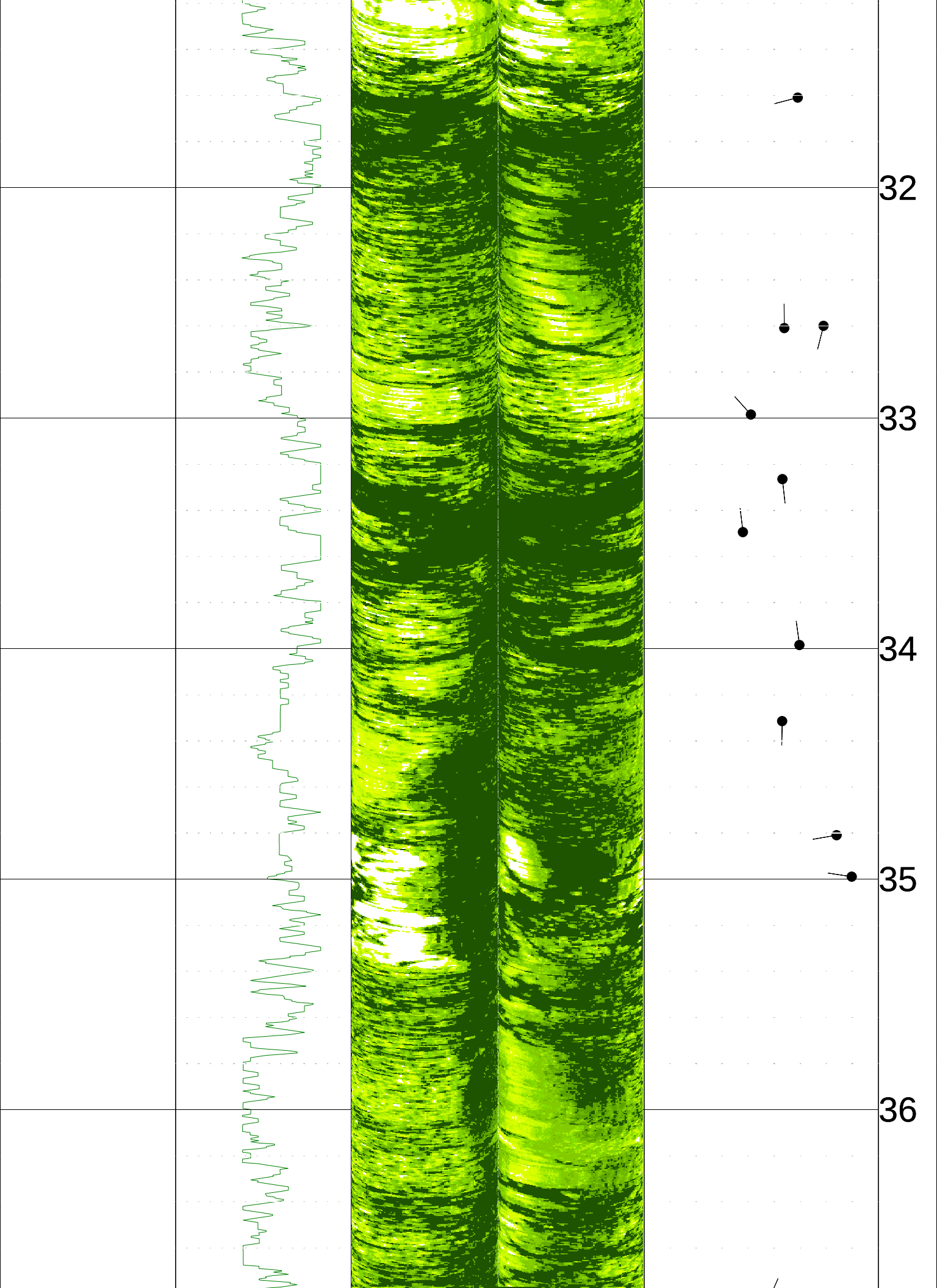
32
33
34
35
36

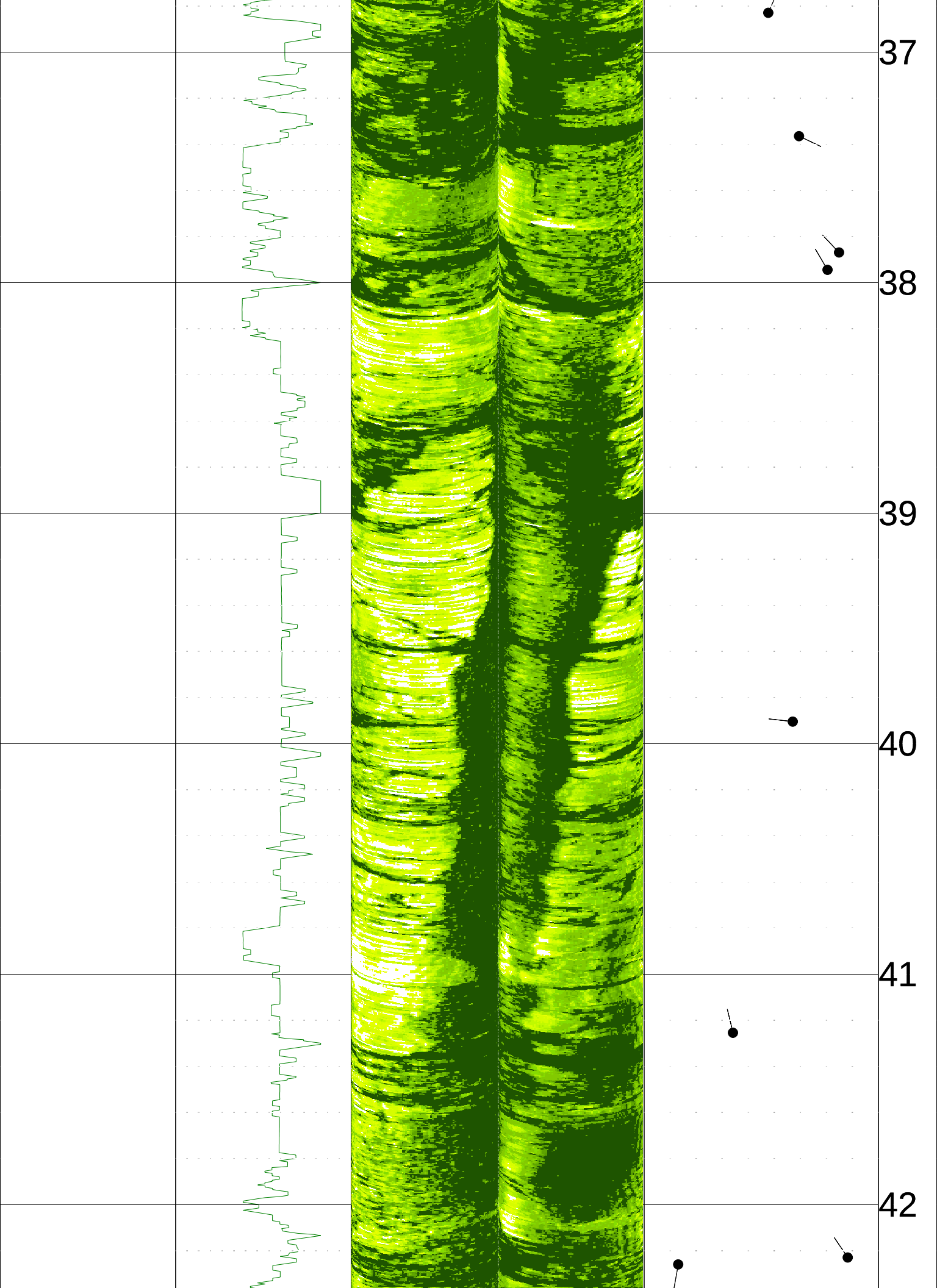
37
38
39
40
41
42

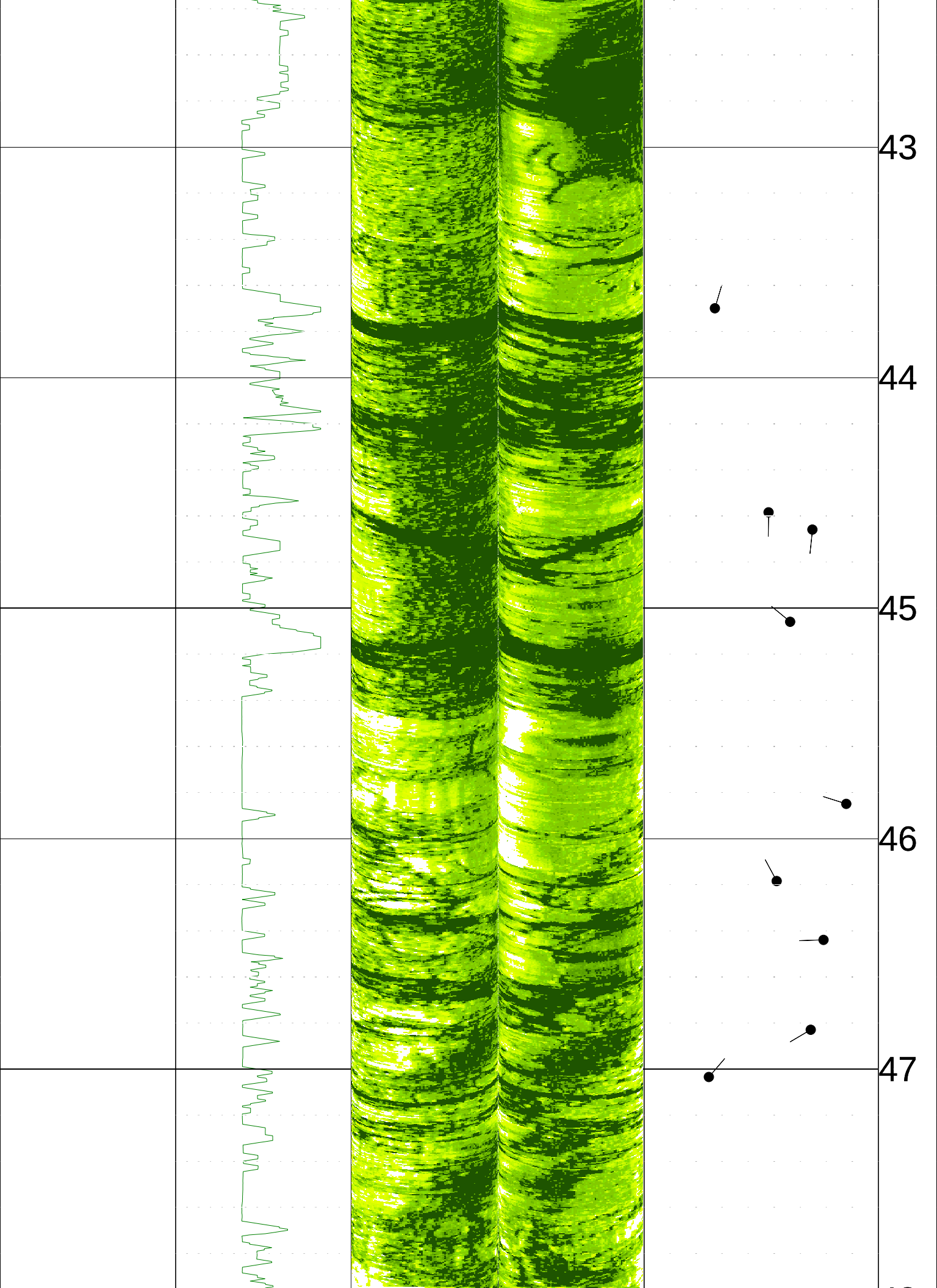
43
44
45
46
47

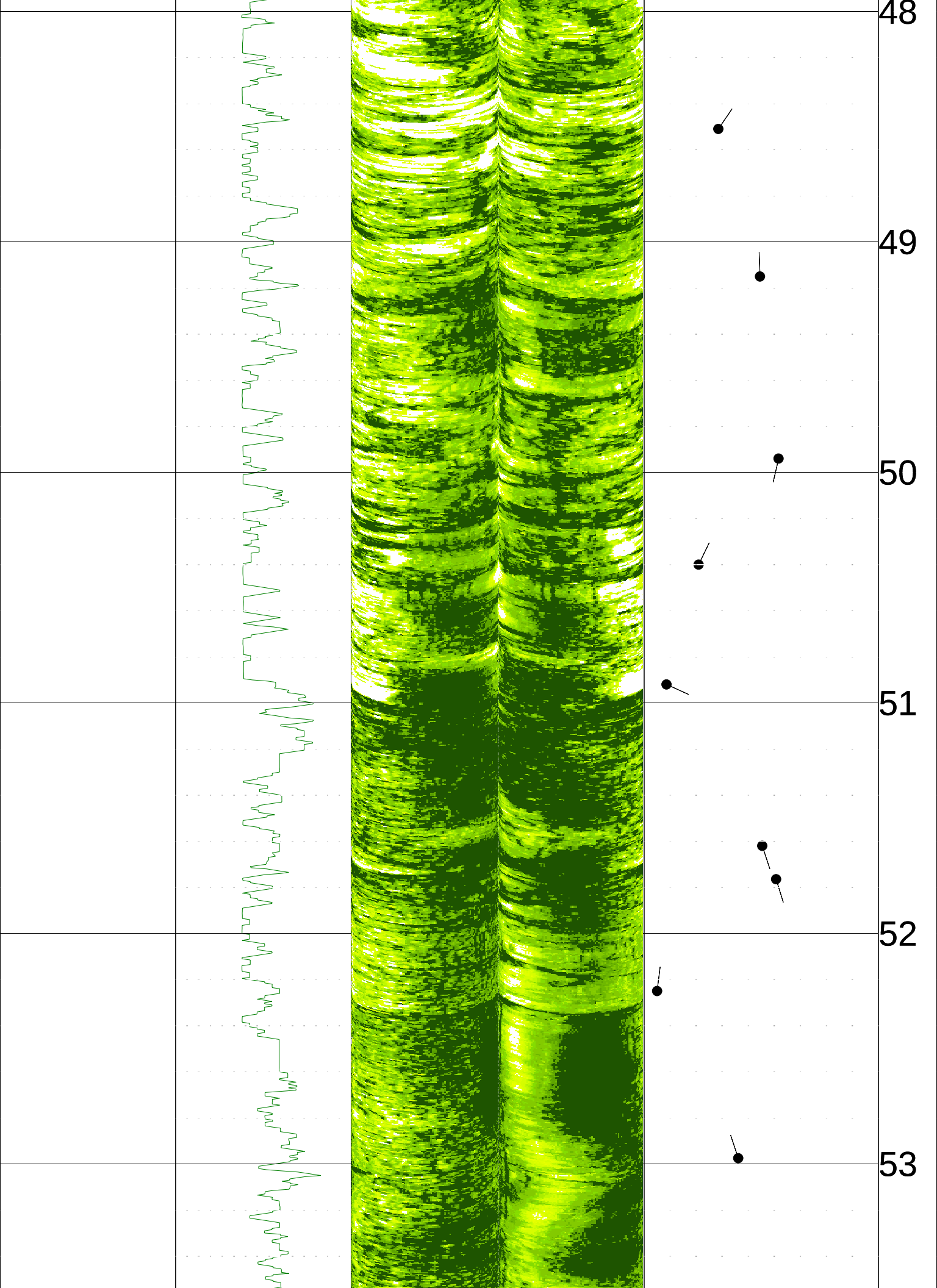
48
49
50
51
52
53

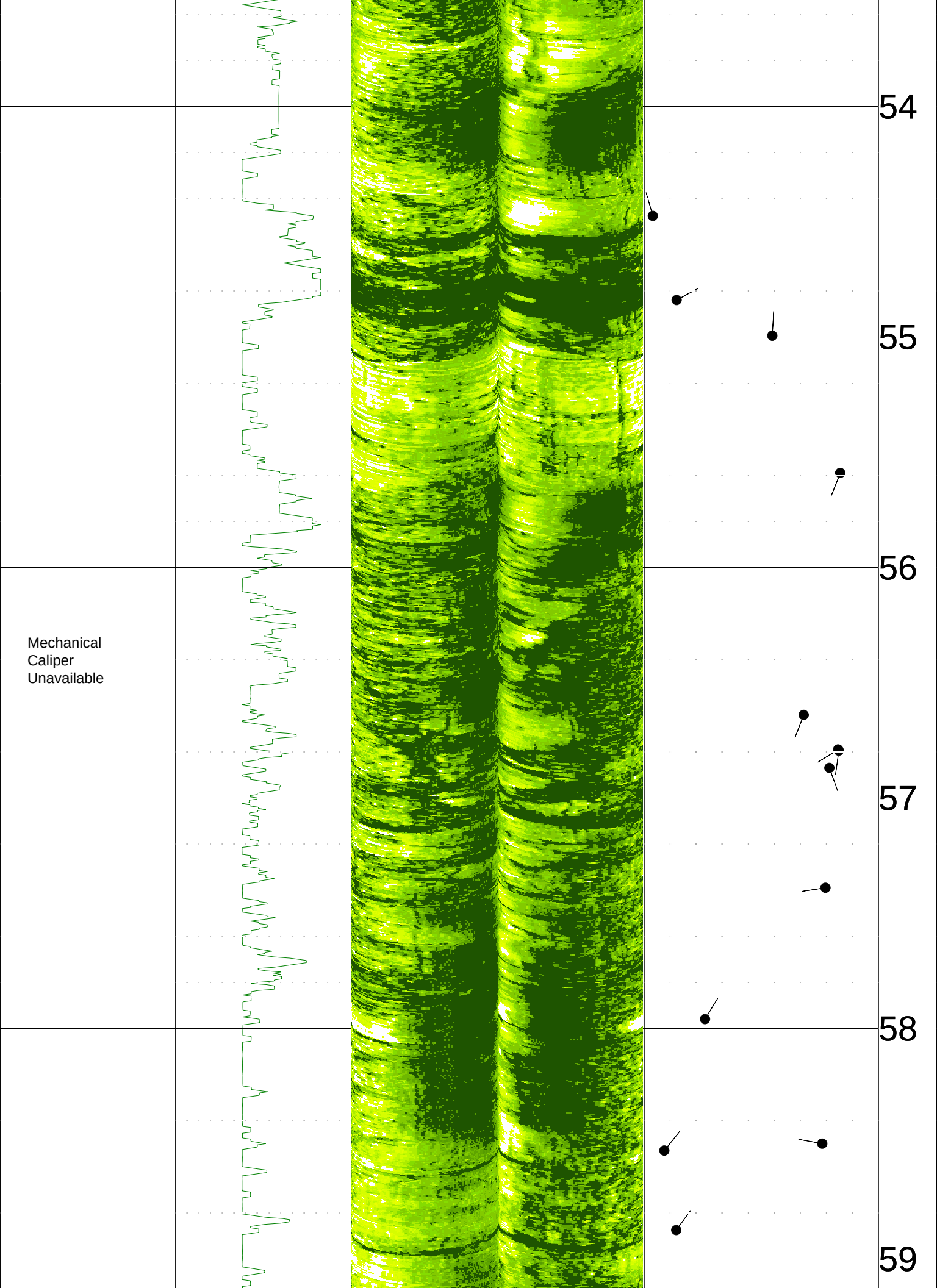
Mechanical
Caliper
Unavailable
54
55
56
57
58
59

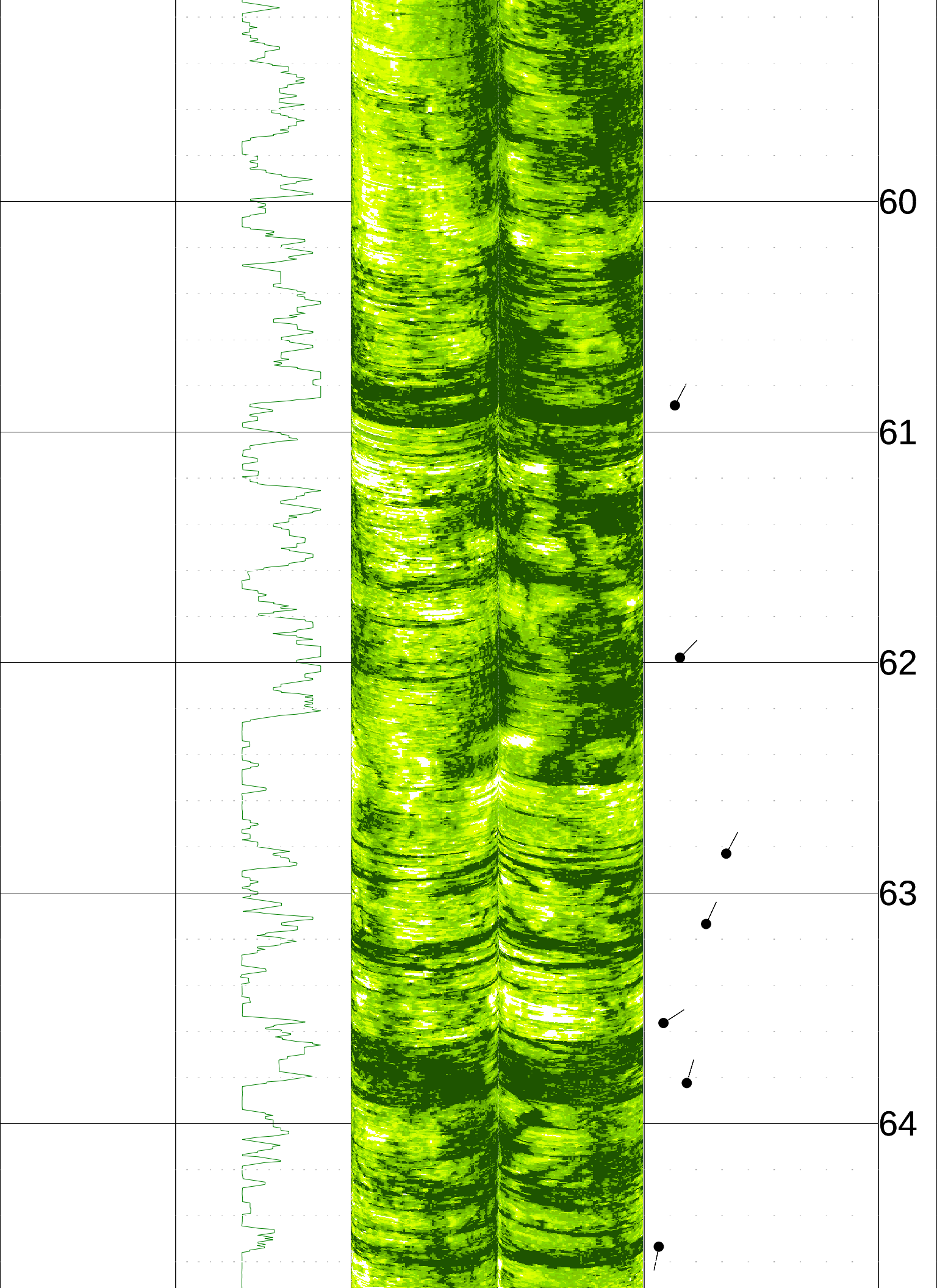
60
61
62
63
64

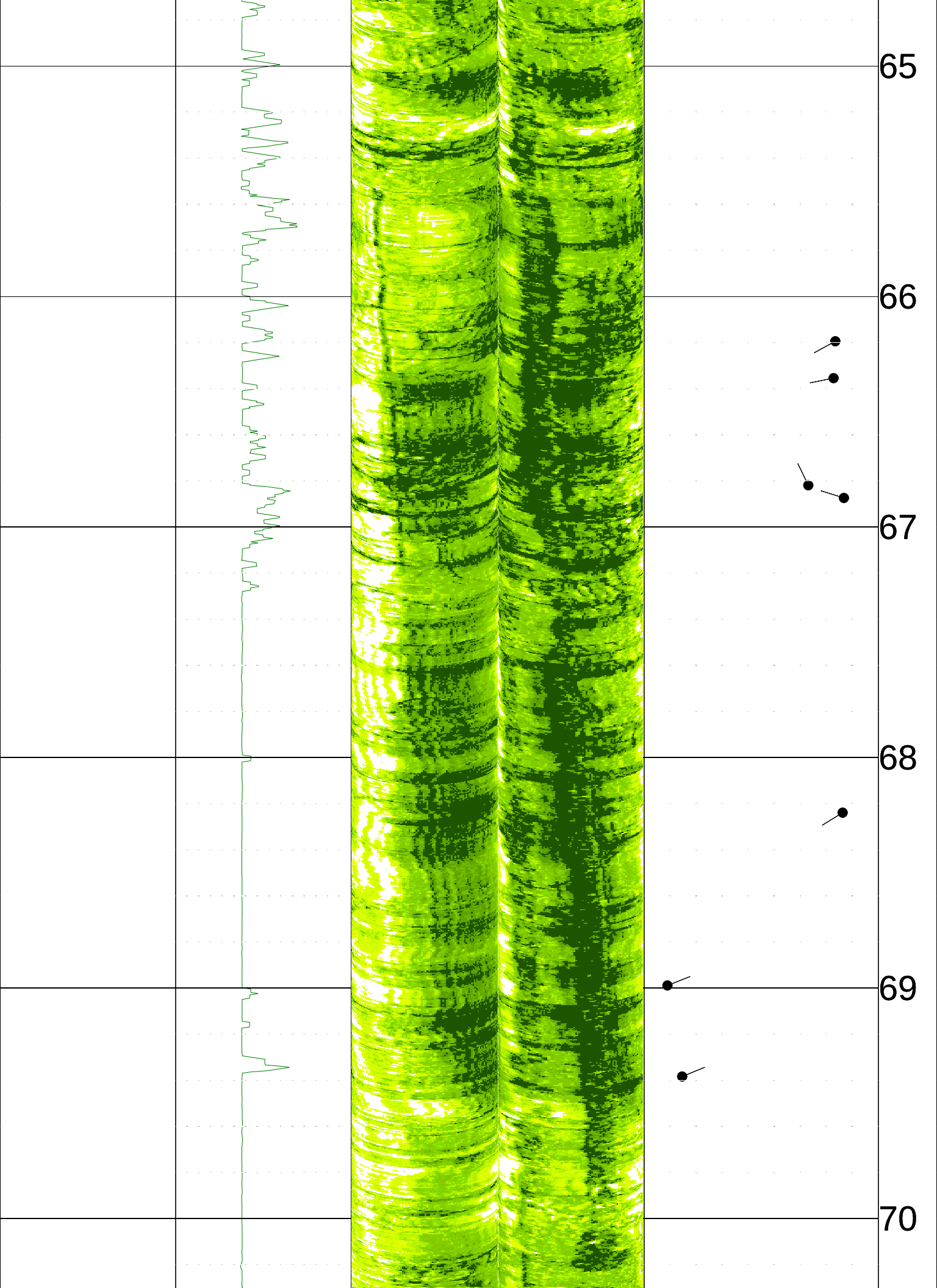
65
66
67
68
69
70

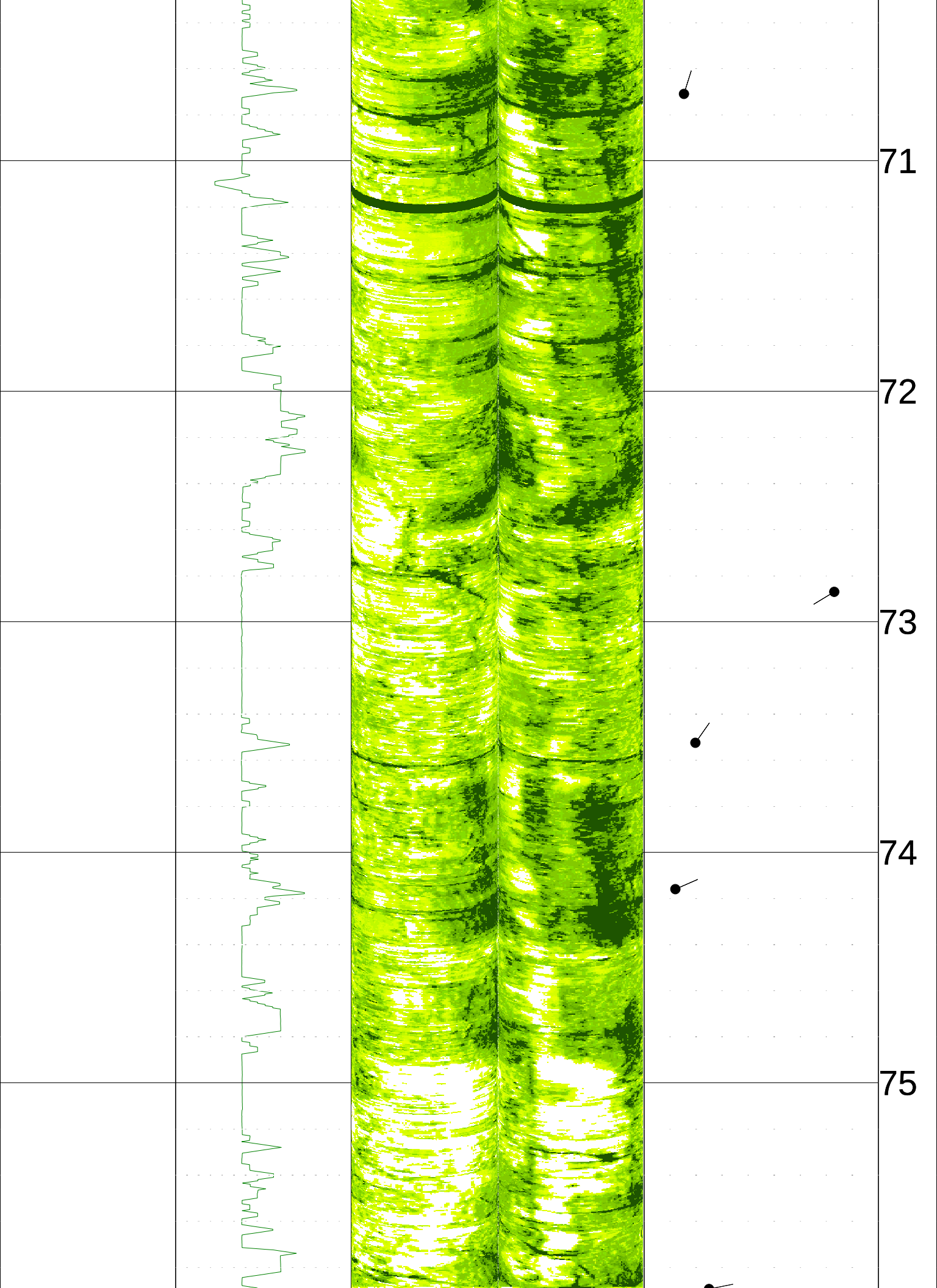
71
72
73
74
75

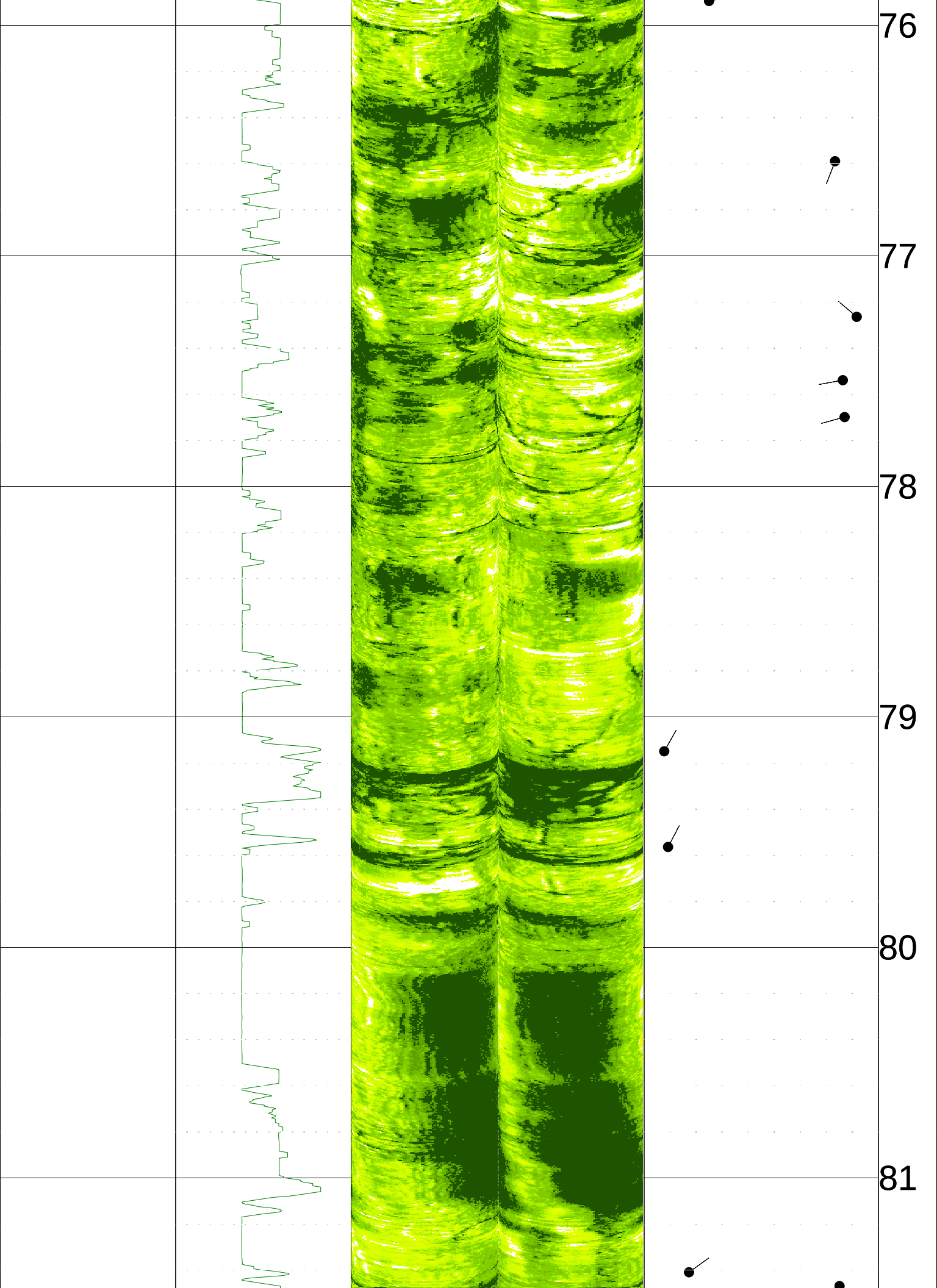
76
77
78
79
80
81

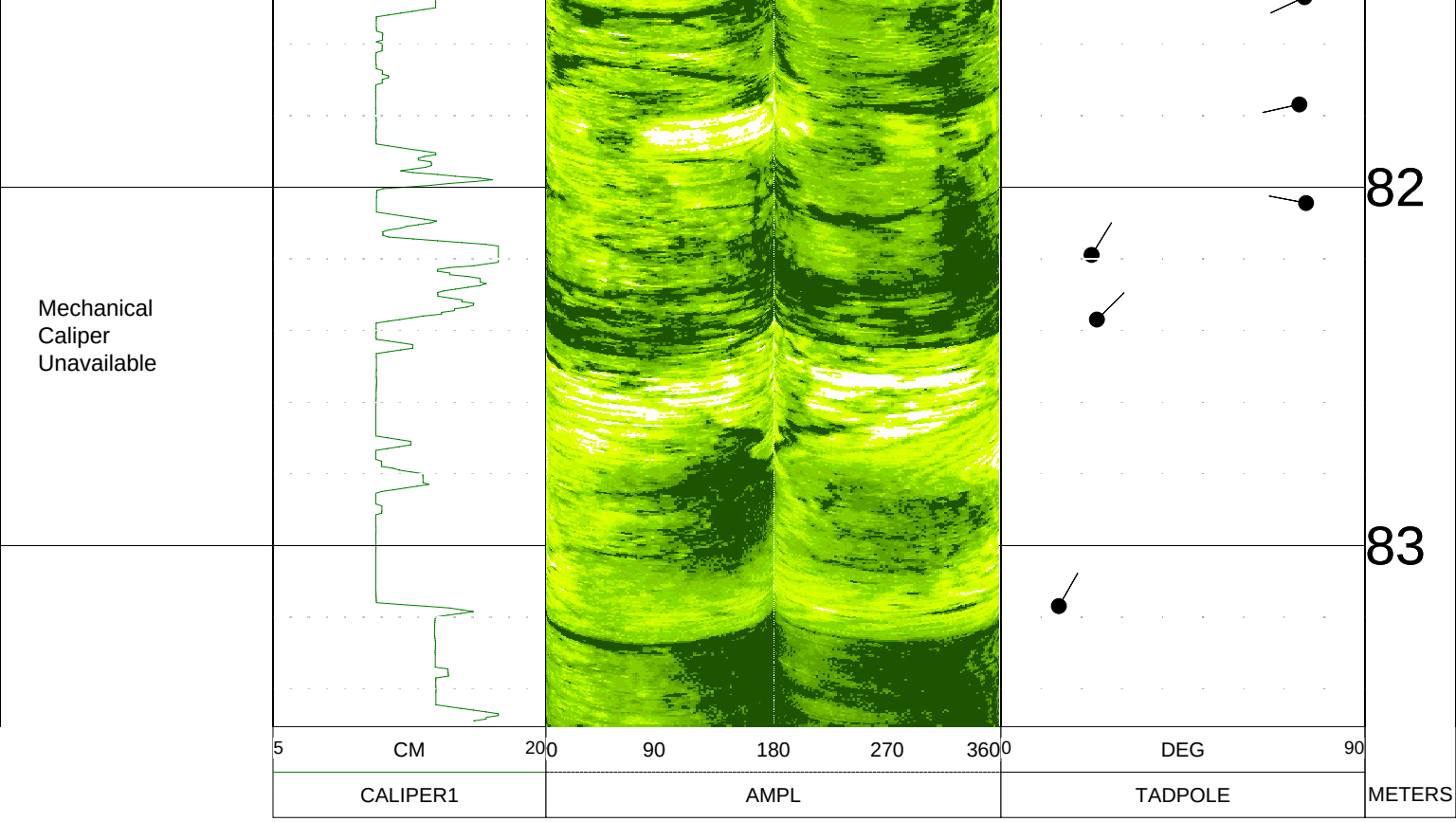
Mechanical
Caliper
Unavailable
82
83
5
CM
20
0
90
180
270
360
0
DEG
90
CALIPER1
AMPL
TADPOLE
METERS

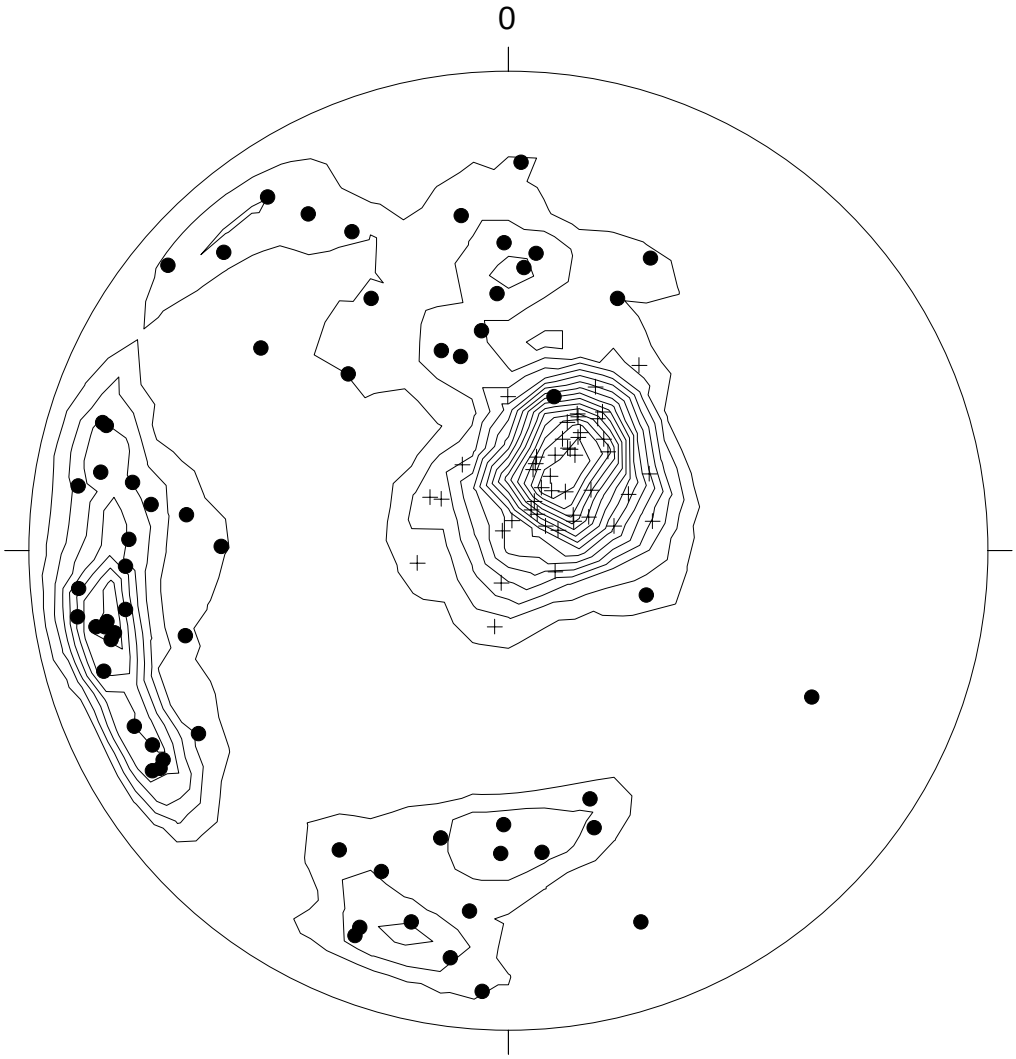


LA 710 Tunnel, boring Z3 B8

+ n=46 (P)
• n=63 (P)

Stereonet contour plot of poles to planes,
Both bedding and fractures

n=109
max. dens.= 16.05 (at 40/ 72)
min. dens.=0.00
Contours at every integer between
1 and 15, inclusive:
(Multiples of random distribution)

Apparent bedding denoted as cross
Apparent fractures denoted as solid circle
Plotted on upper hemisphere


LA 710 Tunnel boring Z3 B11

| | | | | | |
|---|---|---|---|---|---|
| COMPANY | : CALTRANS | | | OTHER SERVICES: | |
| WELL | : Z3 B11 | | | IND-CAL | |
| LOCATION/FIELD | : LA 710 TUNNEL | | | AC TEL | |
| COUNTY | : LA | | | PS LOG | |
| LOCATION | : CA | | | | |
| SECTION | : None | TOWNSHIP | : None | RANGE | : None |
| DATE | : 1/21/09 | PERMANENT DATUM | : None | | |
| DEPTH DRILLER | : 83.82M | | | KB | : NA |
| LOG BOTTOM | : 83.7 | LOG MEASURED FROM: | GL | DF | : NA |
| LOG TOP | : 1.5 | DRL MEASURED FROM: | GL | GL | : NA |
| CASING DIAMETER | : N/A | LOGGING UNIT | : 7311 | | |
| CASING TYPE | : none | FIELD OFFICE | : 7311 | | |
| CASING THICKNESS: | 0 | RECORDED BY | : DH/DL | | |
| BIT SIZE | : 9.8CM | BOREHOLE FLUID | : 0 | FILE | : PROCESSE |
| MAGNETIC DECL. | : 12.85 | RM | : 0 | TYPE | : 9065A |
| MATRIX DENSITY | : 2.71 | RM TEMPERATURE | : 0 | LGDATE | : 1/21/09. |
| NEUTRON MATRIX | : Dolomite | MATRIX DELTA T | : 140 | | |
| | | | | THRESH: | 2500 |

NAT. GAMMA MEASURED AS API UNITS, NOT CPS

EA: 07-187900. GROUND LEVEL ELEVATION NOT ESTIMATE

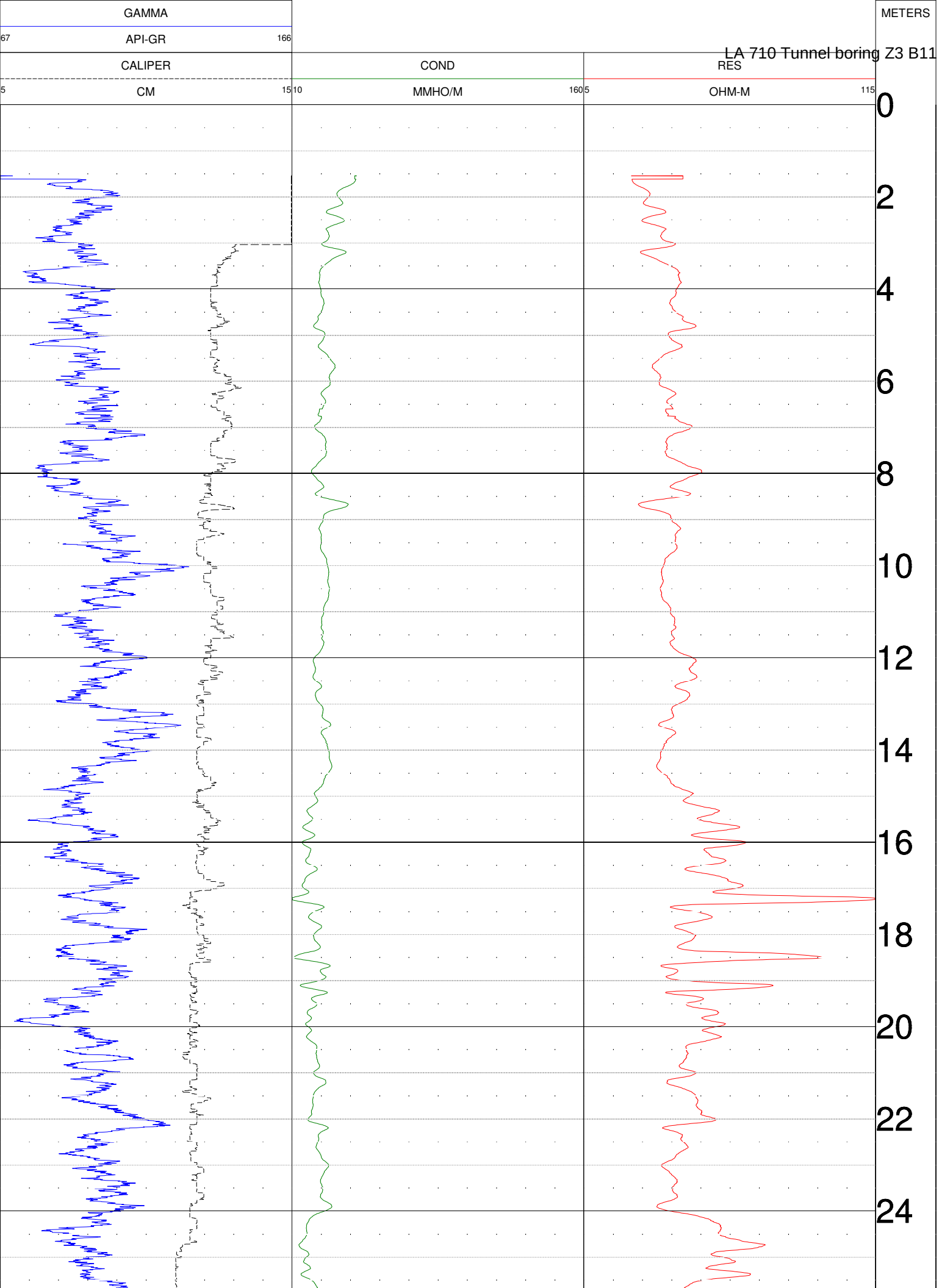
GAMMA
67
API-GR
166
CALIPER
5
CM
15
COND
10
MMHO/M
160
RES
5
OHM-M
115
METERS
LA 710 Tunnel boring Z3 B11
0
2
4
6
8
10
12
14
16
18
20
22
24

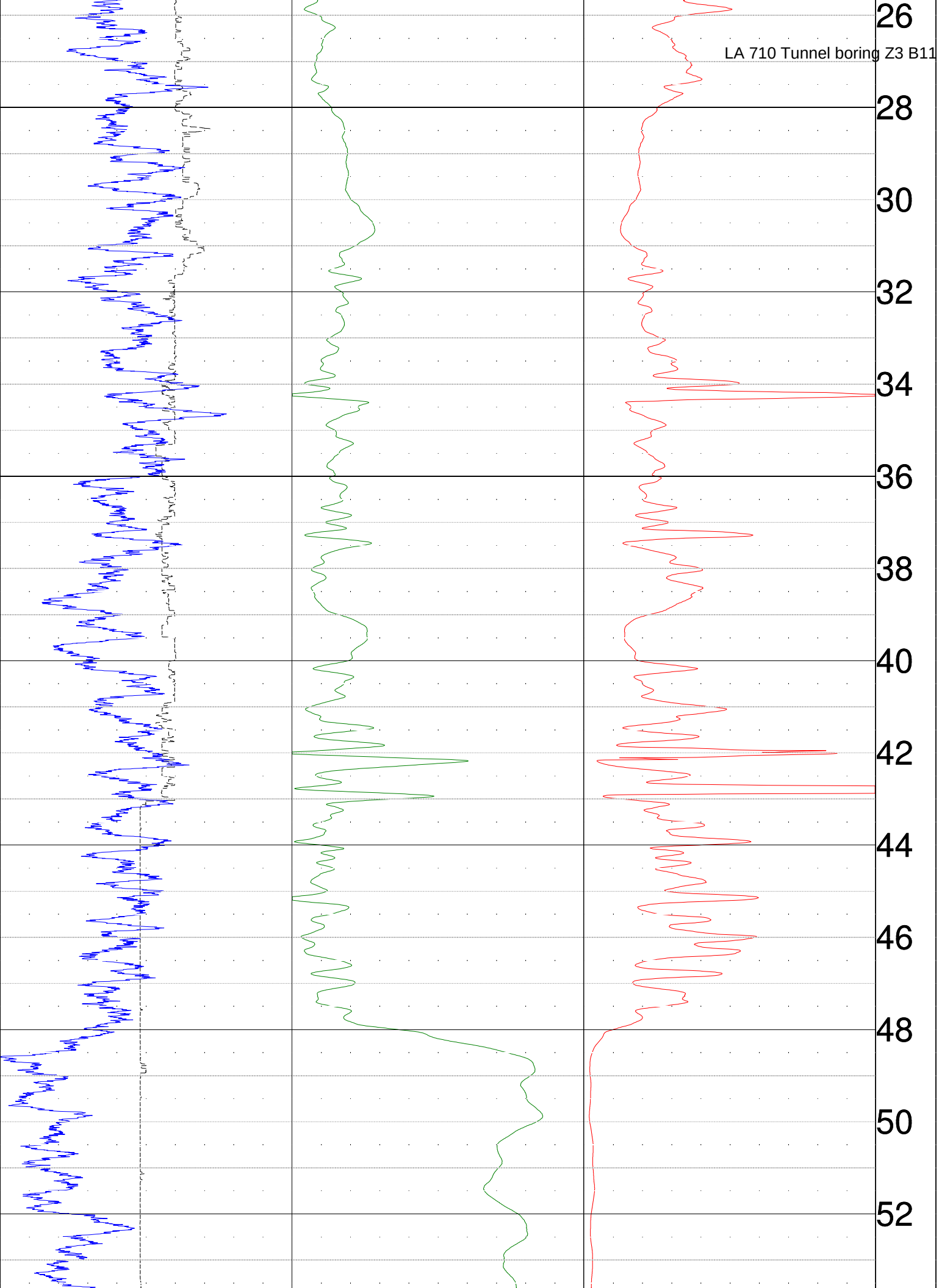
LA 710 Tunnel boring Z3 B11
26
28
30
32
34
36
38
40
42
44
46
48
50
52

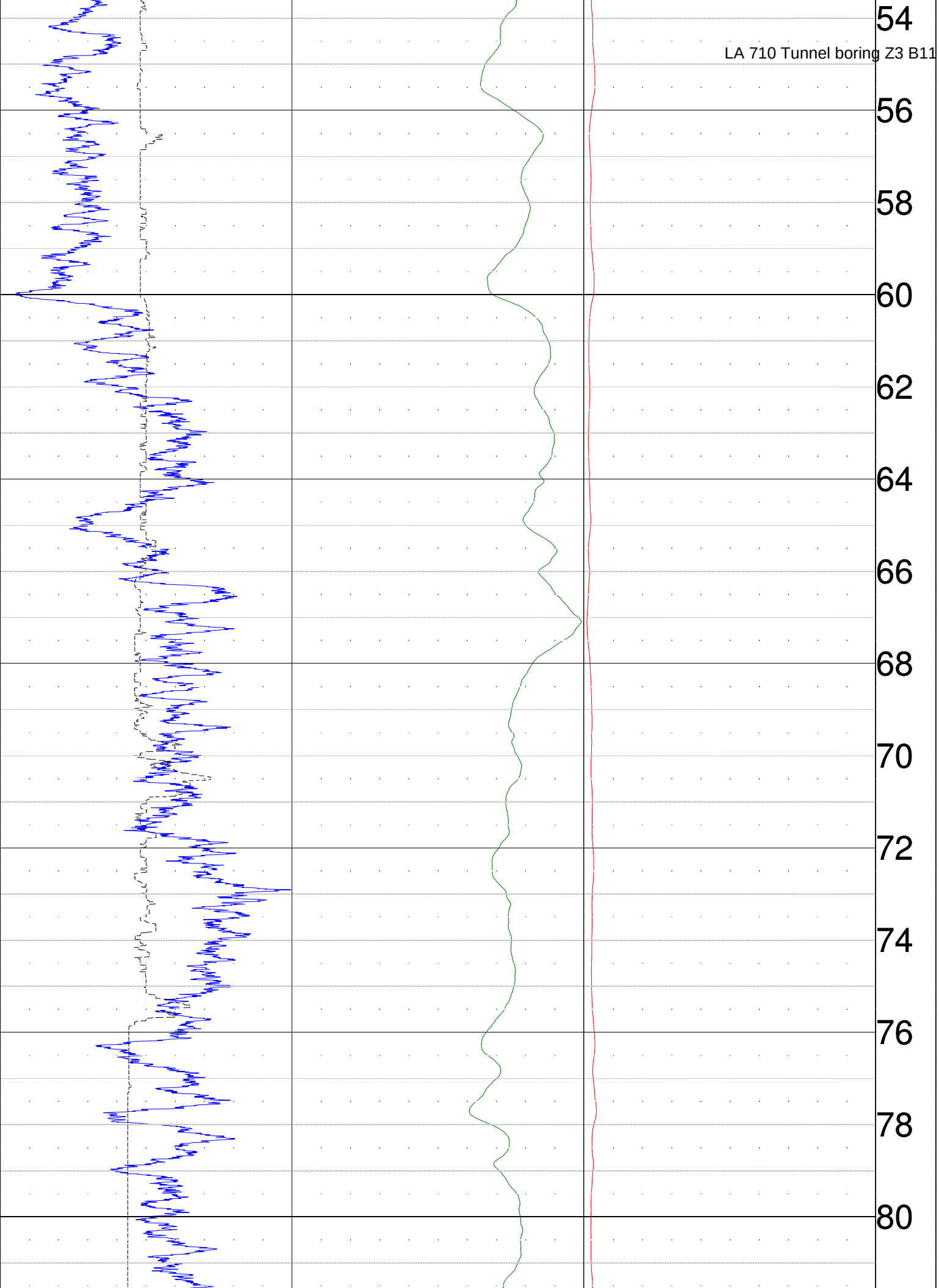
LA 710 Tunnel boring Z3 B11
54
56
58
60
62
64
66
68
70
72
74
76
78
80

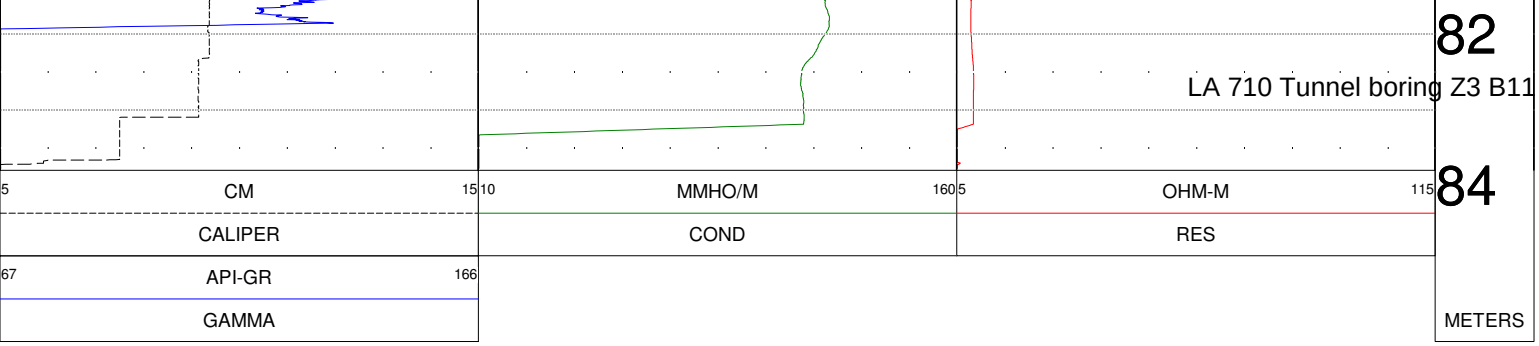
82
LA 710 Tunnel boring Z3 B11
84
5
CM
15
10
MMHO/M
160
5
OHM-M
115
CALIPER
COND
RES
67
API-GR
166
GAMMA
METERS

**Table 2.** LA 710 Tunnel
Boring Z3 B11
PS Suspension Log Data Summary



| Top of Hole Elevation (m) | Depth (m) | Depth (ft) | Vs (m/s) | Vs (ft/s) | Vp (m/s) | Vp (ft/s) | $\gamma$ | $\rho$(Vp) (g/cc) | $\rho$(Vp) ($lb/ft^3$) | G (GPa) | E (GPa) | K (GPa) | G ($10^3 lb/ft^2$) | E ($10^3 lb/ft^2$) | K ($10^3 lb/ft^2$) |
|---|---|---|---|---|---|---|---|---|---|---|---|---|---|---|---|
| Not Provided | 3.5 | 11.5 | | NA | 481 | 1577 | NA | NA | NA | NA | NA | NA | NA | NA | NA |
| | 4 | 13.1 | 253 | 828 | 556 | 1823 | NA | NA | NA | NA | NA | NA | NA | NA | NA |
| | 4.5 | 14.8 | 301 | 988 | 649 | 2130 | NA | NA | NA | NA | NA | NA | NA | NA | NA |
| | 5 | 16.4 | 340 | 1116 | 704 | 2310 | NA | NA | NA | NA | NA | NA | NA | NA | NA |
| | 5.5 | 18.0 | 379 | 1243 | 694 | 2278 | NA | NA | NA | NA | NA | NA | NA | NA | NA |
| | 5.9 | 19.4 | 376 | 1233 | 633 | 2076 | NA | NA | NA | NA | NA | NA | NA | NA | NA |
| | 6.4 | 21.0 | 360 | 1180 | 556 | 1823 | NA | NA | NA | NA | NA | NA | NA | NA | NA |
| | 7 | 23.0 | 316 | 1038 | 556 | 1823 | NA | NA | NA | NA | NA | NA | NA | NA | NA |
| | 7.5 | 24.6 | 316 | 1038 | 571 | 1875 | NA | NA | NA | NA | NA | NA | NA | NA | NA |
| | 8 | 26.2 | 307 | 1006 | 524 | 1718 | NA | NA | NA | NA | NA | NA | NA | NA | NA |
| | 8.5 | 27.9 | 316 | 1038 | 585 | 1919 | NA | NA | NA | NA | NA | NA | NA | NA | NA |
| | 9 | 29.5 | 382 | 1252 | 730 | 2395 | NA | NA | NA | NA | NA | NA | NA | NA | NA |
| | 9.5 | 31.2 | 410 | 1345 | 685 | 2247 | NA | NA | NA | NA | NA | NA | NA | NA | NA |
| | 9.9 | 32.5 | 397 | 1302 | 676 | 2217 | NA | NA | NA | NA | NA | NA | NA | NA | NA |
| | 10 | 32.8 | 382 | 1252 | 641 | 2103 | NA | NA | NA | NA | NA | NA | NA | NA | NA |
| | 10.4 | 34.1 | 376 | 1233 | 625 | 2051 | NA | NA | NA | NA | NA | NA | NA | NA | NA |
| | 10.5 | 34.4 | 362 | 1189 | 602 | 1976 | NA | NA | NA | NA | NA | NA | NA | NA | NA |
| | 11 | 36.1 | 368 | 1206 | 595 | 1953 | NA | NA | NA | NA | NA | NA | NA | NA | NA |
| | 11 | 36.1 | 355 | 1163 | 617 | 2025 | NA | NA | NA | NA | NA | NA | NA | NA | NA |
| | 11.5 | 37.7 | 336 | 1101 | 581 | 1907 | NA | NA | NA | NA | NA | NA | NA | NA | NA |
| | 11.5 | 37.7 | 355 | 1163 | 641 | 2103 | NA | NA | NA | NA | NA | NA | NA | NA | NA |
| | 12 | 39.4 | 329 | 1079 | 568 | 1864 | NA | NA | NA | NA | NA | NA | NA | NA | NA |
| | 12 | 39.4 | 340 | 1116 | 606 | 1988 | NA | NA | NA | NA | NA | NA | NA | NA | NA |
| | 12.5 | 41.0 | 355 | 1163 | 641 | 2103 | NA | NA | NA | NA | NA | NA | NA | NA | NA |
| | 12.5 | 41.0 | 329 | 1079 | 575 | 1886 | NA | NA | NA | NA | NA | NA | NA | NA | NA |
| | 12.9 | 42.3 | 350 | 1147 | 599 | 1965 | NA | NA | NA | NA | NA | NA | NA | NA | NA |
| | 13 | 42.7 | 397 | 1302 | 725 | 2377 | NA | NA | NA | NA | NA | NA | NA | NA | NA |
| | 13.4 | 44.0 | 397 | 1302 | 704 | 2310 | NA | NA | NA | NA | NA | NA | NA | NA | NA |
| | 13.5 | 44.3 | 413 | 1356 | 794 | 2604 | NA | NA | NA | NA | NA | NA | NA | NA | NA |
| | 13.9 | 45.6 | 410 | 1345 | 763 | 2504 | NA | NA | NA | NA | NA | NA | NA | NA | NA |
| | 14 | 45.9 | 424 | 1390 | 833 | 2734 | NA | NA | NA | NA | NA | NA | NA | NA | NA |
| | 14.4 | 47.2 | 417 | 1367 | 781 | 2563 | NA | NA | NA | NA | NA | NA | NA | NA | NA |
| | 14.4 | 47.2 | 424 | 1390 | 885 | 2903 | NA | NA | NA | NA | NA | NA | NA | NA | NA |
| | 14.4 | 47.2 | 420 | 1379 | 877 | 2878 | NA | NA | NA | NA | NA | NA | NA | NA | NA |
| | 14.9 | 48.9 | 427 | 1402 | 781 | 2563 | NA | NA | NA | NA | NA | NA | NA | NA | NA |
| | 15 | 49.2 | 397 | 1302 | 746 | 2448 | NA | NA | NA | NA | NA | NA | NA | NA | NA |
| | 15.5 | 50.9 | 394 | 1292 | 735 | 2412 | NA | NA | NA | NA | NA | NA | NA | NA | NA |

$\gamma$ = Poisson's Ratio  $\rho$(Vp) = Vp-derived density  G = Shear Modulus  E = Young's Modulus  K = Bulk Modulus
Shaded cells denote questionable data.

**Table 2.** LA 710 Tunnel
Boring Z3 B11
PS Suspension Log Data Summary



| Top of Hole Elevation (m) | Depth (m) | Depth (ft) | Vs (m/s) | Vs (ft/s) | Vp (m/s) | Vp (ft/s) | γ | ρ(Vp) (g/cc) | ρ(Vp) ($lb/ft^3$) | G (GPa) | E (GPa) | K (GPa) | G ($10^3 lb/ft^2$) | E ($10^3 lb/ft^2$) | K ($10^3 lb/ft^2$) |
|---|---|---|---|---|---|---|---|---|---|---|---|---|---|---|---|
| | 15.5 | 50.9 | 397 | 1302 | 680 | 2232 | NA | NA | NA | NA | NA | NA | NA | NA | NA |
| | 16 | 52.5 | 376 | 1233 | 781 | 2563 | NA | NA | NA | NA | NA | NA | NA | NA | NA |
| | 16 | 52.5 | 417 | 1367 | 794 | 2604 | NA | NA | NA | NA | NA | NA | NA | NA | NA |
| | 16.5 | 54.1 | 391 | 1282 | 781 | 2563 | NA | NA | NA | NA | NA | NA | NA | NA | NA |
| | 16.5 | 54.1 | 417 | 1367 | 725 | 2377 | NA | NA | NA | NA | NA | NA | NA | NA | NA |
| | 17 | 55.8 | 407 | 1334 | 735 | 2412 | NA | NA | NA | NA | NA | NA | NA | NA | NA |
| | 17 | 55.8 | 413 | 1356 | 775 | 2543 | NA | NA | NA | NA | NA | NA | NA | NA | NA |
| | 17.5 | 57.4 | 400 | 1312 | 746 | 2448 | NA | NA | NA | NA | NA | NA | NA | NA | NA |
| | 17.5 | 57.4 | 397 | 1302 | 690 | 2263 | NA | NA | NA | NA | NA | NA | NA | NA | NA |
| | 17.5 | 57.4 | 392 | 1287 | 685 | 2247 | NA | NA | NA | NA | NA | NA | NA | NA | NA |
| | 18 | 59.1 | 420 | 1379 | 758 | 2485 | NA | NA | NA | NA | NA | NA | NA | NA | NA |
| | 18 | 59.1 | 388 | 1272 | 704 | 2310 | NA | NA | NA | NA | NA | NA | NA | NA | NA |
| | 18.5 | 60.7 | 435 | 1426 | 847 | 2780 | NA | NA | NA | NA | NA | NA | NA | NA | NA |
| | 18.5 | 60.7 | 417 | 1367 | 671 | 2202 | NA | NA | NA | NA | NA | NA | NA | NA | NA |
| | 18.9 | 62.0 | 424 | 1390 | 806 | 2646 | NA | NA | NA | NA | NA | NA | NA | NA | NA |
| | 18.9 | 62.0 | 439 | 1439 | 840 | 2757 | NA | NA | NA | NA | NA | NA | NA | NA | NA |
| | 19.4 | 63.6 | 424 | 1390 | 787 | 2583 | NA | NA | NA | NA | NA | NA | NA | NA | NA |
| | 19.5 | 64.0 | 439 | 1439 | 781 | 2563 | NA | NA | NA | NA | NA | NA | NA | NA | NA |
| | 19.9 | 65.3 | 413 | 1356 | 735 | 2412 | NA | NA | NA | NA | NA | NA | NA | NA | NA |
| | 20 | 65.6 | 446 | 1465 | 769 | 2524 | NA | NA | NA | NA | NA | NA | NA | NA | NA |
| | 20.5 | 67.3 | 435 | 1426 | 758 | 2485 | NA | NA | NA | NA | NA | NA | NA | NA | NA |
| | 20.8 | 68.2 | 521 | 1709 | 962 | 3155 | NA | NA | NA | NA | NA | NA | NA | NA | NA |
| | 21 | 68.9 | 495 | 1624 | 901 | 2956 | NA | NA | NA | NA | NA | NA | NA | NA | NA |
| | 21.5 | 70.5 | 568 | 1864 | 1020 | 3348 | NA | NA | NA | NA | NA | NA | NA | NA | NA |
| | 22 | 72.2 | 581 | 1907 | 990 | 3248 | NA | NA | NA | NA | NA | NA | NA | NA | NA |
| | 22.5 | 73.8 | 526 | 1727 | 917 | 3010 | NA | NA | NA | NA | NA | NA | NA | NA | NA |
| | 23 | 75.5 | 500 | 1640 | 893 | 2929 | NA | NA | NA | NA | NA | NA | NA | NA | NA |
| | 24 | 78.7 | 472 | 1548 | 847 | 2780 | NA | NA | NA | NA | NA | NA | NA | NA | NA |
| | 24.5 | 80.4 | 490 | 1608 | 893 | 2929 | NA | NA | NA | NA | NA | NA | NA | NA | NA |
| | 25 | 82.0 | 476 | 1562 | 758 | 2485 | NA | NA | NA | NA | NA | NA | NA | NA | NA |
| | 25.5 | 83.7 | 459 | 1505 | 855 | 2804 | NA | NA | NA | NA | NA | NA | NA | NA | NA |
| | 26 | 85.3 | 472 | 1548 | 990 | 3248 | NA | NA | NA | NA | NA | NA | NA | NA | NA |
| | 26.5 | 86.9 | 515 | 1691 | 926 | 3038 | NA | NA | NA | NA | NA | NA | NA | NA | NA |
| | 27 | 88.6 | 543 | 1783 | 926 | 3038 | NA | NA | NA | NA | NA | NA | NA | NA | NA |
| | 27.5 | 90.2 | 521 | 1709 | 901 | 2956 | NA | NA | NA | NA | NA | NA | NA | NA | NA |
| | 28 | 91.9 | 505 | 1657 | 847 | 2780 | NA | NA | NA | NA | NA | NA | NA | NA | NA |
| | 28.5 | 93.5 | 476 | 1562 | 855 | 2804 | NA | NA | NA | NA | NA | NA | NA | NA | NA |

γ = Poisson's Ratio  ρ(Vp) = Vp-derived density  G = Shear Modulus  E = Young's Modulus  K = Bulk Modulus
Shaded cells denote questionable data.

**Table 2.** LA 710 Tunnel
Boring Z3 B11
PS Suspension Log Data Summary



| Top of Hole Elevation (m) | Depth (m) | Depth (ft) | Vs (m/s) | Vs (ft/s) | Vp (m/s) | Vp (ft/s) | γ | ρ(Vp) (g/cc) | ρ(Vp) ($lb/ft^3$) | G (GPa) | E (GPa) | K (GPa) | G ($10^3 lb/ft^2$) | E ($10^3 lb/ft^2$) | K ($10^3 lb/ft^2$) |
|---|---|---|---|---|---|---|---|---|---|---|---|---|---|---|---|
| | 29 | 95.1 | 485 | 1593 | 741 | 2430 | NA | NA | NA | NA | NA | NA | NA | NA | NA |
| | 29.5 | 96.8 | 500 | 1640 | 840 | 2757 | NA | NA | NA | NA | NA | NA | NA | NA | NA |
| | 30 | 98.4 | 510 | 1674 | 833 | 2734 | NA | NA | NA | NA | NA | NA | NA | NA | NA |
| | 30.5 | 100.1 | 485 | 1593 | 806 | 2646 | NA | NA | NA | NA | NA | NA | NA | NA | NA |
| | 31 | 101.7 | 463 | 1519 | 1020 | 3348 | NA | NA | NA | NA | NA | NA | NA | NA | NA |
| | 31.5 | 103.3 | 485 | 1593 | 781 | 2563 | NA | NA | NA | NA | NA | NA | NA | NA | NA |
| | 32 | 105.0 | 581 | 1907 | 980 | 3217 | NA | NA | NA | NA | NA | NA | NA | NA | NA |
| | 32.5 | 106.6 | 625 | 2051 | 1053 | 3454 | NA | NA | NA | NA | NA | NA | NA | NA | NA |
| | 33 | 108.3 | 595 | 1953 | 1042 | 3418 | NA | NA | NA | NA | NA | NA | NA | NA | NA |
| | 33.4 | 109.6 | 581 | 1907 | 1075 | 3528 | NA | NA | NA | NA | NA | NA | NA | NA | NA |
| | 34 | 111.5 | 562 | 1843 | 1099 | 3605 | NA | NA | NA | NA | NA | NA | NA | NA | NA |
| | 34.4 | 112.9 | 617 | 2025 | 1149 | 3771 | NA | NA | NA | NA | NA | NA | NA | NA | NA |
| | 35 | 114.8 | 694 | 2278 | 1220 | 4001 | NA | NA | NA | NA | NA | NA | NA | NA | NA |
| | 35.5 | 116.5 | 667 | 2187 | 1190 | 3906 | NA | NA | NA | NA | NA | NA | NA | NA | NA |
| | 36 | 118.1 | 658 | 2158 | 1149 | 3771 | NA | NA | NA | NA | NA | NA | NA | NA | NA |
| | 36.5 | 119.8 | 667 | 2187 | 1190 | 3906 | NA | NA | NA | NA | NA | NA | NA | NA | NA |
| | 37 | 121.4 | 633 | 2076 | 1064 | 3490 | NA | NA | NA | NA | NA | NA | NA | NA | NA |
| | 37.5 | 123.0 | 625 | 2051 | 1042 | 3418 | NA | NA | NA | NA | NA | NA | NA | NA | NA |
| | 38 | 124.7 | 658 | 2158 | 1136 | 3728 | NA | NA | NA | NA | NA | NA | NA | NA | NA |
| | 38.5 | 126.3 | 658 | 2158 | 1149 | 3771 | NA | NA | NA | NA | NA | NA | NA | NA | NA |
| | 39 | 128.0 | 704 | 2310 | 1190 | 3906 | NA | NA | NA | NA | NA | NA | NA | NA | NA |
| | 39.5 | 129.6 | 735 | 2412 | 1316 | 4317 | NA | NA | NA | NA | NA | NA | NA | NA | NA |
| | 40 | 131.2 | 610 | 2001 | 1064 | 3490 | NA | NA | NA | NA | NA | NA | NA | NA | NA |
| | 40.5 | 132.9 | 532 | 1745 | 962 | 3155 | NA | NA | NA | NA | NA | NA | NA | NA | NA |
| | 41 | 134.5 | 526 | 1727 | 917 | 3010 | NA | NA | NA | NA | NA | NA | NA | NA | NA |
| | 41.5 | 136.2 | 495 | 1624 | 893 | 2929 | NA | NA | NA | NA | NA | NA | NA | NA | NA |
| | 42 | 137.8 | 490 | 1608 | 1099 | 3605 | NA | NA | NA | NA | NA | NA | NA | NA | NA |
| | 42.5 | 139.4 | 543 | 1783 | 1220 | 4001 | NA | NA | NA | NA | NA | NA | NA | NA | NA |
| | 43 | 141.1 | 581 | 1907 | 1149 | 3771 | NA | NA | NA | NA | NA | NA | NA | NA | NA |
| | 43.5 | 142.7 | 575 | 1886 | 1053 | 3454 | NA | NA | NA | NA | NA | NA | NA | NA | NA |
| | 44 | 144.4 | 575 | 1886 | 1000 | 3281 | NA | NA | NA | NA | NA | NA | NA | NA | NA |
| | 44.5 | 146.0 | 617 | 2025 | 1176 | 3860 | NA | NA | NA | NA | NA | NA | NA | NA | NA |
| | 45 | 147.6 | 602 | 1976 | 1220 | 4001 | NA | NA | NA | NA | NA | NA | NA | NA | NA |
| | 45.5 | 149.3 | 625 | 2051 | 1250 | 4101 | NA | NA | NA | NA | NA | NA | NA | NA | NA |
| | 46 | 150.9 | 625 | 2051 | 1205 | 3953 | NA | NA | NA | NA | NA | NA | NA | NA | NA |
| | 46.5 | 152.6 | 595 | 1953 | 1149 | 3771 | NA | NA | NA | NA | NA | NA | NA | NA | NA |
| | 47 | 154.2 | 562 | 1843 | 1111 | 3645 | NA | NA | NA | NA | NA | NA | NA | NA | NA |

γ = Poisson's Ratio  ρ(Vp) = Vp-derived density  G = Shear Modulus  E = Young's Modulus  K = Bulk Modulus
Shaded cells denote questionable data.

**Table 2.** LA 710 Tunnel
Boring Z3 B11
PS Suspension Log Data Summary



| Top of Hole Elevation (m) | Depth (m) | Depth (ft) | Vs (m/s) | Vs (ft/s) | Vp (m/s) | Vp (ft/s) | $\gamma$ | $\rho$(Vp) (g/cc) | $\rho$(Vp) ($lb/ft^3$) | G (GPa) | E (GPa) | K (GPa) | G ($10^3 lb/ft^2$) | E ($10^3 lb/ft^2$) | K ($10^3 lb/ft^2$) |
|---|---|---|---|---|---|---|---|---|---|---|---|---|---|---|---|
| | 47.5 | 155.8 | 581 | 1907 | 1220 | 4001 | NA | NA | NA | NA | NA | NA | NA | NA | NA |
| | 48 | 157.5 | 538 | 1764 | 1099 | 3605 | NA | NA | NA | NA | NA | NA | NA | NA | NA |
| | 48.4 | 158.8 | 581 | 1907 | 1020 | 3348 | NA | NA | NA | NA | NA | NA | NA | NA | NA |
| | 48.9 | 160.4 | 595 | 1953 | 1136 | 3728 | NA | NA | NA | NA | NA | NA | NA | NA | NA |
| | 49.5 | 162.4 | 610 | 2001 | 1099 | 3605 | NA | NA | NA | NA | NA | NA | NA | NA | NA |
| | 50 | 164.0 | 595 | 1953 | 1163 | 3815 | NA | NA | NA | NA | NA | NA | NA | NA | NA |
| | 50.5 | 165.7 | 610 | 2001 | 1333 | 4374 | NA | NA | NA | NA | NA | NA | NA | NA | NA |
| | 51 | 167.3 | 463 | 1519 | 1613 | 5292 | 0.46 | 1.94 | 121.09 | 0.416 | 1.210 | 4.492 | 8683 | 25268 | 93807 |
| | 51.5 | 169.0 | 407 | 1334 | 1754 | 5756 | 0.47 | 2.04 | 127.35 | 0.337 | 0.992 | 5.829 | 7040 | 20722 | 121749 |
| | 52.1 | 170.9 | 476 | 1562 | 1786 | 5859 | 0.46 | 2.06 | 128.62 | 0.467 | 1.366 | 5.947 | 9757 | 28524 | 124199 |
| | 52.5 | 172.2 | 476 | 1562 | 1754 | 5756 | 0.46 | 2.04 | 127.35 | 0.463 | 1.351 | 5.662 | 9661 | 28215 | 118254 |
| | 53 | 173.9 | 442 | 1452 | 1786 | 5859 | 0.47 | 2.06 | 128.62 | 0.403 | 1.184 | 6.032 | 8424 | 24722 | 125975 |
| | 53.5 | 175.5 | 420 | 1379 | 1786 | 5859 | 0.47 | 2.06 | 128.62 | 0.364 | 1.070 | 6.085 | 7596 | 22344 | 127080 |
| | 53.9 | 176.8 | 413 | 1356 | 1724 | 5657 | 0.47 | 2.02 | 126.09 | 0.345 | 1.014 | 5.544 | 7203 | 21171 | 115797 |
| | 54.5 | 178.8 | 435 | 1426 | 1695 | 5561 | 0.46 | 2.00 | 124.84 | 0.378 | 1.107 | 5.241 | 7895 | 23129 | 109452 |
| | 55 | 180.4 | 435 | 1426 | 1786 | 5859 | 0.47 | 2.06 | 128.62 | 0.389 | 1.144 | 6.050 | 8134 | 23889 | 126363 |
| | 55.5 | 182.1 | 442 | 1452 | 1852 | 6076 | 0.47 | 2.10 | 131.15 | 0.411 | 1.209 | 6.656 | 8590 | 25251 | 139012 |
| | 56 | 183.7 | 467 | 1533 | 1852 | 6076 | 0.47 | 2.10 | 131.15 | 0.459 | 1.345 | 6.593 | 9581 | 28091 | 137692 |
| | 56.5 | 185.4 | 427 | 1402 | 1852 | 6076 | 0.47 | 2.10 | 131.15 | 0.384 | 1.129 | 6.693 | 8013 | 23588 | 139782 |
| | 57 | 187.0 | 521 | 1709 | 1887 | 6190 | 0.46 | 2.12 | 132.42 | 0.575 | 1.679 | 6.784 | 12017 | 35061 | 141688 |
| | 57.4 | 188.3 | 526 | 1727 | 1887 | 6190 | 0.46 | 2.12 | 132.42 | 0.588 | 1.713 | 6.768 | 12272 | 35780 | 141349 |
| | 58 | 190.3 | 526 | 1727 | 1961 | 6433 | 0.46 | 2.16 | 134.97 | 0.599 | 1.750 | 7.514 | 12508 | 36553 | 156926 |
| | 58.5 | 191.9 | 526 | 1727 | 1887 | 6190 | 0.46 | 2.12 | 132.42 | 0.588 | 1.713 | 6.768 | 12272 | 35780 | 141348 |
| | 59 | 193.6 | 463 | 1519 | 1852 | 6076 | 0.47 | 2.10 | 131.15 | 0.450 | 1.321 | 6.604 | 9404 | 27585 | 137927 |
| | 60 | 196.9 | 500 | 1640 | 1818 | 5965 | 0.46 | 2.08 | 129.88 | 0.520 | 1.518 | 6.184 | 10863 | 31700 | 129158 |
| | 60.5 | 198.5 | 549 | 1803 | 1923 | 6309 | 0.46 | 2.14 | 133.69 | 0.647 | 1.882 | 7.058 | 13503 | 39309 | 147407 |
| | 61.5 | 201.8 | 463 | 1519 | 1818 | 5965 | 0.47 | 2.08 | 129.88 | 0.446 | 1.307 | 6.283 | 9313 | 27294 | 131224 |
| | 62 | 203.4 | 485 | 1593 | 1923 | 6309 | 0.47 | 2.14 | 133.69 | 0.505 | 1.480 | 7.247 | 10540 | 30902 | 151358 |
| | 62 | 203.4 | 485 | 1593 | 1923 | 6309 | 0.47 | 2.14 | 133.69 | 0.505 | 1.480 | 7.247 | 10540 | 30902 | 151358 |
| | 62.5 | 205.1 | 459 | 1505 | 1923 | 6309 | 0.47 | 2.14 | 133.69 | 0.451 | 1.325 | 7.319 | 9412 | 27667 | 152862 |
| | 63 | 206.7 | 385 | 1262 | 1786 | 5859 | 0.48 | 2.06 | 128.62 | 0.305 | 0.899 | 6.163 | 6365 | 18786 | 128721 |
| | 63.5 | 208.3 | 455 | 1491 | 1786 | 5859 | 0.47 | 2.06 | 128.62 | 0.426 | 1.248 | 6.002 | 8890 | 26055 | 125354 |
| | 64 | 210.0 | 459 | 1505 | 1961 | 6433 | 0.47 | 2.16 | 134.97 | 0.455 | 1.338 | 7.706 | 9501 | 27954 | 160935 |
| | 64.5 | 211.6 | 532 | 1745 | 1923 | 6309 | 0.46 | 2.14 | 133.69 | 0.606 | 1.768 | 7.112 | 12655 | 36916 | 148538 |
| | 65 | 213.3 | 455 | 1491 | 1818 | 5965 | 0.47 | 2.08 | 129.88 | 0.430 | 1.261 | 6.305 | 8978 | 26334 | 131671 |
| | 65.5 | 214.9 | 446 | 1465 | 1786 | 5859 | 0.47 | 2.06 | 128.62 | 0.411 | 1.204 | 6.022 | 8576 | 25155 | 125774 |
| | 66 | 216.5 | 431 | 1414 | 1818 | 5965 | 0.47 | 2.08 | 129.88 | 0.387 | 1.137 | 6.362 | 8073 | 23738 | 132878 |

$\gamma$ = Poisson's Ratio  $\rho$(Vp) = Vp-derived density  G = Shear Modulus  E = Young's Modulus  K = Bulk Modulus
Shaded cells denote questionable data.

**Table 2.** LA 710 Tunnel
Boring Z3 B11
PS Suspension Log Data Summary



| Top of Hole Elevation (m) | Depth (m) | Depth (ft) | Vs (m/s) | Vs (ft/s) | Vp (m/s) | Vp (ft/s) | $\gamma$ | $\rho$(Vp) (g/cc) | $\rho$(Vp) ($lb/ft^3$) | G (GPa) | E (GPa) | K (GPa) | G ($10^3 lb/ft^2$) | E ($10^3 lb/ft^2$) | K ($10^3 lb/ft^2$) |
|---|---|---|---|---|---|---|---|---|---|---|---|---|---|---|---|
| | 66.4 | 217.8 | 431 | 1414 | 1818 | 5965 | 0.47 | 2.08 | 129.88 | 0.387 | 1.137 | 6.362 | 8073 | 23738 | 132878 |
| | 66.9 | 219.5 | 427 | 1402 | 1961 | 6433 | 0.48 | 2.16 | 134.97 | 0.395 | 1.165 | 7.786 | 8246 | 24328 | 162608 |
| | 67.5 | 221.5 | 420 | 1379 | 2000 | 6562 | 0.48 | 2.18 | 136.25 | 0.385 | 1.138 | 8.216 | 8047 | 23770 | 171600 |
| | 68 | 223.1 | 459 | 1505 | 1887 | 6190 | 0.47 | 2.12 | 132.42 | 0.446 | 1.311 | 6.956 | 9322 | 27380 | 145282 |
| | 68.5 | 224.7 | 467 | 1533 | 1961 | 6433 | 0.47 | 2.16 | 134.97 | 0.472 | 1.388 | 7.683 | 9860 | 28986 | 160457 |
| | 69 | 226.4 | 510 | 1674 | 1923 | 6309 | 0.46 | 2.14 | 133.69 | 0.557 | 1.630 | 7.177 | 11643 | 34047 | 149887 |
| | 69.5 | 228.0 | 526 | 1727 | 1961 | 6433 | 0.46 | 2.16 | 134.97 | 0.599 | 1.750 | 7.514 | 12508 | 36553 | 156926 |
| | 70 | 229.7 | 549 | 1803 | 1961 | 6433 | 0.46 | 2.16 | 134.97 | 0.653 | 1.902 | 7.442 | 13632 | 39734 | 155427 |
| | 70.5 | 231.3 | 568 | 1864 | 1852 | 6076 | 0.45 | 2.10 | 131.15 | 0.678 | 1.964 | 6.300 | 14164 | 41021 | 131580 |
| | 71 | 232.9 | 581 | 1907 | 2222 | 7291 | 0.46 | 2.29 | 142.69 | 0.773 | 2.261 | 10.257 | 16136 | 47223 | 214227 |
| | 71.5 | 234.6 | 490 | 1608 | 2000 | 6562 | 0.47 | 2.18 | 136.25 | 0.524 | 1.540 | 8.031 | 10953 | 32159 | 167725 |
| | 72 | 236.2 | 538 | 1764 | 2128 | 6981 | 0.47 | 2.24 | 140.11 | 0.649 | 1.902 | 9.295 | 13549 | 39722 | 194125 |
| | 72.5 | 237.9 | 562 | 1843 | 2083 | 6835 | 0.46 | 2.22 | 138.82 | 0.702 | 2.050 | 8.715 | 14658 | 42824 | 182026 |
| | 73 | 239.5 | 481 | 1577 | 2273 | 7456 | 0.48 | 2.31 | 143.99 | 0.533 | 1.574 | 11.203 | 11134 | 32882 | 233976 |
| | 73.5 | 241.1 | 505 | 1657 | 2083 | 6835 | 0.47 | 2.22 | 138.82 | 0.567 | 1.666 | 8.895 | 11846 | 34799 | 185774 |
| | 74 | 242.8 | 562 | 1843 | 2273 | 7456 | 0.47 | 2.31 | 143.99 | 0.728 | 2.137 | 10.943 | 15204 | 44622 | 228550 |
| | 74.5 | 244.4 | 610 | 2001 | 2273 | 7456 | 0.46 | 2.31 | 143.99 | 0.858 | 2.506 | 10.770 | 17910 | 52342 | 224941 |
| | 75 | 246.1 | 562 | 1843 | 2174 | 7132 | 0.46 | 2.26 | 141.40 | 0.715 | 2.093 | 9.751 | 14930 | 43722 | 203650 |
| | 75.5 | 247.7 | 562 | 1843 | 2128 | 6981 | 0.46 | 2.24 | 140.11 | 0.708 | 2.072 | 9.215 | 14794 | 43273 | 192464 |
| | 76 | 249.3 | 549 | 1803 | 2128 | 6981 | 0.46 | 2.24 | 140.11 | 0.678 | 1.984 | 9.256 | 14151 | 41441 | 193321 |
| | 76.5 | 251.0 | 538 | 1764 | 2041 | 6696 | 0.46 | 2.20 | 137.53 | 0.637 | 1.863 | 8.327 | 13300 | 38907 | 173902 |
| | 77 | 252.6 | 455 | 1491 | 2222 | 7291 | 0.48 | 2.29 | 142.69 | 0.472 | 1.396 | 10.658 | 9863 | 29159 | 222591 |
| | 77.4 | 253.9 | 481 | 1577 | 2083 | 6835 | 0.47 | 2.22 | 138.82 | 0.514 | 1.513 | 8.966 | 10734 | 31599 | 187257 |
| | 78 | 255.9 | 562 | 1843 | 2128 | 6981 | 0.46 | 2.24 | 140.11 | 0.708 | 2.072 | 9.215 | 14794 | 43273 | 192465 |
| | 78.4 | 257.2 | 575 | 1886 | 2222 | 7291 | 0.46 | 2.29 | 142.69 | 0.755 | 2.211 | 10.281 | 15768 | 46172 | 214719 |
| | 79 | 259.2 | | NA | 2083 | 6835 | NA | NA | NA | NA | NA | NA | NA | NA | NA |
| | 79.5 | 260.8 | 556 | 1823 | 2128 | 6981 | 0.46 | 2.24 | 140.11 | 0.693 | 2.027 | 9.236 | 14467 | 42342 | 192901 |
| | 80 | 262.5 | 746 | 2448 | 2381 | 7812 | 0.45 | 2.35 | 146.59 | 1.308 | 3.781 | 11.568 | 27313 | 78963 | 241604 |
| | 80.5 | 264.1 | 758 | 2485 | 2222 | 7291 | 0.43 | 2.29 | 142.69 | 1.312 | 3.763 | 9.538 | 27398 | 78590 | 199212 |
| | 81.2 | 266.4 | 658 | 2158 | 2174 | 7132 | 0.45 | 2.26 | 141.40 | 0.980 | 2.842 | 9.397 | 20475 | 59360 | 196258 |
| | 81.7 | 268.0 | 633 | 2076 | 2083 | 6835 | 0.45 | 2.22 | 138.82 | 0.891 | 2.582 | 8.464 | 18603 | 53919 | 176765 |
| | 82.3 | 270.0 | 641 | 2103 | 2174 | 7132 | 0.45 | 2.26 | 141.40 | 0.931 | 2.703 | 9.463 | 19438 | 56463 | 197640 |

$\gamma$ = Poisson's Ratio  $\rho$(Vp) = Vp-derived density  G = Shear Modulus  E = Young's Modulus  K = Bulk Modulus
Shaded cells denote questionable data.

# Figure 1. LA 710 Tunnel
# Boring Z3 B11
# Downhole Interval Velocities

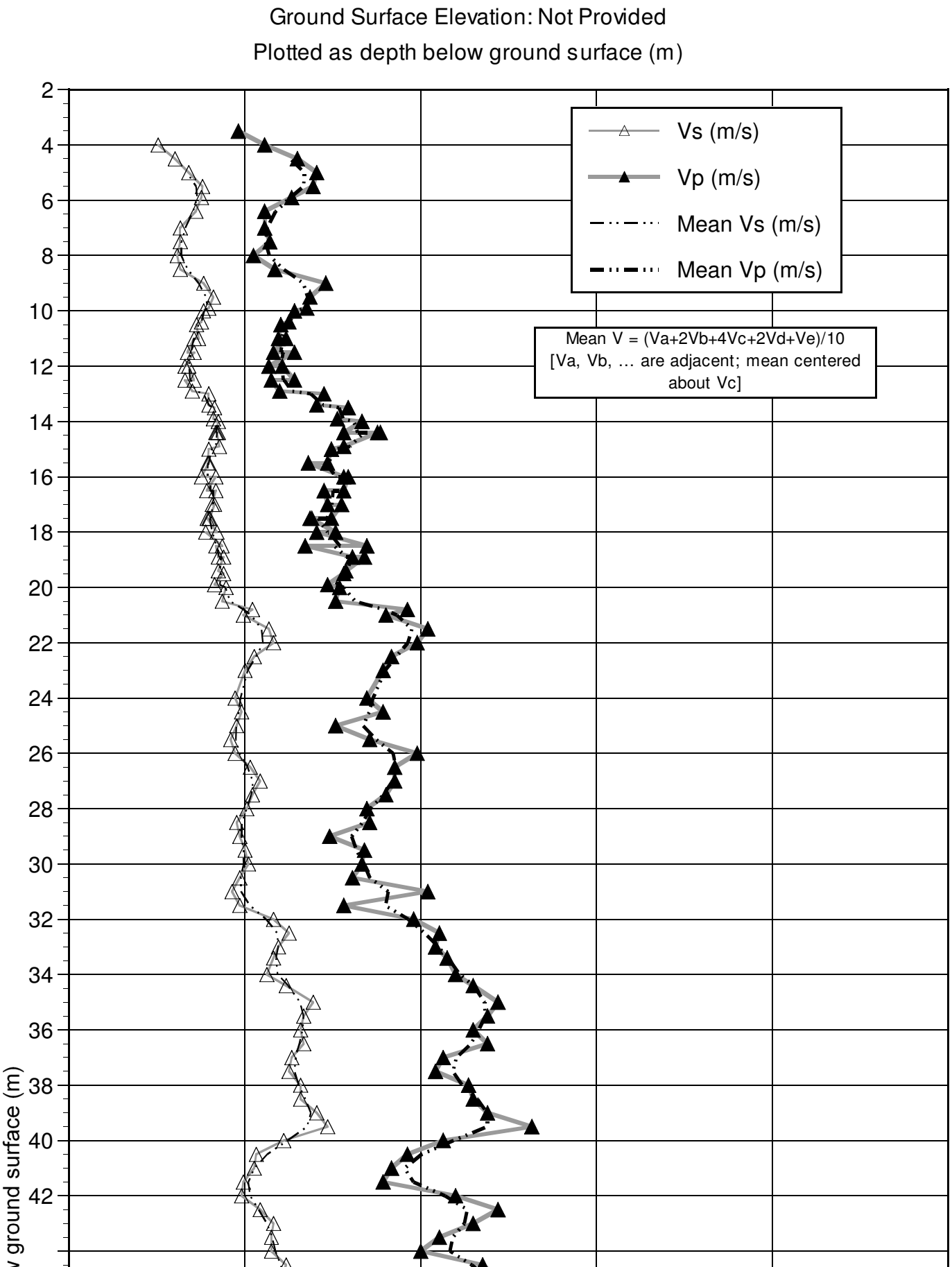

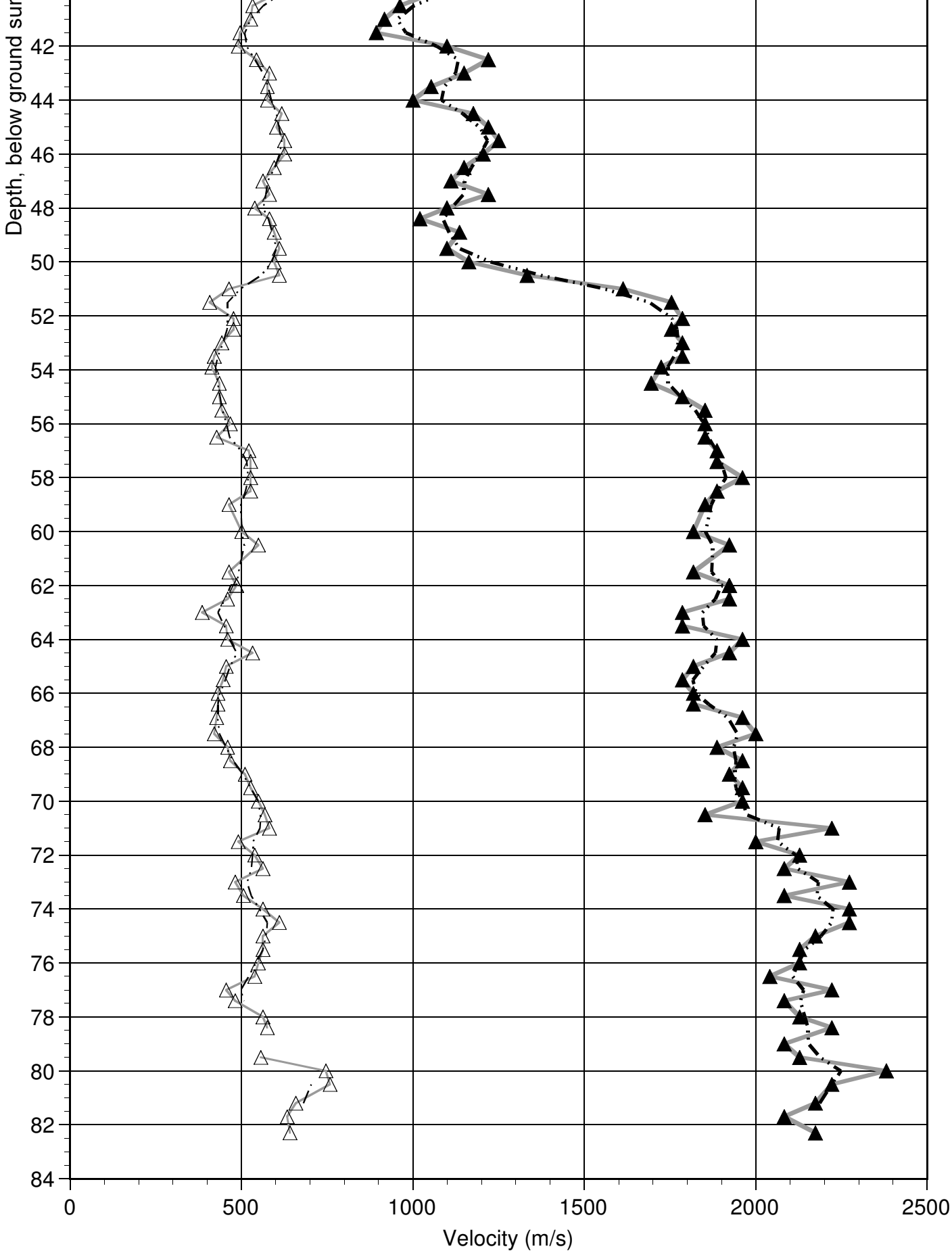
Depth, below ground surface
42
44
46
48
50
52
54
56
58
60
62
64
66
68
70
72
74
76
78
80
82
84
0
500
1000
1500
2000
2500
Velocity (m/s)


# Z3B11

| | | |
|---|---|---|
| COMPANY | : CALTRANS. | OTHER SERVICES: |
| WELL | : Z3B11 | IND-CAL. |
| FIELD | : LA 710 TUNNEL. | AC TEL. |
| COUNTY | : LA | PSLOG |
| STATE | : CA | |

| | |
|---|---|
| LOCATION | : |
| SECTION | : None |
| TOWNSHIP | : None |
| RANGE | : None |
| API NO. | : |
| UNIQUE WELL ID. | : |

| | | | |
|---|---|---|---|
| PERMANENT DATUM | : None | ELEVATION KB | : NA |
| LOG MEASURED FROM | : GL | ELEVATION DF | : NA |
| DRL MEASURED FROM | : GL | ELEVATION GL | : 0 |

| | | | |
|---|---|---|---|
| DATE | : 1/21/09 | RIG NUMBER | : |
| DEPTH DRILLER | : 275 | LOGGER TD | : |
| BIT SIZE | : 98 | ARRIVAL TIME | : |
| LOG TOP | : 4.50 | DEPARTURE TIME | : |
| LOG BOTTOM | : 83.50 | CIRC STOPPED | : 0930 |

| | |
|---|---|
| CASING OD | : |
| CASING BOTTOM | : NA |
| CASING TYPE | : none |
| BOREHOLE FLUID | : 0 |
| RM TEMPERATURE | : 0 |
| MUD RES | : 0 |
| MUD WEIGHT | : |
| WITNESSED BY | : |
| RECORDED BY | : DH/DL |
| REMARKS 1 | : |
| REMARKS 2 | : EA: 07-187900 |

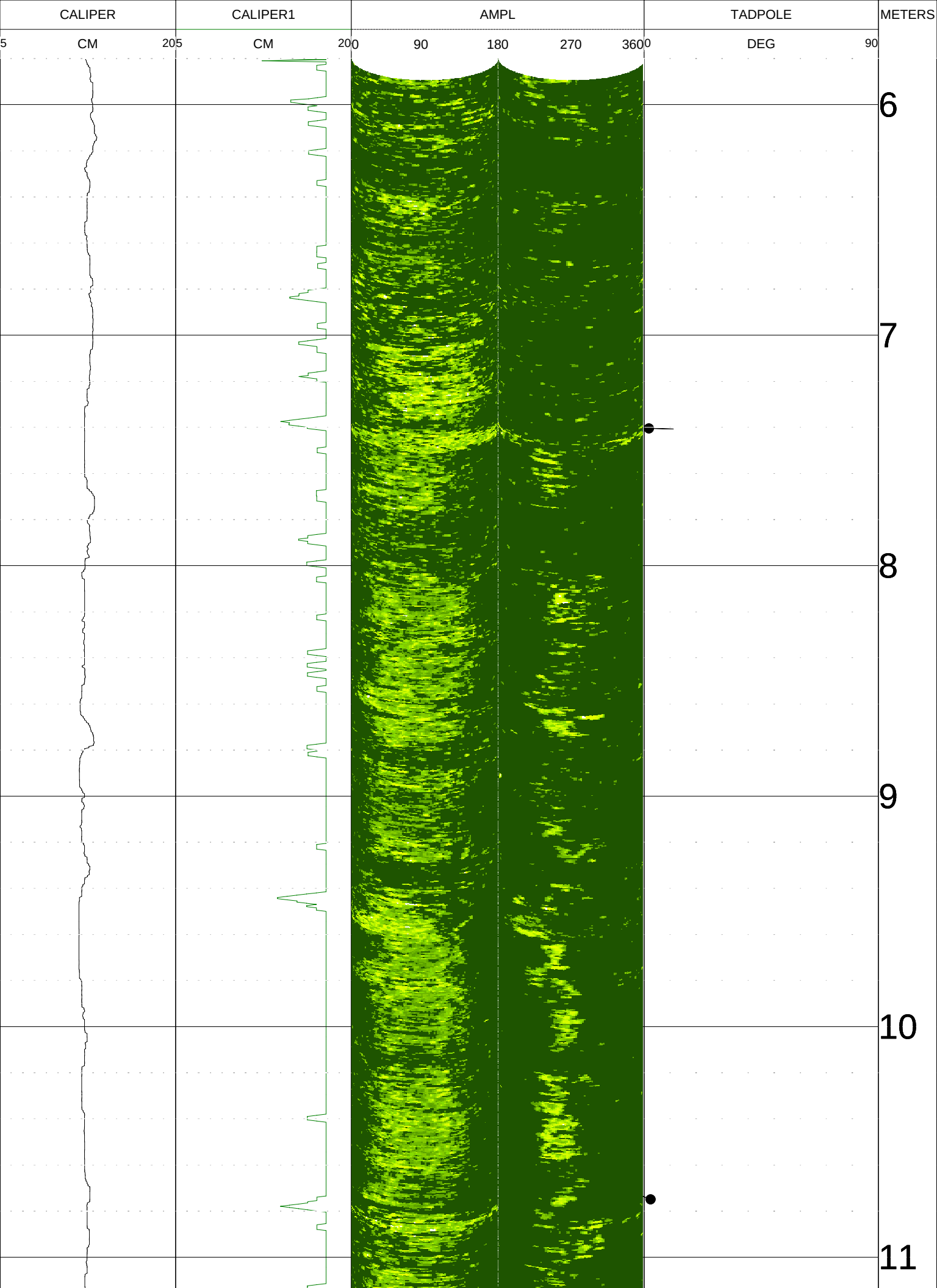
CALIPER
CALIPER1
AMPL
TADPOLE
METERS
5
CM
20
5
CM
20
0
90
180
270
360
0
DEG
90
6
7
8
9
10
11

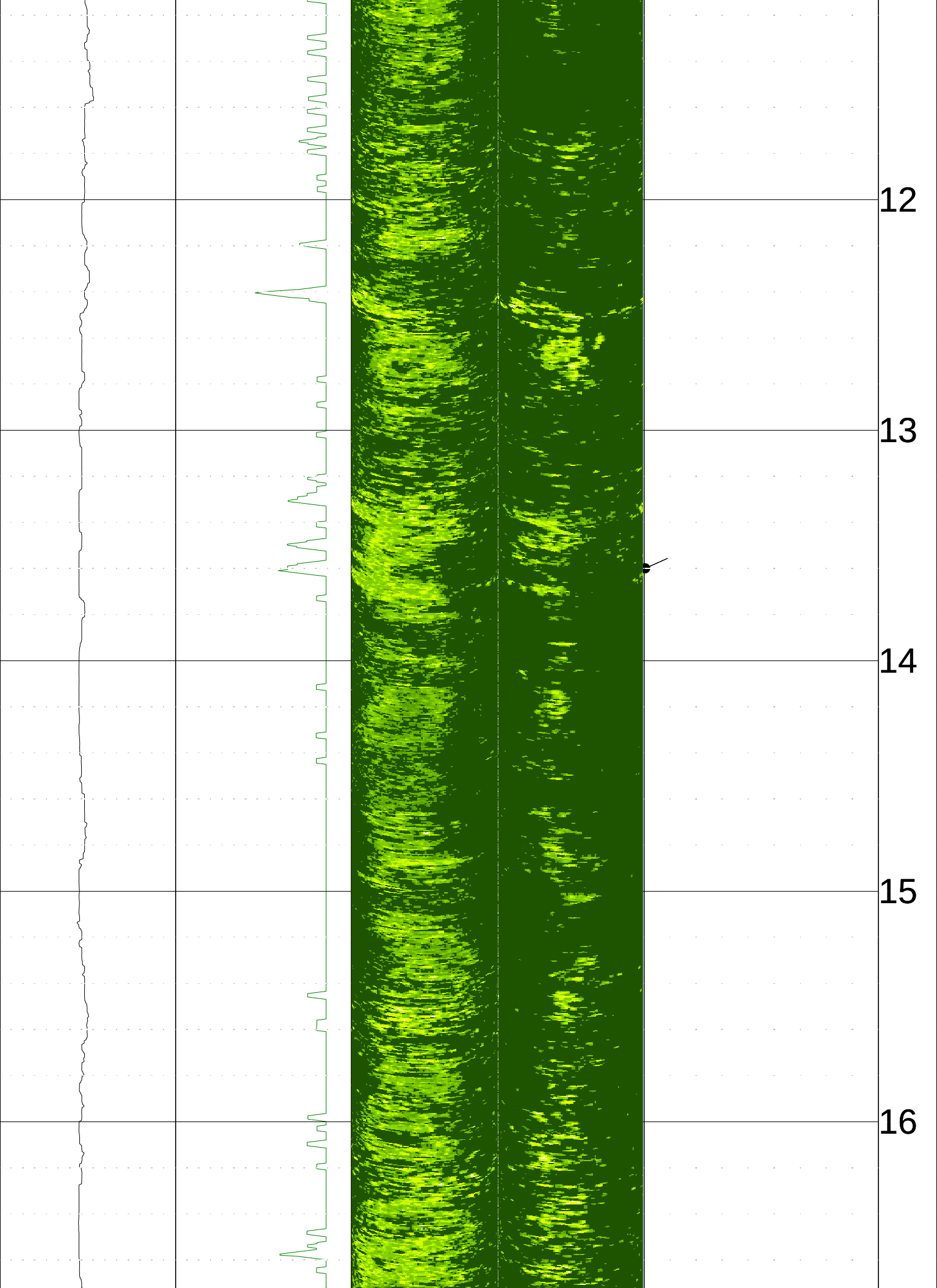
12
13
14
15
16

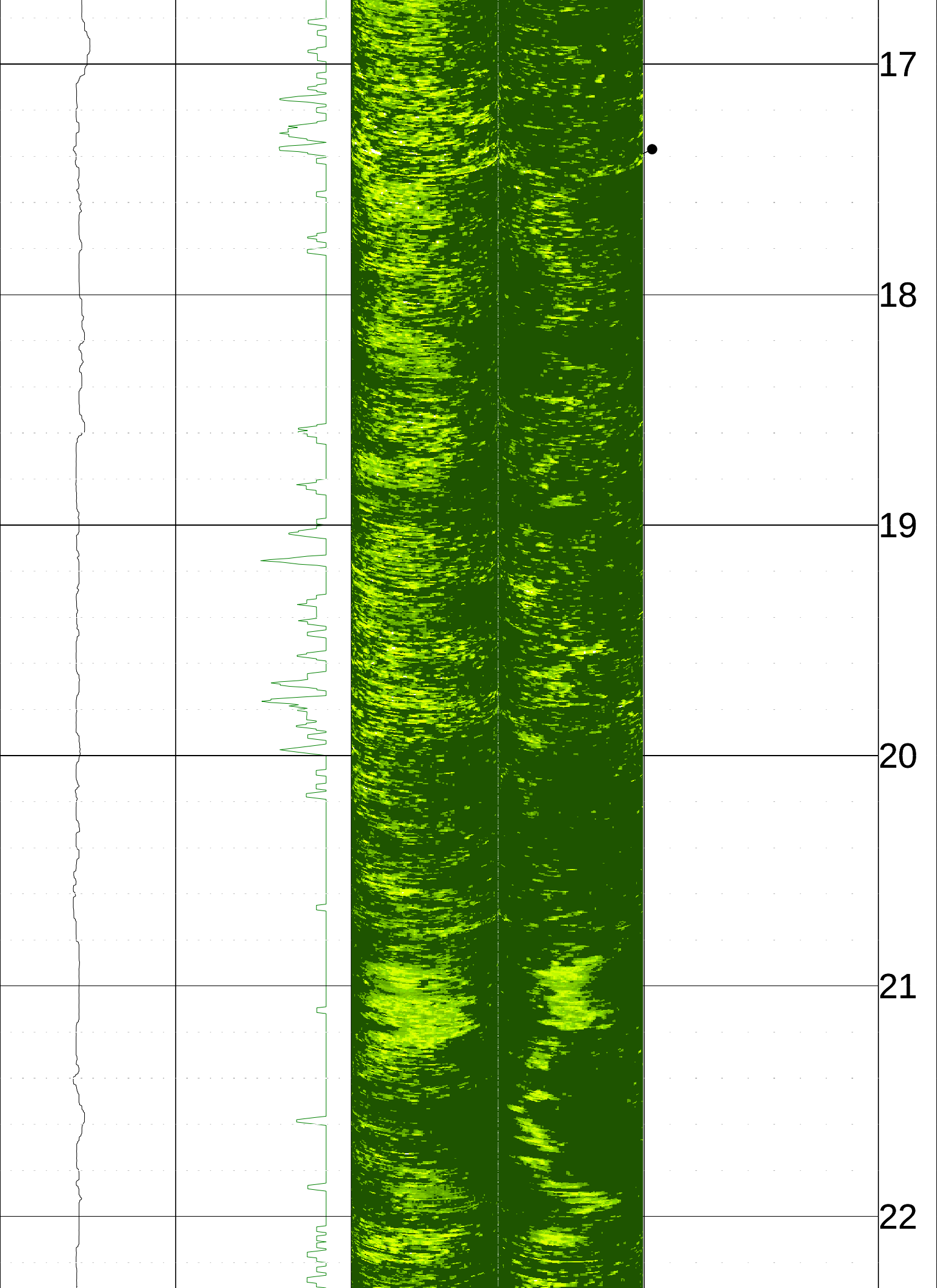
17
18
19
20
21
22

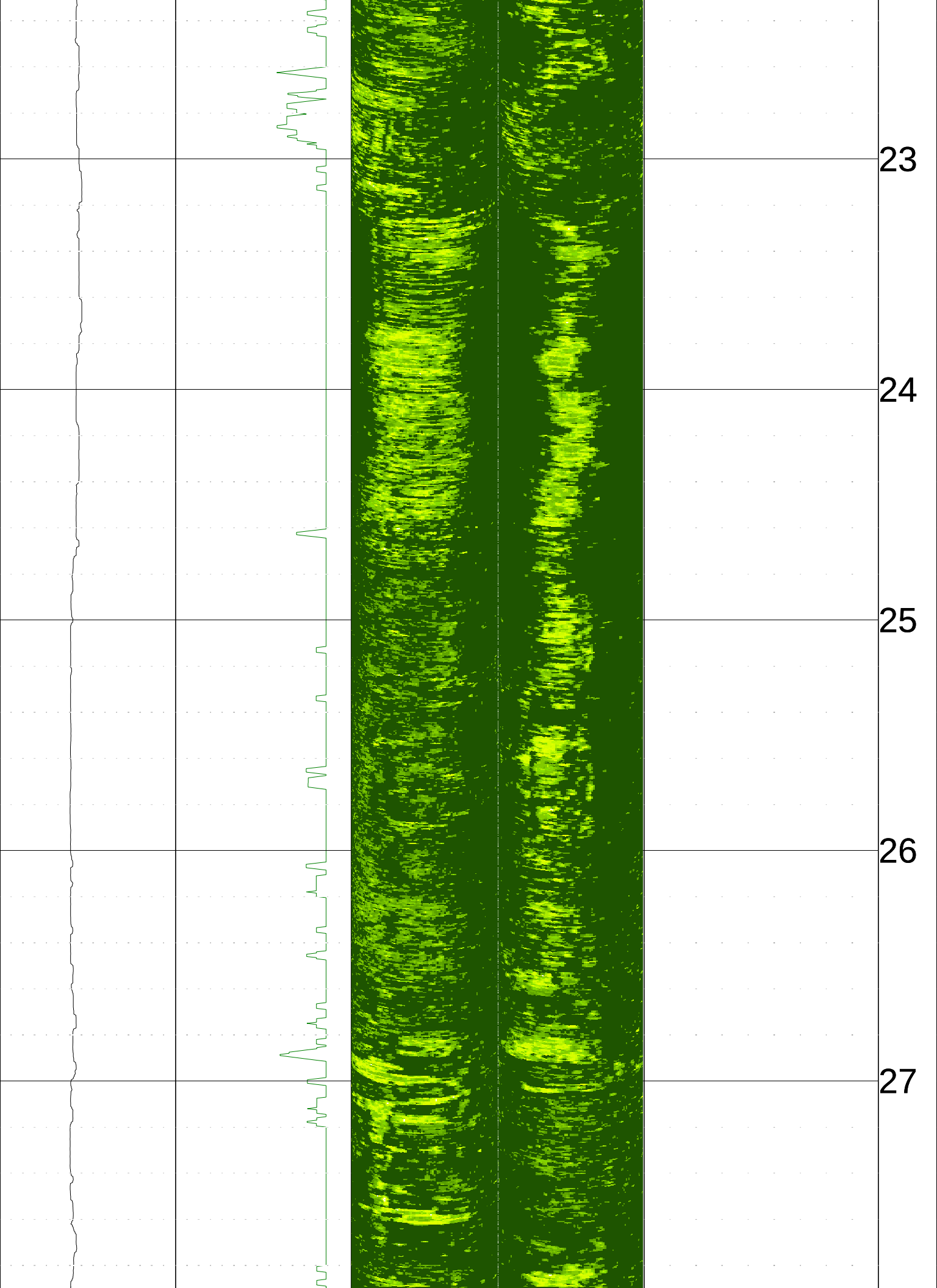
23
24
25
26
27

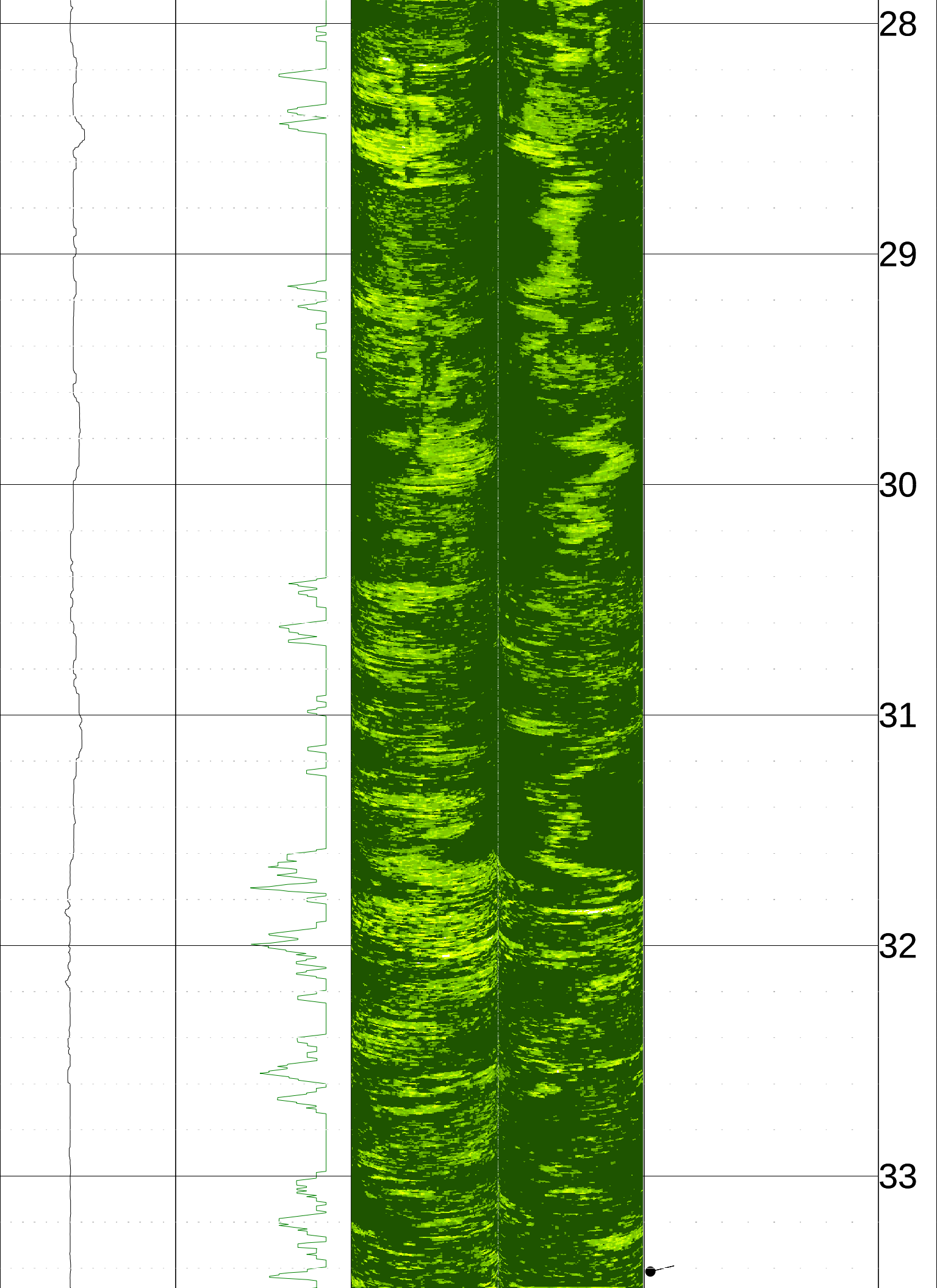
28
29
30
31
32
33

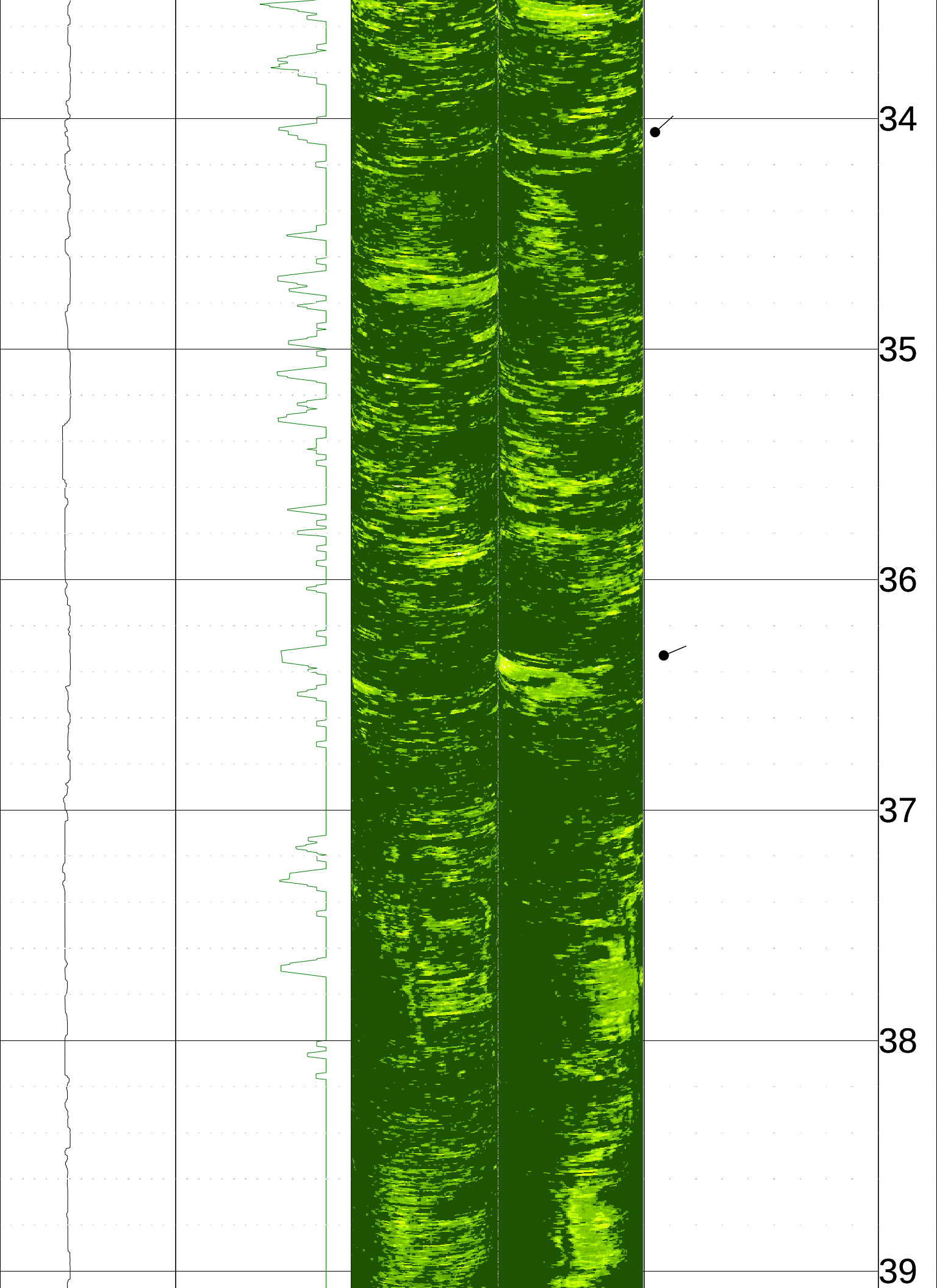
34
35
36
37
38
39

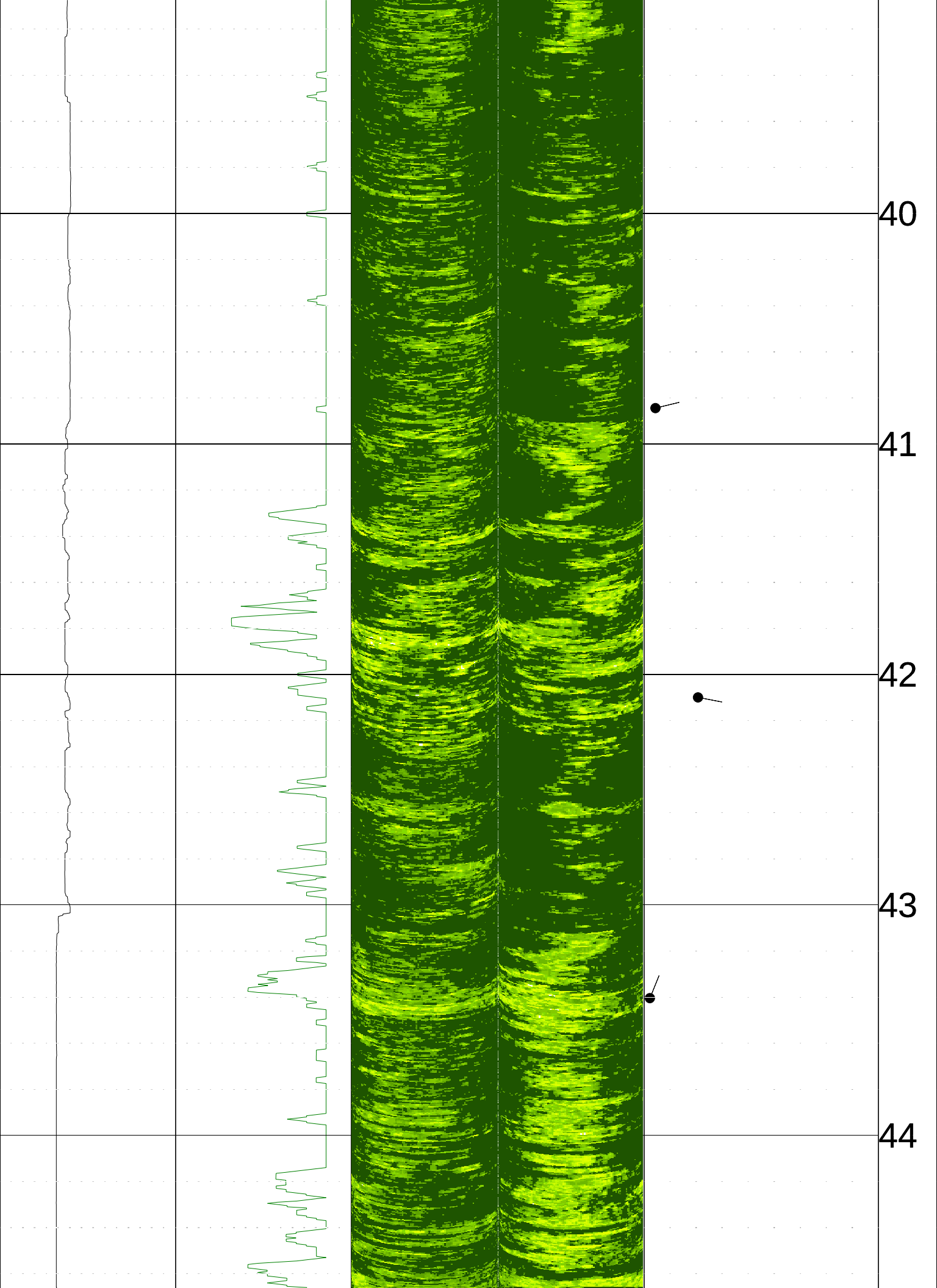
40
41
42
43
44

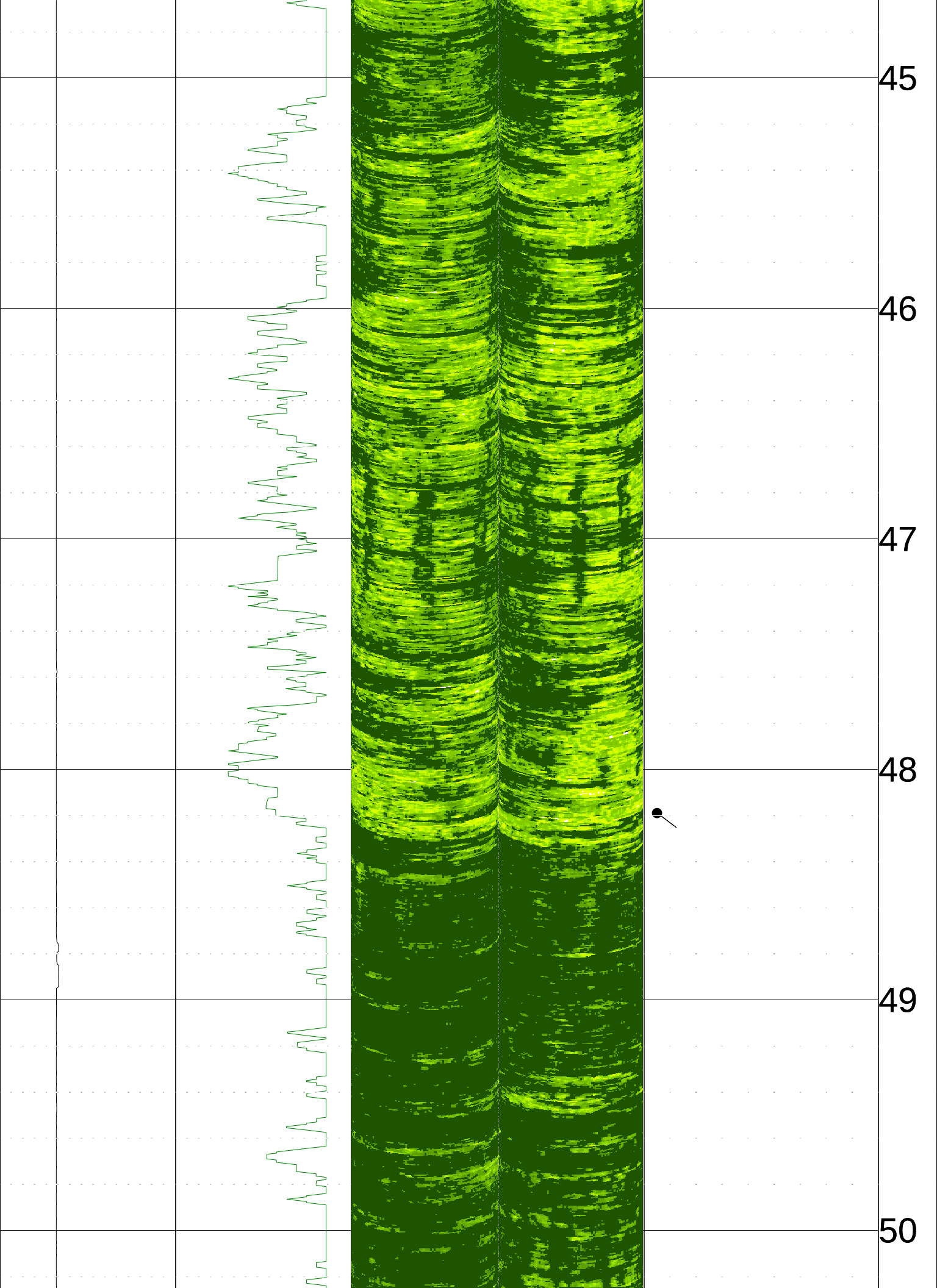
45
46
47
48
49
50

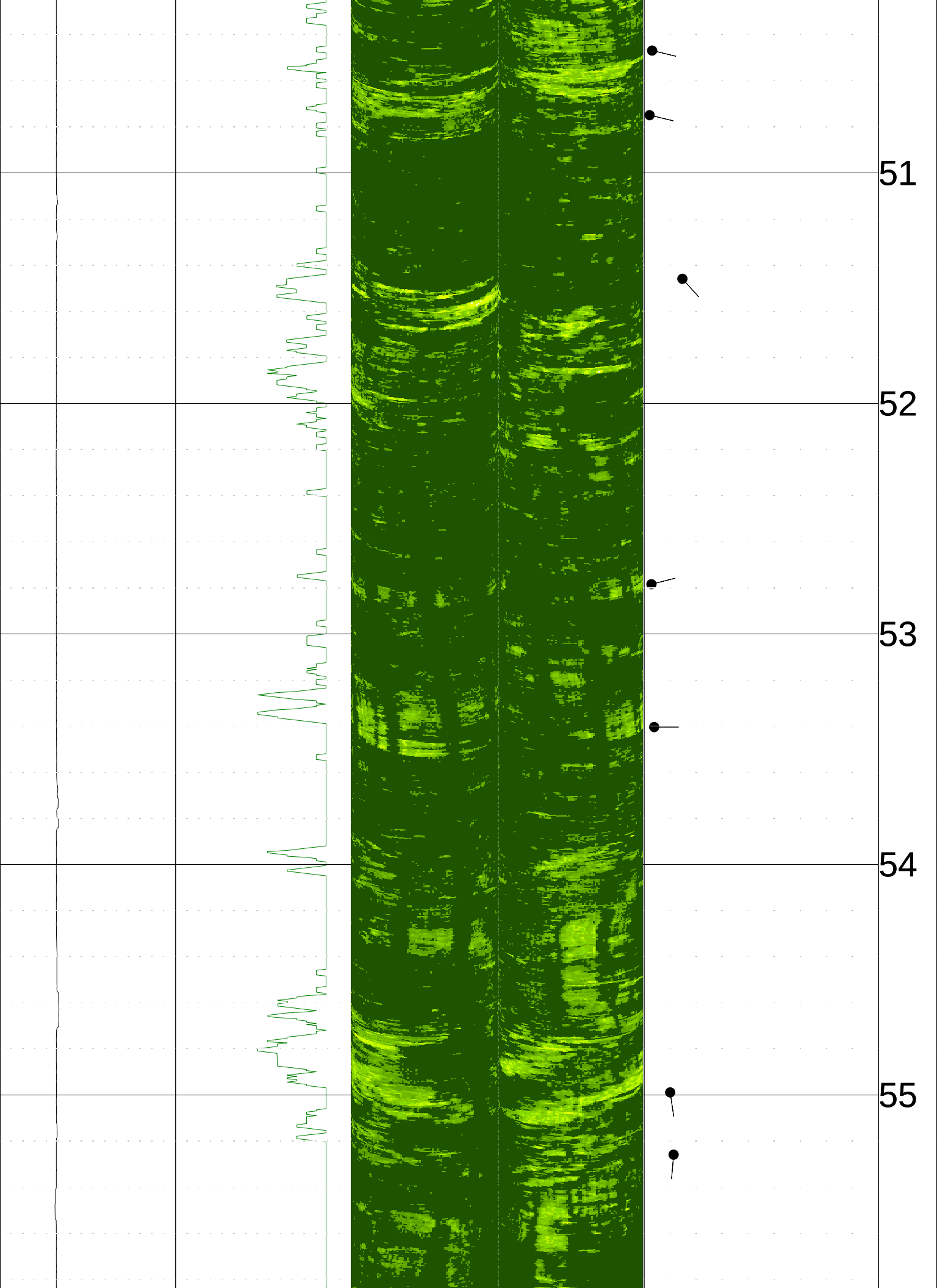
51
52
53
54
55

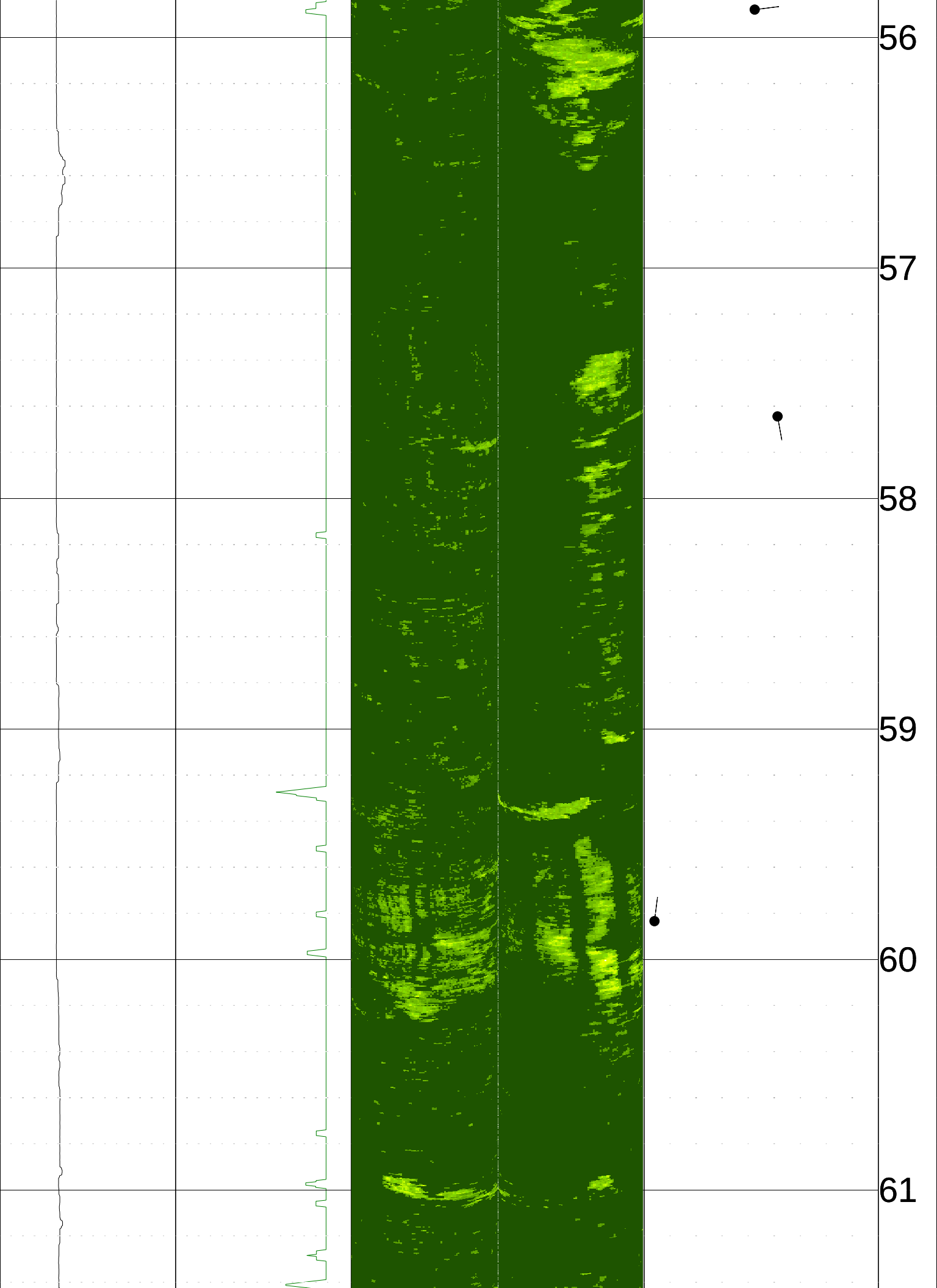
56
57
58
59
60
61

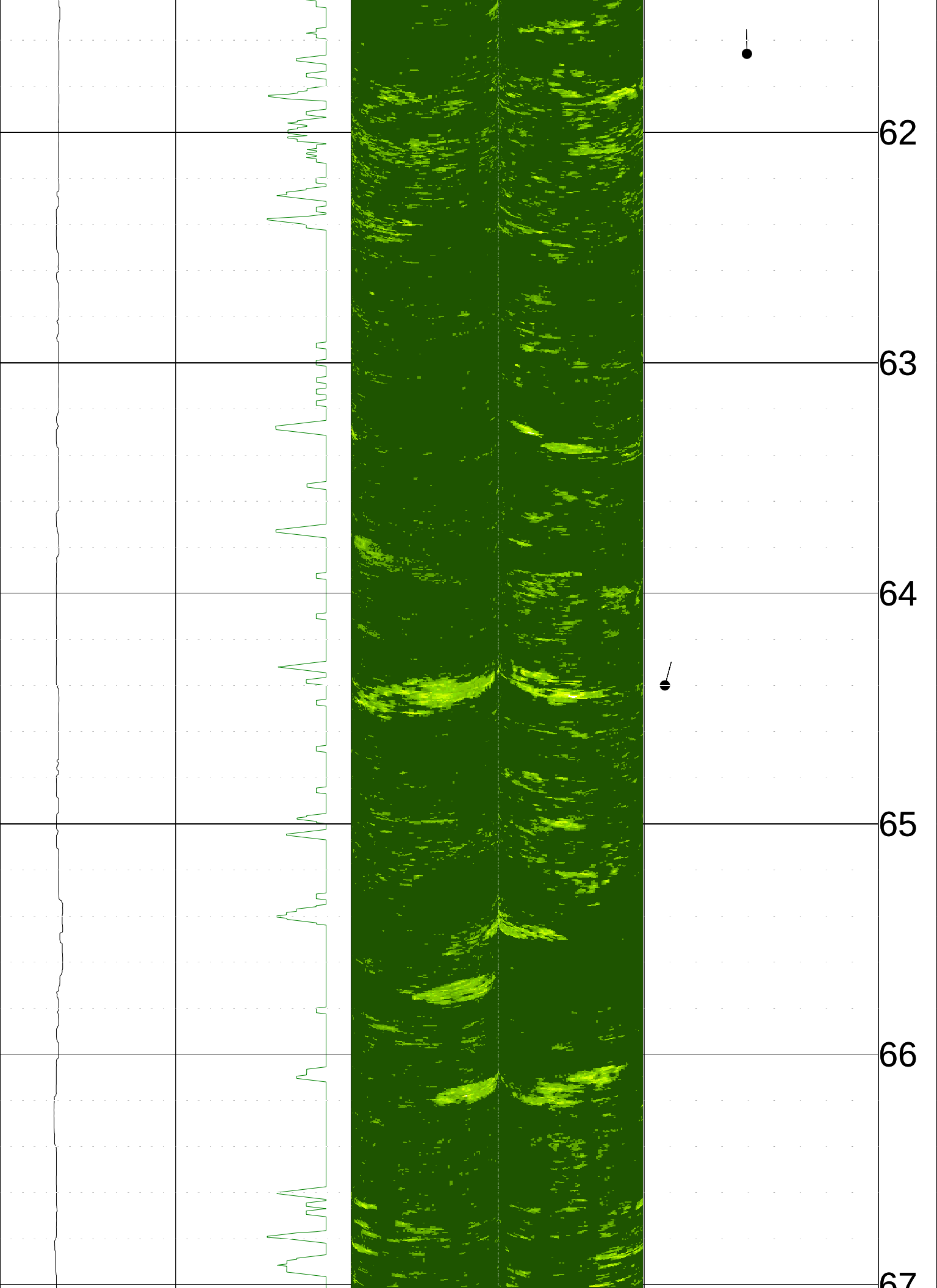
62
63
64
65
66
67

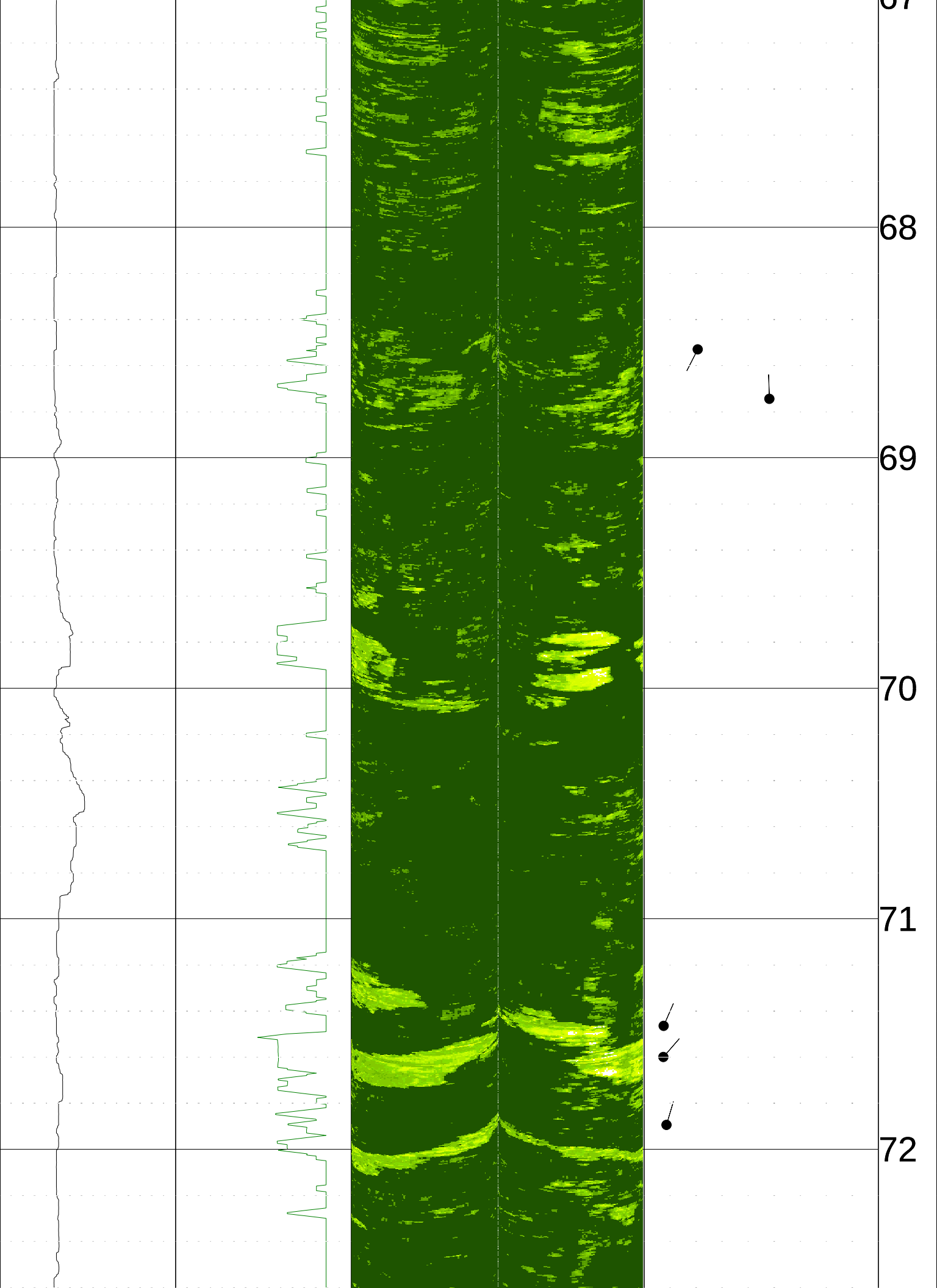
68
69
70
71
72

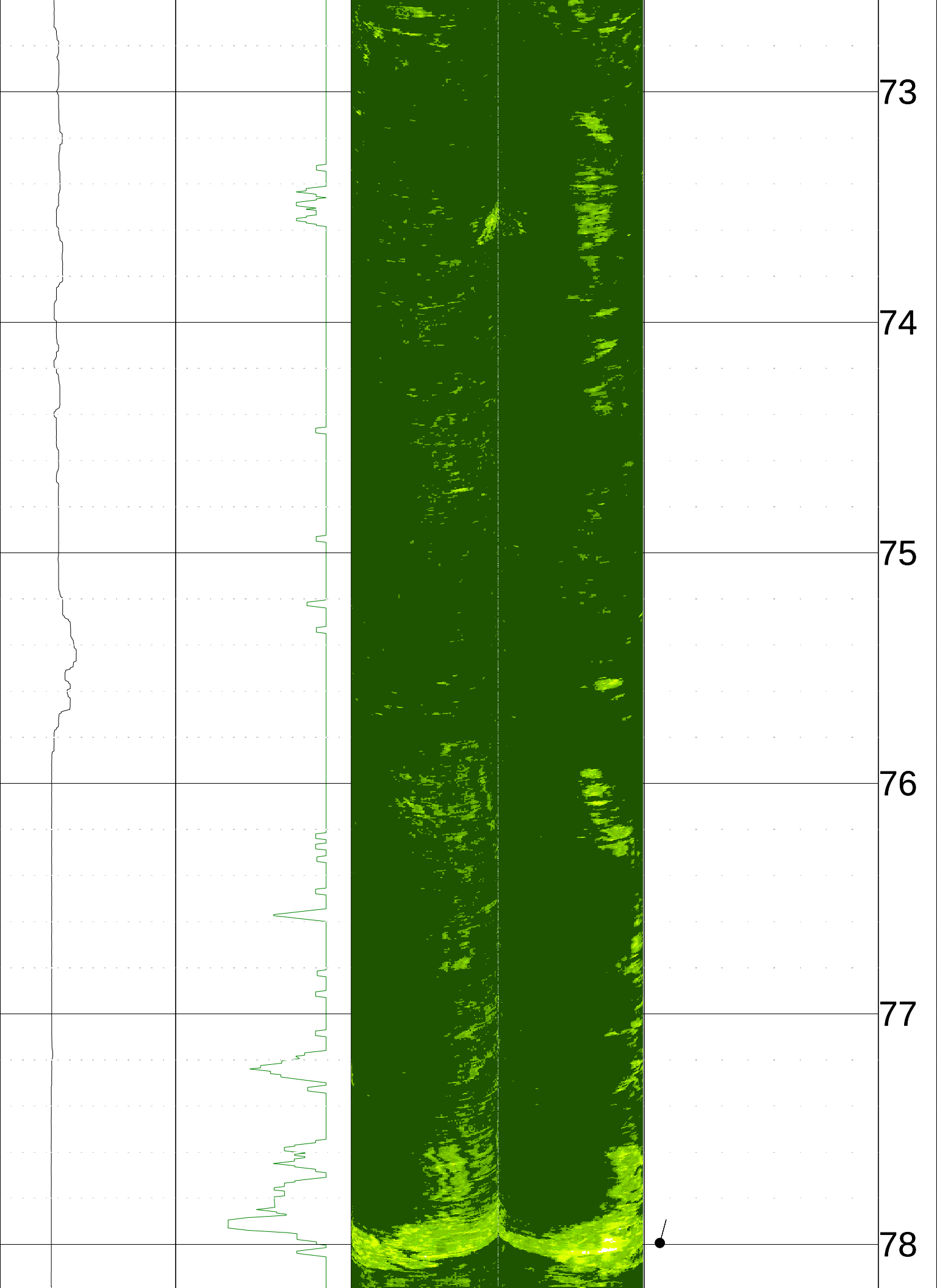
73
74
75
76
77
78

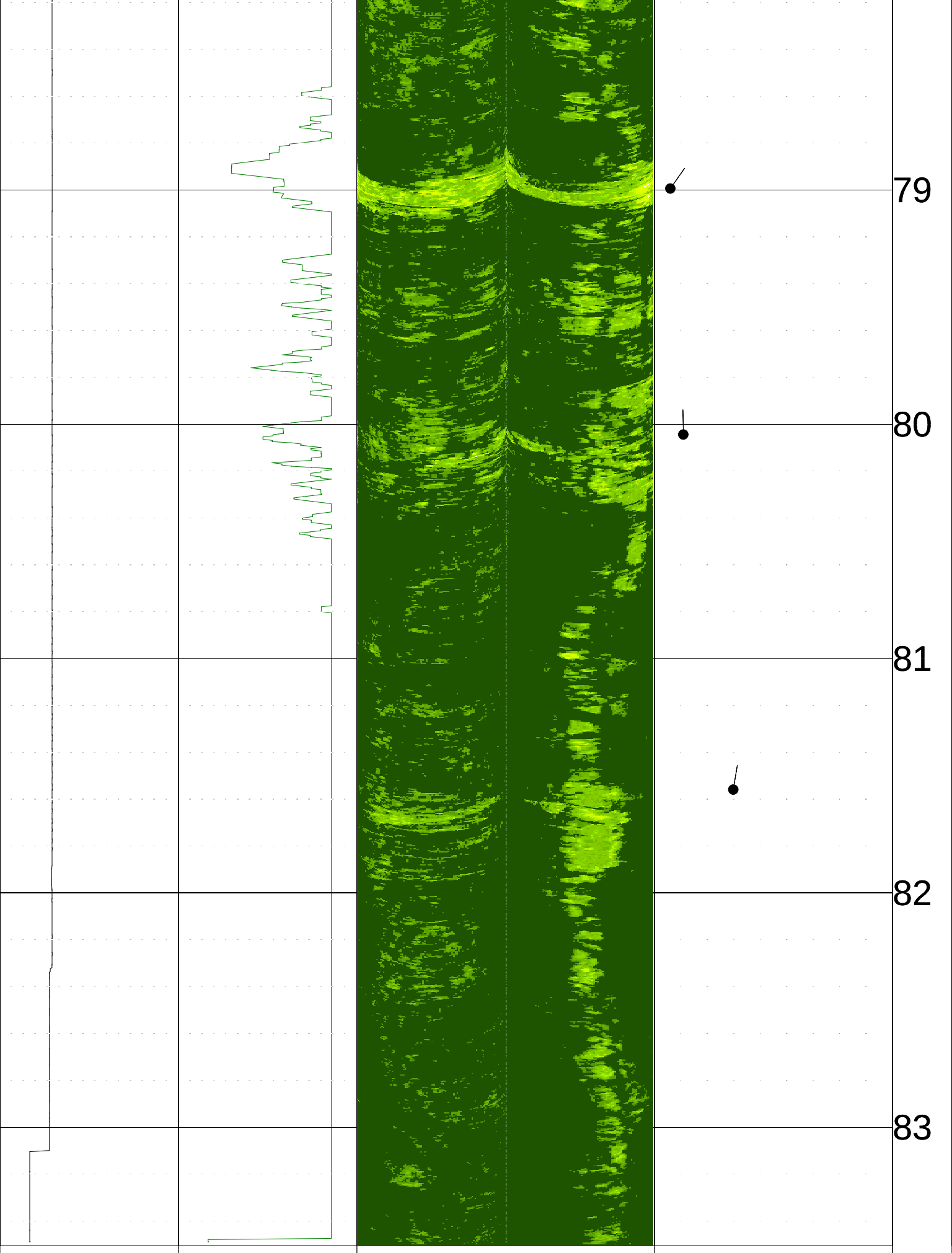
79
80
81
82
83
5
CM
20
5
CM
20
0
90
180
270
360
0
DEG
90
CALIPER
CALIPER1
AMPL
TADPOLE
METERS

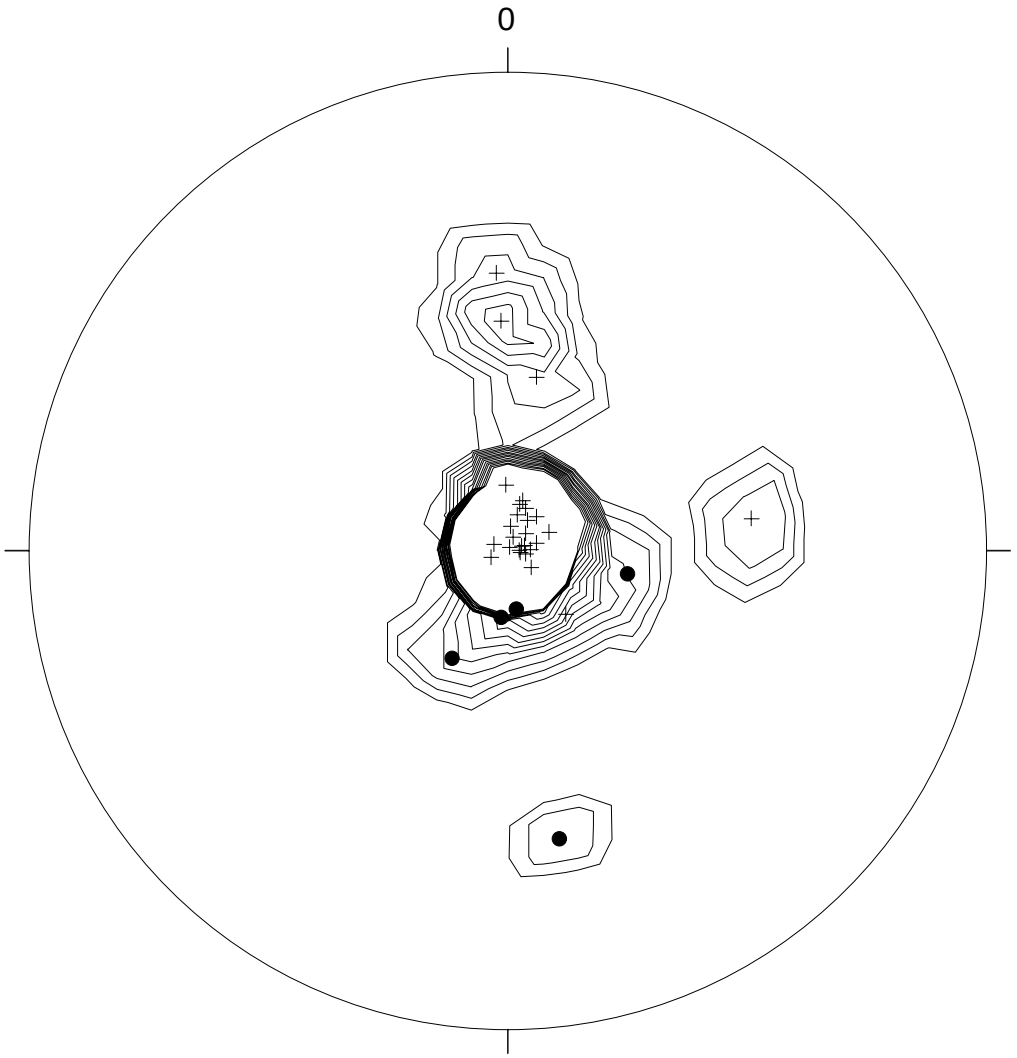


+ n=27 (P)
• n=5 (P)

LA 710 Tunnel, boring Z3 B11

Stereonet contour plot of poles to planes,
Both bedding and fractures

n=32
max. dens.= 77.95 (at 180/ 90)
min. dens.=0.00
Contours at every integer between
1 and 15, inclusive:
(Multiples of random distribution)

Apparent bedding denoted as cross
Apparent fractures denoted as solid circle
Plotted on upper hemisphere

APPENDIX B.1.2

# Seismic Reflection and Surface Wave Data

# Appendix B.1.2
# Seismic Reflection and Surface Wave Data

The following data reports were prepared for the SR 710 Tunnel Technical Study Final Geotechnical Summary Report (CH2M HILL, 2010). However, only data relevant to the SR 710 North Study are provided herein as summarized in Tables B-1 and B-2. The full version of the following appendix is presented in the Technical Study (CH2M HILL, 2010).

TABLE B-1
**Summary of Seismic Reflection Testing**

| Seismic Reflection Line | Approximate Location | City | Purpose/Feature Evaluated |
|---|---|---|---|
| Z3-G1 | South Raymond Avenue (N/O E. Glenarm Street) | Pasadena | San Rafael Fault |
| Z3-G6 | Winchester Avenue (N/O Concord Avenue) | Alhambra | Highland Park Fault |
| Z3-G7 | Westmont Drive (S/O, Valley Boulevard) | Alhambra | Unnamed Fault |
| Z4-G2 | Huntington Drive (SW/O N. Granada Avenue) | Alhambra | Alhambra Wash Fault |
| Z5-G2 | East Shorb Street (E/O S. Hildalgo St.) | Alhambra | Alhambra Wash Fault |
| Z5-G3 | Edgewood Drive (S/O W. Valley Blvd.) | Alhambra | Highland Park Fault |

Source: CH2M HILL, 2010 (EA-07-187900)

TABLE B-2
**Summary of Multichannel Analyses of Surface Waves and ReMi Testing**

| Number | MASW Line | Approximate Location | City |
|---|---|---|---|
| 1 | Z1-S20 | Highbury Avenue (S/O Valley Boulevard) | Los Angeles |
| 2 | Z3-S2 | Palmetto Drive (E/O S. Pasadena Avenue) | Pasadena |
| 3 | Z3-S3 | S. Raymond Avenue, Along Seismic Line Z3-G1 | Pasadena |
| 4 | Z3-S4 | S. Raymond Avenue, Along Seismic Line Z3-G1 | Pasadena |
| 5 | Z3-S5 | Arlington Drive (W/O S. Pasadena Avenue) | Pasadena |
| 6 | Z3-S11 | Meridian Avenue at Buena Vista Street | South Pasadena |
| 7 | Z3-S12 | Brent Avenue at Hope Street | South Pasadena |
| 8 | Z3-S15 | Meridian Avenue (N/O Monterey Road) | South Pasadena |
| 9 | Z3-S16 | Marengo Avenue at Spruce Street | South Pasadena |
| 10 | Z3-S19 | Berkshire Avenue (N/O Kendall Avenue) | South Pasadena |
| 11 | Z3-S20 | Westmont Drive at Keats Street | Alhambra |
| 12 | Z3-S21 | Winchester Avenue, Along Seismic Line Z3-G6 | Alhambra |
| 13 | Z3-S22 | Winchester Avenue, Along Seismic Line Z3-G6 | Alhambra |
| 14 | Z3-S23 | Westmont Drive, Along Seismic Line Z3-G7 | Alhambra |
| 15 | Z3-S24 | Westmont Drive, Along Seismic Line Z3-G7 | Alhambra |
| 16 | Z4-S6 | E. Huntington Drive, Along Seismic Line Z4-G2 | Alhambra |
| 17 | Z4-S7 | E. Huntington Drive, Along Seismic Line Z4-G2 | Alhambra |
| 18 | Z4-S8 | W. McLean Street (NE/O N. Garfield Avenue) | Alhambra |
| 19 | Z4-S9 | N. Bushnell Avenue (N/O Larch Street) | Alhambra |
| 20 | Z4-S10 | S. Date Avenue (S/O W. Commonwealth Avenue) | Alhambra |
| 21 | Z5-S10 | W. Adams Avenue at S. 2nd Street | Alhambra |
| 22 | Z5-S11 | Benito Avenue (N/O W. Shorb Street) | Alhambra |
| 23 | Z5-S12 | Edgewood Drive, Along Seismic Line Z5-G3 | Alhambra |
| 24 | Z5-S13 | Edgewood Drive, Along Seismic Line Z5-G3 | Alhambra |

Source: CH2M HILL, 2010 (EA-07-187900)

GEOVision
geophysical services

# REPORT

# HIGH RESOLUTION SEISMIC REFLECTION SURVEY

## SR-710 Tunnel Technical Study
## Los Angeles County, California

***Prepared for***

**CH2M HILL**
**6 Hutton Centre Drive, # 700**
**Santa Ana, CA 92707**

***Prepared by***

**GEOVision Geophysical Services**
**1124 Olympic Drive**
**Corona, California 92881**
**(951) 549-1234**

**Report 9001-02**

**October 5, 2009**

# TABLE OF CONTENTS

# LIST OF TABLES



# LIST OF FIGURES

# 1 INTRODUCTION

A high-resolution, compressional (P) wave seismic reflection survey was conducted at various sites within the SR-710 Tunnel Study Area, located in Los Angeles County, California. The surveys were conducted from January 13, 2009 to March 24, 2009. The purpose of the seismic reflection survey was to locate geologic structures potentially associated with faulting at each site.

Seventeen (17) seismic reflection lines were located strategically throughout five (5) tunnel study zones, labeled Zones 1 to 5 (Figure 1). The seismic investigation consisted of three (3) seismic lines in Zone 1 (Z1-G3 to Z1-G5), 3 seismic lines in Zone 2 (Z1-G1 to Z2-G3), 7 seismic lines in Zone 3 (Z3-G1 to Z3-G7), 2 seismic lines in Zone 4 (Z4-G1 and Z4-G2), and 2 seismic lines in Zone 5 (Z5-G2 and Z5-G3). The length of the seismic reflection lines ranged from 1,195 to 3,832 feet.

This report contains the results of the seismic reflection investigation conducted at the site. An overview of the seismic reflection method is given in Section 2. Equipment and field procedures are discussed in Section 3. Data processing is discussed in Section 4. Interpretation is presented in Section 5. References and our professional certification are presented in Sections 6 and 7, respectively.

# 2 SEISMIC REFLECTION BACKGROUND

Seismic reflection profiling is a standard subsurface mapping technique employed by the oil and gas exploration industry. The use of this reflection technique in shallow engineering projects has been a relatively recent development, as the formerly high production costs and serious computing requirements were prohibitive. Advances in microelectronics have led to engineering seismographs and PC-based processing that now permit the cost-effective use of reflection seismic methods in a wide variety of applications (Steeples & Miller, 1988).

Details of the general seismic reflection technique can be found in many comprehensive texts, such as Sheriff and Geldart (1995); and, therefore, only a brief synopsis of the technique is included in this report. The seismic reflection method involves projecting a wave down from the surface, and then recording the returning wave back at the surface as it reflects off formations at depth. Seismic energy will also be reflected, refracted, and diffracted at boundaries in the subsurface, in accordance with Snell's Law (Figure 2). The main design consideration for a successful seismic reflection survey is the ability to separate the reflected energy from other arrivals in processing.

Seismic reflection occurs when an acoustic wave front encounters an impedance boundary in the subsurface. Seismic impedance depends on both the velocity and density of the rock, and impedance boundaries occur where these rock properties change abruptly, usually due to changes in lithology. The reflection coefficient, R, across an interface, is expressed by a function relating the acoustic impedance of adjacent layers. R determines the relative amplitude of the reflected wavelet.

$$\mathbf{R} = \frac{\boldsymbol{\sigma}_2 \mathbf{V}_2 - \boldsymbol{\sigma}_1 \mathbf{V}_1}{\boldsymbol{\sigma}_2 \mathbf{V}_2 + \boldsymbol{\sigma}_1 \mathbf{V}_1}$$

where, R = reflection coefficient,

$\sigma_1$, $\sigma_2$ = mass density of the material on each side of the interface, and

$V_1$, $V_2$ = shear wave velocity on each side of the interface.

The sign of the reflection coefficient determines the polarity of the reflected wave. The magnitude of the reflection coefficient is critical to obtaining usable data. The seismic reflection technique will not work if the acoustic contrast is not sufficient to produce a clear reflection, regardless of the survey parameters or processing techniques employed. The ability of the seismic reflection method to detect an individual sedimentary bed is not only a function of the acoustic impedance at the top and bottom of the bed, but also depends on the layer thickness. The minimum resolvable bed thickness is often quoted as 1/4 to 1/8 of the wavelength at the target depth. Wavelength is inversely proportional to frequency.

When a reflecting boundary exists, it is important to optimize the field procedure and acquisition parameters to maximize the quality of the final processed data. Choosing the best field parameters involves determining the relative importance of several competing objectives, such as site constraints, equipment capabilities, and processing needs.

In all geophysical surveys, the objective is to extract the usable data (i.e., in this case, reflections from various lithologic boundaries) from the unwanted background information (source generated and ambient noise). In reflection seismology, it is desirable to record high frequency, high signal-to-noise ratio reflection events from the boundary of interest. The frequency of a reflection event is largely determined by the source input frequency and the filtering effect of the ground. Often, the target reflector frequency is similar to that commonly recorded for coherent noise (in particular, the noise from ground roll), making it difficult or impossible to selectively filter out the noise. Isolation of the reflection events requires careful design of field acquisition parameters, such as the source/receiver geometry, choice of source and receiver types, as well as recording parameters, such as sampling rate and filter settings.

The seismic reflection technique can be divided into two categories based on the type of source used. Compressional (P) waves, propagate through the earth as a change in pressure, and are the same as the sound waves we hear. Particle motion for P-waves is parallel with the direction of propagation of the wave. Shear (S) waves propagate through the earth by shearing adjacent particles. Particle motion in S-waves is perpendicular to the direction of wave propagation.

The frequency content of seismic reflection data is a function of both the energy source and the earth through which the energy travels. Vibratory sources have control of the frequency input to the ground, unlike impulsive sources such as a hammer or explosive. With a vibratory source the frequency input into the ground is a function of the beginning and ending frequencies of the sweep, the length of the sweep and ground coupling. The second factor is the transmission and attenuation of various frequency components in the subsurface, often termed the “earth response”. In general, there are two primary objectives in designing a sweep for high-resolution reflection surveys:

1. To record useful seismic signals at the geophones with as high a frequency as possible.
2. To start the low end of the sweep such that the appropriate depth of penetration is achieved without generating intolerable ground roll.

# 3 PROCEDURES

## 3.1 Seismic Equipment

Key equipment used to collect the high resolution seismic reflection data as shown in Figure 3 included:

- Oyo DAS-1 Seismograph (144 channel system) coupled to a computer with SEISNET acquisition software
- Input/Output Inc. RLS240M roll box
- IVI EnviroVibe energy source
- Oyo Geospace 28 Hz vertical geophones
- Seismic cables and jumper cables

The Oyo DAS-1 Seismograph (DAS) is a 24-bit, 48-channel seismic acquisition system. During this investigation the DAS was coupled to two 48-channel expansion modules to obtain 144-channel recording capability. Coupling the DAS to a computer with the SEISNET seismic acquisition software allows for real-time correlation of the seismic records, filtering, display and printing of shot records and writing of data to CD-ROM.

For this project, an IVI EnviroVibe (Figure 3) was used as the P-wave energy source. Vibratory sources function by oscillating a mass through a user-defined range of frequencies, which are transmitted into the ground. This is known as a "sweep." At the instant the vibrator begins its sweep, the seismograph begins recording the signals received from the geophones. Simultaneously, the sweep being produced by the vibrator is recorded on an auxiliary channel within the seismograph. The seismic record is obtained by cross correlating the recorded signals from the geophones with the known sweep generated by the vibrator.

## 3.2 Site Preparation

The end points, bends and nominal 300 ft intervals of each seismic line were marked using a Nikon total station system. The appropriate group interval (station/geophone spacing) was then marked using a fiberglass tape measure and surveyors paint with typically every $10^{th}$ station labeled for reference during data acquisition. The first station was labeled as station 101 with proceeding stations sequentially numbered along the profile. Group intervals of 5 to 8 ft were used for the P-wave reflection data acquisition. The endpoints and inflection points of each line were surveyed using a Trimble ProXRS GPS system with OmniStar submeter differential corrections. The locations of the seismic lines are summarized in Table 1. Relative elevation profiles for each line were surveyed using a Nikon total station system and converted to elevation using the GPS control (accurate to about 2 meters) at the ends of the line. Geophones were hot glued to the asphalt/concrete surface at the appropriate group interval and cabled into the seismograph. Seismic equipment was then set up for parameter testing and data acquisition as discussed in following sections.

## 3.3 Parameter Testing

Source parameter testing was carried out prior to the respective data acquisition. The receiver interval and geophone array (single geophone) had been determined before the start of the survey. Sweeps of varying frequency bandwidths were recorded into a full (144 trace) off-end or split spread configuration in an effort to bracket the usable frequencies returning to the geophones from the subsurface. The initial testing, aided by frequency filtering in the recording instruments, determined that a sweep range of 20-240 Hz or 20-200 Hz achieved the objectives of broad bandwidth, good depth of penetration and minimal ground roll generation for the P-wave reflection surveys.

With the frequency range selected, the duration and number of sweeps necessary to produce good signal-to-noise content on the shot records remained to be determined. After testing various combinations, it was determined that four, 8 second sweeps provided sufficient energy to overcome ambient noise levels, if at all possible, at the site and satisfy the data acquisition schedule. Longer sweep lengths and additional stacking did not appear to improve signal content on the shot records.

## 3.4 Data Acquisition Parameters

Generalized data acquisition parameters are summarized in Table 2. Specific data acquisition parameters for each seismic line including shot spacing, group interval (geophone spacing), minimum and maximum shot offset, spread geometry, sweep frequency and length and listen time are listed in Table 3.

## 3.5 Data Acquisition Procedures

At the start of data acquisition, the source was positioned between the appropriate receiver stations. The IVI EnviroVib communicated with the seismograph by radio link. When the operator pushed the trigger button in the recording truck, a signal was sent to the vibrator to start the sweep sequence, and the OYO DAS-1 seismograph began recording. During the sweep, a synthetic pilot trace was generated by the vibrator and sent to the seismograph. This pilot sweep is recorded on auxiliary channel 1 for correlation with the recorded data from the geophones. Data was transmitted from the seismograph to a computer where seismic acquisition software was used to correlate data, display data, print selected records, and write data to DVD.

At the beginning of the line an uncorrelated sweep was viewed either on the computer screen or on hardcopy. This provided a check to ensure that the vibrator was operating properly, and that the seismograph was being triggered correctly. Array parameters were checked (i.e., source location, sweep configuration, receiver spacing, etc.) as were all connections. The noise monitor on the seismograph was checked to identify any ambient noise problems and to isolate and correct any noisy or dead receiver channels. The noise monitor was also used to confirm the correct setting on the roll box by lightly tapping the first and last active phone.

P-wave seismic reflection data were acquired using a 5 to 8 ft geophone (group) spacing depending on spatial limitations. Seismic lines were oriented as shown in Figure 1. Conventionally, the first geophone was assigned a station number of 101 (0 ft position). Station numbers are converted to distance along the line by subtracting 101 from the station number and multiplying by the group interval (geophone spacing). Seismic lines were started with the source

located at station 100.5 (half a station/geophone spacing behind the first geophone on the line) and, therefore, the first shot had 0 channels live behind and 144 channels live in front of the vibrator. The vibrator was then "walked" into the line at 1-station increments recording the first 144 stations until there was the desired number of channels behind and in front of the source. Spread geometry for each line is summarized in Table 3. As an example, an asymmetric 48/96 split spread has 48 channels (geophones) behind and 96 channels in front of the source. Once the vibrator was located in the appropriate position, the survey was run in a symmetric or asymmetric split spread configuration. With a split spread, the live channels and vibrator were moved forward at 1-station increments, keeping the vibrator at the center of the active spread until the last live channel was reached. Once the last live channel of the line was reached, the vibrator was "walked" off the spread, in the reverse process to the start of the line. Typically, the last source location had all 144 channels behind the vibrator.

# 4 DATA PROCESSING

The seismic reflection data were processed by Sterling Seismic Services of Denver, Colorado. The processing flow for the data is based on a standard common mid point (CMP) reflection processing sequence with modifications for specific conditions at the survey site. Table 4 shows generalized processing sequence steps leading to the final stacks used for interpretation for the P-wave reflection data.

The seismic section resulting from processing sequences 1 to 16 in Table 4 is referred to as the Final Stack. Additional post processing steps consisting of application of a frequency wavenumber (FX) predictive enhancement filter and spectral balancing over the 40 to 240 Hz frequency range were applied to the seismic sections. These seismic sections were used for interpretation after automatic gain control and application of a 10-20-125-175 Hz band pass filter was completed.

# 5 INTERPRETATION

## *5.1 Overview and Depth Control*

The processed P-wave seismic sections without and with interpretation for the seventeen (17) seismic reflection profiles (Z1-G3 to Z1-G5, Z2-G1 to Z2-G3, Z3-G1 to Z3-G7, Z4-G1 to Z4-G2 and Z5-G2 to Z5-G3) acquired during this investigation are presented in Figures 5 to 38. These figures represent the P-wave seismic reflection data in a trace amplitude format with a band pass filter applied. The trace amplitude format displays the relative signal strength as energy is reflected from various subsurface features using either a color or gray scale display. The seismic sections included herein are displayed using a gray scale color bar with the white and black representing the highest amplitude negative and positive polarity reflections, respectively. The figures are presented with time in seconds on the vertical axis and distance in feet on the horizontal axis. Generally, the seismic images are presented at a scale with only minor estimated vertical exaggeration. A ground surface reference is added to the figures and corresponds to the top of the seismic image, except for Line Z1-G3 where a floating elevation datum was used during processing because of a large bend in the line.

A seismic workstation equipped with either the Seismic Microtechnology, Inc. 2-D interpretation package or SeiSee SEG-Y file viewing package was used for final display of the data. Typical applications of the seismic interpretation packages include: filtering, color display of seismic data, attribute calculation, digital picking (logging) of seismic event travel times, GIS mapping of seismic data, fault tracking and gain functions.

Because the primary purpose of this investigation was to locate potential faults, conversion of the seismic sections from time to depth was not required. However, a rudimentary depth scale was desired to permit identification of potential reflectors (i.e. water table versus top of bedrock). With the exception of seismic lines Z3-G1 and Z3-G3, borehole velocity data were not available to convert the time-sections to approximate depth. Even with borehole control, only rudimentary and approximate depth conversion would be possible in this geologic environment because geologic units are steeply dipping in many areas and, therefore, significant lateral velocity variation may be common. Additionally, a variable water table depth beneath a seismic line would also have a significant impact on depth.

Without borehole control, estimates of depth to groundwater and the P-wave velocity of unsaturated and saturated sediments is necessary to place a rudimentary depth scale on the seismic images. The only available geophysical data to estimate P-wave velocity structure consisted of the seismic reflection shot records and multichannel analysis of surface waves (MASW) soundings located near the ends of the seismic lines. Approximate depth to groundwater was estimated by simple, two or three layer seismic refraction analysis of surface wave seismic records and/or seismic reflection records. The surface wave sounding profiles were generally long enough to estimate depth to groundwater if shallower than 13 m (43 ft). The seismic reflection shot records were long enough to estimate depth to groundwater if shallower than 70 m (230 ft). Ground water depths estimated using this approach are probably only accurate to about 25% of depth because interpretation of unsaturated sediment P-wave velocity was complicated by high velocity asphalt first arrival data. Estimated groundwater depths for each seismic line are summarized in Table 5. Surface wave soundings were conducted near the

ends of the seismic lines to develop S-wave velocity models to depths of 200 ft (60m), or more. To use these S-wave velocity models to develop approximate depth scales on the P-wave seismic sections it was necessary to determine an approximate relationship between P- and S-wave velocities. In the unsaturated zone, P-wave velocity was assumed to be twice the S-wave velocity (Poisson's ratio of 0.33), a reasonable assumption. Borehole velocity logs from 23 boreholes collected as part of this investigation and reported separately were used to develop an approximate relationship between S-wave velocity (Vs) and P-wave velocity (Vp) of the saturated sediments and rock. Figure 4 is a plot of over 3,500 Vs-Vp measurements made in saturated sediments and rock as part of the borehole geophysical logging program. A linear trend was fit to these measurements and used to relate S-wave velocity of saturated sediments derived from surface wave modeling to P-wave velocity. Depths on the seismic sections will be overestimated if the depth to the saturated zone is underestimated or if the saturated zone identified in the refraction survey is a perched water-bearing zone with lower-velocity, unsaturated sediments below. If the water table depth is underestimated by 10 ft (3 m) then the depth to underlying geologic structures could be overestimated by depths of 30 ft (10m), or more.

Geophysical data used for depth control are summarized in Table 5. Seismic lines Z3-G1 and Z3-G3 used borehole velocity logs from Z3-B4 and Z3-B7, respectively, for depth control. The remaining seismic lines used the S-wave velocity models derived from surface wave soundings, modeled approximate groundwater depth, and the Vs-Vp function for saturated sediments and rock derived from all available borehole velocity logs to estimate depth control. Estimated depths were extrapolated to 600 ft assuming a constant P-wave velocity below the maximum depth of the surface wave model or borehole velocity log. Table 3 also contains the bedrock formation expected to be encountered in the vicinity of each seismic line.

Surface wave soundings conducted near the ends of each seismic line, and reported separately, were used to determine if a significant lateral velocity variation occurred along each seismic line. Surface wave soundings, however, were not able to determine if the water table depth was highly variable beneath the line.

As is typical with seismic reflection data, data quality decreases on the edges of the section due to a decrease in data redundancy (fold).

Potential faulting is most easily observed by looking for disruptions in continuous reflectors, diffractions, offset bedding, abrupt changes in apparent dip of bedding, and other potential geologic structures indicative of faulting. Without good reflectively in the seismic section (i.e. multiple parallel reflectors from geologic strata), fault interpretation is limited to identification of diffractions and other discontinuities and may be highly subjective. Depending upon the amount of reflectivity in the seismic section, alternate interpretations of the seismic data will be possible. As an example, multiple offset reflectors are necessary to estimate the orientation of a possible fault and to make conclusive interpretation of the presence of a fault. If only a single strong reflector is present in a seismic section, then apparent small offsets or disruptions in the reflector are not conclusive evidence of faulting and accurate identification of fault orientation is not possible.

## *5.2 Zone 1*

Three 1,912 ft (583 m) seismic reflection profiles, Z1-G3 to Z1-G5, were conducted in Zone 1 as shown on Figure 1.

### 5.2.1 Line Z1-G3

The processed P-wave seismic sections for Line Z1-G3 without and with interpretation are presented in Figures 5 and 6, respectively. An approximate depth scale has been added to Figure 6 using the S-wave velocity model for Z1-S6, estimated groundwater depth of 66 ft (20 m), and approach previously discussed. As shown in Figure 1, surface wave soundings Z1-S5 and Z1-S6 were conducted in the southwestern and northeastern portions of seismic line Z1-G3, respectively. The S-wave velocity models for these soundings are very similar (**GEO***Vision*, 2009) indicating that there may not be significant lateral velocity variation in the immediate vicinity of the seismic line. However, groundwater depth, which impacts P-wave velocity variation, may be highly variable beneath this line because there is over 100 ft (30 m) of elevation change. Therefore, the depth scale shown on Figure 6 may only be applicable to the northeast end of the line and accuracy will be highly dependent on the modeled water table accuracy.

A subhorizontal seismic horizon possibly associated with the top of bedrock or base of a weathering zone within bedrock is interpreted near 0.1 s (~ 50 ft) on the seismic section for line Z1-G3 (Figure 6). This horizon is not a strong continuous reflector and is interpreted as apparent truncation of underlying southwesterly dipping discontinuous reflectors. Bedrock outcrops in the vicinity of the seismic line confirm the apparent southwest dip of seismic reflectors identified in Figure 6. Interpretation of faulting in this seismic image is complicated by the combination of dipping bedding and a significant bend in the seismic line. There are two anomalous zones identified near 850 and 1,150 ft on the seismic line where there are disruptions in bedrock reflectors that could be associated with faulting. However, it is possible that at least one of these anomalies is related to the bend in the seismic line and associated change in apparent (along line) dip of geologic units.

### 5.2.2 Line Z1-G4

The processed P-wave seismic sections for Line Z1-G4 without and with interpretation are presented in Figures 7 and 8, respectively. An approximate depth scale has been added to Figure 8 using the S-wave velocity model for Z1-S15, estimated groundwater depth of 10 ft (3 m), and procedure discussed in the previous section. As shown in Figure 1, surface wave soundings Z1-S14 and Z1-S15 were conducted in the southwestern and northeastern portions of seismic line Z1-G4, respectively. The S-wave velocity models for these soundings are different (**GEO***Vision*, 2009) indicating that there may be significant lateral velocity variation in the immediate vicinity of the seismic line. Additionally, there may be slight variation in groundwater depth beneath this line associated with the 25 ft (8 m) of elevation change. Therefore, the depth scale shown on Figure 8 is only applicable to the northeast end of the line.

A weak, subhorizontal, discontinuous reflector possibly associated with the top of bedrock is interpreted between 0.05 and 0.08 s (~ 40 to 90 ft) on the seismic section for line Z1-G4 (Figure 8). There is poor reflectivity (absence of seismic reflectors) below the interpreted top of bedrock indicating that geologic units are either too steeply dipping for the seismic reflection method to image or that the geologic units are massive rather than interbedded. There is not enough

reflectivity on this seismic line to make an accurate fault interpretation. Possible discontinuities that could be associated with minor faulting are identified in the vicinity of 280, 720 and 1,250 ft on the seismic line; however, there is insufficient reflectivity to make a conclusive interpretation.

### 5.2.3 Line Z1-G5

The processed P-wave seismic sections for Line Z1-G5 without and with interpretation are presented in Figures 9 and 10, respectively. An approximate depth scale has been added to Figure 10 using the S-wave velocity model for Z1-S16, estimated groundwater depth of 10 ft (3 m), and procedure discussed in the previous section. As shown in Figure 1, surface wave soundings Z1-S16 and Z1-S17 were conducted in the northern and southern portions of seismic line Z1-G5, respectively. It was not possible to develop a model for the surface wave data collected at Z1-S17 and, therefore, data on the potential lateral velocity variation along the seismic line is not available.

There is excellent reflectivity on this seismic line with multiple parallel seismic reflectors with which to interpret offset layers or discontinuities potentially associated with faulting. A subhorizontal seismic horizon possibly associated with the top of bedrock or base of a weathering zone within bedrock is interpreted in the 0.07 to 0.085 s range (~ 70 to 120 ft) on the seismic section for line Z1-G5 (Figure 10). This horizon is interpreted by both a discontinuous reflection event and apparent truncation of underlying dipping reflectors. Seismic reflectors associated with subsurface geologic structures appear to have an apparent northerly dip in the southern portion of the line and are subhorizontal/slightly dipping in the northern portion on the line. There is a significant change in dip of reflectors between 700 and 800 ft on the seismic line, which could be associated with faulting. The change in dip of bedding to the north may just be related to a syncline with the axis of the syncline located between a position of about 1,300 and 1,600 ft. The disrupted reflectors in the 700 to 800 ft range, however, may still be related to faulting rather than only folding.

## *5.3 Zone 2*

Three seismic reflection profiles, Z2-G1 to Z2-G3, were conducted in Zone 2 as shown on Figure 1. Lines Z2-G1 and Z2-G3 have lengths of 1,792.5 ft and Line Z2-G3 has a length of 1,434 ft.

### 5.3.1 Line Z2-G1

The processed P-wave seismic sections for Line Z2-G1 without and with interpretation are presented in Figures 11 and 12, respectively. An approximate depth scale has been added to Figure 12 using the S-wave velocity model for Z2-S2, estimated groundwater depth of 10 ft (3 m), and approach previously discussed. As shown in Figure 1, surface wave soundings Z2-S2 and Z2-S3 were conducted in the northern and southern portions of seismic line Z2-G1, respectively. The S-wave velocity models for these soundings are very similar (**GEO***Vision*, 2009) indicating that there may not be significant lateral velocity variation in the immediate vicinity of the seismic line. There is only about 25 ft (8 m) of elevation change along the seismic line and groundwater depth may not be highly variable. Therefore, the approximate depth scale shown on Figure 12 may be applicable to the entire line providing that velocity assumptions and the groundwater depth estimate represent actual site conditions.

A subhorizontal, continuous seismic reflector possibly associated with the top of bedrock is interpreted between 0.055 and 0.07 s (~ 60 to 100 ft) on the line Z2-G1 seismic section (Figure 12). There is only minor reflectivity below the interpreted bedrock surface possibly due to bedrock consisting of massive rather than interbedded geologic units or steeply dipping geologic units. The absence of significant reflectivity within the bedrock unit makes accurate and conclusive fault interpretation difficult. There are two anomalous zones identified between 600 and 650 ft and 1,140 and 1,180 ft on the seismic line that could be associated with potential faulting. Both of these anomalous zones were identified based on disruptions of limited bedrock reflectors.

### 5.3.2 Line Z2-G2

The processed P-wave seismic sections for Line Z2-G2 without and with interpretation are presented in Figures 13 and 14, respectively. An approximate depth scale has been added to Figure 14 using the S-wave velocity model for Z2-S8, estimated groundwater depth of 23 ft (7 m), and approach previously discussed. As shown in Figure 1, surface wave soundings Z2-S7 and Z2-S8 were conducted in the southwestern and northeastern portions of seismic line Z2-G2, respectively. The S-wave velocity models for these soundings are very similar above a depth of 130 ft (40 m) but somewhat different and greater depths (**GEO***Vision*, 2009) indicating that there may be some lateral velocity variation in the immediate vicinity of the seismic line. There is only about 20 ft (6 m) of elevation change along the seismic line and groundwater depth may not be highly variable. The approximate depth scale shown on Figure 12 may primarily apply to the northeastern side of the seismic line providing that velocity assumptions and the groundwater depth estimate represent actual site conditions.

A subhorizontal, continuous seismic reflector possibly associated with the top of bedrock is interpreted between 0.1 and 0.12 s (~ 175 to 225 ft) on the line Z2-G2 seismic section (Figure 12). The surface wave soundings along this seismic line indicate that bedrock may be shallower, possibly in the 125 to 150 ft depth range. An incorrect groundwater depth estimate, the presence of a perched water table and/or lower P-wave velocities in unsaturated and saturates sediments could easily account for this depth discrepancy. There is only minor reflectivity below the interpreted bedrock surface possibly due to bedrock consisting of massive rather than interbedded geologic units or steeply dipping geologic units. The absence of significant reflectivity within the bedrock unit makes accurate and conclusive fault interpretation difficult. There are two anomalous zones identified between 750 and 775 ft and 1,475 and 1,525 ft on the seismic line that could be associated with potential faulting. Both of these anomalous zones were identified based on disruptions of limited bedrock reflectors.

### 5.3.3 Line Z2-G3

The processed P-wave seismic sections for Line Z2-G3 without and with interpretation are presented in Figures 15 and 16, respectively. An approximate depth scale has been added to Figure 16 using the S-wave velocity model for Z2-S10, estimated groundwater depth of 30 ft (9 m), and previously discussed approach. As shown in Figure 1, surface wave soundings Z2-S10 and Z2-S11 were conducted in the northwestern and southeastern portions of seismic line Z2-G3, respectively. The S-wave velocity models for these soundings are very similar (**GEO***Vision*, 2009) indicating that there may not be significant lateral velocity variation in the immediate vicinity of the seismic line. There is, however, about 70 ft (21 m) of elevation change along the

seismic line increasing the possibility of significant variation in groundwater depth, which would cause variation in depth along the seismic line.

A subhorizontal, continuous seismic reflector possibly associated with the top of bedrock is interpreted between 0.06 and 0.075 s (~ 60 to 125 ft) on the line Z2-G3 seismic section (Figure 12). There is some reflectivity below the interpreted bedrock surface indicating that sedimentary units may have a slight apparent dip to the southeast along the seismic line. There are no apparent large offsets in bedrock reflectors indicative of conclusive faulting. There is, however, a minor discontinuity in the upper bedrock reflectors near 650 ft on the seismic line, which could potentially be associated with minor faulting.

## *5.4 Zone 3*

Seven seismic reflection profiles, Z3-G1 to Z3-G7, were conducted in Zone 3 as shown on Figure 1. Lines Z3-G1 and Z3-G3 have lengths of 1,912 ft. Line Z3-G2 has a length of 1,195 ft. Line Z3-G4 has a length of 1,434 ft. Lines Z3-G5 and Z3-G7 have lengths of 1,578 ft and Line Z3-G6 has a length of 1,506 ft.

### 5.4.1 Line Z3-G1

The processed P-wave seismic sections for Line Z3-G1 without and with interpretation are presented in Figures 17 and 18, respectively. An approximate depth scale has been added to Figure 18 using the P-wave velocity log from borehole Z3-B4. As shown in Figure 1, surface wave soundings Z3-S3 and Z3-S4 were conducted in the northern and southern portions of seismic line Z3-G1, respectively. The S-wave velocity models for these soundings are very similar (**GEO***Vision*, 2009) indicating that there may not be significant lateral velocity variation in the immediate vicinity of the seismic line. There is only about 15 ft (4.5 m) of elevation change along the seismic line and groundwater depth may not be highly variable. Therefore, the approximate depth scale shown on Figure 12 may be applicable to the entire line providing that velocity assumptions and the groundwater depth estimate represent actual site conditions.

A subhorizontal, continuous seismic reflector possibly associated with the top of bedrock or weathering contact within bedrock is interpreted between 0.14 and 0.16 s (~ 175 to 270 ft) on the line Z3-G1 seismic section (Figure 18). This reflector appears too deep for groundwater or the bedrock surface, which were encountered in borehole Z3-B4 at about 148 ft (45 m) and 185 ft (56 m), respectively. Assuming some lateral velocity variation in P-wave velocity across the site, the reflector may be associated with the top of crystalline bedrock but could also be associated with an abrupt contact between highly weathered and slightly weathered bedrock.

There is no reflectivity below the interpreted bedrock reflector because bedrock consists of crystalline rock, which has no bedding. The absence of significant reflectivity within the bedrock unit makes conclusive fault interpretation impossible. There are multiple discontinuities in the bedrock reflector, approximately located near 200, 550, 840, 1,100, 1,340 and 1,440 ft. Many of these bedrock discontinuities may be associated with topographic variation of the bedrock surface or bedrock weathering contacts. It is also possible that some of the discontinuities are related to bedrock offsets caused by faulting rather than erosion.

### 5.4.2 Line Z3-G2

The processed P-wave seismic sections for Line Z3-G2 without and with interpretation are presented in Figures 19 and 20, respectively. An approximate depth scale has been added to Figure 20 using the S-wave velocity model for Z3-S6, estimated groundwater depth of 16 ft (5 m), and previously discussed methodology. As shown in Figure 1, surface wave soundings Z3-S6 and Z3-S7 were conducted near the north and south ends of seismic line Z3-G2, respectively. The S-wave velocity models for these soundings differ by more than 10 % (**GEO***Vision*, 2009) indicating that there may be some lateral velocity variation in the immediate vicinity of the seismic line. There is only about 3 ft (1 m) of elevation change along the seismic line and groundwater depth may not be highly variable. The approximate depth scale shown on Figure 12 may vary by 10% or more across the seismic line.

Subhorizontal, continuous seismic reflectors possibly associated with top of bedrock and/or a weathering zone within bedrock are interpreted between 0.03 and 0.04 s (~ 40 to 60 ft) and 0.05 and 0.07 s (~ 100 to 175 ft) on the line Z3-G2 seismic section (Figure 20). The surface wave soundings along this seismic line indicate that bedrock may be associated with the upper reflector with the lower reflector associated with a change in weathering within bedrock or other bedrock structure. There is only minor reflectivity below the interpreted bedrock surface possibly due to bedrock consisting of massive rather than interbedded geologic units or steeply dipping geologic units. The absence of significant reflectivity within the bedrock unit makes accurate and conclusive fault interpretation difficult. There are two anomalous zones identified near 420 and 700 ft on the seismic line that could be associated with potential faulting. Both of these anomalous zones were identified based on disruptions of limited bedrock reflectors.

### 5.4.3 Line Z3-G3

The processed P-wave seismic sections for Line Z3-G3 without and with interpretation are presented in Figures 21 and 22, respectively. An approximate depth scale has been added to Figure 22 using the P-wave velocity log from borehole Z3-B7. As shown in Figure 1, surface wave soundings Z3-S9 and Z3-S10 were conducted near the southwest and northeast ends of seismic line Z3-G3, respectively. The S-wave velocity models for these soundings are significantly different (**GEO***Vision*, 2009) indicating that there may be some lateral velocity variation in the immediate vicinity of the seismic line. There is also about 26 ft (8 m) of elevation change along the seismic line, which may contribute to variable water table depth and associated lateral velocity variation and groundwater depth may not be highly variable. The approximate depth scale shown on Figure 22 is most applicable in the central portion of the seismic line near the borehole.

Subhorizontal, discontinuous seismic reflectors possibly associated with groundwater, top of bedrock and/or a weathering zone within bedrock are interpreted between 0.04 and 0.055 s (~ 60 to 100 ft) and 0.06 and 0.09 s (~ 120 to 270 ft) on the line Z3-G3 seismic section (Figure 22). The surface wave soundings and borehole along this seismic line indicate that bedrock may be associated with the upper reflector, although there may not be an abrupt change in velocity between weathered bedrock and overlying sediments in the vicinity of the seismic line. The lower reflector may be associated with a change in weathering within bedrock or other bedrock structure. There is only minor reflectivity below the interpreted bedrock surface possibly due to bedrock consisting of massive rather than interbedded geologic units or steeply dipping geologic units. The bedrock reflectors identified on the seismic section (Figure 22) occur at depths below

600 ft. The seismic reflection survey was not designed to image to these depths and there is a possibility that the reflection events are associated with coherent noise. The absence of significant reflectivity within the bedrock unit makes accurate and conclusive fault interpretation difficult. There are two anomalous zones identified between 450 and 500 ft and 1,000 and 1,050 ft that could be associated with potential faulting. Both of these anomalous zones were identified based on disruptions of limited bedrock reflectors.

### 5.4.4 Line Z3-G4

The processed P-wave seismic sections for Line Z3-G4 without and with interpretation are presented in Figures 23 and 24, respectively. An approximate depth scale has been added to Figure 24 using the S-wave velocity model for Z3-S13, estimated groundwater depth of 56 ft (17 m), and previously discussed methodology. As shown in Figure 1, surface wave soundings Z3-S13 and Z3-S14 were conducted near the northeast and southwest ends of seismic line Z3-G4, respectively. There is also a borehole (Z3-B9) located near this seismic line, which indicates that crystalline basement rock is present beneath the line. The S-wave velocity models for the surface wave soundings are very similar (**GEO***Vision*, 2009) indicating that there may be only minor lateral velocity variation in the immediate vicinity of the seismic line. There is only about 20 ft (6 m) of elevation change along the seismic line and groundwater depth may not be highly variable.

Subhorizontal, continuous seismic reflectors possibly associated with groundwater and top of crystalline bedrock are interpreted between 0.05 and 0.06 s (~ 30 to 45 ft) and 0.085 and 0.115 s (~ 80 to 200 ft) on the line Z3-G4 seismic section (Figure 24). Nearby borehole Z3-B9 indicates that the lower reflector may be associated with the top of crystalline basement. The upper reflector may be associated with the water table or sediment layer above the water table.

There is no reflectivity below the interpreted bedrock reflector because bedrock consists of crystalline rock, which has no bedding. The absence of significant reflectivity within the bedrock unit makes conclusive fault interpretation impossible. There is a significant drop in the interpreted bedrock surface between 220 and 320 ft, which may be erosional or potentially related to faulting. There are also other disruptions in the possible bedrock reflector near 750, 1,030 and 1,210 ft.

### 5.4.5 Line Z3-G5

The processed P-wave seismic sections for Line Z3-G5 without and with interpretation are presented in Figures 25 and 26, respectively. An approximate depth scale has been added to Figure 26 using the S-wave velocity model for Z3-S17, estimated groundwater depth of 26 ft (8 m), and previously discussed methodology. As shown in Figure 1, surface wave soundings Z3-S17 and Z3-S18 were conducted in the north central and south central portions of seismic line Z3-G5, respectively. The S-wave velocity models for these soundings are generally similar although there is apparent variation in bedrock depth (**GEO***Vision*, 2009) indicating that there may be some lateral velocity variation in the immediate vicinity of the seismic line. There is also about 62 ft (19 m) of elevation change along the seismic line, which may contribute to variable water table depth and associated lateral velocity variation. The approximate depth scale shown on Figure 26 may only apply to the central portion of the seismic line.

A high amplitude, subhorizontal, continuous seismic reflector possibly associated with top of bedrock is interpreted between 0.04 and 0.1 s (~ 140 ft) on the line Z3-G5 seismic section

(Figure 26). The surface wave soundings along this seismic line indicate that bedrock may be located in the 70 to 85 ft (21 to 26 m) depth range. If groundwater were about 15 to 20 ft (4.5 to 6 m) deeper than that used for depth control then the high amplitude reflector would be in the appropriate depth range. The possible bedrock reflector is continuous except for minor discontinuities at 230 and 450 ft, which could be associated with faulting. A more diffuse reflector that may be associated with a possible weathering zone within bedrock is interpreted between 0.14 and 0.17 s (~ 375 to 500 ft). Below the lower reflector, geologic units appear to have apparent dip in a northerly direction. Many of these reflectors are very deep relative to the data acquisition geometry and, therefore, could be related to coherent noise rather than geologic structure. Additionally, several small diffractions appear to line up in the vicinity of 800 ft on the profile beneath the lower reflector. Although unlikely, the possibility that these diffractions are associated with minor faulting cannot be discounted.

### 5.4.6 Line Z3-G6

The processed P-wave seismic sections for Line Z3-G6 without and with interpretation are presented in Figures 27 and 28, respectively. An approximate depth scale has been added to Figure 28 using the S-wave velocity model for Z3-S21, estimated groundwater depth of 52 ft (16 m), and previously discussed methodology. As shown in Figure 1, surface wave soundings Z3-S21 and Z3-S22 were conducted in the northern and southern portions of seismic line Z3-G6, respectively. The S-wave velocity models for these soundings are generally similar (**GEO***Vision*, 2009) indicating that there may not be significant lateral velocity variation in the immediate vicinity of the seismic line. There is about 45 ft (14 m) of elevation change along the seismic line, which may contribute to variable water table depth and associated lateral velocity variation. The approximate depth scale shown on Figure 28 may apply to much of the seismic line.

A subhorizontal, continuous seismic reflector possibly associated with top of bedrock is interpreted between 0.085 and 0.1 s (~ 100 to 115 ft) on the line Z3-G6 seismic section (Figure 28). The surface wave soundings along this seismic line indicate that bedrock may be located in the 92 to 102 ft (28 to 31 m) depth range, which confirms that the reflector may be associated with the top of bedrock. There is excellent reflectively below the interpreted bedrock surface with multiple parallel seismic reflectors with which to interpret offset layers or discontinuities potentially associated with faulting. There is a significant disruption and possible offset of reflectors in the 910 to 950 ft range, which may be associated with faulting. There is also a minor disruption in reflectors between 375 and 440 ft, which could be associated with faulting.

### 5.4.7 Line Z3-G7

The processed P-wave seismic sections for Line Z3-G7 without and with interpretation are presented in Figures 29 and 30, respectively. An approximate depth scale has been added to Figure 30 using the S-wave velocity model for Z3-S23, estimated groundwater depth of 39 ft (12 m), and previously discussed methodology. As shown in Figure 1, surface wave soundings Z3-S23 and Z3-S24 were conducted in the northern and southern portions of seismic line Z3-G7, respectively. The S-wave velocity models for these soundings are different (**GEO***Vision*, 2009) indicating that there may be significant lateral velocity variation in the immediate vicinity of the seismic line. There is about 25 ft (8 m) of elevation change along the seismic line, which may contribute to variable water table depth and associated lateral velocity variation. The

approximate depth scale shown on Figure 28 may only apply to the northern portion of the seismic line.

A subhorizontal, discontinuous seismic reflector possibly associated with top of bedrock is interpreted between 0.06 and 0.085 s (~ 40 to 100 ft) on the line Z3-G7 seismic section (Figure 30). A borehole located in the vicinity of the seismic line (Z1-B8) indicates that the uppermost bedrock zone may be highly weathered and not easily distinguished from overlying sediments based on S-wave velocity. Therefore, the surface wave soundings along this seismic line were only able to indicate that bedrock may be located in the 23 to 118 ft (7 to 36 m) depth range, which is consistent with the interpretation of the bedrock reflector. There is good reflectively below the interpreted bedrock surface in the southern half of the seismic line with multiple parallel seismic reflectors with which to interpret offset layers or discontinuities potentially associated with faulting. There is a significant change in reflectivity in the northern portion of the line associated with a possible fault interpreted between 880 and 920 ft. Additionally, there is also a minor disruption in reflectors around 250 ft on the line, which could also be associated with faulting.

## *5.5 Zone 4*

Two seismic reflection profiles, Z4-G1 and Z4-G2, were conducted in Zone 4 as shown on Figure 1. Lines Z4-G1 and Z4-G2 have lengths of 3,832 and 1,912 ft, respectively.

### 5.5.1 Line Z4-G1

The processed P-wave seismic sections for Line Z4-G1 without and with interpretation are presented in Figures 31 and 32, respectively. An approximate depth scale has been added to Figure 32 using the S-wave velocity model for Z4-S2, estimated groundwater depth of 210 ft (64 m), and approach previously discussed. As shown in Figure 1, surface wave soundings Z4-S2, Z4-S3 and Z4-S4 were conducted in the northern, central and southern portions of seismic line Z4-G1, respectively. The S-wave velocity models for these soundings are very different (**GEO***Vision*, 2009) indicating that there may be significant lateral velocity variation in the immediate vicinity of the seismic line. There is also over 120 ft (37 m) of elevation change along the seismic line, which may contribute to variable groundwater depth and associated lateral velocity variation. Additionally, groundwater depths are not accurately resolved on this seismic line, which may contribute to significant depth errors. The approximate depth scale shown on Figure 32 may only be applicable to the northern portion of the seismic line and may have errors in excess of 25%.

Seismic line Z4-G1 crosses the Raymond Fault Zone. A scarp associated with the fault is located between about 1,200 and 2,000 ft on the seismic line. Bedrock may be located at depths in excess of 500 ft beneath this seismic line and there is no clear seismic reflection associated with the top of bedrock. There is not much reflectively in the seismic section, possibly because the old alluvium overlying bedrock does not have laterally extensive continuous bedding, and/or energy attenuation through the thick unsaturated zone. The absence of significant reflectively makes accurate fault interpretation difficult. There is, however, a significant change in reflectively on the seismic line between 800 and 2,000 ft revealed by abrupt termination change in apparent dip of reflectors at the southern end and change in dip of reflectors and possible large diffractions at the northern end of the zone. Potential faults are identified in the vicinity of 900,

1,500 and 2,000 ft on the seismic line although, given the minimal reflectivity, alternative interpretations are possible.

### 5.5.2 Line Z4-G2

The processed P-wave seismic sections for Line Z4-G2 without and with interpretation are presented in Figures 33 and 34, respectively. An approximate depth scale has been added to Figure 34 using the S-wave velocity model for Z4-S6, estimated groundwater depth of 215 ft (65 m), and approach previously discussed. As shown in Figure 1, surface wave soundings Z4-S6 and Z4-S7 were conducted in the northeastern and southwestern portions of seismic line Z4-G2, respectively. The S-wave velocity models for these soundings are very similar (**GEO***Vision*, 2009) indicating that there may not be significant lateral velocity variation in the immediate vicinity of the seismic line. There is also only 5 ft (1.5 m) of elevation change along the seismic line. Groundwater depths are not accurately resolved beneath this seismic line, however, there is no reason to believe that there is significant depth variation of the water table beneath the line. The approximate depth scale shown on Figure 34 may be applicable to the entire seismic line, providing the assumptions made to estimate depths are reasonably valid.

A high amplitude, subhorizontal, continuous seismic reflector possibly associated with the water table is interpreted between 0.15 and 0.175 s (~ 170 to 220 ft) on the line Z4-G2 seismic section (Figure 34). Another continuous reflector is identified between 0.28 and 0.3 s (~ 525 to 600 ft). The location of this reflector is such that the possibility that it is a multiple reflection from the possible water table cannot be discounted. Other than the two reflectors identified above there is not sufficient reflectivity in the seismic section for detailed fault interpretation. Two possible fault-like anomalies are identified in the seismic section near 1,220 and 1,520 ft. These structures are primarily identified by changes in apparent dip and disruptions of the water table reflector, which may occur if a fault acts as a groundwater barrier. These features cannot be accurately mapped on the seismic section due to absence of reflectivity and, therefore, cannot be confirmed as faults.

## *5.6 Zone 5*

Two seismic reflection profiles, Z5-G2 and Z5-G3, were conducted in Zone 5 as shown on Figure 1. Both lines Z5-G2 and Z5-G3 have a length of 1,912 ft.

### 5.6.1 Line Z5-G2

The processed P-wave seismic sections for Line Z5-G2 without and with interpretation are presented in Figures 33 and 34, respectively. An approximate depth scale has been added to Figure 34 using the S-wave velocity model for Z5-S8, estimated groundwater depth of 184 ft (56 m), and approach previously discussed. As shown in Figure 1, surface wave soundings Z5-S8, and Z5-S9 were conducted in the eastern and western portions of seismic line Z5-G2, respectively. The S-wave velocity models for these soundings are very similar (**GEO***Vision*, 2009) indicating that there may not be significant lateral velocity variation in the immediate vicinity of the seismic line. There is about 36 ft (11 m) of elevation change along the seismic line, which may contribute to variable groundwater depth and some associated lateral velocity variation. Groundwater depth is not well constrained along this seismic line. The approximate depth scale shown on Figure 36 may be applicable to much of the seismic line providing the groundwater depth estimate is reasonably accurate.

The seismic section has good reflectivity with multiple discontinuous reflectors to approximate depths of over 600 ft. Reflectors associated with the water table or bedrock surface were not identified to a high degree of confidence. Bedrock is expected to be very deep in the vicinity of this seismic line. A possible fault-like anomaly was identified in the seismic section at about 740 ft and was identified by disruptions in several reflectors, particularly those in the 600 ft depth range. A more subtle anomalous zone that could be associated with faulting was identified between 1,600 and 1,650 ft.

### 5.6.2 Line Z5-G3

The processed P-wave seismic sections for Line Z5-G3 without and with interpretation are presented in Figures 37 and 38, respectively. An approximate depth scale has been added to Figure 38 using the S-wave velocity model for Z5-S12, estimated groundwater depth of 52 ft (16 m), and approach previously discussed. As shown in Figure 1, surface wave soundings Z5-S12, and Z5-S13 were conducted in the northern and southern portions of seismic line Z5-G3, respectively. The S-wave velocity models for these soundings are very similar (**GEO***Vision*, 2009) indicating that there may not be significant lateral velocity variation in the immediate vicinity of the seismic line. There is only about 16 ft (5 m) of elevation change along the seismic line. The approximate depth scale shown on Figure 38 may be applicable to the entire seismic line providing the groundwater depth estimate is accurate.

A high amplitude, subhorizontal, continuous seismic reflector possibly associated with the top of bedrock is interpreted between 0.14 and 0.16 s (~ 280 to 330 ft) on the line Z5-G3 seismic section (Figure 38). This reflector appears to be much too deep to be associated with the water table, although the reflector could be associated with a continuous geologic layer within alluvial sediments rather than bedrock. There is not significant reflectivity below the interpreted bedrock reflector until depths below 600 ft where possible northward dipping geologic units are identified. Several possible, but not conclusive, fault-like anomalies are identified in the seismic section at 300 and 920 ft and 1,350 to 1,450 ft. These structures were identified by disruption of the potential top of bedrock reflector and underlying reflectors at depth. Reduction of fold (data redundancy) at the ends of the seismic line may contribute to possible incorrect interpretation of the structures at 300 ft and 1,400 ft.

# 6 REFERENCES

Claerbout, J. F., 1985, Imaging the Earth's Interior, Blackwell Scientific Publications.

Geldart, L.P., Telford, W.M., Sheriff, R.E., 1995, Applied Geophysics, Second Edition, Cambridge University Press.

**GEO***Vision* Inc., 2009, Draft Report, Surface Wave Measurements, SR-710 Potential Tunnel Corridors, Los Angeles County, California, prepared for CH2M Hill, July 31, 2009.

Steeples, Don W., and Miller, Richard D., 1988, Seismic Reflection Methods Applied To Engineering, Environmental, and Ground Water Problems, Proc. of SAGEEP, March, Golden, CO, p. 409-460.

Sheriff, R.E., Geldart, L.P., 1985, History, Theory and Data Acquisition, Exploration Seismology, Volume 1, Cambridge University Press.

# 7 CERTIFICATION

All geophysical data, analysis, interpretations, conclusions, and recommendations in this document have been prepared under the supervision of and reviewed by a **GEO*Vision*** California Professional Geophysicist.

October 5, 2009

Antony J. Martin — Date
California Professional Geophysicist GP989
**GEO***Vision* Geophysical Services

* This geophysical investigation was conducted under the supervision of a California Professional Geophysicist using industry standard methods and equipment. A high degree of professionalism was maintained during all aspects of the project from the field investigation and data acquisition, through data processing interpretation and reporting. All original field data files, field notes and observations, and other pertinent information are maintained in the project files and are available for the client to review for a period of at least one year.

  A professional geophysicist's certification of interpreted geophysical conditions comprises a declaration of his/her professional judgment. It does not constitute a warranty or guarantee, expressed or implied, nor does it relieve any other party of its responsibility to abide by contract documents, applicable codes, standards, regulations or ordinances.

# TABLES

## Table 1. Seismic Line Locations

| Line | Station | Position (ft) | Northing (US ft) | Easting (US ft) | Elevation (ft MSL) |
|---|---|---|---|---|---|
| Z1-G3 | 101 | 0 | 1853598 | 6487832 | 579 |
| Z1-G3 | 251 | 1200 | 1854484 | 6488636 | 525 |
| Z1-G3 | 238 | 1096 | 1854396 | 6488580 | 536 |
| Z1-G3 | 340 | 1912 | 1855142 | 6488901 | 477 |
| Z1-G4 | 101 | 0 | 1851571 | 6503615 | 427 |
| Z1-G4 | 340 | 1912 | 1853095 | 6504768 | 450 |
| Z1-G5 | 101 | 0 | 1851287 | 6507737 | 449 |
| Z1-G5 | 340 | 1912 | 1853200 | 6507732 | 459 |
| Z2-G1 | 101 | 0 | 1866438 | 6496103 | 519 |
| Z2-G1 | 175 | 555 | 1866977 | 6496229 | 492 |
| Z2-G1 | 181 | 600 | 1867019 | 6496244 | 493 |
| Z2-G1 | 340 | 1792.5 | 1868182 | 6496515 | 517 |
| Z2-G2 | 101 | 0 | 1860667 | 6500501 | 503 |
| Z2-G2 | 340 | 1792.5 | 1861576 | 6502044 | 519 |
| Z2-G3 | 101 | 0 | 1854399 | 6508688 | 482 |
| Z2-G3 | 333 | 1392 | 1855642 | 6508062 | 541 |
| Z2-G3 | 340 | 1434 | 1855692 | 6508069 | 556 |
| Z3-G1 | 101 | 0 | 1868860 | 6516666 | 739 |
| Z3-G1 | 340 | 1912 | 1870771 | 6516652 | 755 |
| Z3-G2 | 101 | 0 | 1867383 | 6512290 | 685 |
| Z3-G2 | 340 | 1195 | 1868579 | 6512310 | 687 |
| Z3-G3 | 101 | 0 | 1865627 | 6509704 | 584 |
| Z3-G3 | 340 | 1912 | 1866908 | 6511124 | 608 |
| Z3-G4 | 101 | 0 | 1863281 | 6510441 | 612 |
| Z3-G4 | 340 | 1434 | 1864450 | 6511274 | 631 |
| Z3-G5 | 101 | 0 | 1858529 | 6510383 | 579 |
| Z3-G5 | 125 | 144 | 1858674 | 6510377 | 588 |
| Z3-G5 | 158 | 342 | 1858864 | 6510328 | 598 |
| Z3-G5 | 209 | 648 | 1859164 | 6510324 | 614 |
| Z3-G5 | 258 | 942 | 1859462 | 6510322 | 626 |
| Z3-G5 | 302 | 1206 | 1859727 | 6510318 | 633 |
| Z3-G5 | 336 | 1410 | 1859921 | 6510377 | 636 |
| Z3-G5 | 364 | 1578 | 1860066 | 6510461 | 643 |
| Z3-G6 | 101 | 0 | 1851978 | 6513112 | 425 |
| Z3-G6 | 364 | 1578 | 1853555 | 6513105 | 471 |
| Z3-G7 | 101 | 0 | 1848225 | 6513201 | 423 |
| Z3-G7 | 170 | 414 | 1848639 | 6513200 | 432 |
| Z3-G7 | 244 | 858 | 1849084 | 6513199 | 415 |
| Z3-G7 | 300 | 1194 | 1849419 | 6513201 | 418 |
| Z3-G7 | 340 | 1434 | 1849659 | 6513201 | 418 |
| Z3-G7 | 364 | 1578 | 1849803 | 6513202 | 415 |

California State Plane coordinate system, North American Datum 1983, Zone V (0405), US Survey Feet.
Horizontal accuracy is approximately 1m, vertical accuracy is approximately 2m.

## Table 1 (continued) Seismic Line Locations

| Line | Station | Position (ft) | Northing (US ft) | Easting (US ft) | Elevation (ft MSL) |
|---|---|---|---|---|---|
| Z4-G1 | 101 | 0 | 1866934 | 6528963 | 569 |
| Z4-G1 | 180 | 632 | 1867563 | 6528843 | 580 |
| Z4-G1 | 209 | 864 | 1867761 | 6528740 | 584 |
| Z4-G1 | 580 | 3832 | 1869568 | 6528421 | 677 |
| Z4-G2 | 101 | 0 | 1861662 | 6521381 | 556 |
| Z4-G2 | 340 | 1912 | 1862851 | 6522877 | 550 |
| Z4-G3 | 101 | 0 | 1851789 | 6526290 | 398 |
| Z4-G3 | 340 | 1912 | 1851899 | 6528198 | 362 |
| Z5-G3 | 101 | 0 | 1848497 | 6516641 | 420 |
| Z5-G3 | 340 | 1912 | 1850408 | 6516625 | 435 |

California State Plane coordinate system, North American Datum 1983, Zone V (0405), US Survey Feet.
Horizontal accuracy is approximately 1m, vertical accuracy is approximately 2m.

**Table 2. Generalized Data Acquisition Parameters**

| | |
|---|---|
| Shot Spacing | 6 – 8 ft , centered on half stations |
| Geophone Group Interval | 5 – 8 ft |
| Maximum CDP Fold | 72 |
| Maximum Offset | 429 to 956 ft |
| Minimum Offset | 2.5 – 4 ft |
| Spread Geometry | Walk on to asymmetric split spread/symmetric split spread, walk off |
| Seismograph | OYO DAS-1 Recorder |
| Number of Channels | 144 |
| Sample Rate | 0.5 ms |
| Record Length | 8 second sweep, 0.5 – 1 seconds after correlation |
| Field Filters | 3 Hz lo-cut |
| Seismic Source | IVI Envirovibe |
| Geophones | OYO Geospace 28 Hz vertical |

**Table 3. Data Acquisition and Vibrator Parameters**

| Line | Line Length (feet) | Shot Spacing (feet) | Group Interval (feet) | Minimum Offset (feet) | Nominal Maximum Offset (feet) | Normal Spread Geometry | Sweep Frequency (Hz) | Sweep Length (sec) | Listen Time (sec) |
|---|---|---|---|---|---|---|---|---|---|
| Z1-G3 | 1912 | 8 | 8 | 4 | 860 | asymmetric 36/108 split | 20 - 240 | 8 | 1 |
| Z1-G4 | 1912 | 8 | 8 | 4 | 764 | asymmetric 48/96 split | 20 - 240 | 8 | 1 |
| Z1-G5 | 1912 | 8 | 8 | 4 | 764 | asymmetric 48/96 split | 20 - 240 | 8 | 1 |
| Z2-G1 | 1792.5 | 7.5 | 7.5 | 3.75 | 716.25 | asymmetric 48/96 split | 20 - 200 | 8 | 1 |
| Z2-G2 | 1792.5 | 7.5 | 7.5 | 3.75 | 716.25 | asymmetric 48/96 split | 20 - 240 | 8 | 1 |
| Z2-G3 | 1434 | 6 | 6 | 3 | 645 | asymmetric 36/108 split | 20 - 240 | 8 | 1 |
| Z3-G1 | 1912 | 8 | 8 | 4 | 764 | asymmetric 48/96 split | 20 - 240 | 8 | 1 |
| Z3-G2 | 1195 | 5 | 5 | 2.5 | 597.5 | asymmetric 24/120 split | 20 -240 | 8 | 0.5 |
| Z3-G3 | 1912 | 8 | 8 | 4 | 764 | asymmetric 48/96 split | 20 - 240 | 8 | 1 |
| Z3-G4 | 1434 | 6 | 6 | 3 | 573 | asymmetric 48/96 split | 20 - 240 | 8 | 1 |
| Z3-G5 | 1578 | 6 | 6 | 3 | 573 | asymmetric 48/96 split | 20 - 240 | 8 | 1 |
| Z3-G6 | 1506 | 6 | 6 | 3 | 429 | symmetric 72/72 split | 20 - 240 | 8 | 0.5 |
| Z3-G7 | 1578 | 6 | 6 | 3 | 429 | symmetric 72/72 split | 20 - 240 | 8 | 0.5 |
| Z4-G1 | 3832 | 8 | 8 | 4 | 764 | asymmetric 48/96 split | 20 - 200 | 8 | 1 |
| Z4-G2 | 1912 | 8 | 8 | 4 | 764 | asymmetric 48/96 split | 20 - 240 | 8 | 1 |
| Z5-G2 | 1912 | 8 | 8 | 4 | 956 | asymmetric 24/120 split | 20 - 240 | 8 | 1 |
| Z5-G3 | 1912 | 8 | 8 | 4 | 860 | asymmetric 36/108 split | 20 - 240 | 8 | 1 |

**Table 4. Generalized Processing Sequence**

| Sequence # | Description |
|---|---|
| 1 | SEG2 TO INTERNAL FORMAT CONVERSION |
| 2 | VIBROSEIS CORRELATION |
| 3 | GEOMETRY, SURVEY IMPORT AND TRACE EDITING |
| 4 | TRUE AMPLITUDE GAIN RECOVERY |
| 5 | TRACE TO TRACE EDITING |
| 6 | ELEVATION / DATUM STATICS APPLICATION: |
| | DATUM: INTERMEDIATE FLOATING/NMO DATUM |
| | VC: 6000 FEET/SEC |
| 7 | SURFACE CONSISTENT AMPLITUDE ANALYSIS AND COMPENSATION |
| 8 | MINIMUM PHASE CORRECTION FILTER FOR VIBROSEIS DATA |
| 9 | SURFACE CONSISTENT DECONVOLUTION: |
| | TYPE: SPIKING OPERATOR LENGTH: 160 MSEC NOISE: 0.1% |
| 10 | SPECTRAL WHITENING: 20-240 HZ |
| 11 | COMMON DEPTH POINT GATHERS: |
| | CDP BIN SIZE: 2.5 – 4 FEET |
| | PASS 1: VELOCITY AND MUTE ANALYSIS |
| | PASS 1: NORMAL MOVEOUT CORRECTION AND MUTE APPLICATION |
| | PASS 1: SURFACE CONSISTENT AUTOMATIC STATICS APPLICATION |
| | PASS 2: VELOCITY AND MUTE ANALYSIS |
| | PASS 2: NORMAL MOVEOUT CORRECTION AND MUTE APPLICATION |
| | PASS 2: SURFACE CONSISTENT AUTOMATIC STATICS APPLICATION |
| 12 | SURFACE/SOURCE WAVE / LINEAR NOISE ATTENUATION |
| 13 | TIME-VARIANT AMPLITUDE EQUALIZATION |
| | PASS 3: VELOCITY AND MUTE ANALYSIS |
| | PASS 3: NORMAL MOVEOUT CORRECTIONS AND MUTE APPLICATION |
| | PASS 3: SURFACE CONSISTENT AUTOMATIC STATICS APPLICATION |
| 14 | CDP CONSISTENT TRIM STATICS: 4 MSEC MAXIMUM SHIFT |
| 15 | COMMON DEPTH POINT STACK |
| 16 | FINAL DATUM CORRECTION: |
| | DATUM: FIXED FOR EACH LINE |
| | VC: 6000 FEET/SEC |
| 17 | FX PREDICTIVE ENHANCEMENT FILTER |
| 18 | SPECTRAL BALANCING: 40-240 HZ |

## Table 5. Seismic Reflection Depth Control

| Line | Depth Control Source | Estimated Groundwater Depth | | Groundwater Depth Source[1] | Expected Bedrock Type |
|---|---|---|---|---|---|
| | | m | ft | | |
| Z1-G3 | Z1-S6 | 20 | 66 | SR | Puente Fm |
| Z1-G4 | Z1-S15 | 3 | 10 | SW | Puente Fm |
| Z1-G5 | Z1-S16 | 3 | 10 | SW | Puente Fm |
| Z2-G1 | Z2-S2 | 3 | 10 | SW | Topanga Fm |
| Z2-G2 | Z2-S8 | 7 | 23 | SW | Puente Fm/Topanga Fm |
| Z2-G3 | Z2-S10 | 9 | 30 | SW | Puente Fm |
| Z3-G1 | Z3-S3 & Z3-B4 | 45 | 148 | B | Crystalline Basement |
| Z3-G2 | Z3-S6 | 5 | 16 | SW | Topanga Fm |
| Z3-G3 | Z3-S10 & Z3-B7 | 3 | 10 | B/SW | Topanga Fm |
| Z3-G4 | Z3-S13 | 17 | 56 | SR | Topanga Fm/Crystalline Basement |
| Z3-G5 | Z3-S17 | 8 | 26 | SW | Topanga Fm |
| Z3-G6 | Z3-S21 | 16 | 52 | SR | Puente Fm |
| Z3-G7 | Z3-S23 | 12 | 39 | SW | Puente Fm |
| Z4-G1 | Z4-S2 | 64 | 210 | SR | Puente Fm |
| Z4-G2 | Z4-S6 | 65 | 213 | SR | Puente Fm |
| Z5-G2 | Z5-S8 | 56 | 184 | SR | Puente Fm |
| Z5-G3 | Z5-S12 | 16 | 52 | SW | Puente Fm |

1) SR - Seismic Reflection Data, SW - Surface Wave Data, B - Borehole Data

# FIGURES

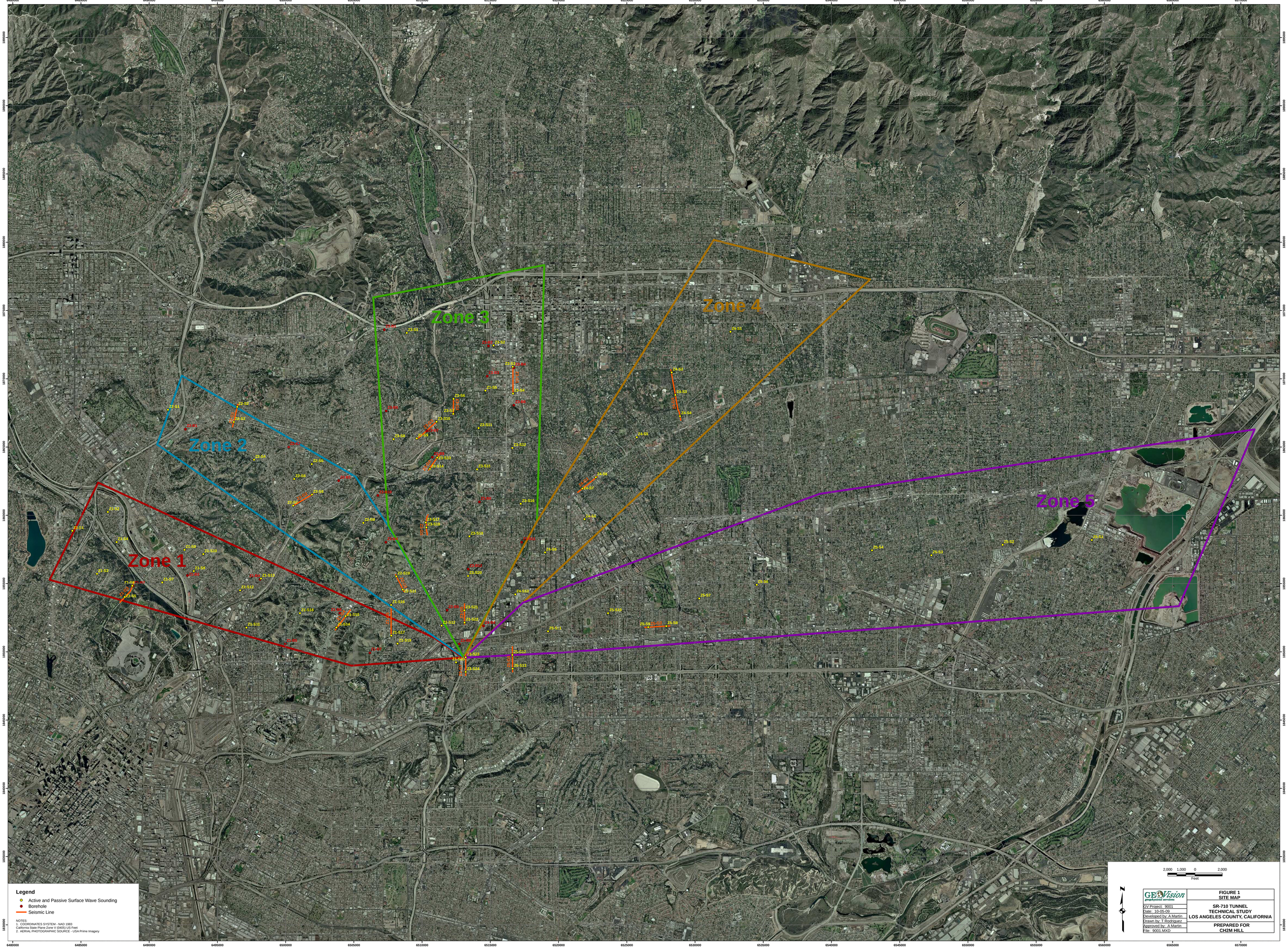
Zone 1
Zone 2
Zone 3
Zone 4
Zone 5
Legend
Active and Passive Surface Wave Sounding
Borehole
Seismic Line
NOTES:
1. COORDINATES SYSTEM - NAD 1983
California State Plane Zone V (0405) US Feet
2. AERIAL PHOTOGRAPHIC SOURCE - USA Prime Imagery
2,000 1,000 0 2,000
Feet
N
GEOVision geophysical services
FIGURE 1
SITE MAP
GV Project: 9001
Date: 10-05-09
Developed by: A Martin
Drawn by: T Rodriguez
Approved by: A Martin
File: 9001.MXD
SR-710 TUNNEL
TECHNICAL STUDY
LOS ANGELES COUNTY, CALIFORNIA
PREPARED FOR
CH2M HILL

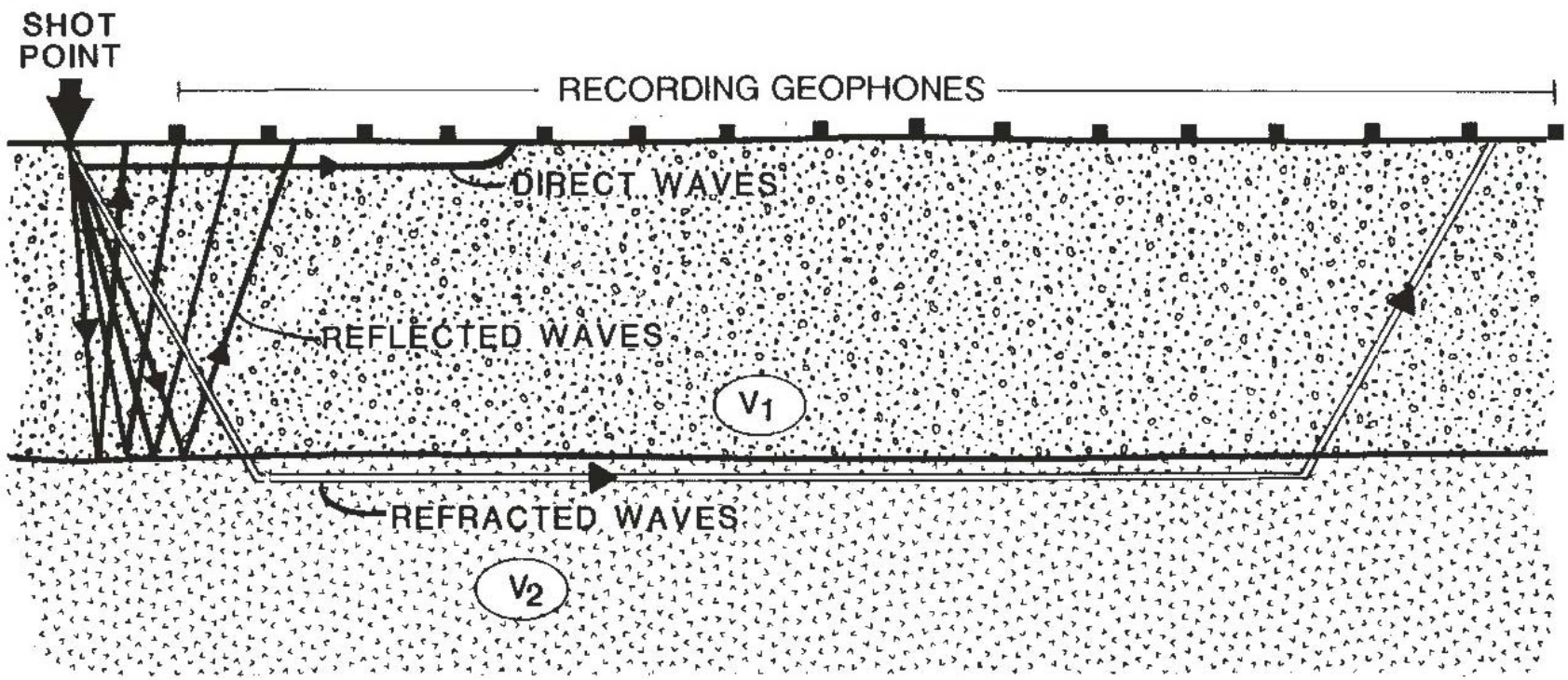


| | |
|---|---|
| GEOVision geophysical services | FIGURE 2<br>SEISMIC RAYPATH GEOMETRY |
| Project # 9001<br>Date: AUG 4, 2009<br>Drawn By: A MARTIN<br>Approved By: | SR-710 TUNNEL TECHNICAL STUDY<br>LOS ANGELES COUNTY, CALIFORNIA |
| File R:\...Project Files\2009\9001ch2mhill\REFLReport\FIGURES\Figure2.cdr | PREPARED FOR<br>CH2M HILL |

TYPICAL SEISMIC LINE


SEISMIC RECORDING SYSTEM

IVI ENVIROVIBE

| | |
|---|---|
| GEOVision geophysical services | FIGURE 3<br>PHOTOGRAPHS OF TYPICAL<br>SEISMIC REFLECTION FIELD SETUP |
| Project # 9001 | SR-710 TUNNEL TECHNICAL STUDY<br>LOS ANGELES COUNTY, CALIFORNIA |
| Date: AUG 4, 2009 | |
| Drawn By: A MARTIN | |
| Approved By: | PREPARED FOR<br>CH2M HILL |
| File R:\...Project Files\2009\9001ch2mhill\REFLReport\FIGURES\Figure3.cdr | |

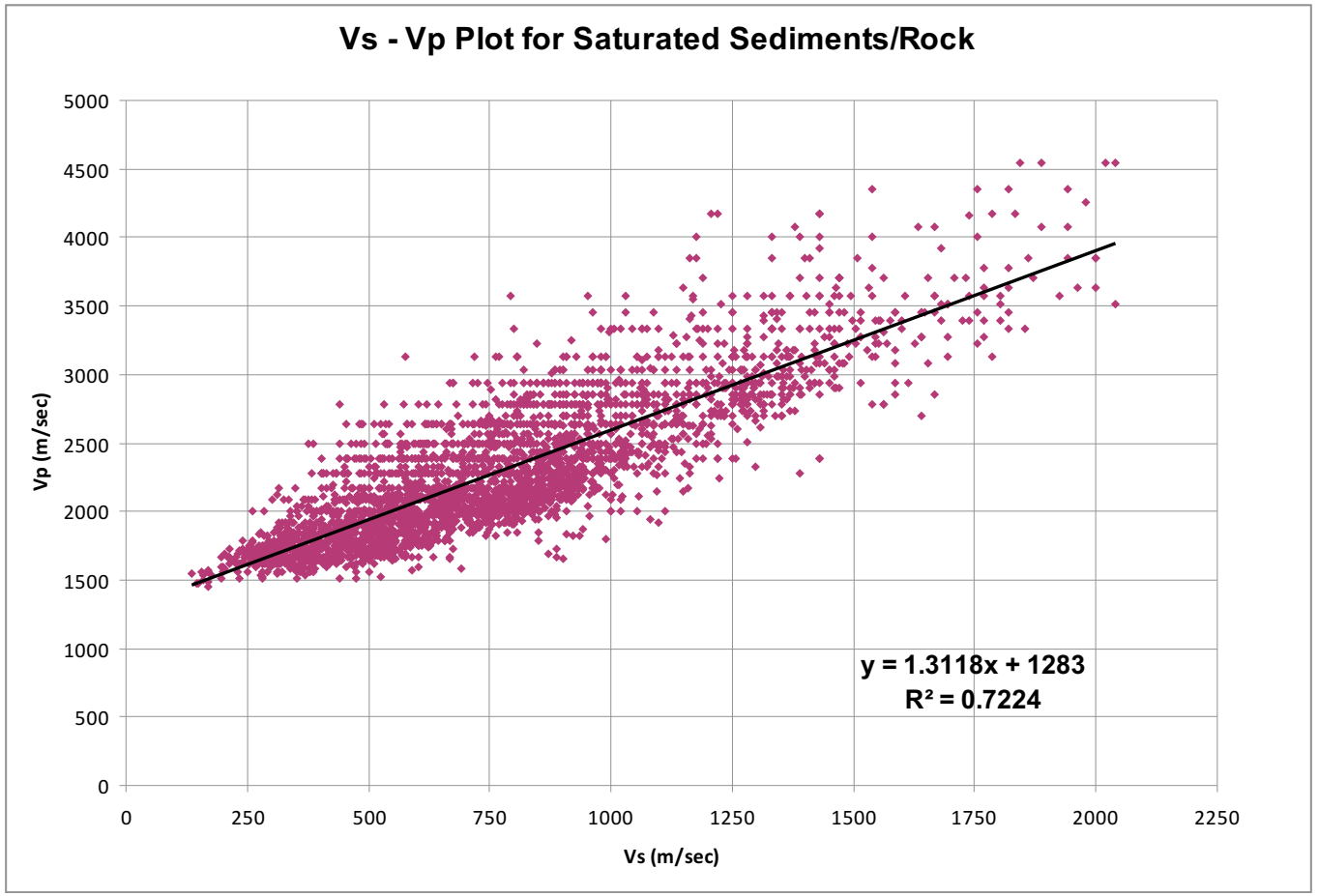


GEOVision geophysical services

| | |
|---|---|
| Project # 9001 | FIGURE 4<br>$V_S$ - $V_P$ PLOT FOR SATURATED SEDIMENTS/ROCK |
| Date: AUG 4, 2009 | SR-710 TUNNEL TECHNICAL STUDY<br>LOS ANGELES COUNTY, CALIFORNIA |
| Drawn By: A MARTIN | |
| Approved By: | PREPARED FOR<br>CH2M HILL |

File R:\...Project Files\2009\9001ch2mhill\REFLReport\FIGURES\Figure4.cdr

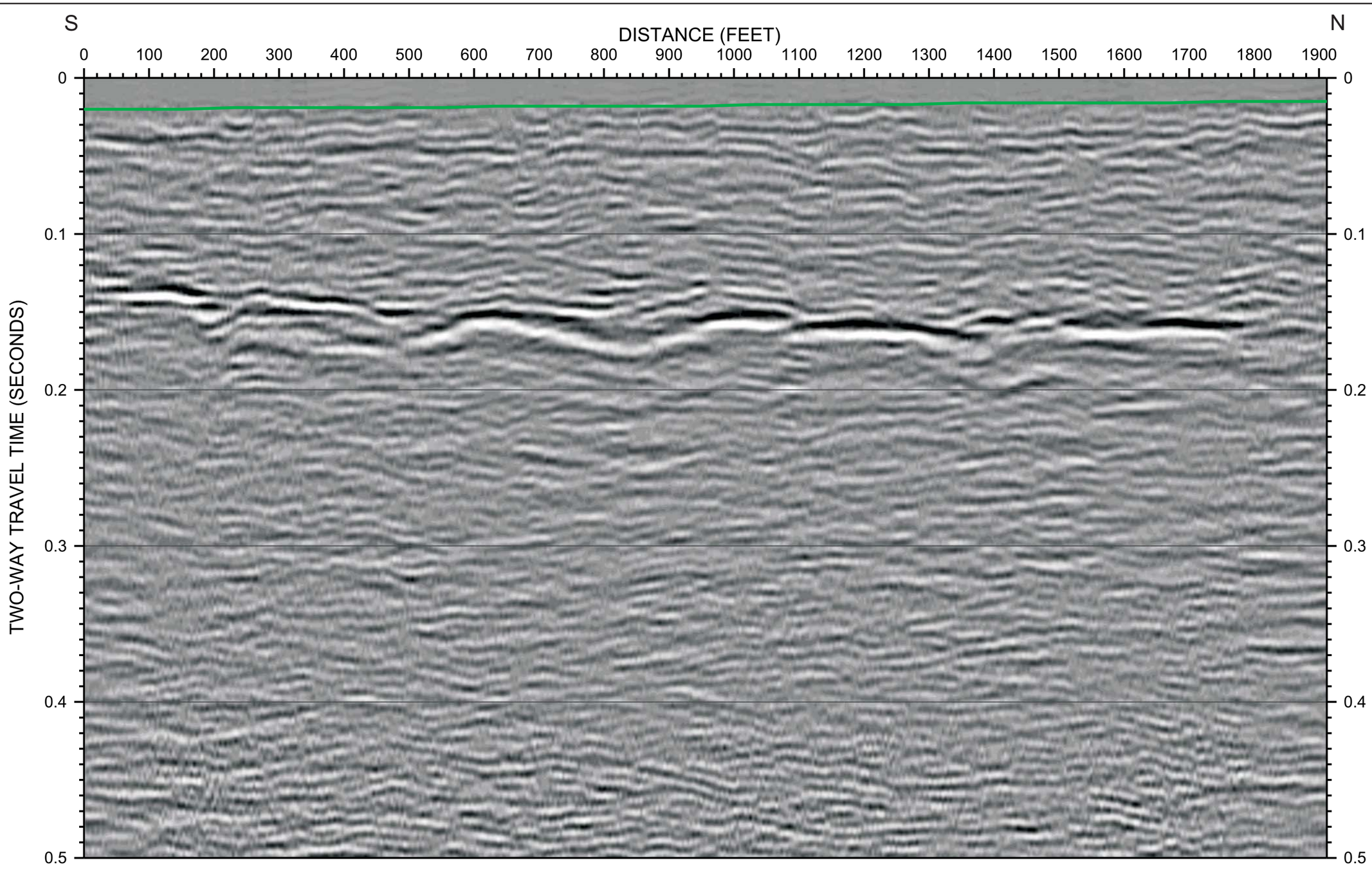


LINE Z3-G1

LEGEND

Ground Surface Reference

GEOVision geophysical services

| | |
|---|---|
| Project # | 9001 |
| Date: | AUG 5, 2009 |
| Drawn By: | A MARTIN |
| Approved By: | |

File R:\...Project Files\2009\9001ch2mhill\REFLReport\FIGURES\Figure17.cdr

FIGURE 17
LINE Z3-G1 SEISMIC SECTION
WITHOUT INTERPRETATION

SR-710 TUNNEL TECHNICAL STUDY
LOS ANGELES COUNTY, CALIFORNIA

PREPARED FOR
CH2M HILL

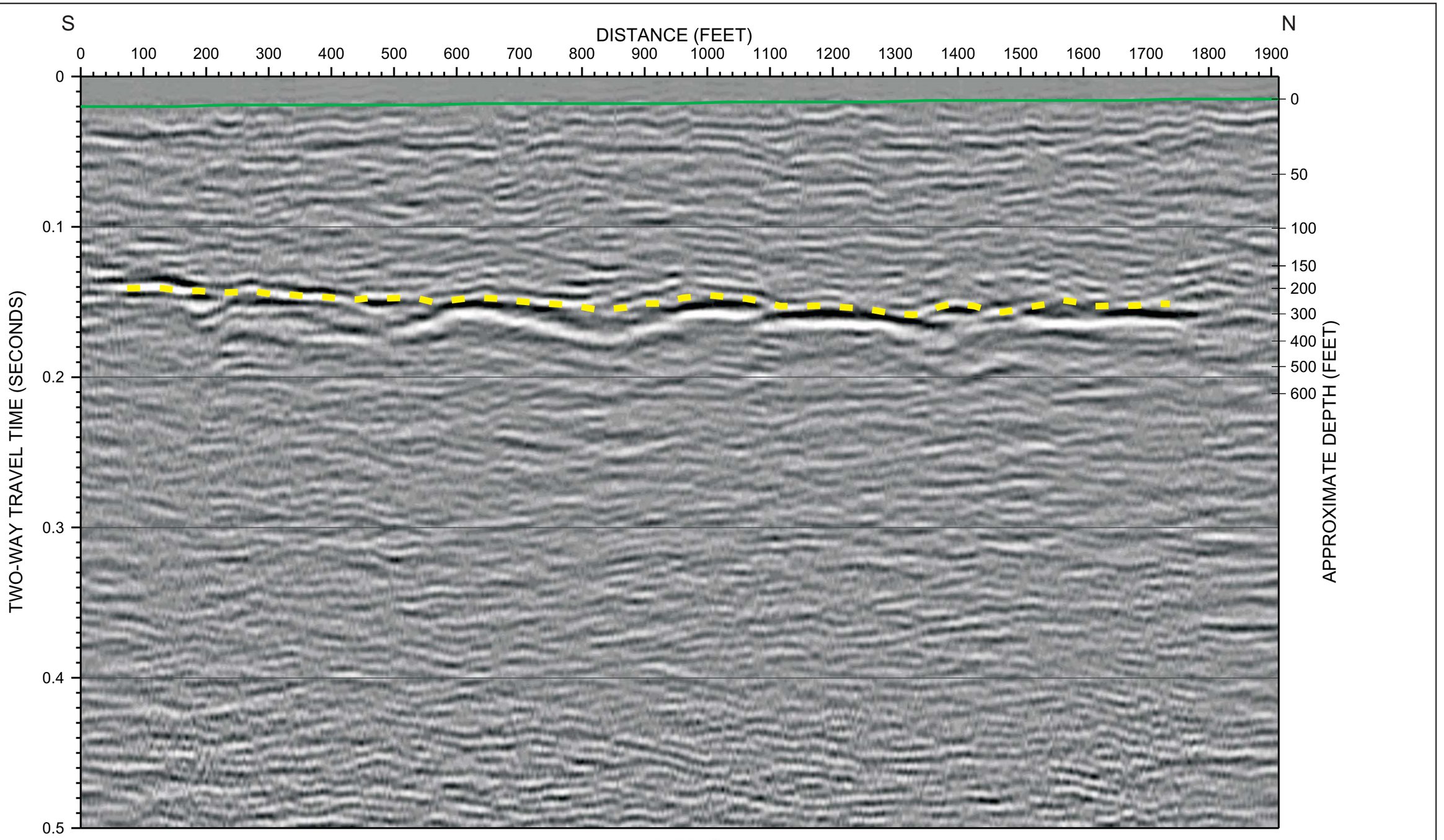


LINE Z3-G1

LEGEND

- Ground Surface Reference
- Interpreted Water Table or Top of Bedrock
- Interpreted Top of Bedrock or Weathering Contact within Bedrock
- Example Seismic Reflector
- Possible Fault, dotted where uncertain

GEOVision geophysical services

| | |
|---|---|
| Project # | 9001 |
| Date: | AUG 5, 2009 |
| Drawn By: | A MARTIN |
| Approved By: | |

File R:\...Project Files\2009\9001ch2mhill\REFLReport\FIGURES\Figure18.cdr

FIGURE 18
LINE Z3-G1 SEISMIC SECTION
WITH INTERPRETATION

SR-710 TUNNEL TECHNICAL STUDY
LOS ANGELES COUNTY, CALIFORNIA

PREPARED FOR
CH2M HILL

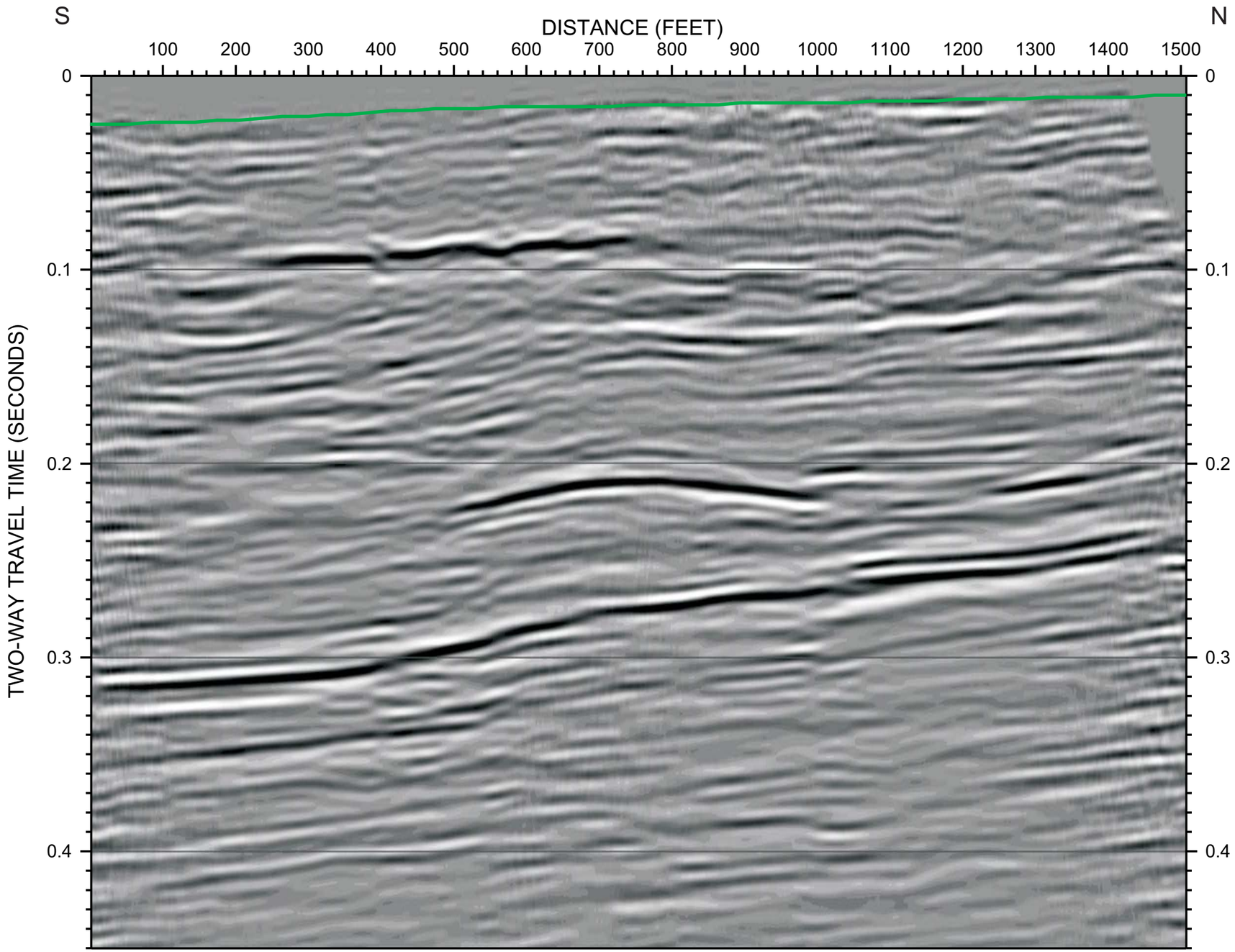


LINE Z3-G6

LEGEND

Ground Surface Reference

GEOVision geophysical services

| | |
|---|---|
| Project # | 9001 |
| Date: | AUG 5, 2009 |
| Drawn By: | A MARTIN |
| Approved By: | |

File R:\...Project Files\2009\9001ch2mhill\REFLReport\FIGURES\Figure27.cdr

FIGURE 27
LINE Z3-G6 SEISMIC SECTION
WITHOUT INTERPRETATION

SR-710 TUNNEL TECHNICAL STUDY
LOS ANGELES COUNTY, CALIFORNIA

PREPARED FOR
CH2M HILL

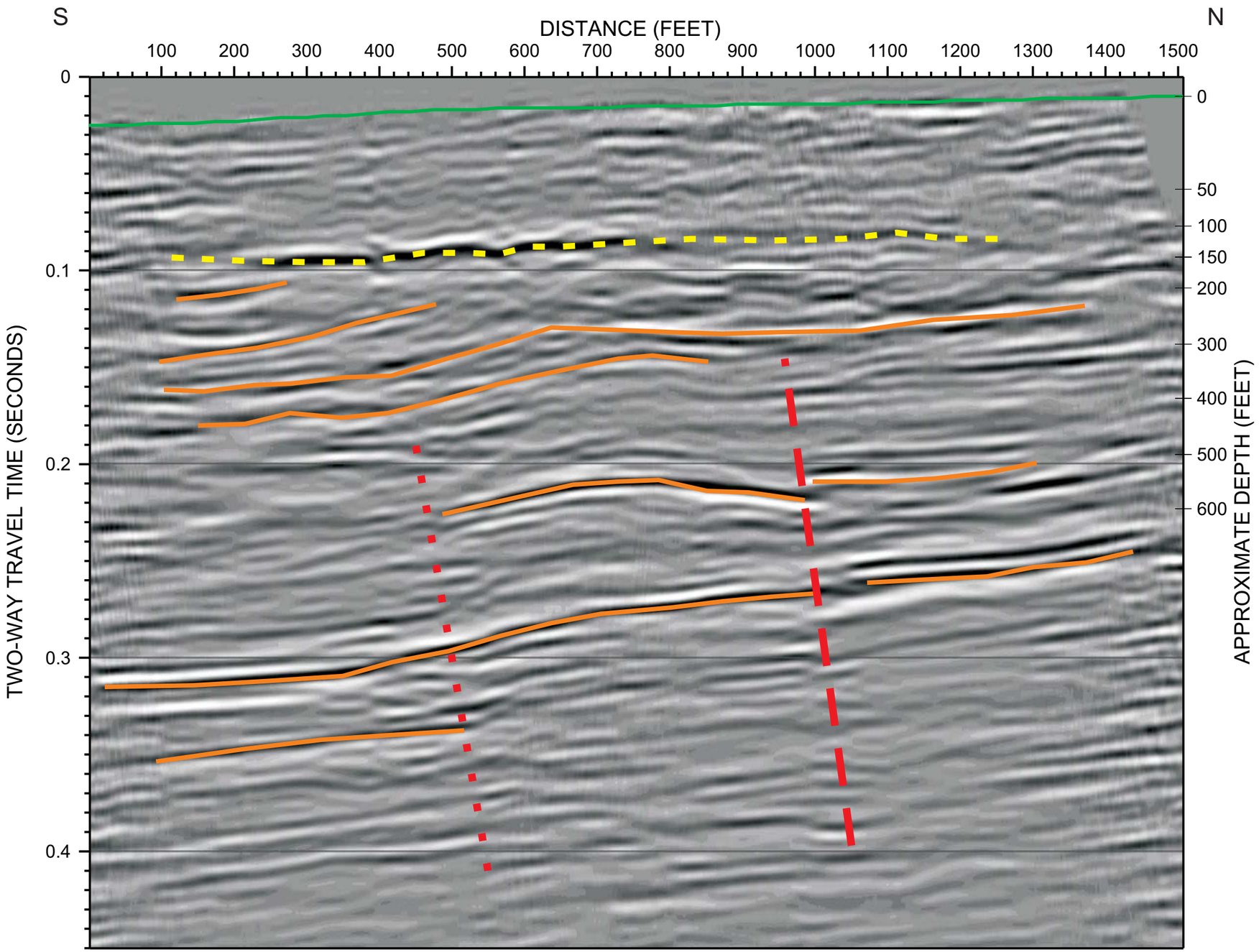


LINE Z3-G6

LEGEND

- Ground Surface Reference
- Interpreted Water Table or Top of Bedrock
- Interpreted Top of Bedrock or Weathering Contact within Bedrock
- Example Seismic Reflector
- Possible Fault, dotted where uncertain

GEOVision geophysical services

| | |
|---|---|
| Project # | 9001 |
| Date: | AUG 5, 2009 |
| Drawn By: | A MARTIN |
| Approved By: | |

File R:\...Project Files\2009\9001ch2mhill\REFLReport\FIGURES\Figure28.cdr

FIGURE 28
LINE Z3-G6 SEISMIC SECTION
WITH INTERPRETATION

SR-710 TUNNEL TECHNICAL STUDY
LOS ANGELES COUNTY, CALIFORNIA

PREPARED FOR
CH2M HILL

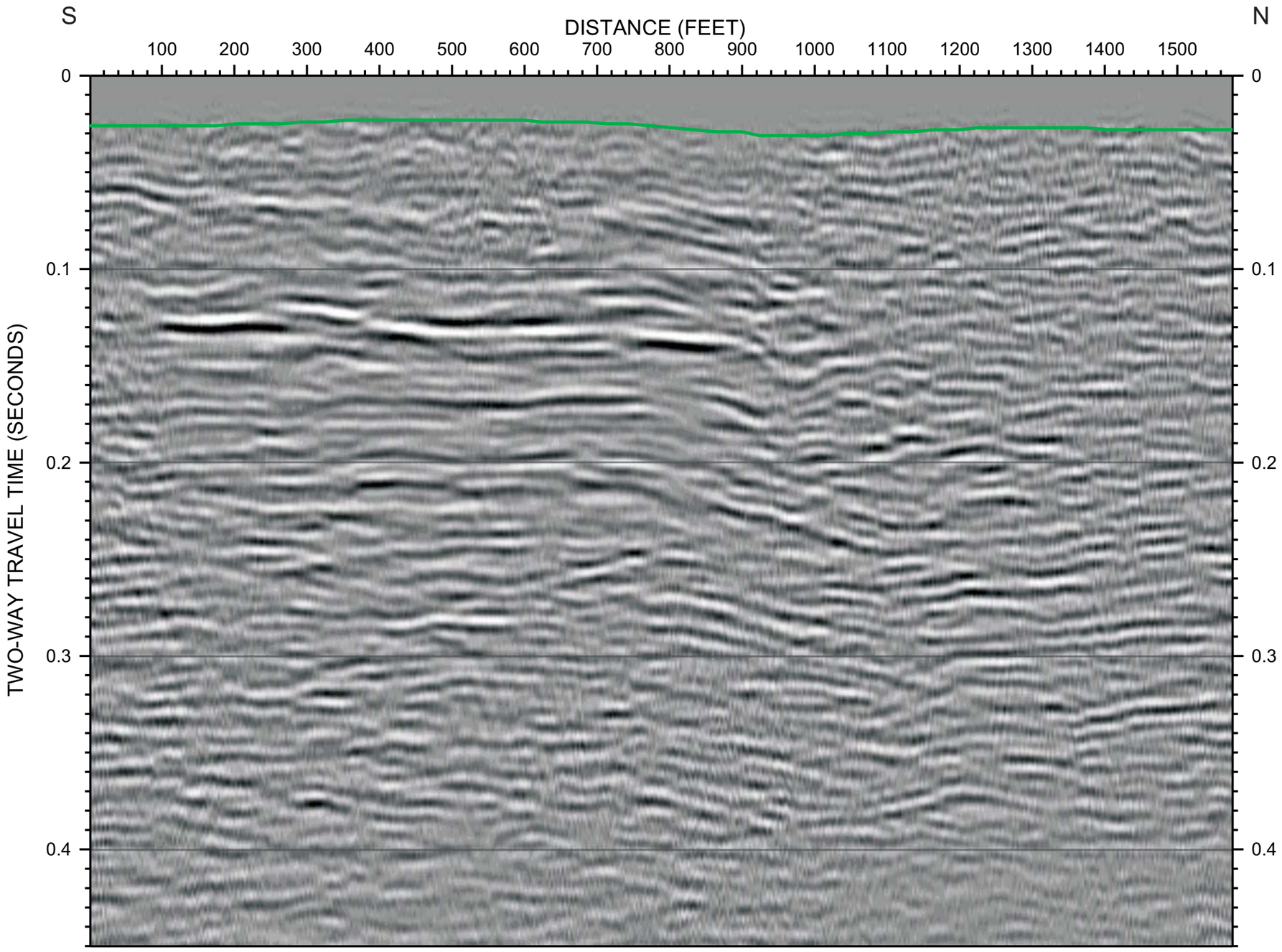


LINE Z3-G7

LEGEND

Ground Surface Reference

GEOVision geophysical services

| | |
|---|---|
| Project # | 9001 |
| Date: | AUG 5, 2009 |
| Drawn By: | A MARTIN |
| Approved By: | |

File R:\...Project Files\2009\9001ch2mhill\REFLReport\FIGURES\Figure29.cdr

FIGURE 29
LINE Z3-G7 SEISMIC SECTION
WITHOUT INTERPRETATION

SR-710 TUNNEL TECHNICAL STUDY
LOS ANGELES COUNTY, CALIFORNIA

PREPARED FOR
CH2M HILL

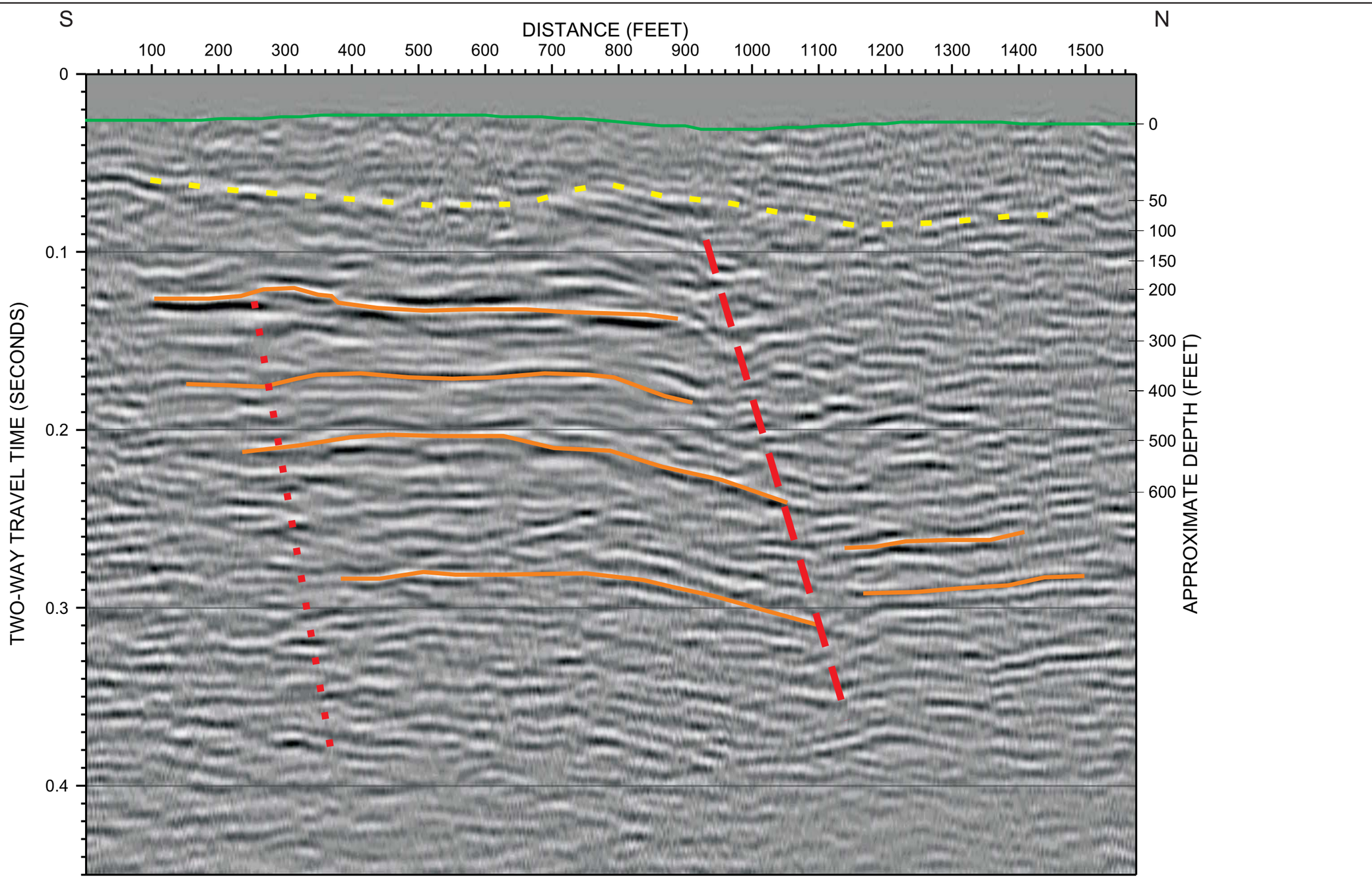


LINE Z3-G7

LEGEND

- Ground Surface Reference
- Interpreted Water Table or Top of Bedrock
- Interpreted Top of Bedrock or Weathering Contact within Bedrock
- Example Seismic Reflector
- Possible Fault, dotted where uncertain

GEOVision geophysical services

| | |
|---|---|
| Project # | 9001 |
| Date: | AUG 5, 2009 |
| Drawn By: | A MARTIN |
| Approved By: | |

File R:\...Project Files\2009\9001ch2mhill\REFLReport\FIGURES\Figure30.cdr

FIGURE 30
LINE Z3-G7 SEISMIC SECTION
WITH INTERPRETATION

SR-710 TUNNEL TECHNICAL STUDY
LOS ANGELES COUNTY, CALIFORNIA

PREPARED FOR
CH2M HILL

SW

NE

DISTANCE (FEET)

0 100 200 300 400 500 600 700 800 900 1000 1100 1200 1300 1400 1500 1600 1700 1800 1900

TWO-WAY TRAVEL TIME (SECONDS)

0 0.1 0.2 0.3 0.4 0.5 0.6

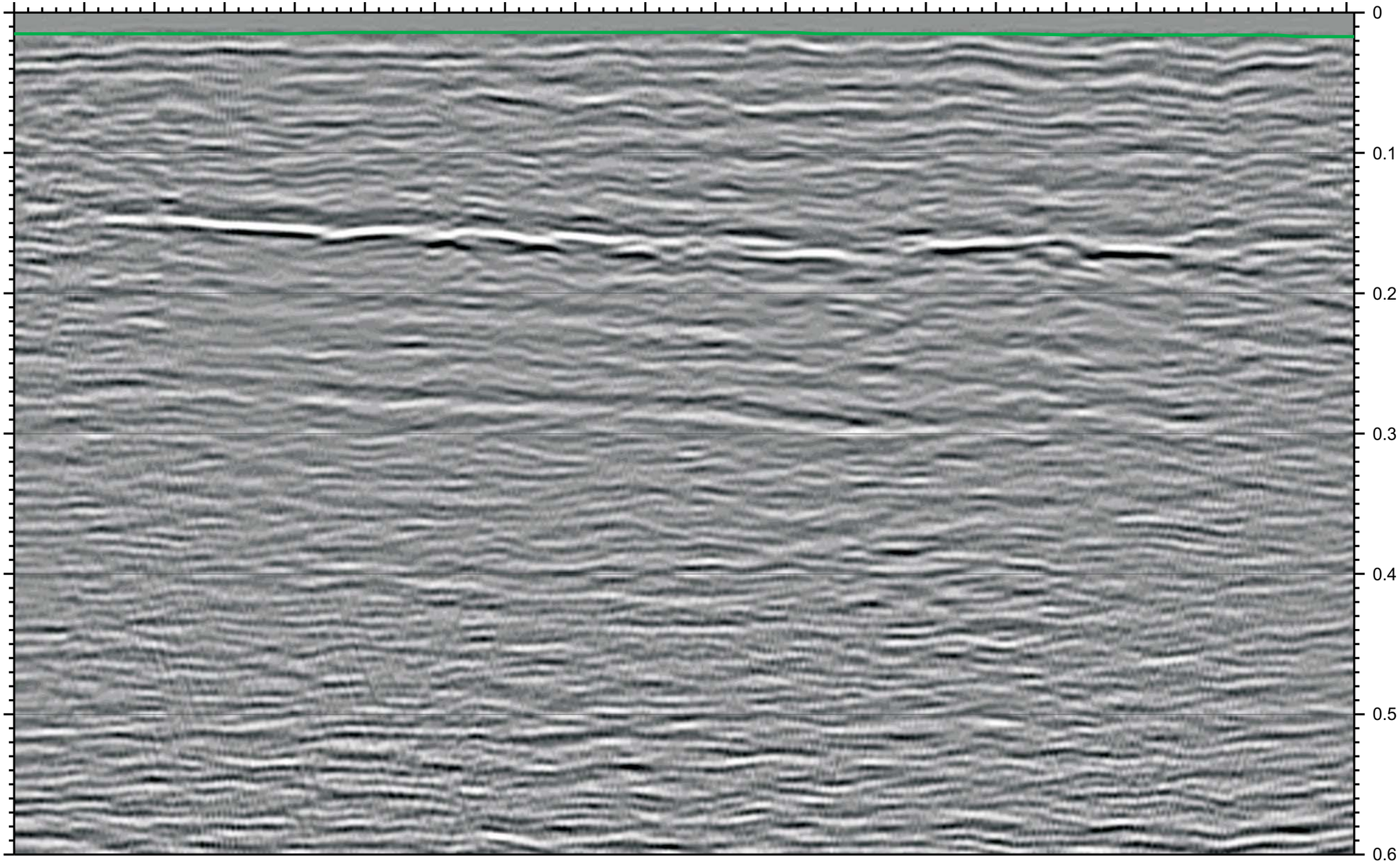

LINE Z4-G2

LEGEND

Ground Surface Reference

GEOVision geophysical services

| | |
|---|---|
| Project # | 9001 |
| Date: | AUG 5, 2009 |
| Drawn By: | A MARTIN |
| Approved By: | |

File R:\...Project Files\2009\9001ch2mhill\REFLReport\FIGURES\Figure33.cdr

FIGURE 33
LINE Z4-G2 SEISMIC SECTION
WITHOUT INTERPRETATION

SR-710 TUNNEL TECHNICAL STUDY
LOS ANGELES COUNTY, CALIFORNIA

PREPARED FOR
CH2M HILL

SW

NE

DISTANCE (FEET)

0 100 200 300 400 500 600 700 800 900 1000 1100 1200 1300 1400 1500 1600 1700 1800 1900

TWO-WAY TRAVEL TIME (SECONDS)

0 0.1 0.2 0.3 0.4 0.5 0.6

APPROXIMATE DEPTH (FEET)

0 50 100 150 200 300 400 500 600

LINE Z4-G2

LEGEND

- Ground Surface Reference
- Interpreted Water Table or Top of Bedrock
- Interpreted Top of Bedrock or Weathering Contact within Bedrock
- Example Seismic Reflector
- Possible Fault, dotted where uncertain

GEOVision geophysical services

Project # 9001
Date: AUG 5, 2009
Drawn By: A MARTIN
Approved By:

File R:\...Project Files\2009\9001ch2mhill\REFLReport\FIGURES\Figure34.cdr

FIGURE 34
LINE Z4-G2 SEISMIC SECTION
WITH INTERPRETATION

SR-710 TUNNEL TECHNICAL STUDY
LOS ANGELES COUNTY, CALIFORNIA

PREPARED FOR
CH2M HILL

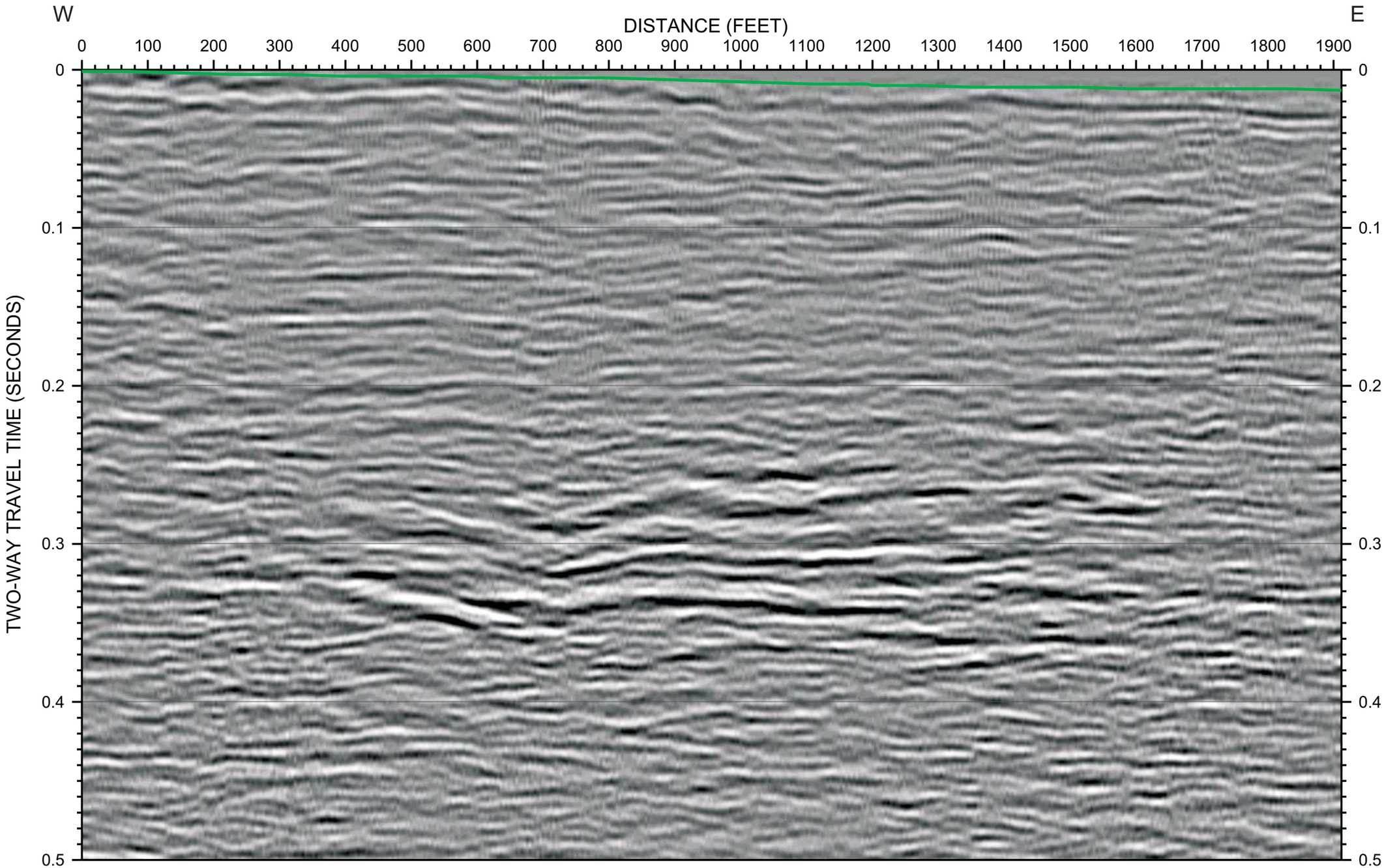


LINE Z5-G2

LEGEND

Ground Surface Reference

GEOVision geophysical services

| | |
|---|---|
| Project # | 9001 |
| Date: | AUG 5, 2009 |
| Drawn By: | A MARTIN |
| Approved By: | |

File R:\...Project Files\2009\9001ch2mhill\REFLReport\FIGURES\Figure35.cdr

FIGURE 35
LINE Z5-G2 SEISMIC SECTION
WITHOUT INTERPRETATION

SR-710 TUNNEL TECHNICAL STUDY
LOS ANGELES COUNTY, CALIFORNIA

PREPARED FOR
CH2M HILL

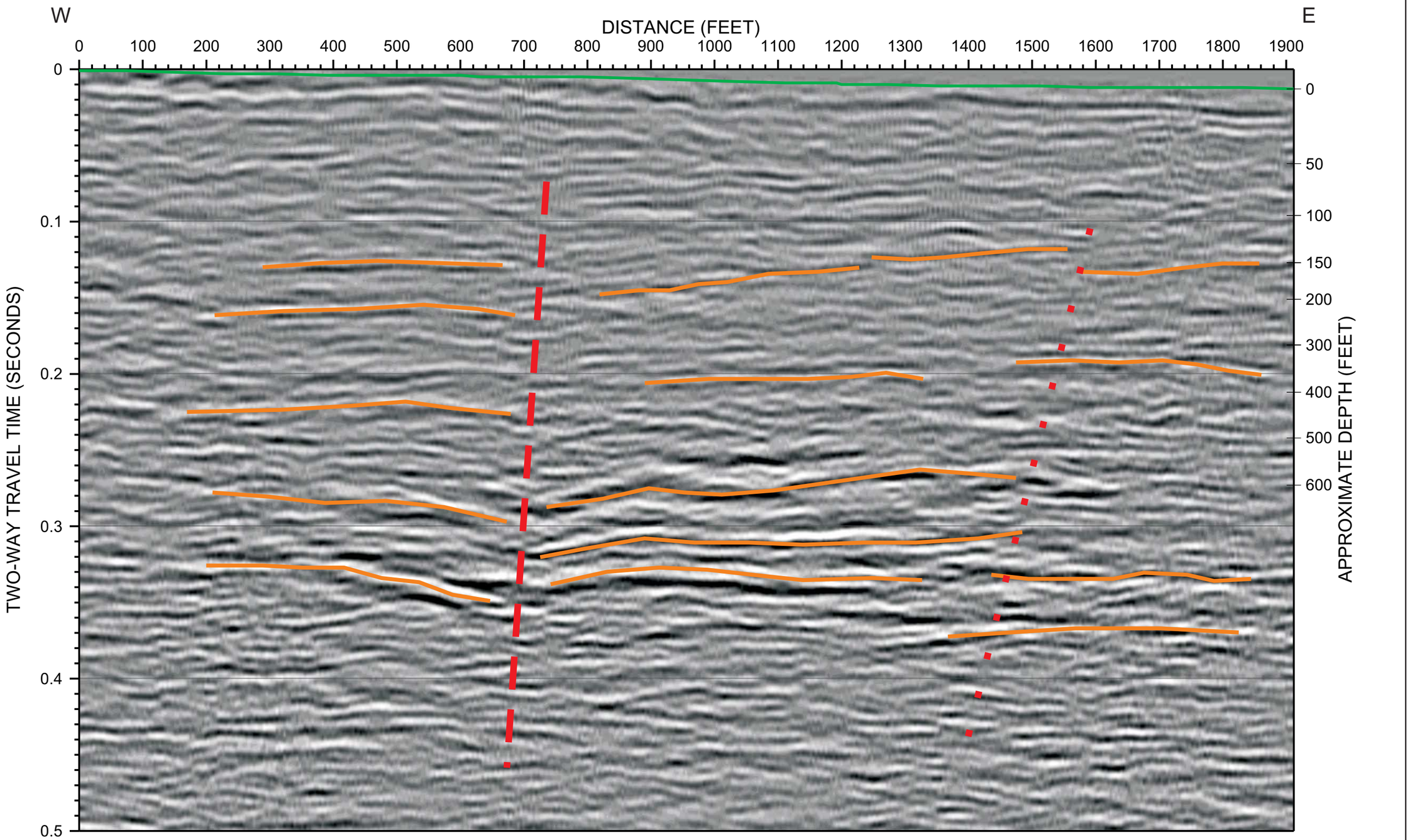


LINE Z5-G2

LEGEND

- Ground Surface Reference
- Interpreted Water Table or Top of Bedrock
- Interpreted Top of Bedrock or Weathering Contact within Bedrock
- Example Seismic Reflector
- Possible Fault, dotted where uncertain

GEOVision geophysical services

| | |
|---|---|
| Project # | 9001 |
| Date: | AUG 5, 2009 |
| Drawn By: | A MARTIN |
| Approved By: | |

File R:\...Project Files\2009\9001ch2mhill\REFLReport\FIGURES\Figure36.cdr

FIGURE 36
LINE Z5-G2 SEISMIC SECTION
WITH INTERPRETATION

SR-710 TUNNEL TECHNICAL STUDY
LOS ANGELES COUNTY, CALIFORNIA

PREPARED FOR
CH2M HILL

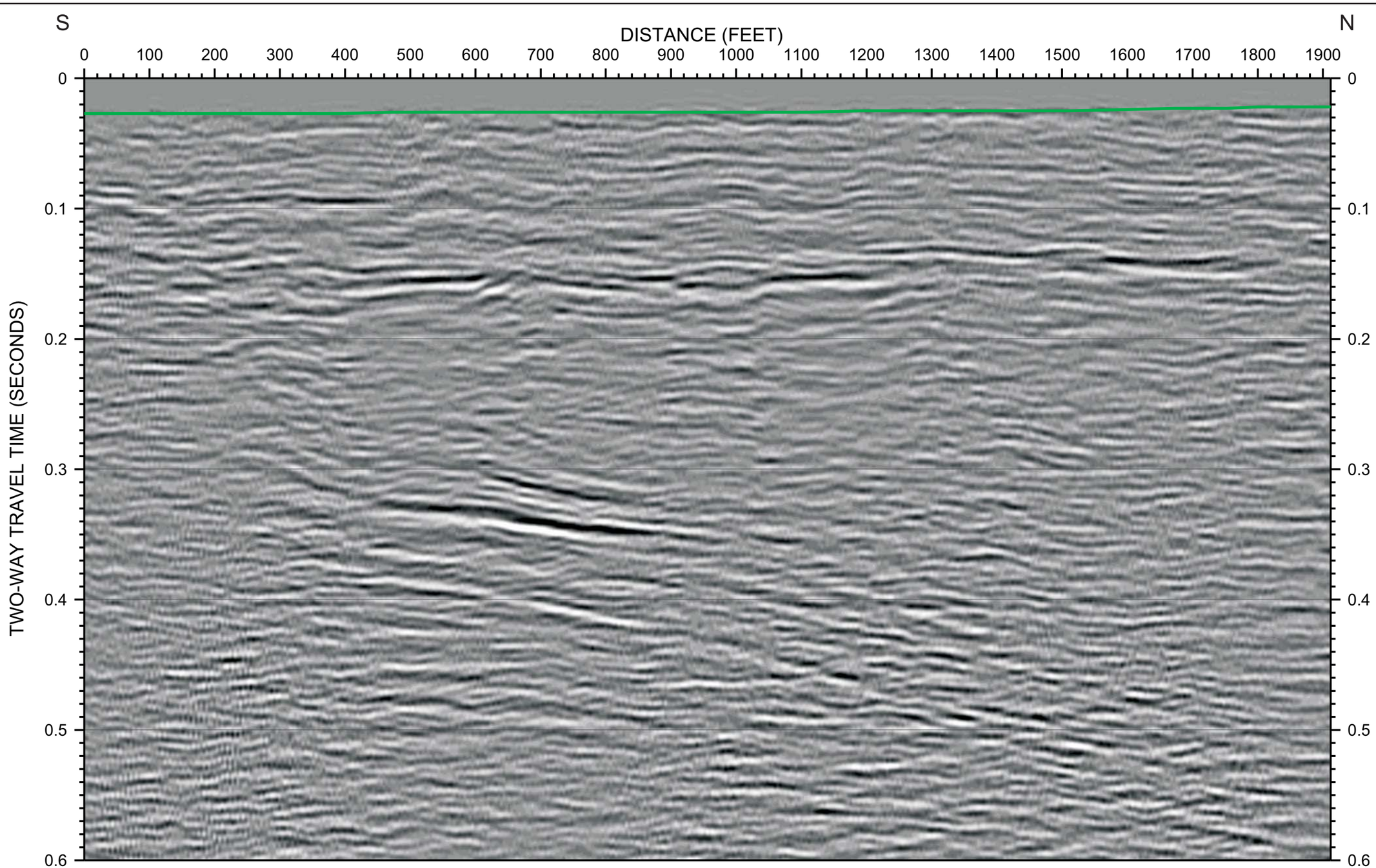


LINE Z5-G3

LEGEND

Ground Surface Reference

GEOVision geophysical services

| | |
|---|---|
| Project # | 9001 |
| Date: | AUG 5, 2009 |
| Drawn By: | A MARTIN |
| Approved By: | |

File R:\...Project Files\2009\9001ch2mhill\REFLReport\FIGURES\Figure37.cdr

FIGURE 37
LINE Z5-G3 SEISMIC SECTION
WITHOUT INTERPRETATION

SR-710 TUNNEL TECHNICAL STUDY
LOS ANGELES COUNTY, CALIFORNIA

PREPARED FOR
CH2M HILL

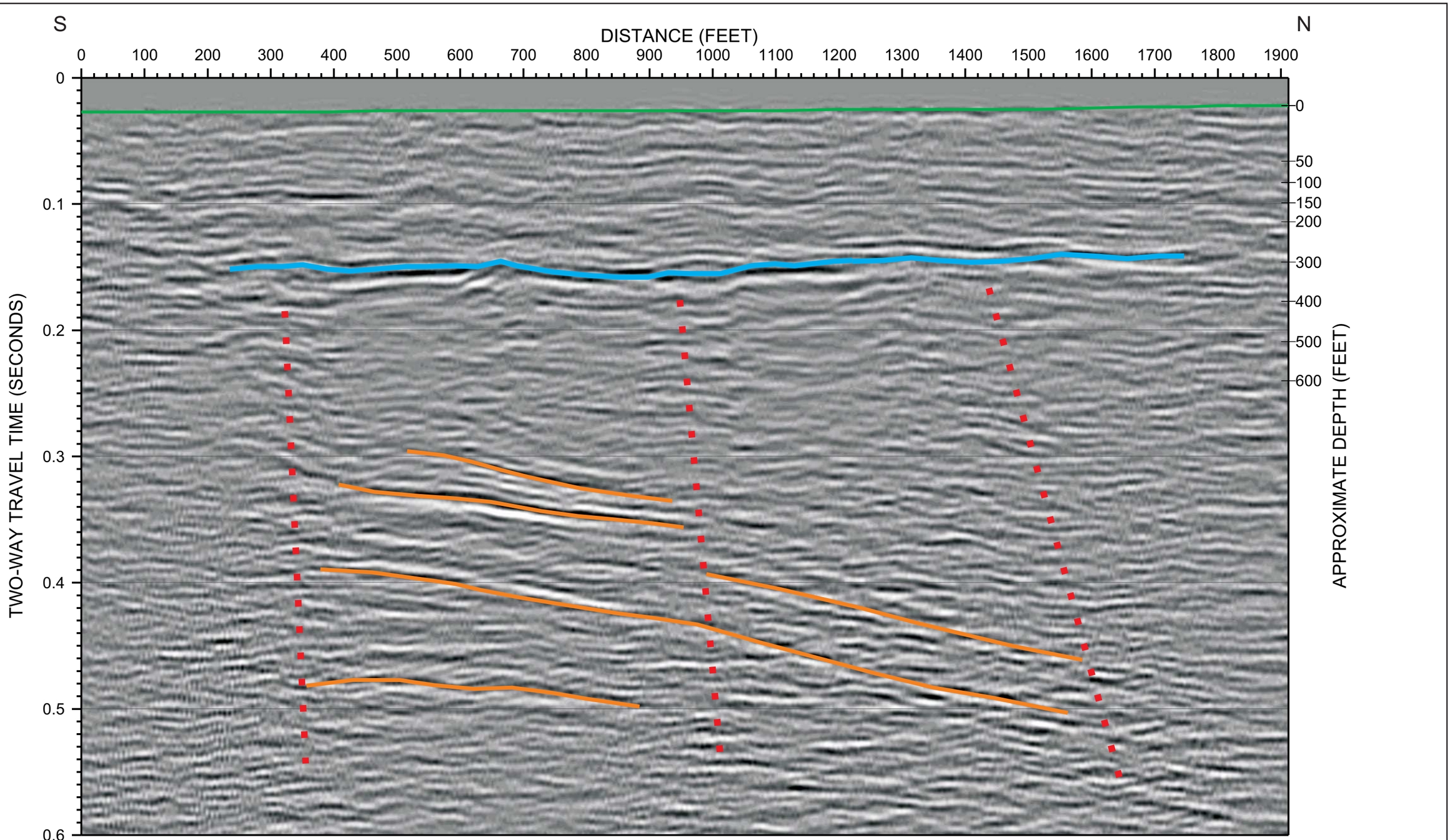


LINE Z5-G3

LEGEND

- Ground Surface Reference
- Interpreted Water Table or Top of Bedrock
- Interpreted Top of Bedrock or Weathering Contact within Bedrock
- Example Seismic Reflector
- Possible Fault, dotted where uncertain

GEOVision geophysical services

| | |
|---|---|
| Project # | 9001 |
| Date: | AUG 5, 2009 |
| Drawn By: | A MARTIN |
| Approved By: | |

File R:\...Project Files\2009\9001ch2mhill\REFLReport\FIGURES\Figure38.cdr

FIGURE 38
LINE Z5-G3 SEISMIC SECTION
WITH INTERPRETATION

SR-710 TUNNEL TECHNICAL STUDY
LOS ANGELES COUNTY, CALIFORNIA

PREPARED FOR
CH2M HILL

# REPORT

# SURFACE WAVE MEASUREMENTS

## SR-710 Tunnel Technical Study
## Los Angeles County, California

***Prepared for***

**CH2M HILL**
**6 Hutton Centre Drive, # 700**
**Santa Ana, CA 92707**

***Prepared by***

**GEOVision Geophysical Services**
**1124 Olympic Drive**
**Corona, California 92881**
**(951) 549-1234**

**Report 9001-01**

**October 5, 2009**

# TABLE OF CONTENTS

# LIST OF TABLES

## LIST OF FIGURES

# 1 INTRODUCTION

In-situ seismic measurements using active and passive surface wave techniques were performed at various sites within the SR-710 Tunnel Study Areas, located in Los Angeles County, California. The measurements were conducted from February 24, 2009 through May 19, 2009. The purpose of this investigation was to provide shear (S) wave velocity profiles to a depth of 60 meters (200 ft) to support site characterization and screening of the five tunnel study zones. Some of the surface wave soundings were acquired near the ends of the 17 seismic reflection profiles acquired during the investigation to provide additional data for seismic interpretation.

The active surface wave technique utilized during this investigation consisted of the multi-channel analysis of surface waves (MASW) method. The passive surface wave techniques utilized consisted of the refraction microtremor and the array microtremor methods. At many sites active surface wave techniques (SASW and MASW) with the utilization of portable energy sources, such as hammers and weight drops, are sufficient to obtain a 30 m S-wave velocity sounding. Larger energy sources, such as a bulldozer, may be used to image to depths of up to 100 m, but are not typically applicable in developed urban environments. Passive surface wave techniques, such as the refraction microtremor method of Louie, 2001 or the array microtremor technique, can be used to extend depth of investigation at sites that have adequate noise levels.

S-wave velocity models developed from surface wave soundings have many potential applications related to site characterization including correlation of seismic properties between boreholes; estimating depth to bedrock (providing there is sufficient contrast in velocity between bedrock and overlying sediments), estimating N-value using emperical correlations between S-wave velocity and N-value, estimation of excavatability or rippability of rock. The S-wave velocity models can also be used to determine average S-wave velocity over depth intervals. For example, the average shear wave velocity of the upper 30 m or 100 ft ($V_S30$) is used in the Uniform Building Code (UBC) and International Building Code (IBC) to separate sites into classes for seismic design.

MASW and refraction microtremor data were collected at 78 locations within the five tunnel study zones, labeled Zones 1 to 5 (Figure 1). Array microtremor data, using an “L” shaped array, were collected at 69 of the locations. The 78 surface wave soundings included 20 soundings in Zone 1, 12 soundings in Zone 2, 24 soundings in Zone 3, 10 soundings in Zone 4 and 12 soundings in Zone 5 as shown on Figure 1. A total of 35 surface wave soundings were conducted on seismic reflection profiles acquired as part of this investigation and reported separately. The remaining 43 surface wave soundings were distributed throughout the tunnel study zones.

This report contains the results of the active and passive surface wave measurements conducted at 78 locations at the site. An overview of the surface wave methods is given in Section 2. Field and data reduction and modeling procedures are discussed in Sections 3 and 4, respectively. Interpretation and results are presented in Section 5. Section 6 presents our conclusions. References and our professional certification are presented in Sections 7 and 8, respectively.

# 2 OVERVIEW OF THE SURFACE WAVE METHODS

A discussion of active and passive surface wave methods is provided in the technical note included as Appendix A. Active surface wave techniques include the spectral analysis of surface waves (SASW) and multi-channel array surface wave (MASW) methods. Passive surface wave techniques include the refraction and array microtremor methods.

The basis of surface wave methods is the dispersive characteristic of Rayleigh waves when propagating in a layered medium. The phase velocity, $V_R$, depends primarily on the material properties ($V_S$, mass density, and Poisson's ratio or compression wave velocity) over a depth of approximately one wavelength. Waves of different wavelengths, $\lambda$, (or frequencies, f) sample different depths. As a result of the variance in the shear stiffness of the layers, waves with different wavelengths travel at different phase velocities; hence, dispersion. A surface wave dispersion curve, or dispersion curve for short, is the variation of $V_R$ with $\lambda$ or f.

The MASW method is an in-situ seismic method for determining shear wave velocity ($V_S$) profiles [Park et al., 1999a and 1999b, Foti, 2000]. Surface wave techniques are non-invasive and non-destructive, with all testing performed on the ground surface at strain levels in the soil in the elastic range (< 0.001%). MASW testing consists of collecting multi-channel seismic data in the field and applying a wavefield transform to obtain the dispersion curve and data modeling.

A detailed description of the MASW method is given by Park, 1999a and 1999b. Ground motions are recorded by 24 or more geophones spaced 1 to 2 m apart and aligned in a linear array and connected to a seismograph. A wavefield transform, such as the f-k or $\tau$-p transform, is applied to the time history data to isolate the surface wave dispersion curve. PICKWIN95, software developed by Oyo Corporation is typically used to process the MASW data and obtain the dispersion curve.

The refraction microtremor technique is a passive surface wave technique developed by Dr. John Louie at University of Nevada, Reno. A detailed description of this technique can be found in Louie, 2001. The refraction microtremor method differs from the more established array microtremor technique in that it uses a linear receiver array rather than a triangular or circular array. Unlike the MASW method, which uses an active energy source (i.e. hammer), the microtremor technique records background noise emanating from ocean wave activity, wind noise, traffic, industrial activity, construction, etc. Refraction microtremor field procedures consist of laying out a linear array of 24, 4.5 to 8 Hz geophones and recording 10, or more, 15 to 60 second noise records. These noise records are reduced using the software package SeisOpt® ReMi™ v2.0 by Optim™ Software and Data Services. This package is used to generate and combine the slowness (p) – frequency (f) transform of the noise records. The surface wave dispersion curve is picked at the lower envelope of the surface wave energy identified in the p-f spectrum.

A detailed discussion of the array microtremor method can be found in Okada, 2003. This technique uses 4 to 24 receivers aligned in a 2-dimensional array. Triangle, circle, semi-circle and "L" shaped arrays are commonly used, although any 2-dimensional arrangement of receivers can be used. Receivers typically consist of 1 to 4.5 Hz geophones. The triangle array, which

consists of several embedded equilateral triangles, is often used as it provides good results with a relatively small number of geophones. With this array the outer side of the triangle should be at least equal to the desired depth of investigation. The "L" array is useful at sites located at the corner of perpendicular intersecting streets. Typically 10 to 20, 30-second noise records are acquired for analysis. The surface wave dispersion curve is estimated by calculating the spatial autocorrelation (SPAC) function for the time-history data. A first-order Bessel function is fit to the SPAC function to obtain the dispersion curve (phase velocity at each frequency). PICKWIN95, software developed by Oyo Corporation is typically used to process the array microtremor data and obtain the dispersion curve.

The active and passive surface wave techniques compliment one another as outlined below:

- SASW/MASW techniques image the shallow velocity structure which cannot be imaged by the microtremor technique and is needed for an accurate $V_S30/V_S100$' estimate.
- Microtremor techniques work best in noisy environments where SASW/MASW depth investigation may be limited.
- In a noisy environment the microtremor technique will usually extend the depth of an SASW/MASW sounding.
- The degree of fit in the overlapping portion of the dispersion curves from the two techniques provides a level of confidence in the results.

The dispersion curves generated from the active and passive surface wave soundings are generally combined and modeled. Typically WinSASW V1, developed at the University of Texas at Austin, or WINSASW V2 (Joh, 2002) is used to model the data, whereby through iterative forward and/or inverse modeling, a $V_S$ profile is found whose theoretical dispersion curve is a close fit to the field data.

The final model profile is assumed to represent actual site conditions. Several options exist for forward modeling: a formulation that takes into account only fundamental-mode Rayleigh wave motion (called the 2-D solution) and one that includes all stress waves and incorporates receiver geometry (3-D solution) [Roesset et al., 1991].

The theoretical model used to interpret the dispersion assumes horizontally layered, laterally invariant, homogeneous-isotropic material. Although these conditions are seldom strictly met at a site, the results of active and/or passive surface wave testing provide a good "global" estimate of the material properties along the array. The results may be more representative of the site than a borehole "point" estimate.

Based on our experience at other sites, the shear wave velocity models determined by surface wave testing are within 20% of the velocities that would be determined by other seismic methods [Brown, 1998]. The average velocity of the upper 30 m or 100 ft, however, is much more accurate than this, often to better than 5%, because it is less sensitive to the layering in the model.

# 3 FIELD PROCEDURES

MASW and refraction microtremor data were collected at 78 locations within the five SR-710 tunnel study zones (Figure 1). The approximate locations of the surface wave soundings are presented in Table 1. Array microtremor data were collected at 69 of the 78 surface wave locations as shown in Table 2.

A typical MASW field layout is shown in Appendix A and Figure 2. MASW equipment used during this investigation consisted of a Geometrics Geode signal enhancement seismograph, 4.5 Hz vertical geophones, seismic cable with 1 to 3 m (3.3 to 9.8 ft) takeouts, a 3 lb hammer, a 16 lb sledge hammer, a truck-mounted accelerated weight drop (AWD) and an aluminum plate. MASW data were acquired along a linear array with 1 to 2 m (3.3 to 6.6 ft) geophone spacing as outlined in Table 2. Shot points were typically located 1, 3 and 5 m (3.3, 9.8 and 16.4 ft) from the end geophone locations. Typically, the 3 lb hammer was used for the 1 m (3.3 ft) offset source locations, a 16 lb sledge hammer was used for the 3 m (9.8 ft) offset source locations, and the 16 lb sledge hammer and/or AWD were used for the 5 m (16.4 ft) offset source locations. Only the hammer energy sources could be used for the MASW survey at some locations because of space or permitting limitations. Data from the transient impacts (hammers) were averaged 5 times to improve the signal-to-noise ratio. Surface waves were monitored by 24 Oyo Geospace 4.5 Hz geophones and recorded by a Geometrics Geode signal enhancement seismograph. Photographs of typical MASW equipment are presented in Appendix A. All field data was saved to hard disk and documented in a field notebook.

Refraction microtremor measurements were made along a linear array of 24, 4.5 Hz geophones with a 6 m (19.7 ft) geophone spacing, as possible. When a 6 m geophone spacing was not possible due to space limitations, it was adjusted to a 4 or 5.5 m (13.1 or 18 ft) spacing as outlined in Table 2. The refraction microtremor arrays were typically located along sidewalks. A typical field layout is shown in Appendix A. A Geometrics Geode, 24 bit, 24-channel seismic recording system was used to record thirty 30 second noise records using a 2 ms sample rate. Data were stored on a laptop computer for later processing and field geometry and associated files names were documented in a field notebook.

Array microtremor measurements were made along a 24-channel “L”-shaped array using 4.5Hz geophones with a geophone spacing of 6 m (19.7 ft) when possible. When a geophone spacing of 6 m was not possible because of space limitations, a 5 or 5.5 m (16.4 or 18 ft) geophone spacing was used as outlined in Table 2. The array microtremor measurements were typically made along sidewalks of intersecting streets. Occasionally, the geometry of the streets required that the intersecting legs of the array were at an angle other than 90 degrees (i.e. “V” shaped rather than “L” shaped array). A Geometrics Geode, 24 bit, 24-channel seismic recording system was used to record thirty 30 second noise records using a 2ms sample rate. Data were stored on a laptop computer for later processing and field geometry and associated files names were documented in a field notebook.

Surface wave sounding locations or seismic lines to which they were tied were surveyed with a Trimble Pro XRS GPS system with OmniStar submeter differential corrections. Estimated accuracy of the locations and elevations are nominally about 1 m (3.3 ft) and 2 m (6.6 ft), respectively.

# 4 DATA REDUCTION AND MODELING

The MASW data were reduced using the software PICKWIN95 developed by Oyo Corporation and the following steps:

- Input seismic record into software.
- Enter receiver spacing, geometry and wavelength restrictions, as necessary.
- Apply wavefield transform to seismic record to convert the data to phase velocity – frequency space.
- Identify and pick dispersion curve.
- Repeat for all shot records and merge dispersion curves.
- Convert dispersion curves to WinSASW format for modeling.

The refraction microtremor data were reduced using the Optim™ Software and Data Services SeisOpt® ReMi™ v4.0 data analysis package. Data reduction steps included the following:

- Conversion of SEG-2 format field files to SEG-Y format.
- Data preprocessing which includes trace-equalization gaining and DC offset removal.
- Erasing receiver geometry present in the file header.
- Computing the velocity spectrum of each record by p-f transformation.
- Combining the individual p-f transforms into one image.
- Picking and saving the velocity spectrum image.
- Conversion of the dispersion curve to WinSASW format for modeling.

The array microtremor and refraction microtremor data were reduced using the software PICKWIN95 developed by Oyo Corporation and the following steps:

- Input all seismic records into software.
- Enter receiver spacing, geometry and wavelength restrictions, as necessary.
- Calculate the SPAC function for each seismic record and average.
- For each frequency calculate the degree of fit of a first-order Bessel function to the SPAC function for a multitude of phase velocities.
- Identify and pick dispersion curve as the best fit of the Bessel function for each frequency.
- Convert dispersion curves to WinSASW format for modeling

Example wavefield transforms of the MASW and microtremor data are presented in Figure 3. The surface wave dispersion curves from the active and passive surface wave data were combined to obtain a composite surface wave dispersion curve. Due to lateral velocity variation at many of the surface wave sounding locations, most likely related to subsurface bedrock topography or the often steeply dipping bedrock units, it was not always possible to combine all of the passive surface wave data sets with the MASW data. The datasets with the best agreement were used to create the composite dispersion curve.

The location of surface wave sounding Z1-S17 was such that reliable active and passive surface wave data were not obtained. An S-wave velocity model was not generated for this sounding.

Once a composite surface wave dispersion curve was developed an iterative forward modeling process was used to generate an S-wave velocity model for the sounding. During this process an initial velocity model was generated based on general characteristics of the dispersion curve. The theoretical dispersion curve was then generated using the 2-D modeling algorithm (fundamental mode Rayleigh wave dispersion module) and compared to the field dispersion curve. Adjustments were then made to the thickness and velocities of each layer and the process repeated until an acceptable fit to the field data was obtained.

Data inputs into the modeling software included layer thickness, S-wave velocity, P-wave velocity and mass density. P-wave velocity and mass density only have a very small influence (i.e. less than 10%) on the S-wave velocity model generated from a surface wave dispersion curve. However, realistic assumptions for P-wave velocity, which is impacted significantly by the location of the water table, and mass density will slightly improve the accuracy of the S-wave velocity model.

Constant mass density values of 1.9 to 2.3 g/cc were used in the velocity profiles for subsurface soils and rock. Within the normal range encountered in geotechnical engineering, variation in mass density has a negligible effect on surface wave dispersion. During data modeling, the compression wave velocity, $V_P$, of unsaturated soils was estimated using a Poisson's ratio, $\nu$, of 0.33 and the relationship:

$$V_P = V_S\,[(2(1-\nu))/(1-2\nu)]^{0.5}.$$

Several approaches were used to estimate groundwater depth in the vicinity of the surface wave soundings. These included a simple, interactive, 2 to 3 layer seismic refraction analysis of MASW shot records and/or selected seismic reflection shot records; review of borehole velocity logs, and interpolation between boreholes or seismic reflection lines. Groundwater depth was assumed for modeling purposes when reasonable estimates could not be made from available surface and borehole geophysical data.

Borehole velocity logs within each of the five tunnel study zones (Zones 1 to 5) were reviewed to correlate P-wave velocity of saturated sediments with S-wave velocity. Borehole velocity and geologic logs were also reviewed to determine if S-wave velocity could be used to differentiate bedrock from overlying sediments. Borehole velocity logs (reported separately) for 6 boreholes (Z1-B3, Z1-B4, Z1-B5, Z1-B6, Z1-B7 and Z1-B8) were available in Zone 1. Borehole velocity logs for 4 boreholes (Z2-B1, Z2-B3, Z2-B4 and Z2-B5) were available in Zone 2. Borehole velocity logs for 12 boreholes (Z3-B1 to Z3-B12) were available in Zone 3. A borehole velocity log for one borehole (Z4-B4) was available in Zone 4. Borehole velocity logs were not available for Zone 5.

# 5 INTERPRETATION AND RESULTS

## *5.1 Zone 1*

Twenty (20) surface wave soundings were conducted within Zone 1 (Z1-S1 to Z1-S20) as shown in Figure 1. Six of these surface wave soundings were located near the ends of seismic reflection lines and the remaining 14 soundings were distributed throughout the zone.

The fit of the theoretical dispersion curve to the experimental data collected at each site and the modeled $V_S$ profiles for Z1-S1 to Z1-S16 and Z1-S18 to Z1-S20 are presented in Figures 4 to 22, respectively. The resolution decreases gradually with depth because of the loss of sensitivity of the dispersion curve to changes in $V_S$ at greater depth. The $V_S$ depth profiles used to match the field data are provided in tabular form as Tables 3 to 21. The location of surface wave sounding Z1-S17 was such that reliable active and passive surface wave data were not obtained and, therefore, an S-wave velocity model was not generated.

The surface wave phase velocities from the microtremor measurements are generally in good agreement with those from the MASW data in the region of overlapping wavelength. Differences in the surface wave dispersion curves between the two techniques result from the passive surface wave data being averaged over much longer arrays with lateral velocity variation having differing affects on the various data sets. The estimated depths of investigation for the combined active and passive surface wave soundings are between 60 and 70 m (197 and 230 ft), as shown on Tables 3 to 21.

For the purpose of data modeling, groundwater depths for 16 of the soundings (Z1-S2, Z1-S4 and Z1-S7 to Z1-S20) were estimated from simple seismic refraction analysis of MASW shot records with groundwater modeled in the 3 to 10 m (10 to 33 ft) depth range. The other 4 soundings (Z1-S1, Z1-S3, Z1-S5 and Z1-S6) were located at higher elevations in areas with outcropping bedrock. The MASW arrays were not long enough to map approximate groundwater depth at these locations. For the purpose of data modeling, groundwater was assumed to be at a depth of 50 m (164 ft) for Z1-S1 and Z1-S3, 45 m (148 ft) for Z1-S5 and 30 m (98 ft) for Z1-S6. Seismic reflection shot records along seismic line Z1-G3 (Figure 1) indicate that groundwater may be shallower along surface wave soundings Z1-S5 and Z1-S6; however, groundwater depth is not expected to have much impact on the S-wave velocity models in this area. Based on review of six (6) Zone 1 borehole velocity logs, the inferred P-wave velocity of saturated sediments was assumed to range from 1,650 to 2,150 m/s (5,413 to 7,054 ft/s) depending upon S-wave velocity. The modeled/assumed saturated sediments can be identified in Tables 3 to 21 based on inferred P-wave velocity of 1,650 m/s (5,413 ft/s), or greater.

Review of 6 available borehole velocity logs in Zone 1 (Z1-B3, Z1-B4, Z1-B5, Z1-B6, Z1-B7 and Z1-B8), geologic maps and borehole geologic logs indicate that bedrock in Zone 1 primarily consists of siltstone, shale and sandstone units of the Puente Formation. Overlying sediments were typically observed to have S-wave velocity below 350 m/s (1,148 ft/s), although sediment velocities up to 450 m/s (1,476 ft/s) were observed. Decomposed and intensely fractured sedimentary rock was found to often have S-wave velocity in the sediment range. Highly to moderately weathered bedrock often had S-wave velocity in the 350 to 600 m/s range (1,148 to

1,969 ft/s) and slightly weathered and fresh rock were found to often have S-wave velocity greater than 700 m/s (2,297 ft/s). Therefore, S-wave velocity above 350 m/s (1,148 ft/s) in the surface wave velocity models (Figures 4 to 22 and Tables 3 to 21) are generally associated with bedrock. Lower velocities will typically be associated with sediments and occasionally decomposed rock.

The average S-wave velocity of the upper 30 and 60 m ($V_S30$ and $V_S60$) and the modeled S-wave velocity at a depth of 60 m (197 ft) for the Zone 1 surface wave soundings are summarized in Table 22. $V_S30$ and $V_S60$ range from 181 to 500 m/s (594 to 1641 ft/s) and 269 to 580 m/s (884 to 1,903 ft/s), respectively. Fifteen (15) of the surface wave soundings have $V_S30$ less than 360 m/s (1,181 ft/s). S-wave velocity at a depth of 60 m (197 ft) ranges from 675 to 850 m/s (2,215 to 2,789 ft/s).

S-wave velocity models were generated for surface wave soundings near each end of two of the three seismic reflection profiles acquired in Zone 1 (Z1-G3 and Z1-G4). Surface wave soundings Z1-S5 and Z1-S6 were conducted in the southwestern and northeastern portions of seismic line Z1-G3, respectively. The S-wave velocity models for these soundings are very similar indicating that there may not be significant lateral velocity variation in the immediate vicinity of the seismic line. Surface wave soundings Z1-S14 and Z1-S15 were conducted in the southwestern and northeastern portions of seismic line Z1-G4, respectively. The S-wave velocity models for these soundings are different with moderately weathered bedrock about 11 m (36 ft) shallower in the vicinity of Z1-S15 located near the northeast end of the line. It should be noted that the surface wave data acquired along Z1-S14 and Z1-S15 were difficult to model due to significant lateral velocity variation of the sediments and highly variable bedrock depths, which cannot adequately be represented by a 1-D model. MASW data and passive "L" array data were in good agreement for Z1-S14 yielding an S-wave velocity model with very low sediment velocity and the lowest Zone 1 $V_S30$ (181 m/s). The low $V_S30$ was primarily the result of the very low sediment velocities in the upper 10 m (33 ft), which were in the 125 to 160 m/s (410 to 525 ft/s) range. The passive linear array data acquired along a 138 m profile at this site were in very poor agreement with the MASW data acquired along a 34.5 m profile and "L" array data and were, therefore, not used for modeling. Explanations for the difference between the different data sets include significant variation of near surface sediment velocity and bedrock depth over the longer passive linear array or negative impact of a directional noise bias on passive linear array data. Models of the passive linear array data (not included) indicate that near surface sediment velocities may be higher and bedrock as much as 6 m (20 ft) shallower adjacent to the MASW array. Only passive "L" array data were used to model Z1-S15, which was similar to Z1-S14, because the MASW data could not be accurately reduced, possibly due to complicated shallow velocity structure, and passive linear array data were noisy, possibly due to limited azimuth of noise sources (i.e. unidirectional rather than omnidirectional noise sources).

Three boreholes are located within about 175 m (574 ft) of surface wave soundings: Z1-B3 about 172 m (565 ft) from Z1-S8, Z1-B4 about 25 m (82 ft) of Z1-S13, and Z1-B6 about 148 m (486 ft) from Z1-S15. Borehole locations are shown on Figure 1. Borehole S-wave velocity data for Z1-B3 are plotted with the surface wave S-wave velocity model for Z1-S8 in Figure 11. This plot illustrates the resolution differences between the two methods with the surface wave velocity models providing more averaged (i.e. thicker layer) velocity models. The two velocity models are in reasonable agreement given the distance between the surface wave sounding and

the borehole and resolution limitations of the surface wave methods relative to borehole PS Suspension velocity log. Borehole S-wave velocity data for Z1-B6 are plotted with the surface wave S-wave velocity model for Z1-S14, located about 330 m (1,083 ft) and the closer Z1-S15 in Figures 17 and 18, respectively. The sediment velocities are much higher in the PS Suspension velocity log, likely due to significant lateral sediment velocity variation discussed previously for these surface wave soundings. The bedrock velocities between the two methods are in good agreement considering likely variation of bedrock depth and weathering. Borehole S-wave velocity data for Z1-B4 are plotted with the surface wave S-wave velocity model for Z1-S13 in Figure 16. The two velocity models are in good agreement considering the resolution capabilities of the two methods and potential lateral velocity variation in this geologic environment. Assuming that the subsurface velocity structure is the same beneath the surface wave sounding as at the borehole location, the surface wave method does not detect a possible 5 m (16 ft) thick low velocity layer at a depth of 19 m (62.3 ft) and as a result overestimates the depth to the higher velocity underlying sedimentary rock. It is not possible to resolve a low velocity layer of this thickness and depth due to the presence of underlying high velocity rock.

## *5.2 Zone 2*

Twelve (12) surface wave soundings were conducted within Zone 2 (Z2-S1 to Z2-S12) as shown in Figure 1. Six of these surface wave soundings were located near the ends of seismic reflection lines and the remaining 6 soundings were distributed throughout the zone.

The fit of the theoretical dispersion curve to the experimental data collected at each site and the modeled $V_S$ profiles for Z2-S1 to Z2-S12 are presented in Figures 23 to 34, respectively. The resolution decreases gradually with depth because of the loss of sensitivity of the dispersion curve to changes in $V_S$ at greater depth. The $V_S$ depth profiles used to match the field data are provided in tabular form as Tables 23 to 34.

The surface wave phase velocities from the microtremor measurements are generally in good agreement with those from the MASW data in the region of overlapping wavelength. Differences in the surface wave dispersion curves between the two techniques result from the passive surface wave data being averaged over much longer arrays with lateral velocity variation having differing affects on the various data sets. The estimated depths of investigation for the combined active and passive surface wave soundings are between 60 and 70 m (197 and 230 ft), as shown on Tables 23 to 34.

For the purpose of data modeling, groundwater depths for 11 of the 12 soundings (Z2-S1 to Z2-S4 and Z2-S6 to Z2-S12) were estimated from simple seismic refraction analysis of MASW shot records with groundwater modeled in the 2 to 9 m (7 to 30 ft) depth range. The MASW array was not long enough at Z2-S5 to map approximate groundwater depth, which was estimated to be greater than 14 m (46 ft) deep. For the purpose of data modeling, groundwater was assumed to be at a depth of 15 m (49 ft) at Z2-S5. Based on review of four (4) Zone 2 borehole velocity logs, the inferred P-wave velocity of saturated sediments was assumed to range from 1,650 to 2,750 m/s (5,413 to 9,022 ft/s) depending upon S-wave velocity. The modeled/assumed saturated sediments can be identified in Tables 23 to 34 based on inferred P-wave velocity of 1,650 m/s (5,413 ft/s), or greater.

Review of 4 available borehole velocity logs in Zone 2 (Z2-B1, Z2-B3, Z2-B4 and Z2-B5) and geologic maps indicates that bedrock in Zone 1 primarily consists of siltstone, claystone, sandstone and conglomerate units of the Fernando, Puente and Topanga Formations. Overlying sediments were typically observed to have S-wave velocity below 350 m/s (1,148 ft/s). Decomposed and intensely fractured sedimentary rock was found to often have S-wave velocity in the sediment range. S-wave velocity of the sedimentary bedrock ranged from about 350 m/s (1,148 ft/s) to over 1,500 m/s (4,921 ft/s). The variable S-wave velocity in the sedimentary rock is a function of degree of weathering, fracturing and lithology. S-wave velocity above 350 m/s (1,148 ft/s) in the surface wave velocity models (Figures 23 to 34 and Tables 23 to 34) is most likely associated with bedrock. Lower velocities will typically be associated with sediments and/or decomposed/highly weathered and fractured rock.

$V_S30$, $V_S60$ and the modeled S-wave velocity at a depth of 60 m (197 ft) for the Zone 2 surface wave soundings are summarized in Table 35. $V_S30$ and $V_S60$ range from 256 to 423 m/s (838 to 1,389 ft/s) and 330 to 552 m/s (1,081 to 1,811 ft/s), respectively. Eight (8) of the 12 surface wave soundings have $V_S30$ less than 360 m/s (1,181 ft/s). S-wave velocity at a depth of 60 m (197 ft) ranges from 420 to 825 m/s (1,378 to 2,707 ft/s).

S-wave velocity models were generated for surface wave soundings near each end of the three seismic reflection profiles acquired in Zone 2 (Z2-G1 to Z2-G3). Surface wave soundings Z2-S3 and Z2-S2 were conducted in the southern and northern portions of seismic line Z2-G1, respectively. The S-wave velocity models for these soundings are very similar, with less than 10% velocity variation in bedrock, indicating that there may not be significant lateral velocity variation in the immediate vicinity of the seismic line. Surface wave soundings Z2-S7 and Z2-S8 were conducted in the southwestern and northeastern portions of seismic line Z2-G2, respectively. The S-wave velocity models for these soundings are similar in the upper 40 m (131 ft) and different at greater depths. The significant lateral velocity variation at depth may be related to changes in bedrock weathering, fracturing or lithology associated with dipping sedimentary units. Surface wave soundings Z2-S10 and Z2-S11 were conducted in the northwestern and southeastern portions of seismic line Z2-G3, respectively. The S-wave velocity models for these soundings are very similar, with less than 10% velocity variation in bedrock, indicating that there may not be significant lateral velocity variation in the immediate vicinity of the seismic line.

No boreholes were drilled in close proximity to any of the surface wave soundings conducted in Zone 2.

## *5.3 Zone 3*

Twenty four (24) surface wave soundings were conducted within Zone 3 (Z3-S1 to Z3-S24) as shown in Figure 1. Fourteen (14) of these surface wave soundings were located near the ends of 7 seismic reflection lines and the remaining 10 soundings were distributed throughout the zone.

The fit of the theoretical dispersion curve to the experimental data collected at each site and the modeled $V_S$ profiles for Z3-S1 to Z3-S24 are presented in Figures 35 to 58, respectively. The resolution decreases gradually with depth because of the loss of sensitivity of the dispersion curve to changes in $V_S$ at greater depth. The $V_S$ depth profiles used to match the field data are provided in tabular form as Tables 36 to 59.

The surface wave phase velocities from the microtremor measurements are generally in good agreement with those from the MASW data in the region of overlapping wavelength. Differences in the surface wave dispersion curves between the two techniques result from the passive surface wave data being averaged over much longer arrays with lateral velocity variation having differing affects on the various data sets. The estimated depths of investigation for the combined active and passive surface wave soundings are between 60 and 75 m (197 and 246 ft), as shown on Tables 36 to 59.

For the purpose of data modeling, groundwater depths for 16 of the 24 soundings (Z3-S1, Z3-S6, Z3-S7, Z3-S9 to Z3-S11, Z3-S13, Z3-S14, Z3-S16 to Z3-S18 and Z3-S20 to Z3-S24) were estimated from simple seismic refraction analysis of MASW or seismic reflection shot records with groundwater modeled in the 3 to 17 m (10 to 56 ft) depth range. Groundwater depths for 4 soundings (Z3-S2 to Z3-S5) were interpreted from nearby borehole velocity logs and interpolated as necessary. Groundwater in the vicinity of these surface wave soundings was modeled in the 30 to 45 m (98 to 148 ft) depth range. The MASW profiles were not long enough to image depth to groundwater at four of the sounding locations (Z3-S8, Z3-S12, Z3-S15 and Z3-S19). Simple seismic refraction analysis of the MASW shot records indicated that groundwater was deeper than 14 m (46 ft) at these locations and for the purpose of modeling groundwater was assumed to be at a depth of 15 m (49 ft). Based on review of 12 Zone 3 borehole velocity logs, the inferred P-wave velocity of saturated sediments was assumed to range from 1,500 to 3,500 m/s (4,921 to 11,483 ft/s) depending upon S-wave velocity. The modeled/assumed saturated sediments can be identified in Tables 36 to 59 based on inferred P-wave velocity of 1,500 m/s (4,921 ft/s), or greater.

Review of 12 available borehole velocity logs in Zone 3 (Z3-B1 to Z3-B12), geologic maps, geologic cross sections and borehole geologic logs indicates that bedrock in Zone 3 consists of siltstone, claystone, sandstone and conglomerate units of the Fernando, Puente and Topanga Formations and crystalline basement rock. Overlying sediments are typically observed to have S-wave velocity in the 175 to 600 m/s (574 to 1,969 ft/s) range. The higher sediment velocities are typically associated with older alluvial deposits encountered in boreholes Z3-B2 to Z3-B4 located north of the Eagle Rock Fault. Typically, a thinner sequence of sediments overlie bedrock south of the Eagle Rock Fault and sediment S-wave velocity rarely exceeded 400 m/s (1,312 ft/s). S-wave velocity of sedimentary rock encountered in the boreholes is in the 325 to 1,850 m/s (1,066 to 6,070 ft/s) range. S-wave velocity of 375 to 450 m/s (1,230 to 1,476 ft/s) is more typical of the lowest velocity for sedimentary rock in many of the boreholes. The variable S-wave velocity in the sedimentary rock is a function of degree of weathering, fracturing and lithology. S-wave velocity of decomposed to weathered crystalline basement rock encountered in boreholes is typically in the 650 to 1,400 m/s (2,133 to 4,593 ft/s) range, but is expected to get much higher as weathering decreases. In areas with crystalline basement north of the Eagle Rock Fault, S-wave velocity over 650 m/s (2,133 ft/s) is probably associated with bedrock with lower velocities associated with overlying sediments. South of the Eagle Rock Fault, S-wave velocity over 400 m/s (1,312 ft/s) will commonly be associated with sedimentary bedrock. Lower velocities will often be associated with sediments; however, there is quite a bit of overlap in sediment and highly weathered sedimentary rock S-wave velocity within Zone 3.

The average S-wave velocity of the upper 30 and 60 m ($V_S30$ and $V_S60$) and the modeled S-wave velocity at a depth of 60 m (197 ft) for the Zone 3 surface wave soundings are summarized

in Table 60. $V_S30$ and $V_S60$ range from 313 to 496 m/s (1,027 to 1627 ft/s) and 361 to 662 m/s (1,184 to 2,172 ft/s), respectively. Twelve (12) of the 24 surface wave soundings have $V_S30$ less than 360 m/s (1,181 ft/s). S-wave velocity at a depth of 60 m (197 ft) in highly variable in Zone 3, ranging from 435 to 1,250 m/s (1,427 to 4,101 ft/s).

S-wave velocity models were generated for surface wave soundings near each end of the 7 seismic reflection profiles acquired in Zone 3 (Z3-G1 to Z3-G7). Surface wave soundings Z3-S3 and Z3-S4 were conducted at the northern and southern ends of seismic line Z3-G1, respectively. The S-wave velocity models for these soundings are very similar and $V_S30$ is almost identical indicating that there is no significant lateral velocity variation along the seismic line. Surface wave soundings Z3-S6 and Z3-S7 were conducted at the northern and southern ends of seismic line Z3-G2, respectively. There is more than a 10% difference in the S-wave velocity models and $V_S30$ for these soundings indicating that there is significant lateral velocity variation along the seismic line, possibly resulting from a geologic structure bisecting the line or steeply dipping geologic units. Surface wave soundings Z3-S9 and Z3-S10 were conducted at the southwestern and northeastern ends of seismic line Z3-G3, respectively. There is a large difference in the S-wave velocity models and $V_S30$ for these soundings indicating that there is significant lateral velocity variation along the seismic line, possibly resulting from a geologic structure bisecting the line or steeply dipping geologic units. Surface wave soundings Z3-S13 and Z3-S14 were conducted in the northeastern and southwestern portions of seismic line Z3-G4, respectively. The S-wave velocity models for these soundings are very similar and $V_S30$ is almost identical indicating that there is no significant lateral velocity variation along the seismic line. Surface wave soundings Z3-S17 and Z3-S18 were conducted in the north central and south central portions of seismic line Z3-G5, respectively. The S-wave velocity models for these soundings are very similar, except for small variation in the depth of high velocity bedrock. There is about an 11% difference in $V_S30$ and $V_S60$ between the two soundings, therefore some lateral velocity variation associated with deepening bedrock or variation of the weathering profile is present. Surface wave soundings Z3-S21 and Z3-S22 were conducted in the northern and southern portions of seismic line Z3-G6, respectively. There is some variation of near surface and deep velocity structure in the S-wave velocity models for these soundings. Additionally, there is about a 6 to 8% difference in $V_S30$ and $V_S60$ between the two soundings and, therefore, some lateral velocity variation occurs along the seismic line. Surface wave soundings Z3-S23 and Z3-S24 were conducted near the northern and southern ends of seismic line Z3-G7, respectively. There is a large difference in the S-wave velocity models and $V_S30$ for these soundings indicating that there is significant lateral velocity variation along the seismic line, possibly resulting from a geologic structure bisecting the line, steeply dipping geologic units or variable bedrock weathering.

Four (4) boreholes are located within about 155 m (509 ft) of surface wave soundings: Z3-B2 about 114 m (375 ft) from Z3-S2, Z3-B4 about 34 m (110 ft) from Z3-S3, Z3-B9 about 110 m (360 ft) from Z3-S13 and Z3-B12 about 155 m (509 ft) from Z3-S20. Additionally, borehole Z3-B7 is located on seismic reflection line Z3-G3 between surface wave soundings Z3-S9 and Z3-S10. Borehole locations are shown on Figure 1.

Borehole S-wave velocity data for Z3-B2 are plotted with the surface wave S-wave velocity model for Z3-S2 in Figure 36. This plot illustrates the resolution differences between the two methods with the surface wave velocity models providing more averaged (i.e. thicker layer) velocity models. The surface wave velocity model generally has much lower S-wave velocity

than the velocity log, which may be the result of lateral velocity variation in the sediments overlying weathered crystalline basement rocks and variable depth to and weathering profile of the basement rock. Borehole S-wave velocity data for Z3-B4 are plotted with the surface wave S-wave velocity model for Z3-S3 in Figure 37. The two velocity models are in good agreement considering the differing resolution capabilities of the two methods. Borehole S-wave velocity data for Z3-B9 are plotted with the surface wave S-wave velocity model for Z3-S13 in Figure 47. The surface wave velocity model generally has slightly lower S-wave velocity than the velocity log, which may be the result of lateral velocity variation between the borehole and surface wave sounding locations. Borehole S-wave velocity data for Z3-B12 are plotted with the surface wave S-wave velocity model for Z3-S20 in Figure 54. The two velocity models are in good agreement considering the differing resolution capabilities of the two methods and distance between the test locations. Borehole S-wave velocity data for Z3-B7 are plotted along the surface wave S-wave velocity models for Z3-S9 and Z3-S10 on Figure 43 and 44, respectively. Both the borehole and surface wave soundings are located on seismic reflection line Z3-G3. As previously discussed, there is significant difference between the two surface wave models. As would be expected, the borehole S-wave velocities lie between the two surface wave models although they are more similar to Z3-S10 below a depth of 30 m (98 ft).

## *5.4 Zone 4*

Ten (10) surface wave soundings were conducted within Zone 4 (Z4-S1 to Z2-S10) as shown in Figure 1. Five of these surface wave soundings were located on seismic reflection lines and the remaining 5 soundings were distributed throughout the zone.

The fit of the theoretical dispersion curve to the experimental data collected at each site and the modeled $V_S$ profiles for Z4-S1 to Z4-S10 are presented in Figures 59 to 68, respectively. The resolution decreases gradually with depth because of the loss of sensitivity of the dispersion curve to changes in $V_S$ at greater depth. The $V_S$ depth profiles used to match the field data are provided in tabular form as Tables 61 to 70.

The surface wave phase velocities from the microtremor measurements are generally in good agreement with those from the MASW data in the region of overlapping wavelength. Differences in the surface wave dispersion curves between the two techniques result from the passive surface wave data being averaged over much longer arrays with lateral velocity variation having differing affects on the various data sets. The estimated depths of investigation for the combined active and passive surface wave soundings are between 60 and 70 m (197 and 230 ft), as shown on Tables 61 to 70.

For the purpose of data modeling, attempts were made to estimate groundwater depth from simple seismic refraction analysis of MASW shot records and seismic records at the ends of two seismic reflection profiles. MASW profiles were not long enough to determine approximate groundwater depth. Groundwater depth was estimated to be on the order of 65 m (213 ft) in the vicinity of seismic reflection profiles Z4-G1 and Z4-G2. Therefore, for data modeling, groundwater was assumed to be 65 m (213 ft) deep in the vicinity of surface wave soundings Z4-S1 to Z4-S7 and then, based on borehole and geophysical control in the adjacent zones, shallow to the southwest between Z4-S8 and Z4-S10. Based on review of a single Zone 4 borehole velocity log, the inferred P-wave velocity of saturated sediments was assumed to range from

1,600 to 1,750 m/s (5,249 to 5,741 ft/s) depending upon S-wave velocity. The modeled/assumed saturated sediments can be identified in Tables 61 to 70 based on inferred P-wave velocity of 1,600 m/s (5,249 ft/s), or greater.

Review of the borehole velocity log for Z4-B4, located in the southwestern corner of Zone 4 (Figure 1), geologic maps and cross sections indicates that bedrock in Zone 4 primarily consists of siltstone, claystone and sandstone units of the Puente Formation and crystalline basement rock. Bedrock is expected to deepen to the northeast and with the exception of the southwestern portion of Zone 4 may exceed 120 m (400 ft) in depth. The borehole velocity log for Z4-B4 indicates that seismic velocity alone may not be useful to distinguish sedimentary rock from overlying sediments. Sediments encountered in the upper 26 m (85 ft) in this borehole have S-wave velocity in the 275 to 550 m/s (902 to 1,804 ft/s) range, whereas decomposed rock immediately beneath the sediments has an S-wave velocity as low as 300 m/s (984 ft/s). Thick sequences of old alluvial sediments in the northeastern portion of Zone 4 may have S-wave velocity increasing with depth to over 600 m/s (1,969 ft/s), similar to the velocities observed in some units of the Puente Formation.

$V_S30$, $V_S60$ and the modeled S-wave velocity at a depth of 60 m (197 ft) for the Zone 4 surface wave soundings are summarized in Table 71. $V_S30$ and $V_S60$ range from 288 to 373 m/s (944 to 1,225 ft/s) and 349 to 484 m/s (1,144 to 1,589 ft/s), respectively. Seven (7) of the 10 surface wave soundings have $V_S30$ less than 360 m/s (1,181 ft/s). S-wave velocity at a depth of 60 m (197 ft) ranges from 475 to 600 m/s (1,558 to 1,969 ft/s) with the exception of Z4-S1, which has a modeled S-wave velocity of 850 m/s (2,789 ft/s) at this depth.

S-wave velocity models were generated for surface wave soundings near each end of the two seismic reflection profiles acquired in Zone 4 (Z4-G1 and Z4-G2). Surface wave soundings Z4-S2 to Z4-S4 were conducted in the northern, central and southern portions of seismic line Z4-G1, respectively. The S-wave velocity models for these soundings are quite variable, as may be expected because the Raymond Fault Zone bisects the seismic line. Surface wave soundings Z4-S6 and Z4-S7 were conducted in the northeastern and southwestern portions of seismic line Z4-G2, respectively. The S-wave velocity models for these soundings are almost identical indicating that there is not significant lateral velocity variation in the immediate vicinity of the seismic line.

No boreholes were drilled in close proximity to any of the surface wave soundings conducted in Zone 4.

## *5.5 Zone 5*

Twelve (12) surface wave soundings were conducted within Zone 5 (Z5-S1 to Z5-S4 and Z5-S6 to S5-S13) as shown in Figure 1. Four of these surface wave soundings were located on seismic reflection lines and the remaining 8 soundings were distributed throughout the zone.

The fit of the theoretical dispersion curve to the experimental data collected at each site and the modeled $V_S$ profiles for Z5-S1 to Z5-S4 and Z5-S6 to Z5-S13 are presented in Figures 69 to 80, respectively. The resolution decreases gradually with depth because of the loss of sensitivity of the dispersion curve to changes in $V_S$ at greater depth. The $V_S$ depth profiles used to match the field data are provided in tabular form as Tables 72 to 83.

The surface wave phase velocities from the microtremor measurements are generally in good agreement with those from the MASW data in the region of overlapping wavelength. Differences in the surface wave dispersion curves between the two techniques result from the passive surface wave data being averaged over much longer arrays with lateral velocity variation having differing affects on the various data sets. The estimated depths of investigation for the combined active and passive surface wave soundings are between 60 and 70 m (197 and 230 ft), as shown on Tables 72 to 83.

For the purpose of data modeling, attempts were made to estimate groundwater depth from simple seismic refraction analysis of MASW shot records and seismic records at the ends of two seismic reflection profiles. MASW profiles were not long enough to determine approximate groundwater depth. Groundwater depth was estimated to be on the order of 56 m (184 ft) and 16 m (52 ft) in the vicinity of seismic reflection profiles Z5-G2 and Z5-G3, respectively. Therefore, for data modeling, groundwater was assumed to be 50 to 56 m (164 to 184 ft) deep in the vicinity of surface wave soundings Z5-S1 to Z5-S9, 40 m (131 ft) at Z5-S10, 25 m (82 ft) at Z5-S11 and 16 m (52 ft) at Z5-S12 and Z5-S13. Subsurface geologic conditions in Zone 5 are expected to be similar to those in Zone 4 and, therefore, the inferred P-wave velocity of saturated sediments was assumed to range from 1,600 to 1,750 m/s (5,249 to 5,741 ft/s) depending upon S-wave velocity. The modeled/assumed saturated sediments can be identified in Tables 72 to 83 based on inferred P-wave velocity of 1,600 m/s (5,249 ft/s), or greater.

Boreholes were not drilled in Zone 5. Review of geologic maps and cross sections indicates that bedrock in Zone 5 primarily consists of siltstone, claystone and sandstone units of the Puente Formation and siltstone and claystone of the Fernando Formation. Bedrock is expected to deepen to the east and, with the exception of the western corner of Zone 5, may significantly exceed 120 m (400 ft) in depth. Because the geology in Zone 5 is expected to be similar to that in Zone 4, it is unlikely that S-wave velocity if useful for distinguishing bedrock from overlying sediments. Additionally, bedrock over most of Zone 5 is much deeper than the surface wave soundings can image.

$V_S30$, $V_S60$ and the modeled S-wave velocity at a depth of 60 m (197 ft) for the Zone 5 surface wave soundings are summarized in Table 84. $V_S30$ and $V_S60$ range from 303 to 392 m/s (994 to 1,287 ft/s) and 362 to 435 m/s (1,187 to 1,429 ft/s), respectively. Eight (8) of the 12 surface wave soundings have $V_S30$ less than 360 m/s (1,181 ft/s). S-wave velocity at a depth of 60 m (197 ft) ranges from 475 to 625 m/s (1,558 to 2,051 ft/s) and in nominally in the 500 to 550 m/s (1,640 to 1,804 ft/s) range.

S-wave velocity models were generated for surface wave soundings near each end of the two seismic reflection profiles acquired in Zone 5 (Z5-G2 and Z5-G3). Surface wave soundings Z5-S8 and Z5-S9 were conducted in the eastern and western portions of seismic line Z5-G2, respectively. The S-wave velocity models for these soundings are typically within 10% of seismic velocity and $V_S30$ and $V_S60$ are within 5% indicating that there is not significant lateral velocity variation in the immediate vicinity of the seismic line. Surface wave soundings Z5-S12 and Z5-S13 were conducted in the northern and southern portions of seismic line Z5-G3, respectively. The S-wave velocity models, $V_S30$ and $V_S60$ for these soundings are typically within 11% of seismic velocity indicating that there is not significant lateral velocity variation in the immediate vicinity of the seismic line.

# 6 CONCLUSIONS

Active and passive surface wave data were collected at 78 locations within the five SR-710 Tunnel Study Zones, located in Los Angeles County, California. The measurements were conducted from February 24, 2009 through May 19, 2009. The purpose of the investigation was to support site characterization and screening efforts and a seismic reflection survey conducted as part of the investigation and reported separately. Surface wave sounding locations are shown on Figure 1 along with the five tunnel study zones, borehole locations and seismic reflection lines. A total of 35 of the surface wave soundings were conducted on seismic reflection lines and the remaining 43 soundings were distributed throughout the tunnel study zones.

The S-wave velocity models derived from the surface wave soundings and summaries are presented as Figures 4 to 80 and Tables 3 to 84. The average S-wave velocity of the upper 30 and 60 m ($V_S30$ and $V_S60$) and the modeled S-wave velocity at a depth of 60 m (197 ft) for the surface wave soundings conducted in Zones 1 to 5 are summarized in Tables 22, 35, 60, 71 and 84, respectively. $V_S30$ and $V_S60$ range from 181 to 500 m/s (594 to 1641 ft/s) and 269 to 662 m/s (884 to 2,172 ft/s), respectively. Fifty (50) of the surface wave soundings have $V_S30$ less than 360 m/s (1,181 ft/s). Modeled S-wave velocity at a depth of 60 m (197 ft) is highly variable ranging from about 420 to 1,250 m/s (1,378 to 4,101 ft/s).

Surface wave data were acquired and modeled at least two locations on each of the 17 seismic reflection lines except for Z1-G5, where one of the surface wave soundings did not yield data that could be modeled. The surface wave soundings indicated than 9 of the seismic lines (Z1-G3, Z2-G1, Z2-G2, Z2-G3, Z3-G1, Z3-G4, Z4-G2, Z5-G2 and Z5-G3) have only minor lateral velocity variation. Therefore, potential geologic structures bisecting these lines do not have a significant impact on subsurface velocity structure. There is significant lateral velocity variation along the other 7 seismic reflection lines (Z1-G4, Z3-G2, Z3-G3, Z3-G5, Z3-G6, Z3-G7 and Z4-G1). The lateral velocity variation along these seismic lines may be the result of a geologic structure, such as a fault, bisecting the line or, alternatively, may be the result of dipping geologic units, variable bedrock depths or variable bedrock weathering profiles.

Review of borehole velocity logs from boreholes primarily located in Zones 1 to 3 indicated that S-wave velocity may be applicable for differentiating sediments from shallow sedimentary rock in Zones 1 and 2. In these zones, S-wave velocity below 350 m/s (1,148 ft/s) was typically found to be associated with sediments, whereas higher velocities were associated with sedimentary rock. However, decomposed rock was occasionally found to have S-wave velocity in the sediment range. The application of S-wave velocity to differentiate sediments from bedrock was more difficult in Zone 3 due to thick accumulations of high velocity, old alluvial sediments in the northern portion of the zone. In areas with crystalline basement north of the Eagle Rock Fault, S-wave velocity over 650 m/s (2,133 ft/s) was found to be typically associated with bedrock and lower velocities associated with overlying sediments. South of the Eagle Rock Fault, S-wave velocity over 400 m/s (1,312 ft/s) was often found to be associated with sedimentary bedrock. However, there was some overlap in S-wave velocity between sediments and weathered sedimentary rock in Zone 3. There was limited borehole control in Zones 4 and 5, and with the exception of the southwestern corner of these zones, bedrock was expected to be much deeper than the exploration limits of the surface wave method.

# 7 REFERENCES


Brown, L.T., 1998, "Comparison of $V_S$ profiles from SASW and borehole measurements at strong motion sites in Southern California", Master's thesis, University of Texas at Austin.

Foti, S., 2000, "Multistation Methods for Geotechnical Characterization using Surface Waves", Ph.D. Dissertation, Politecnico di Torino, Italy.

Joh, S.H., 2002, "WinSASW Version 2.0, Data Interpretation and Analysis for SASW Measurements", Department of Civil Engineering, Chung-Ang University, Anseong, Korea.

Louie, J.N., 2001, "Faster, Better: Shear-Wave Velocity to 100 Meters Depth from Refraction Microtremor Arrays", Bulletin of the Seismological Society of America, vol. 91, no. 2, p. 347-364.

Okada, H, 2003, "The Microtremor Survey Method," Society of Exploration Geophysics Geophysical Monograph Series, Number 12, 135p.

Park, C.B., Miller, R.D. and Xia, J., 1999a, "Multimodal analysis of high frequency surface waves", *Proceedings of the Symposium on the Application of Geophysics to Engineering and Environmental Problems '99*, 115-121.

Park, C.B., Miller, R.D. and Xia, J., 1999b, "Multichannel analysis of surface waves", Geophysics, Vol 64, No. 3, 800-808.

Roesset, J.M., Chang, D.W. and Stokoe, K.H., II, 1991, "Comparison of 2-D and 3-D Models for Analysis of Surface Wave Tests," *Proceedings,* 5th *International Conference on Soil Dynamics and Earthquake Engineering*, Karlsruhe, Germany.

# 8 CERTIFICATION

All geophysical data, analysis, interpretations, conclusions, and recommendations in this document have been prepared under the supervision of and reviewed by a **GEO*Vision*** California Professional Geophysicist.

10/05/09

Antony J. Martin — Date
California Professional Geophysicist GP989
**GEO***Vision* Geophysical Services

* This geophysical investigation was conducted under the supervision of a California Professional Geophysicist using industry standard methods and equipment. A high degree of professionalism was maintained during all aspects of the project from the field investigation and data acquisition, through data processing interpretation and reporting. All original field data files, field notes and observations, and other pertinent information are maintained in the project files and are available for the client to review for a period of at least one year.

  A professional geophysicist's certification of interpreted geophysical conditions comprises a declaration of his/her professional judgment. It does not constitute a warranty or guarantee, expressed or implied, nor does it relieve any other party of its responsibility to abide by contract documents, applicable codes, standards, regulations or ordinances.

# APPENDIX A

## TECHNICAL NOTE

## ACTIVE AND PASSIVE SURFACE WAVE TECHNIQUES

# *ACTIVE AND PASSIVE SURFACE WAVE TECHNIQUES*

GEOVision geophysical services

***Overview***

Active and passive surface wave techniques are relatively new in-situ seismic methods for determining shear wave velocity ($V_S$) profiles. Testing is performed on the ground surface, allowing for less costly measurements than with traditional borehole methods. The basis of surface wave techniques is the dispersive characteristic of Rayleigh waves when traveling through a layered medium. Rayleigh wave velocity is determined by the material properties (primarily shear wave velocity, but also to a lesser degree compression wave velocity and material density) of the subsurface to a depth of approximately 1 to 2 wavelengths. As shown in the adjacent diagram, longer wavelengths penetrate deeper and their velocity is affected by the material properties at greater depth. Surface wave testing consists of measuring the surface wave dispersion curve at a site and modeling it to obtain the corresponding shear wave velocity profile.

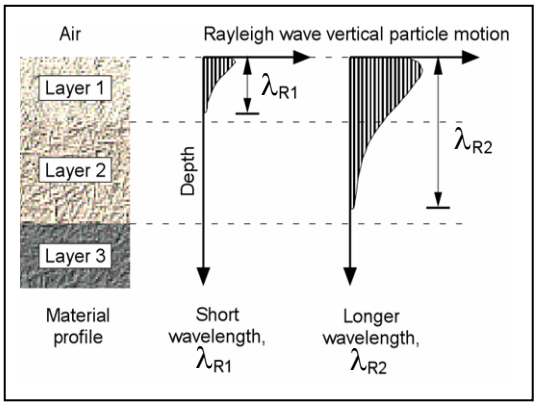


***Active Surface Wave Techniques***

Active surface wave techniques measure surface waves generated by dynamic sources such as hammers, weight drops, electromechanical shakers, vibroseis and bulldozers. These techniques include the spectral analysis of surface waves (SASW) and multi-channel array surface wave (MASW) methods.

***Hammer Energy Sources***

***Accelerated Weight Drop***

***Electromechanical Shaker***

***Bulldozer Energy Source***

*1124 Olympic Drive, Corona, California 92881 ph. 951-549-1234 fx 951-549-1236 www.geovision.com*

The SASW method is optimized for conducting $V_S$ depth soundings. A dynamic source is used to generate surface waves of different wavelengths (or frequencies) which are monitored by two or more receivers at known offsets. An expanding receiver spread and optimized source-receiver geometry are used to minimize near field effects, body wave signal and attenuation. A dynamic signal analyzer is typically used to calculate the phase and coherence of the cross spectrum of the time history data collected at a pair of receivers. During data analysis, an interactive masking process is used to discard low quality data and to unwrap the phase spectrum, as shown in the figure below. The dispersion curve (Rayleigh wave phase velocity versus frequency or alternatively wavelength) is calculated from the unwrapped phase spectrum.

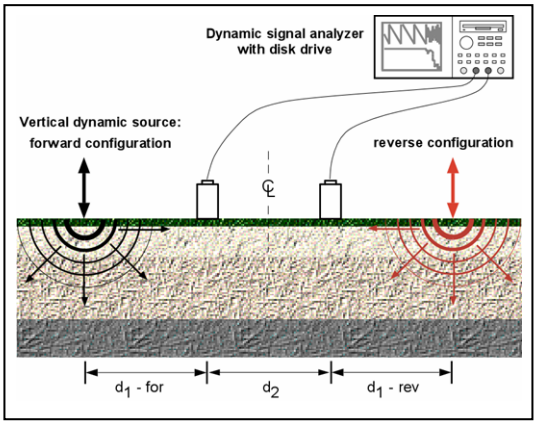


***SASW Setup***

***HP Dynamic Signal Analyzer***

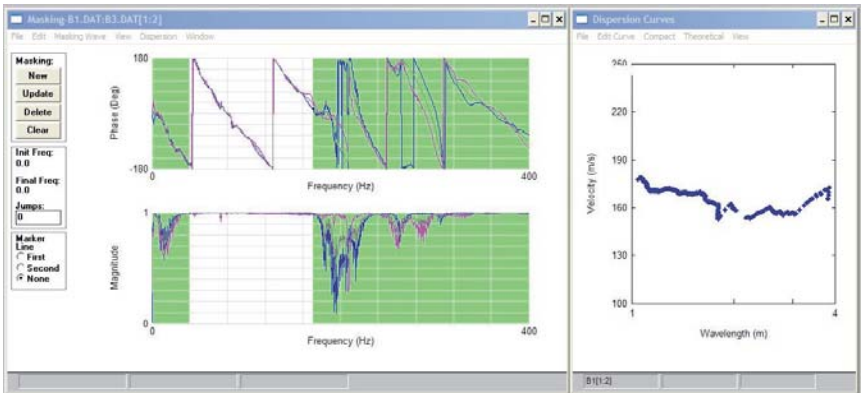


***Masking of Wrapped Phase Spectrum and Resulting Dispersion Curve***

The MASW field layout is similar to that of the seismic refraction technique. Twenty four, or more, geophones are laid out in a linear array with 1 to 2m spacing and connected to a multi-channel seismograph as shown below. This technique is ideally suited to 2D $V_S$ imaging, with data collected in a roll-along manner similar to that of the seismic reflection technique. The source is offset at a predetermined distance from the near geophone usually determined by field testing. The Rayleigh wave dispersion curve is obtained by a wavefield transformation of the seismic record such as the f-k or $\tau$-p transforms. These transforms are very effective at isolating surface wave energy from that of body waves. The dispersion curve is picked as the peak of the surface wave energy in slowness (or velocity) – frequency space as shown. One advantage of the MASW technique is that the wavefield transformation may not only identify the fundamental mode but also higher modes of surface waves. At some sites, particularly those with large velocity inversions, higher surface wave modes may contain more energy than the fundamental mode.

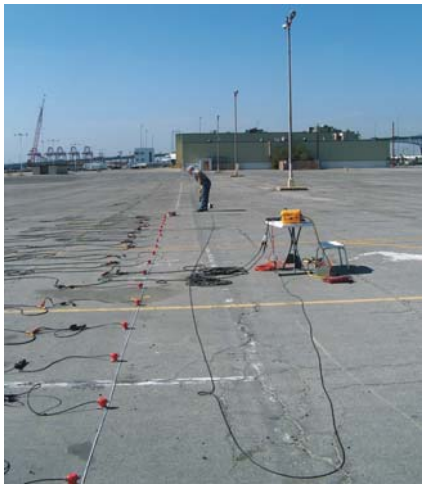

***MASW Field Setup***

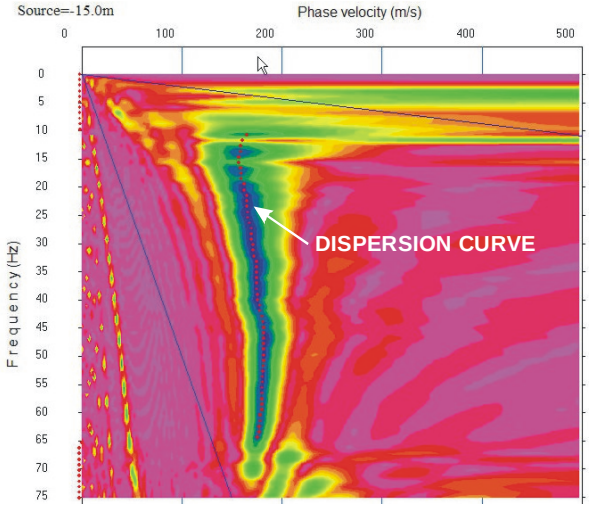


***Wavefield Transform of MASW data***

***Passive Surface Wave Techniques***

Passive surface wave techniques measure noise; surface waves from ocean wave activity, traffic, factories, etc. These techniques include the array microtremor and refraction microtremor (REMI) techniques.

The array microtremor technique typically uses 7 or more 4.5- or 1-Hz geophones arranged in a two-dimensional array. The most common arrays are the triangle, circle, semi-circle and "L" arrays. The triangle array, which consists of several embedded equilateral triangles, is often used as it provides good results with a relatively small number of geophones. With this array the outer side of the triangle should be at least as long as the desired depth of investigation. Typically, fifteen to twenty 30-second noise records are acquired for analysis. The spatial autocorrelation (SPAC) technique is one of several methods that can be used to estimate the Rayleigh wave dispersion curve. A first order Bessel function is fit to the SPAC function to determine the phase velocity for particular frequency. The image shown below shows the degree of fitness of the Bessel function to the SPAC function for a wide range of phase velocity and frequency. The dispersion curve, is the peak (best fit), as shown in the figure below.

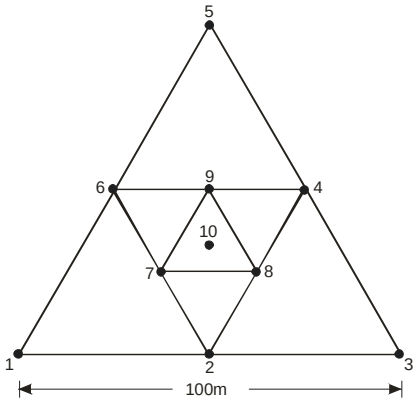


***Triangle Array Geometry***

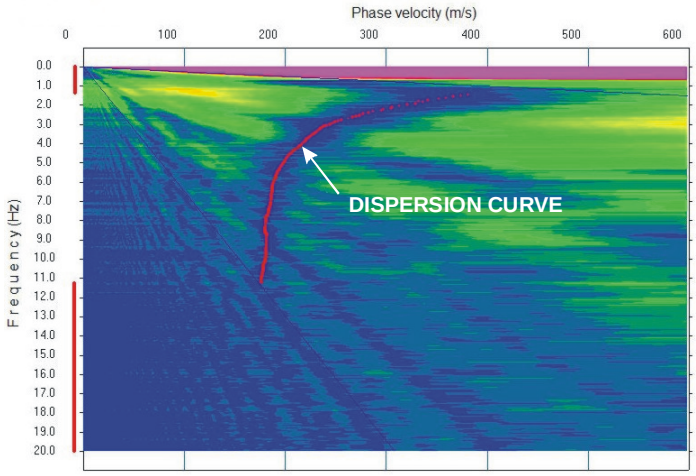


***Dispersion Curve from Array Microtremor Measurements***

The refraction microtremor (REMI) technique uses a field layout similar to the seismic refraction method (hence its name). Twenty-four, 4.5 Hz geophones are laid out in a linear array with a spacing of 6 to 8m and fifteen to twenty 30-second noise records are acquired. A slowness-frequency (p-f) wavefield transform is used to separate Rayleigh wave energy from that of other waves. Because the noise field can originate from any direction, the wavefield transform is conducted for multiple vectors through the geophone array, all of which are summed. The dispersion curve is defined as the lower envelope of the Rayleigh wave energy in p-f space. Because the lower envelope is picked rather than the energy peak (energy traveling along the profile is slower than that approaching from an angle), this technique may be somewhat more subjective than the others, particularly at low frequencies. The SPAC technique can also be used to extract the surface wave dispersion curve from linear array microtremor data providing there are omni-directional noise sources.

***Refraction Microtremor Array Layout***

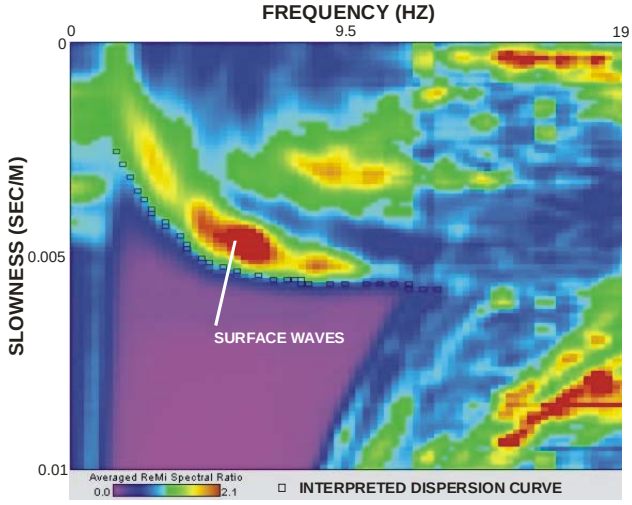


***Wavefield Transform of REMI Data***

***Depth of Investigation***

Active surface wave investigations typically use various sized sledge hammers to image the shear wave velocity structure to depths of up to 15m. Weight drops and electromechanical shakers can often be used to image to depths of 30m. Bulldozers and vibroseis trucks can be used to image to depths as great as 100m. Passive surface wave techniques can often image shear wave velocity structure to depths of over 100m, given sufficient noise sources and space for the receiver array. Large passive arrays, utilizing long-period seismometers with GPS clocks have been used to image shear wave velocity structure to depths of several kilometers.

***Combined Active and Passive Surface Wave Testing***

The combined use of active and passive techniques may offer significant advantages on many investigations. It can be very costly to mobilize large energy sources for 30m/100ft active surface wave soundings. In urban environments, the combined use of active and passive surface wave techniques can image to these depths without the need for large energy sources. We have found that dispersion curves from active and passive surface wave techniques are generally in good agreement, making the combined use of the two techniques viable. It is not recommended that passive surface wave techniques be applied alone for UBC/IBC site classification investigations. Microtremor techniques do not generally characterize near surface velocity, which may have a significant impact of the average shear wave velocity of the upper 30m or 100ft and so should always be used in conjunction with SASW or MASW. An SASW sounding to a depth of 30m requires at least a 60m linear array. If sufficient space is not available for this, it may be possible to use a 45m triangle array on the site or place a 100-200m long REMI array along an adjacent sidewalk or an "L" array at an adjacent street intersection.


***Microtremor Measurements along Sidewalk***

***Modeling***

There are several options for interpreting surface wave dispersion curves, depending on the accuracy required in the shear wave velocity profile. A simple empirical analysis can be done to estimate the average shear wave velocity profile. For greater accuracy, forward modeling of fundamental-mode Rayleigh wave dispersion as well as full stress wave propagation can be performed using several software packages. A formal inversion scheme may also be used. With many of the analytical approaches, background information on the site can be incorporated into the model and the resolution of the final profile may be quantified.

***Applications***

Active and passive surface wave testing can be used to obtain $V_S$ profiles for:

- UBC/IBC site classification for seismic design
- Earthquake site response
- Seismic microzonation
- Liquefaction analysis
- Soil compaction control
- Mapping subsurface stratigraphy
- Locating potentially weak zones in earthen embankments and levees

***Case History***

The figures below show the surface wave dispersion curves and alternative shear wave velocity models for a site in Los Angeles, California. All of the previous figures illustrating SASW, MASW, array and refraction microtremor techniques were from this site. The dispersion curves from all four methods are shown on the left along with the theoretical dispersion curves for alternative S-wave velocity versus depth models on the right. Conditions at this site were very poor for active surface wave techniques because of the presence of very low velocity hydraulic fill. In fact, with active surface wave techniques it was only possible to image to a depth of about 12.5m with energy sources typically capable of imaging to 30m. There is excellent agreement in the dispersion curves generated from all of the methods over the overlapping wavelength ranges. The minor differences probably result from variable velocity of the hydraulic fill within the sampling volume of the specific methods. Two Vs versus depth models were generated to illustrate the difficulty modeling the highly variable, near surface velocity structure evident in the PS log. The two surface wave models yielded similar values for the average shear-wave velocity of the upper 30m ($V_S30$), 201 and 202 m/s, illustrating that Vs30 is much more tightly constrained than the actual layer thicknesses and velocities in the models. $V_S30$ estimated from the PS log (194 m/s) is within 4% of that estimated from the two surface wave models (201 and 202 m/s). The small differences in $V_S30$ between the two methods may easily result from the different sampling regimes (borehole versus large area) rather than errors in either of the methods.

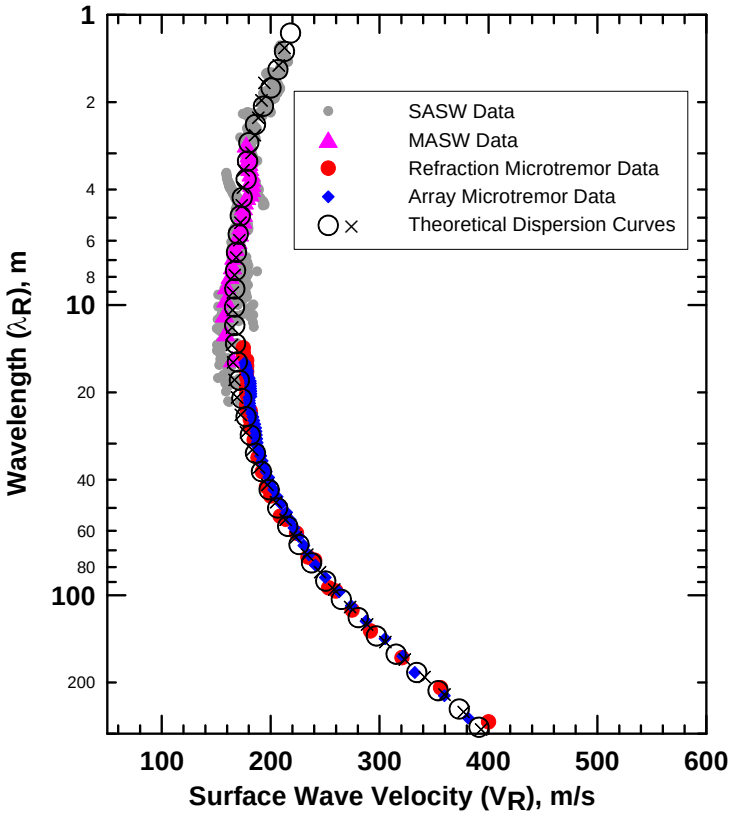


***Field Data and Theoretical Dispersion Curve***

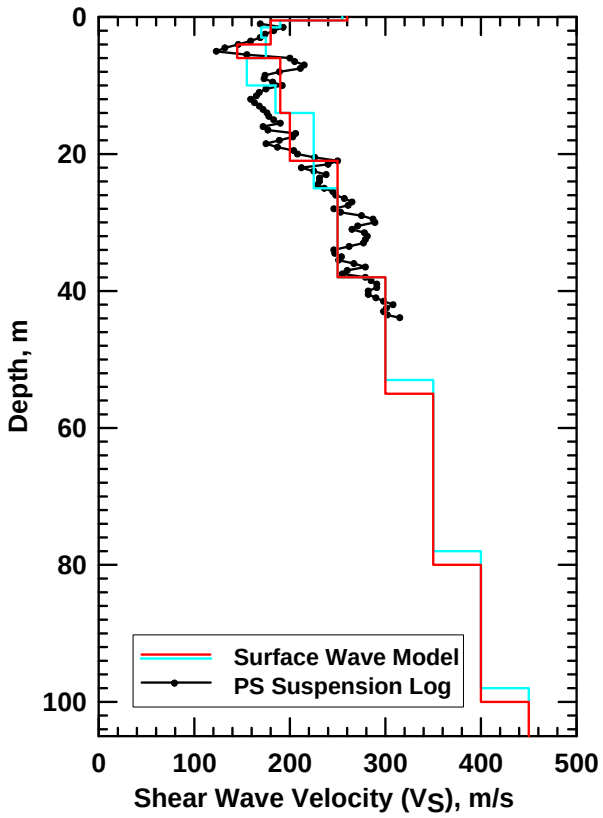


***VS Model***

In contrast to borehole measurements which are point estimates, surface wave testing is a global measurement, that is, a much larger volume of the subsurface is sampled. The resulting profile is representative of the subsurface properties averaged over distances of up to several hundred feet. Although surface wave techniques do not have the layer sensitivity or accuracy (velocity and layer thickness) of borehole techniques; the average velocity over a large depth interval (i.e. the average shear wave velocity of the upper 30m or 100ft) is very well constrained. Because surface wave methods are non-invasive and non-destructive, it is relatively easy to obtain the necessary permits for testing. At sites that are favorable for surface wave propagation, active and passive surface wave techniques allow appreciable cost and time savings.

# TABLES

Table 1 Surface Wave Sounding Locations

| Surface Wave Sounding | Northing (ft) | Easting (ft) | Elevation (ft) | Elevation (m) |
|---|---|---|---|---|
| Z1-S1 | 1858859 | 6484375 | 602 | 184 |
| Z1-S2 | 1860241 | 6486978 | 365 | 111 |
| Z1-S3 | 1855713 | 6486181 | 572 | 174 |
| Z1-S4 | 1858034 | 6487619 | 354 | 108 |
| Z1-S5 | 1854017 | 6488212 | 558 | 170 |
| Z1-S6 | 1854836 | 6488769 | 495 | 151 |
| Z1-S7 | 1855081 | 6490960 | 339 | 103 |
| Z1-S8 | 1855912 | 6493275 | 343 | 105 |
| Z1-S9 | 1857467 | 6492596 | 373 | 114 |
| Z1-S10 | 1857156 | 6493973 | 405 | 124 |
| Z1-S11 | 1851776 | 6497134 | 388 | 118 |
| Z1-S12 | 1854510 | 6496669 | 375 | 114 |
| Z1-S13 | 1855365 | 6498202 | 387 | 118 |
| Z1-S14 | 1851778 | 6503719 | 430 | 131 |
| Z1-S15 | 1852614 | 6504404 | 443 | 135 |
| Z1-S16 | 1853425 | 6507732 | 458 | 140 |
| Z1-S17 | 1851189 | 6507746 | 451 | 137 |
| Z1-S18 | 1852828 | 6501056 | 519 | 158 |
| Z1-S19 | 1850601 | 6508208 | 460 | 140 |
| Z1-S20 | 1849226 | 6512497 | 410 | 125 |
| Z2-S1 | 1867725 | 6491385 | 495 | 151 |
| Z2-S2 | 1867940 | 6496459 | 512 | 156 |
| Z2-S3 | 1866836 | 6496205 | 498 | 152 |
| Z2-S4 | 1864067 | 6497693 | 589 | 179 |
| Z2-S5 | 1863749 | 6501923 | 562 | 171 |
| Z2-S6 | 1862660 | 6500632 | 560 | 171 |
| Z2-S7 | 1860704 | 6500564 | 504 | 154 |
| Z2-S8 | 1861511 | 6501933 | 518 | 158 |
| Z2-S9 | 1859442 | 6505698 | 565 | 172 |
| Z2-S10 | 1855524 | 6508114 | 529 | 161 |
| Z2-S11 | 1854560 | 6508588 | 489 | 149 |
| Z2-S12 | 1851917 | 6511435 | 435 | 133 |
| Z3-S1 | 1873355 | 6508880 | 856 | 261 |
| Z3-S2 | 1872437 | 6515241 | 803 | 245 |
| Z3-S3 | 1870876 | 6516649 | 760 | 232 |
| Z3-S4 | 1868917 | 6516666 | 740 | 226 |
| Z3-S5 | 1869134 | 6514649 | 792 | 241 |
| Z3-S6 | 1868529 | 6512309 | 685 | 209 |
| Z3-S7 | 1867430 | 6512291 | 685 | 209 |

California State Plane coordinate system, North American Datum 1983, Zone V (0405), US Survey Feet
Horizontal accuracy is approximately 1m, vertical accuracy is approximately 2m.

Table 1 (continued) Surface Wave Sounding Locations

| Surface Wave Sounding | Northing (ft) | Easting (ft) | Elevation (ft) | Elevation (m) |
|---|---|---|---|---|
| Z3-S8 | 1865577 | 6507915 | 629 | 192 |
| Z3-S9 | 1865625 | 6509614 | 581 | 177 |
| Z3-S10 | 1866852 | 6511062 | 606 | 185 |
| Z3-S11 | 1866385 | 6514149 | 752 | 229 |
| Z3-S12 | 1864933 | 6516620 | 662 | 202 |
| Z3-S13 | 1864229 | 6511117 | 628 | 191 |
| Z3-S14 | 1863395 | 6510579 | 624 | 190 |
| Z3-S15 | 1863362 | 6514035 | 653 | 199 |
| Z3-S16 | 1860840 | 6517236 | 576 | 176 |
| Z3-S17 | 1859471 | 6510276 | 626 | 191 |
| Z3-S18 | 1859110 | 6510324 | 616 | 188 |
| Z3-S19 | 1858453 | 6513474 | 563 | 171 |
| Z3-S20 | 1855555 | 6513374 | 527 | 161 |
| Z3-S21 | 1853042 | 6513102 | 455 | 139 |
| Z3-S22 | 1852143 | 6513121 | 430 | 131 |
| Z3-S23 | 1849598 | 6513201 | 418 | 127 |
| Z3-S24 | 1848525 | 6513200 | 430 | 131 |
| Z4-S1 | 1873443 | 6532600 | 689 | 210 |
| Z4-S2 | 1870461 | 6528291 | 675 | 206 |
| Z4-S3 | 1868812 | 6528564 | 608 | 185 |
| Z4-S4 | 1867261 | 6528903 | 572 | 174 |
| Z4-S5 | 1865714 | 6525732 | 558 | 170 |
| Z4-S6 | 1862787 | 6522740 | 551 | 168 |
| Z4-S7 | 1861952 | 6521747 | 553 | 168 |
| Z4-S8 | 1859713 | 6521908 | 536 | 164 |
| Z4-S9 | 1857271 | 6519012 | 525 | 160 |
| Z4-S10 | 1854206 | 6516832 | 494 | 150 |
| Z5-S1 | 1858186 | 6559083 | 338 | 103 |
| Z5-S2 | 1857834 | 6552545 | 319 | 97 |
| Z5-S3 | 1857071 | 6547330 | 328 | 100 |
| Z5-S4 | 1857431 | 6542974 | 349 | 106 |
| Z5-S6 | 1854909 | 6534525 | 361 | 110 |
| Z5-S7 | 1853910 | 6530313 | 371 | 113 |
| Z5-S8 | 1851881 | 6527893 | 375 | 114 |
| Z5-S9 | 1851805 | 6526574 | 400 | 122 |
| Z5-S10 | 1852828 | 6523633 | 440 | 134 |
| Z5-S11 | 1851500 | 6519232 | 458 | 139 |
| Z5-S12 | 1849766 | 6516622 | 436 | 133 |
| Z5-S13 | 1848767 | 6516641 | 422 | 129 |

California State Plane coordinate system, North American Datum 1983, Zone V (0405), US Survey Feet
Horizontal accuracy is approximately 1m, vertical accuracy is approximately 2m.

Table 2 Active and Passive Surface Wave Sounding Geometry

| Surface Wave Sounding | MASW Receiver Spacing (m) | Passive Linear Array Receiver Spacing (m) | Passive "L" Array Receiver Spacing (m) |
|---|---|---|---|
| Z1-S1 | 1.5 | 4 | NC |
| Z1-S2 | 1.5 | 6 | 6 |
| Z1-S3 | 1.5 | 6 | 6 |
| Z1-S4 | 1.5 | 6 | 6 |
| Z1-S5 | 1.5 | 6 | 6 |
| Z1-S6 | 1.5 | 6 | NC |
| Z1-S7 | 1.5 | 6 | 6 |
| Z1-S8 | 1.5 | 6 | NC |
| Z1-S9 | 1.5 | 6 | 6 |
| Z1-S10 | 1.5 | 6 | 6 |
| Z1-S11 | 1.5 | 6 | 6 |
| Z1-S12 | 1.5 | 6 | 6 |
| Z1-S13 | 1.5 | 6 | 6 |
| Z1-S14 | 1.5 | 6 | 6 |
| Z1-S15 | 1.5 | 6 | 6 |
| Z1-S16 | 1.5 | 6 | 6 |
| Z1-S17 | 1.5 | 6 | 6 |
| Z1-S18 | 1.5 | 6 | 6 |
| Z1-S19 | 1.5 | 6 | 6 |
| Z1-S20 | 1.5 | 6 | 6 |
| Z2-S1 | 1.5 | 6 | 6 |
| Z2-S2 | 1.5 | 6 | 6 |
| Z2-S3 | 1.5 | 6 | 6 |
| Z2-S4 | 1.5 | 6 | 6 |
| Z2-S5 | 1.5 | 6 | 6 |
| Z2-S6 | 1.5 | 6 | 6 |
| Z2-S7 | 1.5 | 6 | 5 |
| Z2-S8 | 1.5 | 5.5 | 5.5 |
| Z2-S9 | 1.5 | 6 | 6 |
| Z2-S10 | 1.5 | 6 | 6 |
| Z2-S11 | 1.5 | 6 | 6 |
| Z2-S12 | 1.5 | 6 | 6 |
| Z3-S1 | 1.5 | 6 | 6 |
| Z3-S2 | 1.5 | 6 | 6 |
| Z3-S3 | 1.5 | 6 | 6 |
| Z3-S4 | 1.5 | 6 | 6 |
| Z3-S5 | 1.5 | 6 | 6 |
| Z3-S6 | 1.5 | 6 | 6 |
| Z3-S7 | 1.5 | 6 | 6 |

| Surface Wave Sounding | MASW Receiver Spacing (m) | Passive Linear Array Receiver Spacing (m) | Passive "L" Array Receiver Spacing (m) |
|---|---|---|---|
| Z3-S8 | 1.5 | 6 | 6 |
| Z3-S9 | 1.5 | 6 | 6 |
| Z3-S10 | 1.5 | 6 | NC |
| Z3-S11 | 1.5 | 6 | 6 |
| Z3-S12 | 1.5 | 6 | 6 |
| Z3-S13 | 1.5 | 6 | NC |
| Z3-S14 | 1.5 | 6 | 6 |
| Z3-S15 | 1.5 | 6 | 6 |
| Z3-S16 | 1.5 | 6 | 6 |
| Z3-S17 | 1.5 | 6 | 6 |
| Z3-S18 | 1.5 | 6 | 6 |
| Z3-S19 | 1.5 | 6 | 6 |
| Z3-S20 | 1.5 | 6 | 6 |
| Z3-S21 | 1 & 2 | 6 | 6 |
| Z3-S22 | 1.5 | 6 | 6 |
| Z3-S23 | 1 & 2 | 6 | NC |
| Z3-S24 | 1.5 | 6 | 6 |
| Z4-S1 | 1.5 | 6 | 6 |
| Z4-S2 | 1.5 | 6 | NC |
| Z4-S3 | 1.5 | 6 | NC |
| Z4-S4 | 1.5 | 6 | NC |
| Z4-S5 | 1.5 | 6 | 6 |
| Z4-S6 | 1.5 | 6 | 6 |
| Z4-S7 | 1.5 | 6 | 6 |
| Z4-S8 | 1.5 | 6 | 6 |
| Z4-S9 | 1.5 | 6 | 6 |
| Z4-S10 | 1.5 | 6 | 6 |
| Z5-S1 | 1.5 | 6 | 6 |
| Z5-S2 | 1.5 | 6 | 6 |
| Z5-S3 | 1.5 | 6 | 6 |
| Z5-S4 | 1.5 | 6 | 6 |
| Z5-S6 | 1.5 | 6 | 6 |
| Z5-S7 | 1.5 | 6 | 6 |
| Z5-S8 | 1.5 | 6 | 6 |
| Z5-S9 | 1.5 | 6 | 6 |
| Z5-S10 | 1.5 | 6 | 6 |
| Z5-S11 | 1.5 | 6 | 6 |
| Z5-S12 | 1.5 | 6 | 6 |
| Z5-S13 | 1.5 | 6 | 6 |

Note: NC = Not Conducted

Table 20 Velocity Model for Surface Wave Array Z1-S19

| Approx. Elevation of Top of Layer | | Depth to Top of Layer | | Layer Thickness | | S-Wave Velocity | | Inferred P-Wave Velocity | |
|---|---|---|---|---|---|---|---|---|---|
| m | ft | m | ft | m | ft | m/s | ft/s | m/s | ft/s |
| 140 | 518.4 | 0 | 0.0 | 1.5 | 4.9 | 265 | 869 | 530 | 1739 |
| 138.5 | 513.5 | 1.5 | 4.9 | 1.5 | 4.9 | 400 | 1312 | 799.9 | 2624 |
| 137 | 508.5 | 3 | 9.8 | 2 | 6.6 | 550 | 1804 | 1149.9 | 3773 |
| 135 | 502.0 | 5 | 16.4 | 2 | 6.6 | 550 | 1804 | 1850 | 6070 |
| 133 | 495.4 | 7 | 23.0 | 9 | 29.5 | 475 | 1558 | 1850 | 6070 |
| 124 | 465.9 | 16 | 52.5 | 15 | 49.2 | 575 | 1886 | 1850 | 6070 |
| 109 | 416.7 | 31 | 101.7 | 15 | 49.2 | 650 | 2133 | 1850 | 6070 |
| 94 | 367.5 | 46 | 150.9 | >14 | >45.9 | 750 | 2461 | 2150 | 7054 |

Approximate depth of investigation is 60m.

Table 21 Velocity Model for Surface Wave Array Z1-S20

| Approx. Elevation of Top of Layer | | Depth to Top of Layer | | Layer Thickness | | S-Wave Velocity | | Inferred P-Wave Velocity | |
|---|---|---|---|---|---|---|---|---|---|
| m | ft | m | ft | m | ft | m/s | ft/s | m/s | ft/s |
| 125 | 459.3 | 0 | 0.0 | 1.5 | 4.9 | 195 | 640 | 390 | 1280 |
| 123.5 | 454.4 | 1.5 | 4.9 | 1.5 | 4.9 | 285 | 935 | 570 | 1870 |
| 122 | 449.5 | 3 | 9.8 | 3 | 9.8 | 285 | 935 | 1650 | 5413 |
| 119 | 439.6 | 6 | 19.7 | 8 | 26.2 | 300 | 984 | 1650 | 5413 |
| 111 | 413.4 | 14 | 45.9 | 11.5 | 37.7 | 375 | 1230 | 1850 | 6070 |
| 99.5 | 375.7 | 25.5 | 83.7 | 26 | 85.3 | 515 | 1690 | 1850 | 6070 |
| 73.5 | 290.4 | 51.5 | 169.0 | >18.5 | >60.7 | 775 | 2543 | 2150 | 7054 |

Approximate depth of investigation is 70m.

Table 22 Summary of Zone 1 Surface Wave Investigation

| Surface Wave Array | Vs30 (m/s) | Vs30 (ft/s) | Vs60 (m/s) | Vs60 (ft/s) | Vs @ 60m (m/s) | Vs @ 60m (ft/s) |
|---|---|---|---|---|---|---|
| Z1-S1 | 362 | 1188 | 452 | 1481 | 725 | 2379 |
| Z1-S2 | 299 | 982 | 382 | 1254 | 700 | 2297 |
| Z1-S3 | 394 | 1292 | 512 | 1680 | 750 | 2461 |
| Z1-S4 | 315 | 1033 | 423 | 1387 | 700 | 2297 |
| Z1-S5 | 317 | 1039 | 430 | 1412 | 800 | 2625 |
| Z1-S6 | 323 | 1059 | 439 | 1440 | 800 | 2625 |
| Z1-S7 | 295 | 967 | 384 | 1259 | 700 | 2297 |
| Z1-S8 | 280 | 919 | 368 | 1209 | 675 | 2215 |
| Z1-S9 | 302 | 990 | 398 | 1307 | 800 | 2625 |
| Z1-S10 | 328 | 1077 | 437 | 1433 | 800 | 2625 |
| Z1-S11 | 359 | 1177 | 477 | 1565 | 850 | 2789 |
| Z1-S12 | 378 | 1240 | 487 | 1599 | 775 | 2543 |
| Z1-S13 | 354 | 1161 | 455 | 1492 | 800 | 2625 |
| Z1-S14 | 181 | 594 | 269 | 884 | 700 | 2297 |
| Z1-S15 | 230 | 754 | 336 | 1102 | 850 | 2789 |
| Z1-S16 | 249 | 818 | 317 | 1041 | 550 | 1804 |
| Z1-S18 | 273 | 894 | 364 | 1194 | 725 | 2379 |
| Z1-S19 | 500 | 1641 | 580 | 1903 | 750 | 2461 |
| Z1-S20 | 335 | 1099 | 422 | 1384 | 775 | 2543 |

Note: Vs30 = average S-wave velocity of upper 30 m. Vs60 = average S-wave velocity of upper 60 m.

Table 36 Velocity Model for Surface Wave Array Z3-S1

| Approx. Elevation of Top of Layer | | Depth to Top of Layer | | Layer Thickness | | S-Wave Velocity | | Inferred P-Wave Velocity | |
|---|---|---|---|---|---|---|---|---|---|
| m | ft | m | ft | m | ft | m/s | ft/s | m/s | ft/s |
| 261 | 856.3 | 0 | 0.0 | 1.5 | 4.9 | 240 | 787 | 480 | 1575 |
| 259.5 | 851.4 | 1.5 | 4.9 | 3.5 | 11.5 | 360 | 1181 | 720 | 2362 |
| 256 | 839.9 | 5 | 16.4 | 12 | 39.4 | 360 | 1181 | 1750 | 5741 |
| 244 | 800.5 | 17 | 55.8 | 21 | 68.9 | 525 | 1722 | 2100 | 6890 |
| 223 | 731.6 | 38 | 124.7 | 30 | 98.4 | 725 | 2379 | 2100 | 6890 |
| 193 | 633.2 | 68 | 223.1 | >2 | >6.6 | 900 | 2953 | 2400 | 7874 |

Approximate depth of investigation is 70m.

Table 37 Velocity Model for Surface Wave Array Z3-S2

| Approx. Elevation of Top of Layer | | Depth to Top of Layer | | Layer Thickness | | S-Wave Velocity | | Inferred P-Wave Velocity | |
|---|---|---|---|---|---|---|---|---|---|
| m | ft | m | ft | m | ft | m/s | ft/s | m/s | ft/s |
| 245 | 803.8 | 0 | 0.0 | 1.75 | 5.7 | 150 | 492 | 300 | 984 |
| 243.25 | 798.1 | 1.75 | 5.7 | 3.75 | 12.3 | 310 | 1017 | 620 | 2034 |
| 239.5 | 785.8 | 5.5 | 18.0 | 10 | 32.8 | 375 | 1230 | 750 | 2460 |
| 229.5 | 753.0 | 15.5 | 50.9 | 17 | 55.8 | 425 | 1394 | 850 | 2788 |
| 212.5 | 697.2 | 32.5 | 106.6 | 20 | 65.6 | 500 | 1640 | 1925 | 6316 |
| 192.5 | 631.6 | 52.5 | 172.2 | 20 | 65.6 | 650 | 2133 | 2100 | 6890 |
| 172.5 | 565.9 | 72.5 | 237.9 | >2.5 | >8.2 | 1000 | 3281 | 2800 | 9186 |

Approximate depth of investigation is 75m.

Table 38 Velocity Model for Surface Wave Array Z3-S3

| Approx. Elevation of Top of Layer | | Depth to Top of Layer | | Layer Thickness | | S-Wave Velocity | | Inferred P-Wave Velocity | |
|---|---|---|---|---|---|---|---|---|---|
| m | ft | m | ft | m | ft | m/s | ft/s | m/s | ft/s |
| 232 | 761.2 | 0 | 0.0 | 2 | 6.6 | 235 | 771 | 470 | 1542 |
| 230 | 754.6 | 2 | 6.6 | 3.5 | 11.5 | 260 | 853 | 520 | 1706 |
| 226.5 | 743.1 | 5.5 | 18.0 | 16.5 | 54.1 | 405 | 1329 | 810 | 2657 |
| 210 | 689.0 | 22 | 72.2 | 15 | 49.2 | 450 | 1476 | 900 | 2953 |
| 195 | 639.8 | 37 | 121.4 | 8 | 26.2 | 600 | 1969 | 1200 | 3937 |
| 187 | 613.5 | 45 | 147.6 | 12 | 39.4 | 600 | 1969 | 2100 | 6890 |
| 175 | 574.1 | 57 | 187.0 | >13 | >42.7 | 800 | 2625 | 2800 | 9186 |

Approximate depth of investigation is 70m.

Table 39 Velocity Model for Surface Wave Array Z3-S4

| Approx. Elevation of Top of Layer | | Depth to Top of Layer | | Layer Thickness | | S-Wave Velocity | | Inferred P-Wave Velocity | |
|---|---|---|---|---|---|---|---|---|---|
| m | ft | m | ft | m | ft | m/s | ft/s | m/s | ft/s |
| 226 | 741.5 | 0 | 0.0 | 7 | 23.0 | 275 | 902 | 550 | 1804 |
| 219 | 718.5 | 7 | 23.0 | 14 | 45.9 | 390 | 1280 | 780 | 2559 |
| 205 | 672.6 | 21 | 68.9 | 15 | 49.2 | 475 | 1558 | 950 | 3116 |
| 190 | 623.4 | 36 | 118.1 | 9 | 29.5 | 650 | 2133 | 1300 | 4265 |
| 181 | 593.8 | 45 | 147.6 | 11 | 36.1 | 650 | 2133 | 2100 | 6890 |
| 170 | 557.7 | 56 | 183.7 | >14 | >45.9 | 900 | 2953 | 2800 | 9186 |

Approximate depth of investigation is 70m.

Table 40 Velocity Model for Surface Wave Array Z3-S5

| Approx. Elevation of Top of Layer | | Depth to Top of Layer | | Layer Thickness | | S-Wave Velocity | | Inferred P-Wave Velocity | |
|---|---|---|---|---|---|---|---|---|---|
| m | ft | m | ft | m | ft | m/s | ft/s | m/s | ft/s |
| 241 | 790.7 | 0 | 0.0 | 1.75 | 5.7 | 245 | 804 | 490 | 1608 |
| 239.25 | 784.9 | 1.75 | 5.7 | 5.25 | 17.2 | 375 | 1230 | 750 | 2460 |
| 234 | 767.7 | 7 | 23.0 | 10 | 32.8 | 500 | 1640 | 1000 | 3281 |
| 224 | 734.9 | 17 | 55.8 | 10 | 32.8 | 650 | 2133 | 1300 | 4265 |
| 214 | 702.1 | 27 | 88.6 | 3 | 9.8 | 750 | 2461 | 1500 | 4921 |
| 211 | 692.3 | 30 | 98.4 | 7 | 23.0 | 750 | 2461 | 2400 | 7874 |
| 204 | 669.3 | 37 | 121.4 | 10 | 32.8 | 1000 | 3281 | 2800 | 9186 |
| 194 | 636.5 | 47 | 154.2 | >23 | >75.5 | 1200 | 3937 | 2800 | 9186 |

Approximate depth of investigation is 70m.

Table 41 Velocity Model for Surface Wave Array Z3-S6

| Approx. Elevation of Top of Layer | | Depth to Top of Layer | | Layer Thickness | | S-Wave Velocity | | Inferred P-Wave Velocity | |
|---|---|---|---|---|---|---|---|---|---|
| m | ft | m | ft | m | ft | m/s | ft/s | m/s | ft/s |
| 209 | 685.7 | 0 | 0.0 | 2 | 6.6 | 270 | 886 | 540 | 1772 |
| 207 | 679.1 | 2 | 6.6 | 3 | 9.8 | 325 | 1066 | 650 | 2133 |
| 204 | 669.3 | 5 | 16.4 | 2 | 6.6 | 325 | 1066 | 1750 | 5741 |
| 202 | 662.7 | 7 | 23.0 | 8 | 26.2 | 370 | 1214 | 1750 | 5741 |
| 194 | 636.5 | 15 | 49.2 | 8 | 26.2 | 465 | 1526 | 1925 | 6316 |
| 186 | 610.2 | 23 | 75.5 | 17 | 55.8 | 650 | 2133 | 2100 | 6890 |
| 169 | 554.5 | 40 | 131.2 | 20 | 65.6 | 775 | 2543 | 2400 | 7874 |
| 149 | 488.8 | 60 | 196.9 | >10 | >32.8 | 1000 | 3281 | 2800 | 9186 |

Approximate depth of investigation is 70m.

Table 45 Velocity Model for Surface Wave Array Z3-S10

| Approx. Elevation of Top of Layer | | Depth to Top of Layer | | Layer Thickness | | S-Wave Velocity | | Inferred P-Wave Velocity | |
|---|---|---|---|---|---|---|---|---|---|
| m | ft | m | ft | m | ft | m/s | ft/s | m/s | ft/s |
| 185.0 | 607.0 | 0 | 0.0 | 2.5 | 8.2 | 175 | 574 | 350 | 1148 |
| 182.5 | 598.8 | 2.5 | 8.2 | 0.5 | 1.6 | 310 | 1017 | 620 | 2034 |
| 182.0 | 597.1 | 3 | 9.8 | 2.5 | 8.2 | 310 | 1017 | 1750 | 5741 |
| 179.5 | 588.9 | 5.5 | 18.0 | 5 | 16.4 | 440 | 1444 | 1925 | 6316 |
| 174.5 | 572.5 | 10.5 | 34.4 | 20 | 65.6 | 520 | 1706 | 2100 | 6890 |
| 154.5 | 506.9 | 30.5 | 100.1 | >39.5 | >129.6 | 740 | 2428 | 2400 | 7874 |

Approximate depth of investigation is 70m.

Table 46 Velocity Model for Surface Wave Array Z3-S11

| Approx. Elevation of Top of Layer | | Depth to Top of Layer | | Layer Thickness | | S-Wave Velocity | | Inferred P-Wave Velocity | |
|---|---|---|---|---|---|---|---|---|---|
| m | ft | m | ft | m | ft | m/s | ft/s | m/s | ft/s |
| 229.0 | 751.3 | 0 | 0.0 | 2 | 6.6 | 215 | 705 | 430 | 1411 |
| 227.0 | 744.8 | 2 | 6.6 | 3 | 9.8 | 260 | 853 | 520 | 1706 |
| 224.0 | 734.9 | 5 | 16.4 | 4 | 13.1 | 280 | 919 | 560 | 1837 |
| 220.0 | 721.8 | 9 | 29.5 | 1.5 | 4.9 | 325 | 1066 | 650 | 2133 |
| 218.5 | 716.9 | 10.5 | 34.4 | 12.5 | 41.0 | 325 | 1066 | 1750 | 5741 |
| 206.0 | 675.9 | 23 | 75.5 | 20 | 65.6 | 415 | 1362 | 1925 | 6316 |
| 186.0 | 610.2 | 43 | 141.1 | >27 | >88.6 | 625 | 2051 | 2100 | 6890 |

Approximate depth of investigation is 70m.

Table 47 Velocity Model for Surface Wave Array Z3-S12

| Approx. Elevation of Top of Layer | | Depth to Top of Layer | | Layer Thickness | | S-Wave Velocity | | Inferred P-Wave Velocity | |
|---|---|---|---|---|---|---|---|---|---|
| m | ft | m | ft | m | ft | m/s | ft/s | m/s | ft/s |
| 202 | 662.7 | 0 | 0.0 | 1.5 | 4.9 | 200 | 656 | 400 | 1312 |
| 200.5 | 657.8 | 1.5 | 4.9 | 2 | 6.6 | 260 | 853 | 520 | 1706 |
| 198.5 | 651.2 | 3.5 | 11.5 | 3.5 | 11.5 | 235 | 771 | 470 | 1542 |
| 195 | 639.8 | 7 | 23.0 | 8.5 | 27.9 | 340 | 1115 | 680 | 2231 |
| 186.5 | 611.9 | 15.5 | 50.9 | 11.5 | 37.7 | 350 | 1148 | 1750 | 5741 |
| 175 | 574.1 | 27 | 88.6 | 22 | 72.2 | 400 | 1312 | 1925 | 6316 |
| 153 | 502.0 | 49 | 160.8 | >35 | >114.8 | 675 | 2215 | 2100 | 6890 |

Approximate depth of investigation is 70m.

Table 50 Velocity Model for Surface Wave Array Z3-S15

| Approx. Elevation of Top of Layer | | Depth to Top of Layer | | Layer Thickness | | S-Wave Velocity | | Inferred P-Wave Velocity | |
|---|---|---|---|---|---|---|---|---|---|
| m | ft | m | ft | m | ft | m/s | ft/s | m/s | ft/s |
| 199 | 652.9 | 0 | 0.0 | 1.5 | 4.9 | 190 | 623 | 380 | 1247 |
| 197.5 | 648.0 | 1.5 | 4.9 | 2.5 | 8.2 | 260 | 853 | 520 | 1706 |
| 195 | 639.8 | 4 | 13.1 | 2.5 | 8.2 | 300 | 984 | 600 | 1969 |
| 192.5 | 631.6 | 6.5 | 21.3 | 8.5 | 27.9 | 350 | 1148 | 700 | 2297 |
| 184 | 603.7 | 15 | 49.2 | 4 | 13.1 | 350 | 1148 | 1750 | 5741 |
| 180 | 590.6 | 19 | 62.3 | 16 | 52.5 | 400 | 1312 | 1925 | 6316 |
| 164 | 538.1 | 35 | 114.8 | 16 | 52.5 | 500 | 1640 | 2100 | 6890 |
| 148 | 485.6 | 51 | 167.3 | >19 | >62.3 | 750 | 2461 | 2100 | 6890 |

Approximate depth of investigation is 70m.

Table 51 Velocity Model for Surface Wave Array Z3-S16

| Approx. Elevation of Top of Layer | | Depth to Top of Layer | | Layer Thickness | | S-Wave Velocity | | Inferred P-Wave Velocity | |
|---|---|---|---|---|---|---|---|---|---|
| m | ft | m | ft | m | ft | m/s | ft/s | m/s | ft/s |
| 176 | 577.4 | 0 | 0.0 | 2.5 | 8.2 | 225 | 738 | 450 | 1476 |
| 173.5 | 569.2 | 2.5 | 8.2 | 5 | 16.4 | 380 | 1247 | 760 | 2493 |
| 168.5 | 552.8 | 7.5 | 24.6 | 2.5 | 8.2 | 370 | 1214 | 740 | 2427 |
| 166 | 544.6 | 10 | 32.8 | 12 | 39.4 | 370 | 1214 | 1750 | 5741 |
| 154 | 505.2 | 22 | 72.2 | 20 | 65.6 | 425 | 1394 | 1925 | 6316 |
| 134 | 439.6 | 42 | 137.8 | >28 | >91.9 | 500 | 1640 | 1925 | 6316 |

Approximate depth of investigation is 70m.

Table 52 Velocity Model for Surface Wave Array Z3-S17

| Approx. Elevation of Top of Layer | | Depth to Top of Layer | | Layer Thickness | | S-Wave Velocity | | Inferred P-Wave Velocity | |
|---|---|---|---|---|---|---|---|---|---|
| m | ft | m | ft | m | ft | m/s | ft/s | m/s | ft/s |
| 191 | 626.6 | 0 | 0.0 | 2 | 6.6 | 215 | 705 | 430 | 1411 |
| 189 | 620.1 | 2 | 6.6 | 6 | 19.7 | 290 | 951 | 580 | 1903 |
| 183 | 600.4 | 8 | 26.2 | 8 | 26.2 | 290 | 951 | 1750 | 5741 |
| 175 | 574.1 | 16 | 52.5 | 5.5 | 18.0 | 350 | 1148 | 1750 | 5741 |
| 169.5 | 556.1 | 21.5 | 70.5 | 10 | 32.8 | 700 | 2297 | 2100 | 6890 |
| 159.5 | 523.3 | 31.5 | 103.3 | 10 | 32.8 | 800 | 2625 | 2400 | 7874 |
| 149.5 | 490.5 | 41.5 | 136.2 | >28.5 | >93.5 | 1250 | 4101 | 2800 | 9186 |

Approximate depth of investigation is 70m.

Table 53 Velocity Model for Surface Wave Array Z3-S18

| Approx. Elevation of Top of Layer | | Depth to Top of Layer | | Layer Thickness | | S-Wave Velocity | | Inferred P-Wave Velocity | |
|---|---|---|---|---|---|---|---|---|---|
| m | ft | m | ft | m | ft | m/s | ft/s | m/s | ft/s |
| 188 | 616.8 | 0 | 0.0 | 1.5 | 4.9 | 195 | 640 | 390 | 1280 |
| 186.5 | 611.9 | 1.5 | 4.9 | 6.5 | 21.3 | 285 | 935 | 570 | 1870 |
| 180 | 590.6 | 8 | 26.2 | 11 | 36.1 | 285 | 935 | 1750 | 5741 |
| 169 | 554.5 | 19 | 62.3 | 7 | 23.0 | 350 | 1148 | 1750 | 5741 |
| 162 | 531.5 | 26 | 85.3 | 10 | 32.8 | 650 | 2133 | 2100 | 6890 |
| 152 | 498.7 | 36 | 118.1 | 10 | 32.8 | 800 | 2625 | 2400 | 7874 |
| 142 | 465.9 | 46 | 150.9 | >24 | >78.7 | 1250 | 4101 | 2800 | 9186 |

Approximate depth of investigation is 70m.

Table 54 Velocity Model for Surface Wave Array Z3-S19

| Approx. Elevation of Top of Layer | | Depth to Top of Layer | | Layer Thickness | | S-Wave Velocity | | Inferred P-Wave Velocity | |
|---|---|---|---|---|---|---|---|---|---|
| m | ft | m | ft | m | ft | m/s | ft/s | m/s | ft/s |
| 171 | 561.0 | 0 | 0.0 | 1.5 | 4.9 | 260 | 853 | 520 | 1706 |
| 169.5 | 556.1 | 1.5 | 4.9 | 2.5 | 8.2 | 400 | 1312 | 799.9 | 2624 |
| 167 | 547.9 | 4 | 13.1 | 5 | 16.4 | 320 | 1050 | 640 | 2100 |
| 162 | 531.5 | 9 | 29.5 | 6 | 19.7 | 350 | 1148 | 700 | 2297 |
| 156 | 511.8 | 15 | 49.2 | 4 | 13.1 | 350 | 1148 | 1750 | 5741 |
| 152 | 498.7 | 19 | 62.3 | 11 | 36.1 | 375 | 1230 | 1750 | 5741 |
| 141 | 462.6 | 30 | 98.4 | 35 | 114.8 | 550 | 1804 | 2100 | 6890 |
| 106 | 347.8 | 65 | 213.3 | >5 | >16.4 | 705 | 2313 | 2100 | 6890 |

Approximate depth of investigation is 70m.

Table 55 Velocity Model for Surface Wave Array Z3-S20

| Approx. Elevation of Top of Layer | | Depth to Top of Layer | | Layer Thickness | | S-Wave Velocity | | Inferred P-Wave Velocity | |
|---|---|---|---|---|---|---|---|---|---|
| m | ft | m | ft | m | ft | m/s | ft/s | m/s | ft/s |
| 161 | 528.2 | 0 | 0.0 | 2 | 6.6 | 255 | 837 | 510 | 1673 |
| 159 | 521.7 | 2 | 6.6 | 5 | 16.4 | 315 | 1033 | 630 | 2067 |
| 154 | 505.2 | 7 | 23.0 | 3 | 9.8 | 315 | 1033 | 1750 | 5741 |
| 151 | 495.4 | 10 | 32.8 | 10 | 32.8 | 350 | 1148 | 1750 | 5741 |
| 141 | 462.6 | 20 | 65.6 | 15 | 49.2 | 375 | 1230 | 1750 | 5741 |
| 126 | 413.4 | 35 | 114.8 | 30 | 98.4 | 550 | 1804 | 2100 | 6890 |
| 96 | 315.0 | 65 | 213.3 | >5 | >16.4 | 700 | 2297 | 2100 | 6890 |

Approximate depth of investigation is 70m.

Table 56 Velocity Model for Surface Wave Array Z3-S21

| Approx. Elevation of Top of Layer | | Depth to Top of Layer | | Layer Thickness | | S-Wave Velocity | | Inferred P-Wave Velocity | |
|---|---|---|---|---|---|---|---|---|---|
| m | ft | m | ft | m | ft | m/s | ft/s | m/s | ft/s |
| 139 | 456.0 | 0 | 0.0 | 2 | 6.6 | 320 | 1050 | 640 | 2100 |
| 137 | 449.5 | 2 | 6.6 | 8 | 26.2 | 300 | 984 | 600 | 1969 |
| 129 | 423.2 | 10 | 32.8 | 6 | 19.7 | 350 | 1148 | 699.9 | 2296 |
| 123 | 403.5 | 16 | 52.5 | 15 | 49.2 | 350 | 1148 | 1750 | 5741 |
| 108 | 354.3 | 31 | 101.7 | 30 | 98.4 | 450 | 1476 | 1925 | 6316 |
| 78 | 255.9 | 61 | 200.1 | >9 | >29.5 | 650 | 2133 | 2100 | 6890 |

Approximate depth of investigation is 70m.

Table 57 Velocity Model for Surface Wave Array Z3-S22

| Approx. Elevation of Top of Layer | | Depth to Top of Layer | | Layer Thickness | | S-Wave Velocity | | Inferred P-Wave Velocity | |
|---|---|---|---|---|---|---|---|---|---|
| m | ft | m | ft | m | ft | m/s | ft/s | m/s | ft/s |
| 131 | 429.8 | 0 | 0.0 | 3 | 9.8 | 275 | 902 | 550 | 1804 |
| 128 | 419.9 | 3 | 9.8 | 8 | 26.2 | 385 | 1263 | 769.9 | 2526 |
| 120 | 393.7 | 11 | 36.1 | 5 | 16.4 | 350 | 1148 | 700 | 2297 |
| 115 | 377.3 | 16 | 52.5 | 12 | 39.4 | 350 | 1148 | 1750 | 5741 |
| 103 | 337.9 | 28 | 91.9 | 25 | 82.0 | 450 | 1476 | 1925 | 6316 |
| 78 | 255.9 | 53 | 173.9 | >17 | >55.8 | 700 | 2297 | 2100 | 6890 |

Approximate depth of investigation is 70m.

Table 58 Velocity Model for Surface Wave Array Z3-S23

| Approx. Elevation of Top of Layer | | Depth to Top of Layer | | Layer Thickness | | S-Wave Velocity | | Inferred P-Wave Velocity | |
|---|---|---|---|---|---|---|---|---|---|
| m | ft | m | ft | m | ft | m/s | ft/s | m/s | ft/s |
| 127 | 416.7 | 0 | 0.0 | 1.5 | 4.9 | 175 | 574 | 350 | 1148 |
| 125.5 | 411.7 | 1.5 | 4.9 | 2.5 | 8.2 | 285 | 935 | 570 | 1870 |
| 123 | 403.5 | 4 | 13.1 | 3 | 9.8 | 335 | 1099 | 670 | 2198 |
| 120 | 393.7 | 7 | 23.0 | 5 | 16.4 | 375 | 1230 | 749.9 | 2460 |
| 115 | 377.3 | 12 | 39.4 | 24 | 78.7 | 375 | 1230 | 1750 | 5741 |
| 91 | 298.6 | 36 | 118.1 | 26 | 85.3 | 450 | 1476 | 1925 | 6316 |
| 65 | 213.3 | 62 | 203.4 | >8 | >26.2 | 665 | 2182 | 2100 | 6890 |

Approximate depth of investigation is 70m.

Table 59 Velocity Model for Surface Wave Array Z3-S24

| Approx. Elevation of Top of Layer | | Depth to Top of Layer | | Layer Thickness | | S-Wave Velocity | | Inferred P-Wave Velocity | |
|---|---|---|---|---|---|---|---|---|---|
| m | ft | m | ft | m | ft | m/s | ft/s | m/s | ft/s |
| 131 | 429.8 | 0 | 0.0 | 1.5 | 4.9 | 240 | 787 | 480 | 1575 |
| 129.5 | 424.9 | 1.5 | 4.9 | 2.5 | 8.2 | 275 | 902 | 550 | 1804 |
| 127 | 416.7 | 4 | 13.1 | 5 | 16.4 | 325 | 1066 | 650 | 2133 |
| 122 | 400.3 | 9 | 29.5 | 3 | 9.8 | 450 | 1476 | 899.9 | 2952 |
| 119 | 390.4 | 12 | 39.4 | 13 | 42.7 | 450 | 1476 | 1925 | 6316 |
| 106 | 347.8 | 25 | 82.0 | 28 | 91.9 | 525 | 1722 | 1925 | 6316 |
| 78 | 255.9 | 53 | 173.9 | >17 | >55.8 | 700 | 2297 | 2100 | 6890 |

Approximate depth of investigation is 70m.

Table 60 Summary of Zone 3 Surface Wave Investigation

| Surface Wave Array | Vs30 (m/s) | Vs30 (ft/s) | Vs60 (m/s) | Vs60 (ft/s) | Vs @ 60m (m/s) | Vs @ 60m (ft/s) |
|---|---|---|---|---|---|---|
| Z3-S1 | 405 | 1329 | 501 | 1644 | 725 | 2379 |
| Z3-S2 | 355 | 1165 | 423 | 1388 | 650 | 2133 |
| Z3-S3 | 373 | 1223 | 451 | 1479 | 800 | 2625 |
| Z3-S4 | 374 | 1227 | 468 | 1535 | 900 | 2953 |
| Z3-S5 | 496 | 1627 | 662 | 2172 | 1200 | 3937 |
| Z3-S6 | 414 | 1358 | 528 | 1732 | 1000 | 3281 |
| Z3-S7 | 478 | 1568 | 609 | 1998 | 975 | 3199 |
| Z3-S8 | 370 | 1214 | 424 | 1391 | 550 | 1804 |
| Z3-S9 | 313 | 1027 | 361 | 1184 | 435 | 1427 |
| Z3-S10 | 412 | 1352 | 528 | 1732 | 740 | 2428 |
| Z3-S11 | 316 | 1037 | 391 | 1283 | 625 | 2051 |
| Z3-S12 | 314 | 1030 | 377 | 1237 | 675 | 2215 |
| Z3-S13 | 396 | 1299 | 479 | 1572 | 725 | 2379 |
| Z3-S14 | 393 | 1289 | 482 | 1581 | 725 | 2379 |
| Z3-S15 | 337 | 1106 | 412 | 1352 | 750 | 2461 |
| Z3-S16 | 365 | 1198 | 410 | 1345 | 500 | 1640 |
| Z3-S17 | 351 | 1152 | 522 | 1713 | 1250 | 4101 |
| Z3-S18 | 315 | 1033 | 468 | 1535 | 1250 | 4101 |
| Z3-S19 | 351 | 1152 | 428 | 1404 | 550 | 1804 |
| Z3-S20 | 339 | 1112 | 407 | 1335 | 700 | 2297 |
| Z3-S21 | 333 | 1093 | 381 | 1250 | 650 | 2133 |
| Z3-S22 | 354 | 1161 | 411 | 1348 | 700 | 2297 |
| Z3-S23 | 342 | 1122 | 382 | 1253 | 450 | 1476 |
| Z3-S24 | 396 | 1298 | 463 | 1519 | 700 | 2297 |

Note: Vs30 = average S-wave velocity of upper 30 m. Vs60 = average S-wave velocity of upper 60 m.

Table 64 Velocity Model for Surface Wave Array Z4-S4

| Approx. Elevation of Top of Layer | | Depth to Top of Layer | | Layer Thickness | | S-Wave Velocity | | Inferred P-Wave Velocity | |
|---|---|---|---|---|---|---|---|---|---|
| m | ft | m | ft | m | ft | m/s | ft/s | m/s | ft/s |
| 174 | 570.9 | 0 | 0.0 | 3 | 9.8 | 265 | 869 | 530 | 1739 |
| 171 | 561.0 | 3 | 9.8 | 3 | 9.8 | 275 | 902 | 550 | 1804 |
| 168 | 551.2 | 6 | 19.7 | 9 | 29.5 | 285 | 935 | 570 | 1870 |
| 159 | 521.7 | 15 | 49.2 | 25 | 82.0 | 440 | 1444 | 880 | 2887 |
| 134 | 439.6 | 40 | 131.2 | 20 | 65.6 | 500 | 1640 | 1000 | 3281 |
| 114 | 374.0 | 60 | 196.9 | 5 | 16.4 | 600 | 1969 | 1200 | 3937 |
| 109 | 357.6 | 65 | 213.3 | >5 | >16.4 | 600 | 1969 | 1750 | 5741 |

Approximate depth of investigation is 70m.

Table 65 Velocity Model for Surface Wave Array Z4-S5

| Approx. Elevation of Top of Layer | | Depth to Top of Layer | | Layer Thickness | | S-Wave Velocity | | Inferred P-Wave Velocity | |
|---|---|---|---|---|---|---|---|---|---|
| m | ft | m | ft | m | ft | m/s | ft/s | m/s | ft/s |
| 170 | 557.7 | 0 | 0.0 | 2 | 6.6 | 245 | 804 | 490 | 1608 |
| 168 | 551.2 | 2 | 6.6 | 3 | 9.8 | 275 | 902 | 550 | 1804 |
| 165 | 541.3 | 5 | 16.4 | 4 | 13.1 | 250 | 820 | 500 | 1640 |
| 161 | 528.2 | 9 | 29.5 | 11 | 36.1 | 350 | 1148 | 700 | 2297 |
| 150 | 492.1 | 20 | 65.6 | 13 | 42.7 | 400 | 1312 | 800 | 2624 |
| 137 | 449.5 | 33 | 108.3 | 17 | 55.8 | 500 | 1640 | 1000 | 3281 |
| 120 | 393.7 | 50 | 164.0 | 15 | 49.2 | 600 | 1969 | 1200 | 3937 |
| 105 | 344.5 | 65 | 213.3 | >5 | >16.4 | 600 | 1969 | 1750 | 5741 |

Approximate depth of investigation is 70m.

Table 66 Velocity Model for Surface Wave Array Z4-S6

| Approx. Elevation of Top of Layer | | Depth to Top of Layer | | Layer Thickness | | S-Wave Velocity | | Inferred P-Wave Velocity | |
|---|---|---|---|---|---|---|---|---|---|
| m | ft | m | ft | m | ft | m/s | ft/s | m/s | ft/s |
| 168 | 551.2 | 0 | 0.0 | 2 | 6.6 | 265 | 869 | 530 | 1739 |
| 166 | 544.6 | 2 | 6.6 | 3 | 9.8 | 255 | 837 | 510 | 1673 |
| 163 | 534.8 | 5 | 16.4 | 4 | 13.1 | 300 | 984 | 600 | 1969 |
| 159 | 521.7 | 9 | 29.5 | 11 | 36.1 | 350 | 1148 | 700 | 2297 |
| 148 | 485.6 | 20 | 65.6 | 13 | 42.7 | 400 | 1312 | 800 | 2624 |
| 135 | 442.9 | 33 | 108.3 | 20 | 65.6 | 500 | 1640 | 1000 | 3281 |
| 115 | 377.3 | 53 | 173.9 | 12 | 39.4 | 550 | 1804 | 1100 | 3609 |
| 103 | 337.9 | 65 | 213.3 | >5 | >16.4 | 550 | 1804 | 1750 | 5741 |

Approximate depth of investigation is 70m.

Table 67 Velocity Model for Surface Wave Array Z4-S7

| Approx. Elevation of Top of Layer | | Depth to Top of Layer | | Layer Thickness | | S-Wave Velocity | | Inferred P-Wave Velocity | |
|---|---|---|---|---|---|---|---|---|---|
| m | ft | m | ft | m | ft | m/s | ft/s | m/s | ft/s |
| 168 | 551.2 | 0 | 0.0 | 1.5 | 4.9 | 235 | 771 | 470 | 1542 |
| 166.5 | 546.3 | 1.5 | 4.9 | 2.5 | 8.2 | 265 | 869 | 530 | 1739 |
| 164 | 538.1 | 4 | 13.1 | 5 | 16.4 | 300 | 984 | 600 | 1969 |
| 159 | 521.7 | 9 | 29.5 | 11 | 36.1 | 350 | 1148 | 700 | 2297 |
| 148 | 485.6 | 20 | 65.6 | 15 | 49.2 | 400 | 1312 | 800 | 2624 |
| 133 | 436.4 | 35 | 114.8 | 20 | 65.6 | 500 | 1640 | 1000 | 3281 |
| 113 | 370.7 | 55 | 180.4 | 10 | 32.8 | 550 | 1804 | 1100 | 3609 |
| 103 | 337.9 | 65 | 213.3 | >5 | >16.4 | 550 | 1804 | 1750 | 5741 |

Approximate depth of investigation is 70m.

Table 68 Velocity Model for Surface Wave Array Z4-S8

| Approx. Elevation of Top of Layer | | Depth to Top of Layer | | Layer Thickness | | S-Wave Velocity | | Inferred P-Wave Velocity | |
|---|---|---|---|---|---|---|---|---|---|
| m | ft | m | ft | m | ft | m/s | ft/s | m/s | ft/s |
| 164 | 538.1 | 0 | 0.0 | 1.5 | 4.9 | 190 | 623 | 380 | 1247 |
| 162.5 | 533.1 | 1.5 | 4.9 | 2.5 | 8.2 | 250 | 820 | 500 | 1640 |
| 160 | 524.9 | 4 | 13.1 | 6 | 19.7 | 300 | 984 | 600 | 1969 |
| 154 | 505.2 | 10 | 32.8 | 6 | 19.7 | 350 | 1148 | 700 | 2297 |
| 148 | 485.6 | 16 | 52.5 | 15 | 49.2 | 400 | 1312 | 800 | 2624 |
| 133 | 436.4 | 31 | 101.7 | 14 | 45.9 | 500 | 1640 | 1000 | 3281 |
| 119 | 390.4 | 45 | 147.6 | 10 | 32.8 | 600 | 1969 | 1200 | 3937 |
| 109 | 357.6 | 55 | 180.4 | >15 | >49.2 | 600 | 1969 | 1750 | 5741 |

Approximate depth of investigation is 70m.

Table 69 Velocity Model for Surface Wave Array Z4-S9

| Approx. Elevation of Top of Layer | | Depth to Top of Layer | | Layer Thickness | | S-Wave Velocity | | Inferred P-Wave Velocity | |
|---|---|---|---|---|---|---|---|---|---|
| m | ft | m | ft | m | ft | m/s | ft/s | m/s | ft/s |
| 160 | 524.9 | 0 | 0.0 | 1 | 3.3 | 210 | 689 | 420 | 1378 |
| 159 | 521.7 | 1 | 3.3 | 2 | 6.6 | 290 | 951 | 580 | 1903 |
| 157 | 515.1 | 3 | 9.8 | 4.5 | 14.8 | 275 | 902 | 550 | 1804 |
| 152.5 | 500.3 | 7.5 | 24.6 | 6.5 | 21.3 | 350 | 1148 | 700 | 2297 |
| 146 | 479.0 | 14 | 45.9 | 12 | 39.4 | 400 | 1312 | 800 | 2624 |
| 134 | 439.6 | 26 | 85.3 | 24 | 78.7 | 500 | 1640 | 1000 | 3281 |
| 110 | 360.9 | 50 | 164.0 | >20 | >65.6 | 500 | 1640 | 1700 | 5577 |

Approximate depth of investigation is 70m.

Table 70 Velocity Model for Surface Wave Array Z4-S10

| Approx. Elevation of Top of Layer | | Depth to Top of Layer | | Layer Thickness | | S-Wave Velocity | | Inferred P-Wave Velocity | |
|---|---|---|---|---|---|---|---|---|---|
| m | ft | m | ft | m | ft | m/s | ft/s | m/s | ft/s |
| 150.0 | 492.1 | 0 | 0.0 | 1.5 | 4.9 | 245 | 804 | 490 | 1608 |
| 148.5 | 487.2 | 1.5 | 4.9 | 4.5 | 14.8 | 315 | 1033 | 630 | 2067 |
| 144.0 | 472.4 | 6 | 19.7 | 5 | 16.4 | 350 | 1148 | 700 | 2297 |
| 139.0 | 456.0 | 11 | 36.1 | 17 | 55.8 | 410 | 1345 | 820 | 2690 |
| 122.0 | 400.3 | 28 | 91.9 | 7 | 23.0 | 475 | 1558 | 950 | 3116 |
| 115.0 | 377.3 | 35 | 114.8 | 30 | 98.4 | 475 | 1558 | 1700 | 5577 |
| 85.0 | 278.9 | 65 | 213.3 | >5 | >16.4 | 525 | 1722 | 1700 | 5577 |

Approximate depth of investigation is 70m.

Table 71 Velocity Summary of Zone 4 Surface Wave Investigation

| Surface Wave Array | Vs30 (m/s) | Vs30 (ft/s) | Vs60 (m/s) | Vs60 (ft/s) | Vs @ 60m (m/s) | Vs @ 60m (ft/s) |
|---|---|---|---|---|---|---|
| Z4-S1 | 362 | 1188 | 484 | 1589 | 850 | 2789 |
| Z4-S2 | 369 | 1210 | 443 | 1454 | 600 | 1969 |
| Z4-S3 | 288 | 944 | 349 | 1144 | 500 | 1640 |
| Z4-S4 | 341 | 1120 | 398 | 1307 | 600 | 1969 |
| Z4-S5 | 328 | 1076 | 401 | 1315 | 600 | 1969 |
| Z4-S6 | 337 | 1105 | 402 | 1318 | 550 | 1804 |
| Z4-S7 | 337 | 1107 | 399 | 1308 | 550 | 1804 |
| Z4-S8 | 333 | 1093 | 412 | 1353 | 600 | 1969 |
| Z4-S9 | 355 | 1164 | 415 | 1361 | 500 | 1640 |
| Z4-S10 | 373 | 1225 | 418 | 1372 | 475 | 1558 |

Note: Vs30 = average S-wave velocity of upper 30 m. Vs60 = average S-wave velocity of upper 60 m.

Table 78 Velocity Model for Surface Wave Array Z5-S8

| Approx. Elevation of Top of Layer | | Depth to Top of Layer | | Layer Thickness | | S-Wave Velocity | | Inferred P-Wave Velocity | |
|---|---|---|---|---|---|---|---|---|---|
| m | ft | m | ft | m | ft | m/s | ft/s | m/s | ft/s |
| 114 | 374.0 | 0 | 0.0 | 2.5 | 8.2 | 305 | 1001 | 610 | 2001 |
| 111.5 | 365.8 | 2.5 | 8.2 | 3.5 | 11.5 | 335 | 1099 | 670 | 2198 |
| 108 | 354.3 | 6 | 19.7 | 6 | 19.7 | 275 | 902 | 550 | 1804 |
| 102 | 334.6 | 12 | 39.4 | 10 | 32.8 | 400 | 1312 | 800 | 2624 |
| 92 | 301.8 | 22 | 72.2 | 20 | 65.6 | 475 | 1558 | 950 | 3116 |
| 72 | 236.2 | 42 | 137.8 | 14 | 45.9 | 550 | 1804 | 1100 | 3609 |
| 58 | 190.3 | 56 | 183.7 | >14 | >45.9 | 550 | 1804 | 1700 | 5577 |

Approximate depth of investigation is 70m.

Table 79 Velocity Model for Surface Wave Array Z5-S9

| Approx. Elevation of Top of Layer | | Depth to Top of Layer | | Layer Thickness | | S-Wave Velocity | | Inferred P-Wave Velocity | |
|---|---|---|---|---|---|---|---|---|---|
| m | ft | m | ft | m | ft | m/s | ft/s | m/s | ft/s |
| 122 | 400.3 | 0 | 0.0 | 2 | 6.6 | 210 | 689 | 420 | 1378 |
| 120 | 393.7 | 2 | 6.6 | 6 | 19.7 | 315 | 1033 | 630 | 2067 |
| 114 | 374.0 | 8 | 26.2 | 10 | 32.8 | 320 | 1050 | 640 | 2100 |
| 104 | 341.2 | 18 | 59.1 | 35 | 114.8 | 475 | 1558 | 950 | 3116 |
| 69 | 226.4 | 53 | 173.9 | 3 | 9.8 | 500 | 1640 | 1000 | 3281 |
| 66 | 216.5 | 56 | 183.7 | >14 | >45.9 | 500 | 1640 | 1700 | 5577 |

Approximate depth of investigation is 70m.

Table 80 Velocity Model for Surface Wave Array Z5-S10

| Approx. Elevation of Top of Layer | | Depth to Top of Layer | | Layer Thickness | | S-Wave Velocity | | Inferred P-Wave Velocity | |
|---|---|---|---|---|---|---|---|---|---|
| m | ft | m | ft | m | ft | m/s | ft/s | m/s | ft/s |
| 134 | 439.6 | 0 | 0.0 | 2 | 6.6 | 300 | 984 | 600 | 1969 |
| 132 | 433.1 | 2 | 6.6 | 9 | 29.5 | 275 | 902 | 550 | 1804 |
| 123 | 403.5 | 11 | 36.1 | 14 | 45.9 | 375 | 1230 | 750 | 2460 |
| 109 | 357.6 | 25 | 82.0 | 8 | 26.2 | 525 | 1722 | 1050 | 3445 |
| 101 | 331.4 | 33 | 108.3 | 7 | 23.0 | 550 | 1804 | 1100 | 3609 |
| 94 | 308.4 | 40 | 131.2 | 27 | 88.6 | 550 | 1804 | 1700 | 5577 |
| 67 | 219.8 | 67 | 219.8 | >3 | >9.8 | 665 | 2182 | 1750 | 5741 |

Approximate depth of investigation is 70m.

Table 81 Velocity Model for Surface Wave Array Z5-S11

| Approx. Elevation of Top of Layer | | Depth to Top of Layer | | Layer Thickness | | S-Wave Velocity | | Inferred P-Wave Velocity | |
|---|---|---|---|---|---|---|---|---|---|
| m | ft | m | ft | m | ft | m/s | ft/s | m/s | ft/s |
| 139 | 456.0 | 0 | 0.0 | 1.5 | 4.9 | 190 | 623 | 380 | 1247 |
| 137.5 | 451.1 | 1.5 | 4.9 | 3.5 | 11.5 | 285 | 935 | 570 | 1870 |
| 134 | 439.6 | 5 | 16.4 | 7 | 23.0 | 350 | 1148 | 700 | 2297 |
| 127 | 416.7 | 12 | 39.4 | 8 | 26.2 | 400 | 1312 | 800 | 2625 |
| 119 | 390.4 | 20 | 65.6 | 5 | 16.4 | 465 | 1526 | 930 | 3051 |
| 114 | 374.0 | 25 | 82.0 | 30 | 98.4 | 465 | 1526 | 1700 | 5577 |
| 84 | 275.6 | 55 | 180.4 | >15 | >49.2 | 525 | 1722 | 1725 | 5659 |

Approximate depth of investigation is 70m.

Table 82 Velocity Model for Surface Wave Array Z5-S12

| Approx. Elevation of Top of Layer | | Depth to Top of Layer | | Layer Thickness | | S-Wave Velocity | | Inferred P-Wave Velocity | |
|---|---|---|---|---|---|---|---|---|---|
| m | ft | m | ft | m | ft | m/s | ft/s | m/s | ft/s |
| 133 | 436.4 | 0 | 0.0 | 2.5 | 8.2 | 275 | 902 | 550 | 1804 |
| 130.5 | 428.1 | 2.5 | 8.2 | 2 | 6.6 | 255 | 837 | 510 | 1673 |
| 128.5 | 421.6 | 4.5 | 14.8 | 4.5 | 14.8 | 350 | 1148 | 700 | 2297 |
| 124 | 406.8 | 9 | 29.5 | 7 | 23.0 | 450 | 1476 | 900 | 2953 |
| 117 | 383.9 | 16 | 52.5 | 20 | 65.6 | 450 | 1476 | 1600 | 5249 |
| 97 | 318.2 | 36 | 118.1 | >34 | >111.5 | 500 | 1640 | 1700 | 5577 |

Approximate depth of investigation is 70m.

Table 83 Velocity Model for Surface Wave Array Z5-S13

| Approx. Elevation of Top of Layer | | Depth to Top of Layer | | Layer Thickness | | S-Wave Velocity | | Inferred P-Wave Velocity | |
|---|---|---|---|---|---|---|---|---|---|
| m | ft | m | ft | m | ft | m/s | ft/s | m/s | ft/s |
| 129 | 423.2 | 0 | 0.0 | 2.5 | 8.2 | 205 | 673 | 410 | 1345 |
| 126.5 | 415.0 | 2.5 | 8.2 | 2.5 | 8.2 | 300 | 984 | 600 | 1969 |
| 124 | 406.8 | 5 | 16.4 | 7 | 23.0 | 350 | 1148 | 700 | 2297 |
| 117 | 383.9 | 12 | 39.4 | 4 | 13.1 | 400 | 1312 | 800 | 2624 |
| 113 | 370.7 | 16 | 52.5 | 14 | 45.9 | 400 | 1312 | 1600 | 5249 |
| 99 | 324.8 | 30 | 98.4 | 29 | 95.1 | 450 | 1476 | 1700 | 5577 |
| 70 | 229.7 | 59 | 193.6 | >11 | >36.1 | 550 | 1804 | 1725 | 5659 |

Approximate depth of investigation is 70m.

Table 84 Summary of Zone 5 Surface Wave Investigation

| Surface Wave Array | Vs30 (m/s) | Vs30 (ft/s) | Vs60 (m/s) | Vs60 (ft/s) | Vs @ 60m (m/s) | Vs @ 60m (ft/s) |
|---|---|---|---|---|---|---|
| Z5-S1 | 325 | 1065 | 386 | 1265 | 475 | 1558 |
| Z5-S2 | 320 | 1050 | 367 | 1205 | 500 | 1640 |
| Z5-S3 | 320 | 1049 | 381 | 1251 | 500 | 1640 |
| Z5-S4 | 303 | 994 | 362 | 1187 | 500 | 1640 |
| Z5-S6 | 329 | 1080 | 396 | 1299 | 625 | 2051 |
| Z5-S7 | 366 | 1202 | 426 | 1396 | 525 | 1722 |
| Z5-S8 | 364 | 1196 | 428 | 1403 | 550 | 1804 |
| Z5-S9 | 353 | 1157 | 407 | 1335 | 500 | 1640 |
| Z5-S10 | 348 | 1141 | 425 | 1396 | 550 | 1804 |
| Z5-S11 | 367 | 1205 | 414 | 1358 | 525 | 1722 |
| Z5-S12 | 392 | 1287 | 435 | 1429 | 500 | 1640 |
| Z5-S13 | 351 | 1151 | 395 | 1297 | 550 | 1804 |

Note: Vs30 = average S-wave velocity of upper 30 m. Vs60 = average S-wave velocity of upper 60 m.

# FIGURES

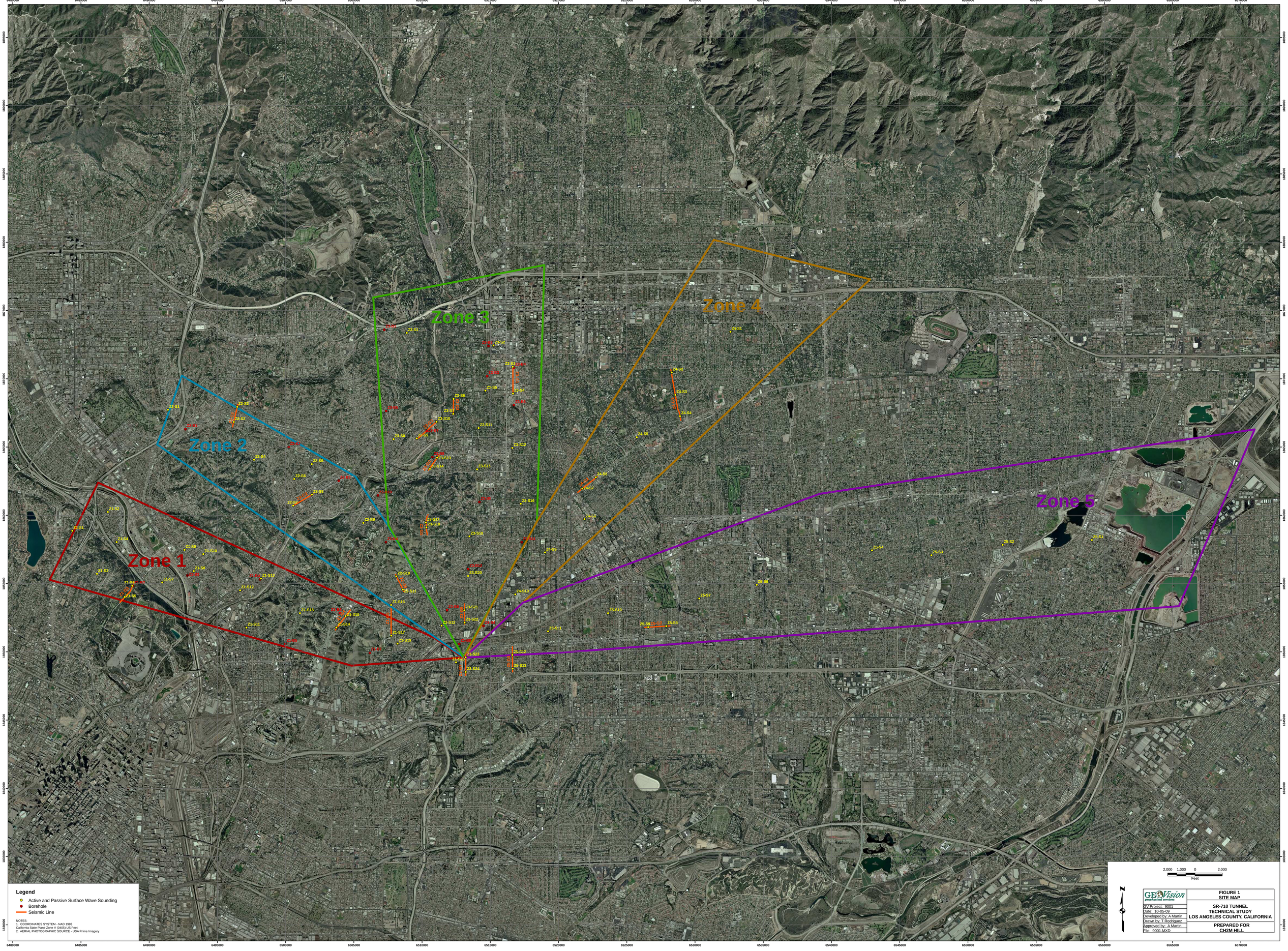
Zone 1
Zone 2
Zone 3
Zone 4
Zone 5
Legend
Active and Passive Surface Wave Sounding
Borehole
Seismic Line
NOTES:
1. COORDINATES SYSTEM - NAD 1983
California State Plane Zone V (0405) US Feet
2. AERIAL PHOTOGRAPHIC SOURCE - USA Prime Imagery
2,000 1,000 0 2,000
Feet
N
GEOVision geophysical services
FIGURE 1
SITE MAP
GV Project: 9001
Date: 10-05-09
Developed by: A Martin
Drawn by: T Rodriguez
Approved by: A Martin
File: 9001.MXD
SR-710 TUNNEL
TECHNICAL STUDY
LOS ANGELES COUNTY, CALIFORNIA
PREPARED FOR
CH2M HILL

TYPICAL PASSIVE SURFACE WAVE SETUP

SEISMIC RECORDER SYSTEM

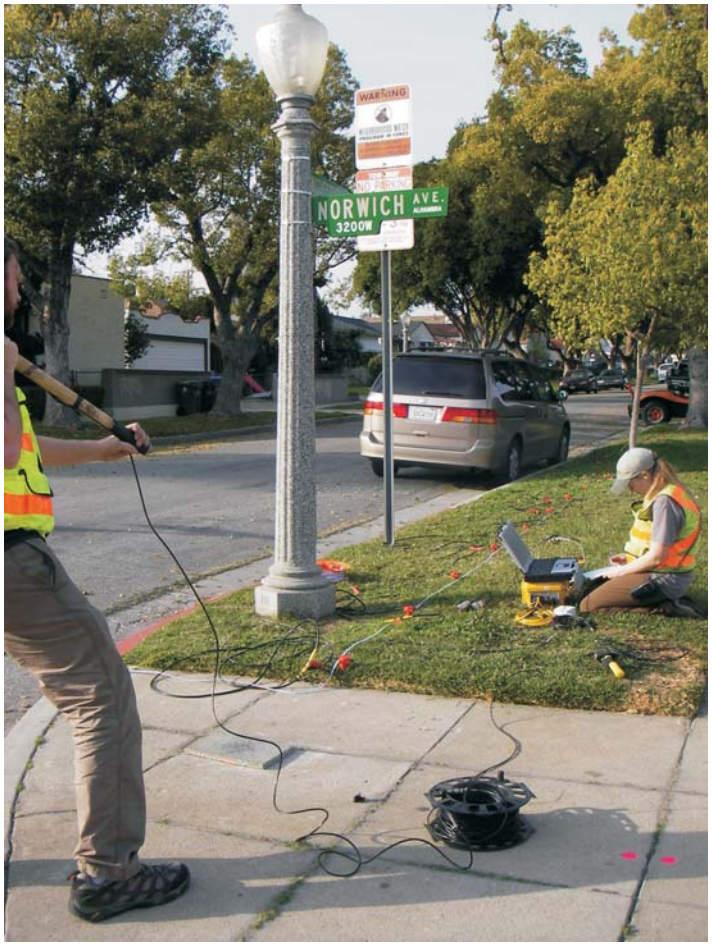


TYPICAL MASW SETUP

| | |
|---|---|
| GEOVision geophysical services | FIGURE 2<br>PHOTOGRAPHS OF PASSIVE AND<br>ACTIVE SURFACE ARRAY FIELD LAYOUT |
| Project # 9001 | SR-710 TUNNEL TECHNICAL STUDY<br>LOS ANGELES COUNTY, CALIFORNIA |
| Date: JUL 17, 2009 | |
| Drawn By: A MARTIN | |
| Approved By: Antony J Martin | PREPARED FOR<br>CH2M HILL |
| File R:\...Project Files\2009\9001ch2mhill\report\figures\Figure2.cdr | |

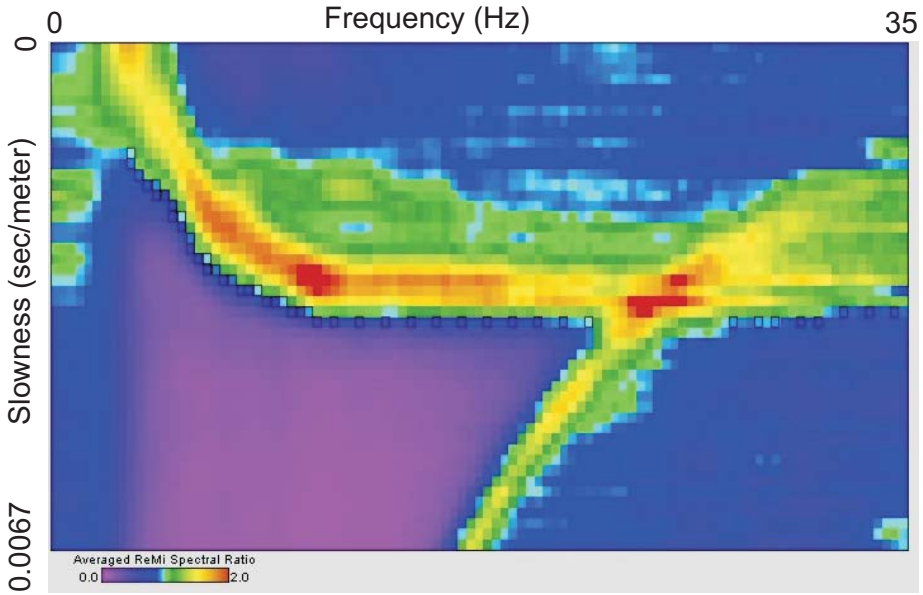


Wavefield Transform of Linear Array Passive Surface Wave Data using Optim SeisOpt ReMi Data Analysis Package (Z2-S2)

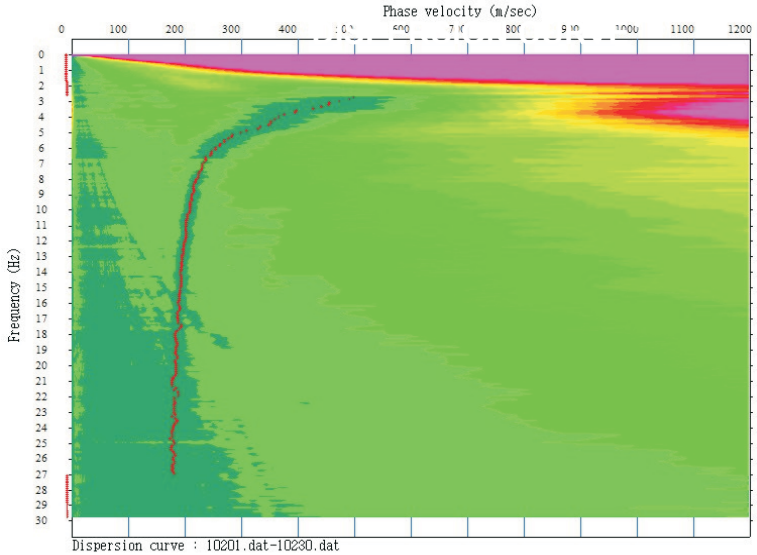


Wavefield Transform of "L" array Passive Surface Wave Data using Spatial Autocorrelation Method (Z1-S16)

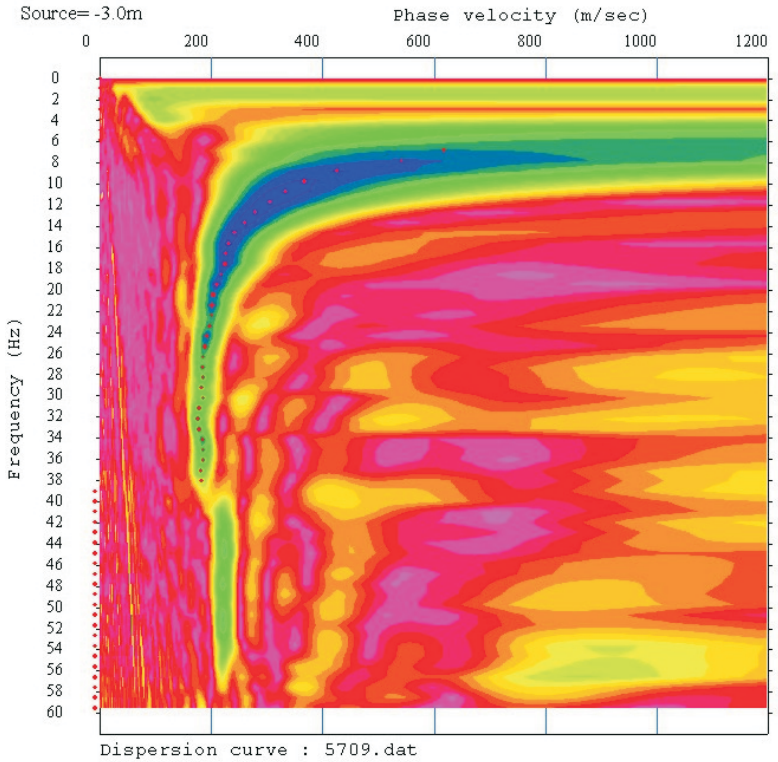


Wavefield Transform of MASW Data (Z2-S6)

| | |
|---|---|
| GEOVision geophysical services | FIGURE 3<br>TYPICAL WAVEFIELD TRANSFORMS OF ACTIVE AND PASSIVE SURFACE WAVE DATA |
| Project # 9001 | SR-710 TUNNEL TECHNICAL STUDY<br>LOS ANGELES COUNTY, CALIFORNIA |
| Date: JUL 20, 2009 | |
| Drawn By: A MARTIN | |
| Approved By: | PREPARED FOR<br>CH2M HILL |
| File R:\...Project Files\2009\9001ch2mhill\report\figures\Figure 3.cdr | |

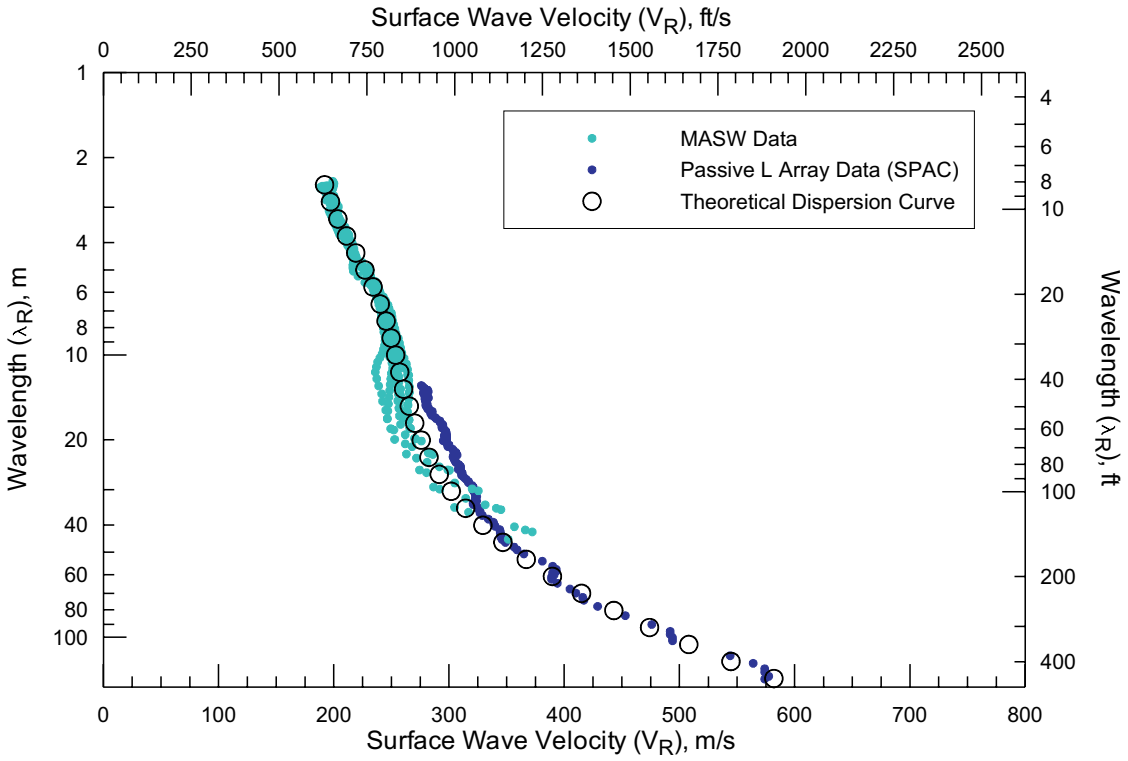


**Comparison of Field Experimental Data and Theoretical Dispersion Curve from Active and Passive Surface Wave Array Z1-S20**

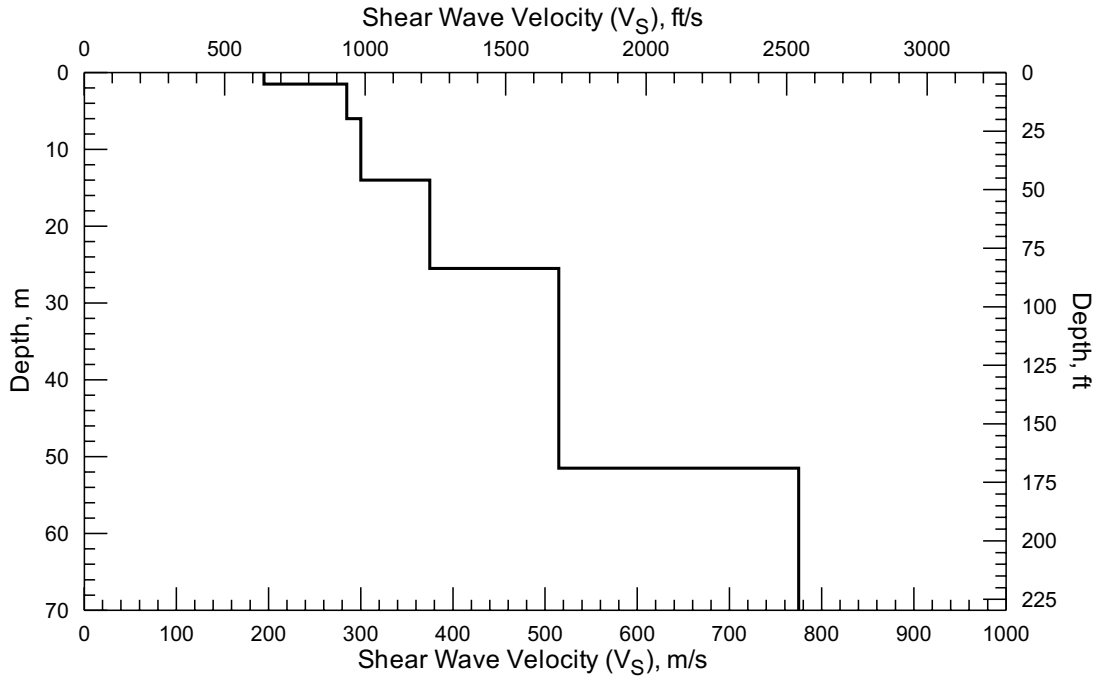


**$V_S$ Model from Active and Passive Surface Wave Array Z1-S20**

| | |
|---|---|
| GEOVision geophysical services | FIGURE 22<br>VELOCITY MODEL FOR ACTIVE AND PASSIVE SURFACE WAVE ARRAY Z1-S20 |
| Project # 9001 | NEAR WEST VALLEY BLVD AND HIGHBURY AVE, LOS ANGELES, CALIFORNIA |
| Date: JUL 17, 2008 | |
| Drawn By: A MARTIN | PREPARED FOR<br>CH2M HILL |
| Approved By: Antony J Martin | |
| File R:\...Project Files\2009\9001ch2mhill\report\figures\Figure22.cdr | |

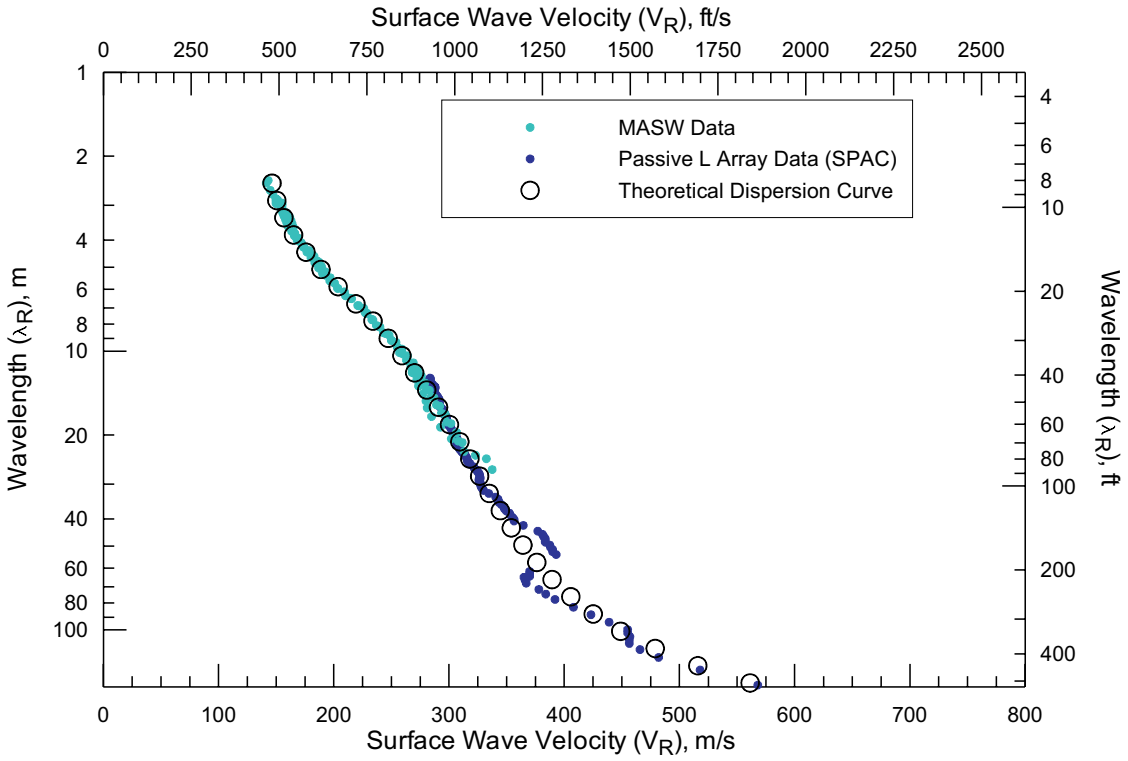


**Comparison of Field Experimental Data and Theoretical Dispersion Curve from Active and Passive Surface Wave Array Z3-S2**

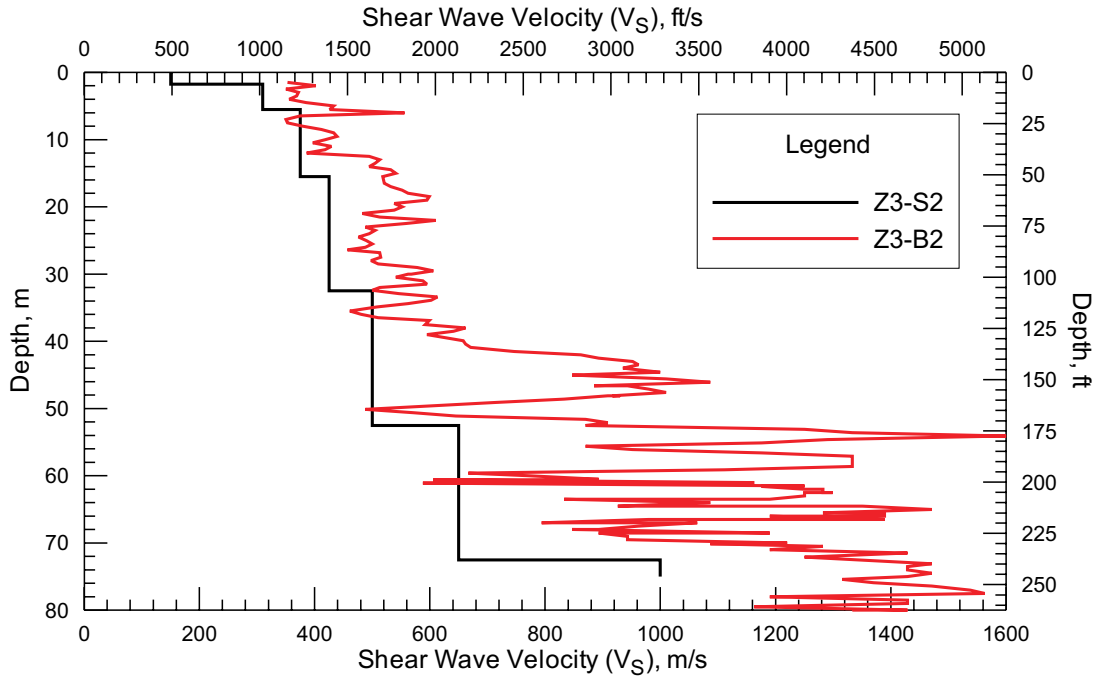


**$V_S$ Model from Active and Passive Surface Wave Array Z3-S2**

| | |
|---|---|
| GEOVision geophysical services | FIGURE 36<br>VELOCITY MODEL FOR ACTIVE AND PASSIVE SURFACE WAVE ARRAY Z3-S2 |
| Project # 9001<br>Date: JUL 24, 2009<br>Drawn By: A MARTIN<br>Approved By: Antony J. Martin<br>File R:\...Project Files\2009\9001ch2mhill\report\figures\Figure36.cdr | PASADENA AVE AND PALMETTO DR,<br>PASADENA, CALIFORNIA |
| | PREPARED FOR<br>CH2M HILL |

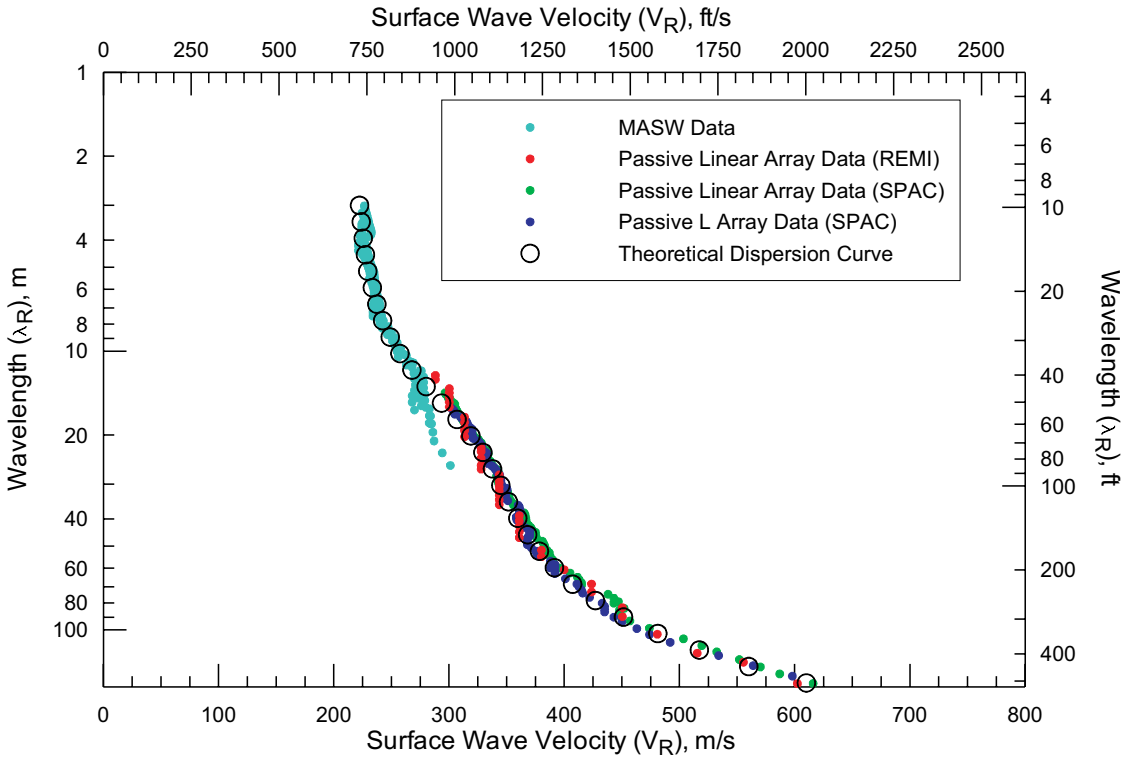


**Comparison of Field Experimental Data and Theoretical Dispersion Curve from Active and Passive Surface Wave Array Z3-S3**

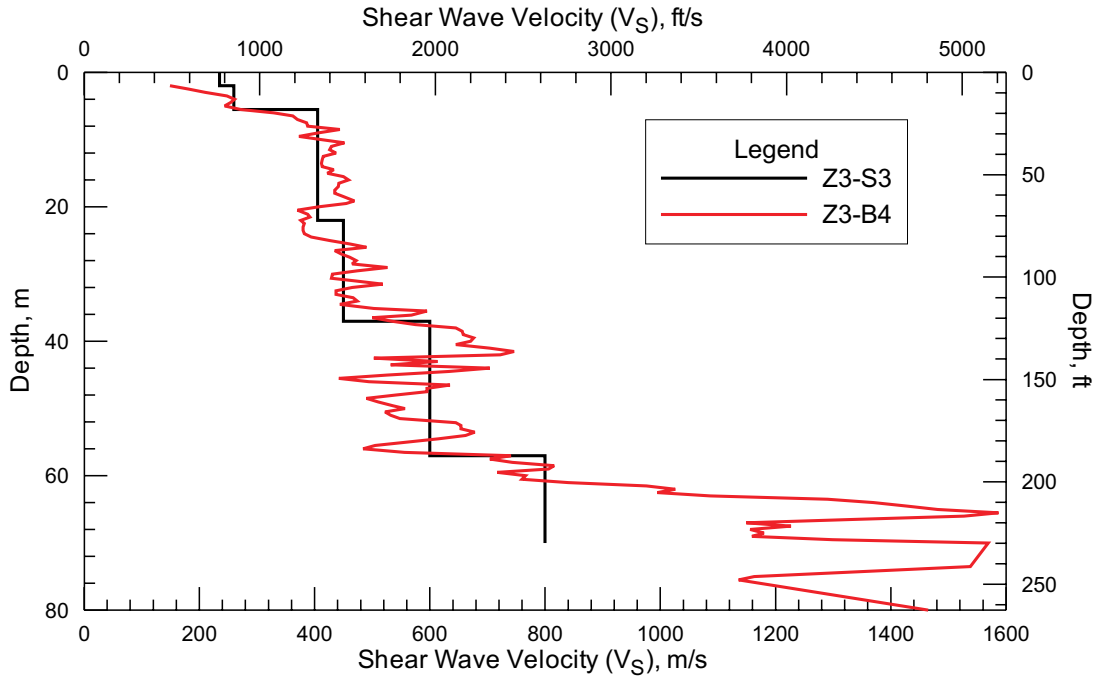


**$V_S$ Model from Active and Passive Surface Wave Array Z3-S3**

| | |
|---|---|
| GEOVision geophysical services | FIGURE 37<br>VELOCITY MODEL FOR ACTIVE AND PASSIVE SURFACE WAVE ARRAY Z3-S3 |
| Project # 9001<br>Date: JUL 24, 2009<br>Drawn By: A MARTIN<br>Approved By: Antony J. Martin<br>File R:\...Project Files\2009\9001ch2mhill\report\figures\Figure37.cdr | RAYMOND AVE AND FILLMORE ST,<br>PASADENA, CALIFORNIA |
| | PREPARED FOR<br>CH2M HILL |

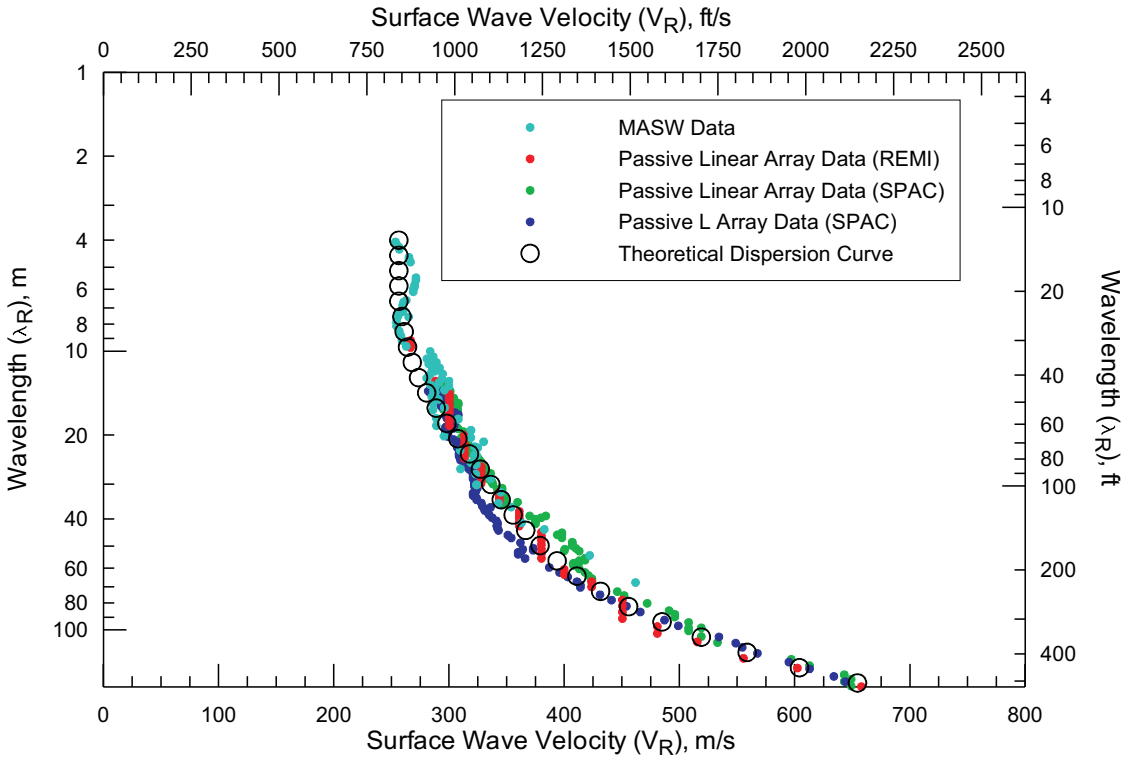


**Comparison of Field Experimental Data and Theoretical Dispersion Curve from Active and Passive Surface Wave Array Z3-S4**

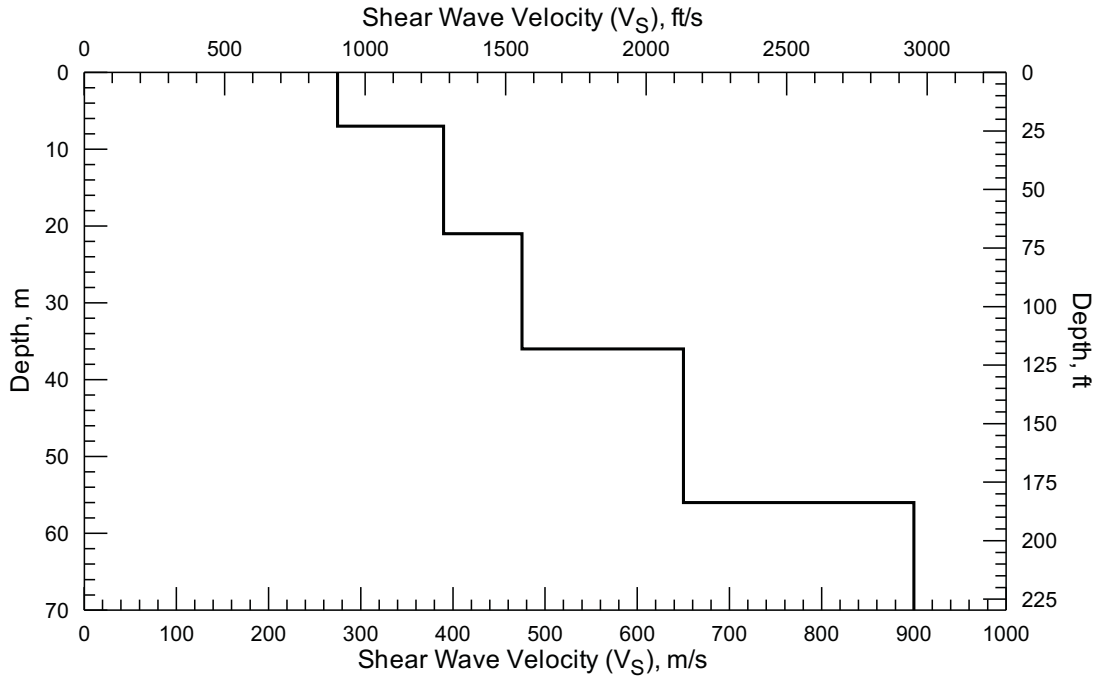


**$V_S$ Model from Active and Passive Surface Wave Array Z3-S4**

| | |
|---|---|
| GEOVision geophysical services | FIGURE 38<br>VELOCITY MODEL FOR ACTIVE AND PASSIVE SURFACE WAVE ARRAY Z3-S4 |
| Project # 9001<br>Date: JUL 24, 2009<br>Drawn By: A MARTIN<br>Approved By: Antony J Martin<br>File R:\...Project Files\2009\9001ch2mhill\report\figures\Figure38.cdr | RAYMOND AVE AND GLENARM ST,<br>PASADENA, CALIFORNIA |
| | PREPARED FOR<br>CH2M HILL |

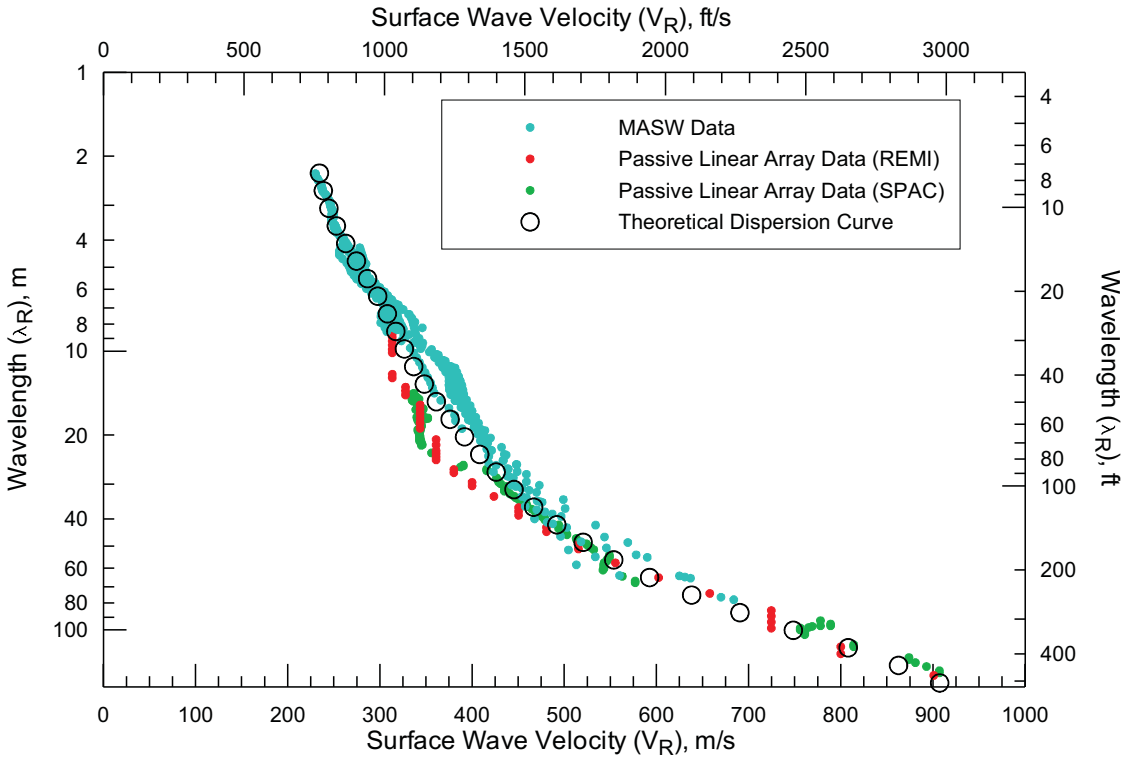


**Comparison of Field Experimental Data and Theoretical Dispersion Curve from Active and Passive Surface Wave Array Z3-S5**

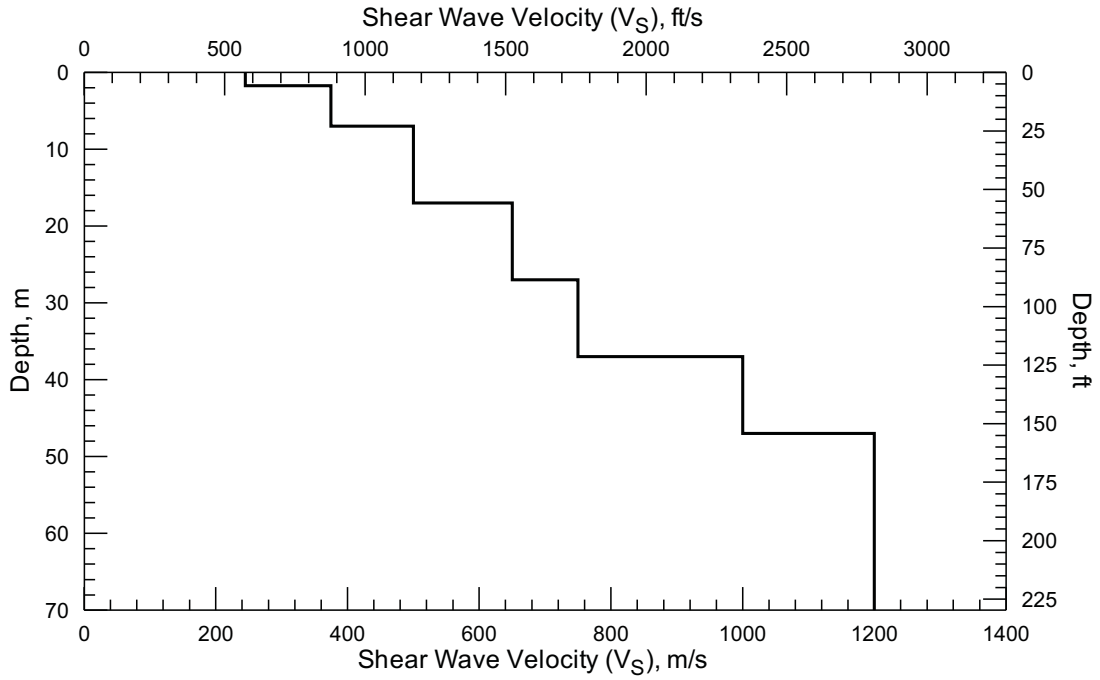


**$V_S$ Model from Active and Passive Surface Wave Array Z3-S5**

| | |
|---|---|
| GEOVision geophysical services | FIGURE 39<br>VELOCITY MODEL FOR ACTIVE AND PASSIVE SURFACE WAVE ARRAY Z3-S5 |
| Project # 9001<br>Date: JUL 24, 2009<br>Drawn By: A MARTIN<br>Approved By: Antony J Martin<br>File R:\...Project Files\2009\9001ch2mhill\report\figures\Figure39.cdr | PASADENA AVE AND ARLINGTON DR,<br>PASADENA, CALIFORNIA |
| | PREPARED FOR<br>CH2M HILL |

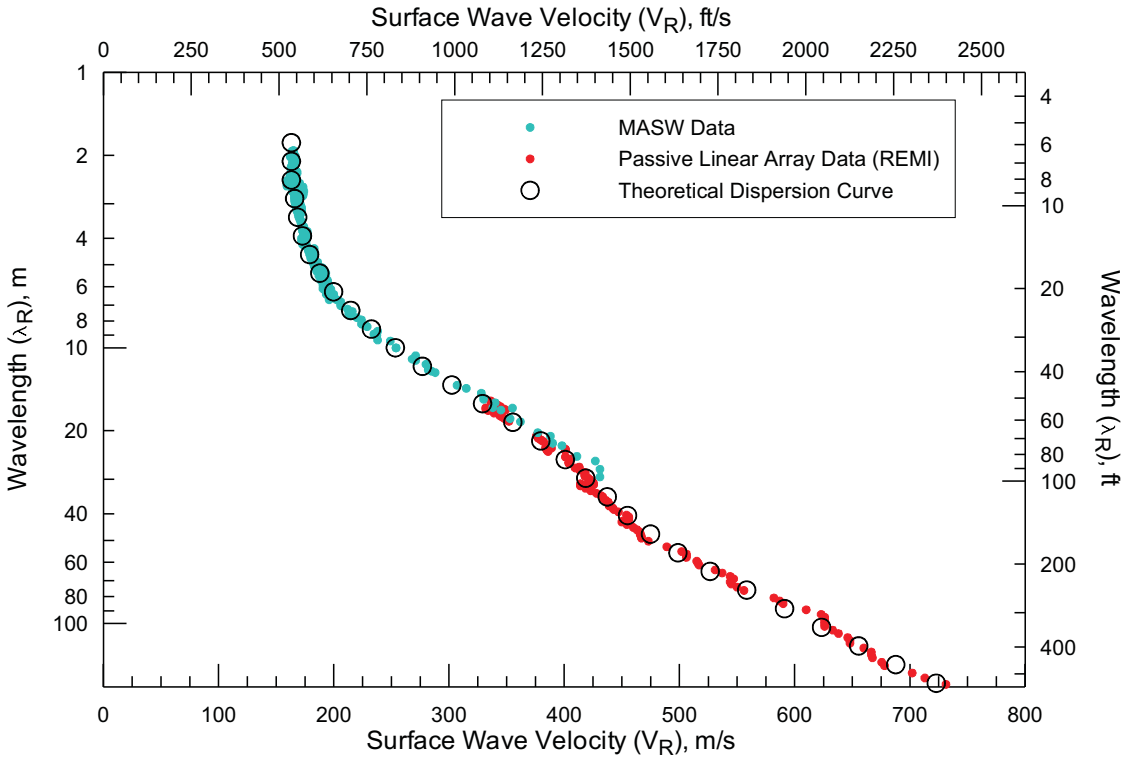


**Comparison of Field Experimental Data and Theoretical Dispersion Curve from Active and Passive Surface Wave Array Z3-S11**

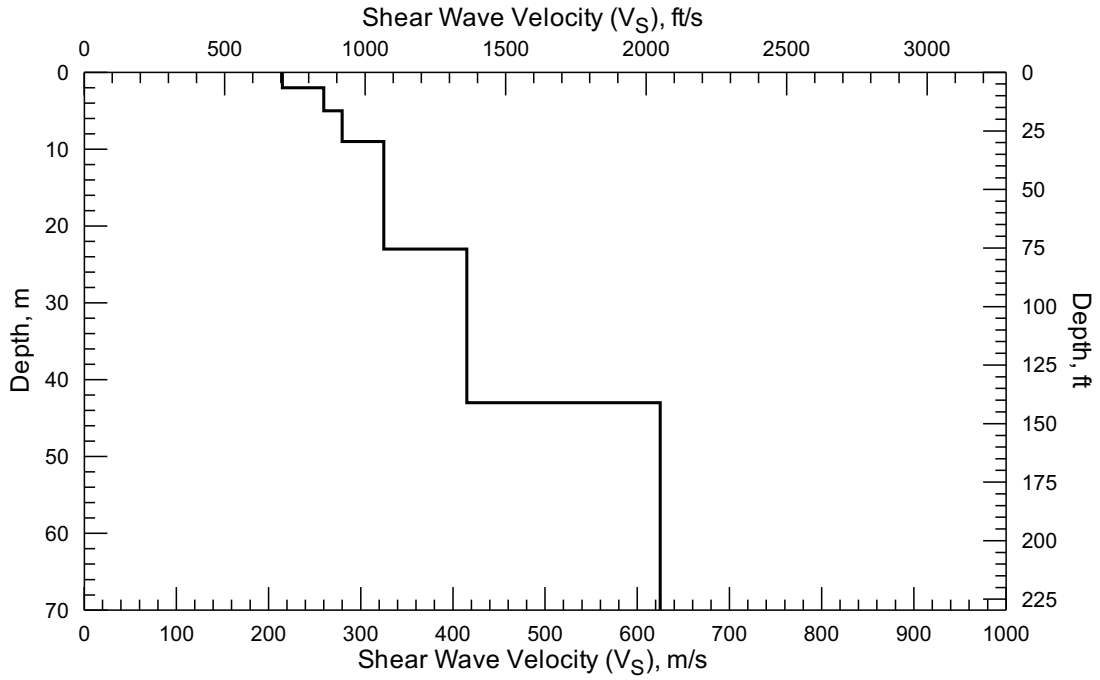


**$V_S$ Model from Active and Passive Surface Wave Array Z3-S11**

| | |
|---|---|
| GEOVision geophysical services | FIGURE 45<br>VELOCITY MODEL FOR ACTIVE AND PASSIVE SURFACE WAVE ARRAY Z3-S11 |
| Project # 9001<br>Date: JUL 24, 2009<br>Drawn By: A MARTIN<br>Approved By: Antony J Martin<br>File R:\...Project Files\2009\9001ch2mhill\report\figures\Figure45.cdr | MERIDIAN AVE AND BUENA VISTA ST,<br>SOUTH PASADENA, CALIFORNIA |
| | PREPARED FOR<br>CH2M HILL |

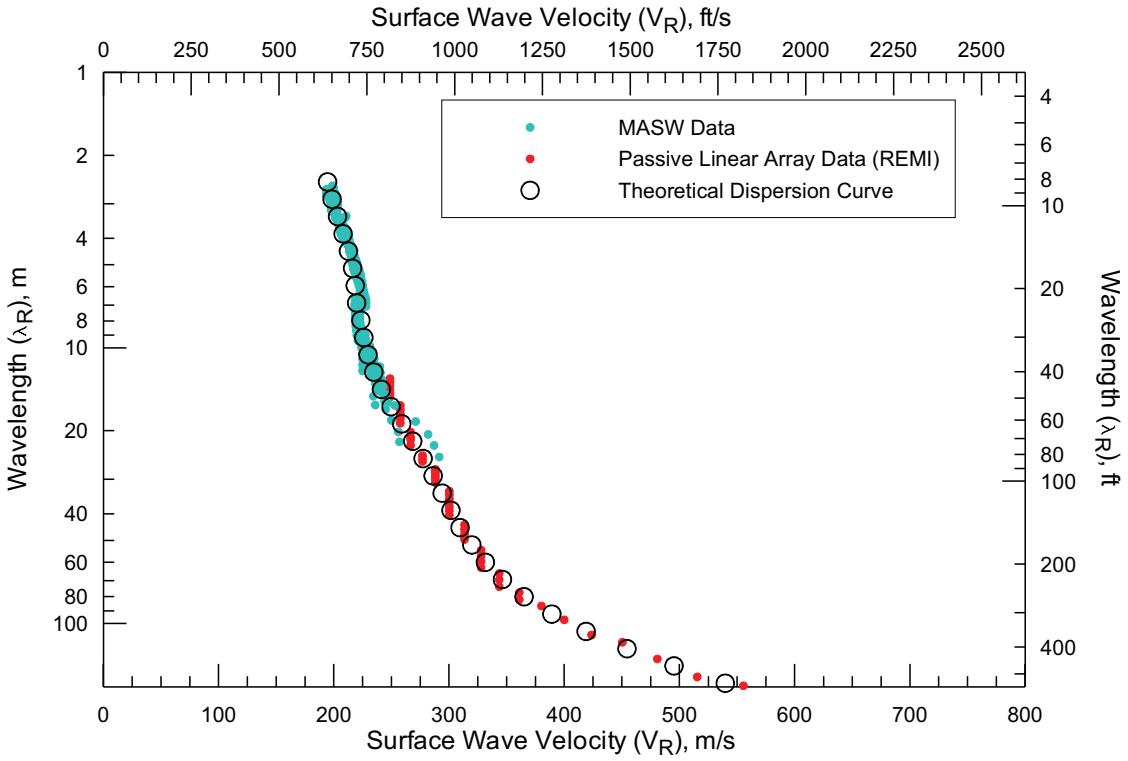


**Comparison of Field Experimental Data and Theoretical Dispersion Curve from Active and Passive Surface Wave Array Z3-S12**

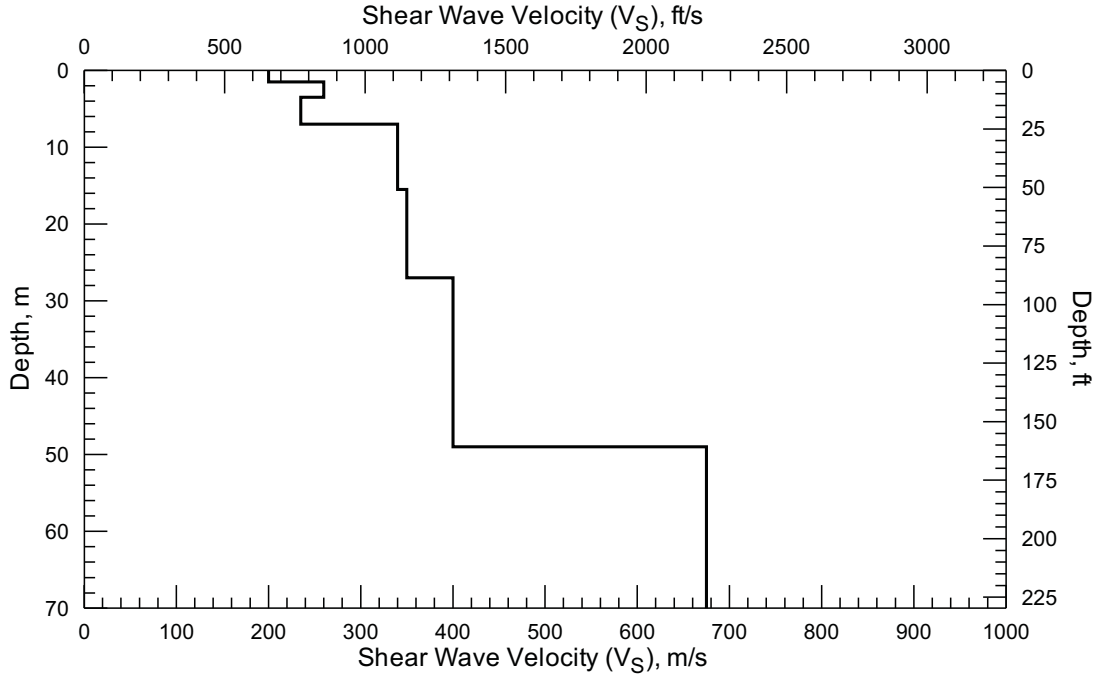


**$V_S$ Model from Active and Passive Surface Wave Array Z3-S12**

| | |
|---|---|
| GEOVision geophysical services | FIGURE 46<br>VELOCITY MODEL FOR ACTIVE AND PASSIVE SURFACE WAVE ARRAY Z3-S12 |
| Project # 9001<br>Date: JUL 24, 2009<br>Drawn By: A MARTIN<br>Approved By: Antony J Martin<br>File R:\...Project Files\2009\9001ch2mhill\report\figures\Figure46.cdr | BRENT AVE AND HOPE ST,<br>SOUTH PASADENA, CALIFORNIA |
| | PREPARED FOR<br>CH2M HILL |

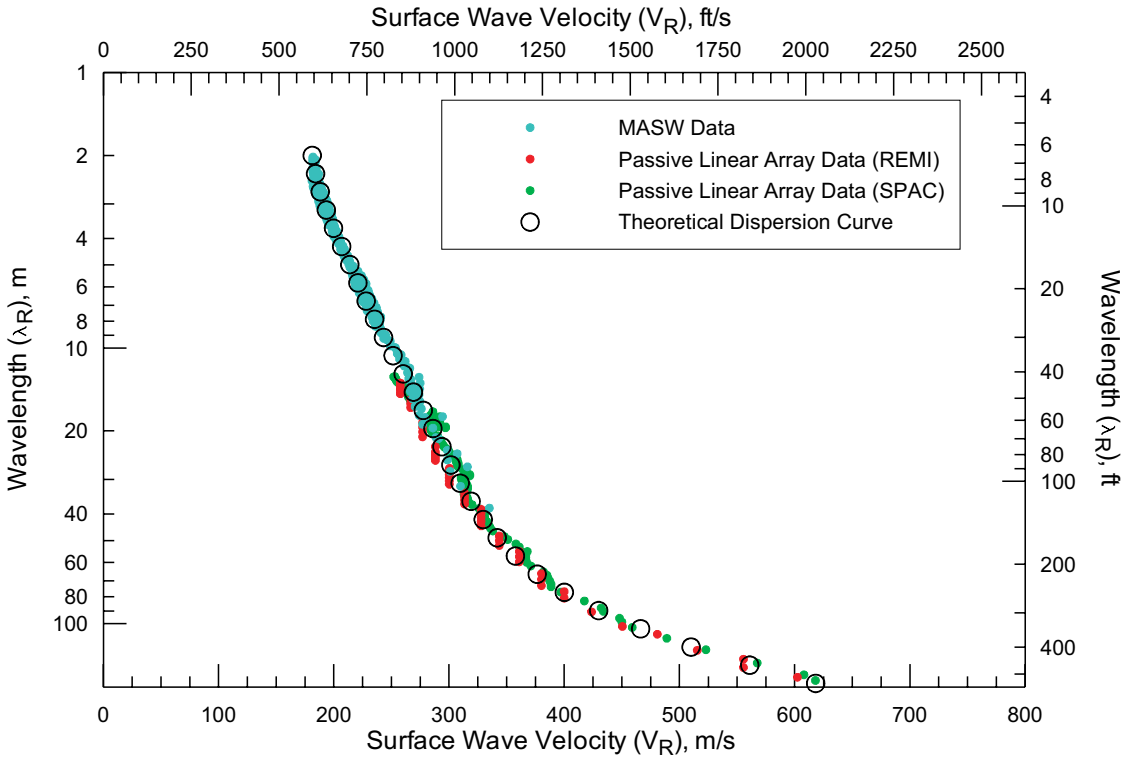


**Comparison of Field Experimental Data and Theoretical Dispersion Curve from Active and Passive Surface Wave Array Z3-S15**

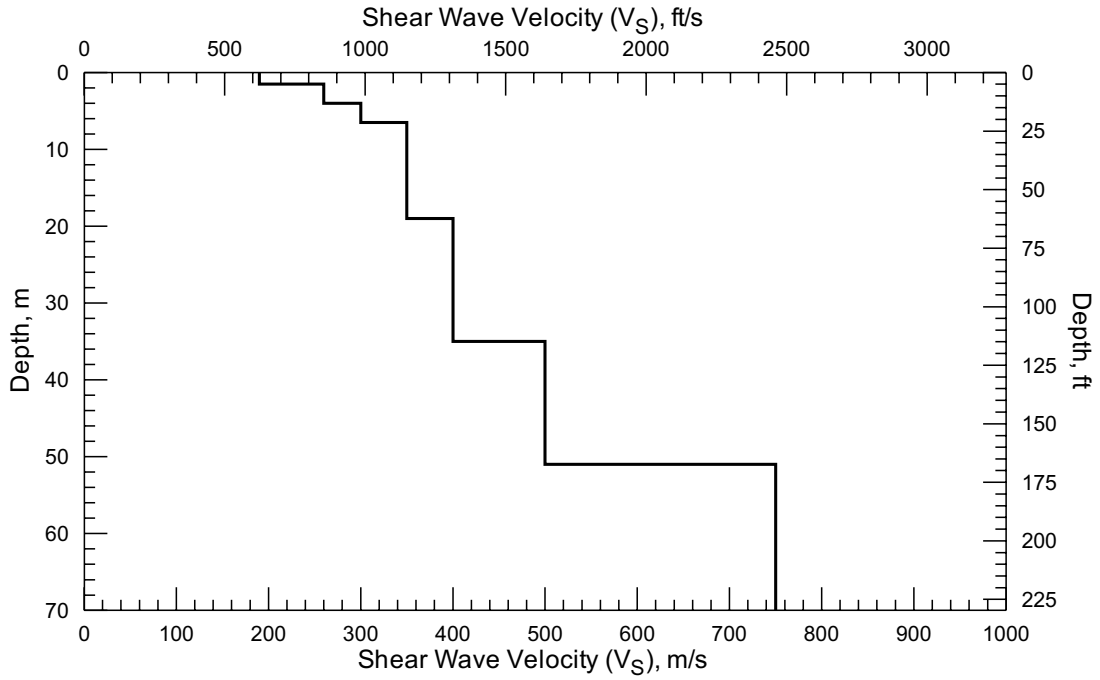


**$V_S$ Model from Active and Passive Surface Wave Array Z3-S15**

| | |
|---|---|
| GEOVision geophysical services | FIGURE 49<br>VELOCITY MODEL FOR ACTIVE AND PASSIVE SURFACE WAVE ARRAY Z3-S15 |
| Project # 9001<br>Date: JUL 27, 2009<br>Drawn By: A MARTIN<br>Approved By: Antony J Martin<br>File R:\...Project Files\2009\9001ch2mhill\report\figures\Figure49.cdr | MONTEREY RD AND MERIDIAN AVE,<br>SOUTH PASADENA, CALIFORNIA |
| | PREPARED FOR<br>CH2M HILL |

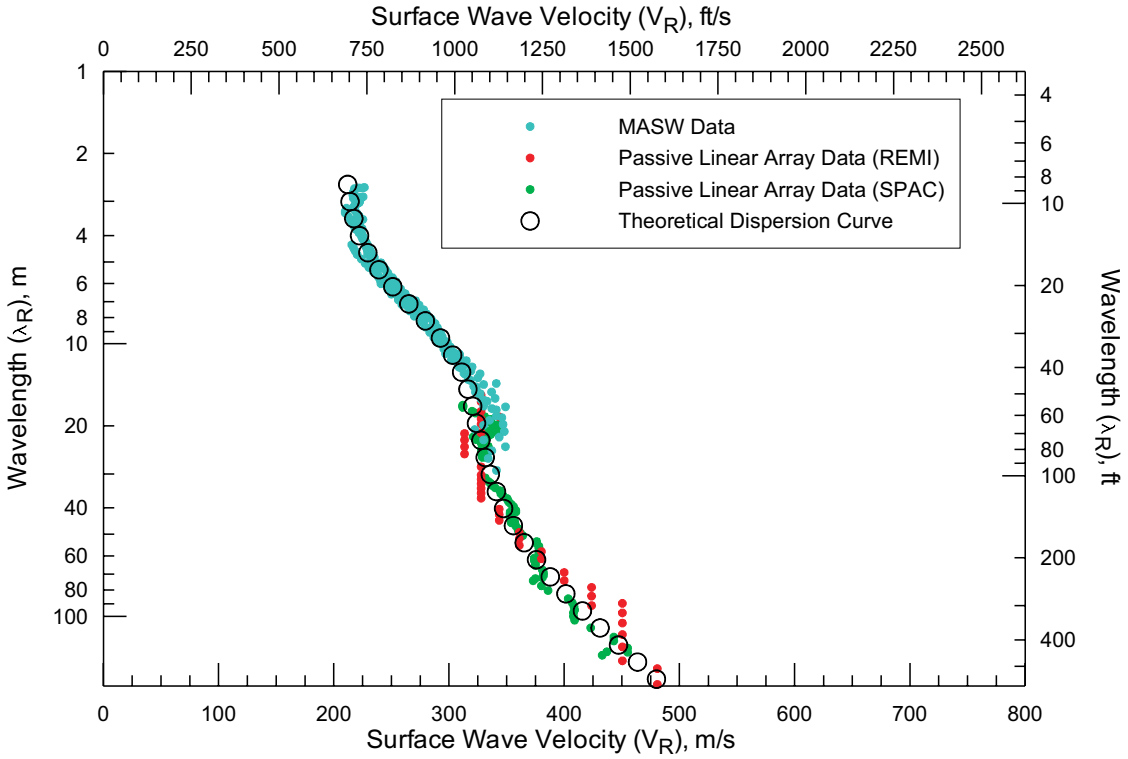


**Comparison of Field Experimental Data and Theoretical Dispersion Curve from Active and Passive Surface Wave Array Z3-S16**

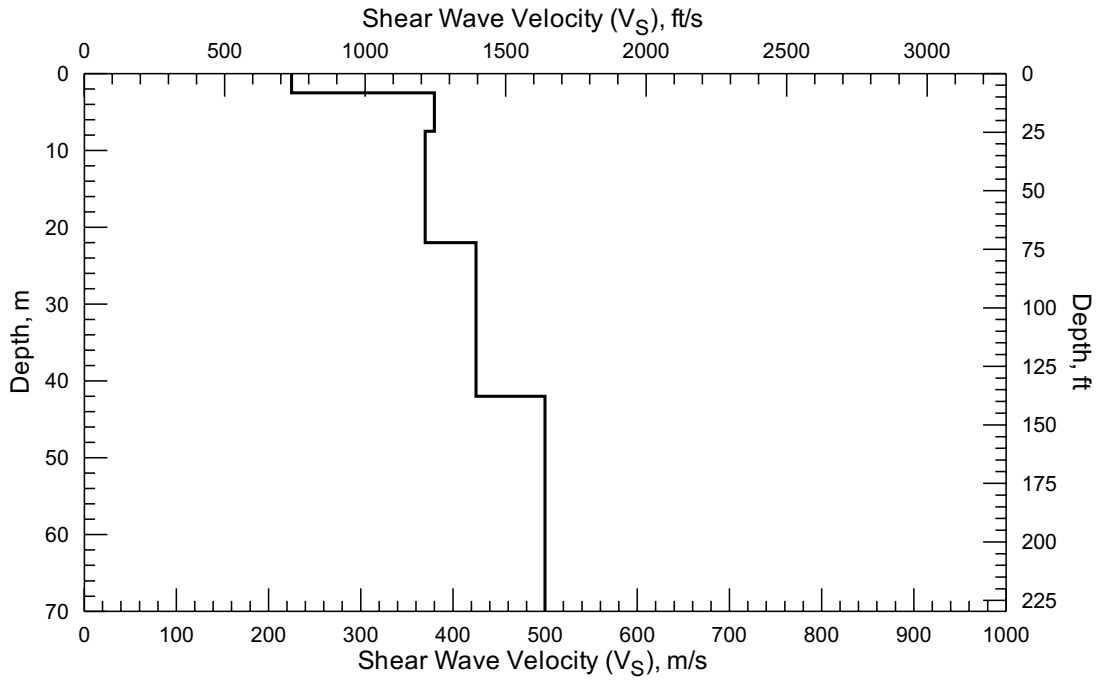


**$V_S$ Model from Active and Passive Surface Wave Array Z3-S16**

| | |
|---|---|
| GEOVision geophysical services | FIGURE 50<br>VELOCITY MODEL FOR ACTIVE AND PASSIVE SURFACE WAVE ARRAY Z3-S16 |
| Project # 9001<br>Date: JUL 27, 2009<br>Drawn By: A MARTIN<br>Approved By: Antony J Martin<br>File R:\...Project Files\2009\9001ch2mhill\report\figures\Figure50.cdr | MARENGO AVE AND SPRUCE ST,<br>SOUTH PASADENA, CALIFORNIA |
| | PREPARED FOR<br>CH2M HILL |

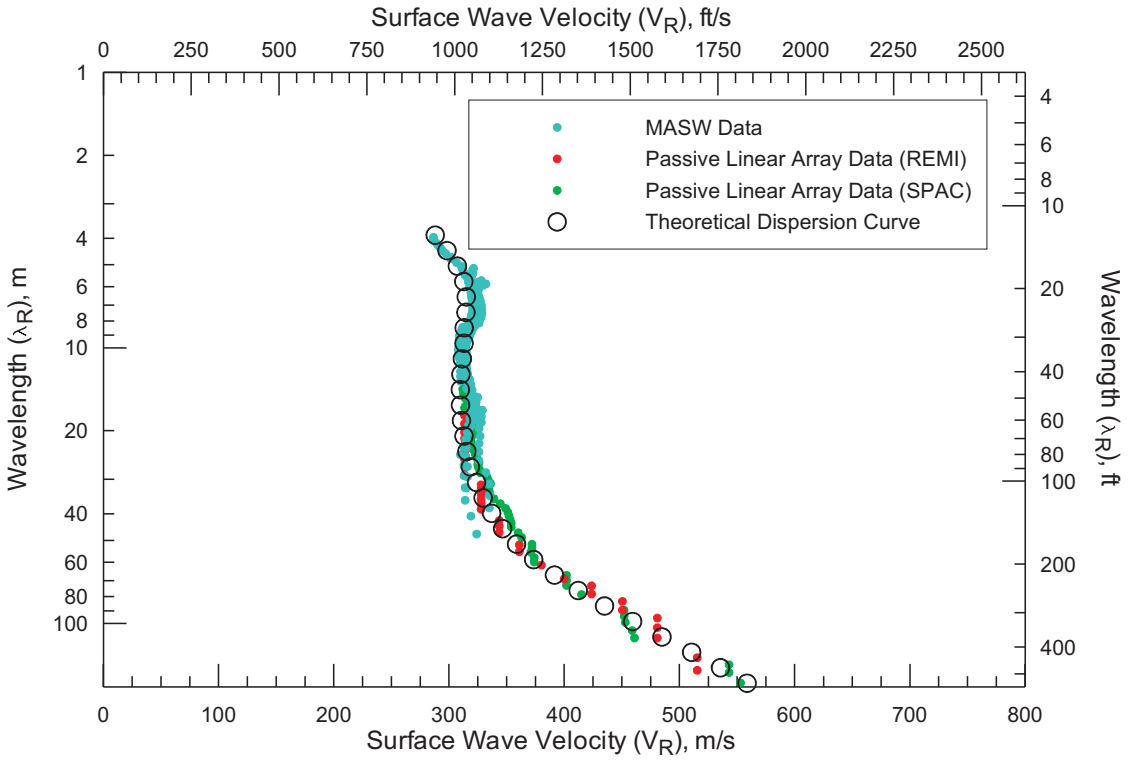


**Comparison of Field Experimental Data and Theoretical Dispersion Curve from Active and Passive Surface Wave Array Z3-S19**

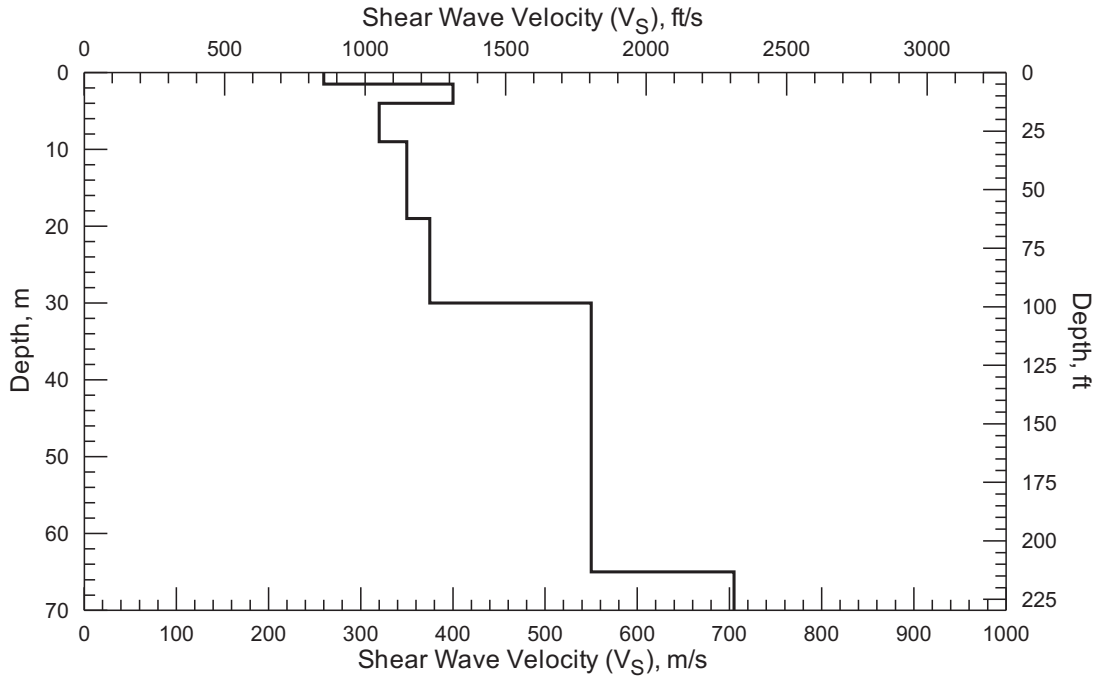


**$V_S$ Model from Active and Passive Surface Wave Array Z3-S19**

| | |
|---|---|
| GEOVision geophysical services | FIGURE 53<br>VELOCITY MODEL FOR ACTIVE AND PASSIVE SURFACE WAVE ARRAY Z3-S19 |
| Project # 9001<br>Date: JUL 27, 2009<br>Drawn By: A MARTIN<br>Approved By: Antony J Martin<br>File R:\...Project Files\2009\9001ch2mhill\report\figures\Figure53.cdr | BERKSHIRE AVE AND KENDALL AVE,<br>LOS ANGELES, CALIFORNIA<br><br>PREPARED FOR<br>CH2M HILL |

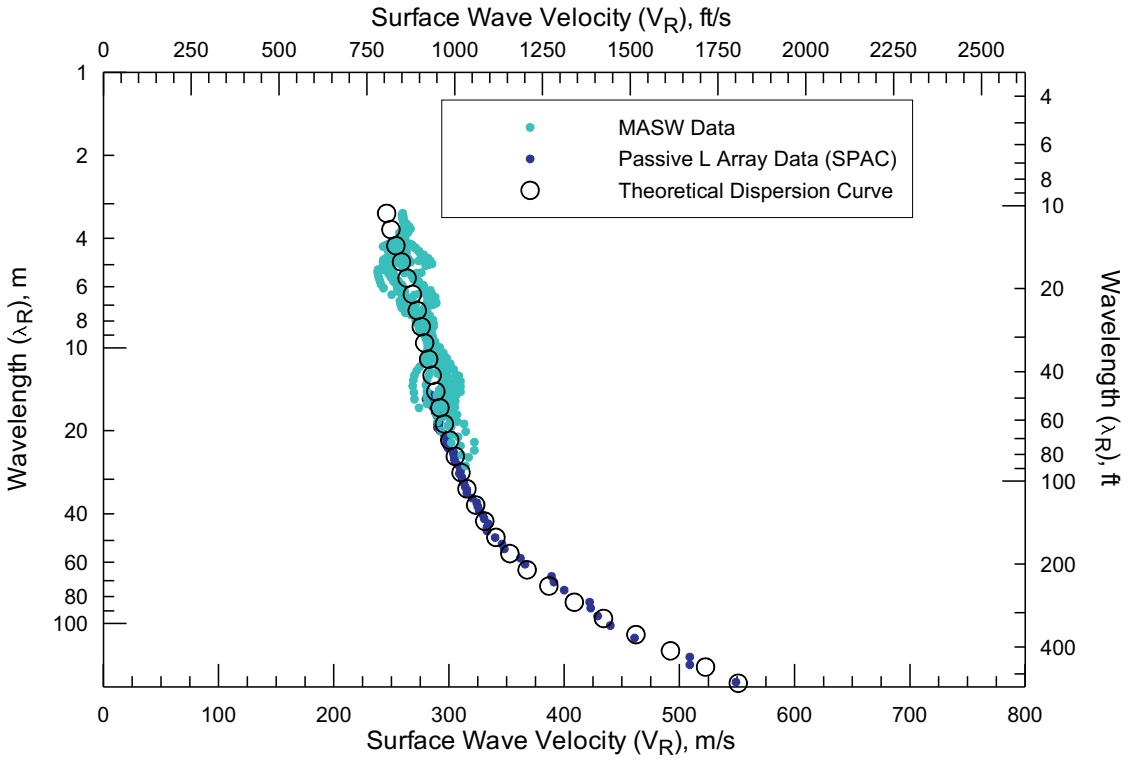


**Comparison of Field Experimental Data and Theoretical Dispersion Curve from Active and Passive Surface Wave Array Z3-S20**

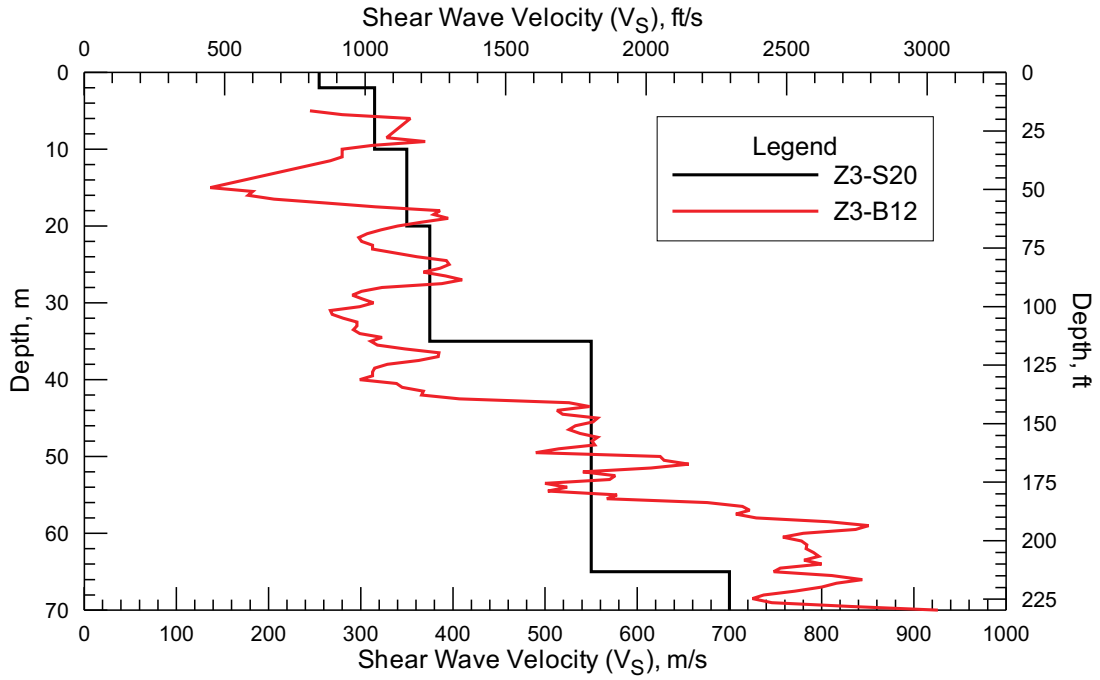


**$V_S$ Model from Active and Passive Surface Wave Array Z3-S20**

| | |
|---|---|
| GEOVision geophysical services | FIGURE 54<br>VELOCITY MODEL FOR ACTIVE AND PASSIVE SURFACE WAVE ARRAY Z3-S20 |
| Project # 9001<br>Date: JUL 27, 2009<br>Drawn By: A MARTIN<br>Approved By: Antony J Martin<br>File R:\...Project Files\2009\9001ch2mhill\report\figures\Figure54.cdr | WESTMONT DR AND KEATS ST,<br>ALHAMBRA, CALIFORNIA |
| | PREPARED FOR<br>CH2M HILL |

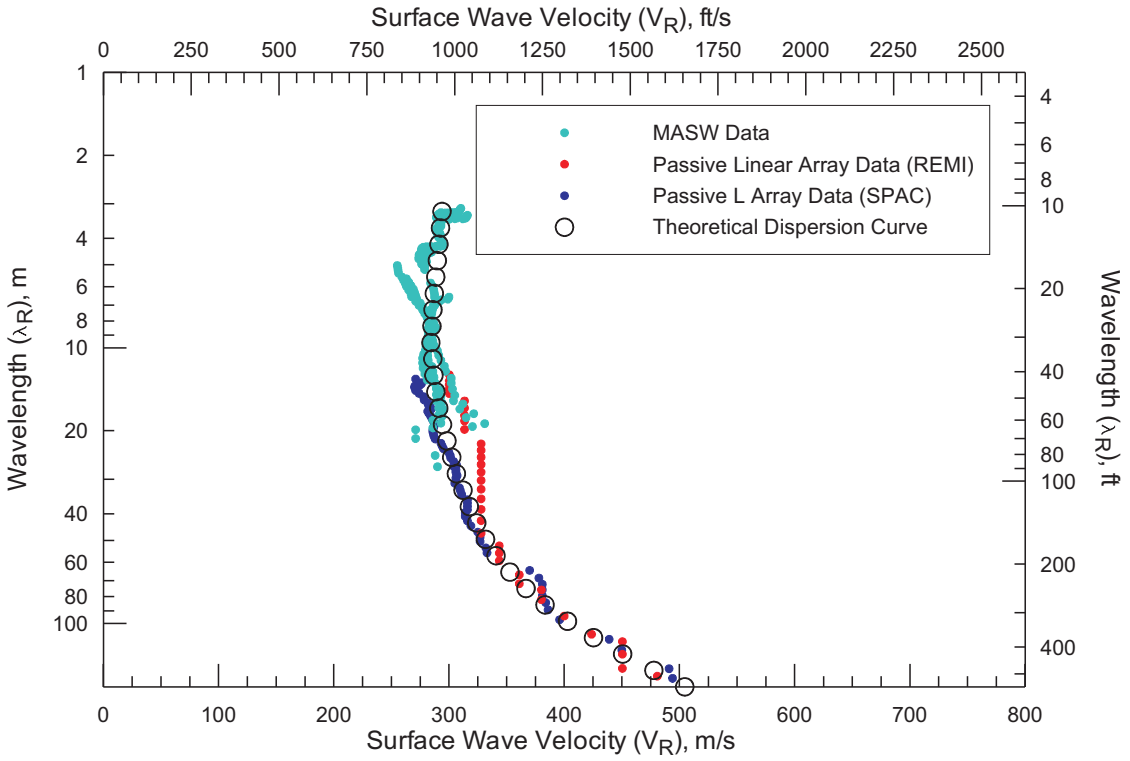


**Comparison of Field Experimental Data and Theoretical Dispersion Curve from Active and Passive Surface Wave Array Z3-S21**

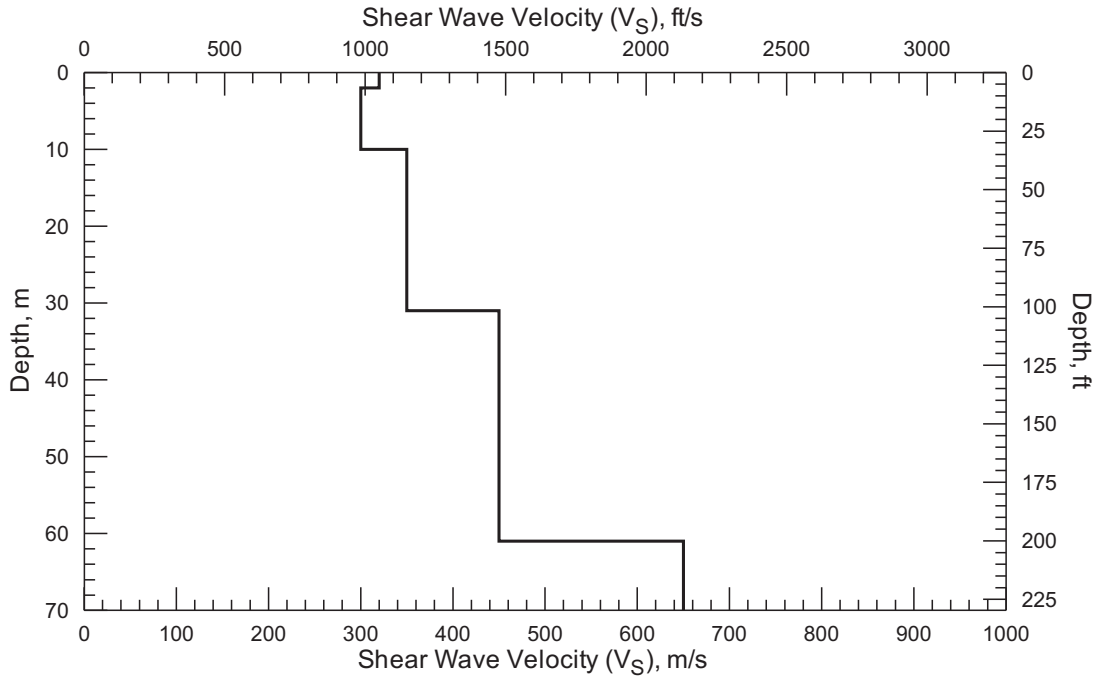


**$V_S$ Model from Active and Passive Surface Wave Array Z3-S21**

| | |
|---|---|
| GEOVision geophysical services | FIGURE 55<br>VELOCITY MODEL FOR ACTIVE AND PASSIVE SURFACE WAVE ARRAY Z3-S21 |
| Project # 9001 | WINCHESTER AVE AND NORWICH AVE, ALHAMBRA, CALIFORNIA |
| Date: JUL 27, 2009 | |
| Drawn By: A MARTIN | |
| Approved By: Antony J Martin | PREPARED FOR<br>CH2M HILL |
| File R:\...Project Files\2009\9001ch2mhill\report\figures\Figure55.cdr | |

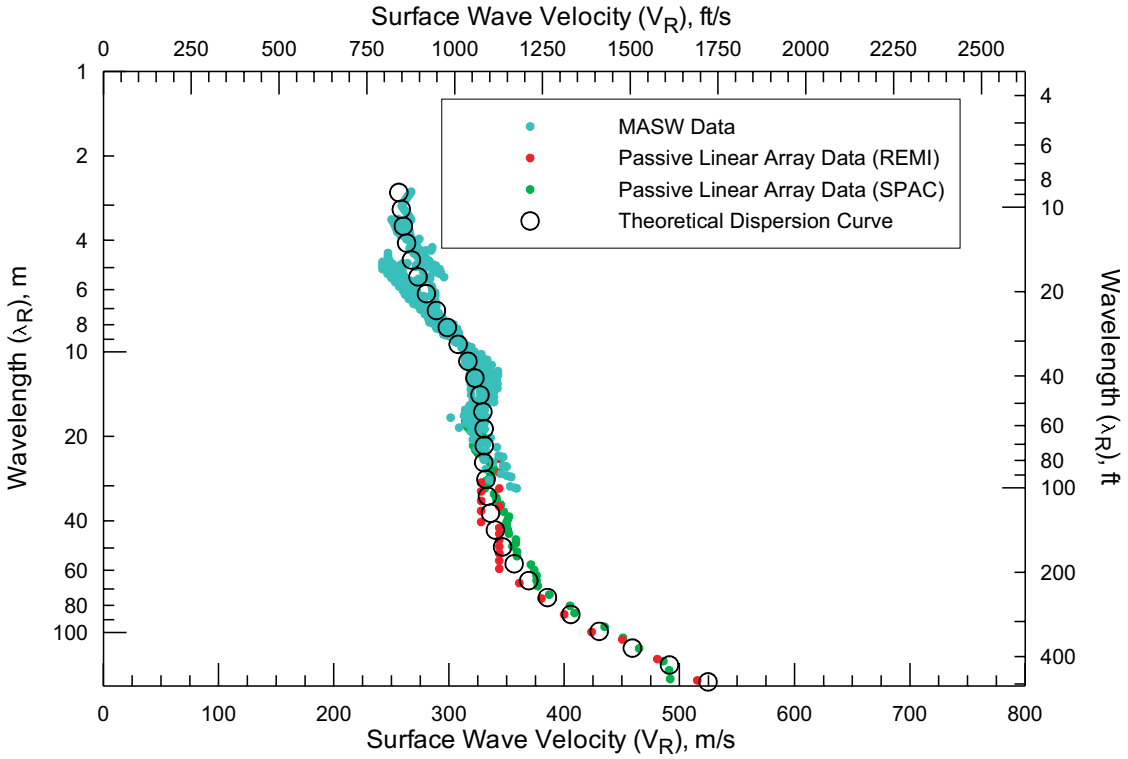


**Comparison of Field Experimental Data and Theoretical Dispersion Curve from Active and Passive Surface Wave Array Z3-S22**

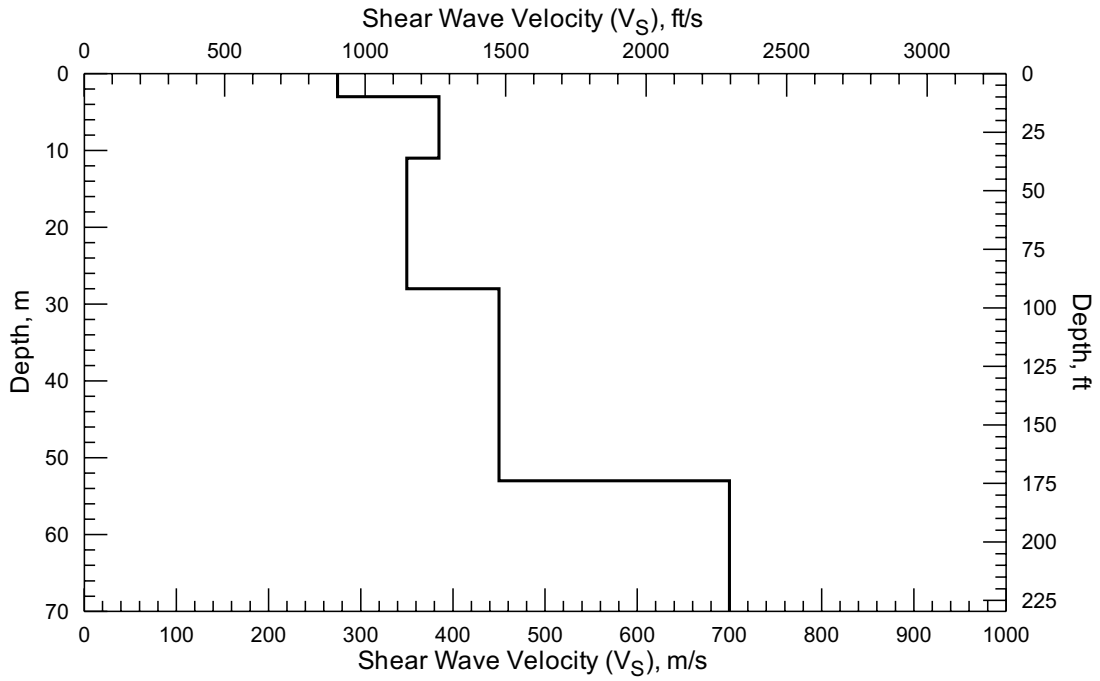


**$V_S$ Model from Active and Passive Surface Wave Array Z3-S22**

| | |
|---|---|
| GEOVision geophysical services | FIGURE 56<br>VELOCITY MODEL FOR ACTIVE AND PASSIVE SURFACE WAVE ARRAY Z3-S22 |
| Project # 9001<br>Date: JUL 27, 2009<br>Drawn By: A MARTIN<br>Approved By: Antony J. Martin<br>File R:\...Project Files\2009\9001ch2mhill\report\figures\Figure56.cdr | WINCHESTER AVE AND CONCORD AVE, ALHAMBRA, CALIFORNIA<br><br>PREPARED FOR<br>CH2M HILL |

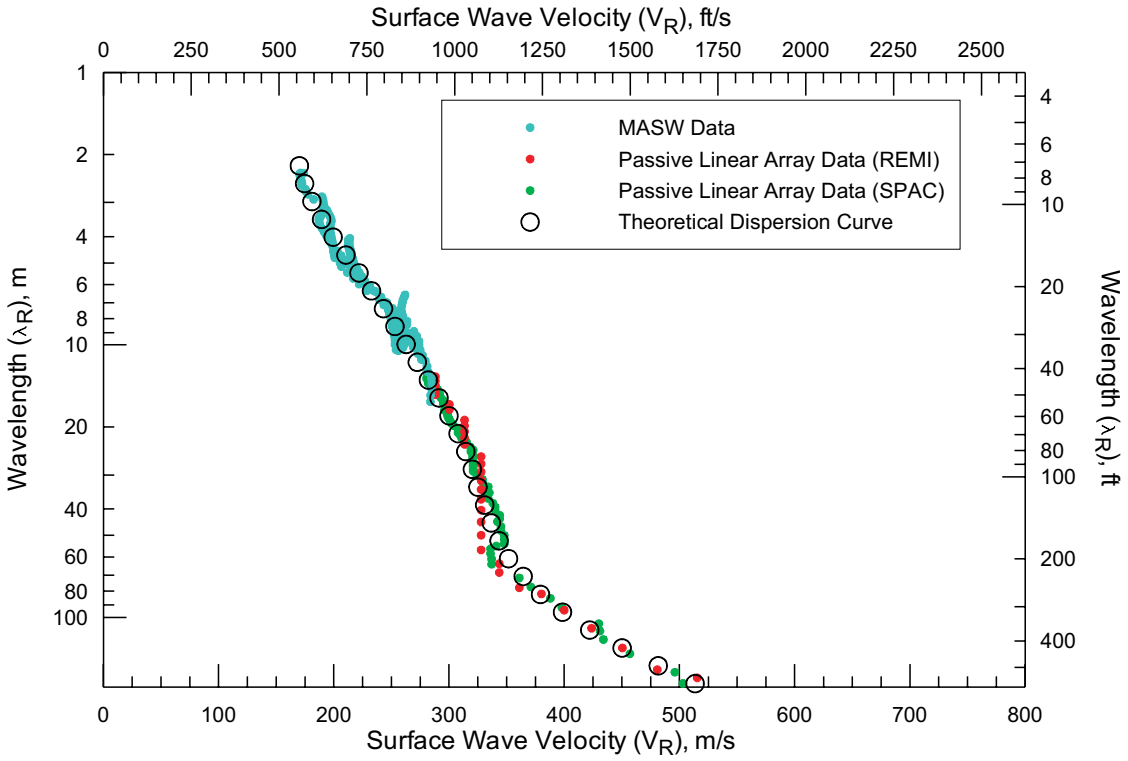


**Comparison of Field Experimental Data and Theoretical Dispersion Curve from Active and Passive Surface Wave Array Z3-S23**

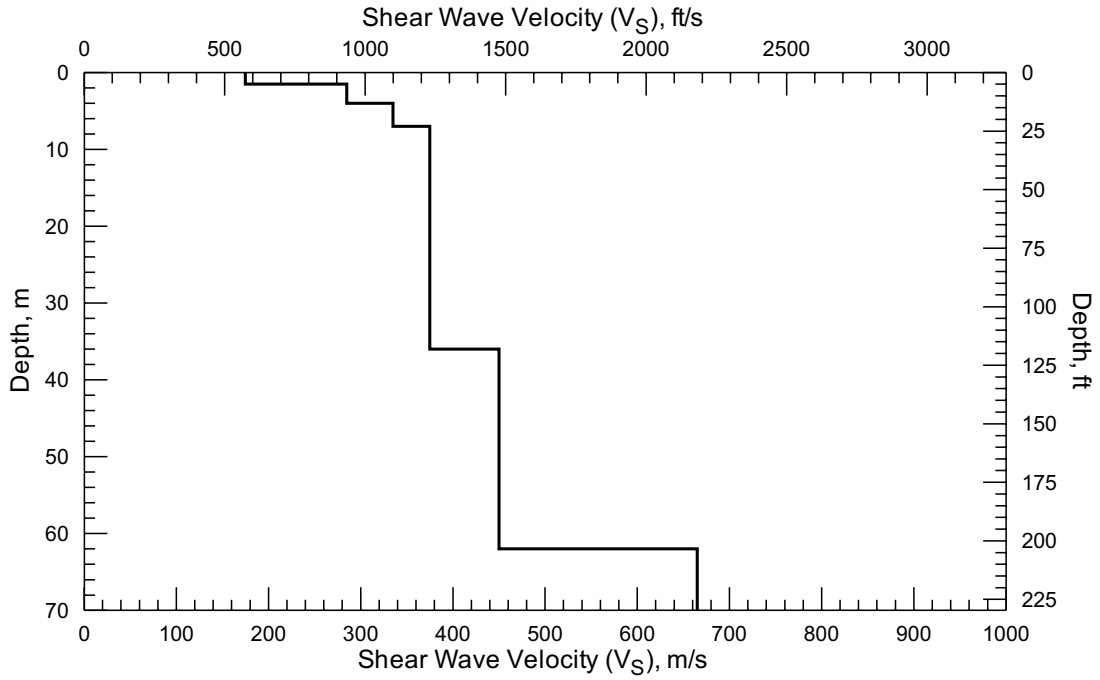


**$V_S$ Model from Active and Passive Surface Wave Array Z3-S23**

| | |
|---|---|
| GEOVision geophysical services | FIGURE 57<br>VELOCITY MODEL FOR ACTIVE AND PASSIVE SURFACE WAVE ARRAY Z3-S23 |
| Project # 9001<br>Date: JUL 27, 2009<br>Drawn By: A MARTIN<br>Approved By: Antony J. Martin<br>File R:\...Project Files\2009\9001ch2mhill\report\figures\Figure57.cdr | WESTMONT DR AND VALLEY BLVD,<br>ALHAMBRA, CALIFORNIA |
| | PREPARED FOR<br>CH2M HILL |

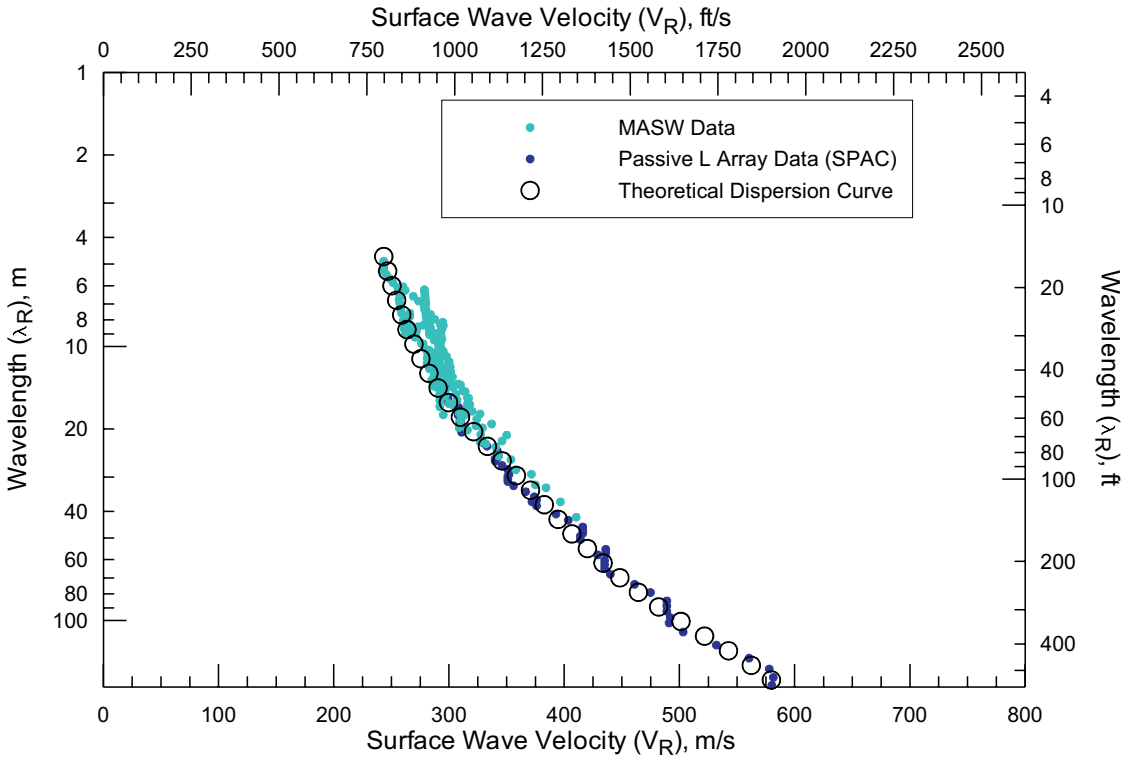


**Comparison of Field Experimental Data and Theoretical Dispersion Curve from Active and Passive Surface Wave Array Z3-S24**

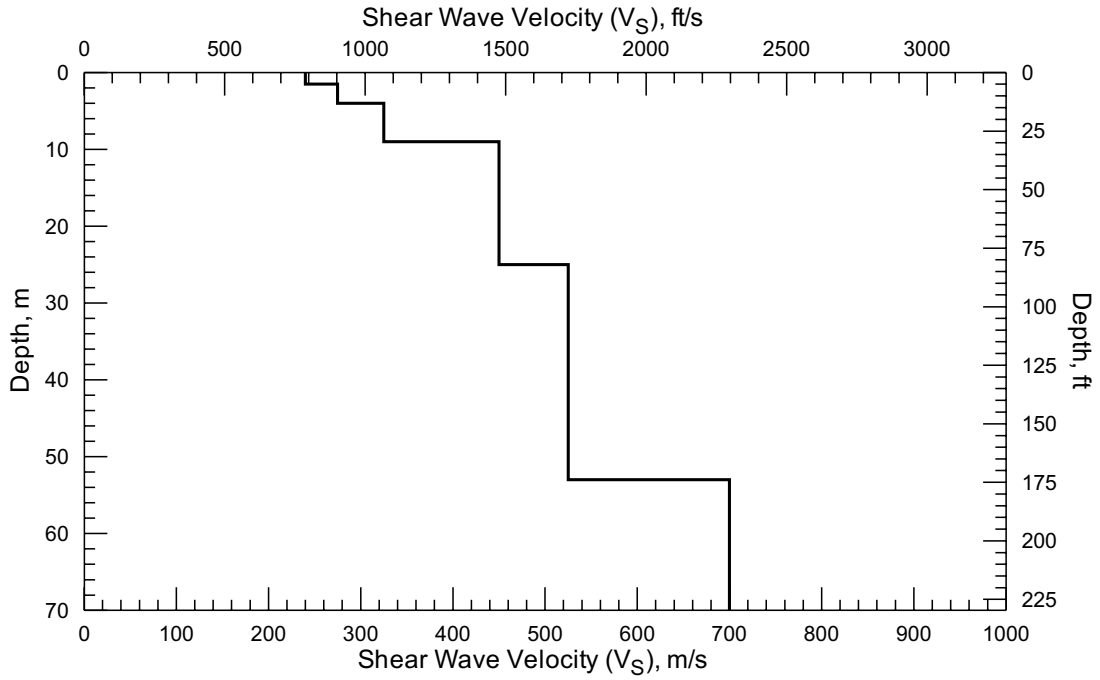


**$V_S$ Model from Active and Passive Surface Wave Array Z3-S24**

| | |
|---|---|
| GEOVision geophysical services | FIGURE 58<br>VELOCITY MODEL FOR ACTIVE AND PASSIVE SURFACE WAVE ARRAY Z3-S24 |
| Project # 9001<br>Date: JUL 27, 2009<br>Drawn By: A MARTIN<br>Approved By: Antony J. Martin<br>File R:\...Project Files\2009\9001ch2mhill\report\figures\Figure58.cdr | WESTMONT DR AND GLENAVEN AVE,<br>ALHAMBRA, CALIFORNIA<br><br>PREPARED FOR<br>CH2M HILL |

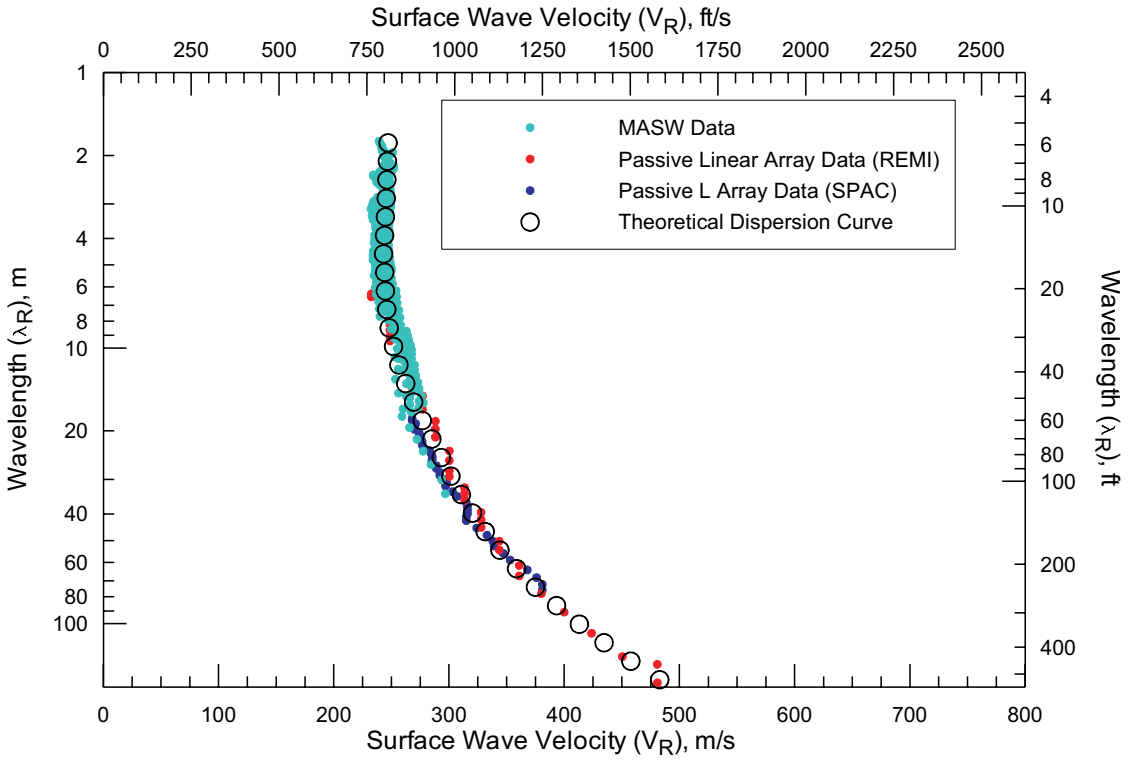


**Comparison of Field Experimental Data and Theoretical Dispersion Curve from Active and Passive Surface Wave Array Z4-S6**

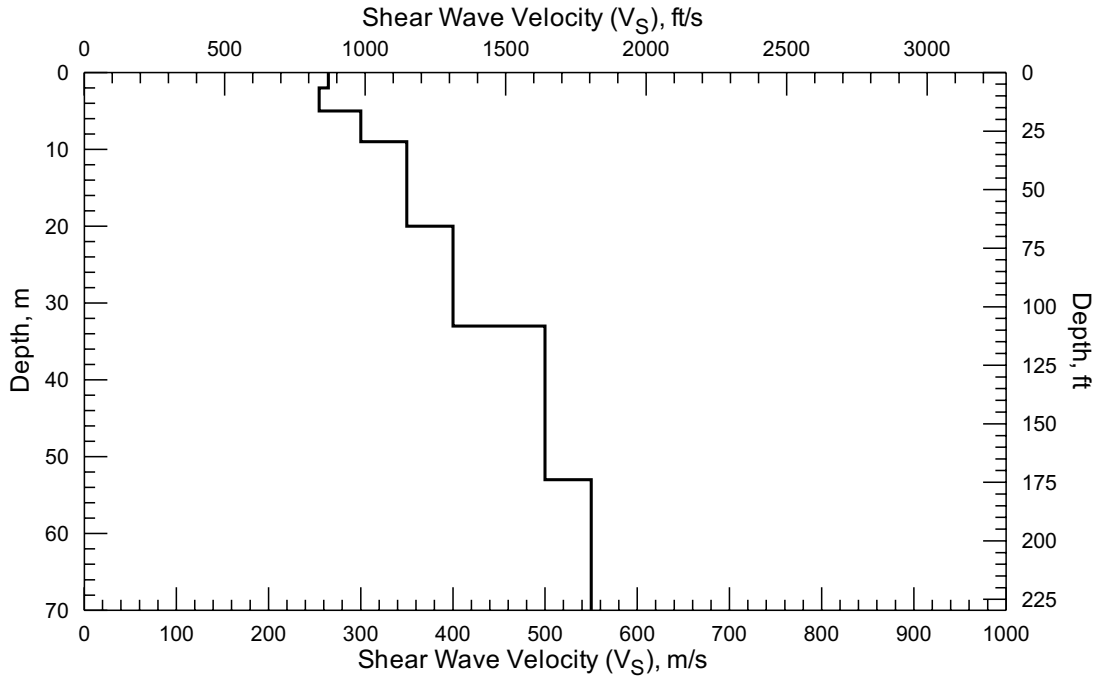


**$V_S$ Model from Active and Passive Surface Wave Array Z4-S6**

| | |
|---|---|
| GEOVision geophysical services | FIGURE 64<br>VELOCITY MODEL FOR ACTIVE AND PASSIVE SURFACE WAVE ARRAY Z4-S6 |
| Project # 9001<br>Date: JUL 29, 2009<br>Drawn By: A MARTIN<br>Approved By: Antony J Martin<br>File R:\...Project Files\2009\9001ch2mhill\report\figures\Figure64.cdr | HUNTINGTON DR AND GRANADA AVE,<br>SAN MARINO, CALIFORNIA |
| | PREPARED FOR<br>CH2M HILL |

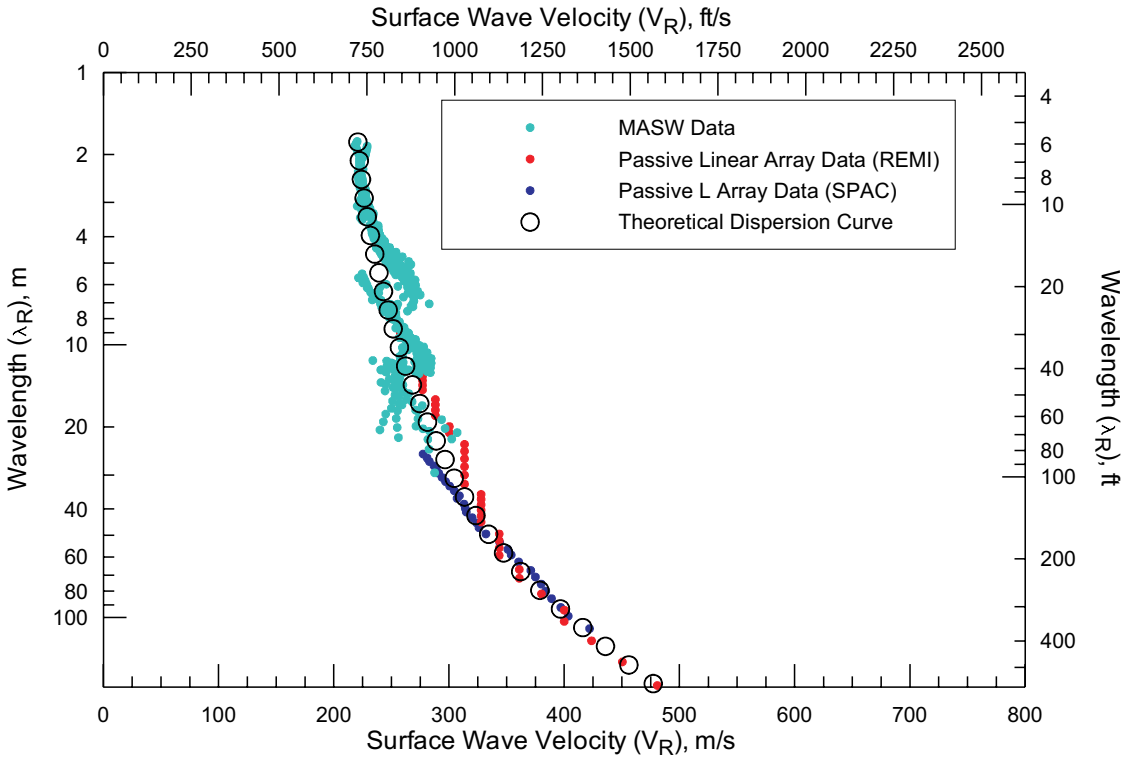


**Comparison of Field Experimental Data and Theoretical Dispersion Curve from Active and Passive Surface Wave Array Z4-S7**

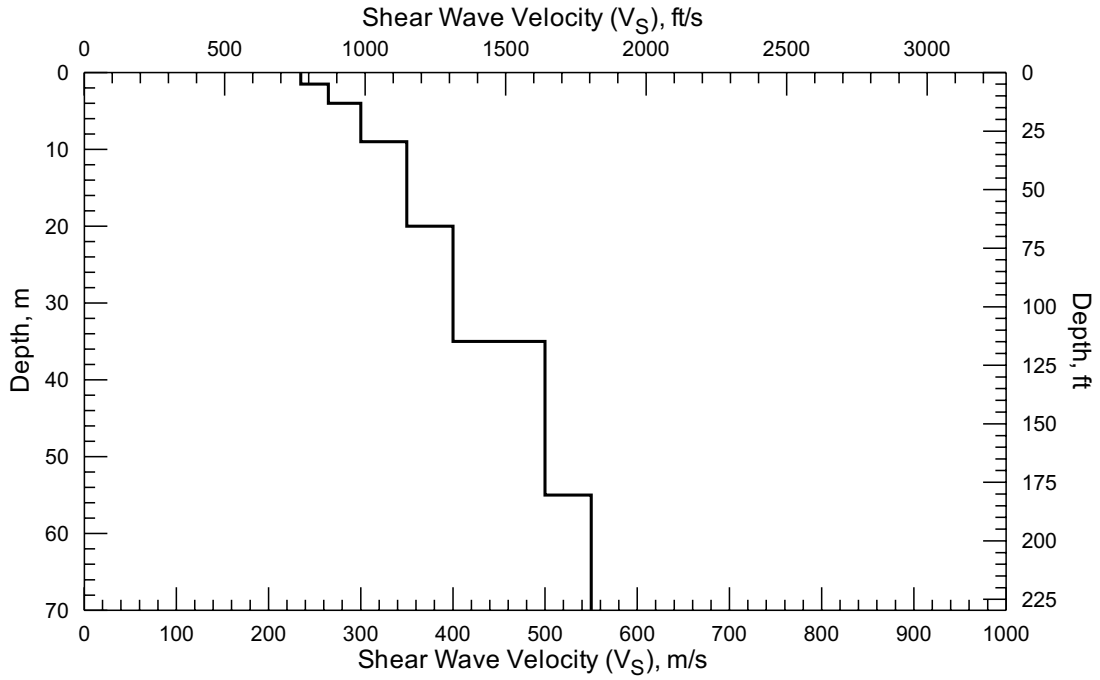


**$V_S$ Model from Active and Passive Surface Wave Array Z4-S7**

| | |
|---|---|
| GEOVision geophysical services | FIGURE 65<br>VELOCITY MODEL FOR ACTIVE AND PASSIVE SURFACE WAVE ARRAY Z4-S7 |
| Project # 9001<br>Date: JUL 29, 2009<br>Drawn By: A MARTIN<br>Approved By: Antony J Martin<br>File R:\...Project Files\2009\9001ch2mhill\report\figures\Figure65.cdr | HUNTINGTON DR AND STORY PL,<br>SAN MARINO, CALIFORNIA |
| | PREPARED FOR<br>CH2M HILL |

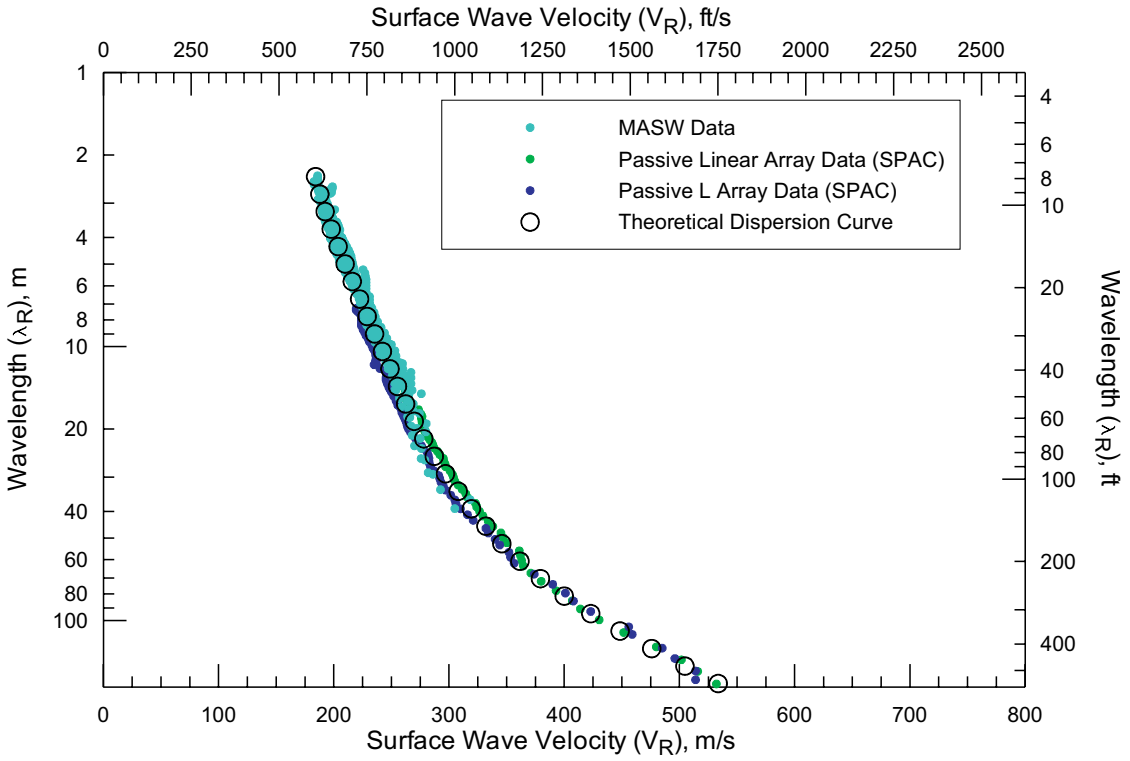


**Comparison of Field Experimental Data and Theoretical Dispersion Curve from Active and Passive Surface Wave Array Z4-S8**

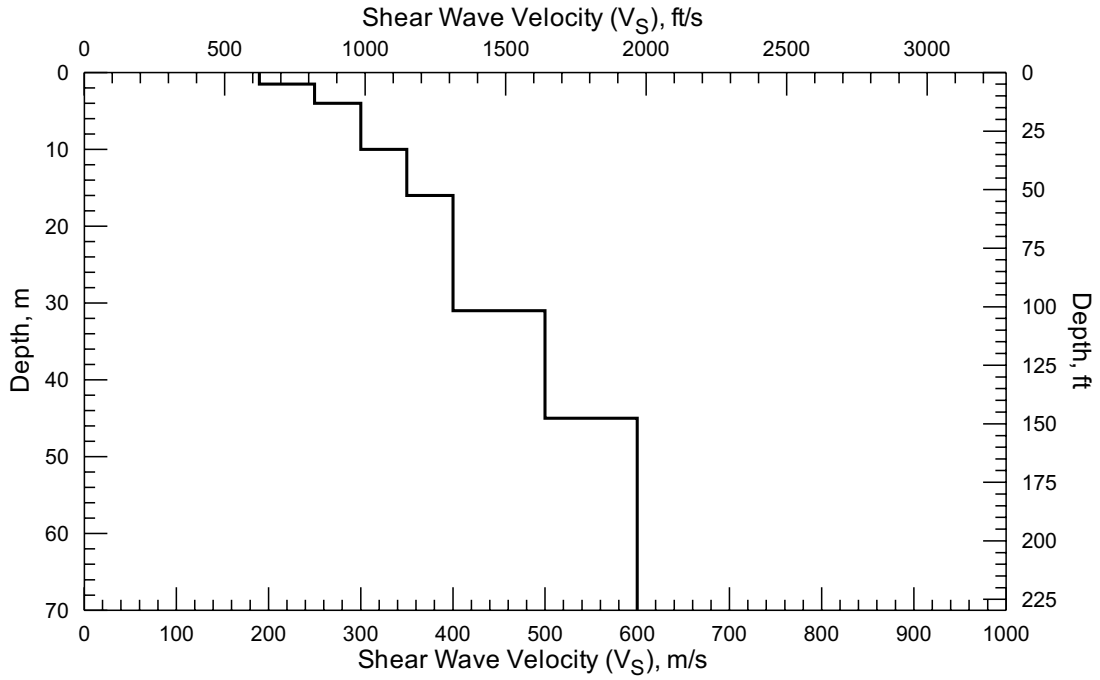


**$V_S$ Model from Active and Passive Surface Wave Array Z4-S8**

| | |
|---|---|
| GEOVision geophysical services | FIGURE 66<br>VELOCITY MODEL FOR ACTIVE AND PASSIVE SURFACE WAVE ARRAY Z4-S8 |
| Project # 9001<br>Date: JUL 29, 2009<br>Drawn By: A MARTIN<br>Approved By: Antony J Martin<br>File R:\...Project Files\2009\9001ch2mhill\report\figures\Figure66.cdr | GARFIELD AVE AND MCLEAN ST,<br>ALHAMBRA, CALIFORNIA |
| | PREPARED FOR<br>CH2M HILL |

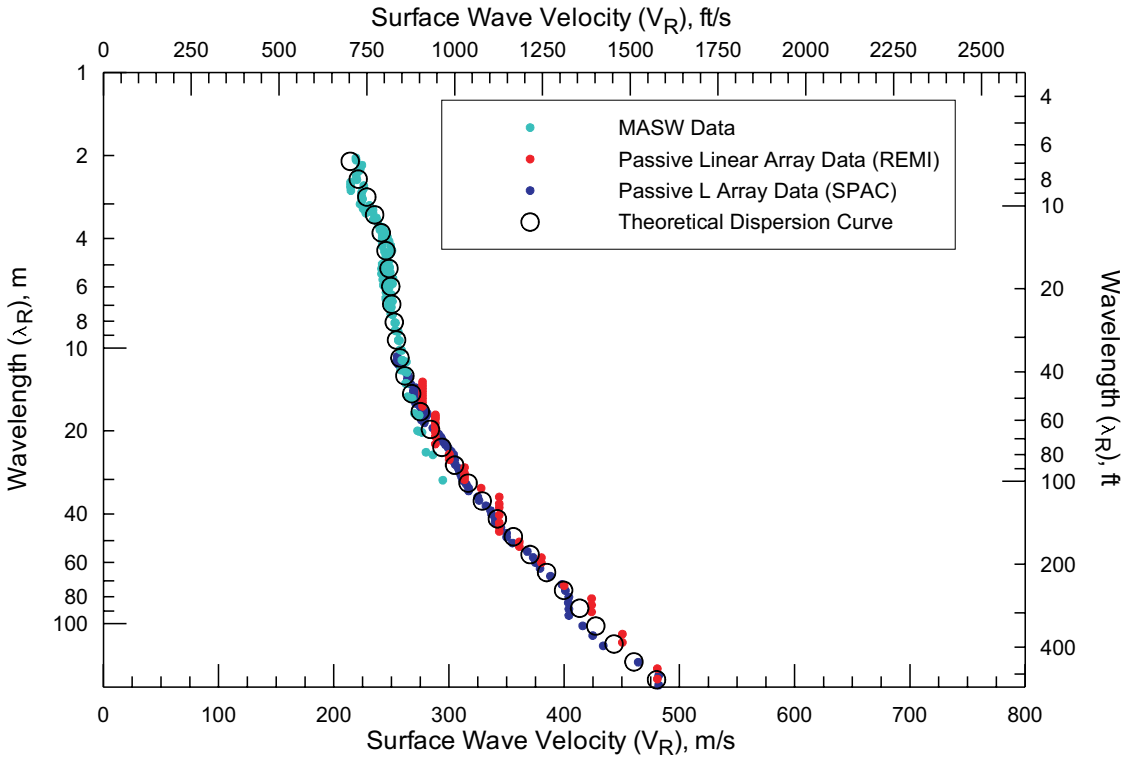


**Comparison of Field Experimental Data and Theoretical Dispersion Curve from Active and Passive Surface Wave Array Z4-S9**

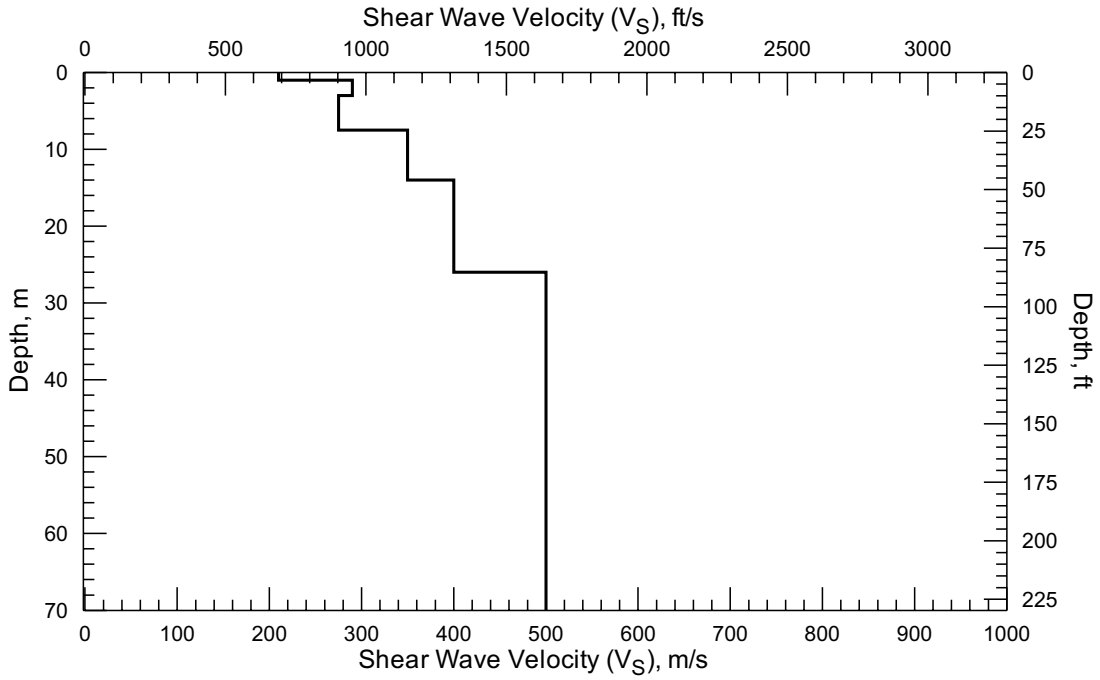


**$V_S$ Model from Active and Passive Surface Wave Array Z4-S9**

| | |
|---|---|
| GEOVision geophysical services | FIGURE 67<br>VELOCITY MODEL FOR ACTIVE AND PASSIVE SURFACE WAVE ARRAY Z4-S9 |
| Project # 9001<br>Date: JUL 29, 2009<br>Drawn By: A MARTIN<br>Approved By: Antony J. Martin<br>File R:\...Project Files\2009\9001ch2mhill\report\figures\Figure67.cdr | BUSHNELL AVE AND LARCH ST,<br>ALHAMBRA, CALIFORNIA |
| | PREPARED FOR<br>CH2M HILL |

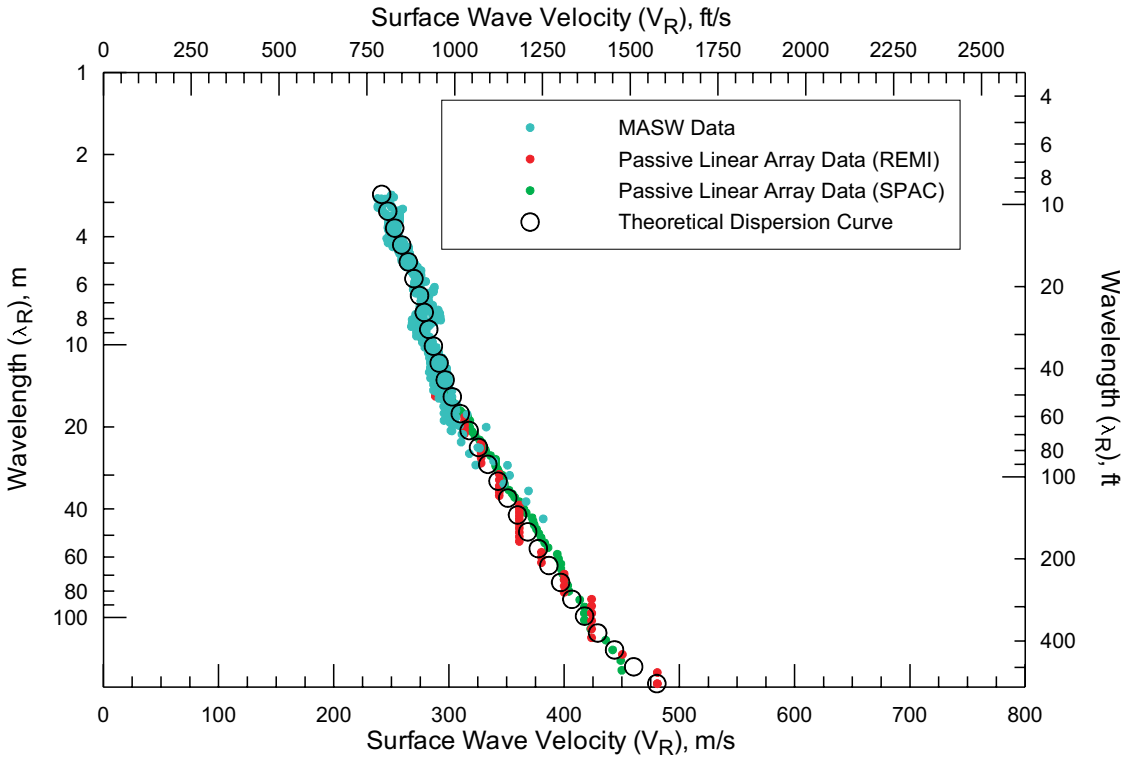


**Comparison of Field Experimental Data and Theoretical Dispersion Curve from Active and Passive Surface Wave Array Z4-S10**

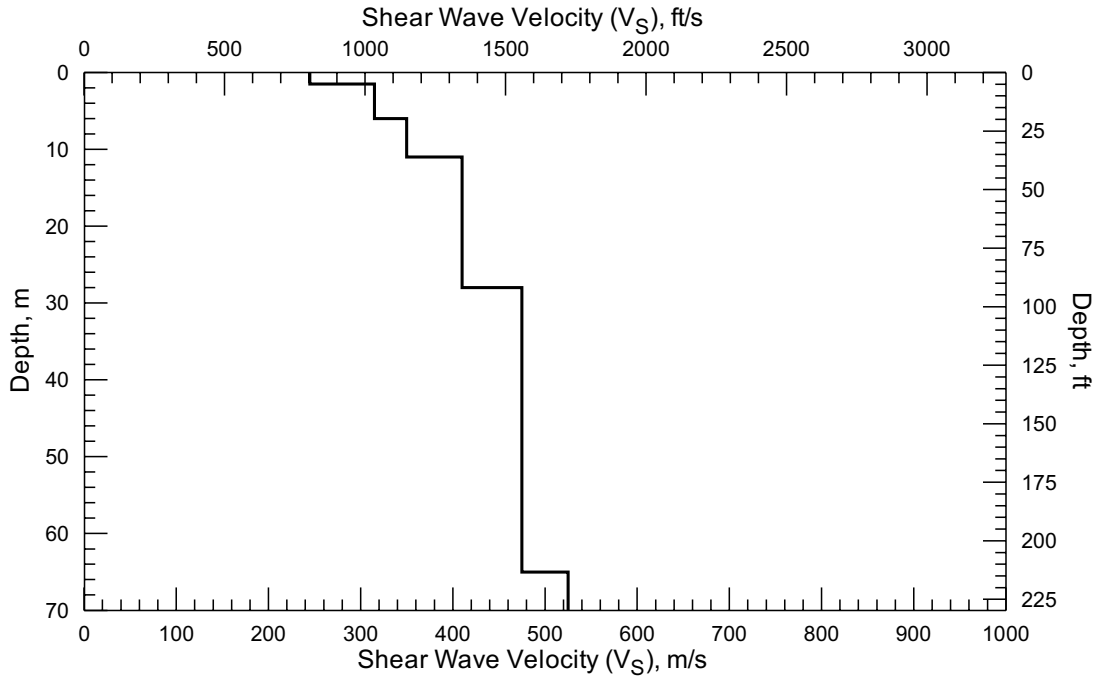


**$V_S$ Model from Active and Passive Surface Wave Array Z4-S10**

| | |
|---|---|
| GEOVision geophysical services | FIGURE 68<br>VELOCITY MODEL FOR ACTIVE AND PASSIVE SURFACE WAVE ARRAY Z4-S10 |
| Project # 9001<br>Date: JUL 29, 2009<br>Drawn By: A MARTIN<br>Approved By: Antony J Martin<br>File R:\...Project Files\2009\9001ch2mhill\report\figures\Figure68.cdr | COMMONWEALTH AVE AND DATE AVE, ALHAMBRA, CALIFORNIA<br><br>PREPARED FOR<br>CH2M HILL |

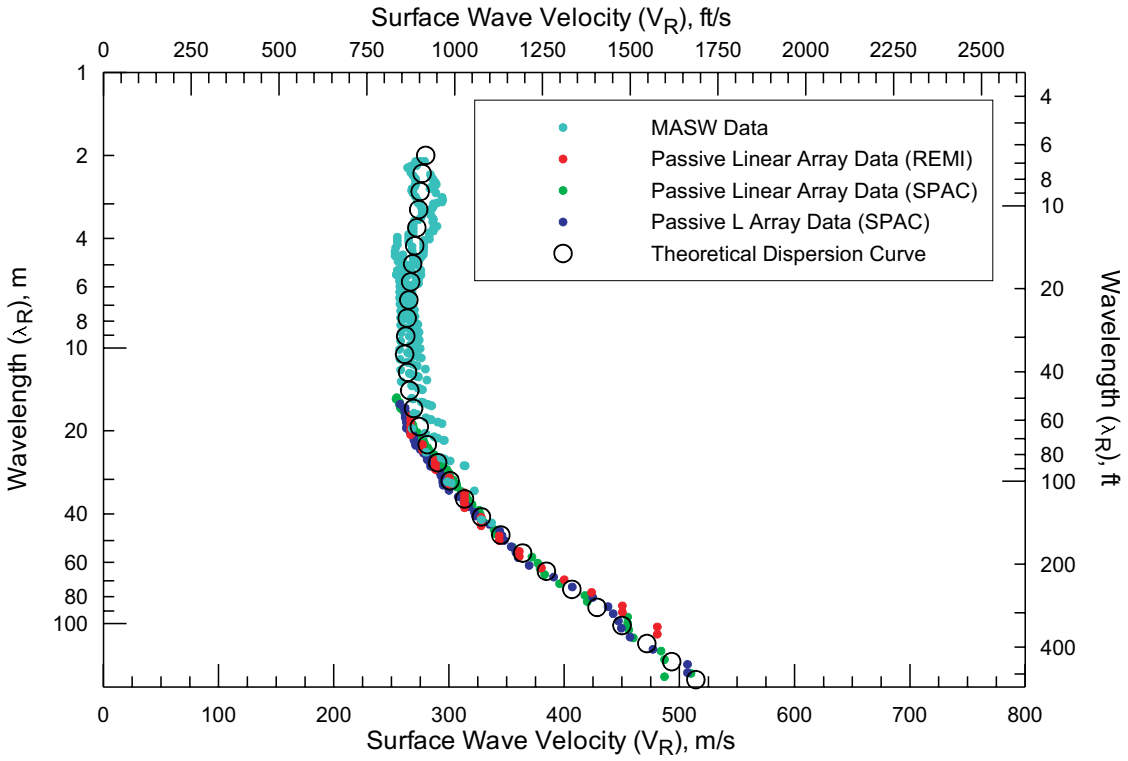


**Comparison of Field Experimental Data and Theoretical Dispersion Curve from Active and Passive Surface Wave Array Z5-S10**

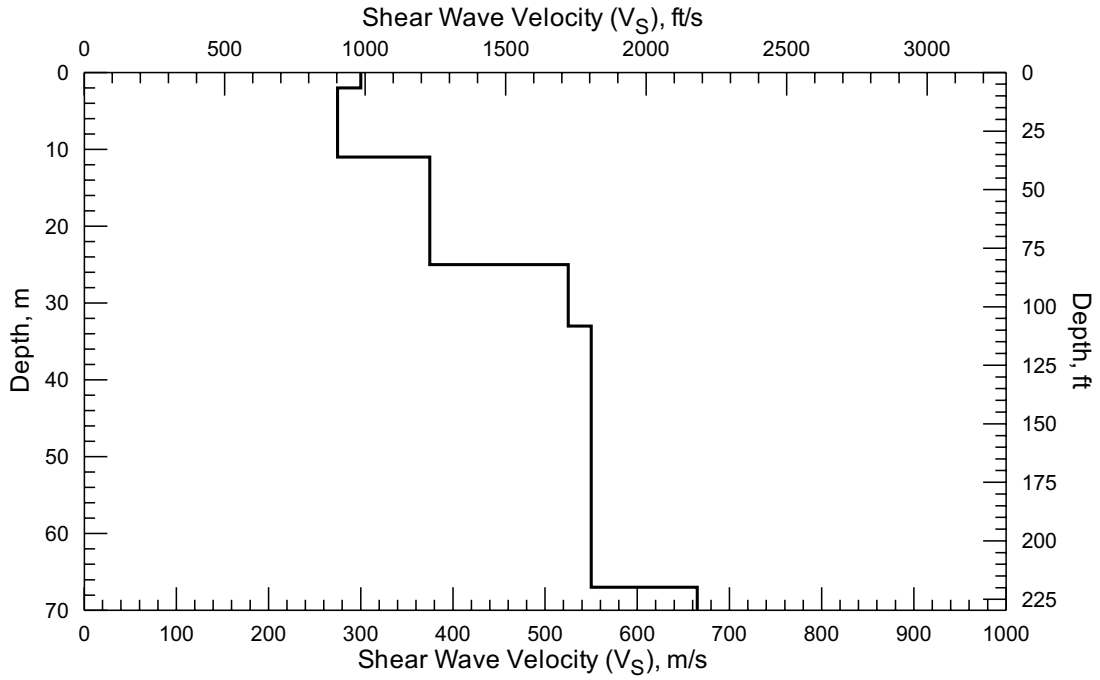


**$V_S$ Model from Active and Passive Surface Wave Array Z5-S10**

| | |
|---|---|
| GEOVision geophysical services | FIGURE 77<br>VELOCITY MODEL FOR ACTIVE AND PASSIVE SURFACE WAVE ARRAY Z5-S10 |
| Project # 9001<br>Date: JUL 29, 2009<br>Drawn By: A MARTIN<br>Approved By: Antony J. Martin | S 2ND ST AND W ADAMS AVE,<br>ALHAMBRA, CALIFORNIA |
| File R:\...Project Files\2009\9001ch2mhill\report\figures\Figure77.cdr | PREPARED FOR<br>CH2M HILL |

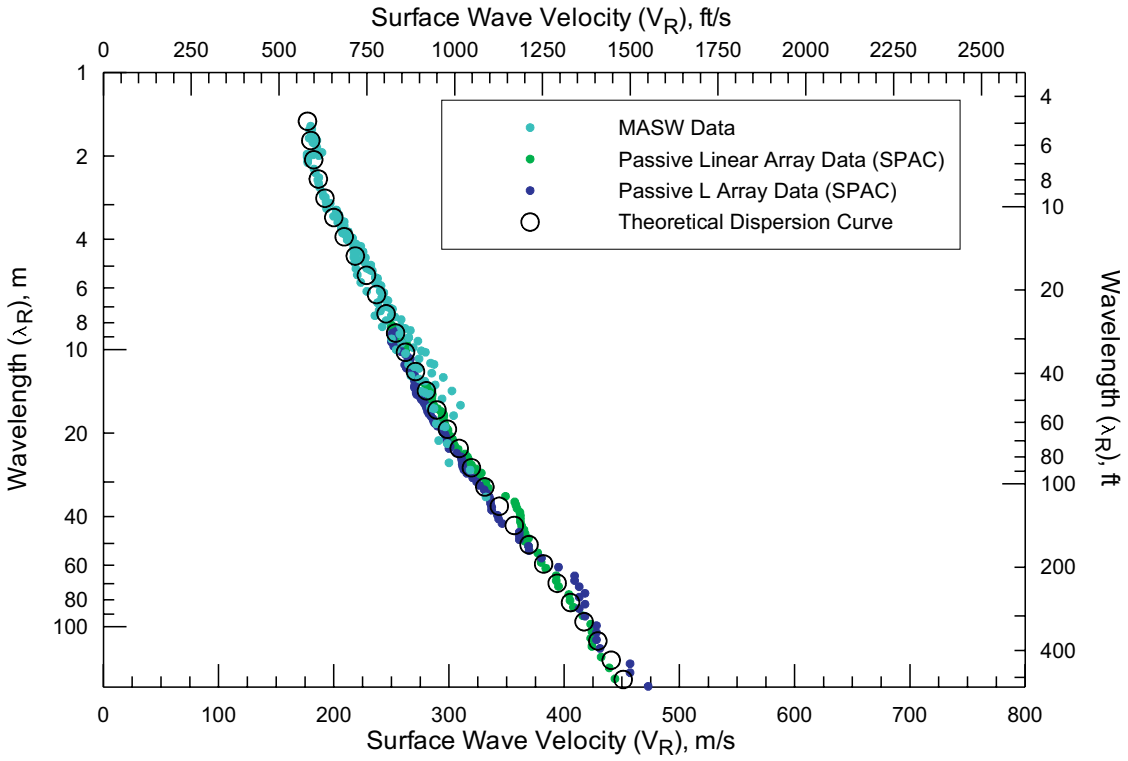


**Comparison of Field Experimental Data and Theoretical Dispersion Curve from Active and Passive Surface Wave Array Z5-S11**

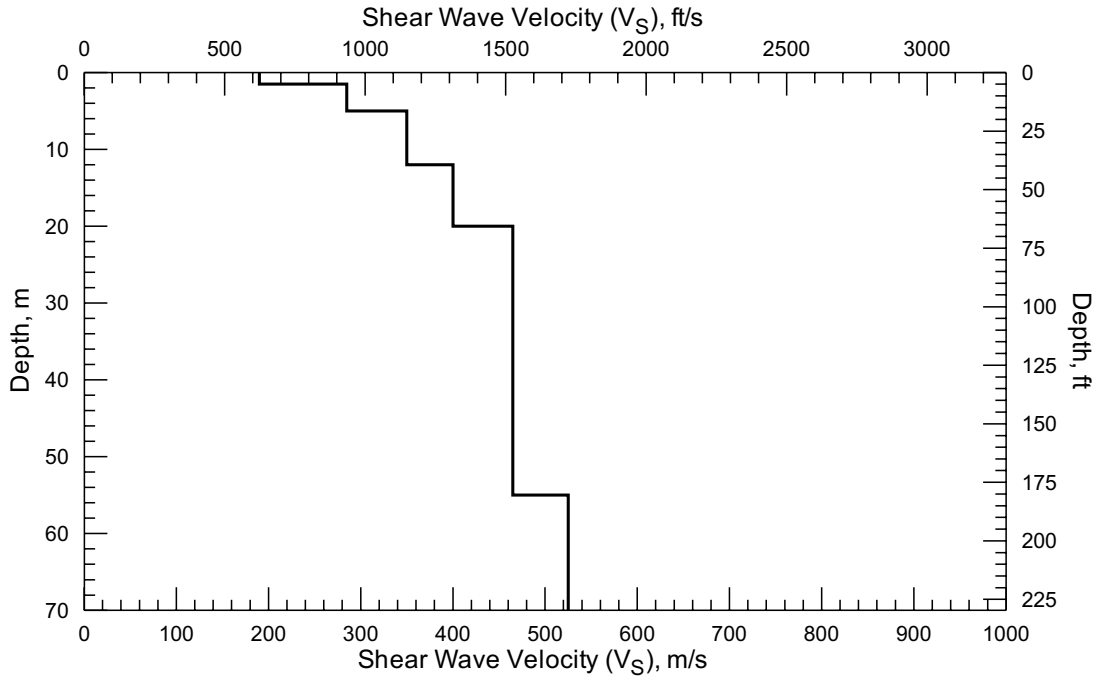


**$V_S$ Model from Active and Passive Surface Wave Array Z5-S11**

| | |
|---|---|
| GEOVision geophysical services | FIGURE 78<br>VELOCITY MODEL FOR ACTIVE AND PASSIVE SURFACE WAVE ARRAY Z5-S11 |
| Project # 9001<br>Date: JUL 29, 2009<br>Drawn By: A MARTIN<br>Approved By: Antony J. Martin | SHORB ST AND BENITO AVE,<br>ALHAMBRA, CALIFORNIA |
| File R:\...Project Files\2009\9001ch2mhill\report\figures\Figure78.cdr | PREPARED FOR<br>CH2M HILL |

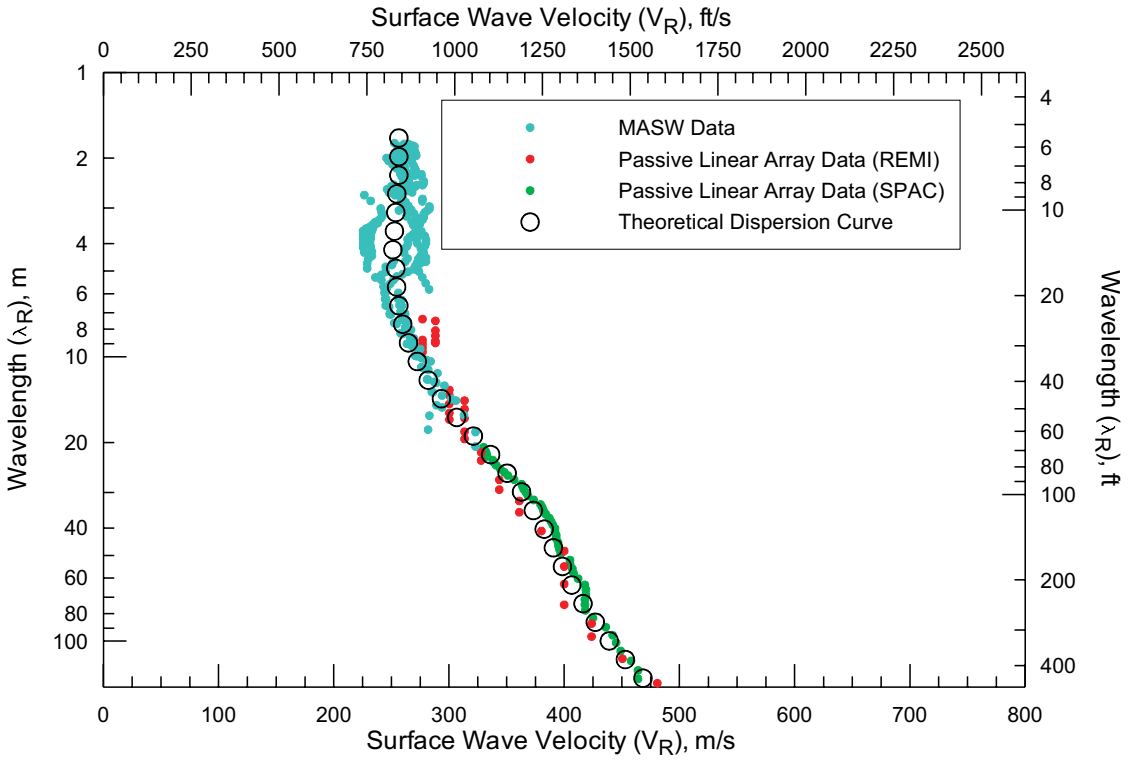


**Comparison of Field Experimental Data and Theoretical Dispersion Curve from Active and Passive Surface Wave Array Z5-S12**

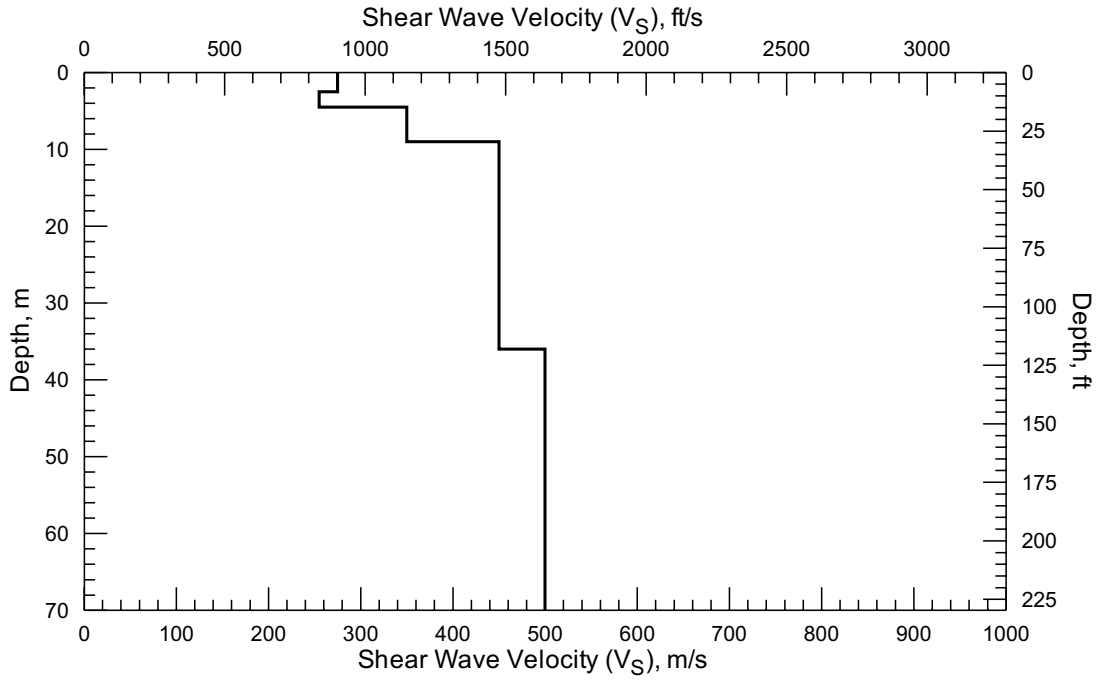


**$V_S$ Model from Active and Passive Surface Wave Array Z5-S12**

| | |
|---|---|
| GEOVision geophysical services | FIGURE 79<br>VELOCITY MODEL FOR ACTIVE AND PASSIVE SURFACE WAVE ARRAY Z5-S12 |
| Project # 9001<br>Date: JUL 29, 2009<br>Drawn By: A MARTIN<br>Approved By: Antony J Martin<br>File R:\...Project Files\2009\9001ch2mhill\report\figures\Figure79.cdr | NORWOOD PL AND EDGEWOOD DR,<br>ALHAMBRA, CALIFORNIA<br><br>PREPARED FOR<br>CH2M HILL |

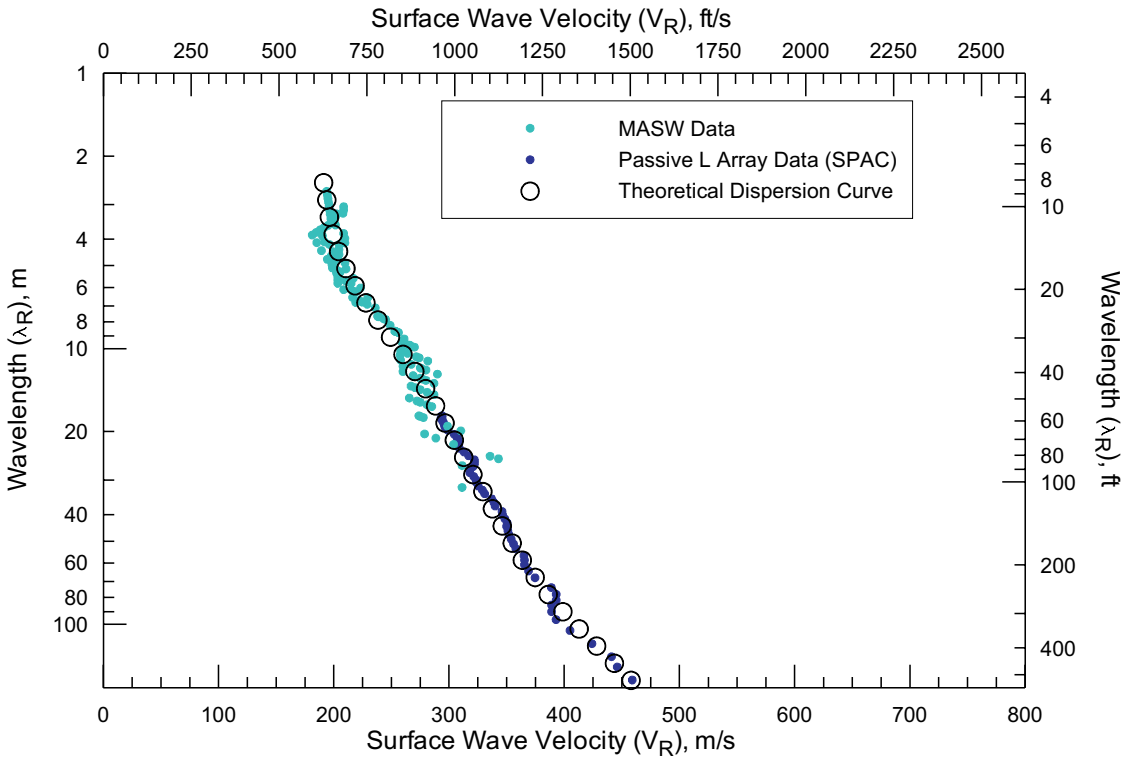


**Comparison of Field Experimental Data and Theoretical Dispersion Curve from Active and Passive Surface Wave Array Z5-S13**

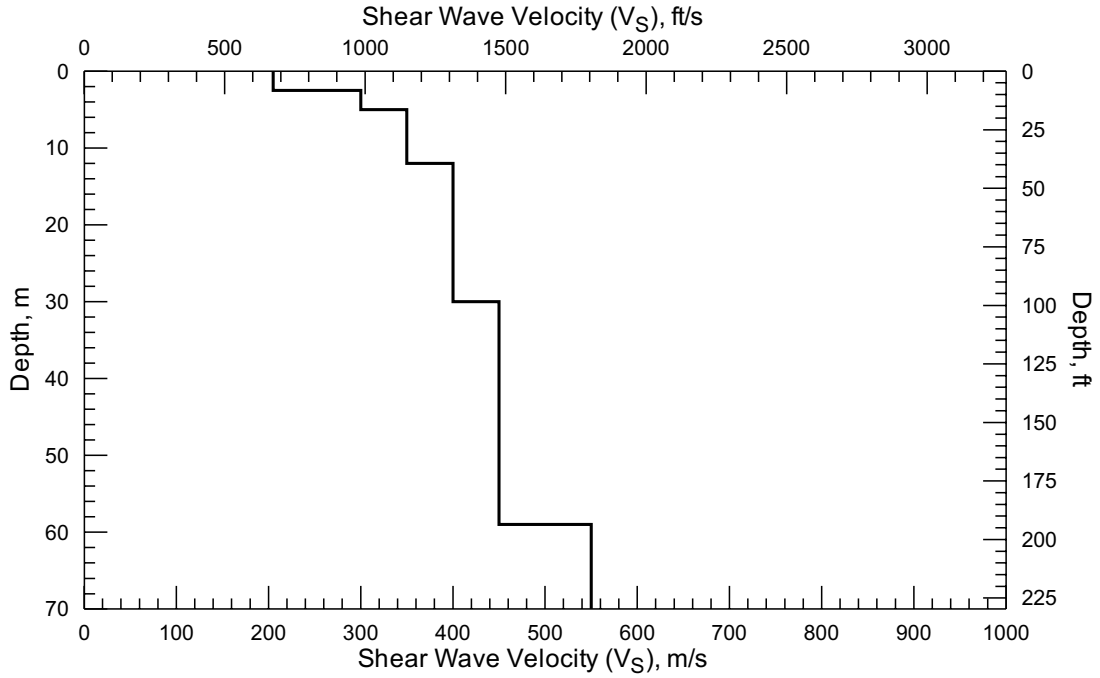


**$V_S$ Model from Active and Passive Surface Wave Array Z5-S13**

| | |
|---|---|
| GEOVision geophysical services | FIGURE 80<br>VELOCITY MODEL FOR ACTIVE AND PASSIVE SURFACE WAVE ARRAY Z5-S13 |
| Project # 9001<br>Date: JUL 29, 2009<br>Drawn By: A MARTIN<br>Approved By: Antony J. Martin<br>File R:\...Project Files\2009\9001ch2mhill\report\figures\Figure80.cdr | ROSS AVE AND EDGEWOOD DR,<br>ALHAMBRA, CALIFORNIA<br><br>PREPARED FOR<br>CH2M HILL |

APPENDIX B.2

# Pressuremeter Results

# Appendix B.2
# Pressuremeter Results

The following data reports were prepared for the SR 710 Tunnel Technical Study Final Geotechnical Summary Report (CH2M HILL, 2010). However, only data relevant to the SR 710 North Study are provided herein as summarized in Table B-3. The full version of the following appendix is presented in the Technical Study (CH2M HILL, 2010).

TABLE B-3
**Summary of Pressuremeter Tests**

| Boring Number | Test Number | Date Performed | Test Depth (feet) | Recovery Percent | RQD | Rock Description |
|---|---|---|---|---|---|---|
| R-09-Z3B2 | SR710-01 | 1/16/2009 | 200.9 | 17 | 0 | Wilson Quartz Diorite (Wqm)/Granitic-type and Gneissic Rock |
| R-09-Z3B2 | SR710-02 | 1/16/2009 | 199.4 | 17 | 0 | Wilson Quartz Diorite (Wqm)/Granitic-type and Gneissic Rock |
| R-09-Z3B2 | SR710-05 | 1/17/2009 | 227 | 100 | 0 | Wilson Quartz Diorite (Wqm)/Granitic-type and Gneissic Rock |
| R-09-Z3B2 | SR710-06 | 1/17/2009 | 225 | 75 | 0 | Wilson Quartz Diorite (Wqm)/Granitic-type and Gneissic Rock |
| R-09-Z3B2 | SR710-09 | 1/18/2009 | 248 | 50 | 0 | Wilson Quartz Diorite (Wqm)/Granitic-type and Gneissic Rock |
| R-09-Z3B2 | SR710-10 | 1/18/2009 | 246.5 | 92 | 0 | Wilson Quartz Diorite (Wqm)/Granitic-type and Gneissic Rock |
| R-09-Z3B6 | SR710-43 | 2/20/2009 | 132 | 20 | 8 | Topanga Formation(Ttcg)/ Conglomerate |
| R-09-Z3B6 | SR710-47 | 2/23/2009 | 166.5 | 44 | 0 | Topanga Formation(Ttcg)/ Conglomerate |
| R-09-Z3B6 | SR710-48 | 2/24/2009 | 188.2 | 98 | 30 | Topanga Formation(Ttcg)/ Conglomerate |

RQD – Rock Quality Designation

# Final Report of
# In Situ Pressuremeter Geotechnical Testing

**Conducted for:**

**SR-710 Tunnel Technical Study**
**Los Angeles County, California**

Submitted to:

**CH2M Hill**
6 Hutton Centre Drive
Suite 700
Santa Ana, California 92707

In Situ Engineering Project Number 812
CH2M Hill Project Number 378312.04.13

August 2009

Testing conducted and report prepared by:


## *In Situ Engineering*

6232 195th Avenue SE

Snohomish, WA 98290 360-568-2807

keith@insituengineering.com

## TABLE OF CONTENTS



**FIGURES**



**TABLES**



**APPENDICES**

## 1.0 INTRODUCTION

This report presents the results of a pressuremeter study, conducted from the 16th of January to 24th of February, 2009, in eleven boreholes within the SR-710 Tunnel Technical Study zones. The pressuremeter testing (PMT) was conducted by In Situ Engineering, Snohomish, WA under contract to CH2M Hill, Santa Ana, California. The drilling and deployment of the pressuremeter was accomplished by two groups; CalTrans, Sacramento, CA, using a CME 85 rig and Cascade Drilling, La Habra, CA using an Ingersoll Rand A-400 and a Failing Speedstar 30K drill rig. In total, 48 pressuremeter tests were attempted, of which 46 produced PMT data. The borehole name, test depths and preliminary material descriptions are presented in Table 1.

## 2.0 PURPOSE

The purpose of this study was to evaluate the *in-situ* modulus of the geologic formations as part of the SR-710 Tunnel Technical Study.

## 3.0 PRESSUREMETER

The pressuremeter used for this study was a pre-bored monocell pressuremeter. Three electronic displacement sensors, spaced 120 degrees apart are located at the center of the pressuremeter. The flexible membrane is placed over the sensors, and clamped at each end. The membrane is covered by a protective sheet of stainless steel strips. The unit is pressurized using compressed nitrogen to deform the adjacent material. The electronic signals from displacement sensors and the pressure sensor are transmitted by cable to the surface. During the test, the average expansion versus pressure is displayed on a computer screen. The pressuremeter is expanded by regulating the flow of compressed nitrogen to the PMT unit.

Fig.1 presents the essential details of the pressuremeter.

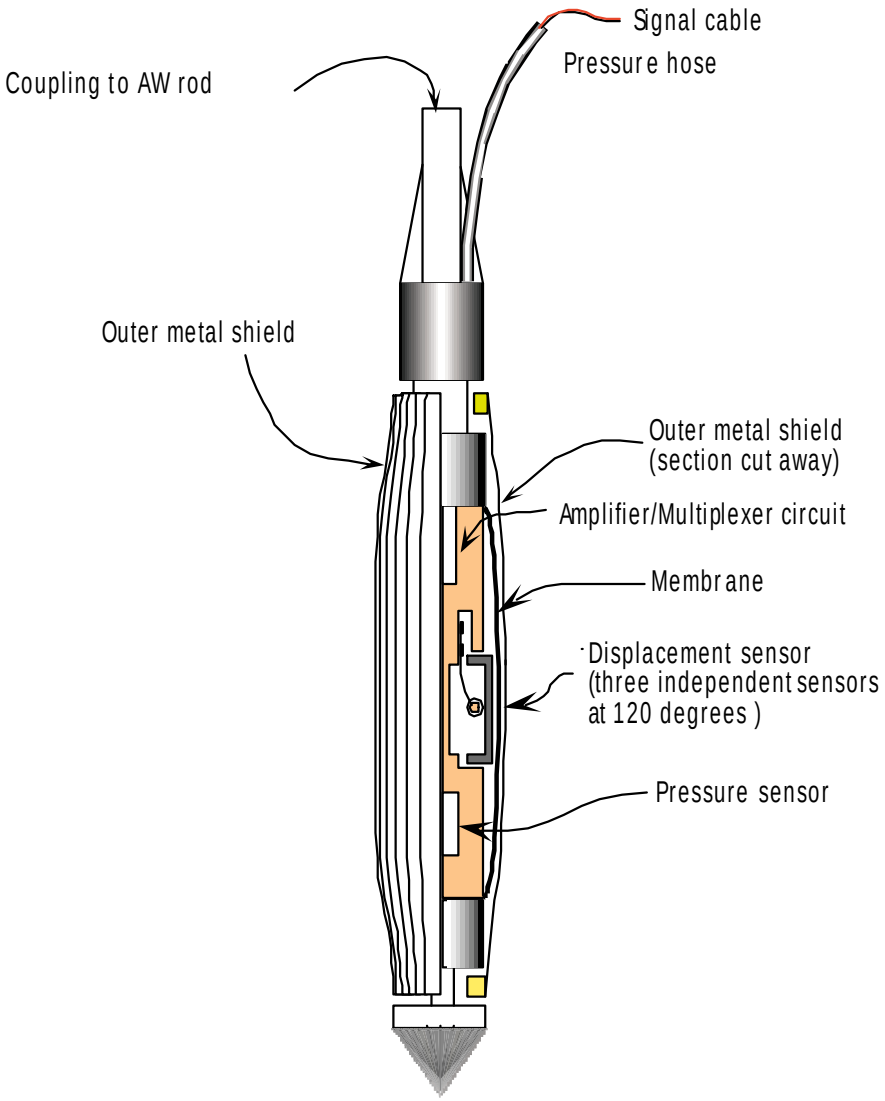


**Fig. 1. Schematic details of the pressuremeter**

## 4.0 HOLE FORMATION

The Cascade Drilling group used a PQ wireline system to advance the borehole. This allowed the hole to be continuously cased. A 5 to 6 foot test pocket for the pressuremeter was drilled using a 2 $^{15}/_{16}$ tricone bit, or NQ core barrel which was able to fit through the PQ core bit. The Caltrans system used an HQ wireline system to advance the main hole. This string had to be withdrawn from the hole and the bit changed to a casing bit to allow a 2 $^{15}/_{16}$ tricone bit, or a NQ core barrel to be used to drill the test pocket for the pressuremeter.

In general the aim is to attempt two pressuremeter tests in the one test pocket. The tests are preformed 18 inches apart. In this manner it is possible to assess the quality of the tests.

The details of the test depth and the initial sample description are given in Table 1. The RQD, percent recovery and rock description provided by CH2M Hill. It should be noted that the preliminary boring numbers shown on the plots in the appendices are different than the final boring numbers shown in the Tables of this report. The final numbers have had a prefix (R-09) added to the number and a dash removed from the final sequence. For instance the final boring number R-09-Z3B2 in Table 1 below is the same as boring number Z3-B2 in the Appendices.

**Table 1 Pressuremeter Test depth and Material Description: Tests 1-48**

| Boring Number | Test Number | Date Performed | Test Depth (feet) | Recovery Percent | RQD | Rock Description |
|---|---|---|---|---|---|---|
| R-09-Z3B2 | SR710-01 | 1/16/2009 | 200.9 | 17 | 0 | Wilson Quartz Diorite (Wqm)/ Granitic and Gneissic Rock |
| R-09-Z3B2 | SR710-02 | 1/16/2009 | 199.4 | 17 | 0 | Wilson Quartz Diorite (Wqm)/ Granitic and Gneissic Rock |
| R-09-Z3B11 | SR710-03 | 1/17/2009 | 192.8 | 100 | 95 | Topanga Formation (Ttsl)/ Siltstone and Mudstone |
| R-09-Z3B11 | SR710-04 | 1/17/2009 | 191.3 | 100 | 95 | Topanga Formation(Ttsl)/ Siltstone and Mudstone |
| R-09-Z3B2 | SR710-05 | 1/17/2009 | 227 | 100 | 0 | Wilson Quartz Diorite (Wqm)/ Granitic and Gneissic Rock |
| R-09-Z3B2 | SR710-06 | 1/17/2009 | 225 | 75 | 0 | Wilson Quartz Diorite (Wqm)/ Granitic and Gneissic Rock |
| R-09-Z3B11 | SR710-07 | 1/18/2009 | 208.4 | 100 | 100 | Topanga Formation (Ttsl)/ Siltstone and Mudstone |
| R-09-Z3B11 | SR710-08 | 1/18/2009 | 206.9 | 100 | 100 | Topanga Formation (Ttsl)/ Siltstone and Mudstone |
| R-09-Z3B2 | SR710-09 | 1/18/2009 | 248 | 50 | 0 | Wilson Quartz Diorite (Wqm)/ Granitic and Gneissic Rock |

| Boring Number | Test Number | Date Performed | Test Depth (feet) | Recovery Percent | RQD | Rock Description |
|---|---|---|---|---|---|---|
| R-09-Z3B2 | SR710-10 | 1/18/2009 | 246.5 | 92 | 0 | Wilson Quartz Diorite (Wqm)/ Granitic and Gneissic Rock |
| R-09-Z2B1 | SR710-11 | 1/19/2009 | 129 | 20 | 20 | Topanga Formation (Ttsl)/ Interbedded Siltstone and Sandstone |
| R-09-Z2B1 | SR710-12 | 1/19/2009 | 127.5 | 20 | 20 | Topanga Formation (Ttsl)/ Interbedded Siltstone and Sandstone |
| R-09-Z2B1 | SR710-13 | 1/20/2009 | 140 | 45 | 35 | Topanga Formation (Ttsl)/ Interbedded Siltstone and Sandstone |
| R-09-Z2B1 | SR710-14 | 1/20/2009 | 138.5 | 45 | 35 | Topanga Formation(Ttsl)/ Interbedded Siltstone and Sandstone |
| R-09-Z1B7 | SR710-15 | 1/20/2009 | 96.5 | 80 | 80 | Puente Formation (Tpds)/ Sandy Siltstone |
| R-09-Z1B7 | SR710-16 | 1/20/2009 | 95 | 80 | 80 | Puente Formation (Tpds)/ Sandy Siltstone |
| R-09-Z1B7 | SR710-17 | 1/21/2009 | 111.5 | 98 | 98 | Puente Formation (Tpds)/ Sandy Siltstone |
| R-09-Z1B7 | SR710-18 | 1/21/2009 | 110 | 98 | 98 | Puente Formation (Tpds)/ Sandy Siltstone |
| R-09-Z1B7 | SR710-19 | 1/21/2009 | 136 | 77 | 68 | Puente Formation (Tpds)/ Sandy Siltstone |
| R-09-Z1B7 | SR710-20 | 1/21/2009 | 134.5 | 77 | 68 | Puente Formation (Tpds)/ Sandy Siltstone |
| R-09-Z1B3 | SR710-21 | 1/28/2009 | 177.3 | 89 | 89 | Puente Formation (Tpss)/ Sandstone |
| R-09-Z1B3 | SR710-22 | 1/28/2009 | 204 | 83 | 79 | Puente Formation (Tpss)/ Sandstone |
| R-09-Z2B2 | SR710-23 | 1/29/2009 | 135.7 | 100 | 100 | Fernando Formation (Tfss-cg)/ Sandstone |
| R-09-Z2B2 | SR710-24 | 1/29/2009 | 134.2 | 100 | 100 | Fernando Formation (Tfss-cg)/ Sandstone |
| R-09-Z2B2 | SR710-25 | 2/4/2009 | 251 | 73 | 0 | Fernando Formation (Tfss-cg)/ Sandstone |
| R-09-Z2B2 | SR710-26 | 2/4/2009 | 249.5 | 73 | 0 | Fernando Formation (Tfss-cg)/ Sandstone |
| R-09-Z1B6 | SR710-27 | 2/4/2009 | 203 | 90 | 75 | Puente Formation (Tpsl)/ Siltstone with interbedded Sandstone |
| R-09-Z1B6 | SR710-28 | 2/5/2009 | 245 | 100 | 92 | Puente Formation (Tpsl)/ Siltstone with interbedded Sandstone |
| R-09-Z3B7 | ST710-29 | 2/6/2009 | 225.8 | 100 | 60 | Topanga Formation (Ttss)/ Sandstone with Interbedded Siltstone |

| Boring Number | Test Number | Date Performed | Test Depth (feet) | Recovery Percent | RQD | Rock Description |
|---|---|---|---|---|---|---|
| R-09-Z3B7 | SR710-30 | 2/6/2009 | 224.3 | 100 | 60 | Topanga Formation (Ttss)/ Sandstone with Interbedded Siltstone |
| R-09-Z1B6 | SR710-31 | 2/6/2009 | 332 | 100 | 100 | Puente Formation (Tpsl)/ Siltstone with interbedded Sandstone |
| R-09-Z1B6 | SR710-32 | 2/6/2009 | 330.5 | 100 | 100 | Puente Formation (Tpsl)/ Siltstone with interbedded Sandstone |
| R-09-Z3B7 | SR710-33 | 2/10/2009 | 252.5 | 97 | 50 | Topanga Formation (Ttss)/ Sandstone with Interbedded Siltstone |
| R-09-Z3B7 | SR710-34 | 2/10/2009 | 251 | 100 | 40 | Topanga Formation (Ttss)/ Sandstone with Interbedded Siltstone |
| R-09-Z3B7 | SR710-35 | 2/10/2009 | 271.6 | 93 | 0 | Topanga Formation (Ttss)/ Sandstone with Interbedded Siltstone |
| R-09-Z3B7 | SR710-36 | 2/10/2009 | 270.1 | 93 | 0 | Topanga Formation (Ttss)/ Sandstone with Interbedded Siltstone |
| R-09-Z1B5 | SR710-37 | 2/19/2009 | 278 | 100 | 100 | Puente Formation (Tpss)/ Sandstone |
| R-09-Z1B5 | SR710-38 | 2/19/2009 | 276.5 | 100 | 100 | Puente Formation (Tpss)/ Sandstone |
| R-09-Z1B4 | SR710-39 | 2/19/2009 | 332** | 100 | 50 | Puente Formation (Tpss)/ Sandstone and Siltstone |
| R-09-Z1B4 | SR710-40 | 2/19/2009 | 330.5** | 100 | 50 | Puente Formation (Tpss)/ Sandstone and Siltstone |
| R-09-Z1B5 | SR710-41 | 2/20/2009 | 347 | 20 | 20 | Puente Formation (Tpss)/ Sandstone |
| R-09-Z1B5 | SR710-42 | 2/20/2009 | 345.5 | 20 | 20 | Puente Formation (Tpss)/ Sandstone |
| R-09-Z3B6 | SR710-43 | 2/20/2009 | 132 | 20 | 8 | Topanga Formation(Ttcg)/ Conglomerate |
| R-09-Z1B5 | SR710-44 | 2/23/2009 | 398 | 100 | 90 | Puente Formation (Tpss)/ Sandstone and Siltstone |
| R-09-Z1B5 | SR710-45 | 2/23/2009 | 396.5 | 100 | 90 | Puente Formation (Tpss)/ Sandstone and Siltstone |
| R-09-Z3B6 | SR710-46 | 2/23/2009 | 168 | 44 | 0 | Topanga Formation(Ttcg)/ Conglomerate |
| R-09-Z3B6 | SR710-47 | 2/23/2009 | 166.5 | 44 | 0 | Topanga Formation(Ttcg)/ Conglomerate |
| R-09-Z3B6 | SR710-48 | 2/24/2009 | 188.2 | 98 | 30 | Topanga Formation(Ttcg)/ Conglomerate |

## 5.0 TEST PROCEDURE

The membrane was expanded by controlling the flow of compressed nitrogen into the pressuremeter, increasing the pressure in small steps until the membrane starts to expand against the borehole wall. Once the average strain of the borehole wall was greater than about 1.5% the pressure is reduced to no more than 40% of the maximum past pressure, then increased again.

The resulting unload-reload loop can be used to evaluate the elastic behavior of the material. In materials which behave in a linear manner, the loops will exhibit little hysteretic behavior. That is, the linear unloading path will follow the reloading path. The loops will be very tight.

The pressure is then advanced in steps until the strain is increased a further 3% before completing a second unload-reload cycle. In many tests the procedure is repeated until a third unload-reload loop is completed. If the disturbance is small, the slope of the loops will tend to be parallel. Figure 2, Test SR710-12, is a typical example.

After the strain exceeds 12%, the pressure is reduced to zero. Adjustments are made for the location of the unload-reload loops as well as the ending strain and pressure for each test based on the expertise of the field operator.

In strong materials such as that shown as SR710-42 (on the right in Fig. 2) the pressure is increased in pressure increments of about 300 to 400 psi.

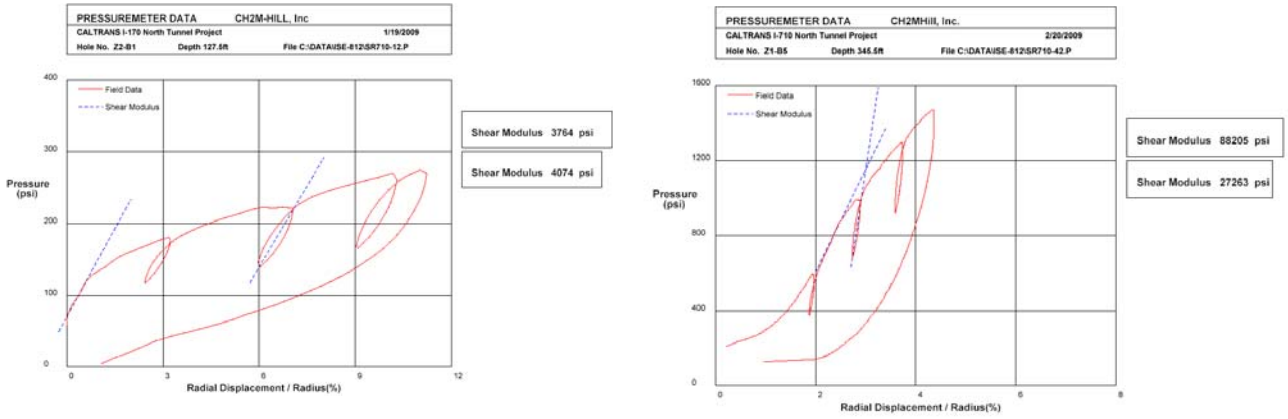


Test SR710-12 SR710-42

**Fig. 2. Test SR710-12 and Tests SR710-42**

(Test SR710-12 in R-09-Z2B1 at 127.5 ft and Test SR710-42 in R-09-Z1B5 at 345.5 ft)

## 6.0 QUALITY OF THE DATA

In general, the pressuremeter testing should reflect the material being tested. If the materials being tested are relatively uniform then adjacent tests should be similar in form. If adjacent tests are distinctly different, then either the material has changed, or some disturbance within the borehole has been encountered while performing the test.

Hence in a qualitative manner the results can be assessed as to whether the data reflects the *in-situ* material properties. In Figure 3 are two adjacent tests at 345.5 and 347 ft in Hole Z1-B5, in the same test pocket.

The maximum pressure reached in both tests is similar; in the order of 1,400 psi after a strain of about 3%. The shape of the final unloading curve, which is less influenced by the initial disturbance, is also similar in the two tests. Both these pieces of data would suggest the material at both locations is similar.

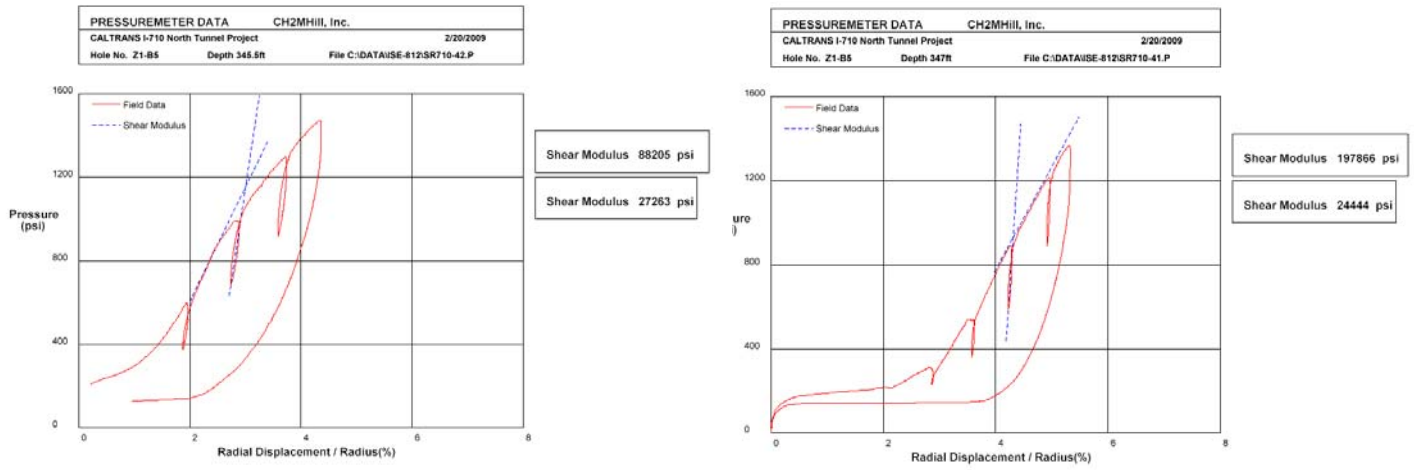


**Fig. 3. Adjacent pressuremeter tests in same pilot hole**

(SR710-42 at 345.5 ft and SR710-41 at 347 ft)

## 7.0 RANGE OF DATA

A variety of material types have been tested in this study. Typical tests examples of the strong and the weak materials are shown in Figure 4. For comparative purposes these tests have all been plotted to the same scale. The shear modulus, as represented by the slopes of the unload-reload loops (Section 9), is 90,000 psi, and 5,000 psi respectively. In terms of stiffness, these materials tested range over 18 to 1. The maximum range in this study ranges from 600,000 psi for Test 6 to 3,000 for Test 11; that is a 200 to 1 range.

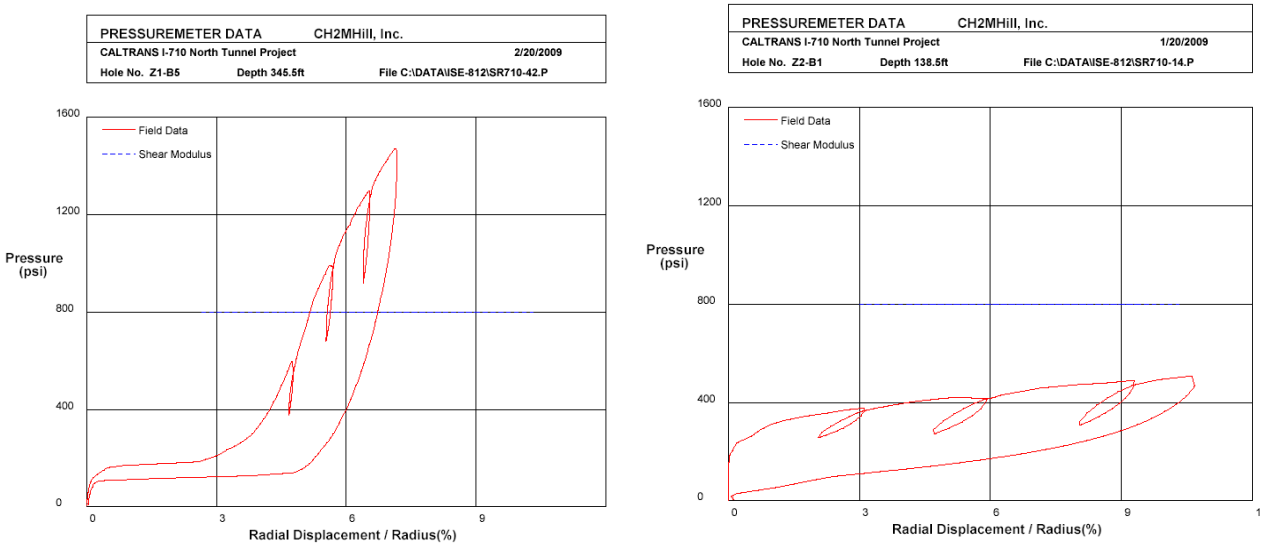


**Fig. 4. Test in Sandstone (SR710-42) and Fractured Diorite (SR710-14)**

## 8.0 STANDARD METHOD OF ANALYSIS OF THE SHEAR MODULUS

If the material surrounding the pressuremeter is assumed to extend to infinity, and assumed to behave as an idealized linear elastic, homogeneous material, which does not fail under shear or tension, then the displacement on the boundary of the pressuremeter, $u_a$, for a given pressure, P, is given by:

$$u_a = P(a)\,(1+\mu) / E \qquad 1)$$

where “E” is the Young’s Modulus, “a” the radius of the pressuremeter cavity, and “μ" the Poisson’s ratio. As the shear modulus, “G”, and the Young’s modulus, “E”, are related by the following relationship:

$$E=2(G)(1+\mu) \qquad 2)$$

Equation 1 reduces to:

$$u_a = 0.5P(a) / G \qquad 3)$$

Hence, the shear modulus G is given by:

$$G = 0.5 * \Delta \text{ Pressure} / \Delta(\text{radial displacement/radius}) \qquad 4)$$

The modulus for the average slope of the initial part of the pressuremeter curve (A-B in Fig.5) expressed as a Young’s modulus (assuming a Poisson's ratio of 0.33) is the same as the “pressuremeter modulus” defined in the American Society for Testing and Materials (ASTM) D4719, Section 9.5. In many tests a straight section in this part of the curve is not defined well enough to enable the modulus to be determined. However, the modulus determined from the unload-reload loops, which is often higher than the initial loading modulus, is more accurately defined and is probably more representative of the *in-situ* modulus for the material. This data is summarized in Table 2.

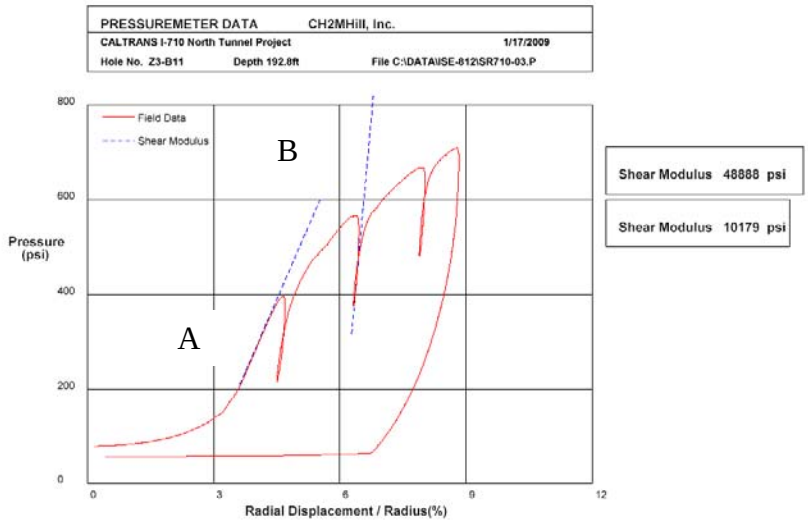


**Fig. 5. Modulus determination for Test SR710-03**

## 9.0 DETERMINATION OF THE LIMIT PRESSURE

From a visual inspection of the typical pressuremeter curve in the clay shown in Fig. 3, the pressure tends to a limit. For Test SR710-03 (Fig. 6) this limit pressure is in the range of 700 psi. To make this limit pressure a quantitative measurement, the limit pressure is defined as that pressure which occurs when the volume of the pressuremeter has doubled. However, few pressuremeter tests ever actually expand this far before reaching the limit of the strain sensing system. The pressuremeters used in this investigation will only expand to about 20% before the displacement limit is reached.

If the material being tested is assumed to behave as an elastic cohesive material, then the equation governing the pressure-displacement curve is given by:

$$P = P_L + (c)\log_e (u_a/_a) \qquad 5)$$

$$P_L = P_o + c + (c)\log_e [G/c] \qquad 6)$$

Where:

$P_L$" is the theoretical limit pressure at infinite expansion

"c" is the undrained cohesive strength,

"$P_O$" is the total *in-situ* lateral stress, and "G" is the shear modulus.

From Equation 5, a plot of pressure P against the log of $u_a/a$ will be a straight line, provided the shear strength remains constant with strain. The slope of this line will provide a measure of the undrained shear strength, c. The Limit Pressure, as defined by the ASTM code D4719, Section 10.6, is the pressure at which the cavity has doubled in size. This doubling in size occurs when $u_a/a$ is equal to 41%. (The origin of the strain used in the log/normal plots is the assumed origin at the *in-situ* stress state). If any disturbance is present, the above method of determining the cohesive strength usually provides an overly optimistic value. In Fig. 6, Test SR710-03 is plotted in the above manner. The above method applies to cohesive materials. However it can be used in granular materials to give an indication of the maximum or limit pressure that can be applied to the ground for the design of foundations. The shear strength determined by this method is not appropriate in granular materials.

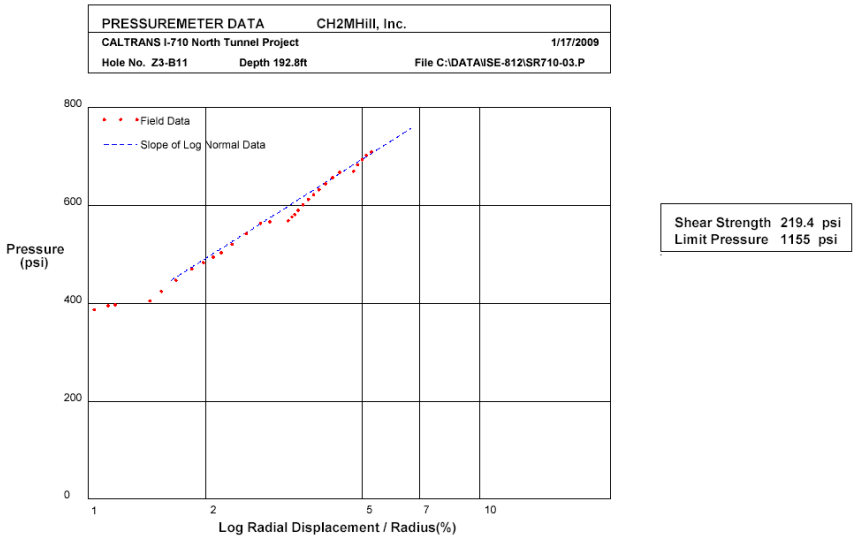


**Fig. 6. Limit Pressure determination for Test SR710-03**

**Table 2 Limit Pressure shear modulus and Shear strength (log method): Tests 1-26**

| Test | Depth (ft) | Hole | Limit Pressure (psi) | Initial Shear modulus (psi) | Unload-reload Shear modulus (psi) | Shear strength (log method) (psi) |
|---|---|---|---|---|---|---|
| SR710-1 | 200.9 | R-09-Z3B2 | 800 | 7,000 | 74,000 | 160 |
| SR710-2 | 199.4 | R-09-Z3B2 | 850 | 5,500 | 47,000 | 180 |
| SR710-5 | 227 | R-09-Z3B2 | 2,400 | 22,400 | 160,000 | 420 |
| SR710-6 | 225 | R-09-Z3B2 | 3,700 | 30,000 | 590,000 | 800 |
| SR710-9 | 248 | R-09-Z3B2 | 3,200 | 32,000 | 273,000 | 600 |
| SR710-10 | 246.5 | R-09-Z3B2 | 2,500 | 34,000 | 332,000 | 470 |
| | | | | | | |
| SR710-3 | 192.8 | R-09-Z3B11 | 1,150 | 9,700 | 46,000 | 220 |
| SR710-4 | 191.3 | R-09-Z3B11 | 1,100 | 7,000 | 44,000 | 220 |
| SR710-7 | 208.4 | R-09-Z3B11 | 660 | 5,500 | 16,000 | 118 |
| SR710-8 | 206.9 | R-09-Z3B11 | 640 | 5,500 | 14,000 | 100 |
| | | | | | | |
| SR710-11 | 129 | R-09-Z2B1 | 315 | 3,000 | 3,000 | 45 |
| SR710-12 | 127.5 | R-09-Z2B1 | 320 | 4,000 | 3,800 | 51 |
| SR710-13 | 140 | R-09-Z2B1 | 600 | na | 5,500 | 40 |
| SR710-14 | 138.5 | R-09-Z2B1 | 560 | 4,800 | 5,200 | 70 |
| | | | | | | |
| SR710-15 | 96.5 | R-09-Z1B7 | 1,700 | 8,900 | 41,400 | 380 |
| SR710-16 | 95 | R-09-Z1B7 | 1,350 | 6,500 | 30,000 | 330 |
| SR710-17 | 111.5 | R-09-Z1B7 | 835 | 6,300 | 31,000 | 137 |
| SR710-18 | 110 | R-09-Z1B7 | 920 | 4,000 | 20,000 | 220 |
| SR710-19 | 136 | R-09-Z1B7 | 1,300 | 6,500 | 50,000 | 270 |
| SR710-20 | 134.5 | R-09-Z1B7 | 2,300 | 15,000 | 60,000 | 590 |
| | | | | | | |
| SR710-21 | 177.3 | R-09-Z1B3 | 3,500 | 24,000 | 107,000 | 700 |
| SR710-22 | 204 | R-09-Z1B3 | 3,870 | 35,000 | 110,000 | 755 |
| | | | | | | |
| SR710-23 | 135.7 | R-09-Z2B2 | 650 | 10,000 | 8,000 | 120 |
| SR710-24 | 134.2 | R-09-Z2B2 | 430 | 1,600 | 3,600 | 90 |
| SR710-25 | 251 | R-09-Z2B2 | 1,100 | 20,000 | 14,000 | 170 |
| SR710-26 | 249.5 | R-09-Z2B2 | 1,550 | 14,000 | 32,000 | 350 |

**Table 2 cont. Limit Pressure shear modulus and Shear strength (log method): Tests 27-48**

| Test | Depth (ft) | Hole | Limit Pressure (psi) | Initial Shear modulus (psi) | Unload-reload Shear modulus (psi) | Shear strength (log method) (psi) |
|---|---|---|---|---|---|---|
| SR710-27 | 203 | R-09-Z1B6 | 1,830 | 14,000 | 70,000 | 310 |
| SR710-28 | 245 | R-09-Z1B6 | 2,600 | 56,000 | 140,000 | 370 |
| SR710-31 | 332 | R-09-Z1B6 | 3,000 | 48,000 | 130,000 | 470 |
| SR710-32 | 330.5 | R-09-Z1B6 | 2,800 | 34,000 | 80,000 | 540 |
| | | | | | | |
| SR710-29 | 225.8 | R-09-Z3B7 | 1,550 | 8,600 | 97,000 | 320 |
| SR710-30 | 224.3 | R-09-Z3B7 | 1,500 | 5,200 | 57,000 | 350 |
| SR710-33 | 252.5 | R-09-Z3B7 | 2,500 | 15,000 | 225,000 | 470 |
| SR710-34 | 251 | R-09-Z3B7 | 1,600 | 7,800 | 74,000 | 354 |
| SR710-35 | 271.6 | R-09-Z3B7 | 1,400 | 9,000 | 76,000 | 290 |
| SR710-36 | 270.1 | R-09-Z3B7 | 1,600 | 7,000 | 45,000 | 330 |
| | | | | | | |
| SR710-37 | 278 | R-09-Z1B5 | 6,000 | 47,000 | 250,000 | 1,280 |
| SR710-38 | 276.5 | R-09-Z1B5 | | hole too large | | |
| SR710-41 | 347 | R-09-Z1B5 | 3,700 | 24,000 | 200,000 | 830 |
| SR710-42 | 345.5 | R-09-Z1B5 | 3,200 | 27,000 | 88,000 | 670 |
| SR710-44 | 398 | R-09-Z1B5 | 2,300 | 16,000 | 84,000 | 500 |
| SR710-45 | 396.5 | R-09-Z1B5 | | hole too large | | |
| | | | | | | |
| SR710-39 | 332 | R-09-Z1B4 | 4,500 | 45,000 | 225,000 | 1,000 |
| SR710-40 | 330.5 | R-09-Z1B4 | 5,000 | 39,000 | 220,000 | 930 |
| | | | | | | |
| SR710-43 | 132 | R-09-Z3B6 | 3,700 | 26,000 | 283,000 | 750 |
| SR710-46 | 168 | R-09-Z3B6 | >2,000 | 69,000 | 450,000 | >1,000 |
| SR710-47 | 166.5 | R-09-Z3B6 | 7,000 | 56,000 | 280,000 | 1,600 |
| SR710-48 | 188.2 | R-09-Z3B6 | 6,500 | 61,000 | 323,000 | 1,400 |

## 10.0 DETERMINATION OF THE STRENGTH PROPERTIES

The PMT data can sometimes be used directly to determine the *in-situ* material properties such as the cohesive strength and the friction angle. To do so, a material model and failure mechanism must be assumed. If it is assumed that the material behaves in an ideal manner, in that the material deforms at constant volume throughout the test, i.e. it does not consolidate or dilate, and the shear strength remains constant, the pressuremeter curve can be interpreted by simple analytical means. The slope of the plot of pressure against the log of the strain can be used to give a direct measure of the shear strength, as discussed in Section 8. Unfortunately, real materials do not quite behave in this manner, and the shear strength determined by this method may not be accurate, particularly in disturbed material, in materials which degrade or partial tests in an enlarged hole. The shear strength determined by plotting on a log scale is not appropriate in frictional materials. However, this method of analysis often forms a basis of rating all materials.

A more realistic method of determining the shear strength in clays is to compare the field PMT data with an ideal model pressuremeter curve based on an assumed set of material parameters. If, for instance, the material is assumed to be cohesive and fails at constant shear strength and at constant volume, then the material parameters required for this model are the shear strength, lateral stress, and shear modulus. Adjustments can be made to those three parameters until a mathematical curve can be fitted to the field data. (Fig. 7 is an example for test SR710-14) Judgment is required to adjust these three parameters to determine the best fit to the data, particularly if there is disturbance present.

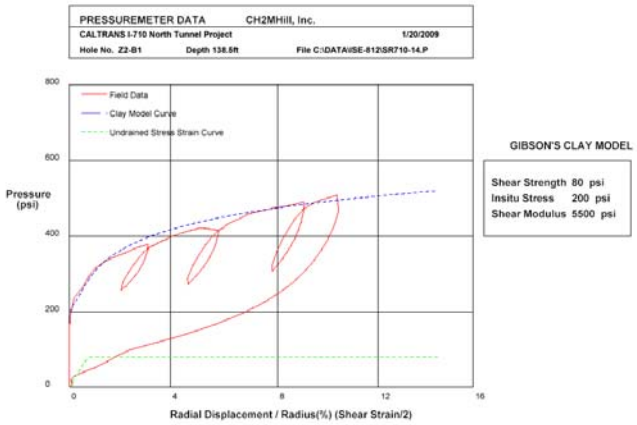


**Fig. 7. Simple constant shear strength model analysis for test SR710-14**

In the frictional materials, if it is assumed that it has a constant friction angle and no cohesion, then a simple model can be used to compare with the field data. Test SR710-03 which is probably a frictional material and not a cohesive material is analyzed in this manner in Fig. 8.

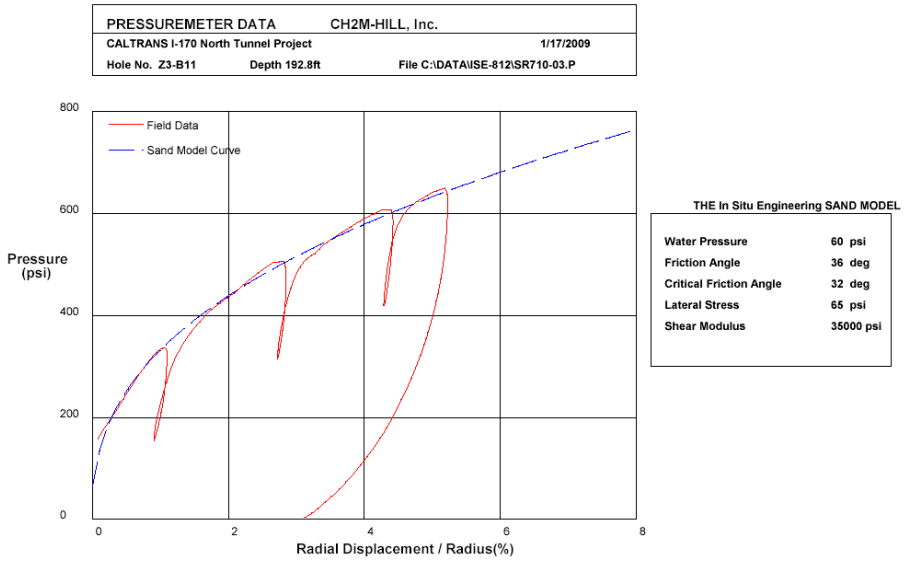


**Fig. 8. Frictional Model for Test SR710-03**

In rock, if it is assumed to be a cohesive material, then a possible model can be developed which uses the initial modulus, as illustrated in Fig 9a. This gives a shear strength of 420 psi. The strength determined in this manner is above that derived by the log method, which give a strength of 380 psi. In dense clays a better modulus to use is the modulus derived from the unload-reload curve. The ideal pressuremeter curve derived for this model is a poor fit to the field data (Fig 9b). However, the strength is lower; it has a minimum value of 240 psi. Hence to gain some understanding of the shear strength, the tests have been analyzed with three methods; the log method and two model methods using the initial shear modulus and the unload-reload shear modulus. Shear Strength values and friction angles are presented in Table 3.

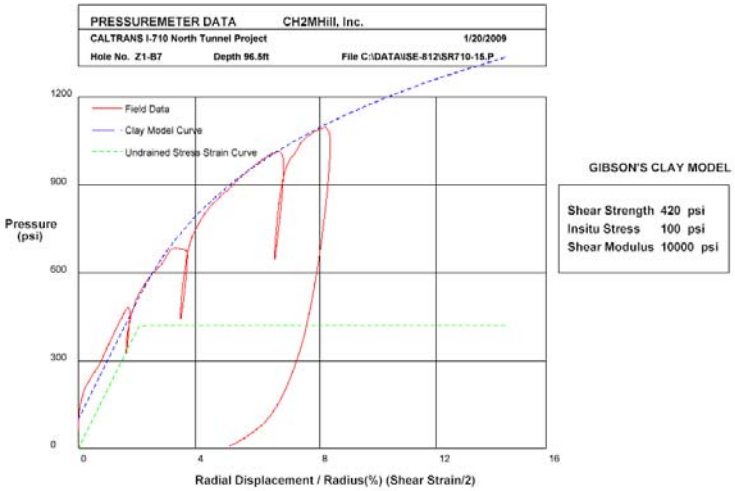


Fig 9a Initial shear modulus

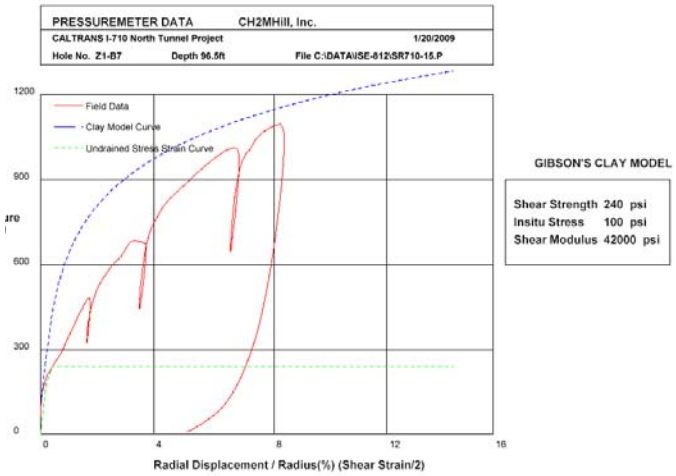


Fig 9b Unload-reload shear modulus

**Fig. 9. Cohesive Models for Test SR710-15**

**Table 3 Material properties from Model Analysis: Tests 1-26**

| Test | Depth (ft) | Hole | Shear strength (model initial modulus) (psi) (Maximum) | Shear strength (model unloading modulus) (psi) (Minimum) | Shear strength log method) (psi) | Friction (model) |
|---|---|---|---|---|---|---|
| SR710-1 | 200.9 | R-09-Z3B2 | 120 | 50 | 160 | |
| SR710-2 | 199.4 | R-09-Z3B2 | 120 | 50 | 180 | |
| SR710-5 | 227 | R-09-Z3B2 | 550 | 220 | 420 | |
| SR710-6 | 225 | R-09-Z3B2 | 900 | 250 | 800 | |
| SR710-9 | 248 | R-09-Z3B2 | 700 | 250 | 600 | |
| SR710-10 | 246.5 | R-09-Z3B2 | 400 | 170 | 470 | |
| | | | | | | |
| SR710-3 | 192.8 | R-09-Z3B11 | 230 | 140 | 220 | 36 |
| SR710-4 | 191.3 | R-09-Z3B11 | 230 | 130 | 220 | |
| SR710-7 | 208.4 | R-09-Z3B11 | 100 | 50 | 118 | |
| SR710-8 | 206.9 | R-09-Z3B11 | 100 | 50 | 100 | |
| | | | | | | |
| SR710-11 | 129 | R-09-Z2B1 | 45 | na | 45 | |
| SR710-12 | 127.5 | R-09-Z2B1 | 50 | na | 51 | |
| SR710-13 | 140 | R-09-Z2B1 | 60 | na | 40 | |
| SR710-14 | 138.5 | R-09-Z2B1 | 80 | na | 70 | |
| | | | | | | |
| SR710-15 | 96.5 | R-09-Z1B7 | 420 | 240 | 380 | |
| SR710-16 | 95 | R-09-Z1B7 | 400 | 200 | 330 | 40 |
| SR710-17 | 111.5 | R-09-Z1B7 | 190 | 90 | 137 | |
| SR710-18 | 110 | R-09-Z1B7 | 250 | 110 | 220 | |
| SR710-19 | 136 | R-09-Z1B7 | 280 | 150 | 270 | |
| SR710-20 | 134.5 | R-09-Z1B7 | >600 | na | 590 | |
| | | | | | | |
| SR710-21 | 177.3 | R-09-Z1B3 | 800 | 400 | 700 | |
| SR710-22 | 204 | R-09-Z1B3 | 850 | 450 | 755 | |
| | | | | | | |
| SR710-23 | 135.7 | R-09-Z2B2 | 110 | na | 120 | |
| SR710-24 | 134.2 | R-09-Z2B2 | 80 | na | 90 | |
| SR710-25 | 251 | R-09-Z2B2 | 200 | na | 170 | |
| SR710-26 | 249.5 | R-09-Z2B2 | 350 | 250 | 350 | |

**Table 3 cont. Material properties from Model Analysis: Tests 27-48**

| Test | Depth (ft) | Hole | Shear strength (model initial modulus) (psi) (Maximum) | Shear strength (model unloading modulus) (psi) (Minimum) | Shear strength log method) (psi) | Friction (model) |
|---|---|---|---|---|---|---|
| SR710-27 | 203 | R-09-Z1B6 | >600 | na | 310 | |
| SR710-28 | 245 | R-09-Z1B6 | 400 | 320 | 370 | |
| SR710-31 | 332 | R-09-Z1B6 | 600 | 300 | 470 | |
| SR710-32 | 330.5 | R-09-Z1B6 | 525 | 350 | 540 | |
| | | | | | | |
| SR710-29 | 225.8 | R-09-Z3B7 | 450 | 170 | 320 | |
| SR710-30 | 224.3 | R-09-Z3B7 | 370 | 150 | 350 | |
| SR710-33 | 252.5 | R-09-Z3B7 | 700 | 250 | 470 | |
| SR710-34 | 251 | R-09-Z3B7 | 450 | 150 | 354 | |
| SR710-35 | 271.6 | R-09-Z3B7 | | | 290 | 35 |
| SR710-36 | 270.1 | R-09-Z3B7 | | | 330 | |
| | | | | | | |
| SR710-37 | 278 | R-09-Z1B5 | 1,200 | na | 1,280 | |
| SR710-38 | 276.5 | R-09-Z1B5 | | | | |
| SR710-41 | 347 | R-09-Z1B5 | 1,000 | na | 830 | |
| SR710-42 | 345.5 | R-09-Z1B5 | 700 | na | 670 | 42 |
| SR710-44 | 398 | R-09-Z1B5 | 650 | 250 | 500 | |
| SR710-45 | 396.5 | R-09-Z1B5 | | | | |
| | | | | | | |
| SR710-39 | 332 | R-09-Z1B4 | 800 | na | 1,000 | 39 |
| SR710-40 | 330.5 | R-09-Z1B4 | 1,100 | na | 930 | |
| | | | | | | |
| SR710-43 | 132 | R-09-Z3B6 | 900 | 400 | 750 | |
| SR710-46 | 168 | R-09-Z3B6 | 1,000 | 350 | >1,000 | |
| SR710-47 | 166.5 | R-09-Z3B6 | 750 | 350 | 1,600 | |
| SR710-48 | 188.2 | R-09-Z3B6 | 750 | na | 1,400 | |

## 11.0 CONCLUSIONS

The objective of this study was to examine the rock properties over an extensive area of proposed routes for the North Tunnel for Interstate I-710. In this analysis the modulus has been considered for each test and some indication of the shear strength has been obtained based on a simple model. In materials that seem to be behaving in a frictional manner, a friction angle has been determined. Once the tunnel alignment has been selected, further analysis could be undertaken to obtain a more complete understanding of the material behavior for tests within range.

## 12.0 REFERENCES

Mair, R.J. and Wood, D.M. 1987. Pressuremeter testing: methods and interpretation. CIRIA Ground Engineering Report. Butterworths, London.

ASTM D4719. 2007. Standard tests method for pressuremeter testing in soils.

# Appendix I - Pressuremeter Data and Standard Interpretation

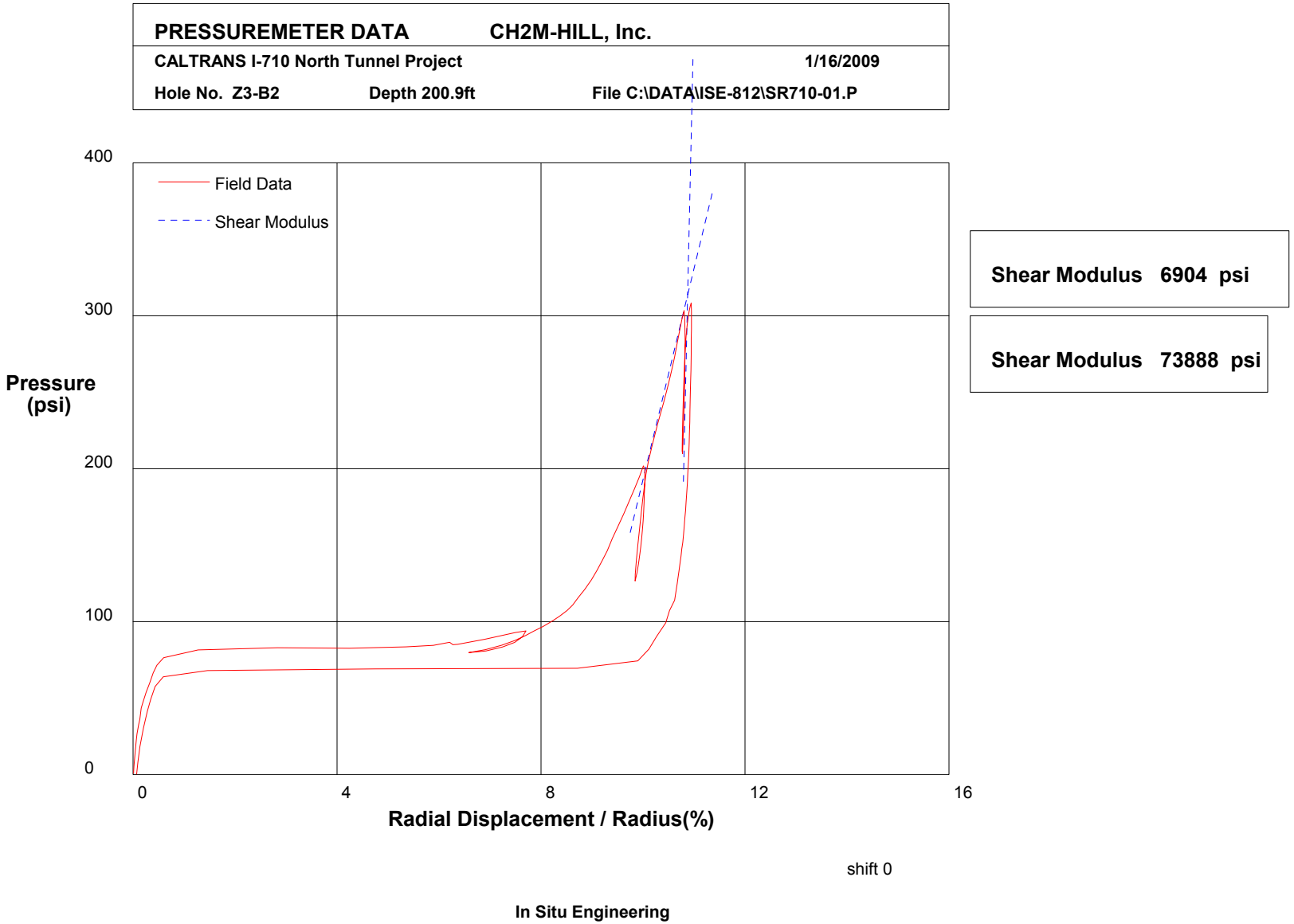

# Appendix I - Pressuremeter Data and Standard Interpretation

**PRESSUREMETER DATA** **CH2MHill, Inc.**

**CALTRANS I-710 North Tunnel Project** **1/16/2009**

**Hole No. Z3-B2** **Depth 200.9ft** **File C:\DATA\ISE-812\SR710-01.P**

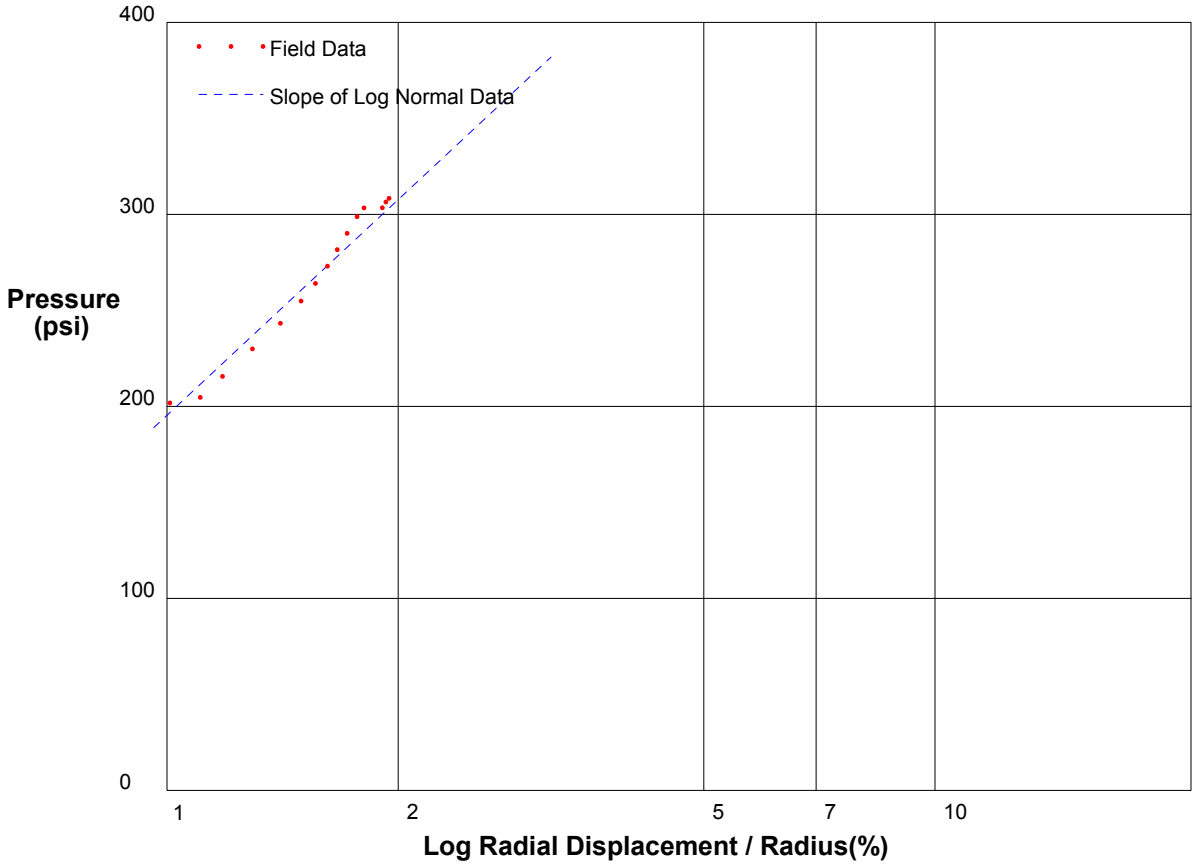


**Shear Strength 162 psi**
**Limit Pressure 797 psi**

shift 9

**In Situ Engineering**

# Appendix I - Pressuremeter Data and Standard Interpretation

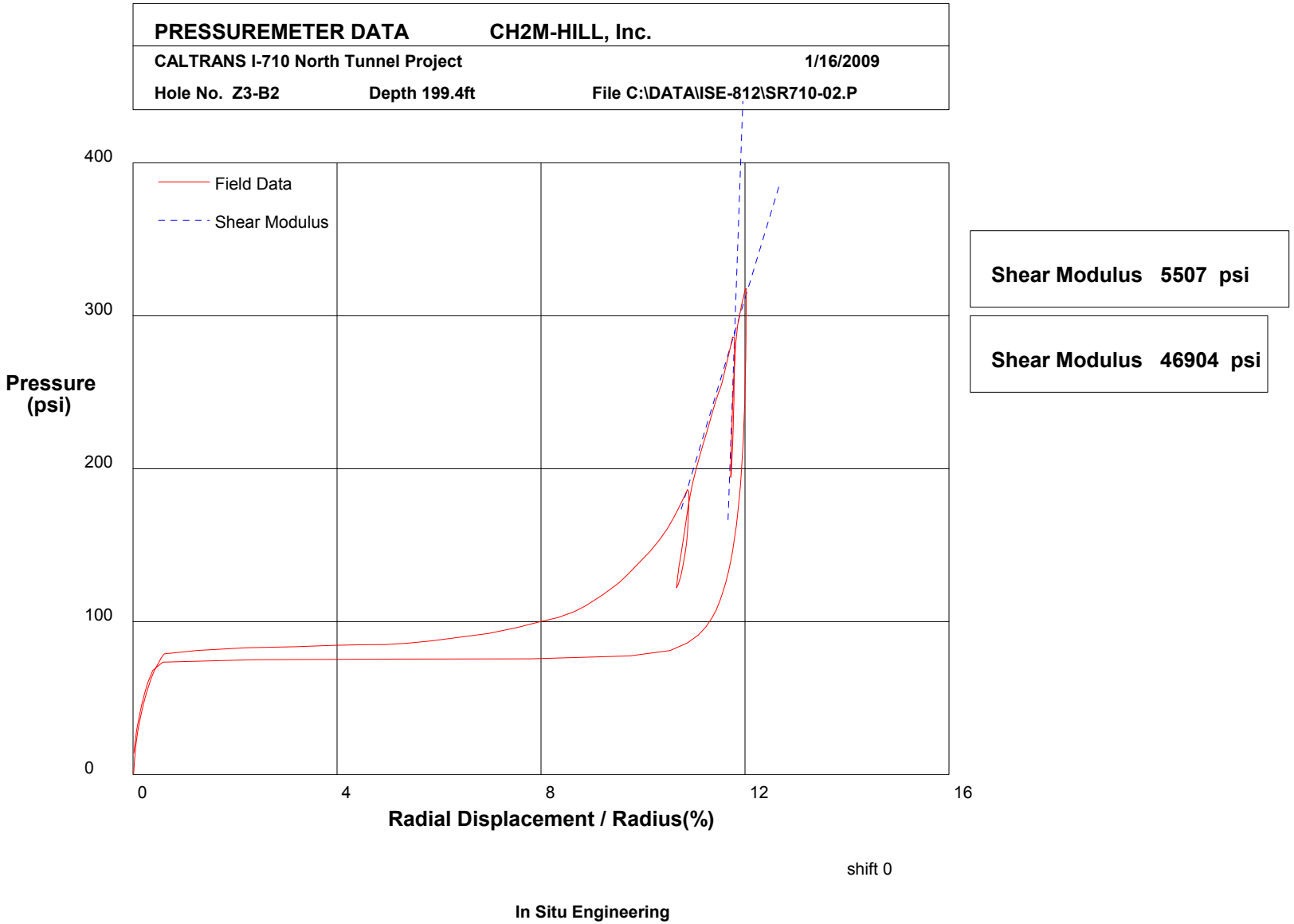

# Appendix I - Pressuremeter Data and Standard Interpretation

**PRESSUREMETER DATA** **CH2MHill, Inc.**

**CALTRANS I-710 North Tunnel Project** **1/16/2009**

**Hole No. Z3-B2** **Depth 199.4ft** **File C:\DATA\ISE-812\SR710-02.P**

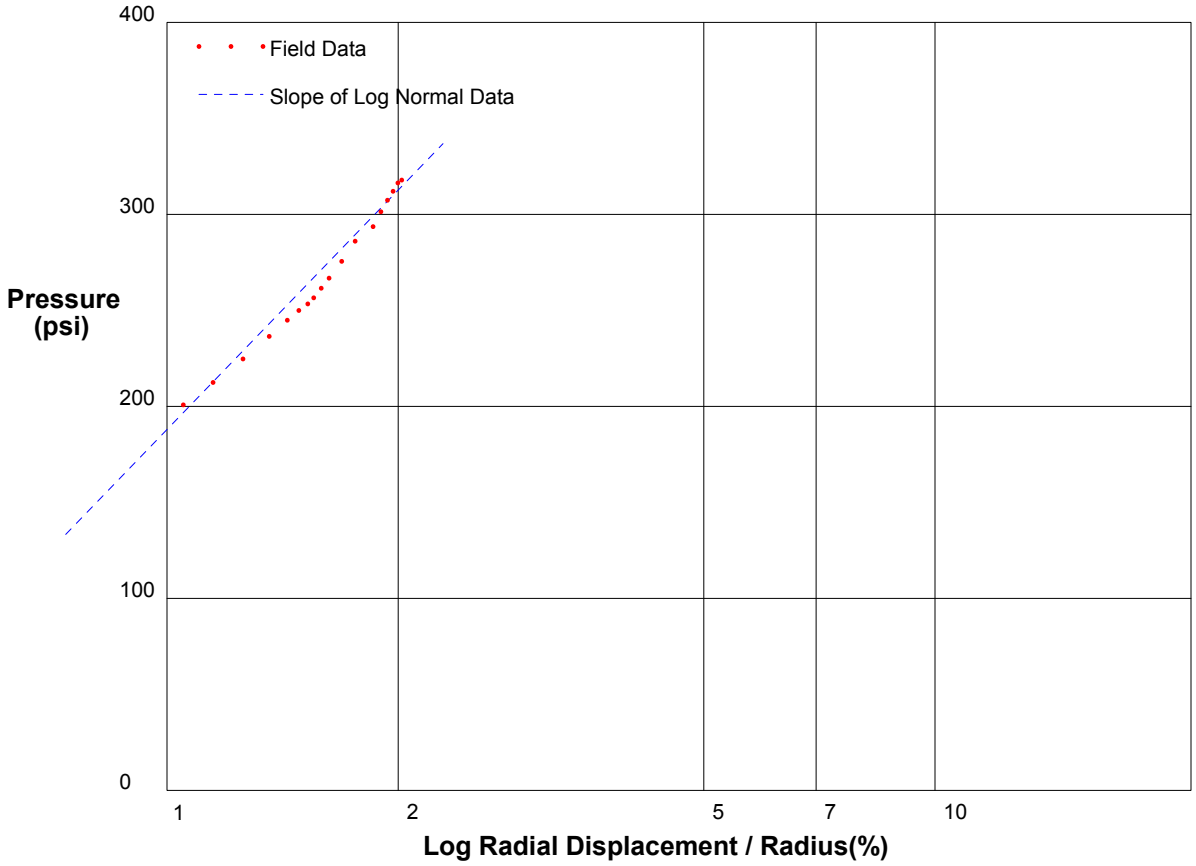


**Shear Strength 179.8 psi**
**Limit Pressure 855 psi**

shift 10

**In Situ Engineering**

# Appendix I - Pressuremeter Data and Standard Interpretation

**PRESSUREMETER DATA** **CH2M-HILL, Inc.**

**CALTRANS I-170 North Tunnel Project** **1/17/2009**

**Hole No. Z3-B11** **Depth 192.8ft** **File C:\DATA\ISE-812\SR710-03.P**

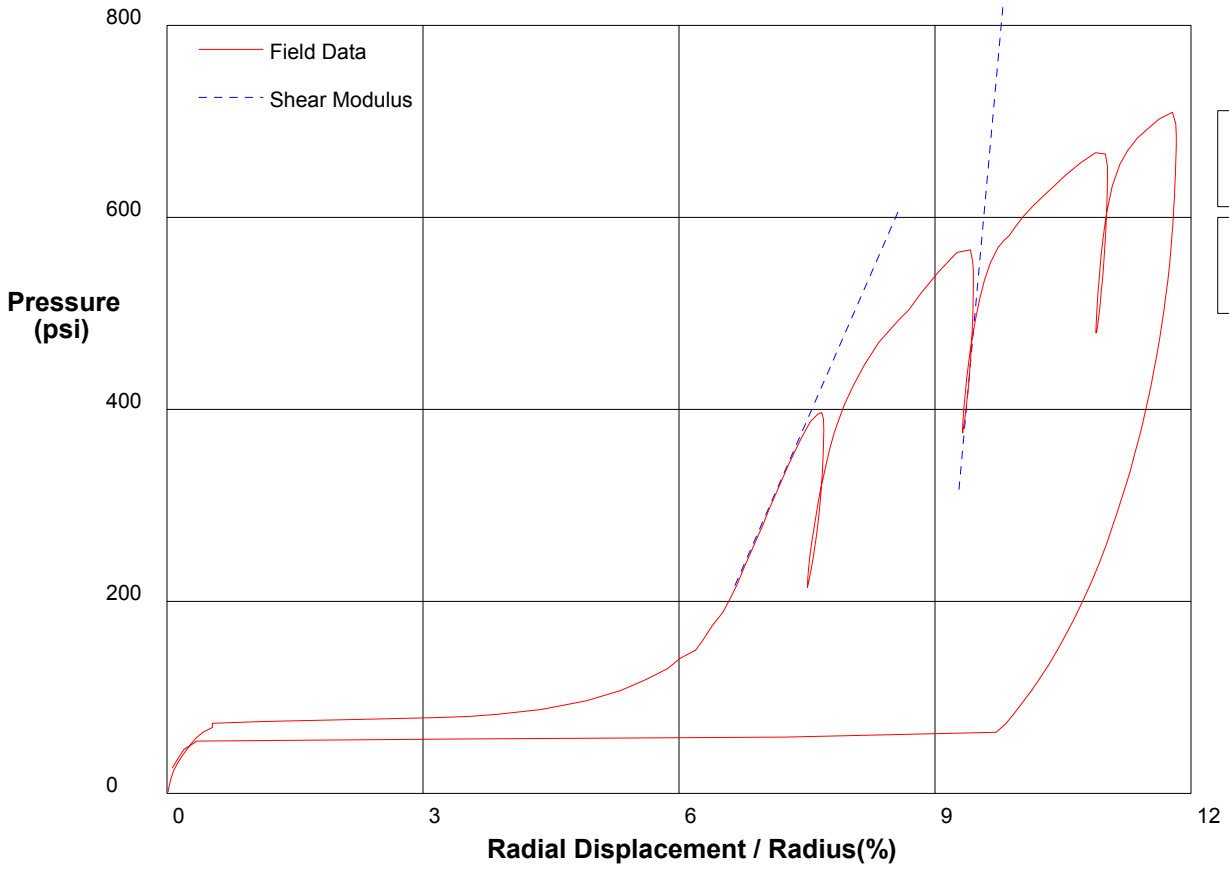


**Shear Modulus 48888 psi**

**Shear Modulus 10179 psi**

shift 0

**In Situ Engineering**

# Appendix I - Pressuremeter Data and Standard Interpretation

**PRESSUREMETER DATA** **CH2MHill, Inc.**

**CALTRANS I-710 North Tunnel Project** **1/17/2009**

**Hole No. Z3-B11** **Depth 192.8ft** **File C:\DATA\ISE-812\SR710-03.P**

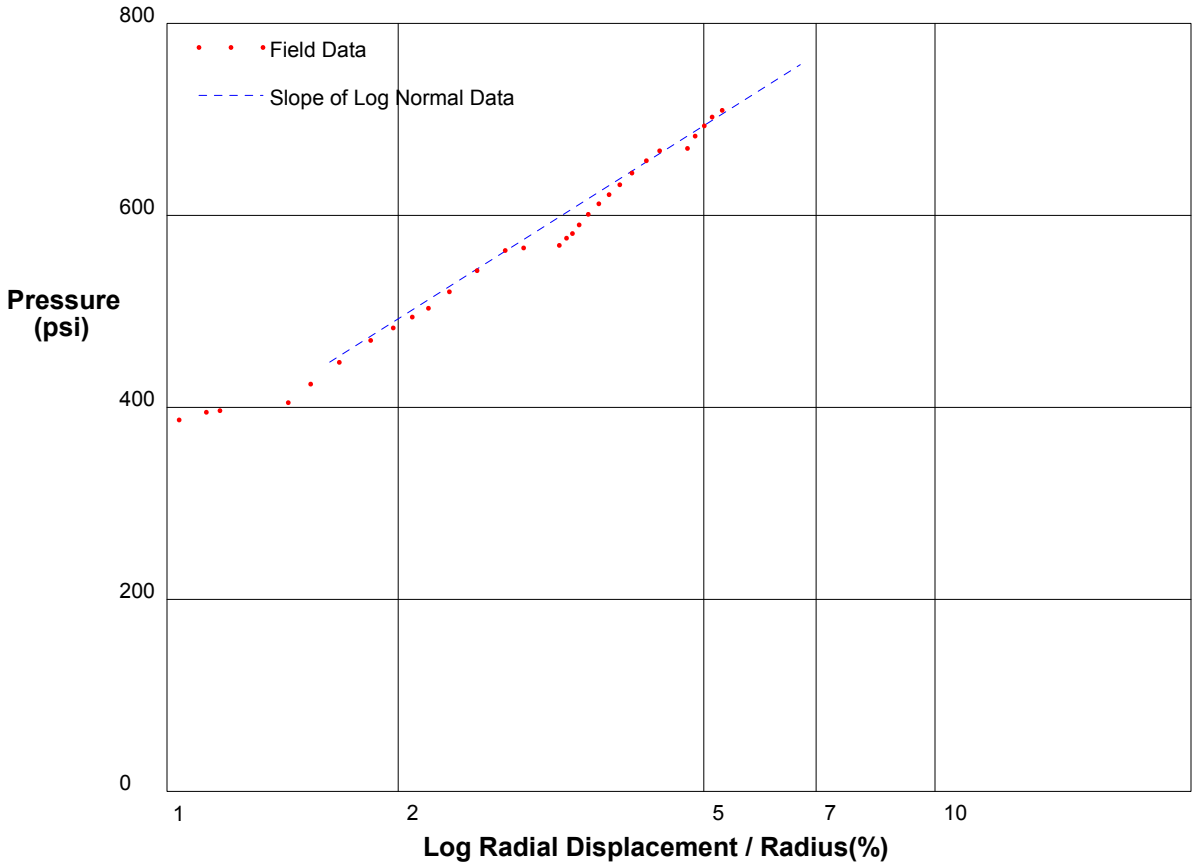


**Shear Strength 219.4 psi**
**Limit Pressure 1155 psi**

shift 6.5

**In Situ Engineering**

# Appendix I - Pressuremeter Data and Standard Interpretation

**PRESSUREMETER DATA** **CH2M-HILL, Inc.**

**CALTRANS I-710 North Tunnel Project** **1/17/2009**

**Hole No. Z3-B11** **Depth 191.3ft** **File C:\DATA\ISE-812\SR710-04.P**

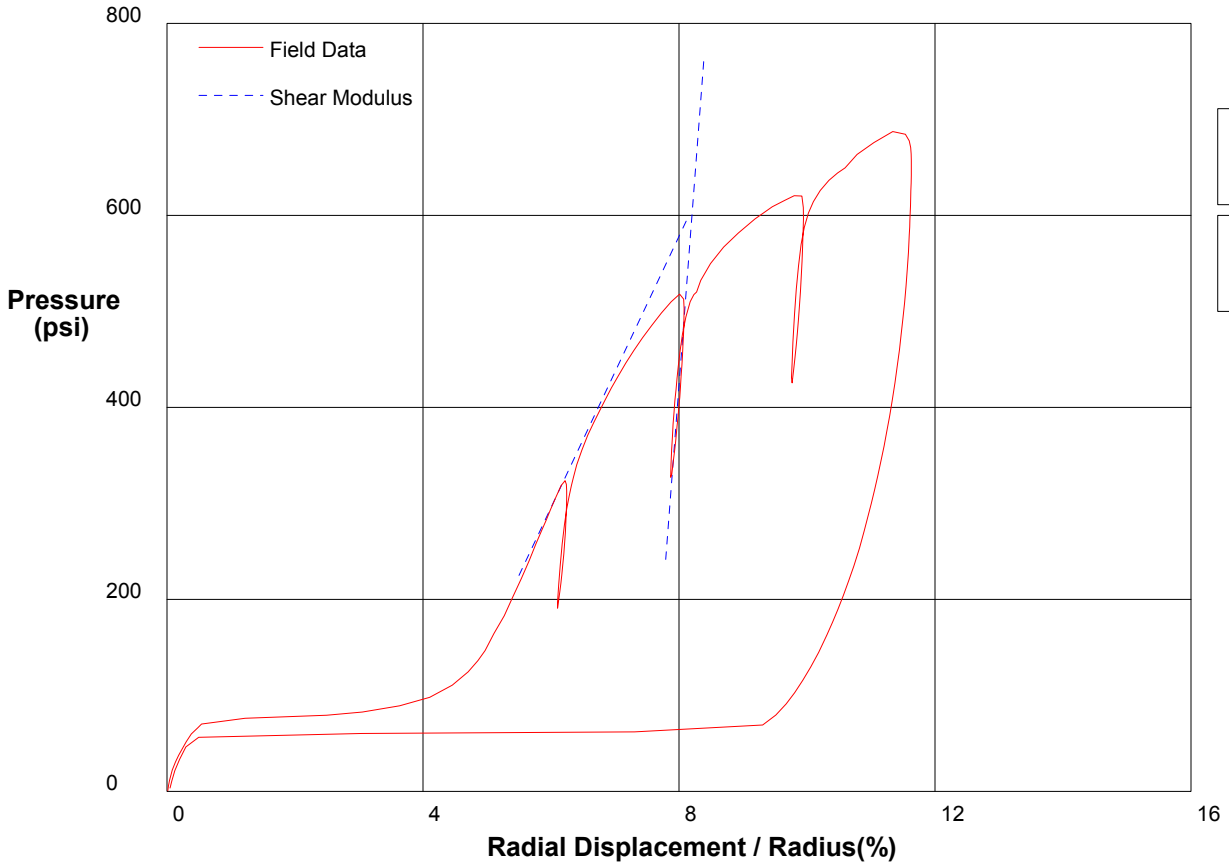


**Shear Modulus 7060 psi**

**Shear Modulus 43563 psi**

shift 0

**In Situ Engineering**

# Appendix I - Pressuremeter Data and Standard Interpretation

**PRESSUREMETER DATA** **CH2MHill, Inc.**

**CALTRANS I-710 North Tunnel Project** **1/17/2009**

**Hole No. Z3-B11** **Depth 191.3ft** **File C:\DATA\ISE-812\SR710-04.P**

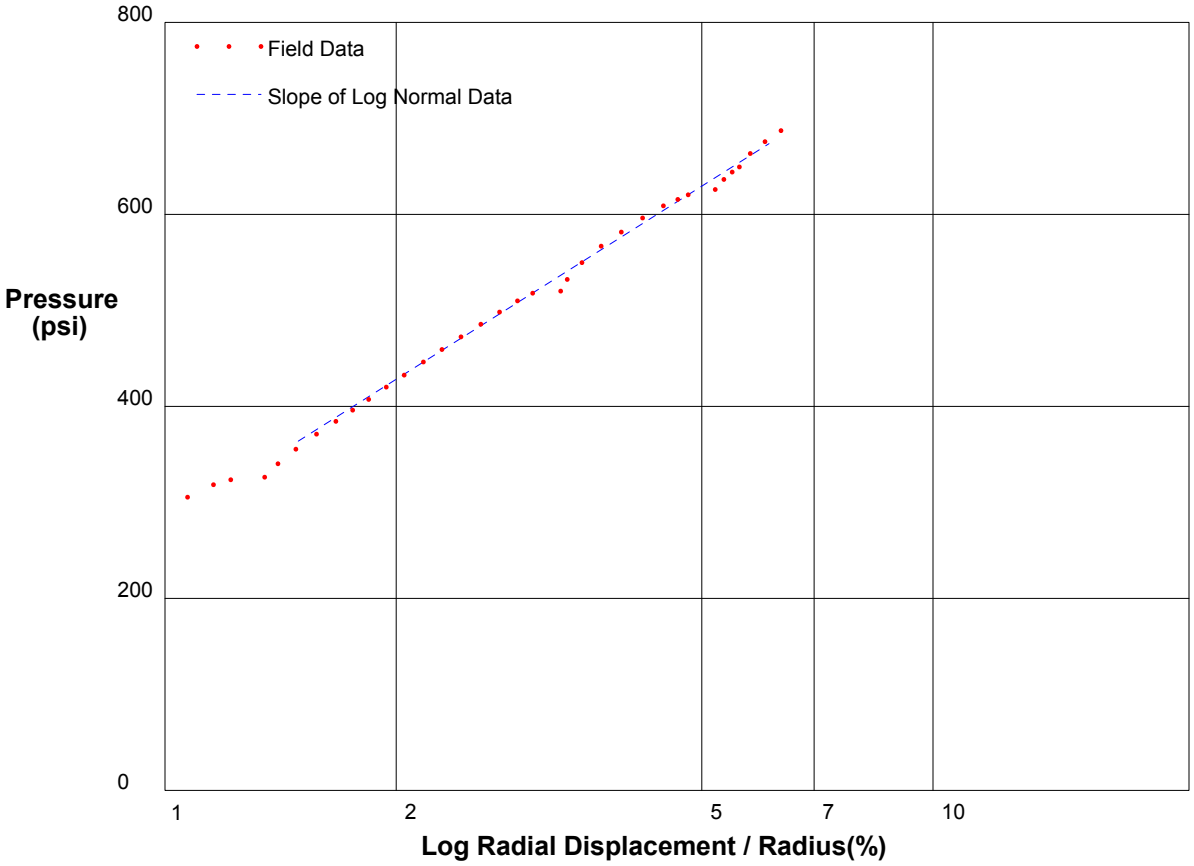


**Shear Strength 219.4 psi**
**Limit Pressure 1091 psi**

shift 5

**In Situ Engineering**

# Appendix I - Pressuremeter Data and Standard Interpretation

**PRESSUREMETER DATA** **CH2M-HILL, Inc.**

**CALTRANS I-710 North Tunnel Project** **1/17/2009**

**Hole No. Z3-B2** **Depth 227ft** **File C:\DATA\ISE-812\SR710-05.P**

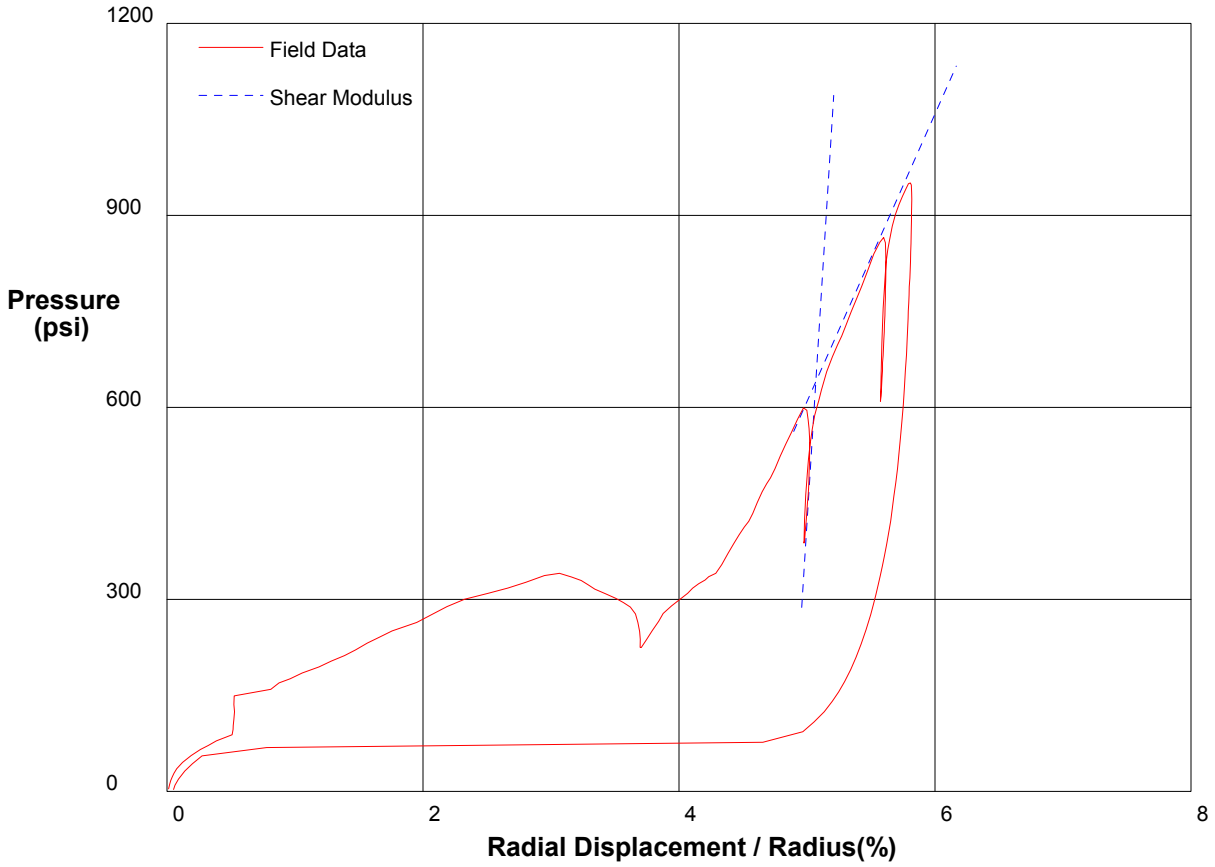


**Shear Modulus 22459 psi**

**Shear Modulus 160000 psi**

shift 0

**In Situ Engineering**

# Appendix I - Pressuremeter Data and Standard Interpretation

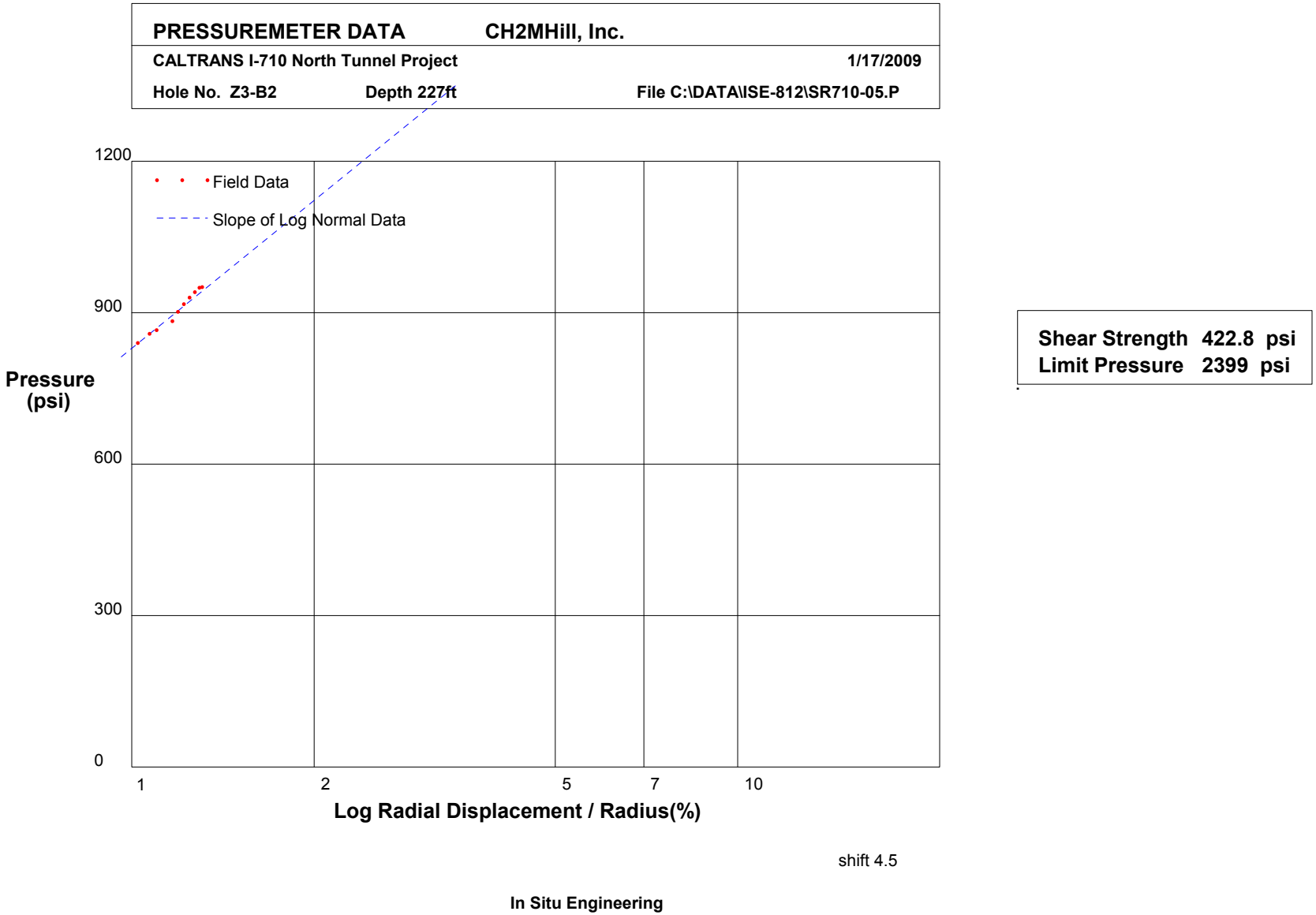

# Appendix I - Pressuremeter Data and Standard Interpretation

**PRESSUREMETER DATA** **CH2M-HILL, Inc.**

**CALTRANS I-710 North Tunnel Project** **1/17/2009**

**Hole No. Z3-B2** **Depth 225ft** **File C:\DATA\ISE-812\SR710-06.P**

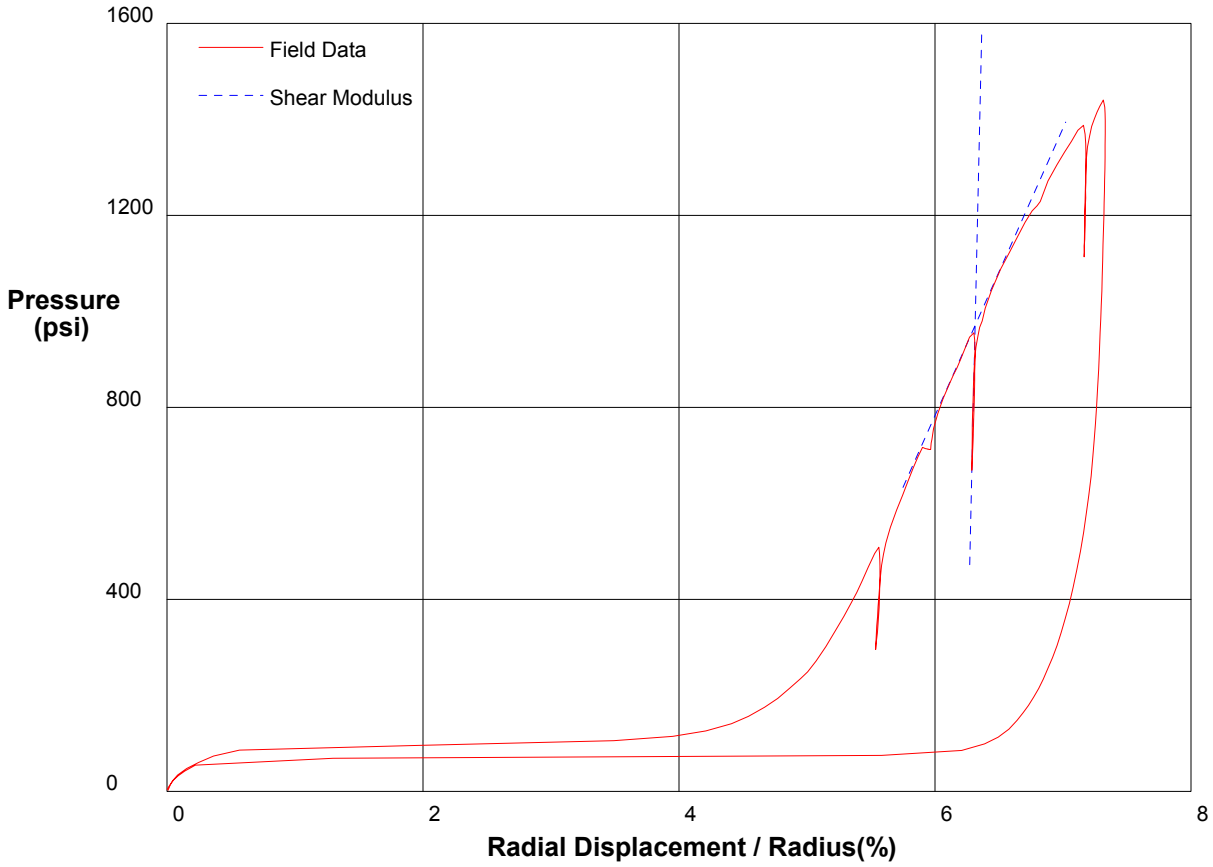


**Shear Modulus 29945 psi**

**Shear Modulus 591111 psi**

shift 0

**In Situ Engineering**

# Appendix I - Pressuremeter Data and Standard Interpretation

**PRESSUREMETER DATA** **CH2MHill, Inc.**

**CALTRANS I-710 North Tunnel Project** **1/17/2009**

**Hole No. Z3-B2** **Depth 225ft** **File C:\DATA\ISE-812\SR710-06.P**

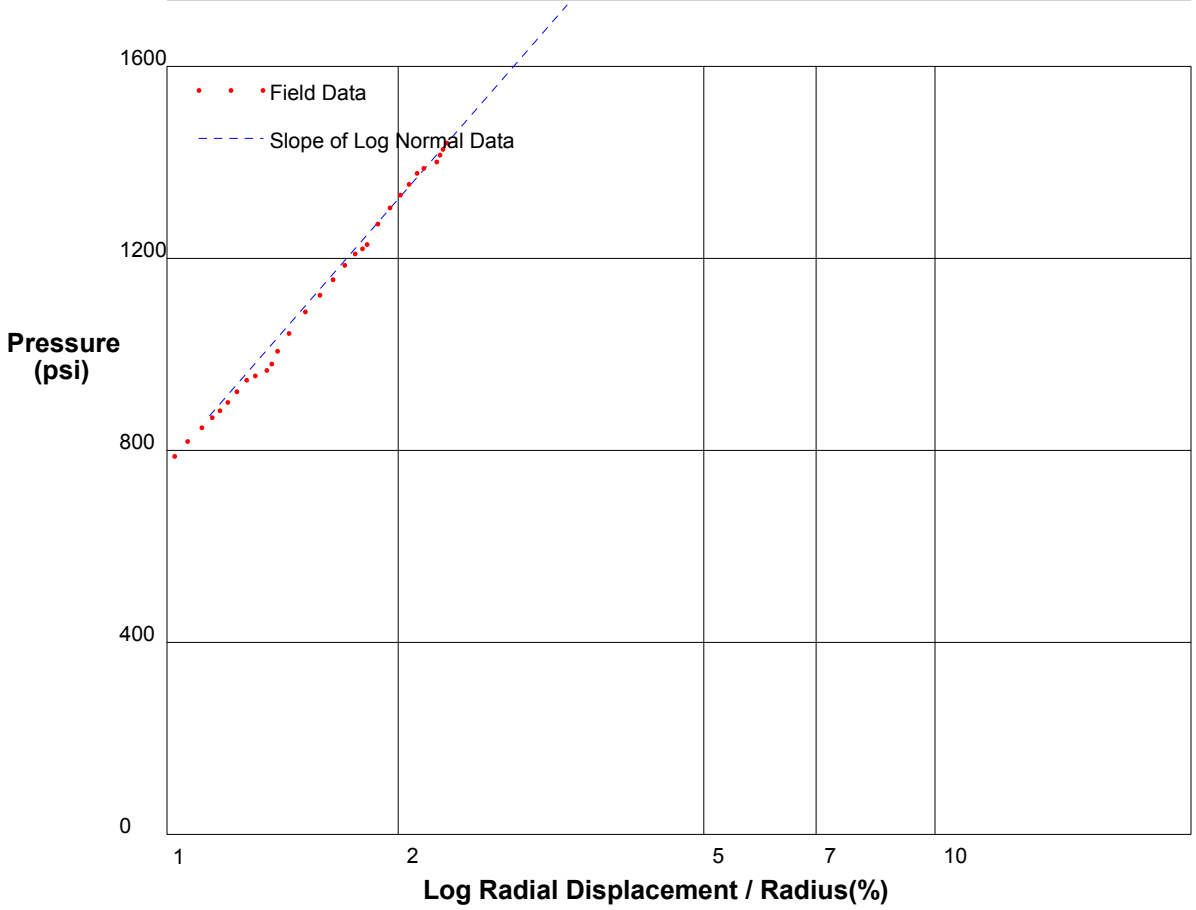


**Shear Strength 798.5 psi**
**Limit Pressure 3735 psi**

shift 5

**In Situ Engineering**

# Appendix I - Pressuremeter Data and Standard Interpretation

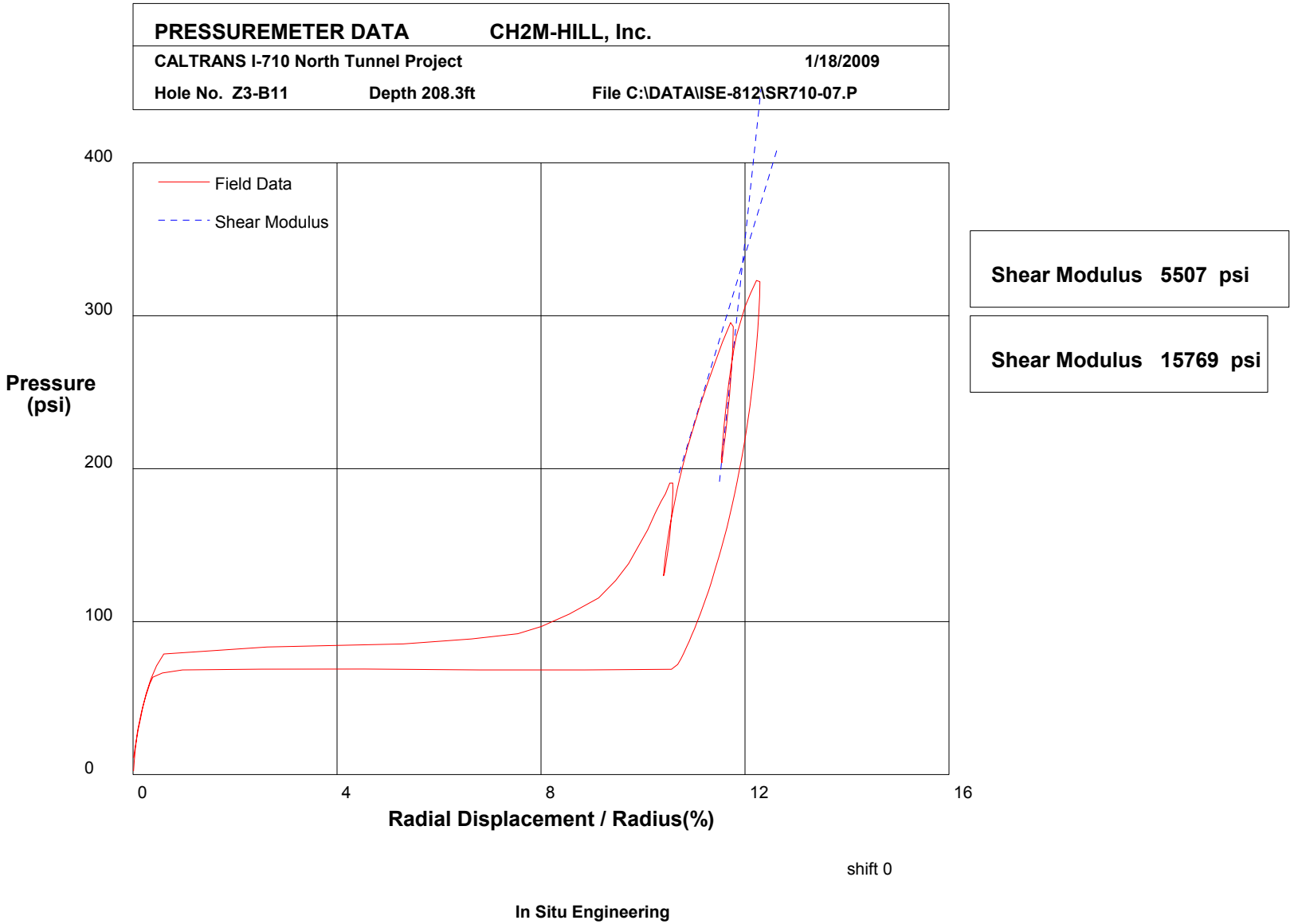

# Appendix I - Pressuremeter Data and Standard Interpretation

**PRESSUREMETER DATA** **CH2MHill, Inc.**

**CALTRANS I-710 North Tunnel Project** **1/18/2009**

**Hole No. Z3-B11** **Depth 208.3ft** **File C:\DATA\ISE-812\SR710-07.P**

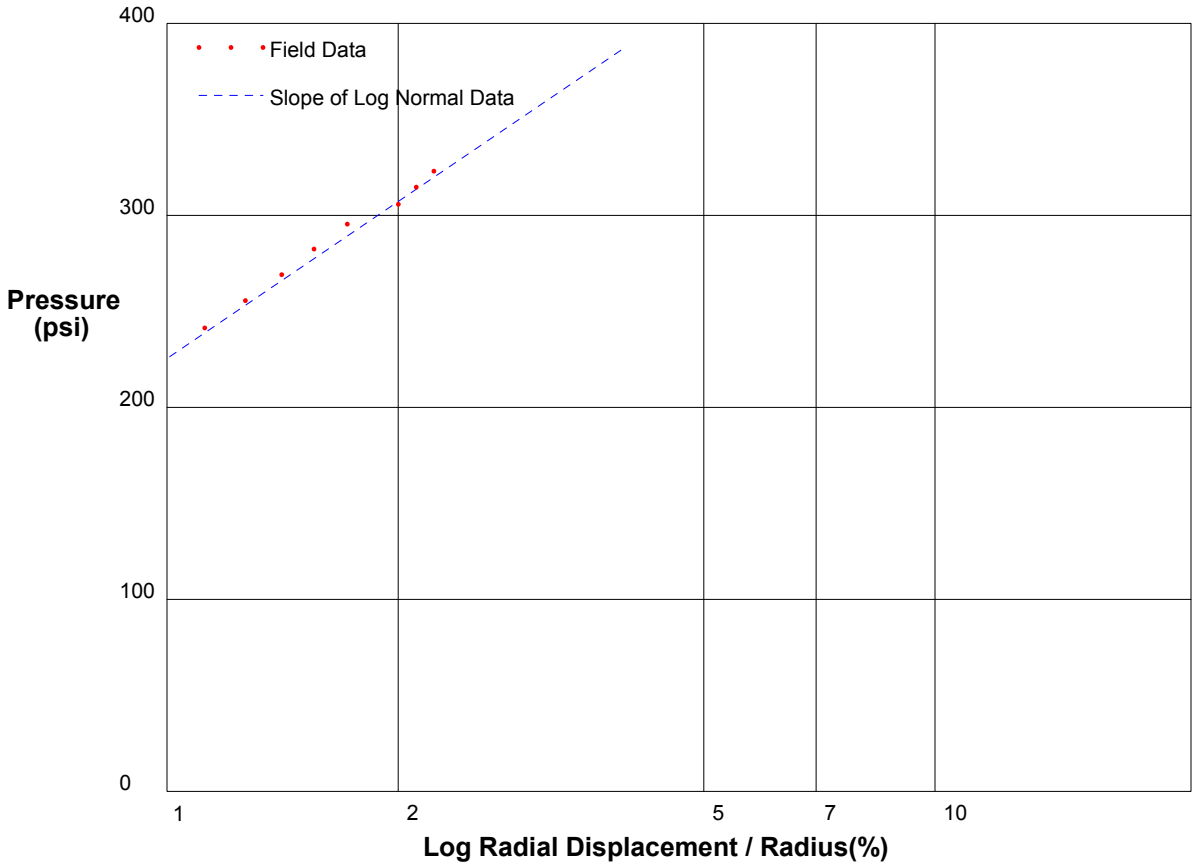


**Shear Strength 118 psi**
**Limit Pressure 663 psi**

shift 10

**In Situ Engineering**

# Appendix I - Pressuremeter Data and Standard Interpretation

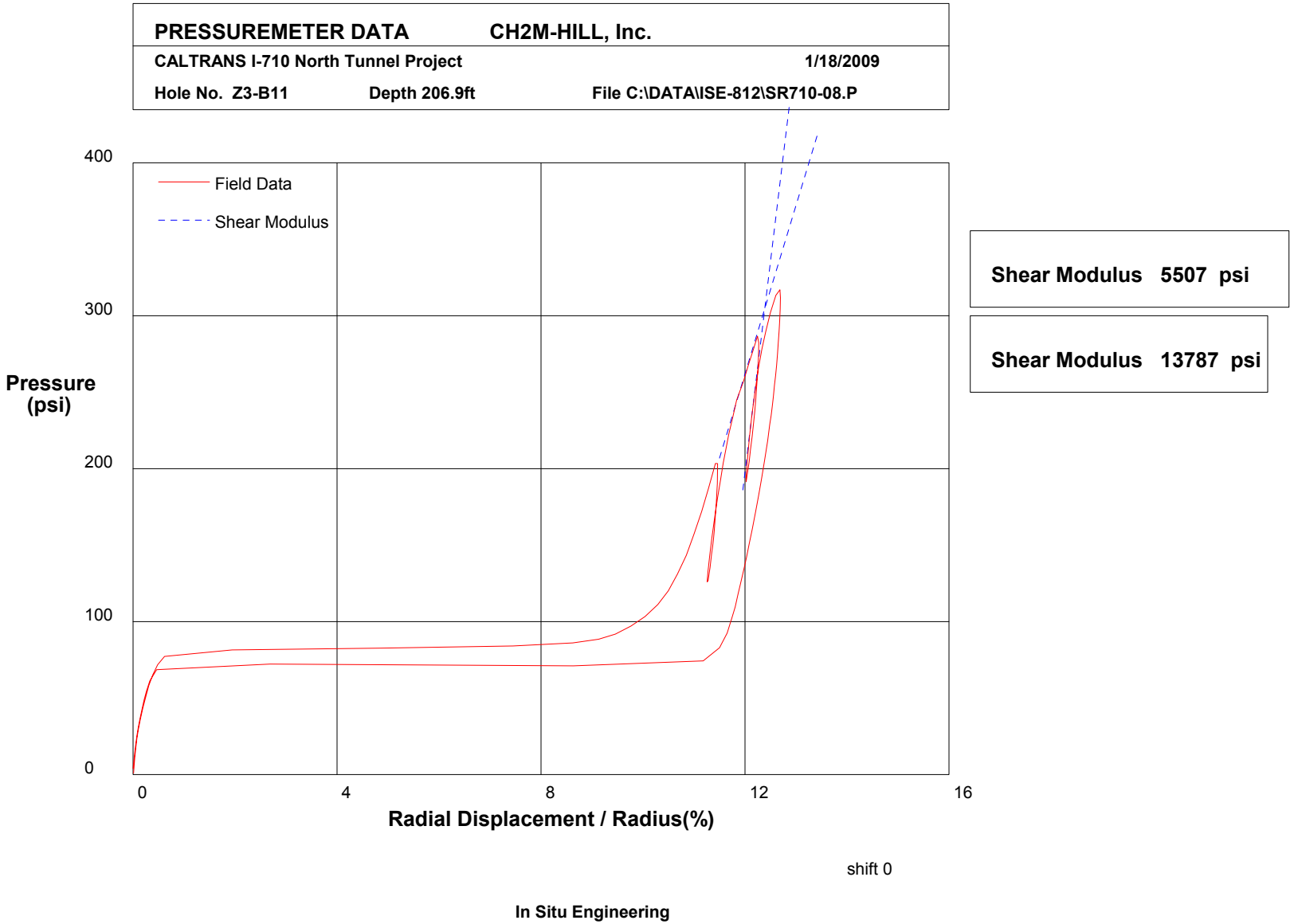

# Appendix I - Pressuremeter Data and Standard Interpretation

**PRESSUREMETER DATA** **CH2MHill, Inc.**

**CALTRANS I-710 North Tunnel Project** **1/18/2009**

**Hole No. Z3-B11** **Depth 206.9ft** **File C:\DATA\ISE-812\SR710-08.P**

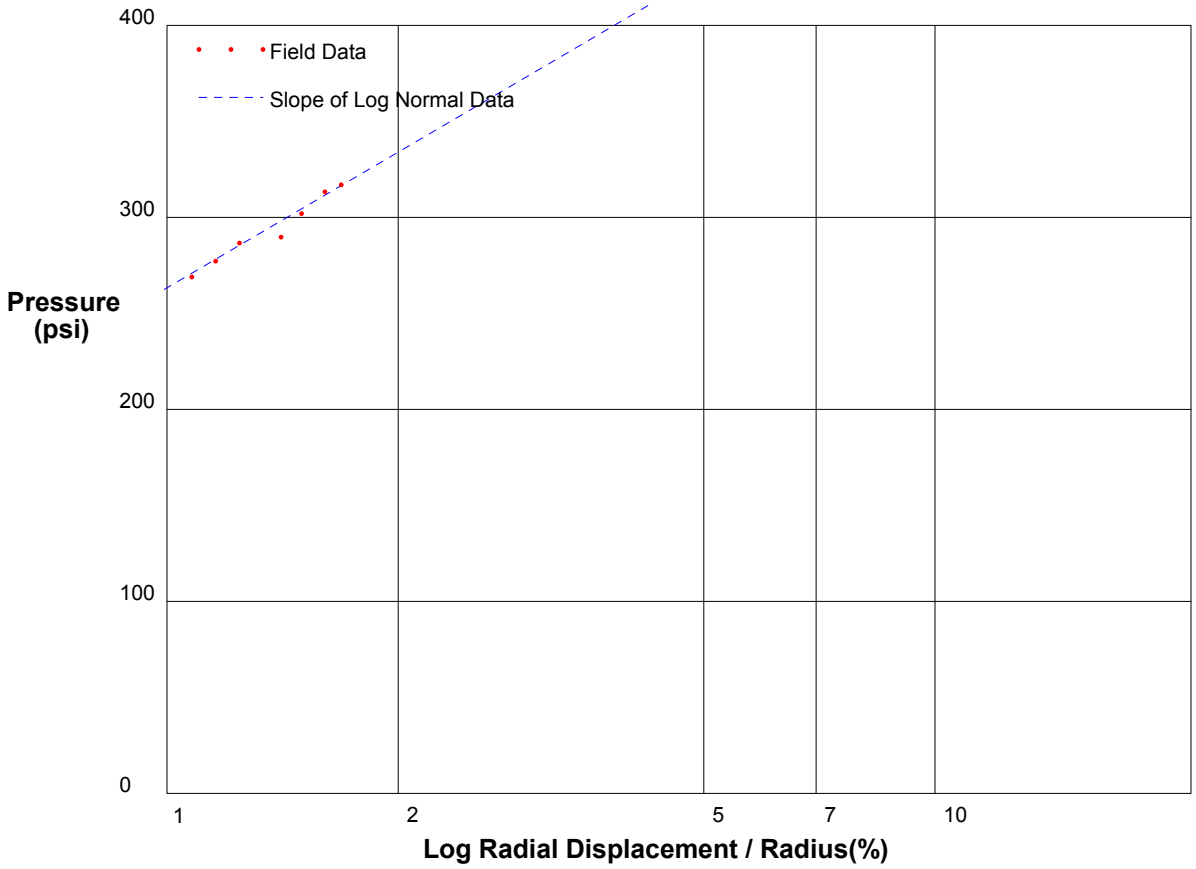


**Shear Strength 101.9 psi**
**Limit Pressure 641 psi**

shift 11

**In Situ Engineering**

# Appendix I - Pressuremeter Data and Standard Interpretation

**PRESSUREMETER DATA** **CH2M-HILL, Inc.**

**CALTRANS I-710 North Tunnel Project** **1/18/2009**

**Hole No. Z3-B2** **Depth 248ft** **File C:\DATA\ISE-812\SR710-09.P**

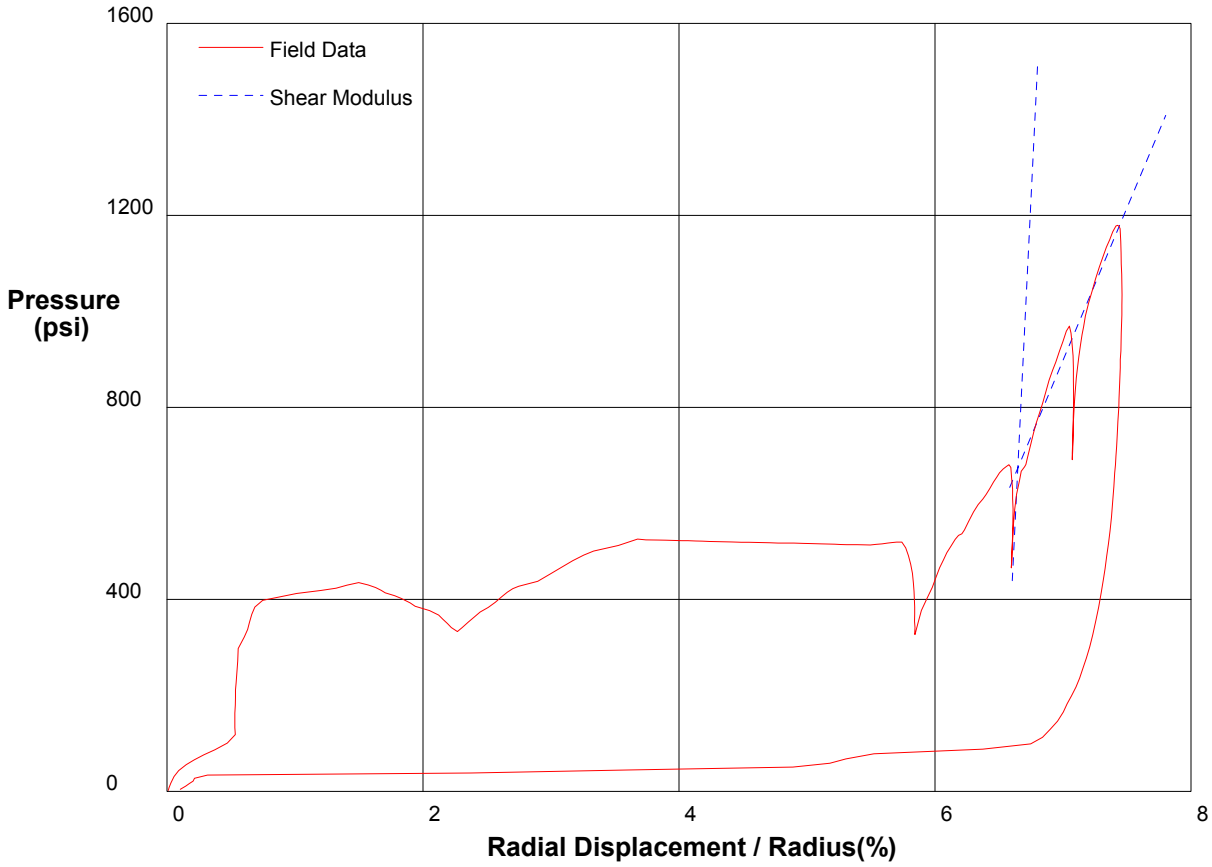


**Shear Modulus 31794 psi**

**Shear Modulus 272982 psi**

shift 0

**In Situ Engineering**

# Appendix I - Pressuremeter Data and Standard Interpretation

**PRESSUREMETER DATA** **CH2MHill, Inc.**

**CALTRANS I-710 North Tunnel Project** **1/18/2009**

**Hole No. Z3-B2** **Depth 248ft** **File C:\DATA\ISE-812\SR710-09.P**

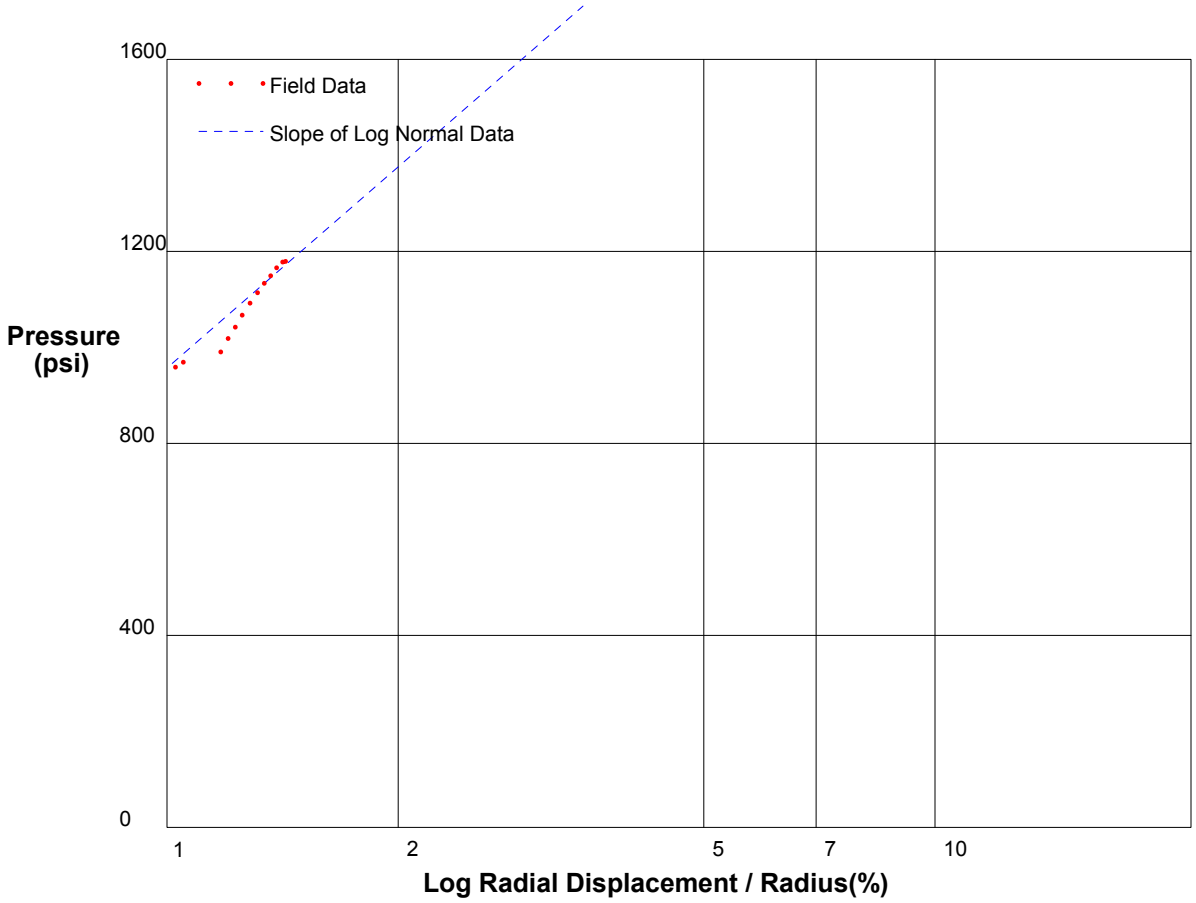


**Shear Strength 604.6 psi**
**Limit Pressure 3202 psi**

shift 6

**In Situ Engineering**

# Appendix I - Pressuremeter Data and Standard Interpretation

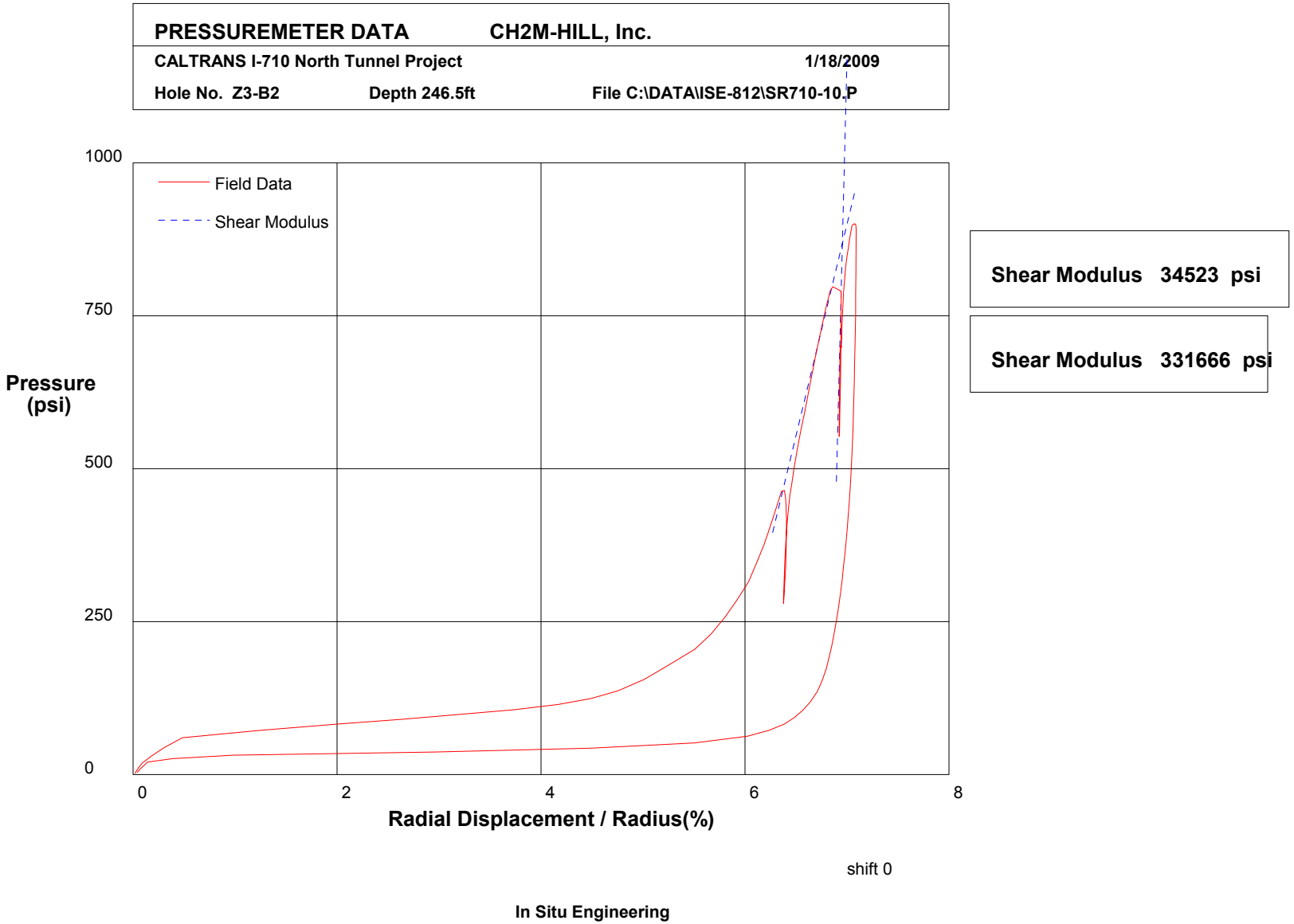

# Appendix I - Pressuremeter Data and Standard Interpretation

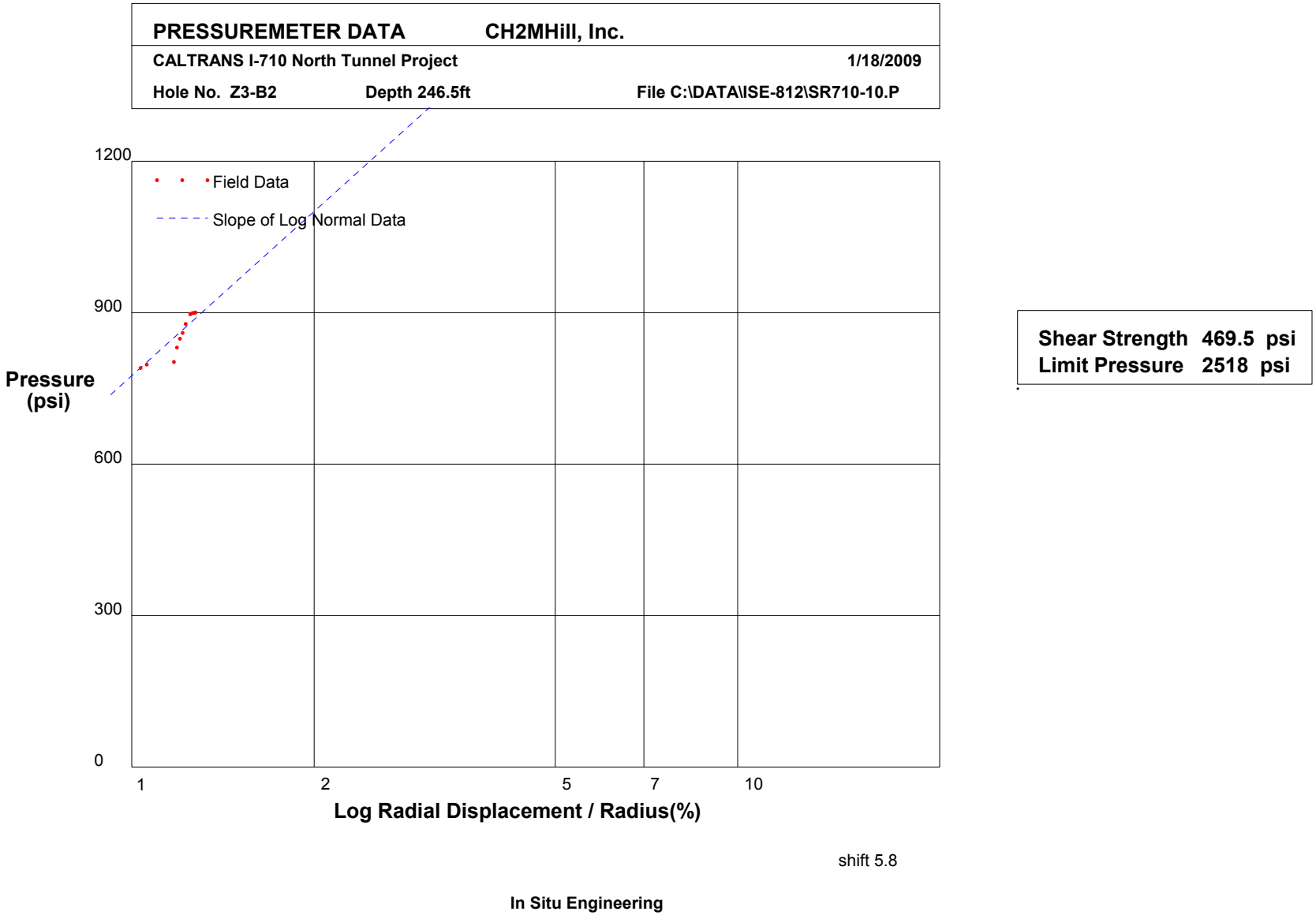

# Appendix I - Pressuremeter Data and Standard Interpretation

**PRESSUREMETER DATA** **CH2MHill, Inc.**

**CALTRANS I-710 North Tunnel Project** **1/19/2009**

**Hole No. Z2-B1** **Depth 129ft** **File C:\DATA\ISE-812\SR710-11.P**

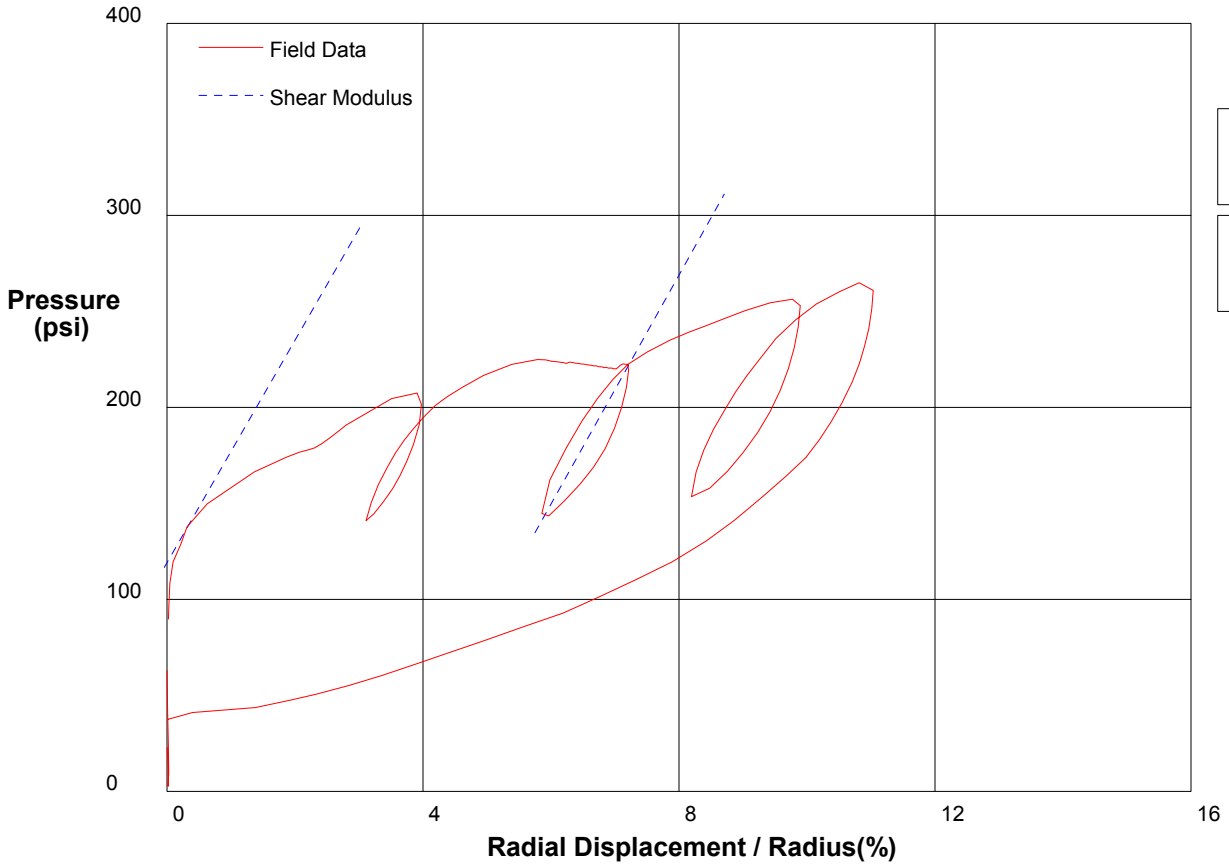


**Shear Modulus 2981 psi**

**Shear Modulus 2897 psi**

shift 0

**In Situ Engineering**

# Appendix I - Pressuremeter Data and Standard Interpretation

**PRESSUREMETER DATA** **CH2M-HILL, Inc.**

**CALTRANS I-710 North Tunnel Project** **1/19/2009**

**Hole No. Z2-B1** **Depth 129ft** **File C:\DATA\ISE-812\SR710-11.P**

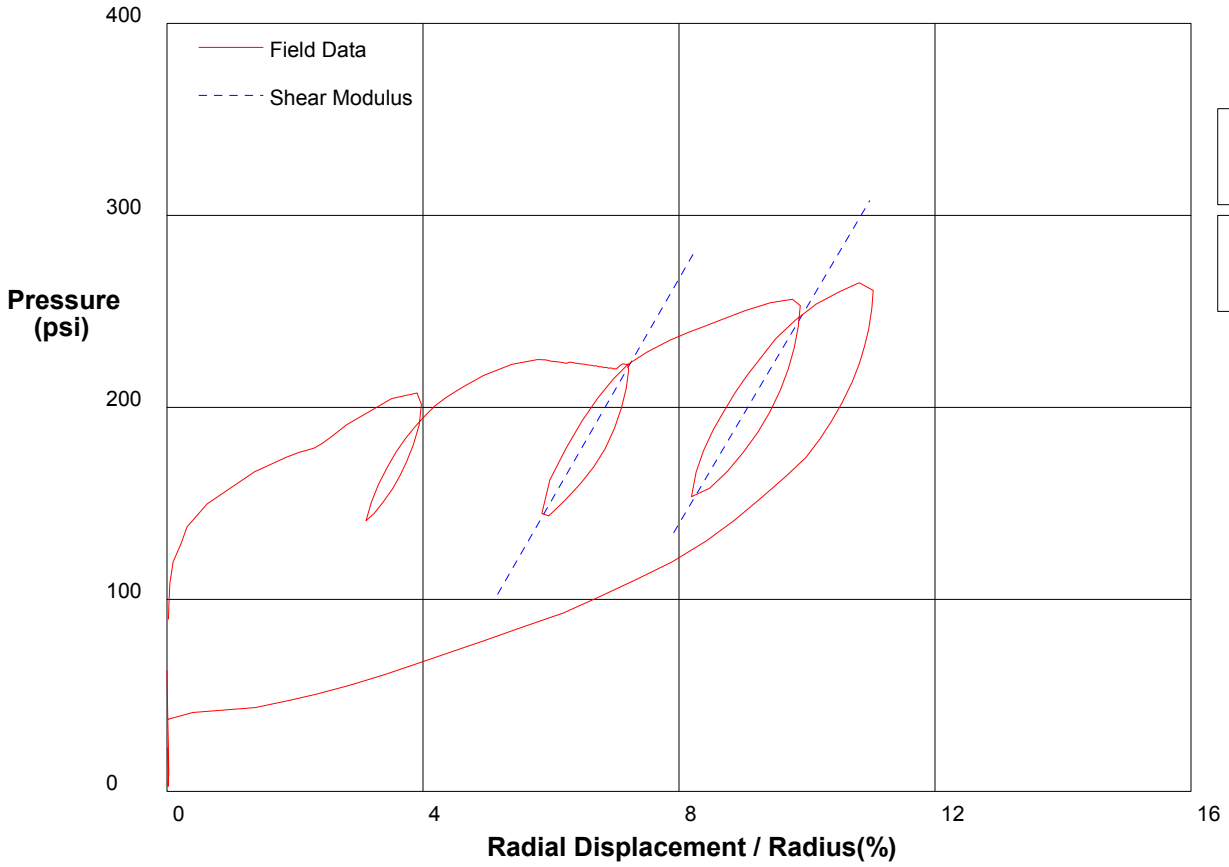


**Shear Modulus 2823 psi**

**Shear Modulus 2897 psi**

shift 0

**In Situ Engineering**

# Appendix I - Pressuremeter Data and Standard Interpretation

**PRESSUREMETER DATA** **CH2MHill, Inc.**

**CALTRANS I-710 North Tunnel Project** **1/19/2009**

**Hole No. Z2-B1** **Depth 129ft** **File C:\DATA\ISE-812\SR710-11.P**

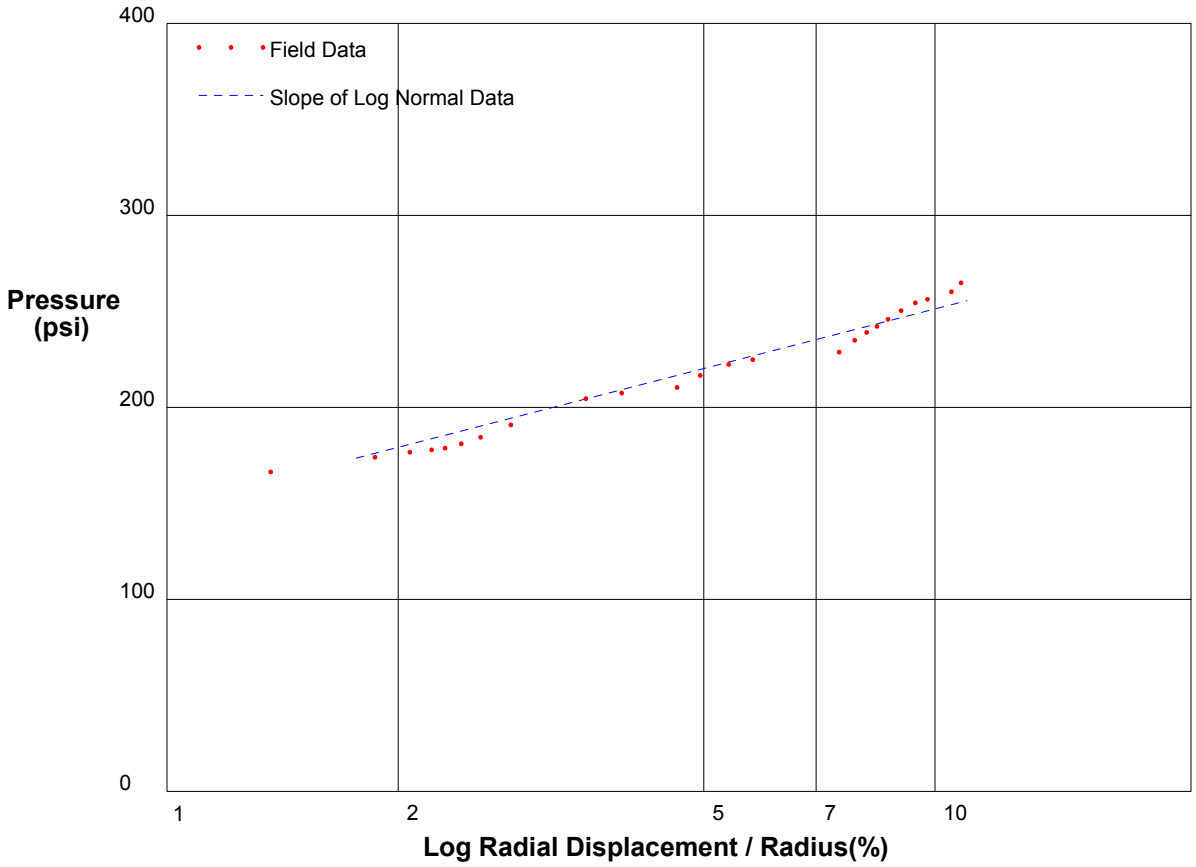


**Shear Strength 44.7 psi**
**Limit Pressure 314 psi**

shift 0

**In Situ Engineering**

# Appendix I - Pressuremeter Data and Standard Interpretation

**PRESSUREMETER DATA** **CH2M-HILL, Inc**

**CALTRANS I-170 North Tunnel Project** **1/19/2009**

**Hole No. Z2-B1** **Depth 127.5ft** **File C:\DATA\ISE-812\SR710-12.P**

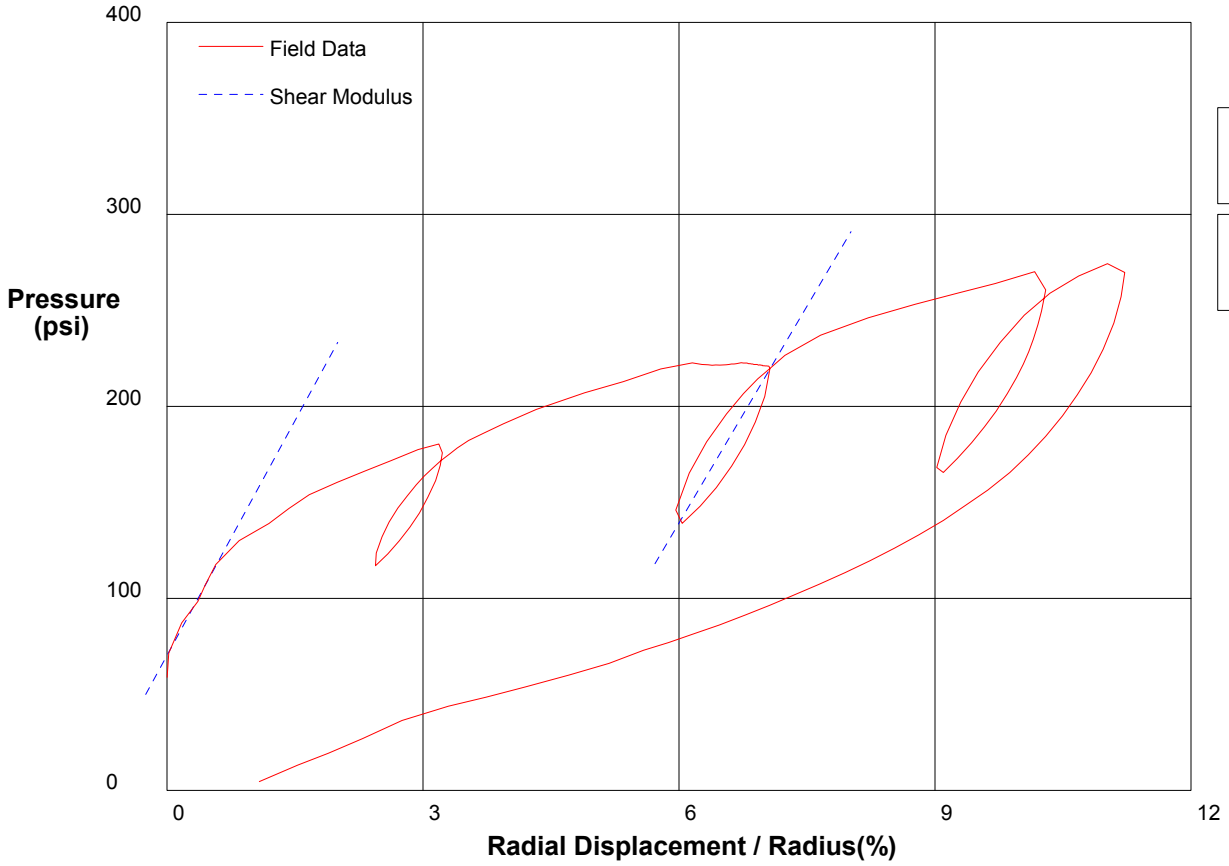


**Shear Modulus 3764 psi**

**Shear Modulus 4074 psi**

shift 0

**In Situ Engineering**

# Appendix I - Pressuremeter Data and Standard Interpretation

**PRESSUREMETER DATA** **CH2MHill, Inc.**

**CALTRANS I-710 North Tunnel Project** **1/19/2009**

**Hole No. Z2-B1** **Depth 127.5ft** **File C:\DATA\ISE-812\SR710-12.P**

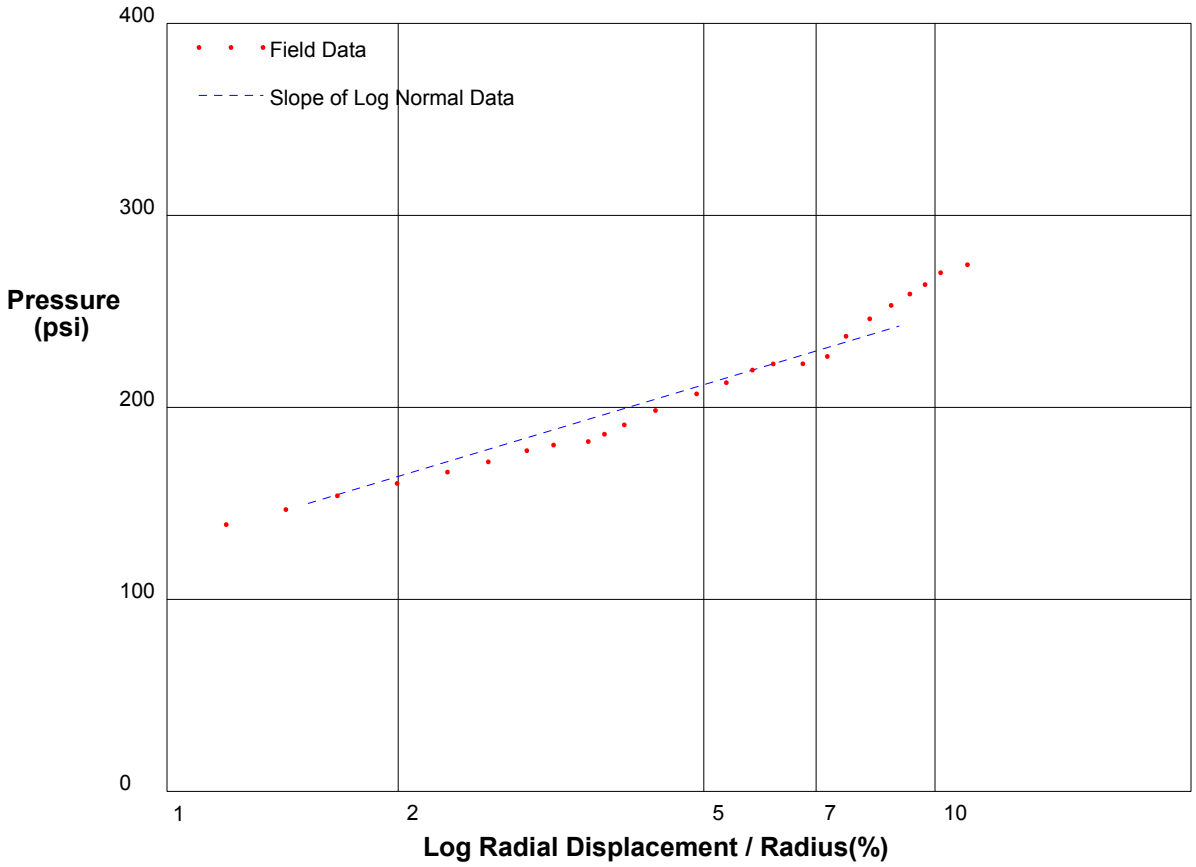


**Shear Strength 52.1 psi**
**Limit Pressure 321 psi**

shift 0

**In Situ Engineering**

# Appendix I - Pressuremeter Data and Standard Interpretation

**PRESSUREMETER DATA** **CH2M-HILL, Inc.**

**CALTRANS I-710 North Tunnel Project** **1/20/2009**

**Hole No. Z2-B1** **Depth 140ft** **File C:\DATA\ISE-812\SR710-13.P**

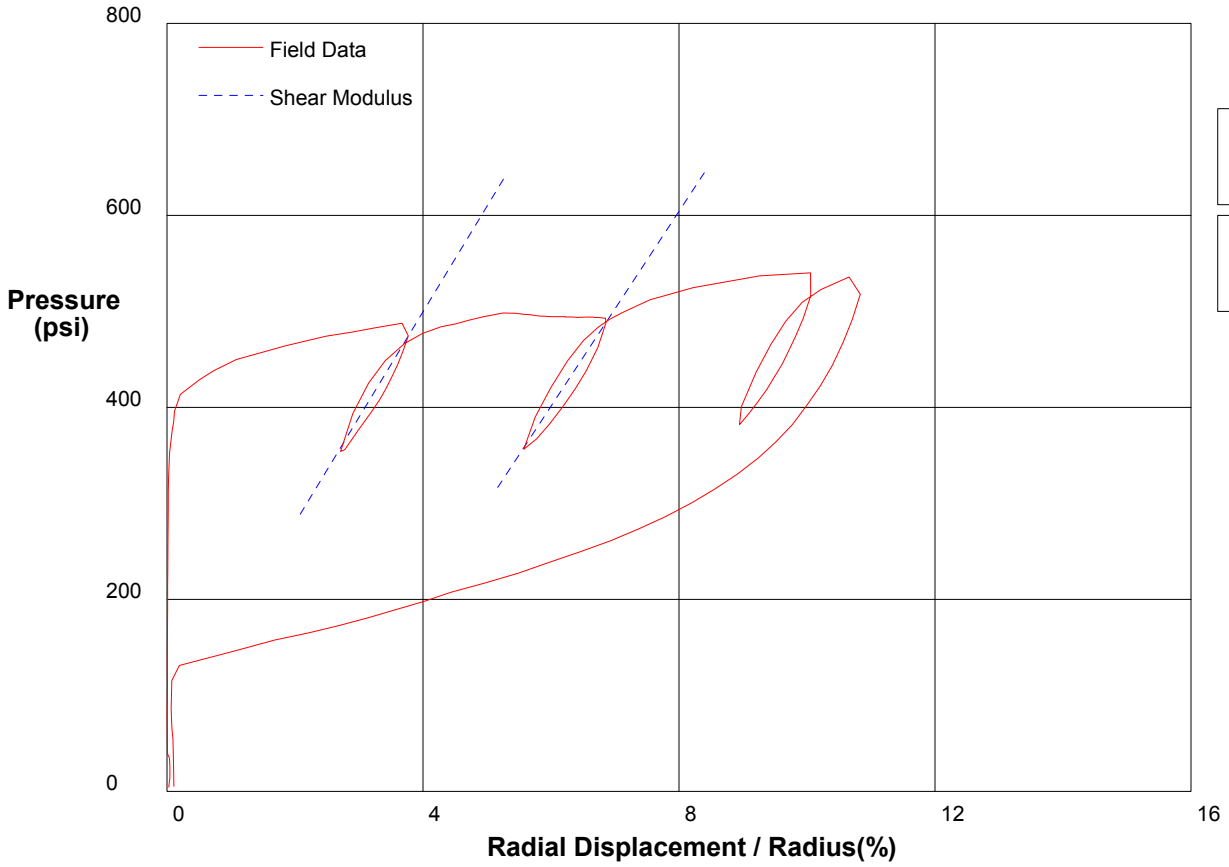


**Shear Modulus 5074 psi**

**Shear Modulus 5497 psi**

shift 0

**In Situ Engineering**

# Appendix I - Pressuremeter Data and Standard Interpretation

**PRESSUREMETER DATA** **CH2MHill, Inc.**

**CALTRANS I-710 North Tunnel Project** **1/20/2009**

**Hole No. Z2-B1** **Depth 140ft** **File C:\DATA\ISE-812\SR710-13.P**

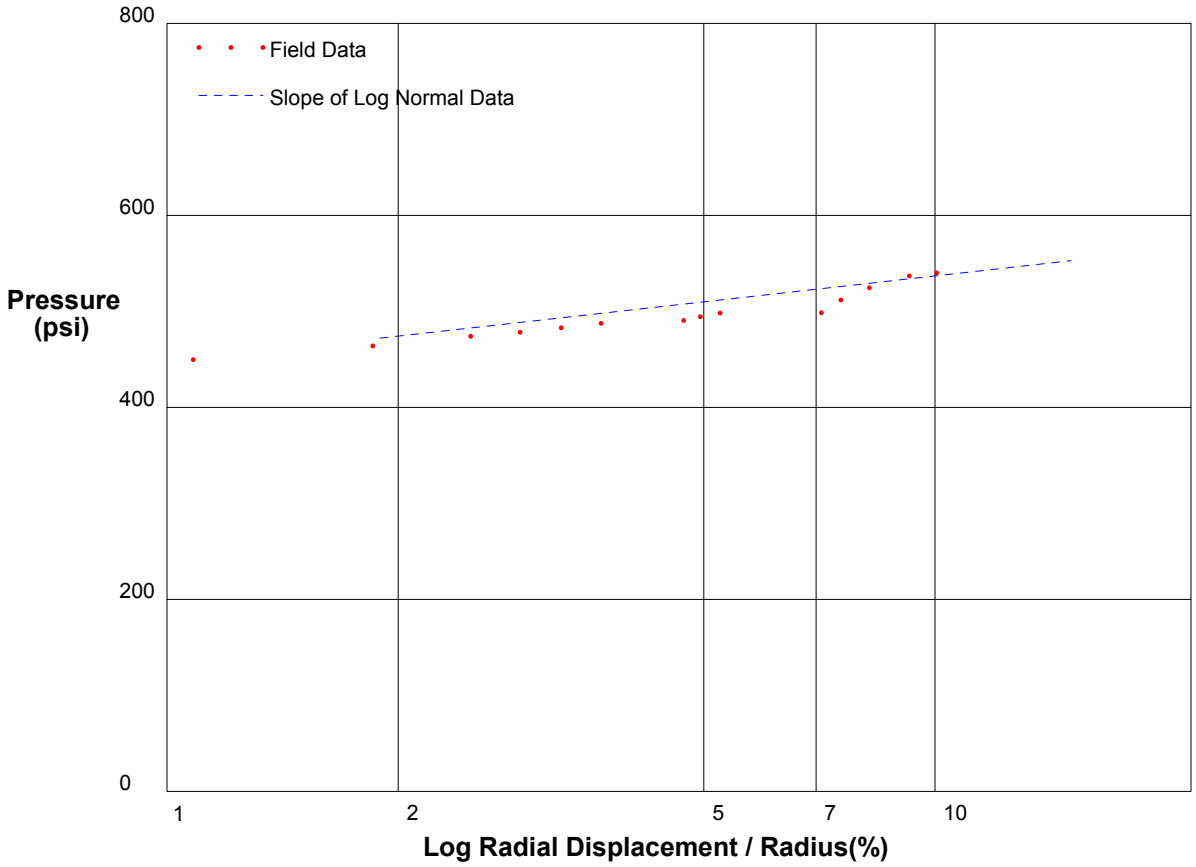


**Shear Strength 38.9 psi**
**Limit Pressure 591 psi**

shift 0

**In Situ Engineering**

# Appendix I - Pressuremeter Data and Standard Interpretation

**PRESSUREMETER DATA** **CH2M-HILL, Inc.**

**CALTRANS I-710 North Tunnel Project** **1/20/2009**

**Hole No. Z2-B1** **Depth 138.5ft** **File C:\DATA\ISE-812\SR710-14.P**

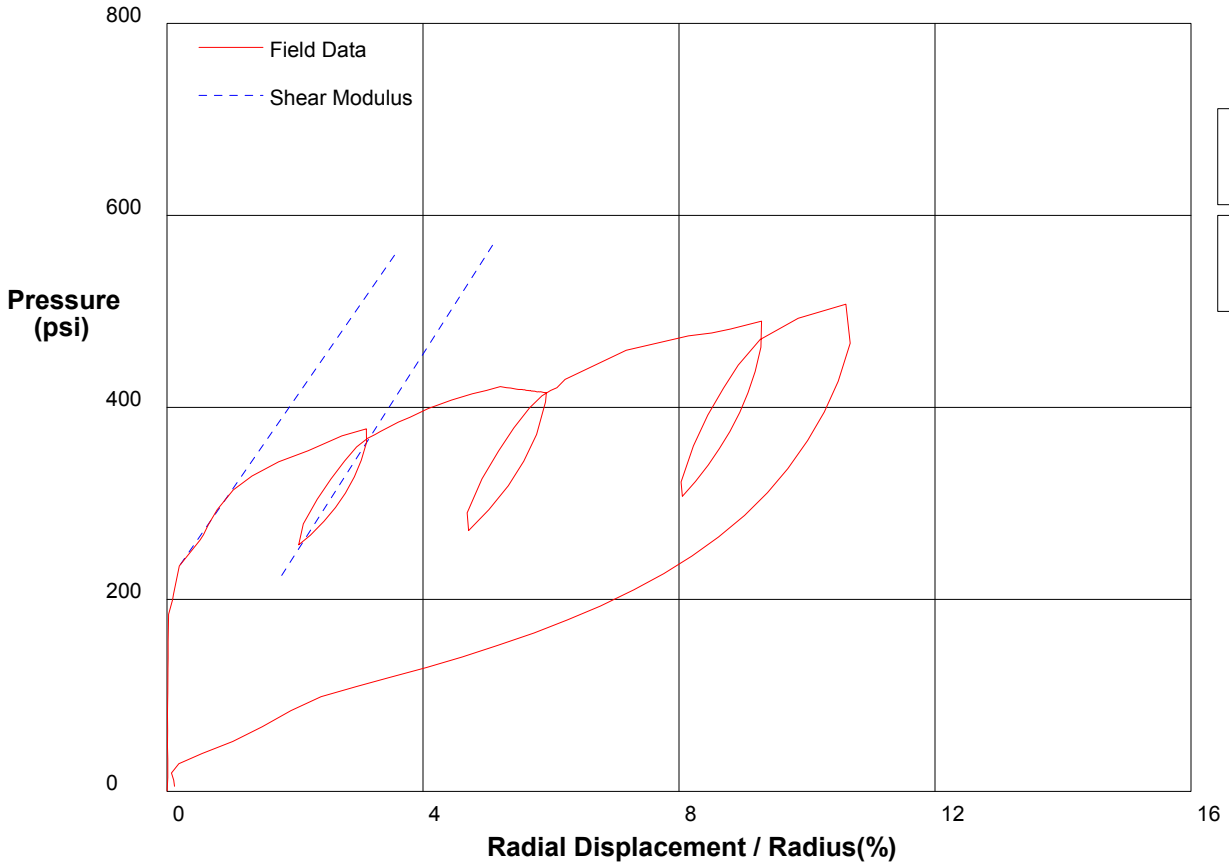


**Shear Modulus 4814 psi**

**Shear Modulus 5220 psi**

shift 0

**In Situ Engineering**

# Appendix I - Pressuremeter Data and Standard Interpretation

**PRESSUREMETER DATA** **CH2MHill, Inc.**

**CALTRANS I-710 North Tunnel Project** **1/20/2009**

**Hole No. Z2-B1** **Depth 138.5ft** **File C:\DATA\ISE-812\SR710-14.P**

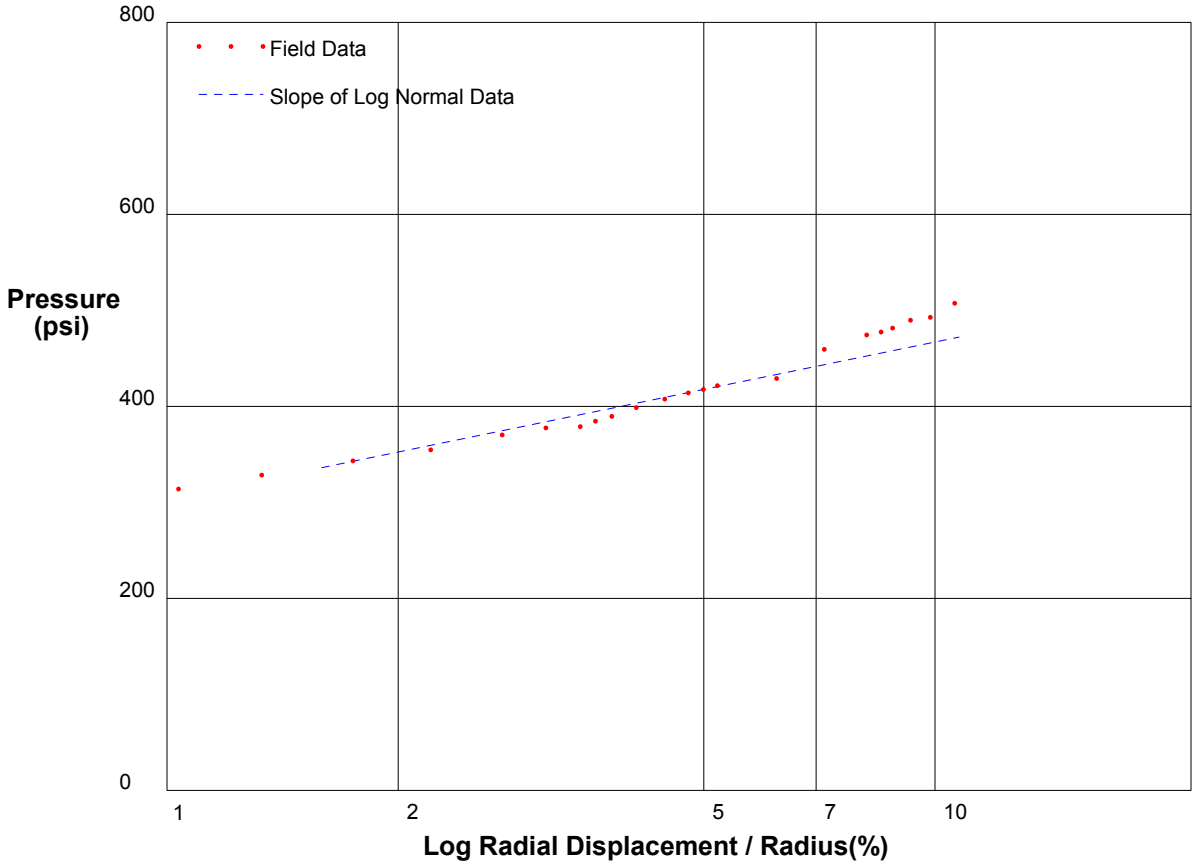


**Shear Strength 71.2 psi**
**Limit Pressure 567 psi**

shift 0

**In Situ Engineering**

# Appendix I - Pressuremeter Data and Standard Interpretation

**PRESSUREMETER DATA** **CH2M-HILL, Inc.**

**CALTRANS I-710 North Tunnel Project** **1/20/2009**

**Hole No. Z1-B7** **Depth 96.5ft** **File C:\DATA\ISE-812\SR710-15.P**

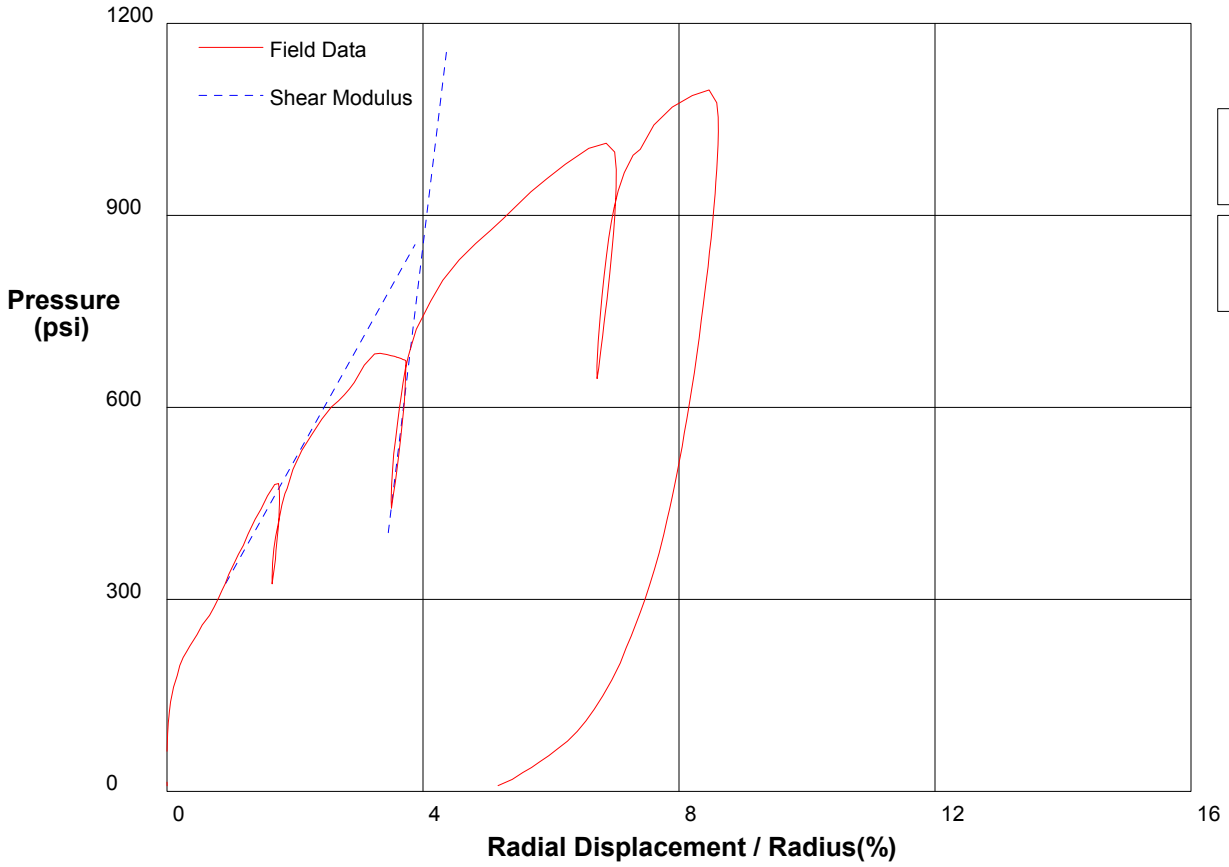


**Shear Modulus 8943 psi**

**Shear Modulus 41363 psi**

shift 0

**In Situ Engineering**

# Appendix I - Pressuremeter Data and Standard Interpretation

**PRESSUREMETER DATA** **CH2MHill, Inc.**

**CALTRANS I-710 North Tunnel Project** **1/20/2009**

**Hole No. Z1-B7** **Depth 96.5ft** **File C:\DATA\ISE-812\SR710-15.P**

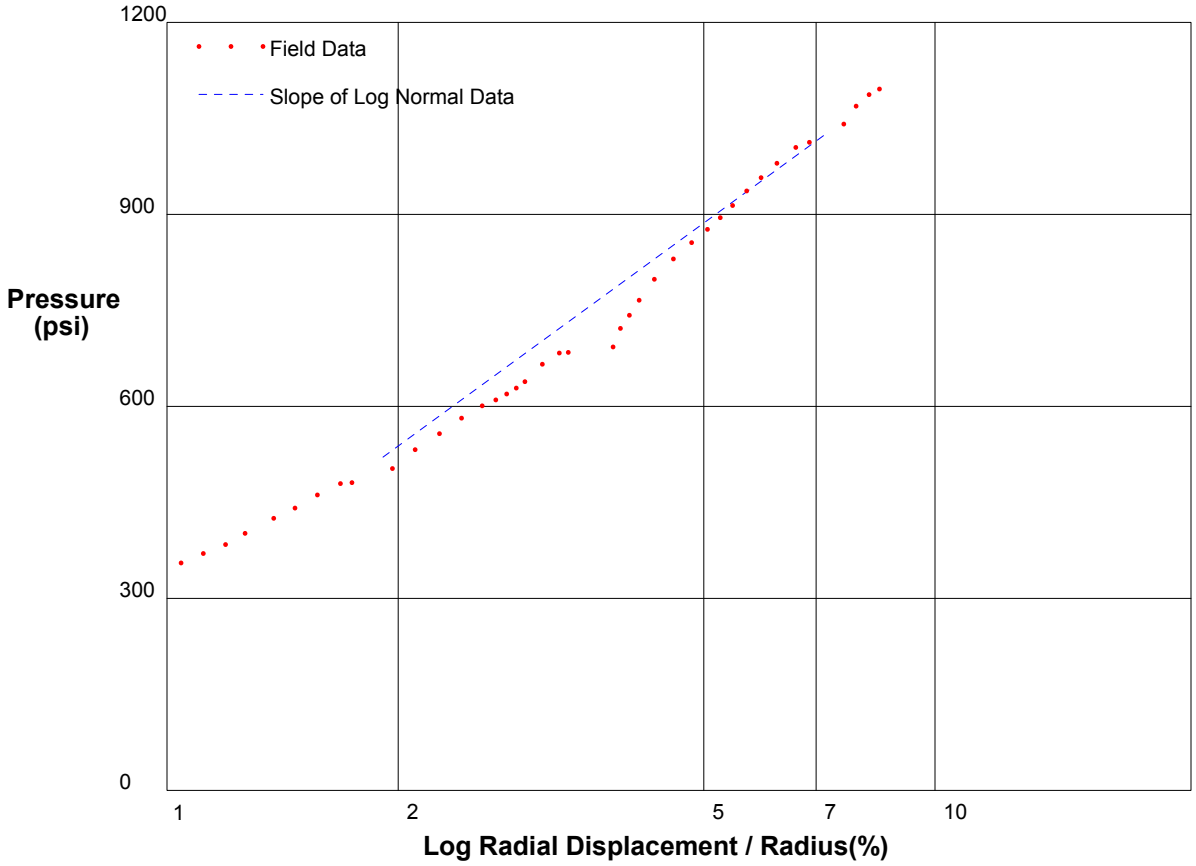


**Shear Strength 380.3 psi**
**Limit Pressure 1686 psi**

shift 0

**In Situ Engineering**

# Appendix I - Pressuremeter Data and Standard Interpretation

**PRESSUREMETER DATA** **CH2M-HILL, Inc.**

**CALTRANS I-710 North Tunnel Project** **1/20/2009**

**Hole No. Z1-B7** **Depth 95ft** **File C:\DATA\ISE-812\SR710-16.P**

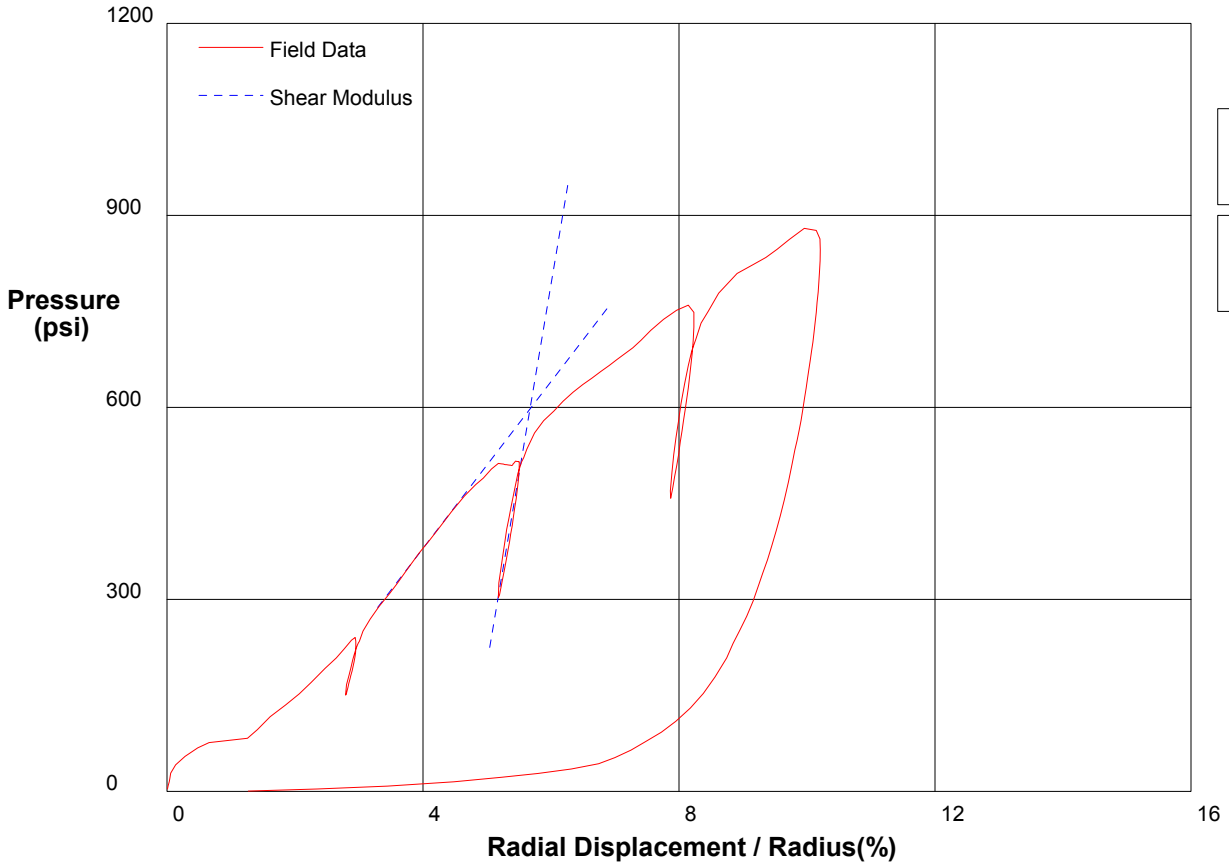


**Shear Modulus 6511 psi**

**Shear Modulus 29576 psi**

shift 0

**In Situ Engineering**

# Appendix I - Pressuremeter Data and Standard Interpretation

**PRESSUREMETER DATA** **CH2MHill, Inc.**

**CALTRANS I-710 North Tunnel Project** **1/20/2009**

**Hole No. Z1-B7** **Depth 95ft** **File C:\DATA\ISE-812\SR710-16.P**

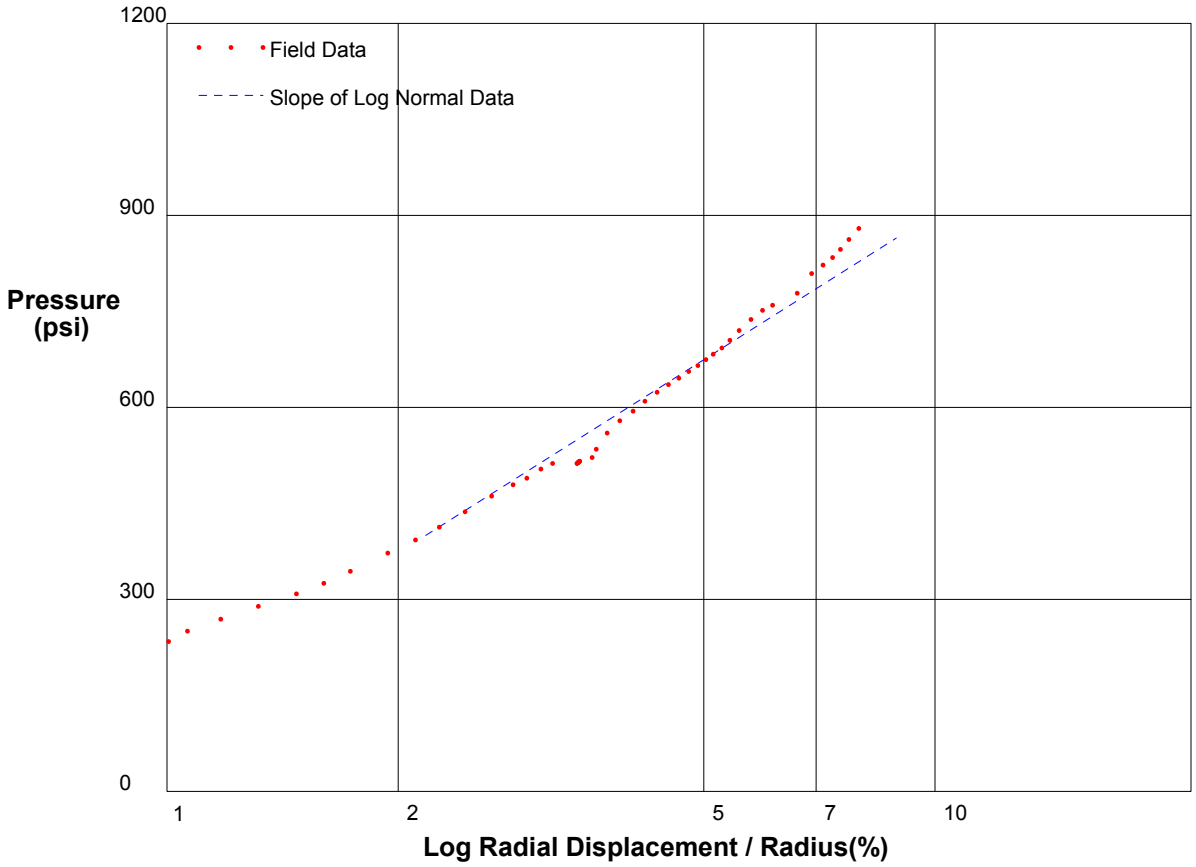


**Shear Strength 329.2 psi**
**Limit Pressure 1367 psi**

shift 2

**In Situ Engineering**

# Appendix I - Pressuremeter Data and Standard Interpretation

**PRESSUREMETER DATA** **CH2M-HILL, Inc.**

**CALTRANS I-710 North Tunnel Project** **1/21/2009**

**Hole No. Z1-B7** **Depth 111.5ft** **File C:\DATA\ISE-812\SR710-17.P**

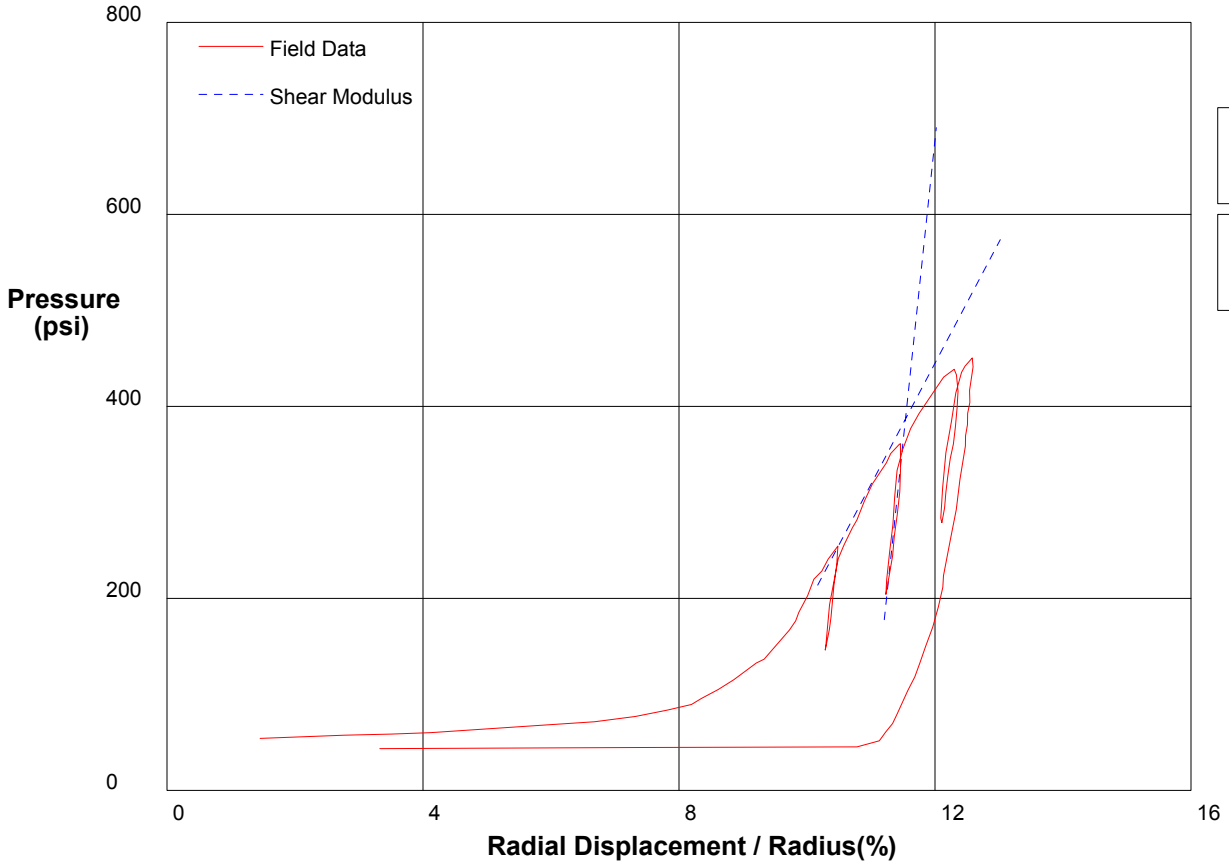


**Shear Modulus 6301 psi**

**Shear Modulus 31538 psi**

shift 0

**In Situ Engineering**

# Appendix I - Pressuremeter Data and Standard Interpretation

**PRESSUREMETER DATA** **CH2MHill, Inc.**

**CALTRANS I-710 North Tunnel Project** **1/21/2009**

**Hole No. Z1-B7** **Depth 111.5ft** **File C:\DATA\ISE-812\SR710-17.P**

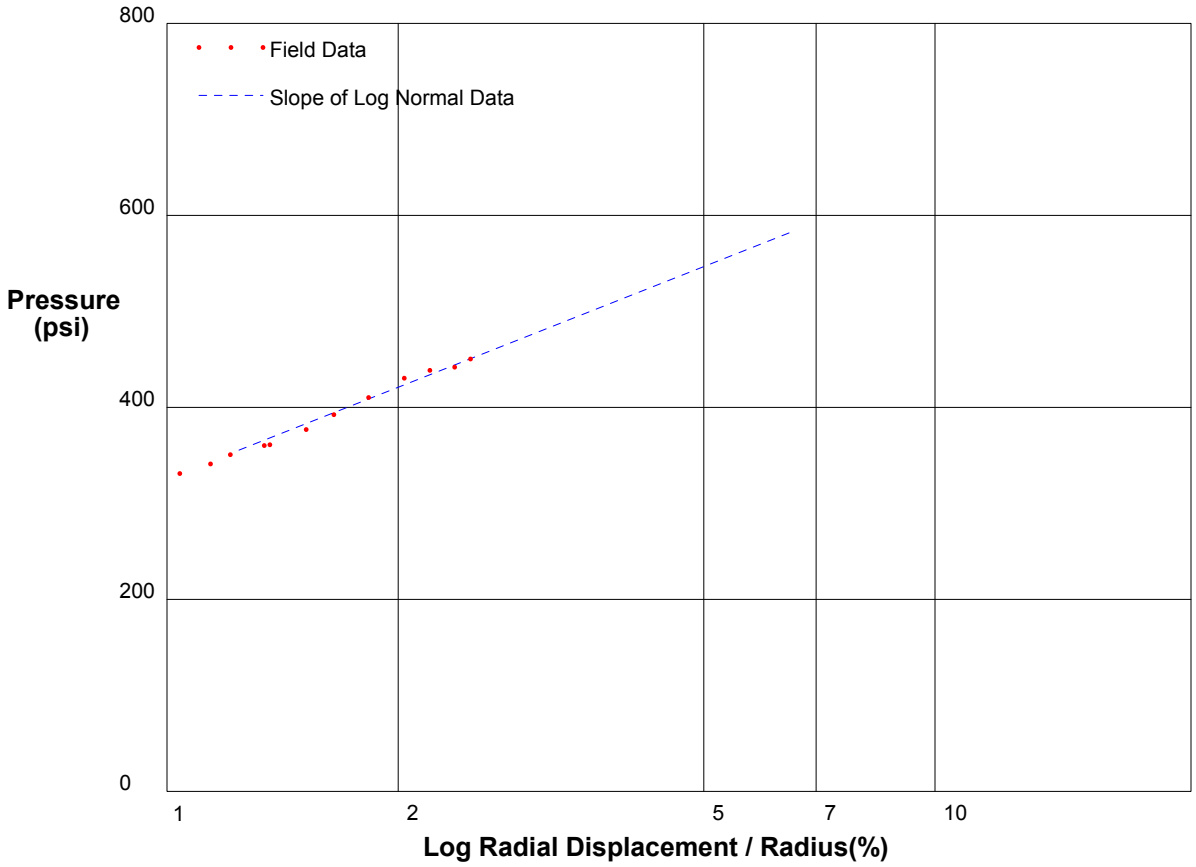


**Shear Strength 137.1 psi**
**Limit Pressure 835 psi**

shift 10.1

**In Situ Engineering**

# Appendix I - Pressuremeter Data and Standard Interpretation

**PRESSUREMETER DATA** **CH2M-HILL, Inc.**

**CALTRANS I-710 North Tunnel Project** **1/21/2009**

**Hole No. Z1-B7** **Depth 110ft** **File C:\DATA\ISE-812\SR710-18.P**

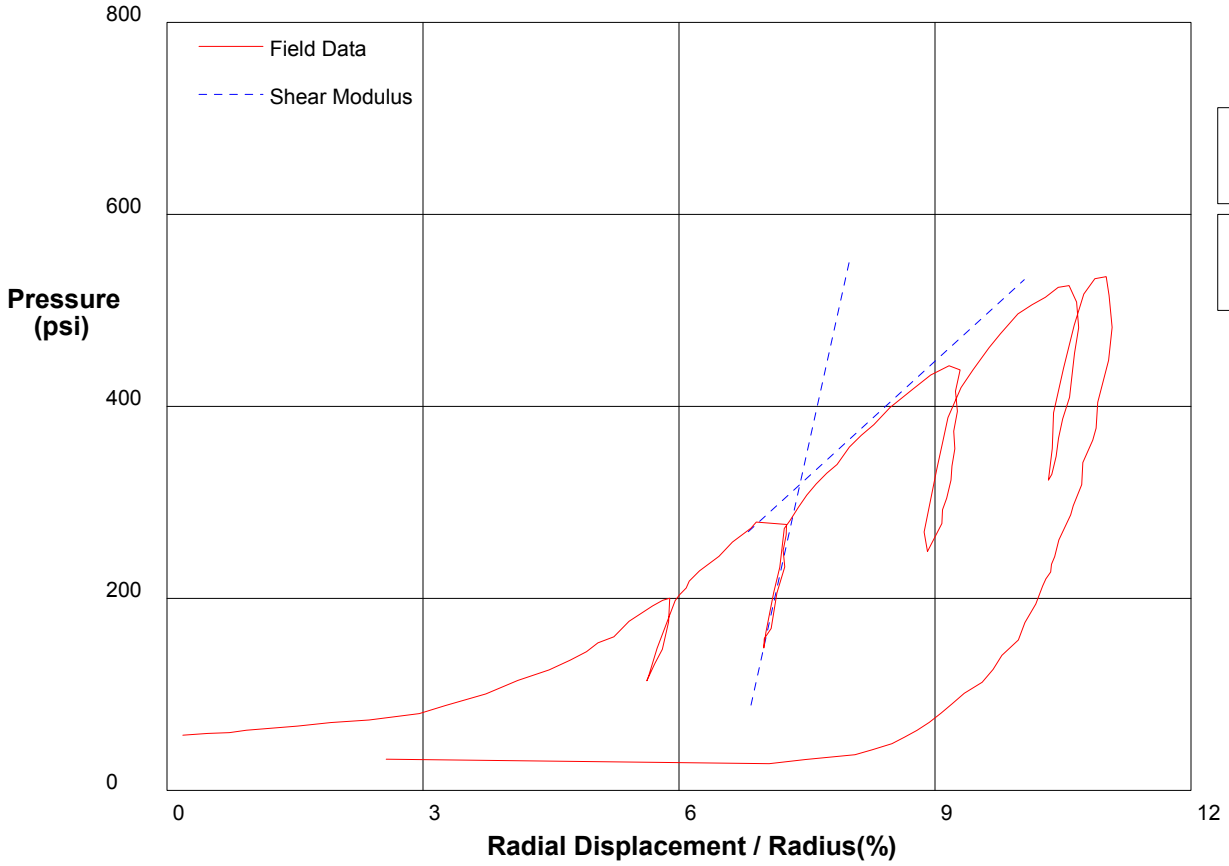


**Shear Modulus 4057 psi**

**Shear Modulus 20060 psi**

shift 0

**In Situ Engineering**

# Appendix I - Pressuremeter Data and Standard Interpretation

**PRESSUREMETER DATA** **CH2MHill, Inc.**

**CALTRANS I-710 North Tunnel Project** **1/21/2009**

**Hole No. Z1-B7** **Depth 110ft** **File C:\DATA\ISE-812\SR710-18.P**

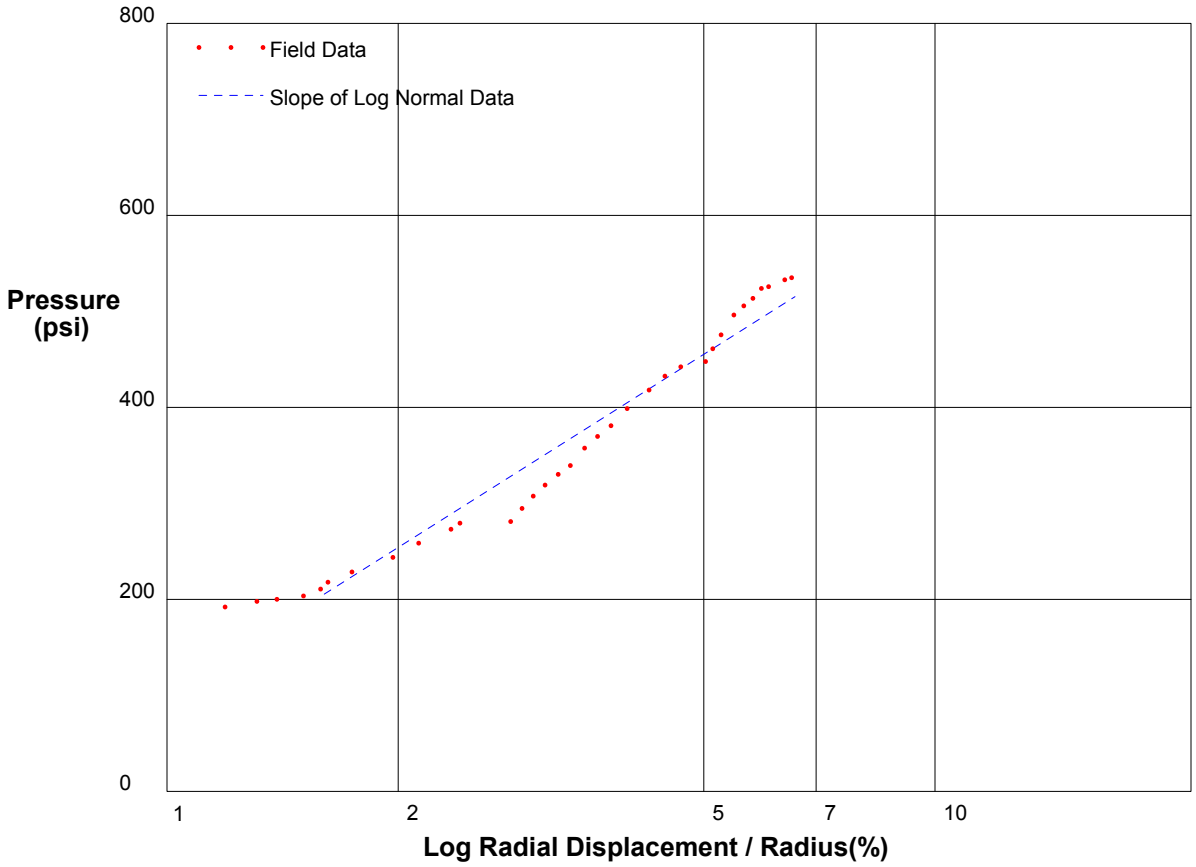


**Shear Strength 219.4 psi**
**Limit Pressure 917 psi**

shift 4.5

**In Situ Engineering**

# Appendix I - Pressuremeter Data and Standard Interpretation

**PRESSUREMETER DATA** **CH2M-HILL, Inc.**

**CALTRANS I-710 North Tunnel Project** **1/21/2009**

**Hole No. Z1-B7** **Depth 136ft** **File C:\DATA\ISE-812\SR710-19.P**

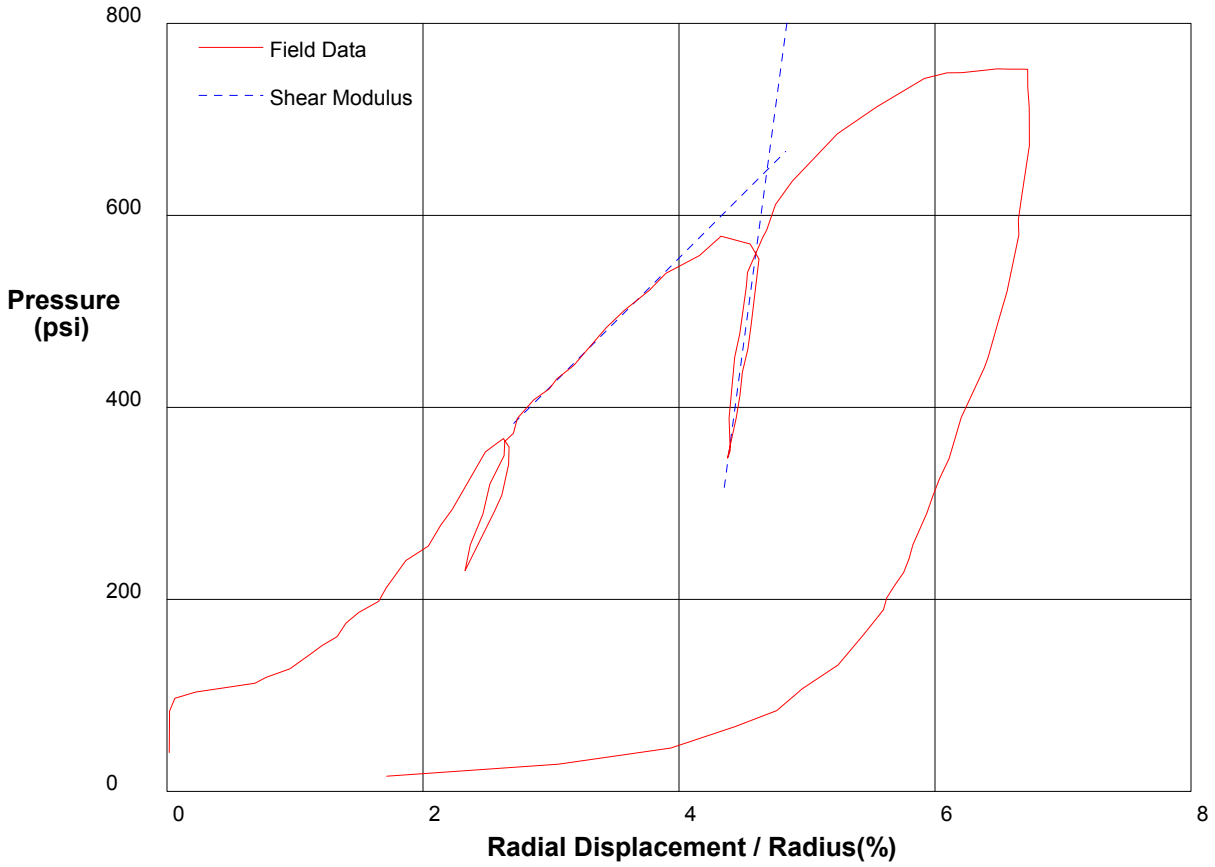


**Shear Modulus 49503 psi**

**Shear Modulus 6666 psi**

shift 0

**In Situ Engineering**

# Appendix I - Pressuremeter Data and Standard Interpretation

**PRESSUREMETER DATA** **CH2MHill, Inc.**

**CALTRANS I-710 North Tunnel Project** **1/21/2009**

**Hole No. Z1-B7** **Depth 136ft** **File C:\DATA\ISE-812\SR710-19.P**

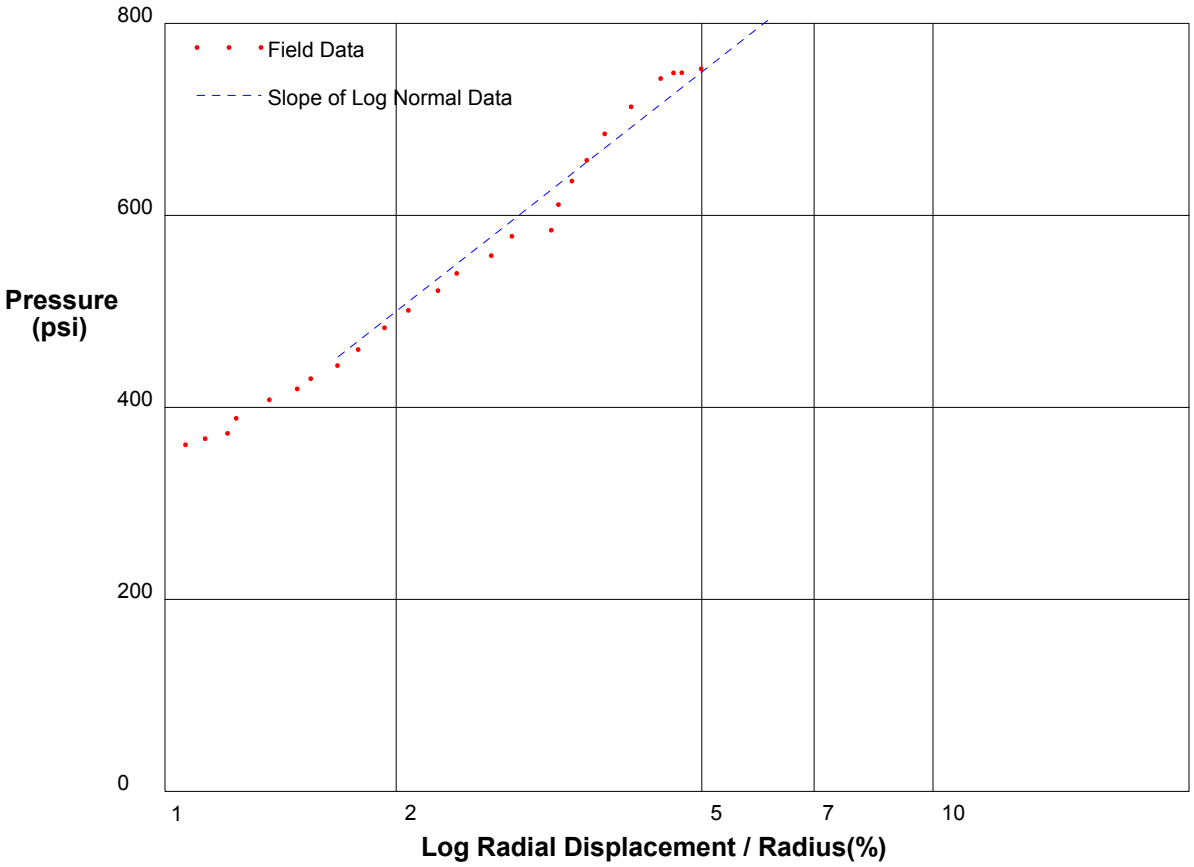


**Shear Strength 272.1 psi**
**Limit Pressure 1321 psi**

shift 1.5

**In Situ Engineering**

# Appendix I - Pressuremeter Data and Standard Interpretation

**PRESSUREMETER DATA** **CH2M-HILL, Inc.**

**CALTRANS I-710 North Tunnel Project** **1/21/2009**

**Hole No. Z1-B7** **Depth 135ft** **File C:\DATA\ISE-812\SR710-20.P**

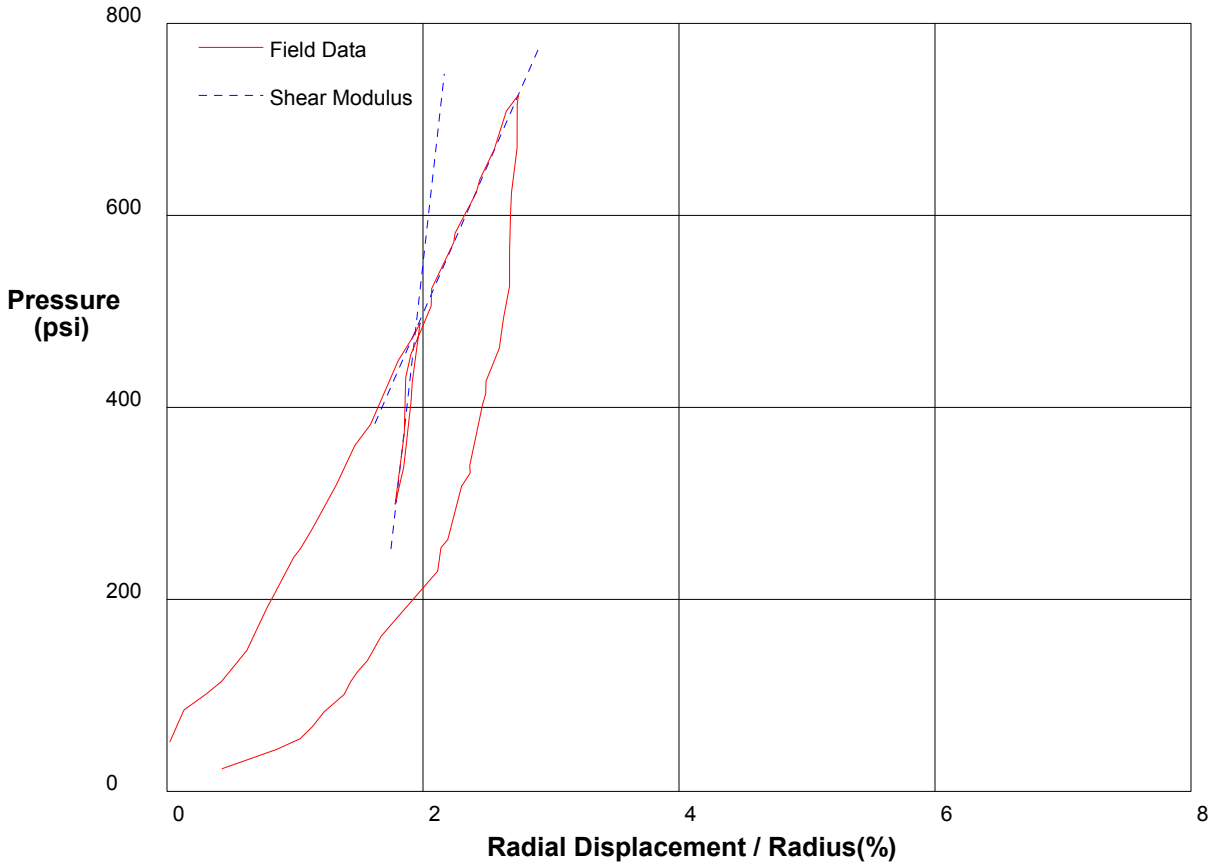


**Shear Modulus 59333 psi**

**Shear Modulus 15268 psi**

shift 0

**In Situ Engineering**

# Appendix I - Pressuremeter Data and Standard Interpretation

**PRESSUREMETER DATA** **CH2MHill, Inc.**

**CALTRANS I-710 North Tunnel Project** **1/21/2009**

**Hole No. Z1-B7** **Depth 135ft** **File C:\DATA\ISE-812\SR710-20.P**

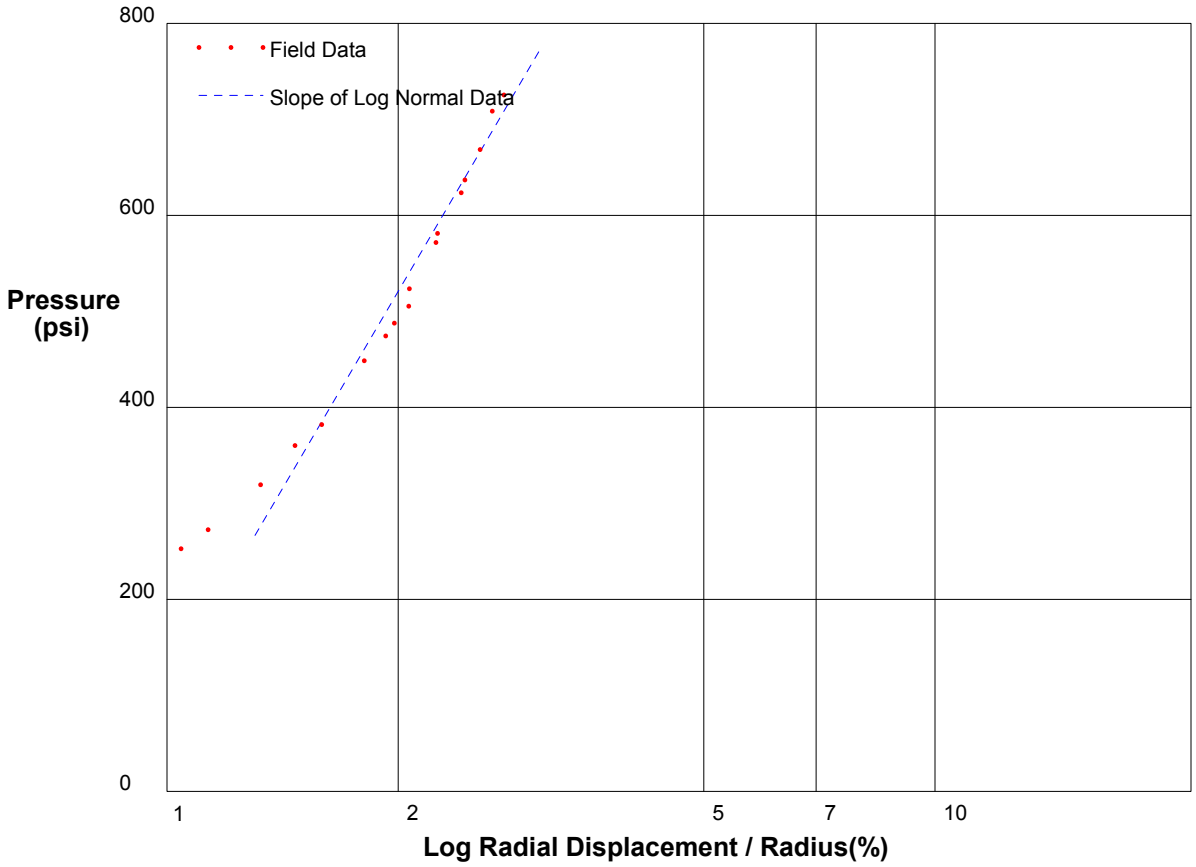


**Shear Strength 592.1 psi**
**Limit Pressure 2309 psi**

shift 0

**In Situ Engineering**

# Appendix I - Pressuremeter Data and Standard Interpretation

**PRESSUREMETER DATA** **CH2MHill, Inc.**

**CALTRANS I-710 North Tunnel Project** **1/28/2009**

**Hole No. Z1-B3** **Depth 177.3ft** **File C:\DATA\ISE-812\SR710-21.P**

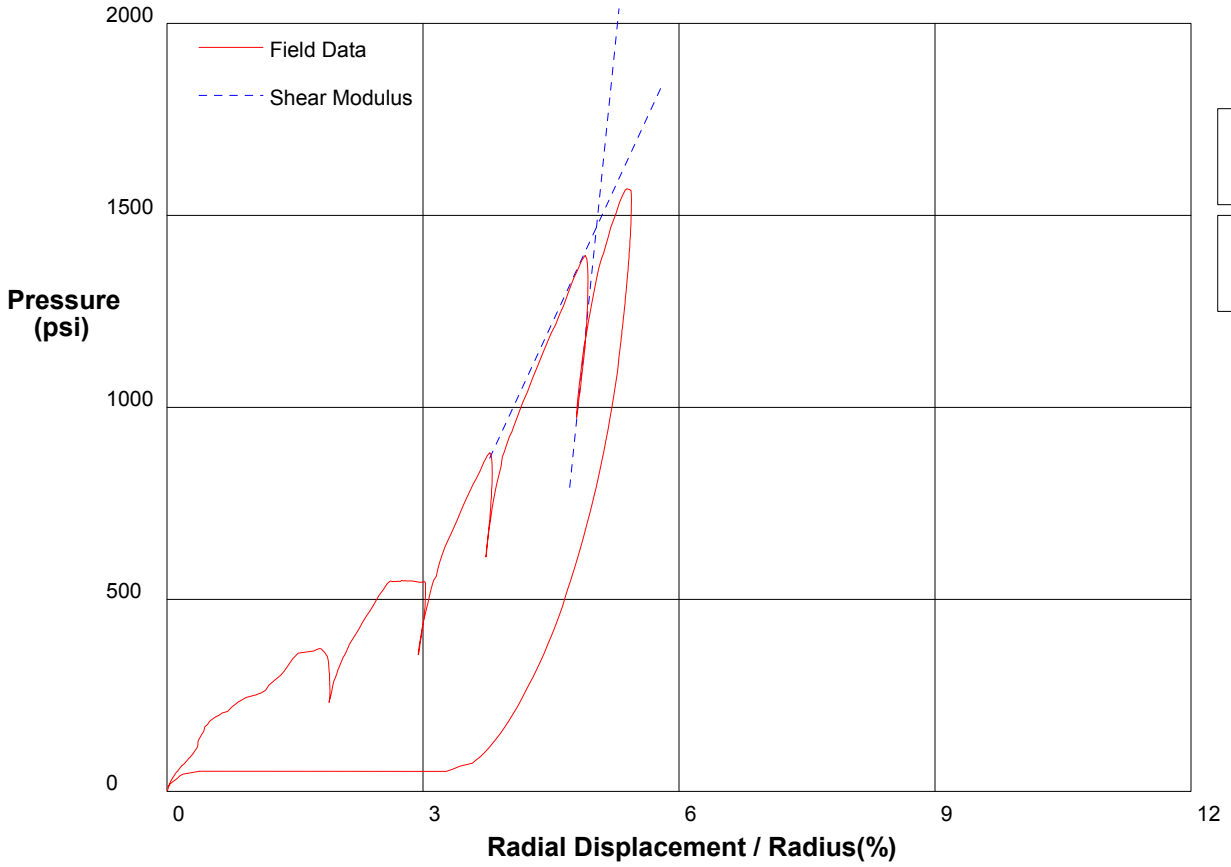


**Shear Modulus 107807 psi**

**Shear Modulus 24031 psi**

shift 0

**In Situ Engineering**

# Appendix I - Pressuremeter Data and Standard Interpretation

**PRESSUREMETER DATA** **CH2M-HILL, Inc.**

**CALTRANS I-710 North Tunnel Project** **1/28/2009**

**Hole No. Z1-B3** **Depth 177.3ft** **File C:\DATA\ISE-812\SR710-21.P**

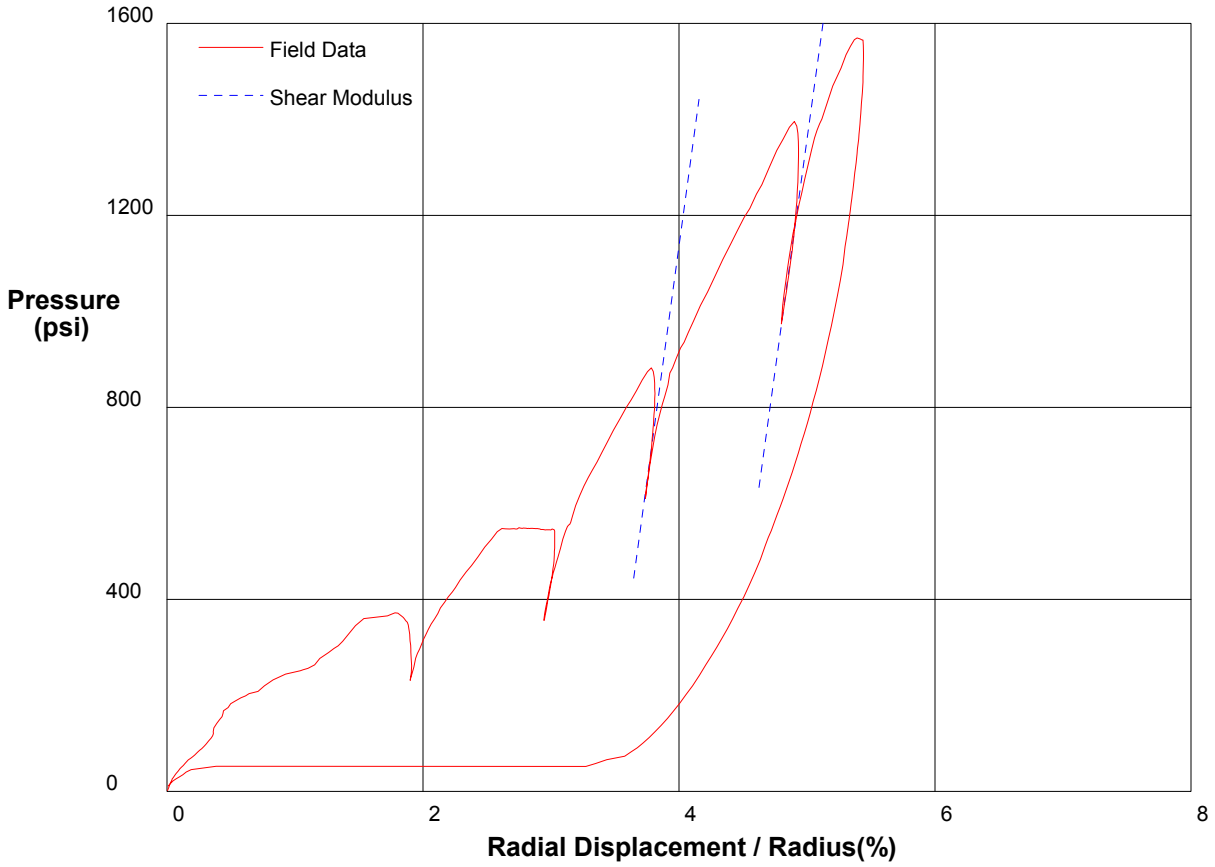


**Shear Modulus 96666 psi**

**Shear Modulus 97687 psi**

shift 0

**In Situ Engineering**

# Appendix I - Pressuremeter Data and Standard Interpretation

**PRESSUREMETER DATA** **CH2MHill, Inc.**

**CALTRANS I-710 North Tunnel Project** **1/28/2009**

**Hole No. Z1-B3** **Depth 177.3ft** **File C:\DATA\ISE-812\SR710-21.P**

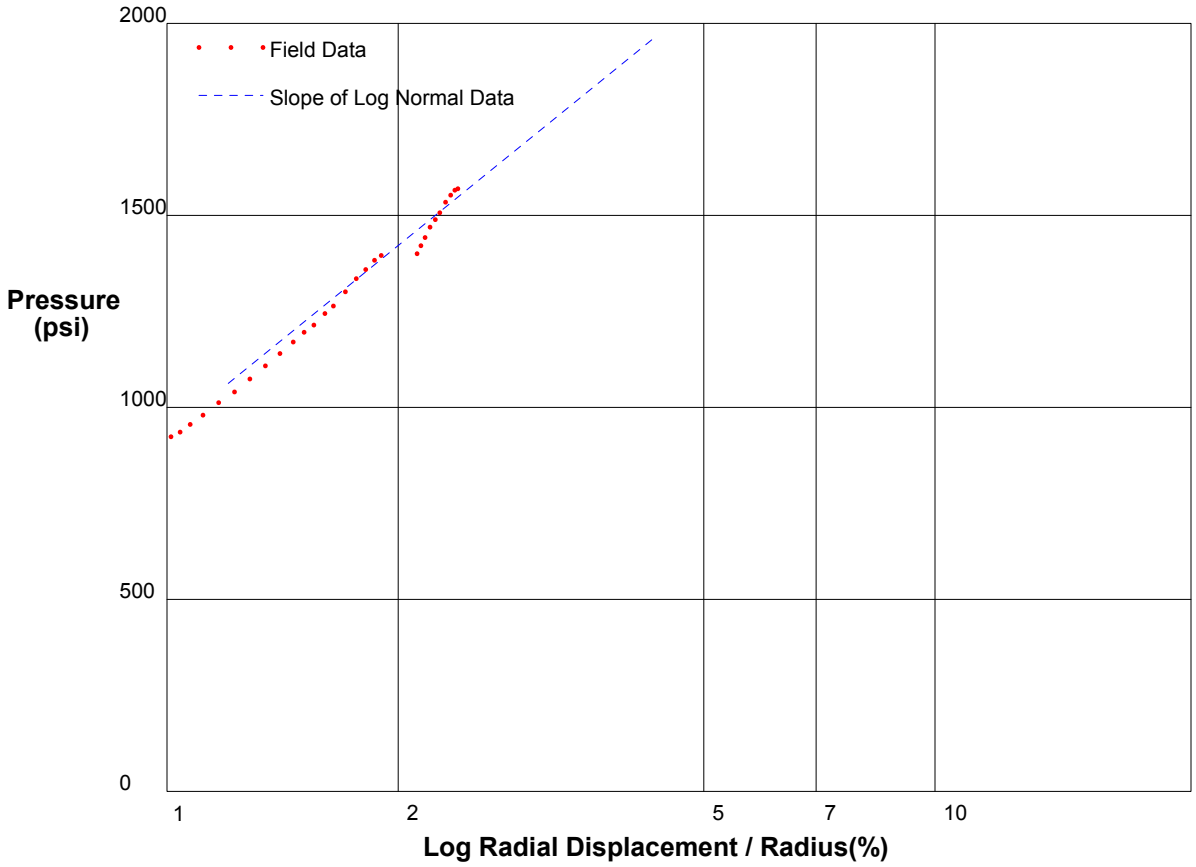


**Shear Strength 704.7 psi**
**Limit Pressure 3549 psi**

shift 3

**In Situ Engineering**

# Appendix I - Pressuremeter Data and Standard Interpretation

**PRESSUREMETER DATA** **CH2MHill, Inc.**

**CALTRANS I-710 North Tunnel Project** **1/28/2009**

**Hole No. Z1-B3** **Depth 204ft** **File C:\DATA\ISE-812\SR710-22.P**

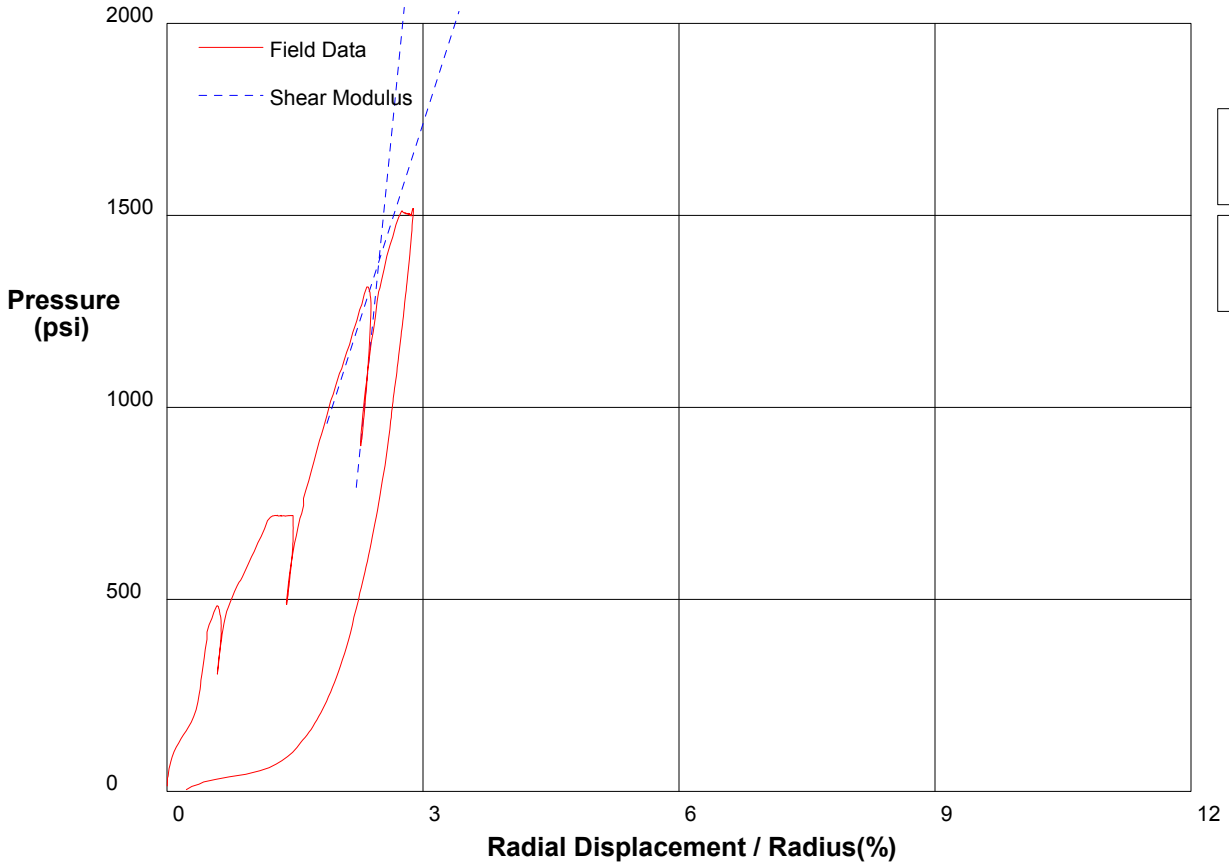


**Shear Modulus 111111 psi**

**Shear Modulus 34680 psi**

shift 0

**In Situ Engineering**

# Appendix I - Pressuremeter Data and Standard Interpretation

**PRESSUREMETER DATA** **CH2M-HILL, Inc.**

**CALTRANS I-710 North Tunnel Project** **1/28/2009**

**Hole No. Z1-B3** **Depth 204ft** **File C:\DATA\ISE-812\SR710-22.P**

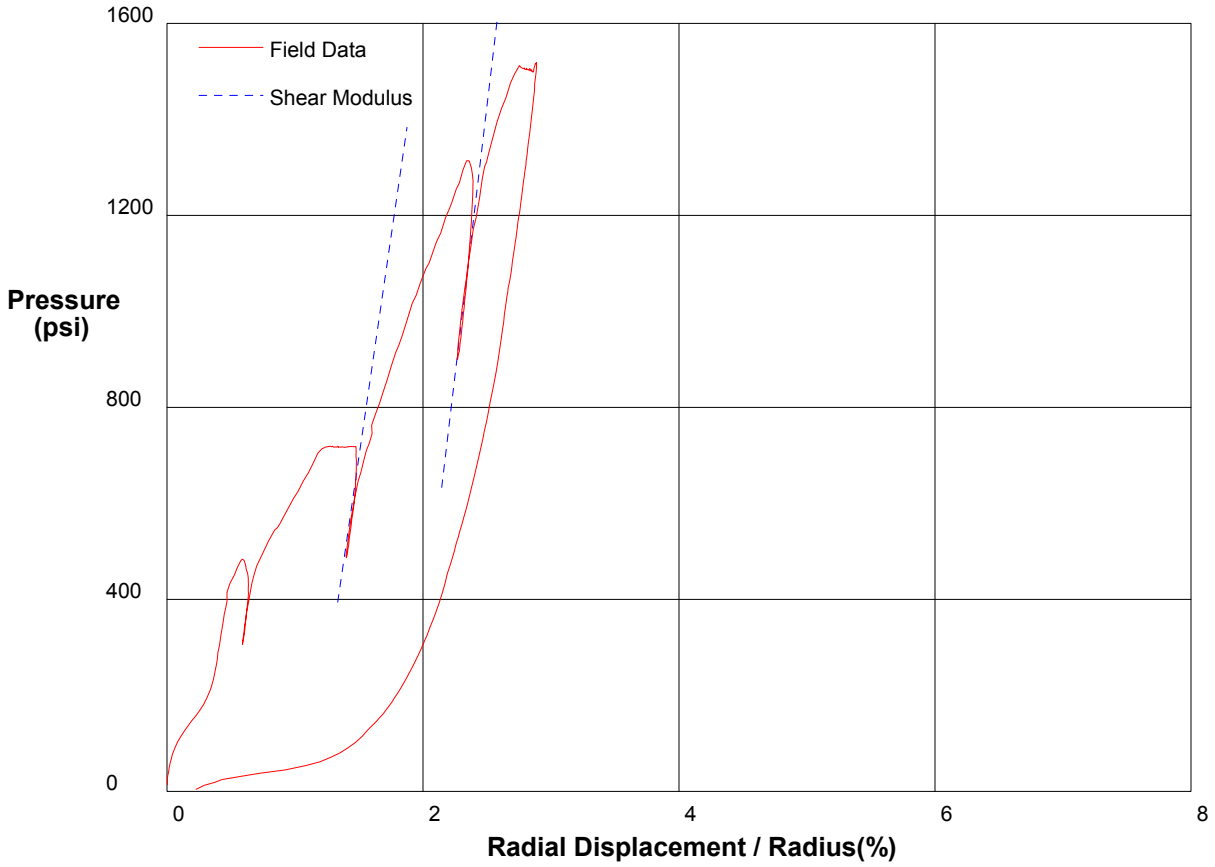


**Shear Modulus 112380 psi**

**Shear Modulus 91282 psi**

shift 0

**In Situ Engineering**

# Appendix I - Pressuremeter Data and Standard Interpretation

**PRESSUREMETER DATA** **CH2MHill, Inc.**

**CALTRANS I-710 North Tunnel Project** **1/28/2009**

**Hole No. Z1-B3** **Depth 204ft** **File C:\DATA\ISE-812\SR710-22.P**

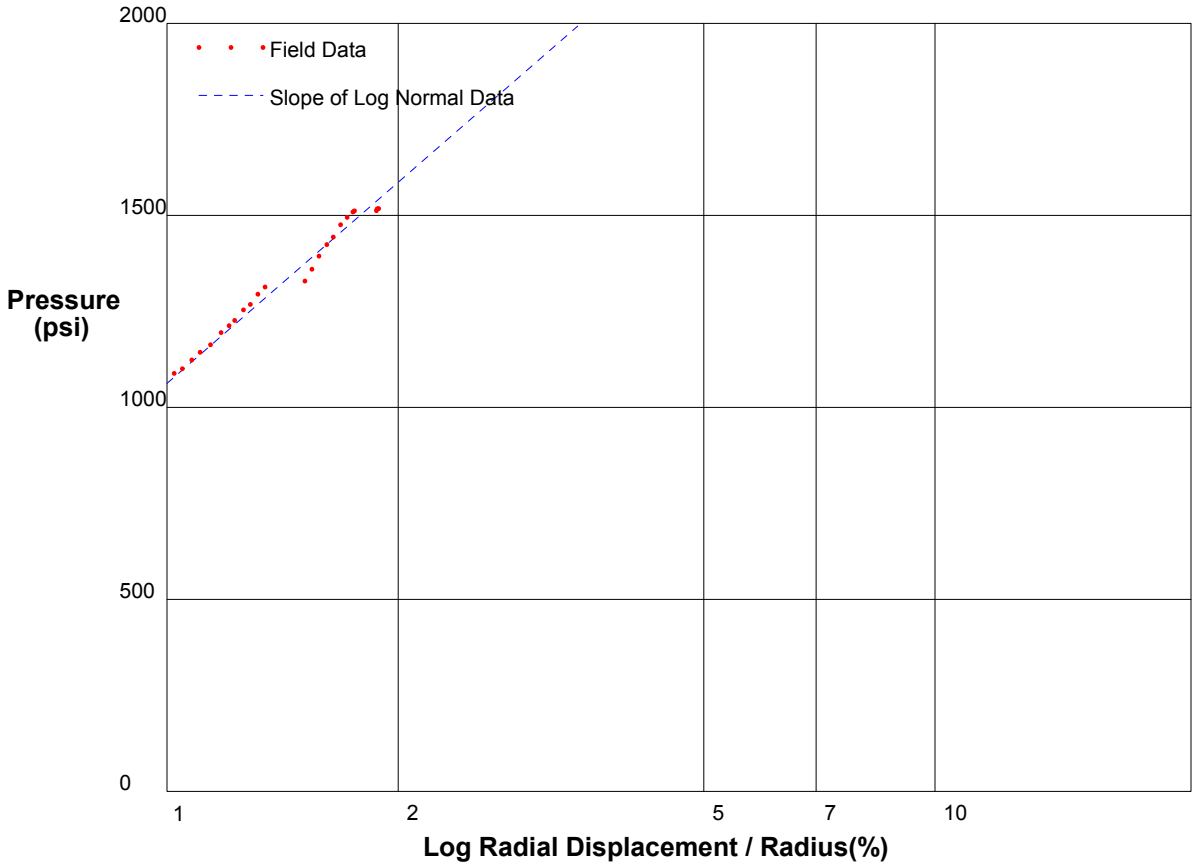


**Shear Strength 755.7 psi**
**Limit Pressure 3869 psi**

shift 1

**In Situ Engineering**

# Appendix I - Pressuremeter Data and Standard Interpretation

**PRESSUREMETER DATA** **CH2MHill, Inc.**

**CALTRANS I-710 North Tunnel Project** **1/29/2009**

**Hole No. Z2-B2** **Depth 135.7ft** **File C:\DATA\ISE-812\SR710-23.P**

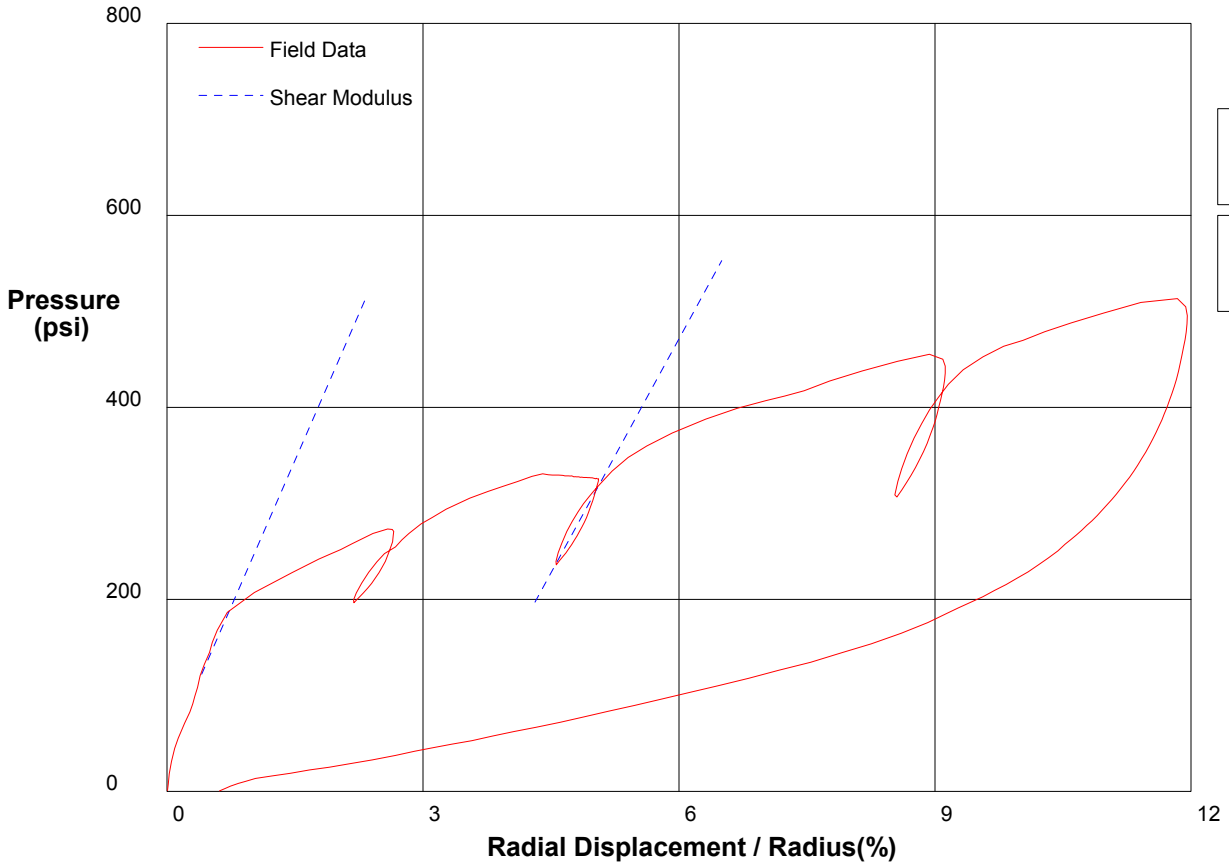


**Shear Modulus 8126 psi**

**Shear Modulus 10179 psi**

shift 0

**In Situ Engineering**

# Appendix I - Pressuremeter Data and Standard Interpretation

**PRESSUREMETER DATA** **CH2M-HILL, Inc.**

**CALTRANS I-710 North Tunnel Project** **1/29/2009**

**Hole No. Z2-B2** **Depth 135.7ft** **File C:\DATA\ISE-812\SR710-23.P**

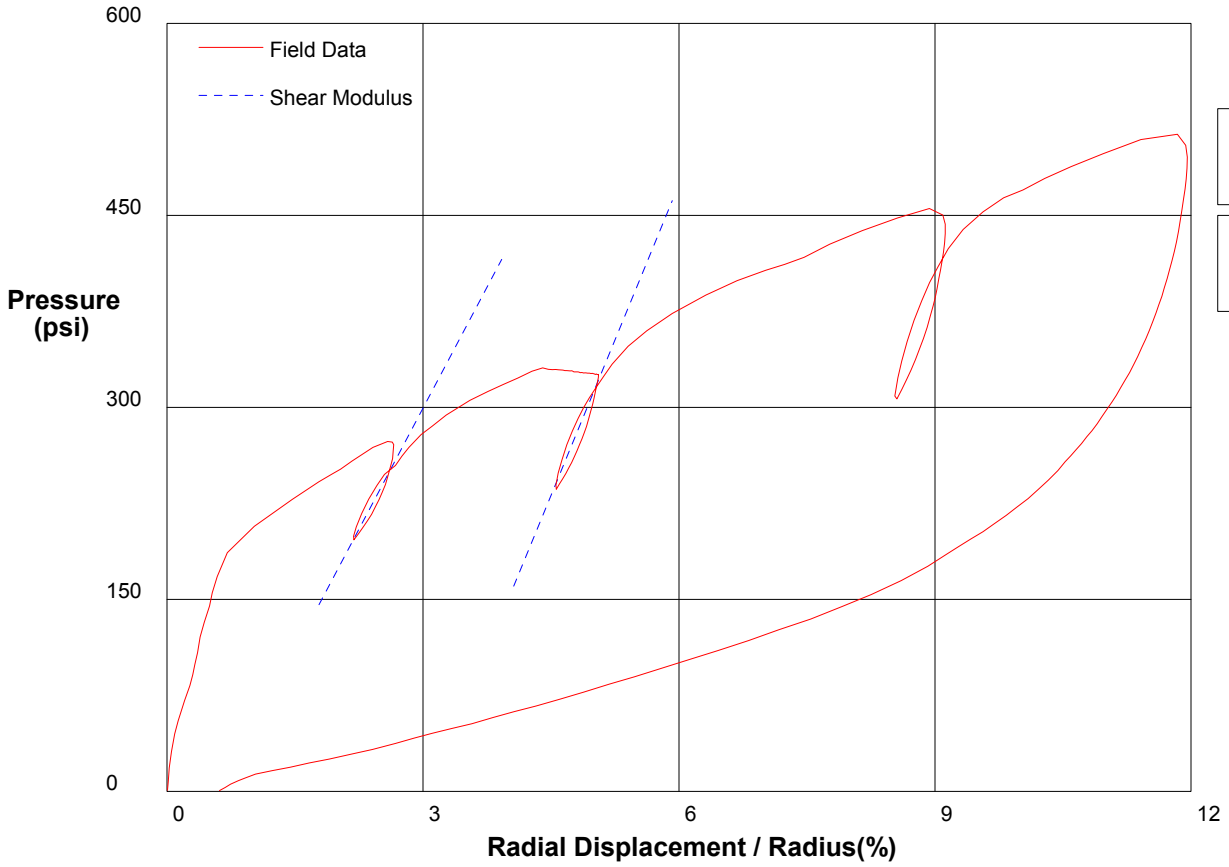


**Shear Modulus 6301 psi**

**Shear Modulus 8095 psi**

shift 0

**In Situ Engineering**

# Appendix I - Pressuremeter Data and Standard Interpretation

**PRESSUREMETER DATA** **CH2M-HILL, Inc.**

**CALTRANS I-710 North Tunnel Project** **1/29/2009**

**Hole No. Z2-B2** **Depth 135.7ft** **File C:\DATA\ISE-812\SR710-23.P**

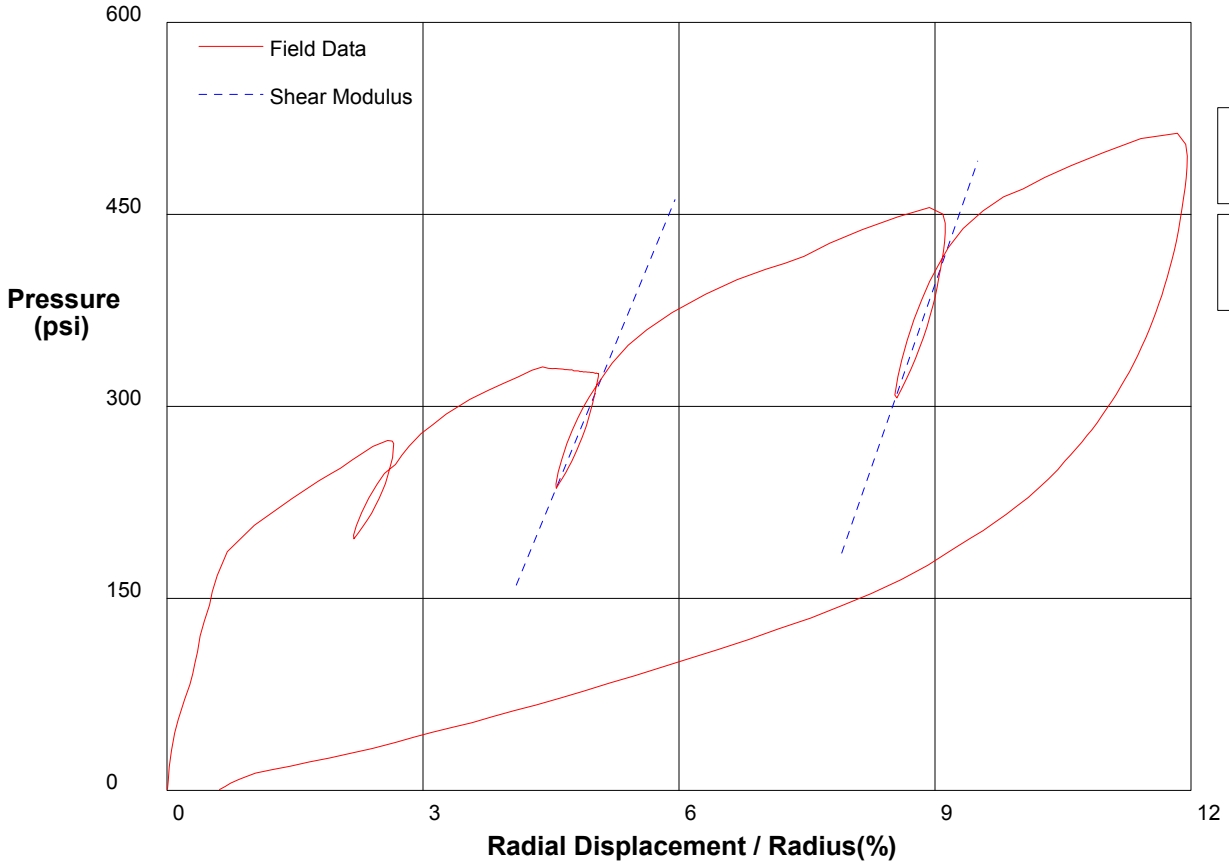


**Shear Modulus 9607 psi**

**Shear Modulus 8095 psi**

shift 0

**In Situ Engineering**

# Appendix I - Pressuremeter Data and Standard Interpretation

**PRESSUREMETER DATA** **CH2MHill, Inc.**

**CALTRANS I-710 North Tunnel Project** **1/29/2009**

**Hole No. Z2-B2** **Depth 135.7ft** **File C:\DATA\ISE-812\SR710-23.P**

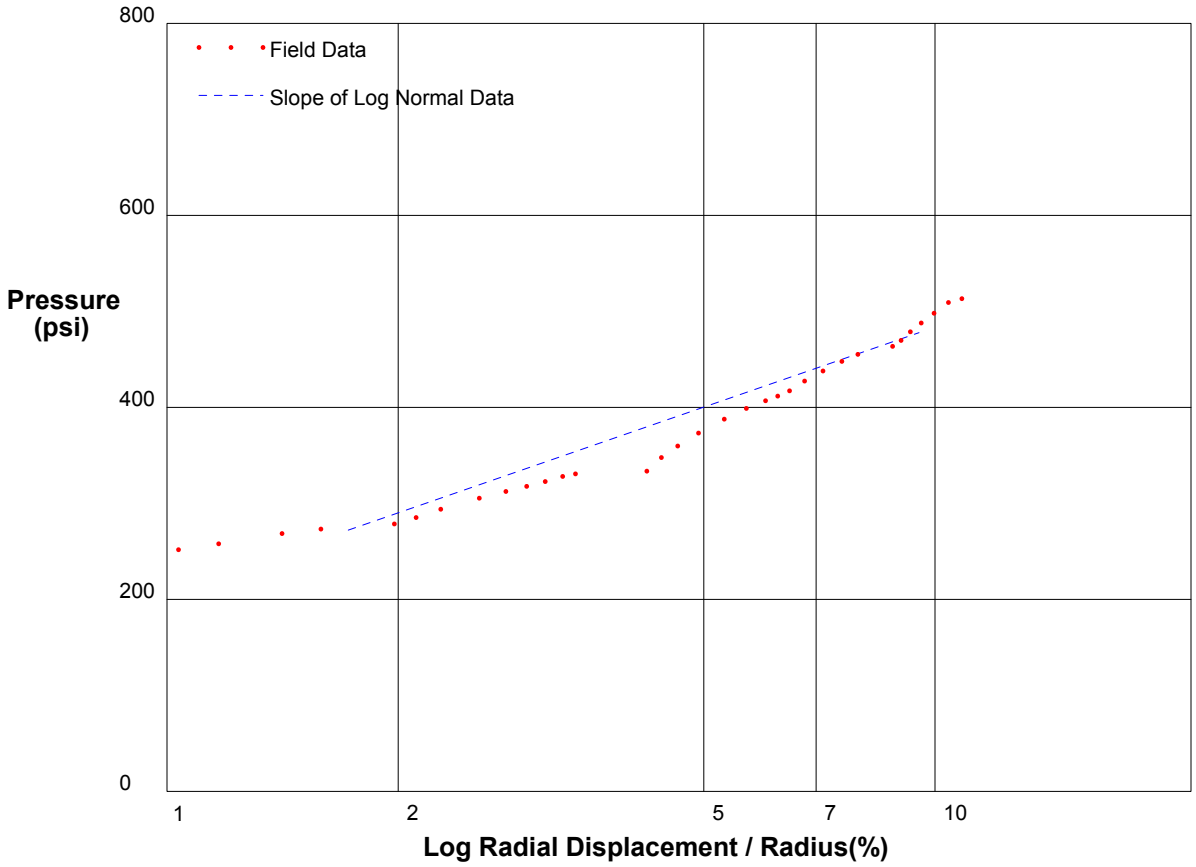


**Shear Strength 120.1 psi**
**Limit Pressure 653 psi**

shift 1

**In Situ Engineering**

# Appendix I - Pressuremeter Data and Standard Interpretation

**PRESSUREMETER DATA** **CH2MHill, Inc.**

**CALTRANS I-710 North Tunnel Project** **1/29/2009**

**Hole No. Z2-B2** **Depth 134.2ft** **File C:\DATA\ISE-812\SR710-24.P**

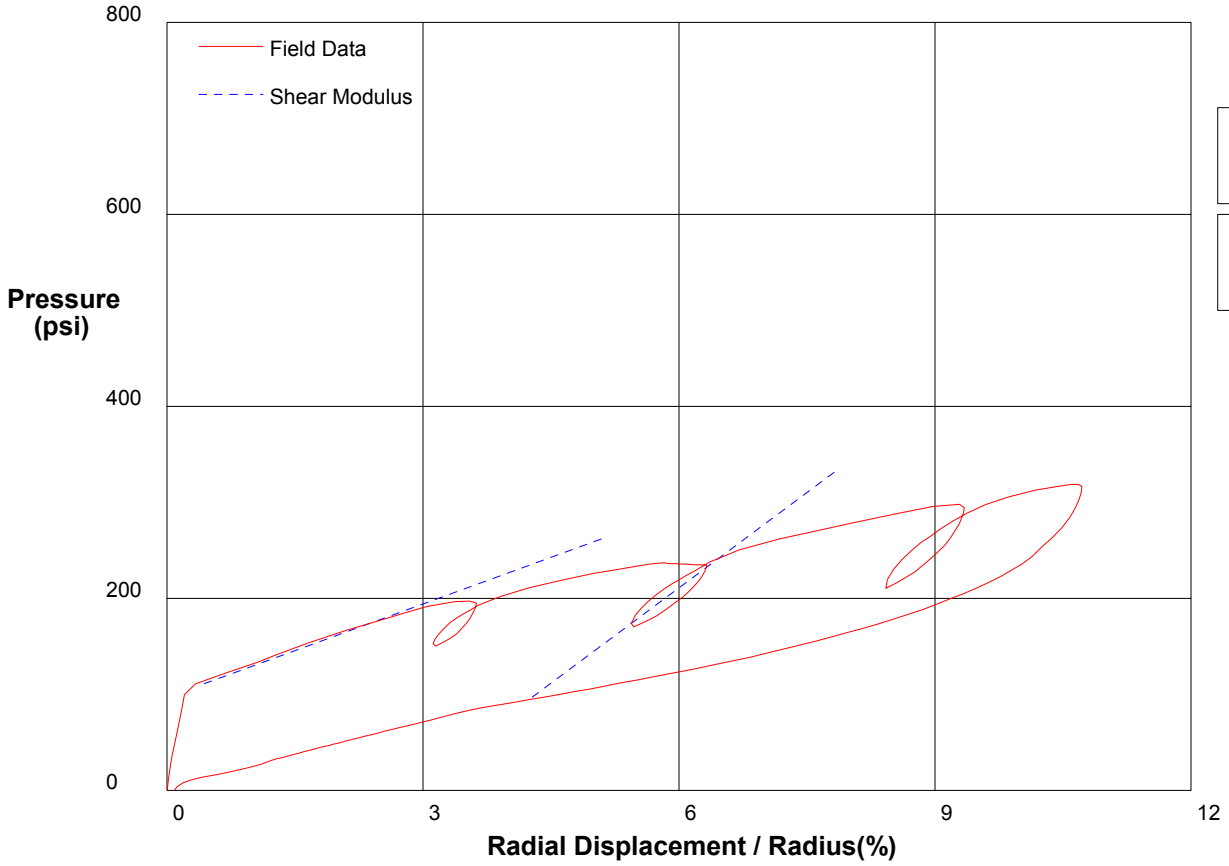


**Shear Modulus 3308 psi**

**Shear Modulus 1620 psi**

shift 0

**In Situ Engineering**

# Appendix I - Pressuremeter Data and Standard Interpretation

**PRESSUREMETER DATA** **CH2M-HILL, Inc.**

**CALTRANS I-710 North Tunnel Project** **1/29/2009**

**Hole No. Z2-B2** **Depth 134.2ft** **File C:\DATA\ISE-812\SR710-24.P**

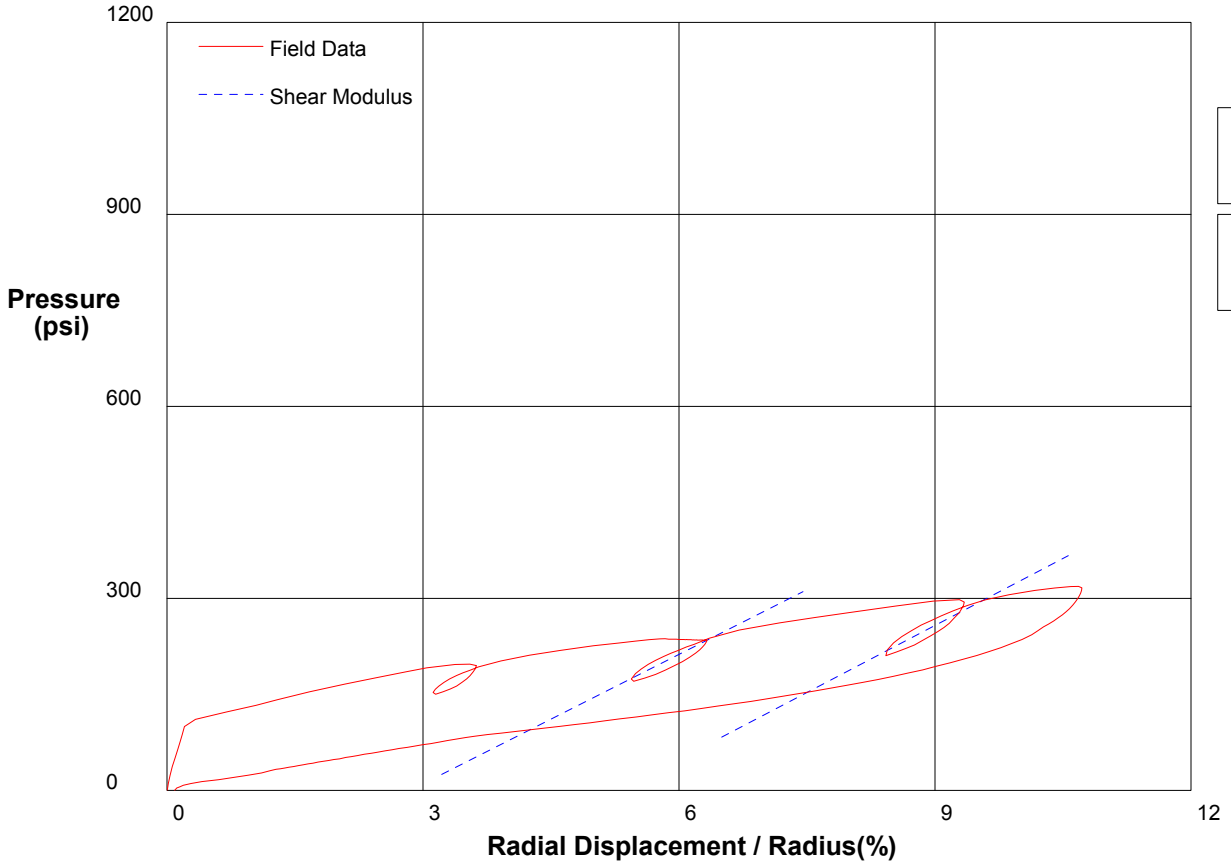


**Shear Modulus 3487 psi**

**Shear Modulus 3370 psi**

shift 0

**In Situ Engineering**

# Appendix I - Pressuremeter Data and Standard Interpretation

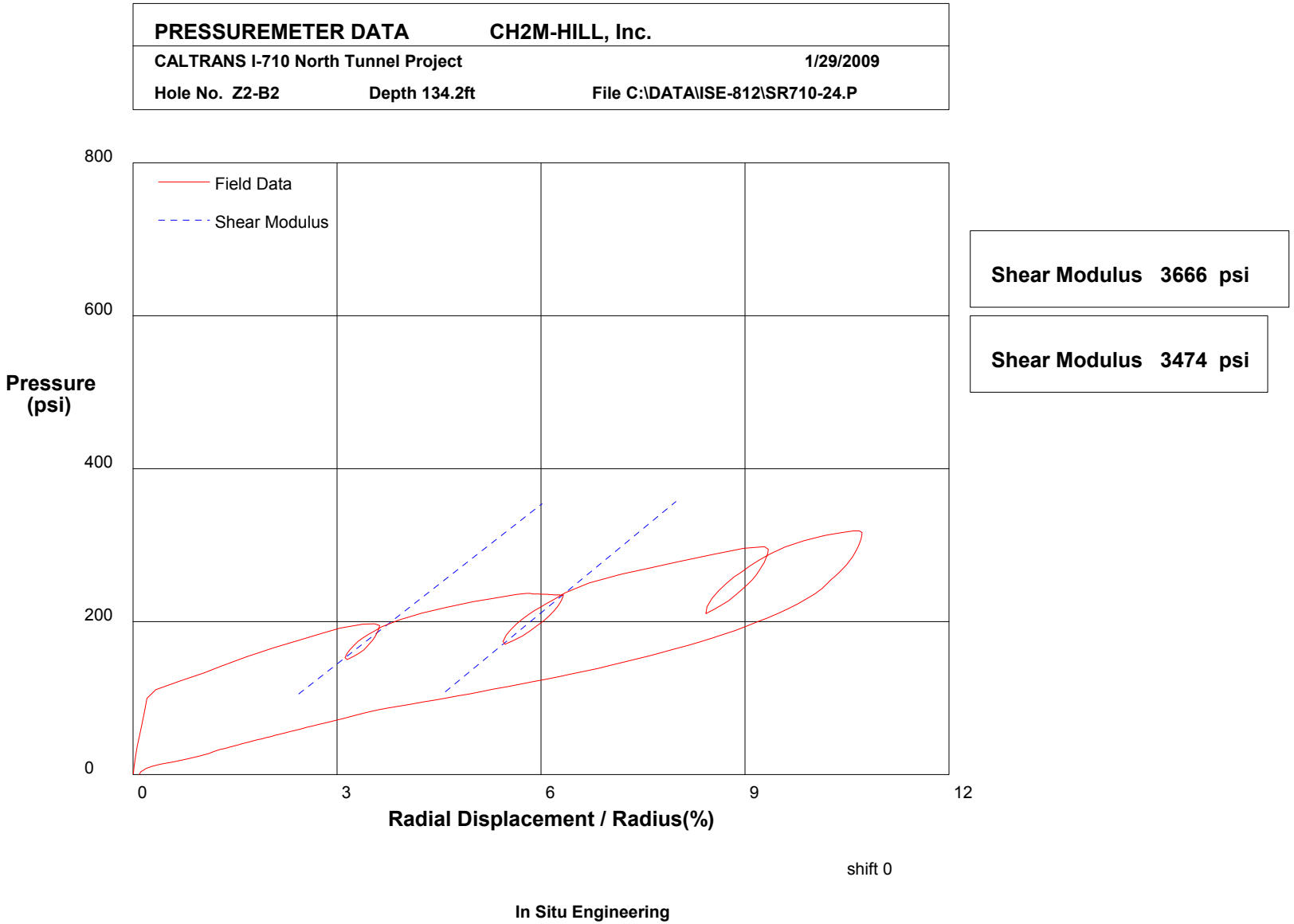

# Appendix I - Pressuremeter Data and Standard Interpretation

**PRESSUREMETER DATA** **CH2MHill, Inc.**

**CALTRANS I-710 North Tunnel Project** **1/29/2009**

**Hole No. Z2-B2** **Depth 134.2ft** **File C:\DATA\ISE-812\SR710-24.P**

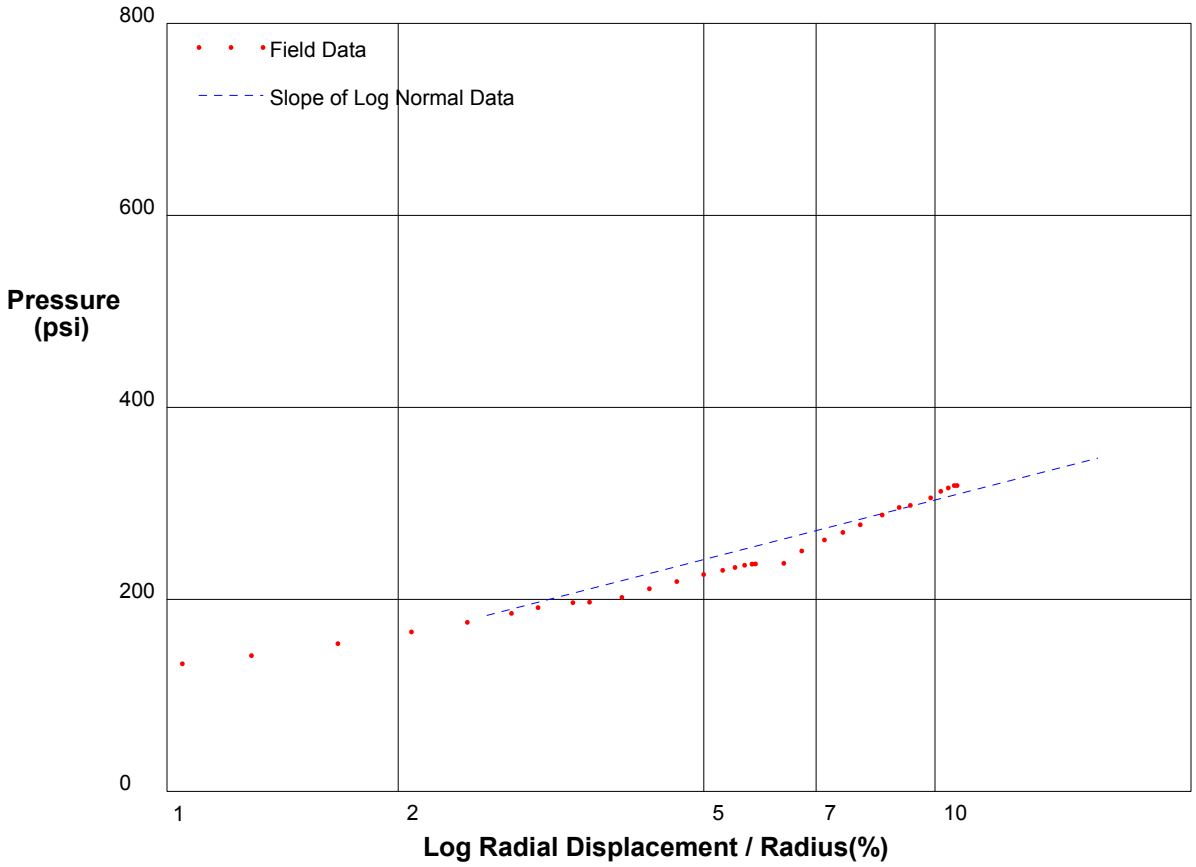


**Shear Strength 89.5 psi**
**Limit Pressure 429 psi**

shift 0

**In Situ Engineering**

# Appendix I - Pressuremeter Data and Standard Interpretation

**PRESSUREMETER DATA** **CH2MHill, Inc.**

**CALTRANS I-710 North Tunnel Project** **2/4/2009**

**Hole No. Z2-B2** **Depth 251ft** **File C:\DATA\ISE-812\SR710-25.P**

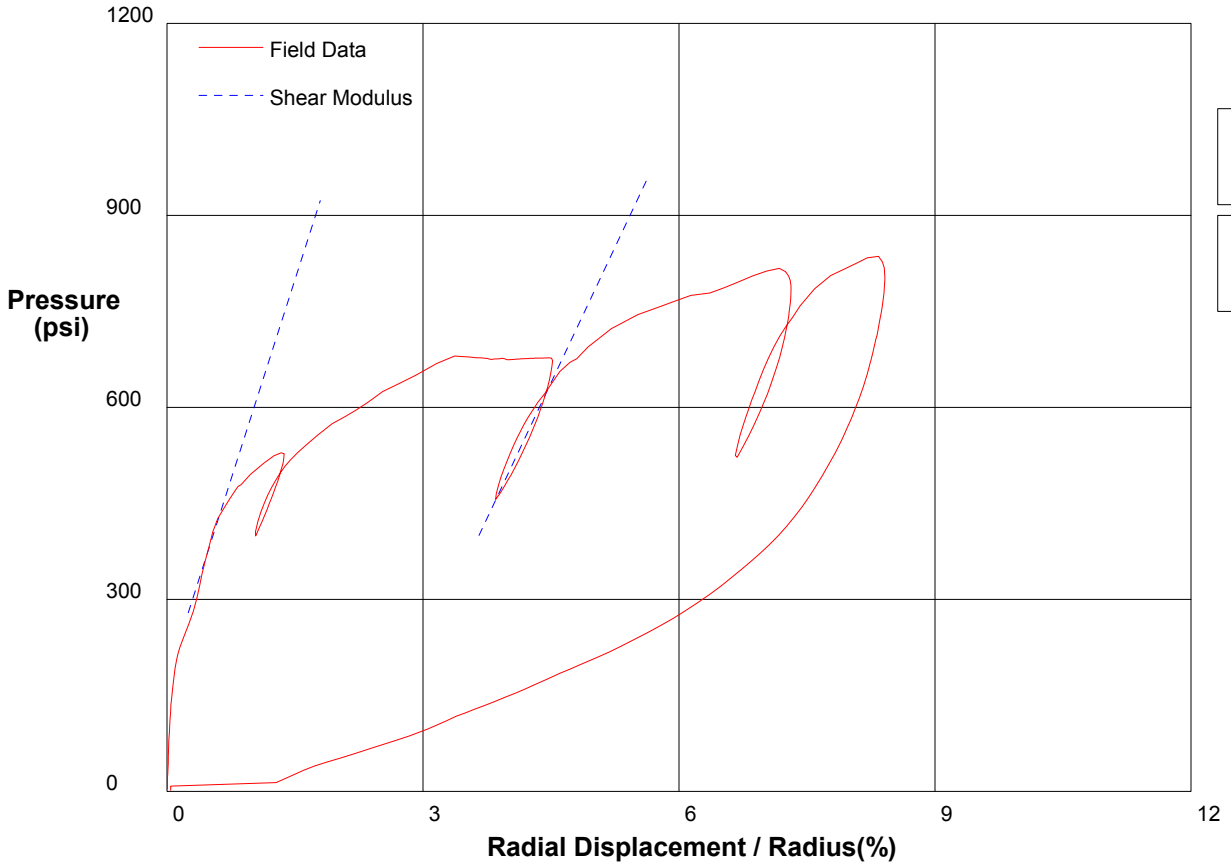


**Shear Modulus 14120 psi**

**Shear Modulus 20808 psi**

shift 0

**In Situ Engineering**

# Appendix I - Pressuremeter Data and Standard Interpretation

**PRESSUREMETER DATA** **CH2M-HILL, Inc.**

**CALTRANS I-710 North Tunnel Project** **2/4/2009**

**Hole No. Z2-B2** **Depth 251ft** **File C:\DATA\ISE-812\SR710-25.P**

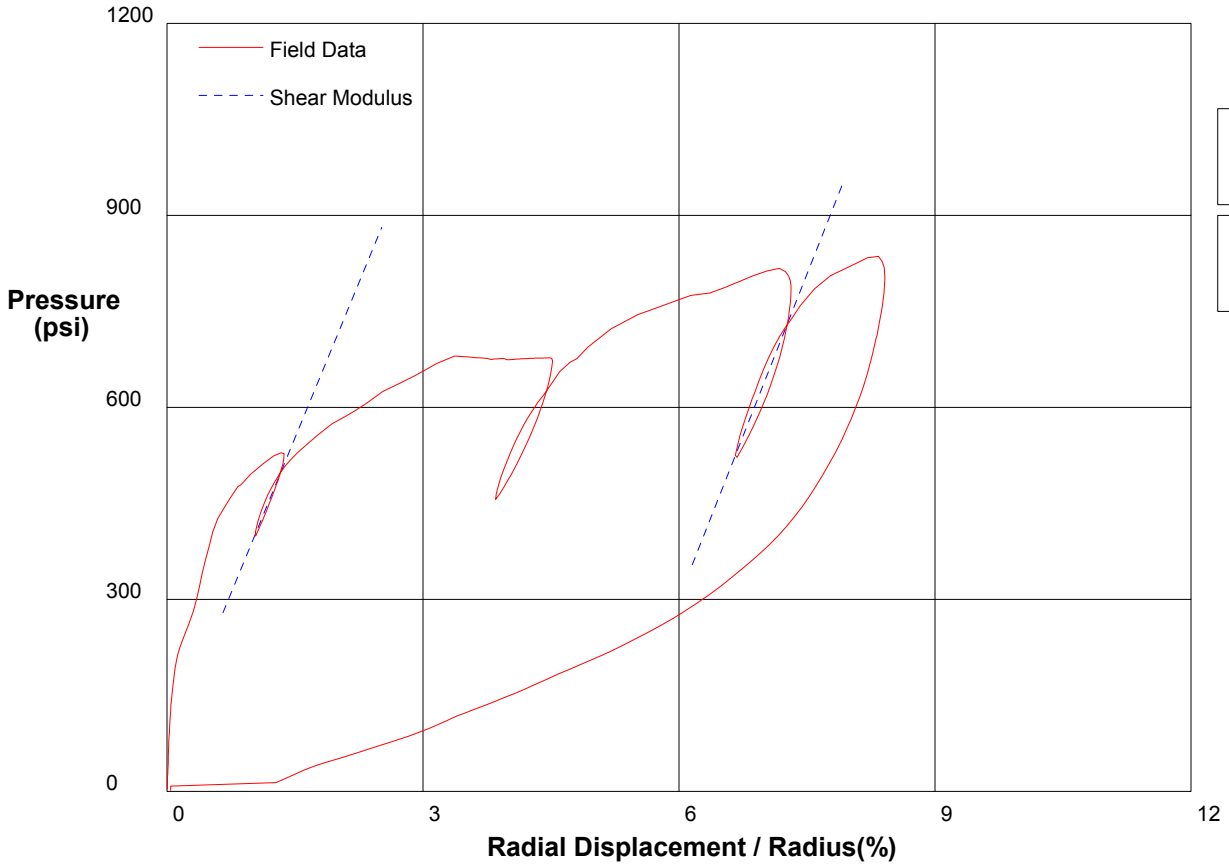


**Shear Modulus 16904 psi**

**Shear Modulus 16190 psi**

shift 0

**In Situ Engineering**

# Appendix I - Pressuremeter Data and Standard Interpretation

**PRESSUREMETER DATA** **CH2M-HILL, Inc.**

**CALTRANS I-710 North Tunnel Project** **2/4/2009**

**Hole No. Z2-B2** **Depth 251ft** **File C:\DATA\ISE-812\SR710-25.P**

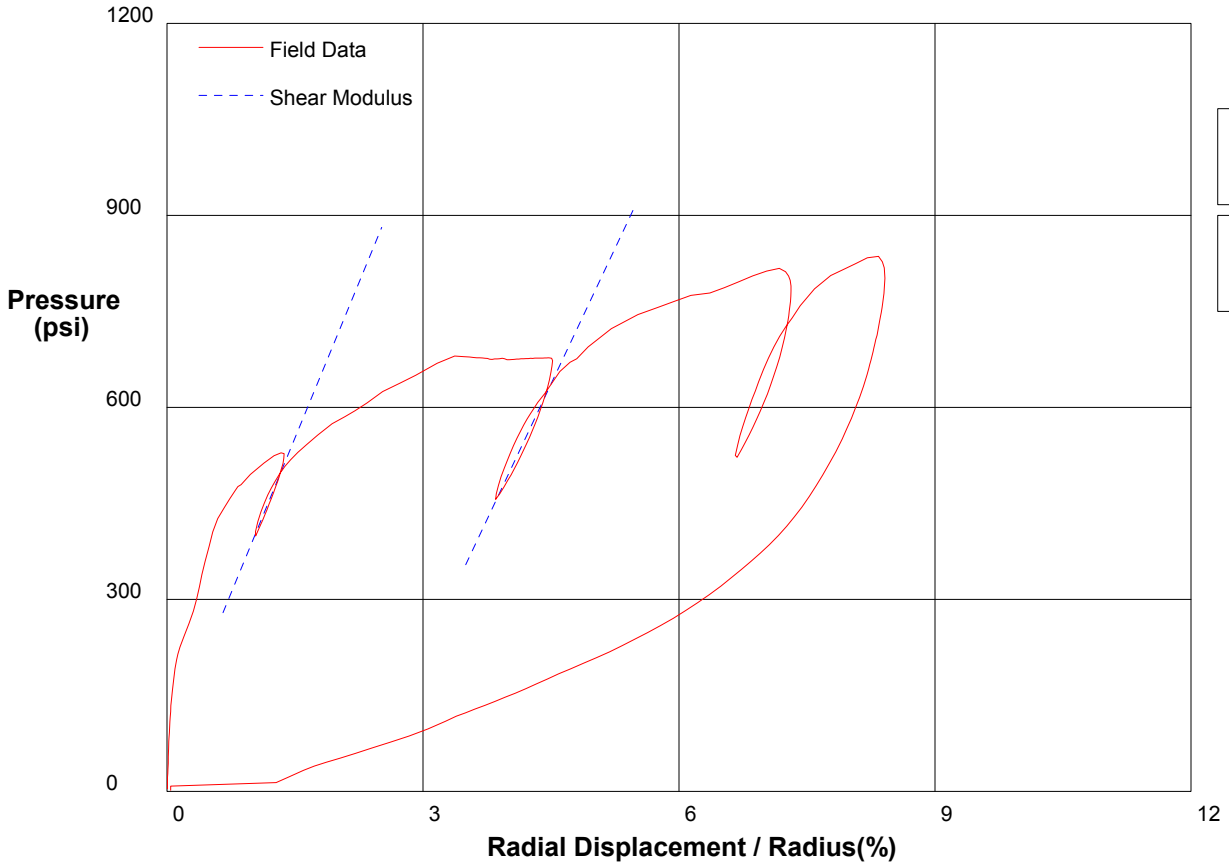


**Shear Modulus 14120 psi**

**Shear Modulus 16190 psi**

shift 0

**In Situ Engineering**

# Appendix I - Pressuremeter Data and Standard Interpretation

**PRESSUREMETER DATA** **CH2MHill, Inc.**

**CALTRANS I-710 North Tunnel Project** **2/4/2009**

**Hole No. Z2-B2** **Depth 251ft** **File C:\DATA\ISE-812\SR710-25.P**

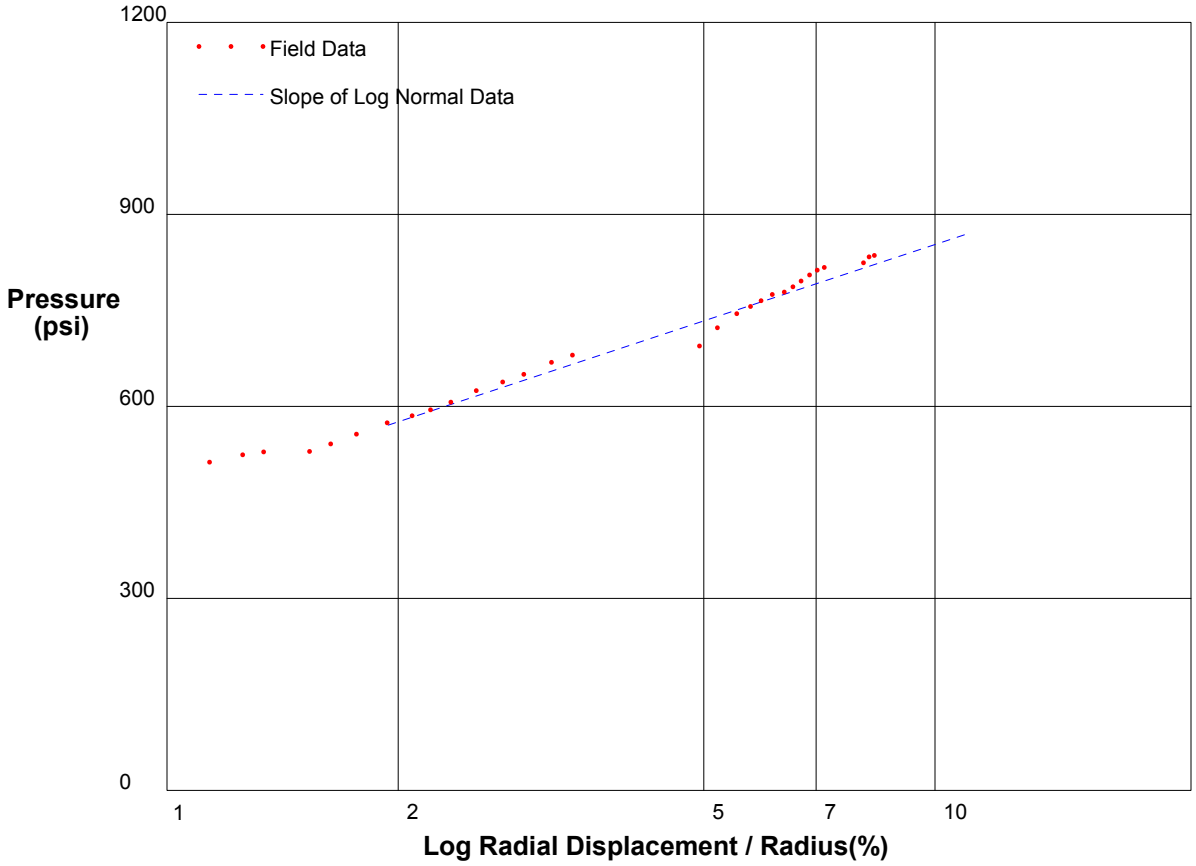


**Shear Strength 172.1 psi**
**Limit Pressure 1095 psi**

shift 0

**In Situ Engineering**

# Appendix I - Pressuremeter Data and Standard Interpretation

**PRESSUREMETER DATA** **CH2MHill, Inc.**

**CALTRANS I-710 North Tunnel Project** **2/4/2009**

**Hole No. Z2-B2** **Depth 249.5ft** **File C:\DATA\ISE-812\SR710-26.P**

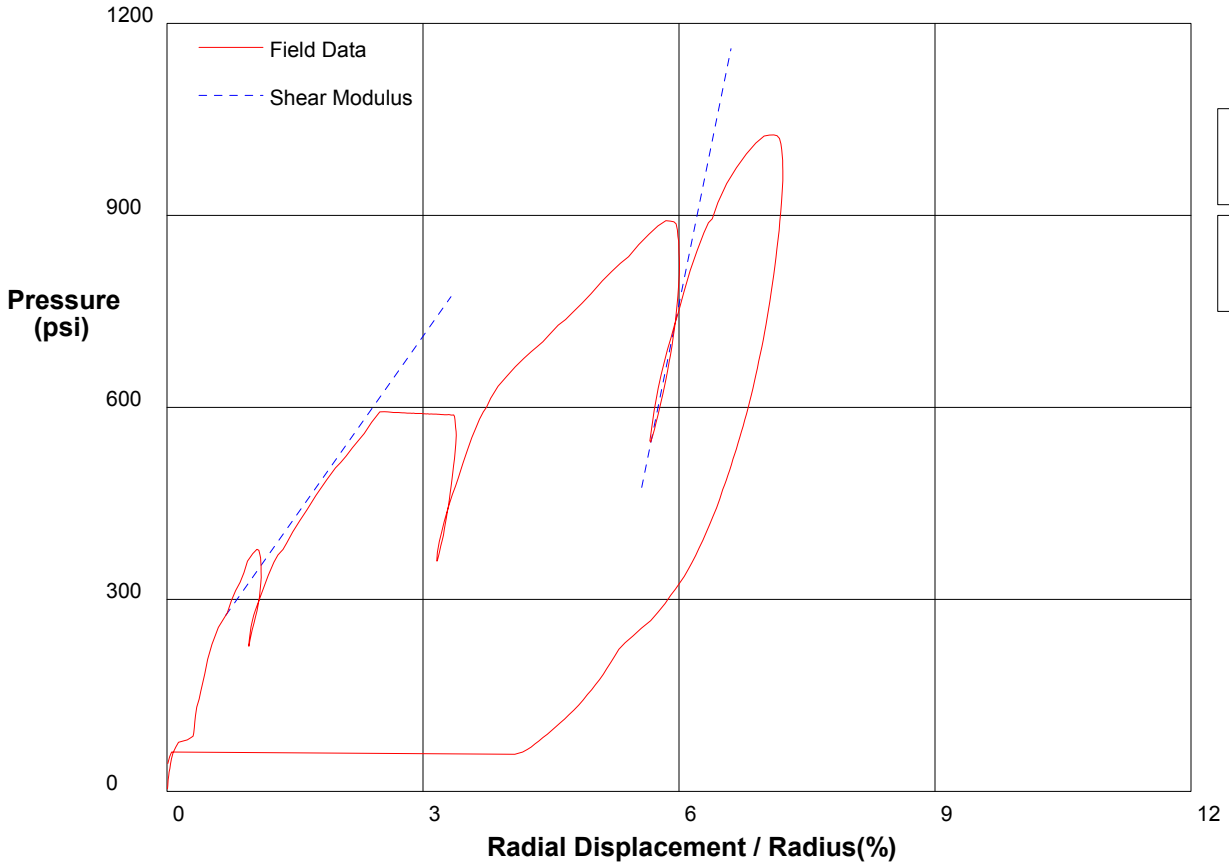


**Shear Modulus 32736 psi**

**Shear Modulus 9428 psi**

shift 0

**In Situ Engineering**

# Appendix I - Pressuremeter Data and Standard Interpretation

**PRESSUREMETER DATA** **CH2M-HILL, Inc.**

**CALTRANS I-710 North Tunnel Project** **2/4/2009**

**Hole No. Z2-B2** **Depth 249.5ft** **File C:\DATA\ISE-812\SR710-26.P**

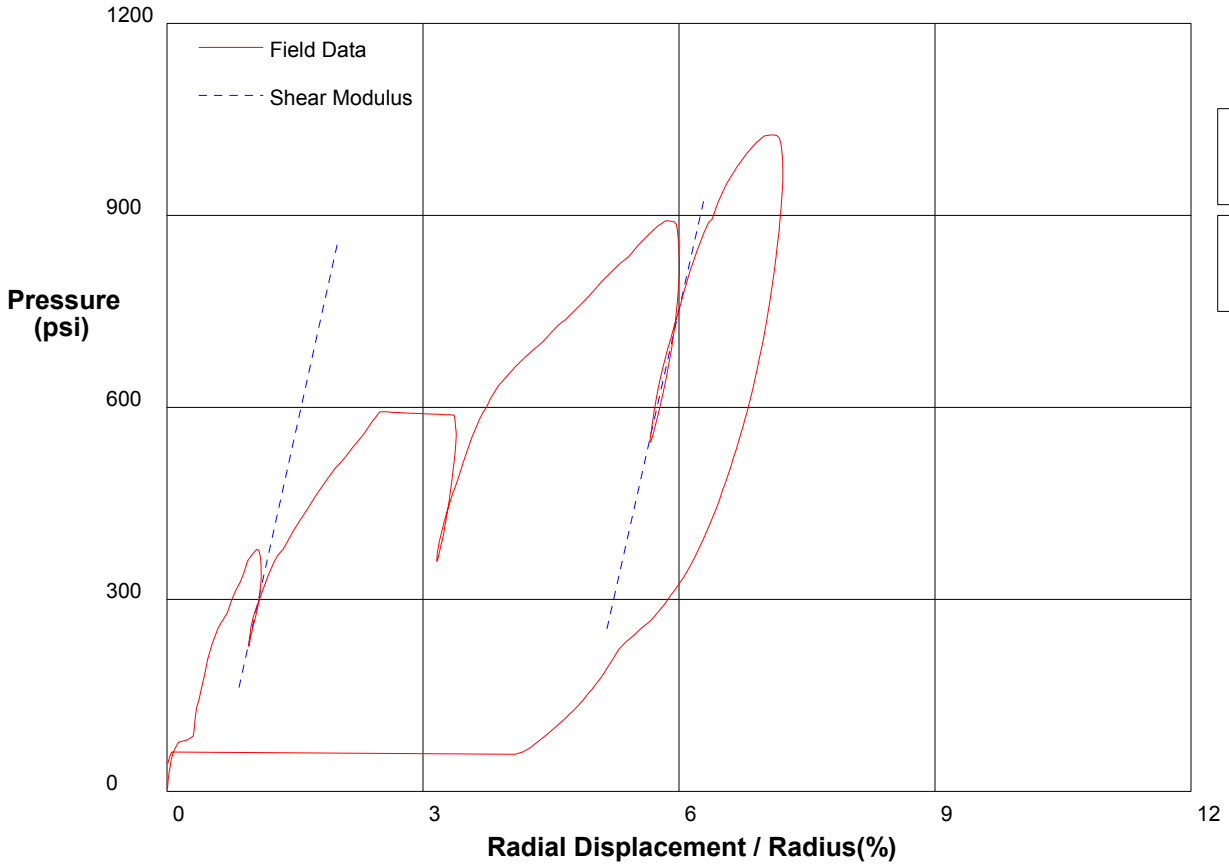


**Shear Modulus 29497 psi**

**Shear Modulus 30090 psi**

shift 0

**In Situ Engineering**

# Appendix I - Pressuremeter Data and Standard Interpretation

**PRESSUREMETER DATA** **CH2M-HILL, Inc.**

**CALTRANS I-710 North Tunnel Project** **2/4/2009**

**Hole No. Z2-B2** **Depth 249.5ft** **File C:\DATA\ISE-812\SR710-26.P**

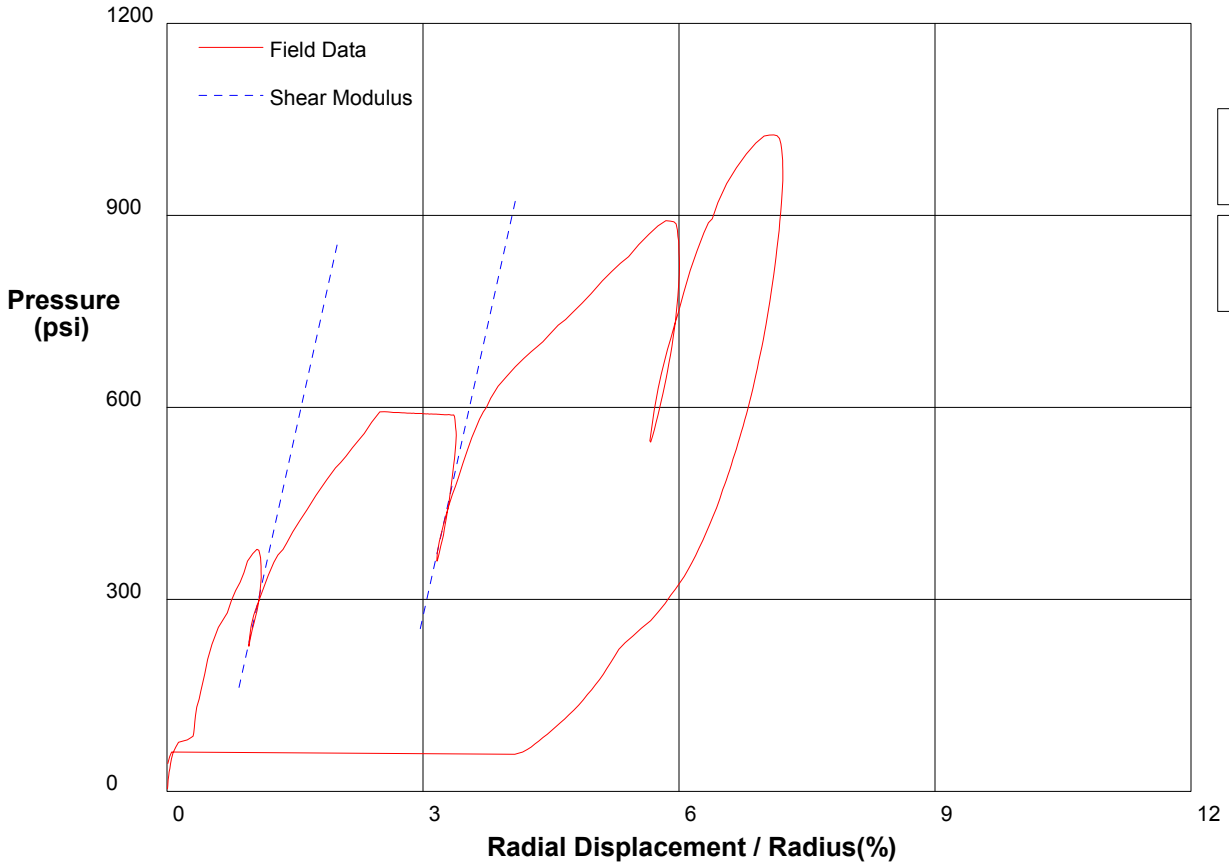


**Shear Modulus 30000 psi**

**Shear Modulus 30090 psi**

shift 0

**In Situ Engineering**

# Appendix I - Pressuremeter Data and Standard Interpretation

**PRESSUREMETER DATA** **CH2MHill, Inc.**

**CALTRANS I-710 North Tunnel Project** **2/4/2009**

**Hole No. Z2-B2** **Depth 249.5ft** **File C:\DATA\ISE-812\SR710-26.P**

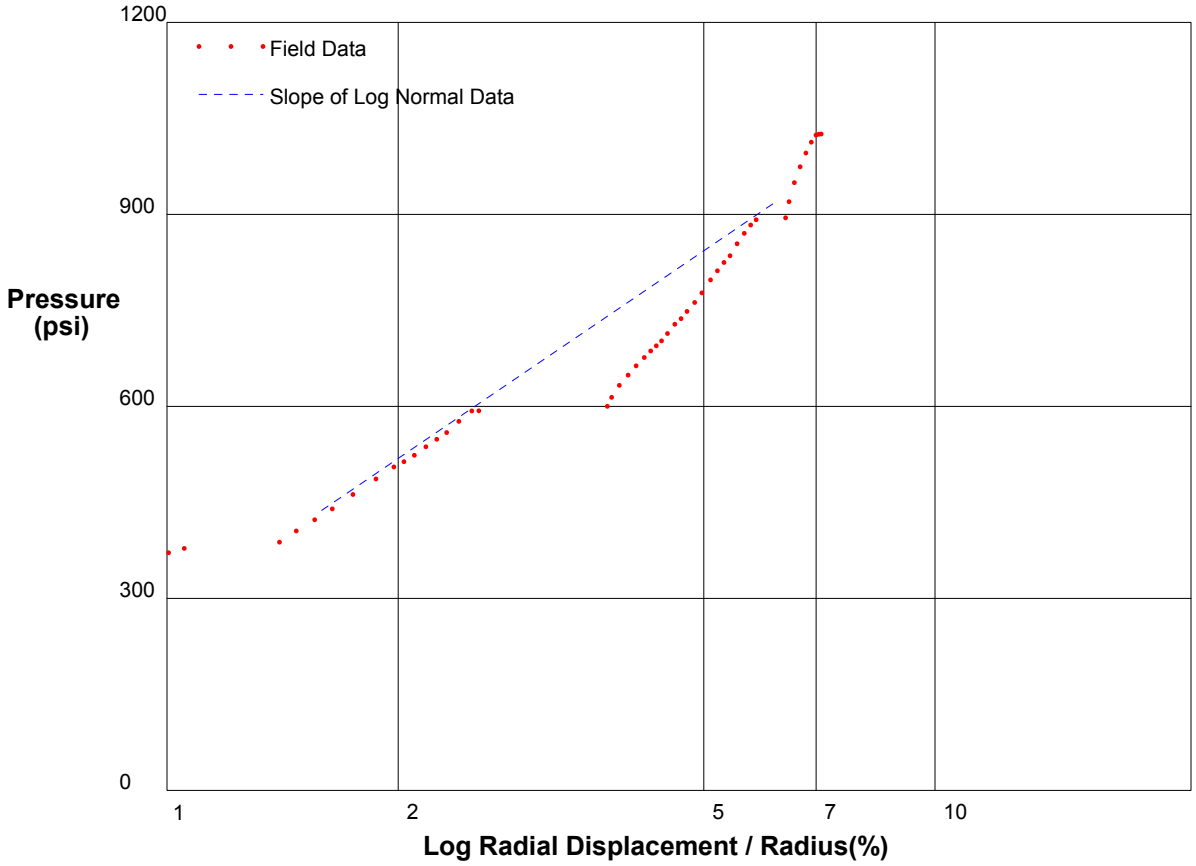


**Shear Strength 354 psi**
**Limit Pressure 1588 psi**

shift 0

**In Situ Engineering**

# Appendix I - Pressuremeter Data and Standard Interpretation

**PRESSUREMETER DATA** **CH2M-HILL, Inc.**

**CALTRANS I-710 North Tunnel Project** **2/4/2009**

**Hole No. Z1-B6** **Depth 203ft** **File C:\DATA\ISE-812\SR710-27.P**

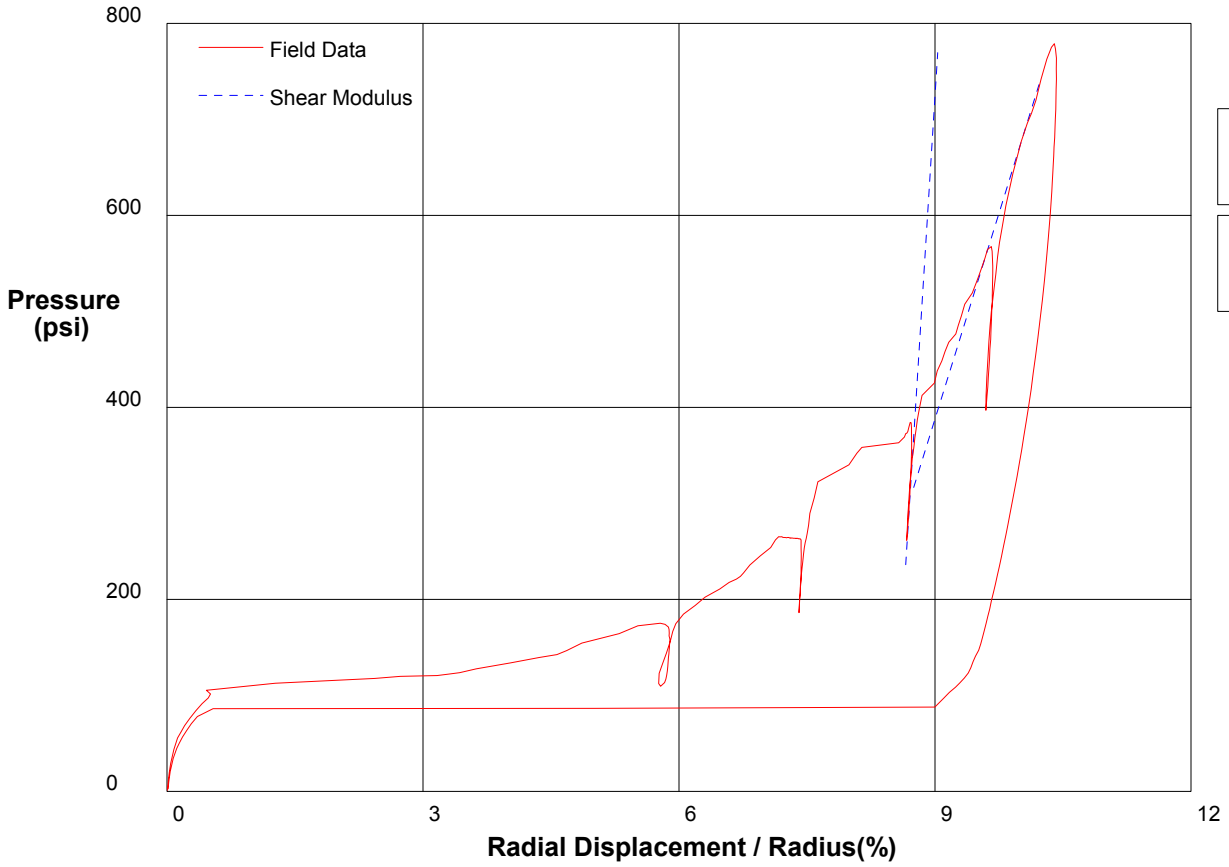


**Shear Modulus 14278 psi**

**Shear Modulus 71111 psi**

shift 0

**In Situ Engineering**

# Appendix I - Pressuremeter Data and Standard Interpretation

**PRESSUREMETER DATA** **CH2M-HILL, Inc.**

**CALTRANS I-710 North Tunnel Project** **2/4/2009**

**Hole No. Z1-B6** **Depth 203ft** **File C:\DATA\ISE-812\SR710-27.P**

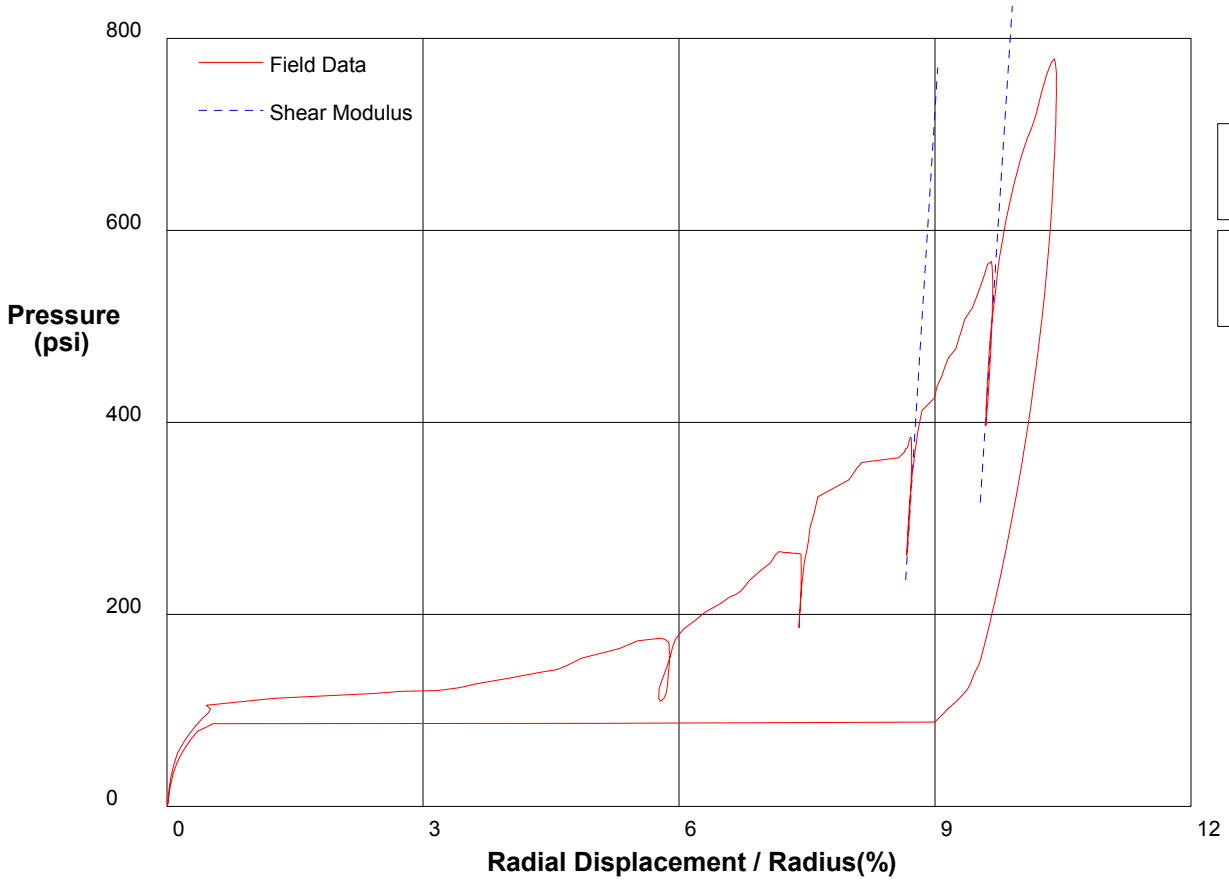


**Shear Modulus 68888 psi**

**Shear Modulus 71111 psi**

shift 0

**In Situ Engineering**

# Appendix I - Pressuremeter Data and Standard Interpretation

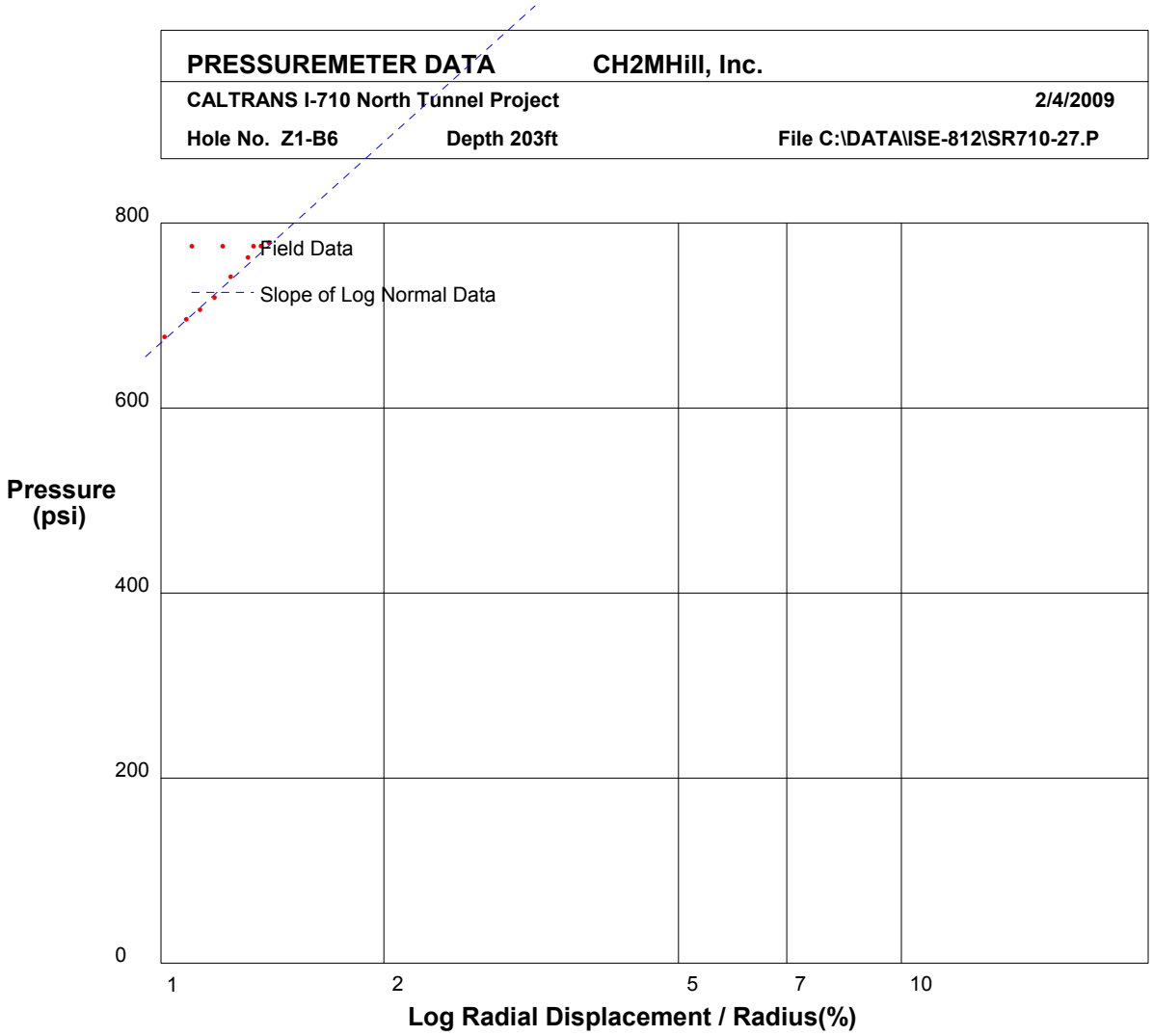


**Shear Strength 313 psi**
**Limit Pressure 1833 psi**

# Appendix I - Pressuremeter Data and Standard Interpretation

**PRESSUREMETER DATA** **CH2MHill, Inc.**

**CALTRANS I-710 North Tunnel Project** **2/5/2009**

**Hole No. Z1-B6** **Depth 245ft** **File C:\DATA\ISE-812\SR710-28.P**

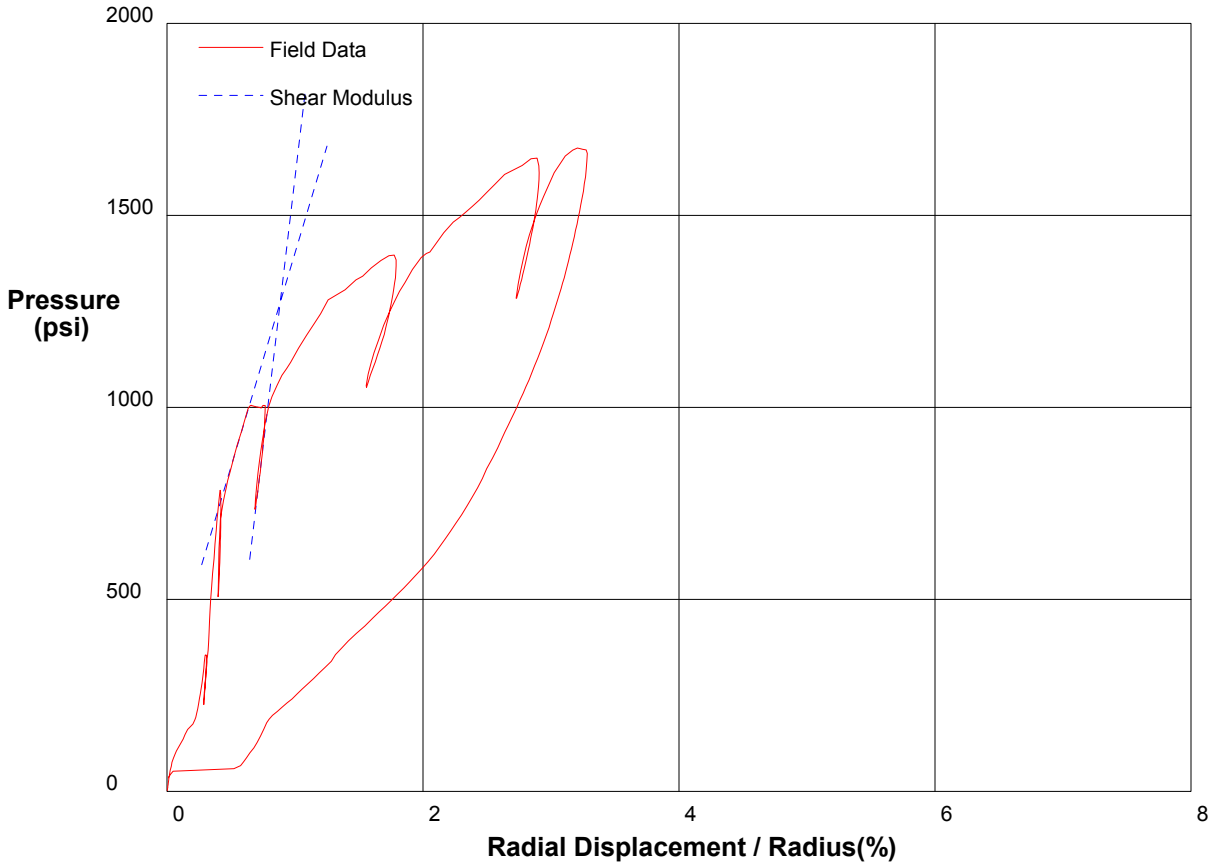


**Shear Modulus 140476 psi**

**Shear Modulus 55673 psi**

shift 0

**In Situ Engineering**

# Appendix I - Pressuremeter Data and Standard Interpretation

**PRESSUREMETER DATA** **CH2M-HILL, Inc.**

**CALTRANS I-710 North Tunnel Project** **2/5/2009**

**Hole No. Z1-B6** **Depth 245ft** **File C:\DATA\ISE-812\SR710-28.P**

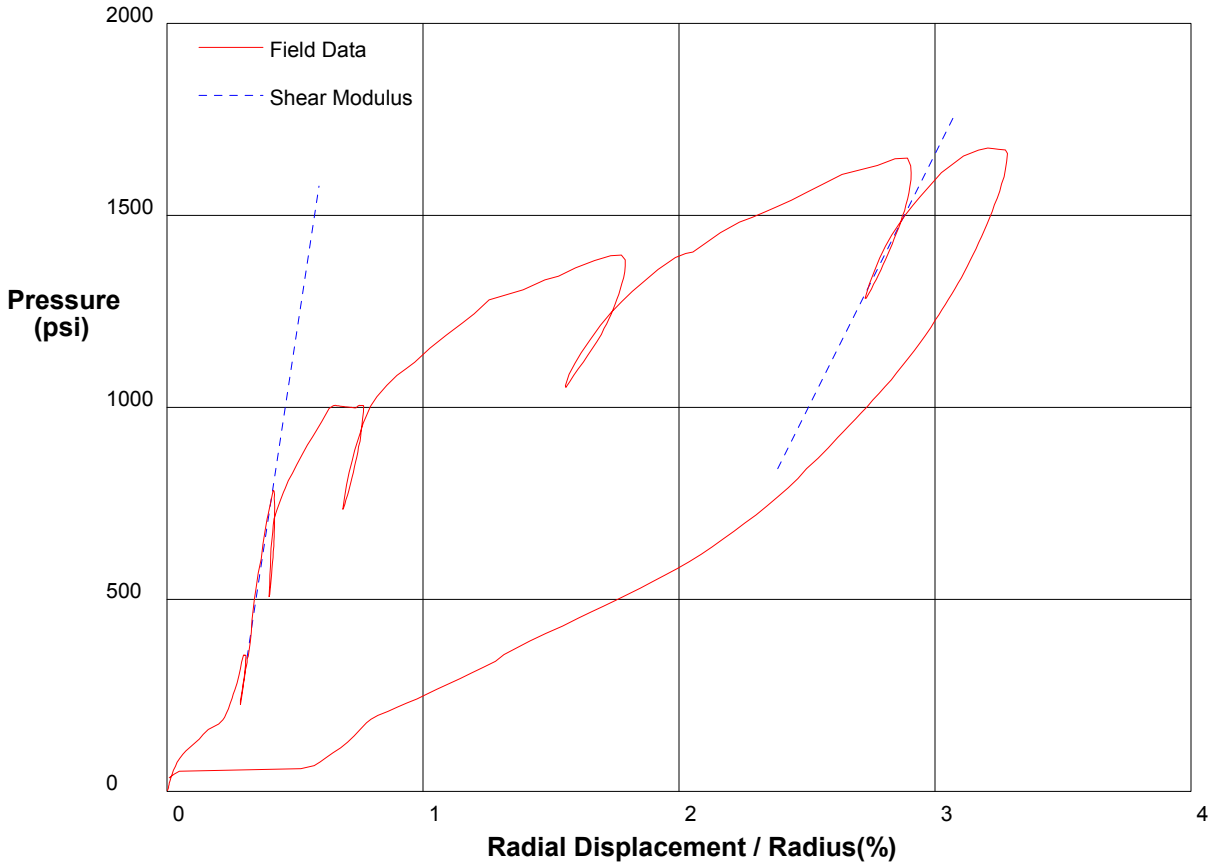


**Shear Modulus 66666 psi**

**Shear Modulus 218518 psi**

shift 0

**In Situ Engineering**

# Appendix I - Pressuremeter Data and Standard Interpretation

**PRESSUREMETER DATA** **CH2M-HILL, Inc.**

**CALTRANS I-710 North Tunnel Project** **2/5/2009**

**Hole No. Z1-B6** **Depth 245ft** **File C:\DATA\ISE-812\SR710-28.P**

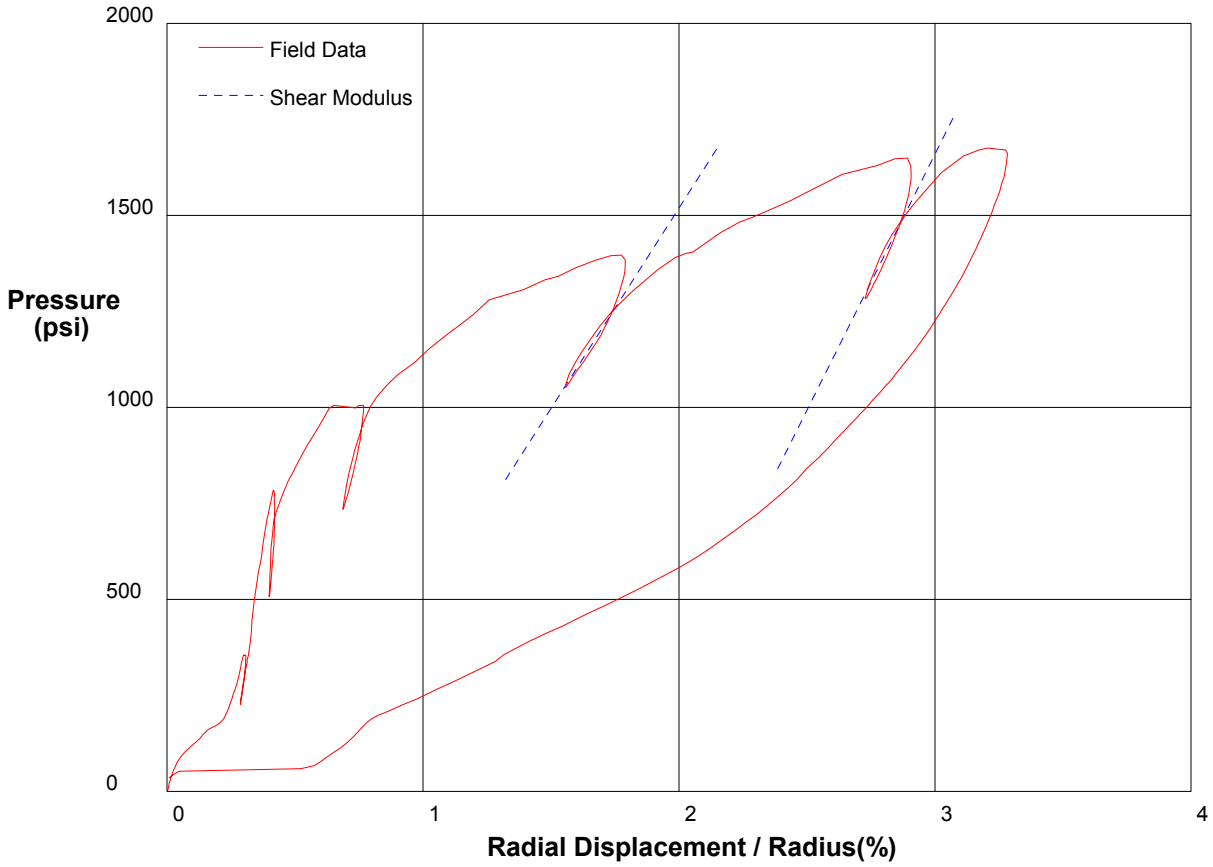


**Shear Modulus 66666 psi**

**Shear Modulus 52201 psi**

shift 0

**In Situ Engineering**

# Appendix I - Pressuremeter Data and Standard Interpretation

**PRESSUREMETER DATA** **CH2M-HILL, Inc.**

**CALTRANS I-710 North Tunnel Project** **2/5/2009**

**Hole No. Z1-B6** **Depth 245ft** **File C:\DATA\ISE-812\SR710-28.P**

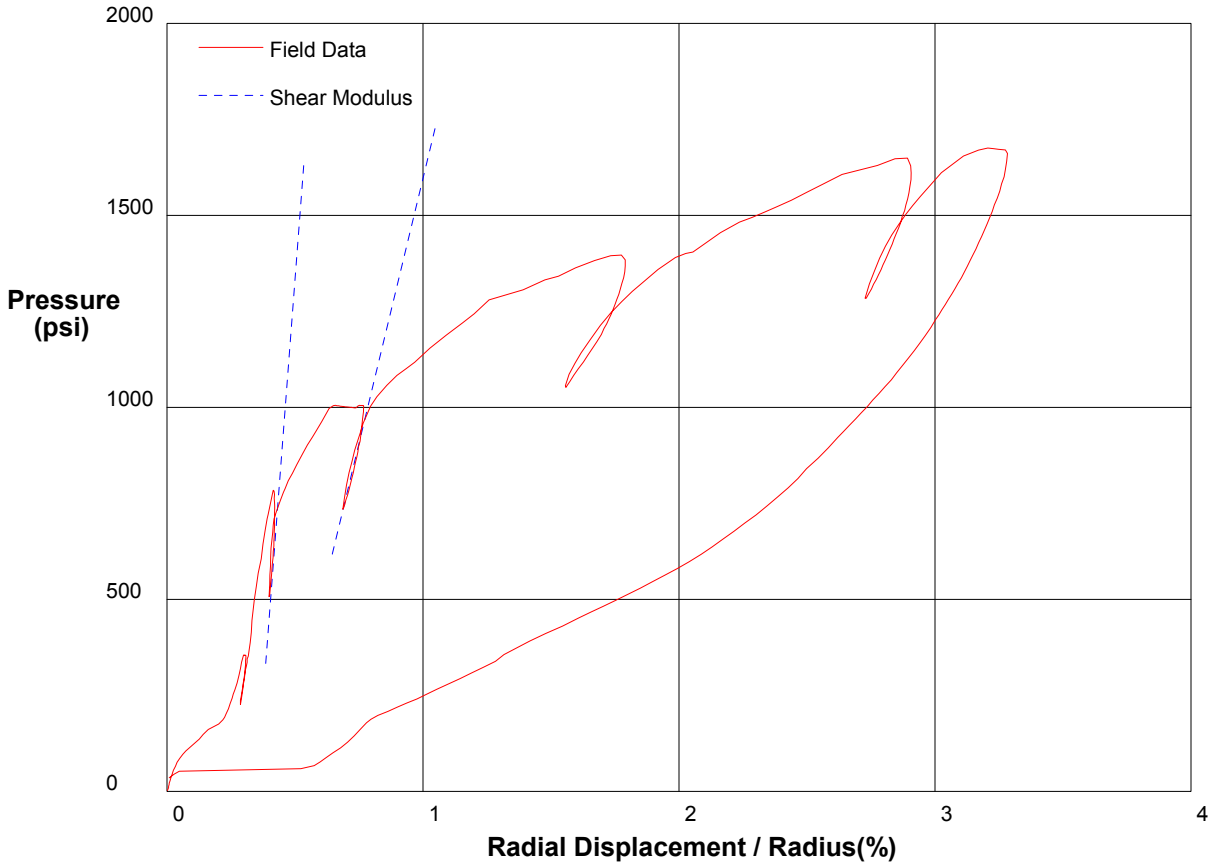


**Shear Modulus 138095 psi**

**Shear Modulus 435632 psi**

shift 0

**In Situ Engineering**

# Appendix I - Pressuremeter Data and Standard Interpretation

**PRESSUREMETER DATA** **CH2MHill, Inc.**

**CALTRANS I-710 North Tunnel Project** **2/5/2009**

**Hole No. Z1-B6** **Depth 245ft** **File C:\DATA\ISE-812\SR710-28.P**

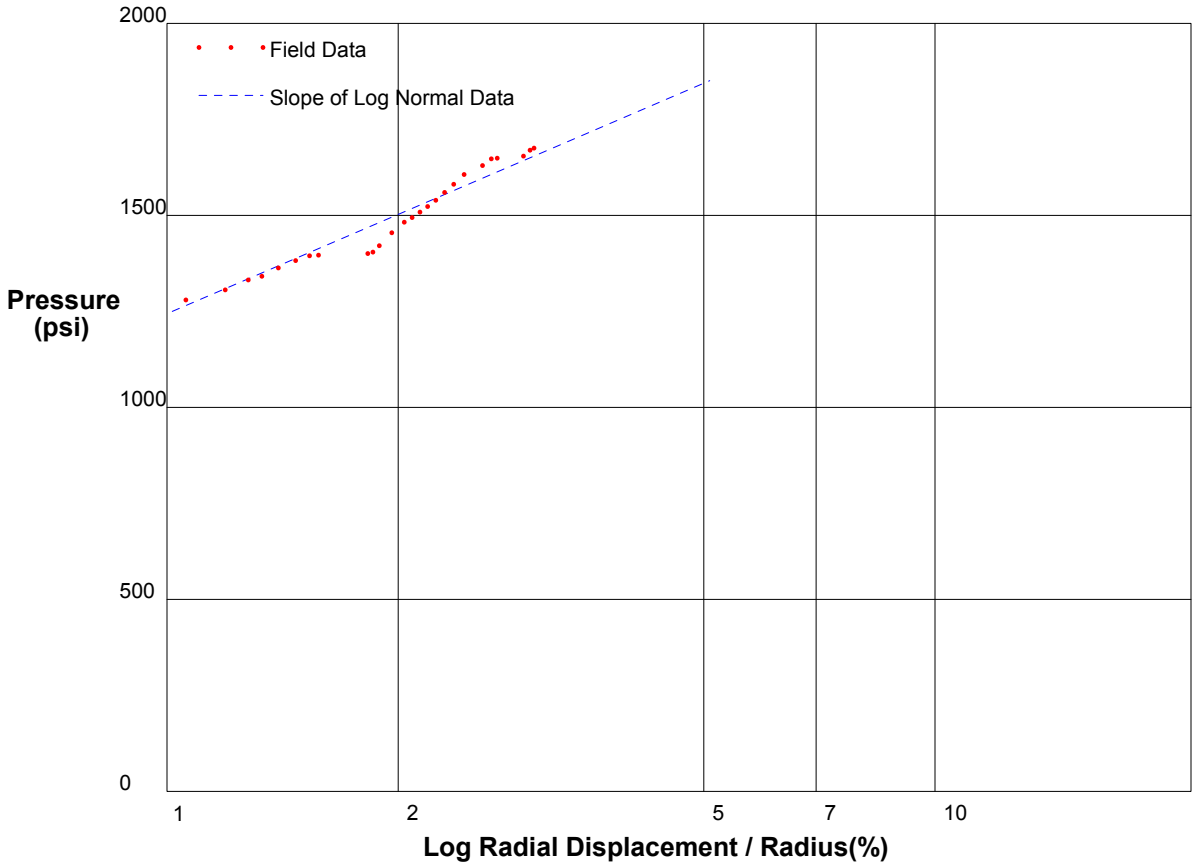


**Shear Strength 372.8 psi**
**Limit Pressure 2628 psi**

shift .2

**In Situ Engineering**

# Appendix I - Pressuremeter Data and Standard Interpretation

**PRESSUREMETER DATA** **CH2MHill, Inc.**

**CALTRANS I-710 North Tunnel Project** **2/6/2009**

**Hole No. Z3-B7** **Depth 225.8ft** **File C:\DATA\ISE-812\SR710-29.P**

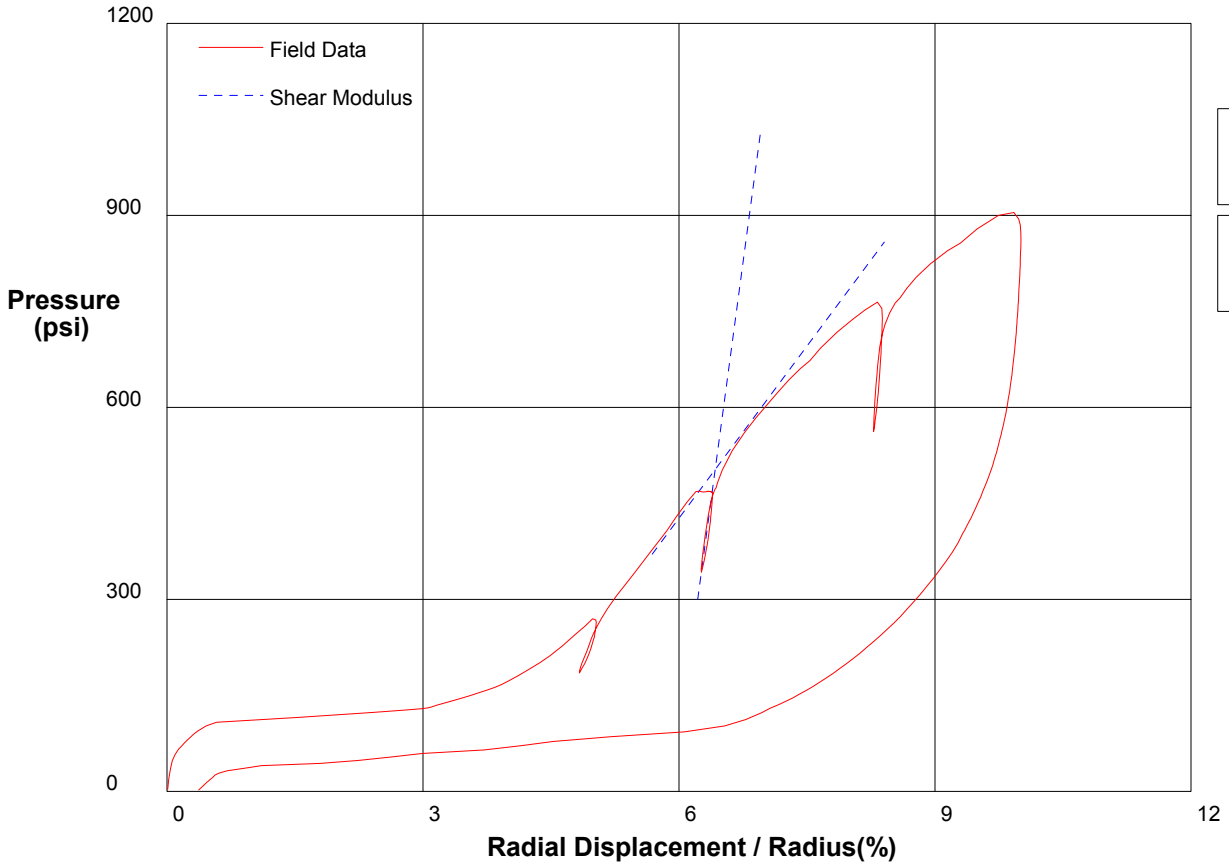


**Shear Modulus 49503 psi**

**Shear Modulus 8965 psi**

shift 0

**In Situ Engineering**

# Appendix I - Pressuremeter Data and Standard Interpretation

**PRESSUREMETER DATA** **CH2MHill, Inc.**

**CALTRANS I-710 North Tunnel Project** **2/6/2009**

**Hole No. Z3-B7** **Depth 225.8ft** **File C:\DATA\ISE-812\SR710-29.P**

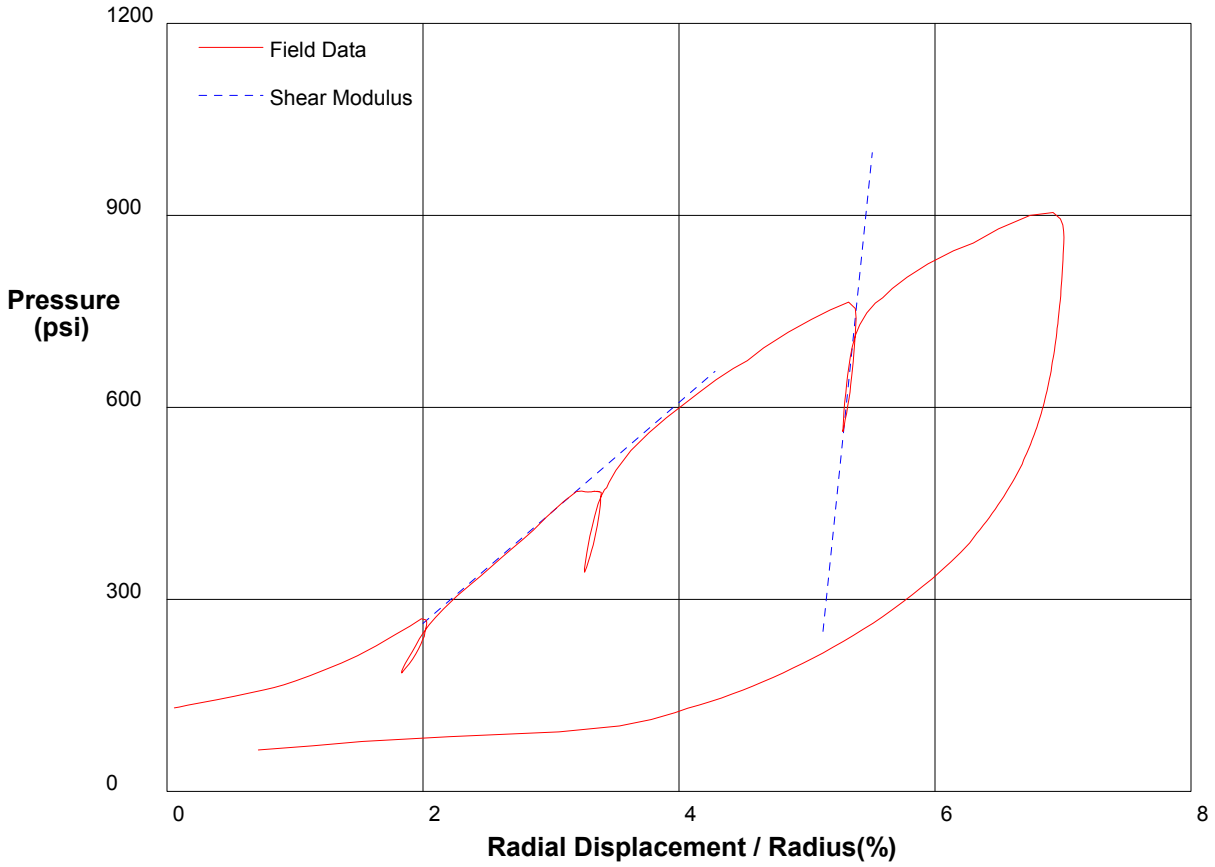


**Shear Modulus 97027 psi**

**Shear Modulus 8630 psi**

shift 3

**In Situ Engineering**

# Appendix I - Pressuremeter Data and Standard Interpretation

**PRESSUREMETER DATA** **CH2MHill, Inc.**

**CALTRANS I-710 North Tunnel Project** **2/6/2009**

**Hole No. Z3-B7** **Depth 225.8ft** **File C:\DATA\ISE-812\SR710-29.P**

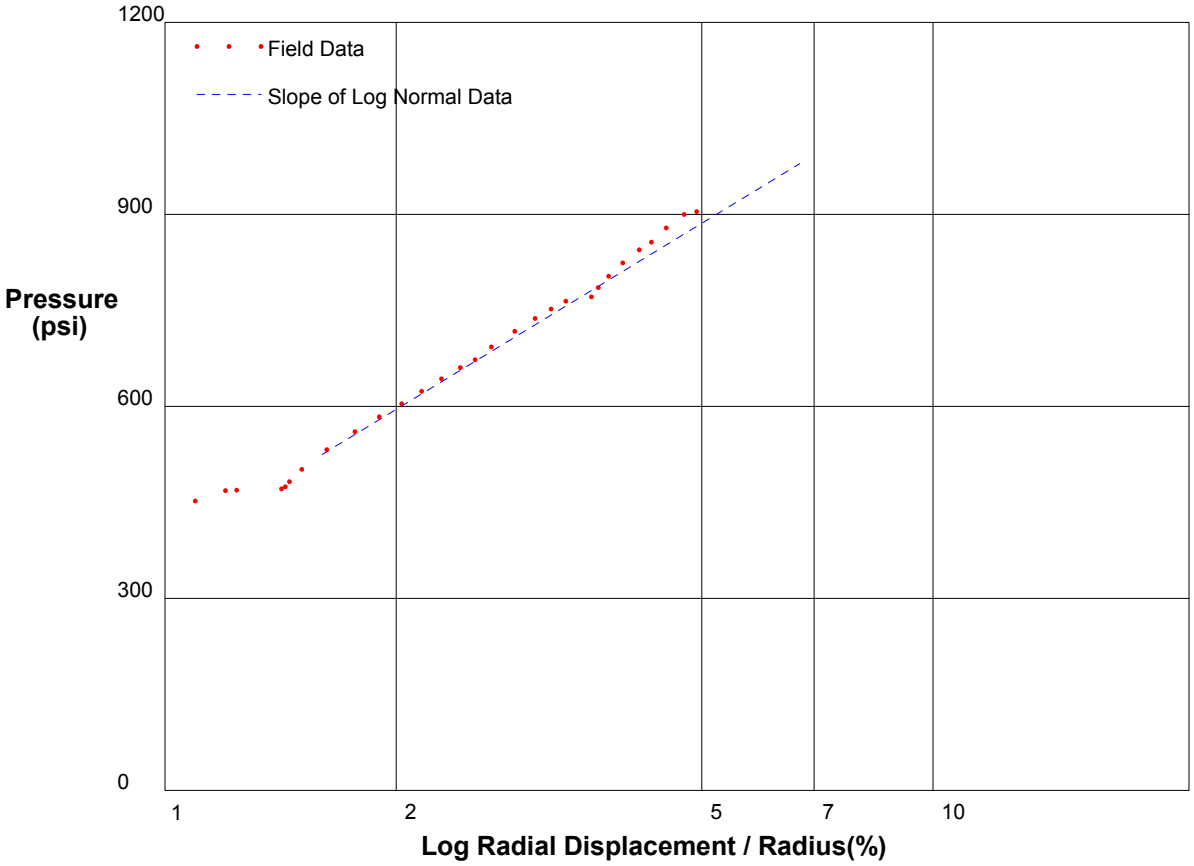


**Shear Strength 317.3 psi**
**Limit Pressure 1553 psi**

shift 5

**In Situ Engineering**

# Appendix I - Pressuremeter Data and Standard Interpretation

**PRESSUREMETER DATA** **CH2MHill, Inc.**

**CALTRANS I-710 North Tunnel Project** **2/6/2009**

**Hole No. Z3-B7** **Depth 224.3ft** **File C:\DATA\ISE-812\SR710-30.P**

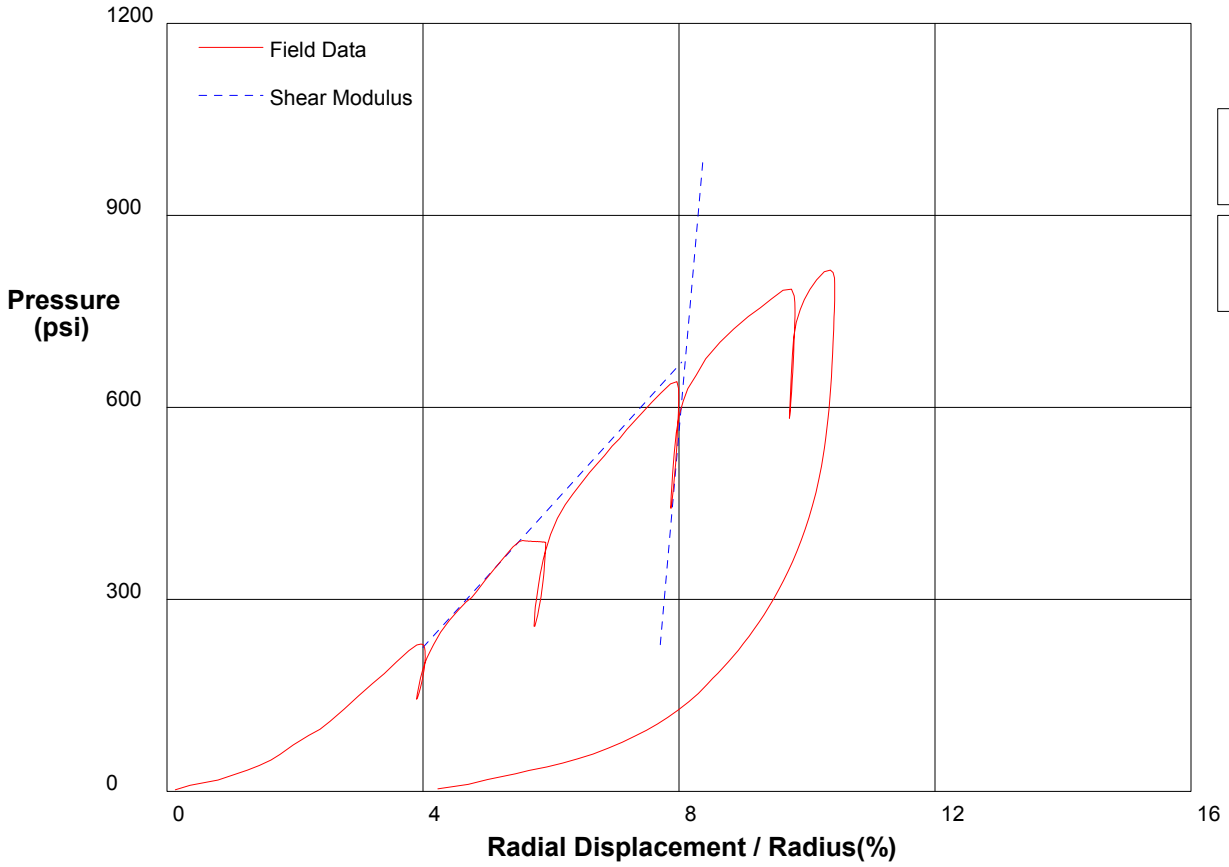


**Shear Modulus 56875 psi**

**Shear Modulus 5515 psi**

shift 0

**In Situ Engineering**

# Appendix I - Pressuremeter Data and Standard Interpretation

**PRESSUREMETER DATA** **CH2MHill, Inc.**

**CALTRANS I-710 North Tunnel Project** **2/6/2009**

**Hole No. Z3-B7** **Depth 224.3ft** **File C:\DATA\ISE-812\SR710-30.P**

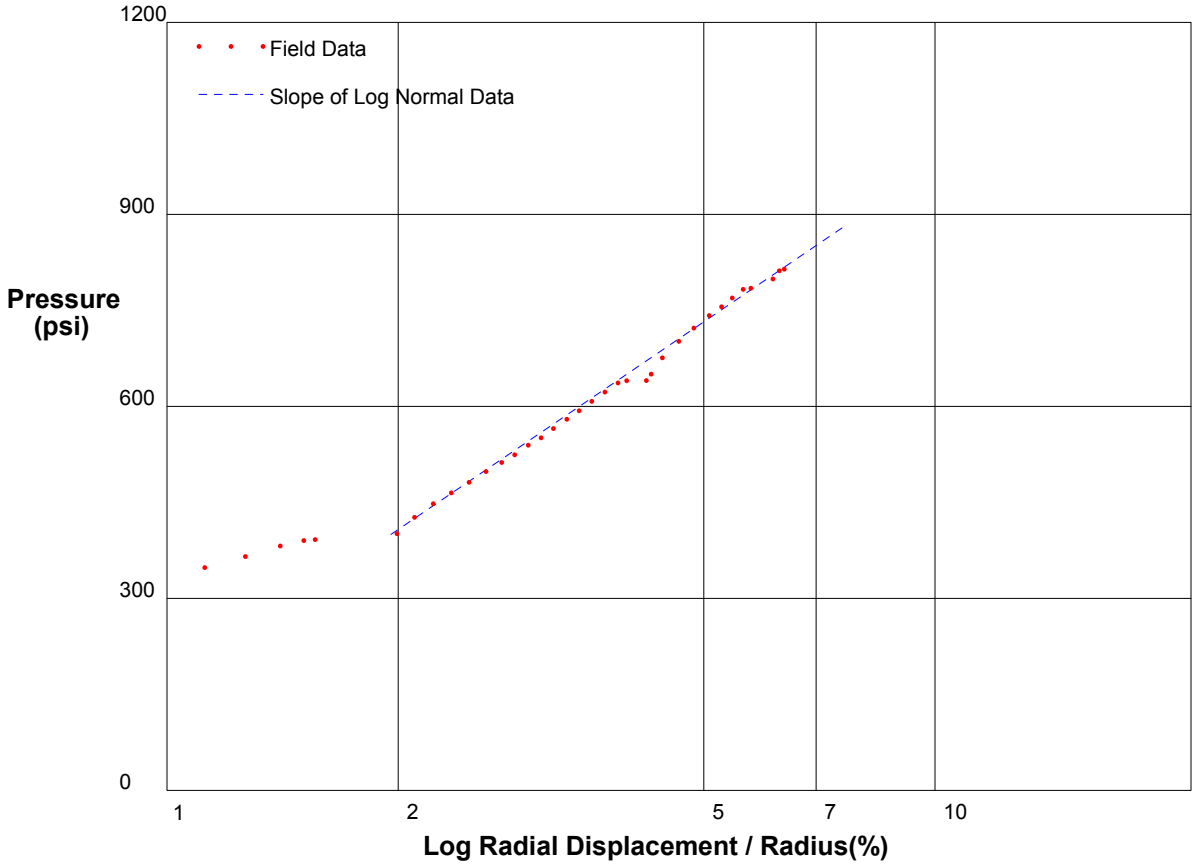


**Shear Strength 354 psi**
**Limit Pressure 1476 psi**

shift 4

**In Situ Engineering**

# Appendix I - Pressuremeter Data and Standard Interpretation

**PRESSUREMETER DATA** **CH2MHill, Inc.**

**CALTRANS I-710 North Tunnel Project** **2/6/2009**

**Hole No. Z1-B6** **Depth 332ft** **File C:\DATA\ISE-812\SR710-31.P**

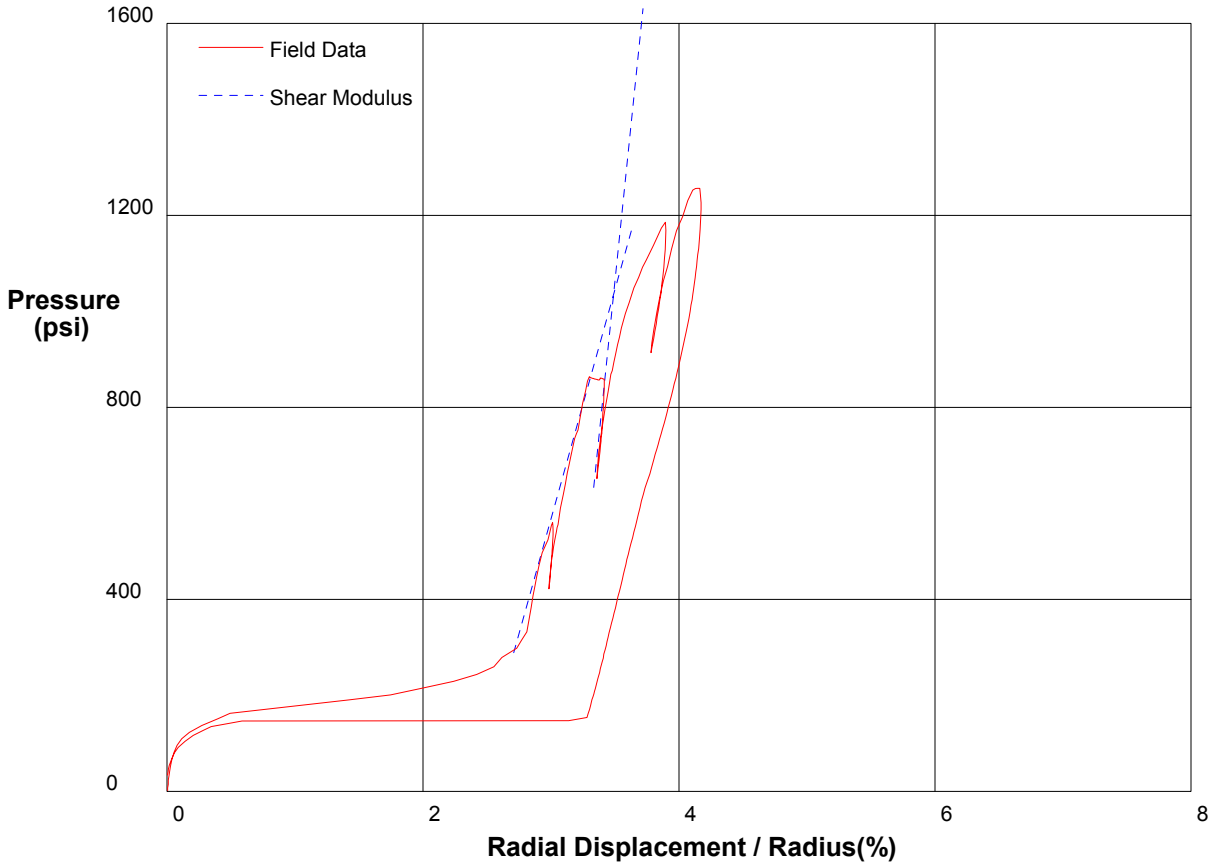


**Shear Modulus 129369 psi**

**Shear Modulus 47790 psi**

shift 0

**In Situ Engineering**

# Appendix I - Pressuremeter Data and Standard Interpretation

**PRESSUREMETER DATA** **CH2MHill, Inc.**

**CALTRANS I-710 North Tunnel Project** **2/6/2009**

**Hole No. Z1-B6** **Depth 332ft** **File C:\DATA\ISE-812\SR710-31.P**

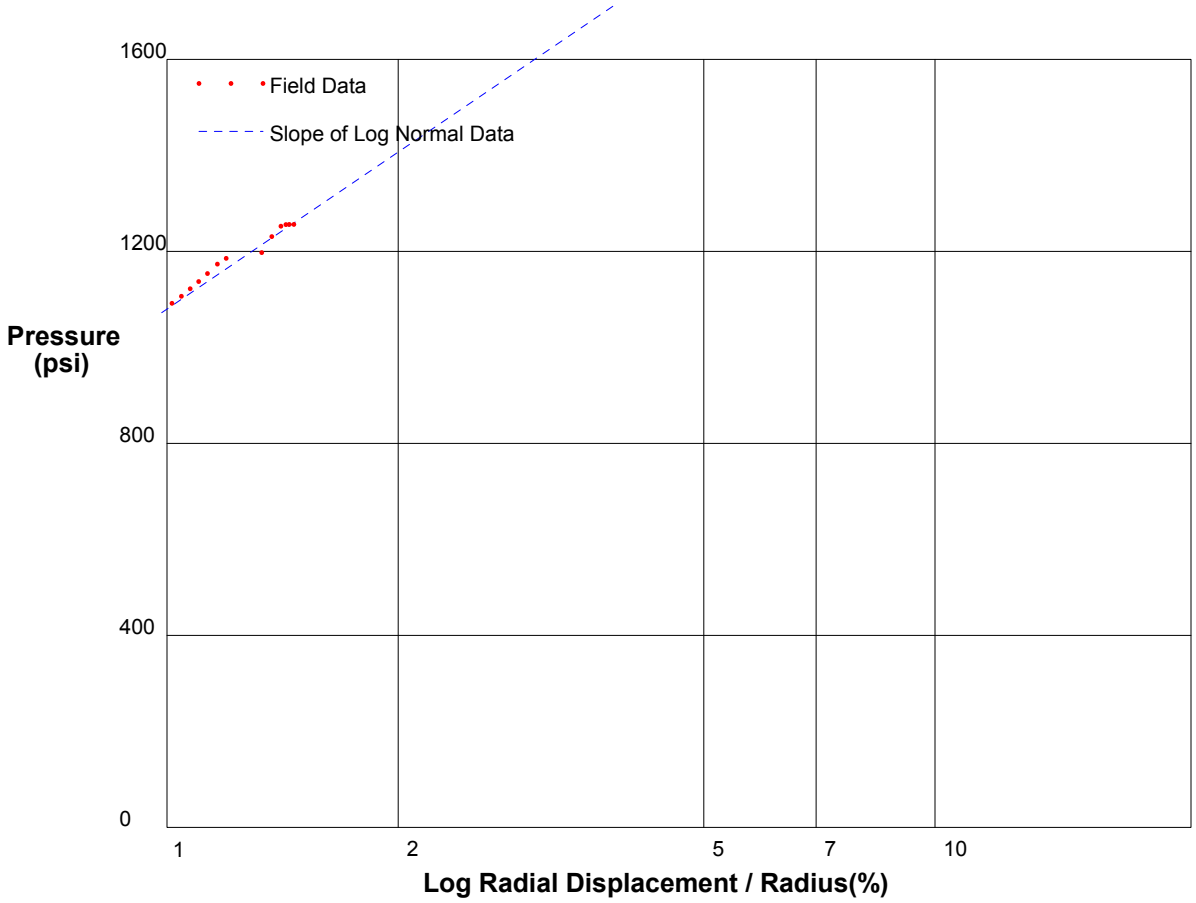


**Shear Strength 472 psi**
**Limit Pressure 2832 psi**

shift 2.7

**In Situ Engineering**

# Appendix I - Pressuremeter Data and Standard Interpretation

**PRESSUREMETER DATA** **CH2MHill, Inc.**

**CALTRANS I-710 North Tunnel Project** **2/6/2009**

**Hole No. Z1-B6** **Depth 330.5ft** **File C:\DATA\ISE-812\SR710-32.P**

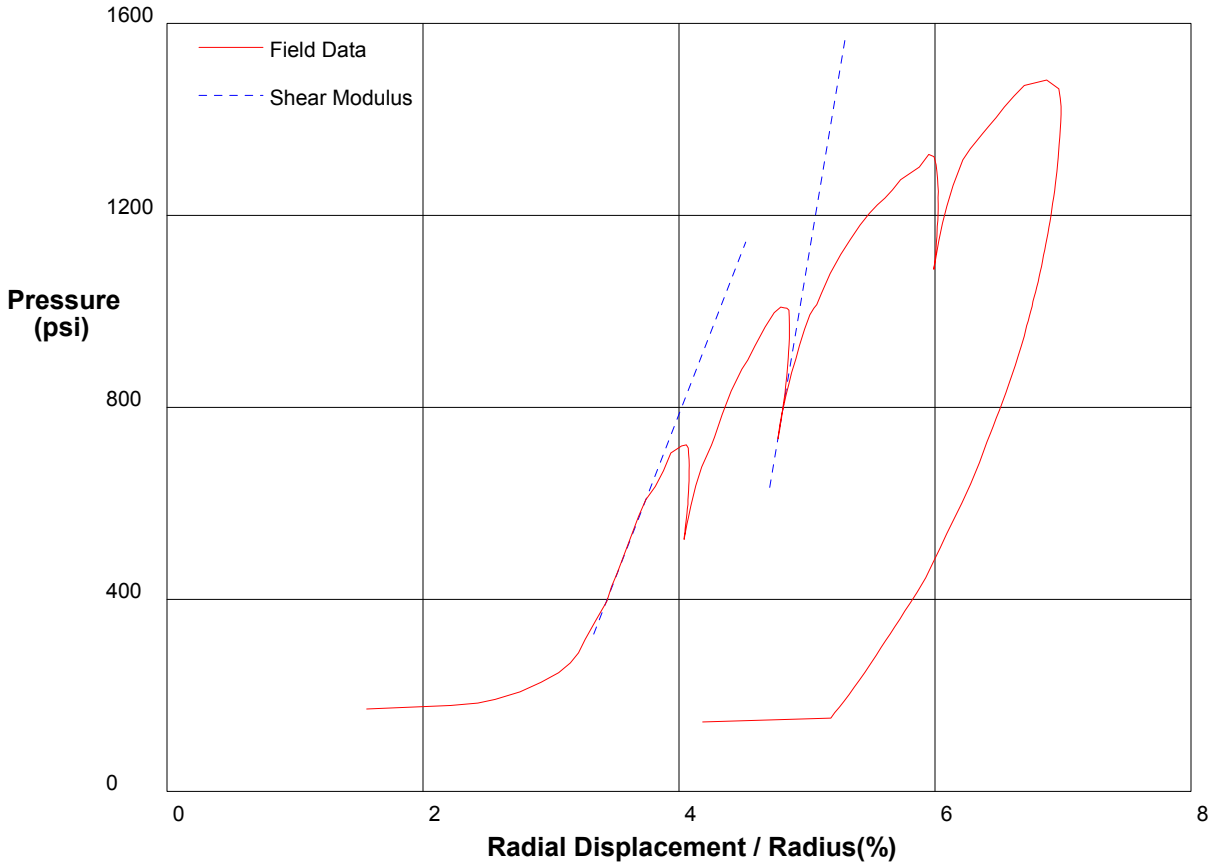


**Shear Modulus 79298 psi**

**Shear Modulus 34385 psi**

shift 4.7

**In Situ Engineering**

# Appendix I - Pressuremeter Data and Standard Interpretation

**PRESSUREMETER DATA** **CH2MHill, Inc.**

**CALTRANS I-710 North Tunnel Project** **2/6/2009**

**Hole No. Z1-B6** **Depth 330.5ft** **File C:\DATA\ISE-812\SR710-32.P**

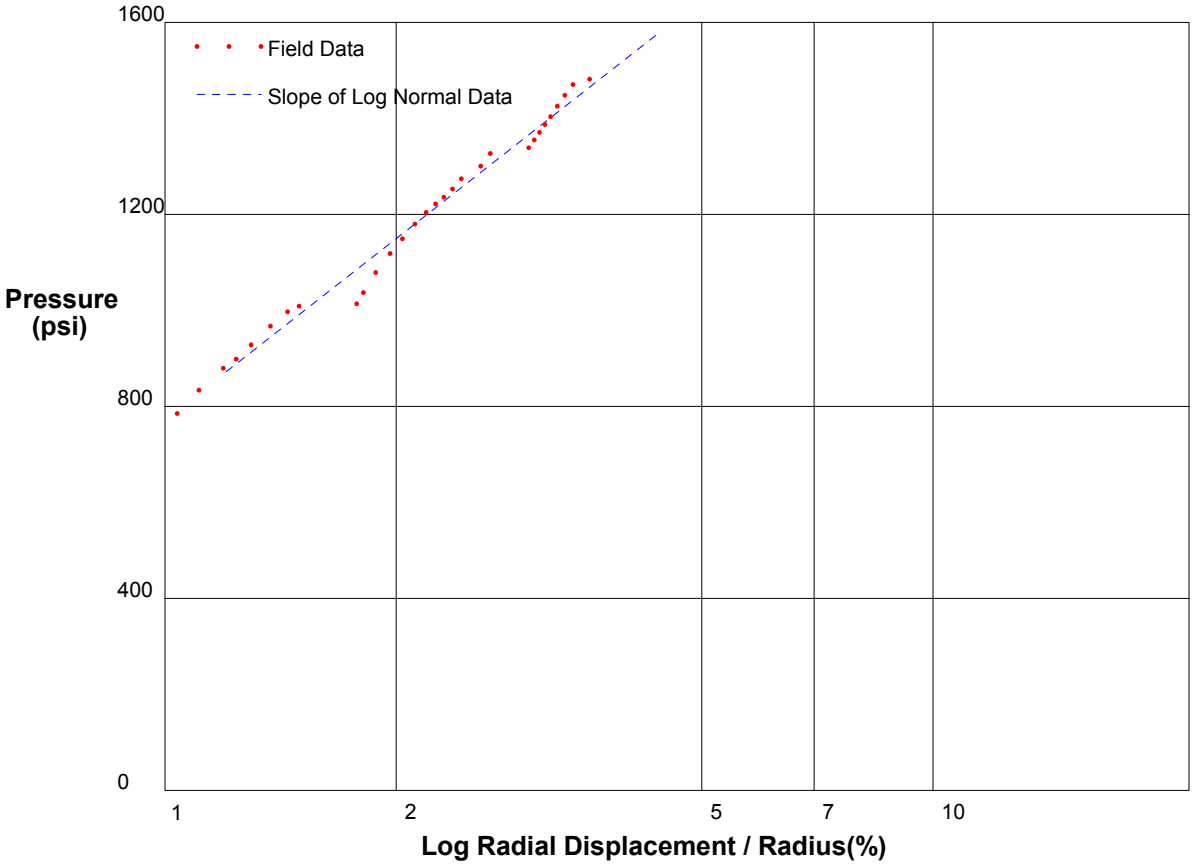


**Shear Strength 544.2 psi**
**Limit Pressure 2793 psi**

shift 8

**In Situ Engineering**

# Appendix I - Pressuremeter Data and Standard Interpretation

**PRESSUREMETER DATA** **CH2MHill, Inc.**

**CALTRANS I-710 North Tunnel Project** **2/10/2009**

**Hole No. Z3-B7** **Depth 252.5ft** **File C:\DATA\ISE-812\SR710-33.P**

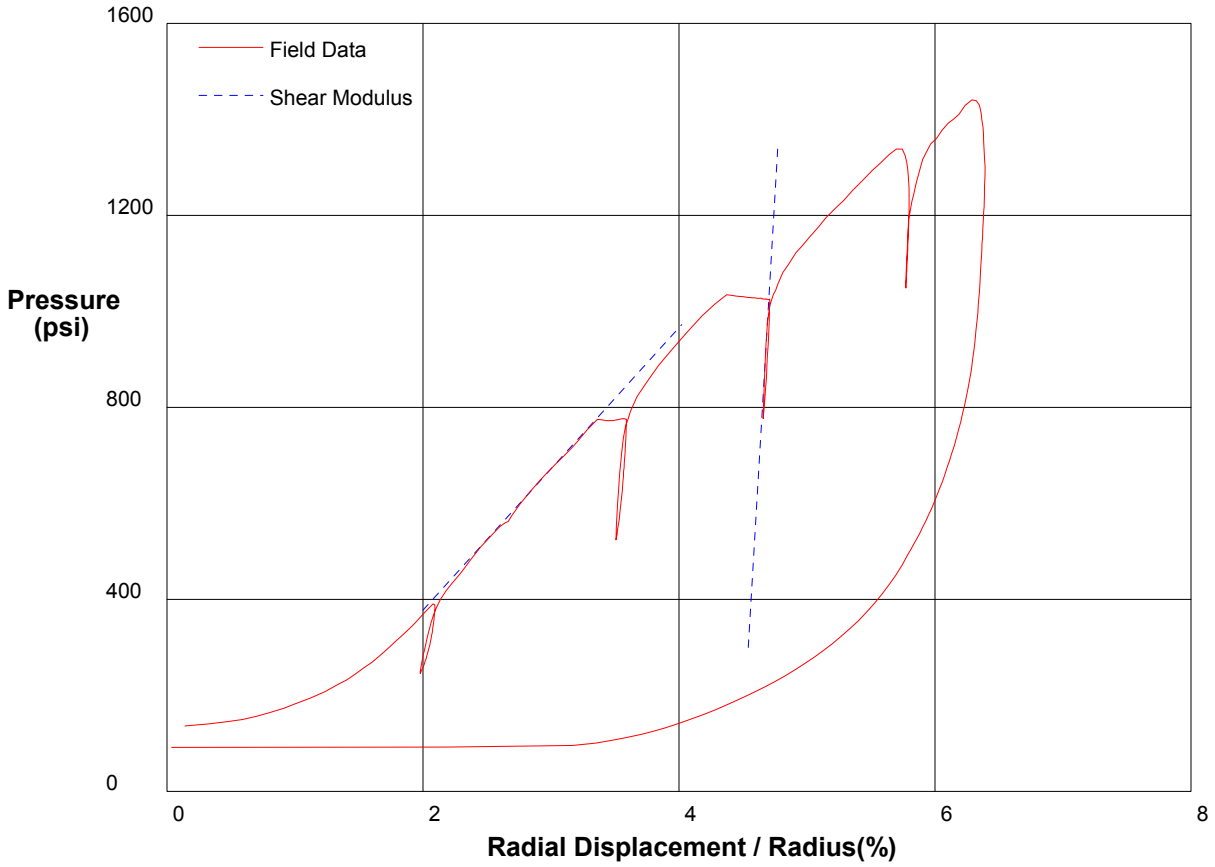


**Shear Modulus 226666 psi**

**Shear Modulus 14707 psi**

shift 4

**In Situ Engineering**

# Appendix I - Pressuremeter Data and Standard Interpretation

**PRESSUREMETER DATA** **CH2MHill, Inc.**

**CALTRANS I-710 North Tunnel Project** **2/10/2009**

**Hole No. Z3-B7** **Depth 252.5ft** **File C:\DATA\ISE-812\SR710-33.P**

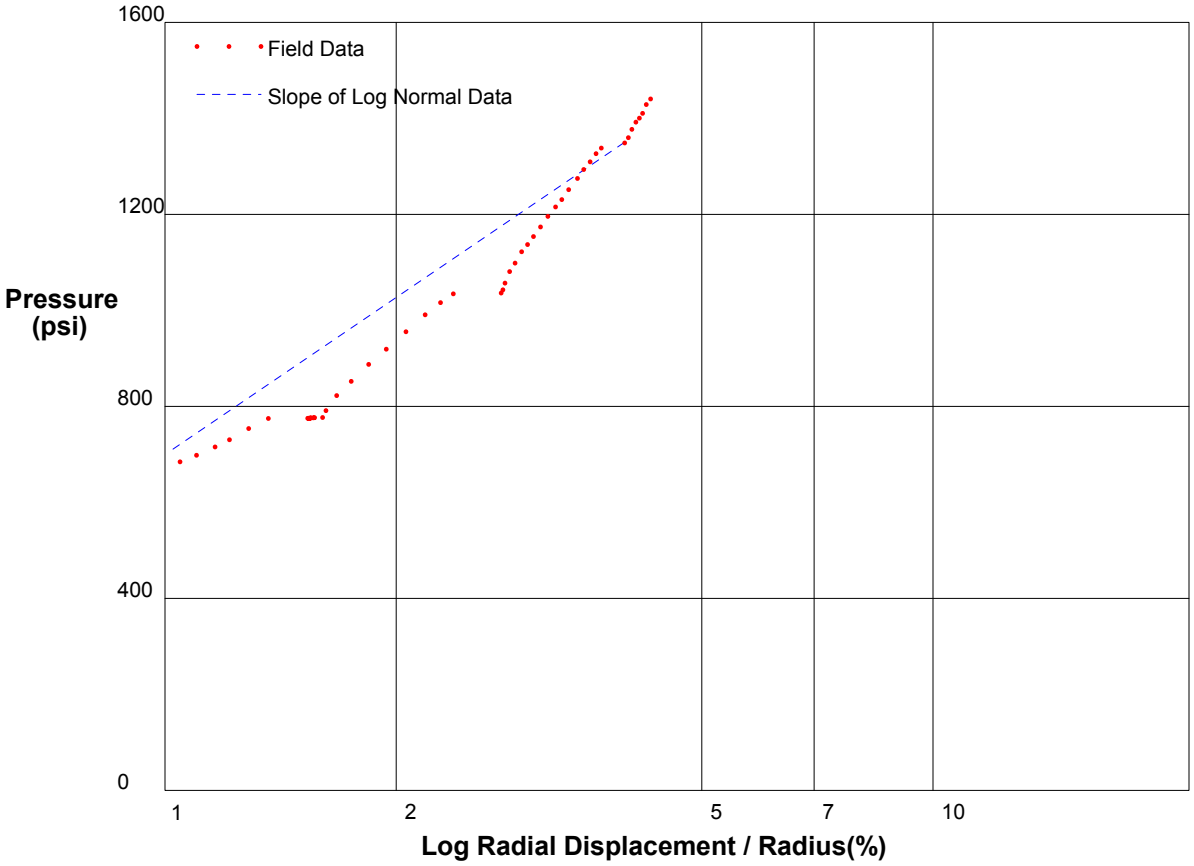


**Shear Strength 472 psi**
**Limit Pressure 2452 psi**

shift 6

**In Situ Engineering**

# Appendix I - Pressuremeter Data and Standard Interpretation

**PRESSUREMETER DATA** **CH2MHill, Inc.**

**CALTRANS I-710 North Tunnel Project** **2/10/2009**

**Hole No. Z3-B7** **Depth 251ft** **File C:\DATA\ISE-812\SR710-34.P**

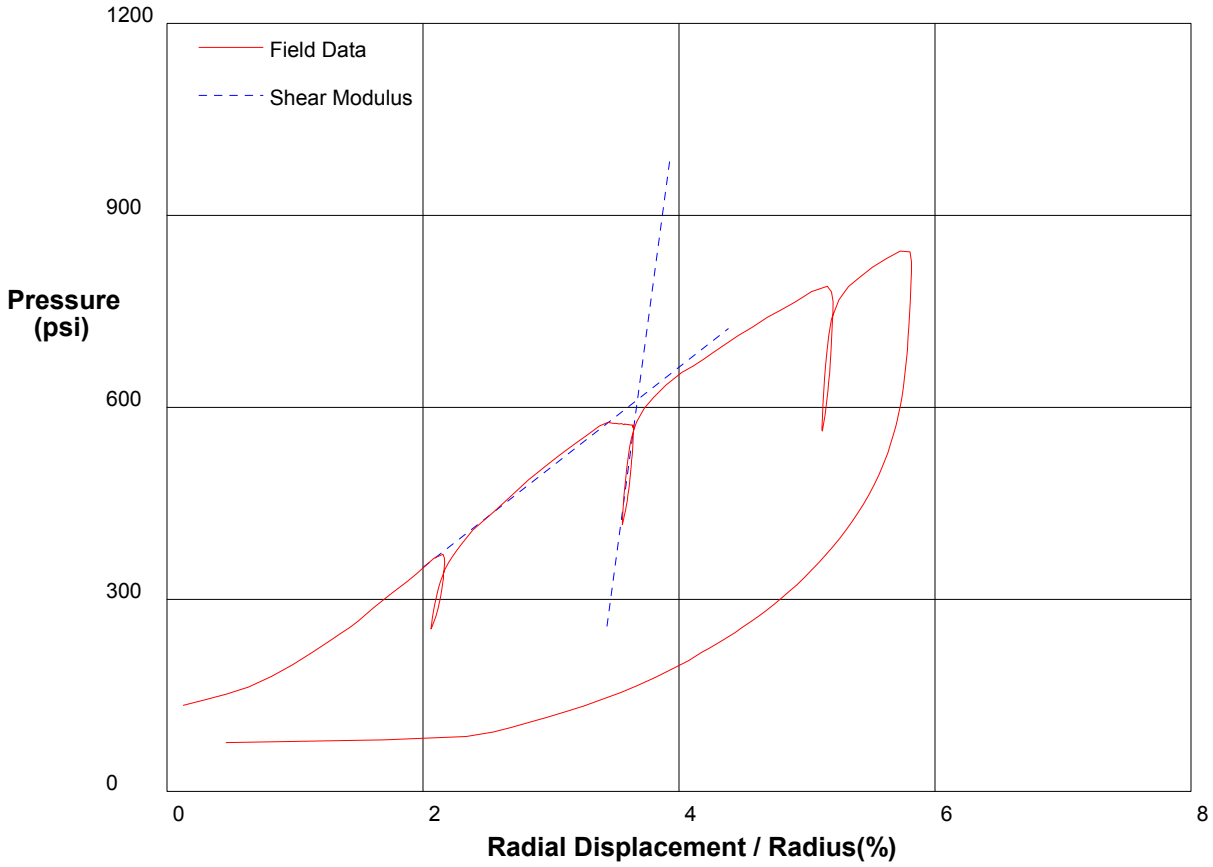


**Shear Modulus 74255 psi**

**Shear Modulus 7816 psi**

shift 5.2

**In Situ Engineering**

# Appendix I - Pressuremeter Data and Standard Interpretation

**PRESSUREMETER DATA** **CH2MHill, Inc.**

**CALTRANS I-710 North Tunnel Project** **2/10/2009**

**Hole No. Z3-B7** **Depth 251ft** **File C:\DATA\ISE-812\SR710-34.P**

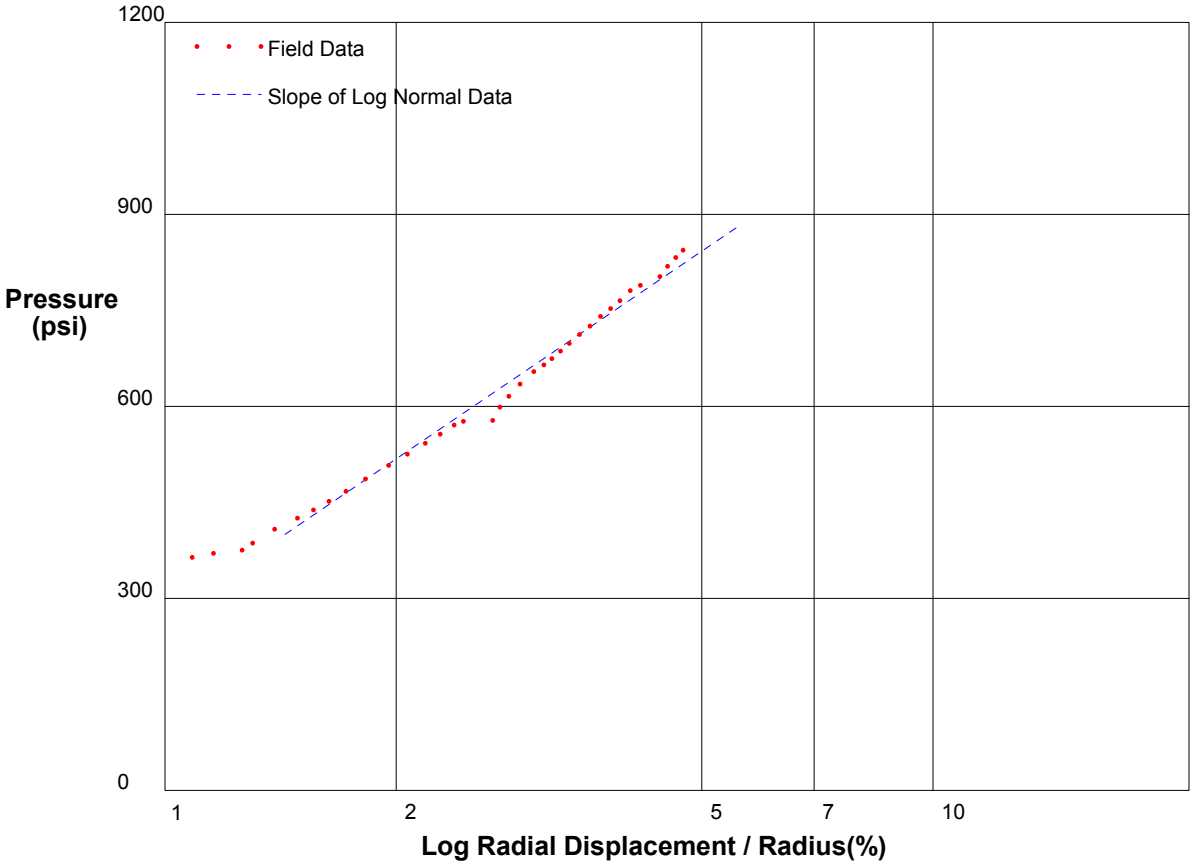


**Shear Strength 354 psi**
**Limit Pressure 1587 psi**

shift 6.2

**In Situ Engineering**

# Appendix I - Pressuremeter Data and Standard Interpretation

**PRESSUREMETER DATA** **CH2MHill, Inc.**

**CALTRANS I-710 North Tunnel Project** **2/10/2009**

**Hole No. Z3-B7** **Depth 271.6ft** **File C:\DATA\ISE-812\SR710-35.P**

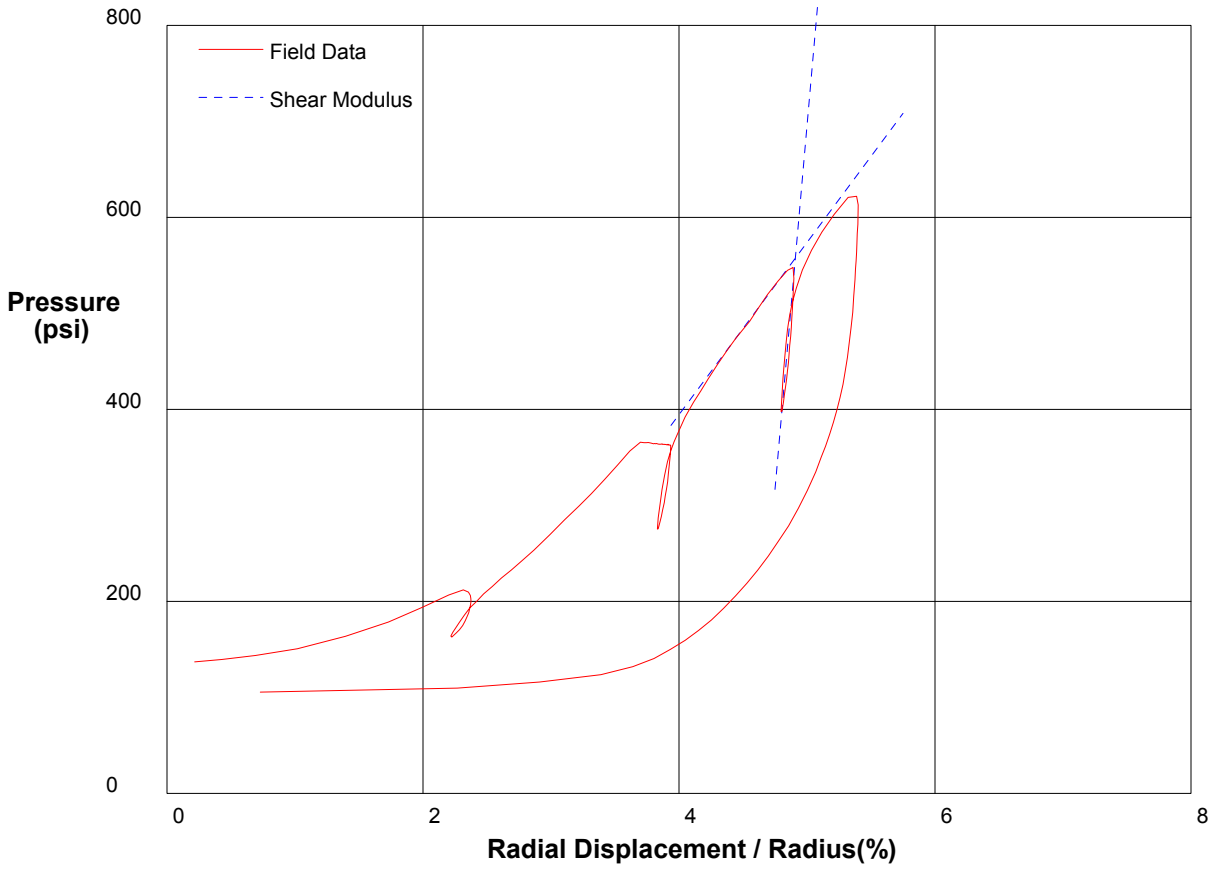


**Shear Modulus 75833 psi**

**Shear Modulus 8965 psi**

shift 7.2

**In Situ Engineering**

# Appendix I - Pressuremeter Data and Standard Interpretation

**PRESSUREMETER DATA** **CH2MHill, Inc.**

**CALTRANS I-710 North Tunnel Project** **2/10/2009**

**Hole No. Z3-B7** **Depth 271.6ft** **File C:\DATA\ISE-812\SR710-35.P**

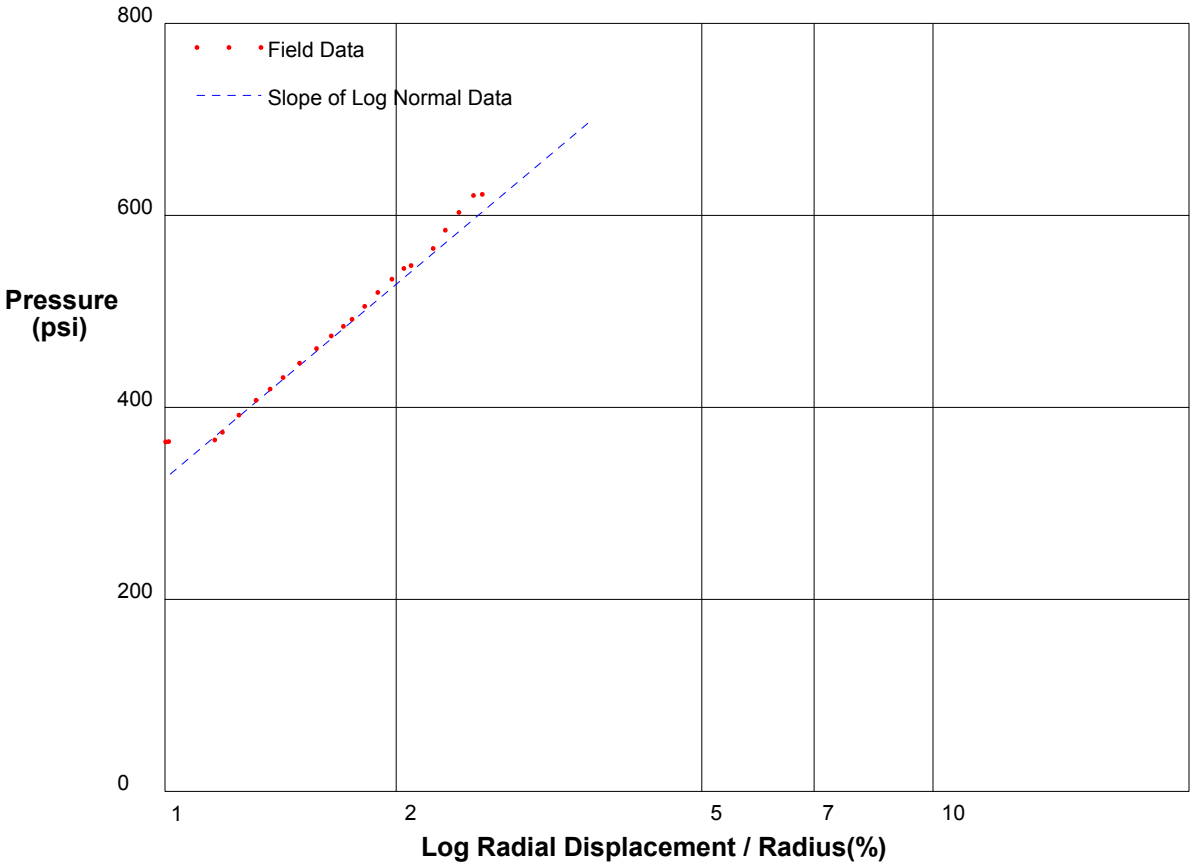


**Shear Strength 291.9 psi**
**Limit Pressure 1410 psi**

shift 10

**In Situ Engineering**

# Appendix I - Pressuremeter Data and Standard Interpretation

**PRESSUREMETER DATA** **CH2MHill, Inc.**

**CALTRANS I-710 North Tunnel Project** **2/10/2009**

**Hole No. Z3-B7** **Depth 270.1ft** **File C:\DATA\ISE-812\SR710-36.P**

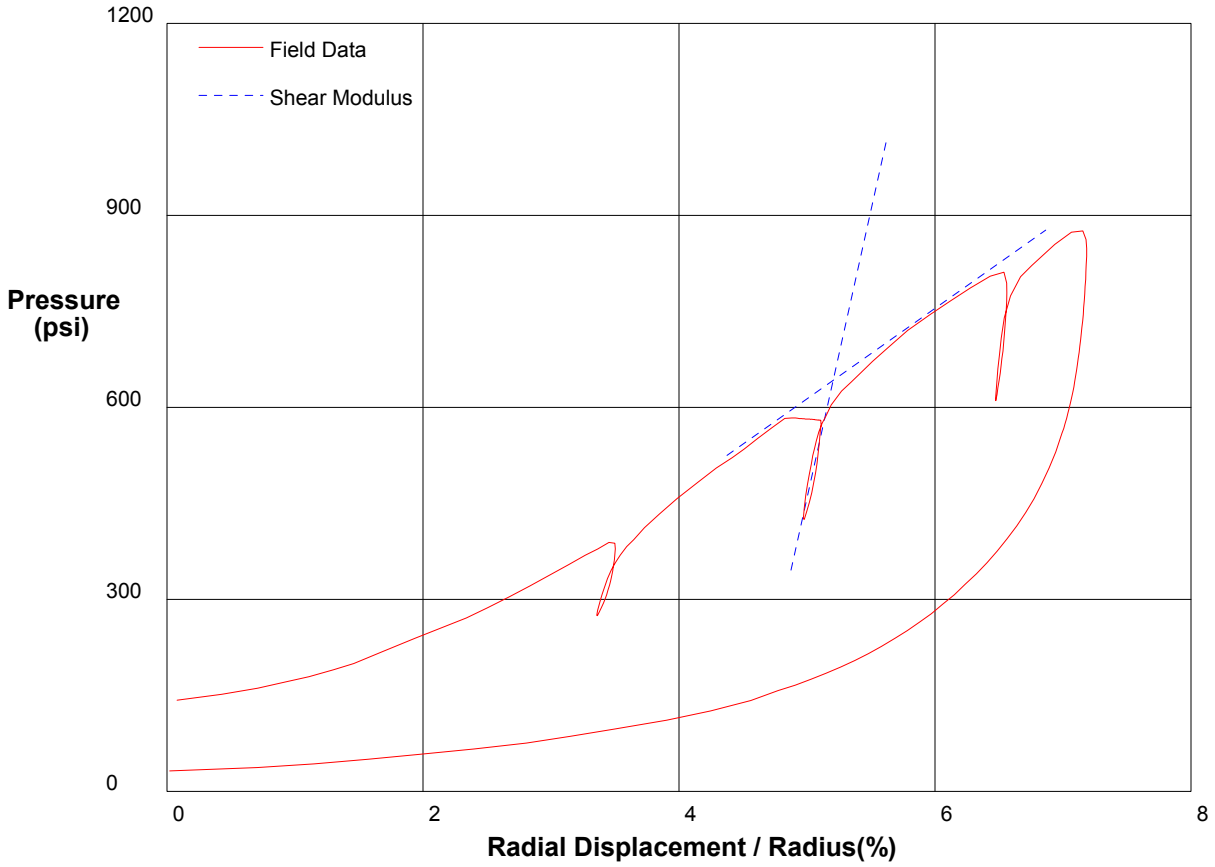


**Shear Modulus 45000 psi**

**Shear Modulus 7071 psi**

shift 4

**In Situ Engineering**

# Appendix I - Pressuremeter Data and Standard Interpretation

**PRESSUREMETER DATA** **CH2MHill, Inc.**

**CALTRANS I-710 North Tunnel Project** **2/10/2009**

**Hole No. Z3-B7** **Depth 270.1ft** **File C:\DATA\ISE-812\SR710-36.P**

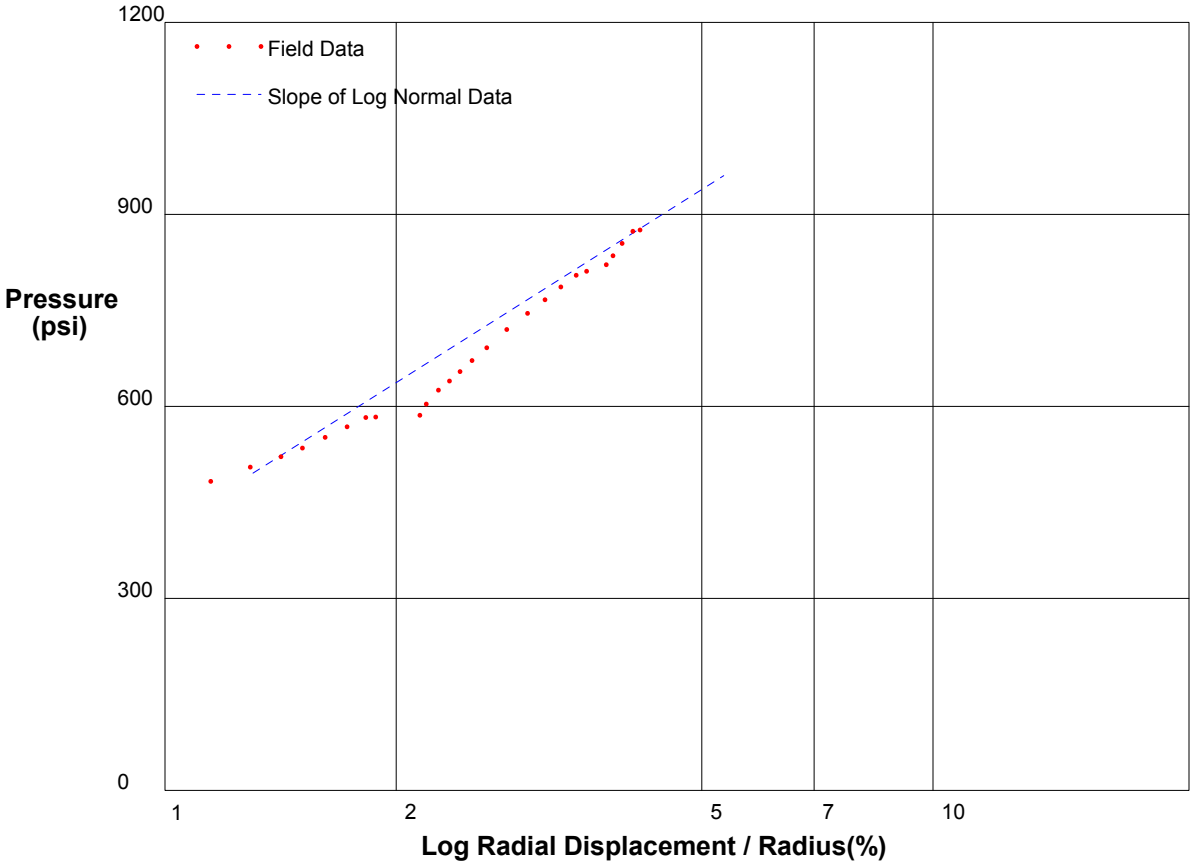


**Shear Strength 329.2 psi**
**Limit Pressure 1631 psi**

shift 7

**In Situ Engineering**

# Appendix I - Pressuremeter Data and Standard Interpretation

**PRESSUREMETER DATA** **CH2MHill, Inc.**

**CALTRANS I-710 North Tunnel Project** **2/19/2009**

**Hole No. Z1-B5** **Depth 278ft** **File C:\DATA\ISE-812\SR710-37.P**

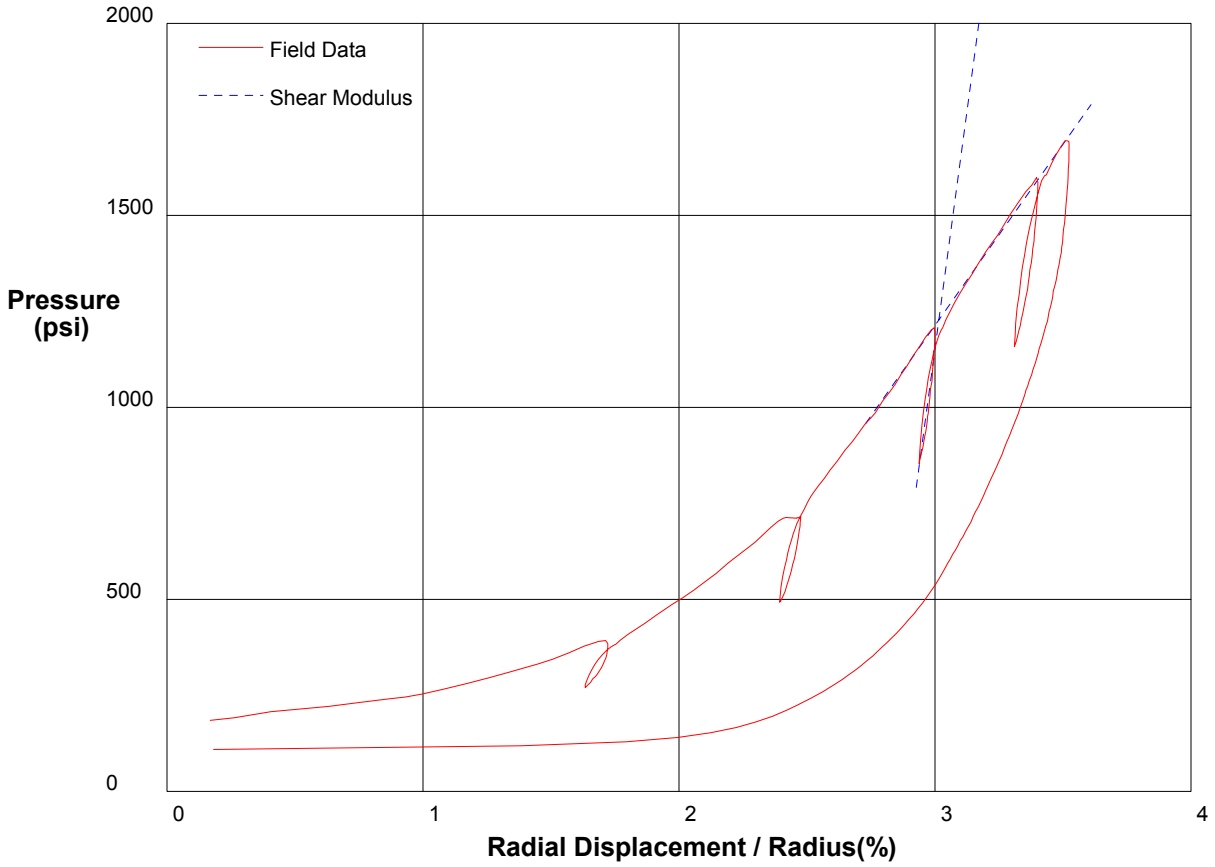


**Shear Modulus 247517 psi**

**Shear Modulus 47140 psi**

shift 2

**In Situ Engineering**

# Appendix I - Pressuremeter Data and Standard Interpretation

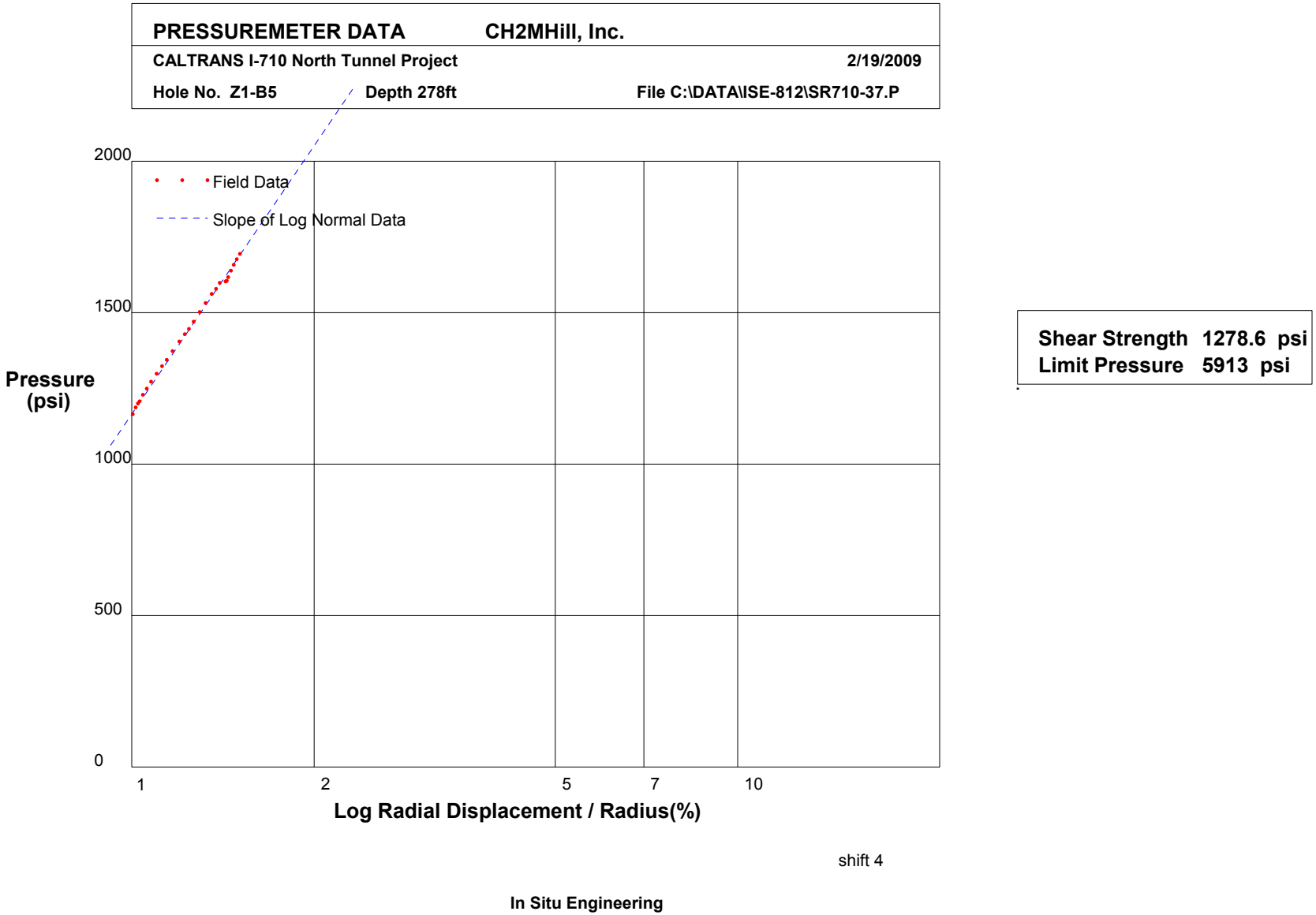

# Appendix I - Pressuremeter Data and Standard Interpretation

**PRESSUREMETER DATA** **CH2MHill, Inc.**

**CALTRANS I-710 North Tunnel Project** **2/19/2009**

**Hole No. Z1-B5** **Depth 276.5ft** **File C:\DATA\ISE-812\SR710-38.P**

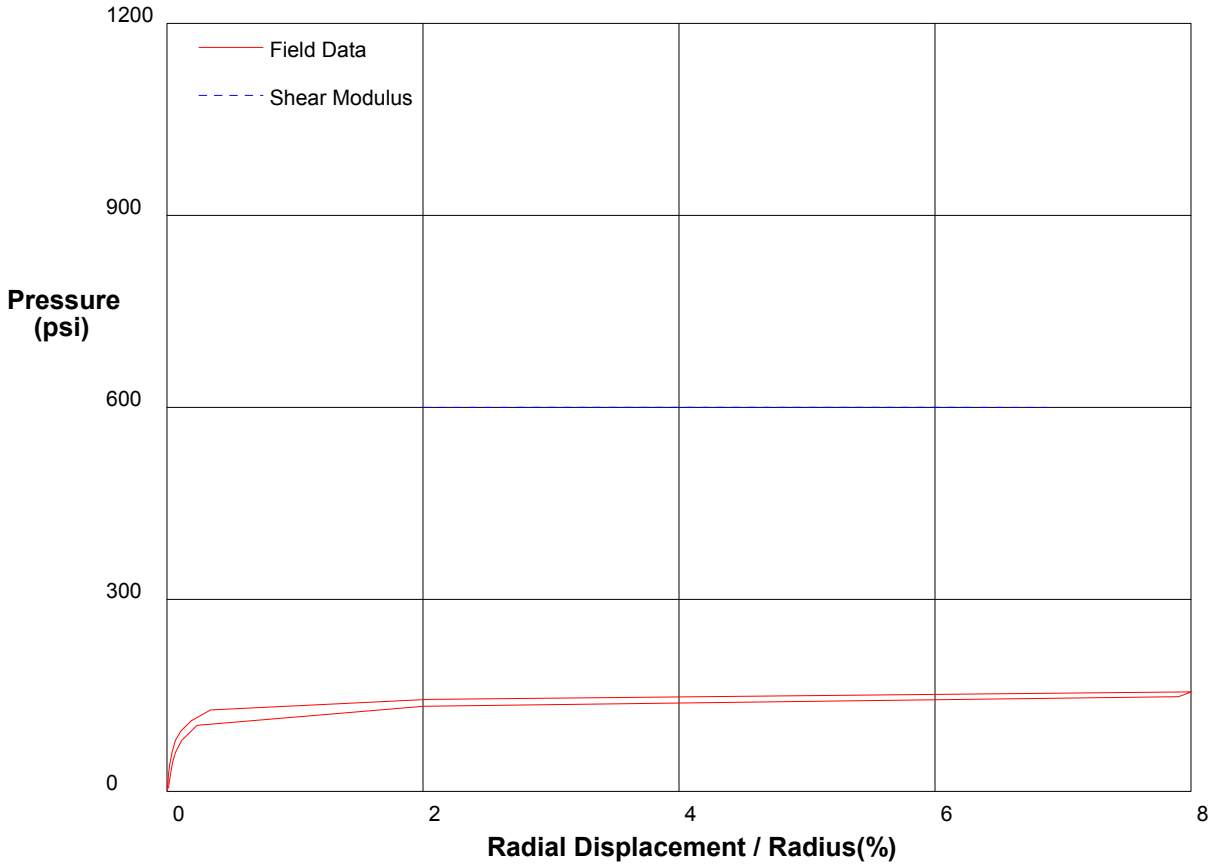


**Shear Modulus 0 psi**

**Shear Modulus 0 psi**

shift 0

**In Situ Engineering**

# Appendix I - Pressuremeter Data and Standard Interpretation

**PRESSUREMETER DATA** **CH2MHill, Inc.**

**CALTRANS I-710 North Tunnel Project** **2/19/2009**

**Hole No. Z1-B4** **Depth 332ft** **File C:\DATA\ISE-812\SR710-39.P**

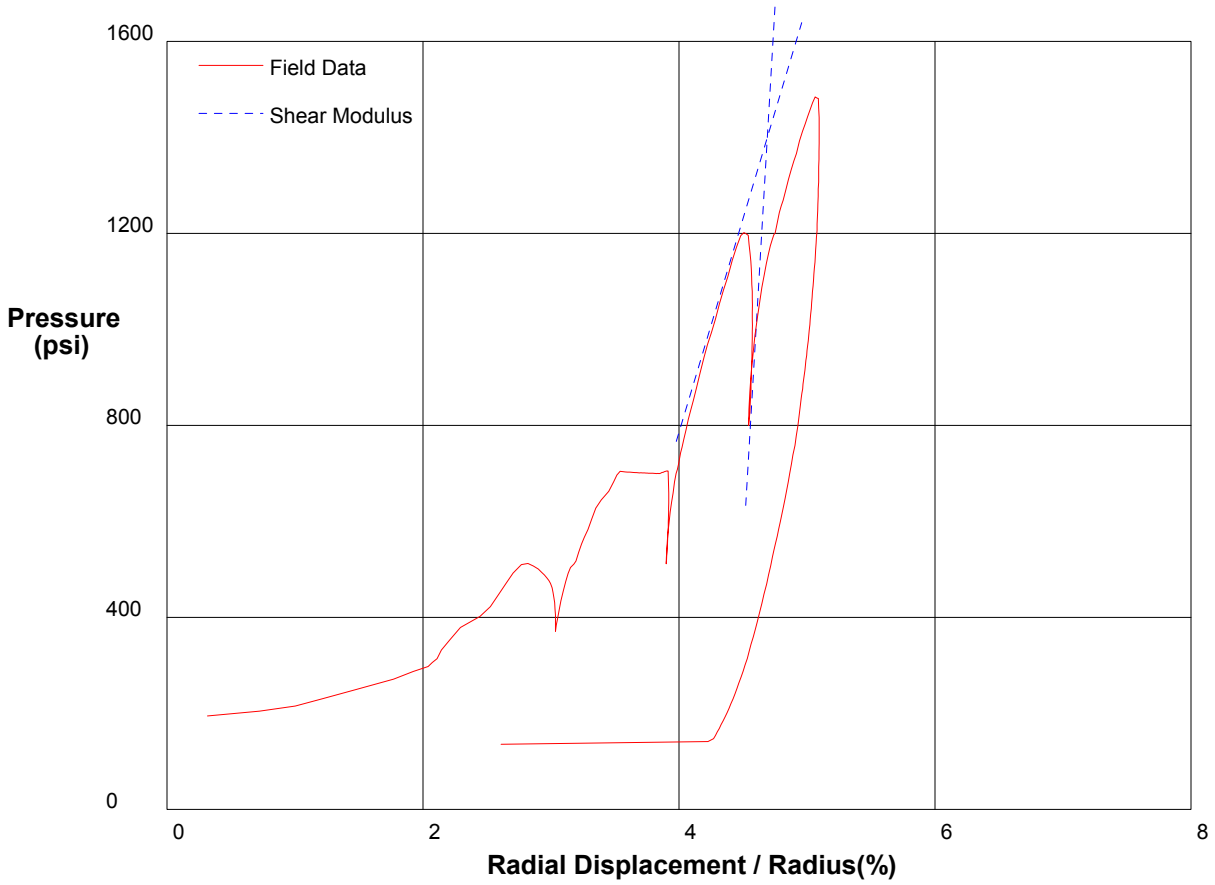


**Shear Modulus 226666 psi**

**Shear Modulus 44539 psi**

shift 2

**In Situ Engineering**

# Appendix I - Pressuremeter Data and Standard Interpretation

**PRESSUREMETER DATA** **CH2MHill, Inc.**

**CALTRANS I-710 North Tunnel Project** **2/19/2009**

**Hole No. Z1-B4** **Depth 332ft** **File C:\DATA\ISE-812\SR710-39.P**

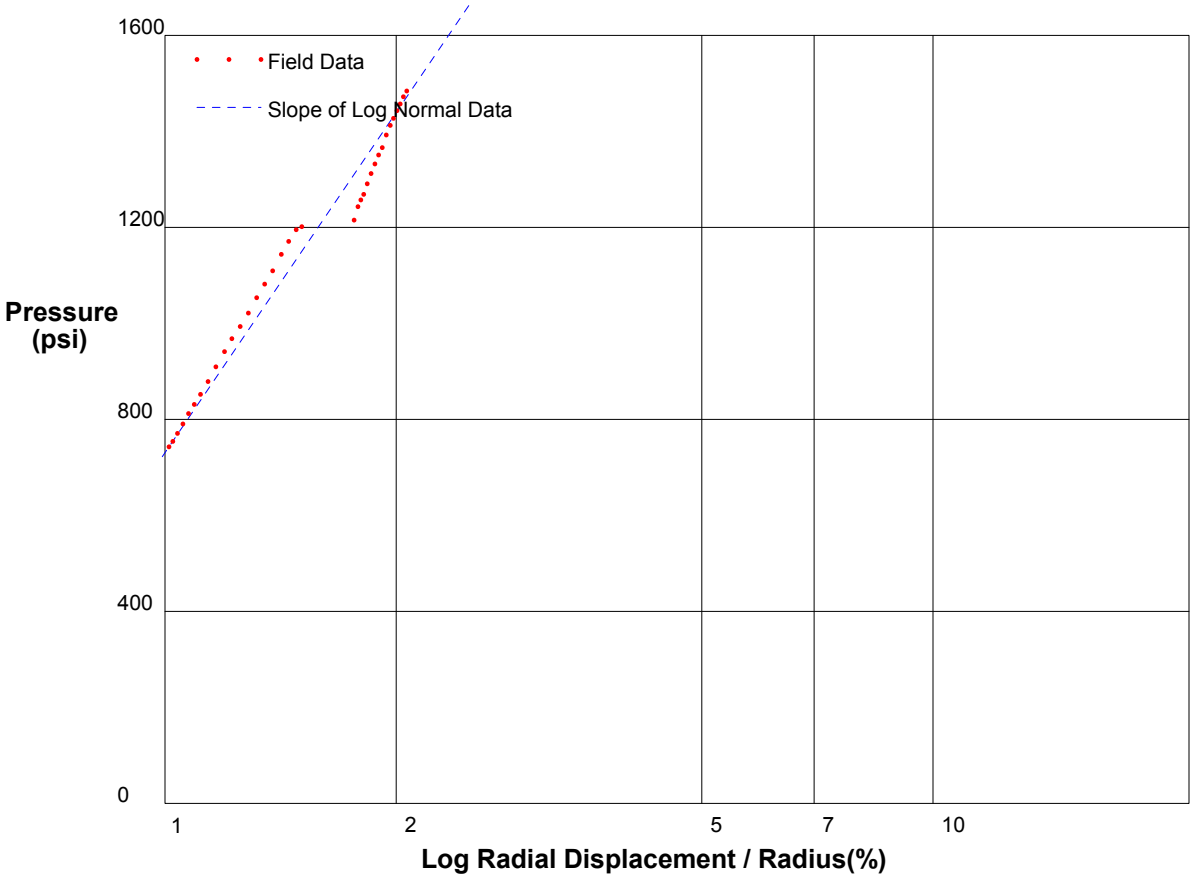


**Shear Strength 1022.9 psi**
**Limit Pressure 4529 psi**

shift 5

**In Situ Engineering**

# Appendix I - Pressuremeter Data and Standard Interpretation

**PRESSUREMETER DATA** **CH2MHill, Inc.**

**CALTRANS I-710 North Tunnel Project** **2/19/2009**

**Hole No. Z1-B4** **Depth 330.5ft** **File C:\DATA\ISE-812\SR710-40.P**

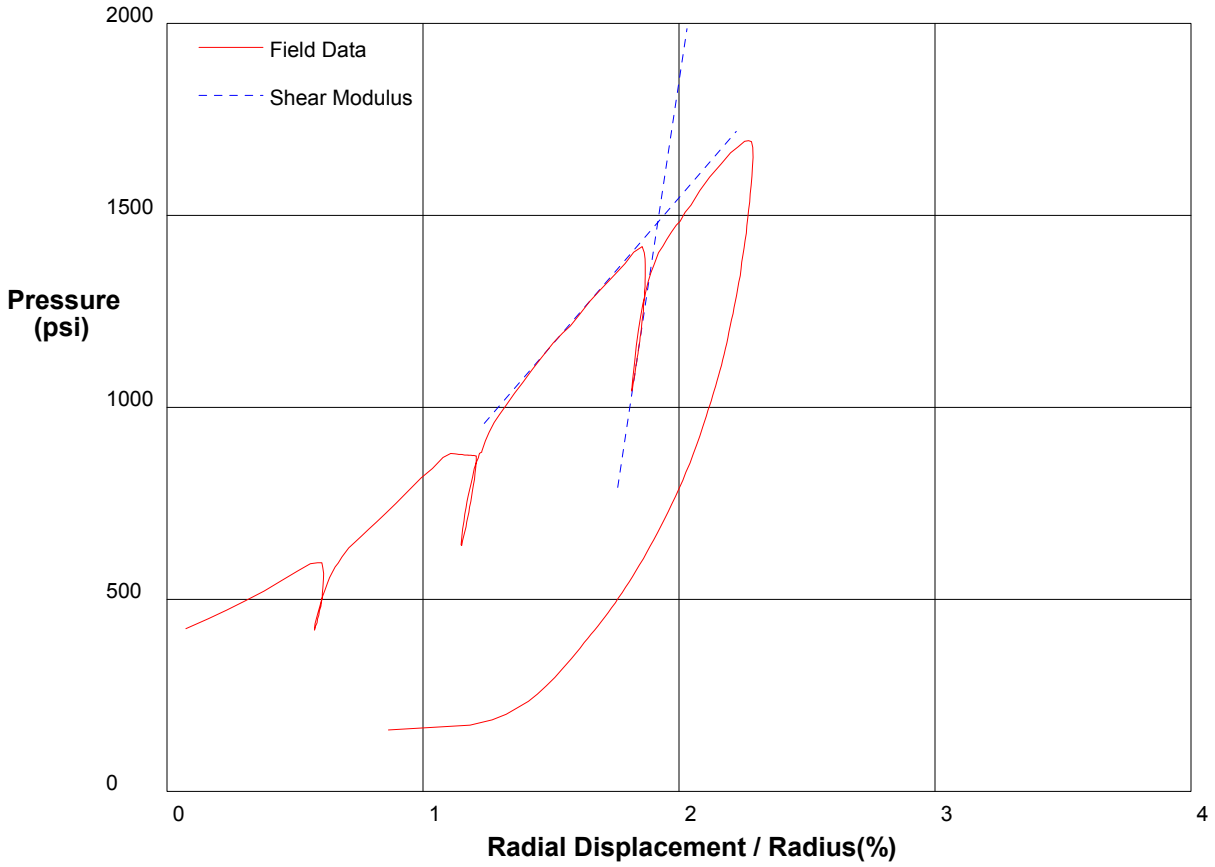


**Shear Modulus 220512 psi**

**Shear Modulus 38624 psi**

shift 4

**In Situ Engineering**

# Appendix I - Pressuremeter Data and Standard Interpretation

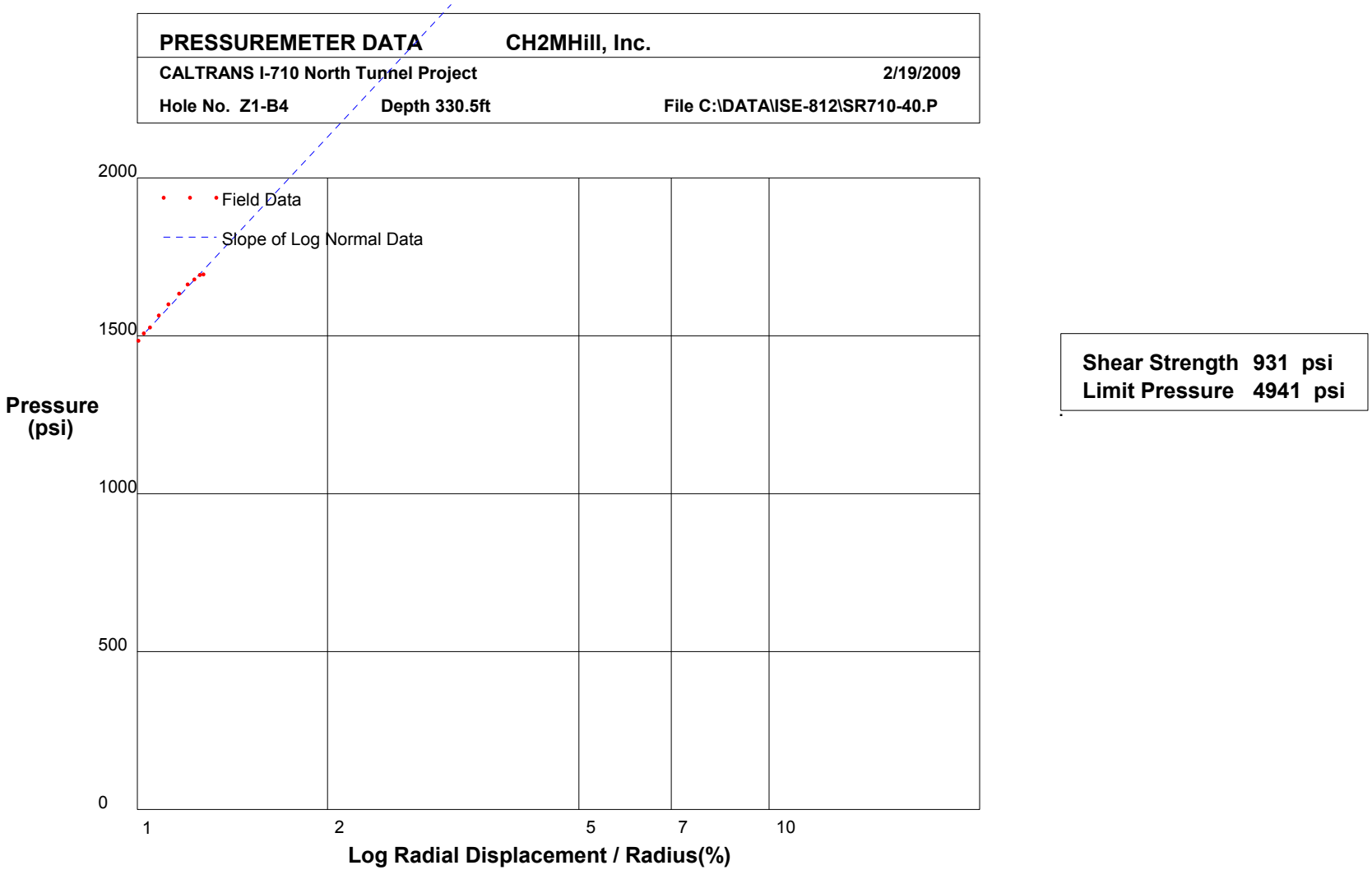

# Appendix I - Pressuremeter Data and Standard Interpretation

**PRESSUREMETER DATA** **CH2MHill, Inc.**

**CALTRANS I-710 North Tunnel Project** **2/20/2009**

**Hole No. Z1-B5** **Depth 347ft** **File C:\DATA\ISE-812\SR710-41.P**

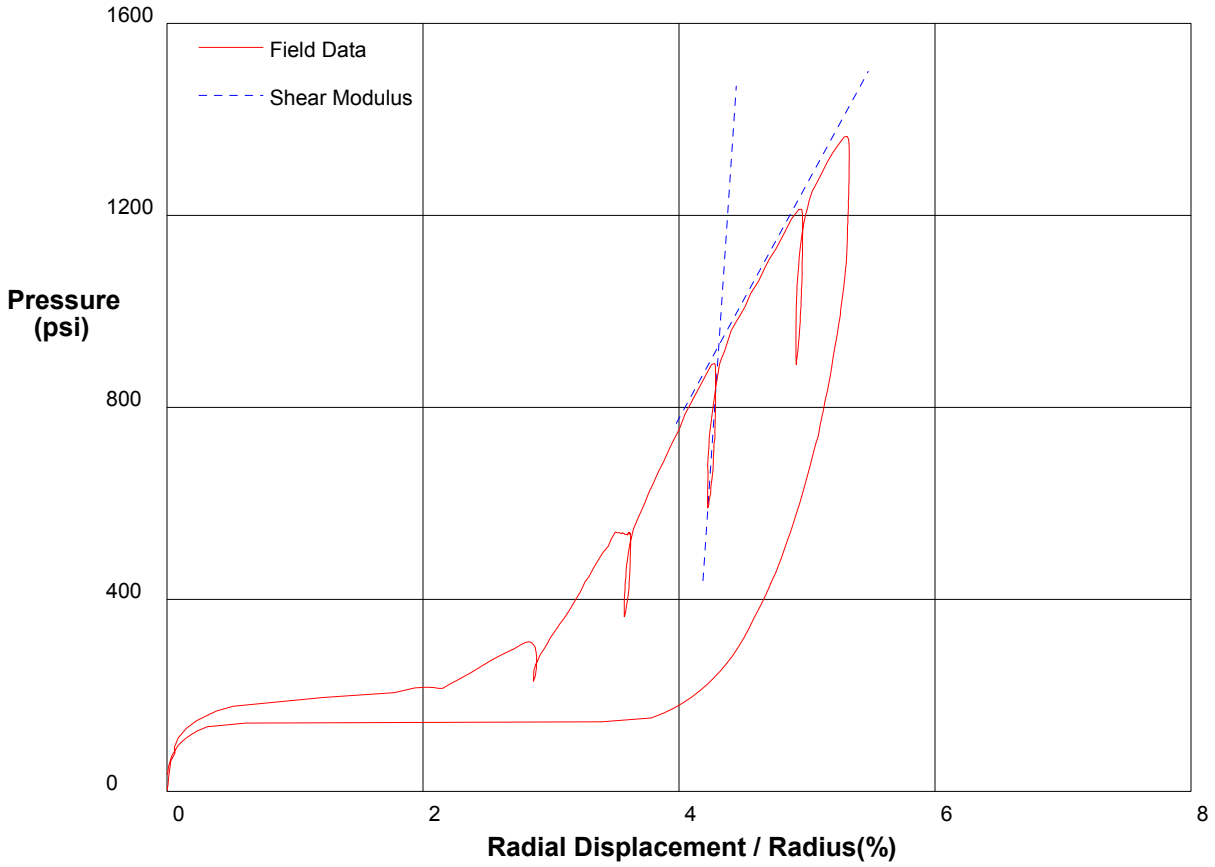


**Shear Modulus 197866 psi**

**Shear Modulus 24444 psi**

shift 0

**In Situ Engineering**

# Appendix I - Pressuremeter Data and Standard Interpretation

**PRESSUREMETER DATA** **CH2MHill, Inc.**

**CALTRANS I-710 North Tunnel Project** **2/20/2009**

**Hole No. Z1-B5** **Depth 347ft** **File C:\DATA\ISE-812\SR710-41.P**

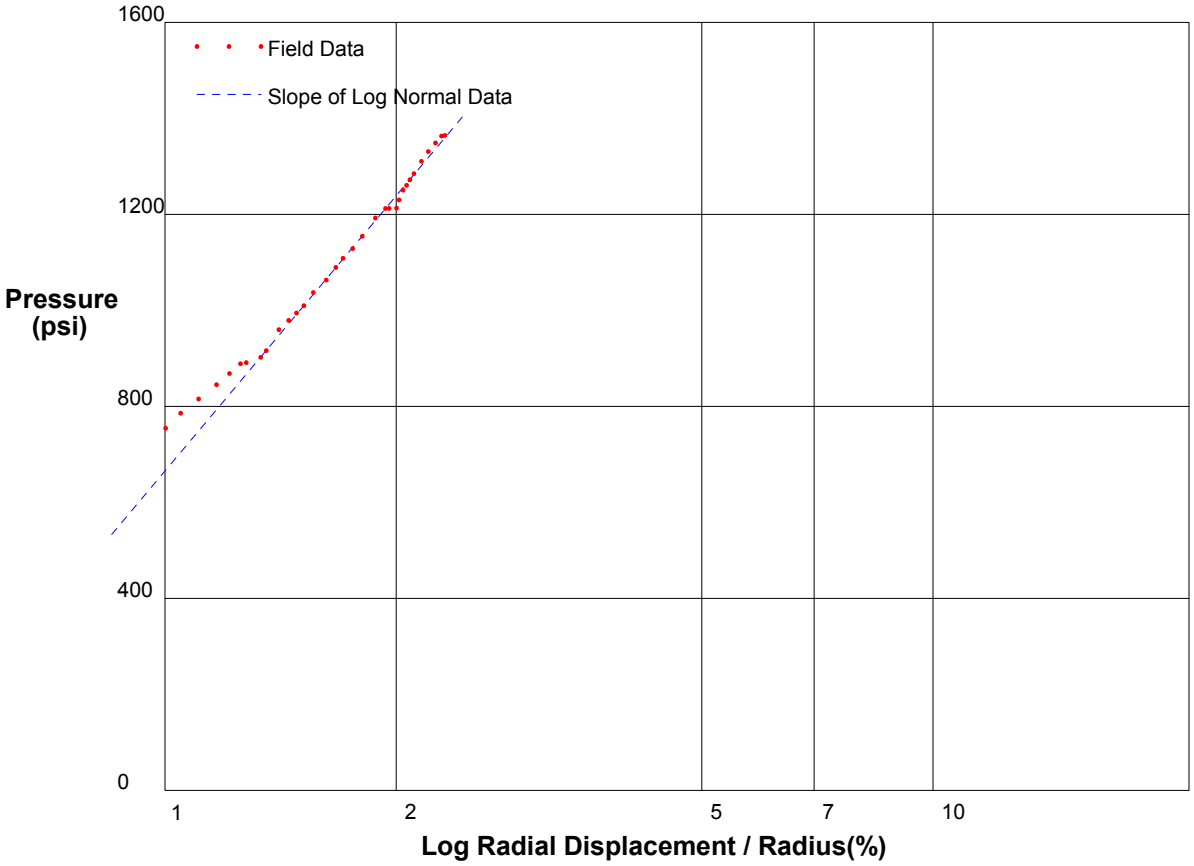


**Shear Strength 826.9 psi**
**Limit Pressure 3736 psi**

shift 3

**In Situ Engineering**

# Appendix I - Pressuremeter Data and Standard Interpretation

**PRESSUREMETER DATA** **CH2MHill, Inc.**

**CALTRANS I-710 North Tunnel Project** **2/20/2009**

**Hole No. Z1-B5** **Depth 345.5ft** **File C:\DATA\ISE-812\SR710-42.P**

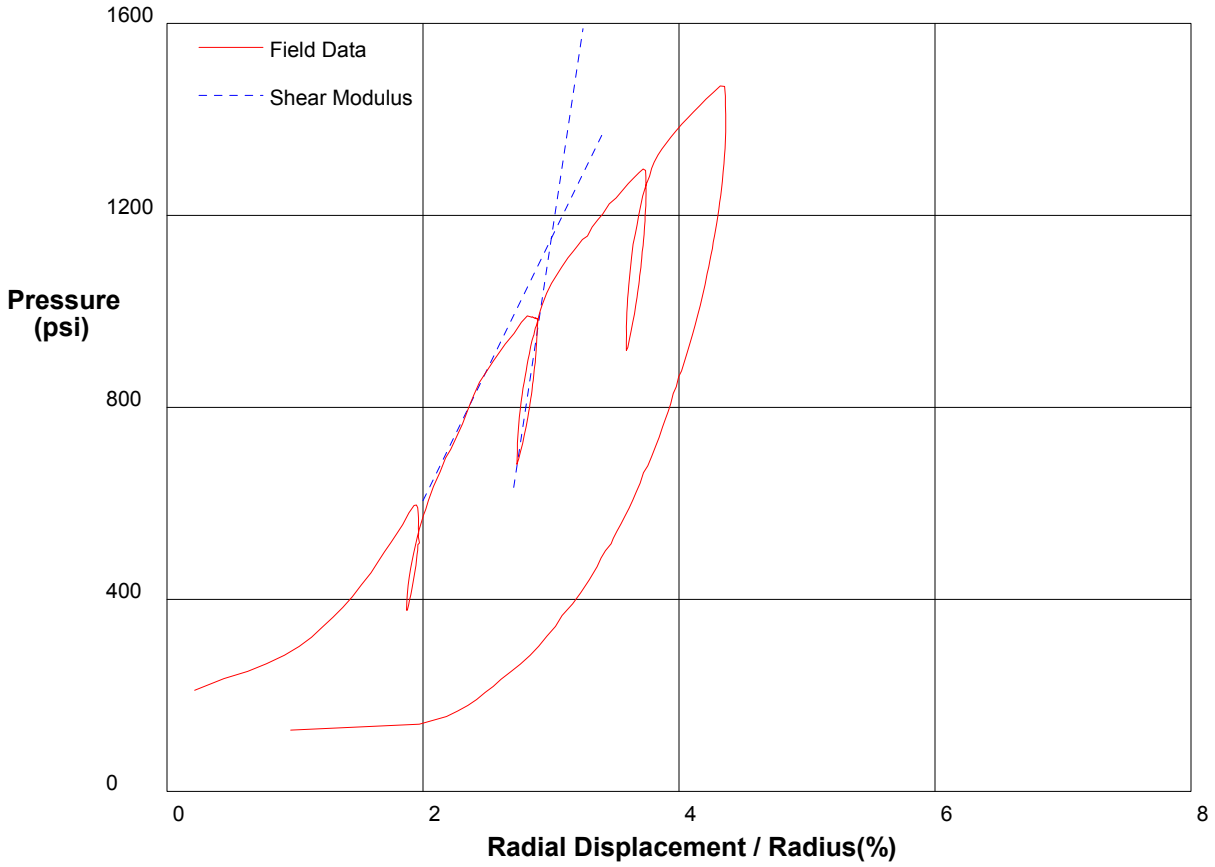


**Shear Modulus 88205 psi**

**Shear Modulus 27263 psi**

shift 2.8

**In Situ Engineering**

# Appendix I - Pressuremeter Data and Standard Interpretation

**PRESSUREMETER DATA** **CH2MHill, Inc.**

**CALTRANS I-710 North Tunnel Project** **2/20/2009**

**Hole No. Z1-B5** **Depth 345.5ft** **File C:\DATA\ISE-812\SR710-42.P**

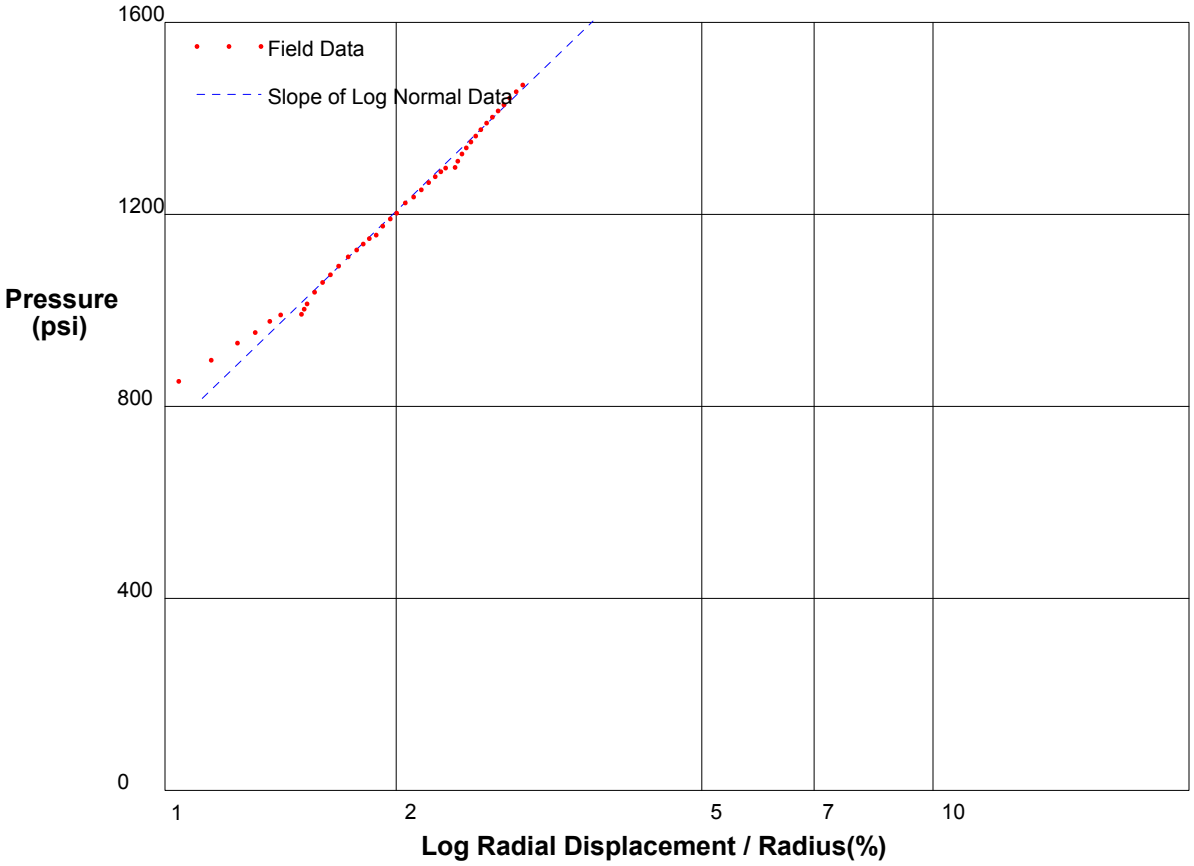


**Shear Strength 671.1 psi**
**Limit Pressure 3233 psi**

shift 4.2

**In Situ Engineering**

# Appendix I - Pressuremeter Data and Standard Interpretation

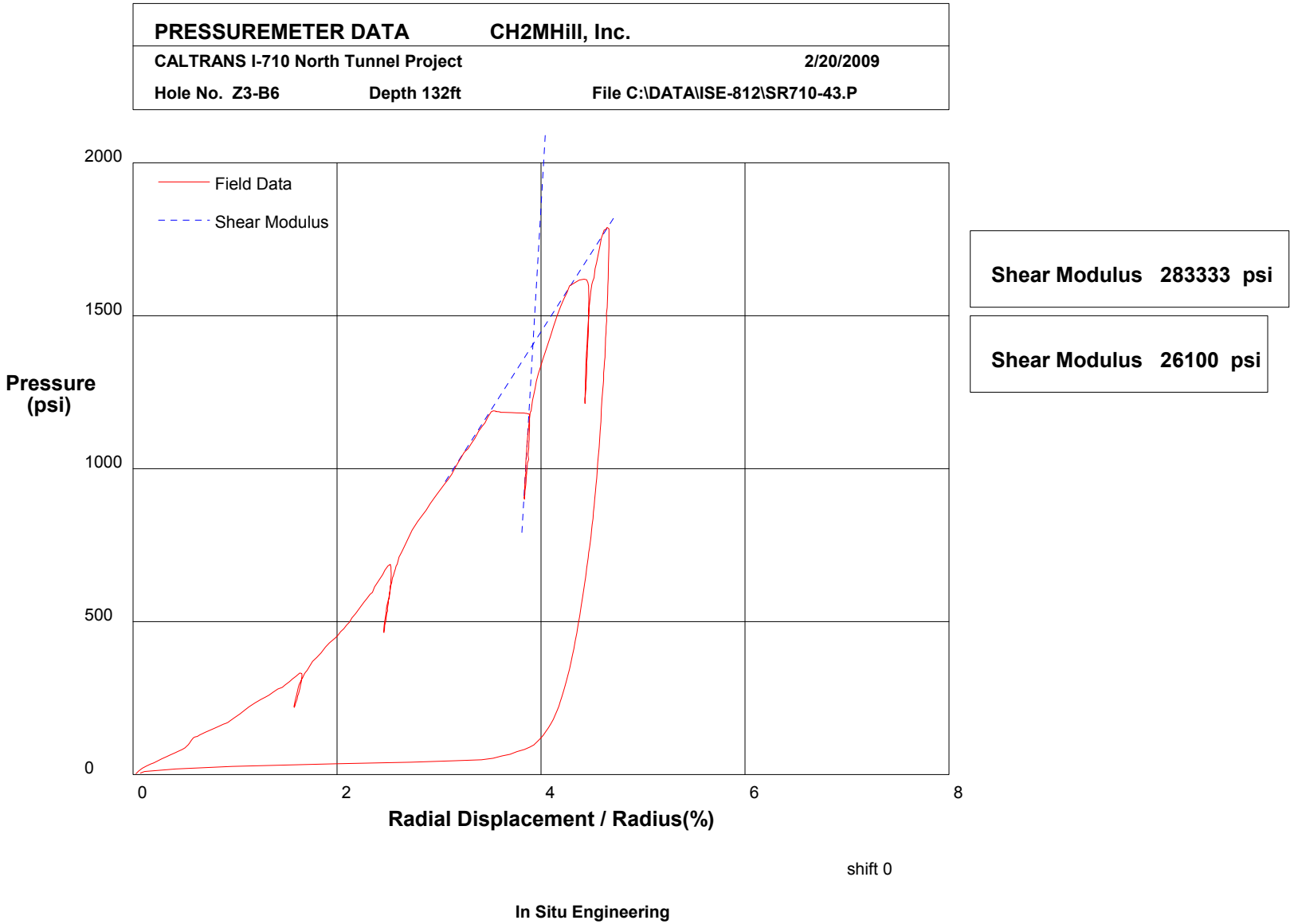

# Appendix I - Pressuremeter Data and Standard Interpretation

**PRESSUREMETER DATA** **CH2MHill, Inc.**

**CALTRANS I-710 North Tunnel Project** **2/20/2009**

**Hole No. Z3-B6** **Depth 132ft** **File C:\DATA\ISE-812\SR710-43.P**

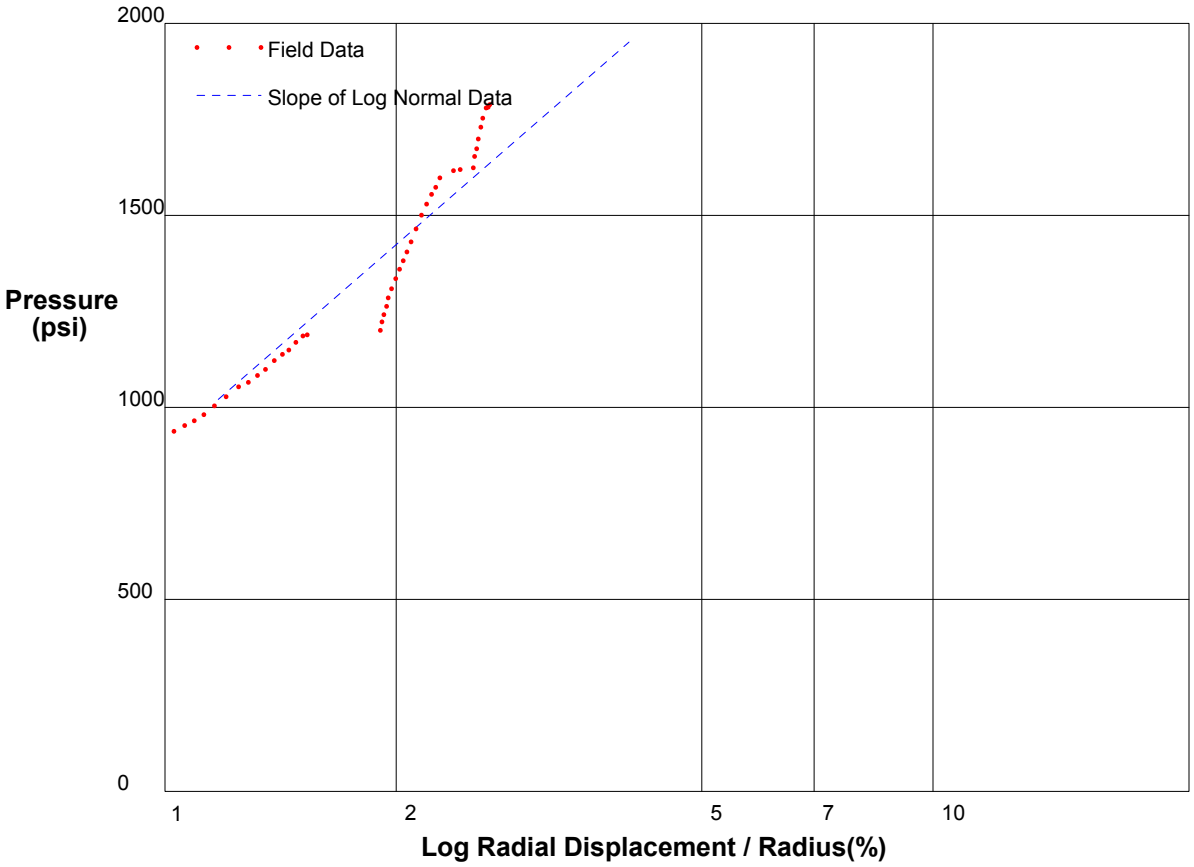


**Shear Strength 755.7 psi**
**Limit Pressure 3706 psi**

shift 2

**In Situ Engineering**

# Appendix I - Pressuremeter Data and Standard Interpretation

**PRESSUREMETER DATA** **CH2MHill, Inc.**

**CALTRANS I-710 North Tunnel Project** **2/23/2009**

**Hole No. Z1-B5** **Depth 398ft** **File C:\DATA\ISE-812\SR710-44.P**

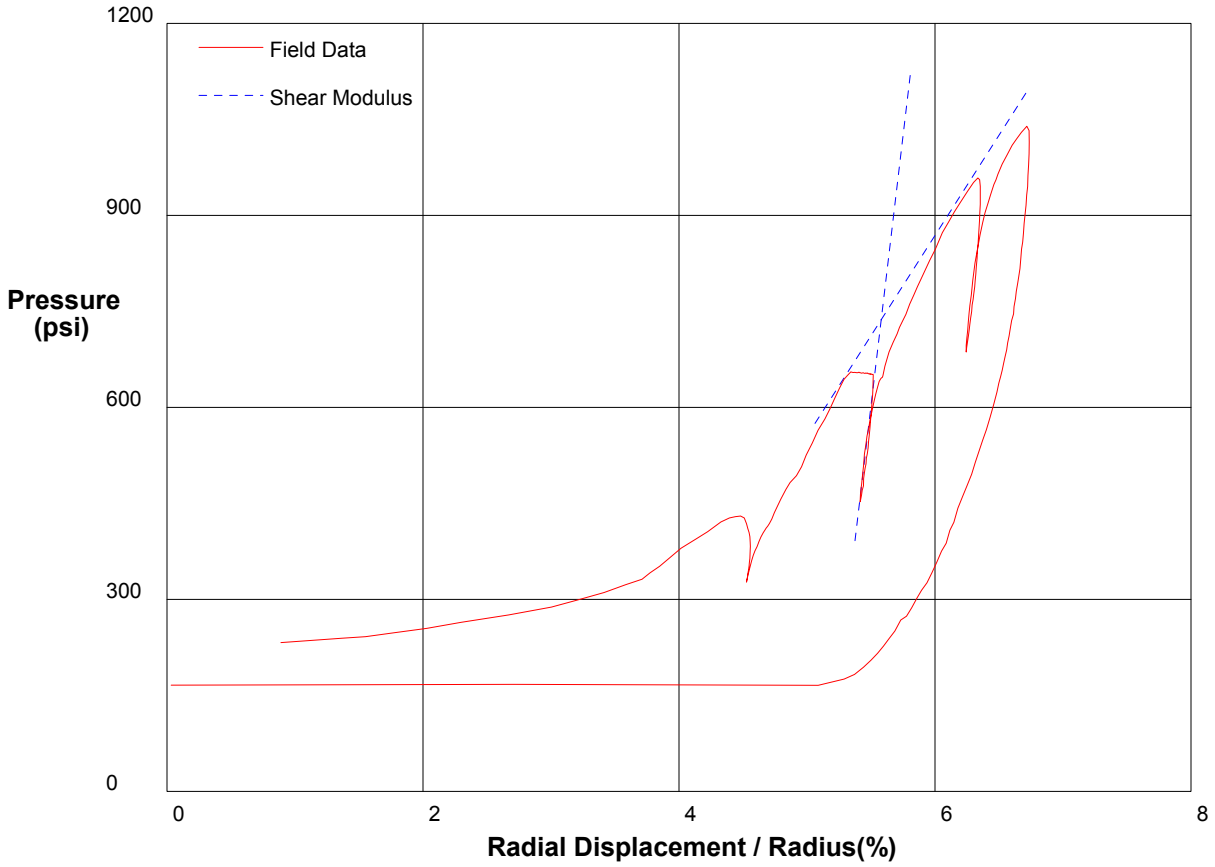


**Shear Modulus 84285 psi**

**Shear Modulus 15660 psi**

shift 1.5

**In Situ Engineering**

# Appendix I - Pressuremeter Data and Standard Interpretation

**PRESSUREMETER DATA** **CH2MHill, Inc.**

**CALTRANS I-710 North Tunnel Project** **2/23/2009**

**Hole No. Z1-B5** **Depth 398ft** **File C:\DATA\ISE-812\SR710-44.P**

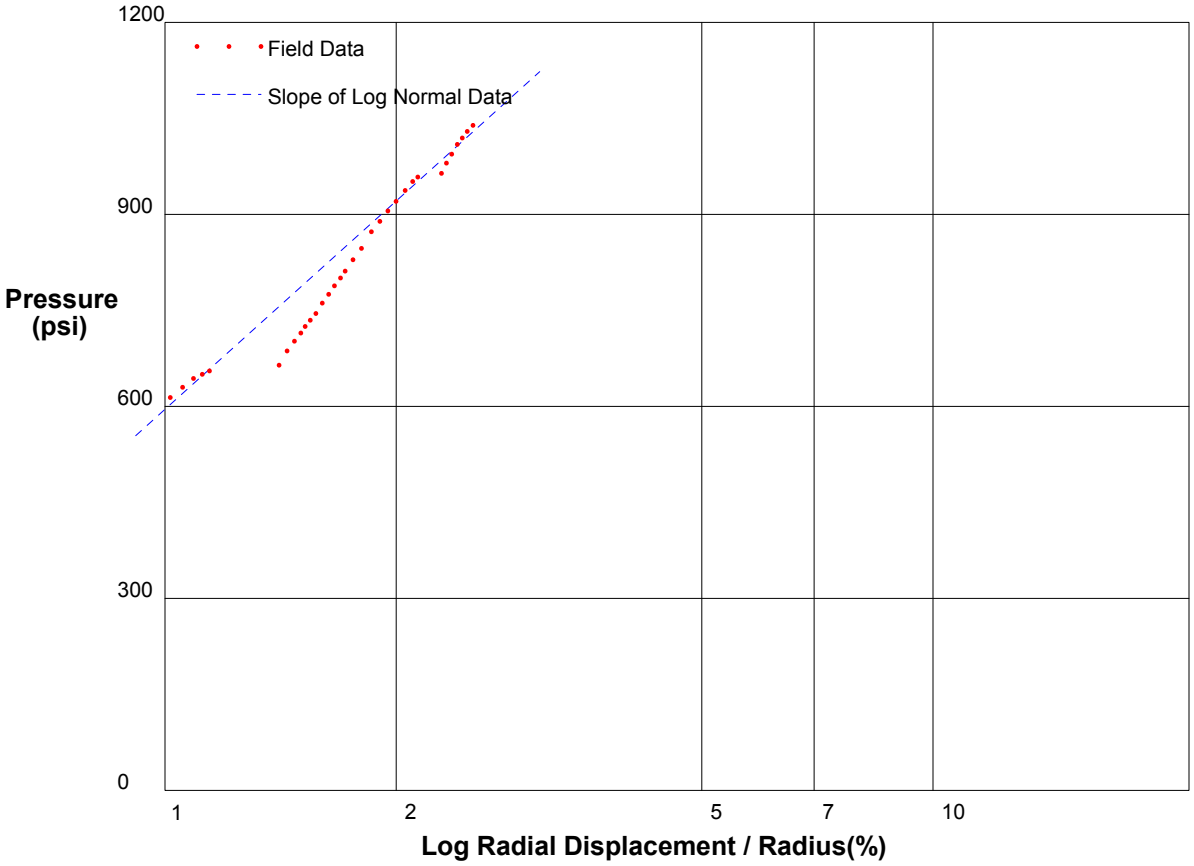


**Shear Strength 469.5 psi**
**Limit Pressure 2339 psi**

shift 5.7

**In Situ Engineering**

# Appendix I - Pressuremeter Data and Standard Interpretation

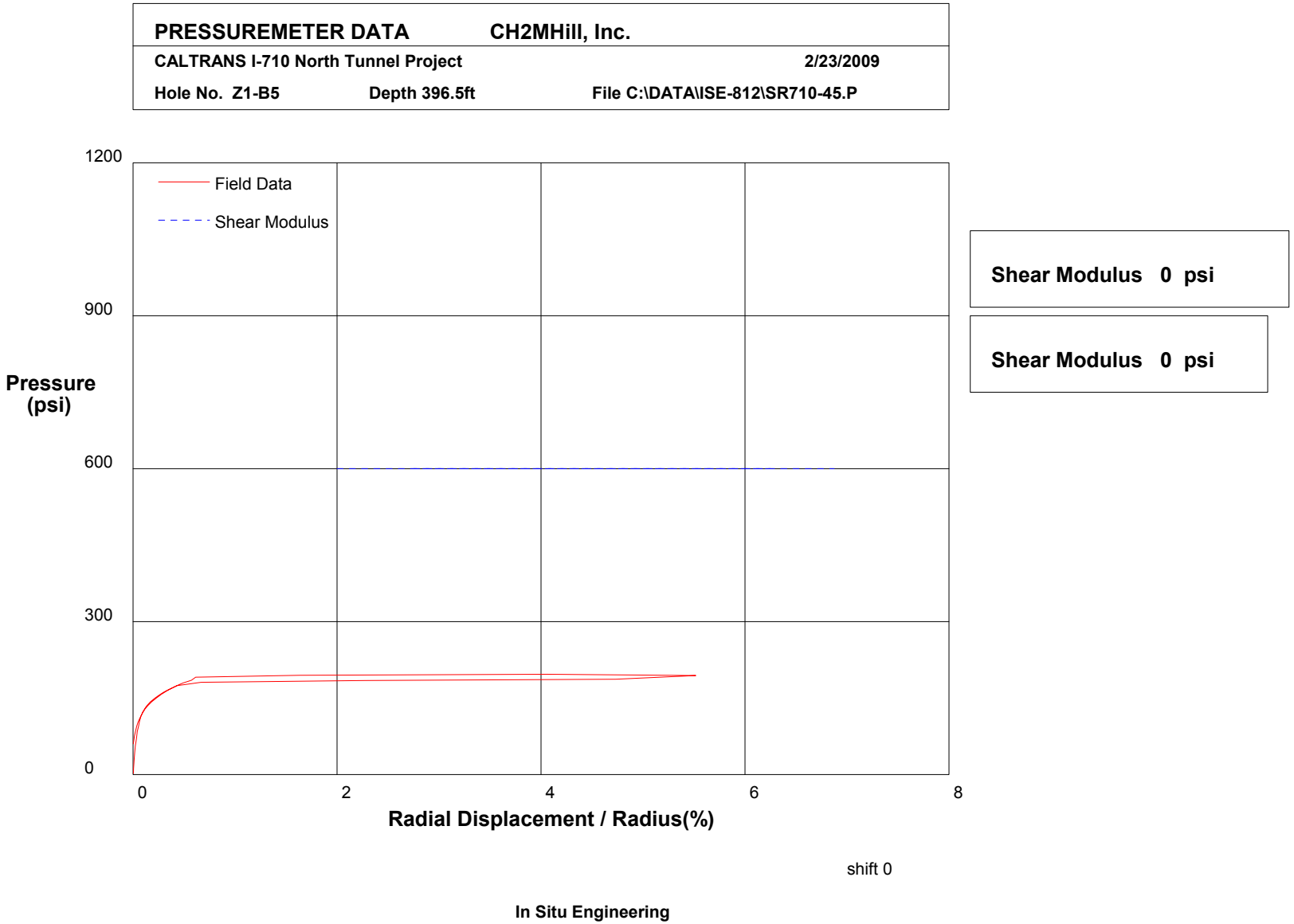

# Appendix I - Pressuremeter Data and Standard Interpretation

**PRESSUREMETER DATA** **CH2MHill, Inc.**

**CALTRANS I-710 North Tunnel Project** **2/23/2009**

**Hole No. Z3-B6** **Depth 168ft** **File C:\DATA\ISE-812\SR710-46.P**

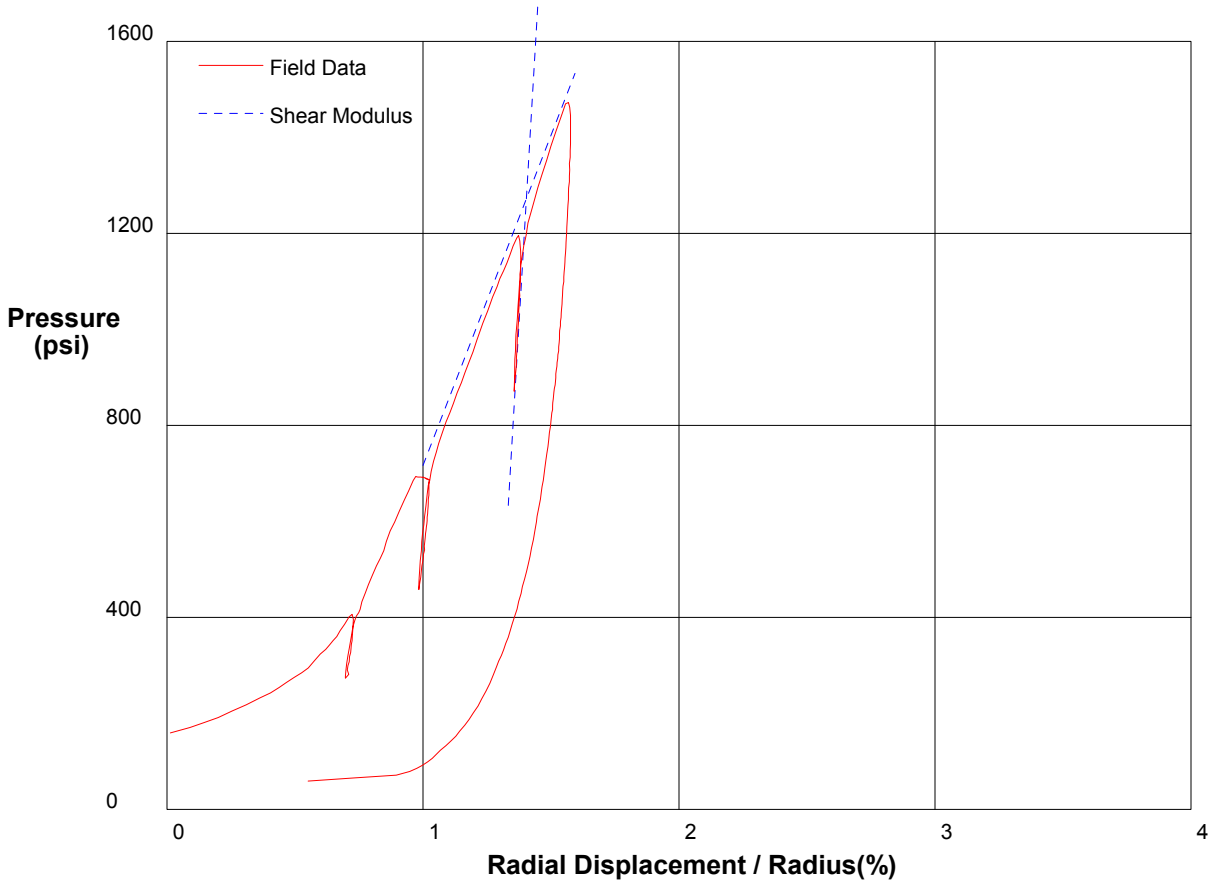


**Shear Modulus 453333 psi**

**Shear Modulus 68771 psi**

shift 2

**In Situ Engineering**

# Appendix I - Pressuremeter Data and Standard Interpretation

**PRESSUREMETER DATA** **CH2MHill, Inc.**

**CALTRANS I-710 North Tunnel Project** **2/23/2009**

**Hole No. Z3-B6** **Depth 166.5ft** **File C:\DATA\ISE-812\SR710-47.P**

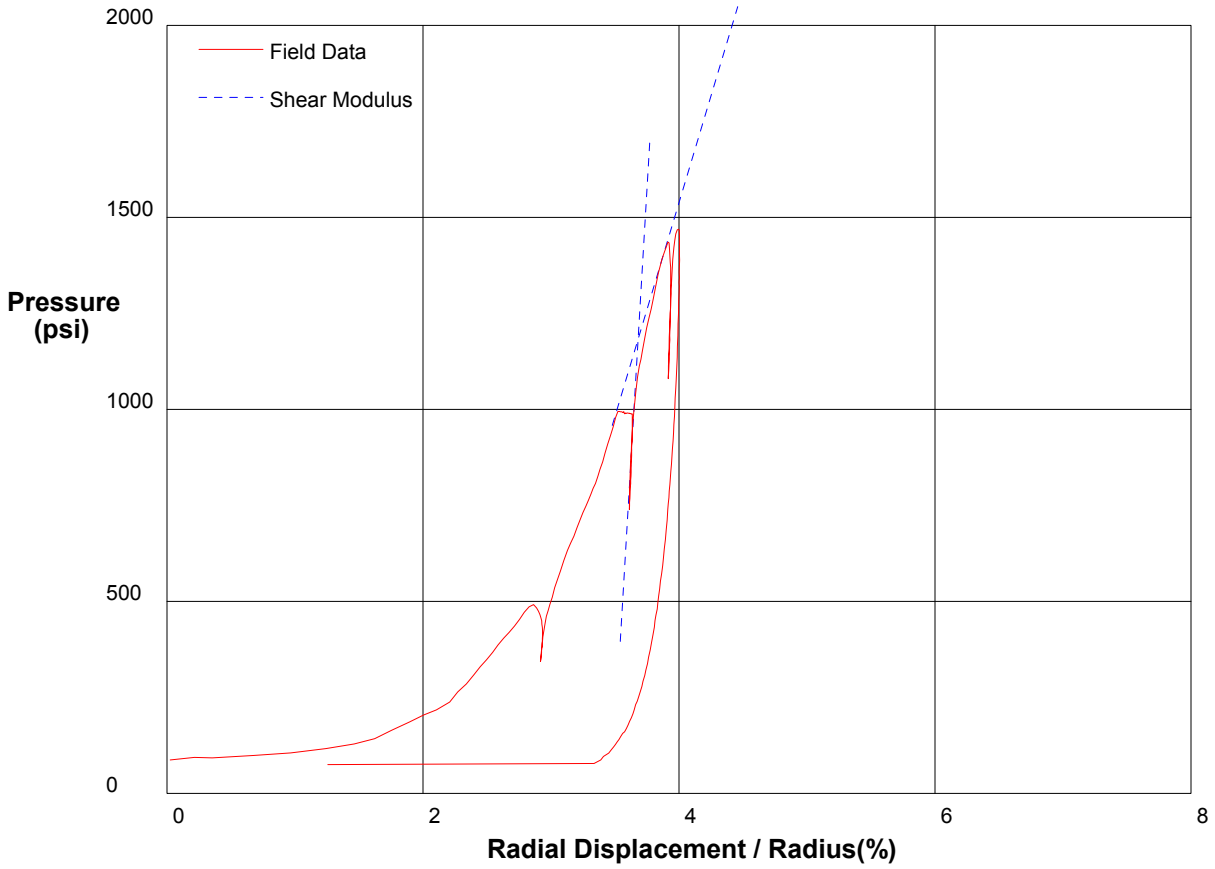


**Shear Modulus 283333 psi**

**Shear Modulus 55673 psi**

shift 3

**In Situ Engineering**

# Appendix I - Pressuremeter Data and Standard Interpretation

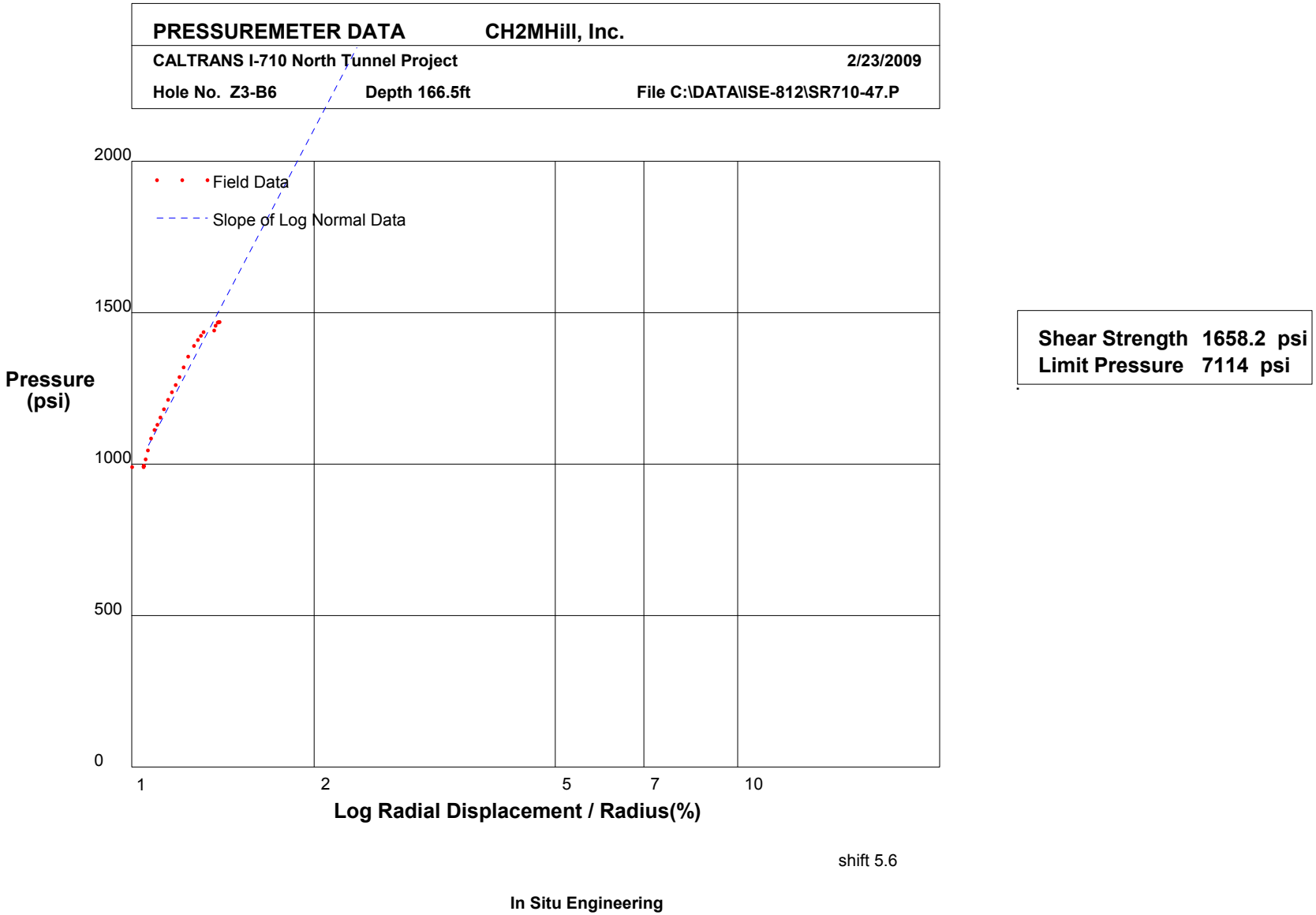

# Appendix I - Pressuremeter Data and Standard Interpretation

**PRESSUREMETER DATA** **CH2MHill, Inc.**

**CALTRANS I-710 North Tunnel Project** **2/24/2009**

**Hole No. Z3-B6** **Depth 188.2ft** **File C:\DATA\ISE-812\SR710-48.P**

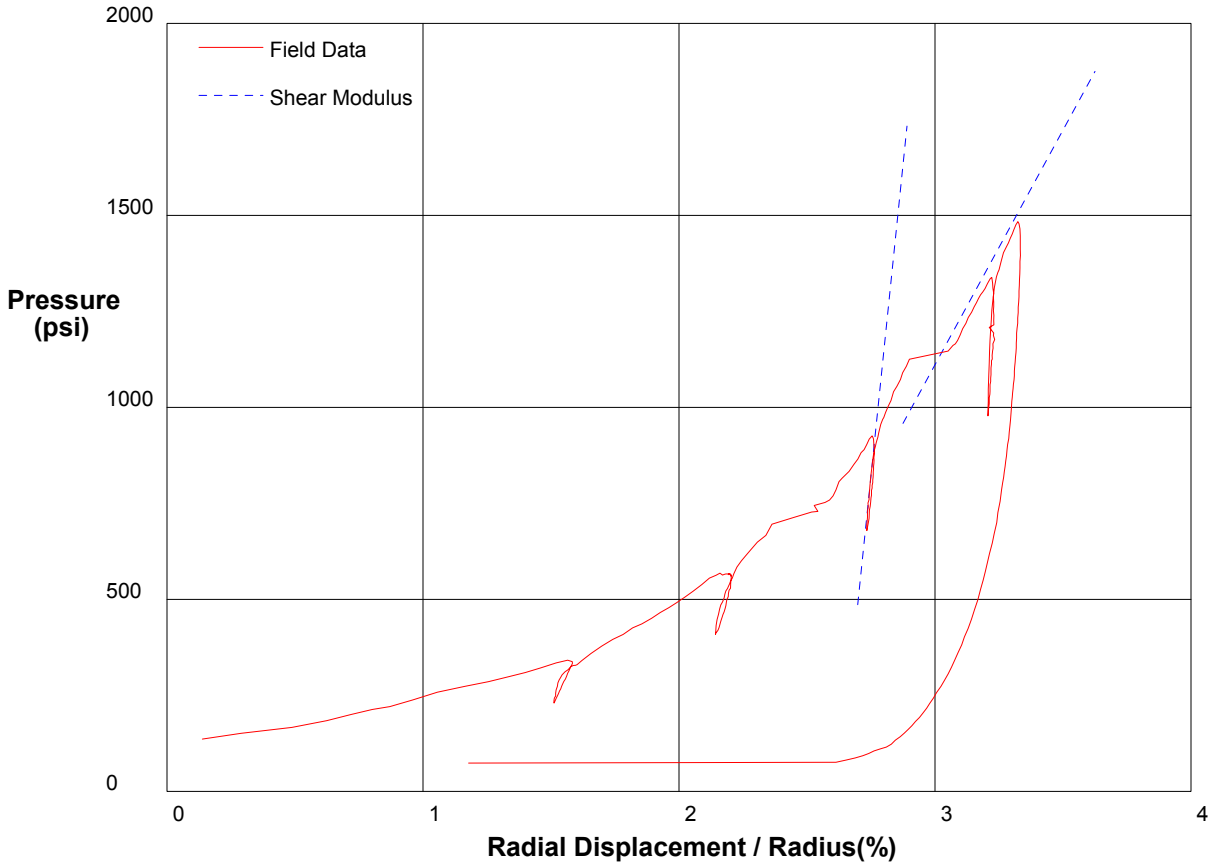


**Shear Modulus 323423 psi**

**Shear Modulus 61111 psi**

shift 1

**In Situ Engineering**

# Appendix I - Pressuremeter Data and Standard Interpretation

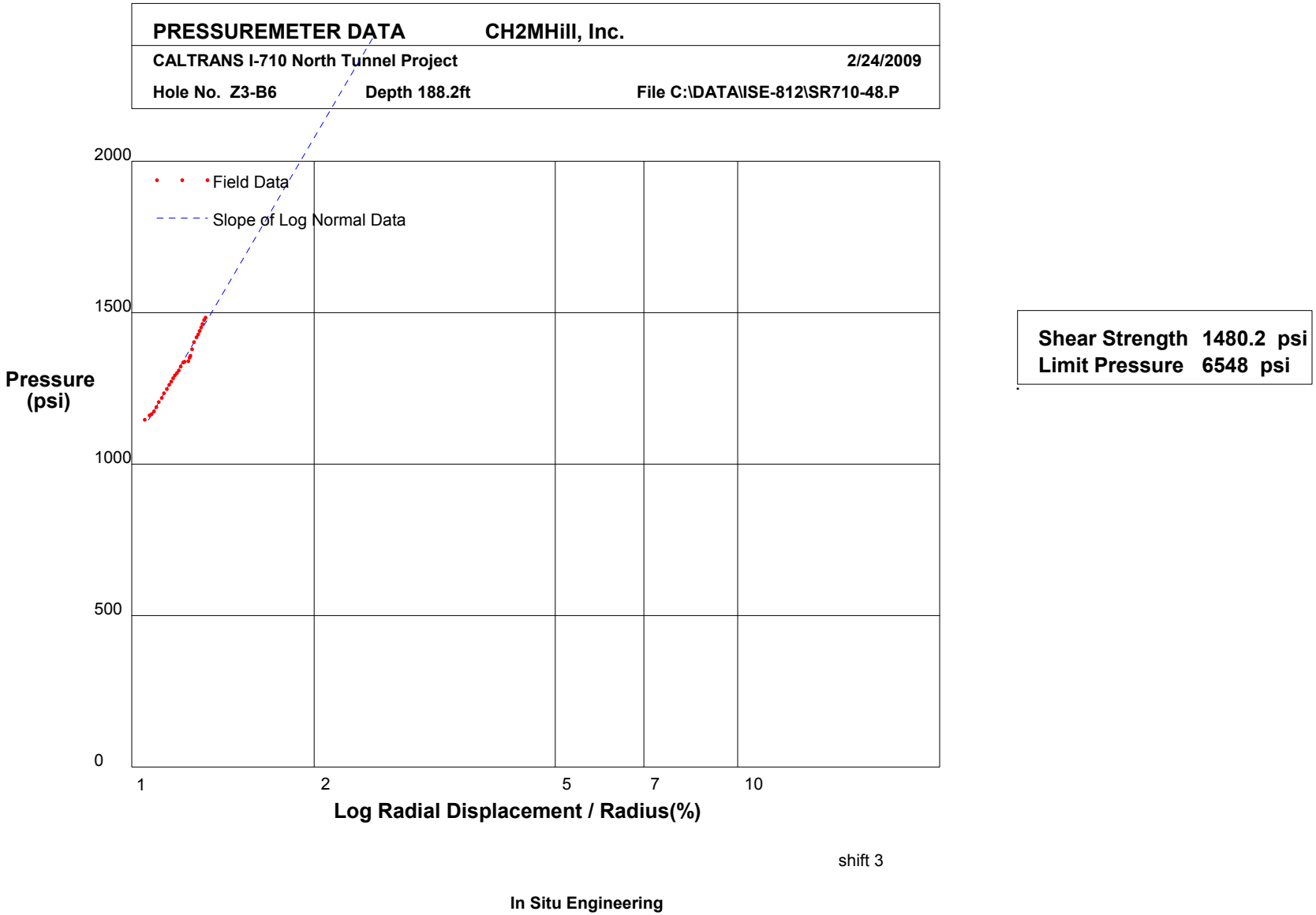

# Appendix II - Pressuremeter Model Interpretation

**PRESSUREMETER DATA** **CH2MHill, Inc.**

**CALTRANS I-710 North Tunnel Project** **1/16/2009**

**Hole No. Z3-B2** **Depth 200.9ft** **File C:\DATA\ISE-812\SR710-01.P**

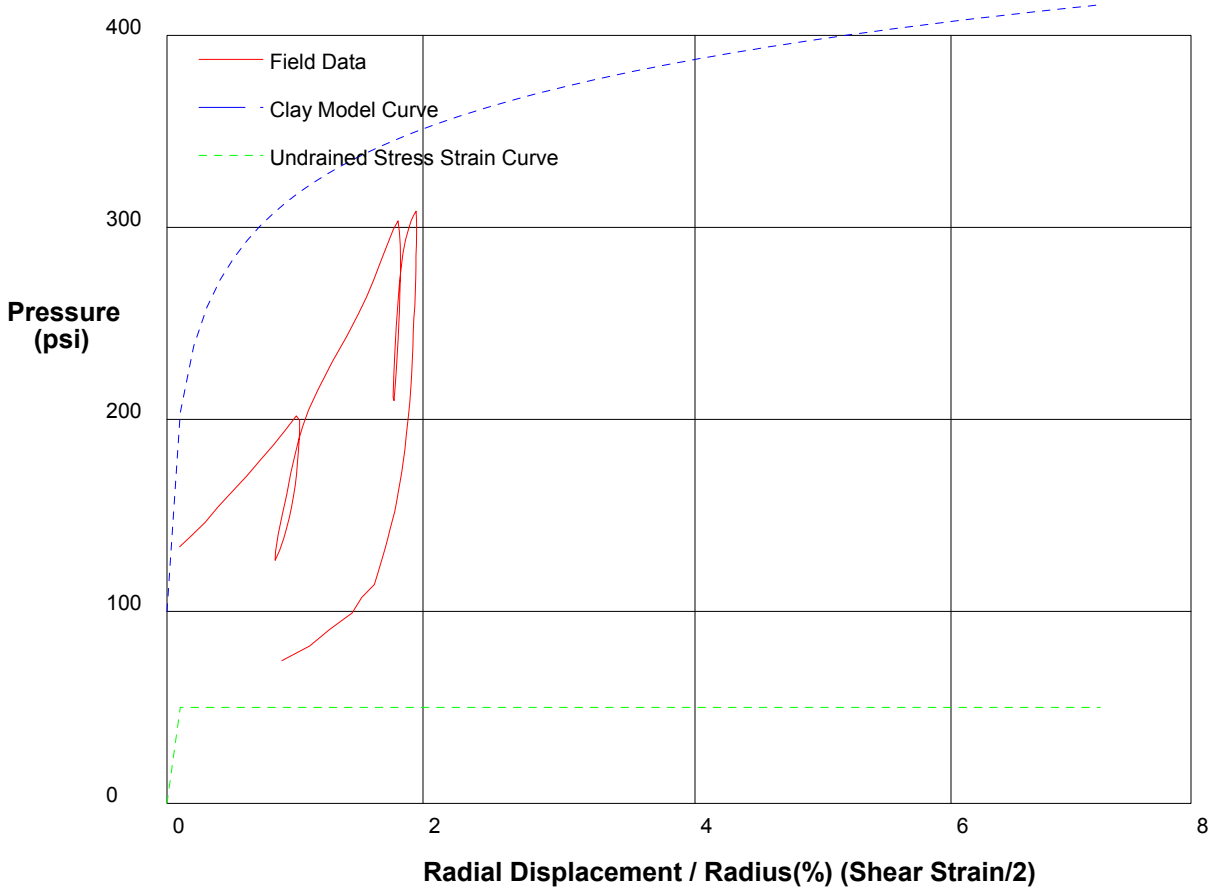


**GIBSON'S CLAY MODEL**

**Shear Strength 50 psi**
**Insitu Stress 100 psi**
**Shear Modulus 70000 psi**

shift 9

**In Situ Engineering**

# Appendix II - Pressuremeter Model Interpretation

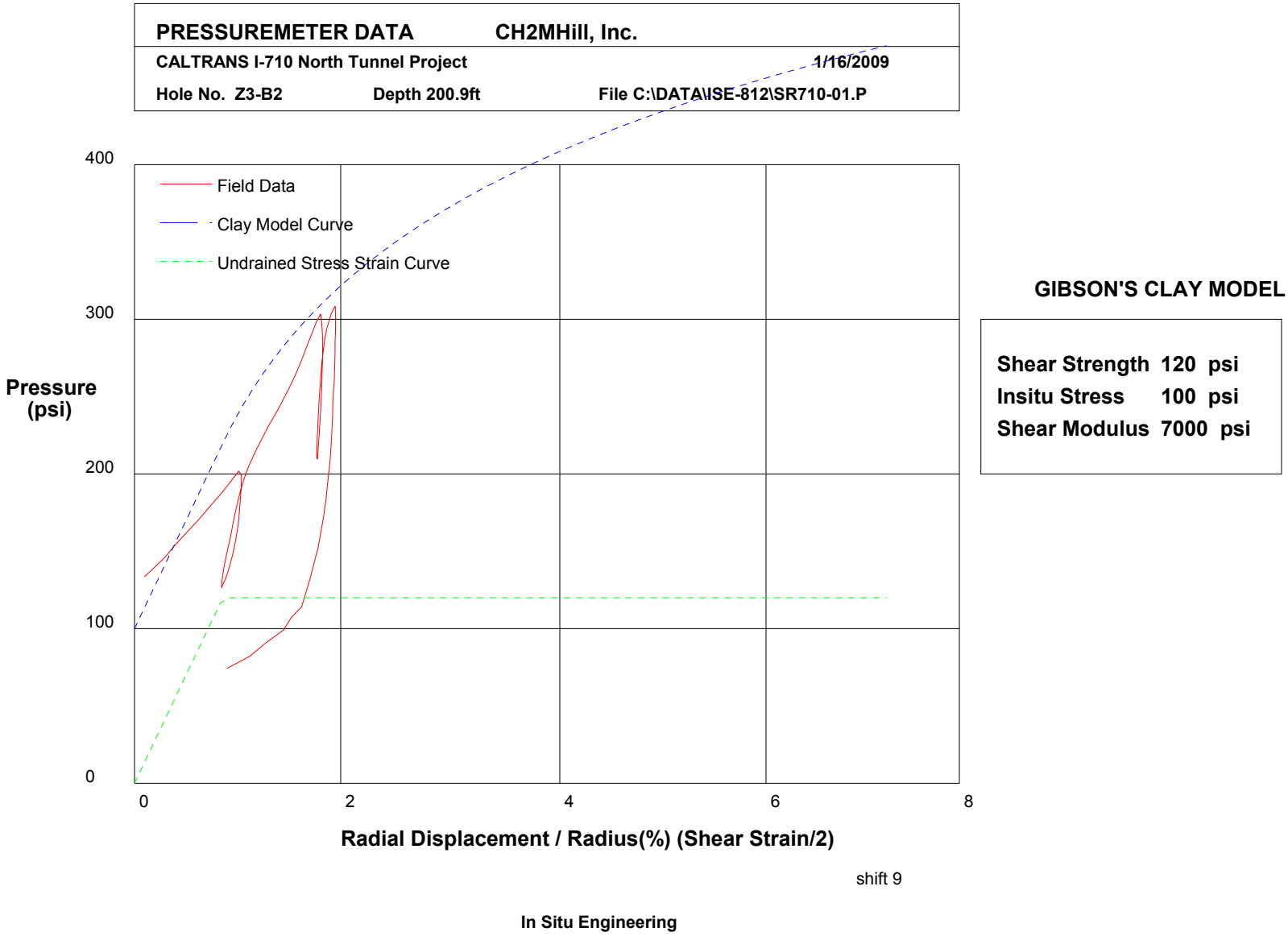

# Appendix II - Pressuremeter Model Interpretation

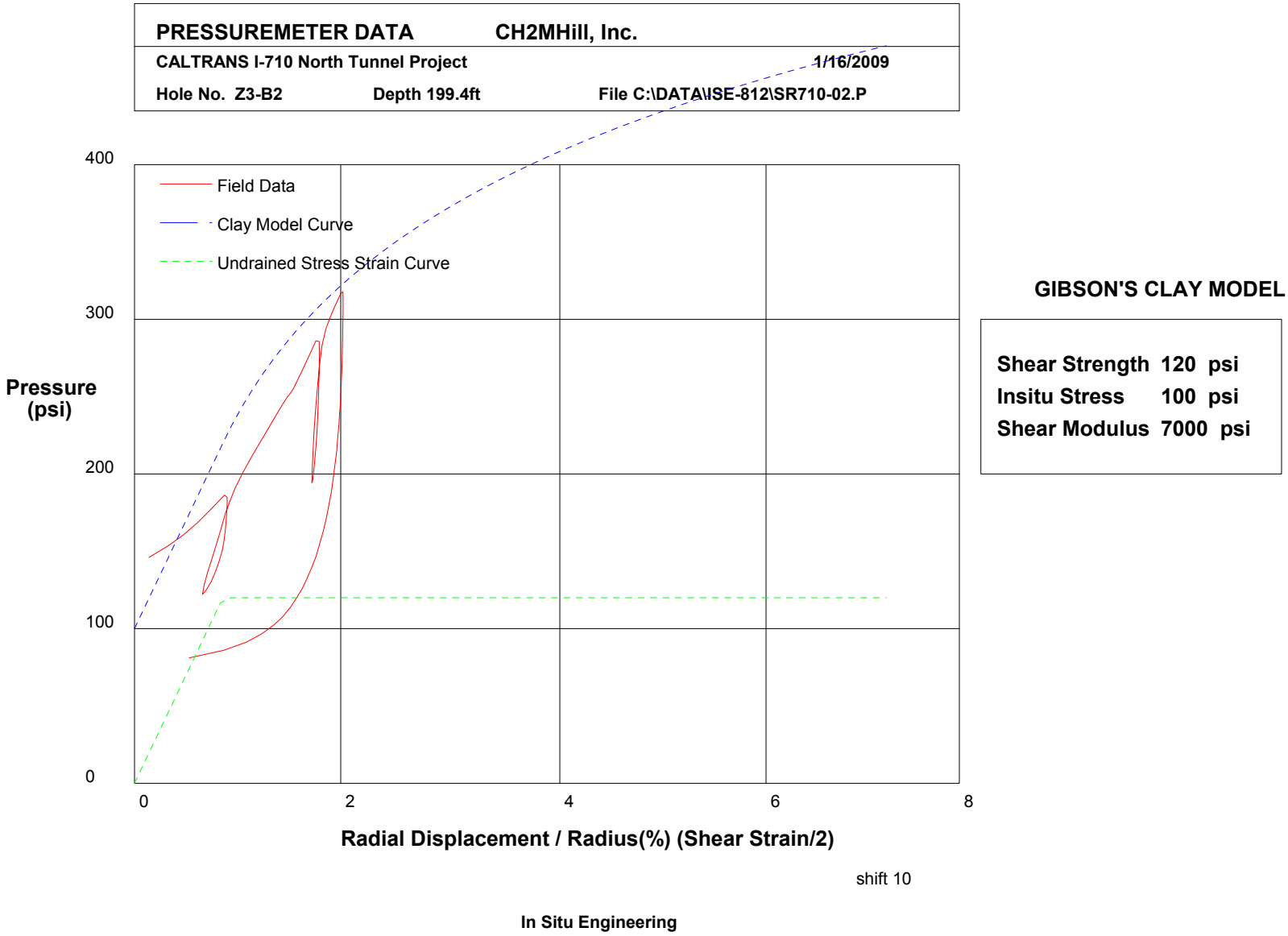

# Appendix II - Pressuremeter Model Interpretation

**PRESSUREMETER DATA** **CH2MHill, Inc.**

**CALTRANS I-710 North Tunnel Project** **1/16/2009**

**Hole No. Z3-B2** **Depth 199.4ft** **File C:\DATA\ISE-812\SR710-02.P**

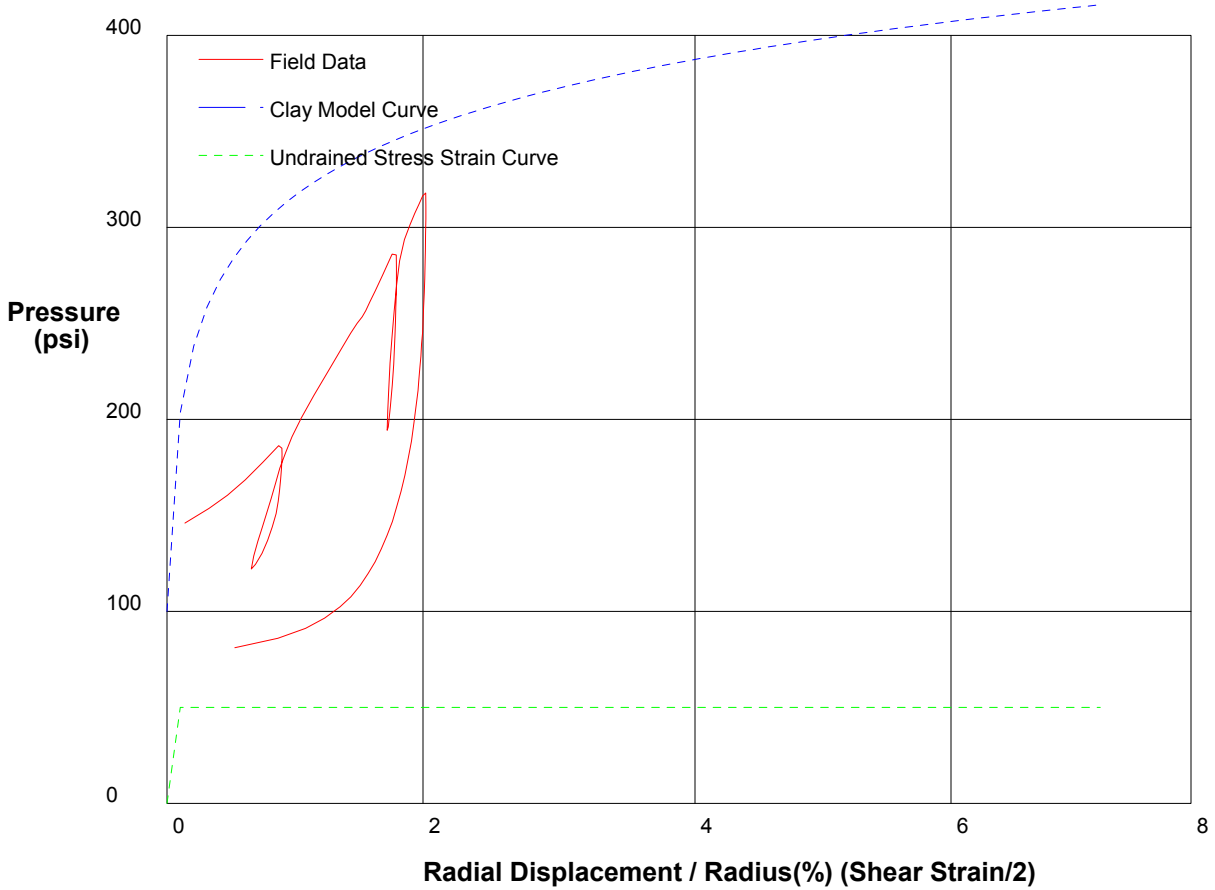


**GIBSON'S CLAY MODEL**

**Shear Strength 50 psi**
**Insitu Stress 100 psi**
**Shear Modulus 70000 psi**

shift 10

**In Situ Engineering**

# Appendix II - Pressuremeter Model Interpretation

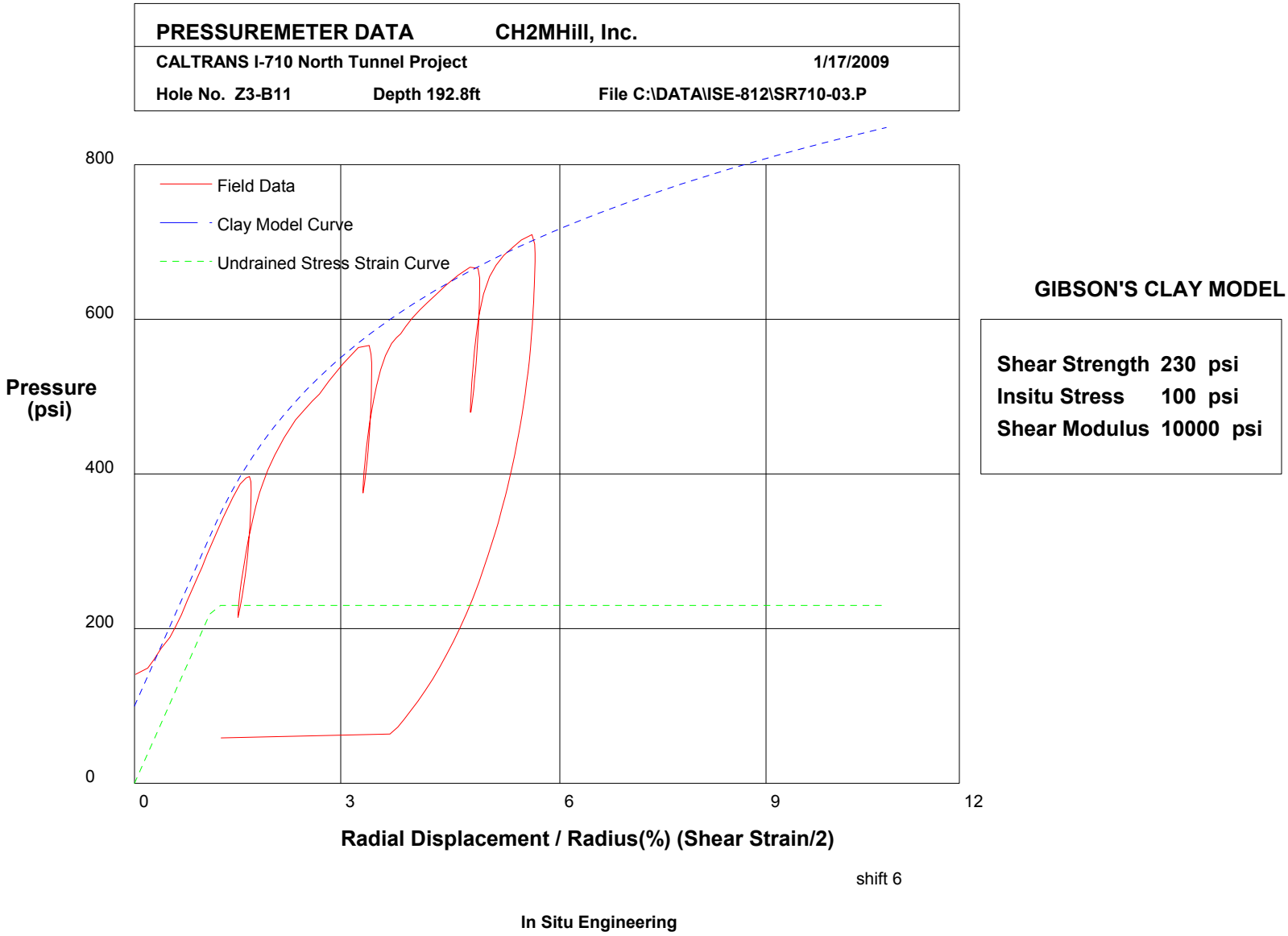

# Appendix II - Pressuremeter Model Interpretation

**PRESSUREMETER DATA** **CH2MHill, Inc.**

**CALTRANS I-710 North Tunnel Project** **1/17/2009**

**Hole No. Z3-B11** **Depth 192.8ft** **File C:\DATA\ISE-812\SR710-03.P**

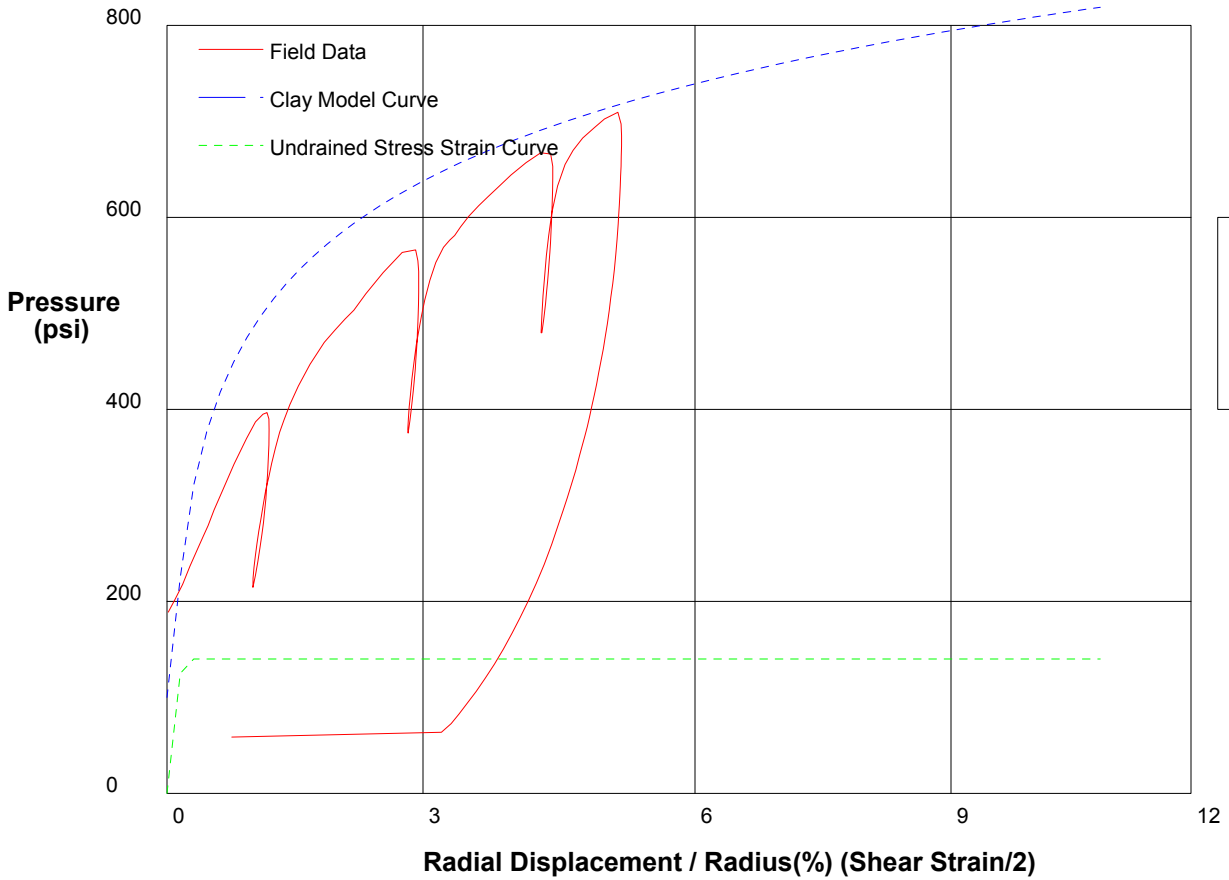


**GIBSON'S CLAY MODEL**

| | |
|---|---|
| **Shear Strength** | **140 psi** |
| **Insitu Stress** | **100 psi** |
| **Shear Modulus** | **40000 psi** |

shift 6.5

**In Situ Engineering**

# Appendix II - Pressuremeter Model Interpretation

**PRESSUREMETER DATA** **CH2M-HILL, Inc.**

**CALTRANS I-170 North Tunnel Project** **1/17/2009**

**Hole No. Z3-B11** **Depth 192.8ft** **File C:\DATA\ISE-812\SR710-03.P**

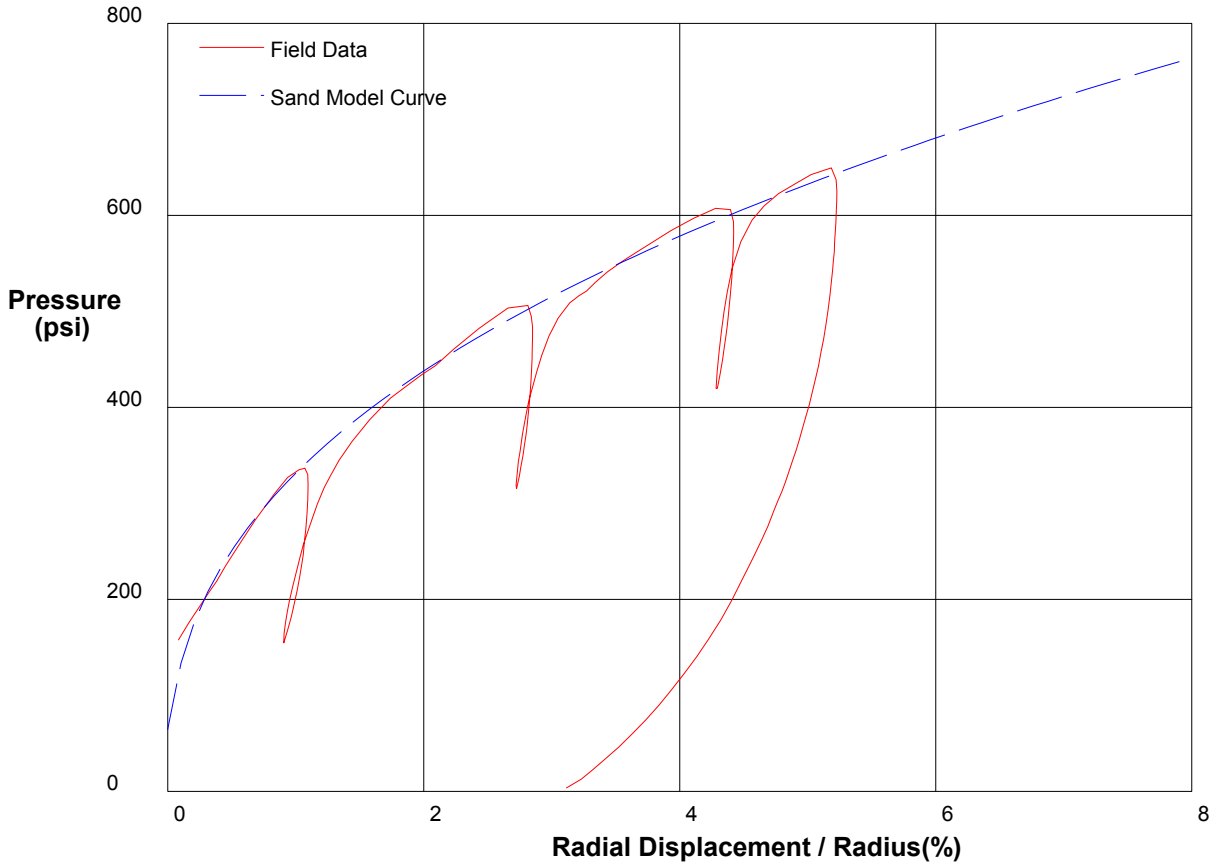


**THE In Situ Engineering SAND MODEL**

| | |
|---|---|
| **Water Pressure** | **60 psi** |
| **Friction Angle** | **36 deg** |
| **Critical Friction Angle** | **32 deg** |
| **Lateral Stress** | **65 psi** |
| **Shear Modulus** | **35000 psi** |

shift 6.6

**In Situ Engineering**

# Appendix II - Pressuremeter Model Interpretation

**PRESSUREMETER DATA** **CH2MHill, Inc.**

**CALTRANS I-710 North Tunnel Project** **1/17/2009**

**Hole No. Z3-B11** **Depth 191.3ft** **File C:\DATA\ISE-812\SR710-04.P**

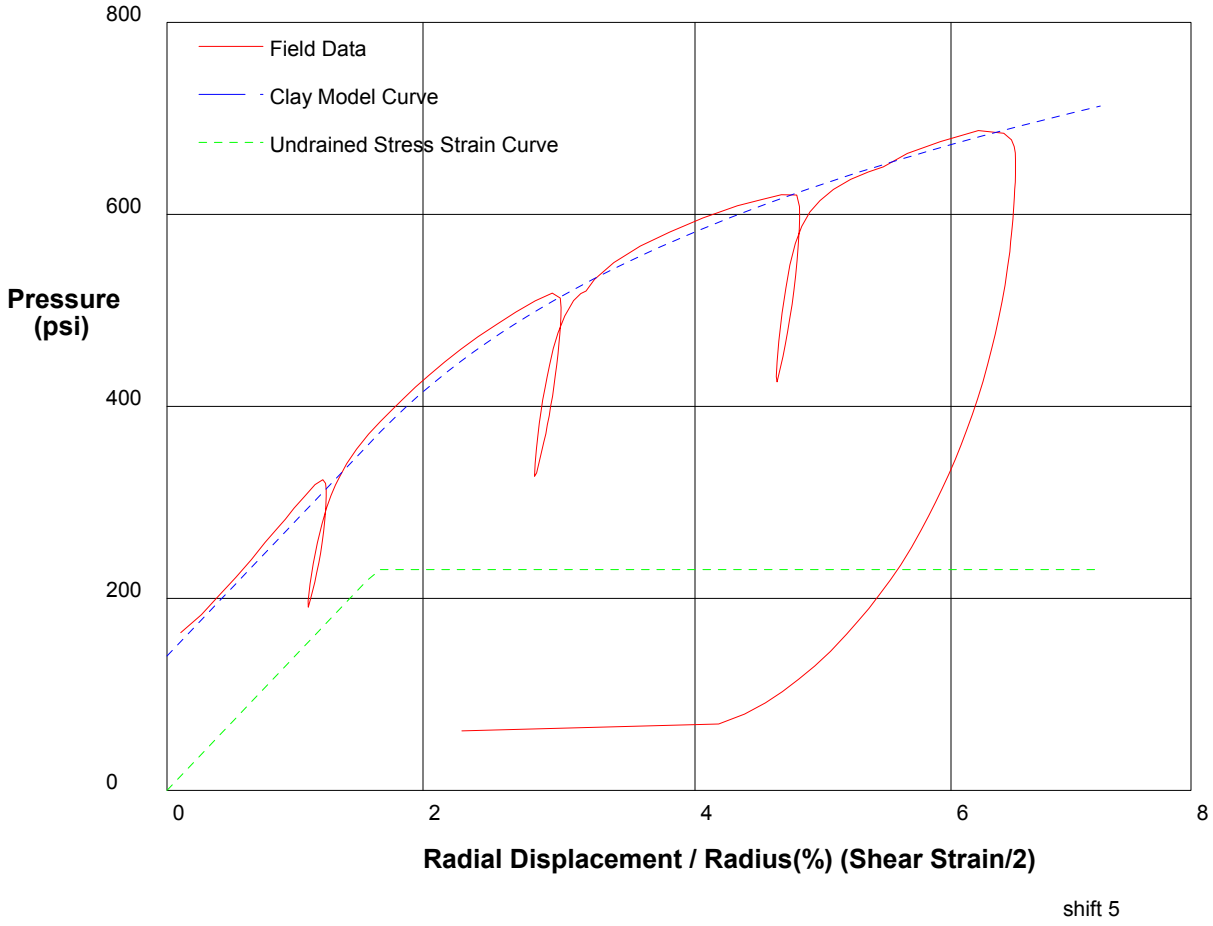


**GIBSON'S CLAY MODEL**

| | |
|---|---|
| **Shear Strength** | **230 psi** |
| **Insitu Stress** | **140 psi** |
| **Shear Modulus** | **7000 psi** |

shift 5

**In Situ Engineering**

# Appendix II - Pressuremeter Model Interpretation

**PRESSUREMETER DATA** **CH2MHill, Inc.**

**CALTRANS I-710 North Tunnel Project** **1/17/2009**

**Hole No. Z3-B11** **Depth 191.3ft** **File C:\DATA\ISE-812\SR710-04.P**

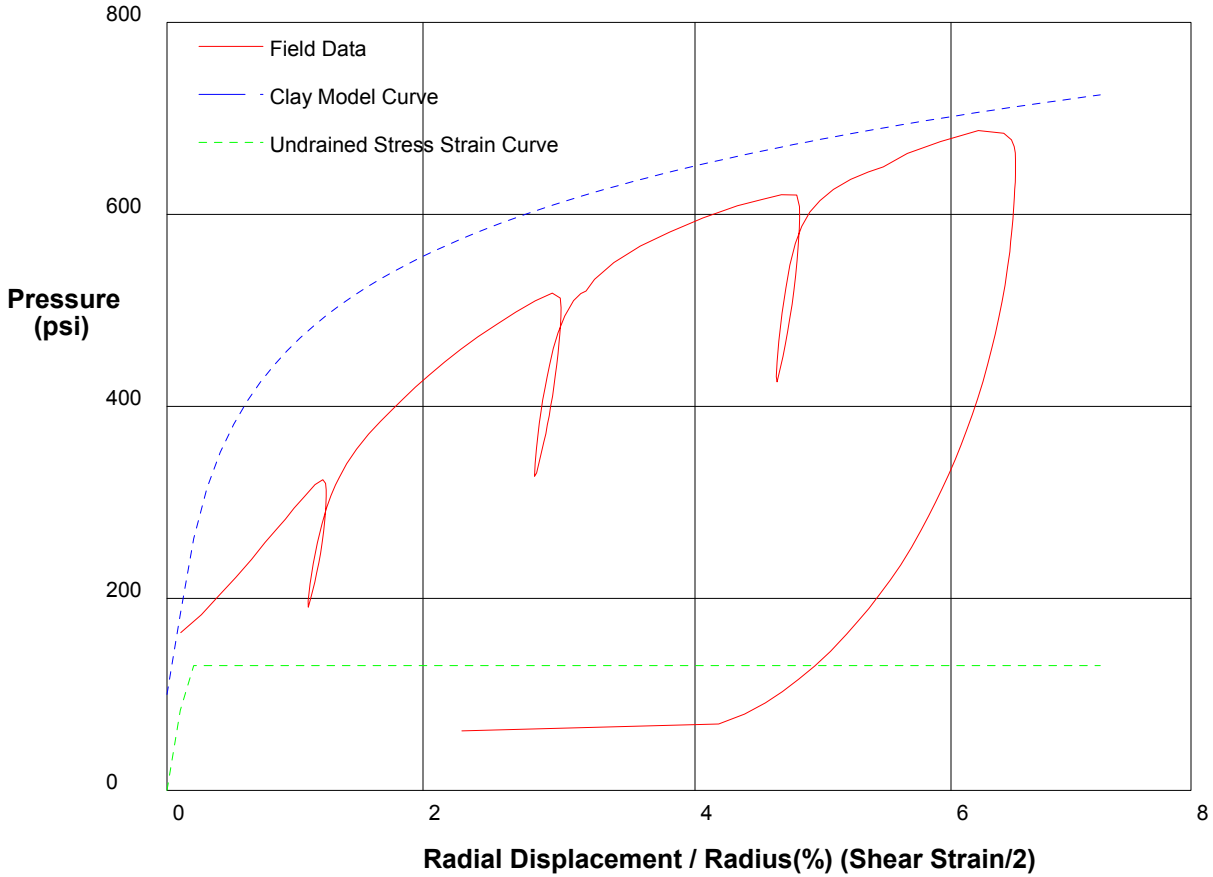


**GIBSON'S CLAY MODEL**

| | |
|---|---|
| **Shear Strength** | **130 psi** |
| **Insitu Stress** | **100 psi** |
| **Shear Modulus** | **40000 psi** |

shift 5

**In Situ Engineering**

# Appendix II - Pressuremeter Model Interpretation

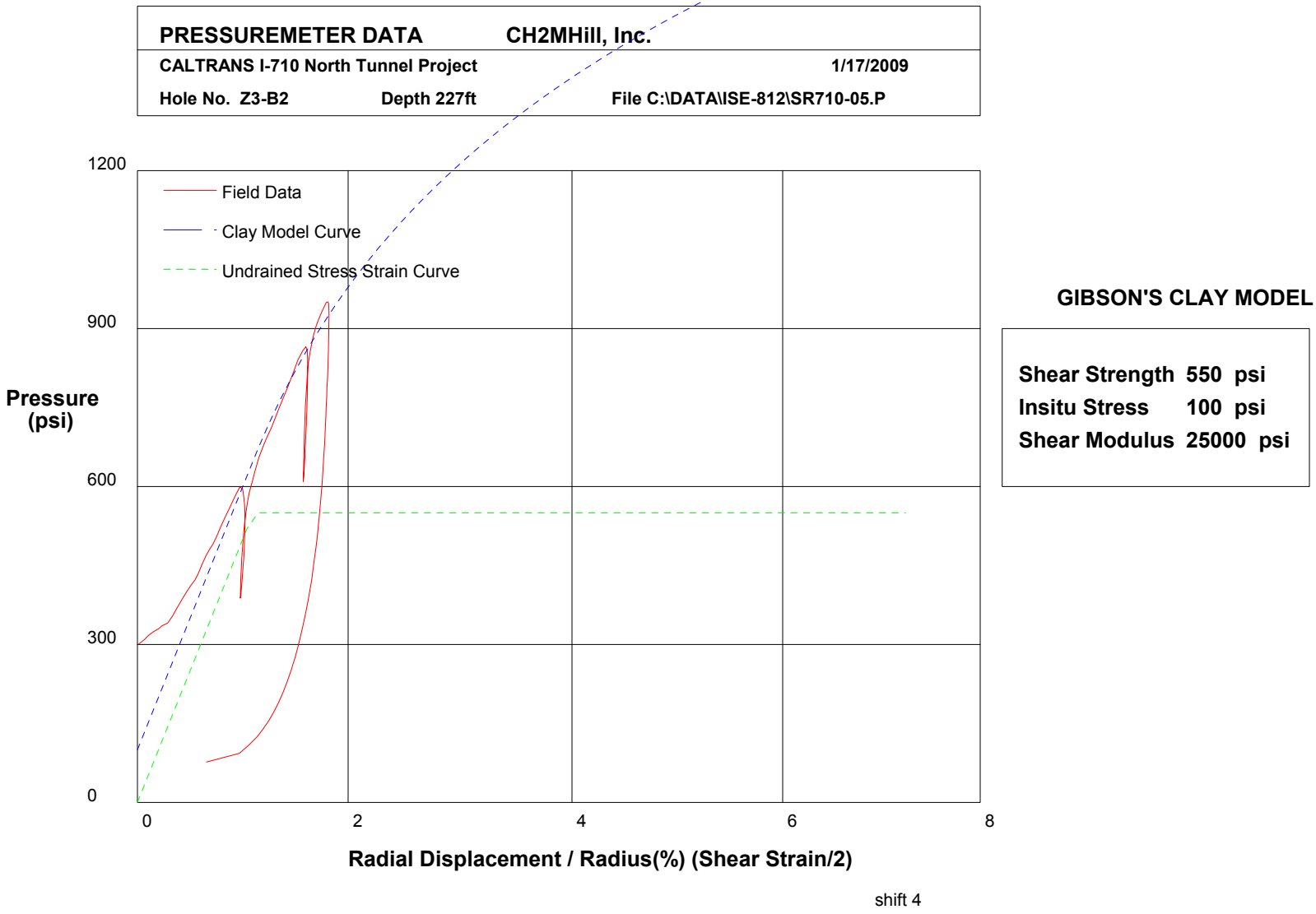

# Appendix II - Pressuremeter Model Interpretation

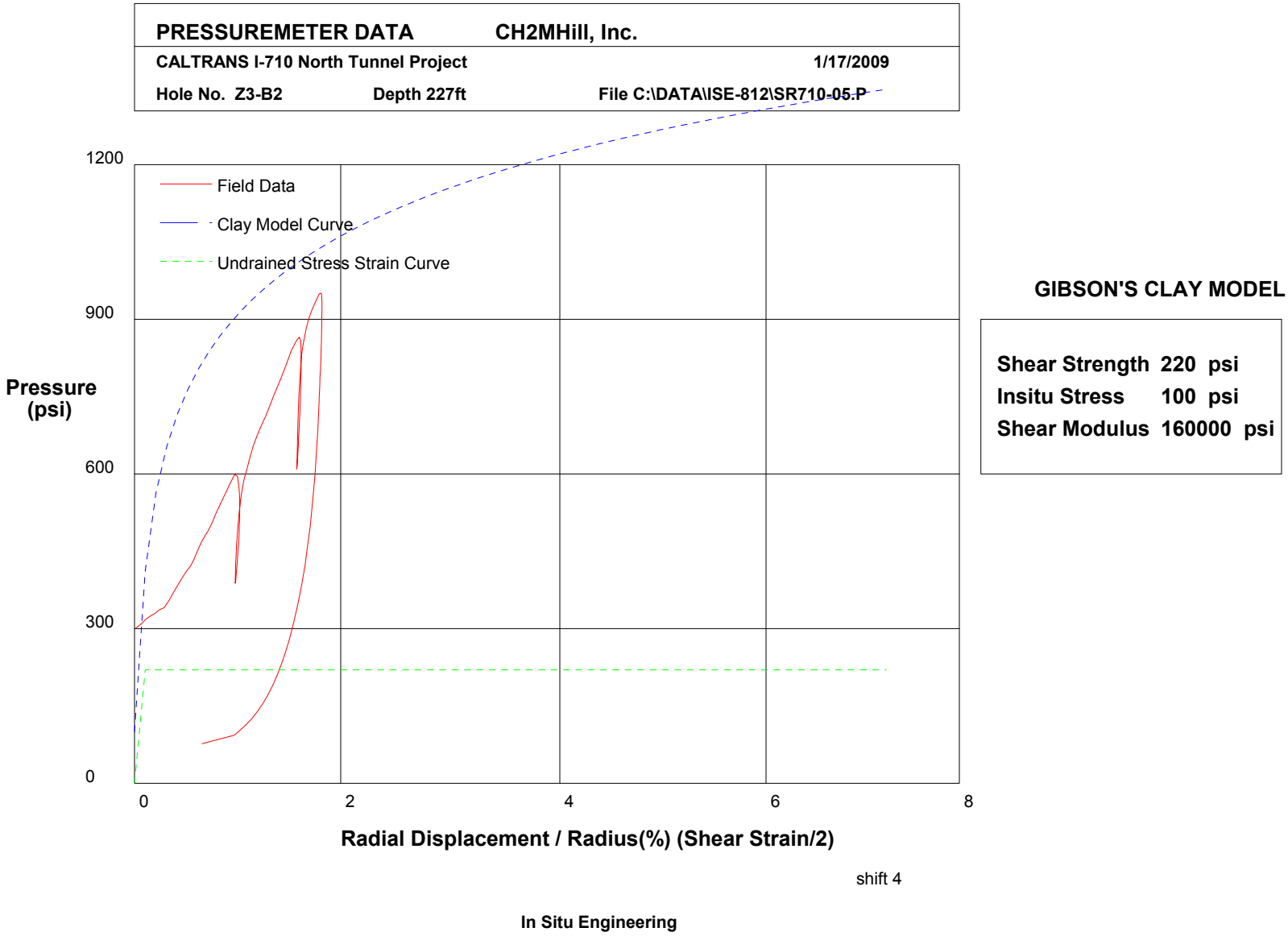

# Appendix II - Pressuremeter Model Interpretation

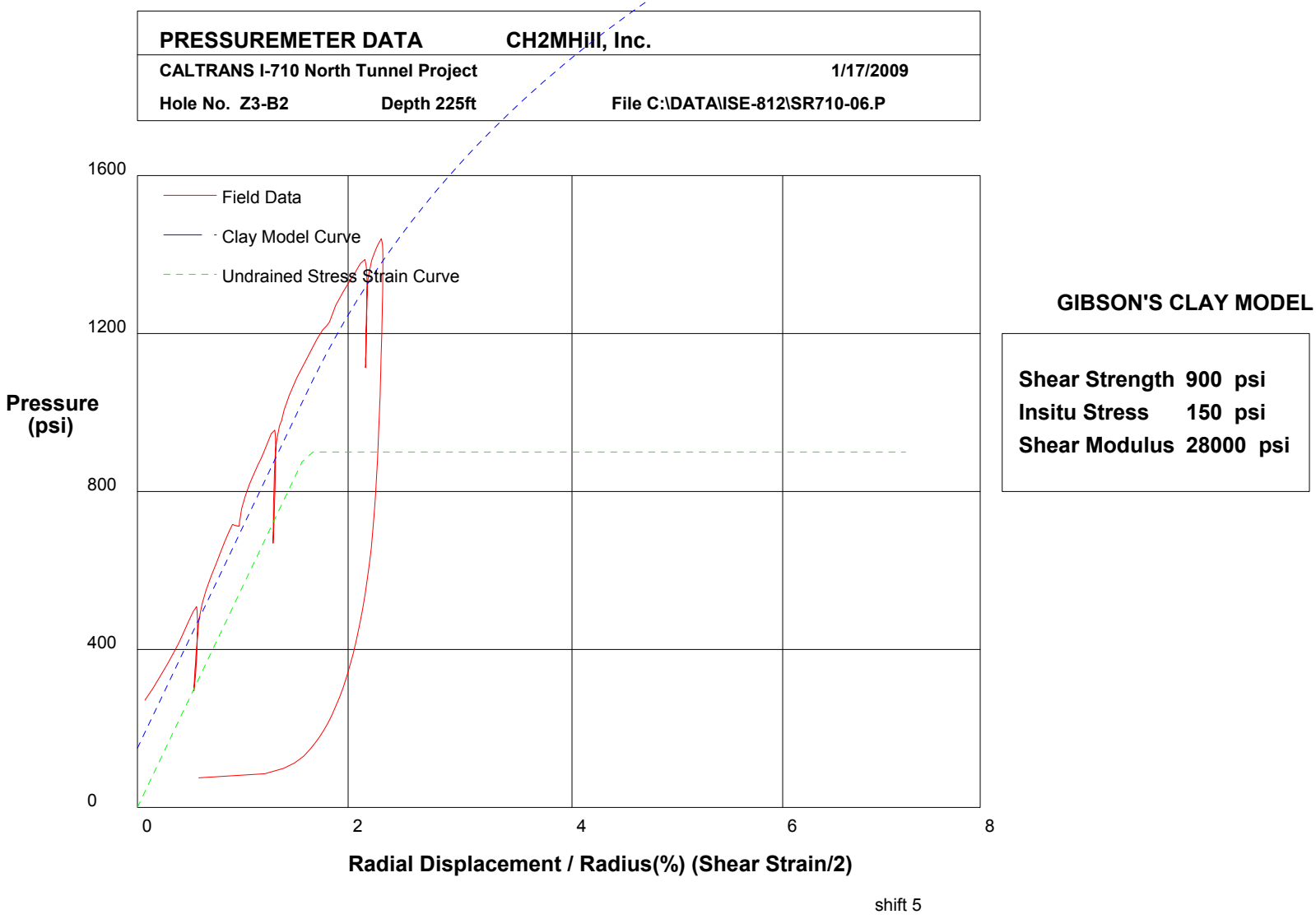


**In Situ Engineering**

# Appendix II - Pressuremeter Model Interpretation

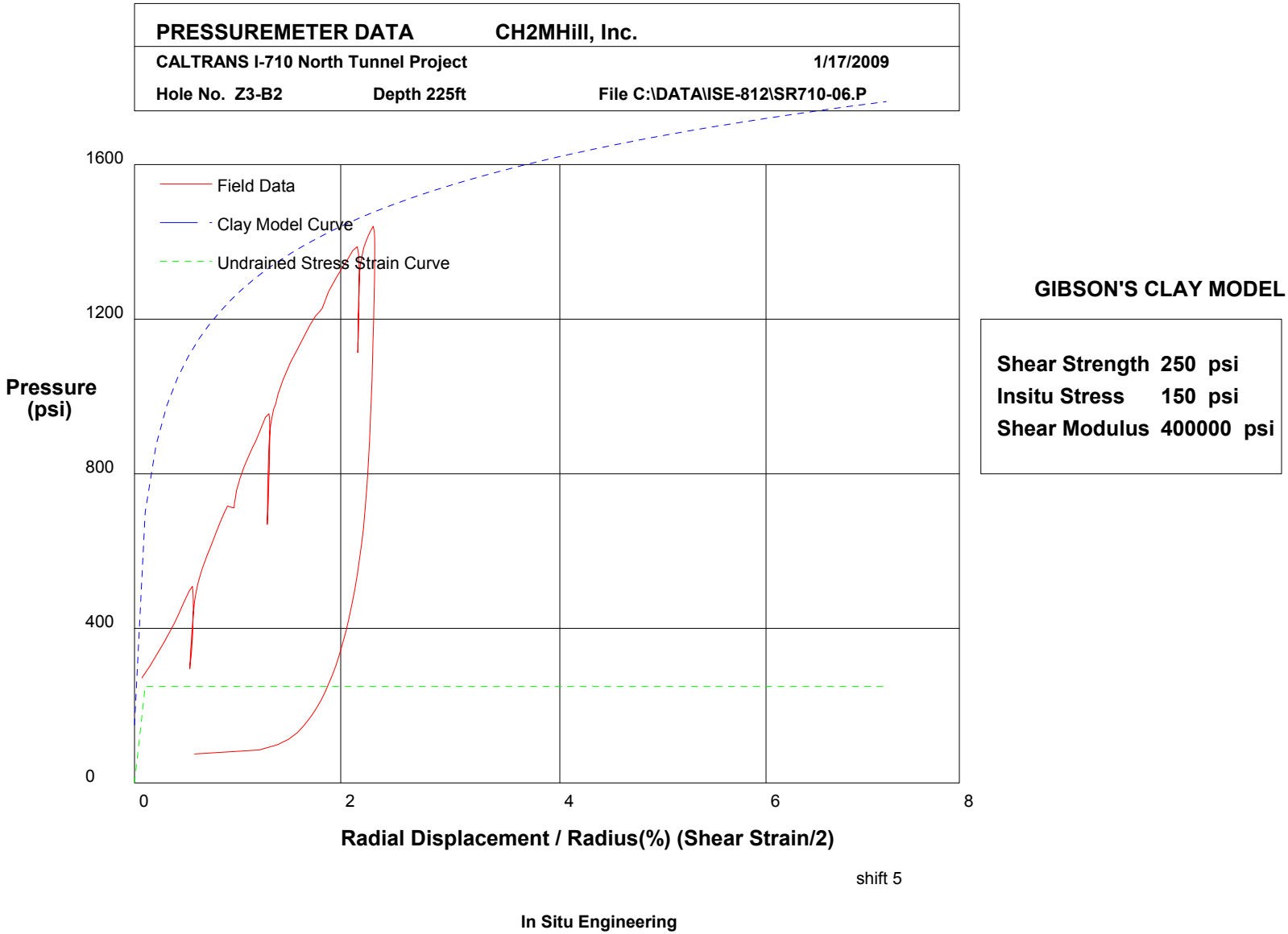

# Appendix II - Pressuremeter Model Interpretation

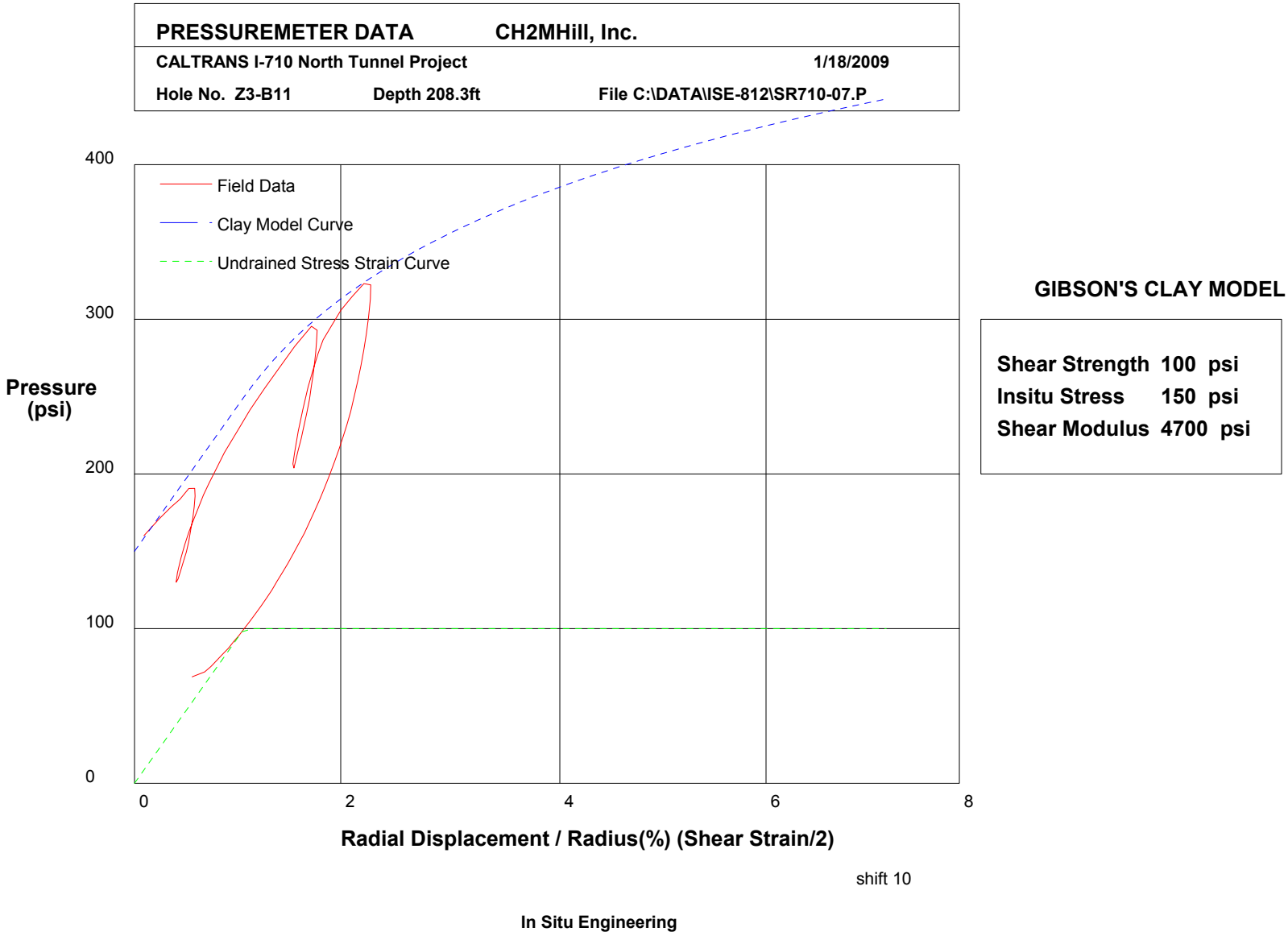

# Appendix II - Pressuremeter Model Interpretation

**PRESSUREMETER DATA** **CH2MHill, Inc.**

**CALTRANS I-710 North Tunnel Project** **1/18/2009**

**Hole No. Z3-B11** **Depth 208.3ft** **File C:\DATA\ISE-812\SR710-07.P**

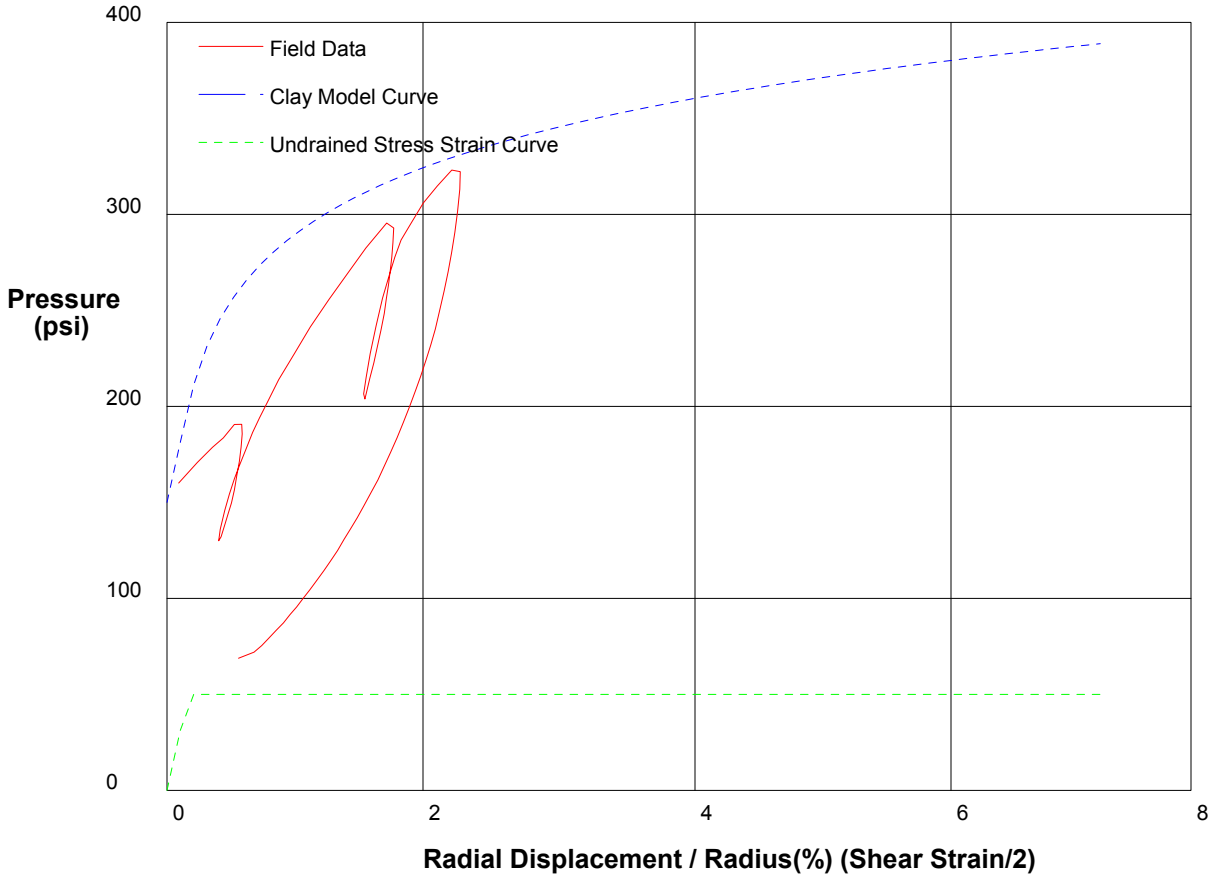


**GIBSON'S CLAY MODEL**

**Shear Strength 50 psi**
**Insitu Stress 150 psi**
**Shear Modulus 15000 psi**

shift 10

**In Situ Engineering**

# Appendix II - Pressuremeter Model Interpretation

**PRESSUREMETER DATA** **CH2MHill, Inc.**

**CALTRANS I-710 North Tunnel Project** **1/18/2009**

**Hole No. Z3-B11** **Depth 206.9ft** **File C:\DATA\ISE-812\SR710-08.P**

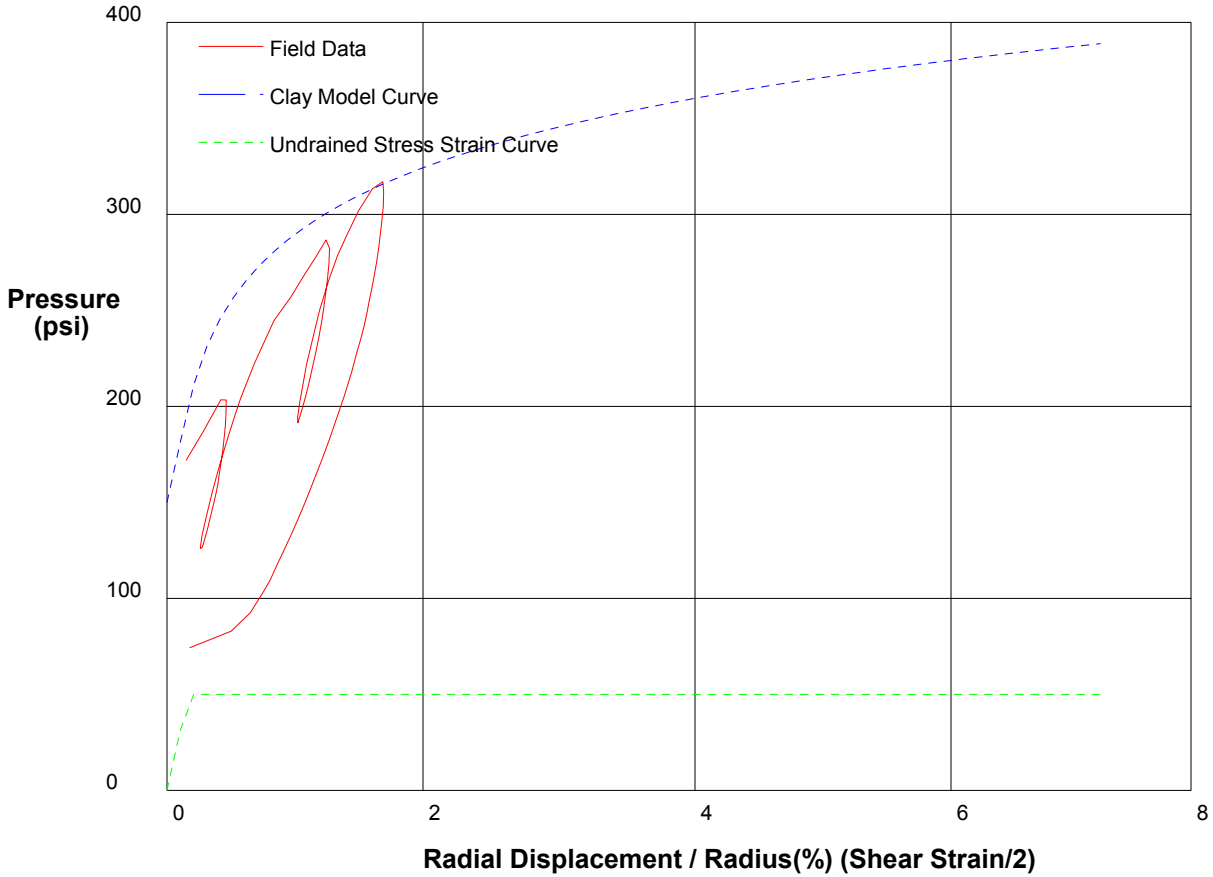


**GIBSON'S CLAY MODEL**

**Shear Strength 50 psi**
**Insitu Stress 150 psi**
**Shear Modulus 15000 psi**

shift 11

**In Situ Engineering**

# Appendix II - Pressuremeter Model Interpretation

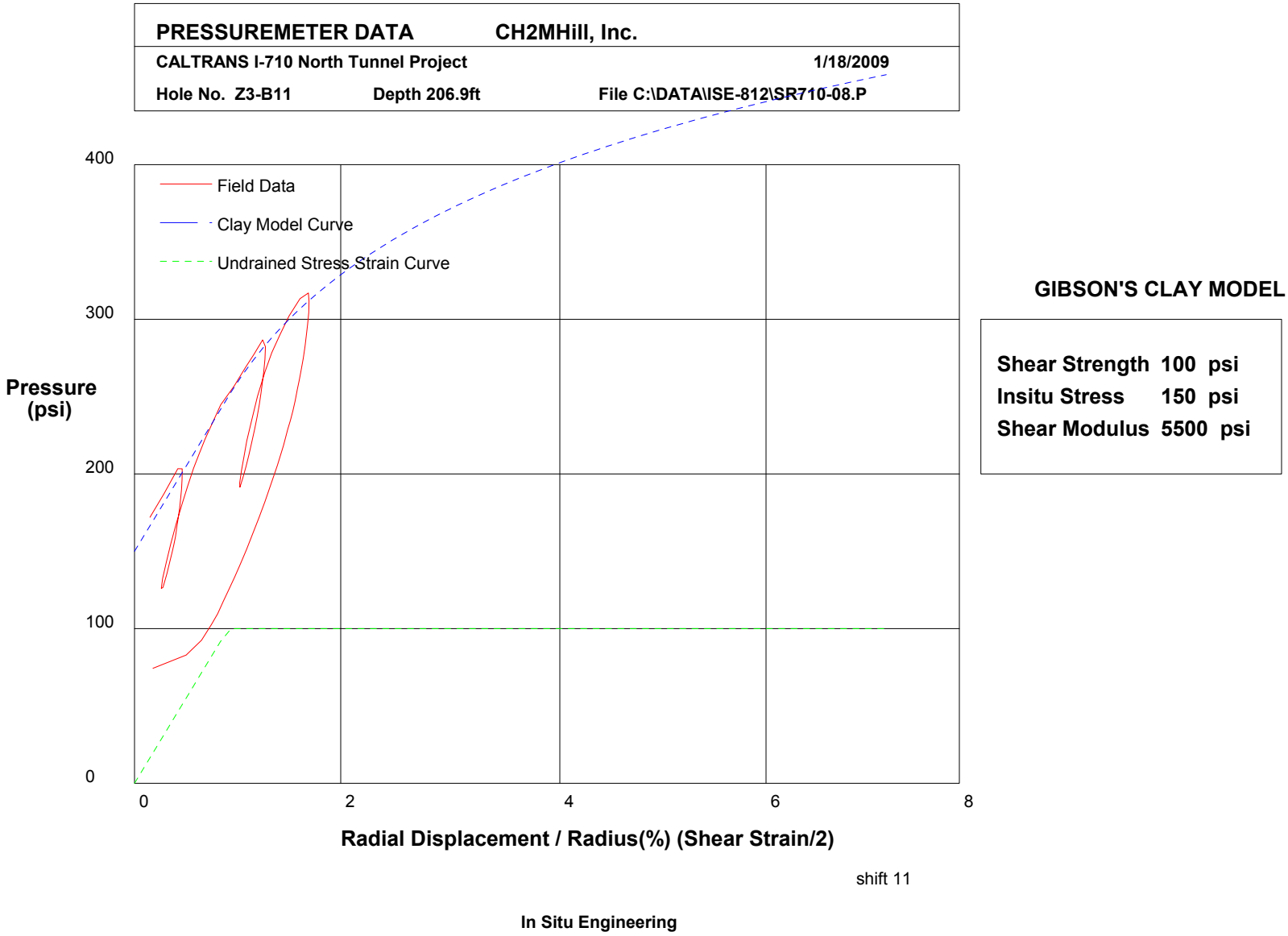

# Appendix II - Pressuremeter Model Interpretation

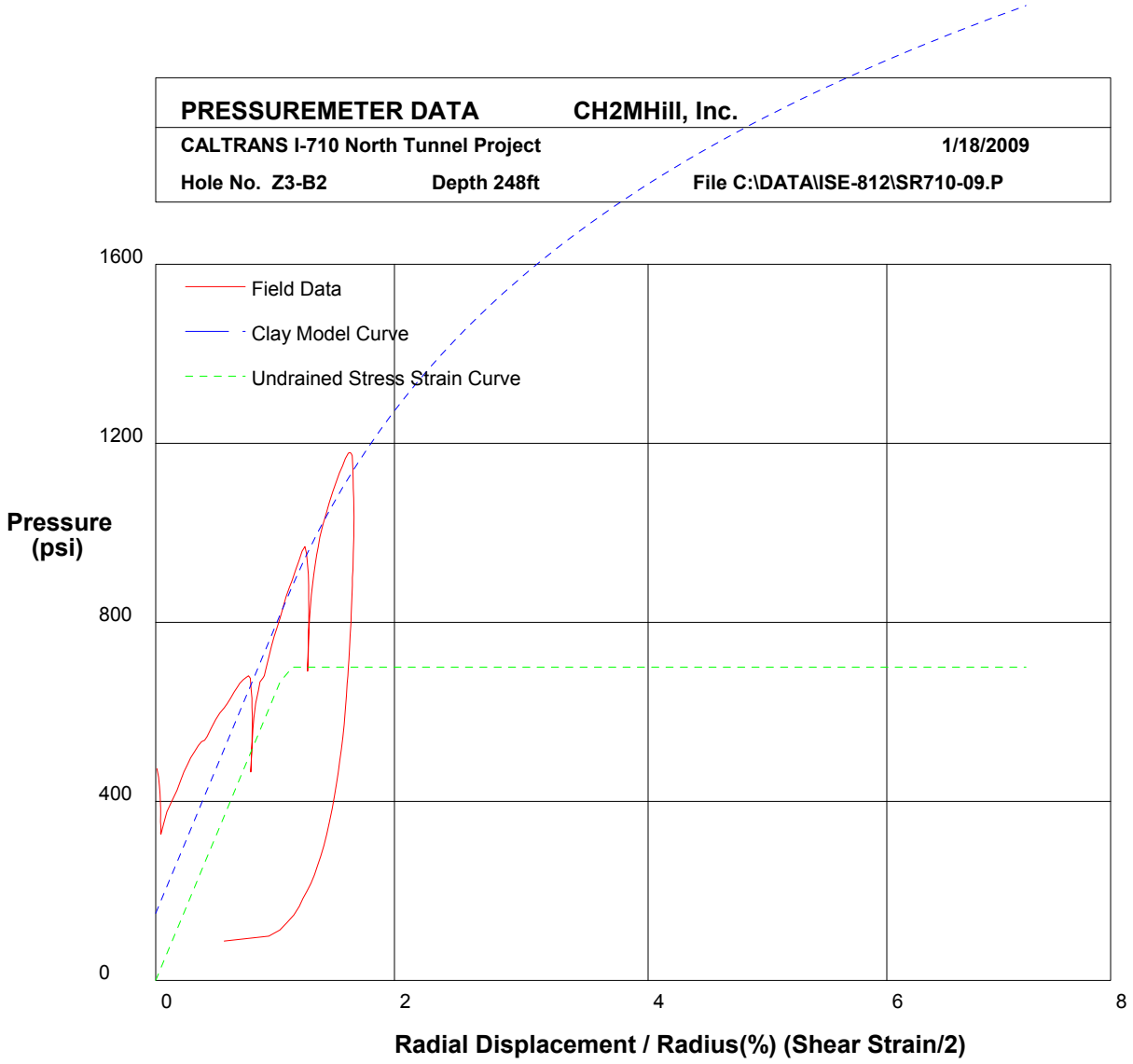


**GIBSON'S CLAY MODEL**

| | |
|---|---|
| **Shear Strength** | **700 psi** |
| **Insitu Stress** | **150 psi** |
| **Shear Modulus** | **32000 psi** |

# Appendix II - Pressuremeter Model Interpretation

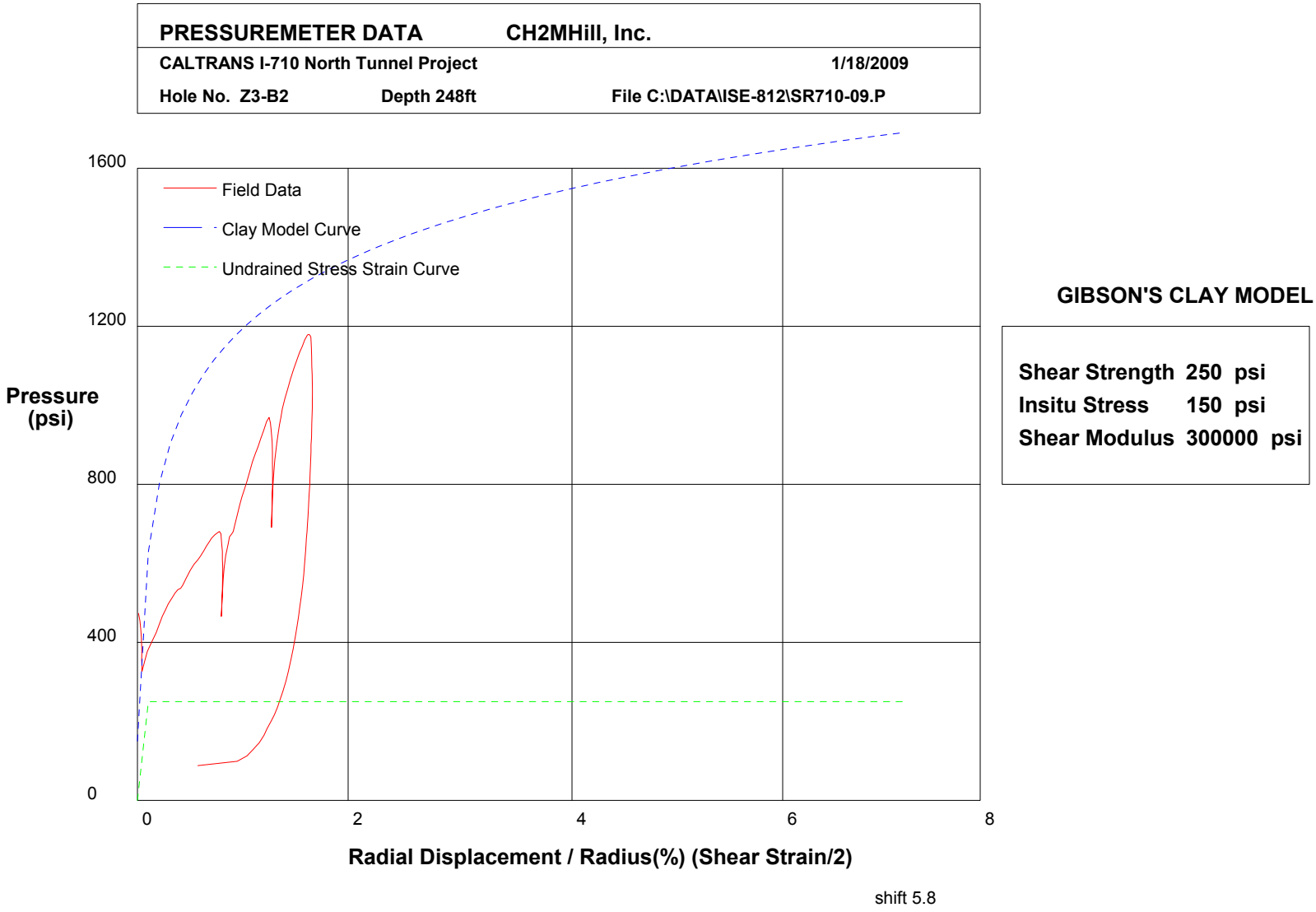

# Appendix II - Pressuremeter Model Interpretation

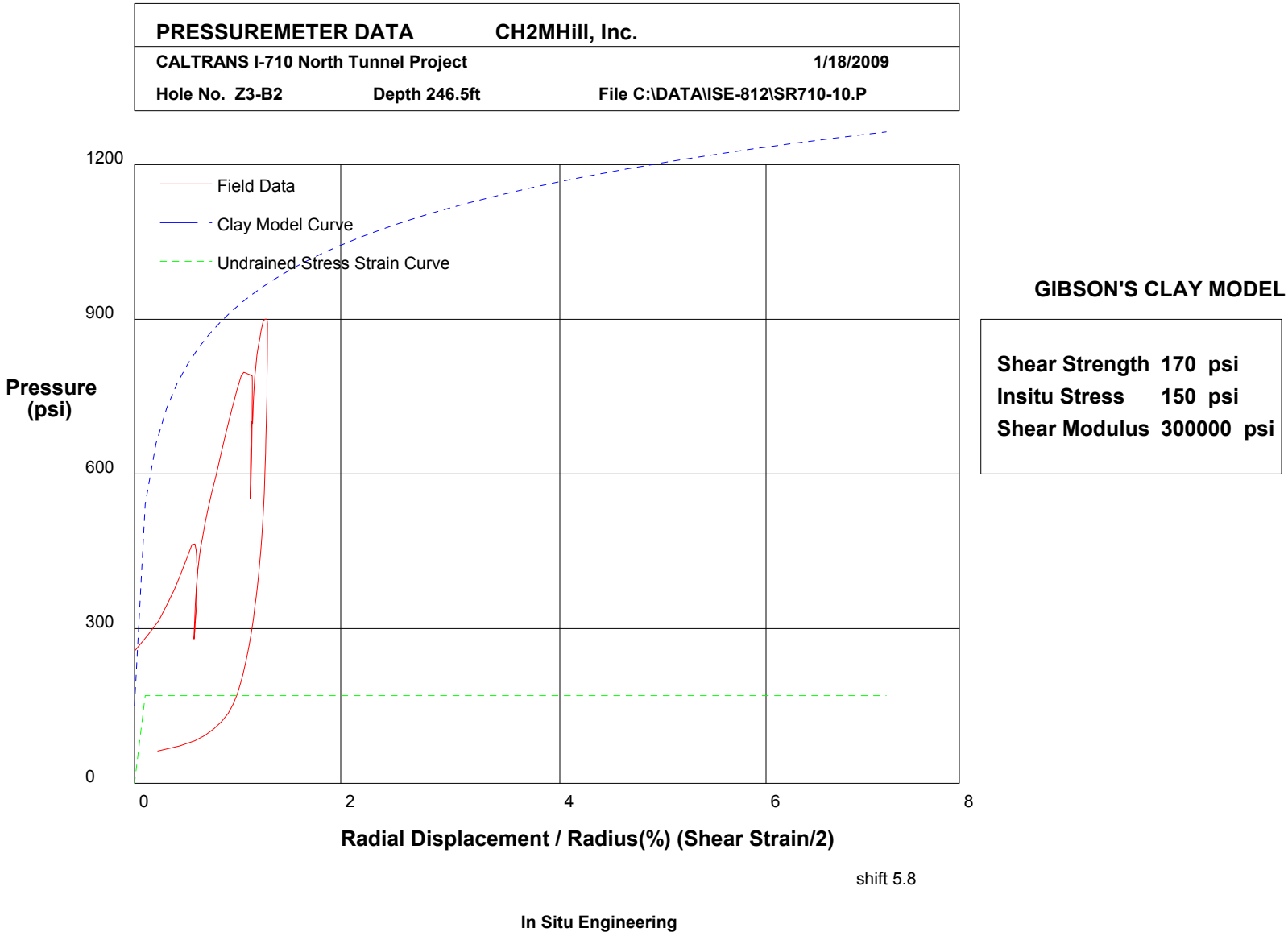

# Appendix II - Pressuremeter Model Interpretation

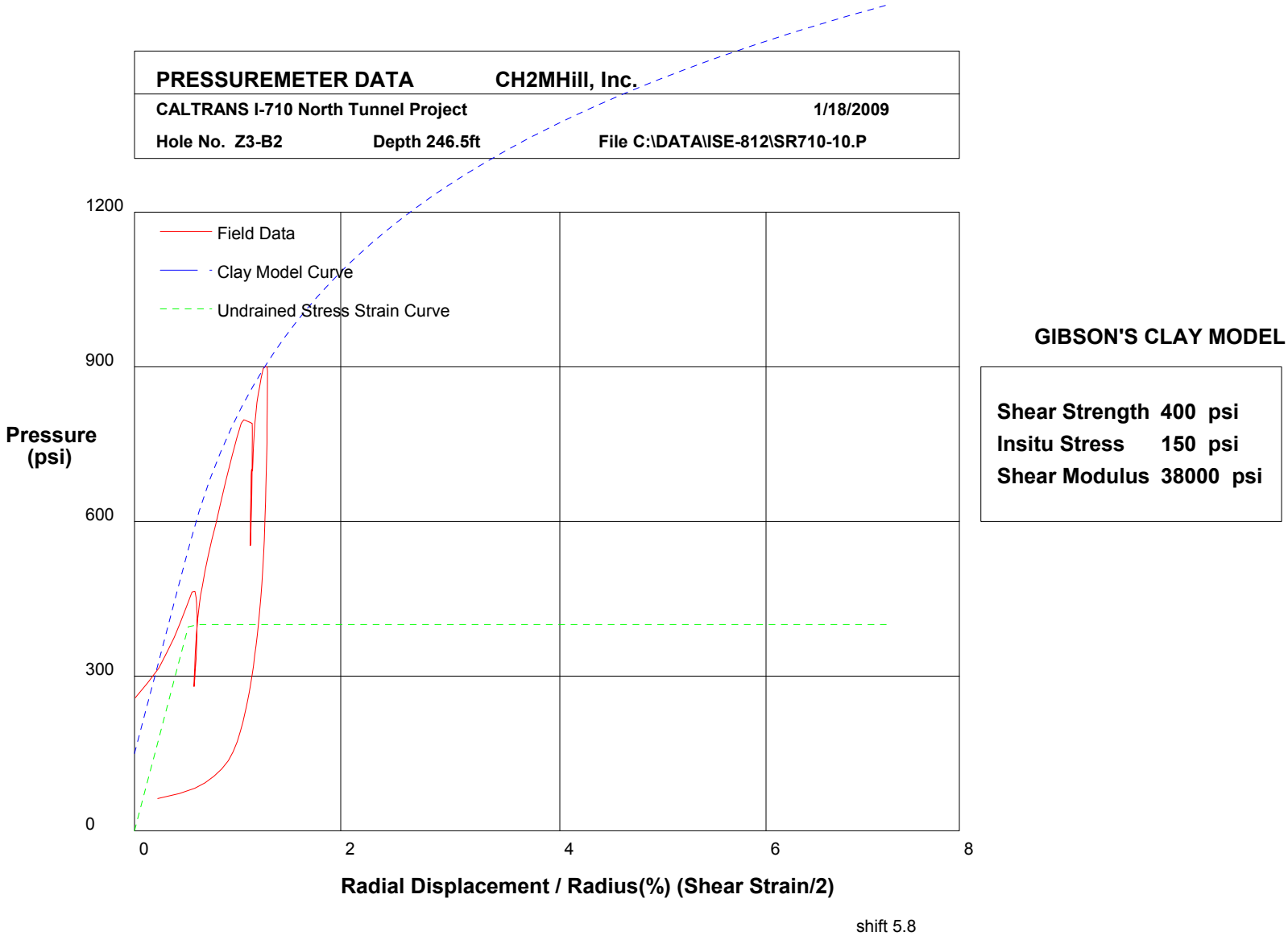

# Appendix II - Pressuremeter Model Interpretation

**PRESSUREMETER DATA** **CH2MHill, Inc.**

**CALTRANS I-710 North Tunnel Project** **1/19/2009**

**Hole No. Z2-B1** **Depth 129ft** **File C:\DATA\ISE-812\SR710-11.P**

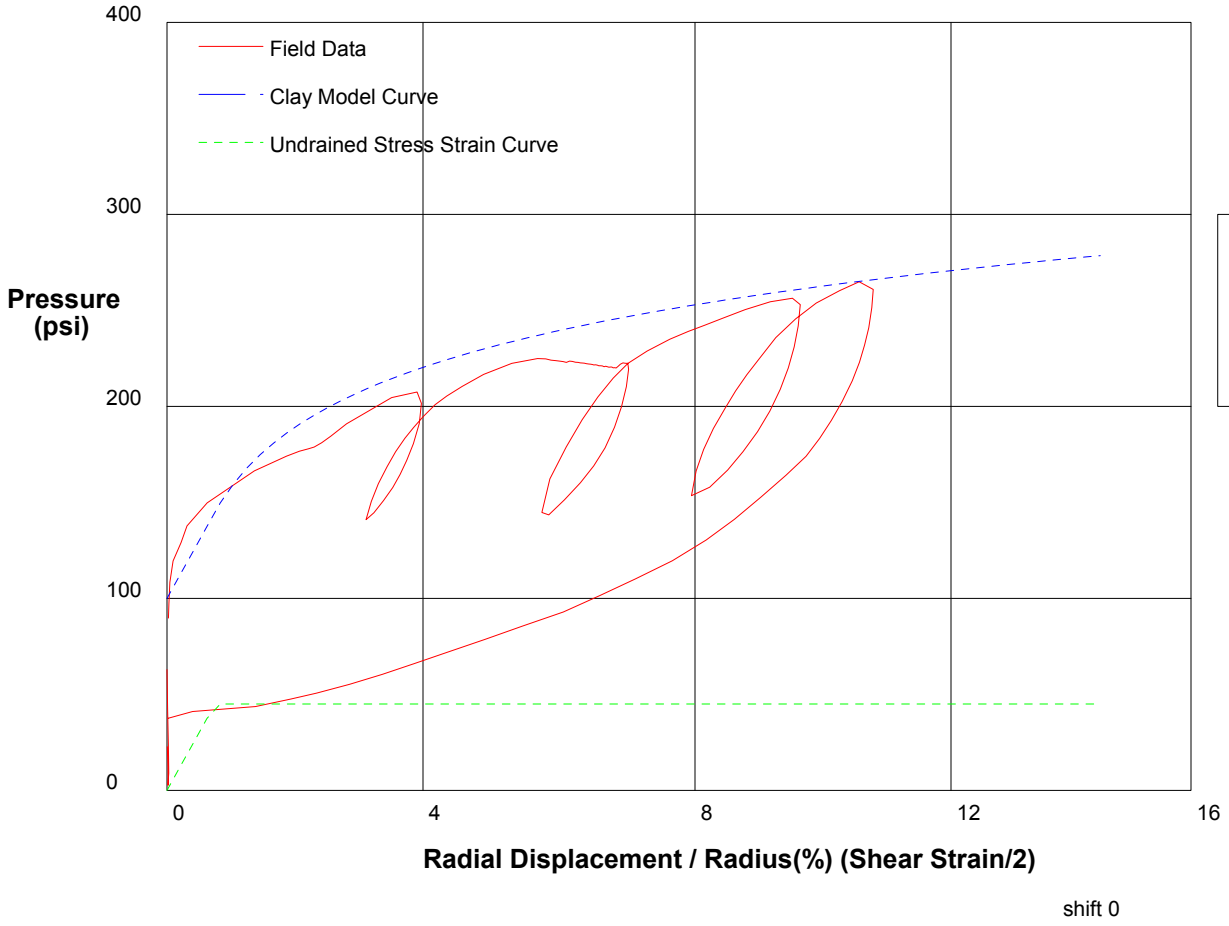


**GIBSON'S CLAY MODEL**

**Shear Strength 45 psi**
**Insitu Stress 100 psi**
**Shear Modulus 3000 psi**

shift 0

**In Situ Engineering**

# Appendix II - Pressuremeter Model Interpretation

**PRESSUREMETER DATA** **CH2MHill, Inc.**

**CALTRANS I-710 North Tunnel Project** **1/19/2009**

**Hole No. Z2-B1** **Depth 127.5ft** **File C:\DATA\ISE-812\SR710-12.P**

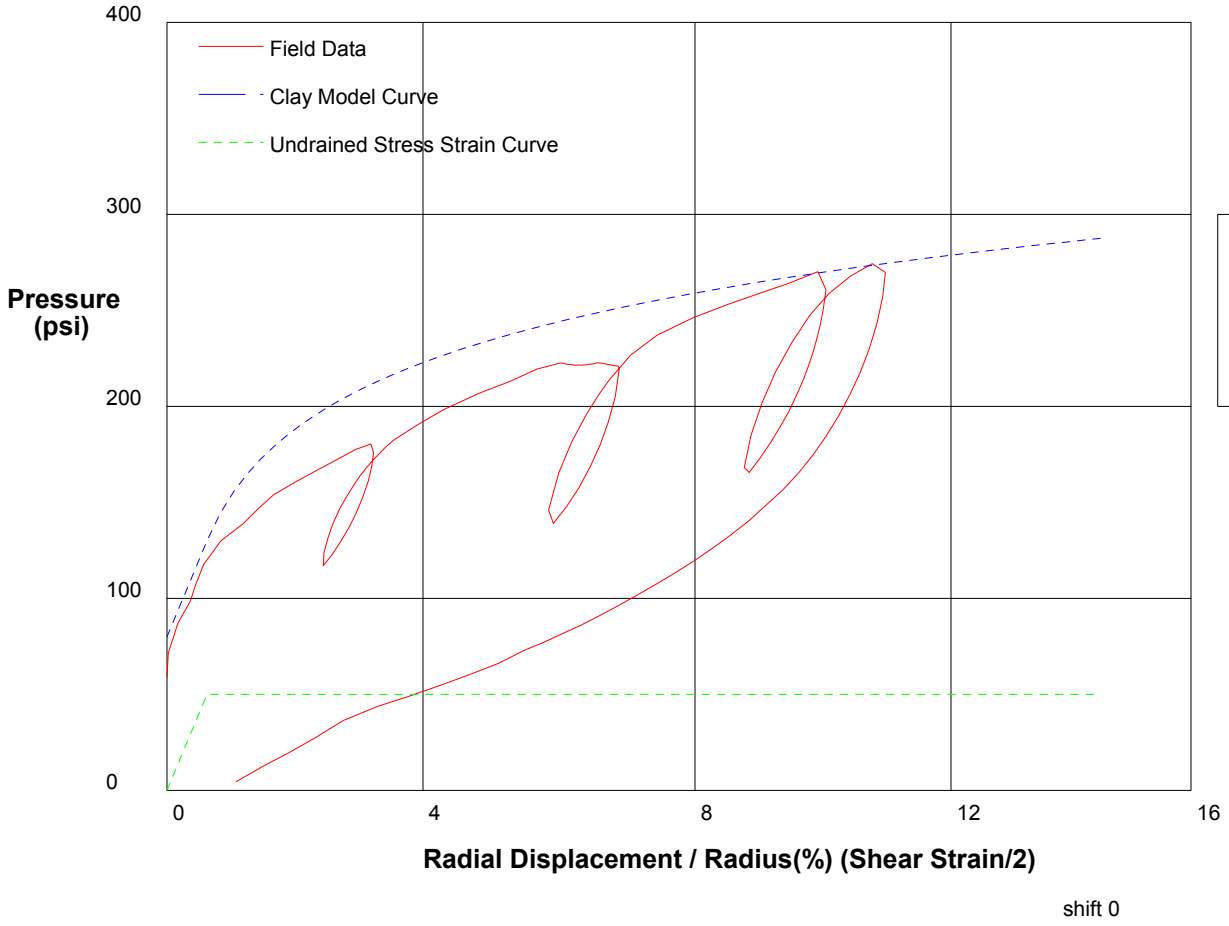


**GIBSON'S CLAY MODEL**

**Shear Strength 50 psi**
**Insitu Stress 80 psi**
**Shear Modulus 4000 psi**

shift 0

**In Situ Engineering**

# Appendix II - Pressuremeter Model Interpretation

**PRESSUREMETER DATA** **CH2MHill, Inc.**

**CALTRANS I-710 North Tunnel Project** **1/20/2009**

**Hole No. Z2-B1** **Depth 140ft** **File C:\DATA\ISE-812\SR710-13.P**

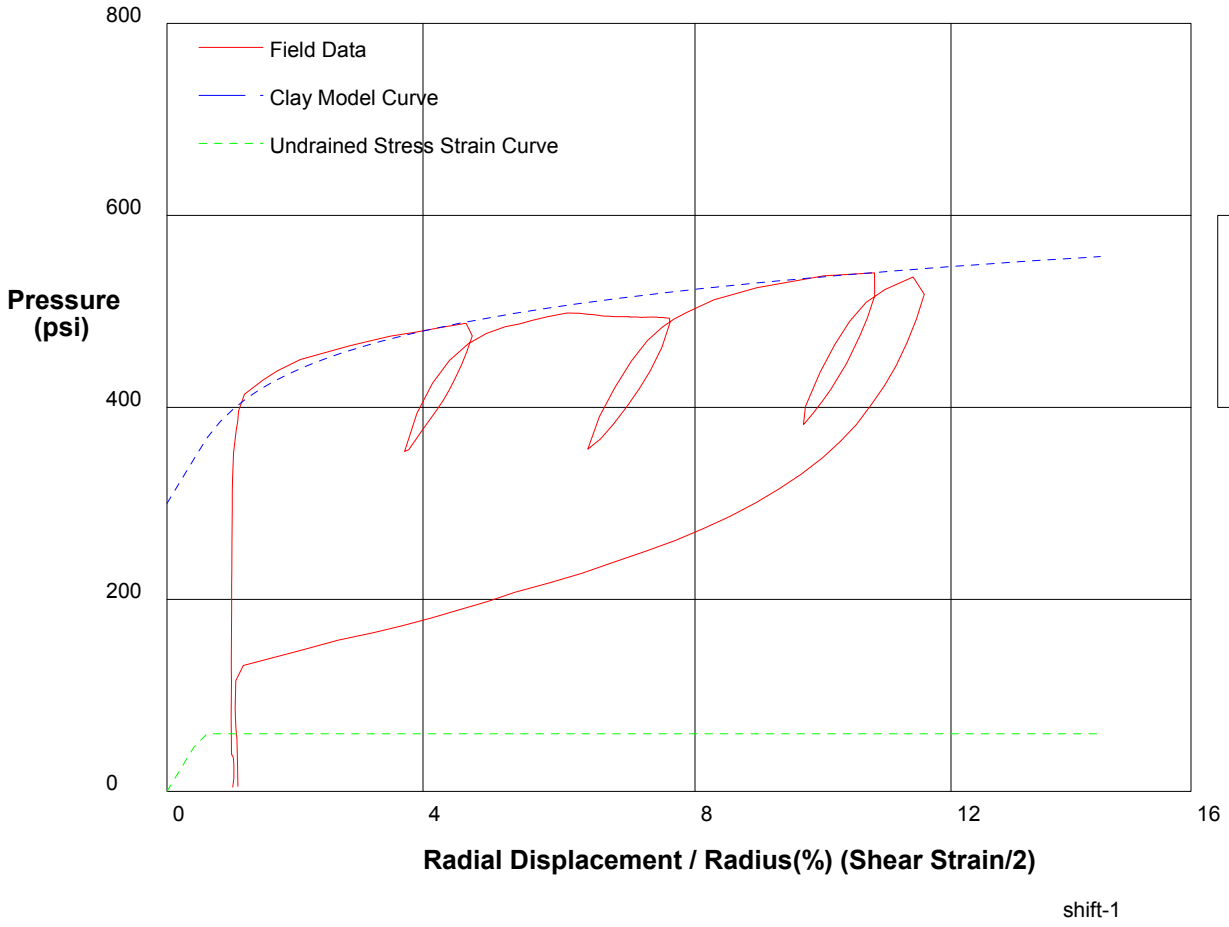


**GIBSON'S CLAY MODEL**

**Shear Strength 60 psi**
**Insitu Stress 300 psi**
**Shear Modulus 5500 psi**

shift-1

**In Situ Engineering**

# Appendix II - Pressuremeter Model Interpretation

**PRESSUREMETER DATA** **CH2MHill, Inc.**

**CALTRANS I-710 North Tunnel Project** **1/20/2009**

**Hole No. Z2-B1** **Depth 138.5ft** **File C:\DATA\ISE-812\SR710-14.P**

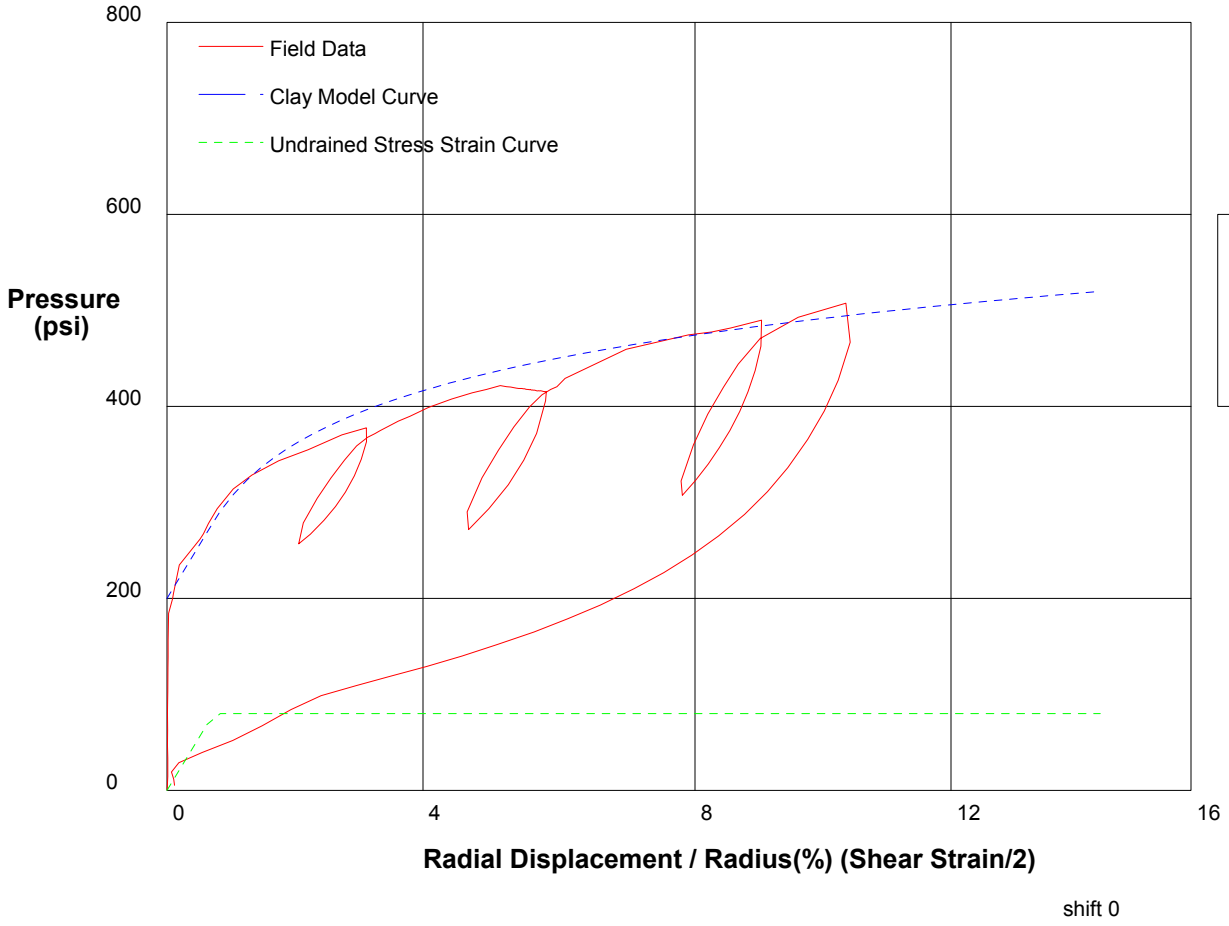


**GIBSON'S CLAY MODEL**

**Shear Strength 80 psi**
**Insitu Stress 200 psi**
**Shear Modulus 5500 psi**

shift 0

**In Situ Engineering**

# Appendix II - Pressuremeter Model Interpretation

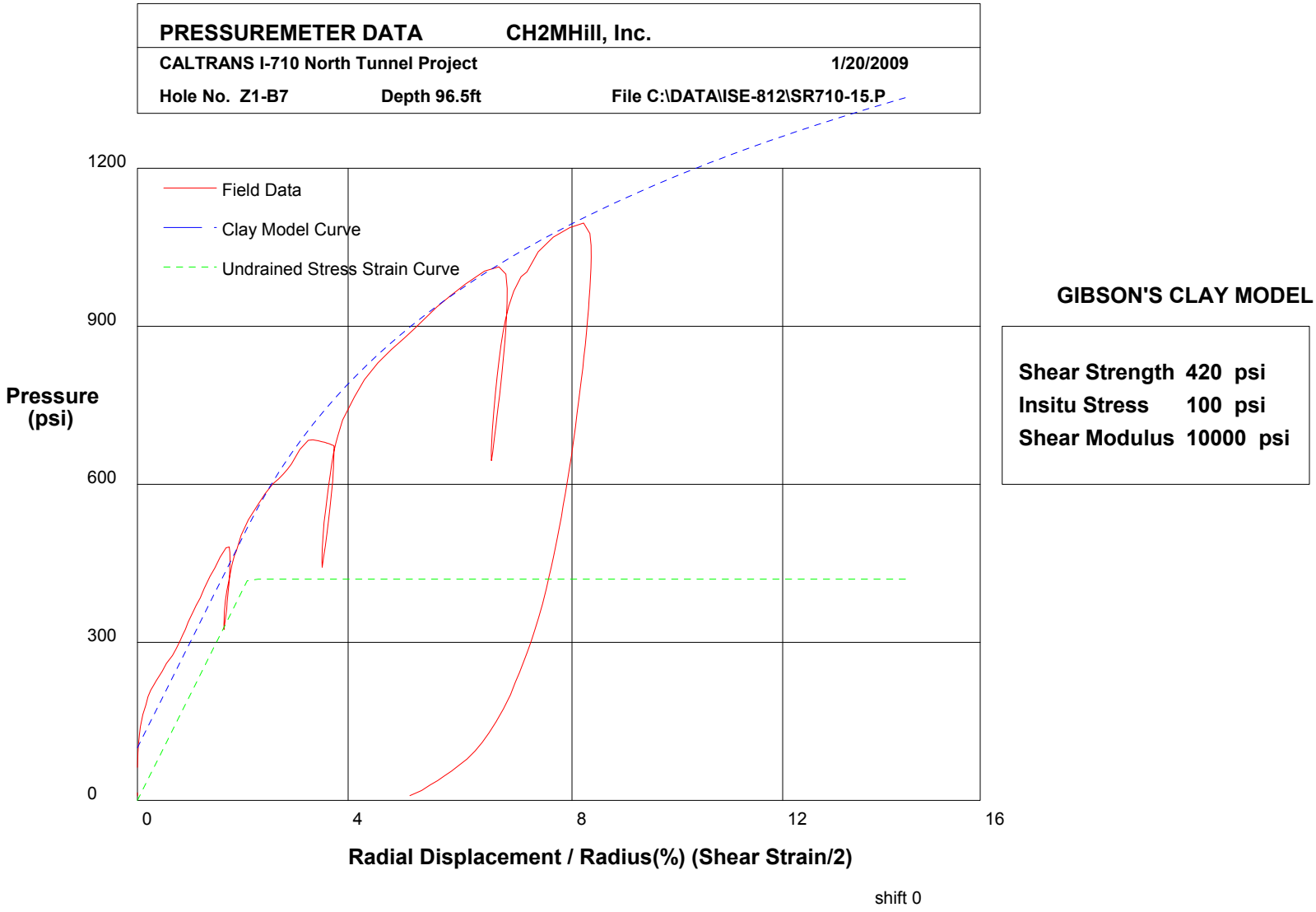

# Appendix II - Pressuremeter Model Interpretation

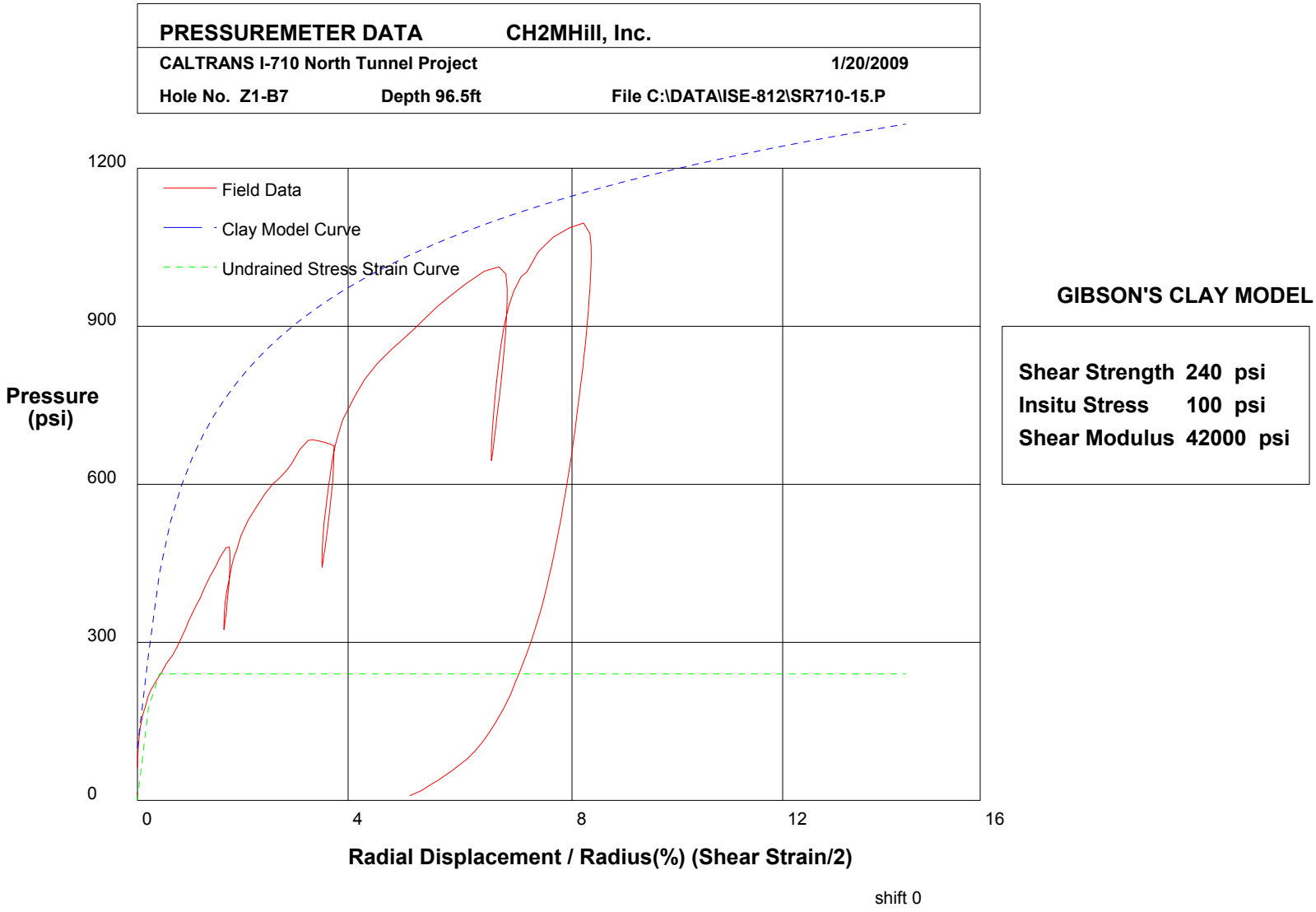

# Appendix II - Pressuremeter Model Interpretation

**PRESSUREMETER DATA** **CH2MHill, Inc.**

**CALTRANS I-710 North Tunnel Project** **1/20/2009**

**Hole No. Z1-B7** **Depth 95ft** **File C:\DATA\ISE-812\SR710-16.P**

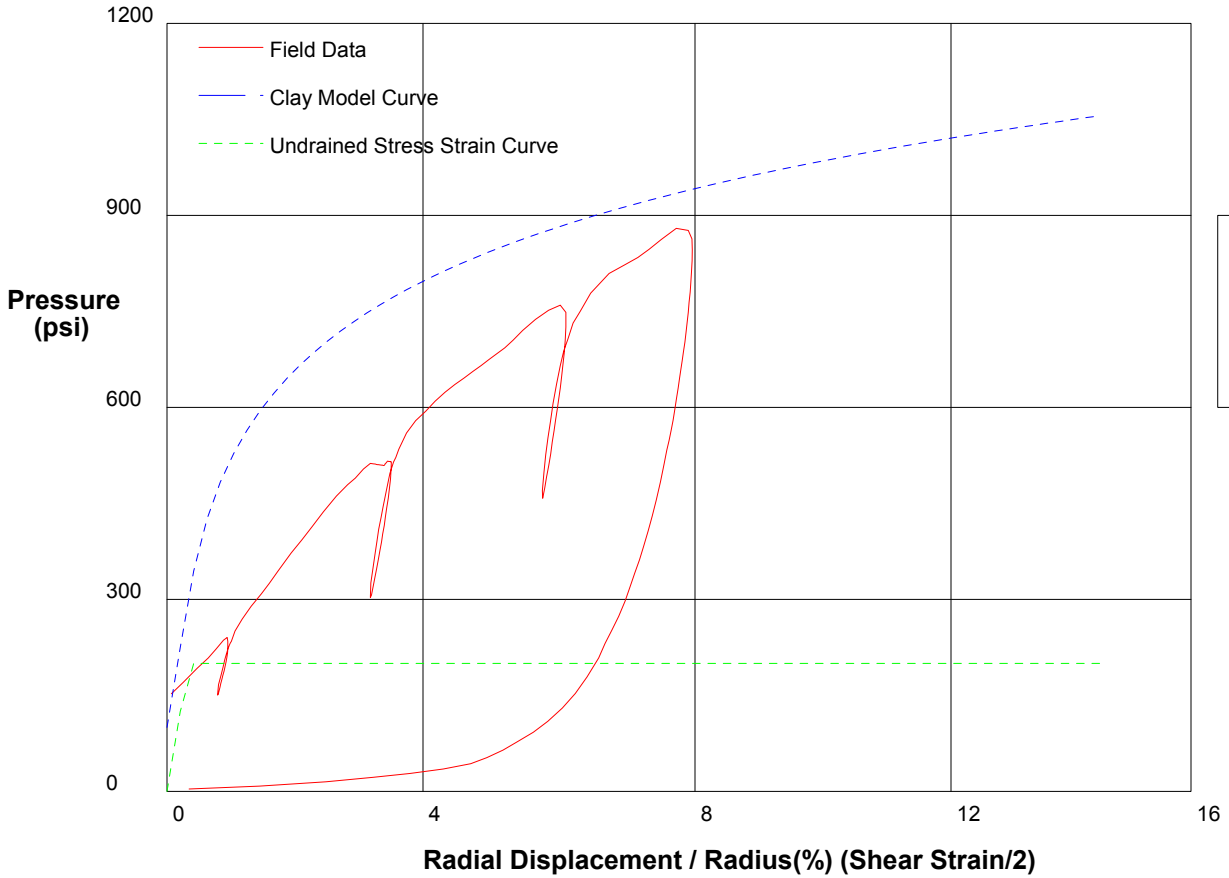


**GIBSON'S CLAY MODEL**

**Shear Strength 200 psi**
**Insitu Stress 100 psi**
**Shear Modulus 30000 psi**

shift 2

**In Situ Engineering**

# Appendix II - Pressuremeter Model Interpretation

**PRESSUREMETER DATA** **CH2MHill, Inc.**

**CALTRANS I-710 North Tunnel Project** **1/20/2009**

**Hole No. Z1-B7** **Depth 95ft** **File C:\DATA\ISE-812\SR710-16.P**

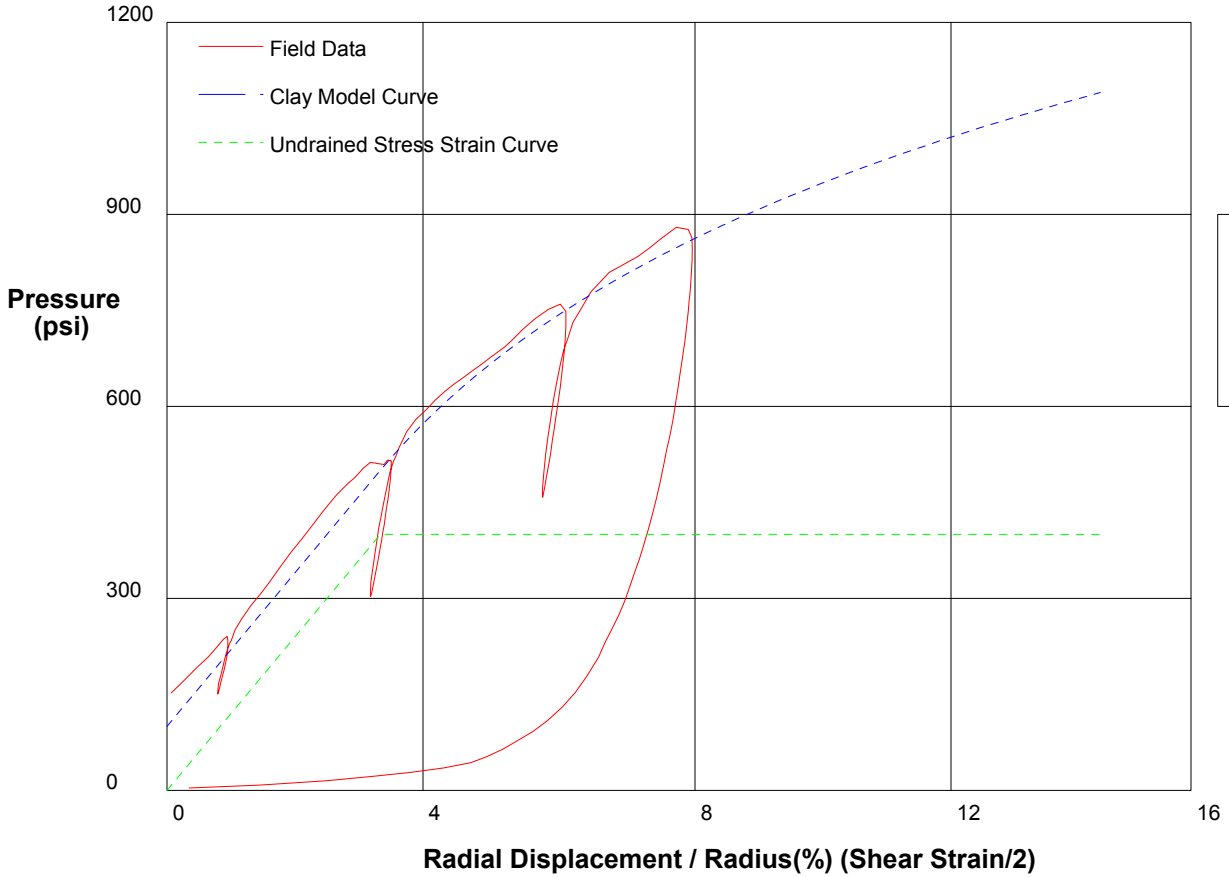


**GIBSON'S CLAY MODEL**

| | |
|---|---|
| **Shear Strength** | **400 psi** |
| **Insitu Stress** | **100 psi** |
| **Shear Modulus** | **6000 psi** |

shift 2

**In Situ Engineering**

# Appendix II - Pressuremeter Model Interpretation

**PRESSUREMETER DATA** **CH2MHill, Inc.**

**CALTRANS I-710 North Tunnel Project** **1/20/2009**

**Hole No. Z1-B7** **Depth 95ft** **File C:\DATA\ISE-812\SR710-16.P**

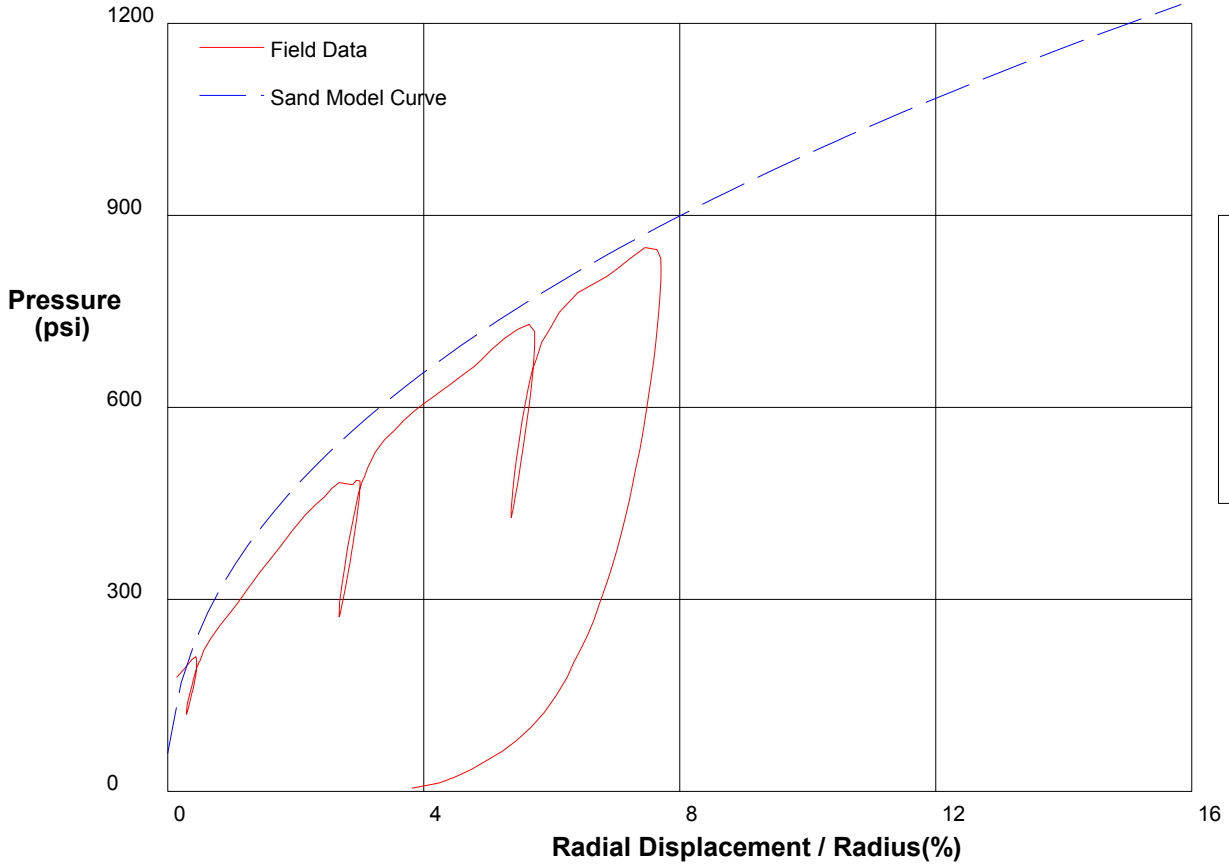


**THE In Situ Engineering SAND MODEL**

| | |
|---|---|
| **Water Pressure** | **30 psi** |
| **Friction Angle** | **40 deg** |
| **Critical Friction Angle** | **32 deg** |
| **Lateral Stress** | **60 psi** |
| **Shear Modulus** | **30000 psi** |

shift 2.5

**In Situ Engineering**

# Appendix II - Pressuremeter Model Interpretation

**PRESSUREMETER DATA** **CH2MHill, Inc.**

**CALTRANS I-710 North Tunnel Project** **1/21/2009**

**Hole No. Z1-B7** **Depth 111.5ft** **File C:\DATA\ISE-812\SR710-17.P**

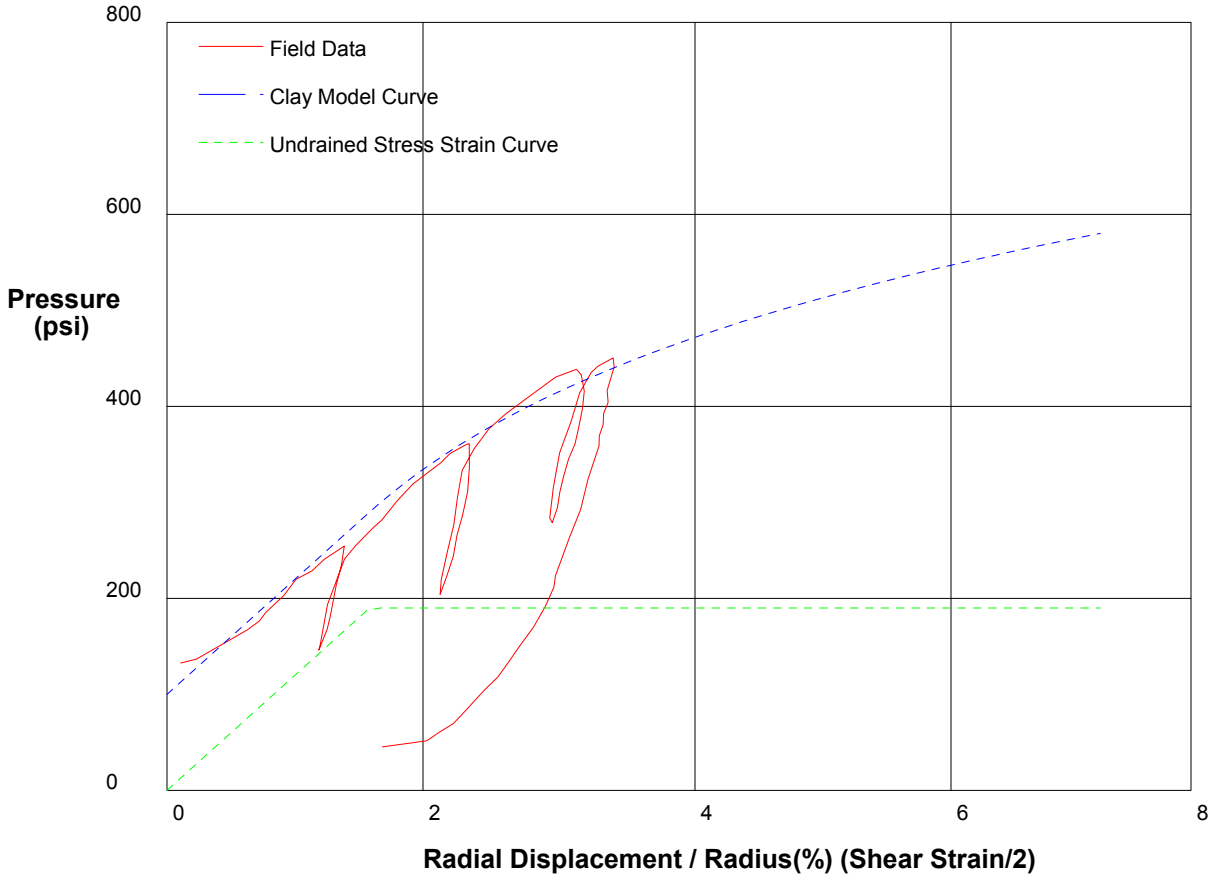


**GIBSON'S CLAY MODEL**

**Shear Strength 190 psi**
**Insitu Stress 100 psi**
**Shear Modulus 6000 psi**

shift 9.1

**In Situ Engineering**

# Appendix II - Pressuremeter Model Interpretation

**PRESSUREMETER DATA** **CH2MHill, Inc.**

**CALTRANS I-710 North Tunnel Project** **1/21/2009**

**Hole No. Z1-B7** **Depth 111.5ft** **File C:\DATA\ISE-812\SR710-17.P**

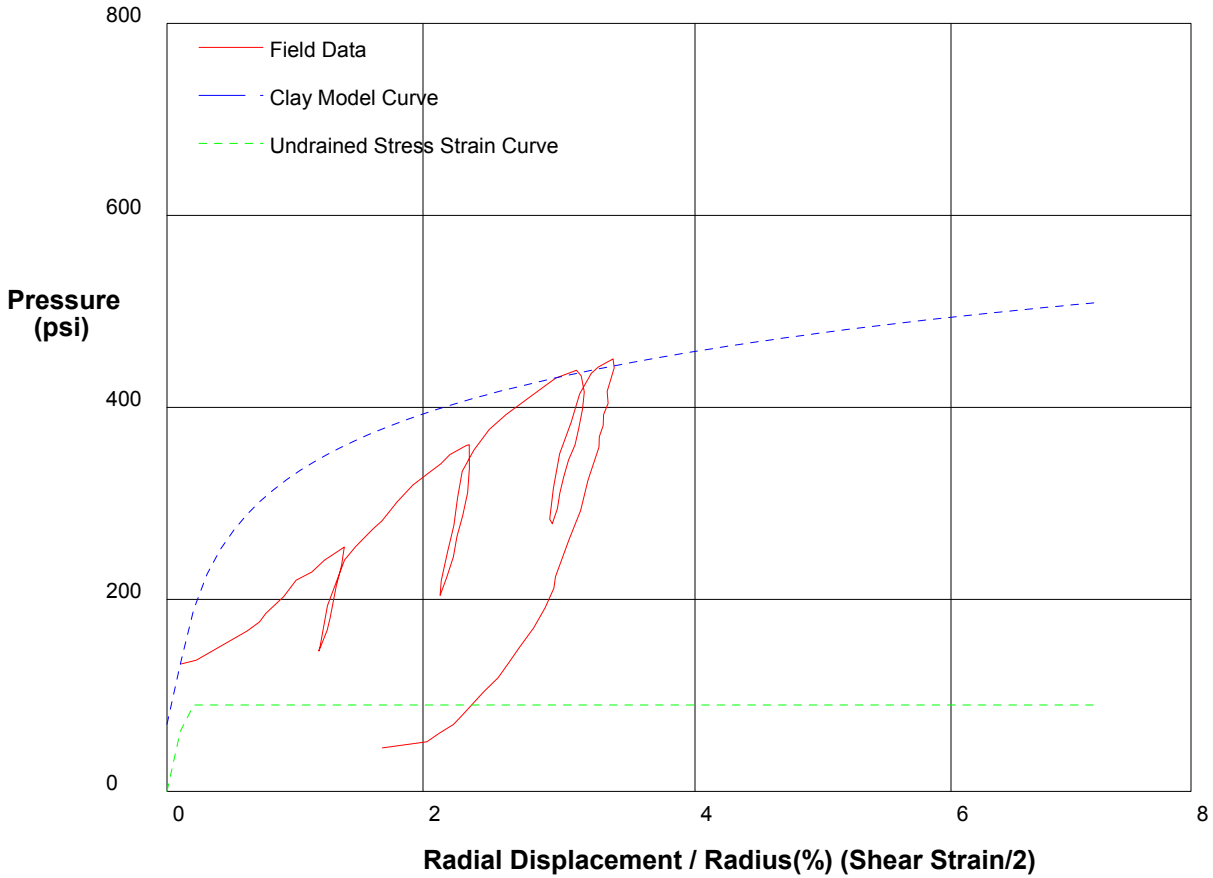


**GIBSON'S CLAY MODEL**

**Shear Strength 90 psi**
**Insitu Stress 70 psi**
**Shear Modulus 30000 psi**

shift 9.1

**In Situ Engineering**

# Appendix II - Pressuremeter Model Interpretation

**PRESSUREMETER DATA** **CH2MHill, Inc.**

**CALTRANS I-710 North Tunnel Project** **1/21/2009**

**Hole No. Z1-B7** **Depth 110ft** **File C:\DATA\ISE-812\SR710-18.P**

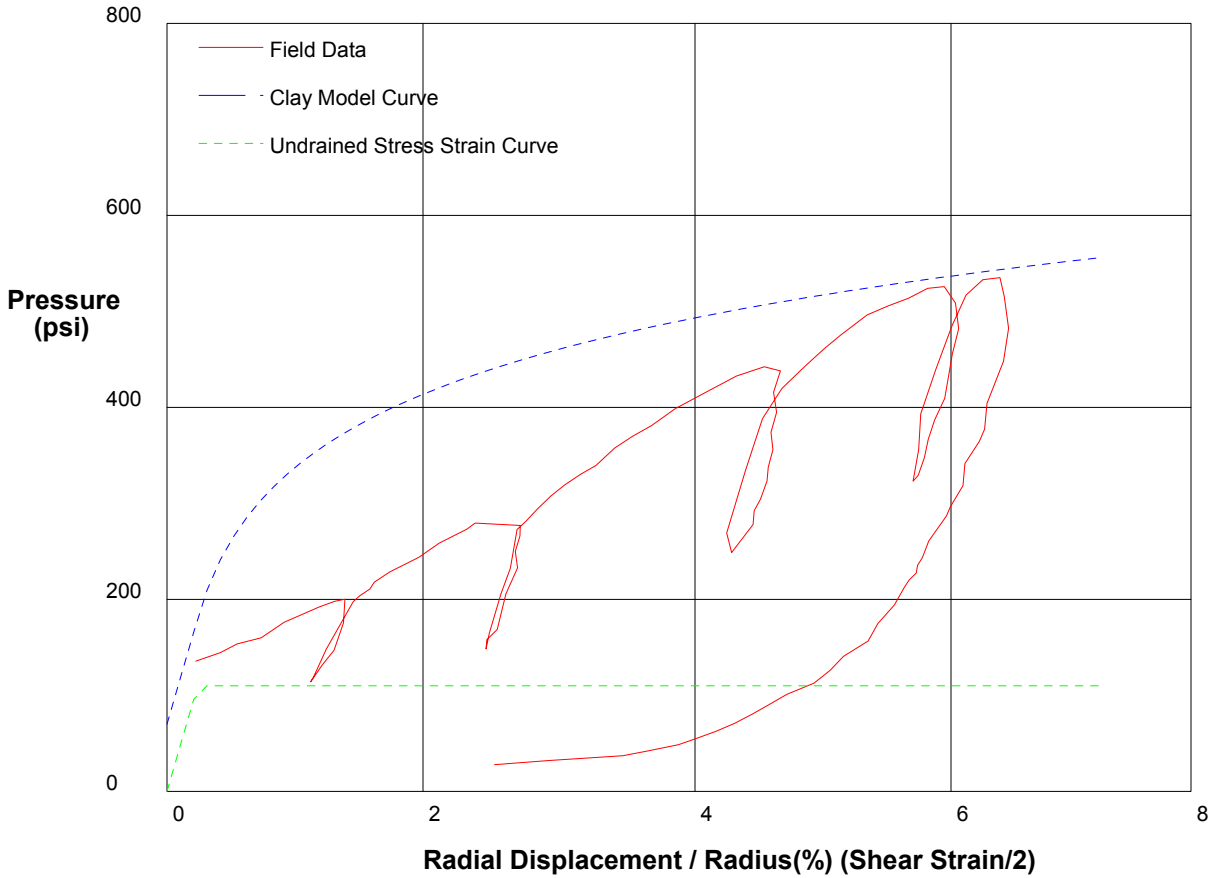


**GIBSON'S CLAY MODEL**

**Shear Strength 110 psi**
**Insitu Stress 70 psi**
**Shear Modulus 23000 psi**

shift 4.5

**In Situ Engineering**

# Appendix II - Pressuremeter Model Interpretation

**PRESSUREMETER DATA** **CH2MHill, Inc.**

**CALTRANS I-710 North Tunnel Project** **1/21/2009**

**Hole No. Z1-B7** **Depth 110ft** **File C:\DATA\ISE-812\SR710-18.P**

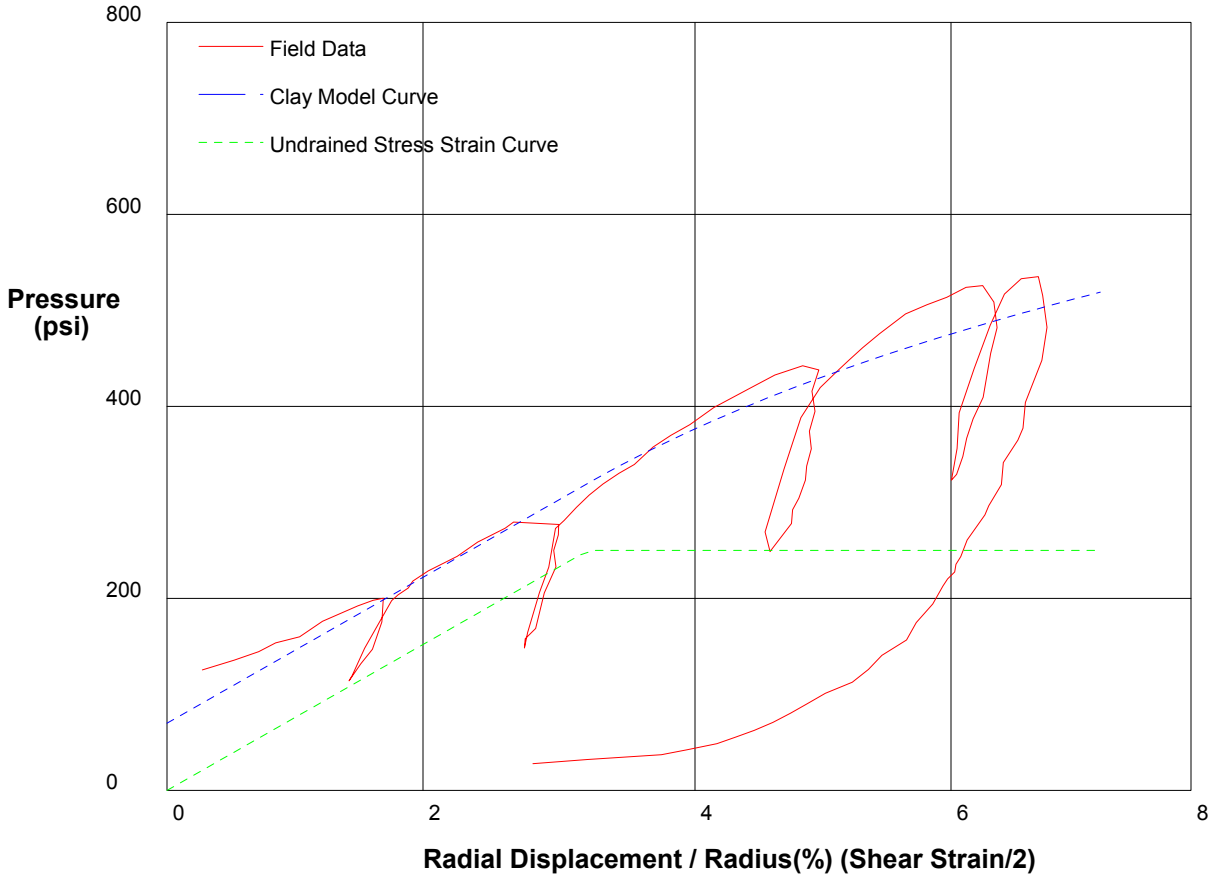


**GIBSON'S CLAY MODEL**

**Shear Strength 250 psi**
**Insitu Stress 70 psi**
**Shear Modulus 3800 psi**

shift 4.2

**In Situ Engineering**

# Appendix II - Pressuremeter Model Interpretation

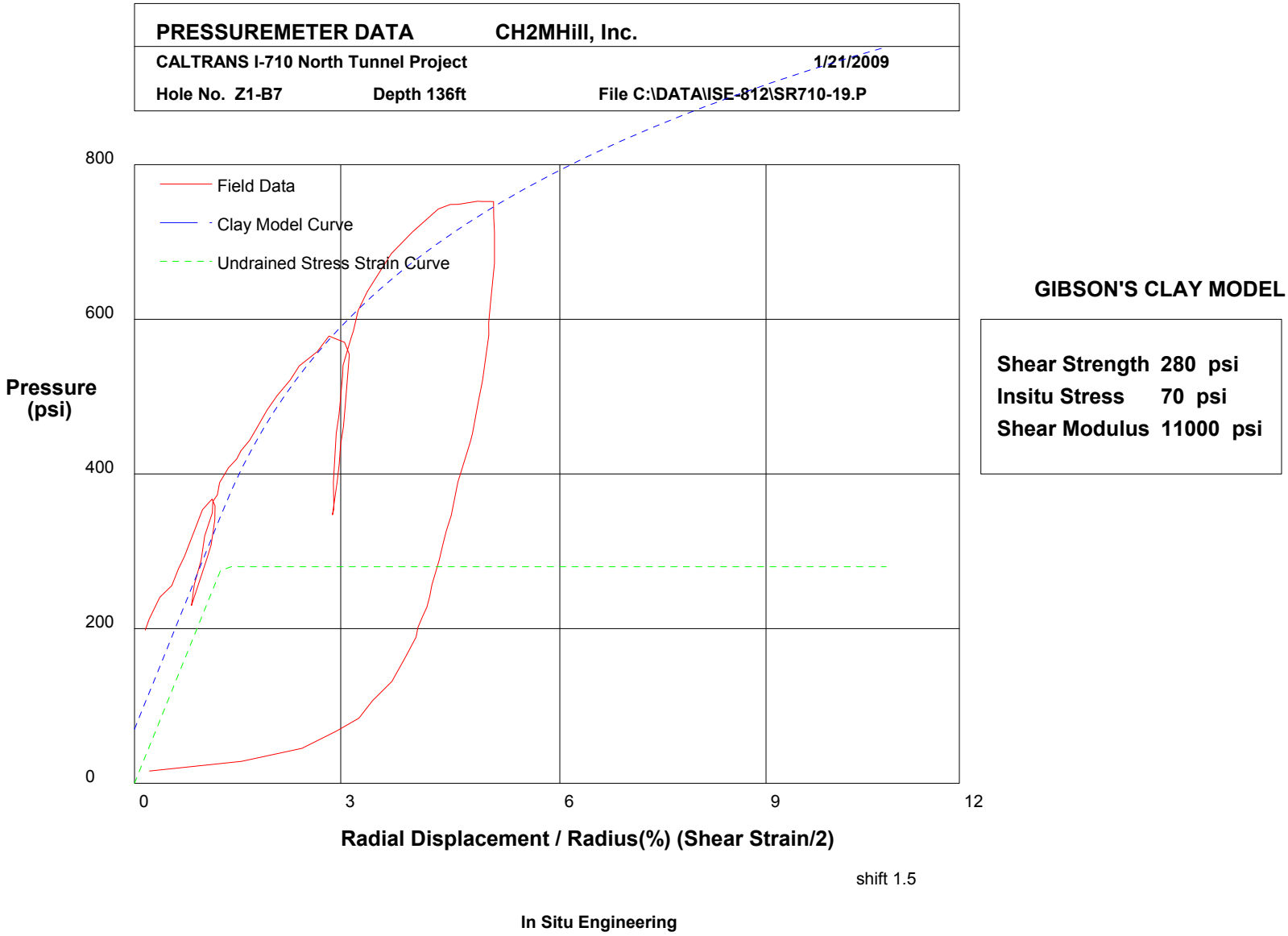

# Appendix II - Pressuremeter Model Interpretation

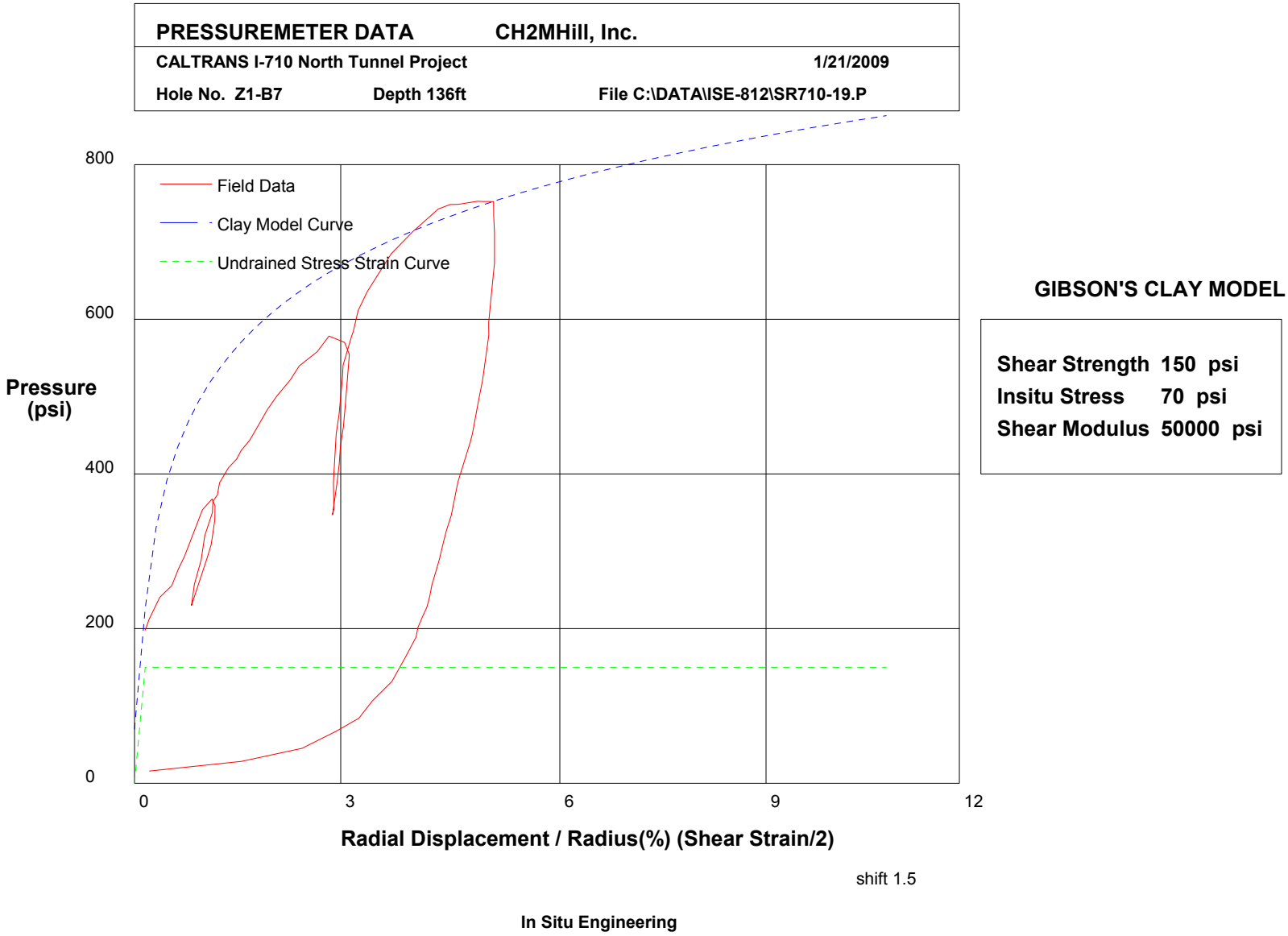

# Appendix II - Pressuremeter Model Interpretation

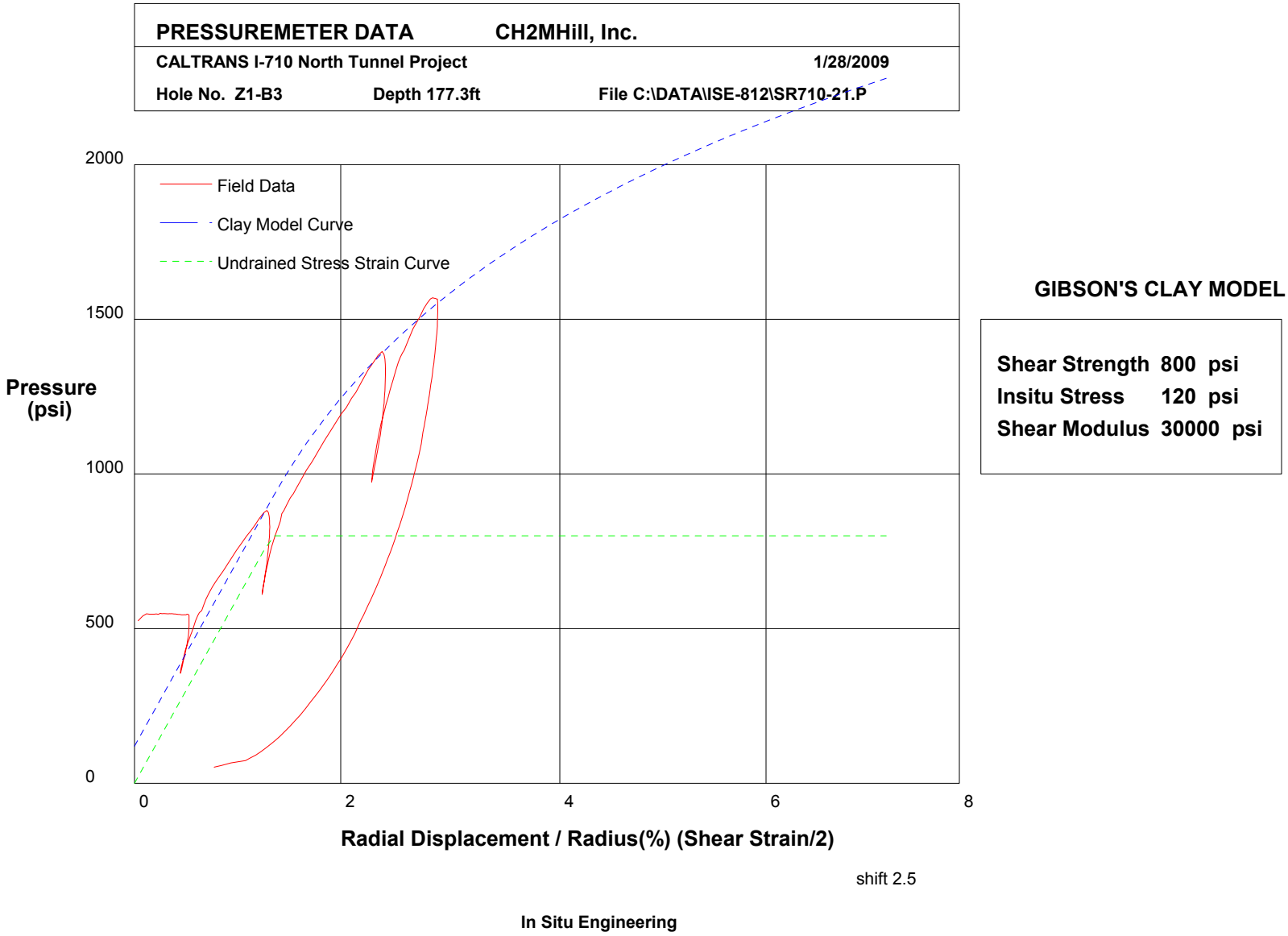

# Appendix II - Pressuremeter Model Interpretation

**PRESSUREMETER DATA** **CH2MHill, Inc.**

**CALTRANS I-710 North Tunnel Project** **1/28/2009**

**Hole No. Z1-B3** **Depth 177.3ft** **File C:\DATA\ISE-812\SR710-21.P**

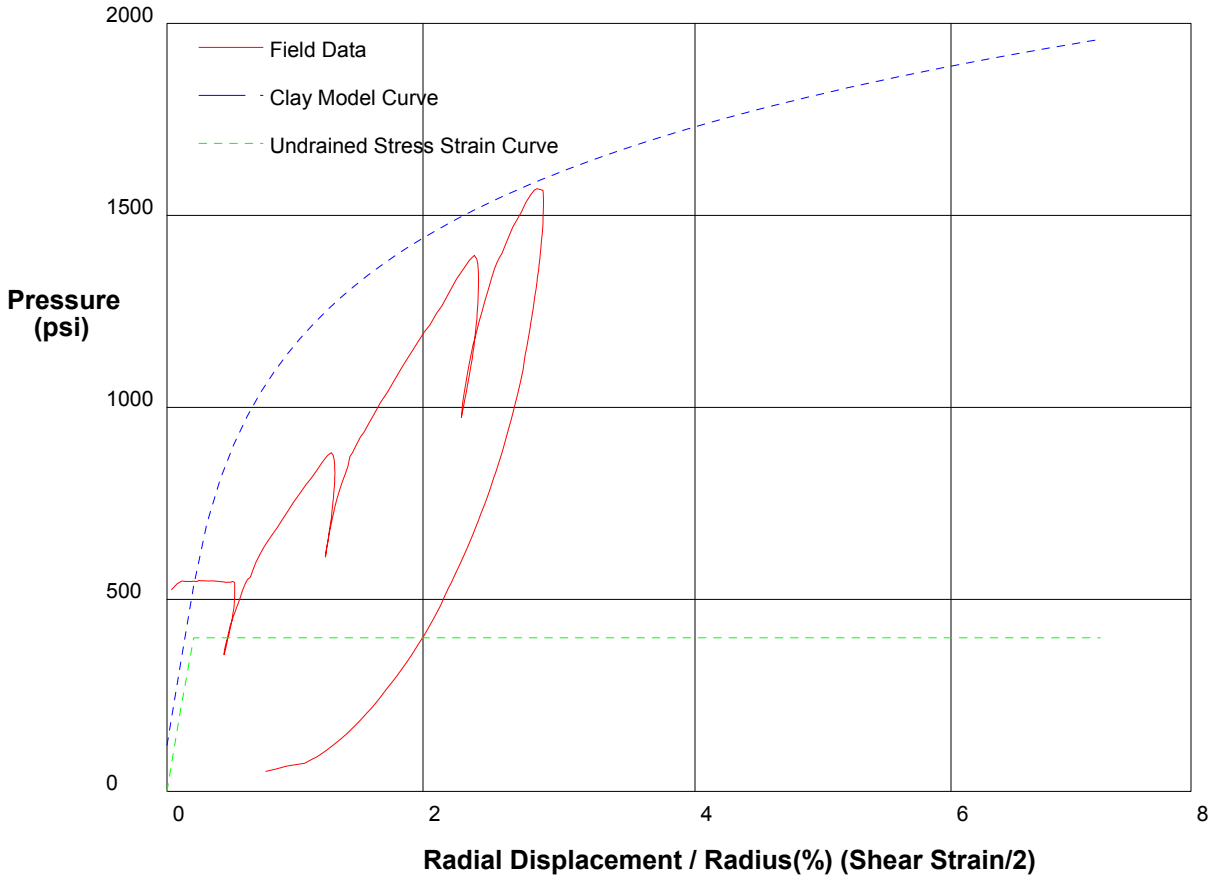


**GIBSON'S CLAY MODEL**

| | |
|---|---|
| **Shear Strength** | **400 psi** |
| **Insitu Stress** | **120 psi** |
| **Shear Modulus** | **100000 psi** |

shift 2.5

**In Situ Engineering**

# Appendix II - Pressuremeter Model Interpretation

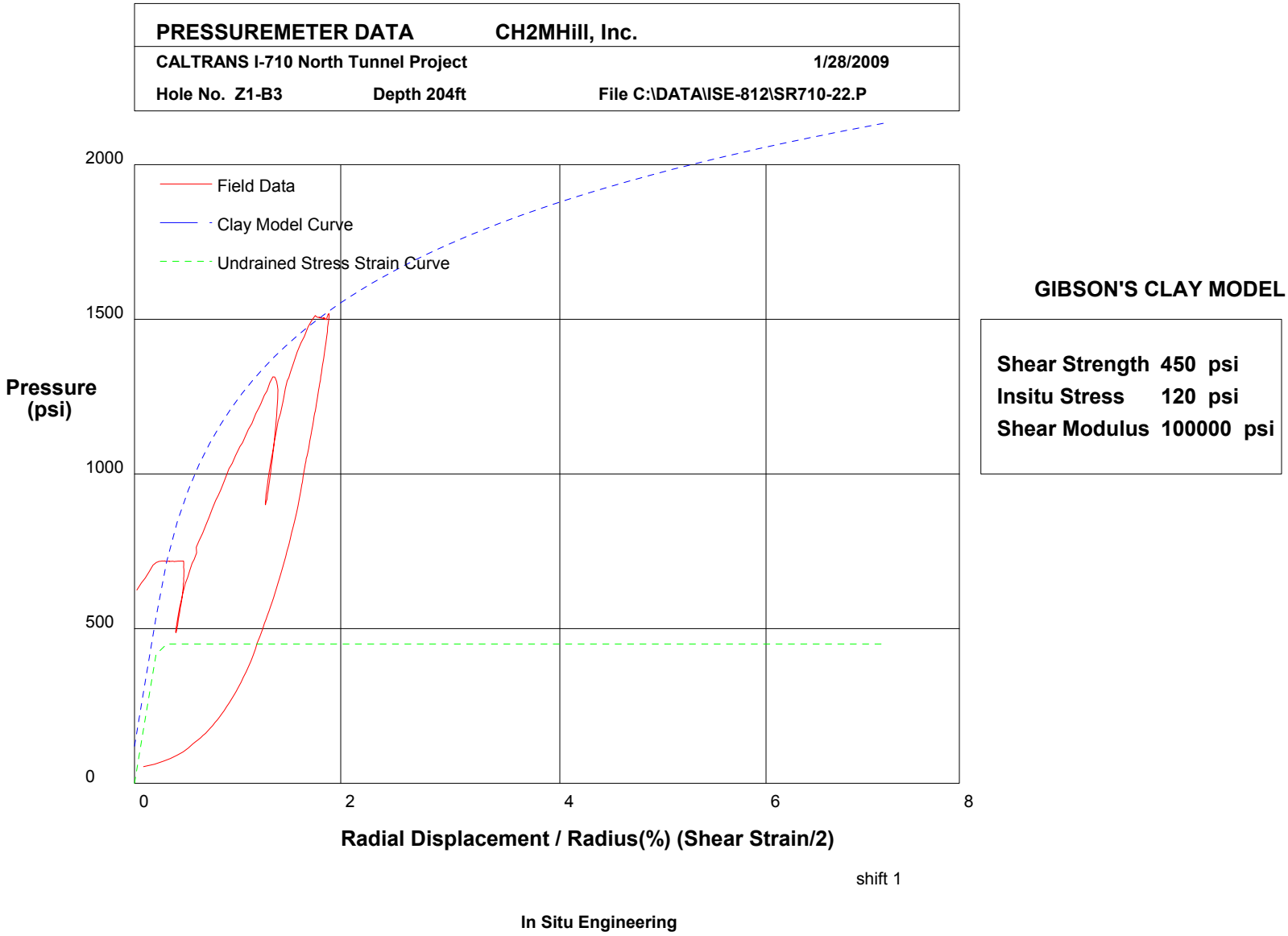

# Appendix II - Pressuremeter Model Interpretation

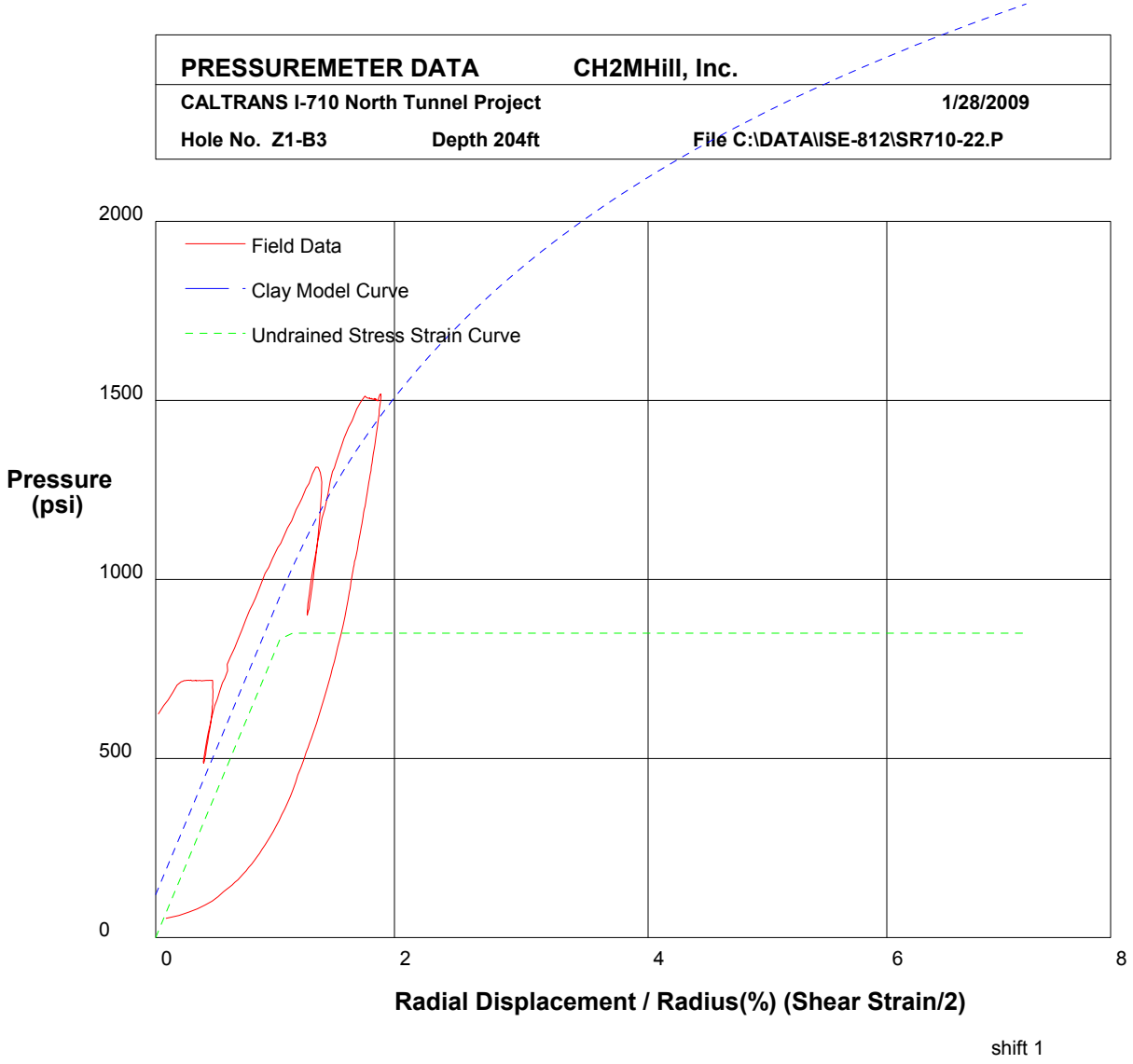


**GIBSON'S CLAY MODEL**

| | |
|---|---|
| **Shear Strength** | **850 psi** |
| **Insitu Stress** | **120 psi** |
| **Shear Modulus** | **40000 psi** |

# Appendix II - Pressuremeter Model Interpretation

**PRESSUREMETER DATA** **CH2MHill, Inc.**

**CALTRANS I-710 North Tunnel Project** **1/29/2009**

**Hole No. Z2-B2** **Depth 135.7ft** **File C:\DATA\ISE-812\SR710-23.P**

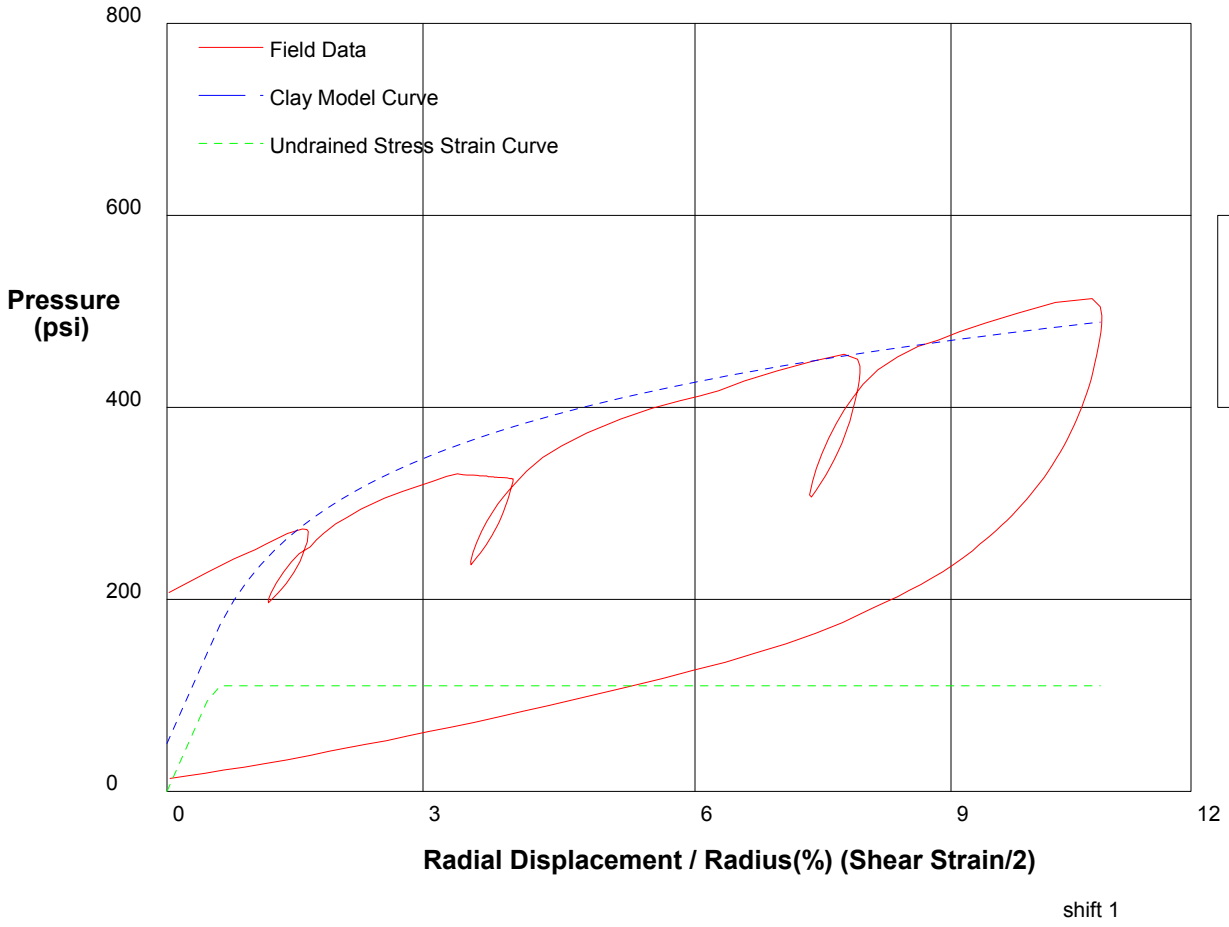


**GIBSON'S CLAY MODEL**

**Shear Strength 110 psi**
**Insitu Stress 50 psi**
**Shear Modulus 10000 psi**

shift 1

**In Situ Engineering**

# Appendix II - Pressuremeter Model Interpretation

**PRESSUREMETER DATA** **CH2MHill, Inc.**

**CALTRANS I-710 North Tunnel Project** **1/29/2009**

**Hole No. Z2-B2** **Depth 134.2ft** **File C:\DATA\ISE-812\SR710-24.P**

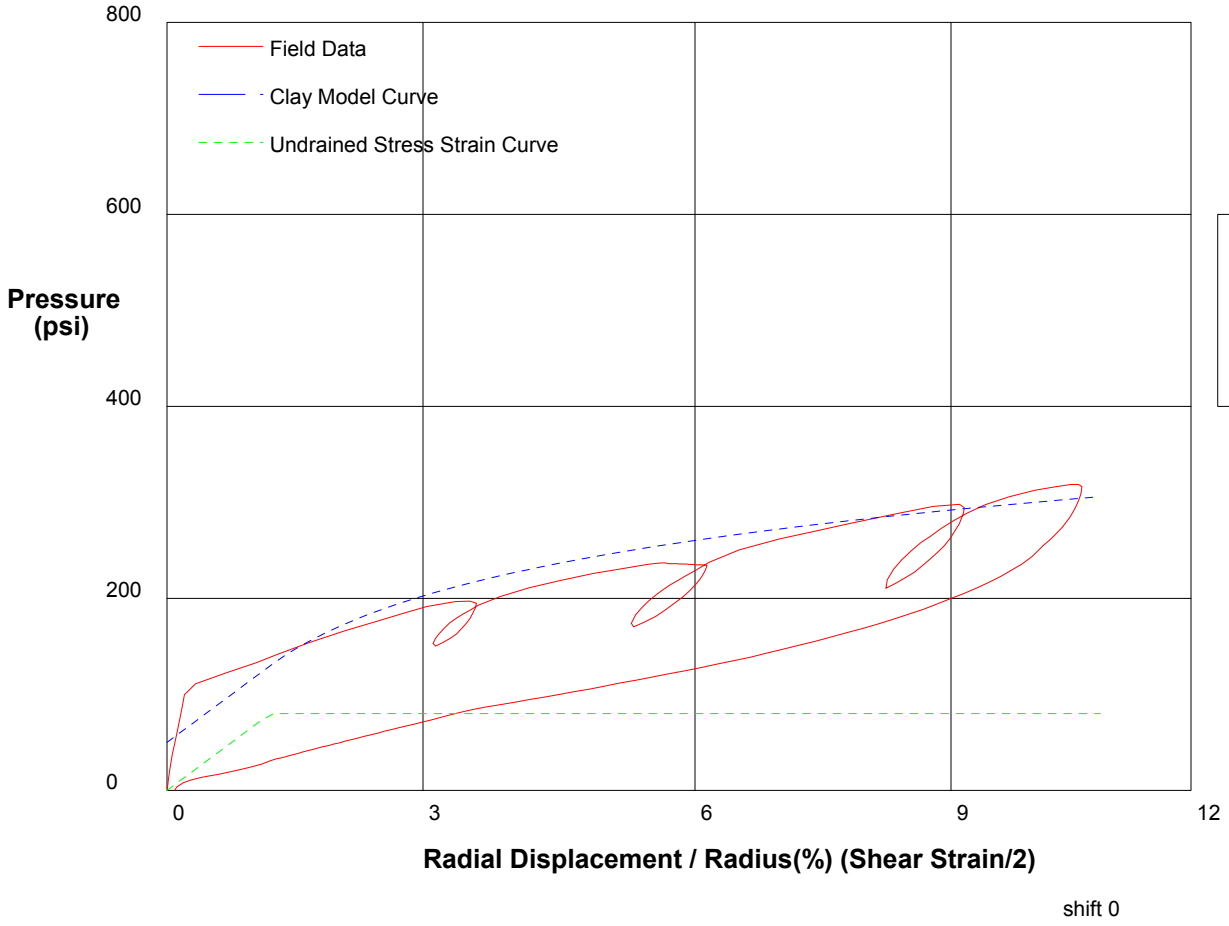


**GIBSON'S CLAY MODEL**

**Shear Strength 80 psi**
**Insitu Stress 50 psi**
**Shear Modulus 3300 psi**

shift 0

**In Situ Engineering**

# Appendix II - Pressuremeter Model Interpretation

**PRESSUREMETER DATA** **CH2MHill, Inc.**

**CALTRANS I-710 North Tunnel Project** **2/4/2009**

**Hole No. Z2-B2** **Depth 251ft** **File C:\DATA\ISE-812\SR710-25.P**

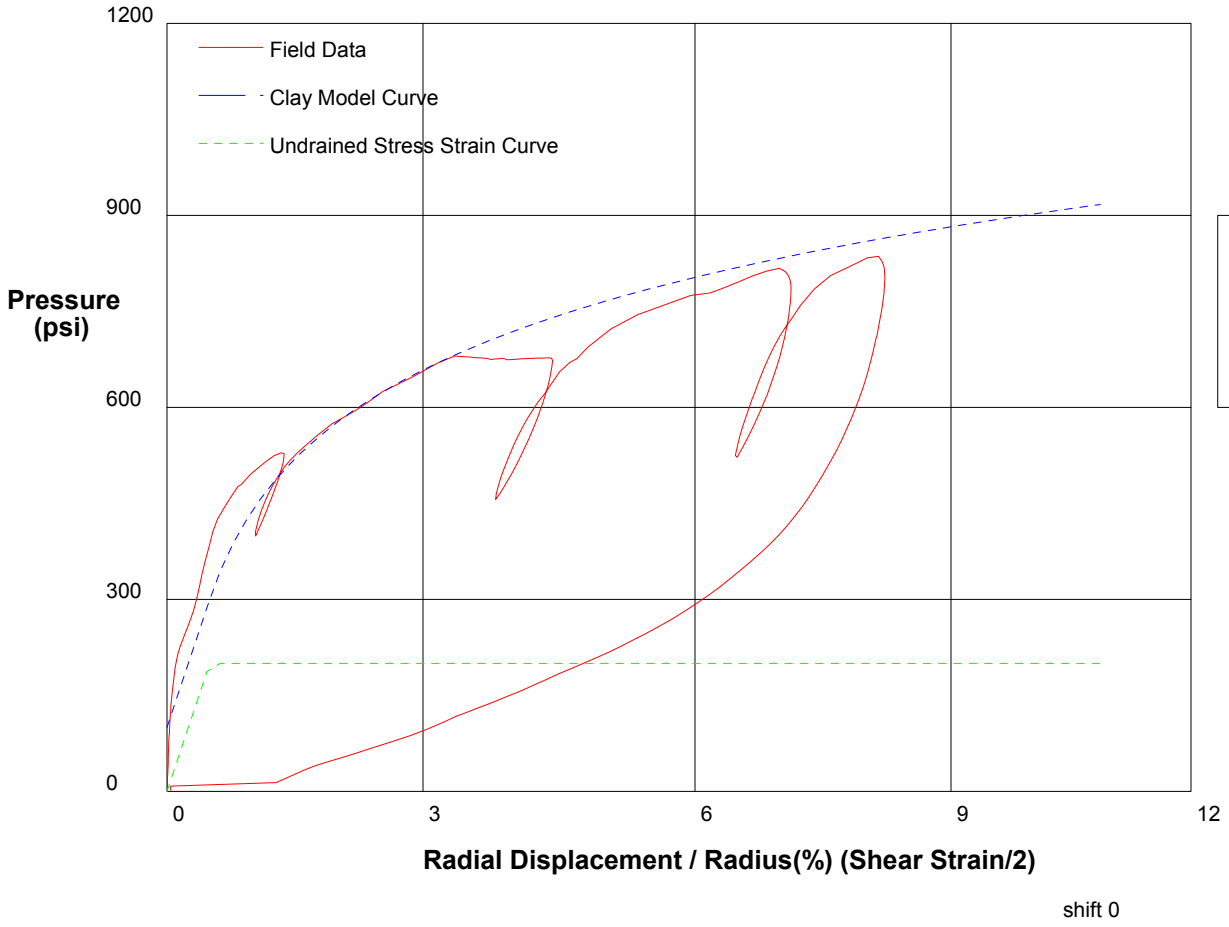


**GIBSON'S CLAY MODEL**

**Shear Strength 200 psi**
**Insitu Stress 100 psi**
**Shear Modulus 20000 psi**

shift 0

**In Situ Engineering**

# Appendix II - Pressuremeter Model Interpretation

**PRESSUREMETER DATA** **CH2MHill, Inc.**

**CALTRANS I-710 North Tunnel Project** **2/4/2009**

**Hole No. Z2-B2** **Depth 249.5ft** **File C:\DATA\ISE-812\SR710-26.P**

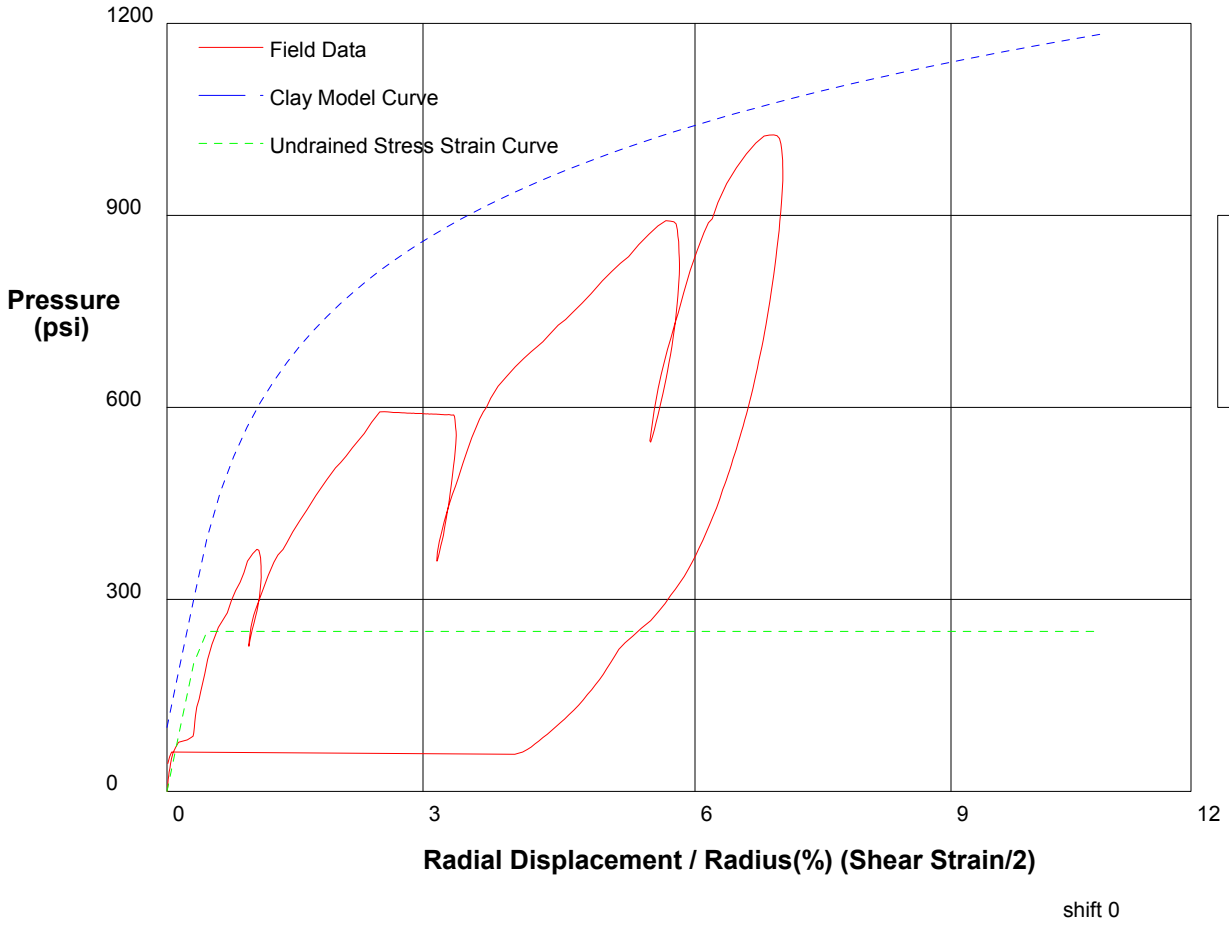


**GIBSON'S CLAY MODEL**

| | |
|---|---|
| **Shear Strength** | **250 psi** |
| **Insitu Stress** | **100 psi** |
| **Shear Modulus** | **32000 psi** |

shift 0

**In Situ Engineering**

# Appendix II - Pressuremeter Model Interpretation

**PRESSUREMETER DATA** **CH2MHill, Inc.**

**CALTRANS I-710 North Tunnel Project** **2/4/2009**

**Hole No. Z2-B2** **Depth 249.5ft** **File C:\DATA\ISE-812\SR710-26.P**

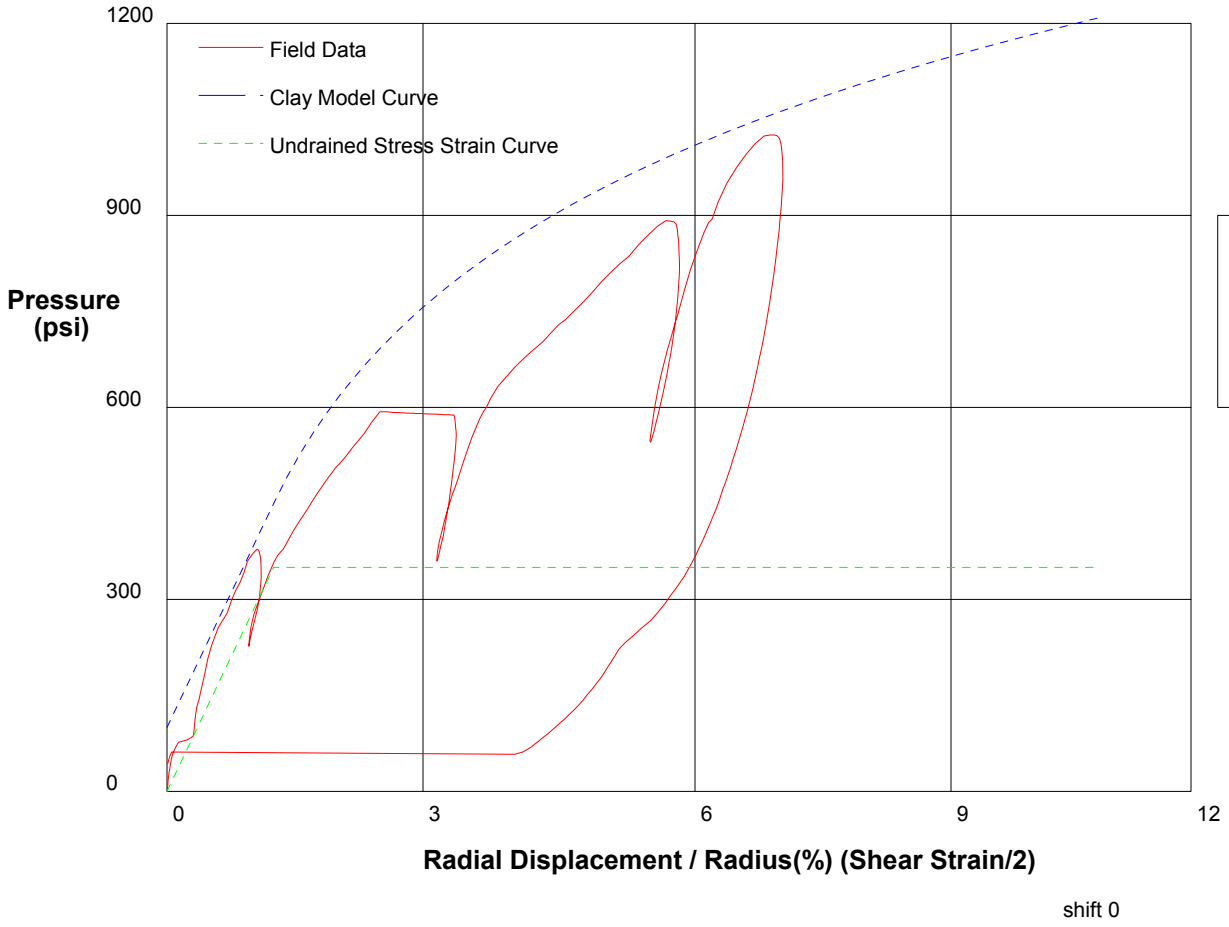


**GIBSON'S CLAY MODEL**

| | |
|---|---|
| **Shear Strength** | **350 psi** |
| **Insitu Stress** | **100 psi** |
| **Shear Modulus** | **14000 psi** |

shift 0

**In Situ Engineering**

# Appendix II - Pressuremeter Model Interpretation

**PRESSUREMETER DATA** **CH2M-HILL, Inc.**

**CALTRANS I-710 North Tunnel Project** **2/5/2009**

**Hole No. Z1-B6** **Depth 245ft** **File C:\DATA\ISE-812\SR710-28.P**

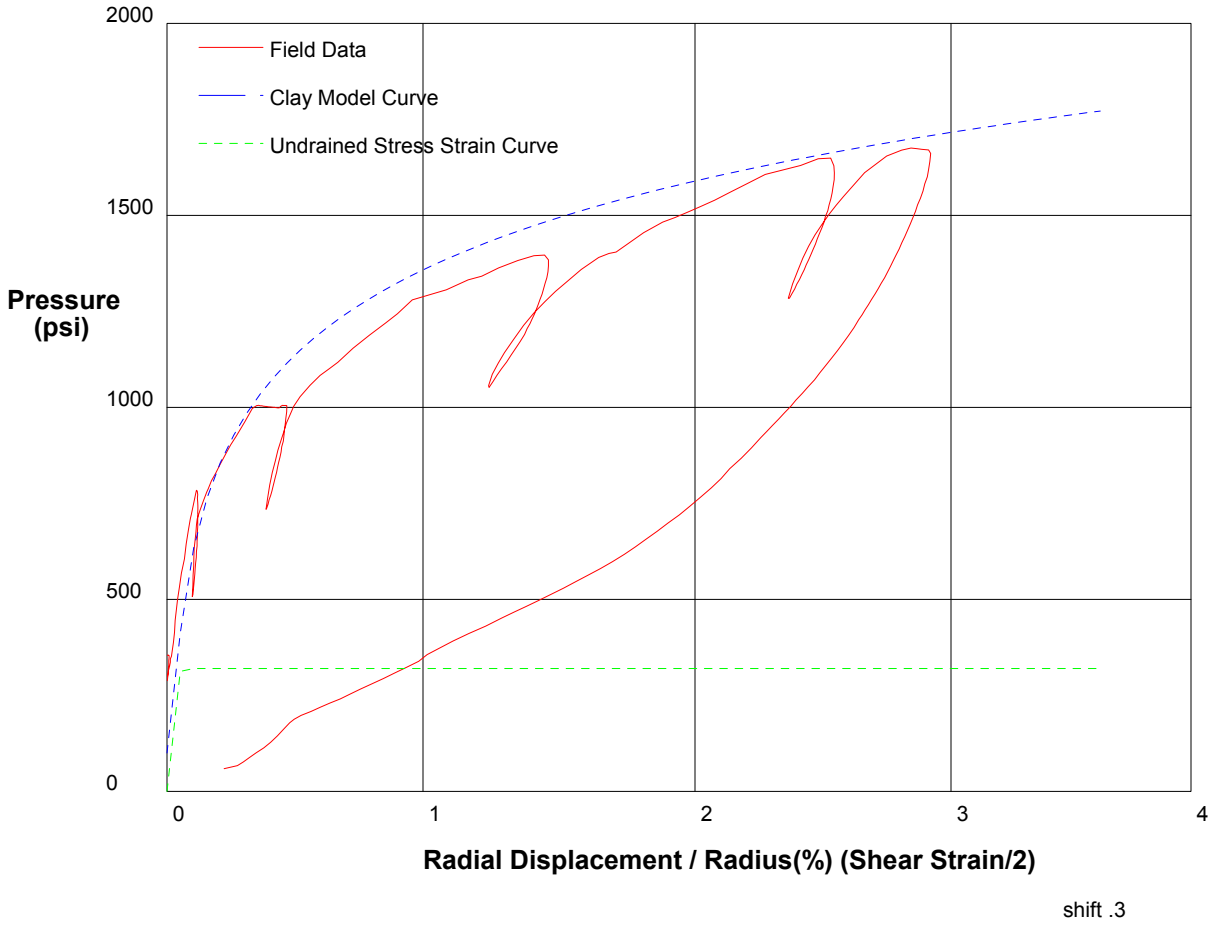


**GIBSON'S CLAY MODEL**

| | |
|---|---|
| **Shear Strength** | **320 psi** |
| **Insitu Stress** | **100 psi** |
| **Shear Modulus** | **300000 psi** |

shift .3

**In Situ Engineering**

# Appendix II - Pressuremeter Model Interpretation

**PRESSUREMETER DATA** **CH2MHill, Inc.**

**CALTRANS I-710 North Tunnel Project** **2/5/2009**

**Hole No. Z1-B6** **Depth 245ft** **File C:\DATA\ISE-812\SR710-28.P**

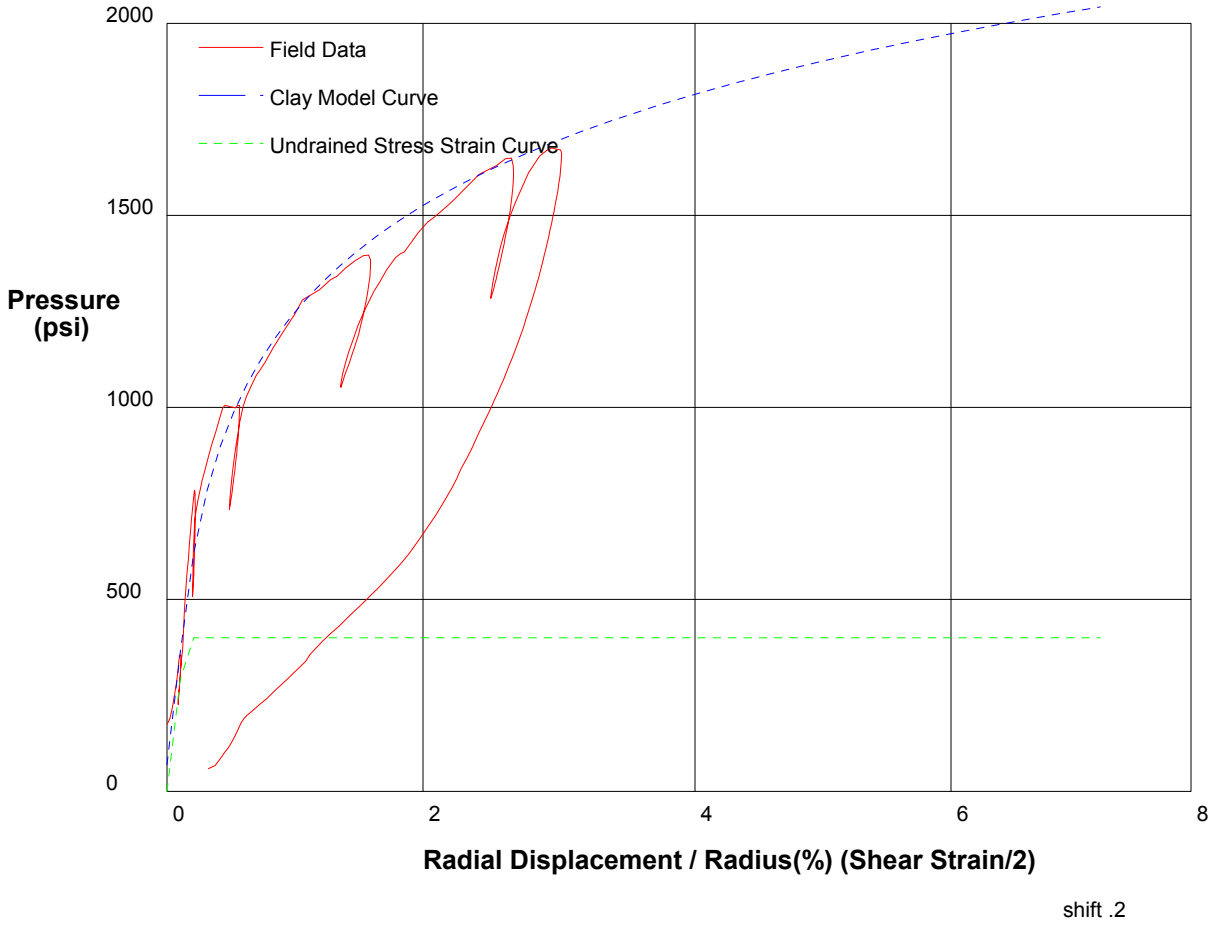


**GIBSON'S CLAY MODEL**

| | |
|---|---|
| **Shear Strength** | **400 psi** |
| **Insitu Stress** | **70 psi** |
| **Shear Modulus** | **140000 psi** |

shift .2

**In Situ Engineering**

# Appendix II - Pressuremeter Model Interpretation

**PRESSUREMETER DATA** **CH2MHill, Inc.**

**CALTRANS I-710 North Tunnel Project** **2/6/2009**

**Hole No. Z3-B7** **Depth 225.8ft** **File C:\DATA\ISE-812\SR710-29.P**

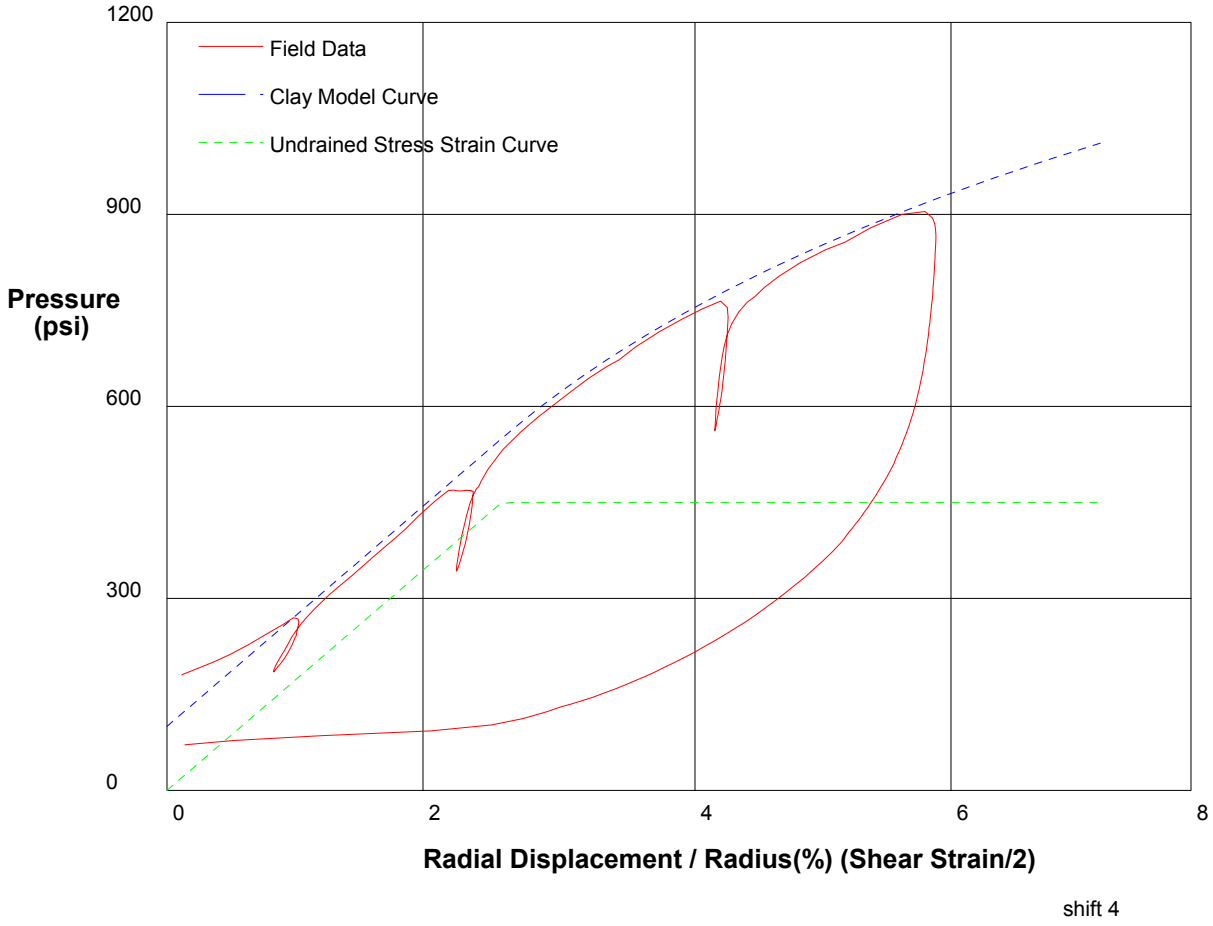


**GIBSON'S CLAY MODEL**

| | |
|---|---|
| **Shear Strength** | **450 psi** |
| **Insitu Stress** | **100 psi** |
| **Shear Modulus** | **8600 psi** |

shift 4

**In Situ Engineering**

# Appendix II - Pressuremeter Model Interpretation

**PRESSUREMETER DATA** **CH2MHill, Inc.**

**CALTRANS I-710 North Tunnel Project** **2/6/2009**

**Hole No. Z3-B7** **Depth 225.8ft** **File C:\DATA\ISE-812\SR710-29.P**

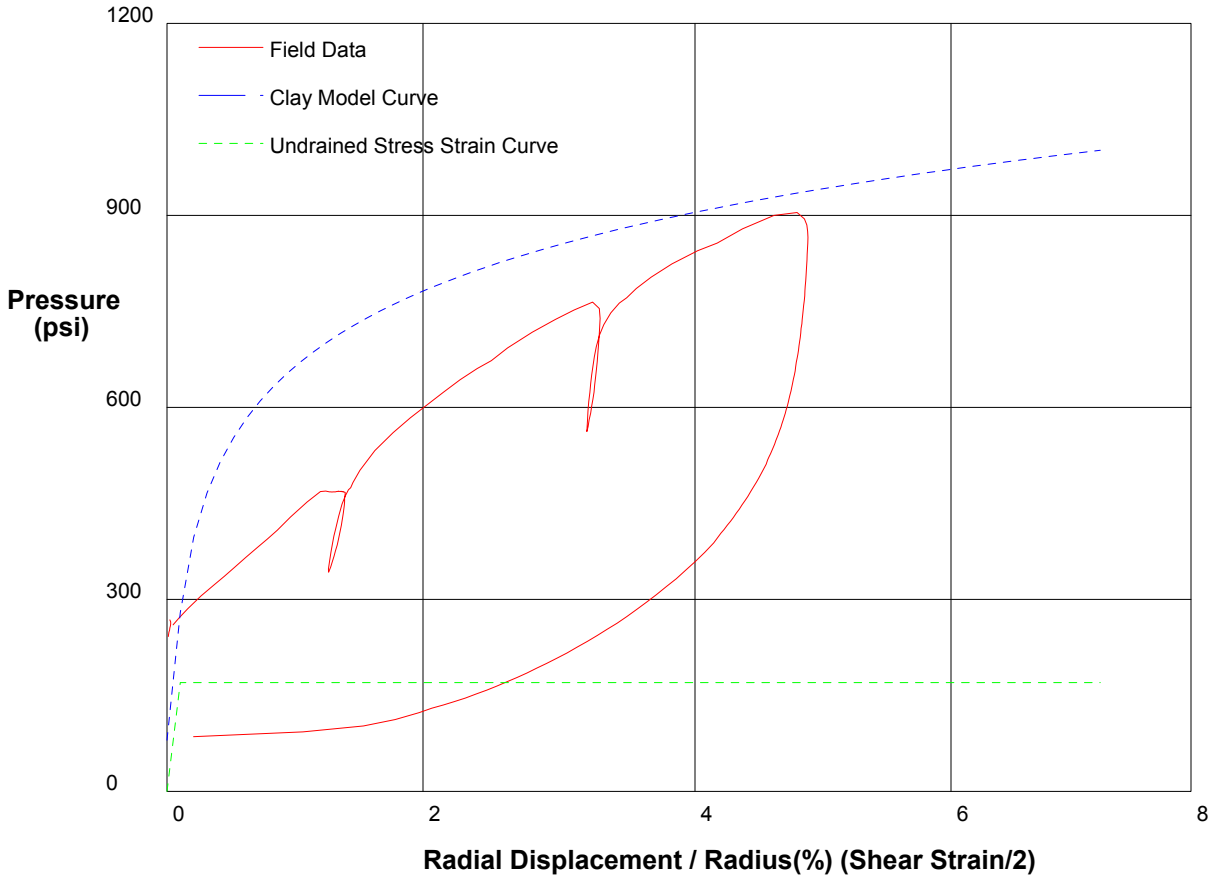


**GIBSON'S CLAY MODEL**

**Shear Strength 170 psi**
**Insitu Stress 80 psi**
**Shear Modulus 97000 psi**

shift 5

**In Situ Engineering**

# Appendix II - Pressuremeter Model Interpretation

**PRESSUREMETER DATA** **CH2MHill, Inc.**

**CALTRANS I-710 North Tunnel Project** **2/6/2009**

**Hole No. Z3-B7** **Depth 225.8ft** **File C:\DATA\ISE-812\SR710-29.P**

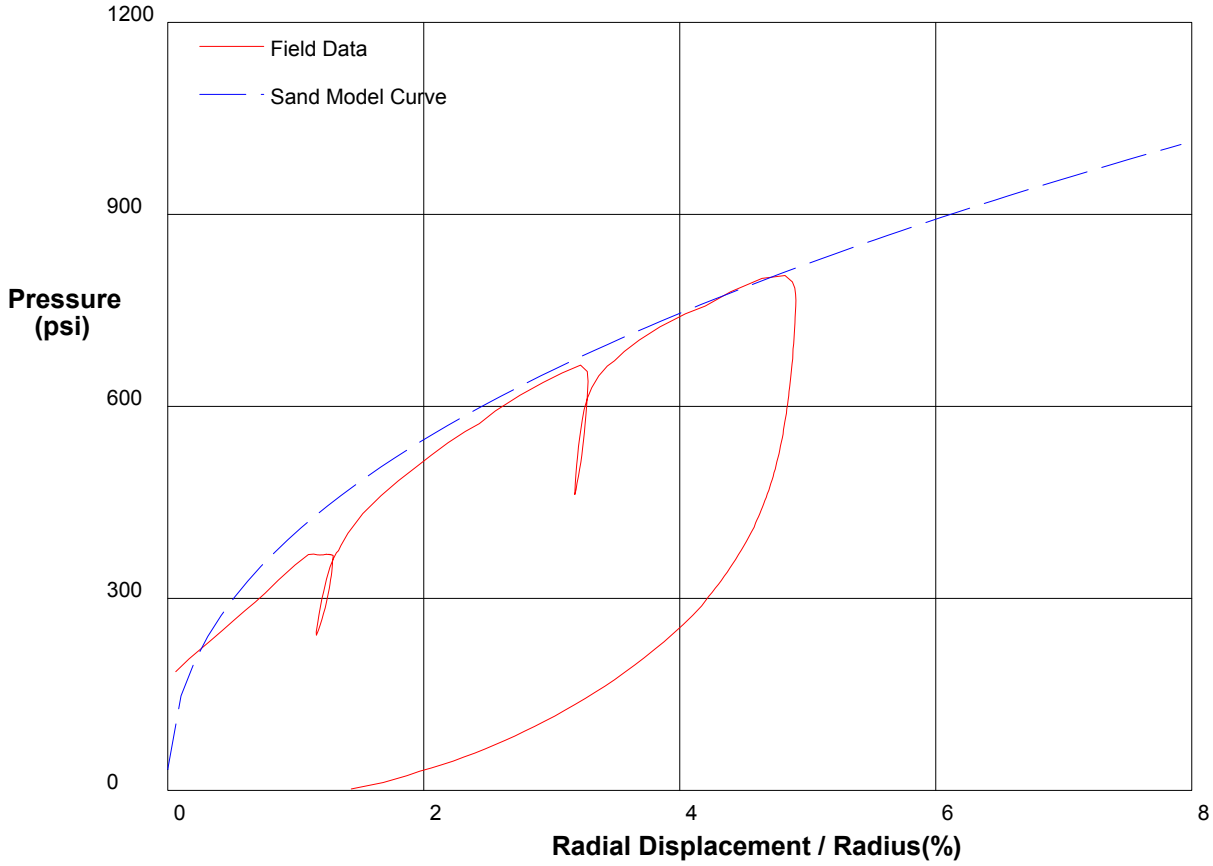


**THE In Situ Engineering SAND MODEL**

| | |
|---|---|
| **Water Pressure** | **100 psi** |
| **Friction Angle** | **39 deg** |
| **Critical Friction Angle** | **32 deg** |
| **Lateral Stress** | **33 psi** |
| **Shear Modulus** | **97000 psi** |

shift 5.1

**In Situ Engineering**

# Appendix II - Pressuremeter Model Interpretation

**PRESSUREMETER DATA** **CH2MHill, Inc.**

**CALTRANS I-710 North Tunnel Project** **2/6/2009**

**Hole No. Z3-B7** **Depth 224.3ft** **File C:\DATA\ISE-812\SR710-30.P**

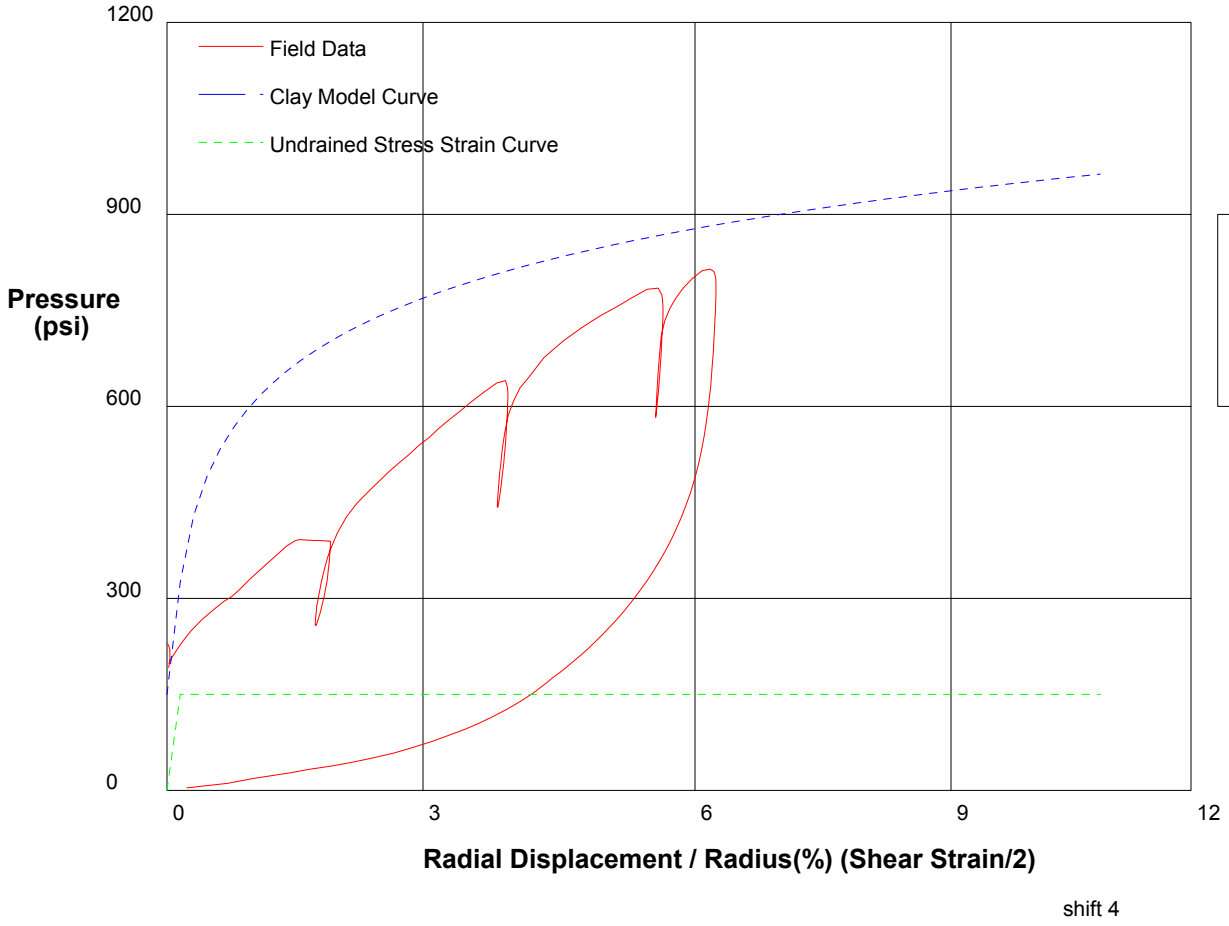


**GIBSON'S CLAY MODEL**

| | |
|---|---|
| **Shear Strength** | **150 psi** |
| **Insitu Stress** | **150 psi** |
| **Shear Modulus** | **57000 psi** |

shift 4

**In Situ Engineering**

# Appendix II - Pressuremeter Model Interpretation

**PRESSUREMETER DATA** **CH2MHill, Inc.**

**CALTRANS I-710 North Tunnel Project** **2/6/2009**

**Hole No. Z3-B7** **Depth 224.3ft** **File C:\DATA\ISE-812\SR710-30.P**

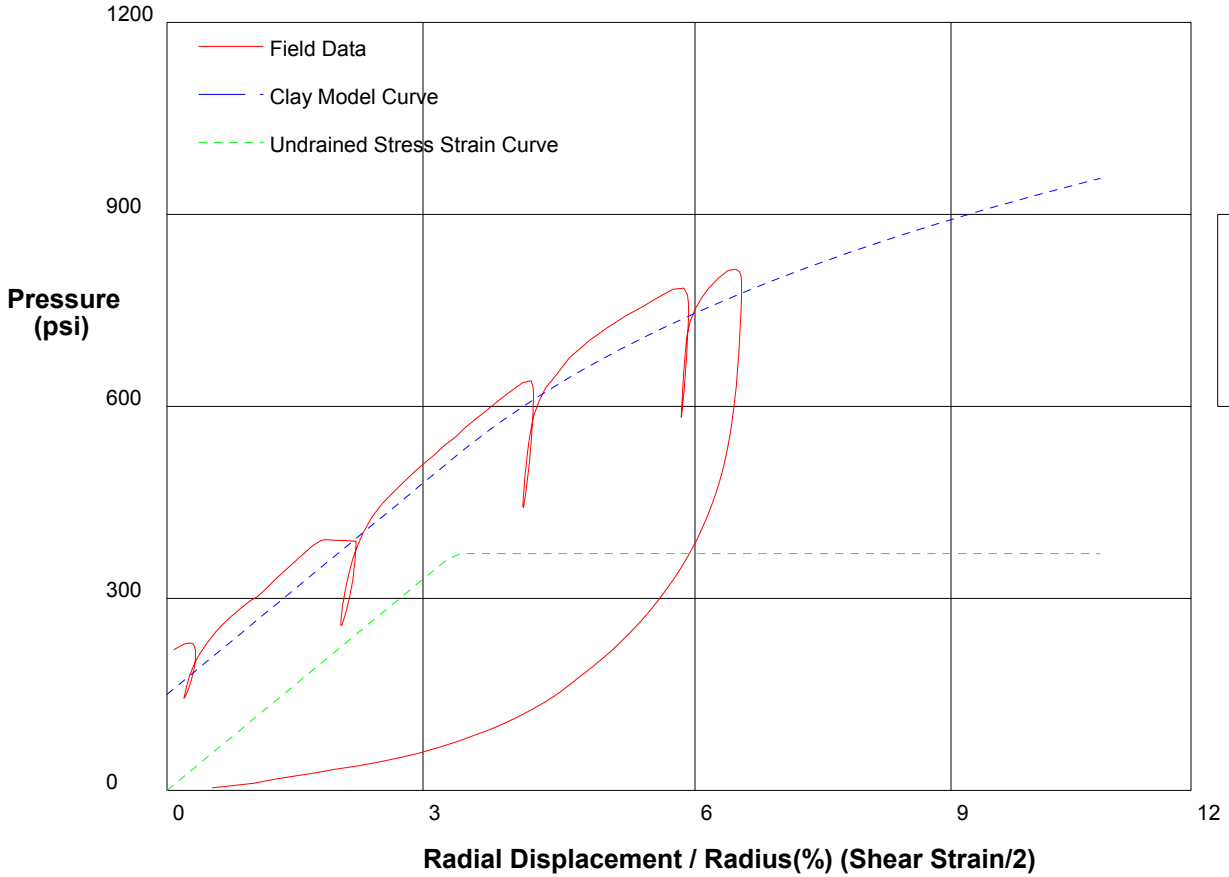


**GIBSON'S CLAY MODEL**

**Shear Strength 370 psi**
**Insitu Stress 150 psi**
**Shear Modulus 5500 psi**

shift 3.7

**In Situ Engineering**

# Appendix II - Pressuremeter Model Interpretation

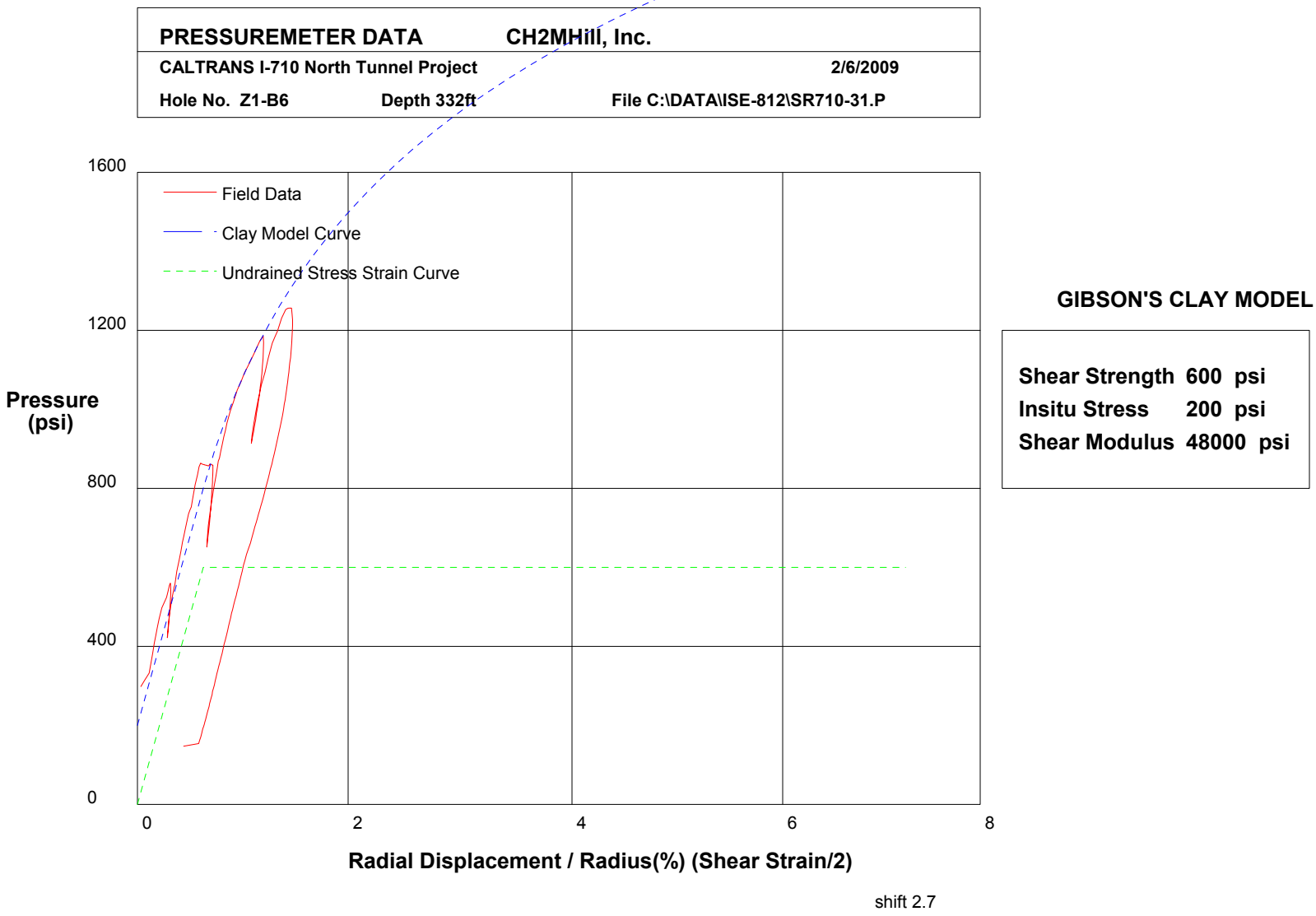


**In Situ Engineering**

# Appendix II - Pressuremeter Model Interpretation

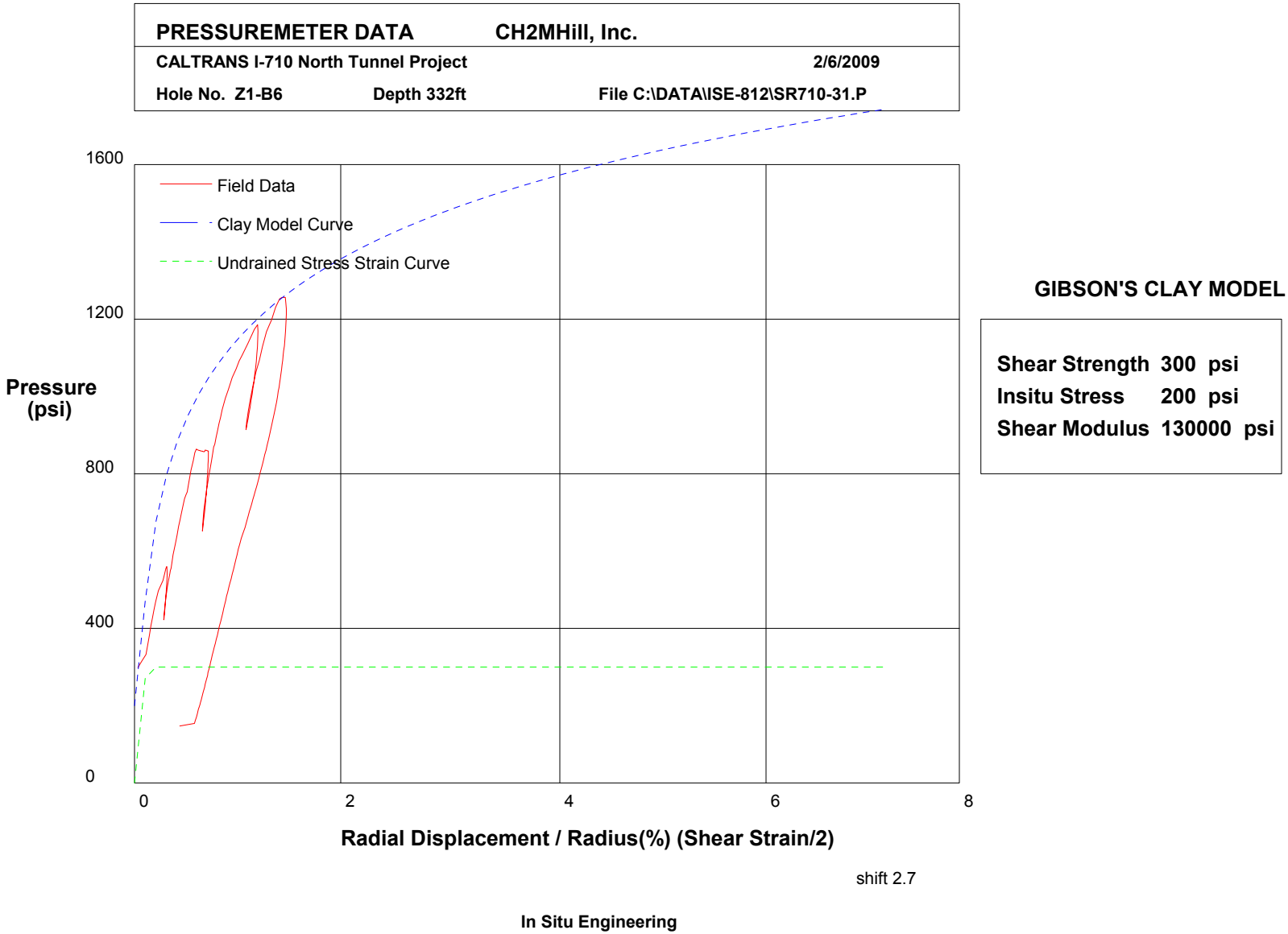

# Appendix II - Pressuremeter Model Interpretation

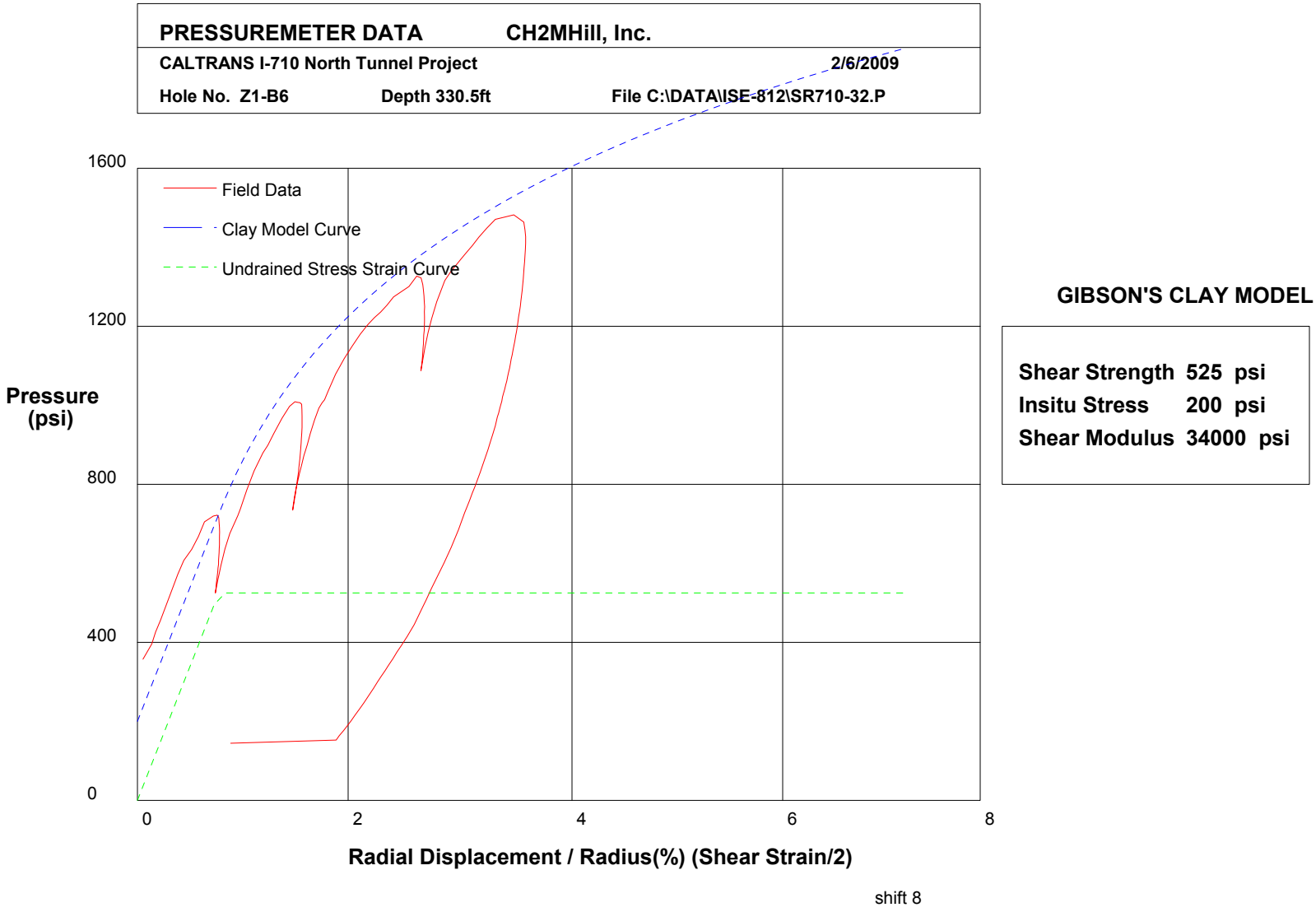

# Appendix II - Pressuremeter Model Interpretation

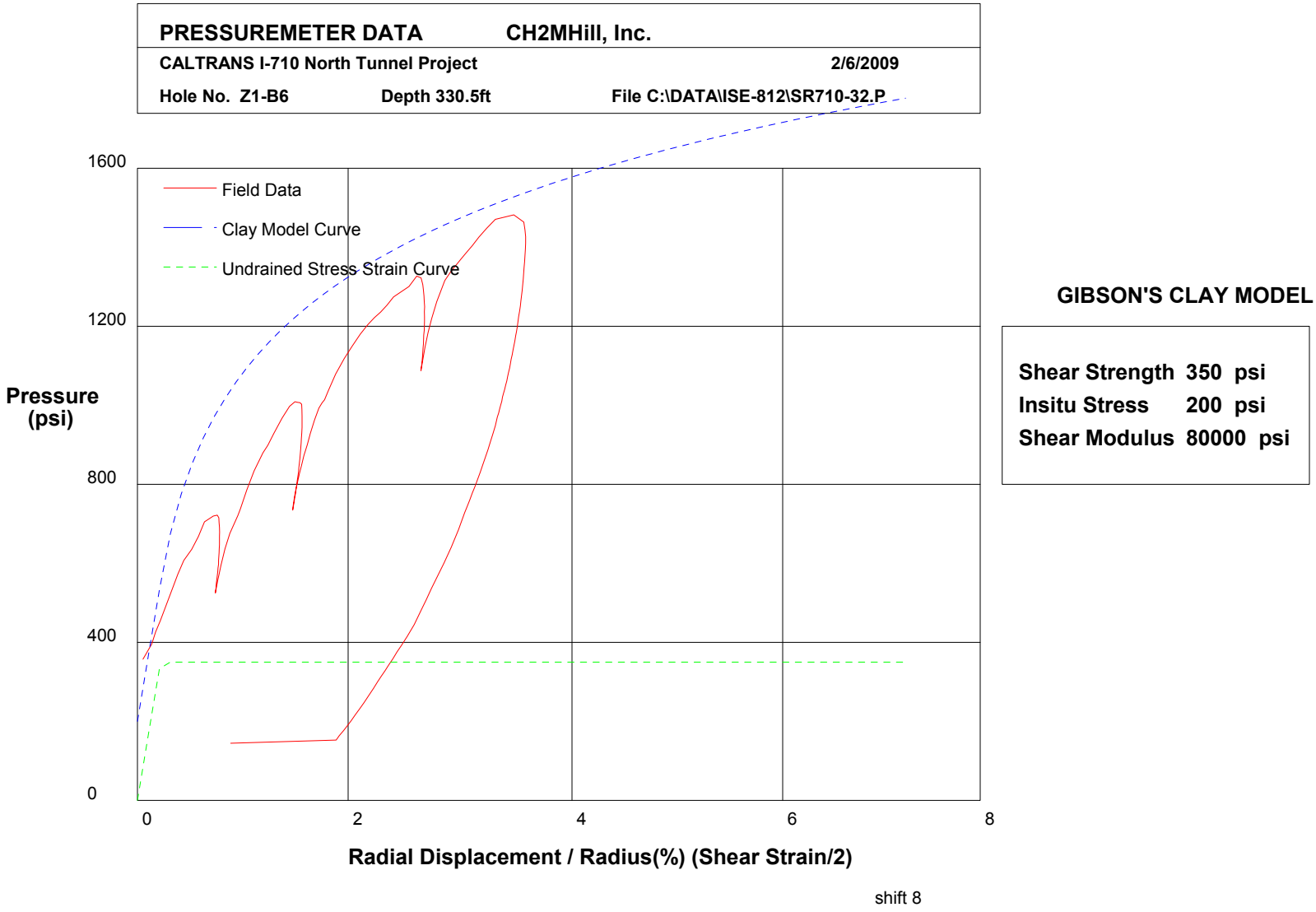

# Appendix II - Pressuremeter Model Interpretation

**PRESSUREMETER DATA** **CH2MHill, Inc.**

**CALTRANS I-710 North Tunnel Project** **2/10/2009**

**Hole No. Z3-B7** **Depth 252.5ft** **File C:\DATA\ISE-812\SR710-33.P**

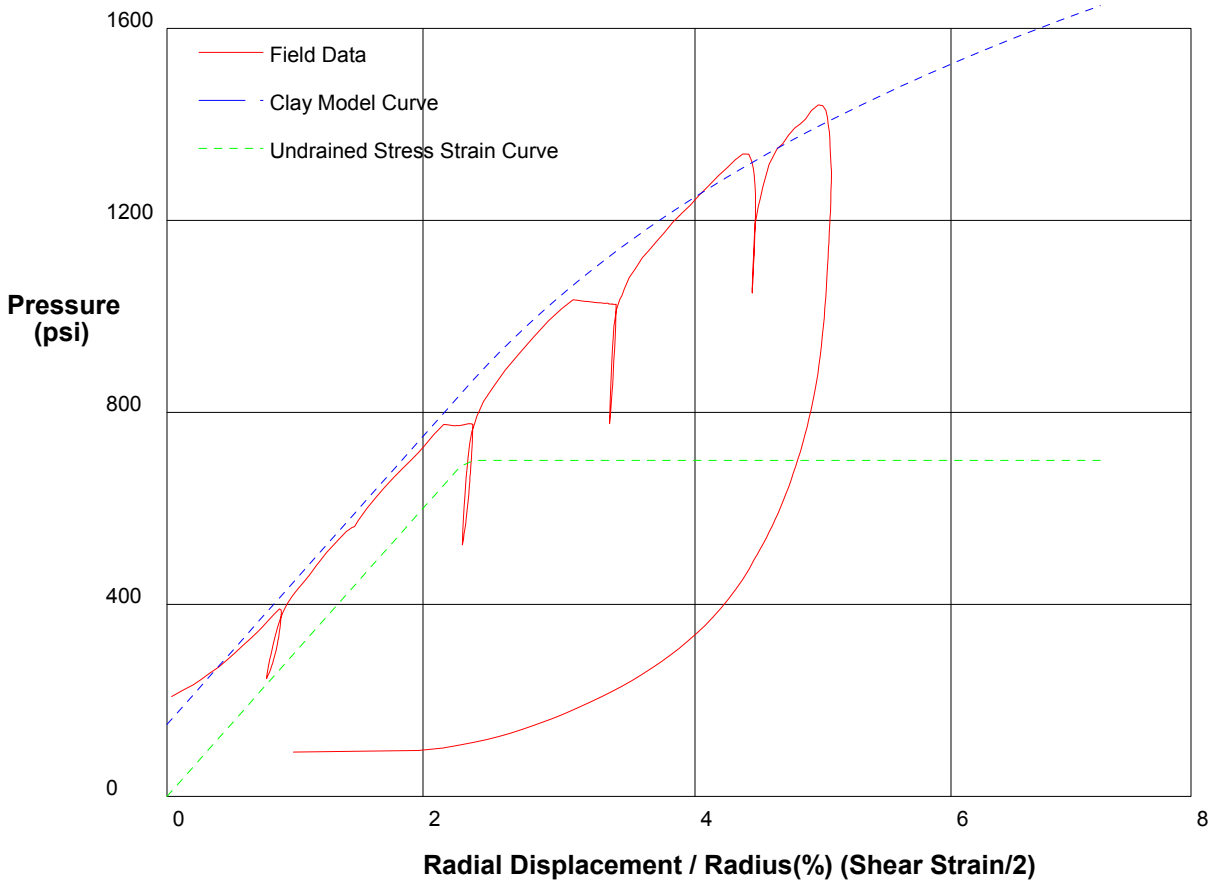


**GIBSON'S CLAY MODEL**

| | |
|---|---|
| **Shear Strength** | **700 psi** |
| **Insitu Stress** | **150 psi** |
| **Shear Modulus** | **15000 psi** |

shift 5.2

**In Situ Engineering**

# Appendix II - Pressuremeter Model Interpretation

**PRESSUREMETER DATA** **CH2MHill, Inc.**

**CALTRANS I-710 North Tunnel Project** **2/10/2009**

**Hole No. Z3-B7** **Depth 252.5ft** **File C:\DATA\ISE-812\SR710-33.P**

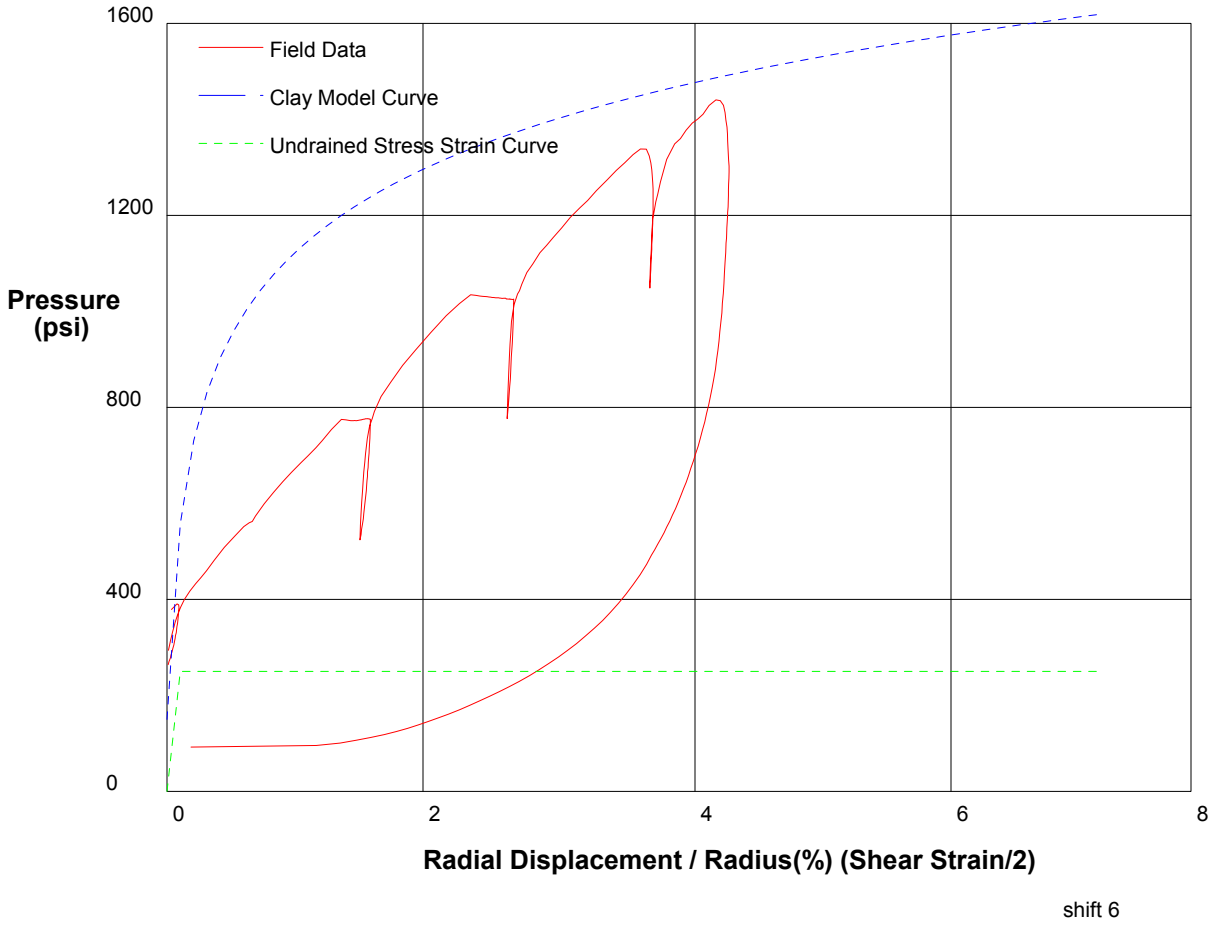


**GIBSON'S CLAY MODEL**

| | |
|---|---|
| **Shear Strength** | **250 psi** |
| **Insitu Stress** | **150 psi** |
| **Shear Modulus** | **225000 psi** |

shift 6

**In Situ Engineering**

# Appendix II - Pressuremeter Model Interpretation

**PRESSUREMETER DATA** **CH2MHill, Inc.**

**CALTRANS I-710 North Tunnel Project** **2/10/2009**

**Hole No. Z3-B7** **Depth 251ft** **File C:\DATA\ISE-812\SR710-34.P**

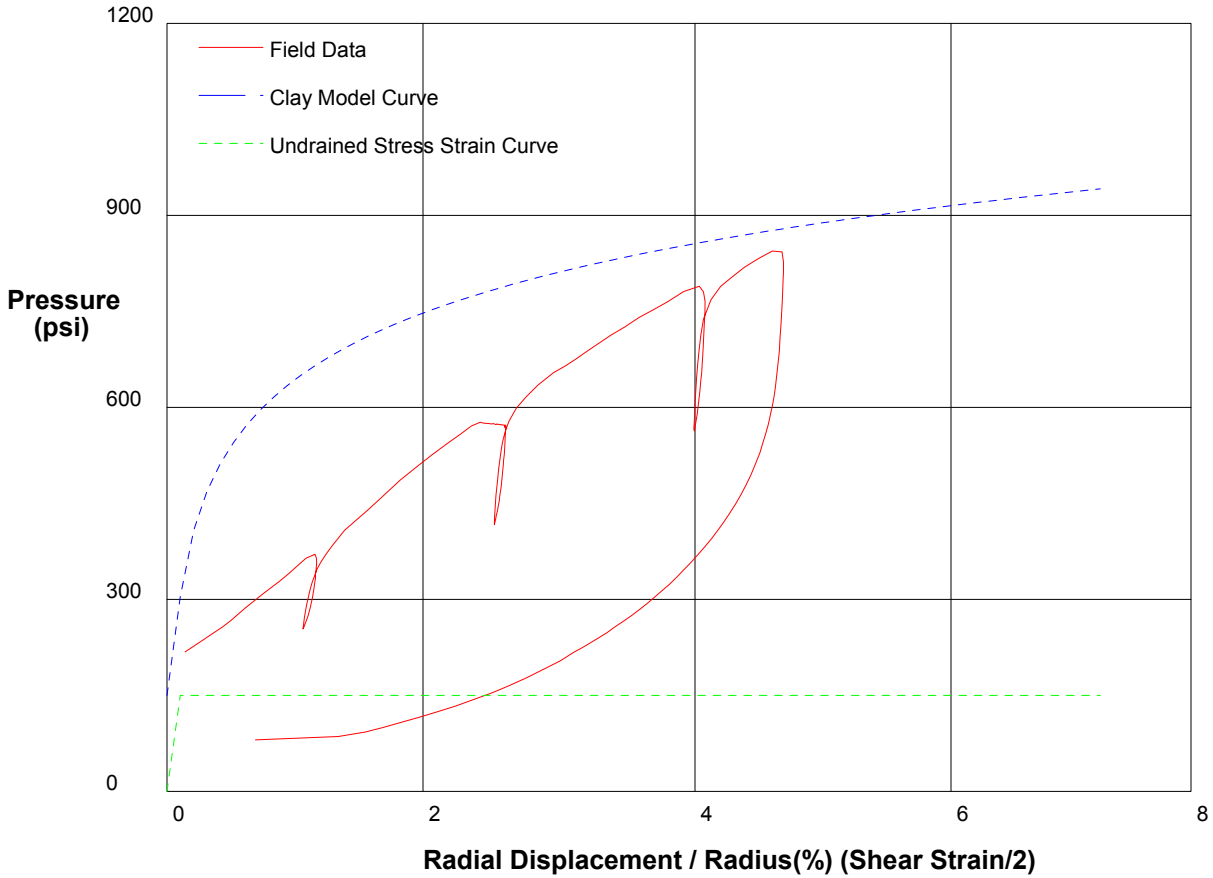


**GIBSON'S CLAY MODEL**

**Shear Strength 150 psi**
**Insitu Stress 150 psi**
**Shear Modulus 74000 psi**

shift 6.2

**In Situ Engineering**

# Appendix II - Pressuremeter Model Interpretation

**PRESSUREMETER DATA** **CH2MHill, Inc.**

**CALTRANS I-710 North Tunnel Project** **2/10/2009**

**Hole No. Z3-B7** **Depth 251ft** **File C:\DATA\ISE-812\SR710-34.P**

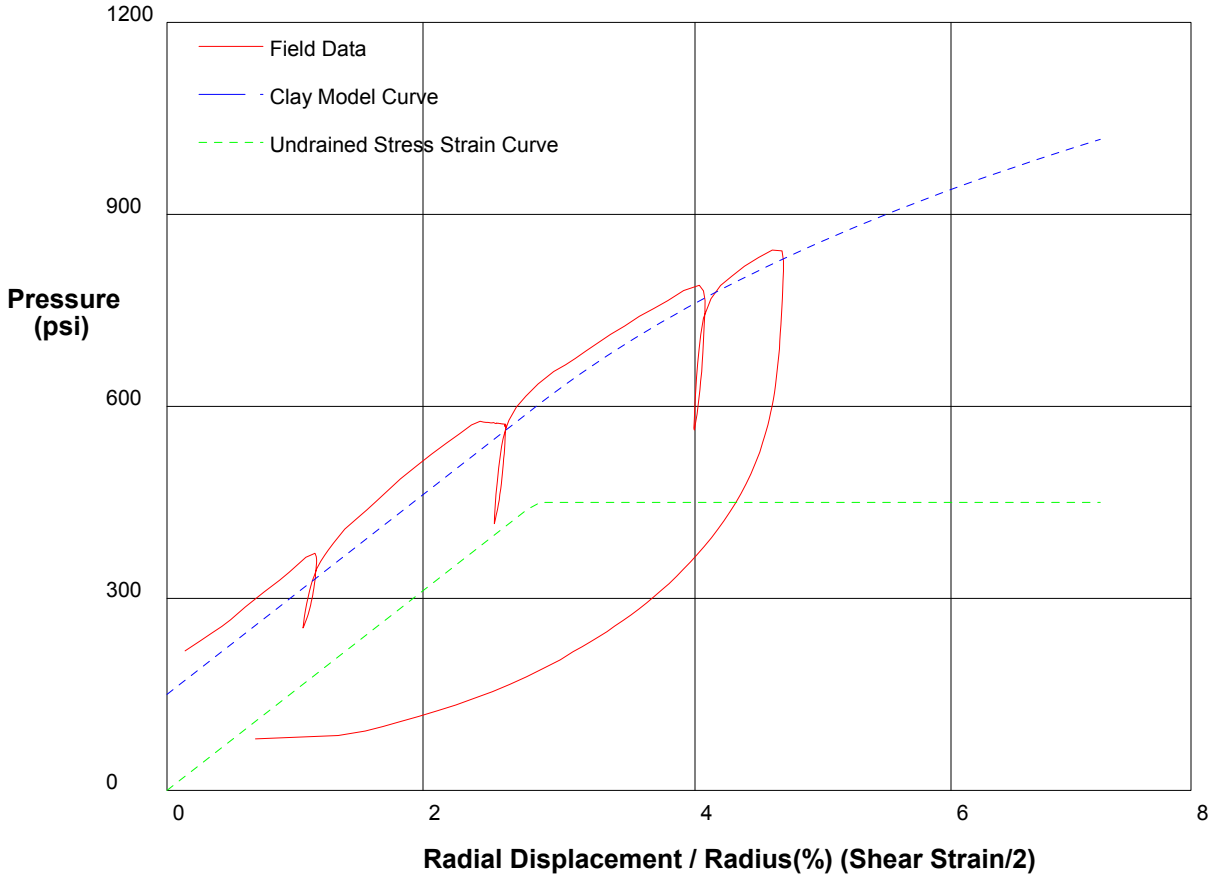


**GIBSON'S CLAY MODEL**

| | |
|---|---|
| **Shear Strength** | **450 psi** |
| **Insitu Stress** | **150 psi** |
| **Shear Modulus** | **7800 psi** |

shift 6.2

**In Situ Engineering**

# Appendix II - Pressuremeter Model Interpretation

**PRESSUREMETER DATA** **CH2MHill, Inc.**

**CALTRANS I-710 North Tunnel Project** **2/10/2009**

**Hole No. Z3-B7** **Depth 251ft** **File C:\DATA\ISE-812\SR710-34.P**

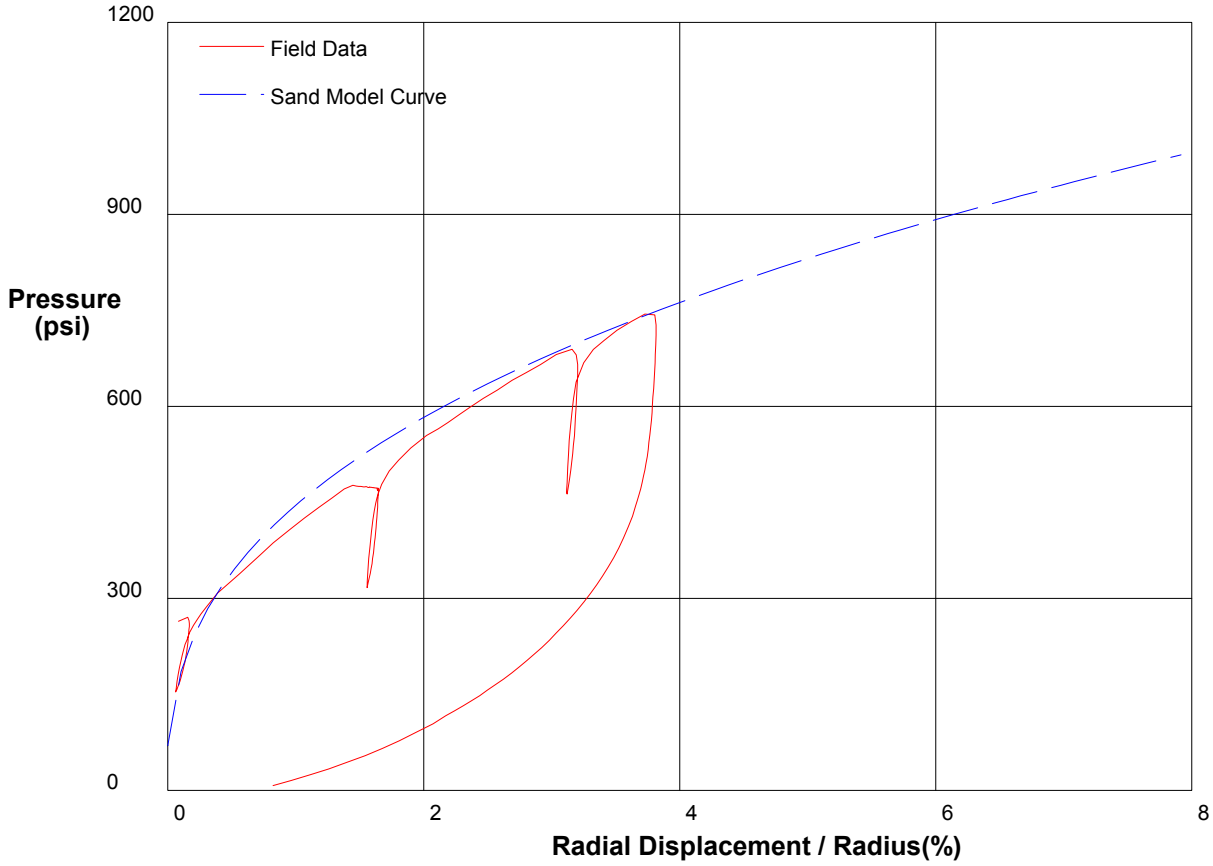


**THE In Situ Engineering SAND MODEL**

| | |
|---|---|
| **Water Pressure** | **100 psi** |
| **Friction Angle** | **35 deg** |
| **Critical Friction Angle** | **32 deg** |
| **Lateral Stress** | **70 psi** |
| **Shear Modulus** | **74000 psi** |

shift 7.2

**In Situ Engineering**

# Appendix II - Pressuremeter Model Interpretation

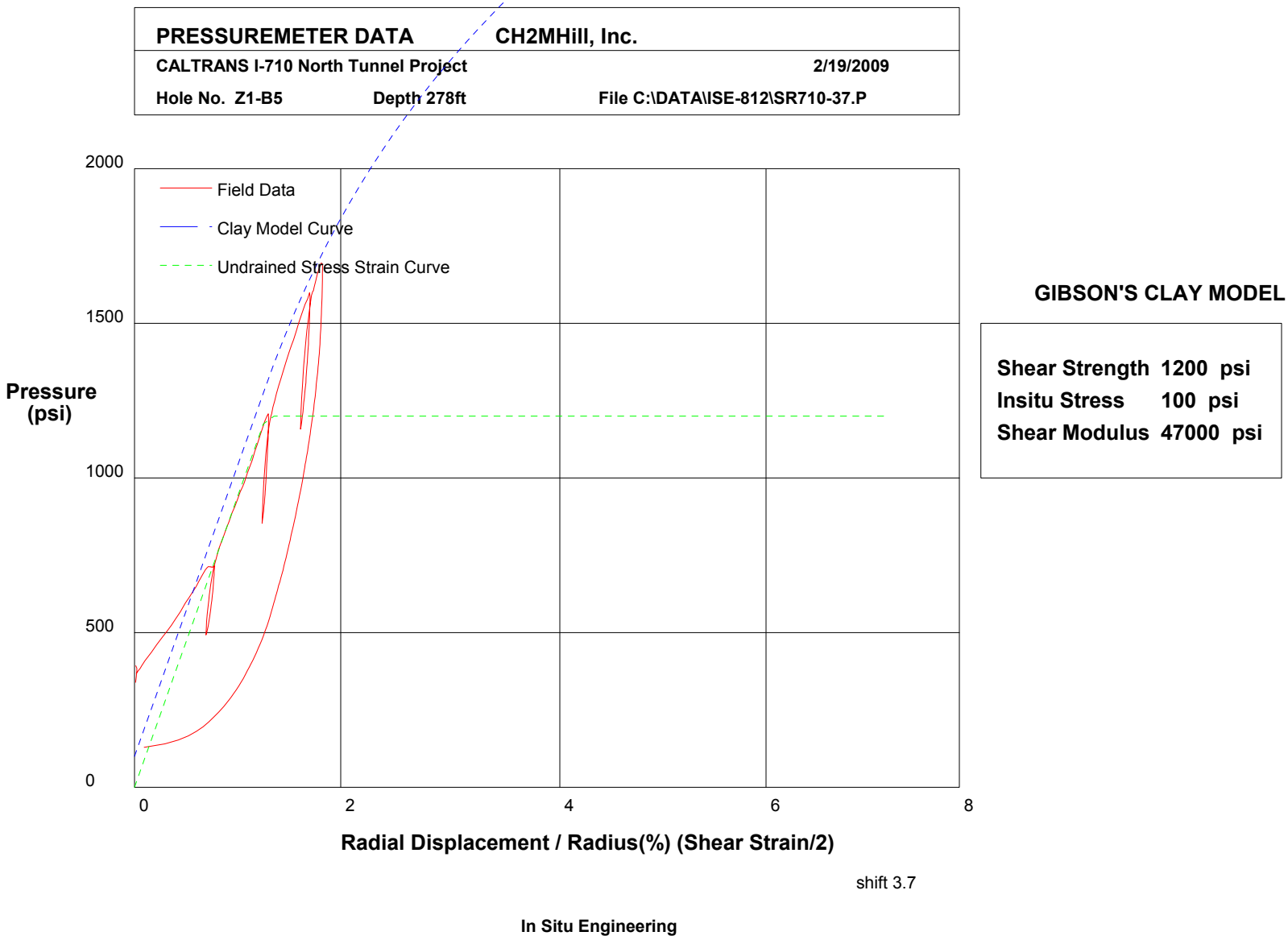

# Appendix II - Pressuremeter Model Interpretation

**PRESSUREMETER DATA** **CH2MHill, Inc.**

**CALTRANS I-710 North Tunnel Project** **2/19/2009**

**Hole No. Z1-B5** **Depth 278ft** **File C:\DATA\ISE-812\SR710-37.P**

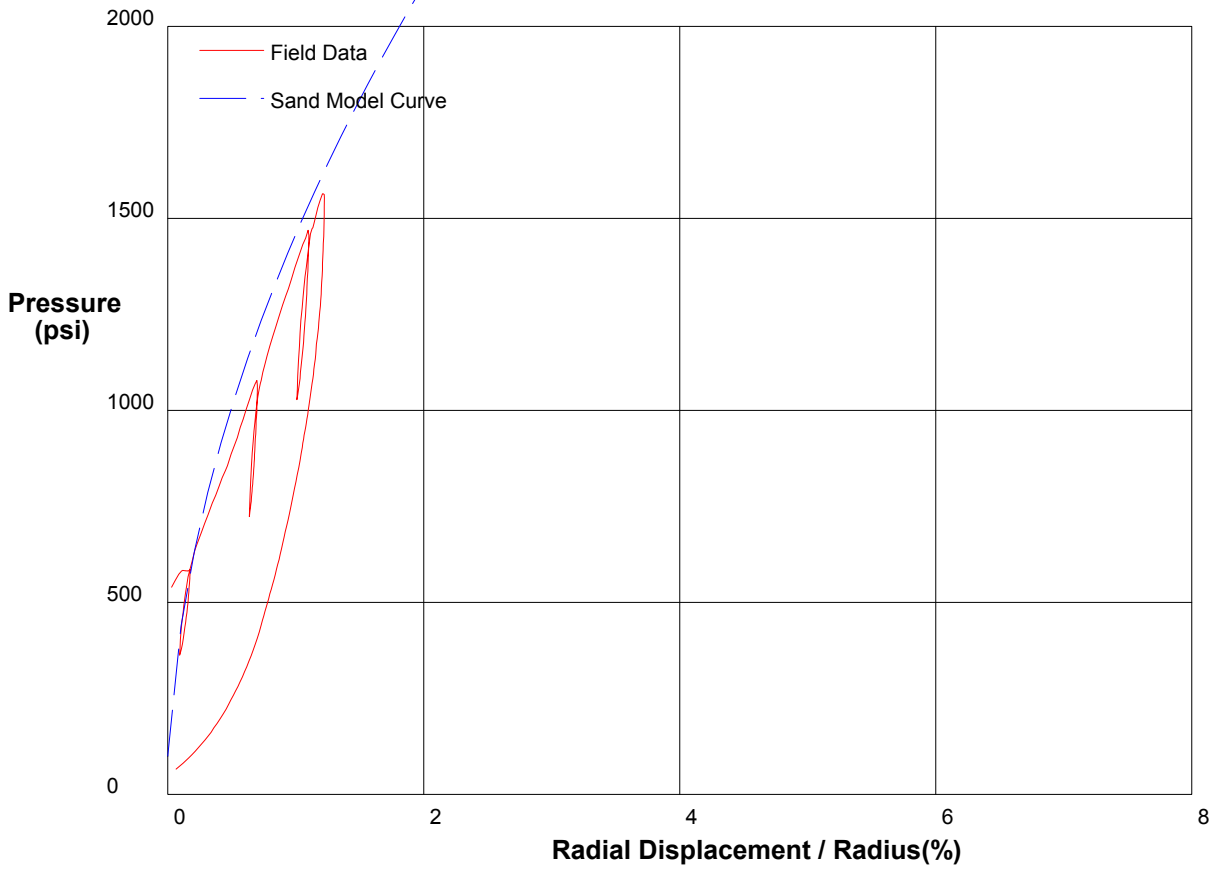


**THE In Situ Engineering SAND MODEL**

| | |
|---|---|
| **Water Pressure** | **130 psi** |
| **Friction Angle** | **45 deg** |
| **Critical Friction Angle** | **32 deg** |
| **Lateral Stress** | **100 psi** |
| **Shear Modulus** | **200000 psi** |

shift 4.3

**In Situ Engineering**

# Appendix II - Pressuremeter Model Interpretation

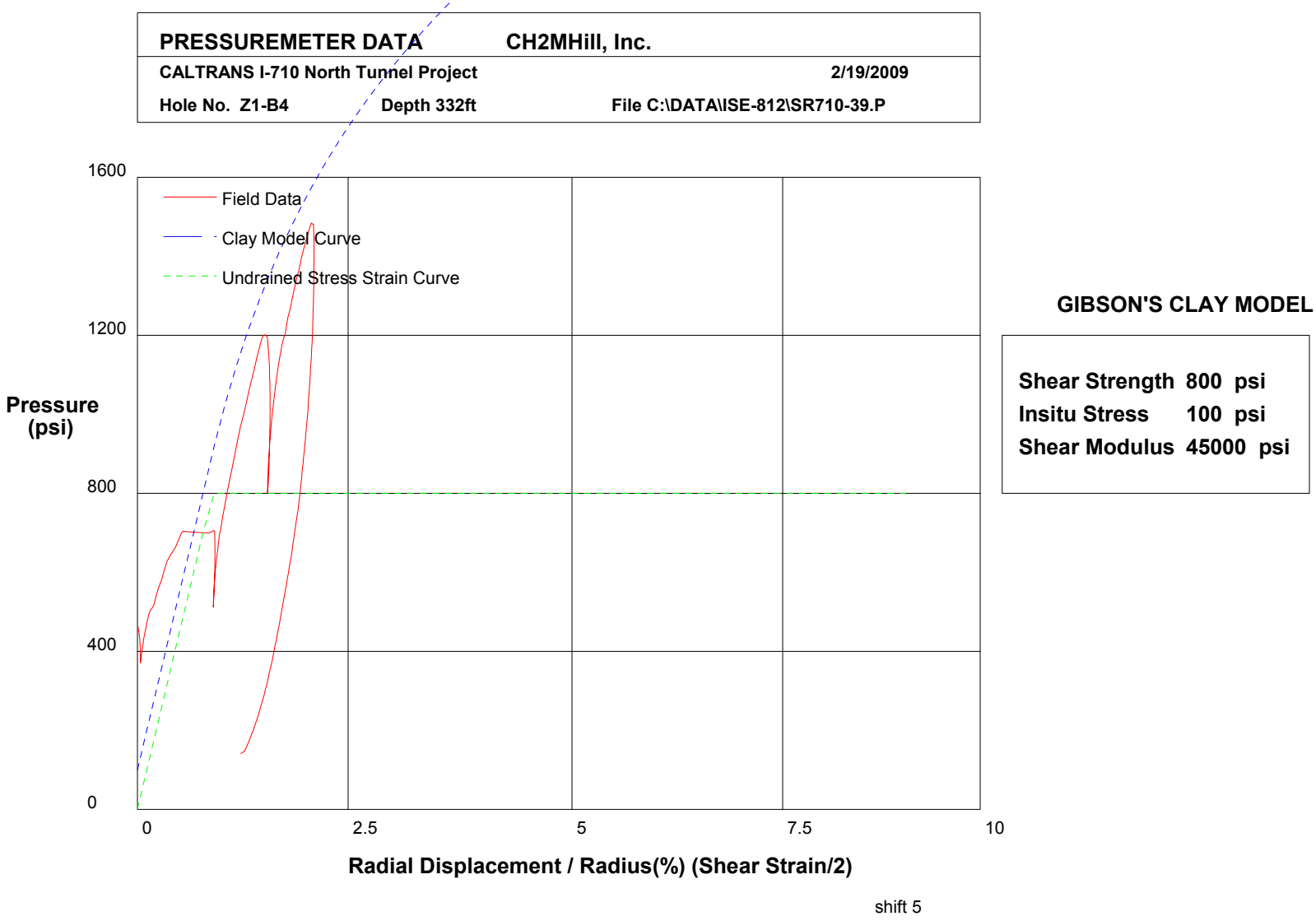

# Appendix II - Pressuremeter Model Interpretation

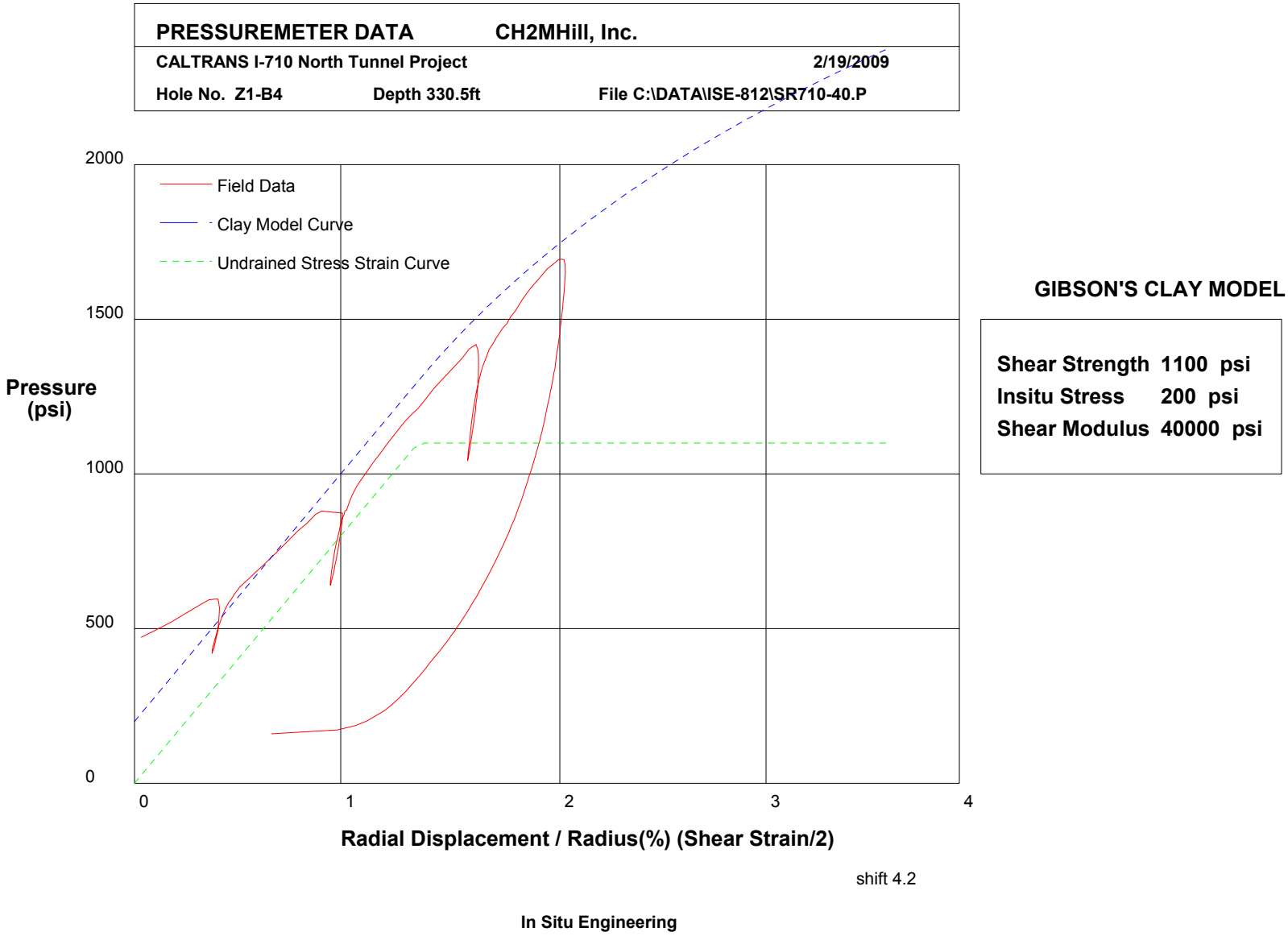

# Appendix II - Pressuremeter Model Interpretation

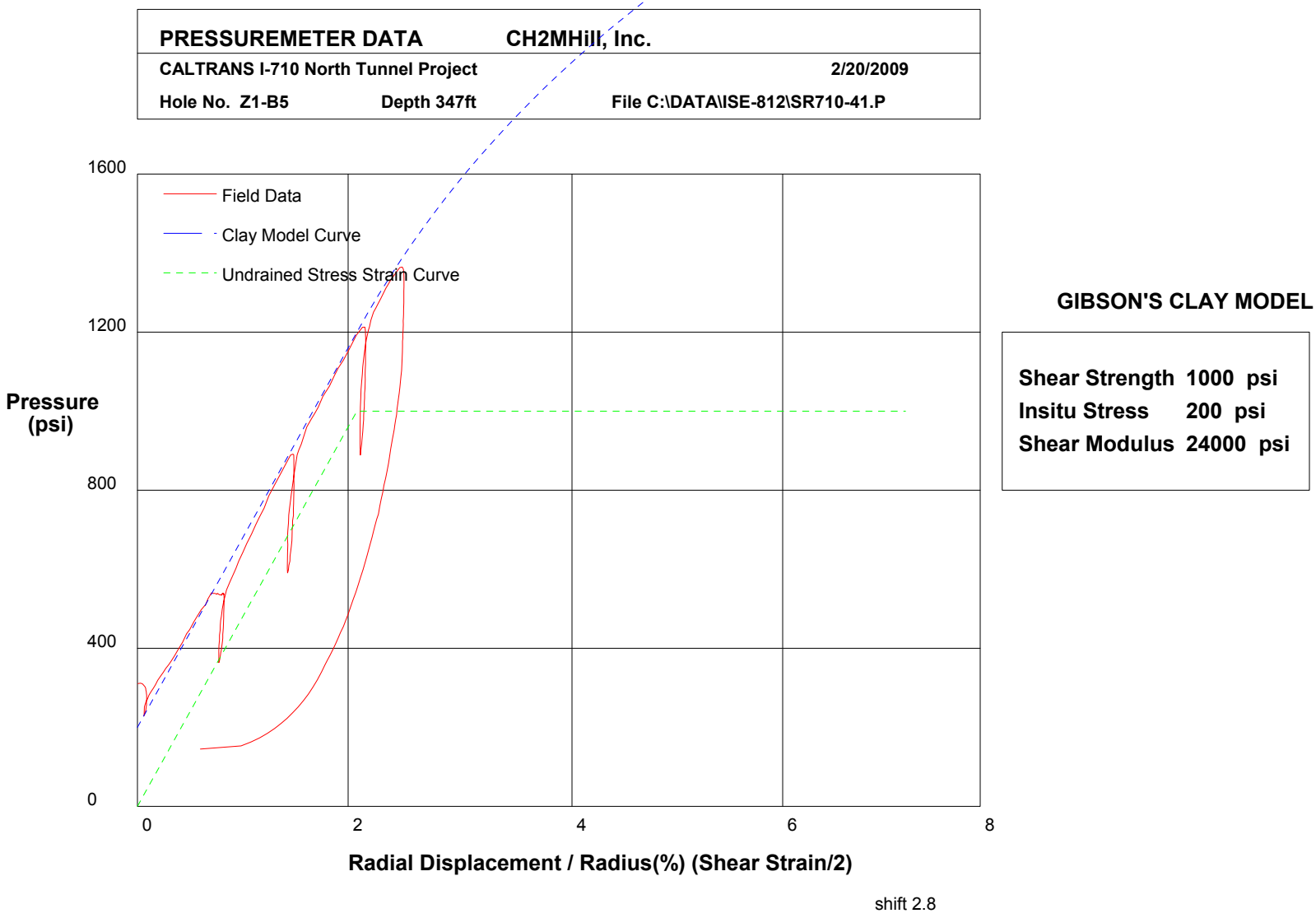

# Appendix II - Pressuremeter Model Interpretation

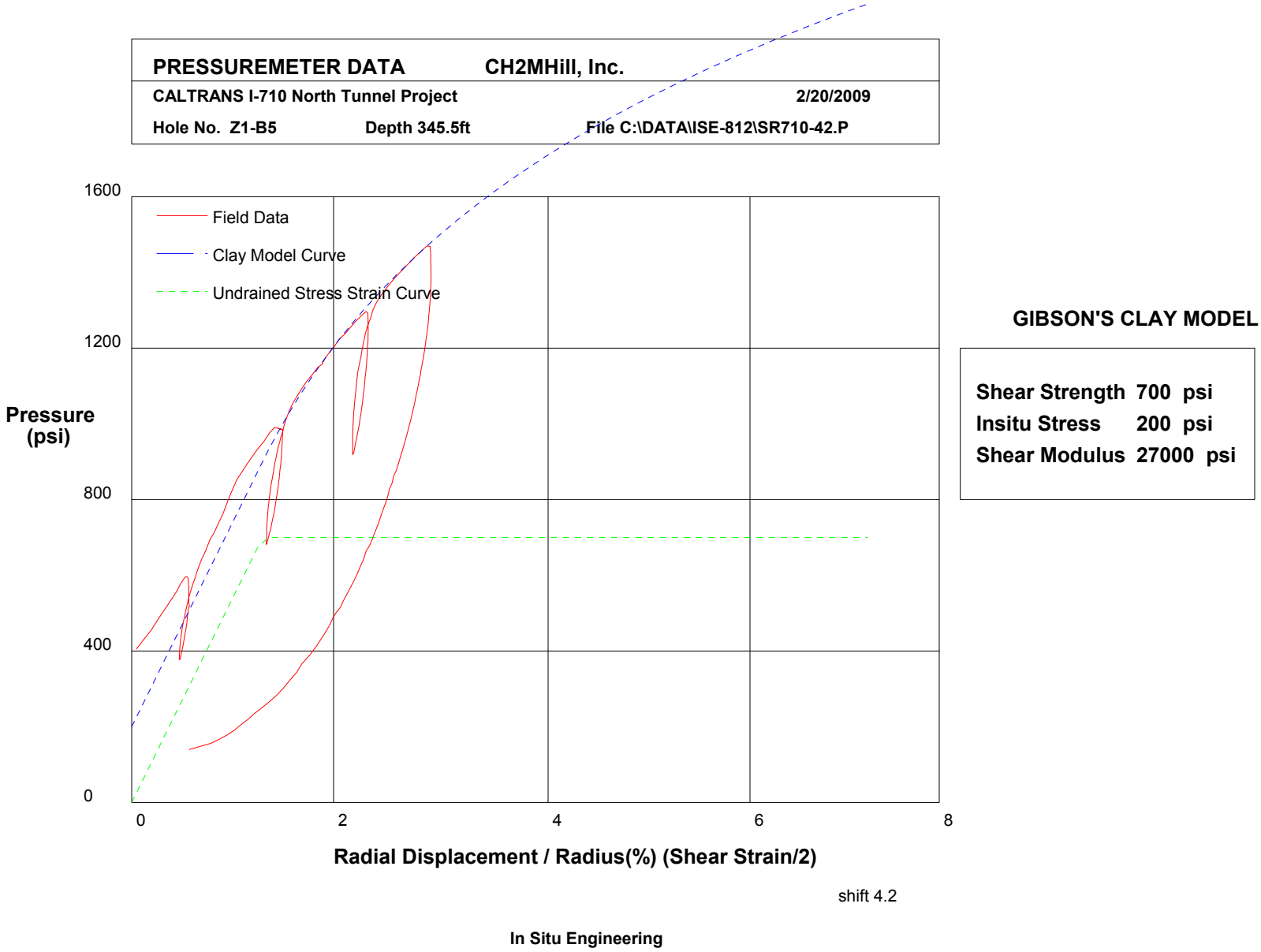

# Appendix II - Pressuremeter Model Interpretation

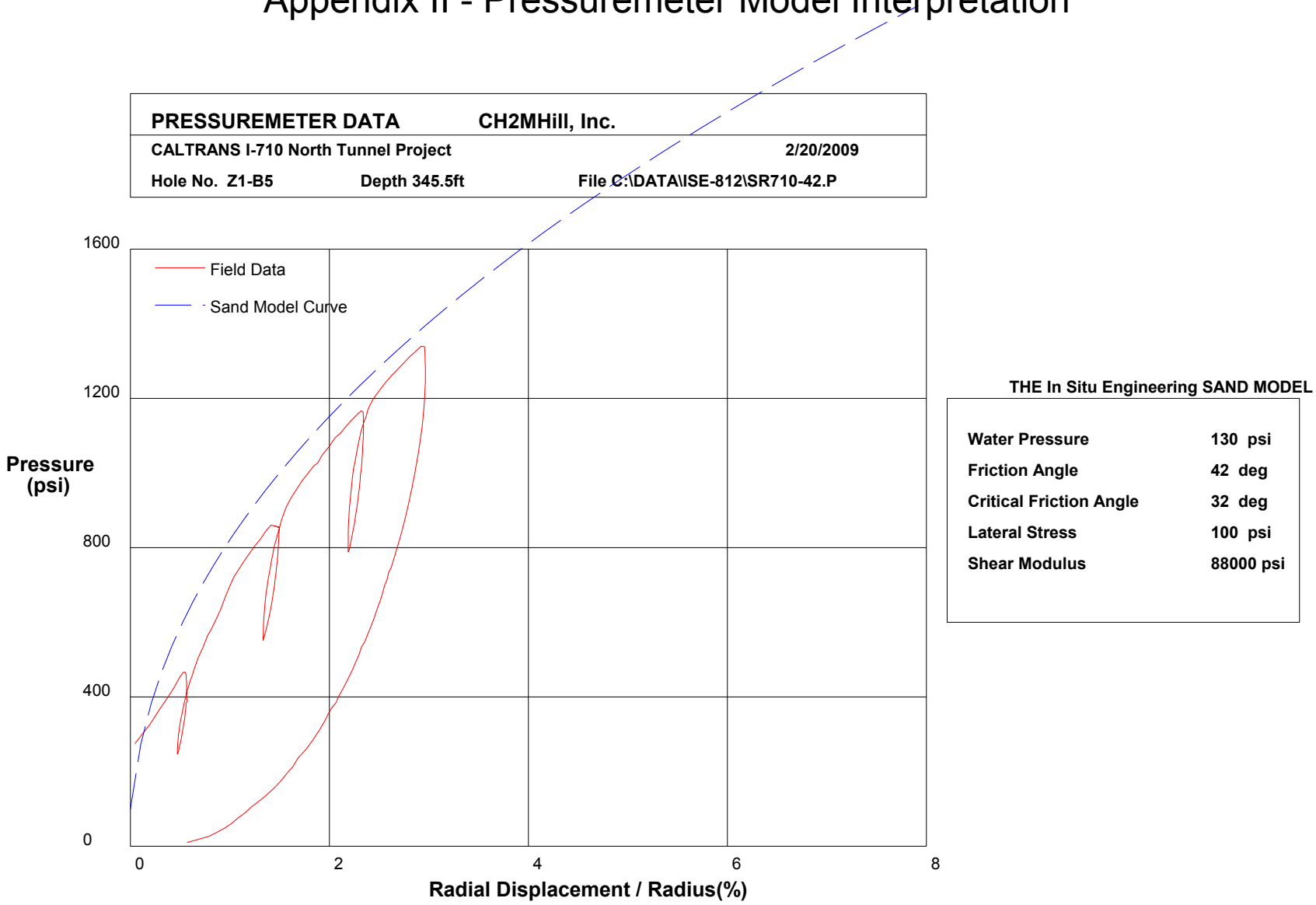

# Appendix II - Pressuremeter Model Interpretation

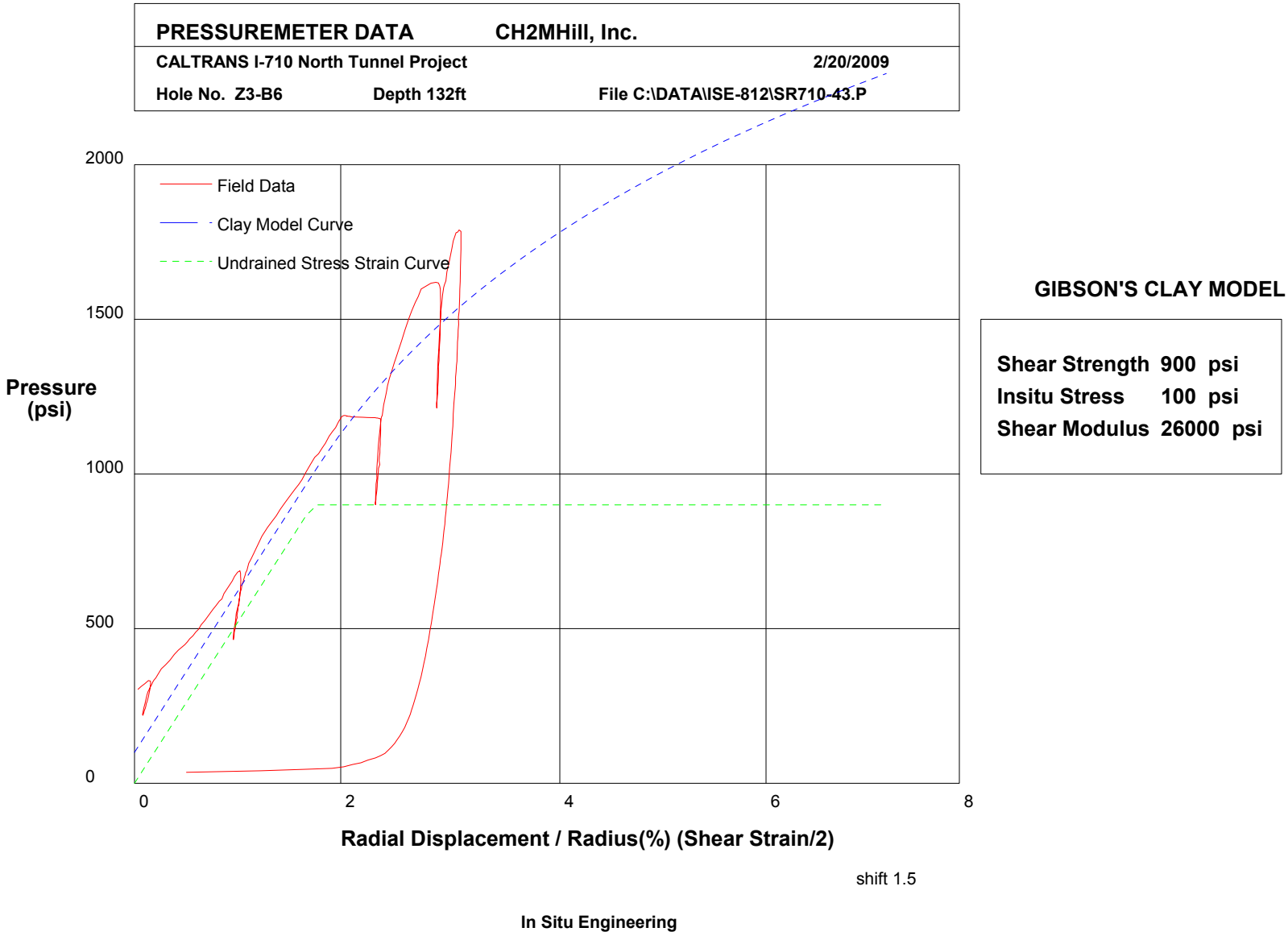

# Appendix II - Pressuremeter Model Interpretation

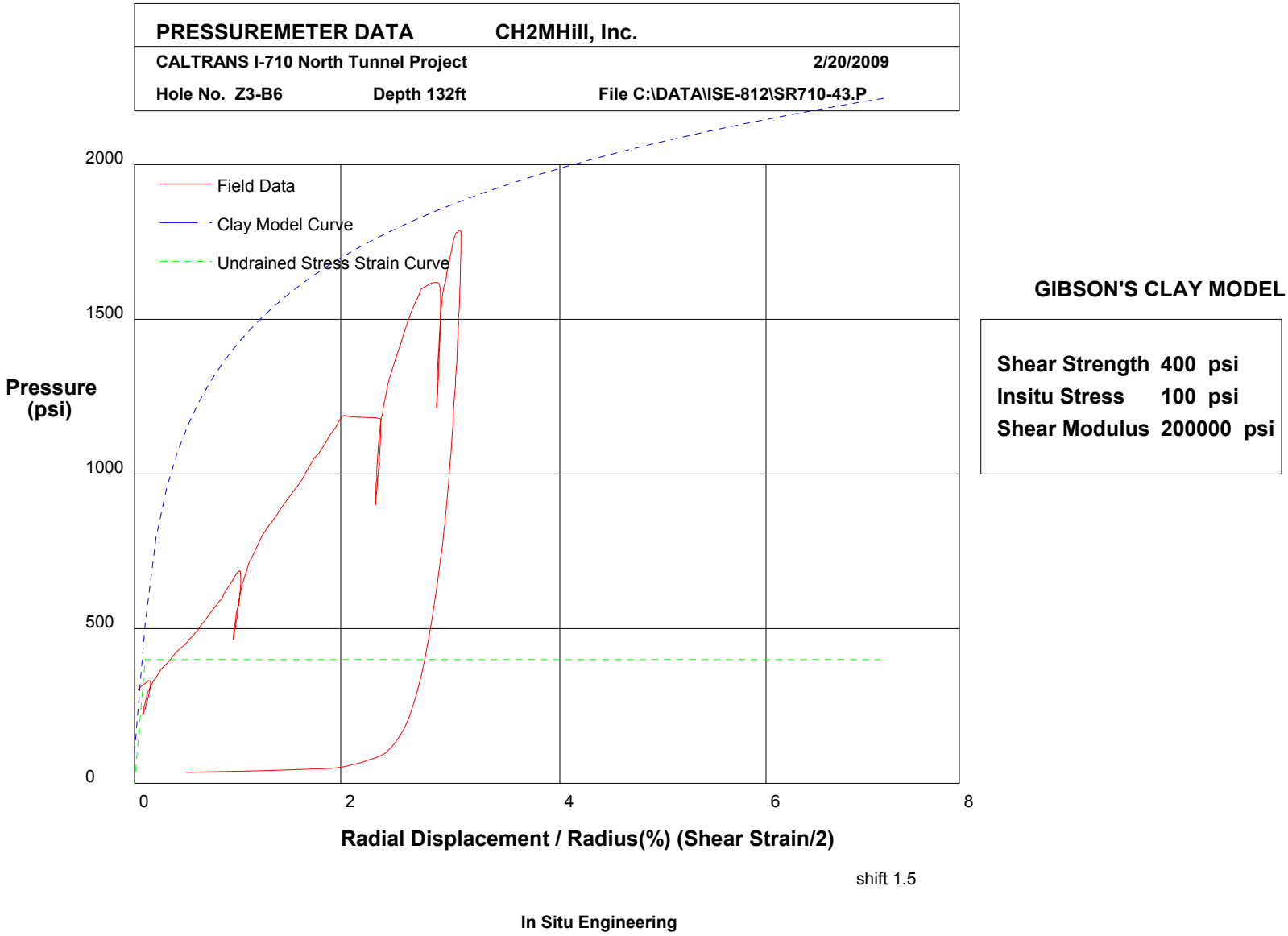

# Appendix II - Pressuremeter Model Interpretation

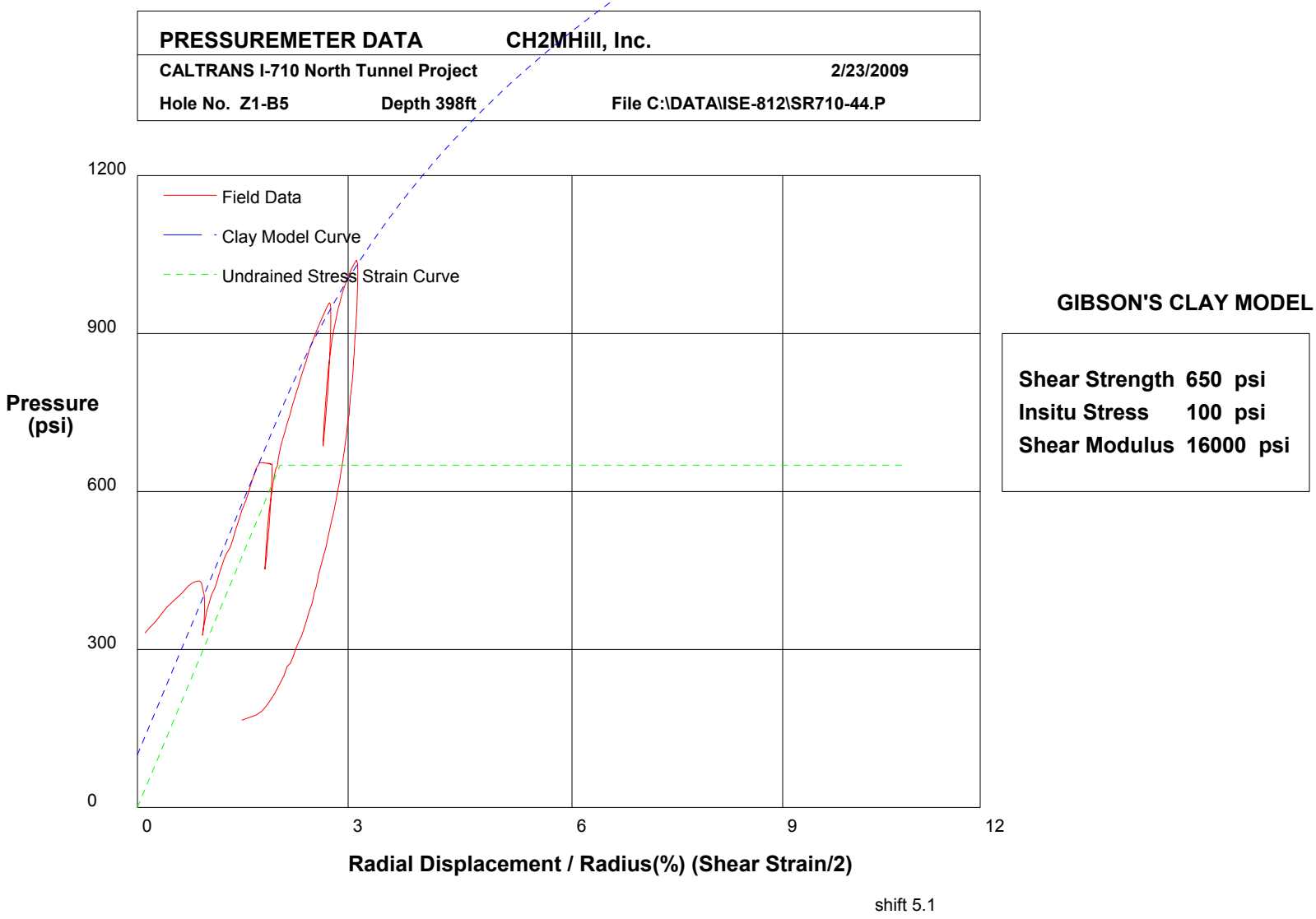

# Appendix II - Pressuremeter Model Interpretation

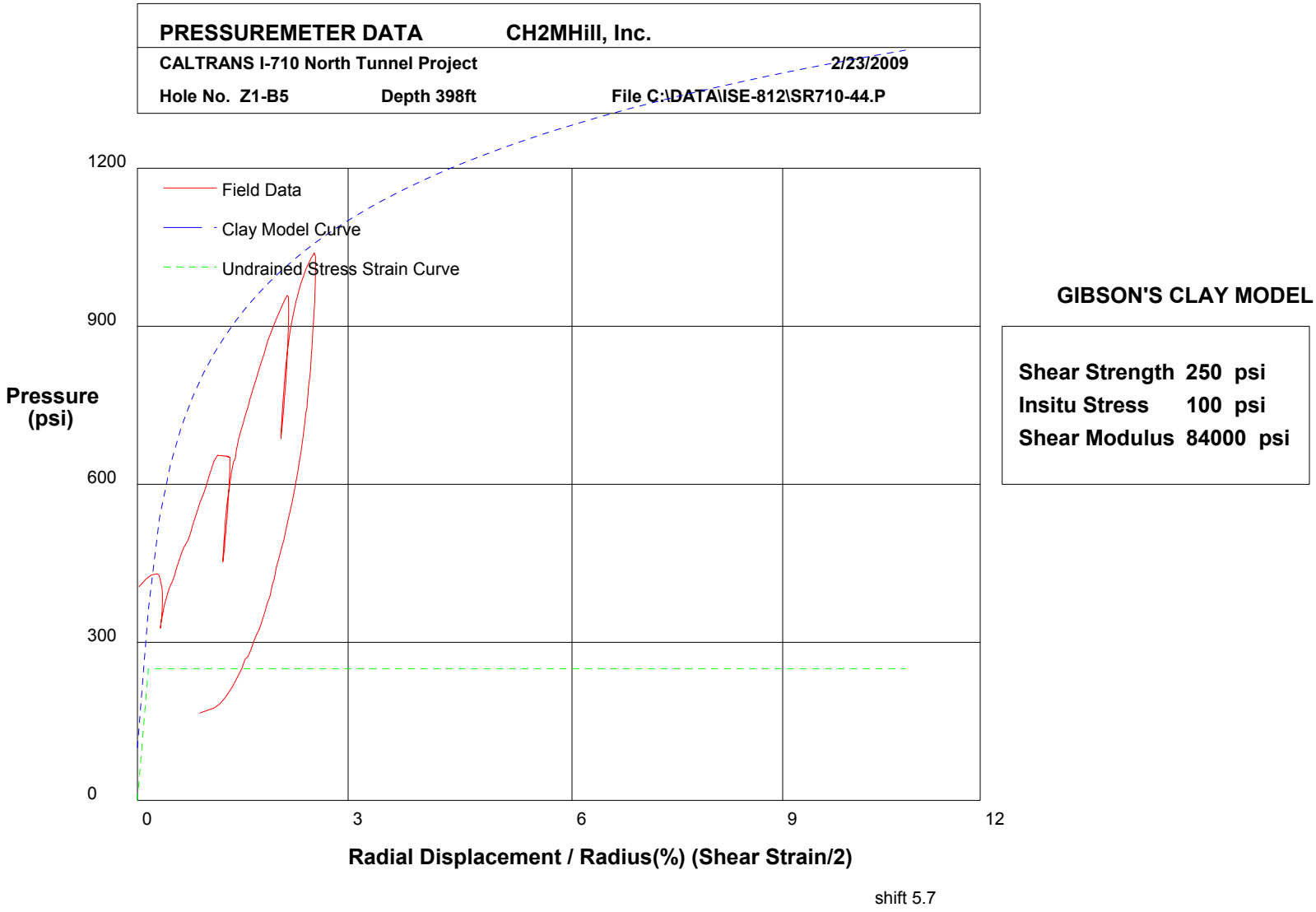

# Appendix II - Pressuremeter Model Interpretation

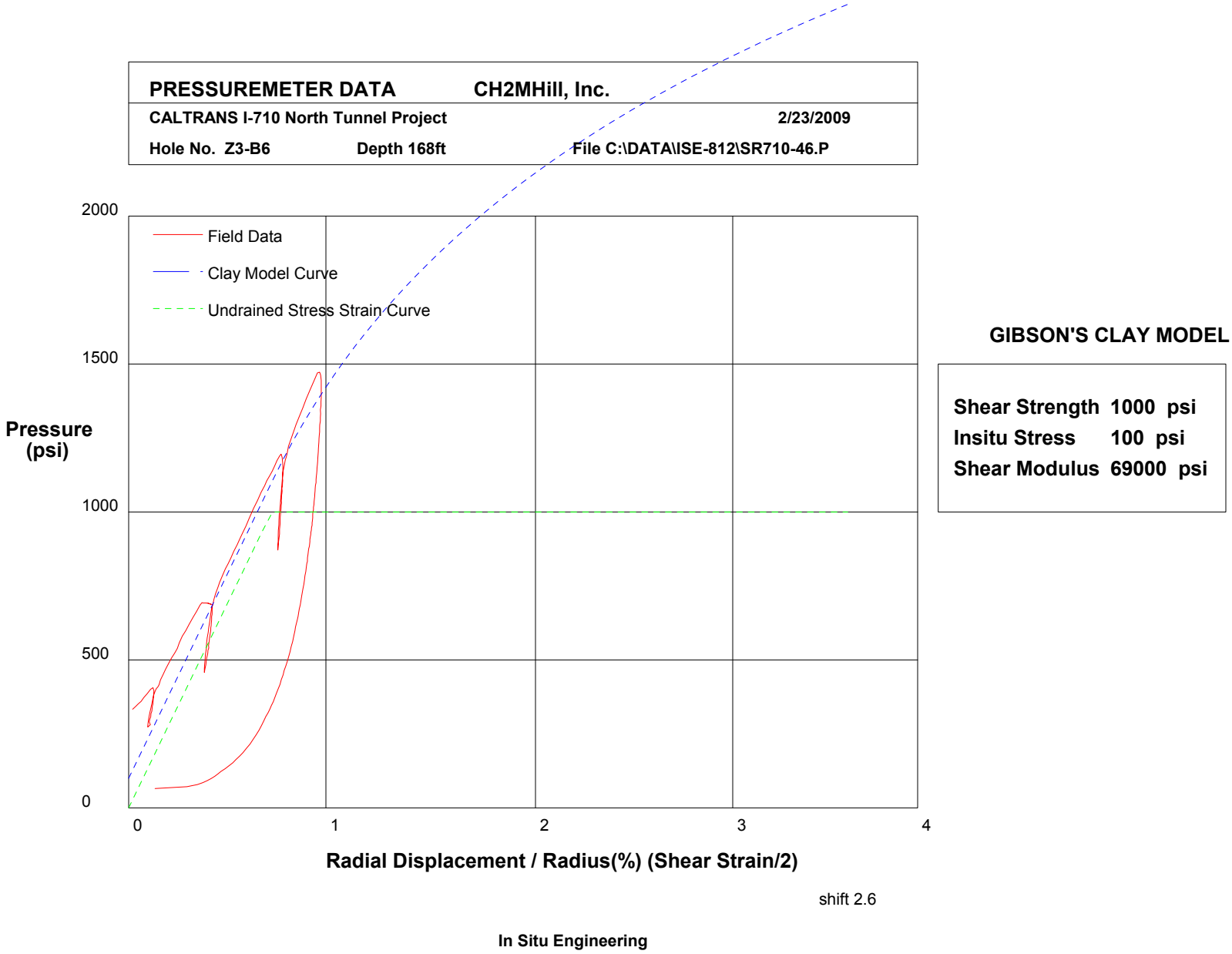

# Appendix II - Pressuremeter Model Interpretation

**PRESSUREMETER DATA** **CH2MHill, Inc.**

**CALTRANS I-710 North Tunnel Project** **2/23/2009**

**Hole No. Z3-B6** **Depth 168ft** **File C:\DATA\ISE-812\SR710-46.P**

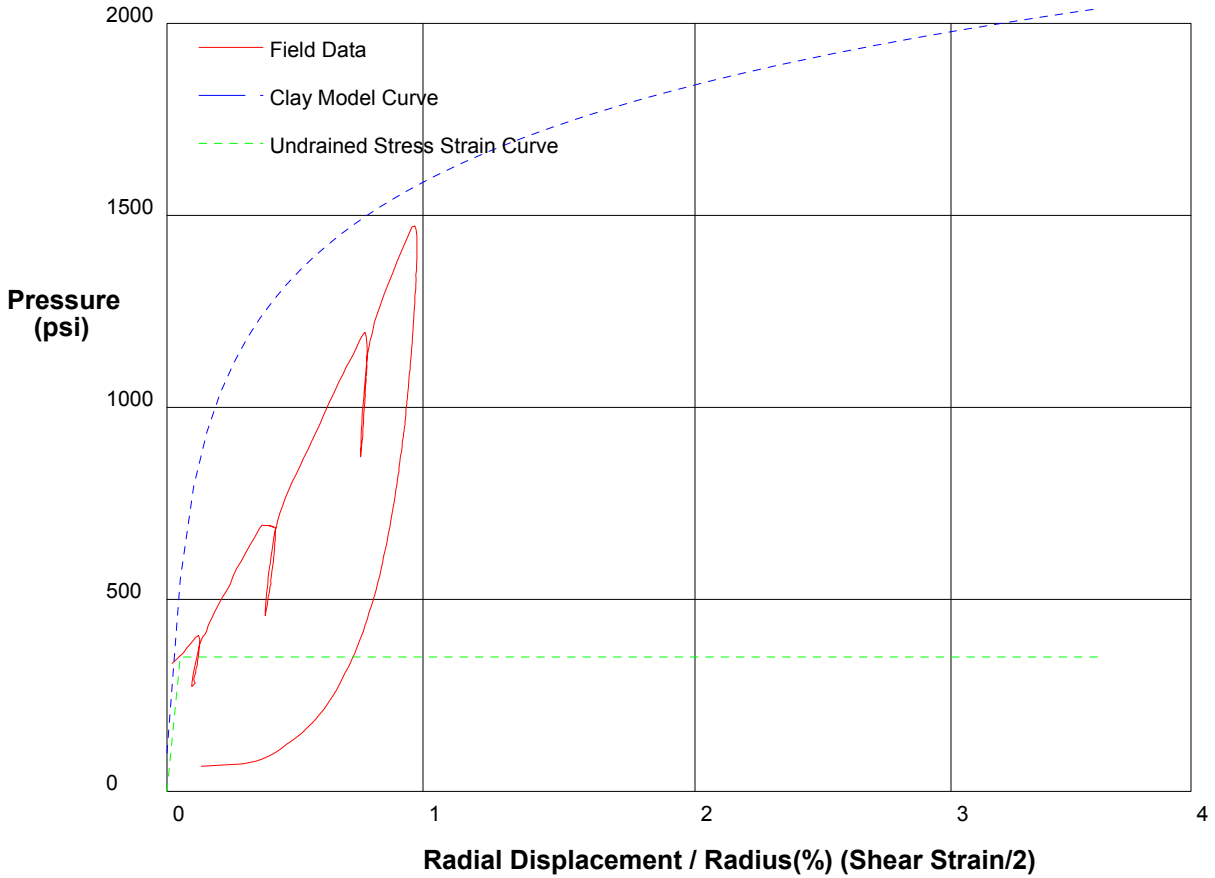


**GIBSON'S CLAY MODEL**

| | |
|---|---|
| **Shear Strength** | **350 psi** |
| **Insitu Stress** | **100 psi** |
| **Shear Modulus** | **450000 psi** |

shift 2.6

**In Situ Engineering**

# Appendix II - Pressuremeter Model Interpretation

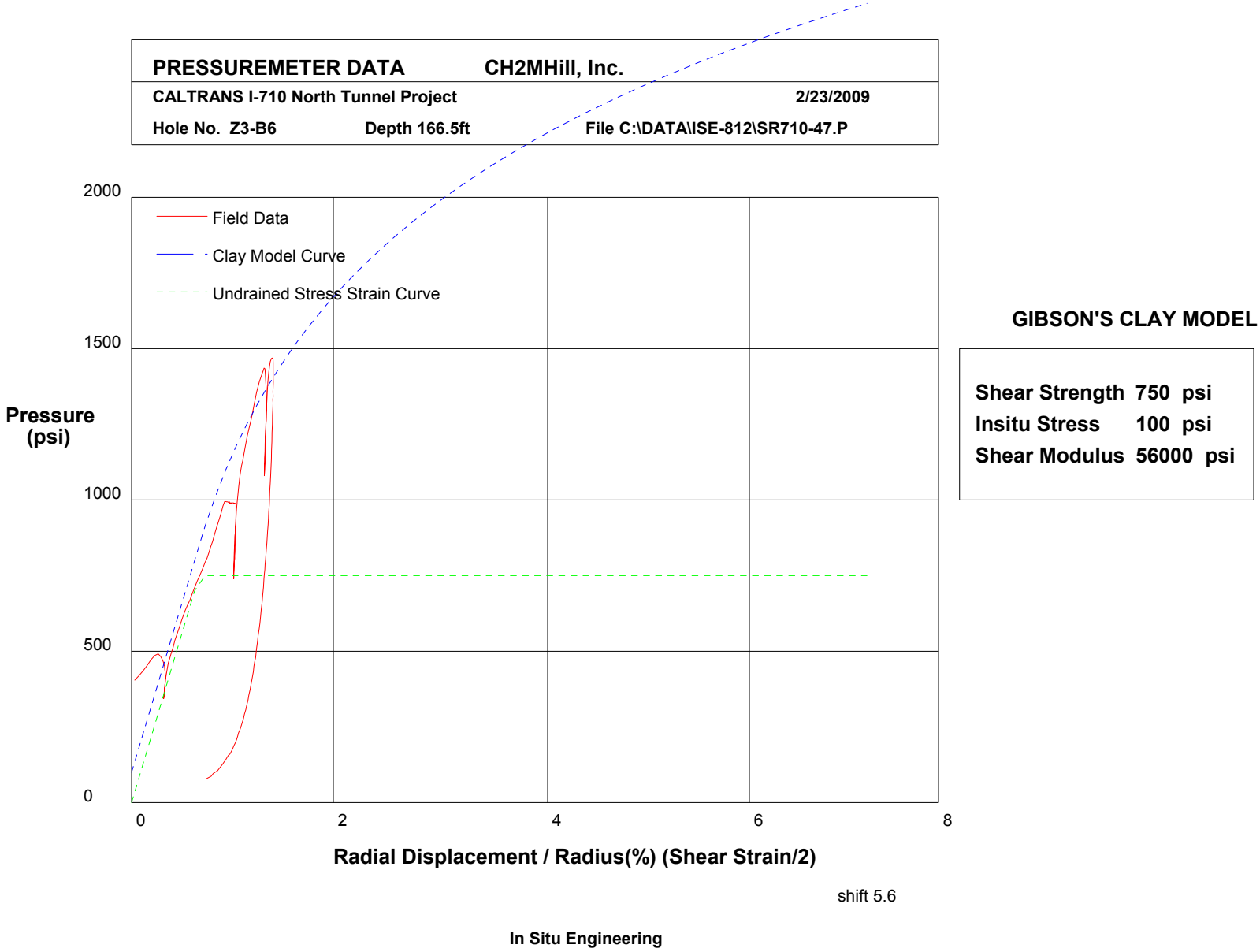

# Appendix II - Pressuremeter Model Interpretation

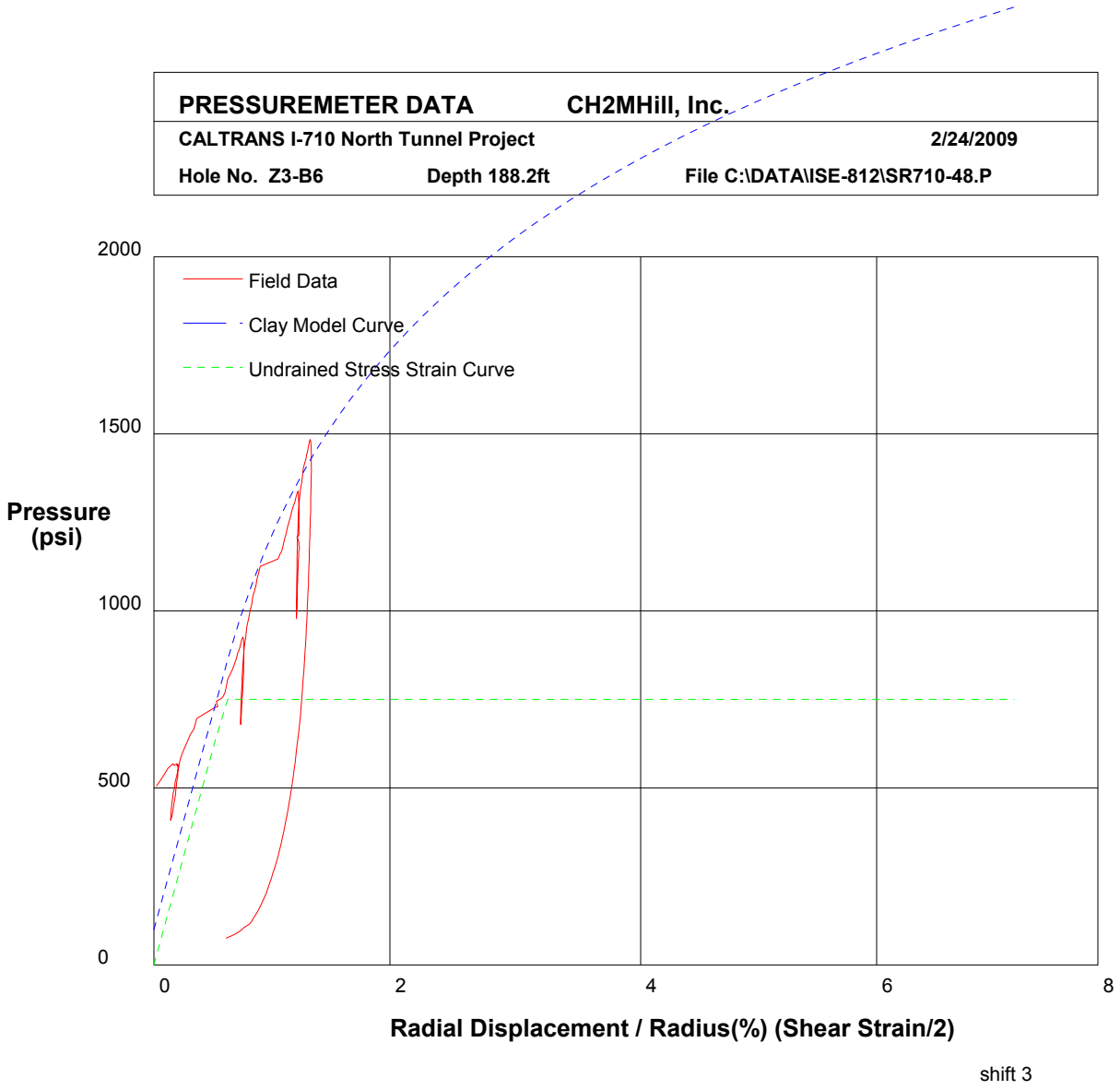


**GIBSON'S CLAY MODEL**

| | |
|---|---|
| **Shear Strength** | **750 psi** |
| **Insitu Stress** | **100 psi** |
| **Shear Modulus** | **61000 psi** |

**In Situ Engineering**

# Appendix II - Pressuremeter Model Interpretation